

Advances in Geophysical and Environmental
Mechanics and Mathematics

AGEM²

Kolumban Hutter
Yongqi Wang

Fluid and Thermodynamics

Volume 2: Advanced Fluid Mechanics
and Thermodynamic Fundamentals

 Springer

Advances in Geophysical and Environmental Mechanics and Mathematics

Series editors

Kolumban Hutter, Zürich, Switzerland

Holger Steeb, Stuttgart, Germany

More information about this series at <http://www.springer.com/series/7540>

Kolumban Hutter · Yongqi Wang

Fluid and Thermodynamics

Volume 2: Advanced Fluid Mechanics
and Thermodynamic Fundamentals

 Springer

Kolumban Hutter
c/o Versuchsanstalt für Wasserbau,
Hydrologie und Glaziologie
ETH Zürich
Zürich
Switzerland

Yongqi Wang
Department of Mechanical Engineering
Technische Universität Darmstadt
Darmstadt, Hessen
Germany

ISSN 1866-8348 ISSN 1866-8356 (electronic)
Advances in Geophysical and Environmental Mechanics and Mathematics
ISBN 978-3-319-33635-0 ISBN 978-3-319-33636-7 (eBook)
DOI 10.1007/978-3-319-33636-7

Library of Congress Control Number: 2016938677

© Springer International Publishing Switzerland 2016

This work is subject to copyright. All rights are reserved by the Publisher, whether the whole or part of the material is concerned, specifically the rights of translation, reprinting, reuse of illustrations, recitation, broadcasting, reproduction on microfilms or in any other physical way, and transmission or information storage and retrieval, electronic adaptation, computer software, or by similar or dissimilar methodology now known or hereafter developed.

The use of general descriptive names, registered names, trademarks, service marks, etc. in this publication does not imply, even in the absence of a specific statement, that such names are exempt from the relevant protective laws and regulations and therefore free for general use.

The publisher, the authors and the editors are safe to assume that the advice and information in this book are believed to be true and accurate at the date of publication. Neither the publisher nor the authors or the editors give a warranty, express or implied, with respect to the material contained herein or for any errors or omissions that may have been made.

Printed on acid-free paper

This Springer imprint is published by Springer Nature
The registered company is Springer International Publishing AG Switzerland

Preface

Fluid and thermodynamics (FTD) are generally taught at technical universities as separate subjects and this separation can be justified simply by reasons of the assigned time; the elements of each subject can be introduced within a semester of ~ 15 weeks. Most likely, these outer educational boundaries may even have well furthered this separation. Intellectually, the two subjects, however, belong together, especially since for all but ideal fluids the second law of thermodynamics imposes constraint conditions on the parameters of the governing equations (generally partial differential equations) that are then used in the fluid dynamic part of the joint effort to construct solutions to physically motivated initial boundary value problems that teach us important facts of the behavior of the motion of the fluid under certain circumstances.

One of the authors (K.H.) found this combination of fluid and thermodynamics as an assigned one-semester course, when he started in 1987 in the Department of Mechanics at Technische Universität Darmstadt (at that time ‘Technische Hochschule’) as successor of the late Prof. Dr. rer.nat. ERNST BECKER (1929–1984). With K.H.’s emphasized interest in continuum mechanics and thermodynamics, this dual understanding of the mathematical description of fluid matter was ideal and the assignment to teach it was a welcome challenge, which was declared as a ‘credo’ to the working environment in both teaching and research in his group.

The course notes of FTD taught to upper-class electrical engineers for 18 years were quickly worked out into the book ‘Fluid und Thermodynamik – eine Einführung’ and published by Springer Verlag, Berlin etc., (ISBN 3-540-59235-0, second edition). All the chapters of this book—some slightly extended—have been translated (by K.H.) into the English language and are interwoven in this treatise with chapters, which, as a whole, should provide a fairly detailed understanding of FTD.

All subjects of this treatise of FTD have been taught in one or another form as lectures in courses to students at Technische Universität Darmstadt, Swiss Federal Institute of Technology in Zürich (ETHZ), and in guest lectures in advanced courses at other universities and research institutions worldwide. The audience in

these courses consisted of students, doctoral candidates and postdoctoral assistants of engineering (civil, mechanical, chemical, mechanics), natural sciences (meteorologists, oceanographers, geophysicists), mathematics, and physics. Some of the topics included are as follows:

- Fluid mechanics,
- Continuum mechanics and thermodynamics,
- Mechanics of environmentally related systems (glacier, ice-sheet mechanics, physical oceanography, lake physics, soil motion, avalanches, debris, and mud flows),
- Vorticity and angular momentum,
- Turbulence modeling (of zeroth, first and second order),
- Regular and singular perturbations,
- Continuum mechanics and thermodynamics of mixtures,
- Continuum mechanics and thermodynamics of COSSERAT continua and COSSERAT mixtures,
- Theoretical glaciology,
- Shallow creeping flows of landslides, glaciers, and ice sheets,

and others. It is hoped that we were successful in designing a coherent picture of the intended text FTD.

Writing the book chapters also profited from books that were written earlier by us and co-authors [1–6].

Fluid and Thermodynamics

Volume 1: Basic Fluid Mechanics

This volume consists of 10 chapters and begins in an introductory **Chap. 1** with some historical facts, definition of the subject field and lists the most important properties of liquids.

This descriptive account is then followed in **Chap. 2** by the simple mathematical description of the fundamental hydrostatic equation and its use in analyses of equilibrium of fluid systems and stability of floating bodies, the derivation of the ARCHIMEDEAN principle and determination of the pressure distribution in the atmosphere.

Chapter 3 deals with hydrodynamics of ideal incompressible (density preserving) fluids. Streamlines, trajectories, and streaklines are defined. A careful derivation of the balances of mass and linear momentum is given and it is shown how the BERNOULLI equation is derived from the balance law of momentum and how it is used in applications. In one-dimensional smooth flow problems the momentum and BERNOULLI equations are equivalent. For discontinuous processes with jumps this is not so. Nevertheless the BERNOULLI equation is a very useful equation in many engineering applications. This chapter ends with the balance law of moment of momentum and its application for EULER's turbine equation.

The conservation law of angular momentum, presented in **Chap. 4**, provides the occasion to define circulation and vorticity and the vorticity theorems, among them those of HELMHOLTZ and ERTEL. The goal of this chapter is to build a fundamental understanding of vorticity.

In **Chap. 5** a collection of simple flow problems in ideal fluids is presented. It is shown how vector analytical methods are used to demonstrate the differential geometric properties of vortex-free flow fields and to evaluate the motion-induced force on a body in a potential field. The concept of virtual mass is defined and two-dimensional fluid potential flow is outlined.

This almanac of flows of ideal fluids is complemented in **Chap. 6** by the presentation of the solution techniques of two-dimensional potential flow by complex-valued function theoretical methods using conformal mappings. Potential flows around two-dimensional air foils, laminar free jets, and the SCHWARZ–CHRISTOFFEL transformations are employed to construct the mathematical descriptions of such flows through a slit or several slits, around air wings, free jets, and in ducts bounding an ideal fluid.

The mathematical physical study of viscous flows starts in **Chap. 7** with the derivation of the general stress–strain rate relation of viscous fluids, in particular NAVIER–STOKES fluids and more generally, non-NEWTONIAN fluids. Application of these equations to viscometric flows, liquid films, POISEUILLE flow, and the slide bearing theory due to REYNOLDS and SOMMERFELD demonstrate their use in an engineering context. Creeping flow for a pseudo-plastic fluid with free surface then shows the application in the glaciological-geological context.

Chapter 8 continues with the study of two-dimensional and three-dimensional simple flow of the NAVIER–STOKES equations. HAGEN–POISEUILLE flow and the EKMAN theory of the wall-near wall-parallel flow on a rotating frame (Earth) and its generalization are presented as solutions of the NAVIER–STOKES equations in the half-space above an oscillating wall and that of a stationary axisymmetric laminar jet. This then leads to the presentation of PRANDTL’s boundary layer theory with flows around wedges and the BLASIUS boundary layer and others.

In **Chap. 9** two- and three-dimensional boundary layer flows in the vicinity of a stagnation point are studied as are flows around wedges and along wedge sidewalls. The flow, induced in the half plane above a rotating plane, is also determined. The technique of the boundary layer approach is commenced with the BLASIUS flow, but more importantly, the boundary layer solution technique for the NAVIER–STOKES equations is explained by use of the method of matched asymptotic expansions. Moreover, the global laws of the steady boundary layer theory are explained with the aid of the HOLSTEIN–BOHLEN procedure. The chapter ends with a brief study of non-stationary boundary layers, in which an impulsive start from rest, flow in the vicinity of a pulsating body, oscillation induced drift current, and non-stationary plate boundary layers are studied.

In **Chap. 10** pipe flow is studied for laminar (HAGEN–POISEUILLE) as well as for turbulent flows; this situation culminates via a dimensional analysis to the well-known MOODY diagram. The volume ends in this chapter with the plane boundary layer flow along a wall due to PRANDTL and VON KÁRMÁN with the famous

logarithmic velocity profile. This last problem is later reanalyzed as the controversies between a power and logarithmic velocity profile near walls is still ongoing research today.

Fluid and Thermodynamics

Volume 2: Advanced Fluid Mechanics and Thermodynamic Fundamentals

This volume consists of 10 chapters and commences in **Chap. 11** with the determination of the creeping motion around spheres at rest in a NEWTONian fluid. This is a classical problem of singular perturbations in the form of matched asymptotic expansions. For creeping flow the acceleration terms in NEWTON's law can be ignored to approximately calculate flow around the sphere by this so-called STOKES approximation. It turns out that far away from the sphere the acceleration terms become larger than those in the STOKES solution, so that the latter solution violates the boundary conditions at infinity. This lowest order correction of the flow around the sphere is due to OSEEN (1910). In a systematic perturbation expansion the outer—OSEEN—series and the inner—STOKES—series with the small REYNOLDS number as perturbation parameter must be matched together to determine all boundary and transition conditions of inner and outer expansions. This procedure is rather tricky, i.e., not easy to understand for beginners. This theory, originally due KAPLUN and to LAGERSTRÖM has been extended, and the drag coefficient for the sphere, which also can be measured is expressible in terms of a series expansion of powers of the REYNOLDS number. However, for REYNOLDS numbers larger than unity, convergence to measured values is poor. About 20–30 years ago a new mathematical approach was designed—the so-called Homotopy Analysis Method; it is based on an entirely different expansion technique, and results for the drag coefficient lie much closer to the experimental values than values obtained with the 'classical' matched asymptotic expansion, as shown in Fig. 11.11. Incidentally the laminar flow of a viscous fluid around a cylinder can analogously be treated, but is not contained in this treatise.

Chapter 12 is devoted to the approximate determination of the velocity field in a shallow layer of ice or granular soil, treated as a non-NEWTONian material flowing under the action of its own weight and assuming its velocity to be so small that STOKES flow can be assumed. Two limiting cases can be analyzed: (i) In the first, the flowing material on a steep slope (which is the case for creeping landslides or snow on mountain topographies with inclination angles that are large). (ii) In the second case the inclination angles are small. Situation (ii) is apt to ice flow in large ice sheets such as Greenland and Antarctica, important in climate scenarios in a warming atmosphere. We derive perturbation schemes in terms of a shallowness parameter in the two situations and discuss applications under real-world conditions.

In shallow rapid gravity driven free surface flows the acceleration terms in NEWTON's law are no longer negligible. **Chapter 13** is devoted to such granular

flows in an attempt to introduce the reader to the challenging theory of the dynamical behavior of fluidized cohesionless granular materials in avalanches of snow, debris and mud, etc. The theoretical description of moving layers of granular assemblies begins with the one-dimensional depth integrated MOHR–COULOMB plastic layer flows down inclines—the so-called SAVAGE–HUTTER theory, but then continues with the general formulation of the model equations referred to topography following curvilinear coordinates with all its peculiarities in the theory and the use of shock-capturing numerical integration techniques.

Chapter 14 on uniqueness and stability provides a first flavor into the subject of laminar-turbulent transition. Two different theoretical concepts are in use and both assume that the laminar–turbulent transition is a question of loss of stability of the laminar motion. With the use of the energy method one tries to find upper bound conditions for the laminar flow to be stable. More successful for pinpointing the laminar-turbulent transition has been the method of linear instability analysis, in which a lowest bound is searched for, at which the onset of deviations from the laminar flow is taking place.

In **Chap. 15**, a detailed introduction to the modeling of turbulence is given. Filter operations are introduced to separate the physical balance laws into evolution equations for the averaged fields on the one hand, and into fluctuating or pulsating fields on the other hand. This procedure generates averages of products of fluctuating quantities, for which closure relations must be formulated. Depending upon the complexity of these closure relations, so-called zeroth, first, and higher order turbulence models are obtained: simple algebraic gradient-type relations for the flux terms, one or two equation models, e.g., k - ε , k - ω , in which evolution equations for the averaged correlation products are formulated, etc. This is done for density preserving fluids as well as so-called BOUSSINESQ fluids and convection fluids on a rotating frame (Earth), which are important models to describe atmospheric and oceanic flows.

Chapter 16 goes back one step by scrutinizing the early zeroth order closure relations as proposed by PRANDTL, VON KÁRMÁN and collaborators. The basis is BOUSSINESQ'S (1872) ansatz for the shear stress in plane parallel flow, τ_{12} , which is expressed to be proportional to the corresponding averaged shear rate $\partial\bar{v}_1/\partial x_2$ with coefficient of proportionality $\rho\varepsilon$, where ρ is the density and ε a kinematic turbulent viscosity or turbulent diffusivity [$\text{m}^2 \text{s}^{-1}$]. In turbulence theory the flux terms of momentum, heat, and suspended mass are all parameterized as gradient-type relations with turbulent diffusivities treated as constants. PRANDTL realized from data collected in his institute that ε was not a constant but depended on his mixing length squared and the magnitude of the shear rate (PRANDTL 1925). This proposal was later improved (PRANDTL 1942) to amend the unsatisfactory agreement at positions where shear rates disappeared. The 1942-law is still local, which means that the REYNOLDS stress tensor at a spatial point depends on spatial velocity derivatives at the *same* position. PRANDTL in a second proposal of his 1942-paper suggested that the turbulent diffusivity should depend on the velocity *difference* at the points where the velocity of the turbulent path assumes maximum and minimum values. This proposal introduces some non-locality, yielded better agreement with data, but

PRANDTL left the gradient-type dependence in order to stay in conformity with BOUSSINESQ. It does neither become apparent nor clear that PRANDTL or the modelers at that time would have realized that non-local effects would be the cause for better agreement of the theoretical formulations with data. The proposal of complete non-local behavior of the REYNOLDS stress parameterization came in 1991 by P. EGOLF and subsequent research articles during ~ 20 years, in which also the local strain rate (= local velocity gradient) is replaced by a difference quotient. We motivate and explain the proposed Difference Quotient Turbulence Model (DQTM) and demonstrate that for standard two-dimensional configurations analyzed in this chapter its performance is superior to other zeroth order models.

The next two chapters are devoted to thermodynamics; first, fundamentals are attacked and, second a field formulation is presented and explored.

Class experience has taught us that thermodynamic fundamentals (**Chap. 17**) are difficult to understand for novel readers. Utmost caution is therefore exercised to precisely introduce terminology such as ‘states’, ‘processes’, ‘extensive’, ‘intensive’, and ‘molar state variables’ as well as concepts like ‘adiabatic’, and ‘diathermal walls’, ‘empirical’ and ‘absolute temperature’, ‘equations of state’, and ‘reversible’ and ‘irreversible processes’. The core of this chapter is, however, the presentation of the First and Second Law of Thermodynamics. The *first law* balances the energies. It states that the time rate of change of the kinetic plus internal energies are balanced by the mechanical power of the stresses and the body forces plus the thermal analogies, which are the flux of heat through the boundary plus the specific radiation also referred to as energy supply. This conservation law then leads to the definitions of the caloric equations of state and the definitions of specific heats. The Second Law of Thermodynamics is likely the most difficult to understand and it is introduced here as a balance law for the entropy and states that all physical processes are irreversible. We motivate this law by going from easy and simple systems to more complex systems by generalization and culminate in this tour with the Second Law as the statement that entropy production rate cannot be negative. Examples illustrate the implications in simple physical systems and show where the two variants of entropy principles may lead to different answers.

Chapter 18 extends and applies the above concepts to continuous material systems. The Second Law is written in global form as a balance law of entropy with flux, supply and production quantities, which can be written in local form as a differential statement. The particular form of the Second Law then depends upon which postulates the individual terms in the entropy balance are subjected to. When the entropy flux equals heat flux divided by absolute temperature and the entropy production rate density is requested to be non-negative, the entropy balance law appears as the CLAUSIUS–DUHEM inequality and its exploitation follows the axiomatic procedure of open systems thermodynamics as introduced by COLEMAN and NOLL. When the entropy flux is left arbitrary but is of the same function class as the other constitutive relations and the entropy supply rate density is identically zero, then the entropy inequality appears in the form of MÜLLER. In both cases the Second Law is expressed by the requirement that the entropy production rate density must be non-negative, but details of the exploitation of the Second Law in the two cases

are subtly different from one another. For standard media such as elastic and/or viscous fluids the results are the same. However, for complex media they may well differ from one another. Examples will illustrate the procedures and results.

Chapter 19 on gas dynamics illustrates a technically important example of a fluid field theory, where the information deduced by the Second Law of Thermodynamics delivers important properties, expressed by the thermal and caloric equations of state of, say, ideal and real gases. We briefly touch problems of acoustics, steady isentropic flow processes and their stream filament theory. The description of the propagation of small perturbations in a gas serves in its one-dimensional form ideally as a model for the propagation of sound, for e.g. in a flute or organ pipe, and it can be used to explain the DOPPLER shift occurring when the sound source is moving relative to the receiver. Moreover, with the stream filament theory the sub- and supersonic flow through a nozzle can be explained. In a final section the three-dimensional theory of shocks is derived as the set of jump conditions on surfaces for the balance laws of mass, momentum, energy, and entropy. Their exploitation is illustrated for steady surfaces for simple fluids under adiabatic flow conditions. These problems are classics; gas dynamics, indeed forms an important advanced technical field that was developed in the twentieth century as a subject of aerodynamics and astronautics and important specialties of mechanical engineering.

Chapter 20 is devoted to the subjects ‘Dimensional analysis, similitude and physical experimentation at laboratory scale’, topics often not systematically taught at higher technical education. However, no insider would deny their usefulness. Books treating these subjects separately and in sufficient detail have appeared since the mid-twentieth century. We give an account of dimensional analysis, define dimensional homogeneity of functions of mathematical physics, the properties of which culminate in BUCKINGHAM’S theorem (which is proved in an appendix to the chapter); its use is illustrated by a diversity of problems from general fluid dynamics, gas dynamics, and thermal sciences, e.g., propagation of a shock from a point source, rising gas bubbles, RAYLEIGH–BÉNARD instability, etc. The theory of physical models develops rules, how to down- or up-scale physical processes from the size of a prototype to the size of the model. The theory shows that in general such scaling transformations are practically never exactly possible, so that scale effects enter in these cases, which distort the model results in comparison to those in the prototype. In hydraulic applications, this leads to the so-called FROUDE and REYNOLDS models, in which either the FROUDE or REYNOLDS number, respectively, remains a mapping invariant but not the other. Application on sediment transport in rivers, heat transfer in forced convection, etc., illustrate the difficulties. The chapter ends with the characterization of dimensional homogeneity of the equations describing physical processes by their governing differential equations. The NAVIER–STOKES–FOURIER–FICK fluid equations serve as illustration.

The intention of this treatise is, apart from presenting its addressed subjects, a clear, detailed, and somewhat rigorous mathematical presentation of FTD on the basis of limited knowledge as a prerequisite. Calculus or analysis of functions of a single or several variables, linear algebra and the basics of ordinary and partial

differential equations are assumed to be known, as is the theory of complex functions. The latter is not universally taught in engineering curricula of universities; we believe that readers not equipped with the theory of complex functions can easily familiarize themselves with its basics in a few weeks' reading effort.

A second goal of this treatise is to frame the individual subjects in their historical content by providing biographical sketches of the inventors of the particular concepts. The science of fluid and thermodynamics began in the Western world more than 2000 years ago, e.g., by ARCHIMEDES in Syracuse. First careful observations on turbulence were described by LEONARDO DA VINCI and on the motion of falling bodies by GALILEO GALILEI. Mathematical description of the motion of physical bodies was begun by ISAAC NEWTON, and DESCARTES. EULER and father JOHANN and son DANIEL BERNOULLI introduced, among others, the continuous methods for ideal, i.e., reversible materials. Most of this research took place in the seventeenth and eighteenth centuries and was perfected in the upcoming nineteenth and twentieth centuries. The recognition of the energy balance equation and the entropy imbalance statement as physical laws are achievements of the nineteenth and first part of the twentieth centuries and are associated with scientists like SADI CARNOT, JULIUS MAYER, HERMANN HELMHOLTZ, RUDOLF CLAUSIUS, PIERRE MAURICE MARIE DUHEM, WILLIAM THOMSON (LORD KELVIN), WILLIARD GIBBS, and MAX PLANK, to name a few.

The solutions of the (initial) boundary value problems which ensue from the emerging equations have been solved by a large number of follow-up scientists from the mid-nineteenth century to present, of whom a few stand out distinguishingly: OSBORNE REYNOLDS, LORD RAYLEIGH, LUDWIG PRANDTL, THEODORE VON KÁRMÁN, G.I. TAYLOR, HERMANN SCHLICHTING, and many others. The history, which evolved from the work of all these scientists, is fascinating. By listing short biographical sketches of those scientists who contributed to the development of fluid and thermodynamics, we hope to guide the reader to a coherent historical development of the fascinating subject of fluid and thermodynamics.

We regard this dual approach as a justified procedure, especially since the twenty-first century university students do no longer sufficiently appreciate the fact, on which shoulders of giants and predecessors we stand.

The books have been jointly drafted by us from notes that accumulated during years. As mentioned before, the Chaps. 1–3, 5, 7, 10, 17–20 are translated (and partly revised) from 'Fluid- und Thermodynamik – eine Einführung'. Many of the other chapters were composed in handwriting and TEXed by K.H. and substantially improved and polished by Y.W. We share equal responsibility for the content and the errors that still remain. Figures, which are taken from others, are reproduced and mostly redrawn, but mentioned in the acknowledgment and/or figure captions. Nevertheless a substantial number of figures have been designed by us. However, we received help for their electronic production: Mr. ANDREAS ROHRER, from the Laboratory of Hydraulics, Hydrology and Glaciology at ETH Zurich (VAW), drew figures for Chaps. 8 and 9 and the student assistants Mr. WALDEMAR SURNIN and Mr. JAN BATTRAM from the Institute of Fluid Dynamics at Technische Universität Darmstadt aided in the production of figures of several other chapters. Mr. ANDREAS

SCHLUMPF from VAW and Ms. ALEXANDRA PAUNICA and Prof. IOANA LUCA drew figures for Chap. 6 and several other chapters.

It is custom of most publishers to ask referees to review book manuscripts shortly before submission for printing by experts of the subjects treated in the forthcoming book. It is, however, also almost consequential that reviewers for a two-volume treatise of more than 1200 pages can hardly be found, simply because of the excessive labor that goes with such an assignment. Nevertheless this burden was taken up by two emeriti, Dr.-Ing. PETER HAUPT, Professor of Mechanics at the University of Kassel, Germany and Dr. rer. nat, Dr. h.c. HANS DIETER ALBER, Professor of Mathematics, Technical University, Darmstadt, Germany. We thoroughly thank these colleagues for their extensive help. Their criticisms and recommendations are gratefully incorporated in the final version of the manuscript.

K.H. wishes to express his sincere thanks to ETH Zurich and in particular to Prof. Dr. R. BOES for the allowance to share a desk as an emeritus professor from Darmstadt at the Laboratory of Hydraulics, Hydrology and Glaciology at ETH Zurich and he equally thanks Profs. Dr. MARTIN FUNK and Dr. WILLI H. HAGER, members of this laboratory, for their support. Y.W. would like to express his thanks to Prof. Dr. MARTIN OBERLACK for the free and constructive collaboration in his fluid dynamic working unit at Technische Universität Darmstadt.

This treatise was planned as a three-volume project, and, indeed, two chapters of a possible volume III have already been written. We still hold up this intention, but the advanced age of one of us does not guarantee that we will be successful in this endeavor. We shall see ...

Finally, we thank Springer Verlag, and in particular Dr. Annett Buettner, for the interest in our FTD treatise and AGEM², in general.

References

1. Hutter, K., Jöhnk, K.: Continuum Methods of Physical Modeling—Continuum Mechanics, Dimensional Analysis, Turbulence, p. 635. Springer, Berlin (2004)
2. Hutter, K., Wang, Y., Chubarenko, I.: Physics of Lakes—Vol. I Foundation of the Mathematical and Physical Background, p. 434. Springer, Berlin (2011a)
3. Hutter, K., Wang, Y., Chubarenko, I.: Physics of Lakes—Vol. II Lakes as Oscillators, p. 646. Springer, Berlin (2011b)
4. Hutter, K., Wang, Y., Chubarenko, I.: Physics of Lakes—Vol. III Methods of Understanding Lakes as Components of the Geophysical Environment, p. 605. Springer, Berlin (2014)
5. Pudasaini, S.P., Hutter, K.: Avalanche Dynamics—Dynamics of Rapid Flows of Dense Granular Avalanches, p. 602. Springer, Berlin (2007)
6. Schneider, L., Hutter, K.: Solid-Fluid Mixtures of Frictional Materials in Geophysical and Geotechnical Context, p. 247. Springer, Berlin (2009)

Zürich
Darmstadt
February 2016

Kolumban Hutter
Yongqi Wang

Contents

11 Creeping Motion Around Spheres at Rest in a Newtonian Fluid	1
11.1 Motivation	3
11.2 Mathematical Preliminaries	5
11.3 Stokes Flow Around a Stagnant Sphere	9
11.3.1 Rigid Sphere and No-Slip Condition on the Surface of the Sphere	9
11.3.2 Cunningham’s Correction	14
11.3.3 Rigid Infinitely Thin Spherical Shell Filled with a Fluid of Different Viscosity	16
11.4 Oseen’s Theory	22
11.4.1 Governing Equations of the Oseen Theory	22
11.4.2 Construction of a Particular Integral of (11.58).	25
11.4.3 ‘Stokes-Lets’ and ‘Oseen-Lets’.	27
11.5 Theory of Lagerstöm and Kaplun.	30
11.5.1 Motivation.	30
11.5.2 Stokes Expansion.	32
11.5.3 Oseen Expansion	34
11.5.4 Matching Procedure	35
11.6 Homotopy Analysis Method—The Viscous Drag Coefficient Computed for Arbitrary Reynolds Numbers.	38
11.6.1 The Mathematical Concept	39
11.6.2 Selection of $\psi_0, \mathcal{H}, \hbar$ and Approximate Solution.	41
11.7 Conclusions and Discussion	43
References	44

12 Three-Dimensional Creeping Flow—Systematic Derivation of the Shallow Flow Approximations 47

12.1 Introductory Motivation 49

12.2 Model Equations 52

 12.2.1 Field Equations 52

 12.2.2 Boundary Conditions 54

12.3 Scaling Procedure 56

12.4 Lowest Order Model Equations for Flow Down Steep Slopes (Strong Steep Slope Shallow Flow Approximation) 66

12.5 A Slightly More General Steep Slope Shallow Flow Approximation (Weak Steep Slope Shallow Flow Approximation) 71

12.6 Phenomenological Expressions for Creeping Glacier Ice 74

12.7 Applications to Downhill Creeping Flows 77

 12.7.1 Computational Procedure. 77

 12.7.2 Profiles and Flows for Isothermal Conditions 79

 12.7.3 Remarks for Use of the Shallow Flow Approximation for Alpine Glaciers 82

12.8 Free-Surface Gravity-Driven Creep Flow of a Very Viscous Body with Strong Thermomechanical Coupling—A Rigorous Derivation of the Shallow Ice Approximation 84

 12.8.1 The Classical Shallow Flow Approximation. 84

 12.8.2 Applications 97

12.9 Discussion and Conclusions 107

References 108

13 Shallow Rapid Granular Avalanches 113

13.1 Introduction. 115

13.2 Distinctive Properties of Granular Materials. 119

 13.2.1 Dilatancy. 120

 13.2.2 Cohesion. 121

 13.2.3 Lubrication 122

 13.2.4 Liquefaction 125

 13.2.5 Segregation, Inverse Grading, Brazil Nut Effect 129

13.3 Shallow Flow Avalanche Modeling 131

 13.3.1 Voellmy’s Avalanche Model 132

 13.3.2 The SH Model, Reduced to Its Essentials 134

13.4 A Three-Dimensional Granular Avalanche Model 141

 13.4.1 Field Equations 141

 13.4.2 Curvilinear Coordinates. 144

 13.4.3 Equations in Dimensionless Form. 147

 13.4.4 Kinematic Boundary Conditions. 149

 13.4.5 Traction Free Condition at the Free Surface. 150

 13.4.6 Coulomb Sliding Law at the Base 150

 13.4.7 Depth Integration 151

13.4.8	Ordering Relations	154
13.4.9	Closure Property	155
13.4.10	Nearly Uniform Flow Profile	158
13.4.11	Summary of the Two-Dimensional SH Equations	159
13.4.12	Standard Form of the Differential Equations	162
13.5	Avalanche Simulation and Verification with Experimental Laboratory Data	165
13.5.1	Introduction	165
13.5.2	Classical and High Resolution Shock Capturing Numerical Methods	165
13.6	Attempts of Model Validation and Verification of Earthquake and Typhoon Induced Landslides	184
	References	192
14	Uniqueness and Stability	197
14.1	Introduction	198
14.2	Kinetic Energy of the Difference Motion	201
14.3	Uniqueness	205
14.4	Stability	206
14.5	Energy Stability of the Laminar Channel Flow	210
14.6	Linear Stability Analysis of Laminar Channel Flow	216
14.6.1	Basic Concepts	216
14.6.2	The Orr–Sommerfeld and the Rayleigh Equations	218
14.6.3	The Eigenvalue Problem	221
	References	224
15	Turbulent Modeling	227
15.1	A Primer on Turbulent Motions	229
15.1.1	Averages and Fluctuations	231
15.1.2	Filters	233
15.1.3	Reynolds Versus Favre Averages	234
15.2	Balance Equations for the Averaged Fields	236
15.3	Turbulent Closure Relations	239
15.3.1	Reynolds Stress Hypothesis and Turbulent Dissipation Rate	239
15.3.2	Averaged Density Field ρ	240
15.3.3	Turbulent Heat Flux q_t and Turbulent Species Mass Flux j_t	241
15.3.4	One- and Two-Equation Models	245
15.4	$k - \varepsilon$ Model for Density Preserving and Boussinesq Fluids	247
15.4.1	The Balance Equations	247
15.4.2	Boussinesq Fluid Referred to a Non-inertial Frame	252

- 15.4.3 Summary of the $k - \epsilon$ Equations 254
- 15.4.4 Boundary Conditions 256
- 15.4.5 Closing Remarks 259
- References 260
- 16 Turbulent Mixing Length Models and Their Applications to Elementary Flow Configurations.** 263
- 16.1 Motivation/Introduction. 265
- 16.2 The Turbulent Plane Wake 271
- 16.3 The Axisymmetric Isothermal Steady Jet. 278
- 16.4 Turbulent Round Jet in a Parallel Co-flow. 295
- 16.5 A Study of Turbulent Plane Poiseuille Flow 300
- 16.6 Discussion 310
- Appendix A: Prandtl’s Mixing Length 313
- References 315
- 17 Thermodynamics—Fundamentals.** 317
- 17.1 Concepts and Some Historical Remarks 320
- 17.2 General Notions and Definitions 337
 - 17.2.1 Thermodynamic System 337
 - 17.2.2 Thermodynamic States, Thermodynamic Processes. 341
 - 17.2.3 Extensive, Intensive, Specific and Molar State Variables. 345
 - 17.2.4 Adiabatic and Diathermic Walls 347
 - 17.2.5 Empirical Temperature, Gas Temperature and Temperature Scales. 349
- 17.3 Thermal Equations of State 353
 - 17.3.1 Ideal Gas. 354
 - 17.3.2 Real Gases 355
 - 17.3.3 The Phenomenological Model of van der Waals. 357
- 17.4 Reversible and Irreversible Thermodynamic Processes 362
 - 17.4.1 Diffusion. 362
 - 17.4.2 Reversible Expansion and Compaction of a Gas. 366
- 17.5 First Law of Thermodynamics. 366
 - 17.5.1 Mechanical Energies. 366
 - 17.5.2 Definitions, Important for the First Law 370
 - 17.5.3 Caloric Equations of State for Fluids and Gases. 378
 - 17.5.4 Simple Applications of the First Law 382
 - 17.5.5 Specific Heats of Real Gases 390
- 17.6 The Second Law of Thermodynamics—Principle of Irreversibility. 392
 - 17.6.1 Preamble. 392
 - 17.6.2 The Second Law for Simple Adiabatic Systems 395

17.6.3	Generalizations for Non-adiabatic Systems.	410
17.7	First Applications of the Second Law of Thermodynamics	412
	References	418
18	Thermodynamics—Field Formulation	421
18.1	The Second Law of Thermodynamics for Continuous Systems	423
18.2	Two Popular Forms of the Entropy Principle.	429
18.2.1	Entropy Principle 1: Clausius–Duhem Inequality	430
18.2.2	Entropy Principle of Ingo Müller	440
18.3	Thermal and Caloric Equations of State	452
18.3.1	Canonical Equations of State	452
18.3.2	Specific Heats and Other Thermodynamic Quantities	458
18.3.3	Application to Ideal Gases.	464
18.3.4	Isentropic Processes in Caloric Ideal Gases	466
18.4	Thermodynamics of an Inviscid, Heat Conducting Compressible Fluid—Toward a Hyperbolic Heat Conduction Equation	467
18.4.1	The Coleman–Noll Approach	468
18.4.2	The Rational Thermodynamics of Ingo Müller.	472
	Appendix: Proof of Liu’s Theorem	479
	References	481
19	Gas Dynamics	483
19.1	Introductory Remarks	485
19.2	Propagation of Small Perturbations in a Gas	486
19.2.1	Fundamental Equations	486
19.2.2	Plane and Spherical Waves	493
19.2.3	Eigen Oscillations Determined with Bernoulli’s Method	502
19.3	Steady, Isentropic Stream Filament Theory	506
19.4	Theory of Shocks.	520
19.4.1	General Concepts	520
19.4.2	Jump Conditions	523
19.4.3	Stationary Shocks in Simple Fluids Under Adiabatic Conditions.	527
19.5	Final Remarks	536
	References	536
20	Dimensional Analysis, Similitude and Physical Experiments at Laboratory Scale	537
20.1	Introductory Motivation	541
20.1.1	Dimensional Analysis	541
20.1.2	Similitude and Model Experiments	543

20.1.3 Systems of Physical Entities 545

20.2 Theory of Dimensional Equations 547

20.2.1 Dimensional Homogeneity. 547

20.2.2 Buckingham’s Theorem 551

20.2.3 A Set of Examples from Fluid Mechanics 556

20.3 Theory of Physical Models 571

20.3.1 Analysis of the Downscaling of Physical
Processes. 571

20.3.2 Applications 577

20.4 Model Theory and Differential Equations 583

20.4.1 Avalanching Motions down Curved and Inclined
Surfaces 584

20.4.2 Navier–Stokes–Fourier–Fick Equations 584

20.4.3 Non-dimensionalization of the NSFF Equations 586

20.5 Discussion and Conclusions 591

Appendix A: Algebraic Theory of Dimensional Analysis 592

References 605

List of Biographies 609

Name Index 611

Subject Index 617

Chapter 11

Creeping Motion Around Spheres at Rest in a Newtonian Fluid

Abstract This volume consists of 10 chapters and commences in this chapter with the determination of the creeping motion around spheres at rest in a NEWTONian fluid. This is a classical problem of singular perturbations in the form of matched asymptotic expansions. For creeping flow the acceleration terms in NEWTON's law can be ignored to approximately calculate flow around the sphere by this so-called STOKES approximation. It turns out that far away from the sphere the acceleration terms become larger than those in the STOKES solution, so that the latter solution violates the boundary conditions at infinity. This lowest order correction of the flow around the sphere is due to OSEEN. In a systematic perturbation expansion the outer—OSEEN—series and the inner—STOKES—series with the small REYNOLDS number as perturbation parameter must be matched together to determine all boundary and transition conditions of inner and outer expansions. This procedure is rather tricky, i.e., not easy to understand for beginners. This theory, originally due to KAPLUN and LAGERSTRÖM has been extended, and the drag coefficient for the sphere, which also can be measured, is expressible in terms of a series expansion of powers of the REYNOLDS number. However, for REYNOLDS numbers larger than unity, convergence to measured values is poor. In the 1990s of the last century a new mathematical approach was designed—the so-called Homotopy Analysis Method; it is based on an entirely different expansion technique, not restricted to small REYNOLDS numbers, and results for the drag coefficient lie much closer to the experimental values than values obtained with the 'classical' matched asymptotic expansion. Incidentally, the laminar flow of a viscous fluid around a cylinder can analogously be treated, but is not contained in this treatise.

Keywords Creeping motion · STOKES approximation · STOKES–OSEEN expansion · Drag coefficient for the sphere as a function of the REYNOLDS number · Homotopy analysis

List of Symbols

Roman Symbols

a	Radius of a circle or sphere
A, B, C, D	Constants of integration when integrating $\mathcal{L}^4\psi = 0$

c_w	General drag coefficient on a sphere
$c_w = 24/\mathbb{R}$	STOKES drag coefficient
ds	Line increment
$d\xi_i, i = 1, 2, 3$	Coordinate increments
$\hat{e}_1, \hat{e}_2, \hat{e}_3$	Unit basis vectors
f	Specific body force
$[H]$	Reference height
HAM	Homotopy Analysis Method
\mathcal{H}	Auxiliary operator in HAM
h_1, h_2, h_3	Metric coefficients in orthogonal curvilinear coordinates
\tilde{h}	Auxiliary parameter in HAM
$In = v_r \frac{\partial v_r}{\partial r}$	Radial inertial acceleration
$\mathbb{K}n$	KNUDSEN number
$\mathcal{L}^2, \mathcal{L}^4$	STOKES operator
$[L]$	Reference length
$\tilde{\mathcal{L}}_\rho^4(\cdot)$	‘Stretched’ STOKES operator
	$\mathcal{L}^4(\cdot)$ see (11.92) and (11.96)
NS...	NAVIER–STOKES...
\mathcal{O}	Order symbol
p, \bar{p}	Pressure, dimensionless—
$q \in [0, 1]$	Embedding parameter in HAM
r	Radial coordinate—distance
$\mathbb{R} = \frac{[L][U]}{\nu}$	REYNOLDS number
$\mathbb{R}' = 2\mathbb{R}$	REYNOLDS number based on $L = 2a$ for spheres
$[U]$	Reference velocity
u_w	Velocity tangential to the wall
$V = \nu \frac{\partial v_r}{\partial r}$	Radial viscous (diffusive) acceleration
$\mathbf{v} = (u, v, w)$	Velocity vector—its components
$\bar{\mathbf{v}} = (\bar{u}, \bar{v}, \bar{w})$	Dimensionless velocity vector—its components
v_z, v_r, v_θ	Axial, radial and azimuthal velocity components
$W = W_1 + W_2$	Drag force exerted on a sphere by a parallel flow
W_1	Pressure drag
W_2	Viscous drag
$\mathbf{x} = (x, y, z)$	Cartesian coordinates, position vector
$\bar{\mathbf{x}} = (\bar{x}, \bar{y}, \bar{z})$	Dimensionless position vector
(z, y, φ)	Cylindrical coordinates, axial, radial, azimuthal

Greek Symbols

$\alpha, \beta, \gamma, \delta$	Constants of integration for the ordinary differential equation $\mathcal{L}^4\psi = 0$
Δ, Δ_H	LAPLACE operator—in 2D
η	Dynamic viscosity
ρ	Mass density

$\rho = \mathbb{R}r$	‘Stretched’ radius for the construction of the OSEEN expansion
$\mu = \cos \theta$	New azimuthal coordinates
λ	Mean free path
ν	Kinematic viscosity
θ	Polar angle in cylindrical coordinates
$\sigma_r, \sigma_\theta, \sigma_\varphi$	Normal stress components in spherical coordinates
$\tau_{r\theta}, \tau_{r\varphi}, \tau_{\theta\varphi}$	Shear stress components in spherical coordinates
ψ	Stream function
ψ^o, ψ^i	Outer and inner expansions respectively, of ψ
$\psi_0(r, \mu)$	Initial guess for $\psi(r, \mu)$ in HAM
$(\psi^o)^i, (\psi^i)^o$	‘Outer-inner’ and ‘inner-outer’ asymptotic representation of ψ
$(\nu \mathcal{L}^2 - U \frac{\partial}{\partial z})(\mathcal{L}^2 \psi)$	OSEEN operator (see Eq. (11.58))

11.1 Motivation

The fundamental equations of this chapter are the NAVIER–STOKES (NS) equations of density preserving fluids, which shall be used here in the form

$$\operatorname{div} \mathbf{v} = 0, \quad \frac{\partial \mathbf{v}}{\partial t} + \operatorname{grad} \frac{|\mathbf{v}|^2}{2} - \mathbf{v} \times \operatorname{curl} \mathbf{v} = -\frac{1}{\rho} \operatorname{grad} p - \nu \operatorname{curl} (\operatorname{curl} \mathbf{v}) + \mathbf{f}$$

as stated in Chap. 7 as (7.33)₁ and (7.39). The first of these equations is the continuity equation, the second the balance of momentum; \mathbf{v} is the velocity field, p the pressure, ρ the constant density, ν the kinematic viscosity and \mathbf{f} the external body force, which henceforth will be ignored. In dimensionless form, when $\mathbf{v} = [U]\bar{\mathbf{v}}$, $(x, y, z) = [L](\bar{x}, \bar{y}, \bar{z})$, $p = [\rho U^2]\bar{p}$, the above equations take for steady state ($\partial \mathbf{v} / \partial t = \mathbf{0}$) the forms

$$\operatorname{div}_{\bar{x}} \bar{\mathbf{v}} = 0, \quad \operatorname{grad}_{\bar{x}} \left| \frac{\bar{\mathbf{v}}}{2} \right|^2 - \bar{\mathbf{v}} \times \operatorname{curl}_{\bar{x}} \bar{\mathbf{v}} = -\operatorname{grad}_{\bar{x}} \bar{p} - \frac{1}{\mathbb{R}} \operatorname{curl}_{\bar{x}} (\operatorname{curl}_{\bar{x}} \bar{\mathbf{v}}), \quad (11.1)$$

in which $\operatorname{grad}_{\bar{x}}$, $\operatorname{div}_{\bar{x}}$ and $\operatorname{curl}_{\bar{x}}$ are operators over $(\bar{x}, \bar{y}, \bar{z})$. Subsequently, their subscripts will be dropped unless the context does not obviously indicate to which variables the operators are referred. Moreover,

$$\mathbb{R} = \frac{[L][U]}{\nu} \quad (11.2)$$

is the REYNOLDS number, defined by the length and velocity scale and the constant viscosity of the fluid. We interpret here the term ‘creeping’ as slow flow, for which

the REYNOLDS number is small, $\mathbb{R} \ll 1$. In the ensuing analysis we shall investigate to what extent this means that the acceleration terms in the momentum equations can be ignored. This is known as the assumption of so-called **Stokes flow**; our analysis, however, will show that flows may still be qualified as creeping when acceleration ought to be accounted for. This requirement leads to the extension of STOKES flow to the **Oseen correction** and at last to an asymptotic expansion, in which successive correction by ‘STOKES-lets’ and ‘OSEN-lets’ are consecutively correcting lower order approximations. This matched asymptotic expansion is the outcome of the so-called LAGERSTRÖM–KAPLUN theory (1957) [5].

Matched asymptotic expansion is a form of a singular perturbation approach, here used for the NAVIER–STOKES (NS) equations. Its solution technique is based on the presence in the governing equations of a small parameter, here the REYNOLDS number $\mathbb{R} \ll 1$. It is, however, known in fluid dynamics that many fluid flows can be characterized as creeping, even if the REYNOLDS number \mathbb{R} is larger than unity. For instance, in pipe flow, laminar flow exists for $\mathbb{R} \leq 2000$ for which the approximate solutions of the NS-equations by perturbation techniques cannot represent realistic results obtained by experiments. In such cases approximate solution procedures must be based on techniques, which are not inherently based on small parameters. In the past 20–30 years such a technique has been proposed and been applied for a number of classical problems of fluid mechanics. It is based on the **homotopy method**. In the ensuing analysis we shall study laminar flow around a stationary sphere by the method of matched asymptotic expansions but shall also demonstrate results obtained with the homotopy method.

STOKES flows are velocity and pressure solutions of the NS-equations, when the acceleration terms are ignored. This does not mean that such flows are automatically steady as time dependence may enter through the boundary conditions. Thus, STOKES flows are solutions of

$$\left. \begin{array}{l} \text{div } \mathbf{v} = 0, \quad -\text{grad } p + \eta \Delta \mathbf{v} = \mathbf{0}, \\ \text{or in dimensionless notation} \\ \text{div } \bar{\mathbf{v}} = 0, \quad -\text{grad } \bar{p} - \frac{1}{\mathbb{R}} \text{curl} (\text{curl } \bar{\mathbf{v}}) = \mathbf{0}. \end{array} \right\} \quad (11.3)$$

By forming the divergence and curl,¹ respectively, of (11.3) we get, owing to $\text{div grad } p = \Delta p$ and $\text{curl grad } p = \mathbf{0}$,

$$\left. \begin{array}{l} \text{div grad } p = \Delta p = 0, \\ \text{curl} (\text{curl} (\text{curl } \mathbf{v})) = \mathbf{0}. \end{array} \right\} \quad (11.4)$$

These are the governing equations of STOKES flow. The pressure obeys the potential equation and the triple rotation of the velocity field vanishes. It is obvious that solutions of (11.4) can only be reasonable approximations to the original equations for small REYNOLDS numbers. For general, *steady* motions, formation of the divergence and rotation of (11.1) yields, respectively,

¹The curl of the momentum equation is often referred to as **vorticity equation**.

$$\left. \begin{aligned} \Delta \left(\frac{p}{\rho} + \left| \frac{\mathbf{v}^2}{2} \right| \right) = 0, \quad \text{curl} (\mathbf{v} \times \text{curl} \mathbf{v}) = \nu \text{curl} (\text{curl} (\text{curl} \mathbf{v})), \\ \text{or in dimensionless notation} \\ \Delta \left(\bar{p} + \left| \frac{\bar{\mathbf{v}}^2}{2} \right| \right) = 0, \quad \text{curl} (\bar{\mathbf{v}} \times \text{curl} \bar{\mathbf{v}}) = \frac{1}{\mathbb{R}} \text{curl} (\text{curl} (\text{curl} \bar{\mathbf{v}})). \end{aligned} \right\} \quad (11.5)$$

In Eq.(11.5)₂ $\mathbb{R} \rightarrow 0$ implies the STOKES equations as expected. However, the complete consistent theory of slow creeping flow around bodies (spheres, cylinders) must employ Eq. (11.5), in which, generally, the squared velocity term in the pressure equations is neglected.

11.2 Mathematical Preliminaries

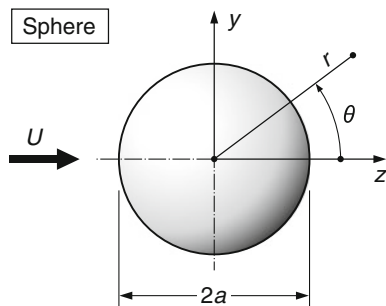
In this section, the NS-equations will be written in cylindrical and spherical coordinates. The goal is to treat parallel flow around a sphere in detail. To this end we shall first write them in cylindrical coordinates (z, y, φ) , see Fig. 11.1. Let us first recall the div—and curl—operators in curvilinear, orthogonal coordinates. These are obtained from the squared line increment

$$ds^2 = h_1^2 d\xi_1^2 + h_2^2 d\xi_2^2 + h_3^2 d\xi_3^2 \quad (11.6)$$

as

$$\begin{aligned} \text{curl} \mathbf{v} &= \frac{1}{h_1 h_2 h_3} \begin{vmatrix} h_1 \hat{e}_1 & h_2 \hat{e}_2 & h_3 \hat{e}_3 \\ \frac{\partial}{\partial \xi_1} & \frac{\partial}{\partial \xi_2} & \frac{\partial}{\partial \xi_3} \\ h_1 v_1 & h_2 v_2 & h_3 v_3 \end{vmatrix}, \\ \text{div} \mathbf{v} &= \frac{1}{h_1 h_2 h_3} \left\{ \frac{\partial}{\partial \xi_1} (v_1 h_2 h_3) + \frac{\partial}{\partial \xi_2} (v_2 h_3 h_1) + \frac{\partial}{\partial \xi_3} (v_3 h_1 h_2) \right\}. \end{aligned} \quad (11.7)$$

Fig. 11.1 Sphere at rest, circumflow by a fluid with constant upstream velocity U in the z -direction. Coordinates are: z —axial; y —perpendicular to z ; r —radial; θ —latitudinal; φ —azimuthal; a is the radius of the sphere



Here, ξ_i ($i = 1, 2, 3$) are curvilinear coordinates. In cylindrical coordinates $(\xi_1, \xi_2, \xi_3) = (z, y, \varphi)$ one has $h_1 = 1$, $h_2 = 1$ and $h_3 = y$; consequently, according to (11.7)₂,

$$\operatorname{div} \mathbf{v} = \frac{\partial v_z}{\partial z} + \frac{1}{y} \frac{\partial(yv_y)}{\partial y} + \frac{1}{y} \frac{\partial v_\varphi}{\partial \varphi} = 0.$$

For steady flow around spheres from a source—constant velocity U parallel to the z -axis at $z = -\infty$ —the flow is axisymmetric, so that $v_\varphi = 0$ and $\partial(\cdot)/\partial\varphi = 0$. For this case the above continuity equation can be identically satisfied by introducing the STOKES stream function $\psi(z, y)$ according to

$$v_z = \frac{1}{y} \frac{\partial \psi}{\partial y}, \quad v_y = -\frac{1}{y} \frac{\partial \psi}{\partial z}. \quad (11.8)$$

Moreover, with the restriction $v_\varphi = 0$ and with (11.8) $\operatorname{curl} \mathbf{v}$ takes the form

$$\operatorname{curl} \mathbf{v} = \left(\frac{\partial v_y}{\partial z} - \frac{\partial v_z}{\partial y} \right) \hat{\mathbf{e}}_\varphi = -\frac{1}{y} \underbrace{\left\{ \frac{\partial^2 \psi}{\partial z^2} + y \frac{\partial}{\partial y} \left(\frac{1}{y} \frac{\partial \psi}{\partial y} \right) \right\}}_{\mathcal{L}^2 \psi} \hat{\mathbf{e}}_\varphi, \quad (11.9)$$

from which the expressions

$$\begin{aligned} \operatorname{curl}(\operatorname{curl} \mathbf{v}) &= \frac{1}{y} \begin{vmatrix} \hat{\mathbf{e}}_z & \hat{\mathbf{e}}_y & y\hat{\mathbf{e}}_\varphi \\ \frac{\partial}{\partial z} & \frac{\partial}{\partial y} & 0 \\ 0 & 0 & -\mathcal{L}^2 \psi \end{vmatrix} = -\frac{1}{y} \frac{\partial \mathcal{L}^2 \psi}{\partial y} \hat{\mathbf{e}}_z + \frac{1}{y} \frac{\partial \mathcal{L}^2 \psi}{\partial z} \hat{\mathbf{e}}_y, \\ \overline{\operatorname{curl}(\operatorname{curl}(\operatorname{curl} \mathbf{v}))} &= \frac{1}{y} \begin{vmatrix} \hat{\mathbf{e}}_z & \hat{\mathbf{e}}_y & y\hat{\mathbf{e}}_\varphi \\ \frac{\partial}{\partial z} & \frac{\partial}{\partial y} & 0 \\ -\frac{1}{y} \frac{\partial \mathcal{L}^2 \psi}{\partial y} & \frac{1}{y} \frac{\partial \mathcal{L}^2 \psi}{\partial z} & 0 \end{vmatrix} \\ &= \left\{ \frac{1}{y} \frac{\partial^2 \mathcal{L}^2 \psi}{\partial z^2} + \frac{\partial}{\partial y} \left(\frac{1}{y} \frac{\partial \mathcal{L}^2 \psi}{\partial y} \right) \right\} \hat{\mathbf{e}}_\varphi \\ &= \frac{1}{y} \left\{ \frac{\partial^2}{\partial z^2} + y \frac{\partial}{\partial y} \left(\frac{1}{y} \frac{\partial}{\partial y} \right) \right\} \mathcal{L}^2 \psi \hat{\mathbf{e}}_\varphi = \frac{1}{y} \mathcal{L}^2 (\mathcal{L}^2 \psi) \hat{\mathbf{e}}_\varphi \\ &= \frac{1}{y} \mathcal{L}^4 \psi \hat{\mathbf{e}}_\varphi \end{aligned} \quad (11.10)$$

follow. For STOKES flow the stream function satisfies the equation²

²We shall call $\mathcal{L}^2(\cdot)$ and $\mathcal{L}^4(\cdot)$ STOKES operators.

$$\mathcal{L}^4\psi = 0. \quad (11.11)$$

Alternatively, it is easy to verify that

$$\begin{aligned} \mathbf{v} \times \text{curl } \mathbf{v} &= -\frac{1}{y}\mathcal{L}^2\psi v_y \hat{\mathbf{e}}_z + \frac{1}{y}\mathcal{L}^2\psi v_z \hat{\mathbf{e}}_y \\ &= \frac{1}{y^2}\mathcal{L}^2\psi \frac{\partial\psi}{\partial z} \hat{\mathbf{e}}_z + \frac{1}{y^2}\mathcal{L}^2\psi \frac{\partial\psi}{\partial y} \hat{\mathbf{e}}_y, \\ \text{curl}(\mathbf{v} \times \text{curl } \mathbf{v}) &= \begin{vmatrix} \hat{\mathbf{e}}_z & \hat{\mathbf{e}}_y & \hat{\mathbf{e}}_\varphi \\ \frac{\partial}{\partial z} & \frac{\partial}{\partial y} & 0 \\ \frac{1}{y^2}\mathcal{L}^2\psi \frac{\partial\psi}{\partial z} & \frac{1}{y^2}\mathcal{L}^2\psi \frac{\partial\psi}{\partial y} & 0 \end{vmatrix} \\ &= \left\{ \frac{\partial}{\partial z} \left(\frac{1}{y^2}\mathcal{L}^2\psi \frac{\partial\psi}{\partial y} \right) - \frac{\partial}{\partial y} \left(\frac{1}{y^2}\mathcal{L}^2\psi \frac{\partial\psi}{\partial z} \right) \right\} \hat{\mathbf{e}}_\varphi \\ &= \left\{ \frac{2}{y^3} \frac{\partial\psi}{\partial z} + \frac{1}{y^2} \left(\frac{\partial\psi}{\partial y} \frac{\partial}{\partial z} - \frac{\partial\psi}{\partial z} \frac{\partial}{\partial y} \right) \right\} \mathcal{L}^2\psi \hat{\mathbf{e}}_\varphi. \end{aligned} \quad (11.12)$$

Substituting the results (11.10) and (11.12) into the vorticity equation (11.5) yields this vorticity equation in cylindrical coordinates as follows:

$$\begin{aligned} \frac{\nu}{y}\mathcal{L}^4\psi &= \frac{1}{y^2} \left\{ \frac{2}{y} \frac{\partial\psi}{\partial z} + \left(\frac{\partial\psi}{\partial y} \frac{\partial}{\partial z} - \frac{\partial\psi}{\partial z} \frac{\partial}{\partial y} \right) \right\} \mathcal{L}^2\psi, \\ \mathcal{L}^2[\cdot] &= \left\{ \frac{\partial^2}{\partial z^2} + y \frac{\partial}{\partial y} \left(\frac{1}{y} \frac{\partial}{\partial y} \right) \right\} [\cdot]. \end{aligned} \quad (11.13)$$

The next step now consists of transforming this equation into spherical coordinates. To this end we again make use of the axial symmetry of the flow, $v_\varphi = 0$, $\partial(\cdot)/\partial\varphi = 0$, and employ the relations

$$\begin{aligned} z &= r \cos \theta, & r &= \sqrt{z^2 + y^2}, \\ y &= r \sin \theta, & \theta &= \arctan(y/z), \end{aligned} \quad (11.14)$$

from which there follows

$$\begin{aligned} \frac{\partial}{\partial z} &= \cos \theta \frac{\partial}{\partial r} - \sin \theta \frac{1}{r} \frac{\partial}{\partial \theta}, \\ \frac{\partial}{\partial y} &= \sin \theta \frac{\partial}{\partial r} + \cos \theta \frac{1}{r} \frac{\partial}{\partial \theta}. \end{aligned} \quad (11.15)$$

With the relations (11.14) and (11.15) the foundations are now laid down to write Eqs. (11.11) and (11.13) in terms of the spherical coordinates (r, θ) . With the intermediate steps

$$\begin{aligned}
\text{(i)} \quad \mathcal{L}^2\psi &= \frac{\partial^2\psi}{\partial z^2} + \frac{\partial^2\psi}{\partial y^2} - \frac{1}{y} \frac{\partial\psi}{\partial y} = \Delta_{(2)}\psi - \frac{1}{y} \frac{\partial\psi}{\partial y} \\
&= \frac{\partial^2\psi}{\partial r^2} + \frac{1}{r} \frac{\partial\psi}{\partial r} + \frac{1}{r^2} \frac{\partial^2\psi}{\partial\theta^2} - \frac{1}{r} \frac{\partial\psi}{\partial r} - \frac{\cos\theta}{r^2 \sin\theta} \frac{\partial\psi}{\partial\theta} \\
&= \frac{\partial^2\psi}{\partial r^2} + \frac{\sin\theta}{r^2} \frac{\partial}{\partial\theta} \left(\frac{1}{\sin\theta} \frac{\partial\psi}{\partial\theta} \right), \tag{11.16} \\
\text{(ii)} \quad \frac{2}{y} \frac{\partial\psi}{\partial z} + \left(\frac{\partial\psi}{\partial y} \frac{\partial}{\partial z} - \frac{\partial\psi}{\partial z} \frac{\partial}{\partial y} \right) \\
&= \frac{2}{r} \left(\cotan\theta \frac{\partial\psi}{\partial r} - \frac{1}{r} \frac{\partial\psi}{\partial\theta} \right) + \frac{1}{r} \frac{\partial\psi}{\partial\theta} \frac{\partial}{\partial r} - \frac{1}{r} \frac{\partial\psi}{\partial r} \frac{\partial}{\partial\theta},
\end{aligned}$$

the steady NS-equation in axisymmetric spherical coordinates and written in terms of the stream function takes the form

$$\nu \mathcal{L}^4\psi = \frac{1}{r^2 \sin\theta} \left\{ \frac{\partial\psi}{\partial\theta} \frac{\partial}{\partial r} - \frac{\partial\psi}{\partial r} \frac{\partial}{\partial\theta} + 2\cotan\theta \frac{\partial\psi}{\partial r} - \frac{2}{r} \frac{\partial\psi}{\partial\theta} \right\} \mathcal{L}^2\psi, \tag{11.17}$$

in which $\mathcal{L}^2\psi$ is given in (11.16). The STOKES approximation is again given by $\mathcal{L}^4\psi = 0$.

Relation (11.17) could also have been obtained by writing (11.6) and (11.7) in terms of the metric in spherical coordinates

$$ds^2 = dr^2 + r^2 d\theta^2 + r^2 \sin^2\theta d\varphi^2. \tag{11.18}$$

According to (11.7)₂, this would have led to

$$\operatorname{div} \mathbf{v} = \frac{1}{r^2} \frac{\partial(r^2 v_r)}{\partial r} + \frac{1}{r \sin\theta} \frac{\partial(v_\theta \sin\theta)}{\partial\theta} + \frac{1}{r \sin\theta} \frac{\partial v_\varphi}{\partial\varphi}. \tag{11.19}$$

For axisymmetric flow ($v_\varphi = 0$) this suggests the introduction of the stream function ψ with the velocity relations

$$v_r = \frac{1}{r^2 \sin\theta} \frac{\partial\psi}{\partial\theta}, \quad v_\theta = -\frac{1}{r \sin\theta} \frac{\partial\psi}{\partial r}, \quad (v_\varphi = 0). \tag{11.20}$$

With these relations the continuity equation (11.19) is identically satisfied. Moreover, this spherical stream function agrees with the earlier stream function modulo an additive constant.

Finally, let us collect at one place those formulae, which will be used in the subsequent sections:

$$\begin{aligned}
v_z &= \frac{1}{y} \frac{\partial \psi}{\partial y}, & v_r &= \frac{1}{r^2 \sin \theta} \frac{\partial \psi}{\partial \theta}, \\
v_y &= -\frac{1}{y} \frac{\partial \psi}{\partial z}, & v_\theta &= -\frac{1}{r \sin \theta} \frac{\partial \psi}{\partial r}, \\
\mathcal{L}^2 \psi &= \frac{\partial^2 \psi}{\partial r^2} + \frac{\sin \theta}{r^2} \frac{\partial}{\partial \theta} \left(\frac{1}{\sin \theta} \frac{\partial \psi}{\partial \theta} \right), & & \text{spherical coordinates,} \\
\text{curl curl } \mathbf{v} &= -\frac{1}{y} \frac{\partial \mathcal{L}^2 \psi}{\partial y} \hat{\mathbf{e}}_z + \frac{1}{y} \frac{\partial \mathcal{L}^2 \psi}{\partial z} \hat{\mathbf{e}}_y, & & \text{cylindrical coordinates.}
\end{aligned} \tag{11.21}$$

11.3 Stokes Flow Around a Stagnant Sphere

11.3.1 Rigid Sphere and No-Slip Condition on the Surface of the Sphere

For creeping STOKES flow around a sphere the following boundary value problem must be solved, see Fig. 11.1.

$$\begin{aligned}
\mathcal{L}^4 \psi &= 0, & & \text{in } \mathcal{R}^3 \setminus V, \\
v_r = v_\theta &= 0, & & \text{for } r = a, \\
\psi &= \frac{U}{2} y^2 = \frac{U}{2} r^2 \sin^2 \theta, & & \text{for } r \rightarrow \infty.
\end{aligned} \tag{11.22}$$

Here, V is the sphere with radius a , and v_r and v_θ are the radial and azimuthal velocity components. The boundary condition (11.22)₃ states that the flow at $r \rightarrow \infty$ merges into the rectilinear flow parallel to the z -axis; indeed $v_z = (1/y)(\partial\psi/\partial y) = U$, according to (11.8)₁; the boundary value problem (11.22) describes the flow exterior to the sphere. The problem was first solved by GEORG GABRIEL STOKES in 1851 [19]; for his brief biography, see Vol. 1, Fig. 7.4.

Let

$$\psi = r^n \sin^2 \theta \tag{11.23}$$

be a trial separation solution. It implies

$$\begin{aligned}
\frac{\partial^2 \psi}{\partial r^2} &= n(n-1)r^{n-2} \sin^2 \theta, \\
\frac{\partial \psi}{\partial \theta} &= 2r^n \sin \theta \cos \theta, \\
\frac{\partial}{\partial \theta} \left(\frac{1}{\sin \theta} \frac{\partial \psi}{\partial \theta} \right) &= \frac{\partial}{\partial \theta} (2r^n \cos \theta) = -2r^n \sin \theta
\end{aligned} \tag{11.24}$$

and, thus, in view of (11.21)

$$\begin{aligned}\mathcal{L}^2\psi &= (n(n-1) - 2) r^{n-2} \sin^2 \theta, \\ \mathcal{L}^4\psi &= (n(n-1) - 2) ((n-2)(n-3) - 2) r^{n-4} \sin^2 \theta.\end{aligned}\quad (11.25)$$

It follows that $\mathcal{L}^4\psi = 0$ is satisfied, if

$$(n(n-1) - 2) = 0 \quad \text{and} \quad ((n-2)(n-3) - 2) = 0$$

with the solution $n = -1, 2, 1, 4$. The most general solution of $\mathcal{L}^4\psi = 0$, thus, has the form

$$\psi = \left(Ar + Br^2 + Cr^4 + \frac{D}{r} \right) \sin^2 \theta = \left(\frac{A}{r} + B + Cr^2 + \frac{D}{r^3} \right) y^2. \quad (11.26)$$

As $r \rightarrow \infty$, the above expression agrees with (11.22)₃, provided that $C = 0$ and $B = U/2$, so that

$$\psi = \left(Ar + \frac{Ur^2}{2} + \frac{D}{r} \right) \sin^2 \theta. \quad (11.27)$$

The second and third terms are the stream functions of the constant rectilinear flow ($\psi = Uy^2/2$, $v_z = U$) and flow due to a dipole ($\psi = (D/r) \sin^2 \theta$ with strength D , respectively, see Vol. 1, Fig. 5.7. They are potential flows and are not responsible for friction; the influence of friction must, therefore, be due to the first term involving A .

Before determining the constants A and D with the aid of boundary conditions at the surface of the sphere, let us first determine a number of additional physical quantities:

- *Velocity:*

$$\begin{aligned}v_r &= \frac{2 \cos \theta}{r^2} \left(Ar + \frac{Ur^2}{2} + \frac{D}{r} \right) = \left(\frac{2A}{r} + U + \frac{2D}{r^3} \right) \cos \theta, \\ v_\theta &= - \left(\frac{A}{r} + U - \frac{D}{r^3} \right) \sin \theta.\end{aligned}\quad (11.28)$$

- *Pressure:* This can be obtained from the equation

$$\text{grad } p = -\eta \text{curl} (\text{curl } \mathbf{v}).$$

Indeed, with the expression immediately above (11.10) one obtains

$$\begin{aligned}\frac{1}{\eta} \frac{\partial p}{\partial y} &= -\frac{1}{y} \frac{\partial \mathcal{L}^2\psi}{\partial z} = -\frac{1}{y} \frac{\partial}{\partial z} \left(-\frac{2A}{r} \sin^2 \theta \right) = -\frac{1}{y} \frac{\partial}{\partial z} \left(-\frac{2Ay^2}{(y^2 + z^2)^{3/2}} \right), \\ \frac{1}{\eta} \frac{\partial p}{\partial z} &= \frac{1}{y} \frac{\partial \mathcal{L}^2\psi}{\partial y} = \frac{1}{y} \frac{\partial}{\partial y} \left(-\frac{2A}{r} \sin^2 \theta \right) = \frac{1}{y} \frac{\partial}{\partial y} \left(-\frac{2Ay^2}{(y^2 + z^2)^{3/2}} \right).\end{aligned}$$

It suffices to transform the first of these expressions; a first step yields

$$\frac{\partial p}{\partial y} = -3\eta Az \frac{2y}{(y^2 + z^2)^{5/2}}$$

and after integration

$$p = -3\eta Az \int_0^y \frac{2y'}{(y'^2 + z^2)^{5/2}} dy' + p^*(z), \quad (11.29)$$

$$p = 2\eta A \frac{z}{(y^2 + z^2)^{3/2}} = 2\eta A \frac{\cos \theta}{r^2},$$

in which $p^* = 0$ has been so selected to yield $p(\infty) = 0$ for normalization. Evidently, the pressure distribution is exclusively given by A (and not the rectilinear flow and the dipole flow).

To evaluate the force exerted by the fluid onto the sphere, the frictional stress components in spherical coordinates are needed. These are given as follows:

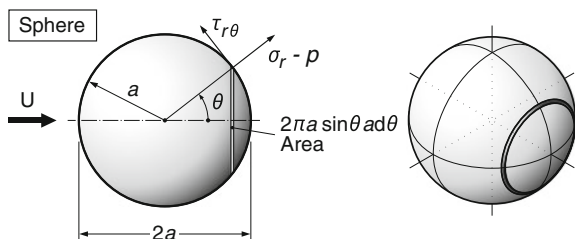
$$\begin{aligned} \sigma_r &= 2\eta \frac{\partial v_r}{\partial r}, \\ \sigma_\theta &= 2\eta \left(\frac{1}{r} \frac{\partial v_\theta}{\partial \theta} + \frac{v_r}{r} \right), \\ \sigma_\varphi &= 2\eta \left(\frac{1}{r \sin \theta} \frac{\partial v_\varphi}{\partial \varphi} + \frac{v_r}{r} + \frac{v_\theta \cotan \theta}{r} \right), \\ \tau_{r\theta} &= \eta \left(\frac{1}{r} \frac{\partial v_r}{\partial \theta} + \frac{\partial v_\theta}{\partial r} - \frac{v_\theta}{r} \right), \\ \tau_{r\varphi} &= \eta \left(\frac{\partial v_\varphi}{\partial r} + \frac{1}{r \sin \theta} \frac{\partial v_r}{\partial \varphi} - \frac{v_\varphi}{r} \right), \\ \tau_{\theta\varphi} &= \eta \left(\frac{1}{r \sin \theta} \frac{\partial v_\theta}{\partial \varphi} + \frac{1}{r} \frac{\partial v_\varphi}{\partial \theta} - \frac{v_\varphi \cotan \theta}{r} \right). \end{aligned} \quad (11.30)$$

The simplifications which emerge for these expressions for axisymmetric flow can easily be identified. If in (11.30)_{1,4} the results of (11.28) and (11.29) are substituted, then the expressions

$$\begin{aligned} \sigma_r &= -4\eta \cos \theta \left(\frac{A}{r^2} + \frac{3D}{r^4} \right), \\ \tau_{r\theta} &= -6\eta \sin \theta \frac{D}{r^4}, \\ \sigma_r - p &= -6\eta \cos \theta \left(\frac{A}{r^2} + \frac{2D}{r^4} \right) \end{aligned} \quad (11.31)$$

are obtained. Due to symmetry of the flow around the sphere the resultant force exerted on the sphere possesses only a component in the direction far upstream of

Fig. 11.2 Stress vectors acting on the surface of the sphere



the sphere; this is the z -direction. Therefore, with reference to **Fig. 11.2**, this leads to

$$W = W_1 + W_2$$

with

$$\begin{aligned} W_1 &= \int_0^\pi (\sigma_r - p) \cos \theta \, 2\pi a^2 \sin \theta \, d\theta \\ &= -6\eta(2\pi a^2) \left(\frac{A}{a^2} + \frac{2D}{a^4} \right) \underbrace{\int_0^\pi \cos^2 \theta \sin \theta \, d\theta}_{2/3} = -8\pi\eta \left(A + \frac{2D}{a^2} \right), \\ W_2 &= - \int_0^\pi \tau_{r\theta} \sin^2 \theta \, 2\pi a^2 \, d\theta = 6\eta \, 2\pi a^2 \frac{D}{a^4} \underbrace{\int_0^\pi \sin^3 \theta \, d\theta}_{4/3} = 8\eta\pi \frac{2D}{a^2}. \end{aligned}$$

Consequently, the total frictional force is given by

$$W = -8\pi\eta A. \quad (11.32)$$

Notice that, owing to our earlier recognition that only terms involving A are contributing to the viscous drag, only those quantities involving A would have to be accounted for in the evaluation of the drag force. That the contributions involving D cancel out in the computation, is a comfortable control of the computation. Notice, moreover, that the above formulae are valid for whatever boundary conditions apply on the spherical surface.

Next, let us determine the constants of integration, A and D . If we require the no-slip condition on the surface, then $v_r(a, \theta) = 0$, $v_\theta(a, \theta) = 0$, so that, in view of (11.28),

$$\frac{A}{a} + \frac{D}{a^3} = -\frac{U}{2}, \quad \frac{A}{a} - \frac{D}{a^3} = -U,$$

from which we obtain

$$A = -\frac{3}{4}Ua, \quad D = \frac{1}{4}Ua^3.$$

so that

$$\begin{aligned} \psi &= \frac{Ua^2}{4} \left(2 \left(\frac{r}{a} \right)^2 + \frac{a}{r} - 3 \frac{r}{a} \right) \sin^2 \theta, \\ v_r &= U \cos \theta \left(1 + \frac{1}{2} \left(\frac{a}{r} \right)^3 - \frac{3a}{2r} \right), \\ v_\theta &= U \sin \theta \left(-1 + \frac{1}{4} \left(\frac{a}{r} \right)^3 + \frac{3a}{4r} \right), \\ p &= -\frac{3}{2}\eta U \cos \theta \frac{a}{r^2}, \\ W &= 6\pi\eta Ua = 3\pi\eta U(2a). \end{aligned} \tag{11.33}$$

This concludes the evaluation of STOKES flow around a sphere. As final remarks we state:

- The STOKES drag consists of two contributions:

$$\begin{aligned} W_1 &= 2\pi\eta Ua, & \text{a pressure drag,} \\ W_2 &= 4\pi\eta Ua, & \text{a viscous drag.} \end{aligned}$$

The denotation ‘pressure drag’ is justified, because for $r = a$, $\sigma_r = 0$.

- A physical interpretation of the STOKES drag is obtained, if one computes the force exerted on a sphere, which moves with REYNOLDS number ‘1’. Indeed,

$$\mathbb{R} = \frac{2aU}{\nu} = 1 \quad \longrightarrow \quad Ua = \frac{\nu}{2} = \frac{\eta}{2\rho} \stackrel{(11.33)_5}{\longrightarrow} W = 3\pi \frac{\eta^2}{\rho}. \tag{11.34}$$

The quantity η^2/ρ is formed only by material quantities, which possess the dimension of a force; it moves a body, large or small, with the REYNOLDS number ‘1’.

- It is customary to characterize the STOKES drag by a dimensionless drag parameter c_w

$$\begin{aligned} c_w &= \frac{W}{\frac{\rho}{2}U^2\pi a^2} = \frac{(6\pi\eta)(2Ua)}{\rho U^2\pi a^2} = \frac{12\nu}{Ua} \\ &= \frac{24}{\mathbb{R}} \quad \text{with} \quad \mathbb{R} = \frac{2aU}{\nu}. \end{aligned} \tag{11.35}$$

- The domain of the validity of the STOKES solution can be found, if a typical viscous diffusive element and a typical convective acceleration term in the NAVIER–STOKES equations are compared to one another. These are for instance

$$v_r \frac{\partial v_r}{\partial r} \quad \text{typical inertial member of the NS-equation,}$$

$$\nu \frac{\partial^2 v_r}{\partial r^2} \quad \text{typical viscous (diffusive) member of the NS-equation}$$

and can be computed with the aid of (11.33) as follows:

$$v_r \frac{\partial v_r}{\partial r} = U^2 \cos^2 \theta \left(1 + \frac{1}{2} \frac{a^3}{r^3} - \frac{3}{2} \frac{a}{r} \right) \left(\frac{3}{2} \frac{a}{r^2} - \frac{3}{2} \frac{a^3}{r^4} \right) \equiv In,$$

$$\nu \frac{\partial^2 v_r}{\partial r^2} = \nu U \cos \theta \left(\frac{6a^3}{r^5} - \frac{3a}{r^3} \right) \equiv V,$$

which implies

$$\frac{In}{V}(\theta = 0) = \frac{Ua}{\nu} \left(\frac{r}{a} \right) \frac{\frac{3}{2} \frac{a}{r} - \frac{3}{2} \frac{a^3}{r^3}}{6 \frac{a^3}{r^3} - 3 \frac{a}{r}} \left(1 + \frac{1}{2} \frac{a^3}{r^3} - \frac{3}{2} \frac{a}{r} \right). \quad (11.36)$$

In the vicinity of the sphere this ratio is of the order of magnitude of the REYNOLDS number $\mathbb{R} = 2Ua/\nu \ll 1$. To ignore the inertial terms in the neighborhood of the sphere is, therefore, justified. However, for $r/a \rightarrow \infty$ the ratio In/V grows indefinitely³; this says that far away from the sphere the inertial forces are no longer negligible. Far away, the inertial as well as the viscous forces have, however, essentially fallen to zero as follows:

$$In(r \rightarrow \infty) = \mathcal{O}(r^{-2}), \quad V(r \rightarrow \infty) = \mathcal{O}(r^{-3}).$$

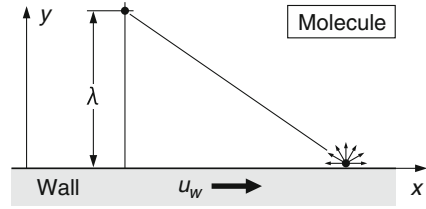
The STOKES theory, therefore, requires amendments.

11.3.2 *Cunningham's Correction*

This correction replaces the no-slip condition at the surface of the sphere by a sliding law. It has its significance in the determination of the charge of an electron according to ROBERT ANDREWS MILLIKAN and HARVEY FLETCHER in 1909 [3]. In their attempt to observe buoyant oil particles under a microscope and to measure the fall velocity one encounters the limitation of the applicability of continuum mechanics. For a fluid sphere 'suspended' in a gas corrections must be incorporated, if the radius of the sphere approaches the order of magnitude of the mean free path λ of the molecules of the gas. The ratio

³At $r = a$, Eq.(11.36) yields $In/V = 0$. Expanding (11.36) in TAYLOR series for small values of $(a - r)/a$ and, respectively, small values of a/r corroborates these statements.

Fig. 11.3 A wall-near particle hitting a boundary, when being ‘glued’ to the boundary by the impact. The wall is locally considered plane and the coordinate perpendicular to the wall is y



$$\mathbb{K}n = \frac{\lambda}{a}$$

is known as **KNUDSEN** number.⁴ For $\mathbb{K}n \ll 1$ the prerequisites of the continuum approximation in the **STOKES** approximation remain still valid, but the fundamental assumption of the no-slip condition at the spherical boundary remains no longer strictly satisfied. For $\mathbb{K}n > 1$ one may still assume the **NS**-equations to remain valid, but must replace the no-slip condition by a *viscous sliding law*. The new boundary condition now reads

$$v_r = 0 \quad v_\theta = \frac{\lambda}{\eta} \tau_{r\theta}, \quad \lambda \text{ mean free path.} \tag{11.37}$$

This sliding law can be motivated as follows, see **Fig. 11.3**. A particle (oil drop in **MILLIKAN**’s experiment) close to the wall possesses the wall-parallel speeds:

$$\left. \begin{array}{l} (i) \text{ prior to the impact: } u_w + \lambda \frac{\partial u}{\partial y} \\ (ii) \text{ after the impact: } 0 \end{array} \right\} \text{mean } u_w = \frac{1}{2} \left(u_w + \lambda \frac{\partial u}{\partial y} \right),$$

of which the mean wall velocity satisfies the equation $u_w = \frac{1}{2} (u_w + \lambda \partial u / \partial y)$ or

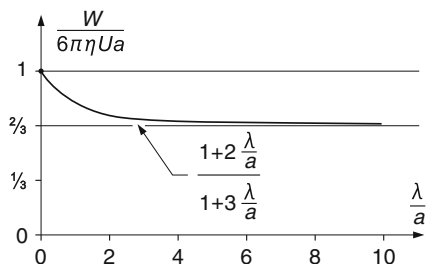
$$u_w = \frac{\lambda}{2} \frac{\partial u}{\partial y} = \frac{\lambda}{\eta} \tau_{xy},$$

if linear **NEWTONIAN** behavior is supposed. The formulae (11.27)–(11.32) remain valid, since they were derived for arbitrary boundary conditions at the surface of the sphere. When (11.37) is used Eqs. (11.28) and (11.31)₂ now yield

$$\begin{aligned} \frac{A}{a} - \frac{D}{a^3} \left(1 + \frac{6\lambda}{a} \right) &= -U, & \left(v_\theta = \frac{\lambda}{\eta} \tau_{r\theta} \right), \\ Aa + \frac{D}{a} &= -\frac{Ua^2}{2}, & (v_r = 0). \end{aligned}$$

⁴After **MARTIN HANS CHRISTIAN KNUDSEN** (15. Feb. 1871–27. May 1949), a physicist who studied primarily molecular gas flows.

Fig. 11.4 Scaled drag force on a sphere, $W/(6\pi\eta Ua)$, plotted against λ/a



These equations, when being solved for A and D have the solution

$$A = -\frac{3}{4}Ua \frac{1 + 2\lambda/a}{1 + 3\lambda/a}, \quad D = \frac{Ua^3}{4} \frac{1}{1 + 3\lambda/a} \tag{11.38}$$

implying

$$W = 6\pi Ua \frac{1 + 2\lambda/a}{1 + 3\lambda/a}, \tag{11.39}$$

see **Fig. 11.4**. This formula shows that for $\lambda = 0$ the STOKES solution is recovered; The sliding boundary condition reduces this at most by a factor of $\frac{2}{3}$. The limit $\lambda \rightarrow \infty$ is interesting. It does *not* produce $W = 0$, which corresponds to perfect sliding; the reason for $W \neq 0$ is that the fluid remains viscous in this case, which produces the viscous drag $W = 4\pi\eta Ua$ without the pressure drag. For $0 < \lambda < \infty$ W lies between $4\pi\eta Ua$ and $6\pi\eta Ua$.

11.3.3 Rigid Infinitely Thin Spherical Shell Filled with a Fluid of Different Viscosity

Very small droplets, which fall or rise in another viscous fluid are often kept in spherical shape due to the effect of surface tension or by impurities attached to the surface. If the fluids within the sphere (with viscosity $\bar{\eta}$) and the exterior fluid (with viscosity η) are immiscible, then the steady motion of the sphere can be determined. In this case a circulating flow occurs also in the interior of the sphere, which, at sufficiently small REYNOLDS numbers satisfies the equation $\mathcal{L}^4\psi = 0$.

Consider first the flow in the interior of the sphere. For this, $\mathcal{L}^4\psi = 0$ has the solution (11.26), or

$$\psi = \left(\alpha r + \beta r^2 + \gamma r^4 + \frac{\delta}{r} \right) \sin^2 \theta \tag{11.40}$$

with the four constants of integration $\alpha, \beta, \gamma, \delta$. Because of the regularity of the solution at $r = 0$, one must have $\delta = 0$, so that

$$\begin{aligned}\frac{\partial \psi}{\partial r} &= (\alpha + 2\beta r + 4\gamma r^3) \sin^2 \theta, \\ \frac{\partial \psi}{\partial \theta} &= (\alpha r + \beta r^2 + \gamma r^4) 2 \sin \theta \cos \theta.\end{aligned}$$

With the aid of (11.21) these expressions allow evaluation of v_r and v_θ as follows:

$$\begin{aligned}v_r &= 2 \cos \theta \left(\frac{\alpha}{r} + \beta + \gamma r^2 \right), \\ v_\theta &= -2 \sin \theta \left(\frac{\alpha}{2r} + \beta + 2\gamma r^2 \right).\end{aligned}$$

To avoid singularities in the velocity components, v_r and v_θ , in the center of the sphere, the constant α must vanish. Thus,

$$\begin{aligned}v_r &= 2 \cos \theta (\beta + \gamma r^2) \quad \longrightarrow \quad \frac{\partial v_r}{\partial \theta} = -2 \sin \theta (\beta + \gamma r^2), \\ v_\theta &= -2 \sin \theta (\beta + 2\gamma r^2) \quad \longrightarrow \quad \frac{\partial v_\theta}{\partial r} = -8 \sin \theta \gamma r,\end{aligned}\tag{11.41}$$

so that the shear stress $\tau_{r\theta}$ is given by, see (11.30),

$$\begin{aligned}\tau_{r\theta} &= \bar{\eta} \left(\frac{1}{r} \frac{\partial v_r}{\partial \theta} + \frac{\partial v_\theta}{\partial r} - \frac{v_\theta}{r} \right) = -2 \sin \theta \left(\frac{\beta}{r} + \gamma r + 4\gamma r - \frac{\beta}{r} - 2\gamma r \right) \bar{\eta} \\ &= -6\bar{\eta}\gamma r \sin \theta.\end{aligned}\tag{11.42}$$

The flow in the space exterior to the sphere is described by formulae (11.27)–(11.30). Let us collect here the relevant statements:

$$\left. \begin{array}{l} \text{exterior : } v_r = 2 \cos \theta \left(\frac{A}{r} + \frac{U}{2} + \frac{D}{r^3} \right), \quad \text{see (11.28),} \\ v_\theta = -\sin \theta \left(\frac{A}{r} + U - \frac{D}{r^3} \right), \quad \text{see (11.28),} \\ \tau_{r\theta} = -6\eta \sin \theta \frac{D}{r^4}, \quad \text{see (11.31),} \\ \text{interior : } v_r = 2 \cos \theta (\beta + \gamma r^2), \quad \text{see (11.41),} \\ v_\theta = -2 \sin \theta (\beta + 2\gamma r^2), \quad \text{see (11.41),} \\ \tau_{r\theta} = -6\bar{\eta}\gamma r \sin \theta, \quad \text{see (11.42).} \end{array} \right\} \tag{11.43}$$

The four constants A, D, β and γ must be determined with the aid of the transition conditions at the surface of the sphere; these conditions read as follows:

1. The radial velocity at the surface vanishes immediately inside and outside the sphere: $v_r(a, \theta) = 0$,

$$\frac{A}{a} + \frac{D}{a^3} = -\frac{U}{2}, \quad (11.44)$$

$$\beta + \gamma a^2 = 0. \quad (11.45)$$

2. The tangential velocity is continuous, $[[v_\theta]] = 0$,

$$\frac{A}{a} + U - \frac{D}{a^3} = 2\beta + 4\gamma a^2. \quad (11.46)$$

3. At the surface of the sphere the shear stresses $\tau_{r\theta}$ are continuous,

$$\eta \frac{D}{a^4} = \bar{\eta} \gamma a. \quad (11.47)$$

The solution of Eqs. (11.44)–(11.47) is given by

$$\begin{aligned} A &= -\frac{Ua}{4} \frac{2 + 3\bar{\eta}/\eta}{1 + \bar{\eta}/\eta}, \\ D &= \frac{Ua^3}{4} \frac{\bar{\eta}/\eta}{1 + \bar{\eta}/\eta}, \\ \gamma &= -\frac{\beta}{a^2} = \frac{U}{4a^2} \frac{1}{1 + \bar{\eta}/\eta}, \end{aligned} \quad (11.48)$$

so that in view of (11.32) the drag force is given by

$$W = 2\pi\eta Ua \frac{2 + 3\bar{\eta}/\eta}{1 + \bar{\eta}/\eta}, \quad (11.49)$$

a result that is due to G.I. TAYLOR⁵ (1932) [20]. Accordingly, $\bar{\eta} \rightarrow \infty$ implies the result for a rigid sphere, $W = 6\pi\eta Ua$; alternatively, for $\bar{\eta} \rightarrow 0$ we obtain instead $W = 4\pi\eta Ua$, the solution for a frictionless surface ($\lambda = 0$); both results are as expected. Moreover, with $\alpha = \delta = 0$ and β, γ as given in (11.48)_{3,4} the stream function in the interior of the sphere is obtained. Indeed, with (11.40) we have

$$\psi = -\frac{U}{4a^2} (a^2 - r^2)r^2 \sin^2 \theta \frac{1}{1 + \bar{\eta}/\eta}. \quad (11.50)$$

⁵For a biography of TAYLOR, see Fig. 11.5.

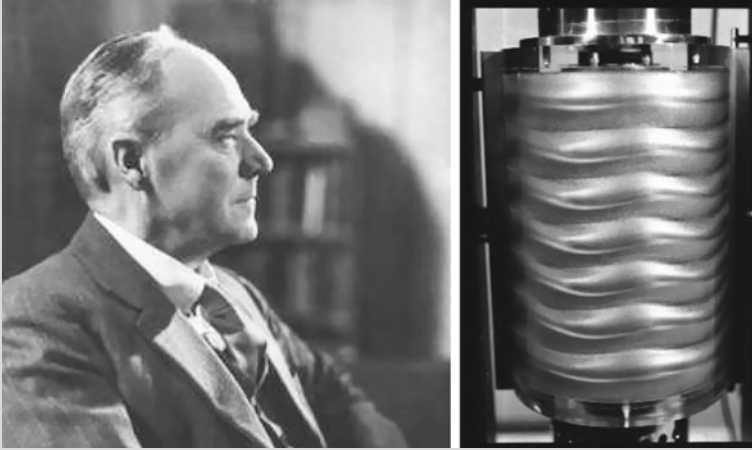


Fig. 11.5 GEOFFREY INGRAM TAYLOR (7. March 1886–17. June 1975). (Right photo) Wavy Taylor vortices in the gap between concentric cylinders, reproduced in laboratory by K.G. ROESNER.

GEOFFREY INGRAM TAYLOR was an applied mathematician and physicist specialized in fluid dynamics and wave theory. Taylor studied mathematics at Trinity College, Cambridge University. With work on shock waves, 1909, he won the Smith's Prize and was elected a fellow at Trinity College in 1910 and a Reader in Dynamical Meteorology in the following year. His publication 'Turbulent motion in fluids' won him the ADAMS Prize in 1915.

During World War II TAYLOR was sent to the Royal Aircraft Factory in Farnborough to apply his knowledge in aerodynamics and meteorology to aircraft design; there he worked on stress in propeller shafts, learned to fly airplanes and made parachute jumps. After World War I, he returned to Cambridge, where he worked on rotating fluids. In 1915 TAYLOR was appointed a Royal Society research professorship. This freed him from teaching and led to a period of very active research on both fluid and solid mechanics (also of crystalline materials), including statistical approaches to turbulence. In 1934 TAYLOR realized—almost simultaneously with POLANYI and OROVAN—that the plastic deformation of ductile material could be explained with the theory of dislocations.

During World War II TAYLOR worked on applications of his expertise to military problems, among others the propagation of blast waves in air and water. His prediction of the strength of the atomic explosion performed as part of the Manhattan Project in the desert of New Mexico is well known. In 1944 he was also knighted.

TAYLOR continued his research after the war, working on the development of supersonic aircraft. He officially retired in 1952 from active duty; he continued to work for twenty more years. He wrote his final paper on electrical activity in thunderstorms in 1969, when he was 83. He suffered a stroke in 1972 and died on 27 June 1975.

The text is based on www.wikipedia.org

Further references:

B. PIPPARD: Sir Geoffrey Taylor, *Physics Today*, Sept 1975, p. 67

G. BATCHELOR: *The life and legacy of G.I. Taylor*. Cambridge University Press, 1994. ISBN 0-521-46121-9

Remarks

- **Figure 11.6** displays the streamlines (panel (a)) and the perspective view (panel (b)) of the function (11.50), called a HILL vortex.
- Formula (11.49) allows evaluation of the rising velocity of a spherical gas bubble with density $\bar{\rho}$ in a heavier fluid according to the equation

$$\underbrace{\frac{4\pi}{3}a^3\rho g}_{\text{Buoyancy}} = \underbrace{\frac{4\pi}{3}a^3\bar{\rho}g}_{\text{Weight}} + \underbrace{2\pi\eta Ua \frac{2+3\bar{\eta}/\eta}{1+\bar{\eta}/\eta}}_{\text{Drag Force}},$$

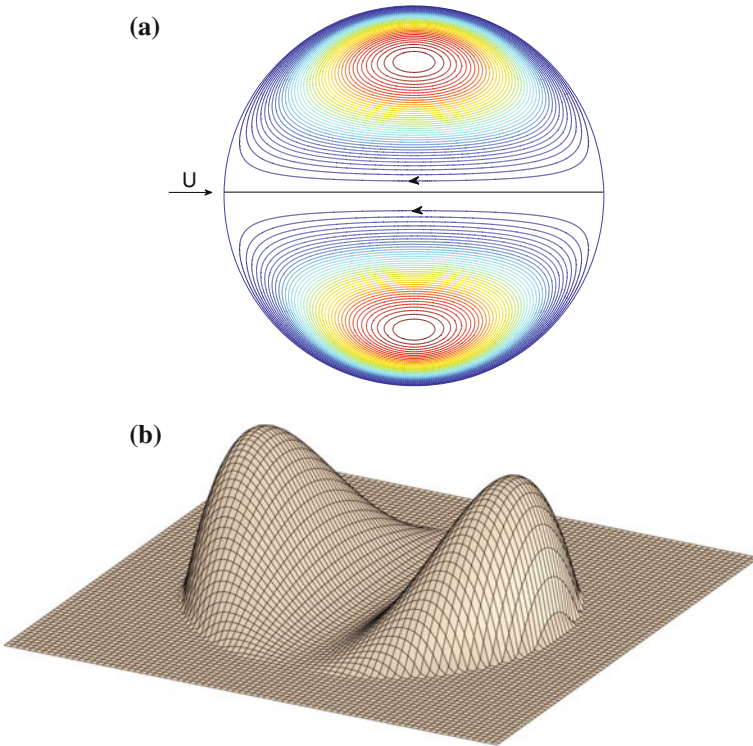


Fig. 11.6 Streamlines (a) and perspective plot of the stream function (b) of a HILL vortex

from which

$$U = \frac{2}{3} \frac{a^2 g}{\nu} \left(1 - \frac{\bar{\rho}}{\rho}\right) \frac{1 + \bar{\eta}/\eta}{2 + 3\bar{\eta}/\eta}, \quad \left(\nu = \frac{\eta}{\rho}\right) \quad (11.51)$$

follows. The limits $\bar{\eta} \rightarrow \infty$ and $\bar{\eta} = 0$ yield

$$\begin{aligned} \bar{\eta} \ll \eta: \quad U &= \frac{1}{3} \frac{a^2 g}{\nu} \left(1 - \frac{\bar{\rho}}{\rho}\right), \\ \bar{\eta} \gg \eta: \quad U &= \frac{2}{9} \frac{a^2 g}{\nu} \left(1 - \frac{\bar{\rho}}{\rho}\right). \end{aligned}$$

Experimentally one often observes for $\bar{\eta} \ll \eta$, the rising velocity for the case $\bar{\eta} \gg \eta$. This corresponds to the no-slip condition and can be explained by a stiffening of the interface due to a gradient of the surface tension by a contamination of the surface.

- GEORGE BATCHELOR (1988) [1] considered the configuration of **Fig. 11.7** to explain the possible existence of air bubbles in ‘fluidized beds’: In a fluid with constant steady speed U at infinity, rigid particles with radius a are suspended having falling velocity W . The particles are surrounded by spherical air bubbles of radius R . In the frame of the moving particles the approaching velocity is given by $U - W$. We then have:

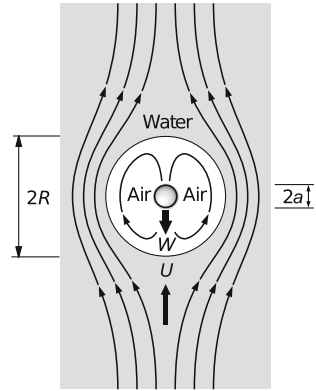
in the exterior region (water)

$$\begin{aligned} v_r &= 2 \cos \theta \left(\frac{A}{r} + \frac{U - W}{2} + \frac{D}{r^3} \right), \\ v_\theta &= -\sin \theta \left(\frac{A}{r} + U - W - \frac{D}{r^3} \right), \\ \tau_{r\theta} &= -6\eta \sin \theta \frac{D}{r^4}; \end{aligned} \quad (11.52)$$

in the inner region (air)

$$\begin{aligned} v_r &= 2 \cos \theta \left(\frac{\alpha}{r} + \beta + \gamma r^2 + \frac{\delta}{r^3} \right), \\ v_\theta &= -2 \sin \theta \left(\frac{\alpha}{r} + \beta + 2\gamma r^2 - \frac{\delta}{r^3} \right) \\ \tau_{r\theta} &= -6\bar{\eta}\gamma r \sin \theta. \end{aligned} \quad (11.53)$$

Fig. 11.7 Spherical particle enclosed in a spherical air bubble rising or falling in a viscous fluid



The constants $A, D, \alpha, \beta, \gamma, \delta$ are so determined that for $r = a$ the velocities $v_r = v_\theta = 0$ and for $r = R, v_r(R^+) = v_r(R^-) = 0$; moreover, for $r = R, v_\theta$ and $\tau_{r\theta}$ must be continuous. These are six equations whose solution is given by BATCHELOR (1988) [1].

11.4 Oseen’s Theory⁶

11.4.1 Governing Equations of the Oseen Theory

The essence of the STOKES theory is the solution of $\mathcal{L}^4\psi = 0$, Eq. (11.11), for the stream function $\psi(z, y)$ from which the axial, v_z , and the radial, v_y , velocity components (11.8) in cylindrical coordinates (z, y) can be determined. It was demonstrated with (11.36) and subsequent discussions that far away from the stationary rigid sphere the inertial (convective) acceleration terms dominate over the viscous (diffusive) terms. This implies that, strictly, the convective acceleration terms must somehow, be accounted for C.W. OSEEN (1910) [15] recognized that far away from the sphere the actual flow around the sphere cannot deviate much from the rectilinear flow $\mathbf{v} \approx U\hat{e}_z$ and approximated for this reason $(\text{grad } \mathbf{v})\mathbf{v}$ by $(\text{grad } \mathbf{v})U\hat{e}_z$, so that

$$(\text{grad } \mathbf{v})\mathbf{v} \approx U \frac{\partial \mathbf{v}}{\partial z}. \tag{11.54}$$

For steady flow, the momentum equation, therefore, takes the form

⁶For a brief biography of CARL WILHELM OSEEN, see **Fig. 11.8**.



Fig. 11.8 CARL WILHELM OSEEN (17. April 1879–7. Nov. 1944)

CARL WILHELM OSEEN was a Swedish theoretical physicist in Uppsala and Director of the NOBEL Institute for theoretical physics. Starting in 1896 he studied at Lund University, where he graduated in 1900; he also studied in Göttingen. 1902 he became a docent and subsequently until 1910 substitute professor of mathematics. Between 1909 and 1933 CARL OSEEN was professor of mechanics and mathematical physics at the University of Uppsala. In 1921 he became a member of the Royal Swedish Academy of Sciences and in 1933 he acquired the head office of the NOBEL Institute, which under ARRHENIUS emphasized on research in chemistry, now concentrated its activities on theoretical physics. 1924 OSEEN became a corresponding member of the Bavarian Academy of Sciences.

CARL WILHELM OSEEN's research focus was the development of the theory of elasticity of liquid crystals. He proposed in 1921 ALBERT EINSTEIN for the NOBEL prize, was among the first Swedish physicists to accept NIELS BOHR's atomic model. Most important for fluid dynamics were the OSEEN equations in viscous fluid flows, which demonstrated for a linear viscous fluid that creeping flow around a sphere far away from the sphere needed to account for the (linearized) advective acceleration terms as illustrated in Sect. 11.4.1. This led later to the famous asymptotic STOKES–OSEEN expansion of bodies, slowly circumflown by a NEWTONian fluid. He also performed pioneering work in the theory of liquid crystals.

The text is based on www.wikipedia.org

$$U \frac{\partial \mathbf{v}}{\partial z} = -\frac{1}{\rho} \text{grad } p - \nu \text{curl}(\text{curl } \mathbf{v}). \quad (11.55)$$

This approximation corresponds to a linearization of the convective acceleration term, if it is assumed that the motion of the fluid deviates only slightly from rectilinear flow in the z -direction. In the neighborhood of the circumflown body this assumption cannot be valid. Here, however, it was recognized that the STOKES approximation was sufficiently accurate, at least for spheres, for which computations have been demonstrated. All the more, it was confirmed that the acceleration terms were indeed negligibly small; it may, therefore be accepted that the error, which is introduced by the OSEEN approximation, is likely of negligible order of magnitude.

It was shown in Sect. 11.1 [between the formulae (11.8), (11.9) and (11.10)] that

$$\begin{aligned} \text{curl } \mathbf{v} &= -\frac{1}{y} \mathcal{L}^2 \psi \hat{\mathbf{e}}_\varphi, \\ \text{curl}(\text{curl}(\text{curl } \mathbf{v})) &= \frac{1}{y} \mathcal{L}^4 \psi \hat{\mathbf{e}}_\varphi. \end{aligned} \quad (11.56)$$

Forming the rotation (curl) of (11.55) yields

$$U \frac{\partial}{\partial z} \text{curl } \mathbf{v} = -\nu \text{curl}(\text{curl}(\text{curl } \mathbf{v})), \quad (11.57)$$

or after substitution of (11.56)

$$\left(\nu \mathcal{L}^2 - U \frac{\partial}{\partial z} \right) \mathcal{L}^2 \psi = 0, \quad (11.58)$$

as the vorticity equation in the OSEEN approximation. Let us also recall the operator $\mathcal{L}^2[\cdot]$,

$$\begin{aligned} \mathcal{L}^2[\cdot] &= \left\{ \frac{\partial^2}{\partial z^2} + y \frac{\partial}{\partial y} \left(\frac{1}{y} \frac{\partial}{\partial y} \right) \right\} [\cdot], \quad \text{in cylindrical coordinates,} \\ &= \left\{ \frac{\partial^2}{\partial r^2} + \frac{\sin \theta}{r^2} \frac{\partial}{\partial \theta} \left(\frac{1}{\sin \theta} \frac{\partial}{\partial \theta} \right) \right\} [\cdot], \quad \text{in spherical coordinates.} \end{aligned} \quad (11.59)$$

We now wish to solve (11.58). This will be done by first seeking a particular solution of the OSEEN equation, which vanishes as $r \rightarrow \infty$; this solution will then be combined with solutions of $\mathcal{L}^2 \psi = 0$ [these are also solutions of (11.58)] for which all boundary conditions are satisfied.

11.4.2 Construction of a Particular Integral of (11.58)

OSEEN started with the representation

$$\mathcal{L}^2 \psi = f(z) \phi(z, y), \quad (11.60)$$

in which (z, y) are the cylindrical coordinates and $\mathcal{L}^2[\cdot]$ is given in (11.59)₁. Thus, one may easily deduce

$$\begin{aligned} \mathcal{L}^4 \psi &= \mathcal{L}^2 (f(z) \phi(z, y)) = f'' \phi + 2f' \phi_z + f \mathcal{L}^2 \phi, \\ \frac{\partial(f\phi)}{\partial z} &= f' \phi + f \phi_z, \end{aligned} \quad (11.61)$$

in which $f' = df/dz$ and $\phi_z = \partial\phi/\partial z$. If Eq. (11.61) are substituted into (11.58), the following equation is obtained

$$\nu \left(f'' \phi + \underbrace{2f' \phi_z + f \mathcal{L}^2 \phi} \right) - U \left(f' \phi + \underbrace{f \phi_z} \right) = 0. \quad (11.62)$$

If we now request somewhat arbitrarily that the underbraced terms together vanish, then

$$2\nu f' - Uf = 0$$

is obtained, a differential equation for f with the solution

$$f = \exp\left(\frac{Uz}{2\nu}\right). \quad (11.63)$$

Back substitution of this exponential function for f into (11.62) leads to the equation

$$\left(\mathcal{L}^2 - \frac{U^2}{4\nu^2} \right) \phi(z, y) = 0. \quad (11.64)$$

OSEEN's ansatz (11.60) has been cleverly so selected that the fourth order differential equation (11.58) is solved by two second order equations, first, Eq. (11.64), which is linear and homogeneous, and, second, by the linear but inhomogeneous equation (11.60).

At this stage of the computations it is advisable to go over to spherical coordinates and to seek a solution of (11.64) in the form

$$\phi = F(r) \sin^2 \theta. \quad (11.65)$$

Substituting this expression in (11.59) leads to

$$\mathcal{L}^2 \phi = \left(F'' - \frac{2}{r^2} F \right) \sin^2 \theta, \quad (11.66)$$

so that in view of (11.64) the radial function must satisfy the ordinary differential equation

$$F'' - \left(\frac{2}{r^2} + \frac{U^2}{4\nu^2} \right) F = 0. \quad (11.67)$$

The reader may demonstrate by substitution that

$$F = C \left(1 + \frac{2\nu}{Ur} \right) \exp \left(-\frac{Ur}{2\nu} \right), \quad C = \text{const.} \quad (11.68)$$

solves (11.67) and enjoys the desired property to vanish as $r \rightarrow \infty$. Hence, with (11.60) and (11.63) we arrive at the intermediate result

$$\mathcal{L}^2 \psi = C \sin^2 \theta \left(1 + \frac{2\nu}{Ur} \right) \exp \left(-\frac{Ur}{2\nu} (1 - \cos \theta) \right). \quad (11.69)$$

This result is significant simply, because, according to (11.56)₁, the operator $-\mathcal{L}^2 \psi / y$ is the vorticity of the motion.

There remains to construct by integration of (11.69) a particular solution for ψ . To this end, we set

$$\psi = g(z, y) \exp \left(\frac{U}{2\nu} z \right). \quad (11.70)$$

Substituting this into (11.59)₁ yields for $\mathcal{L}^2 \psi$

$$\begin{aligned} \mathcal{L}^2 \psi &= \psi_{zz} + \psi_{yy} - \frac{1}{y} \psi_y \\ &= \left(\frac{U^2}{4\nu^2} g + \frac{U}{\nu} g_z + \mathcal{L}^2 g \right) \exp \left(\frac{Uz}{2\nu} \right), \end{aligned} \quad (11.71)$$

in which subscripts y and z denote partial derivatives. Equating (11.69) to (11.71) and transformation of the emerging expression to spherical coordinates results in the following linear and inhomogeneous partial differential equation for g :

$$\begin{aligned} \frac{U^2}{4\nu^2} g + \frac{U}{\nu} \left(\cos \theta \frac{\partial g}{\partial r} - \frac{\sin \theta}{r} \frac{\partial g}{\partial \theta} \right) + \frac{\partial^2 g}{\partial r^2} + \frac{\sin \theta}{r^2} \frac{\partial}{\partial \theta} \left(\frac{1}{\sin \theta} \frac{\partial g}{\partial \theta} \right) \\ = C \sin^2 \theta \left(1 + \frac{2\nu}{Ur} \right) \exp \left(-\frac{Ur}{2\nu} \right). \end{aligned} \quad (11.72)$$

A particular solution of this equation has the form

$$g = \frac{2\nu^2}{U^2} C (1 + \cos \theta) \exp\left(-\frac{U}{2\nu}r\right). \quad (11.73)$$

Back substitution into (11.70) leads to the following particular solution

$$\psi = B(1 + \cos \theta) \left\{ \exp\left(-\frac{Ur}{2\nu}(1 - \cos \theta)\right) - 1 \right\}, \quad B = \text{const.} \quad (11.74)$$

of the OSEEN equation.

11.4.3 'Stokes-Lets' and 'Oseen-Lets'

To the particular solution for ψ in (11.74) we now add the same potential flow solution, which we already employed in the STOKES solution. Thus, we write

$$\begin{aligned} \psi &= \psi_1 + \psi_2, \\ \psi_1 &= \frac{U}{4} \left(2r^2 + \frac{a^3}{r} \right) \sin^2 \theta, \\ \psi_2 &= B(1 + \cos \theta) \left\{ \exp\left(-\frac{Ur}{2\nu}(1 - \cos \theta)\right) - 1 \right\}. \end{aligned} \quad (11.75)$$

ψ_1 satisfies the potential equation $\Delta\psi_1 = 0$, and, therefore, also $\mathcal{L}^2\psi_1 = 0$, as well as the OSEEN equation (11.58). In the immediate neighborhood of the sphere we have $Ur/\nu \ll 1$, and ψ_2 can be approximated as follows:

$$\begin{aligned} \psi_2 &\sim B(1 + \cos \theta) \left\{ 1 - \frac{Ur}{2\nu}(1 - \cos \theta) + \dots - 1 \right\} \\ &\sim -B(1 + \cos \theta) \frac{Ur}{2\nu}(1 - \cos \theta) = -B \frac{Ur}{2\nu} \sin^2 \theta. \end{aligned}$$

Therefore, in the vicinity of the sphere, ψ takes on the form

$$\psi \sim \frac{U}{4} \left(2r^2 + \frac{a^3}{r} \right) \sin^2 \theta - B \frac{U}{2\nu} r \sin^2 \theta. \quad (11.76)$$

This is the same as the STOKES solution (11.33)₁ provided $B = \frac{3}{2}a\nu$. With this choice the boundary condition at the surface of the sphere is only approximately satisfied.

The final result is

$$\psi_{\text{Oseen}} = \frac{U}{4} \left(2r^2 + \frac{a^3}{r} \right) \sin^2 \theta + \underbrace{\frac{3}{2} a \nu (1 + \cos \theta) \left\{ \exp \left(-\frac{Ur}{2\nu} (1 - \cos \theta) \right) - 1 \right\}}_{\text{'Oseen-let'}}. \quad (11.77)$$

As is known from potential theory, the terms in the first line of this expression are due to **doublets** (dipoles) at infinity and the origin of the coordinates. Consequently, the third term due to the particular solution of the OSEEN equation is characteristically called '**Oseen-let**'. In the STOKES solution, the corresponding term is called '**Stokes-let**' and is, according to (11.33)₁, given by

$$\psi_{\text{Stokes}} = \frac{Ua^2}{4} \left(2\frac{r^2}{a^2} + \frac{a}{r} \right) \sin^2 \theta + \underbrace{\frac{3}{4} Uar \sin^2 \theta}_{\text{'Stokes-let'}}. \quad (11.78)$$

We close this section by the following remarks.

- If one computes the drag of the sphere with the solution found this way, one obtains again the result by STOKES,

$$W = 6\pi\eta Ua \quad \text{or} \quad c_w = \frac{24}{\mathbb{R}}. \quad (11.79)$$

However, this result is only obtained, because of the *approximate* satisfaction of the boundary conditions at the surface of the sphere. If the constants of integration, A and D , in the solution of the OSEEN equation are *exactly* satisfied, then one obtains (GOLDSTEIN, 1929, [4])

$$c_w = \frac{24}{\mathbb{R}} \left\{ 1 + \frac{3}{16} \mathbb{R} + \dots \right\}. \quad (11.80)$$

Up to REYNOLDS numbers $\mathbb{R} \approx 1$ this drag coefficient agrees well with experiments.

SIDNEY GOLDSTEIN⁷ [4] went even further in the OSEEN expansion and computed six terms of higher order and obtained

$$c_w = \frac{24}{\mathbb{R}} \left\{ 1 + \frac{3}{16} \mathbb{R} - \frac{19}{1280} \mathbb{R}^2 + \frac{71}{20,480} \mathbb{R}^3 - \frac{30,179}{34,406,400} \mathbb{R}^4 + \frac{122,519}{550,502,400} \mathbb{R}^5 + \dots \right\}. \quad (11.81)$$

⁷For a brief biography of SIDNEY GOLDSTEIN, see **Fig. 11.9**.

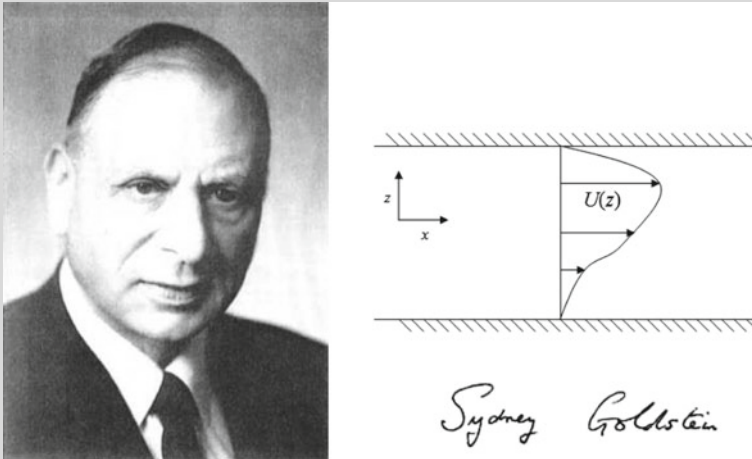


Fig. 11.9 SIDNEY GOLDSTEIN (3. Dec. 1903–22. Jan. 1989). *Right* the TAYLOR–GOLDSTEIN equation describes the dynamics of internal waves in the presence of density stratification and shear flow. A schematic diagram shows the base flow which is parallel to x axis, subject to a small perturbation away from this state which has components in both x, z directions.

SIDNEY GOLDSTEIN started his higher education at the University of Leeds in 1921, where he studied mathematics, but moved to St. John's College, Cambridge, graduating from the mathematical Tripos 1925 and gaining the SMITH's Prize in 1927. He was awarded an Isaac NEWTON Studentship to continue research in applied mathematics and completed his Ph. Degree under Harold JEFFREYS with a thesis entitled 'The theory and application of MATHIEU functions' in 1928. With a ROCKEFELLER Research Fellowship he then spent a year at the University of Göttingen with Ludwig PRANDTL, where he performed laboratory experiments of a fluid in a rotating elliptical container.

In 1929, GOLDSTEIN returned to Cambridge, but accepted in the same year a lectureship in mathematics at the University of Manchester. It had a profound influence on GOLDSTEIN through the heritage of Osborne REYNOLDS and HORACE LAMB. He moved to Cambridge again in 1931 and took over, on LAMB's death, the edition of 'Modern Developments in Fluid Dynamics' which appeared in 1938. He was elected Fellow of the Royal Society in London in 1937. During World War II, GOLDSTEIN worked at the National Physical Laboratory on boundary layer theory. In 1945 GOLDSTEIN moved again to the University of Manchester, where he assumed the chair of Applied Mathematics.

In 1950 GOLDSTEIN accepted the chairmanship of the mathematics department of the Technion at Haifa, but resigned 1955, owing to the administrative overload, and took the chair of Applied Mathematics at Harvard University, Cambridge, USA.

GOLDSTEIN was a very influential fluid dynamicist, best known for his work on steady flow laminar boundary layers and turbulent resistance to rotation of a disk in a fluid. His work in aerodynamics and its influence led Sir JAMES LIGHTHILL to say that he was 'one of those who most influenced progress in fluid dynamics during the 20th century'.

The text is based on www.wikipedia.org and LIGHTHILL [12]. Photo from <http://www.annualreviews.org/>

According to MILTON VAN DYKE (1964) [21] the last term has been corrected by D. SHANKS (1955) [18]. However, owing to the matching requirement of the STOKES–OSEEN expansions, treated in the next section, the higher order terms are not reliable, as we shall see.

- The vorticity, induced by the motion, can be evaluated with the help of (11.77). The resulting expression is

$$\begin{aligned}\operatorname{curl} \mathbf{v} &= -\frac{1}{y} \mathcal{L}^2 \psi \hat{\mathbf{e}}_\varphi = -\frac{1}{r \sin \theta} \left\{ \frac{\partial^2 \psi}{\partial r^2} + \frac{\sin^2 \theta}{r^2} \frac{\partial}{\partial \theta} \left(\frac{1}{\sin^2 \theta} \frac{\partial \psi}{\partial \theta} \right) \right\} \\ &= -\frac{3}{2} Ua \frac{y}{r^3} \left(1 + \frac{Ur}{2\nu} \right) \exp \left(-\frac{Ur}{2\nu} (1 - \cos \theta) \right).\end{aligned}\quad (11.82)$$

Close to the axis, at fixed y , one obtains

- (i) for $\theta \rightarrow 0$: The vorticity decays for large r as r^{-2} ,
- (ii) for $\theta \rightarrow \pi$: For large r the vorticity decays exponentially as $\exp(-Ur/(2\nu))$.

In other words, the vorticity is larger downstream of the sphere than upstream of it. This explains why dead zones have the tendency to arise in the wake.

11.5 Theory of Lagerstöm and Kaplun

11.5.1 Motivation

We have seen that the STOKES theory of the flow exterior to a rigid stagnant sphere fails far away from the sphere at distances

$$r \geq \frac{a}{\mathbb{R}} = \frac{\nu}{U}, \quad \mathbb{R} = \frac{Ua}{\nu}.\quad (11.83)$$

(Note, the REYNOLDS number is here defined with the radius and not the diameter of the sphere.) In terms of the stretched variable

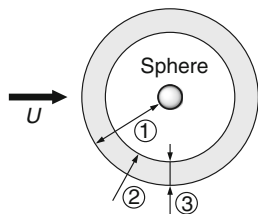
$$s := \frac{r}{a} \mathbb{R}$$

the STOKES solution (11.33)₁ takes the form

$$\frac{\psi}{Ua^2} = \left\{ \frac{1}{2} \frac{s^2}{\mathbb{R}^2} - \frac{3}{4} \frac{s}{\mathbb{R}} + \dots + \frac{1}{4} \frac{\mathbb{R}}{s} + \dots \right\} \sin^2 \theta.\quad (11.84)$$

In this expression dots indicate that the solution (11.84) ought to be interpreted as a beginning series expansion in terms of the REYNOLDS number. We demonstrated in

Fig. 11.10 Validity regimes of the STOKES–OSEEN expansion. ① *Validity regime of the STOKES expansion*, ② *Validity regime of the OSEEN expansion*, ③ *Overlapping region, in which both expansions are asymptotically equal*



earlier sections of this chapter that in the STOKES solution the nonlinear convective members of the full NS-equations were ignored, but when accounted for would dominate the linear term far away from the sphere.

To improve the situation, C.W. OSEEN developed his theory, in which the convective terms were accounted for in such a way that for $r \rightarrow \infty$ they were asymptotically correctly taken into account. OSEEN’s theory is linear; however, because the boundary conditions at the surface of the sphere are not exactly satisfied, additional terms must be incorporated in the STOKES expansion. The OSEEN solution reads

$$\frac{\psi}{Ua^2} = \left\{ \frac{1}{2} \frac{r^2}{a^2} + \frac{1}{4} \frac{a}{r} \right\} \sin^2 \theta - \frac{3}{2} \frac{1 + \cos \theta}{\mathbb{R}} \left(1 - \exp \left(-\frac{r\mathbb{R}}{2a} (1 - \cos \theta) \right) \right). \quad (11.85)$$

Obviously, this is an **outer expansion**, which is valid far away from the sphere (the OSEEN solution is an approximation of this). On the other hand, the STOKES solution is a beginning **inner expansion** with a validity region close to the sphere. The two solutions merge in an **overlapping region** and must be **matched together**, a process, which determines unknown coefficients in the outer and inner expansions, see **Fig. 11.10**.

In order to present this matched asymptotic expansion procedure, let us write the axisymmetric NS-equations in dimensionless form. They read as follows:

$$\begin{aligned} \tilde{\mathcal{L}}^4 \psi &= \frac{\mathbb{R}}{r^2 \sin \theta} \left\{ \frac{\partial \psi}{\partial \theta} \frac{\partial}{\partial r} - \frac{\partial \psi}{\partial r} \frac{\partial}{\partial \theta} + 2 \cot \theta \frac{\partial \psi}{\partial r} - \frac{2}{r} \frac{\partial \psi}{\partial \theta} \right\} \tilde{\mathcal{L}}^2 \psi, \\ \tilde{\mathcal{L}}^2 \psi &= \left\{ \frac{\partial^2}{\partial r^2} + \frac{1}{r^2} \left(\frac{\partial^2}{\partial \theta^2} - \cot \theta \frac{\partial}{\partial \theta} \right) \right\} \psi = \left\{ \frac{\partial^2}{\partial r^2} + \frac{\sin \theta}{r^2} \frac{\partial}{\partial \theta} \left(\frac{\partial / (\partial \theta)}{\sin \theta} \right) \right\} \psi, \\ \mathbb{R} &= \frac{Ua}{\nu}, \\ u_r &= \frac{1}{r^2 \sin \theta} \frac{\partial \psi}{\partial \theta}, \quad u_\theta = \frac{-1}{r \sin \theta} \frac{\partial \psi}{\partial r}. \end{aligned} \quad (11.86)$$

In these expressions all quantities are dimensionless. The boundary conditions, for which these equations must be solved are:

On the surface of the sphere: $u_r = u_\theta = 0$, or in terms of the stream function

$$\psi(1, \theta) = 0, \quad \frac{\partial \psi}{\partial r}(1, \theta) = 0, \quad r = 1. \quad (11.87)$$

At infinity as $r \rightarrow \infty$: $\mathbf{v} = \mathbf{e}_z$, or,

$$\begin{aligned} u_r \cos \theta - u_\theta \sin \theta &= 1, \\ u_r \sin \theta + u_\theta \cos \theta &= 0. \end{aligned}$$

These two equations are identically satisfied if

$$\lim_{r \rightarrow \infty} \psi(r, \theta) = \frac{1}{2} r^2 \sin^2 \theta. \quad (11.88)$$

Equations (11.86)–(11.88) define together the complete boundary value problem.

11.5.2 Stokes Expansion

In the vicinity of the sphere (i.e. in the *inner region*) we write

$$\psi = \psi_i(r, \theta) = \psi_0^i + \mathbb{R}\psi_1^i + \mathbb{R}^2\psi_2^i + \dots. \quad (11.89)$$

When substituting this series expansion into (11.86) a recursive set of principally solvable differential equations is obtained:

$$\begin{aligned} \tilde{\mathcal{L}}^4 \psi_k^i &= g_k, \quad k = 0, 1, 2, \dots, \\ g_k &= \frac{1}{r^2 \sin \theta} \left\{ \left[\frac{\partial \psi^i}{\partial \theta} \frac{\partial}{\partial r} - \frac{\partial \psi^i}{\partial r} \frac{\partial}{\partial \theta} + 2 \cot \theta \frac{\partial \psi^i}{\partial r} - \frac{2}{r} \frac{\partial \psi^i}{\partial \theta} \right] \tilde{\mathcal{L}}^2 \psi^i \right\}_{k-1}. \end{aligned} \quad (11.90)$$

For $k = 0$ the counting index $k - 1$ must be set to zero as must the indexed variables e.g. g_{-1} . The zeroth order equation is simply $\tilde{\mathcal{L}}^4 \psi = 0$ with the solution

$$\psi_0^i = \left(\underbrace{\frac{1}{2} r^2}_I - \underbrace{\frac{3}{4} r}_{II} + \underbrace{\frac{1}{4} \frac{1}{r}}_{III} \right) \sin^2 \theta. \quad (11.91)$$

Hence, the term *I* stands for the rectilinear potential flow with $(\tilde{\mathcal{L}}^2 \psi_0)_I = 0$. Similarly, the term *III* is a dipole (doublet) flow also satisfying $(\tilde{\mathcal{L}}^2 \psi_0)_{III} = 0$. Only the term *II*

delivers a contribution to the relation

$$\text{curl}(\mathbf{v}_{0II}) = -\frac{3}{2} \frac{1}{r^2} \sin \theta \hat{\mathbf{e}}_\varphi.$$

Substitution of (11.91) into (11.90) leads to the differential equation for ψ_1^i

$$\tilde{\mathcal{L}}^4 \psi_1^i = -\frac{9}{4} \left(\frac{2}{r^2} - \frac{3}{r^3} + \frac{1}{r^5} \right) \sin^2 \theta \cos \theta. \tag{11.92}$$

A particular integral, which satisfies the boundary conditions at the surface of the sphere is

$$-\frac{3}{32} \left\{ 2r^2 - 3r + 1 - \frac{1}{r} + \frac{1}{r^2} \right\} \sin^2 \theta \cos \theta. \tag{11.93}$$

Adding to this a solution of the homogeneous equation, which equally satisfies the boundary conditions at the surface of the sphere yields the complete first order inner solution

$$\psi_1^i = C \left\{ 2r^2 - 3r + \frac{1}{r} \right\} \sin^2 \theta - \frac{3}{32} \left(2r^2 - 3r + 1 - \frac{1}{r} + \frac{1}{r^2} \right) \cos \theta \sin^2 \theta, \tag{11.94}$$

in which C is a still undetermined constant.

Remarks

- If one tries to satisfy the velocity boundary conditions at $r \rightarrow \infty$ with (11.94), this cannot be done. Even worse, in the next approximation the velocity would get infinitely large.

The non-existence of the second order approximation of the STOKES expansion is known as **Whitehead Paradox** (1889). WHITEHEAD [24] believed that the paradox could be removed by discontinuities in the solution. Today we know that this is not the case.

- In the analogous problem of the flow around a circular cylinder, the paradox is even stronger. The analogue to (11.91) would here be

$$\psi_0^i = C \left(\underbrace{-\frac{1}{2}r}_I + \underbrace{r \log(r)}_{II} + \underbrace{\frac{1}{2}\frac{1}{r}}_{III} \right) \sin \theta.$$

The second term in this formula is the ‘STOKES-let’. The solution, however, cannot be completed because no choice of the constant C satisfies the upstream boundary condition: $\psi(r, \theta) \sim r \sin \theta$ as $r \rightarrow \infty$. The non-existence of a solution of the STOKES equations in the infinite two-dimensional flow around a circular cylinder is known as STOKES’ paradox. It was recognized by STOKES in 1851 [19].

11.5.3 Oseen Expansion

Our position here is that OSEEN's solution is a limit of a series expansion, which is valid for large r . Because we seek solutions for small REYNOLDS numbers \mathbb{R} , the stretching transformation

$$\rho = r\mathbb{R} \quad (11.95)$$

brings the outer region closer to the sphere. So, the transformation (11.95) is actually a squeezing operation. In these 'stretched' coordinates (11.86) reads

$$\tilde{\mathcal{L}}_\rho^4 \psi = \frac{\mathbb{R}^2}{\rho^2 \sin^2 \theta} \{\cdot\}_\rho \tilde{\mathcal{L}}_\rho^2 \psi, \quad (11.96)$$

in which the index ρ labels the fact that the operator $\{\cdot\}$ has to be taken with respect to ρ (not r). $\{\cdot\}$ is defined in (11.98)₂ below. Notice also that the REYNOLDS number on the right-hand side of (11.96) appears with the common factor \mathbb{R}^2 . This means that in the squeezed coordinates the nonlinear terms receive a larger weight.

In a fashion analogous to Eq. (11.89) one now writes for the outer region

$$\psi = \frac{1}{\mathbb{R}^2} \Psi^o(\rho, \theta) = \frac{1}{\mathbb{R}^2} \{ \Psi_0^o + \mathbb{R} \Psi_1^o + \mathbb{R}^2 \Psi_2^o + \dots \}. \quad (11.97)$$

Substitution of this expansion into (11.96) generates the recursive formula

$$\begin{aligned} \tilde{\mathcal{L}}_\rho^4 \Psi_k^o &= \frac{1}{\rho^2 \sin^2 \theta} \{\cdot\}_\rho \tilde{\mathcal{L}}_\rho^2 \psi_k^o, \\ \{\cdot\} &= \left\{ \frac{\partial \Psi^o}{\partial \theta} \frac{\partial}{\partial \rho} - \frac{\partial \Psi^o}{\partial \rho} \frac{\partial}{\partial \theta} + 2 \cotan \theta \frac{\partial \Psi^o}{\partial \rho} - \frac{2}{\rho} \frac{\partial \Psi^o}{\partial \theta} \right\}. \end{aligned} \quad (11.98)$$

The pre-factor $1/\mathbb{R}^2$ in (11.97) achieves that in (11.98) both sides of the equation have the same \mathbb{R} -weight. The solutions of (11.98) must satisfy the boundary conditions at $r \rightarrow \infty$

$$\begin{aligned} \Psi_0^o &\rightarrow \frac{1}{2} \rho^2 \sin^2 \theta, & \text{for } \rho \rightarrow \infty, \\ \psi_k^o &= 0, \quad k = 1, 2, \dots, & \text{for } \rho \rightarrow \infty. \end{aligned} \quad (11.99)$$

As zeroth order solution of (11.98), for which the right-hand side of (11.98) vanishes, it is tempting to take

$$\Psi_0^o = \frac{1}{2} \rho^2 \sin^2 \theta. \quad (11.100)$$

It satisfies the boundary conditions for $r \rightarrow \infty$ and represents the flow around a sphere with vanishing radius. Comparison of (11.91) with (11.99) also demonstrates that (11.100) represents exactly the dominant effect of the STOKES solution far away from the sphere. For, if one writes the STOKES solution (11.91) in the outer variables

$$\begin{aligned}
(\psi_0^i)^o &= \frac{1}{\mathbb{R}^2} \left\{ \frac{1}{2} \rho^2 - \frac{3}{4} \mathbb{R} \rho + \frac{1}{4} \mathbb{R}^3 \frac{1}{\rho} \right\} \sin^2 \theta \\
&\sim \frac{1}{\mathbb{R}^2} \frac{1}{2} \rho^2 \sin^2 \theta, \quad \text{for } \mathbb{R} \rightarrow 0,
\end{aligned}$$

one obtains exactly the OSEEN solution. If one evaluates the right-hand side of (11.98), one obtains

$$\left\langle \{\cdot\} [\Psi_0^o + \mathbb{R} \Psi_1^o + \dots] \tilde{\mathcal{L}}_\rho^2 [\Psi_0^o + \mathbb{R} \Psi_1^o + \dots] \right\rangle_{k=1}$$

or since $\tilde{\mathcal{L}}_\rho^2 \Psi_0^o = 0$,

$$\begin{aligned}
\langle \cdot \rangle_1 &= \mathbb{R} \left\langle \{\cdot\} [\Psi_0^o] \tilde{\mathcal{L}}_\rho^2 [\Psi_1^o] \right\rangle, \\
\frac{\langle \cdot \rangle_1}{r^2 \sin^2 \theta} &= \mathbb{R} \left\{ -\frac{\sin \theta}{\rho} \frac{\partial}{\partial \theta} + \cos \theta \frac{\partial}{\partial \rho} \right\} \tilde{\mathcal{L}}^2 \Psi_1^o.
\end{aligned}$$

Therefore, the OSEEN differential equation of first order takes the form

$$\tilde{\mathcal{L}}^4 \Psi_1^o = \left\{ -\frac{\sin \theta}{\rho} \frac{\partial}{\partial \theta} + \cos \theta \frac{\partial}{\partial \rho} \right\} \tilde{\mathcal{L}}^2 \Psi_1^o. \quad (11.101)$$

This is exactly the original OSEEN equation in dimensionless form, see (11.58). Its solution has been given as (11.74) and is repeated here:

$$\Psi_1^o = B(1 + \cos \theta) \left\{ \exp \left(-\frac{\rho}{2} (1 - \cos \theta) \right) - 1 \right\}. \quad (11.102)$$

The complete first order OSEEN solution is, therefore, given by

$$\psi^o = \frac{\rho^2}{2\mathbb{R}^2} \sin^2 \theta + \frac{B(1 + \cos \theta)}{\mathbb{R}} \left\{ \exp \left(-\frac{\rho}{2} (1 - \cos \theta) \right) - 1 \right\} + \mathcal{O}(1). \quad (11.103)$$

11.5.4 Matching Procedure

The two STOKES and OSEEN expansions must asymptotically agree with one another in the overlapping region, see Fig. 11.10. To this end one writes the outer expansion in terms of the inner variables and expands the emerging relation in powers of r . This yields

$$\begin{aligned}
(\psi^o)^i &= \frac{1}{2}r^2 \sin^2 \theta + \frac{B(1 + \cos \theta)}{\mathbb{R}} \\
&\times \left\{ 1 - \mathbb{R}(1 - \cos \theta)\frac{r}{2} + \mathbb{R}^2(1 - \cos \theta)^2\frac{r^2}{8} + \dots - 1 \right\} \\
&= \frac{r^2}{2} \sin^2 \theta - \underline{B\frac{r}{2} \sin^2 \theta} + \underline{\underline{\mathbb{R}B\frac{r^2}{8} \sin^2 \theta(1 - \cos \theta)}} + \dots . \quad (11.104)
\end{aligned}$$

Alternatively, the inner STOKES expansion can be written as

$$\begin{aligned}
\psi^i &= \frac{r^2}{2} \sin^2 \theta - \frac{3}{2}\frac{r}{2} \sin^2 \theta + \frac{1}{4}\frac{1}{r} \sin^2 \theta \\
&+ \mathbb{R}C \left\{ 2r^2 - 3r + \frac{1}{r} \right\} \sin^2 \theta \\
&- \mathbb{R}\frac{3}{32} \left\{ 2r^2 - 3r + 1 - \frac{1}{r} + \frac{1}{r^2} \right\} \sin^2 \theta \cos \theta, \quad (11.105)
\end{aligned}$$

see (11.91) and (11.94), the dominant terms of which for large $r \rightarrow \infty$ are

$$\begin{aligned}
\psi_{r \rightarrow \infty}^i &= \frac{r^2}{2} \sin^2 \theta - \underline{\underline{\frac{3}{2}\frac{r}{2} \sin^2 \theta}} + \dots \\
&+ \underline{\underline{C\mathbb{R} \sin^2 \theta 2r^2}} - \frac{3}{16}\mathbb{R}r^2 \sin^2 \theta \cos \theta. \quad (11.106)
\end{aligned}$$

By comparing the underlined terms in (11.104) and (11.106) it is seen that the inner and outer expansions can only be matched, if

$$B = \frac{3}{2}, \quad C = \frac{B}{16} = \frac{3}{32}.$$

The improved inner solution, thus, reads

$$\psi^i = \frac{1}{4}(r-1)^2 \sin^2 \theta \left\{ \left(1 + \frac{3}{8}\mathbb{R}\right) \left(2 + \frac{1}{r}\right) - \frac{3}{8}\mathbb{R} \left(2 + \frac{1}{r} + \frac{1}{r^2}\right) \cos \theta \right\} \quad (11.107)$$

and is now a function of the REYNOLDS number. The streamline $\psi^i = 0$ is now given by the following equations.

1. $\theta = 0, \pi$, corresponding to the axis $y = 0$.
2. $r = 1$, on the surface of the sphere.
3. $\{\cdot\} = 0$, corresponding to the dead water region behind the sphere and given by

$$\cos \theta = \left(\frac{8}{3\mathbb{R}} + 1 \right) \frac{2 + 1/r}{2 + 1/r + (1/r)^2}.$$

The dead water zone can only exist, when $|\cos \theta| < 1$; so, for $r = 1$ we have

$$\frac{3}{4} \left\{ \frac{8}{3\mathbb{R}} + 1 \right\} < 1 \longrightarrow \mathbb{R} > 8. \tag{11.108}$$

This matching procedure can be continued; this was done to second order by I. PROUDMAN and J.R.A. PEARSON (1957) [16]. Their second order drag coefficient is given as

$$c_w = \frac{24}{\mathbb{R}'} \left\{ 1 + \frac{3}{16}\mathbb{R}' + \frac{9}{160}\mathbb{R}'^2 \ln \mathbb{R}' + \mathcal{O}(\mathbb{R}'^3) \right\}, \tag{11.109}$$

$$\mathbb{R}' = \frac{2Ua}{\nu} = 2\mathbb{R}.$$

A third order extension of this matched asymptotic expansion is due to W. CHESTER and D.R. BREACH (1969) [2], and their third order drag formula reads

$$c_w = \frac{24}{\mathbb{R}'} \left\{ 1 + \frac{3}{16}\mathbb{R}' + \frac{9}{160}\mathbb{R}'^2 \left(\ln \mathbb{R}' + \gamma + \frac{2}{3} \ln 2 - \frac{323}{360} \right) + \frac{27}{640}\mathbb{R}'^3 \ln \mathbb{R}' + \mathcal{O}(\mathbb{R}'^4) \right\}, \tag{11.110}$$

where γ is the EULER constant. S.-J. LIAO (2002) [9] writes: ‘it is a little baffling that, when $\mathbb{R}' > 2$ the above 3rd order drag formula is even worse than the 2nd order formula (11.109), as shown in Fig. 11.11’. This figure indicates that the 2nd and 3rd order solutions for c_w obtained by matching approximate inner and outer expansions (by PROUDMAN–PEARSON and CHESTER–BREACH) are less accurate for $\mathbb{R}' \geq 1$ than that of the OSEEN solution. It is thus tempting to try such a comparison with results from higher order outer solutions of OSEEN-type. The six-term solution

$$c_w = \frac{24}{\mathbb{R}'} \left\{ 1 + \frac{3}{16}\mathbb{R}' - \frac{19}{1280}\mathbb{R}'^2 + \frac{71}{20480}\mathbb{R}'^3 - \frac{30179}{34406400}\mathbb{R}'^4 + \frac{122519}{550502400}\mathbb{R}'^5 + \dots \right\} \tag{11.111}$$

was constructed by SIDNEY GOLDSTEIN (1929) [4]. S.-J. LIAO (2002) [9] states: ‘In 1970, MILTON VAN DYKE [22] extended the above drag formula to 24 terms by computer [...] and found that its convergence is limited by a simple pole at $\mathbb{R}' = -4.18172$. Using the EULER transformation, VAN DYKE [22] enlarged its convergence region to infinity. However, the agreement between VAN DYKE’s [22] drag formula (given by EULER transformation) with experimental data is not satisfactory for $\mathbb{R}' > 5$, as shown in Fig. 11.11’. For all mentioned solutions, there is a large disagreement between all above mentioned theoretical drag formulae and experimental data. So, as pointed out by F.M. WHITE in 1991 [23] and quoted by S.-J. LIAO [9], ‘the idea of using creeping flow to expand into the high REYNOLDS number region has not been successful’.

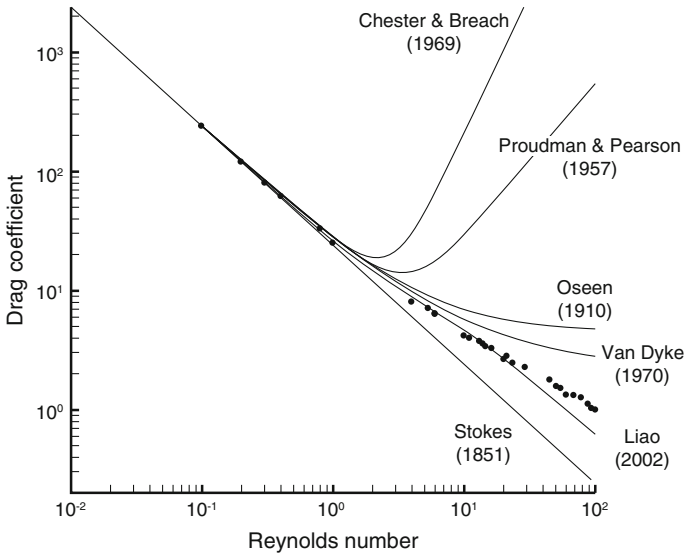


Fig. 11.11 Comparison of experimental data of drag coefficient of a sphere in a uniform stream with theoretical results. Symbols *experimental data*; solid lines *theoretical results by the indicated authors as described in the main text*. Data are taken from T. MAXWORTHY [13], R. OCKENDON and G.A. EVANS [14], F.W. ROOS and W.W. WILLMARTH [17] and C. WIESELSBURGER [25, 26]. Adapted from S.-J. LIAO (2002, 2004) [9, 10]

11.6 Homotopy Analysis Method—The Viscous Drag Coefficient Computed for Arbitrary Reynolds Numbers

As revealed by the above mentioned perturbation approaches, and explicitly demonstrated by Fig. 11.11, the drag coefficient, predicted by them is only in conformity with the experimental results, provided the REYNOLDS number is small, ideally $\mathbb{R}' < 1$ and realistically certainly $\mathbb{R}' < 5$. None of the presented perturbation drag formulae is valid for $\mathbb{R}' > 1$ —more generally for realistic values of \mathbb{R}' up to $\mathbb{R}' < 2000$. It is clear that the two solutions, constructed by matching inner and outer solutions (2nd order: PROUDMAN–PEARSON, 3rd order: CHESTER–BREACH) deviate considerably from the experimental points, when $\mathbb{R}' > 1$. Alternatively, the OSEEN-type solutions (OSEEN [15], VAN DYKE [22]) approximate the experimentally determined drag coefficient much better when $\mathbb{R}' = \mathcal{O}(10^0 - 10^1)$ than the perturbation solutions based on matching. The reason is that ‘the OSEEN equation has nothing to do with any small parameter’ [9].

An approximate solution procedure for the steady flow of a viscous fluid around a fixed body ought to be available which allows construction of approximate sequences of the solutions of the full NS-equations around a fixed body for arbitrary values of the REYNOLDS number. Such a method has been proposed by S.-J. LIAO in 1992

[6]. It is suitable for the solution of nonlinear differential equations and is based on **homotopy**, a technique of topology. It was coined by LIAO the **homotopy analysis method** (HAM) [6]. S.-J. LIAO wrote a number of articles applying this method in fluid mechanics (two-dimensional viscous flow over a semi-infinite flat plate [7], BLASIUS flow [8]). The analysis of the drag force on a stationary sphere due to steady parallel uniform flow of a viscous fluid is presented by him in [9].

11.6.1 The Mathematical Concept

It is not the place here to present the full derivation of the mathematical techniques of HAM applied to the steady viscous flow past a sphere. The reader must consult the pertinent literature for that: [7–11].

Starting point are the NS-equations in spherical coordinates, (11.17), which in dimensionless units and on the basis of the transformation

$$\mu = \cos \theta, \quad 0 \leq \theta \leq 2\pi, \quad \frac{\partial}{\partial \theta} = -\sin \theta \frac{\partial}{\partial \mu} \quad (11.112)$$

yields the boundary value problem

$$\begin{aligned} \mathcal{A}\psi &:= \mathcal{L}^4\psi - \frac{\mathbb{R}}{r^2} \left\{ \frac{\partial\psi}{\partial r} \frac{\partial}{\partial \mu} - \frac{\partial\psi}{\partial \mu} \frac{\partial}{\partial r} + \frac{2\mu}{(1-\mu^2)} \frac{\partial\psi}{\partial r} + \frac{2}{r} \frac{\partial\psi}{\partial \mu} \right\} \mathcal{L}^2\psi = 0, \\ \psi(r, \mu) &= \frac{\partial\psi(r, \mu)}{\partial r} = 0, \quad \text{when } r = 1, \\ \lim_{r \rightarrow +\infty} \psi(r, \mu) &= \frac{1}{2}r^2(1 - \mu^2). \end{aligned} \quad (11.113)$$

\mathcal{A} is called NAVIER–STOKES-operator; r is now dimensionless and the REYNOLDS number $\mathbb{R} = Ua/\nu$ is based on the radius of the sphere.

The key step in HAM consists in constructing a family of boundary value problems involving an embedding parameter $q \in [0, 1]$ and a non-zero auxiliary parameter \hbar as follows:

$$\left. \begin{aligned} (1-q)\mathcal{H}[\Psi(r, \mu, q) - \psi_0(r, \mu)] &= q\hbar\mathcal{A}\Psi(r, \mu, q), \quad r > 1, \\ \Psi(1, \mu, q) &= \frac{\partial\Psi(r, \mu, q)}{\partial r} \Big|_{r=1} = 0, \\ \lim_{r \rightarrow +\infty} \Psi(r, \mu, q) &= \frac{1}{2}r^2(1 - \mu^2), \end{aligned} \right\} \begin{aligned} -1 \leq \mu \leq 1, \\ 0 \leq q \leq 1. \end{aligned} \quad (11.114)$$

Here, the real function $\psi_0(r, \mu)$ is an initial guess for the solution of (11.113)₁ and must satisfy the boundary conditions (11.113)_{2,3}. \mathcal{H} is an auxiliary linear operator, \hbar a non-zero auxiliary parameter and $\Psi(r, \mu, q, \hbar)$ a function of four variables. The function ψ_0 , the operator \mathcal{H} and the non-zero parameter q can be freely assigned.

Of special significance is the embedding parameter q ; it plays an important role and operates like a ‘deus ex machina’ in generating so-called **deformation equations**.

Indeed, consider (11.114) when $q = 0$ and $q = 1$ two limiting values between which q can vary:

$$\begin{aligned} q = 0 &\rightarrow \Psi(r, \mu, 0) = \psi_0(r, \mu), \quad \text{provided } \mathcal{H} \neq 0, \\ q = 1 &\rightarrow \Psi(r, \mu, 1) = \psi(r, \mu), \quad \text{since } \mathcal{A}\Psi(r, \mu, 1) = 0. \end{aligned} \quad (11.115)$$

Thus, the process of q increasing from zero to one is just the process of Ψ varying from $\psi_0(r, \mu)$ to $\psi(r, \mu)$. This is exactly the idea of the homotopy, and this kind of process is called **deformation** in topology; so, (11.113) are called the ‘**zeroth order deformation equations**’, [9]’. They form one boundary value problem for Ψ . The parameter q —our ‘deus ex machina’—however, allows to generate additional boundary value problems, if one assumes that the deformation function $\Psi(r, \mu, q)$ is sufficiently smooth with respect to q to be arbitrarily times differentiable with respect to q . With the notation

$$\psi_0^{[m]}(r, \mu) := \left. \frac{\partial^m \Psi(r, \mu, q)}{\partial q^m} \right|_{q=0}, \quad m = 1, 2, 3, \dots, \quad (11.116)$$

one may then develop $\Psi(r, \mu, q)$ into TAYLOR series about $q = 0$,

$$\begin{aligned} \Psi(r, \mu, q) &= \underbrace{\Psi(r, \mu, 0)}_{(11.115): \psi_0(r, \mu)} + \sum_{m=1}^{+\infty} \underbrace{\frac{\psi_0^{[m]}(r, \mu)}{m!}}_{\psi_m(r, \mu)} q^m \\ &= \psi_0(r, \mu) + \sum_{m=1}^{+\infty} \psi_m(r, \mu) q^m. \end{aligned} \quad (11.117)$$

Assuming that $\psi_0(r, \mu)$, the linear operator \mathcal{H} and the non-zero parameter \hbar are so selected that the TAYLOR series expansion is convergent at $q = 1$, then (11.117) and (11.115) imply

$$\psi(r, \mu) = \psi_0(r, \mu) + \sum_{m=1}^{+\infty} \psi_m(r, \mu). \quad (11.118)$$

This equation is a formal recipe to find the ultimate solution $\psi(r, \mu)$ by successive approximation, if $\psi_m(r, \mu)$, $m = 1, 2, 3, \dots$, can be found. Such equations can be obtained by performing the m th derivatives of the zeroth order deformation equation (11.114) with respect to q , then setting $q = 0$ and finally dividing the resulting equation by $m!$. This yields the boundary value problems for $\psi_m(r, \mu)$, $m = 1, 2, 3, \dots$, which structurally take the forms

$$\left. \begin{aligned} \mathcal{H}[\psi_m(r, \mu)] &= G_m(r, \mu), \quad r \geq 1, \\ \psi_m(1, \mu) &= \frac{\partial \psi_m(r, \mu)}{\partial r} \Big|_{r=1} = 0, \\ \lim_{r \rightarrow +\infty} \frac{1}{r^2} \psi_m(r, \mu) &= 0, \end{aligned} \right\} \begin{aligned} m &\geq 1, \\ -1 &\leq \mu \leq 1, \end{aligned} \quad (11.119)$$

where G_m is given by

$$\begin{aligned} G_m(r, \mu) &= (\chi_m \mathcal{H} + \hbar \mathcal{L}^4) \psi_{m-1} \\ &\quad - \frac{\hbar \mathbb{R}}{r^2} \sum_{k=0}^{m-1} \left\{ \frac{\partial \psi_k}{\partial r} \frac{\partial}{\partial \mu} - \frac{\partial \psi_k}{\partial \mu} \frac{\partial}{\partial r} + \frac{2\mu}{(1-\mu^2)} \frac{\partial \psi_k}{\partial r} \right. \\ &\quad \left. + \frac{2}{r} \frac{\partial \psi_k}{\partial \mu} \right\} \mathcal{L}^2 \psi_{m-1-k}, \end{aligned} \quad (11.120)$$

in which

$$\chi_m = \begin{cases} 0 & \text{when } m \leq 1, \\ 1 & \text{when } m \geq 2. \end{cases} \quad (11.121)$$

The above formulated boundary value problems (11.119) are all *linear* and can be solved consecutively, starting with an estimate for ψ_0 . Then, G_1 is determined by substituting ψ_0 on the right-hand side of (11.120) and solving the emerging linear boundary value problem (11.119) for ψ_1 , etc. In this way an infinite number of functions ψ_m , $m = 1, 2, \dots$ can be determined. In practice, this sequence is truncated at $m = M$ by which an approximation for (11.118) is found. Obviously, this procedure is only useful, provided the sum $\sum_{m=1}^{+\infty} \psi_m(r, \mu)$ is convergent. Fortunately, the HAM provides us with great freedom to select $\psi_0(r, \mu)$, \mathcal{H} and \hbar to express the solution and at the same time to ensure the convergence of (11.118).

To summarize, HAM has transformed the solution of the *nonlinear* boundary value problem (11.113) into an (ideally infinite) set of *linear* boundary value problems. With proper choice of ψ_0 , \mathcal{H} and \hbar these linear boundary value problems lead to convergent series of (11.118) which then represent approximate and increasingly more accurate solutions of the original problem (11.113).

11.6.2 Selection of ψ_0 , \mathcal{H} , \hbar and Approximate Solution

In conformity with the construction of the functions ψ_m , the initial guess $\psi_0(r, \mu)$ must satisfy the boundary conditions (11.114)_{2,3}. The most obvious choice is then the STOKES solution (11.33) [with $a = 1$, $\sin^2 \theta = (1 - \mu^2)$],

$$\psi_0 = \frac{1}{4} \left(2r^2 - 3r + \frac{1}{r} \right) (1 - \mu^2), \quad (11.122)$$

and it is tempting to choose $\mathcal{H}[\cdot]$ proportional to the STOKES operator $\mathcal{L}^4[\cdot]$

$$\mathcal{H}[\cdot] = H(r, \mu) \left(\frac{\partial^2}{\partial r^2} + \frac{(1 - \mu^2)}{r^2} \frac{\partial^2}{\partial \mu^2} \right)^2 [\cdot], \tag{11.123}$$

in which $H(r, \mu)$ is a function of r and μ . LIAO [9] also chose

$$\psi_N(r, \mu) = (1 - \mu^2) \sum_{k=0}^N f_{m,k}(r) \mu^k, \tag{11.124}$$

which is a kind of separation ansatz, and the prefactor $(1 - \mu^2)$ is so selected to have a chance to satisfy the boundary condition when $r \rightarrow \infty$; moreover, N might be infinite or finite. With the choice (11.124), the determination of $\psi_m(r, \mu)$ is transferred to the determination of $f_{m,k}(r)$. At last, a selection for $H(r, \mu)$ is needed; LIAO [9] was successful with the choice⁸

$$H(r, \mu) = r^\sigma, \quad \sigma > 0. \tag{11.125}$$

and picked $\sigma = 1$ for explicit computations.

The remainder consists in the substitution of (11.122)–(11.125) into the deformation equations (11.119) consecutively for $m = 1, 2, 3 \dots$ and in solving the emerging boundary value problems for $f(m, k; \hbar)$, verification of the convergence property of the successive approximations for $\psi(r, \mu)$ as given by (11.118). The higher order approximations have been determined by MATHEMATICA up to the 9th order in the index m resulting in a 10th order drag coefficient. The convergence depends upon the choice of the parameter \hbar ; i.e. depending upon the series; (11.118) is only convergent for $\mathbb{R}' < \mathbb{R}'_{\text{limit}}(\hbar)$. It turned out that the following convergence limits were obtained for the 10th order approximation:

\hbar	-1	-1/2	-1/3
$\mathbb{R}'_{\text{limit}}$	5	9	20

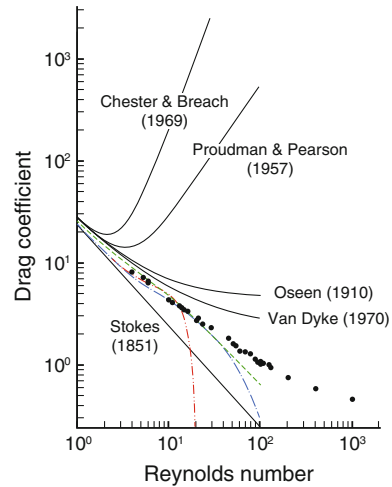
It transpires that $\mathbb{R}'_{\text{limit}}$ -convergence can be improved when negative values approach $0 - \varepsilon, \varepsilon > 0$. LIAO [9] tried by making \hbar REYNOLDS number dependent as follows:

$$\hbar = -\frac{1}{3} \exp(-\mathbb{R}'/30), \quad \text{and} \quad \hbar = -\frac{1}{1 + \mathbb{R}'/4} \tag{11.126}$$

⁸LIAO tried with several different choices and found

1. for $H = 1$ the emerging solution for $m = 1$ does not satisfy the boundary condition at infinity;
2. for $\sigma \leq 0$ the solution (11.119) does not satisfy the uniform-stream condition at infinity.

Fig. 11.12 Comparison of the 10th order HAM drag formula for $\hbar = -1/3$ and \hbar given by (11.126). Dash-double dotted line: $\hbar = -1/3$; dash-dotted line: (11.126a); dashed line: (11.126b). Adapted from S.-J. LIAO (2002, 2004) [9, 10]



The 10th order approximation of the drag coefficient, computed with these representations, is shown in **Fig. 11.12**. It indicates that the theoretical formula agrees well with the experimental data as long as $\mathbb{R}' < 30$. Even though data are available up to $\mathbb{R}' = 1000$, the approximations could not be continued, because of over flow arising in MATHEMATICA at the 11th iteration. Farther reaching computations are not known to us.

11.7 Conclusions and Discussion

This chapter was devoted to a physically simple problem, the determination of the drag force (or better the drag coefficient) exerted on a sphere subjected to a steady parallel flow of a linearly viscous fluid under laminar conditions without separation. The reader will certainly have realized that the solution of the problem is mathematically rather complex, but still not satisfactorily solved. An analogous situation prevails also for the flow across an infinite circular cylinder, but was not dealt with by us.

Apart from the differential properties initially dealt with, the analysis in spherical and cylindrical coordinates of NAVIER–STOKES operators, the topic was begun with the analysis of STOKES flow around a rigid stagnant sphere, i.e., the construction of the solution of the steady NAVIER–STOKES equations, when the acceleration terms in the momentum equations are ignored. This mathematical problem was solved with imposed no-slip and viscous sliding conditions at the surface of the sphere, as well as for the case that the sphere was filled with a fluid or gas of different viscosity. This entailed the formation of a double circulation within the sphere—called HILL

vortex—and also led to the formation of steady suspensions of particle-containing air bubbles in fluidized beds.

Scrutiny of the STOKES solution with estimates of typical convective acceleration terms revealed that far away from the sphere these accelerations outweigh the corresponding values of the STOKES solution. This result means nothing else than that a REYNOLDS number correction to the drag coefficient of the STOKES solution must be determined. The first version of this correction was given by CARL WILHELM OSEEN in 1910. The OSEEN solution yields a linear \mathbb{R} of the drag coefficient.

The constructions of STOKES and OSEEN in regular perturbation series could only be completed by matching the two series step by step by which free coefficients are determined in an overlapping region by the requirement that the two series are asymptotically equal in this region. The solution of this problem kept applied mathematicians busy for about three quarters of the 20th century. However, the results are somewhat disappointing because the results deviate more and more from those obtained by experiments, when the REYNOLDS number exceeds unity as seen from Fig. 11.11. In a way, this cannot be a surprise since ‘small \mathbb{R} ’ is a prerequisite of perturbation formulations in this parameter.

In the 90s of the 20th century, S.-J. LIAO therefore proposed a different method to find approximate series solutions of the NAVIER–STOKES equations for ‘arbitrary values’ of the REYNOLDS number. This is the *Homotopy Analysis Method* (HAM), which can be judged to be a successful approach for the determination of the drag force prior to separation. This rather complex analysis is combined with equally complex numerical techniques. It seems that HAM might prove successful in pushing the results at $\mathbb{R} > 10^1 - 10^2$ closer to measured values.

References

1. Batchelor, G.: A new theory of the instability of a uniform fluidized bed. *J. Fluid Mech.* **193**, 75–100 (1988)
2. Chester, W., Breach, D.R.: On the flow past a sphere at low Reynolds number. *J. Fluid Mech.* **37**, 751–760 (1969)
3. For the history of this experiment see ‘In the case of Robert Andrew Millikan’ by David Goldstein, *American Scientist*, Jan-Feb. 54–60. www.its.caltech.edu/~dg/MillikanII.pdf (2001)
4. Goldstein, S.: The steady flow of viscous fluid past a fixed spherical obstacle at small Reynolds numbers. *Proc. R. Soc. Ser. A* **12**, 225–235 (1929)
5. Kaplun, S., Lagerström, P.A.: Asymptotic expansions of Navier-Stokes solutions for small Reynolds numbers. *J. Math. Mech.* **6**, 585–593 (1957)
6. Liao, S.-J.: The proposed homotopy analysis technique for the solution of nonlinear problems. Ph.D. thesis, Shanghai Jiao Tong University (1992)
7. Liao, S.-J.: A uniformly valid analytic solution of two-dimensional viscous flow over a semi-infinite flat plate. *J. Fluid Mech.* **34**, 101–128 (1999)
8. Liao, S.-J.: An explicit, totally analytic approximate solution for Blasius’ viscous flow problems. *Int. J. Nonlinear Mech.* **34**, 759–778 (1999)
9. Liao, S.-J.: An analytic approximation of the drag coefficient for the viscous flow past a sphere. *Int. J. Non-linear Mech.* **37**, 1–18 (2002)
10. Liao, S.-J.: *Beyond Perturbation - Introduction to the Homotopy Analysis Method*. Chapman & Hall/CRC Press, Boca Raton (2004)

11. Liao, S.-J.: *Homotopy Analysis Method in Nonlinear Differential Equations*. Higher Education Press Beijing, Springer Berlin etc (2011)
12. Lighthill, J.: Sidney Goldstein. *Biogr. Mem. Fellows R. Soc. Lond.* **36**, 175–197 (1990)
13. Maxworthy, T.: Accurate measurements of sphere drag at low Reynolds numbers. *J. Fluid Mech.* **23**, 369–372 (1965)
14. Ockendon, R., Evans, G.A.: The drag on a sphere in low Reynolds number flow. *J. Aerosol Sci.* **3**, 237–242 (1972)
15. Oseen, C.W.: Über die Stokes'sche Formel und die verwandte Aufgabe in der Hydrodynamik. *Arkiv. Mat. Astron. Fys.* **6**, 29 (1910)
16. Proudman, I., Pearson, J.R.A.: Expansions at small Reynolds numbers for the flow past a sphere and a circular cylinder. *J. Fluid Mech.* **2**, 237–262 (1957)
17. Roos, F.W., Willmarth, W.W.: Some experimental results on sphere and disk drag. *AIAA J.* **9**, 285–290 (1971)
18. Shanks, D.: Nonlinear transformations of divergent and slowly convergent sequences. *J. Math. Phys.* **34**, 1–42 (1955)
19. Stokes, G.G.: On the effect of internal friction of fluids on the motion of pendulums. *Trans. Camb. Philos. Soc.* **9**, Part II, 8–106 (1851). Reprinted in *Math. Phys. Pap.* **3**, 1–141, Cambridge University Press, London (1901)
20. Taylor, G.I.: The viscosity of a fluid containing small drops of another fluid. *Proc. R. Soc. Lond.* **138A**, 41–47 (1932)
21. Van Dyke, M.: *Perturbation Methods in Fluid Mechanics*, 229p. Academic Press, New York. (1964). 2nd edn, Parabolic Press
22. Van Dyke, M.: Extension of Goldstein's series for the Oseen drag of a sphere. *J. Fluid Mech.* **44**(2), 365–372 (1970)
23. White, F.M.: *Viscous Fluid Flow*. McGraw Hill, New York (1991)
24. Whitehead, A.N.: Second approximation to viscous motion. *Q. J. Math.* **23**, 143–152 (1889)
25. Wieselsburger, C.: Neuere Feststellungen über die Gesetze des Flüssigkeits- und Luftwiderstandes. *Physikalische Zeitschrift* **22**, 321–328 (1921)
26. Wieselsburger, C.: Weitere Feststellungen über die Gesetze des Flüssigkeits- und Luftwiderstandes. *Physikalische Zeitschrift* **23**, 219–224 (1922)

Chapter 12

Three-Dimensional Creeping Flow— Systematic Derivation of the Shallow Flow Approximations

Abstract This chapter is devoted to the approximate determination of the velocity field in a shallow layer of ice or granular soil, treated as a non-NEWTONian material flowing under the action of its own weight and assuming its velocity to be so small that STOKES flow can be assumed. Two limiting cases can be analyzed: (i) The deforming material flows on a steep slope (which is the case for creeping landslides or snow deposits on mountain topographies with inclination angles that are large). (ii) In the second case the inclination angles are small. Situation (ii) is apt to ice flow in large ice sheets such as Greenland and Antarctica, important in climate scenarios in a warming atmosphere. The two situations require different approximations. Perturbation schemes are derived in terms of a shallowness parameter in the two situations; applications are discussed under real world conditions. Applications focus on thermo-mechanical coupled plane ice sheet flows and to the Greenland ice sheet response to present day climate driving. In shallow, but still slow gravity driven free surface flows the acceleration terms in NEWTON’s law are no longer negligible.

Keywords Viscous material spreading · Thermo-mechanical coupling · STOKES approximation · Free surface shallow creeping flows · Inclined and horizontal gravity driven creep flow.

List of Symbols

Roman Symbols

$A(T)$	Rate factor as a function of temperature T
\mathbb{A}	ARRHENIUS parameter: $\mathbb{A} = \frac{Q}{kT_R}$
$a(x, y, z_S, t)$	Accumulation (rate) function at the free surface $z = z_S$
\mathcal{C}	Dimensionless coefficient in the sliding law
$c(T)$	Specific heat as a function of temperature
$\bar{c}(\theta)$	Dimensionless specific heat as a function of temperature
\mathbf{D}	Stretching tensor, strain rate—, rate of strain— $\mathbf{D} = \frac{1}{2}(\mathbf{L} + \mathbf{L}^T)$
\mathcal{D}	Domain in \mathcal{R}^n , $n = 1, 2, 3$
\mathbb{D}	Dimensionless diffusivity (see (12.18))

$[d]$	Scale for a frequency [1/time]
\mathbb{E}	Ratio of the gravitational potential to the internal energy (see (12.18))
$\mathbb{E}\mathbb{G}$	Dimensionless scale measuring dissipation or strain heating, — in the SIA
$F(\mathbf{t}_{II})$	Creep response function as function of the second stress deviator invariant
\mathbb{F}^2	Squared FROUDE number in the SIA: $\mathbb{F}^2 = \frac{U^2}{g[H]}$
$\hat{\mathbb{F}}^2$	Squared FROUDE number (see (12.18)): $\hat{\mathbb{F}}^2 = \frac{\mathbb{F}^2}{\sin(\alpha)}$
\mathcal{F}	Ratio of nonlinear sliding functions (see (12.9) and (12.24))
f_0, f_1, f_2	Parameters in the quadratic law for the fluidity (see (12.67))
\mathbb{G}	Parameter characterizing the constitutive response of \mathbf{t} (see (12.18)) and in the SIA
g	Gravity vector
$[H]$	Depth/height scale
h_S, h_B	Heat transfer coefficients at the free surface and at the base
$h_{S,B}^{\text{ref}}$	Reference height for h_S and h_B
k	BOLTZMANN constant: $k = 1.3806488 \times 10^{-23}$ [JK ⁻¹]
\mathbb{k}	Dimensionless fluidity at zero shearing (see (12.66))
$\mathbf{L} = \text{grad } \mathbf{v}$	Spatial velocity gradient
$[L_x], [L_y]$	Length scales in the x - and y -directions
$\mathbb{N}_{S,B}$	NUSSELT number for the free surface and the base
n	Exponent of the power law for stress (GLEN: $n = 3$)
N_S	Length of n_S
$\mathbf{n}_S, \mathbf{n}_B$	Normal vectors perpendicular to the surface, —the base
p, \bar{p}	Pressure, dimensionless—
$p = \rho g[H] \cos \alpha$	Pressure scale
Q	Activation energy
Q_x, Q_y	Volume flux in the x - and y -directions
q	Heat flux vector
\mathcal{R}^3	Three dimensional real space
T_A	Atmospheric temperature
T_R	Reference temperature $T_R = 273.15$ °C
\mathfrak{T}	Time scale $\mathfrak{T} = \frac{[L_x]}{[U]}$
\mathbf{t}	CAUCHY stress
$\{t_{xx}, t_{xy}, \dots, t_{zz}\}$	Scales for the components of— $\{t_{xx}, t_{xy}, \dots, t_{zz}\} = \rho g[H] \sin \alpha \{\sigma_x, \tau_{xy}, \dots, \sigma_{zz}\}$
\mathbf{t}_S	Tangential traction vector at the basal surface $\mathbf{t}_S := \mathbf{t}\mathbf{n}_B - \mathbf{t}_n$
\mathbf{t}_n	Traction vector perpendicular to the basal surface $\mathbf{t}_n := (\mathbf{n}_B \cdot \mathbf{t}\mathbf{n}_B)\mathbf{n}_B$
t_{II}	Second stress deviator invariant
$[U], [V]$	Velocity scales in the x - and y -directions
$\mathbf{v} = (u, v, w)$	Velocity vector, components of—

$[W]$	Scale of the velocity component in the z -direction
$\mathbf{x} = (x, y, z)$	Position vector in \mathcal{R}^3 , Cartesian components of \mathbf{x}
$z = z_S(x, y, t)$	Free surface equation
$z = z_B(x, y, t)$	Equation for the basal surface
$\mathbb{Z} = \frac{[\Delta T]}{T_R}$	Dimensionless temperature scale

Greek and Miscellaneous Symbols

α	Inclination angle of the (x, y) -plane relative to the horizontal plane
$[\Delta T]$	Temperature scale
ε	Internal energy
$\varepsilon_x, \varepsilon_y$	Horizontal aspect ratios, $\varepsilon_x = \frac{[H]}{[L_x]}$, $\varepsilon_y = \frac{[H]}{[L_y]}$
η	Ratio of x -scaling/ y -scaling, $\eta = \frac{\varepsilon_x}{\varepsilon_y} = \frac{[L_y]}{[L_x]}$
ρ	Mass density
$\kappa(T)$	Heat conductivity as function of T
$\bar{\kappa}(\theta)$	Heat conductivity as function of θ
μ_{eff}	Effective dynamic viscosity
$\Phi(\mathbf{t}_S ^2, \mathbf{t}_n ^2)$	Drag coefficient, sliding—
θ_A, θ_B	Dimensionless temperature of the atmosphere, —base
Ψ	Essential parameter in defining the sign of the longitudinal velocity component u (see (12.55))
ψ	Parameter in the interval $(0, 1)$: $\psi := \varepsilon_y = \cotan \alpha$
ψ_x	$\mathcal{O}(1)$ -quantity for the non-dimensionalization of the governing equations (12.53): $\psi_x := \varepsilon_x \cotan \alpha$
ψ_y	$\mathcal{O}(1)$ -quantity for the non-dimensionalization of the governing equations (12.53): $\psi_y := \varepsilon_y \cotan \alpha$
$[\tau]$	Scale for horizontal shear stress τ_{xy} : $[\tau] = [\rho g H] \varepsilon$
$\sigma_x, \tau_{xy}, \dots, \sigma_z$	Dimensionless stress deviator components
τ_{II}	Dimensionless second stress deviator invariant
$\partial \mathcal{D}_{S,B}$	Free surface and basal boundary of the domain \mathcal{D}
SFA	Shallow Flow Approximation
SIA	Shallow Ice Approximation
SOSIA	Second Order Shallow Ice Approximation
SSA	Shallow Shelf Approximation
SOSSA	Second Order Shallow Self Approximation

12.1 Introductory Motivation

Section 7.4 in Chap. 7 was devoted to what was said to be among the most complex configurations of the so-called pressure drag flow. A motivation of the simplified equations from the original fluid mechanical equations was presented; it was developed for shallow creeping flows of thermo-mechanically coupled processes of

non-linear viscous heat conducting materials subject to gravity and resting on a more or less horizontal bed. As a typical example the flow of ice in large ice sheets (such as Greenland and Antarctica) was serving as motivating geophysical model, and the simplified initial boundary value problem was explored up to a level at which it is today used in circulation models of climate reconstructions through millennia and future climate scenarios for centennial sea level rise predictions in future Greenhouse scenarios.

The ‘derivation’ of the simplified initial boundary value problems from the balance laws of mass, momentum and energy was neither systematic nor rational, but at best plausible and, in particular, did not suggest a process of improved approximation. Moreover, delineation of the regime of validity of the approximate set of equations was equally not precisely stated. In this chapter we shall partly repeat and partly extend the analysis in Sect. 7.4 of Chap. 7. We shall **non-dimensionalize** the rigorously formulated initial boundary value problem and introduce a **scale analysis** for the various physical quantities and a **coordinate stretching** appropriate for creeping flows down an inclined surface. For such situations it is natural that depth-to-length ratios are different in the downhill direction and perpendicular to it, and that the flow is essentially from higher altitudes to lower ones. This has not been so for the case(s) treated in Chap. 7. The normalized energy equation shows that for the applications considered, in-plane and out-of-plane (transverse) convection is equally important. Alternatively, transverse diffusion and dissipation are both important, whereas ‘in-plane’ diffusion may be ignored to lowest order. The introduction of the scales and the different small aspect ratio parameters allow identification of the **shallow flow approximation** as the lowest order approximation of a **regular perturbation scheme**, using the aspect ratio parameter as perturbation parameter. Furthermore, this analysis makes also clear that free-surface-creeping flow of a very viscous fluid on a more or less horizontal plane (ice sheets on Earth or other planets; honey on the breakfast plate, polymeric fluid spreading) and down a corrie (creep of soil down mountain slopes, etc.) are described by different sets of partial differential equations, each leading to slightly different initial-boundary-value problems. Consequently, there is not a single Shallow Flow Approximation, there are rather several ones, each covering (slightly) different flow configurations.

An early account of shallowness properties by stretched scaling is by KURT OTTO FRIEDRICHS published in 1948 [22], who set the shallow water approximation on a rational mathematical scaling. Such scalings have systematically been introduced in the early eighties of the last century in glacier and ice sheet dynamics almost simultaneously by ANDREW C. FOWLER and D.A. LARSON (1978) [20], K. HUTTER (1981, 1983, 1984) [37, 39, 40], LESLIE W. MORLAND and IAN R. JOHNSON (1980, 1982) [53, 54] and MORLAND (1984) [52]. In this chapter we follow K. HUTTER and LAURENT VULLIET (1985) [43], who applied the method to creeping of soil down slopes in a geotechnical context. These latter authors introduced scalings, which differ from one another depending upon, whether the flow is essentially unidirectional from higher altitudes to lower ones, or whether it forms a divide, separating the flow directions, see **Figs. 12.1, 12.2** and **12.3**. In one case, the plane to which the free basal surface and the flows are referenced, is inclined in the main flow direction



Fig. 12.1 Piedmont glaciers in Southern Axel Heiberg Island. *A series of wide, confined valley glaciers that spread out as wide lobes when they leave narrow mountain valleys to enter a wider valley or a plain, are called Piedmont glaciers. Aerial photo, 1977. ©J. Alean*



Fig. 12.2 Glacier of the ice cap on the beam Martin Mountains, dividing Baffin and Bylot Islands, Canada. *This glacier has an expanded foot, characteristic of a Piedmont glacier, where it widens onto a lowland. Source Natural Resources Canada. © Terrain Sciences Division, Geological Survey of Canada. <http://nsidc.org/cryosphere/glaciers/gallery/piedmont.html>*

with a finite angle; in the second case, this plane is horizontal or has a very small inclination. The asymptotic analysis to the situation to all three cases of Fig. 12.3 is given in this chapter.

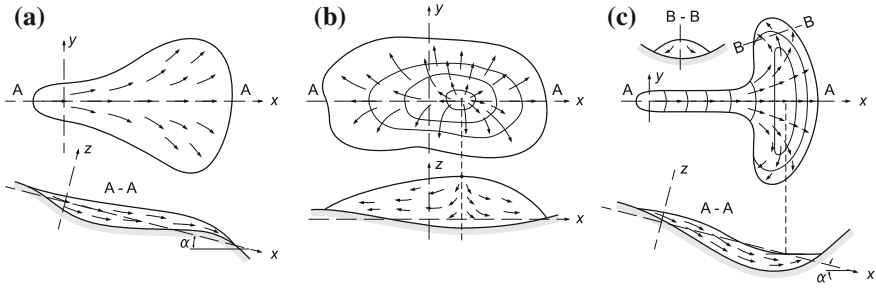


Fig. 12.3 Slow creeping flow of a mass of a very viscous body under its own weight. **a** Flow down an inclined surface. Motion is strictly from higher altitudes to lower ones. Spreading occurs downslope and cross-slope. **b** Spreading of a mass of a viscous body on a flat bed. Motion is from a dome (or divide in 2 dimensions) into all directions. **c** Downward motion on a sloping bottom, but such that the front is pushed upward beyond the lowest point of the topography. The main flow is from above to below in the positive x -direction, but there are domains (cross section $B-B$) where backward flow can arise. Based on [43]

12.2 Model Equations

Consider a three-dimensional domain $\mathcal{D} \in \mathcal{R}^3$ with bounding surfaces $\partial\mathcal{D}_S$ (free surface) and $\partial\mathcal{D}_B$ (base). Let x, y, z be Cartesian coordinates (see **Fig. 12.4**); x, y are in a plane which is inclined relative to a horizontal plane with inclination angle α ; x is in the direction of steepest descent and positive downwards; y is perpendicular to it and thus horizontal. We regard the (x, y) -plane to be a best planar fit to the basal surface. The third coordinate, z is perpendicular to x, y and points upwards. The top free surface and the basal surface¹ will be denoted by $z = z_S(x, y, t)$ and $z = z_B(x, y)$, respectively, and the domain \mathcal{D} is assumed to be continuously filled with a density preserving heat conducting body under slow creeping motion, of which the constitutive response is characteristically that of a fluid. We assume the material in \mathcal{D} to be in thermodynamic non-equilibrium and subject to heat exchange both at the free and basal surfaces, but we ignore phase changes. Our interest is in the evolution of the domain $\mathcal{D}(t)$ and the velocity and temperature distributions within it.

12.2.1 Field Equations

Governing equations are the balance laws of mass (continuity), momentum and energy,²

¹For simplicity, we treat here the basal surface as rigid and non-moving ; the more general case is left to the reader as an exercise.

²A derivation of the energy equation is given in Chap. 17, ‘Thermodynamics—Fundamentals’.

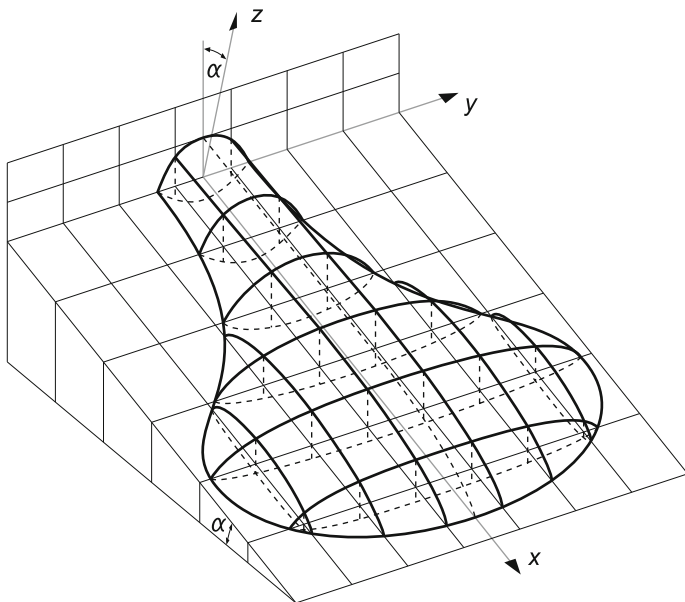


Fig. 12.4 Definition of configuration and coordinate system. *The direction of steepest descent defines the x-coordinate of a Cartesian coordinate system. The y-axis is horizontal, perpendicular to the x-axis. The (x, y)-axes form a plane; perpendicular to it is the third, z-axis, positive upward. The bottom topography (dashed lines), assumed to be un-deformable and the moving deformable free surface (solid lines) bound the moving mass that enters the space from a narrow valley, from [43]*

$$\begin{aligned}
 \operatorname{div} \mathbf{v} &= 0, \\
 \rho \frac{d\mathbf{v}}{dt} &= -\operatorname{grad} p + \operatorname{div} \mathbf{t} + \rho \mathbf{g}, \\
 \rho \frac{d\varepsilon}{dt} &= -\operatorname{div} \mathbf{q} + \operatorname{tr}(\mathbf{tD}),
 \end{aligned}
 \tag{12.1}$$

in which \mathbf{v} is the velocity vector of which the components in the Cartesian coordinates x, y, z will be denoted as u, v, w . $\rho, p, \mathbf{t}, \mathbf{g}$ are the density, pressure, stress deviator and gravity vector; ε and \mathbf{q} denote the internal energy and the heat flux vector and \mathbf{D} is the stretching tensor, which is defined by $\mathbf{D} = \operatorname{sym}(\operatorname{grad} \mathbf{v})$. Moreover, ‘grad’, ‘div’ and ‘tr’ are the gradient, divergence and trace operators and d/dt is the material time derivative, which is given by

$$\frac{d(\cdot)}{dt} = \frac{\partial(\cdot)}{\partial t} + \operatorname{grad}(\cdot)\mathbf{v}.
 \tag{12.2}$$

Occasionally we shall also use the notations

$$\mathbf{L} = \operatorname{grad} \mathbf{v}, \quad \mathbf{D} = \frac{1}{2}(\mathbf{L} + \mathbf{L}^T).$$

In order that the balance laws become field equations, they must be complemented by constitutive relations. In this chapter we shall restrict ourselves to a fluid with negligible elastic, but strong thermo-viscous response of the form

$$\begin{aligned}\varepsilon &= \int_0^T c(T') dT', \\ \mathbf{q} &= -\kappa(T) \text{grad } T, \\ \mathbf{D} &= A(T)F(t_{II})\mathbf{t}, \quad t_{II} = \frac{1}{2}\text{tr}(\mathbf{t}^2).\end{aligned}\tag{12.3}$$

Here, $c(T)$ is the temperature dependent heat capacity and $\kappa(T)$ the heat conductivity, typical of a heat conducting fluid. The third of Eq. (12.3) assumes that stretching \mathbf{D} and stress deviator \mathbf{t} are collinear with a coefficient which is separated into a stress dependent **creep response function** F (which is assumed to depend only on the second stress deviator invariant t_{II}) and a temperature dependent **rate factor** $A > 0$. Later on the significance of one of several hidden variables will also be studied; they may alter the constitutive relations. Explicit expressions for F and A will be given below. Here, it may suffice to mention that physically reasonable F 's and A 's have $F(t_{II}) \geq 0$, $A(T) > 0$, for all t_{II} and T . With $F(0) \neq 0$ the creep law exhibits finite viscosity at zero stress, for $F(0) = 0$ it is infinite, and singular behavior must be expected. This case will be excluded. Furthermore, for creeping flow at elevated temperatures, A varies in general several orders of magnitude within a relatively small range of temperature, suggesting a strong thermomechanical coupling.

12.2.2 Boundary Conditions

These must be formulated at the free surface and at the bed and comprise kinematic and dynamic statements. The free surface $z = z_S(x, y, t)$ will be assumed to be stress free and to exchange heat with the environment. With the exterior unit normal vector \mathbf{n}_S and with

$$N_S = \left[1 + \left(\frac{\partial z_S}{\partial x} \right)^2 + \left(\frac{\partial z_S}{\partial y} \right)^2 \right]^{1/2}\tag{12.4}$$

the kinematic surface equation becomes

$$N_S^{-1} \frac{\partial z_S}{\partial t} + \mathbf{n}_S \cdot \mathbf{v} = a(x, y, z_S, t), \quad \text{at } z = z_S(x, y, t),\tag{12.5}$$

in which $a(x, y, z_S(x, y, t), t)$ is the so-called **accumulation rate function**, expressing the addition of mass at the free surface, perpendicular to the surface. For $a = 0$, Eq. (12.5) simply expresses that the free surface is material. The boundary conditions

of zero traction and heat exchange are written in the form³

$$\begin{aligned} \mathbf{t}\mathbf{n}_S - p\mathbf{n}_S &= \mathbf{0}, \\ \mathbf{q} \cdot \mathbf{n}_S &= h_S(T - T_A), \end{aligned} \quad \text{at } z = z_S(x, y, t). \quad (12.6)$$

For non-vanishing accumulation rate, $a \neq 0$, these are approximate. T_A is the air temperature outside a thermal boundary layer and h_S is the heat transfer coefficient, which may itself be a function of the surface temperature and other variables of the environment (say a boundary layer wind speed).

Boundary conditions at the *un-deformable* base $z = z_B(x, y)$ comprise a kinematic statement, if a slip is permitted, and a thermal heat transfer statement. The analogues of Eqs. (12.5) and (12.6)₂ are, therefore,⁴

$$\begin{aligned} \mathbf{v} \cdot \mathbf{n}_B &= 0, \\ \mathbf{q} \cdot \mathbf{n}_B &= h_B(T - T_G), \end{aligned} \quad \text{at } z = z_B(x, y, t), \quad (12.7)$$

where T_G is the ground temperature outside the basal thermal boundary layer and h_B is the basal heat transfer coefficient. It remains to conjecture a *sliding law* that is compatible with the kinematic condition (12.7)₁. Postulating collinearity of basal velocity and shear traction, we define

$$\mathbf{t}_S := \mathbf{t}\mathbf{n}_B - \mathbf{t}_n, \quad \mathbf{t}_n := (\mathbf{n}_B \cdot \mathbf{t}\mathbf{n}_B)\mathbf{n}_B \quad (12.8)$$

and write

$$\mathbf{v} = -\Phi(|\mathbf{t}_S|^2, |\mathbf{t}_n|^2)\mathbf{t}_S, \quad \text{at } z = z_B(x, y), \quad (12.9)$$

in which $\Phi \geq 0$ is a possible non-linear function of the magnitudes of the shear and normal tractions at the base. Physically we must have $\Phi > 0$ for non-zero \mathbf{t}_S or \mathbf{t}_n , but one may have $\Phi(0, 0) = 0$, or $\Phi(0, 0) \neq 0$. It is easily seen that (12.9) satisfies the tangency condition (12.7)₁; furthermore, $\Phi \equiv 0$ corresponds to no-slip and $\Phi \rightarrow \infty$ yields perfect sliding. This completes the formulation of the formal boundary value problem.

³For a material surface these expressions are accurate, but for a non-material surface (12.6) ignores the impulse due to the mass flow across the surface. This is generally justified.

⁴The first of relations (12.7) assumes that there is no mass flow through the surface, e.g. no melting of ice if glaciers or ice sheets are considered.

12.3 Scaling Procedure

Non-dimensionalization of the above field equations are motivated by the fact that domains, in which such creep flows usually take place (lava flows from volcanoes, wide glacier flows, melts, etc.), are long and wide but shallow. We, thus scale the horizontal and vertical coordinates and corresponding velocities differently and write for these, for the time, the stresses and temperature

$$\begin{aligned}
 x &= [L_x]\bar{x}, & u &= [U]\bar{u}, & t_{xx} &= \rho g[H] \sin \alpha \sigma_x, \\
 y &= [L_y]\bar{y}, & v &= [V]\bar{v}, & t_{xy} &= \rho g[H] \sin \alpha \tau_{xy}, \\
 z &= [H]\bar{z}, & w &= [W]\bar{w}, & & \text{etc.}, \\
 & & a &= [W]\bar{a}, & & \\
 t &= [\mathfrak{T}]\bar{t}, & T &= T_R + [\Delta T]\theta, & p &= \rho g[H] \cos \alpha \bar{p},
 \end{aligned} \tag{12.10}$$

in which $[L_x]$, $[L_y]$, $[H]$ are length scales in the x , y and z -directions, $[\mathfrak{T}]$ is a typical time, $[U]$, $[V]$ and $[W]$ are characteristic velocities in the x , y and z -directions. Moreover, T_R is a constant reference temperature and $[\Delta T]$ a temperature range within the material occupying the domain \mathcal{D} . Note that pressure has been scaled with $\rho g[H] \cos \alpha$ and components of the stress deviator with $\rho g[H] \sin \alpha$, because it is supposed that the basal tractions (normal pressure, shear traction) are basically responding to a hydrostatic pressure distribution. This will naturally limit the flow configurations in the approximations treated below. Greek and overbarred quantities are dimensionless.

We now focus attention to processes of which the velocity components arise in proportion of the length scales in the x -, y - and z -directions, $[L_x]$, $[L_y]$ and $[H]$, respectively. This suggests the identifications

$$\frac{[V]}{[U]} = \frac{[L_y]}{[L_x]}, \quad \frac{[W]}{[U]} = \frac{[H]}{[L_x]}, \quad [\mathfrak{T}] = \frac{[L_x]}{[U]}. \tag{12.11}$$

The choices (12.11)_{1,2} say that the geometric stretchings and the velocity stretchings are the same. So, localized features, i.e., formations of local vortices are not optimally incorporated and, in a stretching based approximation, eliminated. On the other hand, it is readily seen that with (12.11)_{1,2} the dimensionless continuity equation, $\operatorname{div}_x \mathbf{v} = 0$ is preserved, $\operatorname{div}_{\bar{x}} \bar{\mathbf{v}} = 0$. Moreover, (12.11)₃ together with (12.11)_{1,2} and the scaling (12.10) show that

$$\frac{d\mathbf{v}}{dt} \longrightarrow \rho g \hat{\mathbb{F}}^2 \frac{d\bar{\mathbf{v}}}{d\bar{t}}, \quad \frac{d\bar{\mathbf{v}}}{d\bar{t}} = \frac{\partial \bar{\mathbf{v}}}{\partial \bar{t}} + (\operatorname{grad}_{\bar{x}} \bar{\mathbf{v}}) \cdot \bar{\mathbf{v}}, \tag{12.12}$$

where $\hat{\mathbb{F}}$ is defined in (12.18) (below) or for any scalar variable (\cdot)

$$\frac{d(\cdot)}{dt} \longrightarrow \alpha_{(\cdot)} \frac{d(\cdot)}{d\bar{t}}, \tag{12.13}$$

in which $\alpha_{(\cdot)}$ is an isotropic stretching measure. Thus, mass balance is fully preserved and substantive derivatives of the velocity vector or any scalar variable are isotropically stretched or squeezed. This is indication that these quantities are well transformed under the chosen scalings. We shall soon see that this is different for flux terms.

It is straightforward, even though a bit cumbersome, to show that the component form of the field Eq. (12.1) and constitutive relations (12.3) in dimensionless form become

$$\begin{aligned}
\frac{\partial \bar{u}}{\partial \bar{x}} + \frac{\partial \bar{v}}{\partial \bar{y}} + \frac{\partial \bar{w}}{\partial \bar{z}} &= 0, \\
\hat{\mathbb{F}}^2 \frac{d\bar{u}}{d\bar{t}} &= \varepsilon_x \left(-\cotan \alpha \frac{\partial \bar{p}}{\partial \bar{x}} + \frac{\partial \sigma_x}{\partial \bar{x}} \right) + \varepsilon_y \frac{\partial \tau_{xy}}{\partial \bar{y}} + \frac{\partial \tau_{xz}}{\partial \bar{z}} + 1, \\
\hat{\mathbb{F}}^2 \eta \frac{d\bar{v}}{d\bar{t}} &= \varepsilon_x \frac{\partial \tau_{xy}}{\partial \bar{x}} + \varepsilon_y \left(-\cotan \alpha \frac{\partial \bar{p}}{\partial \bar{y}} + \frac{\partial \sigma_y}{\partial \bar{y}} \right) + \frac{\partial \tau_{yz}}{\partial \bar{z}}, \\
\hat{\mathbb{F}}^2 \varepsilon_x \tan \alpha \frac{d\bar{w}}{d\bar{t}} &= \varepsilon_x \tan \alpha \frac{\partial \tau_{xz}}{\partial \bar{x}} + \varepsilon_y \tan \alpha \frac{\partial \tau_{yz}}{\partial \bar{y}} - \left(\frac{\partial \bar{p}}{\partial \bar{z}} + \tan \alpha \frac{\partial \sigma_z}{\partial \bar{z}} + 1 \right), \\
\bar{c}(\theta) \frac{d\theta}{d\bar{t}} &= \mathbb{D} \left[\varepsilon_x^2 \frac{\partial}{\partial \bar{x}} \left(\bar{\kappa}(\theta) \frac{\partial \theta}{\partial \bar{x}} \right) + \varepsilon_y^2 \frac{\partial}{\partial \bar{y}} \left(\bar{\kappa}(\theta) \frac{\partial \theta}{\partial \bar{y}} \right) + \frac{\partial}{\partial \bar{z}} \left(\bar{\kappa}(\theta) \frac{\partial \theta}{\partial \bar{z}} \right) \right] \\
&\quad + \mathbb{E} \mathbb{G} 2 \bar{A}(\theta) \mathbb{f}(\tau_{II}) \tau_{II}, \tag{12.14}
\end{aligned}$$

$$\frac{\partial \bar{u}}{\partial \bar{x}} = \mathbb{G} \bar{A}(\theta) \mathbb{f}(\tau_{II}) \sigma_x,$$

$$\frac{\partial \bar{v}}{\partial \bar{y}} = \mathbb{G} \bar{A}(\theta) \mathbb{f}(\tau_{II}) \sigma_y,$$

$$\frac{\partial \bar{w}}{\partial \bar{z}} = \mathbb{G} \bar{A}(\theta) \mathbb{f}(\tau_{II}) \sigma_z,$$

$$\frac{\partial \bar{u}}{\partial \bar{y}} + \eta^2 \frac{\partial \bar{v}}{\partial \bar{x}} = 2\eta \mathbb{G} \bar{A}(\theta) \mathbb{f}(\tau_{II}) \tau_{xy},$$

$$\frac{\partial \bar{u}}{\partial \bar{z}} + \varepsilon_x^2 \frac{\partial \bar{w}}{\partial \bar{x}} = 2\varepsilon_x \mathbb{G} \bar{A}(\theta) \mathbb{f}(\tau_{II}) \tau_{xz},$$

$$\frac{\partial \bar{v}}{\partial \bar{z}} + \varepsilon_y^2 \frac{\partial \bar{w}}{\partial \bar{y}} = 2\varepsilon_y \mathbb{G} \bar{A}(\theta) \mathbb{f}(\tau_{II}) \tau_{yz},$$

in which

$$\tau_{II} = \frac{1}{2} (\sigma_x^2 + \sigma_y^2 + \sigma_z^2) + \tau_{xy}^2 + \tau_{yz}^2 + \tau_{zx}^2, \tag{12.15}$$

$$\frac{d}{d\bar{t}} = \frac{\partial}{\partial \bar{t}} + \frac{\partial}{\partial \bar{x}} \bar{u} + \frac{\partial}{\partial \bar{y}} \bar{v} + \frac{\partial}{\partial \bar{z}} \bar{w}$$

are the dimensionless stress deviator invariant and the dimensionless material time derivative and

$$\varepsilon_x = \frac{[H]}{[L_x]}, \quad \varepsilon_y = \frac{[H]}{[L_y]}, \quad \eta = \frac{\varepsilon_x}{\varepsilon_y} = \frac{[L_y]}{[L_x]} \quad (12.16)$$

are aspect ratios. Furthermore,

$$\begin{aligned} \mathbb{f}(\tau_{II}) &:= \frac{F((\rho g[H] \sin \alpha)^2 \tau_{II})}{F((\rho g[H] \sin \alpha)^2 \cdot 1)}, \\ \bar{A}(\theta) &:= \frac{A(T)}{A(T_R)} = \frac{A(T_R + [\Delta T]\theta)}{A(T_R)} := \frac{A'(\theta)}{A(T_R)}, \\ \bar{\kappa}(\theta) &:= \frac{\kappa(T)}{\kappa(T_R)} = \frac{\kappa(T_R + [\Delta T]\theta)}{\kappa(T_R)} := \frac{\kappa'}{\kappa(T_R)}, \\ \bar{c}(\theta) &:= \frac{c(T)}{c(T_R)} = \frac{c(T_R + [\Delta T]\theta)}{c(T_R)} := \frac{c'(\theta)}{c(T_R)} \end{aligned} \quad (12.17)$$

are a dimensionless creep response function, rate factor, heat conductivity and heat capacity, all positive functions. Moreover, $\hat{\mathbb{F}}$, \mathbb{G} , \mathbb{D} and \mathbb{E} are dimensionless characteristic numbers, defined by

$$\begin{aligned} \hat{\mathbb{F}}^2 &:= \frac{[U^2]}{g[L_x] \sin \alpha} \\ \mathbb{G} &:= \frac{[L_x]}{[U]} \rho g \sin \alpha [H] A(T_R) F((\rho g[H] \sin \alpha)^2), \\ \mathbb{D} &:= \frac{[L_x]}{[U]} \frac{\kappa(T_R)}{\rho c(T_R) [H^2]}, \\ \mathbb{E} &:= \frac{g[H] \sin \alpha}{c(T_R) [\Delta T]}. \end{aligned} \quad (12.18)$$

$\hat{\mathbb{F}}$ is a FROUDE⁵ number, \mathbb{D} a dimensionless diffusivity, \mathbb{G} a parameter characterizing the constitutive response of stress, and the product $\mathbb{E}\mathbb{G}$ measures the significance of dissipation or strain heating.

Let us pause and inspect equations (12.14) more closely: (12.14)₁ is the dimensionless mass balance equation for a density preserving body; (12.14)_{2,3} are the (x, y) -parallel components of the momentum balance, whilst (12.14)₄ is that perpendicular to the (x, y) -plane. We take the position that the dimensionless variables in Eq. (12.14) are of order unity, whereas the factors $\hat{\mathbb{F}}$, $\hat{\mathbb{F}} \tan \alpha$, \mathbb{D} , \mathbb{E} , \mathbb{G} and $\varepsilon_x, \varepsilon_y, \eta$ take

⁵In continental Europe $\hat{\mathbb{F}}$ is defined as FROUDE number, in English speaking countries it is more often $\hat{\mathbb{F}}^2$. For a biographical sketch of Froude, see Fig. 7.25 in Vol. 1.

Table 12.1 Magnitudes of physical quantities and orders of magnitude for typical scales for glaciers, soil, lava and steel-melt flows, after [43]

Quantity	Dimension ^a	Glacier ice ^b	Soil ^d	Lava flows ^c	Steel melt ^f
g	[m (*) ⁻²]	9.76×10^{15}	9.81	9.81	9.81
ρ	[kg m ⁻³]	900	2000	2500	7500
T_R	[°K]	273.15	–	1773	1773
$\kappa(T_R)$	[J K ⁻¹ m ⁻¹ (*) ⁻¹]	7×10^7	–	2 – 4	30
$c(T_R)$	[J kg ⁻¹ K ⁻¹]	2×10^3	–	1.225×10^3	650
μ_{eff}	[kg m ⁻¹ (*) ⁻¹]	^c $7.5 \times (10^{18} - 10^{23})$	^c 3.2×10^{20}	0.2	0.2
n	[–]	3	3	1	1
[ΔT]	[°K]	20	–	100	100
[U]	[m (*) ⁻¹]	100 – 1000	$10^{-2} - 10^{-1}$	$10^{-2} - 10^{-1}$	0.5
[d] ⁻¹	[(*)]	10 – 10 ²	10 – 10 ³	10 ² – 10 ³	0.2
[H]	[m]	10 ² – 10 ³	10 – 10 ²	1 – 5	0.1
α	[°]	3 – 30	10 – 20	5	5
$A(T_R)$	[(*) ⁻¹ ((*) ² m kg) ⁿ]	1.73×10^{-61}	1.6×10^{-24}	1.3×10^{-7}	–
	[bar ⁻ⁿ (*) ⁻¹]	=0.17	–	–	–

^aThe asterisk stands for seconds (soil, steel melts, lava flows) or years (glaciers)

^bData are taken from K. HUTTER [39]

^cCalculated on the basis of a power law constitutive law: $\mu_{\text{eff}}^{-1} = A(T_R)(\rho g [H] \sin \alpha)^{n-1}$

^dData are taken from ANONYMOUS [3]. Temperature hardly affects the flow and the stress distribution

^eData are taken from A. RITTMANN [59] but (mostly) from T. MURASE & A.R. MCBIRNEY [56]

^fData are taken from F. RICHTER [58]

values as dictated by the material properties and the chosen scales, see **Tables 12.1** and **12.2**. The proper choice of these quantities is a delicate matter and must be selected such that the dimensionless (overbarred) variables assume order unity values in the processes to which they are projected. Equation (12.14)₅ is the dimensionless form of the internal energy balance. The two terms on its right-hand side describe **diffusion due to FOURIER-type heat flux** and **dissipation due to strain heating** (or dissipation). Interestingly, and different from the behavior of the convective operator in (12.12) and (12.13), the diffusive operator in braces exhibits anisotropic contributions in the three coordinate directions. Indeed, the (x , y)-parallel diffusion terms are weighted with the aspect ratios ε_x^2 and ε_y^2 whereas the z -component has the weighting factor 1. If ε_x and ε_y are small, the corresponding terms may be negligible. The introduced scaling process favors diffusion perpendicular to the main flow direction. We emphasize once more, the dimensionless stresses, velocities and temperature, as well as dimensionless material functions, listed in (12.17) are all of order unity, if scales are properly selected.

Table 12.2 Approximate values of the dimensionless parameters arising in the field equation for the typical scales and the physical parameters listed in Table 12.1, after [43]

	Glaciers ^c			Soil		Lava flows ^c		Steel melt ^d
$[H] = (\text{in [m]})$	100	500	1000	10	80	1	5	0.1
$\hat{\rho}^2 = \frac{[U]^2}{g[H] \sin \alpha}$	$< 10^{-11}$			$< 10^{-10}$		$\leq 10^{-7}$		$< 0.75 \times 10^{-3}$
$\mathbb{G} = \frac{\rho g [H] \sin \alpha}{[d] \mu_{\text{eff}}}$	1.2×10^1	1.5×10^3	1.2×10^4	0.5×10^2	2×10^4	5.3×10^4	2.65×10^5	2.25×10^2
$\mathbb{D} = \frac{\kappa(T_R)}{\rho(T_R)[H^2 d]}$	^a 4 ^b 4×10^{-1}	1.5×10^{-1} 1.5×10^{-2}	4×10^{-2} 4×10^{-3}	–		6.4×10^{-5}	2.5×10^{-6}	2
$\mathbb{E} = \frac{g[H] \sin \alpha}{c(T_R)[\Delta T]}$	0.25×10^{-2}	1.25×10^{-2}	2.5×10^{-2}	–		2.4×10^{-5}	9.6×10^{-5}	4.5×10^{-7}
$\mathbb{E}\mathbb{G}$	3×10^{-2}	1.8×10^1	3×10^2	–		0.12	2.5	1.01×10^{-4}

^a $[d] = 10^{-2}$ [1/a]

^b $[d] = 10^{-1}$ [1/a]

^cSome of the numerical values for \mathbb{D} suggest existence of a thermal boundary layer at the basal boundary

^dThe numerical values for \mathbb{D} and $\mathbb{E}\mathbb{G}$ suggest that ignoring dissipation in the energy equation is justified

With the physical parameters and the scales listed in Table 12.1, the dimensionless parameters (12.18) take on the order of magnitudes listed in Table 12.2. Accordingly, $\hat{\mathbb{F}}$ is very small, justifying the STOKES approximation, which ignores the acceleration terms in NEWTON's law. Hence, the momentum equations reduce to force balances. In the evaluation of the quantities of Table 12.2 we have used

$$A(T_R)F((\rho g[H] \sin \alpha)^2)^{-1} = \mu_{\text{eff}}, \quad (12.19)$$

which is an effective viscosity, and have introduced $[d] \equiv [U]/[L_x]$, which is a representative scale for the stretching. This choice is preferable to the independent selection of $[L_x]$, because strain rates can directly be measured and typical values be estimated. $[L_x]$ is then simply a deduced quantity, an order of magnitude for a length over which dimensionless stresses and strain rates vary by order unity. A value for this typical length follows from the recognition that $\mathbb{G} = \mathcal{O}(\varepsilon_x^{-1})$ as explained below and yields $[L_x] = [H^2]\rho g \sin \alpha / (\mu_{\text{eff}}[d])$. Table 12.2 also indicates that \mathbb{G} is large, and \mathbb{D} and \mathbb{E} are not small, in general; so, in the energy equation neither diffusion nor dissipation should be ignored in comparison to advection.

Substituting the scales (12.10) into the *free surface boundary conditions* (12.5)–(12.7) and using relations (12.11) and (12.16) yields the boundary conditions in dimensionless form. At the upper surface $\bar{z} = \bar{z}_S(\bar{x}, \bar{y}, \bar{t})$ they are

$$\begin{aligned} \frac{\partial \bar{z}_S}{\partial \bar{t}} + \frac{\partial \bar{z}_S}{\partial \bar{x}} \bar{u} + \frac{\partial \bar{z}_S}{\partial \bar{y}} \bar{v} - \bar{w} &= \bar{a}(\bar{x}, \bar{y}, \bar{z}_S, \bar{t}), \\ \varepsilon_x (-\sigma_x + \cotan \alpha \bar{p}) \frac{\partial \bar{z}_S}{\partial \bar{x}} - \varepsilon_y \tau_{xy} \frac{\partial \bar{z}_S}{\partial \bar{y}} + \tau_{xz} &= 0, \\ -\varepsilon_x \tau_{xy} \frac{\partial \bar{z}_S}{\partial \bar{x}} + \varepsilon_y (-\sigma_y + \cotan \alpha \bar{p}) \frac{\partial \bar{z}_S}{\partial \bar{y}} + \tau_{yz} &= 0, \\ -\varepsilon_x \tau_{xz} \frac{\partial \bar{z}_S}{\partial \bar{x}} - \varepsilon_y \tau_{yz} \frac{\partial \bar{z}_S}{\partial \bar{y}} + (-\sigma_z + \cotan \alpha \bar{p}) &= 0, \\ \bar{\kappa}(\theta) \left[\frac{\partial \theta}{\partial \bar{z}} - \varepsilon_x^2 \frac{\partial \theta}{\partial \bar{x}} \frac{\partial \bar{z}_S}{\partial \bar{x}} - \varepsilon_y^2 \frac{\partial \theta}{\partial \bar{y}} \frac{\partial \bar{z}_S}{\partial \bar{y}} \right] &= -\mathbb{N}_S \bar{h}_S (\theta - \theta_A) \mathbb{N}_S, \end{aligned} \quad (12.20)$$

in which \mathbb{N}_S is the *free surface NUSSELT number*,⁶

⁶For a biographical sketch of NUSSELT, see Fig. 12.5.



Fig. 12.5 ERNST KRAFT WILHELM NUSSULT (25. Nov. 1882–1. Sept. 1957)

ERNST KRAFT WILHELM NUSSULT was a German mechanical engineer with specialization in thermodynamics. He studied at the University Berlin Charlottenburg and the Technische Hochschule (TH) in Munich. He received his habilitation degree in 1909 and the titular professorship of the TH Dresden in 1915. After some years of practical engineering work, he was called as full professor of Theoretical Machine Design at the TH Karlsruhe (1920–1925). From 1925–1952, he held the position of Head and Professor of the ‘Institute of Theoretical Machine Design’ and the ‘Laboratory of Heat Engines’ at the TH Munich.

WILHELM NUSSULT was an internationally recognized researcher and teacher of great esteem. His and his pupils’ publications were primarily devoted to specialties of technical thermodynamics. In his famous early paper ‘Das Grundgesetz des Wärmeübergangs’ (The fundamental law of heat transfer) in 1915 he laid the theoretical basis of this law, now summarized by the dimensionless NUSSULT number (12.21). The Universities of Danzig (now Gdańsk, Poland) and Dresden honored him with honorary doctorates and in 1953 he became a Member of the Bavarian Academy of Sciences.

Text and photo based on: https://www.mach.kit.edu/wilhelm_nusselt.php

$$\mathbb{N}_S := \frac{h_S^{\text{ref}} [H]}{\kappa(T_R)}, \quad \text{with } h_S = h_S^{\text{ref}} \bar{h}_S \quad (12.21)$$

and

$$N_S = \left[1 + \varepsilon_x^2 \left(\frac{\partial \bar{z}_S}{\partial \bar{x}} \right)^2 + \varepsilon_y^2 \left(\frac{\partial \bar{z}_S}{\partial \bar{y}} \right)^2 \right]^{1/2} .$$

Equation (12.20)₁ is the dimensionless version of the kinematic surface equation; it is form-invariant under the applied scalings. The next three equations are the boundary conditions of stress expressing continuity of shear and normal tractions, and the last equation expresses the heat transfer from the body to the environment. The limits $\mathbb{N}_S \rightarrow \infty$ and $\mathbb{N}_S \rightarrow 0$ imply prescribed surface temperature and vanishing heat flow, respectively.

The derivation of the *basal boundary conditions* is more involved. With the definition (12.8) and the scalings

$$(\mathbf{t}_S, \mathbf{t}_n) = \rho g[H] \sin \alpha (\bar{\mathbf{t}}_S, \bar{\mathbf{t}}_n) \quad (12.22)$$

one can readily show that at $\bar{z} = \bar{z}_B(\bar{x}, \bar{y})$

$$\begin{aligned} \bar{t}_{S_x} &= -\frac{1}{N_B} \left[\tau_{xz} + \varepsilon_x \frac{\partial \bar{z}_B}{\partial \bar{x}} (-\sigma_x + \cotan \alpha \bar{p}) - \varepsilon_y \frac{\partial \bar{z}_B}{\partial \bar{y}} \tau_{xy} \right] \\ &\quad + \frac{1}{N_B^3} \left[\varepsilon_x \frac{\partial \bar{z}_B}{\partial \bar{x}} (-\sigma_z + \cotan \alpha \bar{p}) + \mathcal{O}(\varepsilon_x^2, \varepsilon_x \varepsilon_y, \dots) \right], \\ \bar{t}_{S_y} &= -\frac{1}{N_B} \left[\tau_{yz} - \varepsilon_x \frac{\partial \bar{z}_B}{\partial \bar{x}} \tau_{xy} + \varepsilon_y \frac{\partial \bar{z}_B}{\partial \bar{y}} (-\sigma_y + \cotan \alpha \bar{p}) \right] \\ &\quad + \frac{1}{N_B^3} \left[\varepsilon_y \frac{\partial \bar{z}_B}{\partial \bar{y}} (-\sigma_z + \cotan \alpha \bar{p}) + \mathcal{O}(\varepsilon_y^2, \varepsilon_x \varepsilon_y, \dots) \right], \\ \bar{t}_{S_z} &= -\frac{1}{N_B} \left[(\sigma_z - \cotan \alpha \bar{p}) - \varepsilon_x \frac{\partial \bar{z}_B}{\partial \bar{x}} \tau_{xz} - \varepsilon_y \frac{\partial \bar{z}_B}{\partial \bar{y}} \tau_{yz} \right] \\ &\quad + \frac{1}{N_B^3} \left[(\sigma_z - \cotan \alpha \bar{p}) - 2\varepsilon_x \frac{\partial \bar{z}_B}{\partial \bar{x}} \tau_{xz} - 2\varepsilon_y \frac{\partial \bar{z}_B}{\partial \bar{y}} \tau_{yz} \right. \\ &\quad \left. + \mathcal{O}(\varepsilon_x^2, \varepsilon_y^2, \varepsilon_x \varepsilon_y, \dots) \right], \end{aligned} \quad (12.23)$$

with

$$N_B = \left[1 + \varepsilon_x^2 \left(\frac{\partial \bar{z}_B}{\partial \bar{x}} \right)^2 + \varepsilon_y^2 \left(\frac{\partial \bar{z}_B}{\partial \bar{y}} \right)^2 \right]^{1/2},$$

in which \mathcal{O} is the order symbol and the dots indicate higher order terms. The terms in the second lines of each of (12.23) comprise the x -, y - and z -components of \mathbf{t}_n . The explicit derivation of (12.23) from Eq. (12.8) is somewhat involved, but it is not difficult. Defining

$$\mathcal{F} := \frac{\Phi \left((\rho g[H] \sin \alpha)^2 |\bar{\mathbf{t}}_S|^2, (\rho g[H] \sin \alpha)^2 |\bar{\mathbf{t}}_n|^2 \right)}{\Phi \left((\rho g[H] \sin \alpha)^2 \cdot 1, (\rho g[H] \sin \alpha)^2 \cdot 1 \right)} \quad (12.24)$$

and using the scales (12.10) and (12.22), straightforward manipulations with (12.9) yield the dimensionless sliding law in the form

$$\begin{aligned} \bar{u}_B &= -\mathcal{CF} \left(|\bar{\mathbf{t}}_S|^2, |\bar{\mathbf{t}}_n|^2 \right) \bar{t}_{S_x}, & \text{at } \bar{z} = \bar{z}_B(\bar{x}, \bar{y}), \\ \eta \bar{v}_B &= -\mathcal{CF} \left(|\bar{\mathbf{t}}_S|^2, |\bar{\mathbf{t}}_n|^2 \right) \bar{t}_{S_y}, \end{aligned} \quad (12.25)$$

in which

$$\mathcal{C} := \frac{c \Phi(c^2, c^2)}{[U]}, \quad c := \rho g [H] \sin \alpha. \quad (12.26)$$

The third velocity component at the base follows from the tangency condition $\mathbf{v}_B \cdot \mathbf{n}_B = 0$ and reads in dimensionless form

$$\bar{w}_B = \bar{u}_B \frac{\partial \bar{z}_B}{\partial \bar{x}} + \bar{v}_B \frac{\partial \bar{z}_B}{\partial \bar{y}}. \quad (12.27)$$

Moreover, the thermal boundary condition (12.7)₂ becomes

$$\bar{\kappa}(\theta) \left[\frac{\partial \theta}{\partial \bar{z}} - \varepsilon_x^2 \frac{\partial \theta}{\partial \bar{x}} \frac{\partial \bar{z}_B}{\partial \bar{x}} - \varepsilon_y^2 \frac{\partial \theta}{\partial \bar{y}} \frac{\partial \bar{z}_B}{\partial \bar{y}} \right] = \mathbb{N}_B h_B (\theta - \theta_B) N_B, \quad \text{at } \bar{z} = \bar{z}_B(\bar{x}, \bar{y}), \quad (12.28)$$

in which

$$\mathbb{N}_B := \frac{h_B^{\text{ref}} [H]}{\kappa(T_R)}, \quad \text{with } h_B = h_B^{\text{ref}} \bar{h}_B \quad (12.29)$$

is the *basal NUSSELT number* and N_B is defined immediately below (12.23). Again the limits $\mathbb{N}_B \rightarrow \infty$ and $\mathbb{N}_B \rightarrow 0$ incorporate the cases of prescribed temperature and vanishing heat flow.

The transformation of the boundary value problem to dimensionless form is now complete. However, it is convenient to complement the above equations by the **depth integrated continuity equation**. From (12.14)₁ we may deduce

$$\int_{\bar{z}_B}^{\bar{z}_S} \left(\frac{\partial \bar{u}}{\partial \bar{x}} + \frac{\partial \bar{v}}{\partial \bar{y}} \right) d\bar{z} + \bar{w}_{\bar{z}_S} - \bar{w}_{\bar{z}_B} = 0,$$

or, when using in the integral term on the left-hand side the LEIBNIZ rule,

$$\begin{aligned} & \underbrace{\frac{\partial}{\partial \bar{x}} \int_{\bar{z}_B}^{\bar{z}_S} \bar{u}(\bar{x}, \bar{y}, \bar{z}, \bar{t}) d\bar{z}}_{Q_{\bar{x}}} + \underbrace{\frac{\partial}{\partial \bar{y}} \int_{\bar{z}_B}^{\bar{z}_S} \bar{v}(\bar{x}, \bar{y}, \bar{z}, \bar{t}) d\bar{z}}_{Q_{\bar{y}}} \\ & - \underbrace{\left(\frac{\partial \bar{z}_S}{\partial \bar{x}} \bar{u}_{\bar{z}_S} + \frac{\partial \bar{z}_S}{\partial \bar{y}} \bar{v}_{\bar{z}_S} - w_{\bar{z}_S} \right)}_{-\frac{\partial \bar{z}_S}{\partial \bar{t}} + N_S \bar{a}(\bar{x}, \bar{y}, \bar{z}_S, \bar{t})} + \underbrace{\left(\frac{\partial \bar{z}_B}{\partial \bar{x}} \bar{u}_{\bar{z}_B} + \frac{\partial \bar{z}_B}{\partial \bar{y}} \bar{v}_{\bar{z}_B} - \bar{w}_{\bar{z}} \right)}_{=0 \text{ [for } \bar{z}=\bar{z}_B(\bar{x}, \bar{y})]} = 0, \end{aligned} \quad (12.30)$$

so that

$$\frac{\partial \bar{z}_S}{\partial \bar{t}} + \frac{\partial Q_{\bar{x}}}{\partial \bar{x}} + \frac{\partial Q_{\bar{y}}}{\partial \bar{y}} = N_S \bar{a} \quad (12.31)$$

with

$$Q_{\bar{x}} := \int_{\bar{z}_B}^{\bar{z}_S} \bar{u}(\bar{x}, \bar{y}, \bar{z}, \bar{t}) d\bar{z}, \quad Q_{\bar{y}} := \int_{\bar{z}_B}^{\bar{z}_S} \bar{v}(\bar{x}, \bar{y}, \bar{z}, \bar{t}) d\bar{z}, \quad (12.32)$$

which are the **volume fluxes** in the \bar{x} - and \bar{y} -directions, respectively.

Equations (12.14), (12.20), (12.25) and (12.28) constitute the boundary value problem in dimensionless form. It involves several dimensionless parameters; $\mathbb{G} \gg 1$ is large, and in view of the fact that we expect $[L_x] \gg [H]$, $[L_y] \gg [H]$, but $[L_y] \leq [L_x]$, one has $\varepsilon_x \ll 1$ and $\varepsilon_y \ll 1$, but $\eta \leq \mathcal{O}(1)$. Moreover, since α is small (5° – 20°), $\tan \alpha \ll 1$, but $\cotan \alpha$ is large.

Clearly, various distinguished limits can be analyzed, but here we assume that the downhill motion causes a dimensionless shear stretching of order unity. Because A and F have been scaled such that \bar{A} and \bar{f} are order unity quantities, Eq. (12.14)₁₀ then requires that $\mathbb{G} = \mathcal{O}(\varepsilon_x^{-1})$, for otherwise the order unity left-hand side of (12.14)₁₀ would not be balanced by an order unity right-hand side. Since \mathbb{G} is large, this implies small ε_x , but the value of ε_x defines also, over which lengths an order unity dimensionless stress causes an order unity dimensionless stretching. Analogously, Eq. (12.14)₁₁ implies $\mathbb{G} = \mathcal{O}(\varepsilon_y^{-1})$, so that $\varepsilon_x \approx \varepsilon_y$.⁷ In reality, see Fig. 12.3, it is expected that $\varepsilon_x \leq \varepsilon_y$, and in fact, we will assume so; more specifically, it is required that $\varepsilon_x \cotan \alpha$ is small, perhaps of order ε_y , while $\varepsilon_y \cotan \alpha$ and $\varepsilon_x/\varepsilon_y = \eta$ are $\mathcal{O}(1)$. This essentially delimits application of subsequent developments to flow situations of Fig. 12.3a. This means physically that the *flow is primarily downhill*. The inclination angle must clearly be bounded away from zero. We shall see that this scaling makes approximate equations applicable e.g. to mountainous glacier flows and creeping landslides down mountain slopes. Furthermore, for STOKES flow ($\hat{\mu}^2 \rightarrow 0$), the momentum Eq. (12.14)_{2,3,4} reduce to force balances: in the downhill direction the shear stresses are, to lowest order, balanced by the gravity force component in that direction.⁸ The z -momentum equation reduces to the hydrostatic pressure equation. In the y -direction, however, shear stresses should be balanced by the transverse \bar{y} -pressure gradients for otherwise τ_{yz} would identically vanish in view of the boundary condition (12.20)₃. This would then contradict with the fact that a sidewise shear stretching is possible. Thus, in order to balance in equation (12.14)₃ the vertical shear stress gradient $\partial \tau_{yz} / \partial \bar{z}$ with the pressure gradient, one must necessarily have $\varepsilon_y \cotan \alpha = \mathcal{O}(1)$.

⁷If we would assume \mathbb{G} to be $\mathcal{O}(1)$, whilst $\varepsilon_x, \varepsilon_y$ are small, Eq. (12.14)_{10,11} would to lowest order request that the horizontal velocity components would be independent of the z -variable (plug flow), which for any shearing deformation must be unrealistic.

⁸Strictly this assumes that $\tan \alpha (\partial \sigma_z) / (\partial \bar{z})$ is small as compared to unity, see (12.14)₄, which shall be assumed.

12.4 Lowest Order Model Equations for Flow Down Steep Slopes (Strong Steep Slope Shallow Flow Approximation)

The purpose of the non-dimensionalization of the model equations in Sect. 12.2 has been to obtain field equations and boundary conditions in which the independent variables and their space and time derivatives are pure numbers with order of magnitude equal to unity; these are possibly pre-multiplied with dimensionless quantities of which the numerical values are dictated by the scalings and material quantities (coefficients). These can have values from very small to very large and may then suggest procedures of approximation e.g. by dropping terms that are thought to be of negligible influence. This was done in Chap. 7 in an ad-hoc manner. Here, with the employed scaling and the non-dimensionalization of the boundary value problem, the procedure is more rational and, thus guarantees, since small parameters are present, that systematic simplifications can be implemented. The discussion in the last paragraph of Sect. 12.3 suggests that the following distinguished limit should be studied:

$$\begin{aligned}
 \hat{\mathbb{F}} &\rightarrow 0, && \text{STOKES approximation,} \\
 \mathbb{G} &= \mathcal{O}(\varepsilon_x^{-1}), \\
 \varepsilon_x \cotan \alpha &= \phi \varepsilon_y, && \phi \text{ finite, bounded away from zero,} \\
 \varepsilon_y \cotan \alpha &= \psi, && \psi \text{ finite, bounded away from zero,} \\
 \eta &= \frac{\varepsilon_x}{\varepsilon_y} = \text{finite,} && \text{finite, bounded away from zero.}
 \end{aligned} \tag{12.33}$$

All other dimensionless quantities are regarded as finite. With (12.33), the boundary value problem (12.14), (12.20), (12.25), (12.28) can be expressed as operator equations involving the small parameters $\varepsilon_x, \varepsilon_y$ in terms of which perturbation solutions can be sought. Here we are less ambitious and only deal with the lowest order approximation, $\varepsilon_x \rightarrow 0, \varepsilon_y \rightarrow 0$. The constitutive relations (12.14)_{6–11} then imply (bars, characterizing dimensionless quantities, will henceforth be omitted):

$$\begin{aligned}
 \sigma_x &= \sigma_y = \sigma_z = \tau_{xy} = 0, \\
 \frac{\partial u}{\partial z} &= 2A(\theta)\mathbb{f}(\tau_{II})\tau_{xz}, && \text{in } \mathcal{D}, \\
 \frac{\partial v}{\partial z} &= \frac{1}{\eta}2A(\theta)\mathbb{f}(\tau_{II})\tau_{yz},
 \end{aligned} \tag{12.34}$$

in which

$$\tau_{II} = \tau_{xz}^2 + \tau_{yz}^2. \tag{12.35}$$

The momentum equations reduce to

$$\begin{aligned}
 \frac{\partial \tau_{xz}}{\partial z} + 1 &= 0, \\
 -\psi \frac{\partial p}{\partial y} + \frac{\partial \tau_{yz}}{\partial z} &= 0, && \text{in } \mathcal{D}, \\
 \frac{\partial p}{\partial z} + 1 &= 0,
 \end{aligned} \tag{12.36}$$

and the mechanical boundary conditions of stress on the free surface, (12.20), become

$$\tau_{xz} = 0, \quad \tau_{yz} = 0, \quad p = 0, \quad \text{on } \partial\mathcal{D}_S, \quad (12.37)$$

whereas on the immobile basal surface, (12.25) and (12.27) remain unchanged,

$$\begin{aligned} u_B &= \mathcal{CF}(\cdot, \cdot)\tau_{xz}, \\ \eta v_B &= \mathcal{CF}(\cdot, \cdot)\tau_{yz}, \quad \text{on } \partial\mathcal{D}_B, \\ w_B &= u_B \frac{\partial z_B}{\partial x} + v_B \frac{\partial z_B}{\partial y}, \end{aligned} \quad (12.38)$$

except that \mathcal{F} is now given by

$$\mathcal{F} = \mathcal{F} \left((\tau_{xz}^2 + \tau_{yz}^2), \left(\cotan^2(\alpha) p^2 + \psi^2 p^2 \left(\frac{\partial z_B}{\partial y} \right)^2 \right) \right). \quad (12.39)$$

The thermal equations will later be dealt with. Equation (12.36) subject to the boundary conditions (12.37) can be integrated and the results be substituted into (12.34)_{2,3}. For a known temperature field the emerging equations for u and v can then be integrated subject to the boundary conditions (12.38). This process yields

$$\begin{aligned} \tau_{xz}(x, y, z, t) &= (z_S(x, y, t) - z), \\ \tau_{yz}(x, y, z, t) &= -\psi \frac{\partial z_S(x, y, t)}{\partial y} (z_S(x, y, t) - z), \\ p(x, y, z, t) &= (z_S(x, y, t) - z), \end{aligned} \quad (12.40)$$

and

$$\begin{aligned} u(x, y, z, t) &= \mathcal{CF}(\cdot, \cdot) (z_S(x, y, t) - z_B(x, y)) \\ &\quad + 2 \int_{z_B}^z A(\theta(x, y, z, t)) \mathbb{f}(\tau_{II}(x, y, \zeta, t)) \cdot (z_S(x, y, t) - \zeta) d\zeta, \end{aligned} \quad (12.41)$$

$$\begin{aligned} v(x, y, z, t) &= -\mathcal{CF}(\cdot, \cdot) \frac{\psi}{\eta} \frac{\partial z_S(x, y, t)}{\partial y} (z_S(x, y, t) - z_B(x, y)) \\ &\quad - \frac{2\psi}{\eta} \frac{\partial z_S(x, y, t)}{\partial y} \int_{z_B}^z A(\theta(x, y, z, t)) \mathbb{f}(\tau_{II}(x, y, \zeta, t)) \\ &\quad \cdot (z_S(x, y, t) - \zeta) d\zeta, \end{aligned}$$

in which

$$\begin{aligned} \tau_{II}(x, y, z, t) &= \left(1 + \psi^2 \left(\frac{\partial z_S(x, y, t)}{\partial y}\right)^2\right) (z_S(x, y, t) - z)^2, \\ \mathcal{F}(\cdot, \cdot) &= \mathcal{F} \left\{ (z_S(x, y, t) - z_B(x, y))^2 \left(1 + \psi^2 \left(\frac{\partial z_S(x, y, t)}{\partial y}\right)^2\right), \right. \\ &\quad \left. (z_S(x, y, t) - z_B(x, y))^2 \left(\cotan^2(\alpha) + \psi^2 \left(\frac{\partial z_B}{\partial y}\right)^2\right) \right\}. \end{aligned} \quad (12.42)$$

Finally, once u and v are determined from (12.41), w can be determined by depth integrating the continuity equation from $\zeta = z_B$ to $\zeta = z$; with the aid of (12.38)₃ this yields

$$w = u_B \frac{\partial z_B}{\partial x} + v_B \frac{\partial z_B}{\partial y} - \int_{z_B}^z \left(\frac{\partial u}{\partial x}(x, y, \zeta) + \frac{\partial v}{\partial y}(x, y, \zeta) \right) d\zeta, \quad (12.43)$$

or with (12.41) in which $z = z_B$,

$$\begin{aligned} w(x, y, z, t) &= \mathcal{C}\mathcal{F}(\cdot, \cdot) (z_S(x, y, t) - z_B(x, y)) \\ &\quad \times \left[\frac{\partial z_B(x, y)}{\partial x} - \frac{\psi}{\eta} \cdot \frac{\partial z_S(x, y, t)}{\partial y} \frac{z_B(x, y)}{\partial y} \right] \\ &\quad - \int_{z_B}^z \left(\frac{\partial u(x, y, \zeta, t)}{\partial x} + \frac{\partial v(x, y, \zeta, t)}{\partial y} \right) d\zeta, \end{aligned} \quad (12.44)$$

in which u and v are to be substituted from (12.41). As would be expected, w (in physical dimensions) is small.

It is appropriate here to pause and to review what has been achieved. For given geometry, Eq. (12.40) permit evaluation of the dimensionless stresses. Accordingly, the ‘downhill’ shear stress and the overburden pressure are simply given by the overburden depth. Because the latter is always positive, τ_{xz} cannot change signs. Alternatively, τ_{yz} , the cross-slope shear stress, is proportional to the product of overburden depth and surface gradient, $\partial z_S/\partial y$, which may be positive or negative. This suggests that $u > 0$, whereas $v \geq 0$ depending on whether $\partial z_S/\partial y \leq 0$. Because $\mathcal{F} \geq 0$, $A > 0$ and $\mathbb{f} \geq 0$ for all arguments, these properties are readily corroborated with the aid of (12.41). A fortiori, (12.41)₂ implies that $v = 0$ whenever $\partial z_S/\partial y = 0$. Because this last equation defines the ‘ridge’, it follows that along the ridge the flow is in the x -direction at all depths. Moreover, from (12.41) we deduce

$$\frac{v}{u} = -\frac{\psi}{\eta} \frac{\partial z_S(x, y, t)}{\partial y}, \quad (12.45)$$

independent of z and z_B . Therefore, for fixed x and y the in-plane velocity vector does not rotate as one moves downward parallel to the z -axis.⁹ To obtain a complete picture of the velocity field in the (x, y) -plane, it suffices to construct vector plots of the surface velocities (u, v) or associated streamlines and profiles of speed for fixed x and y .

Note also that determination of all fields in Eqs.(12.40)–(12.42) and (12.44) requires knowledge of the phenomenological functions \mathcal{F} , A , \mathbb{f} and \mathcal{C} , as well as the temperature distribution as functions of space and time. Moreover, the surface geometry must also be known. Given this information the stresses τ_{xz} , τ_{yz} , the pressure p and velocity components u, v, w can be determined by only using quadratures in the z -direction. Thus, for the solution of the complete problem the heat equation and the kinematic wave equation must be solved along with (12.40)–(12.42). To lowest order in ε_x and ε_y the temperature boundary value problem (12.14)₅, (12.20)₅ and (12.28) reduces to the boundary value problem

$$\begin{aligned} c(\theta) \left(\frac{\partial \theta}{\partial t} + \frac{\partial \theta}{\partial x} u + \frac{\partial \theta}{\partial y} v + \frac{\partial \theta}{\partial z} w \right) & \quad \text{in } \mathcal{D}, \\ = \mathbb{D} \frac{\partial}{\partial z} \left(\kappa(\theta) \frac{\partial \theta}{\partial z} \right) + 2\mathbb{E}GA(\theta)\mathbb{f}(\tau_{II})\tau_{II}, & \quad (12.46) \end{aligned}$$

$$\kappa(\theta) \frac{\partial \theta}{\partial z} = -N_S h_S (\theta - \theta_A), \quad \text{on } \partial \mathcal{D}_S, \quad (12.47)$$

$$\kappa(\theta) \frac{\partial \theta}{\partial z} = N_S h_S (\theta - \theta_B), \quad \text{on } \partial \mathcal{D}_B$$

subject to the initial condition

$$\theta(x, y, z, 0) = \theta_0(x, y, z) \quad \text{in } \mathcal{D}. \quad (12.48)$$

On the other hand, the evolution equation for the free surface (12.31) can with (12.45) be given in the form

⁹In field campaigns of glacier or soil flows, vertical bore holes are equipped with inclinometers at various depths with the aid of which the velocity profiles can be determined. In such measurements it is possible to verify whether all inclinometers lie indeed in a vertical plane. If this is not the case, one reason could be that the basal sliding law is not isotropic. In that case (12.9) and (12.25) would have to be changed.

$$\begin{aligned} \frac{\partial z_S}{\partial t} + \frac{\partial Q_x}{\partial x} - \frac{\psi}{\eta} \frac{\partial}{\partial y} \left(\frac{\partial z_S}{\partial y} Q_x \right) &= a(x, y, z_S, t), \quad \text{in } PD, \\ Q_x &= \mathcal{CF}(\cdot) (z_S - z_B)^2 \\ &+ 2 \int_{z_B}^{z_S} A(\theta(x, y, \zeta, t)) \cdot \mathbb{f}(\tau_{II}(x, y, \zeta, t)) (z_S(x, y, t) - \zeta)^2 d\zeta \end{aligned} \quad (12.49)$$

to be solved in the projection onto the (x, y) -plane, PD of \mathcal{D} , and subject to the boundary condition $z_S = z_B$ along the grounding line $\partial\mathcal{D}_S \cap \partial\mathcal{D}_B$. Equation (12.46) is an unsteady advection-diffusion-reaction equation for temperature in a three dimensional domain. Analogously, because the third term on the left of (12.49)₁ depends explicitly on $\partial z_S/\partial y$, but also because \mathcal{F} and \mathbb{f} contain it implicitly (compare (12.42)), Eq. (12.46) is a forced advection-diffusion equation in the two-dimensional domain PD . In view of (12.49)₂ one has

$$Q_x = \tilde{Q} \left(z_S, \frac{\partial z_S}{\partial y}, \cdot \right),$$

so that (12.49)₁ may be written as

$$\begin{aligned} \frac{\partial z_S}{\partial t} + \frac{\partial \tilde{Q}}{\partial z_S} \left[\frac{\partial z_S}{\partial x} - \frac{\psi}{\eta} \left(\frac{\partial z_S}{\partial y} \right)^2 \right] + \frac{\partial \tilde{Q}}{\partial(\partial z_S/\partial y)} \frac{\partial^2 z_S}{\partial x \partial y} \\ + \left\{ -\frac{\psi}{\eta} \left[\tilde{Q} + \frac{\partial \tilde{Q}}{\partial(\partial z_S/\partial y)} \frac{\partial z_S}{\partial y} \right] \right\} \frac{\partial^2 z_S}{\partial y^2} = a(x, y, z_S, t), \end{aligned} \quad (12.50)$$

from which it is now seen that the surface elevation equation is parabolic and quasi-linear. However, it is also singular at the grounding line, because for $z_S = z_B$, $\tilde{Q} = 0$, $\partial \tilde{Q}/\partial z_S = 0$, $\partial \tilde{Q}/\partial(\partial z_S/\partial y) = 0$, for the proof of which (12.49)₂ and (12.42) are used. Furthermore,

$$\begin{aligned} \frac{\partial \tilde{Q}}{\partial(\partial z_S/\partial y)} &= 2\mathcal{C}\psi^2 (z_S - z_B)^4 \mathcal{F}'(\cdot) \frac{\partial z_S}{\partial y} \\ &+ 4\psi \frac{\partial z_S}{\partial y} \int_{z_B}^{z_S} A(\theta) \mathbb{f}'(\tau_{II}(x, y, \zeta, t)) (z_S - \zeta)^4 d\zeta, \end{aligned}$$

in which $\mathbb{f}'(\xi) := d\mathbb{f}(\xi)/d\xi$ and $\mathcal{F}'(\xi, \cdot) = \partial\mathcal{F}(\xi, \cdot)/\partial\xi$. Any physically reasonable constitutive relations and sliding laws have $\mathbb{f}' > 0$ and $\mathcal{F}' > 0$, so that

$$\frac{\partial \tilde{Q}}{\partial(\partial z_S/\partial y)} > 0 \iff \frac{\partial z_S}{\partial y} > 0 \iff v > 0, \quad \frac{\partial \tilde{Q}}{\partial z_S} > 0, \quad \text{if } z_S > z_B. \quad (12.51)$$

Thus, the term in braces in (12.50) is always negative, which verifies the positive diffusive nature of the equation for both steady and non-steady flows and demonstrates the invariance of Eq. (12.50) to the sign of $\partial z_S/\partial y$ as would be expected.

12.5 A Slightly More General Steep Slope Shallow Flow Approximation (Weak Steep Slope Shallow Flow Approximation)

It was demonstrated earlier that the preceding scaling analysis does not apply to situations of panels b and c in Fig. 12.3. Whereas the situation of Fig. 12.3b needs to be treated quite differently (see the subsequent section), that of Fig. 12.3c can relatively easily be included. However, it requires a different ordering of equations, namely $\varepsilon_x \approx \varepsilon_y$ as well as

$$\varepsilon_x \cotan \alpha = \psi_x \approx \varepsilon_y \cotan \alpha = \psi_y = \mathcal{O}(1), \quad (12.52)$$

All other order of magnitude relations remain valid. With (12.52), Eq. (12.14)_{2,3,4} appear now in the forms

$$\begin{aligned} -\psi_x \frac{\partial \bar{p}}{\partial \bar{x}} + \frac{\partial \tau_{xz}}{\partial \bar{z}} + 1 &= 0, \\ -\psi_y \frac{\partial \bar{p}}{\partial \bar{y}} + \frac{\partial \tau_{yz}}{\partial \bar{z}} &= 0, \\ \frac{\partial \bar{p}}{\partial \bar{z}} - 1 &= 0. \end{aligned} \quad (12.53)$$

Integrating these equations, subject to the boundary conditions $\bar{p}(\cdot, \bar{z}_S) = \tau_{xz}(\cdot, \bar{z}_S) = \tau_{yz}(\cdot, \bar{z}_S) = 0$ yields the stress distribution

$$\begin{aligned} \bar{p}(\bar{x}, \bar{y}, \bar{z}, \bar{t}) &= (\bar{z}_S(\bar{x}, \bar{y}, \bar{t}) - \bar{z}), \\ \tau_{xz}(\bar{x}, \bar{y}, \bar{z}, \bar{t}) &= \left(1 - \psi_x \frac{\partial \bar{z}_S(\bar{x}, \bar{y}, \bar{t})}{\partial \bar{x}} \right) (\bar{z}_S(\bar{x}, \bar{y}, \bar{t}) - \bar{z}), \\ \tau_{yz}(\bar{x}, \bar{y}, \bar{z}, \bar{t}) &= -\psi_y \frac{\partial \bar{z}_S(\bar{x}, \bar{y}, \bar{t})}{\partial \bar{y}} (\bar{z}_S(\bar{x}, \bar{y}, \bar{t}) - \bar{y}). \end{aligned} \quad (12.54)$$

Moreover, substituting these into (12.34)_{2,3} and integrating the emerging relations with respect to ζ from $\zeta = \bar{z}_B$ to $\zeta = \bar{z}$ and observing the basal boundary conditions (12.38) yields

$$\begin{aligned} \bar{u}(\bar{x}, \bar{y}, \bar{z}, \bar{t}) &= \mathcal{CF}(\cdot, \cdot) \left(1 - \psi_x \frac{\partial \bar{z}_S(\bar{x}, \bar{y}, \bar{t})}{\partial \bar{x}} \right) (\bar{z}_S(\bar{x}, \bar{y}, \bar{t}) - \bar{z}_B(\bar{x}, \bar{y})) \\ &\quad + 2 \left(1 - \psi_x \frac{\partial \bar{z}_S(\bar{x}, \bar{y}, \bar{t})}{\partial \bar{x}} \right) \mathcal{I}(\bar{z}, \bar{z}_S(\bar{x}, \bar{y}, \bar{t}), \bar{z}_B(\bar{x}, \bar{y})), \end{aligned} \quad (12.55)$$

$$\begin{aligned} \bar{v}(\bar{x}, \bar{y}, \bar{z}, \bar{t}) &= -\mathcal{CF}(\cdot, \cdot) \frac{\psi_y}{\eta} \frac{\partial \bar{z}_S(\bar{x}, \bar{y}, \bar{t})}{\partial \bar{y}} (\bar{z}_S(\bar{x}, \bar{y}, \bar{t}) - \bar{z}_B(\bar{x}, \bar{y})) \\ &\quad - 2 \frac{\psi_y}{\eta} \frac{\partial \bar{z}_S(\bar{x}, \bar{y}, \bar{t})}{\partial \bar{y}} \mathcal{I}(\bar{z}, \bar{z}_S(\bar{x}, \bar{y}, \bar{t}), \bar{z}_B(\bar{x}, \bar{y})), \end{aligned}$$

in which

$$\begin{aligned} \tau_{II}(\bar{x}, \bar{y}, \bar{z}, \bar{t}) &= \left[\left(1 - \psi_x \frac{\partial \bar{z}_S(\bar{x}, \bar{y}, \bar{t})}{\partial \bar{x}} \right)^2 + \psi_y^2 \left(\frac{\partial \bar{z}_S(\bar{x}, \bar{y}, \bar{t})}{\partial \bar{y}} \right)^2 \right] \\ &\quad \times (\bar{z}_S(\bar{x}, \bar{y}, \bar{t}) - \bar{z})^2, \\ \mathcal{F}(\cdot, \cdot) &= \mathcal{F} \left[(\bar{z}_S(\bar{x}, \bar{y}, \bar{t}) - \bar{z}_B(\bar{x}, \bar{y}))^2 \left(\left(1 - \psi_x \frac{\partial \bar{z}_S(\bar{x}, \bar{y}, \bar{t})}{\partial \bar{x}} \right)^2 \right. \right. \\ &\quad \left. \left. + \psi_y^2 \left(\frac{\partial \bar{z}_S(\bar{x}, \bar{y}, \bar{t})}{\partial \bar{y}} \right)^2 \right), (\bar{z}_S(\bar{x}, \bar{y}, \bar{t}) - \bar{z}_B(\bar{x}, \bar{y}))^2 \right. \\ &\quad \left. \times \left(\cotan^2 \alpha \times \psi_x^2 \left(\frac{\partial \bar{z}_B(\bar{x}, \bar{y})}{\partial \bar{x}} \right)^2 + \psi_y^2 \left(\frac{\partial \bar{z}_B(\bar{x}, \bar{y})}{\partial \bar{y}} \right)^2 \right) \right], \end{aligned} \quad (12.56)$$

$$\begin{aligned} \mathcal{I}(\bar{z}, \bar{z}_S(\bar{x}, \bar{y}, \bar{t}), \bar{z}_B(\bar{x}, \bar{y})) \\ = \int_{\bar{z}_B}^{\bar{z}} \bar{A}(\theta(\bar{x}, \bar{y}, \zeta, \bar{t})) \mathfrak{f}(\tau_{II}(\bar{x}, \bar{y}, \zeta, \bar{t})) (\bar{z}_S(\bar{x}, \bar{y}, \bar{t}) - \zeta) d\zeta. \end{aligned}$$

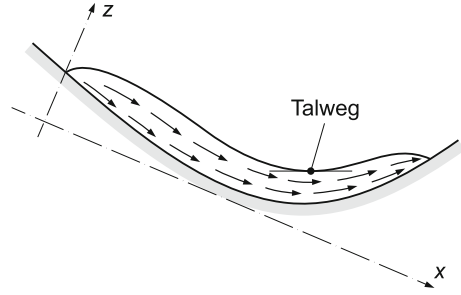
It follows, as before, that $v \geq 0$ depending on whether $\partial \bar{z}_S(\bar{x}, \bar{y}, \bar{t})/\partial \bar{y} \leq 0$, but \bar{u} is no longer strictly positive as before. In fact, the sign of \bar{u} depends on that of

$$\Psi := \left[1 - \psi_x \frac{\partial \bar{z}_S(\bar{x}, \bar{y}, \bar{t})}{\partial \bar{x}} \right]. \quad (12.57)$$

Over most part of the domain we have $\Psi > 0$, so $\bar{u} > 0$, in particular at the thalweg position, where the flow crosses from one valley side to the other, **Fig. 12.6** and the motion may proceed uphill on the other side of the valley. Only where

$$\psi_x \frac{\partial \bar{z}_S(\bar{x}, \bar{y}, \bar{t})}{\partial \bar{x}} > 1$$

Fig. 12.6 Flow near the thalweg position. The flow crosses from one valley side to the other and the motion may proceed uphill on the other side of the valley



a return flow does occur as shown on Fig. 12.3c (cross section $B-B$). Because in view of (12.55)

$$\frac{v}{u} = -\frac{\psi_y \partial \bar{z}_S / \partial \bar{y}}{\eta (1 - \psi_x \partial \bar{z}_S / \partial \bar{x})}, \quad (12.58)$$

which is independent of z , the in-plane velocity vector does not rotate with depth as before, and the kinematic surface equation becomes

$$\frac{\partial \bar{z}_S}{\partial \bar{t}} + \frac{\partial}{\partial \bar{x}} \left(\left(1 - \psi_x \frac{\partial \bar{z}_S}{\partial \bar{x}} \right) Q_x \right) - \frac{\psi_y}{\eta} \frac{\partial}{\partial \bar{y}} \left(Q_x \frac{\partial \bar{z}_S}{\partial \bar{y}} \right) = \bar{a}, \quad (12.59)$$

where Q_x is defined in (12.49)₂. Alternatively, since

$$Q_x = \tilde{Q}_x \left(\bar{z}_S, \frac{\partial \bar{z}_S}{\partial \bar{x}}, \frac{\partial \bar{z}_S}{\partial \bar{y}}, \cdot \right), \quad (12.60)$$

one has as evolution equation of \bar{z}_S

$$\begin{aligned} \frac{\partial \bar{z}_S}{\partial \bar{t}} + \left(1 - \psi_x \frac{\partial \bar{z}_S}{\partial \bar{x}} \right) \frac{\partial \tilde{Q}}{\partial \bar{z}_S} \frac{\partial \bar{z}_S}{\partial \bar{x}} - \frac{\psi_y}{\eta} \frac{\partial \tilde{Q}}{\partial \bar{z}_S} \left(\frac{\partial \bar{z}_S}{\partial \bar{y}} \right)^2 \\ - \left[- \left(1 - \psi_x \frac{\partial \bar{z}_S}{\partial \bar{x}} \right) \frac{\partial \tilde{Q}}{\partial (\partial \bar{z}_S / \partial \bar{x})} + \psi_x \tilde{Q} \right] \frac{\partial^2 \bar{z}_S}{\partial \bar{x}^2} \\ - \left[- \left(1 - \psi_x \frac{\partial \bar{z}_S}{\partial \bar{x}} \right) \frac{\partial \tilde{Q}}{\partial (\partial \bar{z}_S / \partial \bar{y})} + \frac{\psi_y}{\eta} \frac{\partial \tilde{Q}}{\partial (\partial \bar{z}_S / \partial \bar{x})} \frac{\partial \bar{z}}{\partial \bar{y}} \right] \frac{\partial^2 \bar{z}_S}{\partial \bar{x} \partial \bar{y}} \\ - \frac{\psi_y}{\eta} \left[\tilde{Q} + \frac{\partial \tilde{Q}}{\partial (\partial \bar{z}_S / \partial \bar{y})} \frac{\partial \bar{z}}{\partial \bar{y}} \right] \frac{\partial^2 \bar{z}_S}{\partial \bar{y}^2} = \bar{a}(\bar{x}, \bar{y}, \bar{z}_S, \bar{t}). \end{aligned} \quad (12.61)$$

This is a quasi-linear advection-diffusion-reaction equation. Its invariance to the sign of $\partial \bar{z}_S / \partial \bar{y}$ can be proven, but a demonstration of the positive diffusive nature has not been possible under all flow situations even though it is likely.

Because computations are only slightly more difficult with this scaling than the previous one they are best performed with this equation set.

12.6 Phenomenological Expressions for Creeping Glacier Ice

The model is completed by presenting explicit expressions for the functions $A(\theta)$, f (τ_{II}) and $\mathcal{F}(|t_S|^2, |t_n|^2)$. Typical of thermo-viscous bodies at elevated temperature is an ARRHENIUS-type rate factor¹⁰

¹⁰For a biographical sketch of SVANTE AUGUST ARRHENIUS, see **Fig. 12.7**. This might be the point where climatologically other significant work of SVANTE ARRHENIUS ought to be mentioned. This is justified in a chapter in which the dynamics of ice sheets, in particular their nutrition and wastage of mass and energy, is described by the accumulation of mass and the flow of heat through the free surface by radiation from the outer space. From a climatological point of view, ARRHENIUS was probably the first scientist to draw attention to the anthropogenic effect caused by the greenhouse gases. Indeed: ‘ARRHENIUS developed a theory to explain the ice ages, and in 1896, was the first scientist to attempt to calculate how changes in the levels of *carbon dioxide* in the atmosphere could alter the surface temperature through the *greenhouse effect*. He was influenced by the work of others, including JOSEPH FOURIER, JOHN TYNDALL or CLAUDE POUILLET. ARRHENIUS used the infrared observations of the moon by FRANK WASHINGTON VERY and SAMUEL PIERPONT LANGLEY at the Allegheny Observatory in Pittsburgh to calculate the absorption of infrared radiation by atmospheric CO_2 and water vapour. Using the STEFAN–BOLTZMANN law, he formulated his greenhouse law. In its original form, ARRHENIUS’ greenhouse law reads as follows:

if the quantity of carbonic acid [CO_2] increases in geometric progression, the augmentation of the temperature will increase nearly in arithmetic progression.

The following equivalent formulation of ARRHENIUS’ greenhouse law is still used today:

$$\Delta F = \alpha \ln(C/C_0).$$

Here C is carbon dioxide (CO_2) concentration measured in parts per million by volume (ppmv); C_0 denotes a baseline or unperturbed concentration of CO_2 , and ΔF is the radiative forcing, measured in watts per square meter. The constant α has been assigned a value between five and seven.

Based on information from his colleague ARVID HÖGBOM, ARRHENIUS was the first person to predict that emissions of carbon dioxide from the burning of fossil fuels and other combustion processes were large enough to cause global warming. In his calculation he included the feedback from changes in water vapor as well as latitudinal effects, but he omitted clouds, convection of heat upward in the atmosphere, and other essential factors. His work is currently seen less as an accurate prediction of global warming than as the first demonstration that it should be taken as a serious possibility.

ARRHENIUS’ absorption values for CO_2 and his conclusions met criticism by KNUT ANGSTRÖM in 1900, who published the first modern infrared spectrum of CO_2 with two absorption bands, and published experimental results that seemed to show that absorption of infrared radiation by the gas in the atmosphere was already “saturated” so that adding more could make no difference. ARRHENIUS replied strongly in 1901 (*Annalen der Physik*), dismissing the critique altogether. He touched the subject briefly in a technical book titled ‘*Lehrbuch der kosmischen Physik*’ (1903) (*Course book on cosmic physics*). He later wrote ‘*Världarnas utveckling*’ (1906) (English: ‘*Worlds in the Making*’ (1908)) directed at a general audience, where he suggested that the human emission of CO_2 would be strong enough to prevent the world from entering a new ice age, and that a warmer earth would be needed to feed the rapidly increasing population.’ Based on www.wikipedia.org.

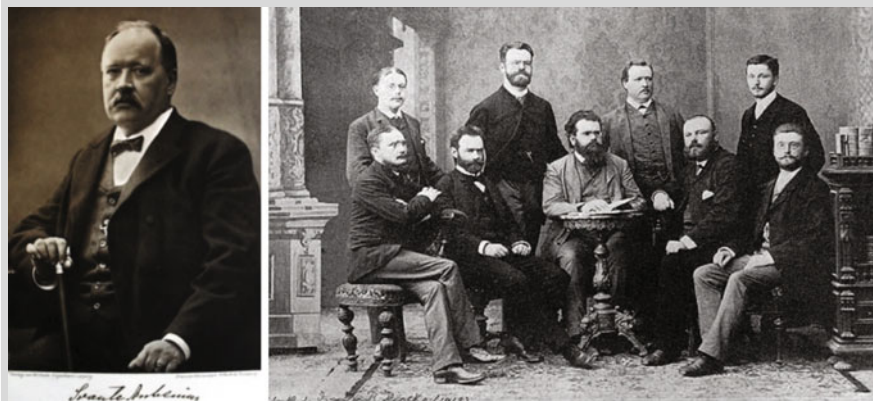


Fig. 12.7 SVANTE AUGUST ARRHENIUS (19. Feb. 1859–2. Oct. 1927) (*Right photo*) ARRHENIUS visiting BOLTZMANN in Graz 1887

SVANTE AUGUST ARRHENIUS was a Swedish scientist, originally a physicist, but often referred to as a chemist, and one of the founders of the science of physical chemistry. He received the NOBEL Prize for Chemistry in 1903, becoming the first Swedish NOBEL laureate, and in 1905 became director of the NOBEL Institute where he remained until his death.

ARRHENIUS was born at Vik, near Uppsala, Sweden [...]. At the age of three, ARRHENIUS taught himself to read without the encouragement of his parents, and by watching his father's addition of numbers in his account books, became an arithmetical prodigy. At age eight, he entered the local cathedral school, starting in the fifth grade, distinguishing himself in physics and mathematics, and graduating as the youngest and most able student in 1876.

He studied at the Physical Institute of the Swedish Academy of Sciences under the physicist ERIK EDLUND, working on the conductivities of electrolytes. In 1884, he submitted a 150-p dissertation on electrolytic conductivity to Uppsala for the doctorate and received only a fourth class degree, but upon his defense it was reclassified as third class. His main statement was that neither pure salts nor pure water are conductors, but solutions of salts in water are. Later, extensions of this very work would earn him the Nobel Prize in Chemistry. European scientists, such as RUDOLF CLAUSIUS, WILHELM OSTWALD, and J.H. VAN'T HOFF, were far more impressed.

ARRHENIUS received a travel grant from the Swedish Academy of Sciences, which enabled him to study with OSTWALD in Riga (Latvia), with FRIEDRICH KOHLRAUSCH in Würzburg, Germany, with LUDWIG BOLTZMANN in Graz, Austria, and with VAN'T HOFF in Amsterdam.

In 1889 he explained the fact that most reactions require added heat energy to proceed by formulating the concept of *activation energy*, an energy barrier that must be overcome before two molecules will react.

In 1891 he became a lecturer at the Stockholm University College, being promoted to professor of physics in 1895, and rector in 1896. In 1900, ARRHENIUS aided in setting up the NOBEL Institutes and the NOBEL Prizes. For the rest of his life, he was a member of the Nobel Committee on Physics and a de facto member of the Nobel Committee on Chemistry [...]. In 1901 he was elected to the Swedish Academy of Sciences. He became a Fellow of the Royal Society, London, in 1910 and [...] in 1911 he was elected a Foreign Honorary Member of the American Academy of Arts and Sciences [...].

The text is based on www.wikipedia.org

$$A(T) = A_0 \exp\left(-\frac{Q}{kT}\right), \quad (12.62)$$

where Q is what is called the *activation energy*, k is the BOLTZMANN constant and A_0 is a constant. Formula (12.62) follows from rate process theory and describes the dependence of the viscosity upon the temperature. However, for processes close to a phase transition (say melting for cold glacier ice) ARRHENIUS relations are known to be inaccurate. Exponential curve fitting may be advantageous in this case. Thus, we have either the ARRHENIUS relation

$$A(\theta) = \exp(\mathbb{A}\hat{\theta}), \quad \hat{\theta} = \frac{1}{1 + \mathbb{Z}\theta}, \quad (12.63)$$

$$\mathbb{A} = \frac{Q}{kT_R}, \quad \mathbb{Z} = \frac{[\Delta T]}{T_R},$$

in which Q is the activation energy measured in electron volts [eV], k is BOLTZMANN's constant ($k = 1.3806488 \times 10^{-23}$ [J K⁻¹]) and T_R is the reference temperature, measured in degrees Kelvin. An alternative parameterization, not related to the ARRHENIUS relation, and also appropriate for ice close to the melting point e.g. for $263 \text{ K} < T < 273.15 \text{ K}$ is

$$A(\theta) = a \exp(\alpha\theta) + b \exp(\beta\theta), \quad (12.64)$$

in which a , b and α , β are constants which can be determined from creep experiments at various different temperatures. GEORGE SMITH and LESLIE W. MORLAND [63] have analyzed ice creep data and obtain with the choices $T_R = 273.15 \text{ K}$ and $[\Delta T] = 20 \text{ K}$

$$\begin{aligned} a &= 0.7242, & \alpha &= 11.9567, \\ b &= 0.3438, & \beta &= 2.9494. \end{aligned} \quad (12.65)$$

The dimensionless creep response function \mathbb{f} is often prescribed as a simple power law (NORTON's, GLEN's law, OSTWALD-DE WAELE law, ...); however, the perturbation scheme that is based on the present scalings can be shown to become invalid, because of singularities that develop at higher order terms, see HUTTER (1983) [39], R.E. JOHNSON and R.M. MCMEEKING (1984) [47]. It is, therefore, advantageous to use polynomial representations, which exhibit finite viscosity at zero stretching or stress deviator. The simplest proposition (HUTTER [37, 40]) is

$$\mathbb{f}(\tau_{II}) = \frac{\tau_{II}^{(n-1)/2} + \mathbb{k}}{1 + \mathbb{k}} \quad \text{with} \quad \mathbb{k} = \frac{1/\eta_0}{(\rho g[H])^{m-1}}, \quad (12.66)$$

in which η_0 is the viscosity (dimension Nsm^{-2}) at zero stretching and $n > 1$ is a stress exponent, usually having values from 1 to 10, for ice $n = 1.7\text{--}4$, generally $n = 3$, and $k \approx 0.1$ or less. Clearly, for $k \rightarrow 0$, Eq. (12.66) corresponds to a power law (NORTON, GLEN, OSTWALD-DE WAELE, ...). The modern trend is to use polynomial representations, i.e.,

$$\mathbb{f}(\tau_{II}) = f_0 + f_1\tau_{II} + f_2\tau_{II}^2, \quad (12.67)$$

with materially dependent coefficients f_0, f_1, f_2 . For ice GEORGE SMITH and LESLIE W. MORLAND obtained

$$f_0 = 0.3336, \quad f_1 = 0.3200, \quad f_2 = 0.0296 \quad \text{for ice.} \quad (12.68)$$

The sliding law is the least known of the three functions A, \mathbb{f} and \mathcal{F} , because it expresses the effect of the small scale boundary layer flow close to the ground that is dominated by the roughness elements on the outer flow distant from the base. Here, we simply suggest the phenomenological relation

$$\mathcal{F}(|\mathbf{t}_S|^2, |\mathbf{t}_n|^2) = +\sqrt{|\mathbf{t}_n|^2} \mu^{-1} = |\mathbf{t}_n| \mu^{-1}, \quad (12.69)$$

in which μ is a dimensionless constant ‘viscosity’, whose dimensional counterpart has the dimension of a velocity, or

$$\mathcal{F}(|\mathbf{t}_S|^2, |\mathbf{t}_n|^2) = \mathcal{B}(|\mathbf{t}_n|^2)(|\mathbf{t}_S|^2)^{(m-1)/2}. \quad (12.70)$$

\mathcal{B} is sometimes chosen to be a constant and $m \geq 1$. The non-linear relation (12.70) is more general than (12.69), in which the basal shear traction \mathbf{t}_S is linearly related to the tangential velocity \mathbf{v}_B , but the limit behavior $\mathbf{t}_S \rightarrow \mathbf{0}$ linearly with \mathbf{t}_n has been shown to be compatible with a finite surface slope profile up to the grounding line (LESLIE W. MORLAND and IAN R. JOHNSON, [53, 54]). This will be assumed here, for otherwise a separate margin analysis is required that involves FROBENIUS expansions, see HUTTER [39]. In addition, lowest order approximations could not be uniformly valid. All this has already been discussed in principle in Chap. 7, Sect. 7.4.

12.7 Applications to Downhill Creeping Flows

12.7.1 Computational Procedure

Equations (12.46), (12.47) and (12.50) are viewed as initial value problems, which must be solved by forward marching in time. To this end, an initial profile $z_S^0 = z_S(x, y, t_0)$ must be prescribed along with an initial accumulation function $a_0 = a(x, y, z_S^0, t_0)$ and temperature field $\theta_0 = \theta(x, y, z, t_0)$, which is compatible with

the boundary conditions (12.47). While initial functional values for z_S^0 and a_0 may be obtained straightforwardly either from own measurements or from the literature, those for θ_0 must be constructed from e.g. a prescription of measured or estimated temperature θ_0 and temperature gradient $\partial\theta_0/\partial z$ along the free surface and the base, respectively. With (12.47) it suffices to prescribe $\theta_S^0(x, y, z_S, t_0)$ and $\theta_B^0(x, y, z_B, t)$.

Implementation of initial conditions requires thought. In applications of the model equations to glacier and ice sheet flows the initial temperature and free surface fields cannot be exactly prescribed, but must be reasonably guessed, because data are generally not sufficiently available. One way is to assume a judiciously selected surface geometry and a constant temperature distribution, say -10°C throughout the ice domain and to prescribe a temporally constant accumulation function $a(x, y, z_S, t_0)$, $t_0 = \text{initial time}$; with this choice one then determines the velocity and stress fields with (12.40)–(12.42) and integrates (12.46)–(12.49) or (12.50) for some time until steady state is reached. This approach treats the initial fields $(u, v, T, z_S, \theta)_0$ as strictly steady, which in realistic climate scenarios is likely never occurring, but since processes in ice sheets are extremely slowly varying, the details of the initial temperature distribution and geometry will not considerably affect these fields at later times, provided integrations are begun sufficiently in the past. In general, 10^4 – 10^5 years of integration into steady state are needed to reach reliable initial conditions for ice sheet profiles and temperature distributions. For glaciers at most a few hundred years are needed.

This process of generating initial conditions may be accelerated if one starts with a prescribed initial geometry and given temperature fields on the free and basal surfaces close to reality and uses a heat transfer model (such as (12.47) that delivers estimates for θ_S^0 and θ_B^0). In this spirit the temperature representation in the fluid domain is chosen as a cubic polynomial in z with coefficients, which depend on x and y ,

$$\theta_0 = c_0(x, y) + c_1(x, y)z + c_2(x, y)z^2 + c_3(x, y)z^3, \quad (12.71)$$

where evaluation of θ_0 and $\theta'_0 = \partial\theta_0/\partial z$ on $z = z_S$ and $z = z_B$ yields four equations in four unknowns c_0, c_1, \dots, c_3 , which can be solved. For plane flow (no y -dependence) the solution is (see MORLAND and SMITH (1984) [55])

$$\begin{aligned} c_0(x, y) &= \theta_B^0 - \theta_B^0 + r_1 z_B^2 - r_2 z_B^3, \\ c_3(x, y) &= r_2, \\ c_1(x, y) &= \theta_B^0 - 2r_1 z_B + 3r_2 z_B^2, \\ c_2(x, y) &= r_1 - 3r_2 z_B, \end{aligned} \quad (12.72)$$

and

$$\begin{aligned} r_1 &= (z_S - z_B)^{-2} \left[3(\theta_S^0 - \theta_B^0) - (z_S - z_B)(2\theta_B^0 + \theta_S^0) \right], \\ r_2 &= (z_S - z_B)^{-3} \left[2(\theta_B^0 - \theta_S^0) - (z_S - z_B)(2\theta_B^0 + \theta_S^0) \right]. \end{aligned} \quad (12.73)$$

θ_S^0 and θ_B^0 are the prescribed initial surface and basal temperatures, respectively, and

$$\theta_S^{0'} = -\frac{\mathbb{N}_B h_S (\theta_S^0 - \theta_A^0)}{\kappa (\theta_S^0)}, \quad \theta_B^{0'} = \frac{\mathbb{N}_B h_B (\theta_B^0 - \theta_G^0)}{\kappa (\theta_B^0)}. \quad (12.74)$$

θ_A^0 and θ_B^0 are the constant ambient and ground temperatures, respectively. This selection of an initial temperature distribution may also be useful in three-dimensional ice sheets if reliable temperature distributions for θ_S and θ_B are known.

With (12.71)–(12.74) starting conditions are given for the evaluation of the stresses (12.40), the velocities (12.41) and (12.44). From (12.46), (12.47) and (12.50) $\partial\theta/\partial t$ and $\partial z_S/\partial t$ can then be calculated over the entire domains $\mathcal{D}(t_0)$ and $P\mathcal{D}(t_0)$, respectively. Marching forward in time permits evaluation of θ and z_S one time step ahead, which defines $\mathcal{D}(t_1)$ and $P\mathcal{D}(t_1)$, when $t_1 = t_0 + \Delta t$, etc. Steady conditions, if they exist, are best sought by searching for a large time solution which becomes independent of t as $t \rightarrow \infty$. Details of the numerical method are described in a dissertation by L. VULLIET (1986) [64].

12.7.2 Profiles and Flows for Isothermal Conditions

The simplest application of the presented shallow flow approximation is restriction to isothermal conditions. In this case the thermal initial-boundary-value problem (12.46), (12.47) is superfluous and the rate factor $A(\theta)$ arising in (12.41), (12.42) may be set equal to the constant 1. Given the initial profile for $z = z_S$ and $z = z_B$ (the latter being rigid), the stress and velocity fields can be determined by simple quadratures of (12.40)–(12.42), and $z = z_S$ can be updated by forward evaluation of $z = z_S$ with Eq. (12.50).

Computations were performed with an initial geometry similar to that of Fig. 12.4. The domain (at $t = 0$) is defined by

$$\begin{aligned} z_S &= \left(1 - \left(\frac{y}{y_B(x)}\right)^2\right) d \tanh(b(x_e - x)) + \tan \gamma (x_e - x), \\ z_B &= -\left(1 - \left(\frac{y}{y_B(x)}\right)^2\right) d \tanh(b(x_e - x)) + \tan \gamma' (x_e - x), \\ y_B(x) &= a(x_e - x) \exp\left(-\frac{x_e - x}{c}\right), \end{aligned} \quad (12.75)$$

in which $y_B(x)$ is an auxiliary variable and

$$\begin{aligned} a &= 4, & d &= 100 \text{ m}, \\ b &= 2.7 \times 10^{-3} \text{ m}^{-1}, & x_e &= 1000 \text{ m}, \\ c &= 200 \text{ m}, & \alpha &= 10^\circ \end{aligned} \quad (12.76)$$

and

$$\begin{aligned}\tan \gamma &= \tan \alpha - \frac{d}{dx_e} (\tanh(bx_e)), \\ \tan \gamma' &= \frac{2d}{x_e} \tanh(bx_e) + \tan \gamma.\end{aligned}\tag{12.77}$$

Here, x is the down-slope and y the cross-slope variable; for constant x the profiles (12.75) are parabolas of degree 2 both for the free and bottom surfaces, the former of concave, the latter of convex geometry. The variable $y_B(x)$ measures the cross-slope curvature that can be varied in the downslope direction. The selection (12.75)₃ makes $y_B(x)$ to grow linearly for small $(x_e - x)$ and to exponentially decay for $(x_e - x) \rightarrow \infty$. The profiles $z = z_S(x, y)$ and $z = z_B(x, y)$ are symmetric in y ; so, symmetric flow states are to be expected under constant gravity force application.

Finite difference techniques were used to discretize the geometry with mesh sizes $\Delta x = 40$ m, $\Delta y = 20$ m and a total of 595 grid points. The integrations in the z -direction were performed using the trapezoidal rule and dividing the depth into 40 intervals. Computations indicated that these could even be decreased without essential loss of accuracy. Computations in time were performed, using an increment $\Delta t = 10^{-3}[\mathfrak{T}]$ where $[\mathfrak{T}]$ is the characteristic time given below, but the graphs were produced for $t = 0, t = 40\Delta t, t = 80\Delta t, \dots$ only.

The constitutive and scaling properties, summarized in **Table 12.3**, are grossly representative for landslides or glaciers, but were chosen somewhat arbitrarily.

Figure 12.8a–c show surface velocities in scaled coordinates for the three consecutive times mentioned above. A conspicuous spreading of the domain at early times can be observed, which is expected, given the pronounced initial cross-profile velocities. Once this spreading has taken place, velocities become mainly longitudinal as seen in **Fig. 12.8b** and **c**. For comparison, **Figs. 12.9a–c** show the same in physical space.

In order to better see the evolution in time of the free surface we show in **Figs. 12.10a–b** the geometries at the cross sections $A-A$ and $B-B$ again in scaled coordinates. The initial parabolic shape of the profile (solid lines) is flattened-out in the cross-profile direction, which results in the more pronounced longitudinal velocity distribution seen earlier. A closer view on output for early times showed that this spreading takes place very quickly and slows down at later times (shown here).

Figure 12.11 displays in physical coordinates (i) the evolution in time of the domain in the cross section $C-C$ (see **Fig. 12.8**) and (ii) a few selected velocity profiles including their evolution in time. A pronounced thinning of the domain and reduction in speeds in the upper part is observed, which is counterbalanced by a corresponding thickening, advance and velocity increase close to the snout. Moreover, for the physical conditions implemented in this case the downslope velocity is composed of some sliding and primarily differential shearing.

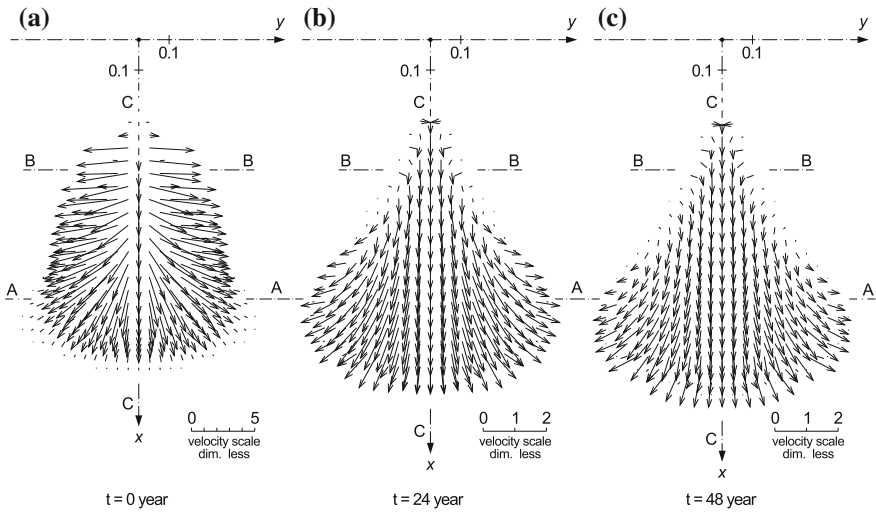


Fig. 12.8 Dimensionless surface velocities of an isothermal deformation of a mass of a very viscous power law fluid, moving down an inclined surface. The basal surface is given by $z = z_B$ and initial profile geometry given by $z = z_S$ (see (12.75)–(12.77)) released from rest. Panels a–c show the surface velocity field at $t = 0$, $t = 24$, and $t = 48$ years. Note the different velocity scales in panel (a) from the other panels. After [43] with changes

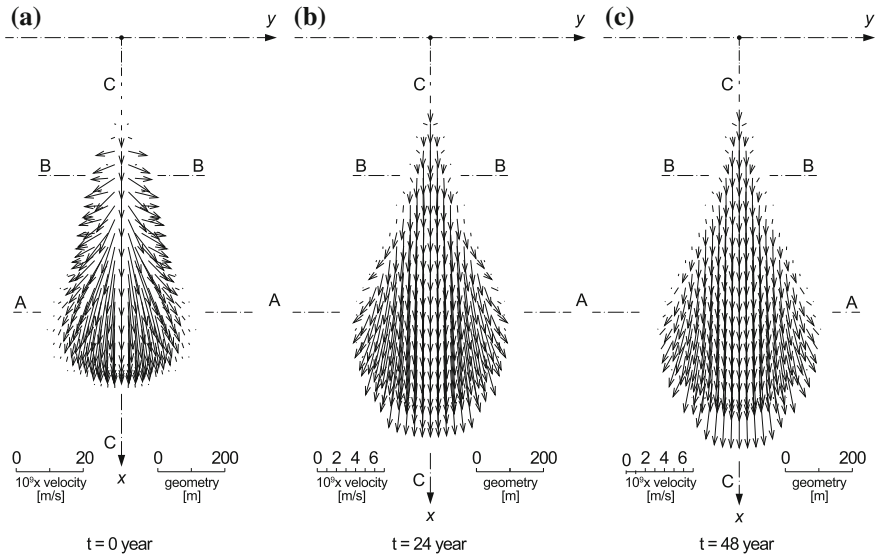


Fig. 12.9 Surface velocity distributions in physical space corresponding to Fig. 12.8. The snapshots are again for the times 0, 24, 48 years. Note also the different velocity scales in panels a–c. After [43] with changes

Table 12.3 Physical constants and scales used in the computations for Figs. 12.8, 12.9, 12.10 and 12.11, from [43]

Viscosity	$\eta_0^{-1} = 6.24 \times 10^{-15}$	[m s kg ⁻¹]
Rate factor	$A = 2.76 \times 10^{-29}$	[s ⁵ m ³ kg ⁻³]
Creep exponent	$n = 3$	[-]
Sliding law exponent	$m = 1$	[-]
Sliding coefficient	$B = 10^{-13}$	[m s kg ⁻¹]
Density ρ	$\rho = 2000$	[kg m ⁻³]
Characteristic depth	$[H] = 50$	[m]
Characteristic length	$[L_y] = 600$	[m]
Typical stretching	$[d] = [U/L_x] = 5.314 \times 10^{-11}$	[s ⁻¹]
Inclination angle α	$= 10$	[°]
$\mu_{\text{eff}} = A^{-1}(\rho g [H] \sin \alpha)^{-2}$	$= 9.41 \times 10^{13}$	[m s kg ⁻¹]
$[L_x] = \rho g \sin \alpha [H^2] / ([d] \mu_{\text{eff}})$	$= 1000$	[m]
$[U] = [d L_x]$	$= 5.314 \times 10^{-8}$	[m s ⁻¹]
	$= 1.7$	[m a ⁻¹]
$[V] = [L_y U / L_x]$	$= 3.18 \times 10^{-8}$	[m s ⁻¹]
	$= 1.0$	[m a ⁻¹]
$[W] = [H U / L_x]$	$= 2.66 \times 10^{-9}$	[m s ⁻¹]
	$= 0.08$	[m a ⁻¹]
$[\mathfrak{T}] = [L_x / U]$	$= 1.88 \times 10^6$	[s]
	$= 600$	[a]

12.7.3 Remarks for Use of the Shallow Flow Approximation for Alpine Glaciers

The above shallow flow approximation has been developed in the 80s of the last century when electronic computational facilities were much less developed than they are now. For creeping landslides over time scales of a few decades to, say, a century, they are useful when a fairly smooth rigid rocky basal surface can be identified. In such geotechnical applications it generally suffices, if the isothermal, reduced module of the discretized version of the equations is employed. In steep hanging glaciers at high altitudes in the Alps the ice is generally cold, so that the thermomechanical equations must be solved. This then entails the prescription of not only the thermal boundary condition at the free surface, but equally also on the rock bed, which generally is hard to determine both geometrically and thermally. In the past the no-slip boundary condition was imposed; but in the present and future climate warming the basal temperature at some regions of the basal surface may reach the melting temperature which then requires imposition of a sliding law.

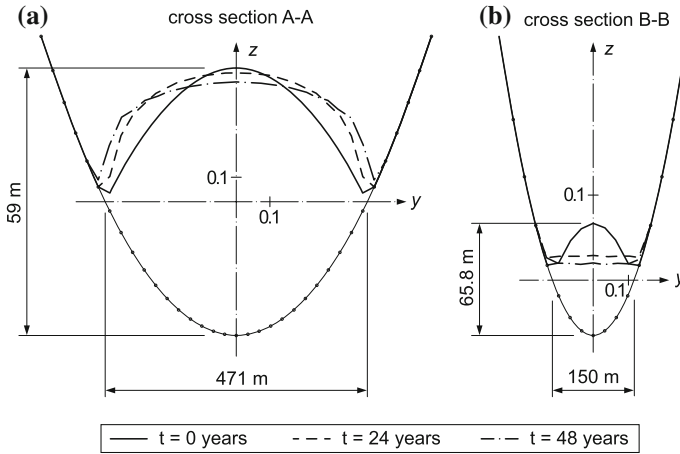


Fig. 12.10 Cross sections A–A and B–B (see Figs. 12.8 and 12.9). Panel (a) shows the parabolic basal topography, and the surface profiles for $t = 0$ years (solid lines), $t = 24$ years (dashed lines) and $t = 48$ years (dashed-dotted lines). Panel b shows the analogous results for cross section B–B. After [43] with changes

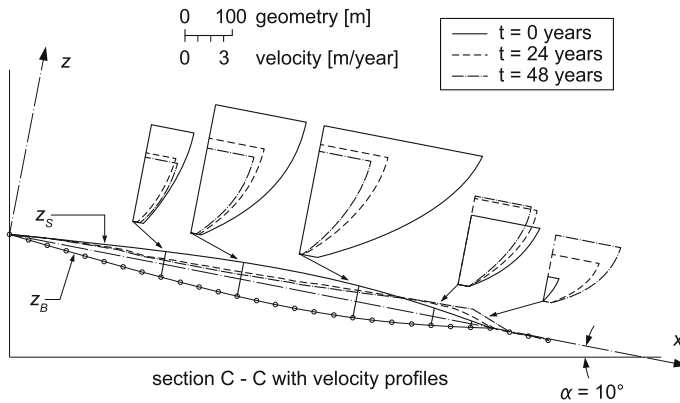


Fig. 12.11 Longitudinal cut C–C (see Figs. 12.8 and 12.9) along the symmetry line. The figure shows the profiles normal to the x -axis at the indicated positions from bottom to the free surface for $t = 0$ (solid lines), $t = 24$ (dashed lines) and $t = 48$ years (dashed-dotted lines). After [43] with changes

For estimation of such endangering scenarios into the immediate future (a few decades), the shallow flow approximation in glaciers is somewhat questionable. With today’s computational facilities and available software it may be advantageous to employ the original equations in the STOKES approximation. For computations over a few decades these may today well be a competitive more realistic alternative.

12.8 Free-Surface Gravity-Driven Creep Flow of a Very Viscous Body with Strong Thermomechanical Coupling—A Rigorous Derivation of the Shallow Ice Approximation

The scaling analysis introduced in Sect. 12.3 has as one of its intentions the replacement of the physical variables by dimensionless analogues so that the initial boundary value problems could be written in terms of quantities that are dimensionless. The difficulty of this procedure lies in the appropriate selection of the coordinates (x, y) , which here are the ‘best fit’ to the boundary topography $z = z_B(x, y)$. This was in the present analysis a plane, inclined at an angle α to the horizontal plane. This suggested in Eq. (12.10) a scaling for the stresses, which involves the angle α and led to the dimensionless set of Eq. (12.14), which involve terms with $\tan \alpha$ and $\cotan \alpha$ as factors. The analysis then showed that the associated Shallow Flow Approximation [Eqs. (12.40)–(12.42) and (12.44)–(12.50)] is only meaningful for α bounded away from zero. The case $\alpha = 0$ involves singularities ($\lim_{\alpha \rightarrow 0} \cotan \alpha \rightarrow \infty$). So, for a creeping mass of a non-NEWTONian fluid on a horizontal plane or a topography close to this, a new scale analysis must be made.

12.8.1 The Classical Shallow Flow Approximation

Because spreading in the two horizontal directions is likely of the same order of magnitude, it is tempting to choose $[L_x] = [L_y]$ and $[U] = [V]$ and to non-dimensionalize the dynamical equations as follows:

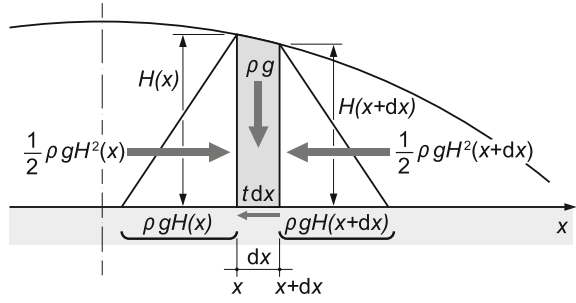
$$\begin{aligned}
 \{x, y, z, t\} &= \left\{ [L]\bar{x}, [L]\bar{y}, [H]\bar{z}, \frac{[W]}{[H]}\bar{t} \right\}, \\
 \{u, v, w, a\} &= \{[U]\bar{u}, [U]\bar{v}, [W]\bar{w}, [W]\bar{a}\}, \\
 \{p, t_{xx}, t_{yy}, t_{zz}\} &= [\rho g H] \{ \bar{p}, \varepsilon^2 \sigma_x, \varepsilon^2 \sigma_y, \varepsilon^2 \sigma_z \}, \\
 \{t_{xy}, t_{xz}, t_{yz}\} &= [\rho g H] \{ \varepsilon^2 \tau_{xy}, \varepsilon \tau_{xz}, \varepsilon \tau_{yz} \}, \\
 T &= T_0 + [\Delta T] \theta \\
 A(T) f(\Pi_\sigma) &= \frac{[D]}{[\sigma]} \bar{A} \bar{f}(\bar{\Pi}_\sigma),
 \end{aligned} \tag{12.78}$$

where we have chosen the aspect ratio

$$\varepsilon = \frac{[H]}{[L]} = \frac{[W]}{[U]}. \tag{12.79}$$

So, the aspect ratios of the length scales and velocity scales are the same. Note, moreover, that the scales of the stresses are weighted with ε and ε^2 , respectively. The

Fig. 12.12 Creeping flow of a fluid on a horizontal basis. Under hydrostatic conditions the pressure forces at x and $x + dx$ are in equilibrium with the basal shear stresses, explaining the scale for t_{xz} and t_{yz}



pressure is scaled with a reference overburden pressure $[\rho g H]$. Relative to this, the normal components of the stress deviator are $\mathcal{O}(\varepsilon^2)$ smaller and the vertical shear stresses are $\mathcal{O}(\varepsilon)$ smaller. These weights are at first not evident but can be made plausible. To this end, consider plane flow as shown in **Fig. 12.12**. Let the stress distribution be hydrostatic, so that the indicated column of length dx is subjected to the triangular pressure forces $\frac{1}{2}\rho g H^2(x)$, $-\frac{1}{2}\rho g H^2(x + dx)$ and the basal shear stress $t dx$. A horizontal force balance then yields, after Taylor-series expansion restricted to linear terms,

$$t dx = \rho g H \left(-\frac{\partial H}{\partial x} \right) dx,$$

or when non-dimensionalized

$$t = [\tau] \bar{\tau} = [\rho g H] \frac{[H]}{[L]} \bar{h}(\bar{x}) \left(-\frac{\partial \bar{h}}{\partial \bar{x}} \right)$$

implying

$$[\tau] = [\rho g H] \varepsilon \tag{12.80}$$

This result explains, why the scales for t_{xz} and t_{yz} must be of order $[\rho g H] \varepsilon$.

There are further reasons for this scaling. To see this, we write the force balances¹¹ in scaled form, using (12.78), but not implementing the $\mathcal{O}(\varepsilon^2)$ -weights in the stresses $\sigma_x, \sigma_y, \sigma_z, \tau_{xy}$. These yield

$$\begin{aligned} -\varepsilon \frac{\partial \bar{p}}{\partial \bar{x}} + \varepsilon \frac{\partial \bar{\sigma}_x}{\partial \bar{x}} + \varepsilon \frac{\partial \bar{\tau}_{xy}}{\partial \bar{y}} + \varepsilon \frac{\partial \tau_{xz}}{\partial \bar{z}} &= 0, \\ -\varepsilon \frac{\partial \bar{p}}{\partial \bar{y}} + \varepsilon \frac{\partial \bar{\tau}_{xy}}{\partial \bar{x}} + \varepsilon \frac{\partial \bar{\sigma}_y}{\partial \bar{y}} + \varepsilon \frac{\partial \tau_{yz}}{\partial \bar{z}} &= 0, \\ -\frac{\partial \bar{p}}{\partial \bar{z}} + \varepsilon^2 \frac{\partial \tau_{xz}}{\partial \bar{x}} + \varepsilon^2 \frac{\partial \tau_{yz}}{\partial \bar{y}} + \frac{\partial \bar{\sigma}_z}{\partial \bar{z}} &= 1, \end{aligned} \tag{12.81}$$

¹¹We omit the accelerations as they play no role for the arguments.

Here,

$$\{t_{xx}, t_{yy}, t_{zz}, t_{xy}\} = [\rho g H] \{\tilde{\sigma}_x, \tilde{\sigma}_y, \tilde{\sigma}_z, \tilde{\tau}_{xy}\} \quad (12.82)$$

We know from physics of such flows that the tilde-quantities (12.82) must be small. In Eq. (12.81), these are identified by writing them in color. This observation justifies to lowest order the use of the hydrostatic pressure Eq. (12.81)₃ in the form $\partial \bar{p} / \partial \bar{z} = -1$. Consequently, we may either assume $\tilde{\sigma}_z = (\varepsilon \sigma_z)$ or $\tilde{\sigma}_z = (\varepsilon^2) \sigma_z$, but only the latter choice makes sense as we expect the next order to be ε^2 . Indeed, the continuity equation, $\text{div } \mathbf{v} = 0$, paired with the constitutive law $\mathbf{D} \propto \boldsymbol{\sigma}$ implies that the normal stresses $\tilde{\sigma}_x, \tilde{\sigma}_y, \tilde{\sigma}_z$ must all be of the same order $\mathcal{O}(\varepsilon^2)$. Finally, this also implies that $\tilde{\tau}_{xy}$ is of the order $\mathcal{O}(\varepsilon^2)$, since the (x, y) coordinates may be arbitrarily oriented on the horizontal plane. So, we now have

$$\{\tilde{\sigma}_x, \tilde{\sigma}_y, \tilde{\sigma}_z, \tilde{\tau}_{xy}\} = \varepsilon^2 \{\sigma_x, \sigma_y, \sigma_z, \tau_{xy}\}. \quad (12.83)$$

The scalings (12.78) are now justified. The component forms of the field Eq. (12.1) and constitutive relations (12.3) take with these scalings the forms

$$\begin{aligned} \frac{\partial \bar{u}}{\partial \bar{x}} + \frac{\partial \bar{v}}{\partial \bar{y}} + \frac{\partial \bar{w}}{\partial \bar{z}} &= 0, \\ \frac{\mathbb{F}^2}{\varepsilon} \frac{d\bar{u}}{d\bar{t}} &= \left(-\frac{\partial \bar{p}}{\partial \bar{x}} \right) + \varepsilon^2 \left(\frac{\partial \sigma_x}{\partial \bar{x}} + \frac{\partial \tau_{xy}}{\partial \bar{y}} \right) + \frac{\partial \tau_{xz}}{\partial \bar{z}}, \\ \frac{\mathbb{F}^2}{\varepsilon} \frac{d\bar{v}}{d\bar{t}} &= \left(-\frac{\partial \bar{p}}{\partial \bar{y}} \right) + \varepsilon^2 \left(\frac{\partial \sigma_y}{\partial \bar{y}} + \frac{\partial \tau_{xy}}{\partial \bar{x}} \right) + \frac{\partial \tau_{yz}}{\partial \bar{z}}, \\ \mathbb{F}^2 \varepsilon \frac{d\bar{w}}{d\bar{t}} &= \left(-\frac{\partial \bar{p}}{\partial \bar{z}} \right) + \varepsilon^2 \left(\frac{\partial \tau_{xz}}{\partial \bar{x}} + \frac{\partial \tau_{yz}}{\partial \bar{y}} \right) + \varepsilon^2 \frac{\partial \sigma_z}{\partial \bar{z}} - 1, \\ \bar{c}(\theta) \frac{d\theta}{d\bar{t}} &= \mathbb{D} \left\{ \varepsilon^2 \left[\frac{\partial}{\partial \bar{x}} \left(\bar{\kappa}(\theta) \frac{\partial \theta}{\partial \bar{x}} \right) + \frac{\partial}{\partial \bar{y}} \left(\bar{\kappa}(\theta) \frac{\partial \theta}{\partial \bar{y}} \right) \right] + \frac{\partial}{\partial \bar{z}} \left(\bar{\kappa}(\theta) \frac{\partial \theta}{\partial \bar{z}} \right) \right\} \\ &\quad + \mathbb{E} 2 \bar{A}(\theta) \mathbb{f}(\tau_{II}) \tau_{II}, \end{aligned} \quad (12.84)$$

$$\frac{\partial \bar{u}}{\partial \bar{x}} = \mathbb{G} \bar{A}(\theta) \mathbb{f}(\tau_{II}) \sigma_x,$$

$$\frac{\partial \bar{v}}{\partial \bar{y}} = \mathbb{G} \bar{A}(\theta) \mathbb{f}(\tau_{II}) \sigma_y,$$

$$\frac{\partial \bar{w}}{\partial \bar{z}} = \mathbb{G} \bar{A}(\theta) \mathbb{f}(\tau_{II}) \sigma_z,$$

$$\frac{\partial \bar{u}}{\partial \bar{y}} + \frac{\partial \bar{v}}{\partial \bar{x}} = 2 \mathbb{G} \bar{A}(\theta) \mathbb{f}(\tau_{II}) \tau_{xy},$$

$$\frac{\partial \bar{u}}{\partial \bar{z}} + \varepsilon^2 \frac{\partial \bar{w}}{\partial \bar{x}} = 2 \mathbb{G} \bar{A}(\theta) \mathbb{f}(\tau_{II}) \tau_{xz},$$

$$\frac{\partial \bar{v}}{\partial \bar{z}} + \varepsilon^2 \frac{\partial \bar{w}}{\partial \bar{y}} = 2 \mathbb{G} \bar{A}(\theta) \mathbb{f}(\tau_{II}) \tau_{yz},$$

in which

$$\tau_{II} = \tau_{xz}^2 + \tau_{yz}^2 + \varepsilon^2 \left[\frac{1}{2} (\sigma_x^2 + \sigma_y^2 + \sigma_z^2) + \tau_{xy}^2 \right] \quad (12.85)$$

is the dimensionless second order stress deviator invariant and

$$\begin{aligned} \mathbb{f}(II_\sigma) &= \frac{F([\rho g H]^2 \tau_{II})}{F([\rho g H]^2 \cdot 1)}, \\ \bar{A}(\theta) &= \frac{A(T)}{A(T_R)} = \frac{A(T_R + [\Delta T]\theta)}{A(T_R)} = \frac{A'(\theta)}{A(T_R)}, \\ \bar{\kappa}(\theta) &= \frac{\kappa(T)}{\kappa(T_R)} = \frac{\kappa(T_R + [\Delta T]\theta)}{\kappa(T_R)} = \frac{\kappa'(\theta)}{\kappa(T_R)}, \\ \bar{c}(\theta) &= \frac{c_p(T)}{c_p(T_R)} = \frac{c_p(T_R + [\Delta T]\theta)}{c_p(T_R)} = \frac{c'(\theta)}{c_p(T_R)} \end{aligned} \quad (12.86)$$

are the analogous quantities already defined in (12.17). They show no dependence on the inclination angle α . Moreover,

$$\begin{aligned} \mathbb{F}^2 &= \frac{[U^2]}{g[H]}, \\ \mathbb{G} &= \frac{\varepsilon^2}{S_\Sigma D_\Delta}, \quad S_\Sigma = \frac{[\sigma]}{[\rho g H]}, \quad D_\Delta = \frac{[W]/[H]}{[D]}, \end{aligned} \quad (12.87)$$

$$\begin{aligned} \mathbb{D} &= \frac{\kappa(T_R)[L]}{\rho c_p(T_R)[U][H^2]} = \frac{\kappa(T_R)}{\rho c_p(T_R)[W][H]}, \\ \mathbb{E} &= \frac{A}{S_E D_\Delta}, \end{aligned} \quad (12.88)$$

\mathbb{F}^2 is the (squared) FROUDE number, \mathbb{D} is a dimensionless thermal diffusivity, \mathbb{G} a parameter characterizing the constitutive response of stress; S_Σ is a stress ratio of a material stress to an overburden stress; D_Δ is a vertical strain rate and \mathbb{E} measures the significance of dissipation or strain heating.

The field Eq. (12.84) are supposed to be so non-dimensionalized that all expressions printed in black are order unity quantities whereas the colored quantities have values as dictated by the chosen scales and given by (12.87). These latter quantities appear in color in (12.84). In applications to large ice sheets, say Greenland and Antarctica, the various scales and the physical parameters for polycrystalline ice have values as listed in **Table 12.4**. With them, it is a straightforward exercise to see that $\varepsilon = \mathcal{O}(10^{-3} - 10^{-2})$, $\mathbb{F}^2 = \mathcal{O}(10^{-18} - 10^{-14})$, so that $\mathbb{F}^2/\varepsilon = \mathcal{O}(10^{-16} - 10^{-11})$ and $\mathbb{F}^2\varepsilon = \mathcal{O}(10^{-21} - 10^{-16})$. Similar estimates for the remaining quantities suggest that ‘with some tolerance’ $(\mathbb{D}, \mathbb{E}, \mathbb{G}) = \mathcal{O}(10^{-1} - 10^1)$. These estimates should not be looked at as strict ranges of values, but rather as guidelines suggesting the following approximations:

Table 12.4 Characteristic scales and physical parameters for large ice sheets such as Greenland and Antarctica

$[U]$	$10^2\text{--}10^3$ m/a	Characteristic horizontal speed
$[W]$	1–10 m/a	Characteristic vertical speed
$[L]$	500–4000 km	Characteristic ice sheet extent
$[H]$	500–3000 m	Typical ice sheet depth
$[\sigma]$	10^5 Pa	Typical material stress
$[g]$	$9.81\text{ m s}^{-2} = 9.76 \times 10^{15}\text{ m a}^{-2}$	Gravity constant
$[\rho]$	910 kg m^{-3}	Ice density
$[\Delta T]$	20–30 °C	Ice sheet temperature range
$[c_p]$	$2 \times 10^3\text{ J kg}^{-1}\text{ K}^{-1}$	Specific heat of ice at 273.15 °K
T_R	273.15 °K	Melting temperature of ice

1. In the momentum equations the acceleration terms can be ignored, since \mathbb{F}^2/ε and $\mathbb{F}^2\varepsilon$ are both substantially smaller than any other terms in Eq. (12.84). Dropping the acceleration terms is called the STOKES approximation.
2. This STOKES approximation is satisfied to a very high degree; in other words, if ε is used as a perturbation parameter and regular perturbation solutions are sought for $\Phi = \{\bar{u}, \bar{v}, \bar{w}, \bar{p}, \theta\}$ in the spirit that

$$\Phi = \Phi_0 + \varepsilon\Phi_1 + \varepsilon^2\Phi_2 + \dots \approx \sum_{\nu=0}^N \varepsilon^\nu \Phi_\nu, \quad (12.89)$$

then the STOKES approximation remains an acceptable assumption at least to second ($N = 2$) or third ($N = 3$) order.¹² The approximation $N = 0$ is called in glaciology the **Shallow Ice Approximation (SIA)**, whereas $N = 2$ characterizes the **Second Order Shallow Ice Approximation (SOSIA)**.¹³

3. Looking at (12.84)_{2–4} it is seen that the convective heat transport is fully accounted for in any approximation ($N < \infty$) (as are, incidentally also the convective accelerations, but this is irrelevant in a STOKES approximation). By contrast, the horizontal momentum and heat fluxes can be dropped in the SIA and SOSIA approximations as compared to the corresponding fluxes in the normal, z -direction. Similarly, (12.84)_{10,11} imply that in the SIA the horizontal stretching can be dropped.
4. In the z -component of the momentum equation, all flux terms, except $\partial\bar{p}/\partial\bar{z}$ are $\mathcal{O}(\varepsilon^2)$ and can be dropped in the SIA. What then remains is the **hydrostatic**

¹²This is often not so for applications in rheology.

¹³Note that SIA and SOSIA are meant here to apply to ice sheets, but neither to (steep) glaciers nor floating ice shelves.

pressure equation, $\partial\bar{p}/\partial\bar{z} = 1$. Corrections to this behavior only enter at the SOSIA. Moreover, to account for vertical accelerations would require a higher order model with $N = 3$ or $N = 4$. This has so far never been attempted. An alternative would be to employ a non-stretched non-dimensionalization of the governing equation and employing depth integration of these equations as is done in hydraulics with the BOUSSINESQ equations against the DE SAINT VENANT equations, but for creeping flow this has not yet been done, see [11, 42], to our knowledge.

5. In the limit as $\varepsilon \rightarrow 0$, Eq. (12.84) take the limiting forms

$$\begin{aligned} \frac{\partial\bar{u}}{\partial\bar{x}} + \frac{\partial\bar{v}}{\partial\bar{y}} + \frac{\partial\bar{w}}{\partial\bar{z}} &= 0, \\ -\frac{\partial\bar{p}}{\partial\bar{x}} + \frac{\partial\tau_{xz}}{\partial\bar{z}} &= 0, \\ -\frac{\partial\bar{p}}{\partial\bar{y}} + \frac{\partial\tau_{yz}}{\partial\bar{z}} &= 0, \\ -\frac{\partial\bar{p}}{\partial\bar{z}} - 1 &= 0, \\ \bar{c}\frac{d\theta}{d\bar{t}} &= \mathbb{D}\frac{\partial}{\partial\bar{z}}\left(\bar{\kappa}(\theta)\frac{\partial\theta}{\partial\bar{z}}\right) + 2\mathbb{E}\bar{A}(\theta)\mathfrak{f}(\tau_{II})\tau_{II}, \\ \frac{\partial\bar{u}}{\partial\bar{z}} &= 2\mathbb{G}\bar{A}(\theta)\mathfrak{f}(\tau_{II})\tau_{xz}, \\ \frac{\partial\bar{v}}{\partial\bar{z}} &= 2\mathbb{G}\bar{A}(\theta)\mathfrak{f}(\tau_{II})\tau_{yz} \end{aligned} \tag{12.90}$$

and

$$\begin{aligned} \frac{\partial\bar{u}}{\partial\bar{x}} &= \mathbb{G}\bar{A}(\theta)\mathfrak{f}(\tau_{II})\sigma_x, \\ \frac{\partial\bar{v}}{\partial\bar{y}} &= \mathbb{G}\bar{A}(\theta)\mathfrak{f}(\tau_{II})\sigma_y, \\ \frac{\partial\bar{w}}{\partial\bar{z}} &= \mathbb{G}\bar{A}(\theta)\mathfrak{f}(\tau_{II})\sigma_z, \\ \frac{\partial\bar{u}}{\partial\bar{y}} + \frac{\partial\bar{v}}{\partial\bar{x}} &= 2\mathbb{G}\bar{A}(\theta)\mathfrak{f}(\tau_{II})\tau_{xy}. \end{aligned} \tag{12.91}$$

Equations (12.90) and (12.91) have been separated for reasons which will soon become apparent; relations (12.90) are the proper SIA-equations, (12.91) are only needed for the higher order models $N \geq 2$.

By contrast, (12.85) reduces to

$$\tau_{II} = \tau_{xz}^2 + \tau_{yz}^2. \tag{12.92}$$

It appears as if also this reduced second stress deviator invariant should be dropped. This should not be done, however; for $\mathbb{f}(0) \neq 0$ a NEWTONian fluid model would emerge at the SIA-level; for $\mathbb{f}(0) = 0$, e.g. a power law fluid, (12.90)_{6,7} yield $(\partial\bar{u}/\partial\bar{z}, \partial\bar{v}/\partial\bar{z}) = (0, 0)$, implying a constant vertical profile of the horizontal velocity components. This contradicts inclinometer observations in vertical ice bore holes. This second interpretation is also correct from a scaling analysis viewpoint, since $\tau_{II} = \mathcal{O}(1 - 10^1)$, which is not small.

6. Inspecting the field Eqs. (12.84) and (12.85), one may conclude as if the perturbation solutions would step in orders ε^2 , i.e., $\Phi = \sum_{\nu=0}^N \varepsilon_\nu^2 \Phi_\nu$ so that odd order solutions would vanish. Whether such behavior prevails can be seen, once the boundary conditions are formulated. Ordinarily, it is assumed that the first order quantities, Φ_1 , vanish, which we regard as questionable.

Boundary conditions are to be formulated at the free and basal surfaces and are stated as (12.5), (12.6) and (12.7)–(12.9), respectively. These statements will be derived here in Cartesian coordinates (x, y horizontal, z vertical) and using the scales (12.78), (12.79). Somewhat lengthy, but straightforward calculations then show the following:

- (i) For the *free surface* $\bar{z} = \bar{z}_S(\bar{x}, \bar{y}, \bar{t})$ the surface boundary conditions are given by

$$\begin{aligned}
 & \frac{\partial \bar{z}_S}{\partial \bar{t}} + \frac{\partial \bar{z}_S}{\partial \bar{x}} \bar{u} + \frac{\partial \bar{z}_S}{\partial \bar{y}} \bar{v} - \bar{w} = N_S \bar{a}, \\
 & \bar{p} \frac{\partial \bar{z}_S}{\partial \bar{x}} + \tau_{xz} - \varepsilon^2 \left(\sigma_x \frac{\partial \bar{z}_S}{\partial \bar{x}} + \tau_{xy} \frac{\partial \bar{z}_S}{\partial \bar{y}} \right) = 0, \\
 & \bar{p} \frac{\partial \bar{z}_S}{\partial \bar{y}} + \tau_{yz} - \varepsilon^2 \left(\sigma_y \frac{\partial \bar{z}_S}{\partial \bar{y}} + \tau_{xy} \frac{\partial \bar{z}_S}{\partial \bar{x}} \right) = 0, \\
 & \bar{p} - \varepsilon^2 \left(\sigma_z - \tau_{xz} \frac{\partial \bar{z}_S}{\partial \bar{x}} - \tau_{yz} \frac{\partial \bar{z}_S}{\partial \bar{y}} \right) = 0, \\
 & \bar{\kappa}(\theta) \left\{ \frac{\partial \theta}{\partial \bar{z}} - \varepsilon^2 \left(\frac{\partial \theta}{\partial \bar{x}} \frac{\partial \bar{z}_S}{\partial \bar{x}} + \frac{\partial \theta}{\partial \bar{y}} \frac{\partial \bar{z}_S}{\partial \bar{y}} \right) \right\} = \mathbb{N}_S (\theta - \theta_A) N_S.
 \end{aligned} \tag{12.93}$$

Equation (12.93)₁ is the kinematic surface condition, in which \bar{a} is the dimensionless accumulation function; (12.93)_{2,3,4} are the two horizontal and one vertical force balance equations, and (12.93)₅ is the boundary condition of heat, in which

$$N_S = \left\{ 1 + \varepsilon^2 \left[\left(\frac{\partial \bar{z}_S}{\partial \bar{x}} \right)^2 + \left(\frac{\partial \bar{z}_S}{\partial \bar{y}} \right)^2 \right] \right\}^{1/2}. \tag{12.94}$$

\mathbb{N}_S is the free surface NUSSELT number, defined as

$$\mathbb{N}_S = \frac{h_S^{\text{ref}}[H]}{\kappa(T_R)}. \quad (12.95)$$

For $\mathbb{N}_S \rightarrow \infty$, the thermal boundary condition reads $\theta = \theta_A$ and is of DIRICHLET type, whilst for $\mathbb{N}_S \rightarrow 0$ it is of NEUMANN type.

(ii) For the *rigid basal surface*, $\bar{z}_B(\bar{x}, \bar{y} - \bar{z}) = 0$, Eqs. (12.7)–(12.9) allow the derivation of the following dimensionless laws:

$$\begin{aligned} \bar{u}_B &= \mathcal{C}\mathcal{F}_B(|\bar{\mathbf{t}}_S|^2, |\bar{\mathbf{t}}_n|^2)(\bar{\mathbf{t}}_S)_x, \\ \bar{v}_B &= \mathcal{C}\mathcal{F}_B(|\bar{\mathbf{t}}_S|^2, |\bar{\mathbf{t}}_n|^2)(\bar{\mathbf{t}}_S)_y, \\ \bar{w}_B &= \bar{u}_B \frac{\partial \bar{z}_B}{\partial \bar{x}} + \bar{v}_B \frac{\partial \bar{z}_B}{\partial \bar{y}}, \\ \bar{\kappa}(\theta) \left\{ \frac{\partial \theta}{\partial \bar{z}} - \varepsilon^2 \left(\frac{\partial \theta}{\partial \bar{x}} \frac{\partial \bar{z}_B}{\partial \bar{x}} + \frac{\partial \theta}{\partial \bar{y}} \frac{\partial \bar{z}_B}{\partial \bar{y}} \right) \right\} &= \mathbb{N}_B(\theta - \theta_A)N_B, \end{aligned} \quad (12.96)$$

in which

$$\begin{aligned} N_B &= \left\{ 1 + \varepsilon^2 \left[\left(\frac{\partial \bar{z}_B}{\partial \bar{x}} \right)^2 + \left(\frac{\partial \bar{z}_B}{\partial \bar{y}} \right)^2 \right] \right\}^{1/2}, \\ \mathbb{N}_B &= \frac{h_B^{\text{ref}}[H]}{\kappa(T_R)}. \end{aligned} \quad (12.97)$$

The index $(\cdot)_B$ refers to the bottom surface. Equation (12.96)_{1,2} express the sliding law, according to which the tangential velocity at the base is collinear to the tangential traction with a dimensionless sliding function $\mathcal{F}(|\bar{\mathbf{t}}_S|^2, |\bar{\mathbf{t}}_n|^2)$, which depends on the dimensionless tangential and normal surface tractions $|\bar{\mathbf{t}}_S|$ and $|\bar{\mathbf{t}}_n|$, respectively. Symbolically, and in physical space, the sliding law is expressed as $\mathbf{v}_B = -F(|\mathbf{t}_S|^2, |\mathbf{t}_n|^2)\mathbf{t}_S$, where

$$\mathbf{t}_S := \mathbf{t}_{n_B} - \mathbf{t}_n, \quad \mathbf{t}_n := (\mathbf{n}_B \cdot \mathbf{t}_{n_B})\mathbf{n}_B \quad (12.98)$$

and

$$\mathcal{F}_B(|\bar{\mathbf{t}}_S|^2, |\bar{\mathbf{t}}_n|^2) = \frac{\Phi_B(c^2|\bar{\mathbf{t}}_S|^2, c^2|\bar{\mathbf{t}}_n|^2)}{\Phi_B(c^2, c^2)}, \quad c := [\rho g H] \quad (12.99)$$

as well as $\mathbf{t}_S = c\bar{\mathbf{t}}_S$, $\mathbf{t}_n = c\bar{\mathbf{t}}_n$; the drag coefficient is

$$\mathcal{C}_B = \frac{c\Phi(c^2, c^2)}{[U]}\varepsilon. \quad (12.100)$$

Please note the definition of c in (12.99), which is different from that in (12.26)₂. Moreover,

$$(\mathbf{t}_S)_{x,y} = [\rho g H] \varepsilon (\bar{\mathbf{t}}_S)_{\bar{x},\bar{y}}, \quad (\mathbf{t}_n)_{x,y} = [\rho g H] \varepsilon (\bar{\mathbf{t}}_n)_{\bar{x},\bar{y}} \quad (12.101)$$

with

$$\begin{aligned} (\bar{\mathbf{t}}_S)_x &= \frac{1}{N_B} \left\{ \left(-\bar{p} \frac{\partial \bar{z}_S}{\partial \bar{x}} - \tau_{xz} \right) + \varepsilon^2 \left(\sigma_x \frac{\partial \bar{z}_B}{\partial \bar{x}} + \tau_{xy} \frac{\partial \bar{z}_B}{\partial \bar{y}} \right) \right\} - \frac{1}{N_B} |\bar{\mathbf{t}}_n| \frac{\partial \bar{z}_B}{\partial \bar{x}}, \\ (\bar{\mathbf{t}}_S)_y &= \frac{1}{N_B} \left\{ \left(-\bar{p} \frac{\partial \bar{z}_S}{\partial \bar{y}} - \tau_{yz} \right) + \varepsilon^2 \left(\sigma_y \frac{\partial \bar{z}_B}{\partial \bar{y}} + \tau_{xy} \frac{\partial \bar{z}_B}{\partial \bar{x}} \right) \right\} - \frac{1}{N_B} |\bar{\mathbf{t}}_n| \frac{\partial \bar{z}_B}{\partial \bar{y}}, \\ |\bar{\mathbf{t}}_n| &= \frac{1}{N_B^2} \left\langle - \left[\bar{p} + \varepsilon^2 \left(\tau_{xz} \frac{\partial \bar{z}_B}{\partial \bar{x}} + \tau_{yz} \frac{\partial \bar{z}_B}{\partial \bar{y}} - \sigma_z \right) \right] \right. \\ &\quad + \left\{ \varepsilon^2 \left(-\bar{p} \frac{\partial \bar{z}_B}{\partial \bar{x}} - \tau_{xz} \right) + \mathcal{O}(\varepsilon^3) \right\} \frac{\partial \bar{z}_B}{\partial \bar{x}} \\ &\quad \left. + \left\{ \varepsilon^2 \left(-\bar{p} \frac{\partial \bar{z}_B}{\partial \bar{y}} - \tau_{yz} \right) + \mathcal{O}(\varepsilon^3) \right\} \frac{\partial \bar{z}_B}{\partial \bar{y}} \right\rangle. \end{aligned} \quad (12.102)$$

Equations (12.93)–(12.102) show that to second order approximation in ε , only ε^0 and ε^2 -terms arise. Only when higher order perturbation solutions $N \geq 3$ are sought, odd order ε terms will arise. So, as long as the SIA and SOSIA solutions are sought, the first order FOSIA can be set identically equal to zero [unless, of course, the basal topography $z = z_B(x, y)$ has small wave length $\mathcal{O}(\varepsilon)$ variations, a case which is generally excluded.]

Specifically, in the SIA the **boundary conditions** are as follows.

(i) At the *free surface* $\bar{z} = \bar{z}_S(\bar{x}, \bar{y}, \bar{t})$:

$$\begin{aligned} \frac{\partial \bar{z}_S}{\partial \bar{t}} + \frac{\partial \bar{z}_S}{\partial \bar{x}} \bar{u} + \frac{\partial \bar{z}_S}{\partial \bar{y}} \bar{v} - \bar{w} &= N_S \bar{a}, \quad N_S = 1, \\ \left. \begin{aligned} \bar{p} \frac{\partial \bar{z}_S}{\partial \bar{x}} + \tau_{xz} &= 0, \\ \bar{p} \frac{\partial \bar{z}_S}{\partial \bar{y}} + \tau_{yz} &= 0, \\ \bar{p} &= 0 \end{aligned} \right\} \text{implying} \left\{ \begin{aligned} \bar{p} &= 0, \\ \tau_{xz} &= 0, \\ \tau_{yz} &= 0, \end{aligned} \right. \quad (12.103) \\ \bar{\kappa}(\theta) \frac{\partial \theta}{\partial \bar{z}} &= N_S (\theta - \theta_A). \end{aligned}$$

(ii) At the *fixed bottom surface* $\bar{z}_B(\bar{x}, \bar{y}) - \bar{z} = 0$ we obtain the sliding condition in the form

$$\begin{aligned} \bar{u}_B &= \mathcal{C}_B \mathcal{F}_B (|\bar{\mathbf{t}}_S|^2, |\bar{\mathbf{t}}_n|^2) \tau_{xz}^B, \\ \bar{v}_B &= \mathcal{C}_B \mathcal{F}_B (|\bar{\mathbf{t}}_S|^2, |\bar{\mathbf{t}}_n|^2) \tau_{yz}^B, \\ \bar{w} &= \bar{u}_B \frac{\partial \bar{z}_B}{\partial \bar{x}} + \bar{v}_B \frac{\partial \bar{z}_B}{\partial \bar{y}}. \end{aligned} \quad (12.104)$$

The classical shallow ice approximation SIA is now governed by Eqs.(12.90)–(12.92), (12.103), (12.104). Integrating the momentum Eq.(12.90)_{2–4}, subject to the boundary conditions (12.103)_{2–4}, yields

$$\begin{aligned}\bar{p}(\bar{x}, \bar{y}, \bar{z}, \bar{t}) &= (\bar{z}_S(\bar{x}, \bar{y}, \bar{t}) - \bar{z}), \\ \bar{\tau}_{xz}(\bar{x}, \bar{y}, \bar{z}, \bar{t}) &= -\frac{\partial \bar{z}_S(\bar{x}, \bar{y}, \bar{t})}{\partial \bar{x}} (\bar{z}_S(\bar{x}, \bar{y}, \bar{t}) - \bar{z}), \\ \bar{\tau}_{yz}(\bar{x}, \bar{y}, \bar{z}, \bar{t}) &= -\frac{\partial \bar{z}_S(\bar{x}, \bar{y}, \bar{t})}{\partial \bar{y}} (\bar{z}_S(\bar{x}, \bar{y}, \bar{t}) - \bar{z}).\end{aligned}\quad (12.105)$$

Assuming that $\theta(\bar{x}, \bar{y}, \bar{z}, \bar{t}) \in \mathcal{D}$ is known, Eq.(12.90)_{6,7} can now be integrated subject to the boundary conditions (12.104). This yields

$$\begin{aligned}\bar{u}(\bar{x}, \bar{y}, \bar{z}, \bar{t}) &= \bar{u}_B(\bar{x}, \bar{y}, \bar{t}) - 2\mathbb{G} \frac{\partial \bar{z}_S}{\partial \bar{x}} \int_{\bar{z}_B(\bar{x}, \bar{y})}^{\bar{z}} \bar{A}(\theta(\bar{x}, \bar{y}, \zeta, \bar{t})) \mathbb{f}(\tau_{II}(\bar{x}, \bar{y}, \zeta, \bar{t})) \\ &\quad \times (\bar{z}(\bar{x}, \bar{y}, \bar{t}) - \zeta) \, d\zeta,\end{aligned}\quad (12.106)$$

$$\begin{aligned}\bar{v}(\bar{x}, \bar{y}, \bar{z}, \bar{t}) &= \bar{v}_B(\bar{x}, \bar{y}, \bar{t}) - 2\mathbb{G} \frac{\partial \bar{z}_S}{\partial \bar{y}} \int_{\bar{z}_B(\bar{x}, \bar{y})}^{\bar{z}} \bar{A}(\theta(\bar{x}, \bar{y}, \zeta, \bar{t})) \mathbb{f}(\tau_{II}(\bar{x}, \bar{y}, \zeta, \bar{t})) \\ &\quad \times (\bar{z}(\bar{x}, \bar{y}, \bar{t}) - \zeta) \, d\zeta,\end{aligned}$$

where

$$\begin{aligned}\bar{u}_B(\bar{x}, \bar{y}, \bar{t}) &= -\mathcal{CF} \left[(\bar{z}_S - \bar{z}_B)^2 \mathcal{F} \left(\left(\frac{\partial \bar{z}_S}{\partial \bar{x}} \right)^2 + \left(\frac{\partial \bar{z}_S}{\partial \bar{y}} \right)^2 \right), (\bar{z}_S - \bar{z}_B)^2 \right] \\ &\quad \times \frac{\partial \bar{z}_S}{\partial \bar{x}} (\bar{z}_S - \bar{z}_B), \\ \bar{v}_B(\bar{x}, \bar{y}, \bar{t}) &= -\mathcal{CF} \left[(\bar{z}_S - \bar{z}_B)^2 \mathcal{F} \left(\left(\frac{\partial \bar{z}_S}{\partial \bar{x}} \right)^2 + \left(\frac{\partial \bar{z}_S}{\partial \bar{y}} \right)^2 \right), (\bar{z}_S - \bar{z}_B)^2 \right] \\ &\quad \times \frac{\partial \bar{z}_S}{\partial \bar{y}} (\bar{z}_S - \bar{z}_B),\end{aligned}\quad (12.107)$$

$$\tau_{II} = \tau_{xz}^2 + \tau_{yz}^2 = (\bar{z}_S(\bar{x}, \bar{y}, \bar{t}) - \zeta)^2 \left(\left(\frac{\partial \bar{z}_S}{\partial \bar{x}} \right)^2 + \left(\frac{\partial \bar{z}_S}{\partial \bar{y}} \right)^2 \right). \quad (12.108)$$

Moreover, the continuity equation (12.90)₁ together with (12.104)₃ allow evaluation of the velocity component \bar{w} as follows:

$$\bar{w}(\bar{x}, \bar{y}, \bar{z}, \bar{t}) = \bar{w}_B(\bar{x}, \bar{y}, \bar{z}_B(\bar{x}(\bar{y}), \bar{t})) - \int_{\bar{z}_B(\bar{x}, \bar{y})}^{\bar{z}} \left(\frac{\partial \bar{u}}{\partial \bar{x}} + \frac{\partial \bar{v}}{\partial \bar{y}} \right) (\bar{x}, \bar{y}, \zeta, \bar{t}) d\zeta. \quad (12.109)$$

Scrutiny of formulae (12.106)–(12.108) shows that the horizontal velocity $\bar{\mathbf{v}}_H = (\bar{u}, \bar{v})$ is structurally given by

$$\bar{\mathbf{v}}_H(\bar{x}, \bar{y}, \bar{z}, \bar{t}) = -\mathfrak{J}(\bar{x}, \bar{y}, \bar{z}, \bar{t}) \text{grad}_H \bar{z}_S(\bar{x}, \bar{y}, \bar{t}), \quad (12.110)$$

in which $\mathfrak{J}(\bar{x}, \bar{y}, \bar{z}, \bar{t})$ is a scalar function, which can simply be inferred from (12.106)–(12.109). This formula gives rise to the following theorem:

Fundamental SIA Theorem

1. At a fixed position (\bar{x}, \bar{y}) the horizontal velocity \mathbf{v}_H points in the direction of *steepest descent* at all depths $\bar{z}_B \leq \bar{z} \leq \bar{z}_S$. In other words, in a vertical bore hole, the velocity \mathbf{v}_H does not rotate around the vertical bore hole axis when one moves down the hole.
2. Positions of zero horizontal velocity agree with positions of horizontal tangent planes of the surface $\bar{z} = \bar{z}_S(\bar{x}, \bar{y}, \bar{t})$. In three dimensions these are positions of **domes** or **troughs** or saddle points; in two dimensions, these positions are **ice divides**.
3. Since the flow in the vicinity of troughs is towards the trough minimum, such depressions are filled with time. Troughs are unsteady features of the surface topography.
4. Vertical surfaces through crests are separating surfaces of **cryological or hydrological basins**, i.e., there is no flow of ice across such surfaces. The ice velocity vector is strictly within the vertical surface crest.

If any observations are not in conformity with the statements of this fundamental theorem, then the prerequisites of the SIA do not hold. One such condition would be non-isotropic sliding,¹⁴ in which sliding velocity and basal shear traction would not be collinear. Interpreted this with different emphasis we can state that *in the SIA the basal velocity is always pointing in the direction of the free surface slope, no matter how the basal surface is oriented.*

It is evident that in the evaluation of the stresses (12.105)_{2,3} and the velocity components (12.106)–(12.109) only algebraic and differential operations and quadrature formulae are involved. With these variables being determined the thermal boundary value problem is given by (12.90)₅, (12.93)₅, (12.96)₄, or

¹⁴For instance, if the basal interface would be a ‘corrugated sheet’, the basal drag coefficient would be orthogonal, i.e. different parallel and orthogonal to the sheet orientation.

$$\begin{aligned}
\bar{c}(\theta) \left\{ \frac{\partial \theta}{\partial \bar{t}} + \frac{\partial \theta}{\partial \bar{x}} \bar{u} + \frac{\partial \theta}{\partial \bar{y}} \bar{v} + \frac{\partial \theta}{\partial \bar{z}} \bar{w} \right\} &= \mathbb{D} \frac{\partial}{\partial \bar{z}} \left(\bar{\kappa} \frac{\partial \theta}{\partial \bar{z}} \right) + 2\mathbb{E} \bar{A} \mathbb{f}(\tau_{II}) \tau_{II}, \quad \text{in } \mathcal{D}, \\
\bar{\kappa} \frac{\partial \theta}{\partial \bar{z}} &= \mathbb{N}_S(\theta - \theta_A), \quad \text{on } \bar{z} = \bar{z}_S, \\
\bar{\kappa} \frac{\partial \theta}{\partial \bar{z}} &= \mathbb{N}_B(\theta - \theta_G), \quad \text{on } \bar{z} = \bar{z}_B.
\end{aligned} \tag{12.111}$$

This boundary value problem for θ is generally non-linear in all terms of the field equations and boundary conditions. However, when \bar{c} and $\bar{\kappa}$ are constants, the only nonlinearity is in the reaction term $\bar{A}(\theta)$, which for an ARRHENIUS parameterization is exponential. In any case, for given $\bar{z} = \bar{z}_S(\bar{x}, \bar{y}, \bar{t})$ and $\bar{z} = \bar{z}_B(\bar{x}, \bar{y})$, the boundary value problem (12.111) is solvable, at least numerically.

The next step is to perform a forward integration step in time of the geometry of the moving mass. To this end the continuity equation (12.90)₁ is integrated over depth from $\bar{z} = \bar{z}_B(\bar{x}, \bar{y})$ to $\bar{z} = \bar{z}_S(\bar{x}, \bar{y}, \bar{t})$, thereby incorporating the kinematic surface equations (12.93)₁ and (12.96)₃. This computation parallels that derived to obtain (12.31). The result is

$$\frac{\partial \bar{z}_S}{\partial \bar{t}} + \frac{\partial \bar{Q}_x}{\partial \bar{x}} + \frac{\partial \bar{Q}_y}{\partial \bar{y}} = N_S \bar{a}, \tag{12.112}$$

(this equation is exact!) with

$$\begin{aligned}
\bar{Q}_x(\bar{x}, \bar{y}, \bar{t}) &:= \bar{u}_B(\bar{x}, \bar{y}, \bar{t}) (\bar{z}_S(\bar{x}, \bar{y}, \bar{t}) - \bar{z}_B(\bar{x}, \bar{y})) \\
&\quad - 2\mathbb{G} \frac{\partial \bar{z}_S}{\partial \bar{x}} \int_{\bar{z}_B}^{\bar{z}_S} d\bar{z} \int_{\bar{z}_B}^{\bar{z}} \bar{A}(\theta(\bar{x}, \bar{y}, \zeta, \bar{t})) \mathbb{f}(\tau_{II}(\cdot, \zeta)) (\bar{z}_S(\bar{x}, \bar{y}, \bar{t}) - \zeta) d\zeta \\
&= \bar{u}_B(\bar{x}, \bar{y}, \bar{t}) (\bar{z}_S(\bar{x}, \bar{y}, \bar{t}) - \bar{z}_B(\bar{x}, \bar{y})) \\
&\quad - 2\mathbb{G} \frac{\partial \bar{z}_S(\bar{x}, \bar{y}, \bar{t})}{\partial \bar{x}} \int_{\bar{z}_B}^{\bar{z}_S} (\bar{z}_S(\bar{x}, \bar{y}, \bar{t}) - \bar{z})^2 \bar{A}(\theta(\bar{x}, \bar{y}, \zeta, \bar{t})) \mathbb{f}(\tau_{II}(\cdot, \bar{z})) d\bar{z},
\end{aligned} \tag{12.113}$$

$$\begin{aligned}
\bar{Q}_y(\bar{x}, \bar{y}, \bar{t}) &:= \bar{v}_B(\bar{x}, \bar{y}, \bar{t}) (\bar{z}_S(\bar{x}, \bar{y}, \bar{t}) - \bar{z}_B(\bar{x}, \bar{y})) \\
&\quad - 2\mathbb{G} \frac{\partial \bar{z}_S(\bar{x}, \bar{y}, \bar{t})}{\partial \bar{y}} \int_{\bar{z}_B}^{\bar{z}_S} (\bar{z}_S(\bar{x}, \bar{y}, \bar{t}) - \bar{z})^2 \bar{A}(\theta(\bar{x}, \bar{y}, \zeta, \bar{t})) \mathbb{f}(\tau_{II}(\cdot, \bar{z})) d\bar{z}.
\end{aligned} \tag{12.114}$$

Using integration by parts, the double integral in (12.113) has been transformed into a single integral. Moreover, it is easily seen that

$$\begin{aligned}\bar{Q}_x &= \tilde{Q}_x \left(\bar{z}(\bar{x}, \bar{y}, \bar{t}), \frac{\partial \bar{z}_S(\bar{x}, \bar{y}, \bar{t})}{\partial \bar{x}}, \frac{\partial \bar{z}_S(\bar{x}, \bar{y}, \bar{t})}{\partial \bar{y}} \right), \\ \bar{Q}_y &= \tilde{Q}_y \left(\bar{z}(\bar{x}, \bar{y}, \bar{t}), \frac{\partial \bar{z}_S(\bar{x}, \bar{y}, \bar{t})}{\partial \bar{x}}, \frac{\partial \bar{z}_S(\bar{x}, \bar{y}, \bar{t})}{\partial \bar{y}} \right).\end{aligned}\tag{12.115}$$

This, together with (12.112), implies the evolution equation

$$\begin{aligned}& \frac{\partial \bar{z}_S}{\partial \bar{t}} + \frac{\partial \tilde{Q}_x}{\partial \bar{z}_S} \frac{\partial \bar{z}_S}{\partial \bar{x}} + \frac{\partial \tilde{Q}_y}{\partial \bar{z}_S} \frac{\partial \bar{z}_S}{\partial \bar{y}} \\ & - \left\{ \frac{\partial \tilde{Q}_x}{\partial (\partial \bar{z}_S / \partial \bar{x})} \frac{\partial^2 \bar{z}_S}{\partial \bar{x}^2} + \left(\frac{\partial \tilde{Q}_x}{\partial (\partial \bar{z}_S / \partial \bar{y})} + \frac{\partial \tilde{Q}_y}{\partial (\partial \bar{z}_S / \partial \bar{x})} \right) \frac{\partial^2 \bar{z}_S}{\partial \bar{x} \partial \bar{y}} \right. \\ & \quad \left. + \frac{\partial \tilde{Q}_y}{\partial (\partial \bar{z}_S / \partial \bar{y})} \frac{\partial^2 \bar{z}_S}{\partial \bar{y}^2} \right\} \\ & = N_S \bar{a}\end{aligned}\tag{12.116}$$

for the surface. It provides information about the detailed structure of (12.112). In a numerical program, in which \bar{Q}_x and \bar{Q}_y are computed in a finite difference grid, it is certainly more direct to compute $\Delta \bar{z}_S / \Delta \bar{t}$ in a forward time step from (12.112) rather than from (12.116). This yields the new free surface $\bar{z}_S(\bar{x}, \bar{y}, \bar{t} + \Delta \bar{t})$ as $\bar{z}_S(\bar{x}, \bar{y}, \bar{t}) + \Delta \bar{z}_S$ and thus fixes the conditions for the next step forward in time. With the new geometry computations can be started again at time $\bar{t} + \Delta \bar{t}$ with the determination of the stresses $\{\bar{p}, \tau_{xz}, \tau_{yz}\}$ by using (12.105) the velocity components $\{\bar{u}, \bar{v}, \bar{w}\}$ with (12.106)–(12.109), the updated temperature field (12.111) and $\Delta \bar{z}_S$, etc. This principal procedure is applied as such in quite a number of software programs, which were developed in the last decade of the 20th century. Early pioneers having done this are K. HERTERICH et al. [50], R. CALOV [7–9], P. HUYBRECHTS [46] and R. GREVE [23] and others. Today’s software incorporates besides *cold ice* (i.e. ice of which the temperature distribution is below the melting point) also *temperate ice* (with the temperature exactly at the melting point), which are separated by a singular surface which operates as a so-called STEFAN surface at which ice may melt or water may freeze. The SIA formulation for such polythermal ice is structurally analogous to the SIA without phase changes; for literature on this see HUTTER [38, 39, 41, 45], GREVE [23–25, 27]. An open source program due to RALF GREVE bears the name SICOPOLIS (for **S**imulation **C**ode for **P**olythermal **I**ce **S**heets) and has been applied in many scenarios of climate reconstructions of the large ice sheets on Earth through the last ice ages and for prognostic views into hundred and more years of ice sheets subject to different climate scenarios. The newest version of SICOPOLIS is complemented by an ice-shelf module¹⁵ to make it applicable to Antarctica, which is surrounded by two large and many smaller ice shelves, SATO [60], SATO and GREVE [61].

¹⁵For the theory of ice shelves see MAGNUS WEIS et al. (1999) [67].

Before turning to applications mention should be made of the fact that equations (12.91) were not used in establishing the zeroth order SIA-solutions. It is interesting that exactly these terms provide indications as to the possible limitation of the zeroth order SIA, terms which are not contributing at all to the solutions (12.106)–(12.109). In fact, these formulae allow evaluation of $\sigma_x, \sigma_y, \sigma_z, \tau_{xy}$ as follows:

$$\{\sigma_x, \sigma_y, \sigma_z, \tau_{xy}\} = \frac{\left\{ \frac{\partial \bar{u}}{\partial \bar{x}}, \frac{\partial \bar{v}}{\partial \bar{y}}, \frac{\partial \bar{w}}{\partial \bar{z}}, \frac{1}{2} \left(\frac{\partial \bar{u}}{\partial \bar{y}} + \frac{\partial \bar{v}}{\partial \bar{x}} \right) \right\}}{\mathbb{G} \bar{A}(\theta) \mathbb{f}(\tau_{II})}. \quad (12.117)$$

Critical in this formula is the creep response function $\mathbb{f}(\tau_{II})$ with the second stress deviator invariant τ_{II} given in (12.92) as argument. At a dome, ice divide and on the free surface $\tau_{II} = 0$, since $(\tau_{xz}, \tau_{yz}) = (0, 0)$; so, if $\mathbb{f}(0) = 0$, then the stresses (12.117) are infinitely large at these positions in this case. A finite viscosity law has $\mathbb{f}(0) \neq 0$, for which the above stresses remain regular at a dome, divide and on the free surface. This was already spelled out and consequences discussed in Chap. 7 Sect. 7.4 and Fig. 7.32.

12.8.2 Applications

(a) Plane steady ice sheet flow. The first applications of the SIA-equations were restricted to plane ice flow in two dimensions and to steady state. LESLIE W. MORLAND and GEORGE SMITH (1984) [55] prescribed the temperature distribution within the ice according to (12.72)–(12.74). They chose $[H] = 2000$ m, $[L] = 400$ km ($\varepsilon = 0.005$) and employed an accumulation pattern given by

$$\bar{a} = \begin{cases} 12.5 (\bar{z}_S - \bar{h}_e) \frac{\bar{h}_e}{\bar{h}_e^0} & (\bar{z}_S < \bar{h}_e), \\ \left\{ 12.5(\bar{z}_S - \bar{h}_e) - 76(\bar{z}_S - \bar{h}_e)^2 \right. \\ \left. + 136(\bar{z}_S - \bar{h}_e)^3 \right\} \frac{\bar{h}_e}{\bar{h}_e^0} & (\bar{h}_e \leq \bar{z}_S \leq \bar{h}_e + 0.25), \\ 0.5 \frac{\bar{h}_e}{\bar{h}_e^0} & (\bar{z}_S \geq \bar{h}_e + 0.25), \end{cases} \quad (12.118)$$

with $\bar{h}_e^0 = \bar{h}_e = 1$ and $[H] = 1000$ m the ‘equilibrium height’. In general $\bar{h}_e = \bar{h}_e(\bar{x}, \bar{y})$, but MORLAND and SMITH chose $\bar{h}_e = \text{const.} = 1$. Equation (12.118) corresponds to a linear decrease of the surface melting with height, if $\bar{z}_S < \bar{h}_e$, a cubic growth of precipitation for $\bar{h}_e \leq \bar{z}_S \leq \bar{h}_e + 0.25$ and a constant value of snow accumulation above $\bar{h}_e + 0.25$. MORLAND and SMITH chose the surface temperature to decrease 0.8 K per 100 m and the vertical atmospheric surface temperature gradient to vanish, corresponding to zero heat loss at the surface. Alternative values of $-(1-2.5)$ K per 100 m are assumed for the vertical temperature gradient at the base,

reflecting respective geothermal heat fluxes of $(0.8-2.0) \times 10^6 \text{ J m}^{-2} \text{ a}^{-1}$, if frictional heating and dissipation are negligible at the base.

These choices specifically led

- at the *free surface* to

$$T_S = T_M - 16 \text{ (K)} \bar{h}(\bar{\xi}), \quad \frac{dT_S}{d\bar{y}} = 0, \quad \bar{\xi} = \varepsilon \bar{x}, \quad (12.119)$$

where T_M is the margin temperature by choice of the margin as coordinate origin and

- at the *basal surface* to

$$\frac{dT_b}{d\bar{y}} = -20 \text{ K}, \quad T_M = (-2, -6) \text{ }^\circ\text{C}. \quad (12.120)$$

Figures 12.13 and **12.14** display computational results ‘for uniform bed temperatures $T_b = -2 \text{ }^\circ\text{C}$ and $T_b = -6 \text{ }^\circ\text{C}$ in the prescribed temperature pattern. The temperature variation with height at three sections, together with the resulting profile, basal velocity and relative longitudinal velocity at three sections, are shown [...]. For the moderately warmer bed (Fig. 12.13) the temperature influence on the rate factor is reflected by the increased differential motion, but there is negligible change of span and only a modest decrease in maximum thickness in comparison with Fig. 12.14 [...]. The change of the velocity distribution accompanying the temperature variation influences the large scale features significantly. Moreover, the enhanced velocity gradients extend well beyond a negligible boundary layer’, [55].

The most significant inferences that can be drawn from the MORLAND-SMITH analysis in steady state is as follows:

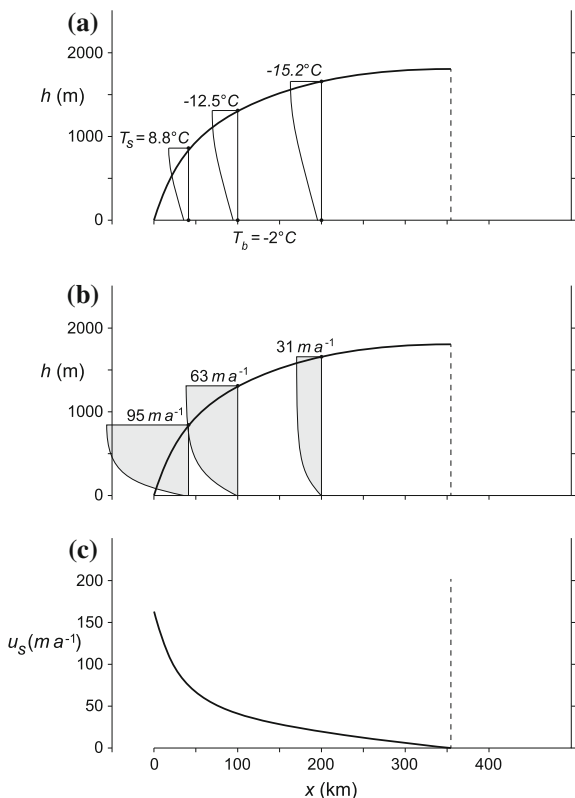
1. The flow pattern obtained with realistic temperature distributions are vastly different from corresponding steady patterns in the ice sheet that are subjected to isothermal conditions.
2. The enhanced velocity gradients in the warmer basal regions (of the temperature patterns considered) do not include a high shear rate boundary layer with negligible shear rate through the bulk flow. That is, *the viscous response of the ice is not confined, in general, to a thin boundary layer.*

A second, more complete study of the steady response of the two-dimensional SIA equations is due to SIDNEY YAKOWITZ et al. (1985) [68] and K. HUTTER et al. (1986) [44]. In their computations the temperature distribution was not prescribed but computed along with the ice sheet profile, the velocity distribution (u, v, w) and the general flow pattern. So, in these computations the temperature distribution satisfies the heat equation together with the thermal boundary conditions, [55] at the free and basal surfaces.

HUTTER et al. [44] chose MORLAND and SMITH’s [55] accumulation function (12.118) with

$$\bar{h}_e = \bar{h}_e^0 (1 - p_1 \bar{x} - p_2 \bar{x}^2) \quad (12.121)$$

Fig. 12.13 Steady state ice sheet flows with prescribed temperature distribution. Solution for temperature variation with uniform bed temperature $T_b = -2^\circ\text{C}$: **a** profile and temperature variation; **b** longitudinal velocities relative to the basal velocity; **c** basal velocity distribution, redrawn from [55] with changes



and a simplified version of it, namely

$$\bar{a} = \begin{cases} a(\bar{z}_S - \bar{h}_e), & \left(\bar{z}_S < \bar{h}_e + \frac{b}{a} \frac{\bar{h}_e}{\bar{h}_e^0} \right), \\ b \frac{\bar{h}_e}{\bar{h}_e^0}, & \left(\bar{z}_S > \bar{h}_e + \frac{b}{a} \frac{\bar{h}_e}{\bar{h}_e^0} \right), \end{cases} \quad (12.122)$$

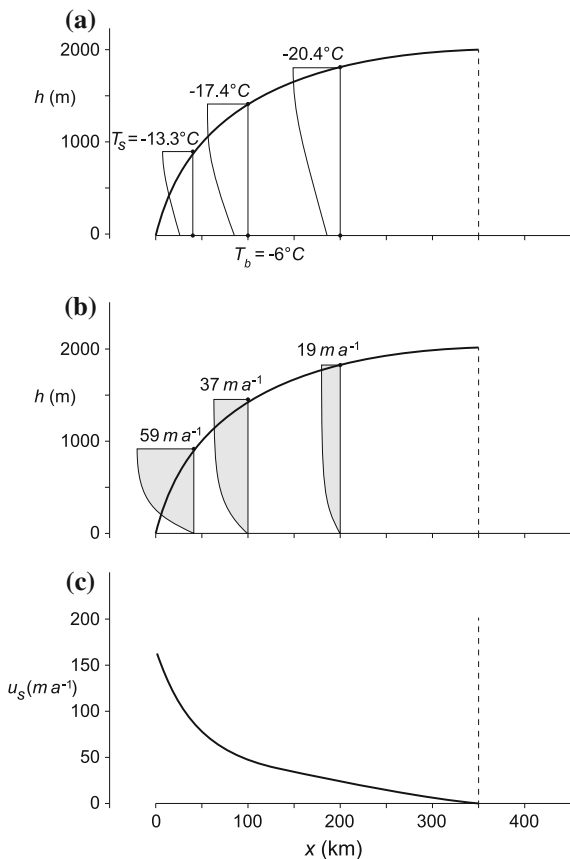
Furthermore, the surface temperature in $^\circ\text{C}$ is parameterized as

$$T_S = T_M - T_M^{(1)} \bar{z}_S - T_M^{(2)} \bar{x}. \quad (12.123)$$

In these formulae $\bar{x} = 0$ marks the ice divide and the parameters have the values

$$\begin{aligned} -40^\circ\text{C} \leq T_M \leq 0^\circ\text{C}, & \quad 0^\circ\text{C} \leq T_M^{(1)} \leq 2^\circ\text{C}, & \quad 0^\circ\text{C} \leq T_M^{(2)} \leq 2^\circ\text{C}, \\ 0.375 \leq \bar{h}_e^0 \leq 0.75, & \quad 0 \leq p_1 \ll 0.15, & \quad 0 < p_2 \ll 0.1. \end{aligned} \quad (12.124)$$

Fig. 12.14 Steady state ice sheet flows with prescribed temperature distribution. Solution for temperature variation with uniform bed temperature $T_b = -6^\circ\text{C}$: **a** profile and temperature variation; **b** longitudinal velocities relative to the basal velocity; **c** basal velocity distribution, redrawn from [55] with changes



Moreover, at the flat basal surface, $\bar{z}_b = 0$, a constant heat flow was imposed according to

$$\theta_z = \frac{G_0[H]}{[20 \text{ K}]}, \quad \text{with } 0 \leq \theta_z < 10, \tag{12.125}$$

in which G_0 is the geothermal temperature gradient, typically $1^\circ\text{K}/100 \text{ m} = 10^{-2} \text{ }^\circ\text{K m}^{-2}$ (implying for $[H] = 2000 \text{ m}$, $\theta_z = 1$).

Figure 12.15 summarizes the results of a typical run for conditions described in the figure legend. ‘In this figure the top two graphs (panels a and b) display the temperature distribution in the form of isotherms and vertical profiles, respectively. They show the pattern one would expect, given the available data from observations and earlier approximate models [...]. Figure 12.15d–f summarize the results obtained for the dimensionless velocity distribution. Graph (c) shows vertical profiles for the longitudinal velocity U , graph (d) the difference between U and the sliding velocity U_B , characterizing the flow component due to viscous deformation. This difference will be called gliding velocity. In view of the scales shown as insets on these graphs,

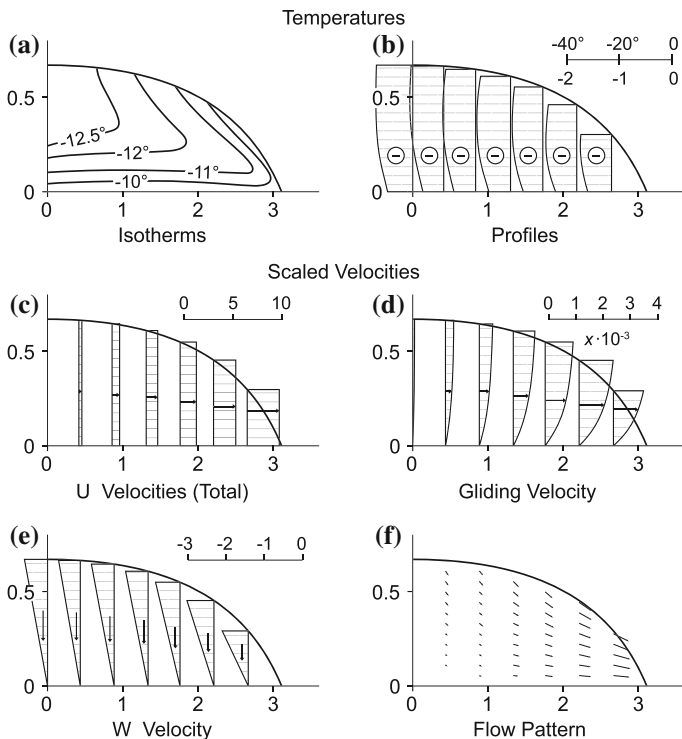


Fig. 12.15 Steady-state temperature distribution and flow pattern. Distributions of the temperature and (scaled) velocities for computations using $\bar{h}_e^0 = 0.5$, $p_1 = 0.1$, $p_2 = 0$, $T_M = -2^\circ\text{C}$, $T_M^{(1)} = -16^\circ\text{C}$, $T_M^{(2)} = 0.2^\circ\text{C}$. The temperature distribution, indicated in $^\circ\text{C}$, is shown for the top two graphs, **a** displaying a few selected isotherms, and **b** showing vertical profiles with the temperature scale drawn as an inset. The plots **c–f** depict the non-dimensional and scaled velocities. The first figure **c** shows vertical profiles of the total horizontal velocity; figure **d** shows the same profiles for the difference $(U - U_B)$, called gliding velocity, while figure **e** gives vertical profiles of the vertical velocity W . Dimensionless scales for all three are given as insets. Finally, figure **f** gives the vector plot for the velocities, indicating the flow pattern within the ice sheet. Scales are not indicated, from HUTTER et al. [44], © J. Glaciology, reproduced with changes

we see that the gliding velocity is approximately 0.5% or less of the sliding velocity [...]. Note the continuous growth of the gliding velocity as one moves upwards away from the bed. This behavior is, of course, corroboration that the applied software has produced reliable results beyond two places of accuracy’ [44].

‘Figure 12.15e displays vertical profiles of the dimensionless vertical velocity. The linear profile has often been conjectured in glaciology and was first used by GORDEN ROBIN [16] to explain the contribution of vertical convection to the temperature distribution. Here, it is a proven result of the computation [but it is theoretically not compelling]. Notice also that [the vertical velocity] W is downwards everywhere, including the ablation zone, contrary to what one might expect’.

‘The flow pattern along the free surface is still as expected, namely *into* the ice within the ablation zone. This is demonstrated in Fig. 12.15f, which is a vector plot of the velocity distribution [...] that gives a fairly reliable view of the streamline pattern’, [44].

The temperature distribution within the ice sheet is mainly governed by the relative weights of diffusion versus vertical convection (compare graphs a & b of Fig. 12.15 with graphs a & b and c & d in Fig. 12.16, respectively). ‘In this figure, α is a measure for vertical convection and β for vertical diffusion. Evidently, when β is small, vertical convection dominates, vertical temperature profiles change slowly in the upper part of the ice sheet but relatively quickly close to the base, [44]. The boundary layer can clearly be seen (Fig. 12.15 [...]). One detail in these temperature distributions should be emphasized; over most of the ice sheet the temperature profile for fixed \bar{x} shows an inversion; in other words, along a vertical line, the temperature is coldest not at the surface but at a certain depth [...]. The location of the inversion point relative to the surface varies with position (it is close to the surface towards the snout). Its existence is to a large extent the result of the fact that thermal diffusivities are small. Figure 12.16 corroborates this statement. When $\beta = 0.1$ (top of Fig. 12.16), vertical temperature profiles are still curved but more tapered than seen from the isotherm plots. The basal boundary layer has disappeared, advection no longer dominates over diffusion but both compete with comparable amounts. Finally, when $\beta = 1$ (bottom of Fig. 12.16) diffusion over-rides advection. This is why isotherms are essentially horizontal and temperature profiles linear in this case’, [44].

HUTTER et al. [44] present a whole range of applications, in which the external forcing (accumulation rate, surface temperature; geothermal heat) and internal parameters (basal sliding; rate factor, creep response function) are varied. As an example, Fig. 12.17 displays isotherm depth plots for varied accumulation functions according to Eq. (12.122) for parameters a and b as indicated as insets in the figure. The three accumulation functions are nearly equal but the isotherm plots in Fig. 12.17 indicate considerably different temperature distributions as is well seen from the isotherms close to the base.

(b) The SIA applied to the Greenland ice sheet. The SIA has been applied to the larger ice sheets on Earth, (i) to obtain the present day geometry, velocity and temperature distributions by integrating the SIA equation. Early computational attempts are given in [7–9, 25, 29, 30, 44, 66]. RALF GREVE and UTE C. HERZFELD (2013) [28] performed computations subject to the following condition:

- Realistic initial conditions at pre-Eemian times (before $\approx 175,000$ years) and responding to reasonable parameterizations of the precipitation/melting scenarios at the moving and deforming free surface through the ice age(s) until the present time.
- Incorporated in this model must be polythermal modules, separately accounted for cold and temperate ice with their equations, in disjoint domains, which join at the **cold-temperate-transition surface** at which the CLAUSIUS–CLAPEYRON behavior must hold, [23–25, 27, 29, 38, 39, 41, 45].

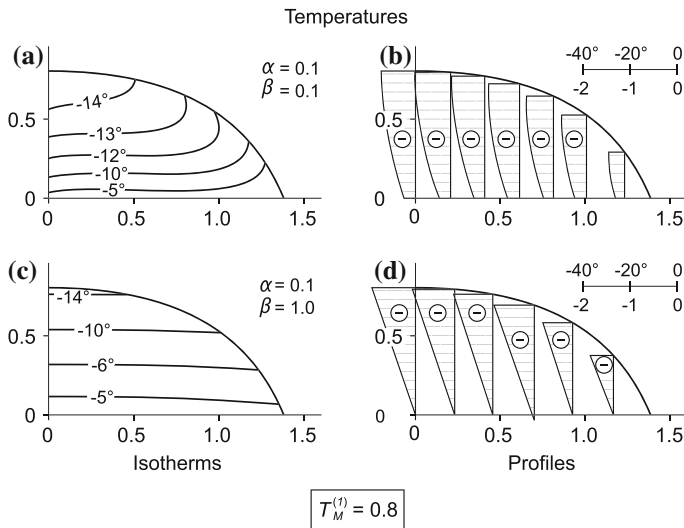


Fig. 12.16 Temperature distribution under steady flow conditions. In the computations the accumulation rate function (12.118) was used with $\tilde{h}_e^0 = 0.5$, $p_1 = 0.1$, $p_{(2)} = 0$, $T_M = -20^\circ\text{C}$, $T_M^{(1)} = 16^\circ\text{C}$ and $T_M^{(2)} = 0^\circ\text{C}$. The two coefficients α and β are defined as

$$\alpha = \frac{g[H]}{c_p \Delta T}, \quad \beta = \frac{\lambda}{\rho c_p [H][W]}$$

and are measures for convection and vertical diffusion, respectively. Here: $g = 9.81 \text{ m s}^{-2}$, $c_p = 2 \times 10^3 \text{ m}^2 \text{ s}^{-2} \text{ K}^{-1}$, $\lambda = 2.2 \text{ N kg}^{-1} \text{ K}^{-1}$, $\rho = 910 \text{ kg m}^{-3}$, $[H] = 500\text{--}3000 \text{ m}$, $\Delta T = 20 \text{ K}$, $[W] = 1 \text{ m a}^{-1}$, from HUTTER et al. [44], © J. Glaciology, reproduced with changes

- Because the heavy weights of the large ice sheets deform the solid earth on which they sit, the isostatic depression and rebound of the lithosphere due to the changing ice load must be evaluated along with the varied mass distribution of the sheet. Early models employed a relaxation type response of lithosphere pillars into the asthenosphere, [7, 8]. R. GREVE and U.C. HERZFELD [28] apply the elastic-lithosphere relaxing-asthenosphere approach due to E. LE MEUR and PHILIPPE HUYNBRECHTS [51] or R. GREVE [26]. This models the lithosphere as a viscoelastic plate (or shell).
- Of significance is the digital elevation model of the present day topography of the Greenland ice sheet. Early models used a 40 km grid; today's ice sheet data by J.L. BAMBER et al. (2001) [4] have grid spacing of 5 km. This is still not sufficiently fine to capture local morphological features such as deep canyons and canyon systems. HERZFELD et al. [35, 36] devised an algorithm for preserving important sub-scale morphologic features at grids of lower resolution. In the model computations of R. GREVE and U.C. HERZFELD [28] these sub-scale features are incorporated into the 5 km grid of J.L. BAMBER et al. [4].

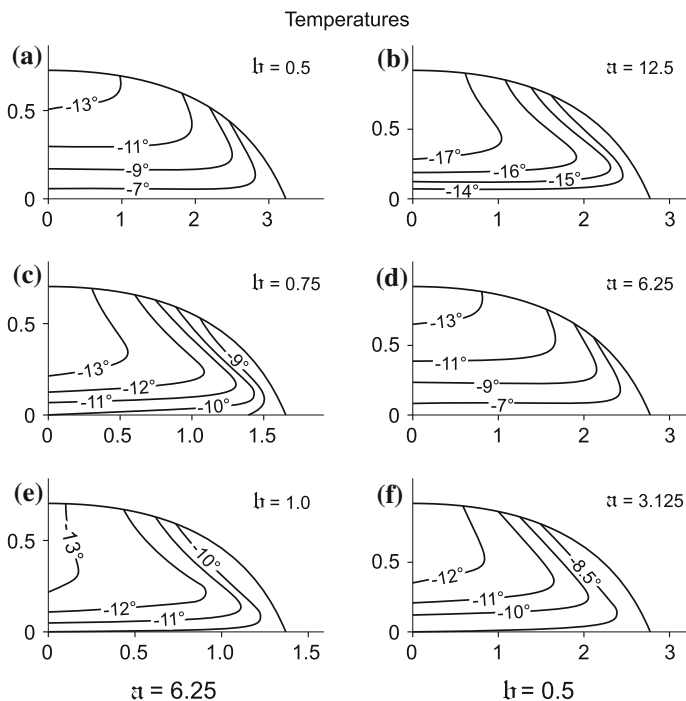


Fig. 12.17 Isotherm distribution for different surface accumulation functions. An explanation of the considerable temperature change with accumulation. Shown are isotherm plots determined by using the accumulation function (12.122). Thermal and basal conditions are the same as for Fig. 12.15. Panels **a, c, e** (left) show the isotherm distributions when the parameter b is varied; figures **b, d, f** show those when α is varied, from HUTTER et al. [44] © J. Glaciology, reproduced with changes

The remaining details of the model, how the climate input is modeled and the ‘spin-up’ of the model reaches acceptable initial pre-Eemian geometry, temperature and velocity distributions as well as the integration to the present time are described in sufficient details in [28]. Here, we confine attention to a comparison of the present day features of the computed Greenland ice sheet and compare it with corresponding features, obtained from the present day observations.

‘The result of the paleo-climatic spin-up run at the highest resolution of 5 km [...] for the present [time] are shown in **Fig. 12.18**. Comparison of the simulated (panel a) and observed (panel b; data by I. JOUGHIN et al. 2010 [48]) surface velocities reveals that the general pattern with the low-velocity (<10 m/year) ‘backbone’, the general acceleration towards the coast and the organization into drainage systems is reproduced very well. The most conspicuous discrepancy is in the region of the northeast Greenland ice stream (NEGIS), which appears only very weakly in the simulation.

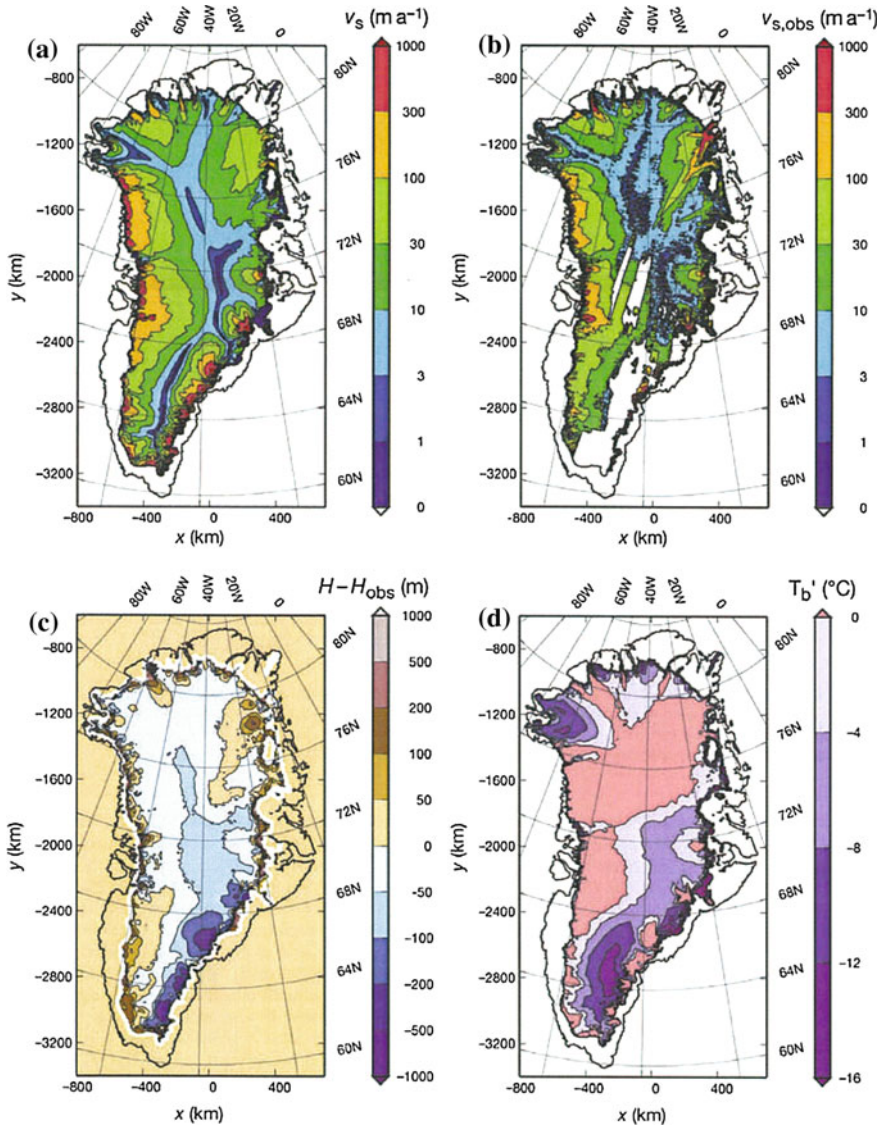


Fig. 12.18 Results of the paleo-climatic spin-up of the Greenland Ice Sheet at 5 km resolution over 150,000 years. **a** Simulated v_s and **b** (observed $v_{s,obs}$; JOUGHIN et al. 2010 [48]) present-day surface velocities. **c** Difference of simulated (h) and observed (h_{obs}) present-day ice thicknesses **d** simulated present-day basal temperature relative to pressure melting. From [28] © *Annals of Glaciology*, reproduced with changes

This is reflected in the difference of simulated and observed ice thicknesses (panel c). This misfit is generally small (<100 m) due to the fixed-topography constraint during most of the spin-up run. However, some areas stick out, and one

Table 12.5 Basal temperatures at the four positions of ice drill sites in Greenland, computed by GREVE and HERZFELD [28] and measured according to the listed references

Site	Computed basal temperature [°C]	Measured basal temperature [°C]	References
GRIP	−8.66	−8.56	Dansgaard et al. (1993) [15]
			Dahl-Jensen et al. (1998) [12]
North GRIP	−2.64 (pressure melting)	−2.4	Dahl-Jensen et al. (2003) [13]
			North GRIP members (2004) [57]
Camp century	−13.96	−13.00	Dansgaard et al. (1969) [14]
			Gundestrup et al. (1987, 1993) [32, 33]
Dye 3	−14.08	−13.22	Gundestrup & Handsen (1984) [31]

of them is the NEGIS area, where simulated ice thicknesses are too large as a consequence of the under-predicted drainage towards the coast. The same holds for the area of PETERMANN Glacier in the northwest. In contrast, along the southeastern ice margin simulated ice thicknesses are generally too small, which may be due to over-predicted ice flow (difficult to judge because of gaps in the observational coverage) or inaccuracies in the surface mass balance. Most of the rapid topographic adjustments that lead to these local misfits arise early during the short transient run [...] over 100 years at the end of the spin-up sequence. After these 100 years, the ice-sheet geometry has largely stabilized, and no spurious rapid adjustments occur in the future-climate runs [...].’ [28].

‘Basal temperatures (panel d) are at the pressure-melting point for $\approx 44\%$ of the ice covered area, including all major draining basins’. At the ice core sites, the computed basal temperatures agree very well with those measured (**Table 12.5**). R. GREVE and U.C. HERZFELD say that the good agreement is mainly due to the choice of the geothermal heat flux. They also analyze the surface velocities, particularly in the vicinity of linear deep troughs. From the results obtained at 20, 10 and 5 km resolutions it becomes apparent that the 5 km resolution performs best, but still not sufficiently satisfactorily, consult [28].

(c) Shallow flow approximations—research into the future. Antarctica is the largest ice mass on Earth consisting of a grounded shallow portion to which a number of floating **ice shelves** is attached; its two largest ones are the Ross Ice Shelf and the Rønne-Filchner Ice Shelf, more than 1000 km in horizontal extent and of varied depth between 50 to less than 2000 m thickness. To first order approximation ice shelves behave like **viscous membranes**, which are, via ice streams, nourished by the inland ice and wasted by the calving processes at their fronts. In the vicinity of the **grounding line** at the sheet-shelf transition, they exert a buttress to the sheet, which affects the flow from the sheet to the shelf; so, sheet and shelf are dynamically coupled. In addition, Antarctica has relatively large portions of temperate ice and needs to be treated as a polythermal ice mass.

In spite of these complexities, early attempts to the understanding of the dynamics of Antarctica ignored the shelves or used an extremely simple patching-together model and employed the SIA by restricting Antarctica to the grounded portion, see [10, 34, 46]. A physically acceptable model for ice masses with sheet-shelf combinations must employ the shallow flow approximations for the grounded portion(s)—these are the SIA and SOSIA—and the corresponding approximations for the shelves—these are the **shallow shelf approximation, SSA** and the **second order shallow shelf approximation, SOSSA**. The theoretical basis for these approximations is given by DAMBARU BARAL (1999) [5], who delivers systematic derivations of the SIA, SOSIA for grounded ice sheets as well as of the SSA, SOSSA for floating shelves. D. BARAL, K. HUTTER and R. GREVE (2001) [6] present the asymptotic theory for sheets, M. WEIS, R. GREVE and K. HUTTER (1999) re-iterate on the SSA. The SOSSA is so far only available in [5].

A first analysis beyond these limited computations has been presented by EGHOLM et al. (2011) [17]. Work at greater depth by AHLKRONA et al. (2013) [1, 2] compares various asymptotic results (including SIA and SOSIA) with those from a STOKES model (ELMER [18]). It is found that the regular perturbation of the SIA and SOSIA gloss over the high viscosity boundary layer (in the inner regions near the free surface and the vicinity of domes and divides) as mentioned in plane flows by JOHNSON & MCMEEKING (1984) [47] and in three dimensional flow by SCHOOF and HINDMARSH (2010) [62].

Reliable computations of sheet-shelf combinations with equations of the shallow flow approximations are given by SATO (2012) [60] in his dissertation and a brief account by SATO and GREVE (2012) [61]. Their technique is to patch together the SIA- and SSA-equations at the grounding line. Systematically, this is not possible with the SIA-SSA equations alone as explained by KIRCHNER et al. (2011) [49]. For a consistent asymptotic matching of the sheet and shelf dynamics the higher order models SOSIA-SOSSA are the least order models which must be applied. Preliminary work by KIRCHNER et al. (2011) [49] and work in progress by AHLKRONA, KIRCHNER and LÖTSTEDT (personal communication, 2014) suggests that the grounding line sheet-shelf transition requires more than a regular straightforward SOSIA-SOSSA matching procedure.

12.9 Discussion and Conclusions

This chapter has been devoted to systematic derivations of approximate models of gravity driven free surface creeping flows of very viscous fluid-like materials, which are initially, or develop with time into, shallow geometries. The physical circumstances were motivated by creeping soil on mountain slopes, which may move several centimeters to meters per year, or by the moving of large ice masses sitting on solid ground such as glaciers in mountainous territory or ice sheets covering large areas or even continents, such as piedmont glaciers and the Greenland ice sheet and Antarctica. The physics of such flows is graphically illustrated in Fig. 12.3; the flow

pattern is dictated primarily by the hydrostatic pressure. Scrutiny of the governing equations indicates that the mean slope angle of the basal topography is crucial in developing approximate model equations. This difference is quantified by the differences in scaling analyses, in which the sinus of the mean slope angle enters the characteristic dimensionless quantities such as the FROUDE number, when the flow is down steep slopes, but is missing, when the fluid-like mass moves on horizontal topography (see (12.18) and (12.87)). This different scaling procedure has led to distinct approximations. It strictly implies mathematically that the flow of a shallow creeping mass down a mountain valley into an approximately horizontal bed cannot be described by a single mathematical model. The two approximate models of this chapter must be patched together accordingly.

This, however, has not been done so far. Instead, the notion ‘shallowness’ should be defined relative to a curvilinear imbedding, in which the coordinate metric is based upon the underlying topography. This has been done for rapid shallow flows (see Chap. 13), where the acceleration term in the momentum equation is important. As we have seen, when estimating the orders of magnitude of the acceleration terms, the STOKES approximation (i.e., the neglect of the acceleration terms in the momentum equation) is valid in the studied geophysical applications to a very high degree. This makes the use of non-Cartesian metric not so important. For cases, when higher order shallow flow approximations request to account for the non-hydrostatic acceleration terms (e.g., in some engineering applications this would likely be different).

This discussion leads to the question, whether approximate formulations in the spirit of SIA and SOSIA should simply be dismissed and be replaced today (i.e. the year 2015) by general software modules, which directly integrate the STOKES equations. Such software has indeed been developed (e.g. ELMER, ...) and applied to ice flow problems. The disadvantage of such software is that CPU-times for computations are excessively long, far too long that climate reconstructions over several 100,000 years cannot be performed. As long as faster and more efficient software is not available, the use of the approximate computations as dealt with in this chapter, are to be preferred.

References

1. Ahlkrone, J., Kirchner, N., Lötsted, P.: A numerical study of scaling relations for non-Newtonian thin-film flows with applications in ice sheet modelling. *Q. J. Appl. Math.* **66**(4), 417–435 (2013)
2. Ahlkrone, J., Kirchner, N., Lötsted, P.: Accuracy of the zeroth and second order shallow ice approximation - numerical and theoretical results. *Geosci. Model Dev. Discuss.* **6**, 2135–2152 (2013)
3. Anonymous: *Projet d’Ecole: Detection et utilization des terrains instables. Rapport d’activité.* Ecole Polytechnique Federal de Lausanne (1981, 1982, 1983)
4. Bamber, J.L., Laberry, R.L., Gogineni, S.P.: A new ice thickness and bed data set for the Greenland ice sheet. 1. Measurement, data reduction and errors. *J. Geophys. Res.* **106**(D24), 33773–33780 (2001)

5. Baral, D.: Asymptotic theories of large scale motion, temperature and moisture distributions in land based polythermal ice shields and in floating ice shelves - A critical review and new developments. Ph.D. theses, Darmstadt University of Technology, Darmstadt, Germany (1999)
6. Baral, D.R., Hutter, K., Greve, R.: Asymptotic theories of large scale motion, temperature and moisture distributions in land based polythermal ice sheets. A critical review and new developments. *Appl. Mech. Rev.* **54**(3), 215–256 (2001)
7. Calov, R.: Das thermomechanische Verhalten des Grönländischen Eisschildes unter der Wirkung verschiedener Klimaszenarien – Antworten eines theoretisch-numerischen Modells. Ph.D. thesis, Technische Universität Darmstadt, Germany, 171 p (1993)
8. Calov, R., Hutter, K.: The thermomechanical response of the Greenland ice sheet to various climate scenarios. *Clim. Dyn.* **12**(4), 243–260 (1996)
9. Calov, R., Hutter, K.: Large scale motion and temperature distributions in land-based ice shields; the Greenland ice sheet in response to various climate scenarios. *Arch. Mech.* **49**(50), 919–962 (1997)
10. Calov, R., Savvin, A., Greve, R., Hansen, I., Hutter, K.: Simulation of the Antarctic with a 3d polythermal ice sheet model - a support of the EPICA project. *Ann. Glaciol.* **27**, 201–206 (1998)
11. Castro-Orgaz, O., Hutter, K., Giráldez, J.V., Hager, W.H.: Nonhydrostatic granular flow over 3D terrain: new Boussinesq-type gravity waves? *J. Geophys. Res. - Earth Surf.* **120**(1), 1–28 (2015)
12. Dahl-Jensen, D., et al.: Past temperatures directly from the Greenland ice sheet. *Science* **282**(5387), 268–271 (1998)
13. Dahl-Jensen, D., Gundestrup, N., Gogineni, S.P., Miller, H.: Basal melt at NorthGRIP modeled from borehole, ice-core and radio-echo sounder observations. *Ann. Glaciol.* **37**, 207–212 (2003)
14. Dansgaard, W., Johnsen, S.J., Møller, J., Langway Jr., C.C.: One thousand centuries of climatic record from Camp century on the Greenland ice sheet. *Science* **166**(3903), 377–381 (1969)
15. Dansgaard, W., et al.: Evidence for general instability of past climate from a 250 kyr ice core record. *Nature* **364**(6434), 218–220 (1993)
16. de Q Robin, G.: Ice movement and temperature distributions in glaciers and ice sheets. *J. Glaciol.* **2**(18), 523–532 (1955)
17. Egholm, D.L., Knudsen, M.F., Clark, C.D., Leemann, J.E.: Modeling the flow of glaciers in steep terrains: the integrated second-order-shallow ice approximation (iSOSIA). *J. Geophys. Res.* **116**, F022012 (2011)
18. Elmer manual (2012). <http://www.nic.funet.fi/pub/sci/physics/elmer/doc/ElmerModelsManual.pdf>
19. Fowler, A.: On the transport of moisture in polythermal glaciers. *Geophys. Astrophys. Fluid Dyn.* **28**, 99–140 (1984)
20. Fowler, A.C., Larson, D.A.: On the flow of polythermal glaciers, I. Model and preliminary analysis. *Proc. R. Soc. Lond. Ser. A* **363**, 217–242 (1978)
21. Fowler, A.C., Larson, D.A.: On the flow of polythermal glaciers, II. Surface wave analysis. *Proc. R. Soc. Lond. Ser. A* **370**, 155–171 (1980)
22. Friedrichs, K.O.: On the derivation of the shallow water theory. Appendix to: the formation of breakers and bores, by J.J. Stoker. *Commun. Pure Appl. Math.* **1**, 81–85 (1948)
23. Greve, R.: Thermomechanisches Verhalten polythermer Eisschilde – Theorie, Analytik, Numerik. Ph.D. thesis, Technische Universität Darmstadt, Deutschland. *Berichte aus der Geo-Wissenschaft*, Shaker Verlag, Aachen, Deutschland (1995)
24. Greve, R.: A continuum-mechanical formulation for shallow polythermal ice sheets. *Philos. Trans. R. Soc. Lond.* **A355**(1762), 924–974 (1997)
25. Greve, R.: Application of a polythermal three-dimensional ice sheet model to the Greenland ice sheet: response to steady-state and transient climate scenarios. *J. Clim.* **10**(5), 901–918 (1997)
26. Greve, R.: Glacial isostasy: models for the response of the eEarth to varying ice loads. In: Straughan, B., Greve, R., Ehrentraut, H., Wang, Y. (eds.) *Continuum Mechanics and Applications in Geophysics and the Environment*, pp. 307–325. Springer, Berlin (2001)
27. Greve, R., Blatter, H.: *Dynamics of Ice Sheets and Glaciers*, p. 287. Springer, Berlin (2009)

28. Greve, R., Herzfeld, U.C.: Resolution of ice streams and outlet glaciers in large-scale simulations of the Greenland ice sheet. *Ann. Glaciol.* **54**(63), 209–220 (2013)
29. Greve, R., Hutter, K.: Polythermal three-dimensional modeling of the Greenland ice sheet with varied geothermal heat flux. *Ann. Glaciol.* **21**, 8–12 (1995)
30. Greve, R., Weis, M., Hutter, K.: Paleoclimatic evolution and present conditions of the Greenland ice sheet in the vicinity of summit: an approach by large scale modeling. *Paleoclimates* **2**(2–3), 133–161 (1998)
31. Gundestrup, N.S., Hansen, B.L.: Bore-hole survey at Dye 3. South Greenland. *J. Glaciol.* **30**(106), 282–288 (1984)
32. Gundestrup, N.S., Clausen, H.B., Hansen, B.L., Rand, J.: Camp century survey 1986. *Cold Reg. Sci. Technol.* **14**(3), 281–288 (1987)
33. Gundestrup, N.S., Dahl-Jensen, D., Hansen, B.L., Kelty, J.: Borehole survey at Camp century 1989. *Cold Reg. Sci. Technol.* **21**(2), 187–193 (1993)
34. Hansen, I., Greve, R., Hutter, K.: Application of a polythermal ice model to the Antarctic ice sheet. Steady-state solution and response to Milancovic' cycles. In: Lee, Y., Halle, W. (eds.) *Proceedings of Fifth International Symposium on Thermal Engineering and Sciences for Cold Regions*. Ottawa, 19–22 May, pp. 89–96 (1996)
35. Herzfeld, U.C., Wallin, B.F., Leuschen, C.J., Plummer, J.: An algorithm for generalizing topography to grids while preserving subscale morphologic characteristics - creating a glacier bed DEM for Jacobshavn trough as low-resolution input for dynamic ice-sheet models. *Comput. Geosci.* **37**(11), 1793–1801 (2011)
36. Herzfeld, U.C., Fasdtook, J., Greve, R., McDonald, B., Wallin, B.F., Chen, P.A.: On the influence of outlet glaciers in Greenland bed topography on results from dynamic ice sheet models. *Ann. Glaciol.* **53**(60 Pt2), 281–293 (2012)
37. Hutter, K.: The effect of longitudinal strain on the shear stress of an ice sheet. In defense of using stretched coordinates. *J. Glaciol.* **25**(95), 39–56 (1981)
38. Hutter, K.: A mathematical model of polythermal glaciers and ice sheets. *Geophys. Astrophys. Fluid Dyn.* **21**, 201–224 (1982)
39. Hutter, K.: *Theoretical Glaciology*. D. Reidel Publishing Company, Dordrecht, Boston, Lancaster, XXXII+510 p (1983)
40. Hutter, K.: Ice and snow mechanics, a challenge to theoretical and applied mechanics. In: *Proceedings of the XVI-ICTAM Congress*, North Holland Publishing Company, Copenhagen (1984)
41. Hutter, K.: Thermo-mechanically coupled ice sheet response: cold, polythermal, temperate. *J. Glaciol.* **39**(131), 65–86 (1993)
42. Hutter, K., Castro-Orgaz, O.: Non-hydrostatic free surface flows: Saint Venant versus Boussinesq depth integrated dynamic equations for river and granular flows. In: Albers, B., Kuczma, M. (eds.) *Continuous Media with Microstructure*. Springer, Berlin (2016)
43. Hutter, K., Vulliet, L.: Gravity driven slow creeping flow of a thermoviscous body at elevated temperature. *J. Therm. Stress.* **8**, 99–138 (1985)
44. Hutter, K., Yakowitz, S., Szidarovsky, F.: A numerical study of plane ice-sheet flow. *J. Glaciol.* **32**(111), 139–160 (1986)
45. Hutter, K., Blatter, H., Funk, M.: A model of polythermal glaciers. *J. Geophys. Res.* **93**(10B), 12205–12214 (1988)
46. Huybrechts, P.: A 3D model for the Antarctic ice sheet: a sensitivity study on the glacial-interglacial contrast. *Clim. Dyn.* **5**, 79–90 (1990)
47. Johnson, R.E., McMeeking, R.M.: Near surface flow in glaciers obeying Glen's flow law. *Quart. J. Mech. Appl. Math.* **37**, 273–291 (1984)
48. Joughin, I., Smitj, B.E., Howat, I.M., Scambos, T., Moon, T.: Greenland flow variability from ice sheet-wide velocity mapping. *J. Glaciol.* **56**(197), 415–430 (2010)
49. Kirchner, N., Hutter, K., Jakobsson, M., Gyllencreutz, R.: Capabilities and limitations of numerical ice sheet models: a discussion for Earth scientists and modelers. *Quat. Sci. Rev.* **30**(25–26), 3691–3704 (2011)

50. Kuhle, M., Herterich, K., Calov, R.: On the ice age glaciation of the Tibetan highland and its transformation into a 3D model. *GeoJournal* **19**(2), 201–206 (1989)
51. LeMeur, E., Huybrechts, P.: A comparison of different ways of dealing with isostasy: examples from modelling the Antarctic ice sheet during the last glacial cycle. *Ann. Glaciol.* **23**, 309–317 (1996)
52. Morland, L.W.: Thermomechanical balances of ice sheet flows. *J. Geophys. Astrophys. Fluid Dyn.* **29**(1–4), 237–266 (1984)
53. Morland, L.W., Johnson, I.R.: Steady motion of ice sheets. *J. Glaciol.* **25**(95), 229–246 (1980)
54. Morland, L.W., Johnson, I.R.: Effects of bed inclination and topography on steady ice sheets. *J. Glaciol.* **28**(98), 71–90 (1982)
55. Morland, L.W., Smith, G.D.: Influence of non-uniform temperature distribution of the steady motion of ice sheets. *J. Fluid Mech.* **140**, 113–133 (1984)
56. Musase, T., McBirney, A.R.: Properties of some common igneous rocks and their melts at high temperatures. *Geol. Soc. Am. Bull.* **84**(9), 3563–3592 (1973)
57. North Greenland Ice Core Project (NorthGRIP) Members: High-resolution record of Northern Hemisphere climate extending into the last interglacial period. *Nature* **431**(7005), 147–151 (2004)
58. Richter, F.: *Physikalische Eigenschaften von Stählen und ihre Temperaturabhängigkeit. Polynome und graphische Darstellungen. Stahleisen – Sonderberichte Heft 10.* Verlag Stahleisen M.B.H. Düsseldorf (1983)
59. Rittmann, A.: *Vulkane und ihre Tätigkeit*, 2nd edn. Ferdinand Enke Verlag, Stuttgart (1960)
60. Sato, T.: Dynamics of the Antarctic ice sheet with coupled ice shelves. Ph.D. thesis, Division of Earth System Science, Graduate School of Environmental Science, Hokkaido University. 1–110 pp (2012)
61. Sato, T., Greve, R.: Sensitivity experiments for the Antarctic ice sheet with varied sub-ice-shelf melting rates. *Ann. Glaciol.* **53**(60), 221–227 (2012)
62. Schoof, C., Hindmarsh, R.C.A.: Thin-film flows with wall slip: an asymptotic analysis of higher order glacier flow models. *Quart. J. Mech. Appl. Math.* **63**, 73–114 (2010)
63. Smith, G.D., Morland, L.W.: Viscous relations for the steady creep of polycrystalline ice. *Cold Reg. Sci. Technol.* **5**, 141–150 (1980)
64. Vulliet, L.: *L'instabilité des pentes en fonction du temps.* Ecole Polytechnique Fédérale de Lausanne (1986)
65. Weis, M.: Theory and finite element analysis of shallow ice shelves. Ph.D. thesis, Darmstadt University of Technology, Darmstadt, Germany (2001)
66. Weis, M., Hutter, K., Calov, R.: 250.000 years in the history of the Greenland ice sheet. *Ann. Glaciol.* **23**, 359–363 (1996)
67. Weis, M., Greve, R., Hutter, K.: Theory of shallow ice shelves. *Contin. Mech. Thermodyn.* **11**(1), 15–50 (1999)
68. Yakowitz, S., Hutter, K., Szidarowsky, F.: Elements of computational theory of glaciers. *J. Comput. Phys.* **66**, 132–150 (1986)

Chapter 13

Shallow Rapid Granular Avalanches

Abstract This chapter is devoted to rapid granular flows in an attempt to introduce the reader to the challenging theory of the dynamical behavior of fluidized beds. The peculiar behavior of such materials is exhibited in typical responses such as ‘dilatancy’, ‘liquefaction’, (size) ‘segregation’, ‘normal and inverse grading’ etc. The fluid mechanical description of cohesionless granular materials—dry or wet—in avalanches of snow, debris and mud also applicable to transport of dry granular materials in industrial production chains, follows continuum and discrete descriptions. The theoretical modeling of moving layers of granular assemblies begins with the one-dimensional depth integrated MOHR–COULOMB plastic layer flows down inclines—the earliest description being the so-called VOELLMY model (1955), extended by the SAVAGE–HUTTER theory (1989) and its extensions—but then continues with the general formulation of the model equations referred to topography-following curvilinear coordinates, with all its peculiarities in the theory and the use of shock-capturing numerical integration techniques. Detailed comparison of computational results with laboratory chute flows and field events demonstrate the suitability of the various models.

Keywords Dilatancy · Segregation · Liquefaction · Shallow flow models · Curvilinear coordinates · Shock capturing numerical techniques · Laboratory chute flows · Field events of large landslides

List of Symbols

Roman Symbols

A_x, A_y	Spatial matrices in the hyperbolic partial differential equation (13.120): $A_x = \partial f / \partial \omega$, $A_y = \partial g / \partial \omega$
a, \mathbf{a}	Acceleration—vector
$b(x, y) =: z$	Equation for the basal surface relative to a reference ruled surface
$C = \rho g / \xi$	Viscous friction coefficient
D	Stretching tensor, strain rate tensor (deviator)
$F^{s,b}(\mathbf{x}, t) = 0$	Equation of the free/basal surface

\mathbf{f}	Flux matrix associated with \mathbf{w} (see (13.112) and (13.113))
\bar{f}	Depth average of f : $\bar{f} = \frac{1}{h} \int_b^s f dz$
g	Gravity constant
\mathbf{g}_i	Covariant basis vector: $\mathbf{g}_i = \frac{\partial \mathbf{r}}{\partial x_i}$
\mathbf{g}^i	Contravariant basis vector
$g_{ij} = \mathbf{g}_i \cdot \mathbf{g}_j$	Covariant metric coefficients
$\mathbf{g}_j^* := \mathbf{g}_j / \mathbf{g}_j $	Unit basis vector
$h(x), h(x, y, t)$	Height of a granular mass—of a moving mass relative to the reference surface
$H, [H]$	Scaling length perpendicular to the (x, y) -plane
K_x^b, K_y^b	Earth pressure coefficient at the basal surface: $K_x^b := \frac{p_{xx}^b}{p_{zz}^b}$, $K_y^b := \frac{p_{yy}^b}{p_{zz}^b}$
$K_{\text{act/pas}}$	Active/passive earth pressure coefficients
$K_{x_{\text{act/pas}}^b}, K_{y_{\text{act/pas}}^b}$	Active/passive earth pressure coefficients at the base
$L, [L]$	Scaling length in the directions parallel to the (x, y) -plane
m_x, m_y	Specific momentum in the x - and y -directions: $m_x = hu_x$, $m_y = hv_y$
m_δ	Coefficient in the parametrization of the bed friction angle
N	Force normal to an internal cut at a point in a body
$\mathbf{n}^{s,b}$	Unit normal vector on a free/basal surface of the body
\mathcal{O}	Order symbol
p	Pressure, overburden –
p_L	Longitudinal pressure
$\mathbf{p}^{s,b}$	Pressure tensor evaluated at the free/basal surface of a body
$p_{xx}, p_{xy}, \dots, p_{zz}$	Components of the pressure tensor
p_{zz}	‘Hydrostatic pressure’: $p_{zz} = (s - z) \cos \zeta$
\mathcal{R}	Typical radius of curvature
$\mathbf{r}(x, y, z)$	Position vector of a body point
$\mathbf{r}^r(x, y)$	Position vector to a point on the reference surface
\mathbf{S}	Shear force tangential to an internal cut at a point of a body
$\text{sgn}(u)$	Sign of u : $\text{sgn}(u) = 1$ if $u > 0$, $= 0$ if $u = 0$ and $= -1$ if $u < 0$
$s(x, y) = z$	Equation for the free surface of a body
t	Time
\mathbf{u}, u	Velocity vector, downslope velocity of a sliding body point
u_{max}	Maximum velocity of a sliding body
\mathbf{w}	Array of independent variables of a partial differential equation in conservative form (see (13.112) and (13.113))
x	Position of a sliding body
x, y, z	Coordinates (not necessarily Cartesian)
x_f, x_r	Front and rear end positions of an avalanche
x, y, z	Cartesian coordinates

Greek and Miscellaneous Symbols

$ \alpha , \beta , \gamma < 1$	Exponents in the order relations $\mathcal{O}(\varepsilon^\alpha)$, $\mathcal{O}(\varepsilon^\beta)$, $\mathcal{O}(\varepsilon^\gamma)$
γ	Shear angle in e.g. simple shearing, $2\times$ (shear rate)
$\Gamma_{\ell m}^k$	CHRISTOFFEL symbol of second kind
$\Delta_b = \nabla F^b $	Basal surface quantity (see (13.75))
δ, δ_0	Bed friction angle, constant bed friction angle
$\varepsilon = \frac{H}{L} \ll 1$	Aspect ratio
ξ	MANNING-GAUKLER-STRICKLER coefficient
$\zeta, \tilde{\zeta}$	Inclination angle(s)
κ	Coefficient of a REINER-RIWLIN fluid
$\kappa = \partial\zeta/\partial x_1$	Curvature in the downslope direction
$\lambda = L/\mathcal{R}$	Typical measure of the radius of curvature of the topography
μ	Dynamic viscosity,
$\mu = \tan \delta_0$	Friction coefficient formed with a typical angle of friction
ρ	Density of a fluid—of a granular heap,
ρ_a	Density of air
σ, σ_D	CAUCHY stress tensor—deviator
τ	Shear stress, basal shear stress
ϕ	Angle of internal friction, typical parameter measuring the curvature of the basal topography
Ψ	Typical parameter measuring the curvature of the basal topography
II_D	Second invariant of \mathbf{D} : $II_D = \frac{1}{2}\text{tr}\mathbf{D}^2$
∇	Gradient operator: $\nabla := \mathbf{g}^k \frac{\partial}{\partial x_k}$
NOC scheme	Non-oscillatory central difference scheme
SH model	SAVAGE-HUTTER model
TVD method	Total variation diminishing method

13.1 Introduction

In the geophysical environment avalanches occur in a variety of circumstances. Such rapid mass flows might occur in the form of rock and snow avalanches, as landslides of catastrophic soil release, debris and mud flows, gravity driven motions of volcanic ash and as turbidity currents (under water avalanches). Industrial examples are flows of cereals, pharmaceuticals, coal and cement in storage facilities, production lines, power stations and construction sites. All these cases do have many common features and their mathematical description can be based on similar physical principles. Thus, not surprisingly, nearly the same concepts have been applied to avalanching mass movements in different fields of science and engineering specialties.

The model equations, which will be our focus in this chapter, are depth integrated versions of the balance laws of mass and momentum, and as such involve idealizing approximations e.g., the shallowness of the geometries of the moving masses. They are in most parts based on a dry granular concept and employ a one-constituent

continuum formulation. The derivation of the depth integrated equations is based on mathematical simplifications, notably a scaling analysis, in which a shallowness parameter, expressed as the ratio of a typical flow depth to avalanche extent, $\varepsilon = [H]/[L]$, may be used to construct approximate field equations in the limit as $\varepsilon \rightarrow 0$. Such models must be tested against experiments in the laboratory and possibly in Nature, in order to identify their range of applicability.

Snow avalanche conditions are usually caused by the combination of heavy snow fall, wind and changing temperatures. The number of avalanches falling annually in the USA is on the order of 10^5 , and the number of avalanches falling annually worldwide is on the order of 10^6 . Of the about 100 people who are annually caught by avalanches in the USA about 17 are killed and the average annual property damage is 400,000 USD. Yearly death casualties are about 25 in Switzerland and Austria, 31 in France, 20–30 in Italy, 30 in Japan, 10–15 in Norway, 10 in Germany and 7 in Canada, according to B.R. ARMSTRONG and K. WILLIAMS [3] and these figures have not appreciably decreased in the last 30 years. **Figures 13.1, 13.2 and 13.3** show manifestations of *dense flow avalanches* and *powder snow avalanches*.

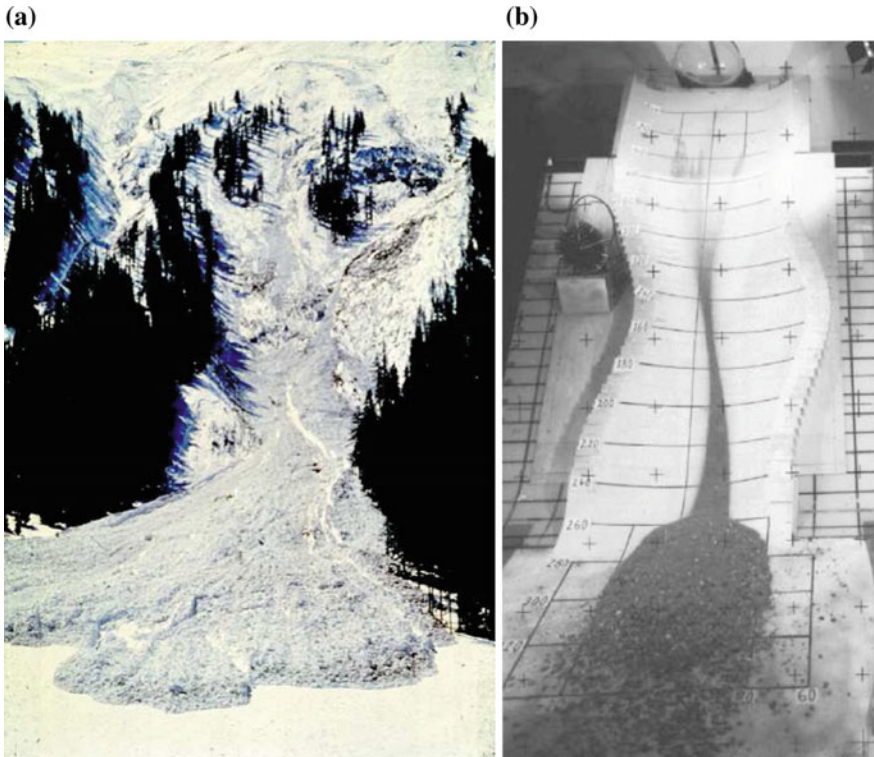


Fig. 13.1 Deposits of avalanches in two different situations. **a** *Deposit of a real snow avalanche in the Alps (Courtesy of the Swiss Federal Institute of Snow and Avalanche Research, SLF, Davos* **b** *Laboratory avalanche simulation with a mixture of sand and gravel [29]*

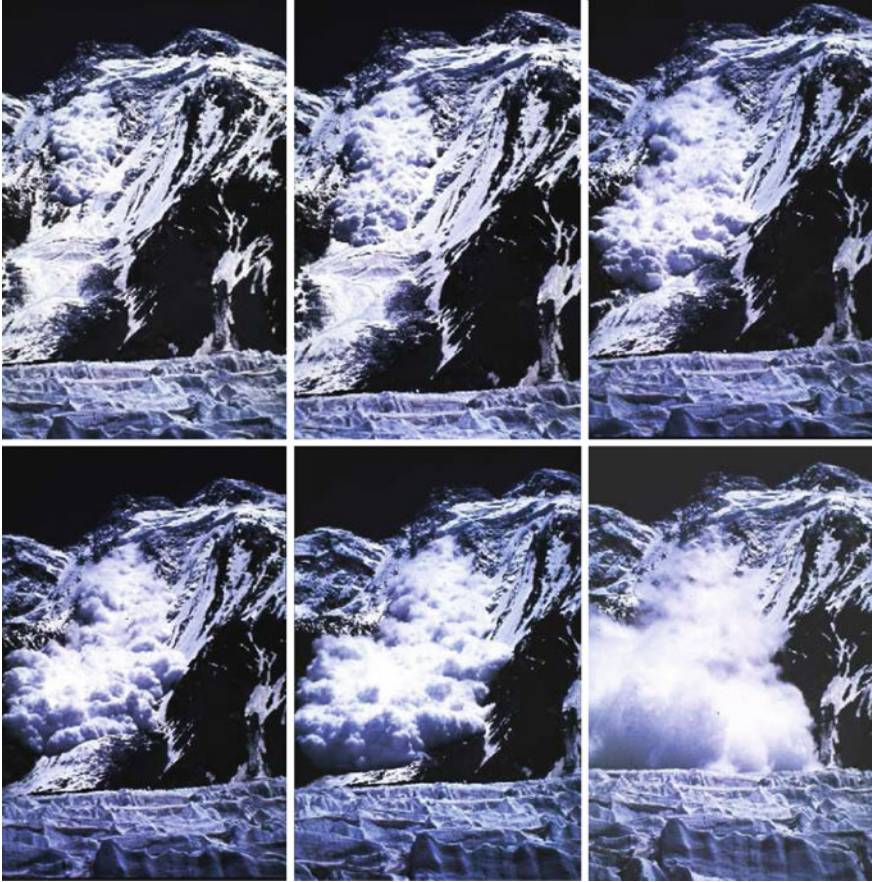


Fig. 13.2 A sequence of snapshots of a powder snow avalanche in the Himalaya Courtesy F. TSCHIRKI, Swiss Federal Institute of Snow and Avalanche Research, Davos, Switzerland

Avalanches also occur in the form of the motion of soil or rock down mountain sides, sometimes mixed with uprooted bushes, trees and often containing water. When water does not play any significant role in the motion of the granular masses, geologists also talk of avalanches or rock falls. If water is likely to be the triggering element of the soil in motion, then the terminology is *debris flow*, even if eventually i.e. during the catastrophic motion of the granular mass, the water can be ignored as a dynamic element. *Mud flows* are flows of soil and added debris that is substantially mixed with interstitial fluid, which contributes to the dynamics of the solid-fluid mixture. **Figure 13.4** shows a view of the village Gondo in southern Switzerland as it has been hit by the spitting mud flow of 14 October 2000. The heavy rainfall of 48 h prior to the event triggered the 10.000 m^3 mud flow.



Fig. 13.3 Photographs of a powder avalanche taken from a helicopter. *This avalanche was artificially released by blasts from the helicopter.* Courtesy Swiss Federal Institute of Snow and Avalanche Research, SLF, Davos, Switzerland

Volcanic eruptions (e.g. Mount Saint Helens in Washington State, USA, 1980) often generate gravity currents of hot ash down the mountain side. These debris flows are referred to as *pyroclastic* and are often also called *lahars*, because of their considerable heat and burning temperatures. Earth quakes are often equally triggering landslides or debris flows. **Figure 13.5** depicts the devastating debris slide in January 2001 in Las Colinas, El Salvador. This landslide may have buried as many as 500 homes.



Fig. 13.4 Destruction by mud flow and landslide: 10.000 m³ spitting mud flow in Gondo (South Switzerland) on 14 October 2000 caused 14 deaths and destroyed a dozen buildings, including the 400 years old Stockalper tower. © Berner Zeitung



Fig. 13.5 Deposit of a devastating debris slide in Las Colinas (on the outskirts of San Salvador), January 2001. This landslide was induced by an earthquake and buried as many as 500 homes, from <http://www.crealp.ch>

13.2 Distinctive Properties of Granular Materials

Many rapid mass movements in geophysical flows have a granular structure. Among these are snow avalanches and landslides that are formed from rock falls, ice avalanches that evolve from fragmented ice junks, which broke off from steep glaciers, debris flows of soil soaked with water during and in the aftermaths of a heavy

rain storm. Air or water borne *density currents*, such as powder snow avalanches, dust clouds above deserts by wind, and sub-aquatic water suspended turbulent mass flows also define a class of granular flows, but these are structurally distinct from dense granular flows and must be treated by mixture concepts. By contrast, in dense granular flows the interstitial fluid or gas plays a small, generally negligible dynamic role. It is this latter class of gravity driven granular flows, which will be more closely analyzed in this chapter.

13.2.1 Dilatancy

Deformations in a granular body are almost always accompanied by corresponding volume changes. OSBORNE REYNOLDS in 1885 [71] called this phenomenon *dilatancy*. If an array of identical spheres (or parallel circular cylinders in two dimensions) at closest packing is subject to a load so as to cause a shear deformation, then from pure geometric considerations those particles must ride one over the other, and it follows that an increase in volume of the bulk material will occur, see **Fig. 13.6**. Dilatancy in this case is due to kinematic constraints.

Dilatancy is the cause that granular materials exhibit what in rheology is called ‘*normal stress effect*’. This means that shearing of a granular pack, in which the expansion of the sheared specimen is constrained, will automatically induce a normal stress perpendicular to the direction of shearing. A constitutive postulate must account for this property; for instance, in a density preserving fluid a stress strain rate relation of the form $\sigma_D = 2\mu(H_D)\mathbf{D}$, where σ_D is the stress deviator, \mathbf{D} is the stretching tensor, $H_D = \frac{1}{2}\text{tr}\mathbf{D}^2$, does not exhibit normal stresses, but the REINER-RIVLIN fluid

$$\sigma_D = 2\mu\sigma + \kappa \left\{ \mathbf{D}^2 - \frac{2}{3}H_D\mathbf{I} \right\} \quad (13.1)$$

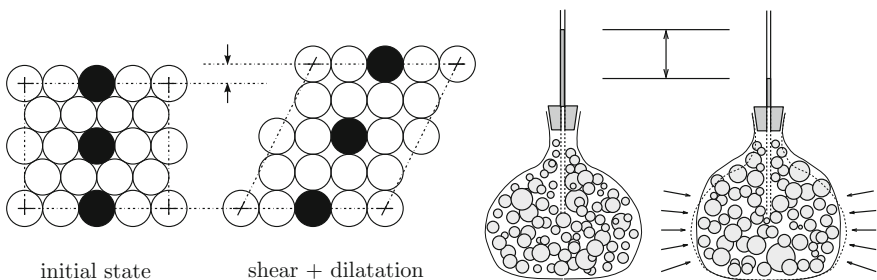


Fig. 13.6 *Left* shearing of a closed packing of *spheres* or *circular cylinders* generates a volume expansion. *Right* displacing a saturated mixture of grains with the pore space filled with water at closest packing by pressing the belly from outside will enlarge the pore space in the belly, so that the water in the capillary will drop, from [86]. © Springer Verlag, reproduced with permission

does so. Indeed, in simple shearing we have

$$\mathbf{D} = \begin{pmatrix} 0 & \gamma/2 & 0 \\ \gamma/2 & 0 & 0 \\ 0 & 0 & 0 \end{pmatrix}, \quad \mathbf{D}^2 = \begin{pmatrix} \gamma^2/4 & 0 & 0 \\ 0 & \gamma^2/4 & 0 \\ 0 & 0 & 0 \end{pmatrix}, \quad II_{\mathbf{D}} = \frac{\gamma^2}{4} \quad (13.2)$$

and, therefore according to (13.1)

$$\begin{aligned} \sigma_{\mathbf{D}} &= 2\mu \begin{pmatrix} 0 & \gamma/2 & 0 \\ \gamma/2 & 0 & 0 \\ 0 & 0 & 0 \end{pmatrix} + \kappa \left[\begin{pmatrix} \gamma^2/4 & 0 & 0 \\ 0 & \gamma^2/4 & 0 \\ 0 & 0 & 0 \end{pmatrix} - \frac{2}{3} \frac{\gamma^2}{4} \begin{pmatrix} 0 & 0 & 0 \\ 0 & 1 & 0 \\ 0 & 0 & 1 \end{pmatrix} \right] \\ &= 2\mu \begin{pmatrix} 0 & \gamma/2 & 0 \\ \gamma/2 & 0 & 0 \\ 0 & 0 & 0 \end{pmatrix} + \frac{\kappa}{3} \begin{pmatrix} \gamma^2/4 & 0 & 0 \\ 0 & \gamma^2/4 & 0 \\ 0 & 0 & 0 \end{pmatrix} \end{aligned} \quad (13.3)$$

with normal stresses $\sigma_x = \frac{\kappa}{12}\gamma^2$, $\sigma_y = \frac{\kappa}{12}\gamma^2$, $\sigma_z = 0$. With $\kappa = 0$, (13.3) does not exhibit normal stress effects.

13.2.2 Cohesion

In a granular deposit the contact forces between particles can be normal and tangential to the tangent plane in the contact point. If the normal forces are restricted to pressures, the granular material is said to be *cohesionless*. If also some tension is active, then the contact is *cohesive*. Tensile forces can e.g. be induced in a soil deposit by partly wetting the particles. Surface tension that is active in the menisci then gives rise to cohesive behavior of the deposited mass, compare **Fig. 13.7**. In this particular application the forces are also called *capillary forces*. The effect arises e.g. in water

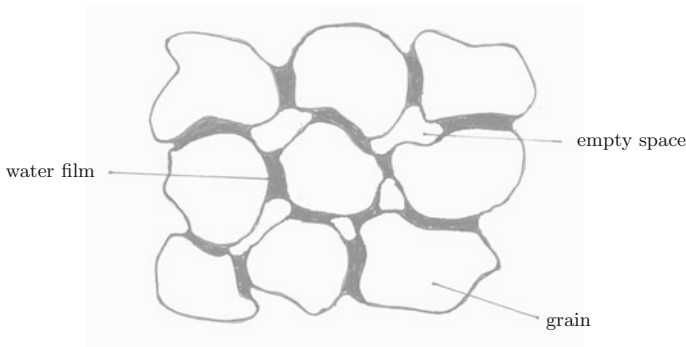


Fig. 13.7 In wet soil the water accumulates in liquid films in the pore space between grains

saturated soil immediately above the ground-water surface, when the soil is only partly saturated in the so-called *capillary fringe*.

Cohesion is a physical mechanism that is likely more significant for snow, soil and rock masses at rest or in creeping deformations than in rapid motion. Dynamic processes tend to break the bonds that exist because of the liquid bridges between the particles. Once broken, the tension forces between the grains are not likely to be re-established, because the sliding motion and the bouncing of the particles are too strong that surface tension at the menisci in the fluid between particles can be established.

13.2.3 Lubrication

There are several distinct mechanisms, which reduce friction in granular materials in motion. One of them is *lubrication* and expresses the reduction of frictional resistance by introducing an additional medium, the lubricant between the surfaces of two bodies that are displaced relative to one another. For granular gravity driven mass flows lubrication is particularly important, because it is likely responsible for large run-out distances of the avalanching mass down low slope angles. Air or water can act as lubricating media, or lubrication can be process-induced, e.g. when the particles in the vicinity of the sliding surface experience increased pulsations, which increase their fluctuation energy (i.e., granular temperature), enlarge the mean free path between the particles and, thus, reduce the friction.

In flow avalanches of snow, lubrication may arise in form of a liquid water film between the surfaces of the sliding snow and the ground. These kinds of lubrication, the frictional energy between the sliding snow at the base and the stagnant base may continuously generate melt water as its own lubricant. In very large landslides (of several millions of m³ of rocks) the frictional heat at the sliding surface may cause basal temperatures of more than 1000 K, so that the gravel may melt and act as lubricant between the rock avalanche and the stagnant base. T. ERISMANN and G. ABELE [27] demonstrate for the historic avalanche event at K ofels (Austria) that rock material in this sliding motion must have melted during motion and subsequently again solidified, while being deposited. Geologists call such sintered ‘volcanic rocks’ “*frictionites*”.

It is quite clear that the thermal component of avalanching flows of lahars, volcanic ash, lava possibly with phase changes, need to be described by energy considerations apart from balances of mass and momentum. Theoretical descriptions of these flows are very scarce. A model on lava flow in the spirit of the ‘cold’ avalanche theories dealt with in this chapter is by K. HUTTER and O. BAILLIFART [44].

A particular limit of lubricated sliding is *un-lubricated sliding*. By this one usually means sliding that operates without the action of a lubricant. The best known case of such un-lubricated friction is so-called *solid friction* according to the classical

COULOMB¹ law. It postulates that the *resistance opposed to a sliding motion of a granular body is proportional to the compressive force acting at right angle to the contact surface*. The factor of proportionality is called the *coefficient of friction*, which is assumed to be characteristic for the surface (but not the load, relative velocity and time).

When using the simple COULOMB law, the motion of a mass point along an inclined plane, see **Fig. 13.9**, is described by

$$a = g (\sin \zeta - \mu \cos \zeta), \quad (13.4)$$

in which a is the acceleration, ζ the slope angle, μ the coefficient of friction of the material with the basal surface and g the gravity constant. In (13.4) $g \sin \zeta$ is the driving gravity force and $g\mu \cos \zeta$ the un-lubricated frictional force resisting the motion. This dry friction force does not depend on the velocity difference between avalanche sole and solid bed. Such a viscous drag will likely depend on the square of this velocity difference with a drag coefficient C . Thus, (13.4) changes to

$$\underbrace{a}_{\text{acc.}} = \underbrace{g \sin \zeta}_{\text{velocity parallel gravity force}} - \underbrace{g\mu \cos \zeta}_{\text{Coulomb friction}} - \underbrace{Cu^2}_{\text{viscous friction}}. \quad (13.5)$$

With

$$a = \frac{du}{dt} = \frac{d^2x}{dt^2} \quad (13.6)$$

Equations (13.5) and (13.6) can directly be integrated with the results,

- For (13.4):

$$\begin{aligned} u &= g (\sin \zeta - \mu \cos \zeta) t + u_0, \\ x &= \frac{g}{2} (\sin \zeta - \mu \cos \zeta) t^2 + u_0 t + x_0. \end{aligned} \quad (13.7)$$

- For (13.5):

$$\begin{aligned} u &= \sqrt{\frac{g (\sin \zeta - \mu \cos \zeta)}{C}} \tanh \left\{ \sqrt{C g (\sin \zeta - \mu \cos \zeta)} (t - t_0) \right\}, \\ x &= \ln \cos \sqrt{\frac{g (\sin \zeta - \mu \cos \zeta)}{C}} (t - t_0) + x_0. \end{aligned} \quad (13.8)$$

¹For a biographical sketch of COULOMB, see **Fig. 13.8**.



Fig. 13.8 CHARLES-AUGUSTINE DE COULOMB (14. June 1736–23 Aug. 1806)

CHARLES-AUGUSTINE DE COULOMB was a French physicist best known for developing COULOMB's law, describing the *electrostatic attraction and repulsion of electric charges*, but he also did important work on *dry friction*. He went to school in the Collège Mazarin in Paris where, at the Ecole de Génie militaire de Mézière, he received a profound education in mathematics, astronomy, chemistry and botany, as well as philosophy, language and literature. He graduated in 1761 and then spent his next 20 years in the military with engineering assignments: structural, fortifications, soil mechanics. From 1764 to 1772 he was in Martinique, where he was in charge of building the new fort Bourbon. Later, he had similar assignments in France and abroad. In 1789, on the outbreak of the revolution, he resigned his appointment and retired in a small estate, which he possessed in Blois, but he was recalled to Paris for a time order to take part in the new determination of *weights and measures*, which had been decreed by the Revolutionary government

AUGUSTINE COULOMB's scientific achievements are manifold and substantial. He is known for:

- (i) his law on solid friction;
- (ii) the law on internal friction of liquids;
- (iii) the development of the first ever formulated shear stress-normal stress interaction in soil mechanics and the introduction of the earth pressure coefficient;
- (iv) his outstanding work on the experimental demonstration of the electrostatic force-distant law between two electric charges ($(1/\text{distance squared})$ law), which is one of the universal physical laws

The text is based on www.wikipedia.org

Interesting are the limit values of the velocities as $t \rightarrow \infty$. They are

$$\left. \begin{aligned} u &\rightarrow \sqrt{\frac{g(\sin \zeta - \mu \cos \zeta)}{C}} t \text{ for (13.7)}_1 \\ u &\rightarrow \sqrt{\frac{g(\sin \zeta - \mu \cos \zeta)}{C}} \text{ for (13.8)}_1 \end{aligned} \right\} \text{ as } t \rightarrow \infty. \quad (13.9)$$

Equation (13.7)₁ tells us that the velocity of the sliding mass grows linearly with time; it never comes to a constant limiting value. By contrast, we conclude from (13.8)₁ or (13.8)₂ that for velocity-dependent sliding an avalanching mass reaches a steady asymptotic flow state with constant velocity.

It is not clear whether the asymptotic velocity will be constant or whether an infinite increase of the velocity will persist. Experiments by W. ECKART et al. (2003) [21] and CH. ANSEY and M. MEUNIER, 2003, [4] do not come to a conclusion whether viscous sliding may be dropped and only COULOMB sliding is relevant.

13.2.4 Liquefaction

Liquefaction, also called fluidization, is a transitional state of water saturated soils, which may occur during and in aftermaths of earthquakes or as a result of artificial explosions in loose saturated sand deposits. Liquefaction manifests itself in a sudden change of the saturated soil from an essentially solid material state to a fluid behavior or something in-between. This transition sets in some time in the last stretch of an earthquake or immediately thereafter and lasts for some minutes. It tapers off due to

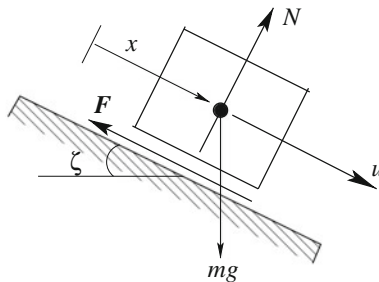


Fig. 13.9 Motion of a rigid body down an inclined plane *The frictional force consists of two contributions, a COULOMB type, $|\mathbf{F}_{\text{COULOMB}}| = \mu N$ and a velocity dependent contribution $F_{\text{viscous}} = Cu^2$. In this case $N = (\rho - \rho_a)g \cos \zeta$, $F_{\text{viscous}} = (\rho - \rho_a)g \sin \zeta$ and $C = \rho g/\xi$. Here, ρ_a is the density of the atmosphere*

the solidification or consolidation processes, which set-in simultaneously with the fluidization and the concurrent partial separation of the solid and fluid constituents. Soil deposits, which have been subject to liquefaction in the past e.g. by an earthquake may not be sufficiently consolidated after settlement to be absolutely stable and safe against further fluidization in future oscillating or impact events.

It must be the geotechnician's intention to describe the implications, which can be possibly deduced from observations of the processes and remains of destructions caused by earthquake-induced events, now identified as liquefaction. The description of these observations leads to implications of the physical behavior of the saturated soil as a material and, subsequently, to a proposal of a possible constitutive modeling, which is subject to consistency requirements with the Second Law of Thermodynamics and later scrutinized in numerical applications of geotechnical scenarios.

An excellent description of the liquefaction of soils by earthquakes is by N. AMBRASEYES and S. SARMA [1]. In their introductory statement they write:

“Liquefaction of deposits caused by earthquakes is not an uncommon phenomenon. It accounts for submarine slides and subsequent turbidity currents (N. MORGENSTERN, 1967) [64], for landslides and flows of subaerial deposits (A. CASAGRANDE, 1936) [10]; it is a phenomenon that may even explain the mechanism that allowed the debris of some of the larger prehistoric and more recent slides, of many cubic miles of material, to travel distances of over 20 km (J. HARRISON and N. FALCON, 1937) [36]. On flat ground, sand blows, mud volcanoes and extensive flooding of the ground by exuded water, are the results of liquefaction. Also, the settlements of man-made structures, in some cases to the extent that the ground becomes level with windowsills, can be produced by liquefaction of the foundation materials. Underground structures such as septic and storage tanks, sewage conduits and manholes, water mains, even piles driven into the ground, have floated up, many feet above ground level, after the earthquake. Most of these effects do not usually appear until toward the end or several minutes after the earthquake and they persist for some time.” These authors analyzed observations of ten earthquakes between 1899 and 1966 and their detailed description points at typical behavioral patterns, which occur in the saturated top layers of soils, when an earthquake passes these locations:

- Between few and up to a large number of vertical jets of water, 0.5–2.0 m high, emerged from motion-induced fissures in the plain. These spouts are mixed with sand, peats or coals.
- Such ejections began during the earthquake and generally lasted 3–5 min, sometimes up to 30 min or more after the shaking had been ceased.
- These mud volcanoes, also called cold volcanoes, may have arisen just once and then died out or they spurted intermittently, i.e., ejections would stop and then resume action after a few seconds later.
- Drainage channels, up to 5 and more meters deep, had their bottom lifted until they became level with their banks. Similarly, wells overflowed as their bottoms were blowing-up and flooded plains. In some places, the material brought up by

the fluid mixture, was the same as that of the stratum encountered by wells as deep as ~ 25 m.

- 2–3 mins after the beginning and towards the end of the earthquake, the ground around some buildings began to crack and to open-up in places. A minute or two later, water began to come up around the buildings. Structures of all kinds sank into the ground. In some cases they stayed intact but sank into the ground, were tilted and/or slid on the foundation, in others they were destroyed by the excessive differential vertical displacements of parts of the foundation.
- Underground structures (septic tanks, storage tanks, petrol tanks, sewage conduits and manholes, etc.) floated-up or sank into the ground.
- Other surface structures (bridge abutments) were differentially lifted and thus destroyed by the excessive strains induced by this.

Qualitatively similar observations are equally stated (but less systematically documented) by D. KOLYMBAS (1998, 2013) [50, 51] also for earthquakes beyond 1964, e.g. the Loma Prieta earthquake in San Francisco, 1989 (see J.P. BARDET and F. KAPUSKAR, 1993, [5] and Japanese earthquakes analyzed by E. KURIBAYASHI and F. TATSUOKA (1977) [54]). The general observations in KOLYMBAS' papers do not go beyond the above summary of stated effects about near surface devastations. **Figure 13.10** displays some destruction that occurred as a result of the liquefaction of the saturated soils subject to earthquakes and **Fig. 13.11** illustrates a cold volcano under action.

N. AMBRASEYS and S. SARMA [1] further observed that (i) artesian and oil wells at depth of more than 100m were not affected and (ii) ground movements show that soon after the beginning of the earthquake this ground shaking subsided. This indicates that, as soon as deeper strata liquefied, they ceased to transmit the earthquake vibrations to the overlying deposits.

It, thus, appears that at depth of approximately 100 m or more, the seismic excitation seems not to be strong enough to sufficiently liquefy the stratum material. Our present ad-hoc interpretation is that the exciting seismic wave is primarily a surface wave (RAYLEIGH or/and LOVE-wave), which attenuates with depth below the surface. This, in turn, also means that fluidization is only partial but not complete. The individual grains are still partly in contact with one another; consequently, solid friction between some particles is still effective so that frictional solid shear stresses can still be transmitted among some particles. Hence, 'soon after the beginning of the earthquake the ground shaking subsides' as a consequence of the associated dissipation. With this interpretation, it is then equally clear that deeper, partly 'liquefied strata cease to transmit vibrations to the overlying deposits'. So, it appears that full liquefaction is restricted to surface near layers, if it really develops fully. Below a certain depth only partial fluidization exists, of which the relative amount decreases with depth and causes induced vibrations to attenuate at a faster rate than at shallow depth. The inference which follows from this may be stated as follows:

The fluidization in a binary solid-fluid mixture theory ought to be incorporated in the constitutive relation for the granular stress by a scalar variable, which expresses the granular stress as a functional that depends on a scalar variable $0 \leq li \leq 1$ such that for $li = 0$ a full solid stress representation emerges, while for $li = 1$ the



Fig. 13.10 (Upper-left) Overturned buildings after the devastating earthquake in Niigata, Japan, 1964. (Upper-right) Debris moraines in Tuyk Valley, Alaarcha basin North Tien Shan, Kirgizstan. © Prof. Aizen. (Lower left) Broken asphalt road and lifted manhole by Chuetsu Earthquake, 2004, Oijya, Niigata, Japan, reproduced from NGU Free Documentation License. (Lower right) Canterbury Earthquake, 04. Sept. 2010, New Zealand. Concrete sump, popped up out of the road due to liquefaction, Lower Styx Road, Canterbury, licensed under the Creative Commons Attribution Share 2.0

functional represents a stress formula for which full liquefaction is present for which no solid stress contribution survives.

Two limiting processes are seemingly responsible for the observations during, and in the aftermaths of, a strong earthquake. The *first* is a direct response of the soil to the driving surface-near (visco)-elastic wave and can be characterized as *acoustic fluidization* with high particle oscillations due to the strong and rapid oscillations. The *second* process, responsible for the post-earthquake water ejections, cannot be interpreted as an acoustic wave response since no driving mechanism is active. Consolidation and water ejection may be explained in this phase by the collapse of medium to high solid volume-fraction-soil lenses in an otherwise still loosely packed but denser matrix medium. During lens collapses, grains dripping from the matrix into the lenses will fill them with grains, so that the water must escape, eventually forming the cold volcanoes. For a regular distribution of the lenses continuous water ejection may take place. When the lenses are of different size, and irregularly

Fig. 13.11 Liquefaction by densification through explosives in the Lausitz, Eastern Germany.
© WALTER KUNZE and DIMITRIOS KOLYMBAS



distributed lens collapses may occur in an uncorrelated fashion and lead to intermittent water ejection. Both these processes are associated with dissipation due to solid and liquid response to it with solid and liquid stress contribution that is monitored by the fluidization parameter, li .

13.2.5 Segregation, Inverse Grading, Brazil Nut Effect

It is common experience for everyone who wishes to mix different types of granular particles that it is very difficult to achieve homogeneous mixing of several sorts of grains, whereas it is, in general, fairly easy to achieve homogeneous mixing with miscible fluids (e.g. water and ink). A system containing particles of different properties usually tends to show segregation. The nature of it depends on many factors, such as size, geometry and surface properties of the particles, the size of the velocity gradients and on boundary conditions. The dominant effect of segregation is the ratio of particle size between large and small particles in the mixture. However, the structure of the contact forces (resilience) and the smoothness or bumpiness of the surfaces of the particles also exercises an effect on the characterization of the segregation structure. Shaking a box of muesli before use brings any of the large nuts to the surface and rinsing with a spoon a jar of dried frozen coffee transports the large grains to the top. Such separations need dynamic action, i.e., particles must move and/or bounce against each other to activate the interaction between the particles.

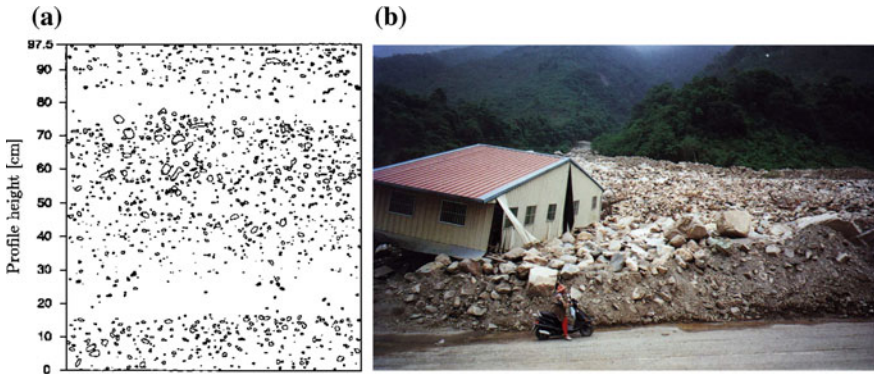


Fig. 13.12 **a** Sketch of a profile from a deposit of a pyroclastic flow due to the volcanic eruption of Mount Saint Helens, Washington USA, 1980. The profile is taken from a position about 6.7 km north of the crater and 1 km southwest of Spirit Lake. One complete ‘flow unit’ is shown that is over- and underlayed by other flow units. The profile depicts a clear reverse grading, in which larger grains are at the upper portion of the flow unit, while smaller grains are in its lower parts. Each flow unit corresponds to the passage of one pyroclastic flow (Courtesy S. STRAUB [77]). **b** Debris flow deposit from a disastrous flow event on 31. July-01 August 1996 in Taiwan. The front side of the road has been cleared. The picture demonstrates also particle size separation. The free surface of the deposit is covered by large boulders, whilst the lower part consists of the fine material, from [86]

This phenomenon is known as *Brazil nut effect* and has much importance in industrial and geological processes. When a granular material consisting of grains differing in size, shape, density, etc., is agitated or deformed in the presence of a gravitational field, *segregation* or *grading of particles* can occur. In gravity driven shear flows with a free surface it is observed that the fine particles collect at the lower parts of the layers, whereas the largest particles move towards the free surface. In the geological literature, this phenomenon is called *reverse* or *inverse grading*.

Such particle size separations are often observed in snow avalanches, debris flows and pyroclastic flow deposits. In dynamical systems of such flows one generally observes that the large particles move to the front and to the top surface, whilst the small particles accumulate at the bottom and in the rear part of the avalanche. In deposits of *pyroclastic flows* due to volcanic eruptions or in marine sediments of *turbidity currents* depositions show often a repetitive occurrence of ‘flow units’ with the fine particles at the bottom and particle size increasing as one moves higher up until a level is reached where a new flow unit commences as shown in **Fig. 13.12a**. Each flow unit corresponds to a passage of an avalanche, manifesting inverse grading.

Similar structures of inverse grading can also be seen in debris and (less obvious) in mud flows. Figure **13.12b** shows a debris deposit in which large particles cover the top, whereas the lower main part is composed of smaller size particles.

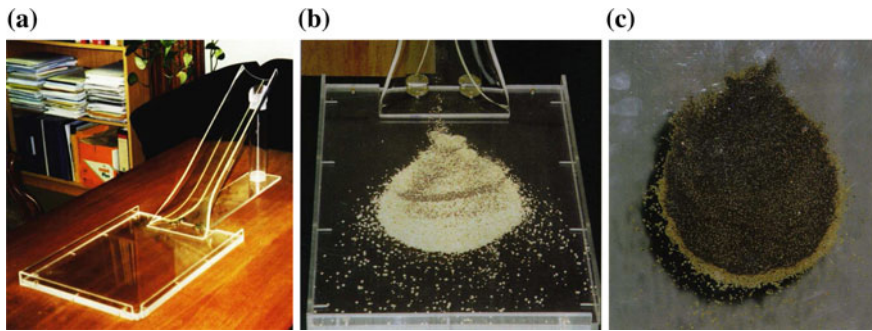


Fig. 13.13 Experiment, demonstrating inverse grading in an avalanche deposition of a bi-disperse granular mixture. The particles were initially almost uniformly mixed, and segregated due to their motion. **a** Small scale laboratory model with a parabolic chute inclined at 45° , continuously merging into a horizontal plane. **b** Photograph from above, of the deposited binary mixture consisting of small (*dark*) and large (*pale*) particles. The large particles are primarily at the *top* and in the front. **c** Photograph of the deposited mixture from *below*. A frontal horse shoe ring of *pale*, large particles is clearly seen, but the remainder of the basal deposit is made up of *dark* small particles, from [70]

Figure 13.13 shows a table-top experiment of an avalanche flowing down a Plexiglas-chute into a horizontal deposition area. The granular mass consists of particles with two different sizes: small (*dark*) and large (*pale*) particles. The granular mass is initially mixed; this mass is suddenly released at the top of the chute and the deposition on the horizontal Plexiglas is photographed from above and below the deposit. The panel in the middle shows the deposition from above in pale whitish color, indicating that the large particles ended up on the top of the deposit, Fig. 13.13b. Panel (c) shows the photo from below; primarily the dark particles which are of small size are seen. The horse-shoe type ring shows the pale big particles in the front part of the deposit. The figure corroborates our earlier statement that the large particles are in the front and on top, whereas the small ones are primarily at the bottom.

Finally, it should be stated that *normal* grading also exists but such situations are much less frequent.

13.3 Shallow Flow Avalanche Modeling

In this subsection we shall present the dominant avalanche models as they have been derived in the second half of the 20th century, beginning with VOELLMY's one-dimensional hydraulic or simple mass point model and ending with those models which are presently under use as depth integrated two-dimensional shallow flow models—for that see e.g. PUDASAINI and HUTTER [70], who give a detailed account of the subject and also present a historical review of it.



Fig. 13.14 ADOLF VOELLMY (15. July 1900–20. Feb. 1990)

Dr. ADOLF VOELLMY is born in Murten, a town in Freiburgian Switzerland. He was educated as an engineer at the ‘Technikum Burgdorf’ (a junior college) and entered the ‘Federal Institute of Technology’ (ETH) in Zurich by compulsory entrance examination, where he graduated as a civil engineer and earned the Dr. sc. tech. with a dissertation on ‘Eingebettete Rohre’ (‘Embedded pipes’). Following a transitory period on construction sites, he entered the ‘Eidgenössische Materialprüfungsanstalt’ (EMPA) (‘Swiss Laboratories for Materials Science and Technology’) in Dübendorf, where he acted since 1931 as Section Head and retired in December 1965.

His overall working attitude was outlined by himself in his dissertation: ‘The ensuing investigations follow the trustworthy approach applied in technology, namely to obtain, on the basis of simple assumptions, a principally correct picture about the static circumstances, and subsequently to experimentally verify some typical implications that are based on these knowingly simplified assumptions, in order, thus, to gain concrete, albeit restricted guidelines for computations. A solution will only correspond to the practical needs, if it is simultaneously to the point as well as simple.’

ADOLF VOELLMY was a calm, alert listener, whose opinions were moderately stated but objective, based on rational, well thought out arguments.

Photo: Archive EMPA. The text is based on [2].

13.3.1 Voellmy’s Avalanche Model

A. VOELLMY,² an engineer working at the Swiss Institute of Materials Testing (Eidgenössische Materialprüfungsanstalt, EMPA) in 1955 presented the first theoretical

²For a biographical sketch of ADOLF VOELLMY, see **Fig. 13.14**.

analysis of avalanche dynamics that was internationally recognized.³ His work remained largely unnoticed. VEOLLYMY's work appeared in a paper 'Über die Zerstörkraft von Lawinen' (about the destructive power of avalanches) in four consecutive parts and is based on a consultancy assignment to EMPA by the private company 'VOBAG AG' (in Vorarlberg, Austria) to analyze the damage done on properties in the Vorarlberg in the avalanche event of January 1954. Part 2 of the series of papers is relevant to us as it deals with the dynamics of snow masses.

Consider a snow layer of height h on a rigid plane inclined at the angle ζ relative to the horizontal plane. For the snow layer of density ρ immersed in an atmosphere of density $\rho_a = 0.127 \text{ kg m}^{-3}$ NEWTON's second law, formulated parallel to the sliding plane, see Fig. 13.9 reads

$$\rho h \frac{du}{dt} = \underbrace{g(\rho - \rho_a) h \sin \zeta}_{\text{driving force}} - \underbrace{(g(\rho - \rho_a) h \cos \zeta) \mu}_{\text{friction}} - \underbrace{\frac{\rho g}{\xi} u^2}_{\text{turb. friction}}. \quad (13.10)$$

In this equation the resistive force has two contributions, a dry friction COULOMB resistive force with (drag) coefficient μ and a turbulent MANNING-GAUKLER-STRICKLER term proportional to the squared velocity with coefficient ξ (ms^{-2}). By a routine computation (13.10) can be transformed to

$$\frac{du}{dt} = \frac{g}{h\xi} \left\{ \underbrace{\xi \left(1 - \frac{\rho_a}{\rho} \right) h (\sin \zeta - \mu \cos \zeta)}_{u_{\max}^2} - u^2 \right\} = \frac{g}{h\xi} \{u_{\max}^2 - u^2\}; \quad (13.11)$$

$$u_{\max} := \sqrt{\xi \left(1 - \frac{\rho_a}{\rho} \right) h (\sin \zeta - \mu \cos \zeta)}.$$

With the further variable transformation

$$y = \frac{u}{u_{\max}} \quad \text{and} \quad \tau := \frac{u_{\max}}{k} t, \quad k = \frac{h\xi}{g} \quad (13.12)$$

Equation (13.11) takes the form

$$\frac{dy}{d\tau} = 1 - y^2 \quad \longrightarrow \quad y = \tanh \tau \quad \Longrightarrow \quad u = u_{\max} \tanh \left(\frac{u_{\max}}{k} t \right) \quad (13.13)$$

for a motion starting from rest at $t = 0$. The avalanche velocity follows a hyperbolic tangent law and leads to an asymptotic velocity $u = u_{\max}$ at $t \rightarrow \infty$. The travel distance s is obtained as

³This is historically actually not correct. A French forest engineer, P. MOUGIN published in 1922 his results on the physical characteristics of snow and proposed a simple model to compute avalanche velocity and impact pressure: an avalanche was considered to be a sliding block experiencing a COULOMB friction force. For more details see [70].

$$s(t) = \int_0^t u(t') dt' = k \int_0^{\tau} \tanh(\tau') d\tau' = k \ln \left[\cosh \left(\frac{u_{\max}}{k} t \right) \right]. \quad (13.14)$$

To estimate the time t^* , which it takes to reach 80% of the limit velocity u_{\max} , one must invert the equation

$$\tanh \left(\frac{u_{\max}}{k} t^* \right) = 0.8 \quad (13.15)$$

for $u_{\max} t^*/k$ and substitute this value into (13.14). A. VOELLMY estimated $s^* \approx 0.5k = 0.5h\xi/g$. With $\xi = 500 \text{ ms}^{-2}$ and $g = 10 \text{ ms}^{-2}$ one obtains $s^* \approx 25h$: The avalanche travels 25 times its height to reach 80% of its maximum speed.

The above formulae can be simplified if the density of air is ignored as compared to the snow density ρ and if also the COULOMB friction force is ignored in comparison to the viscous force ($\mu = 0$). Then,

$$v_{\max}^2 \approx \xi h \sin \zeta.$$

The above are the few central lines of A. VOELLMY's text, extended by us to explain a few computational steps that fills only about half a page in the Swiss Civil Engineering Magazine (Schweizerische Bauzeitung) [84]. The entire paper is a landmark, because beyond the presentation of the above derivation, it contains a wealth of side issues that are touched, which demonstrate a superb physical understanding of the dynamical problem concerning fundamental as well as applied aspects of the stated problem.

13.3.2 The SH Model, Reduced to Its Essentials

The VOELLMY model received in the 60 and 70s of the 20th century a number of additions and improvements, in particular in attempts to design a model that could be applied to curved down-slopes. One rather important issue, however, was not touched, namely the fact that real avalanches do deform in the course of their motion, and VOELLMY's model as a mass point model does not have the flexibility to account for the geometric changes, which a moving granular mass experiences during its motion. In plane down-slope flow the toe of the avalanche will flow differently from its rear and correspondingly, the velocities inside the avalanche and the geometry will also accordingly adjust to these conditions. The new model, incorporating the geometric variations under movement, was developed in 1986 with publication in 1989⁴ by STEWARD B. SAVAGE and K. HUTTER [72]; it became so popular that extensions of it were immediately following and are still in the process of being developed. The

⁴The paper was not at all well received by the referees and had to go through a nearly 3-year process of revisions and extensions. K.H. still thinks, the original draft was more to the point than the published version, which now also contains a number of side issues.

model became known as SAVAGE-HUTTER (SH) model. In this subsection we present a derivation following an engineering approach of simple mechanics and will later present a slight generalization of the model derived from first principles.

Consider plane two-dimensional flow of a granular mass down an inclined plane and assume the flow to be density preserving. Isolate a column of length dx and formulate the mass and x -momentum balance equations for this element, see Fig. 13.15. Assume, moreover, that the down-slope velocity is constant over depth, so that $u = u(x, t)$. Equating the growth rate of mass within the column due to the growth in height to the inflow of mass from above and outflow from below yields

$$\begin{aligned} \frac{\partial}{\partial t} (\rho h(x, t)) dx &= \rho h(x, t)u(x, t) - \rho h(x + dx, t)u(x + dx, t) \\ &= -\frac{\partial}{\partial x} (\rho h(x, t)u(x, t)) dx + \mathcal{O}((dx)^2), \end{aligned} \quad (13.16)$$

or after dropping the constant mass density ρ ,

$$\frac{\partial h}{\partial t} + \frac{\partial(hu)}{\partial x} = 0. \quad (13.17)$$

In (13.16) TAYLOR series expansion was employed with higher terms being dropped in the second term of the first line. This will be done as well in the ensuing developments of many mathematical expressions without mentioning it.

Balance of momentum in the x -direction will be formulated following NEWTON's second law. With the x -momentum of the column given by $\rho h u dx$ we write

- Time rate of change of $\rho h u dx$:

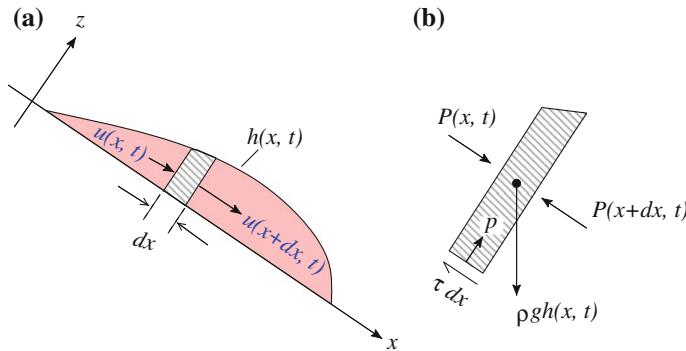


Fig. 13.15 Plane flow of a finite mass of granular material down an inclined plane **a** Sketch of the geometry, coordinate system and an infinitesimal column for which mass and momentum balances are formulated. **b** Free body diagram of the column with acting forces, where $P(x, t) = \int_0^{h(x,t)} p_L(x, z, t) dz$ and $P(x + dx, t) = \int_0^{h(x+dx,t)} p_L(x + dx, z, t) dz$, from [70]

$$\frac{\partial}{\partial t} ((\rho h u)(x, t)) dx, \quad (13.18)$$

- Flux of x -momentum through the column walls:

$$\begin{aligned} & \rho h(x, t)u^2(x, t) - \rho h(x + dx, t)u^2(x + dx, t) \\ &= -\frac{\partial}{\partial x} (\rho h(x, t)u^2(x, t)) dx + \mathcal{O}((dx)^2), \end{aligned} \quad (13.19)$$

- Forces in the x -direction applied on the column:

$$\begin{aligned} \text{(i)} &= \rho g h \sin \zeta \quad (\text{driving component of gravity}), \\ \text{(ii)} &= -\tau dx \quad (\text{basal friction}), \\ \text{(iii)} &= \int_0^{h(x,t)} p_L(x, z, t) dz - \int_0^{h(x+dx,t)} p_L(x + dx, z, t) dz \\ & \quad (\text{sum of longitudinal pressures}). \end{aligned} \quad (13.20)$$

The next step is the evaluation of the longitudinal pressure, p_L , in terms of the overburden pressure. This step is based on the recognition that in soils the *overburden pressure*

$$p(x, z, t) = \rho g (h(x, t) - z) \cos \zeta,$$

obtained from a force balance perpendicular to the x -direction, differs from the longitudinal pressure p_L by the *earth pressure coefficient* $K_{\text{act/pas}}$, viz.,

$$p_L(x, z, t) = K_{\text{act/pas}} p(x, z, t) \quad (13.21)$$

with

$$K_{\text{act/pas}} = \begin{cases} K_{\text{act}}, & \text{if } \partial u / \partial x > 0, \\ K_{\text{pas}}, & \text{if } \partial u / \partial x < 0, \end{cases} \quad (13.22)$$

where K_{act} and K_{pas} correspond to the extensive and compressive modes of deformation. With the representation (13.21) Eq. (13.20)₃ can be approximated as

$$-\frac{\rho g}{2} \cos \zeta \frac{\partial}{\partial x} (K_{\text{act/pas}} h^2(x, t)) dx + \mathcal{O}(dx)^2).$$

Applying a COULOMB-type friction law for the shear traction at the base yields

$$\tau(x, t) dx = -\rho g h(x, t) \cos \zeta \operatorname{sgn}(u) \tan \delta,$$

in which δ is the bed friction angle. Adding all contributions of (13.20), this yields

$$x - \text{force} = \left\{ \rho g h(x, t) (\sin \zeta - \operatorname{sgn}(u) \tan \delta \cos \zeta) - \frac{\rho g}{2} \frac{\partial}{\partial x} (K_{\text{act/pas}} h^2(x, t)) \cos \zeta \right\} dx + \mathcal{O}(dx^2). \quad (13.23)$$

If we now collect (13.18) + (13.19) = (13.23) and drop the common factor ρdx in the emerging equation, we have

$$\begin{aligned} & \frac{\partial}{\partial t} (hu) + \frac{\partial}{\partial x} (hu^2) \\ & = g \left\{ (\sin \zeta - \operatorname{sgn} u \tan \delta \cos \zeta) h - \frac{1}{2} \frac{\partial}{\partial x} (K_{\text{act/pas}} h^2(x, t)) \cos \zeta \right\}. \end{aligned} \quad (13.24)$$

Equations (13.17) and (13.24) constitute a system of two partial differential equations for the unknown longitudinal velocity $u(x, t)$ and the distribution of the height $h(x, t)$. They appear here in conservative form. Applying product differentiation in the respective terms on the left-hand side and right-hand side of (13.24) and using the mass balance Eq. (13.17) in the emerging equation yields instead of (13.24) the alternative equation

$$\begin{aligned} & \rho \left(\frac{\partial u}{\partial t} + u \frac{\partial u}{\partial x} \right) \\ & = \rho g (\sin \zeta - \operatorname{sgn} u \tan \delta \cos \zeta) - \rho g K_{\text{act/pas}} \frac{\partial h}{\partial x} \cos \zeta, \end{aligned} \quad (13.25)$$

in which the constant density ρ has been re-substituted to make NEWTON's second law more explicit as (mass times acceleration) = (sum of the forces). Equations (13.17) and (13.25) are the SAVAGE-HUTTER equations as derived by them in [72] in a more rigorous fashion. When $p = p_L$ ($K_{\text{act/pas}} = 1$) the pressure distribution is that of a liquid. In this form the equations correspond to the usual hydraulic models and are often called DE SAINT-VENANT or BOUSSINESQ equations. They were used in this form by the avalanche scientists in the Soviet Union, see S.S. GRIGORIYAN et al. [33–35] and M.E. EGLIT et al. [22–24, 26].

Equation (13.25) appears in a physically transparent form. The force terms on the right-hand side are the gravity driving force (first term), a COULOMB sliding force resisting the motion and slowing it down (second term) and a force (third term), which for $\partial h / \partial x < 0$ enhances the acceleration and for $\partial h / \partial x > 0$ reduces it. So, looking at Fig. 13.15, the last term on the right-hand side accelerates the moving mass on the frontal part and decelerates it in the rear part of the pile; the moving pile becomes longer with growing time on a plane with slope angle ζ . Omitting this term from (13.25) reduces the equation to the momentum balance of a rigid mass model that cannot account for geometric changes of the moving mass. Except for the turbulent viscous term, this is analogous to the VOELLMY model.

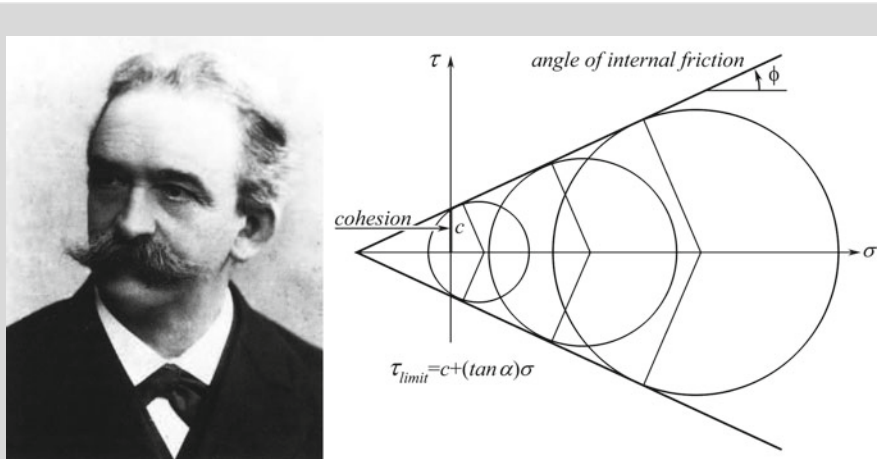


Fig. 13.16 CHRISTIAN OTTO MOHR (8. Oct. 1835 – 2. Oct. 1918)

CHRISTIAN OTTO MOHR was a German structural engineer who started his engineering education with 16 years at the Polytechnicum Hannover. 1855 he started to work as an engineer for the Royal Hanoverian State Railway System. As an assistant working for this governmental company he published in 1860 a paper on the statics of continuous bending beams. This work became instantly known, since it simplified the determination of the stress distribution in such structures. After moving to the Oldenburg State Railways, OTTO MOHR was the first structural engineer to design a steel bridge in Germany; its characteristics were to have been consequently composed of a truss of triangles, which allowed him to apply a simple computational scheme for the internal stresses, which was in 1863 further perfected by AUGUST RITTER.

1867, at the young age of 32, OTTO MOHR was appointed professor of applied mechanics and road and earth mechanics at the University of Stuttgart. He is said to have delivered attractive lectures of theoretical mechanics, so that his lectures were well attended. Scientifically, he reached a considerable simplification of the computation of the bending curve of beams by inventing his graphical construction by a string polygon. OTTO MOHR also developed the WILLOT-MOHR diagram and the MAXWELL-MOHR method for analyzing statically indeterminate structures. Best known is OTTO MOHR's graphical method to construct in a body point under plane stress the principal stresses by the MOHR stress circle, which is now taught to every engineering student in the basic courses of strength of materials. In 1873, OTTO MOHR assumed a chair of engineering science at the Polytechnicum Dresden, where he stayed until his retirement in 1900. He continued working scientifically, and his yield criterion for failure, alluded to in the main text by us is published in [62].

The above figure shows for plane stress that failure at a material point will occur when the MOHR circle touches the failure line $\tau = c + (\tan \phi)\sigma$.

The text is based on www.wikipedia.org

There still remains the identification of the earth pressure coefficient under active and passive pressure conditions. To this end, we consider the granulate to be a cohesionless COULOMB material with angle of internal friction $\phi > \delta$, where δ is the bed friction angle. The state of stress $(p, -\tau)$ for a plane material element (**Fig. 13.17a**)

at the base must lie on a straight line through the origin inclined at the angle $(-\delta)$ (Fig. 13.17b). All other elements that are rotated relative to the element shown in Fig. 13.17a must lie on circles through the point $(p, -\tau)$, which are also tangential to the lines through the origin with inclination $\pm\phi$; there are two such circles, a bigger, passive, and a smaller, active-one. The stress states (p_L, τ) on the perpendicular elements lie on opposite sides of these MOHR-circles,⁵ as indicated in Fig. 13.17b. The center of the bigger MOHR-circle lies at $\frac{1}{2}(p_L + p)$ and its radius is given by $r = (\tau^2 + \frac{1}{4}(p_L - p)^2)^{1/2}$. Moreover, from the geometry of the circles in Fig. 13.17b we identify

$$\frac{\tau}{p} = \tan \delta, \quad \sin^2 \phi = \frac{\tau^2 + \frac{1}{4}(p_L - p)^2}{\frac{1}{4}(p_L + p)^2}. \quad (13.26)$$

Substituting (13.26)₁ into (13.26)₂ and observing that $p_L/p = K_{\text{act/pas}}$ leads to a quadratic equation for $K_{\text{act/pas}}$ with the solution

$$K_{\text{act/pas}} = 2 \sec^2 \phi \left(1 \mp (1 - \cos^2 \phi \sec^2 \delta)^{1/2} \right) - 1, \quad (13.27)$$

in which the upper (lower) signs apply for K_{act} (K_{pas}) and $\sec \phi = 1/\cos \phi$. This shows that only two phenomenological constants, the angle of internal friction, ϕ , and the bed friction angle, δ , describe the earth pressure coefficient, the only two material parameters arising in this SH model. A further advantage of this model is also, that in applications δ and ϕ can relatively easily be estimated.

The above equations have been written in dimensional form. It is always advantageous to put them in dimensionless form because in that form characteristic dimensionless quantities arise explicitly, which point at the significance of the physical processes that are described by the equations. We shall introduce dimensionless quantities for the variables $\{x, z, h, u, t\}$ in the form

$$\{x, z, h, u, t\} = \left\{ L\hat{x}, H\hat{z}, H\hat{h}, \sqrt{gL}\hat{u}, \sqrt{(L/g)\hat{t}} \right\}, \quad (13.28)$$

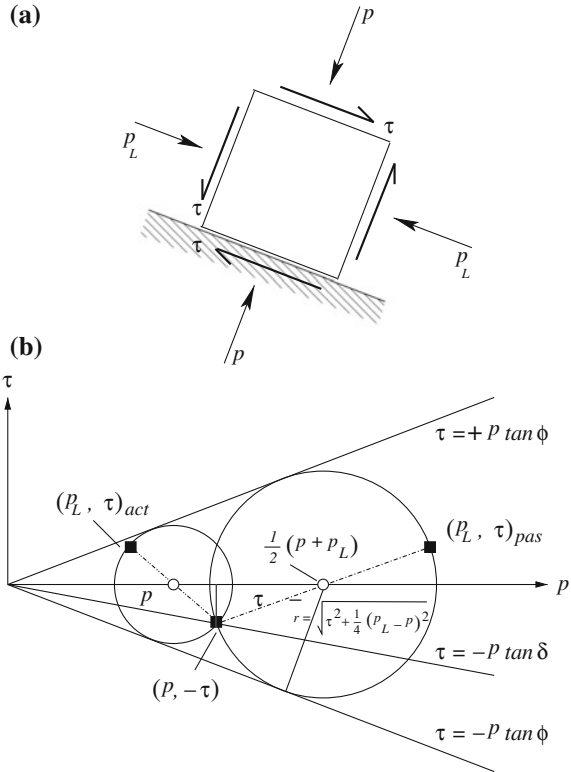
in which L and H are length and depth scales, $\sqrt{L/g}$ is a time scale, reminiscent of the free fall and, \sqrt{gL} is a free fall velocity and the $(\hat{\cdot})$ -quantities are dimensionless variables. Substitution of the transformations (13.28) into (13.17) and (13.24) or (13.25) transform these into

- in conservative form:

$$\begin{aligned} \frac{\partial h}{\partial t} + \frac{\partial hu}{\partial x} &= 0, \\ \frac{\partial hu}{\partial t} + \frac{\partial hu^2}{\partial x} &= (\sin \zeta - \text{sgn}(u) \tan \delta \cos \zeta)h - \frac{\partial}{\partial x} \left(\frac{\varepsilon}{2} K_{\text{act/pas}} h^2 \cos \zeta \right), \end{aligned} \quad (13.29)$$

⁵For a biographical sketch of C.O. MOHR, see Fig. 13.16.

Fig. 13.17 a Material plane element at the basal plane with the stresses $(p, -\tau)$ and (p_L, τ) , acting at the faces as indicated. **b** MOHR circles, representing active and passive stress states: The element touching the base, the side element, $p_L/p = K_{act/pas}$ follows from trigonometric relations (13.26)



- in non-conservative form:

$$\begin{aligned} \frac{\partial h}{\partial t} + \frac{\partial hu}{\partial x} &= 0, \\ \frac{\partial u}{\partial t} + u \frac{\partial u}{\partial x} &= (\sin \zeta - \operatorname{sgn}(u) \tan \delta \cos \zeta) - \varepsilon \cos \zeta K_{act/pas} \frac{\partial h}{\partial x}, \end{aligned} \tag{13.30}$$

in which the hat symbols have been deleted, and

$$\varepsilon = H/L \ll 1. \tag{13.31}$$

ε is very small, generally $\varepsilon = 10^{-3} - 10^{-2}$.

Equations (13.29) and (13.30) show no other characteristic parameters than $K_{act/pas}$, which stands for normal stress effects. ε is also dimensionless and measures as an aspect ratio the significance of the shallowness of the avalanching mass. Thus, apart from the angle of internal friction no other parameter such as the FROUDE and REYNOLDS numbers enter the equations. Since ϕ and δ are easy to keep invariant under down-scaling processes to laboratory dimensions one concludes that the SH

equations are scale invariant. Reason for this is that no turbulent viscous resistive forces are included in the SH equations.

13.4 A Three-Dimensional Granular Avalanche Model

In this section we shall not present a rigorous derivation of the SH equations; for that we refer the reader to the original paper by S.B. SAVAGE and K. HUTTER [72]. Here we derive a slight generalization of it due to J.M.N.T. GRAY et al. [30], namely the flow of avalanches over shallow parabolic three-dimensional topography. This will lead to the first, still somewhat academic, description of the flow of a finite mass of granular material down a valley or corrie. A reference surface that follows the mean down-slope bed topography is used to define an orthogonal curvilinear coordinate system $Oxyz$, see Fig. 13.18. The z -axis is normal to the reference (ruled) surface, and the x - and y -coordinates are tangential to it with the x -axis oriented in the down-slope direction. The down-slope inclination angle ζ is used to define the reference surface as a function of the down-slope coordinate x . The reference surface does not vary with the cross-slope coordinate y . The chute geometry is superposed by defining the height $z = b(x, y, t)$ above the reference surface, $z = 0$, as illustrated in Fig. 13.18. Even though the local down-slope direction may not coincide with the direction of the x -coordinate, for notational simplicity, the components in the x -direction are referred to as down-slope components and components in the y -direction as cross-slope components. Here we will present a detailed derivation of the model equations, which will reduce to the SH equations with adequate simplifications.

13.4.1 Field Equations

The avalanche is assumed to be a density preserving material⁶ with constant density ρ_0 throughout the body. Then, the mass and momentum conservation laws reduce to

$$\nabla \cdot \mathbf{u} = 0, \quad (13.32)$$

$$\rho_0 \left\{ \frac{\partial \mathbf{u}}{\partial t} + \nabla \cdot (\mathbf{u} \otimes \mathbf{u}) \right\} = -\nabla \cdot \mathbf{p} + \rho_0 \mathbf{g}, \quad (13.33)$$

where \mathbf{u} is the velocity, \otimes is the tensor product, \mathbf{p} is the pressure tensor (negative CAUCHY stress tensor) and the \mathbf{g} -vector is the gravity constant. The granular

⁶Experiments by THILO KOCH [49] have shown in this case that the avalanche volume expands immediately after the start of the motion by approximately 10% and then remains approximately constant during the entire motion.

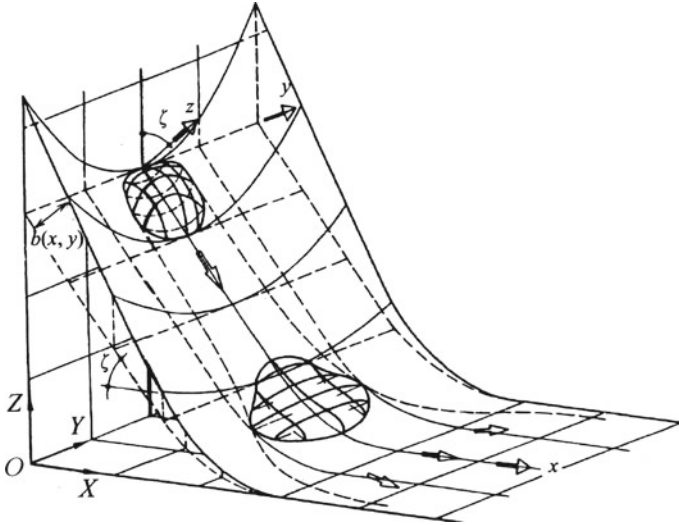


Fig. 13.18 The rectangular Cartesian coordinate system $OXYZ$ aligned so that the Z -axis is parallel but opposite in direction to the gravity acceleration vector, and the Y -axis is parallel to the cross-slope reference surface coordinate y . The basal topography (solid lines), on which the avalanche slides, $F^b(x, y, t) = 0$, is defined by its height above the curvilinear reference surface $F^b = b(x, y, t) - z$ (dashed lines). The shallow complex three-dimensional geometry is therefore superposed on the two-dimensional reference surface, from [30]. © Proc. Royal Soc. London

avalanche is assumed to satisfy a MOHR–COULOMB *yield criterion*, in which the internal shear stress \mathbf{S} and the normal pressure N on the plane element, see Fig. 13.19, are related by

$$|\mathbf{S}| = N \tan \phi, \quad (13.34)$$

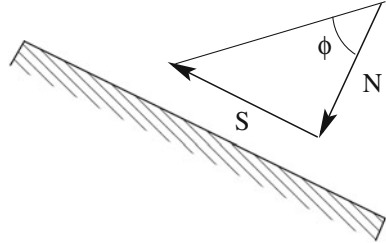
where ϕ is the angle of internal friction. The conservation laws (13.32) and (13.33) are complemented by *kinematic boundary conditions* at the free surface $F^s(\mathbf{x}, t) = 0$, and at the base, $F^b(\mathbf{x}, t) = 0$, of the avalanche,

$$F^s(\mathbf{x}, t) = 0, \quad \frac{\partial F^s}{\partial t} + \mathbf{u}^s \cdot \nabla F^s = 0, \quad (13.35)$$

$$F^b(\mathbf{x}, t) = 0, \quad \frac{\partial F^b}{\partial t} + \mathbf{u}^b \cdot \nabla F^b = 0, \quad (13.36)$$

where the superscripts ‘ s ’ and ‘ b ’ indicate that a variable is to be evaluated at the surface and the base, respectively. There are also *dynamical boundary conditions* that must be satisfied. The *free surface* of the avalanche is *traction free*, while at the base satisfies a COULOMB *dry friction sliding law* will hold. That is

Fig. 13.19 Sketch showing the relation between the internal shear stress S and the normal pressure N on a plane element in the granular body



$$F^s(\mathbf{x}, t) = 0, \quad \mathbf{p}^s \mathbf{n}^s = \mathbf{0}, \quad (13.37)$$

$$F^b(\mathbf{x}, t) = 0, \quad \mathbf{p}^b \mathbf{n}^b - \mathbf{n}^b (\mathbf{n}^b \cdot \mathbf{p}^b \mathbf{n}^b) = (\mathbf{u}^b / |\mathbf{u}^b|) (\mathbf{n}^b \cdot \mathbf{p}^b \mathbf{n}^b) \tan \delta, \quad (13.38)$$

where the surface and basal normal vectors are

$$\mathbf{n}^s = \frac{\nabla F^s}{|\nabla F^s|}, \quad \mathbf{n}^b = \frac{\nabla F^b}{|\nabla F^b|}. \quad (13.39)$$

Remarks

1. Notice that $\mathbf{p}\mathbf{n}$ is the negative traction vector, $\mathbf{n} \cdot \mathbf{p}\mathbf{n}$ is the normal pressure and $\mathbf{p}\mathbf{n} - \mathbf{n}(\mathbf{n} \cdot \mathbf{p}\mathbf{n})$ is the negative shear traction. Thus, the COULOMB dry friction law, (13.38), expresses the fact that the magnitude of the basal shear stress equals the normal basal pressure multiplied by the coefficient of friction, $\tan \delta$, called the *basal friction angle*.
2. The basal shear traction is assumed to point in the opposite direction to the basal velocity \mathbf{u}^b in (13.38). This implicitly assumes that the basal topography is fixed, so that $\mathbf{u}^b \cdot \mathbf{n}^b = 0$ by (13.36). This implies that the basal velocity \mathbf{v}^b is tangential to the basal surface. It also states that entrainment of snow from the ground is ignored. Defining the direction of the shear stress in this way introduces a singularity into the equation at $\mathbf{u}^b = \mathbf{0}$.
3. This singularity can be avoided by replacing $\mathbf{u}^b / |\mathbf{u}^b|$ by the vector valued function

$$\mathbf{f}_\alpha = (f_u, f_v), \quad (13.40)$$

where

$$f_u = \tanh(\alpha u), \quad f_v = \tanh(\alpha v), \quad (13.41)$$

where $\alpha > 1$ is a real number. This parameterization removes the singularity at $\mathbf{u}^b = \mathbf{0}$. Moreover, as $\alpha \rightarrow \infty$, \mathbf{f}_α approaches the function $\mathbf{u}^b / |\mathbf{u}^b|$.

In actual modeling computations this restriction causes problems at the onset of the motion and near the end of the avalanche motion when the moving mass comes to a rest.

13.4.2 Curvilinear Coordinates⁷

The complex topography is modeled by defining an orthogonal curvilinear reference surface, and then superposing the shallow basal topography on it, as shown in Fig. 13.18. For precise explanation, a rectangular Cartesian coordinate system $O'XYZ$ is defined with unit basis vectors \mathbf{i} , \mathbf{j} , \mathbf{k} aligned so that the vector \mathbf{k} is parallel, but in the opposite sense, to the gravity vector \mathbf{g} , and \mathbf{k} lies in the vertical plane, in which the reference surface varies. A simple curvilinear coordinate system $oxyz$ is introduced. In this coordinate system, the position vector \mathbf{r} is given by

$$\mathbf{r} = \mathbf{r}^r(x, y) + z\mathbf{n}^r, \quad (13.42)$$

where \mathbf{r}^r is the position vector of the reference surface and \mathbf{n}^r is the unit normal vector to this surface. In Cartesian coordinates

$$\mathbf{n}^r = \sin \zeta \mathbf{i} + \cos \zeta \mathbf{k}, \quad (13.43)$$

where ζ is the inclination angle of the normal vector relative to the Z -axis. For ease of notation the identification $(x, y, z) = (x^1, x^2, x^3)$ is made. These are the contravariant components in the curvilinear coordinate system (see e.g. [48]), and the associated covariant basis vectors, \mathbf{g}_i are given by

$$\mathbf{g}_i = \frac{\partial \mathbf{r}}{\partial x^i}. \quad (13.44)$$

The gradients $\partial \mathbf{r} / \partial x^1$ and $\partial \mathbf{r} / \partial x^2$ are the tangent vectors to the reference surface in the x^1 - and x^2 -directions, respectively. Thus, choosing the orthogonal vectors with the x -axis in the $O'XZ$ -plane, it follows that $\partial \mathbf{r} / \partial x^1 = \cos \zeta \mathbf{i} - \sin \zeta \mathbf{k}$ and $\partial \mathbf{r} / \partial x^2 = \mathbf{j}$, so that

$$\begin{aligned} \mathbf{g}_1 &= (1 - \kappa x^3) (\cos \zeta \mathbf{i} - \sin \zeta \mathbf{k}), \\ \mathbf{g}_2 &= \mathbf{j}, \\ \mathbf{g}_3 &= \sin \zeta \mathbf{i} + \cos \zeta \mathbf{k}, \end{aligned} \quad (13.45)$$

where the curvature is defined as

$$\kappa = -\frac{\partial \zeta}{\partial x^1}. \quad (13.46)$$

The covariant metric coefficients are defined as $g_{ij} = \mathbf{g}_i \cdot \mathbf{g}_j$, so that in view of (13.45)

⁷In this section and henceforth knowledge of the basic elements of tensor calculus are supposed known. There is a great number of books on this e.g. R. BOWEN and C.C. WANG [7], I.S. SOKOLNIKOFF [76], E. KLINGBEIL [48], L. BRILLOUIN [8].

$$(g_{ij}) = \begin{pmatrix} (1 - \kappa x^3)^2 & 0 & 0 \\ 0 & 1 & 0 \\ 0 & 0 & 1 \end{pmatrix}. \quad (13.47)$$

Since the off-diagonal elements of this metric tensor are all zero, this simple curvilinear coordinate system is called orthogonal. The covariant unit vectors are defined as $\mathbf{g}_i^* = \mathbf{g}_i / \sqrt{g_{(ii)}}$, where the EINSTEIN summation convention is dropped for the indices in parentheses. The contravariant basis vectors \mathbf{g}^j are constructed by

$$\mathbf{g}_i \cdot \mathbf{g}^j = \delta_i^j, \quad (13.48)$$

and this formula delivers for (13.45)

$$\begin{aligned} \mathbf{g}^1 &= \frac{(\cos \zeta \mathbf{i} - \sin \zeta \mathbf{k})}{1 - \kappa x^3}, \\ \mathbf{g}^2 &= \mathbf{j}, \\ \mathbf{g}^3 &= \sin \zeta \mathbf{i} + \cos \zeta \mathbf{k}. \end{aligned}$$

Moreover, the associated contravariant metric coefficients are given by the metric

$$(g^{ij}) = (\mathbf{g}^i \cdot \mathbf{g}^j) = \begin{pmatrix} 1/(1 - \kappa x^3)^2 & 0 & 0 \\ 0 & 1 & 0 \\ 0 & 0 & 1 \end{pmatrix}.$$

It is clear that in contrast to the unit vectors \mathbf{i} , \mathbf{j} , \mathbf{k} , the covariant vectors \mathbf{g}_i vary as functions of position. We need the CHRISTOFFEL⁸ symbols of second kind to transfer the equations of motion from coordinate free form to the curvilinear coordinate system; they are defined as

$$\Gamma_{lm}^k = \frac{1}{2} g^{(kk)} (g_{mk,l} + g_{kl,m} - g_{lm,k}), \quad (13.49)$$

and the EINSTEIN summation convention is again dropped for the indices in parentheses. For the curvilinear coordinates (13.47) the components of the CHRISTOFFEL symbol are

$$\begin{aligned} \mathbf{\Gamma}^1 &= \frac{-1}{1 - \kappa z} \begin{pmatrix} \kappa' & 0 & \kappa \\ 0 & 0 & 0 \\ \kappa & 0 & 0 \end{pmatrix}, & \mathbf{\Gamma}^2 &= \begin{pmatrix} 0 & 0 & 0 \\ 0 & 0 & 0 \\ 0 & 0 & 0 \end{pmatrix}, \\ \mathbf{\Gamma}^3 &= (1 - \kappa z) \begin{pmatrix} \kappa & 0 & 0 \\ 0 & 0 & 0 \\ 0 & 0 & 0 \end{pmatrix}, \end{aligned} \quad (13.50)$$

where $\kappa' = \partial \kappa / \partial x^1$.

⁸For a portrait and a short biography of E.B. CHRISTOFFEL, see Vol. 1, Chap. 6, Fig. 6.35.

Further, the vector differential operator ∇ is defined as

$$\nabla := \mathbf{g}^k \frac{\partial}{\partial x^k}, \quad (13.51)$$

with components given by the contravariant basis \mathbf{g}^k ; the gradient of a given scalar field F is $\nabla F = F_{,k} \mathbf{g}^k$. For the curvilinear coordinate system defined in (13.47) in terms of the covariant unit basis, this can be expressed as

$$\nabla F = \frac{1}{1 - \kappa z} \frac{\partial F}{\partial x} \mathbf{g}_1^* + \frac{\partial F}{\partial y} \mathbf{g}_2^* + \frac{\partial F}{\partial z} \mathbf{g}_3^* \quad (13.52)$$

in terms of the variables (x, y, z) . Here, $\mathbf{g}_j^* = \mathbf{g}_j / |\mathbf{g}_j|$, $j = 1, 2, 3$ are unit vectors and the prefactors of \mathbf{g}_j^* are called the *physical components* of the gradient of F .

The divergence of the vector field $\mathbf{u} = u^i \mathbf{g}_i$ is expressed as

$$\nabla \cdot \mathbf{u} = \left(\mathbf{g}^k \frac{\partial}{\partial x^k} \right) \cdot (u^i \mathbf{g}_i) = u^i_{,i} + u^i \Gamma_{ik}^k, \quad \Gamma_{ik}^k = \mathbf{g}^k \cdot \mathbf{g}_{i,k}. \quad (13.53)$$

The vector physical components u^{i*} of \mathbf{u} are defined by $u^{i*} = u^i \sqrt{g_{(ii)}}$. The divergence of a vector \mathbf{u} in curvilinear coordinates is now computed by substituting this into (13.53) together with the CHRISTOFFEL symbols (13.50) as

$$\nabla \cdot \mathbf{u} = \frac{\partial}{\partial x} \left(\frac{u^{1*}}{1 - \kappa z} \right) + \frac{\partial u^{2*}}{\partial y} + \frac{\partial u^{3*}}{\partial z} - \frac{u^{1*} \kappa' z}{(1 - \kappa z)^2} - \left(\frac{u^{3*} \kappa}{1 - \kappa z} \right). \quad (13.54)$$

In a similar manner, for a given symmetric rank-2 tensor $\mathbf{p} = p^{ij} \mathbf{g}_i \otimes \mathbf{g}_j$, the divergence can be computed as

$$\nabla \cdot \mathbf{p} = \left(\mathbf{g}^k \frac{\partial}{\partial x^k} \right) \cdot (p^{ij} \mathbf{g}_i \otimes \mathbf{g}_j) = (p^{ki}_{,k} + p^{ji} \Gamma_{jk}^k + p^{kj} \Gamma_{jk}^i) \sqrt{g_{(ii)}} \mathbf{g}_i^*. \quad (13.55)$$

As before, the physical components p^{ij*} of a second order tensor \mathbf{p} are related to the contravariant components by $p^{ij*} = p^{ij} (\sqrt{g_{(ii)}} \sqrt{g_{(jj)}})$. This, together with the CHRISTOFFEL symbols (13.50), after substitution into (13.55) implies the following curvilinear form of $\nabla \cdot \mathbf{p}$:

$$\begin{aligned} \nabla \cdot \mathbf{p} = & \left(\frac{\partial}{\partial x} \left(\frac{p^{11*}}{1 - \kappa z} \right) + \frac{\partial p^{12*}}{\partial y} + \frac{\partial p^{13*}}{\partial z} - \frac{\kappa' z p^{11*}}{(1 - \kappa z)^2} - \frac{2\kappa p^{13*}}{1 - \kappa z} \right) \mathbf{g}_1^* \\ & + \left(\frac{\partial}{\partial x} \left(\frac{p^{12*}}{1 - \kappa z} \right) + \frac{\partial p^{22*}}{\partial y} + \frac{\partial p^{23*}}{\partial z} - \frac{\kappa' z p^{12*}}{(1 - \kappa z)^2} - \frac{2\kappa p^{23*}}{1 - \kappa z} \right) \mathbf{g}_2^* \\ & + \left(\frac{\partial}{\partial x} \left(\frac{p^{13*}}{1 - \kappa z} \right) + \frac{\partial p^{23*}}{\partial y} + \frac{\partial p^{33*}}{\partial z} - \frac{\kappa' z p^{13*}}{(1 - \kappa z)^2} \right) \mathbf{g}_3^* \end{aligned}$$

$$- \kappa \left(\frac{p^{33*} - p^{11*}}{1 - \kappa z} \right) \mathbf{g}_3^* \quad (13.56)$$

13.4.3 Equations in Dimensionless Form

Let us now write the mass and momentum balance equations in the curvilinear coordinates using the basis \mathbf{g}_1^* , \mathbf{g}_2^* , \mathbf{g}_3^* . With respect to this basis the components of the velocity vector are u , v , w , so that $\mathbf{u} = u\mathbf{g}_1^* + v\mathbf{g}_2^* + w\mathbf{g}_3^*$. Similarly, the physical components of the symmetric pressure tensor \mathbf{p} are p_{xx} , p_{yy} , p_{zz} , p_{xy} , p_{yz} , p_{zx} , where the convention that subscripts define covariant quantities is now dropped,⁹ i.e. p_{xx} , etc., are now and henceforth physical components. The physical variables are non-dimensionalized by using the scaling transformations

$$\begin{aligned} (x, y, z, F^s, F^b, t) &= (L\hat{x}, L\hat{y}, H\hat{z}, H\hat{F}_b, H\hat{F}_s, \sqrt{(L/g)\hat{t}}), \\ (u, v, w) &= \sqrt{gL} (\hat{u}, \hat{v}, \varepsilon\hat{w}), \\ (p_{xx}, p_{yy}, p_{zz}) &= \rho_0 g H (\hat{p}_{xx}, \hat{p}_{yy}, \hat{p}_{zz}), \\ (p_{xy}, p_{xz}, p_{yz}) &= \rho_0 g H \mu (\hat{p}_{xy}, \hat{p}_{xz}), \\ (\kappa) &= \mathcal{R}\hat{\kappa}, \end{aligned} \quad (13.57)$$

where the variables $\hat{(\cdot)}$ are dimensionless. The scalings (13.57) assume that the avalanche has a typical length tangential to the reference surface and a typical thickness H normal to it, and \mathcal{R} is a typical radius of curvature of the reference geometry. Assuming a granular static balance, the typical normal pressures at the base of the avalanche are of the order¹⁰ $\rho_0 g H$, and the COULOMB dry friction law suggests that the basal shear stresses are of the order $\rho_0 g H \tan \delta_0$, where δ_0 is a typical basal angle of friction. Finally, the down-slope curvature κ is in the order of $1/\mathcal{R}$. These scalings introduce three non-dimensional parameters, namely

$$\varepsilon = H/L, \quad \lambda = L/\mathcal{R}, \quad \mu = \tan \delta_0, \quad (13.58)$$

where ε is the *aspect ratio* of the avalanche, λ is a *measure of the radius of curvature* of the reference geometry with respect to the length of the avalanche and μ is the *coefficient of friction* associated to the base.

The mass balance equation (13.32) can be written in curvilinear coordinates by using the transformation rule (13.53) for the divergence of a vector field. Applying

⁹For orthogonal coordinate systems there is no difference between co- and contravariant components of vectors and tensors anyhow.

¹⁰This scaling for the normal pressure tacitly assumes a ‘hydrostatic nature of the pressure’ in a granular heap. This is in fact untypical of granular systems for which the pressure is not the overburden weight but saturates after a certain depth.

the scalings (13.57) and (13.58), it follows that the non-dimensional curvilinear form of the mass balance equation (13.54) is

$$\nabla \cdot \mathbf{u} = \frac{\partial}{\partial x}(u\psi) + \frac{\partial v}{\partial y} + \frac{\partial w}{\partial z} - \varepsilon\lambda\kappa'zu\psi^2 - \varepsilon\lambda\kappa w\psi = 0, \quad (13.59)$$

where the hats are now dropped and

$$\psi = \frac{1}{\sqrt{1 - \varepsilon\lambda\kappa z}}. \quad (13.60)$$

The momentum balance equation (13.33) can be written in curvilinear coordinates by using relation (13.56) to transform the tensor $\mathbf{u} \otimes \mathbf{u}$ and the pressure tensor \mathbf{p} . Let g_1 , g_2 and g_3 be the physical components of the gravitational acceleration along the x -, y - and z -axes, respectively. Assume, moreover, that $\mathbf{g} = (g_1, g_2, g_3)$. For the present coordinate system $g_1 = g \sin \zeta$, $g_2 = 0$ and $g_3 = -g \cos \zeta$. It follows that the non-dimensional curvilinear components of the momentum balance in the down-slope, cross-slope and normal directions to the reference surface are

$$\begin{aligned} & \frac{\partial u}{\partial t} + \frac{\partial}{\partial x}(u^2\psi) + \frac{\partial}{\partial y}(uv) + \frac{\partial}{\partial z}(uw) - \varepsilon\lambda\kappa'zu^2\psi^2 - 2\varepsilon\lambda\kappa uv\psi \\ &= \sin \zeta - \varepsilon \frac{\partial}{\partial x}(p_{xx}\psi) - \varepsilon\mu \frac{\partial p_{xy}}{\partial y} - \mu \frac{\partial p_{xz}}{\partial z} + \varepsilon^2\lambda\kappa'zp_{xx}\psi^2 + 2\varepsilon\lambda\mu\kappa p_{xz}\psi, \end{aligned} \quad (13.61)$$

$$\begin{aligned} & \frac{\partial v}{\partial t} + \frac{\partial}{\partial x}(uv\psi) + \frac{\partial}{\partial y}(v^2) + \frac{\partial}{\partial z}(vw) - \varepsilon\lambda\kappa'zuv\psi^2 - \varepsilon\lambda\kappa v w\psi \\ &= -\varepsilon\mu \frac{\partial}{\partial x}(p_{xy}\psi) - \varepsilon \frac{\partial p_{yy}}{\partial y} - \mu \frac{\partial p_{yz}}{\partial z} + \varepsilon^2\lambda\mu\kappa'zp_{xy}\psi^2 + \varepsilon\lambda\mu\kappa p_{yz}\psi, \end{aligned} \quad (13.62)$$

$$\begin{aligned} & \varepsilon \left\{ \frac{\partial w}{\partial t} + \frac{\partial}{\partial x}(uw\psi) + \frac{\partial}{\partial y}(vw) + \frac{\partial}{\partial z}(w^2) \right\} - \varepsilon^2\lambda\kappa'z uw\psi^2 - \lambda\kappa(\varepsilon^2w^2 - u^2)\psi \\ &= \cos \zeta - \varepsilon\mu \frac{\partial}{\partial x}(p_{xz}\psi) - \varepsilon\mu \frac{\partial p_{yz}}{\partial y} - \frac{\partial p_{zz}}{\partial z} + \varepsilon^2\lambda\mu\kappa'zp_{xz}\psi^2 + \varepsilon\lambda\kappa(p_{zz} - p_{xx})\psi, \end{aligned} \quad (13.63)$$

respectively. Further simplification of these equations is possible, but they are left in the given form as this proves to be particularly useful when the free surface and basal boundary conditions are included once the depth integration process is performed.

13.4.4 Kinematic Boundary Conditions

The free surface of the avalanche, $F^s = 0$, and the basal topography over which the avalanche is assumed to slide, $F^b = 0$, are defined by their respective heights above the curvilinear reference:

$$F^s \equiv z - s(x, y, t) = 0, \quad F^b \equiv -z + b(x, y, t) = 0. \quad (13.64)$$

Consider the basal surface $F^b(\mathbf{x}, t) = 0$, $z = b(x, y, t)$; briefly $F^b \equiv b - z = 0$ in dimensional form. Then,

$$\frac{\partial F^b}{\partial t} + \mathbf{u}^b \cdot \nabla F^b = 0 \quad (13.65)$$

describes the kinematic surface condition. It is emphasized that \mathbf{u}^b is here the material velocity of particles at the base, but then processes of bed erosion or sedimentation are excluded. In case these processes are included, \mathbf{u}^b in (13.65) would have to be replaced by \mathbf{w} , say, the non-material velocity with which the base is moving when erosion from, and deposition of the material to, the base are accounted for. This not being considered, we deduce from (13.51), (13.64)₂, and (13.65) the following kinematic condition for the basal surface (13.51),

$$\frac{\partial b}{\partial t} + \left(\frac{1}{1 - \kappa z} \right)^b u^b \frac{\partial b}{\partial x} + v^b \frac{\partial b}{\partial y} - w^b = 0. \quad (13.66)$$

Similarly, the kinematic condition for the free surface is

$$\frac{\partial s}{\partial t} + \left(\frac{1}{1 - \kappa z} \right)^s u^s \frac{\partial s}{\partial x} + v^s \frac{\partial s}{\partial y} - w^s = 0. \quad (13.67)$$

Now we will derive the non-dimensional form of the kinematic conditions. From (13.57) and (13.66) we have

$$\frac{\partial(Hb)}{\partial(\sqrt{L/gt})} + \left(\frac{1}{1 - \frac{H}{R}\kappa z} \right)^b \frac{\partial(Hb)}{\partial(Lx)} + \sqrt{gL}v^b \frac{\partial(Hb)}{\partial(Ly)} - \sqrt{gL}\varepsilon w^b = 0.$$

We can derive a similar equation for the free surface. Using (13.58), it follows from (13.66) and (13.67) that the non-dimensional curvilinear form of the surface and basal kinematic conditions are

$$z = b(x, y, t), \quad \frac{\partial b}{\partial t} + \psi^b u^b \frac{\partial b}{\partial x} + v^b \frac{\partial b}{\partial y} - w^b = 0, \quad (13.68)$$

$$z = s(x, y, t), \quad \frac{\partial s}{\partial t} + \psi^s u^s \frac{\partial s}{\partial x} + v^s \frac{\partial s}{\partial y} - w^s = 0, \quad (13.69)$$

where hats have been dropped.

13.4.5 Traction Free Condition at the Free Surface

From (13.52), (13.57) and (13.58), we obtain the non-dimensional form of the gradient of the free surface as follows

$$\nabla F^s = \varepsilon \left(\frac{1}{1 - \varepsilon \lambda \kappa z} \right)^s \frac{\partial s}{\partial x} \mathbf{g}_1^* + \varepsilon \frac{\partial s}{\partial y} \mathbf{g}_2^* + \frac{\partial s}{\partial z} \mathbf{g}_3^*. \quad (13.70)$$

From (13.37) and the definition (13.51) of the gradient of a scalar field, the traction-free condition reads

$$\frac{p^{ij*}}{\sqrt{g_{(jj)}}} \frac{\partial F^s}{\partial x^j} \mathbf{g}_i^* = 0. \quad (13.71)$$

Hence, the traction free boundary condition at the free surface of the avalanche has down-slope, cross-slope and normal physical components as follows

$$\begin{aligned} -\varepsilon \psi^s p_{xx}^s \frac{\partial s}{\partial x} - \varepsilon \mu p_{xy}^s \frac{\partial s}{\partial y} + \mu p_{xz}^s &= 0, \\ -\varepsilon \mu \psi^s p_{xy}^s \frac{\partial s}{\partial x} - \varepsilon p_{yy}^s \frac{\partial s}{\partial y} + \mu p_{yz}^s &= 0, \\ -\varepsilon \mu \psi^s p_{xz}^s \frac{\partial s}{\partial x} - \varepsilon \mu p_{yz}^s \frac{\partial s}{\partial y} + p_{zz}^s &= 0, \end{aligned} \quad (13.72)$$

written here again in dimensionless form.

13.4.6 Coulomb Sliding Law at the Base

The COULOMB basal sliding law (13.38) implies the relation

$$\mathbf{p}^b \mathbf{n}^b = (\mathbf{n}^b \cdot \mathbf{p}^b \mathbf{n}^b) \{ (u^b / |\mathbf{u}^b|) \tan \delta + \mathbf{n}^b \}.$$

It follows from this that the down-slope, cross-slope and normal components of the above relation, respectively, are

$$\begin{aligned} \varepsilon \psi^b p_{xx}^b \frac{\partial b}{\partial x} + \varepsilon \mu p_{xy}^b \frac{\partial b}{\partial y} - \mu p_{xz}^b &= (\mathbf{n}^b \cdot \mathbf{p}^b \mathbf{n}^b) \left(\Delta_b \frac{u^b}{|\mathbf{u}^b|} \tan \delta + \varepsilon \psi \frac{\partial b}{\partial x} \right), \\ \varepsilon \mu \psi^b p_{xy}^b \frac{\partial b}{\partial x} + \varepsilon p_{yy}^b \frac{\partial b}{\partial y} - \mu p_{yz}^b &= (\mathbf{n}^b \cdot \mathbf{p}^b \mathbf{n}^b) \left(\Delta_b \frac{v^b}{|\mathbf{u}^b|} \tan \delta + \varepsilon \frac{\partial b}{\partial y} \right), \\ \varepsilon \mu \psi^b p_{xz}^b \frac{\partial b}{\partial x} + \varepsilon \mu p_{yz}^b \frac{\partial b}{\partial y} - p_{zz}^b &= (\mathbf{n}^b \cdot \mathbf{p}^b \mathbf{n}^b) \left(\Delta_b \frac{\varepsilon w^b}{|\mathbf{u}^b|} \tan \delta - 1 \right), \end{aligned} \quad (13.73)$$

where $|\mathbf{u}| = (u^2 + v^2 + \varepsilon^2 w^2)^{1/2}$, the basal unit normal vector \mathbf{n}^b is given by

$$\Delta_b \mathbf{n}^b = \nabla F^b, \quad \Delta_b := |\nabla F^b|, \quad (13.74)$$

and the associated normalization factor is

$$\Delta_b = \left\{ 1 + \varepsilon^2 (\psi^b)^2 \left(\frac{\partial b}{\partial x} \right)^2 + \varepsilon^2 \left(\frac{\partial b}{\partial y} \right)^2 \right\}^{1/2}. \quad (13.75)$$

This completes the transformation from the coordinate independent form of the COULOMB sliding law to curvilinear coordinates using the non-dimensional variables defined in (13.57).

13.4.7 Depth Integration

The difference between the height of the free surface $s(x, y, t)$ and the height of the basal topography $b(x, y, t)$, defines the thickness, or depth, of the avalanche

$$h(x, y, t) = s(x, y, t) - b(x, y, t), \quad (13.76)$$

measured along the normal direction of the reference surface. A crucial step in deriving the equations of motion for a shallow granular material is the process of integration of the mass and momentum balance equations through this thickness. In order to perform this step, it is useful to define the mean value of the function $f = f(x, y, z, t)$ through the avalanche thickness

$$\bar{f} = \frac{1}{h} \int_b^s f dx, \quad (13.77)$$

where the overbar is a shorthand notation for the mean of the depth integrated function f . In the process of depth integration, we need the LEIBNIZ rule to change the order of integration and differentiation. According to this rule, if $G(x, t)$ and $\partial G(x, t)/\partial t$ are continuous with respect to x and t and if both $a(t)$ and $b(t)$ are differentiable with respect to t , then the following holds true

$$\frac{d}{dt} \int_{a(t)}^{b(t)} G(x, t) dx = \int_{a(t)}^{b(t)} \frac{\partial G(x, t)}{\partial t} dx + \left[G(x, t) \frac{dx}{dt} \right]_{a(t)}^{b(t)}, \quad (13.78)$$

where the square bracket defines the difference of the enclosed function at the two limiting points of integration, $[f]_a^b = f^b - f^a$. On using LEIBNIZ' rule the mass balance (13.59) is integrated through the avalanche depth. This yields

$$\int_b^s \left\{ \frac{\partial u \psi}{\partial x} + \frac{\partial v}{\partial y} + \frac{\partial w}{\partial z} \right\} dz$$

$$= \frac{\partial}{\partial x} (h \overline{u \psi}) + \frac{\partial}{\partial y} (h \bar{v}) - \left[u \psi \frac{\partial z}{\partial x} + v \frac{\partial z}{\partial y} - w \right]_b^s = 0. \quad (13.79)$$

The function contained in square brackets in (13.79) has a number of terms in common with the equations expressing the kinematic boundary conditions (13.68) and (13.69). From (13.68), (13.69) and (13.76) we obtain

$$0 = \frac{\partial h}{\partial t} + \left[u \psi \frac{\partial z}{\partial x} + v \frac{\partial z}{\partial y} - w \right]_b^s. \quad (13.80)$$

From (13.79) and (13.80) it follows that the depth-integrated form of the mass balance (13.59) takes the simple form

$$\frac{\partial h}{\partial t} + \frac{\partial}{\partial x} (h \overline{u \psi}) + \frac{\partial}{\partial y} (h \bar{v}) - \varepsilon \lambda \kappa' h \overline{z u \psi^2} - \varepsilon \lambda \kappa \overline{w \psi} = 0. \quad (13.81)$$

This is the depth-integrated mass balance of the density preserving fluid.

The process of depth integration of the momentum balance equations (13.61)–(13.63) is performed in a number of steps. Considering first four terms in (13.61) and integrating these yields

$$a_x := \int_b^s \left\{ \frac{\partial u}{\partial t} + \frac{\partial}{\partial x} (u^2 \psi) + \frac{\partial}{\partial y} (u v) + \frac{\partial}{\partial z} (u w) \right\} dz$$

$$= \left[\frac{\partial}{\partial t} (h \bar{u}) + \frac{\partial}{\partial x} (h \overline{u^2 \psi}) + \frac{\partial}{\partial y} (h \bar{u v}) \right]$$

$$- \underbrace{\left[u \left(\frac{\partial z}{\partial t} + u \psi \frac{\partial z}{\partial x} + v \frac{\partial z}{\partial y} - w \right) \right]_b^s}_{=0 \text{ (see (13.68), (13.69))}}.$$

Hence,

$$a_x = \frac{\partial}{\partial t} (h \bar{u}) + \frac{\partial}{\partial x} (h \overline{u^2 \psi}) + \frac{\partial}{\partial y} (h \bar{u v}). \quad (13.82)$$

Analogously, from the last term of the right-hand side of (13.61), we deduce

$$b_x := \int_b^s \left\{ \varepsilon \frac{\partial}{\partial x} (p_{xx} \psi) + \varepsilon \mu \frac{\partial}{\partial y} (p_{xy}) + \mu \frac{\partial}{\partial z} (p_{xz}) \right\} dz$$

$$= \varepsilon \frac{\partial}{\partial x} \left(h \overline{p_{xx} \psi} \right) + \varepsilon \mu \frac{\partial}{\partial y} \left(h \overline{p_{xy}} \right) - \left[\varepsilon p_{xx} \psi \frac{\partial z}{\partial x} + \varepsilon \mu p_{xy} \frac{\partial z}{\partial y} - \mu p_{xz} \right]_b^s.$$

With (13.72)₁ and (13.73)₁, this expression reduces to

$$b_x = \varepsilon \frac{\partial}{\partial x} \left(h \overline{p_{xx} \psi} \right) + \varepsilon \mu \frac{\partial}{\partial y} \left(h \overline{p_{xy}} \right) + \left(\mathbf{n}^b \cdot \mathbf{p}^b \mathbf{n}^b \right) \left(\Delta_b \frac{u^b}{|\mathbf{u}^b|} \tan \delta + \varepsilon \psi \frac{\partial b}{\partial x} \right), \quad (13.83)$$

where the COULOMB dry friction law and the down-slope component of the basal normal pressure have entered through the boundary conditions. In a similar fashion we can derive the depth-integrated cross-slope and normal components of the momentum balances. It follows that the depth-integrated down-slope, cross-slope and normal components of the momentum balance laws, respectively, take the forms

$$\begin{aligned} & \frac{\partial}{\partial t} (h \bar{u}) + \frac{\partial}{\partial x} \left(h \overline{u^2 \psi} \right) + \frac{\partial}{\partial y} (h \bar{u} \bar{v}) - \varepsilon \lambda \kappa' h \overline{zu^2 \psi^2} - 2\varepsilon \lambda \kappa h \overline{uw \psi} \\ &= h \sin \zeta - \left(\Delta_b \frac{u^b}{|\mathbf{u}^b|} \tan \delta + \varepsilon \psi \frac{\partial b}{\partial x} \right) \left(\mathbf{n}^b \cdot \mathbf{p}^b \mathbf{n}^b \right) - \varepsilon \psi \frac{\partial}{\partial x} (h \overline{p_{xx}}) \\ & \quad - \varepsilon \frac{\partial}{\partial x} \left(h \overline{p_{xx} \psi} \right) - \varepsilon \mu \frac{\partial}{\partial y} (h \overline{p_{xy}}) + \varepsilon^2 \lambda \kappa' h \overline{zuv \psi^2} + 2\varepsilon \lambda \kappa h \overline{p_{xz} \psi}, \end{aligned} \quad (13.84)$$

$$\begin{aligned} & \frac{\partial}{\partial t} (h \bar{v}) + \frac{\partial}{\partial x} (h \overline{uv \psi}) + \frac{\partial}{\partial y} (h \bar{v}^2) - \varepsilon \lambda \kappa' h \overline{zuv \psi^2} - \varepsilon \lambda \kappa h \overline{zvw \psi} \\ &= - \left(\Delta_b \frac{v^b}{|\mathbf{u}^b|} \tan \delta + \varepsilon \frac{\partial b}{\partial x} \right) \left(\mathbf{n}^b \cdot \mathbf{p}^b \mathbf{n}^b \right) - \varepsilon \mu \frac{\partial}{\partial x} (h \overline{p_{xy} \psi}) \\ & \quad - \varepsilon \frac{\partial}{\partial y} \left(h \overline{p_{yy} \psi} \right) - \varepsilon^2 \lambda \mu \kappa' h \overline{z p_{xy} \psi^2} + \varepsilon \lambda \kappa' h \overline{p_{yz} \psi}, \end{aligned} \quad (13.85)$$

$$\begin{aligned} & \varepsilon \left\{ \frac{\partial}{\partial t} (h \bar{w}) + \frac{\partial}{\partial x} (h \overline{uw \psi}) + \frac{\partial}{\partial y} (h \bar{v} \bar{w}) \right\} - \varepsilon^2 \lambda \kappa' h \overline{z uw \psi^2} \\ & \quad - \lambda \kappa h \overline{(\varepsilon^2 w^2 - u^2) \psi} \\ &= -h \cos \zeta - \left(\Delta_b \frac{\varepsilon w^b}{|\mathbf{u}^b|} \tan \delta - 1 \right) \left(\mathbf{n}^b \cdot \mathbf{p}^b \mathbf{n}^b \right) \\ & \quad - \varepsilon \mu \frac{\partial}{\partial x} (h \overline{p_{xz} \psi}) - \varepsilon \mu \frac{\partial}{\partial y} (h \overline{p_{yz}}) + \varepsilon^2 \lambda \kappa' h \overline{z p_{xz} \psi^2} \\ & \quad + \varepsilon \lambda \kappa h \overline{(p_{zz} - p_{xx}) \psi}. \end{aligned} \quad (13.86)$$

The formal depth-integration process is now complete. The depth-integrated mass balance (13.81), and the depth integrated down-slope and cross-slope momentum balances (13.84) and (13.85), form the basis of the (shallow) granular flow equations.

The depth integrated normal component of the momentum equation, (13.86) thereby serves as an auxiliary equation defining the pressure.

13.4.8 Ordering Relations

Equations (13.81), (13.84)–(13.86) constitute four scalar field equations for h , u , v and w as unknowns. However, they contain more than just these unknowns, because many ‘correlation terms’ arise, which are thickness averages of product quantities of h , u , v and w . The number of these unknown variables can be reduced by introducing a further approximation that is based on the ordering of the various terms arising in the stated equations. Such orders of magnitude are now assumed for the parameters λ and μ . Realistic avalanche lengths are generally larger than typical curvature radii of the topographic surfaces. Of course, this is not unanimously so, but $0 < \lambda < 1$ is almost everywhere correct. Similarly, δ_0 as a typical basal friction angle is smaller than 45° (usually between 20° and 30°), so, also $0 < \mu < 1$ must hold. Since the aspect ratio is generally much smaller than unity, $\varepsilon \ll 1$, such corrections are fulfilled for

$$\lambda = \mathcal{O}(\varepsilon^\alpha), \quad \mu = \mathcal{O}(\varepsilon^\beta), \quad (13.87)$$

where $0 < \alpha, \beta < 1$ are realistic for typical curvature radii and coefficients of basal friction. As long as no formal perturbation expansion involving higher order terms is pursued, the exponents α and β need not further be specified except that $\alpha \neq 1$ and $\beta \neq 1$. As typical values of these parameters we can take $\alpha = \beta = \frac{1}{2}$, $\varepsilon = 10^{-2}$ and $\mu = 10^{-1}$. The functions ψ from (13.60) and Δ_b from (13.75), respectively, can be estimated by

$$\psi = 1 + \mathcal{O}(\varepsilon^{1+\alpha}), \quad \Delta_b = 1 + \mathcal{O}(\varepsilon^2). \quad (13.88)$$

With these orderings, the depth-integrated mass balance equation (13.81) reduces to

$$\frac{\partial h}{\partial t} + \frac{\partial}{\partial x}(h\bar{u}) + \frac{\partial s}{\partial y}(h\bar{v}) = 0 + \mathcal{O}(\varepsilon^{1+\alpha}). \quad (13.89)$$

The down-slope and cross-slope components of the depth-integrated momentum balances (13.84) and (13.85) must be approximated to leading and first order in the small parameter ε in order to obtain a realizable theory, which includes some constitutive properties of granular material. These equations contain a term that is multiplied by the factor $\mathbf{n}^b \cdot \mathbf{p}^b \mathbf{n}^b$. From the normal component of the momentum balance (13.86), it follows that

$$\mathbf{n}^b \cdot \mathbf{p}^b \mathbf{n}^b = h \cos \zeta + \lambda \kappa h \overline{u^2} + \mathcal{O}(\varepsilon) = h \cos \zeta + \mathcal{O}(\varepsilon^\alpha), \quad (13.90)$$

to order ε^α . Applying this to the depth-integrated momentum balance equations in the two principal flow directions, relations (13.84) and (13.85) reduce the latter to

$$\begin{aligned} & \frac{\partial}{\partial t} (h \bar{u}) + \frac{\partial}{\partial x} (h \bar{u}^2) + \frac{\partial}{\partial y} (h \bar{u}v) \\ &= h \sin \zeta - \frac{u^b}{|\mathbf{u}^b|} h \tan \delta \left(\cos \zeta + \lambda \kappa \bar{u}^2 \right) - \varepsilon \frac{\partial}{\partial x} (h \bar{p}_{xx}) - \varepsilon \cos \zeta h \frac{\partial b}{\partial x} \\ & \quad + \mathcal{O}(\varepsilon^{1+\gamma}), \end{aligned} \quad (13.91)$$

$$\begin{aligned} & \frac{\partial}{\partial t} (h \bar{v}) + \frac{\partial}{\partial x} (h \bar{u}v) + \frac{\partial}{\partial y} (h \bar{v}^2) \\ &= -\frac{v^b}{|\mathbf{u}^b|} h \tan \delta \left(\cos \zeta + \lambda \kappa \bar{u}^2 \right) - \varepsilon \frac{\partial}{\partial y} (h \bar{p}_{yy}) - \varepsilon \cos \zeta h \frac{\partial b}{\partial y} \\ & \quad + \mathcal{O}(\varepsilon^{1+\gamma}), \end{aligned} \quad (13.92)$$

where $\gamma = \min(\alpha, \beta)$ that satisfies the inequality $0 < \gamma < 1$ and $\mathbf{u} = (u, v, 0)^T$ is the two-dimensional tangential velocity at the bed. It is important to mention here that ignoring $\mathcal{O}(\varepsilon)$ and to drop $\mathcal{O}(\varepsilon^{1+\gamma})$ -terms and higher order terms yields the mass point model. So, it is physically very significant to carry the theory to $\mathcal{O}(\varepsilon)$ and only to drop higher order terms. From the normal component of the momentum balance we then obtain the equation for the pressure as

$$\frac{\partial p_{zz}}{\partial z} = -\cos \zeta + \mathcal{O}(\varepsilon^\alpha). \quad (13.93)$$

Integrating this equation with respect to z and applying the traction free boundary condition, $p_{zz}^b = 0 + \mathcal{O}(\varepsilon^\alpha)$, from (13.93), we receive the following pressure distribution that is linear in the normal direction as follows:

$$p_{zz} = (s - z) \cos \zeta + \mathcal{O}(\varepsilon^\alpha), \quad (13.94)$$

which is consistent with (13.73)₃ and (13.90) and equivalent to the hydrostatic pressure assumption.

13.4.9 Closure Property

Further reduction of Eqs. (13.91) and (13.92) requires constitutive information about the pressure tensor \mathbf{p} and the depth-integrated tangential velocity \mathbf{u} . Note that the component p_{zz} need only be approximated to order ε^α as it is used to simplify the depth integrated down-slope and cross-slope pressure terms \bar{p}_{xx} and \bar{p}_{yy} , which are already order ε -terms in Eqs. (13.91) and (13.92).

The SH theory assumes that a very simple state of stress prevails within the avalanche. Following common practice in soil mechanics we assume that the pressure terms p_{xx} and p_{yy} can be expressed in terms of the overburden pressure p_{zz} with the aid of the MOHR-circle. This holds at the base and at the stress free surface. So, its validity through depth is justified by the continuity requirement. Because the predominant shearing takes place in vertical surfaces perpendicular to the direction of steepest descent, it may, as a rough approximation, be justified to assume that the lateral confinement pressure p_{yy} is close to a principal stress, p_1 , say, see Fig. 13.20. Furthermore, it shall be assumed that one of the other principal stresses acting in the (x, z) -surface, p_2 and p_3 , equals p_1 . This is an ad-hoc assumption that is not guaranteed by any physical argument, but it reduces the three MOHR-circles that describe all possible combinations of normal stresses and shear stresses to only one MOHR-circle as in the case of two dimensional flow. Thus, to a given stress state (p_{xx}^b, p_{xy}^b) at the base, two MOHR-circles can be constructed to satisfy both the basal sliding law and the internal yield criterion simultaneously. Their construction is shown in Fig. 13.21.

The principal stresses, p_2 and p_3 in the xz -plane are given by

$$(p_x, p_z) = \frac{1}{2} \left\{ (p_{xx} + p_{zz}) \pm \sqrt{(p_{xx} - p_{zz})^2 + 4\tau_{xz}^2} \right\}, \tag{13.95}$$

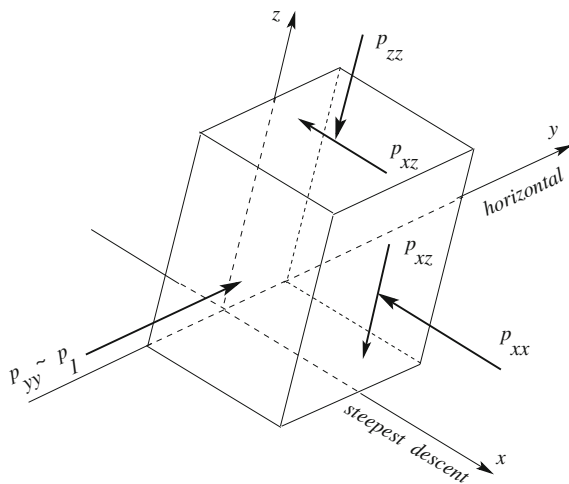


Fig. 13.20 Infinitesimal cubic element cut out of the avalanche with surface perpendicular to the coordinates. The motion is predominantly in the direction of steepest descent and the dominant shearing is acting on planes normal to the x - and z -directions. This gives rise to the dominant shear stresses $\tau_{xz} = -p_{xz}$ and normal pressures p_{xx}, p_{yy}, p_{zz} . Shear stresses τ_{xy}, τ_{yz} also arise but are much smaller than τ_{xz} . Thus, p_{yy} is approximately equal to p_1 , one of the principal stresses. (When τ_{xy}, τ_{yz} are exactly zero, then p_{yy} is exactly p_1). The other two principal stresses, p_2, p_3 act on surface elements, of which the surface normals lie in the (xz) -plane, from [70]

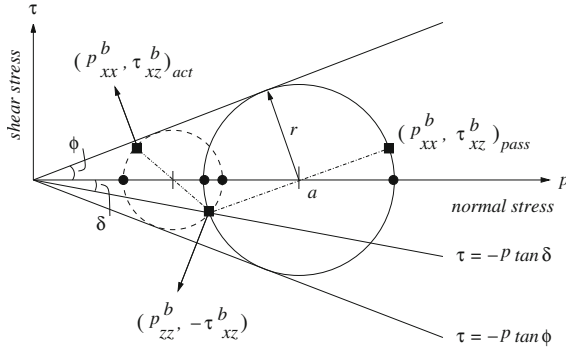


Fig. 13.21 MOHR-circle diagram representing the stress state within the avalanche. The yield criterion corresponds to the two straight lines at angles $\pm\phi$ to the horizontal. Similarly, the COULOMB basal dry friction is indicated by the line at an angle $-\delta$ to the horizontal. The passive basal stress state is indicated by the solid circle of radius r and the center at $p = a$. The circle is both tangent to the yield curves and passes through the point $(p_{zz}, -p_{zz} \tan \delta)$. The broken-line circle represents a second active stress state that also satisfies these conditions. Full squares indicate the possible stress states in the xz -plane. Full circles show possible stress states for p_{yy} , from [70]

and the cross-slope principal stress $p_{yy} = p_2$ or $p_{yy} = p_3$, depending on the nature of the deformation. The MOHR circles can be constructed which satisfy both the sliding law and the angle of internal friction at the same time. In the original works of SAVAGE-HUTTER [72] the basal normal pressure equals p_{zz}^b and the shear stress equals $-p_{xz}^b$. The basal down-slope normal pressure equals p_{zz}^b and the shear stress equals $-p_{xz}^b = \tau_{xz}^b$. The basal down-slope pressure p_{xx}^b can therefore assume two values, one on the smaller circle, $p_{xx}^b \leq p_{zz}^b$, and one on the larger circle $p_{xx}^b \geq p_{zz}^b$, which are related to *active* and *passive* stress states, respectively. Since there are four possible values for the principal stresses, p_x^b and p_z^b , there are four values for the basal cross-slope pressure p_{yy}^b . The earth pressure coefficients K_x^b and K_y^b are defined as follows:

$$K_x^b = \frac{p_{xx}^b}{p_{zz}^b}, \quad K_y^b = \frac{p_{yy}^b}{p_{zz}^b}. \tag{13.96}$$

To determine the values of these pressure coefficients, elementary geometric arguments with the MOHR-circle representation in Fig. 13.21 can be used. The reader may corroborate the formulae

$$K_{x_{act/pas}}^b = 2 \sec^2 \phi \left\{ 1 \mp (1 - \cos^2 \phi \sec^2 \delta)^{1/2} \right\} - 1, \tag{13.97}$$

$$\left(K_{y_{act/pas}}^x \right)^b = \frac{1}{2} \left\{ K_x^b + 1 \mp \left((K_x^b - 1)^2 + 4 \tan^2 \delta \right)^{1/2} \right\}, \tag{13.98}$$

for $K_{x_{act/pas}}^b$ and $\left(K_{y_{act/pas}}^x \right)^b$, which are real for $\delta \leq \phi$.

To uniquely determine the value of the earth pressure coefficient associated with a particular deformation, the earth pressure coefficient K_x is defined to be *active* or *passive* according to whether the down-slope motion is dilating or compacting as given by

$$K_x^b = \begin{cases} K_{x_{\text{act}}}, & \partial u / \partial x > 0, \\ K_{x_{\text{pas}}}, & \partial u / \partial x < 0. \end{cases} \quad (13.99)$$

Analogously, the earth pressure coefficients in the lateral direction are computed by considering whether the down-slope and cross-slope deformations are dilatational or compressive:

$$K_y^b = \begin{cases} K_{y_{\text{act}}}^{x_{\text{act}}}, & \partial u / \partial x > 0, \quad \partial v / \partial y > 0, \\ K_{y_{\text{act}}}^{x_{\text{pas}}}, & \partial u / \partial x < 0, \quad \partial v / \partial y > 0, \\ K_{y_{\text{pas}}}^{x_{\text{act}}}, & \partial u / \partial x > 0, \quad \partial v / \partial y < 0, \\ K_{y_{\text{pas}}}^{x_{\text{pas}}}, & \partial u / \partial x < 0, \quad \partial v / \partial y < 0. \end{cases} \quad (13.100)$$

At the traction free surface of the avalanche the MOHR–COULOMB yield criterion collapses to order ε^α to a single point and the down-slope and cross-slope normal surface pressures are

$$p_{xx}^s = 0 + \mathcal{O}(\varepsilon^\gamma), \quad p_{yy}^s = 0 + \mathcal{O}(\varepsilon^\gamma). \quad (13.101)$$

Having the values of p_{xx} and p_{yy} at the base and at the free surface, intermediate values are now interpolated accordingly. The SH theory assumes that the down-slope and cross-slope pressures vary linearly with normal pressure through the avalanche depth. This is achieved to leading order by the following expression

$$p_{xx} = K_x^b p_{zz} + \mathcal{O}(\varepsilon^\gamma), \quad p_{yy} = K_y^b p_{zz} + \mathcal{O}(\varepsilon^\gamma). \quad (13.102)$$

Substituting p_{zz} from (13.94) and integrating the emerging expressions through the avalanche depth, the depth-integrated pressures in the down-slope and cross-slope directions are, respectively, given by

$$\begin{aligned} \overline{p_{xx}} &= \frac{1}{2} K_x \cos \zeta h + \mathcal{O}(\varepsilon^\gamma), \\ \overline{p_{yy}} &= \frac{1}{2} K_y \cos \zeta h + \mathcal{O}(\varepsilon^\gamma). \end{aligned} \quad (13.103)$$

13.4.10 Nearly Uniform Flow Profile

Since the constitutive properties that are used in the SH theory provide no link between stress and strain rate, it is assumed that the velocity profiles are approx-

imately uniform through the avalanche depth; this is essentially BOUSSINESQ's assumption, and it means that primarily sliding and little differential shearing takes place, explicitly,

$$\bar{u} = u^b + \mathcal{O}(\varepsilon^{1+\gamma}), \quad \bar{v} = v^b + \mathcal{O}(\varepsilon^{1+\gamma}). \quad (13.104)$$

In this case the velocity product can be factorized as

$$\overline{uv} = u^b v^b + \mathcal{O}(\varepsilon^{1+\gamma}). \quad (13.105)$$

The assumption of plug flow is supported by measurements in large scale and laboratory avalanches, see e.g. [17, 30, 61, 79]. On the other hand, one may also assume power law velocity profiles with vanishing basal velocity (corresponding to no sliding and all differential shearing). This then yields $\overline{u^2} = \alpha \bar{u}^2$. For a parabolic profile $\alpha = 1.20$ and for plug flow $\alpha = 1$. Since it is likely that sliding is present, the active shear zone is confined to a thin basal layer and the velocity profile is blunt. This fact justifies the $\mathcal{O}(\varepsilon^{1+\gamma})$ error term in the above formulae. Explicit computations were performed by K. HUTTER et al. (2005) [43]. They justify the use of $\alpha = 1$.

13.4.11 Summary of the Two-Dimensional SH Equations

In this subsection we now collect the avalanche equations in the shallow flow approximation in which terms of order $\mathcal{O}(\varepsilon^{1+\gamma})$, $\gamma > 0$ are dropped.

Equations in conservative form. From (13.104) it follows that the mass balance equation (13.89) reduces to

$$\frac{\partial h}{\partial t} + \frac{\partial}{\partial x}(hu) + \frac{\partial}{\partial y}(hv) = 0. \quad (13.106)$$

With the assumptions (13.103), (13.104) and (13.105), the depth-integrated down-slope and cross-slope momentum balance laws yield

$$\frac{\partial}{\partial t}(hu) + \frac{\partial}{\partial x}(hu^2) + \frac{\partial}{\partial y}(huv) = hs_x - \frac{\partial}{\partial x}\left(\frac{\beta_x h^2}{2}\right), \quad (13.107)$$

$$\frac{\partial}{\partial t}(hv) + \frac{\partial}{\partial x}(huv) + \frac{\partial}{\partial y}(hv^2) = hs_y - \frac{\partial}{\partial y}\left(\frac{\beta_y h^2}{2}\right), \quad (13.108)$$

accurate to order $\mathcal{O}(\varepsilon^{1+\gamma})$, and where the superscript 'b' has been dropped. The factors β_x and β_y are defined as

$$\beta_x = \varepsilon \cos \zeta K_x, \quad \beta_y = \varepsilon \cos \zeta K_y, \quad (13.109)$$

respectively. The terms s_x and s_y represent the *net driving accelerations* in the down-slope and cross-slope directions, respectively, and are given by

$$s_x = \sin \zeta - \frac{u}{|\mathbf{u}|} \tan \delta (\cos \zeta + \lambda \kappa u^2) - \varepsilon \cos \zeta \frac{\partial b}{\partial x}, \quad (13.110)$$

$$s_y = -\frac{v}{|\mathbf{u}|} \tan \delta (\cos \zeta + \lambda \kappa u^2) - \varepsilon \cos \zeta \frac{\partial b}{\partial y}, \quad (13.111)$$

where $|\mathbf{u}| = (u^2 + v^2)^{1/2}$. The first term on the right-hand side of (13.110) is due to the gravitational acceleration and has no contribution in the lateral, y -direction. The second terms of both Eqs. (13.110) and (13.111) emerge from the COULOMB dry friction and the third terms are associated with the contribution of the basal topography. The system of Eqs. (13.106)–(13.108), including (13.109)–(13.111), constitute a *two dimensional conservative system of partial differential equations*. It is useful here to quote the definition of a conservative system of partial differential equations:

Definition: A system of partial differential equations is said to be in conservative form, if it can be written as

$$\frac{\partial \mathbf{w}}{\partial t} + \frac{\partial \mathbf{f}}{\partial \mathbf{x}} = \mathbf{s}, \quad (13.112)$$

where \mathbf{w} and \mathbf{s} are vector-valued quantities and \mathbf{f} is a matrix. Else, it is said to be in non-conservative form.

For (13.106)–(13.111) \mathbf{w} , \mathbf{f} , \mathbf{s} are given by

$$\mathbf{w} = \begin{pmatrix} h \\ hu \\ hv \end{pmatrix}, \quad \mathbf{f} = \begin{pmatrix} hu & hv \\ u^2 + \beta_x h^2/2 & huv \\ huv & v^2 + \beta_y h^2/2 \end{pmatrix}, \quad \mathbf{s} = \begin{pmatrix} 0 \\ hs_x \\ hs_y \end{pmatrix}. \quad (13.113)$$

In this form of writing the governing partial differential equations \mathbf{w} is the vector of conservative variables, \mathbf{f} is the matrix of transport flux elements and the vector \mathbf{s} represents the elements of source terms.

Equations in non-conservative form. For smooth solutions the mass balance equation (13.106) can be used to simplify the convective terms in the momentum equations (13.107) and (13.108). Provided the earth pressure coefficients satisfy the relations $\partial K_x / \partial x = \mathcal{O}(\varepsilon^\gamma)$ and $\partial K_y / \partial y = \mathcal{O}(\varepsilon^\gamma)$, then

$$\begin{aligned} \frac{\partial}{\partial x} \left(\frac{1}{2} K_x h^2 \cos \zeta \right) &= h K_x \cos \zeta \frac{\partial h}{\partial x} + \mathcal{O}(\varepsilon^\gamma), \\ \frac{\partial}{\partial y} \left(\frac{1}{2} K_y h^2 \cos \zeta \right) &= h K_y \cos \zeta \frac{\partial h}{\partial y} + \mathcal{O}(\varepsilon^\gamma). \end{aligned} \quad (13.114)$$

Now, substituting (13.103)–(13.105) and (13.114) into the depth-integrated momentum Eqs. (13.91), and (13.92), and making use of the depth-integrated mass balance equation (13.106) with

$$\frac{d}{dt} = \frac{\partial}{\partial t} + u \frac{\partial}{\partial x} + v \frac{\partial}{\partial y}$$

yields

$$\frac{du}{dt} = \sin \zeta - \frac{u}{|u|} \tan \delta (\cos \zeta + \lambda \kappa u^2) - \varepsilon \cos \zeta \left(K_x \frac{\partial h}{\partial x} + \frac{\partial b}{\partial x} \right), \quad (13.115)$$

$$\frac{dv}{dt} = -\frac{v}{|u|} \tan \delta (\cos \zeta + \lambda \kappa u^2) - \varepsilon \cos \zeta \left(K_y \frac{\partial h}{\partial y} + \frac{\partial b}{\partial y} \right), \quad (13.116)$$

provided $h \neq 0$. The system of equations (13.106), (13.115) and (13.116), constitutes a *non-conservative system of equations*, derived originally by J.M.N.T. GRAY et al. [30] to generalize the one-dimensional SH theory, [72, 73]. Given the basal topography $b(x, y, t)$, a reference surface (slope) $\zeta(x)$ and the material parameters δ and ϕ , both these systems of equations allow three independent variables h , u and v to be computed once the initial conditions are prescribed.

To put everything at one place, this generalized SH avalanche model can be phrased in the following way:

Consider the following assumptions [70]:

- (a) **Topography:** A reference surface can be described by an orthogonal curvilinear coordinate system $\mathcal{O}xyz$, in which the z -axis is normal to the surface and the x - and y -axes are tangential to it, with the x -axis oriented down slope. The function $\zeta = \zeta(x)$ represents the down-slope inclination to the horizontal and $\kappa = -\partial \zeta / \partial x$ is the curvature. Suppose $z = b(x, y, t)$ is the chute geometry above this surface and $z = s(x, y, t)$ the free surface, so that $h = s - b$ represents the avalanche thickness along the z -axis.
- (b) **Material:** The avalanche is assumed to consist of a shallow, density preserving, cohesionless, dry and dense continuous material.
- (c) **Closure:** Assume that the material satisfies the COULOMB dry friction law at the slide and the MOHR–COULOMB plastic yield in the interior; moreover, the dominant deformation takes place in the down-slope direction. Furthermore, the down-slope and the cross-slope pressures vary linearly with the normal pressure through the depth of the avalanche, and shearing occurs in a very small basal layer so that the velocity distribution is almost uniform over the depth.
- (d) **Parameters:** Let δ and ϕ be the bed and internal friction angles, respectively, of the granular material and let $K_{x,y} = K_{x,y}(\delta, \phi)$ be functions constructed by using the MOHR circle with respect to the closure property of the form

$$K_x = 2\sec^2\phi \left\{ 1 \mp (1 - \cos^2\phi \sec^2\delta)^{1/2} \right\} - 1,$$

$$K_y = \frac{1}{2} \left\{ K_x + 1 \mp ((K_x - 1)^2 + 4 \tan^2\delta)^{1/2} \right\}.$$

Let, moreover, H , L and $\mathcal{R} = 1/\kappa_0$ be a typical avalanche thickness, length and radius of curvature. Define $\varepsilon = H/L$, $\lambda = L/\mathcal{R}$, and

$$\beta_{x,y} = \varepsilon \cos \zeta K_{x,y},$$

$$s_x = \sin \zeta - \frac{u}{|\mathbf{u}|} \tan \delta (\cos \zeta + \lambda \kappa u^2) - \varepsilon \cos \zeta \frac{\partial b}{\partial x},$$

$$s_y = -\frac{v}{|\mathbf{u}|} \tan \delta (\cos \zeta + \lambda \kappa u^2) - \varepsilon \cos \zeta \frac{\partial b}{\partial y},$$

where $\mathbf{u} = (u, v)$ is the depth-averaged surface parallel velocity with components u and v along the x - and y -axes, respectively.

- (e) **Smoothness:** Suppose that all field variables are sufficiently smooth that the order of differentiation and integration can be interchanged. Then, under a realistic non-dimensionalization, the dynamics of a granular avalanche can be described by the following set of equations:

$$\frac{\partial h}{\partial t} + \frac{\partial}{\partial x} (hu) + \frac{\partial}{\partial y} (hv) = 0,$$

$$\frac{\partial}{\partial t} (hu) + \frac{\partial}{\partial x} (hu^2) + \frac{\partial}{\partial y} (huv) = hs_x - \frac{\partial}{\partial x} \left(\frac{\beta_x h^2}{2} \right), \quad (13.117)$$

$$\frac{\partial}{\partial t} (hv) + \frac{\partial}{\partial x} (huv) + \frac{\partial}{\partial y} (hv^2) = hs_y - \frac{\partial}{\partial y} \left(\frac{\beta_y h^2}{2} \right),$$

accurate to order $\varepsilon^{1+\gamma}$, $0 < \gamma < 1$.

13.4.12 Standard Form of the Differential Equations

System (13.117) can be put into the standard form

$$\frac{\partial \mathbf{w}}{\partial t} + \frac{\partial \mathbf{f}}{\partial x} + \frac{\partial \mathbf{g}}{\partial y} = \mathbf{s}, \quad (13.118)$$

where \mathbf{w} denotes the vector of conservative variables and \mathbf{f} and \mathbf{g} represent the transport fluxes in the x - and y -directions, respectively. Let us define the conservative variables as h , $m_x = hu$ and $m_y = hv$. Then, the SH Eq. (13.117) can be written in the form (13.118), where \mathbf{f} , \mathbf{g} and \mathbf{s} are given by

$$\begin{aligned} \mathbf{w} &= \begin{pmatrix} h \\ m_x \\ m_y \end{pmatrix}, & \mathbf{f} &= \begin{pmatrix} m_x \\ (m_x)^2/h + \beta_x h^2/2 \\ m_x m_y/h \end{pmatrix}, \\ \mathbf{g} &= \begin{pmatrix} m_y \\ m_x m_y/h \\ (m_y)^2/h + \beta_y h^2/2 \end{pmatrix}, & \mathbf{s} &= \begin{pmatrix} 0 \\ h s_x \\ h s_y \end{pmatrix}. \end{aligned} \quad (13.119)$$

To compute the characteristic speed for the system (13.118) and (13.119), we rewrite it as

$$\frac{\partial \mathbf{w}}{\partial t} + \begin{pmatrix} \mathbf{A}_x & \mathbf{0} \\ \mathbf{0} & \mathbf{A}_y \end{pmatrix} \begin{pmatrix} \frac{\partial \mathbf{w}}{\partial x} \\ \frac{\partial \mathbf{w}}{\partial y} \end{pmatrix} = \mathbf{s}, \quad (13.120)$$

where

$$\begin{aligned} \mathbf{A}_x &= \frac{\partial \mathbf{f}}{\partial \mathbf{w}} = \begin{pmatrix} 0 & 1 & 0 \\ -(m_x)^2/h^2 + \beta_x h & 2m_x/h & 0 \\ -m_x m_y/h^2 & m_y/h & m_x/h \end{pmatrix}, \\ \mathbf{A}_y &= \frac{\partial \mathbf{g}}{\partial \mathbf{w}} = \begin{pmatrix} 0 & 0 & 1 \\ -m_x m_y/h^2 & m_y/h & m_x/h \\ -(m_y)^2/h^2 + \beta_y h & 0 & 2m_y/h \end{pmatrix}. \end{aligned} \quad (13.121)$$

Next, we evaluate the eigenvalues of the matrix \mathbf{A} defined by

$$\mathbf{A} = \begin{pmatrix} \mathbf{A}_x & \mathbf{0} \\ \mathbf{0} & \mathbf{A}_y \end{pmatrix}. \quad (13.122)$$

The characteristic equation for this system, i.e.,

$$\det(\mathbf{A} - \lambda \mathbf{I}_6) = \det(\mathbf{A}_x - \lambda \mathbf{I}_3) \det(\mathbf{A}_y - \lambda \mathbf{I}_3) = 0 \quad (13.123)$$

(note \mathbf{I}_3 and \mathbf{I}_6 are 3×3 and 6×6 unit matrices) possesses the following six eigenvalues (see [80])

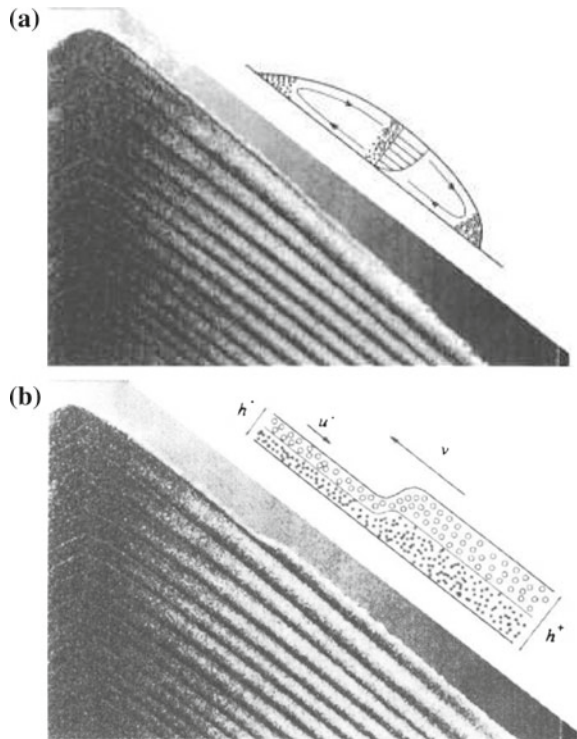
$$\begin{aligned} \lambda_1 &= u, & \lambda_{3,5} &= m_x/h \pm \sqrt{\beta_x h}, \\ \lambda_2 &= v, & \lambda_{4,6} &= m_y/h \pm \sqrt{\beta_y h}, \end{aligned} \quad (13.124)$$

The first two solutions, $\lambda_{1,2}$, yield as characteristic speed the particle velocity $c_p^2 = (u^2 + v^2)$ and as characteristic directions the streamline directions. The remaining eigenvalues $\lambda_{3,\dots,6}$ constitute the other four different characteristic speeds in four different directions

$$\begin{aligned}
 C^{++} &= (\lambda_3^2 + \lambda_4^2)^{1/2}, & C^{+-} &= (\lambda_3^2 + \lambda_6^2)^{1/2}, \\
 C^{-+} &= (\lambda_5^2 + \lambda_4^2)^{1/2}, & C^{--} &= (\lambda_5^2 + \lambda_6^2)^{1/2}.
 \end{aligned}
 \tag{13.125}$$

Here, C^{++} is the fastest and C^{--} the slowest characteristic speed. The flow is called *supercritical* for $c_p > C^{--}$ and *subcritical* for $c_p < C^{--}$. When a finite avalanching mass of granular material moves down a steep slope, reaches a supercritical speed and then approaches the run-out zone, where a considerable deceleration occurs, it experiences a sudden transition from supercritical to subcritical flow. Any such transition from a supercritical to a subcritical flow state produces a shock. These shock fronts are experienced by the avalanching body when the avalanche depth and speed go quickly from small heights and large speeds to large heights and small speeds, see **Fig. 13.22**. This is the reason why numerical schemes must be implemented in these generalized SH equations, which are capable of capturing possible shocks.

Fig. 13.22 Schematic diagrams and photographs of **a** downward moving and **b** upward propagating dispersed shock wave *The material below the shock is at rest or near rest, whilst the grains in panel (a) and above the shock are flowing rapidly down-slope. The experiment was conducted between parallel plates which prevent lateral spreading of the avalanche and exert an additional wall friction that slows the avalanche to observable speed. A mixture of (white) sugar crystals and (dark) spherical iron powder is used with mixing ratio by volume of $\sim 1 : 1$. Kinetic sieving mechanism sorts the grains by their size*



13.5 Avalanche Simulation and Verification with Experimental Laboratory Data

13.5.1 Introduction

In this section numerical methods shall be used to solve typical initial value problems (IVPs) for avalanche motions of the free boundary value problems derived and stated in Sect. 13.4. Results from such computations will then be compared with data exploited from laboratory experiments to validate the computational models by accordingly adjusting the phenomenological parameters (here the angle of internal friction, ϕ , and the bed friction angle, δ). This will eventually lead to an acceptable verification of the model equations for the geo-material configurations of the topographies to which the model of Sect. 4 is applicable. Our presentation is only a brief account of certain aspects of the research that was performed in the past approximately 30 years; a more detailed and fairly complete approach is given by SHIVA P. PUDASAINI and KOLUMBAN HUTTER [70].

Both attempts of arriving at acceptable numerical schemes for adequately solving IVPs of the partial differential equations (PDEs) of Sect. 13.4, (13.117) or (13.118), (13.119) and performing adequate laboratory experiments have been research endeavors as substantial as the derivation of the avalanche models themselves. We shall only be able to provide a selection of important results: In the numerical issues we will show the peak of a long interesting climb to the ultimate or perhaps pre-ultimate approach, and on the experimental side, only final results will be shown, leaving all the peculiar details aside. A more complete account can again be obtained from S.P. PUDASAINI and K. HUTTER [70]. We wish to acknowledge the unlimited help of students and post-doctoral assistants, who provided support through the years.

13.5.2 Classical and High Resolution Shock Capturing Numerical Methods

Twenty five years ago the one-dimensional SH equations [72] were numerically attacked by employing EULERian and LAGRANGEan discretization techniques to find approximate solutions. The equations are close in form to the shallow water equations (SWE); however, they are in fact quite cumbersome to integrate. Reasons for this are:

- “When a pile of granular material is released from rest on a slope, the material near the rear end often tends to initially move up the slope. Similarly, near the rear end in the deposition zone material is still approaching the deposited mass; often parts of the mass at the rear end move backwards before they come to a complete rest.

- Because the motion is dominantly advective (=convective), acceleration terms critically decide about the stability of a numerical scheme, one must be careful to use appropriate up-winding (in EULERian finite discretization) to avoid numerical instability.
- The avalanche model equations are very close in structure to the SWEs, but the geometries of the avalanches are different from those of the usual water wave problem, and so the wave solutions differ considerably from those of the SW-waves.
- The flow of a granular mass can be regarded as a moving interface and embodies all the associated difficulties of such bodies”, from [70], with changes.

In this regard it should also be realized that the accuracy of the numerical solution, in particular for the resolution of steep gradients, it is important that the equations are formulated in the conservative form; i.e., the momentum equations should be stated as

“time rate of change of momentum = sum of the forces” and not as
 “mass times acceleration = sum of the forces”.

(I)EULERian and LAGRANGEan Integration Schemes

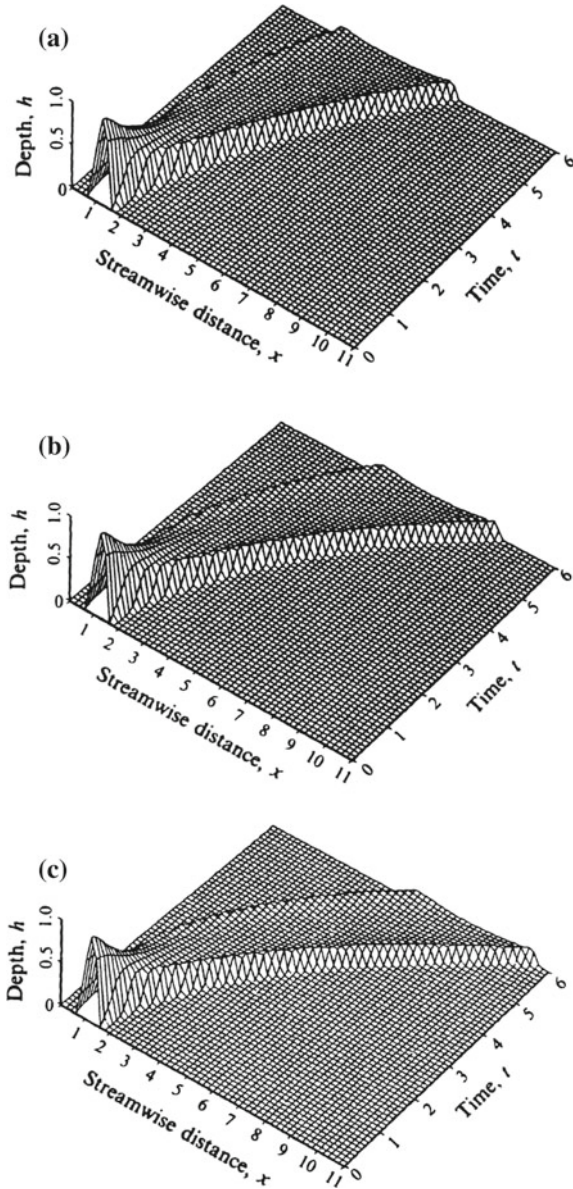
(a)EULERian approach. Among several implicit and explicit schemes to test one-dimensional hyperbolic systems of the form

$$\frac{\partial \mathbf{w}}{\partial t} + \frac{\partial \mathbf{f}(\mathbf{w})}{\partial x} = \mathbf{s}. \quad (13.126)$$

S.B. SAVAGE and K. HUTTER [72] used in their solution approach of the SH equations a method similar to that of R.W. MACCORMACK [58], comprising a two-step explicit finite difference scheme. From the solution known at time $t = n\Delta t$, the values of h and u at the new time $(n + 1)\Delta t$ can be predicted by employing one-sided upwind differences to approximate the first derivatives. Corrections are made in the second step to predict values using opposite one-sided differences for first derivatives. The method is second order accurate and stable for adequately chosen time steps. The method generates evolutions of avalanches down an inclined plane from a hump at rest into a moving and extending M -wave not a hump,¹¹ see Fig. 13.23. Experience has shown that the commonly used EULERian scheme is fraught with several difficulties; among these are, see [70]:

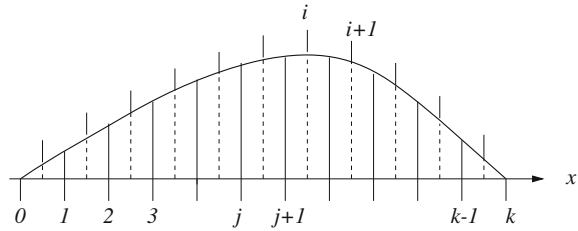
¹¹The spatially one dimensional SH equations allow construction of two types of exact similarity solutions. One is a parabolic hump with vanishing depths at the front and rear ends, called a parabolic hump, the other is also of parabolic shape but with finite maximum depths at the end point, called by S.B. SAVAGE and K. HUTTER M -wave [70, 72] as seen in the experiments (for details see [72, 73] ([70], Fig. 7.2 on p. 302)). **Figure 13.23** indicates that the parabolic hump seems to develop into a profile close to an M -wave.

Fig. 13.23 Results obtained from R.W. MACCORMACK'S explicit EULERian finite difference scheme for the evolution of the motion of a finite mass of granular material starting from rest down a bed with inclination angle $\zeta = 32^\circ$, an angle of internal friction $\phi = 29^\circ$ and bed friction angle $\delta = 22^\circ$ (a), 16° (b), 10° (c), from [72]. © J. Fluid Mech



- The scheme uses a fixed spatial grid that extends upstream and downstream of the moving pile.
- Even at those parts of the bed, where no material exists and the depth is zero, the equations of motion yield non-vanishing velocities upstream and downstream of

Fig. 13.24 Definition of mesh cell notation for the LAGRANGE an numerical scheme The indices i refer to cell centers, j to cell boundaries



the pile. This causes sudden changes in the velocities up- and downstream of the pile, a destabilizing effect in the numerical integrations.

- When using artificial viscosity to control such instabilities, the velocities in the region outside of that occupied by the pile began to affect the results in the region of the pile itself.

(b)LAGRANGEan approach. In the one-dimensional Lagrange an scheme one divides the length of the avalanche into equal elements, see **Fig. 13.24**

$$\begin{aligned}
 x_j^n &= x_j^{n-1} + x_j^{n-1/2} \Delta t, \quad (j = 1, 2, \dots, N), \\
 x_i^n &= \frac{1}{2} (x_j^n + x_{j+1}^n), \quad (j = 1, 2, \dots, N)
 \end{aligned}
 \tag{13.127}$$

and integrates in a first step the mass balance equation (13.30)₁

$$\frac{\partial h}{\partial t} + \frac{\partial hu}{\partial x} = 0
 \tag{13.128}$$

from x_{i-1} to x_i to obtain

$$\frac{d}{dt} \int_{x_{i-1}}^{x_i} h \, dx = \frac{d F_i}{d x_i} = 0,
 \tag{13.129}$$

where F_i is the area of the i th cell, i.e., the area of any numerically advected cell is conserved. Approximating F_i by $h_i(x_i - x_{i-1})$, (13.129) implies

$$h_i^n (x_i^n - x_{i-1}^n) = h_i^{n-1} (x_i^{n-1} - x_{i-1}^{n-1}), \quad (i = 1, 2, \dots, N),
 \tag{13.130}$$

which is an equation for h_i^n , since all other quantities are known.

The depth averaged momentum equation in non-conservative form, (13.30)₂ is used to solve for the new values of velocities at the cell boundary points. Since the left-hand side of this equation contains $\partial h/\partial x$, the boundary cells must separately be handled. The finite difference representation for this yields

$$u_j^{n+1/2} = u_j^{n-1/2} + \Delta t \left[\sin \zeta - \operatorname{sgn} \left(u_j^{n-1/2} \right) \cos \zeta \tan \delta - \varepsilon K_{\text{act/pas}} \cos \zeta P_j^n \right], \quad (13.131)$$

where

$$P_j^n = \begin{cases} h_0^n / (x_0^n - x_1^n), & \text{for } j = 0, \\ (h_i^n - h_{i-1}^n) / (x_i^n - x_{i-1}^n), & \text{for } j = 1, 2, \dots, N-1, \\ h_{N-1}^n / (x_N^n - x_{N-1}^n), & \text{for } j = N \end{cases}$$

and

$$x_i^n = \frac{1}{2} (x_j^n + x_{j+1}^n), \quad (13.132)$$

$$K_{\text{act/pas}} = \begin{cases} K_{\text{act}}, & \text{for } u_{j+1} - u_j \geq 0, \\ K_{\text{pas}}, & \text{for } u_{j+1} - u_j < 0. \end{cases} \quad (13.133)$$

Numerical computations using (13.130)–(13.133) remained only stable if the artificial viscosity

$$\mu \frac{\partial u^2}{\partial x^2} = \mu \left(u_{j+1}^{n-1/2} - 2u_j^{n-1/2} + u_{j-1}^{n-1/2} \right) / (x_{j+1}^n - x_{j-1}^n)^2 \quad (13.134)$$

was added to the right-hand side of (13.131) with $0.01 < \mu < 0.05$.

Numerical solutions of the one-dimensional SH equations were constructed in [72] by the above described LAGRANGEan approach, in which the computational grid was advected with the material; the construction of the solution is simple, efficient and reliable. It was applied and compared with laboratory experiments for one- and two-dimensional flows down various basal geometries from initiation to run-out, see e.g. [31, 41, 42, 47, 72, 73]. **Figure 13.25** shows time slices of length profiles from $t = 0$ to $t = 5$ (dimensionless time) for an avalanche down an inclined plane.

Since Eqs. (13.130)–(13.133) are based on the momentum equation in non-conservative form, these finite difference equations are not explicitly shock-capturing. Steep gradients and spurious oscillations of the field variables must be handled by numerical diffusion, using the latter judiciously, where instability prone oscillations occur. This has been reasonably successful, but it is unsatisfactory and calls for better schemes.

(II) High Resolution Shock-Capturing Numerical Methods for One- and Two-Dimensional Avalanche Modeling.

(a) A quick review for the need of TVD and discontinuous Galerkin methods. In a continuum-mechanical approach, the governing equations for granular-fluid flows comprise of a strongly convective hyperbolic system, especially for the granular phase. Successful numerical modeling of strongly convective hyperbolic equations is one of the most challenging problems in computational fluid mechanics, particu-

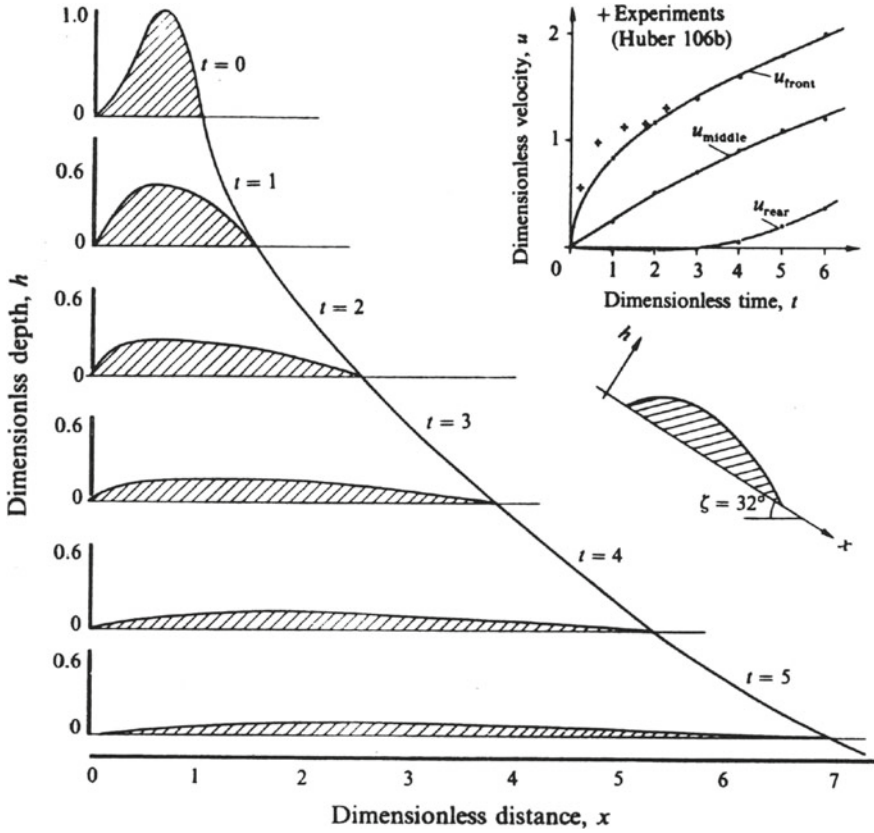


Fig. 13.25 Height h plotted against distance x for LAGRANGEAN calculations of avalanche length profiles at six different times. With increasing time the profile tends to become closer to parabolic. Also shown in the inset are the *front*, *middle* and *rear end* velocities. The points indicate computed values (from [72]), whilst the crosses are from A. HUBER [37]. Computations were performed for $\zeta = 32^\circ$, $\phi = 20^\circ$, $\delta = 22^\circ$ and $\varepsilon = 0.3218$, from [72]. © J. Fluid Mech

larly when large gradients of the physical variables occur, e.g. for a moving front or possibly arising shock waves in a granular avalanche. Shock formation is an essential mechanism in granular flows on an inclined surface merging into a horizontal run-out zone or encountering an obstacle when the velocity becomes subcritical from its supercritical state. In the past decades numerical techniques have been developed to solve hyperbolic equations for typical moving boundary value problems of granular flows. Most of these techniques are based on LAGRANGEAN moving mesh finite-difference schemes. In these LAGRANGEAN schemes explicit artificial numerical diffusion is often incorporated to maintain stability. In doing so the quality of resolution deteriorates. In fact, the adequacy of these numerical solutions can be challenged because of uncontrolled spreading due to this numerical diffusion. Without adding extra artificial diffusion the formation of the shock results in numerical insta-

bilities of the LAGRANGEan moving grid technique. This also occurs for an EULERian integration technique if traditional high-order schemes are employed. Although traditional first-order finite difference methods, e.g. the upstream schemes, are monotonic and stable, due to inherent numerical diffusion, they are strongly dissipative, causing the solution to become also smeared out and often grossly inaccurate. It is therefore natural to apply conservative high-resolution numerical techniques. Modern high-resolution schemes are based on flux/slope limiters which switch between linear high-order (usually second or third order) and low-order (usually first order) discretizations adaptively depending on the smoothness of the solution. To a certain extent, such schemes are able to resolve the steep gradients and moving fronts often observed in experiments but not captured by the LAGRANGEan finite difference scheme and traditional EULERian finite difference schemes. Y. WANG and K. HUTTER (2001) [85] compared a series of more than ten most frequently used numerical schemes with respect to convectively dominated problems. Numerical results showed that the high-resolution modified total variation diminishing (TVD) LAX-FRIEDRICHS method is the most competent method for convectively dominated problems with a steep spatial gradient of the variables. The TVD algorithm can ensure that the total variation of the variables does not increase with time, thus no spurious numerical oscillations are generated. The numerical solution can be second- or even third-order accurate in the smooth parts of the solution, but only first-order near regions with large gradients. Shock capturing TVD techniques have been developed to solve numerically the SH equations for single-phase granular flows [79, 87], two-phase fluid-solid mixtures with negligible difference of particle fluid and solid velocities [69]. Although this numerical approach can demonstrate fairly good numerical results, the accuracy of a high-resolution discretization inevitably degrades to the first order at local extrema. Furthermore, an insuperable difficulty arises when granular flows around a wall obstacle are investigated where high-resolution schemes require more boundary conditions than those provided physically.

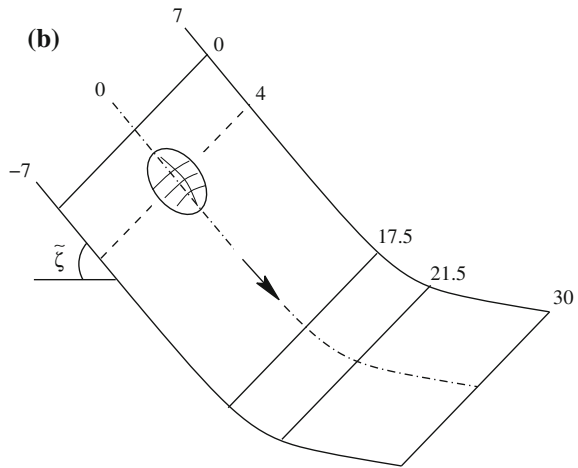
Within the last decade, the Discontinuous Galerkin (DG) method [14] has been rather successfully established for solving hyperbolic conservation laws, especially in computational fluid dynamics [6, 19, 32, 74]. There are especially two reasons for this ascent which obviates essential limitations of classical techniques such as finite volume or finite difference methods. DG cleverly combines

- (i) an arbitrary order $p \in \mathbb{N}$ in the numerical discretization error $\mathcal{O}(h^p)$ with
- (ii) a local flux evaluation which is at most to be computed from adjacent cells.

Here h refers to the local grid spacing, and p the order of the DG basis polynomials. Item (i) is in strong contrast to the established schemes which are substantially limited to $\mathcal{O}(h^n)$ with $n \leq 2$ for unstructured grids, and even on Cartesian grids n is rather limited to small values because of the increasing number of stencils for increasing n . Item (ii) avoids the necessity of more boundary conditions required in high-resolution schemes. At present, the DG scheme has still not been applied to simulate granular flows.

(b) Comparison of the performances of the various schemes. Comparison of the performances of the various numerical schemes will be conducted with the laboratory

Fig. 13.26 **a** Laboratory avalanche chute consisting of upper inclined plane merging continuously into a horizontal plane. **b** Idealized bottom topography with dimensionless distance along the lower coordinate to test the various numerical schemes, from [13].
© Min-Ching Chiou



chute displayed in **Fig. 13.26**. A hemispherical shell holding the material together at the upper end of the chute is suddenly released so that the bulk material commences to slide on an inclined flat plane at 35° into a horizontal run-out plane by a smooth transition. The computational domain is the rectangle $x \in [0, 30]$ and $y \in [-7, 7]$ in dimensionless length units, where the inclined section lies in the interval $x \in [0, 17.5]$ and the horizontal region lies where $x \geq 21.5$ with a smooth change of the topography in the transition zone $x \in [17.5, 21.5]$. Furthermore, the inclination angle is prescribed as

$$\tilde{\zeta}(x) = \begin{cases} \tilde{\zeta}_0, & 0 \leq x \leq 17.5, \\ \tilde{\zeta}_0 (1 - (x - 17.5)/4), & 17.5 < x < 21.5, \\ 0^\circ, & x \geq 21.5, \end{cases} \quad (13.135)$$

with $\tilde{\zeta}_0 = 35^\circ$. Simulations are performed with an angle of internal friction $\phi = 30^\circ$ and a bed friction angle $\delta = 30^\circ$. The material is suddenly released at $t = 0$ from the hemispherical shell with initial radius $r_0 = 1.85$ in dimensional length-units. The center of the cap is initially located at $(x_0, y_0) = (4, 0)$. The results of the numerical simulations will below be tested against laboratory avalanche experiments.

Numerical results are obtained with the central difference scheme applied to (13.118) and (13.119) with the artificial diffusion term

$$\mu_x \frac{\partial^2 \mathbf{w}}{\partial x^2} + \mu_y \frac{\partial^2 \mathbf{w}}{\partial y^2}$$

added to the right-hand sides with viscosities $\mu_x = \mu_y = 0.02$; for smaller viscosities the simulation becomes unstable. The central difference schemes, as well as many other traditional higher order difference methods, introduce *dispersive effects* to the equations, which are susceptible to numerical instabilities and lead to unphysical oscillations in the numerical solutions. These are usually located behind the advancing front and are damped with growing distance from the front. The three dimensional evolution of the avalanche geometry at three different dimensionless times, $t = 6, 9, 12$ is shown **Fig. 13.27**. It displays the free surface distribution at these times when $\mu_x = \mu_y = 0.02$. When sufficiently large artificial diffusion is added to dampen the spurious oscillations, a numerical solution without superimposed numerical oscillation can be obtained. However, in such cases the corresponding solution will be highly diffusive. The simulated granular flow will then spread over a much wider area than with higher order difference schemes, finer resolution, less numerical diffusion, and it will probably also be less physically realistic.

Computations, performed with the non-oscillatory central difference scheme (NOC) and use of the Minmod TVD limiter have performed much more stably,

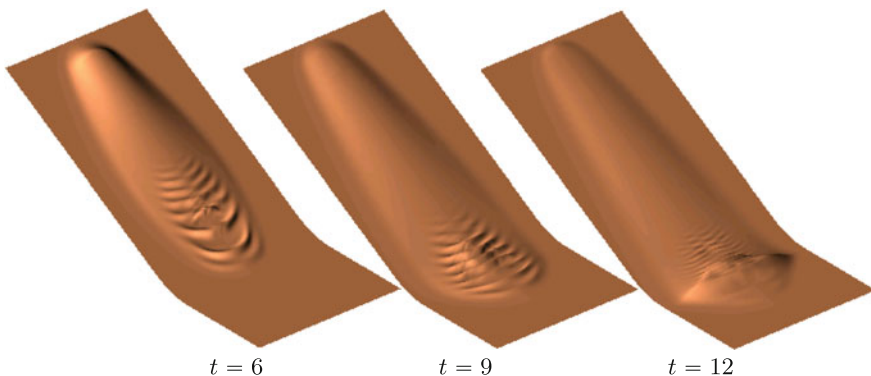


Fig. 13.27 Three dimensional geometries of the avalanche at three dimensionless times $t = 6, 9, 12$, obtained with the traditional difference scheme and $\mu_x = \mu_y = 0.02$, from [87] © Zeitschrift für Angewandte Mathematik und Mechanik

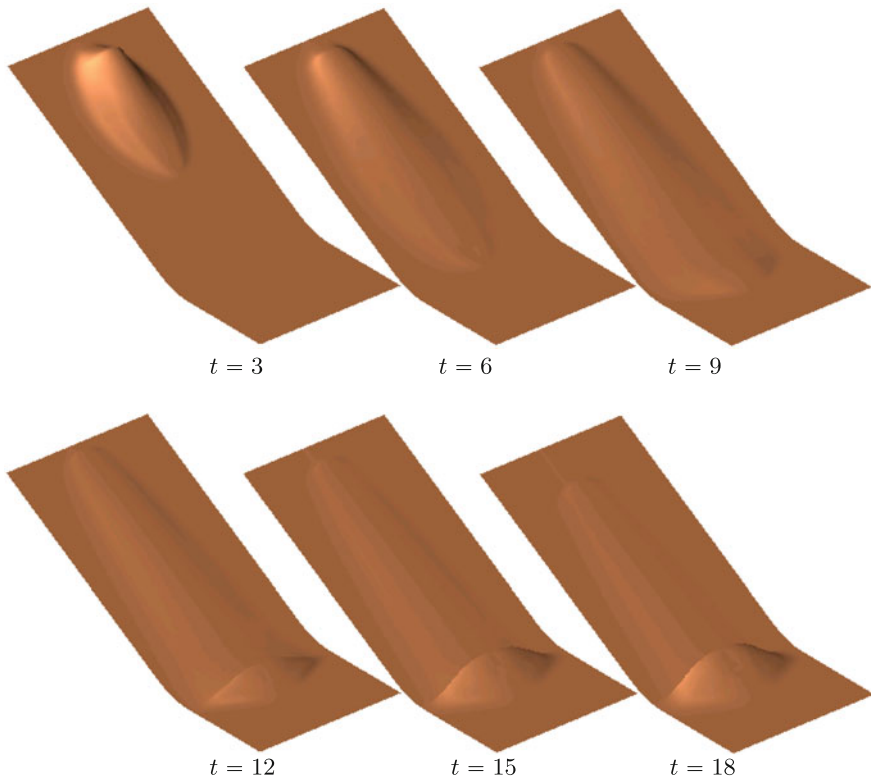


Fig. 13.28 Three-dimensional geometries of the avalanche at six different dimensionless times $t = 3, 6, 9, 12, 15, 18$, obtained with the NOC scheme and the Minmod limiter *In this example the down-slope inclination angle is defined as*

$$\tilde{\zeta}(x) = \begin{cases} \tilde{\zeta}_0, & 0 \leq x < x_\ell, \\ \tilde{\zeta}_0, & \left(\frac{x_r - x}{x_r - x_\ell} \right), \\ 0^\circ, & x > x_r \end{cases}, \quad (13.136)$$

with $\tilde{\zeta} = 45^\circ, x_\ell = 11.5, x_r = 44.5, (x_0, y_0) = (3, 0), y \in [-5, 5]$ and $\phi = 43^\circ, \delta = 33^\circ$, from [87]. © Zeitschrift für Angewandte Mathematik und Mechanik

Fig. 13.28, as can be seen from the humps at dimensionless times = 3, 6, 9, 12, 15, 18 and without the explicit use of additional numerical viscosity.

One of the important questions is the influence of obstructions upon the flow of avalanches. In practice, often constructions are erected in possible avalanche tracks to divert the motion of an avalanche or reduce its dynamics and so to protect property which can possibly be damaged by it. The effect of a tetrahedron positioned in an avalanche track was tested by M.C. CHIOU, Y. WANG and K. HUTTER (2005) [12], shown in **Fig. 13.29**. It can be seen that for a sufficiently high obstacle, all the granular

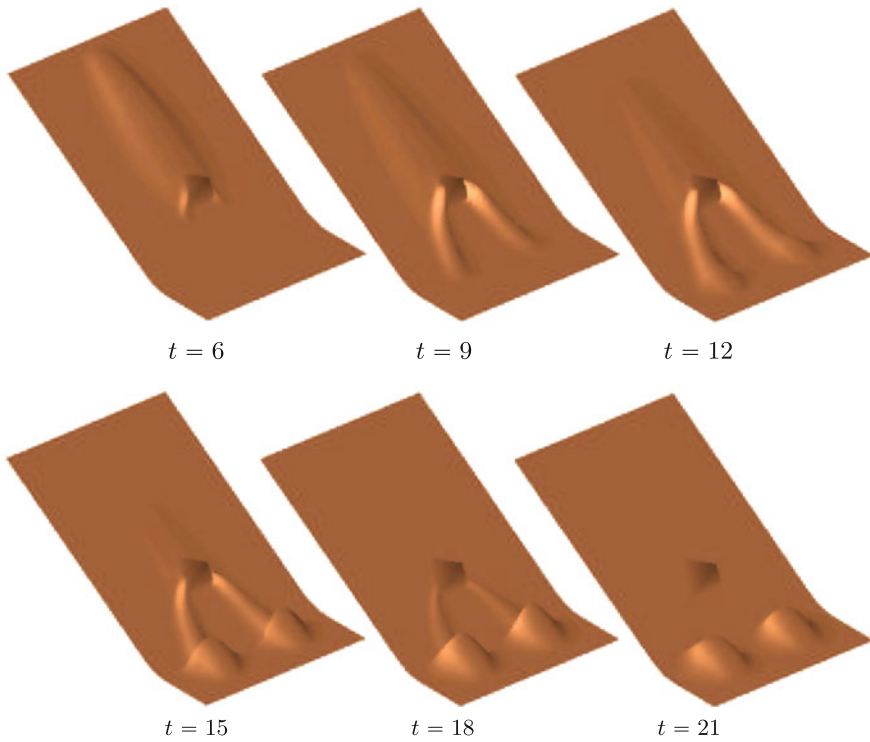


Fig. 13.29 Three-dimensional geometries of an avalanche past a tetrahedral wedge located on the inclined plane for different dimensionless times, from [12]. © Acta Mech. Springer Verlag, reproduced with permission

material approaching the obstacle is diverted to its sides and flows around the obstacle downwards. A so-called granular vacuum is formed behind the tetrahedron, hence the obstacle can prevent the zone directly behind it from being attacked by the granular flow.

The generalized SH equations with COULOMB-type frictional stress parameterization are a hyperbolic system of equations and, consequently, susceptible to solutions involving shocks. **Figure 13.30** shows supercritical flows of a layer of grains down an inclined plane being diverted (i) by a straight or curved wall, perpendicular to the plane, (ii) by a circular cylinder and (iii) by a regular tetrahedron. The shocks are clearly visible in the photographs and show that the flow regimes before and behind the shock differ from one another. The shock structure is sketched and indicates that the flow speed, orientation of the shock and height of the granular layer behind the shock adjust to the wall.¹² In the case of the division of the flow by the side faces of

¹²The shocks arise at singular surfaces across which certain variables suffer jump discontinuities, here for the avalanche thickness and for the surface tangential velocity components. The equations, which hold between the field variables on the two sides of such surfaces are known as

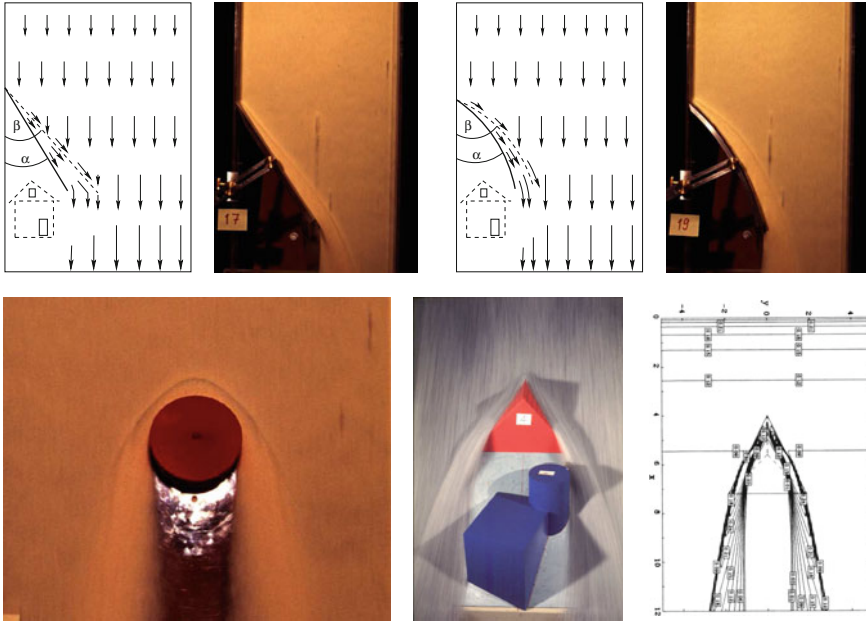


Fig. 13.30 Sketches and snapshots of supercritical granular flows down inclined planes, which are diverted by obstructing walls (*straight* and *curved*, but perpendicular to the inclined planes), a circular cylinder and a regular tetrahedron. *Top row* from [78], *bottom row* from [79]. © Yih-Chin Tai

the tetrahedron into two separate granular side discharge units generate in-between a granular vacuum protecting an object (here the blue building). Computational analysis in the last panel shows that the SH equations reproduce the shock structure in this case characteristically correctly.

Numerical solutions of the SH equations have been constructed by the shock-capturing NOC, second order finite difference scheme using the Minmod limiter. A great number of such computations have been performed to study the performance of the numerical scheme for the motion of a finite mass down the laboratory chute having bottom topographies typically as shown in Fig. 13.18 or Fig. 13.26 with various cross flow parabolic curvatures, see [70] and literature in there. In this way strongly or weakly channelized flows down inclines merging into a horizontal channel or plane can be tested with regard to the spreading of the granular mass and the details of trim lines and depositions in location and form.

Figure 13.31¹³ depicts the thickness contours of the avalanching body taken from [70], originally published in [68], at ten non-dimensional time steps. ‘The flow

(Footnote 12 continued)

RANKINE-HUGONIOT relations and follow from the jump relations of the balance laws of mass and momentum. In the shock capturing numerical schemes they are automatically incorporated in the integration technique.

¹³Text follows closely [70].

of the finite mass of granular material is down a circular channel into a horizontal channel of the same cross-flow shape. The bulk body commences to slide and deform continuously along the chute as long as the bed friction resistive force is smaller than the down-slope component of the gravity force. The first few panels in this figure show clearly that, once the cap holding the mass is opened, the avalanche accelerates and spreads rapidly in the down-slope direction due to the channeling effect in the cross-slope direction. The avalanche decelerates rapidly as soon as it enters the run-out zone, which starts at $t \geq 4.5$, because of the continued mass flux from the tail, its front is then able to spread laterally as evident in panels 5 – 7 for $t = 6.0, 7.5, 9.0$ '.

'After $t = 7.5$, due to the channeling effect of the cross section, the tail of the avalanche reduces in width, but the head expands in width in the run-out zone. Owing to the reduction of the avalanche speed from supercritical to subcritical conditions the transition zone into the horizontal induces a shock associated with the height of the avalanche that is moving upstream from time $t = 9.0$ onward. The avalanche comes to rest after $t = 13.5$. The first three panels of Fig. 13.31 indicate that due to the dilatation, the granular body is extending in all directions, if mainly in the downhill direction. At $t = 6.0$ the front part has completely reached the transition zone. Therefore, the mass at the front is contracting due to the effect of the passive earth pressure coefficient, but the mass in the tail is still extending. At $t = 7.5$, deposition of mass starts in the vicinity of the lower end of the transition zone. Owing to the effect of the curvature, the flowing body starts contracting longitudinally and extending laterally. After $t = 9.0$, a steep surface-height gradient starts to develop on the tail side of the avalanche. *Although the body is almost at standstill, the mass from the tail is continuously flowing down and is deposited on the tail side of the body. This is the main mechanism for the development of the shock front moving upstream.* The physical explanation for this is that from the front there is a strong resistive force from the bed that prevents the body from sliding further. Thus, mass arriving from the upper part of the channel must be deposited at the back of the body. Consequently, the stopped body must extend upward. The last three panels show the continuous development of the backward moving shock. At the same time, there is almost no motion at the front. Due to the partial lateral confinement, the extension of the body in the cross-slope direction is almost negligible', [70].

S.P. PUDASAINI and K. HUTTER [70] discuss a great number of results from computations for granular avalanches down inclines into a horizontal deposition zone, using various cross-channel curvatures to estimate the dependences of the deposition geometries on these parameters. S.P. PUDASAINI also looks at the dynamics of granular masses down helically curved channels and gives quantifications on run-out distances and spreading of the granular masses in the deposition zone. Moreover, he demonstrates that avalanche run-out distances depend strongly on the dependence of the bed friction angle on the pressure [67].

Comparison with channelized laboratory avalanche flows. S.P. PUDASAINI and K. HUTTER ([70], pp 425 ff) summarize a great many laboratory experiments for flows down a sliding surface that is a straight parabolic channel down an inclined plane merging into a horizontal plane. Specifically, such models have been used

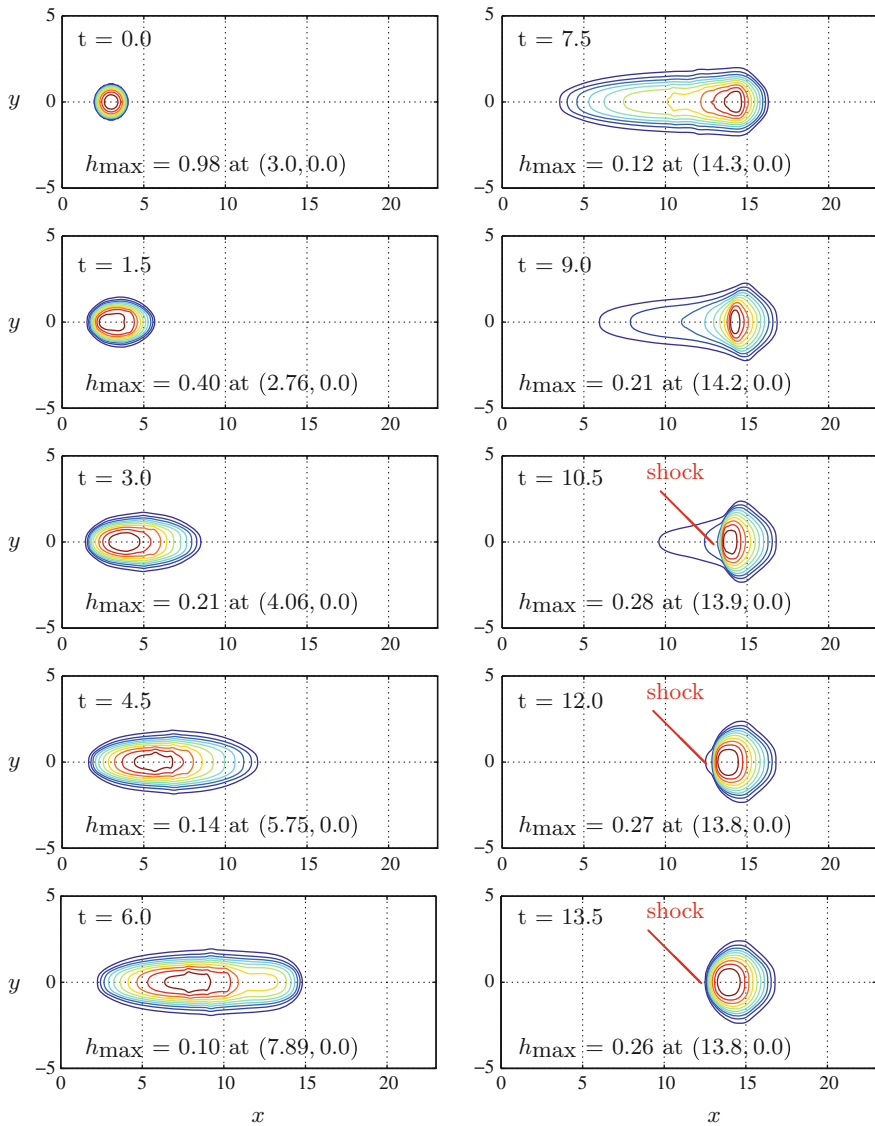


Fig. 13.31 A sequence of numerical snapshots of the avalanching motion of a granular material with internal and basal friction angles $\phi = 43^\circ$ and $\delta = 33^\circ$, for different time slices. *Contours of equal thickness are plotted at ten time intervals using ‘unrolled’ projected non-dimensional curvilinear coordinates (x, y) . The transition zone lies between $x = 11.5$ to $x = 14.5$. The 45° inclined section lies on the left and the horizontal part lies on the right of each panel. The thalweg of the valley is indicated by the line $y = 0$. The panels demonstrate the deformation and settling of avalanches in doubly curved channels, from S.P. PUDASAINI et al. [68]. © Annals of Glaciology*

to test the validity of the theoretical model for this slightly complex geometry. A reference surface is defined, which consists of a plane with inclination angle $\zeta = 40^\circ$, which is connected to a horizontal run-out zone by a cylindrical transition zone. The x -axis is aligned with the direction of steepest descent of the reference surface and the y -axis points in the cross slope direction. Superimposed on the inclined section of the chute is a shallow parabolic cross-slope topography, $b = y^2/(2R)$ with $R = 110\text{ cm}$ forming a channel which partly confines the avalanche motion. The inclined parabolic chute lies in the range $x < 175\text{ cm}$, the plane run-out zone lies in the range $215\text{ cm} < x < 320\text{ cm}$ and the transition zone smoothly joins these two regions. The partly confined chute channels the flow and results in significantly longer maximum run-out distances than in an unconfined chute. Below we discuss the results of J.M.N.T. GRAY et al. [30].

The experiment was performed with quartz chips of mean diameter of 2–4 mm, an angle of internal friction $\phi = 40^\circ$ and a basal friction angle $\delta = 30^\circ$. The granular material was released from rest on the parabolic inclined section of the chute by means of a cap having the form of a hemispherical surface and fitted to the basal surface topography. In an experiment, once the cap is suddenly released, the avalanche accelerates and spreads rapidly in the down-slope direction. As it enters the run-out zone, it rapidly decelerates and spreads out laterally when the partial confinement of the topography ceases. The avalanche comes to rest after 1.79 s.

Figure 13.32 shows a comparison of the marginal curves (black closed lines) of the experimental avalanche with the computed topography (shaded area), demonstrating that the computed speeds of the rear parts of the avalanche are considerably under-predicted. The last panel in the figure also shows that the experimental avalanche has come to rest while the rear part of the computed avalanche is still in motion. The most likely cause for this is that the basal sliding law is considerably more complicated than COULOMB dry friction with constant friction angle.

In order to demonstrate that a change in the bed friction sliding law can qualitatively bring theory and experiment into better agreement, the numerical computations have been repeated using a variable bed friction angle. In the front quarter of the avalanche the bed friction angle is held constant as before, but it is linearly reduced in the rear according to

$$\delta = \begin{cases} \delta_0, & x \geq x_f - \frac{1}{4}(x_f - x_r), \\ \delta_0 - m_\delta(x_f - x) - \frac{1}{4}(x_f - x_r), & x < x_f - \frac{1}{4}(x_f - x_r), \end{cases} \quad (13.137)$$

where δ_0 is the constant bed friction angle, $m_\delta = 10^\circ\text{ m}^{-1}$ is the bed friction reduction factor and x_f and x_r are the positions of the front and rear of the avalanche, respectively. The avalanche thickness distributions computed by using the modified bed friction relation (13.137) are illustrated in **Fig. 13.33**. The reduced bed friction angle in the avalanche tail allows the rear of the avalanche to accelerate more rapidly under the action of gravity and the agreement with the experimental boundary is considerably better. For more details and further comparison with laboratory data see [30, 67, 70, 88].

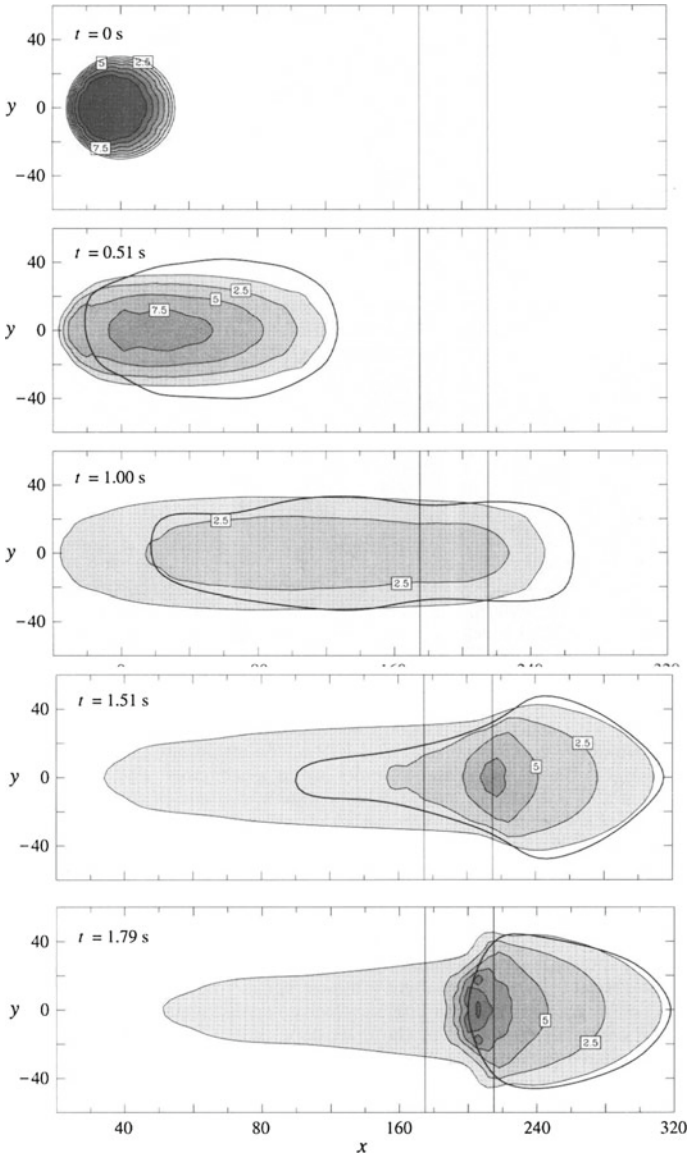


Fig. 13.32 Computed avalanche thickness, illustrated at five time slices using ‘unrolled’ projected curvilinear coordinates (x, y). Contours of equal thickness are indicated in cm and thickness ranges are differently shaded. The time is indicated in the top left-hand corner and all lengths are in cm. The solid lines at $x = 175$ cm and at 215 cm indicate the position of the transition zone. The 40° inclined parabolic section lies on the left and the horizontal plane on the right of each panel. The line $y = 0$ is the thalweg. The thick solid line indicates the position of the avalanche edge in the laboratory experiment, determined from photographs, from [30]. © Proc. Royal Soc. London

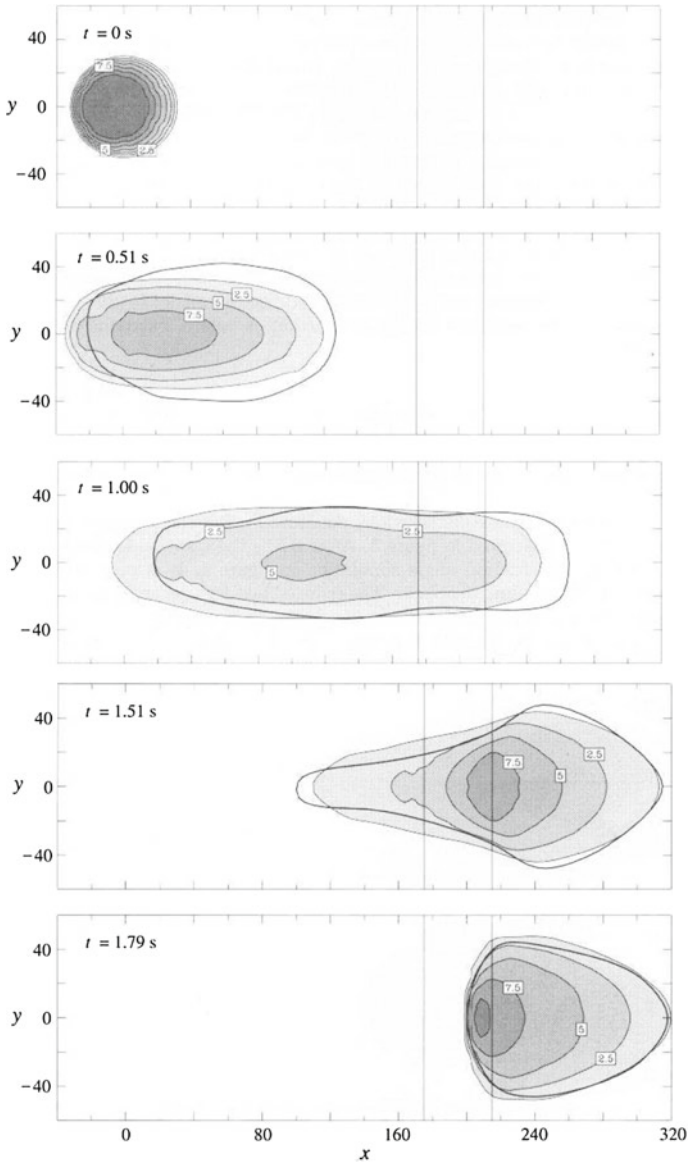


Fig. 13.33 Same as in Fig. 13.32 but the avalanche thickness is computed by using the modified basal friction angle (13.137) and comparison with the experimental avalanche boundary, from [30]. © Proc. Royal Soc. London

It was pointed out earlier that the SH equations or any of their extensions are very similar in form to the *Shallow Water Equations* of fluid mechanics. The essential difference lies in the assumed constitutive properties and the basal topography.

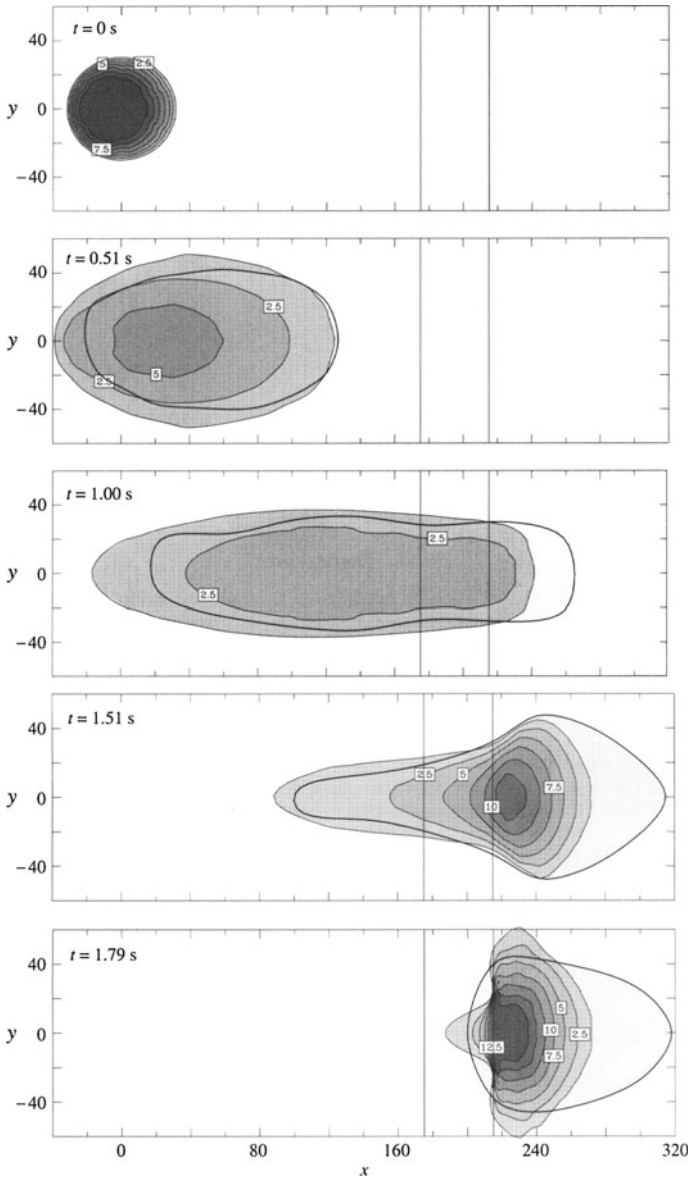


Fig. 13.34 Computed avalanche thickness using the *shallow water avalanche model*, illustrated at the indicated time slices (in the upper left corners) For the computations, $K_x = K_y = 1$ were used. The dark lines in the panels outline the experimental avalanche margins of the experiment of Fig. 13.32 or Fig. 13.33, from [30]. © Proc. Royal Soc. London

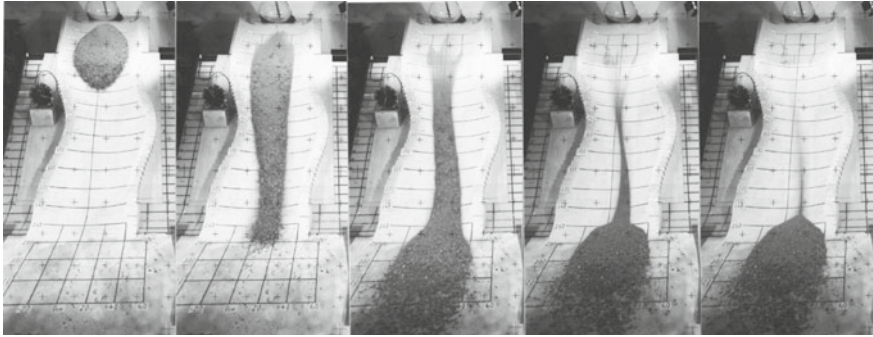


Fig. 13.35 Laboratory gully for simulations of granular avalanches. On a plane inclined by 40° a parabolically shaped channel is mounted where the thalweg deviates sinusoidally from the direction of steepest descent. A mixture of 40 kg sand and gravel is released from a Plexiglass hemispherical cap at the upper edge of the channel. A clock on the left in the pictures measures the time, its long arm performs one revolution per second. The photographs show five shots of the moving avalanche. Note that the originally well-mixed gravel mass is de-mixed with the coarse particles in the front and the small ones in the rear, from [30]. © Proc. Royal Soc. London

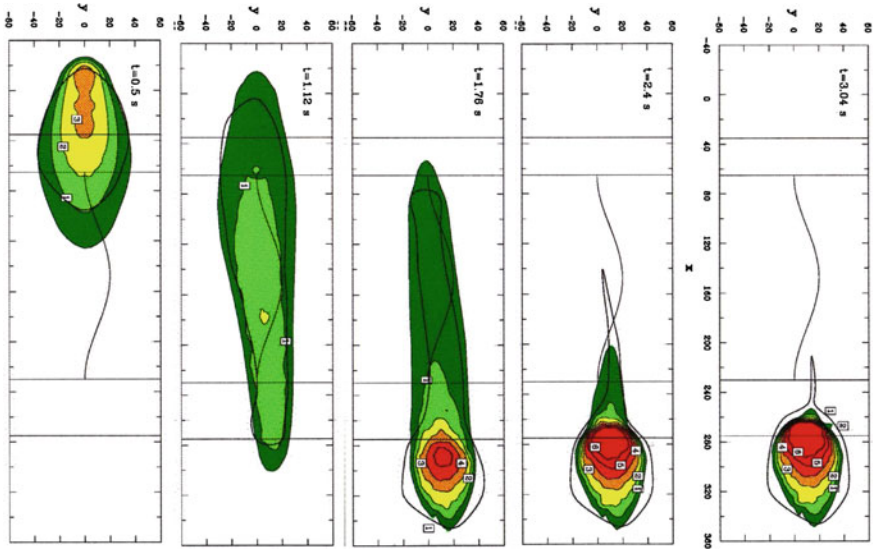


Fig. 13.36 Plane view of the unrolled chute of the top panels with the avalanche motion from top to bottom. The horizontal lines show where the sinusoidal thalweg begins (above at $x = 65$ cm), ends at $x = 320$ cm) and where the horizontal plane begins (below = 275 cm). The times in the panels indicate the moments since the avalanche was released from rest. The graphs show the topographies in different shadings (with numbers indicating the thickness in cm, as obtained via numerical computations the black solid lines show the margins of the avalanche piles as determined from the photographs, from [30]. © Proc. Royal Soc. London

It was also mentioned that the SH equations reflect shallow water properties when $K_x = K_y = 1$. A one-dimensional version of such a hydraulic avalanche model was developed by M.E. EGLIT et al. [22–26], however, with no numerical computations and no experimental verification. A repetition of the computations of our avalanche model on the doubly curved topography with $K_x = K_y = 1$ yielded instructive results of which the essentials are displayed in **Fig. 13.34**. It is evident from this figure that under rapid dilatational motion the computed avalanche shapes do not considerably deviate from that of the experiment. In the deposition zone, where contracting flow conditions prevail, deviations from the experimental results are substantial. The travel distance is too short and the avalanche spread too wide. *COULOMB frictional behavior is therefore, very significant in catching the correct dynamical behavior of the avalanche.*

Selecting earth pressure coefficients unequal to unity is tantamount to accepting normal stress effects in the constitutive relations. These stress anisotropies evidently become significant when the avalanche enters the horizontal run-out zone (and somewhat earlier), as seen in the fifth panel of **Fig. 13.34**. Without the passive earth pressure coefficient to act against sidewise spreading, the computed deposition of the granular avalanche is too wide and its front is behind that of the experiments.

Let us close this analysis with small scale laboratory avalanches, in which the thalweg is not only curved in a vertical plane defining the direction of the steepest descent, but also to the side. **Figure 13.35** shows a laboratory gully for laboratory avalanche simulations, where the thalweg deviates sinusoidally from the direction of steepest descent. The parabolic channel merges after 240 cm into the horizontal plane in the foreground and thus gives up the parabolic profile. A mixture of 40 kg gravel and sand is released from a hemispherical Plexiglas cap and moves down the gully; by the sidewise sinusoidal deviation of the thalweg from the direction of steepest descent; the moving granular flow deviates from the symmetric motion down the direction of steepest descent. This un-symmetry is clearly seen in the five photographs of **Fig. 13.35**. The early longitudinal stretching and the formation of a tail of fine material that still moves, when the front of the avalanche has already settled down are typical. **Figure 13.36** displays a comparison of the experiment with computational results, here also based on the LAGRANGEan integration technique, used by J.M.N.T. GRAY et al. [30].

13.6 Attempts of Model Validation and Verification of Earthquake and Typhoon Induced Landslides

In the previous sections the coordinate systems underlying the governing equations have in general not exactly followed the true topography but only nearly so; deviations from the actual topographies were accounted for by especially introducing the base geometry via an equation $F^b(\mathbf{x}, t) = 0$. It seems obvious that curvilinear coordinates should be employed, which are constructed with the aid of the digital elevation data of the geographical information system provided in the area of potential

landslide occurrences, which are now almost everywhere available to an accuracy of 5 m. These coordinate-based approaches have been introduced by F. BOUCHUT and M. WESTDICKENBERG [9] and were applied to the MOHR–COULOMB constitutive model by Y.- CH. TAI and CH.- Y. KUO (2008) [81] and I. LUCA et al. (2009) [55, 56], Y.-CH. TAI et al. (2012) [83]. The governing equations of these models are derived by constructing a terrain-fitted coordinate system, in which the flow depth is defined in the direction normal to the basal surface. Along this depth-wise direction the inertial effects are of a small negligible magnitude, which leads to a hydrostatic pressure assumption. The last 10–15 years have witnessed a search of papers dealing with these descriptions.

Models achieving equivalent approximate descriptions and applied to the chosen constitutive class of these authors are by H. CHEN and C.F. LEE (2000) [11], S. MCDUGALL and O. HUNGR (2004) [59] and O. HUNGR and S. MCDUGALL (2009) [40] and R.P. DENLINGER and R.M. IVERSON (2004) [16] and R.M. IVERSON and R.P. DENLINGER (2004) [45], R.P. IVERSON et al. (2004) [46] and S. DE TONI and P. SCOTTON (2005) [18].

The aforementioned references employ either EULERIAN or LAGRANGEAN finite differences paired with the use of non-oscillatory numerical schemes and TVD slope limiters (see G.S. JIANG and E. TADMOR (1997) [63] or for an overview [70]). They require as a preliminary step derivation of the governing equations (balances of mass, momentum,...) referred to the basal topography fitted coordinates. In the newer approach Y.- CH. TAI et al. (2012) [83] “the model equations are written for the Cartesian components of the momentum and stresses in the terrain-fitted coordinates. The difference between the present model and traditional description of [the] governing equations over curvilinear coordinates is that the new model avoids the calculation of the Christoffel symbols; see for comparison I. LUCA et al. [55, 56]. This form is not the first seen in the literature, but it is a special form (the EULERIAN description limit) of the Unified Coordinate (UC) formalism [W.H. HUI and S. KOURDRIAKOV (2002) [39]; W.H. HUI (2007) [38]]. As a fuller example Y.- CH. TAI and CH.- Y. KUO [81] and Y.- CH. TAI et al. [83] further elaborate on the capability of moving coordinates in the UC method for their two-dimensional model with erosion and deposition”, after C.- Y. KUO et al. (2011) [53].

Apart from a great number of validation attempts for table top, see [15, 46], and laboratory avalanches of the 1–5 m size, [59], using the constitutive class of the SH model—performances are reported in this chapter and to a much larger extent by S.P. PUDASAINI and K. HUTTER [70] and, incorporating also entrainment and deposition phenomena, by Y.- CH. TAI and Y.C. LIN (2008) [82] and S. MCDUGALL and O. HUNGR [60]—large scale chute experiments (of 95 m length) were done by IVERSON and DENLINGER (2004) [45] and PUDASAINI et al. [69].

The book by I. LUCA, Y.- CH. TAI and CH.- Y. KUO [57] gives a detailed summary of the numerical methods and validation and verification of the models equations, [57].

R.P. DENLINGER and R.M. IVERSON performed their outdoor experiments in a rectangular chute of 2 m width and ca 70 m down-slope length and 31.5° inclination angle, merging into a 25 m long plane inclined 2.5°. They used a 10 m³ mass of a gravel-water mixture suddenly released from a head gate at the top of

the chute. Because of the pressure of the water a mixture model was formulated and reduced to a classical avalanche model extended by accounting for the pore pressure. Two models, physically equivalent, but with [69], and without [15], accounting for the curvature effects along the trajectory are derived by R.P. DENLINGER and R.M. IVERSON [16] and S.P. PUDASAINI et al. [69]. Results are comparable to one another, though those of S.P. PUDASAINI et al. seem to match measurements a bit better, see Fig. 13.37.

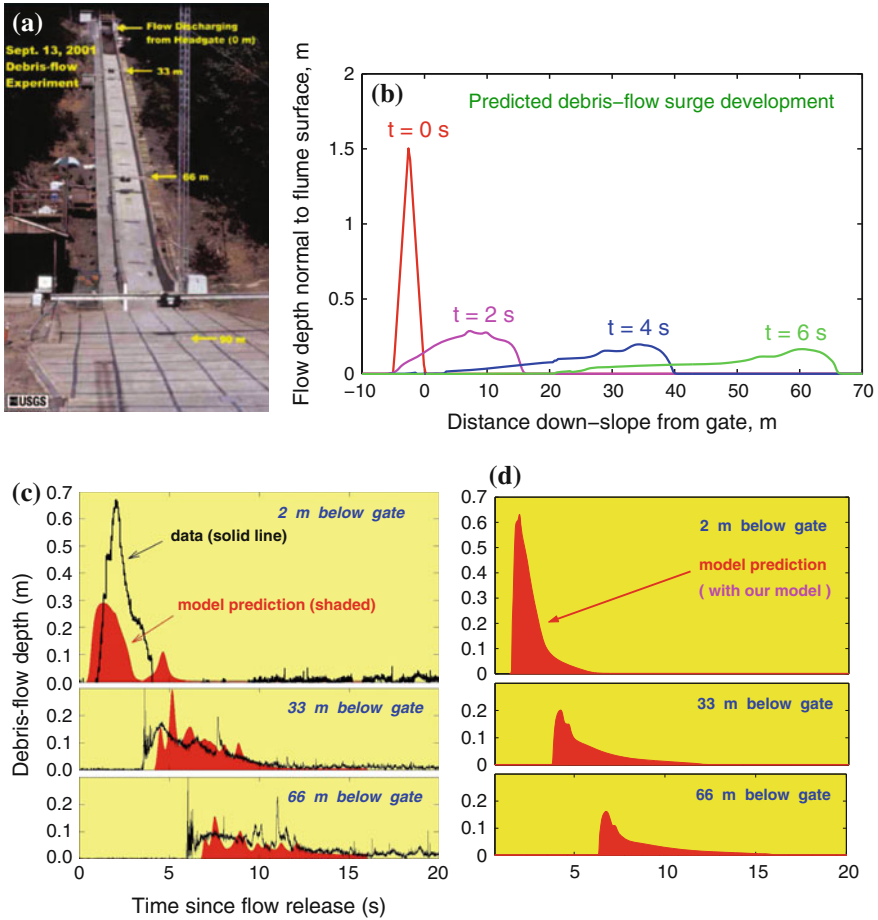


Fig. 13.37 a 95 m long chute-horizonal plane combination of USGS, photographed here on 1st September 2001 for solid-water debris flow tests. For details see [15]. **b** Predicted profiles of debris flow surges along the down-slope coordinate in the middle of the channel in panel (a) at four successive times on the inclined rectangular flume with inclination angle of 31.4° , [69]. **c, d** Comparison between measurements and two model predictions. **c** Experimental data of flow depth at three cross sections of a water saturated debris flow at USGS, 24. July 1995, and numerical results predicted by R.P. DENLINGER and R.M. IVERSON [15]. **d** Numerical results predicted by S.P. PUDASAINI et al. [69]. © Natural Hazards and Earth System Sciences

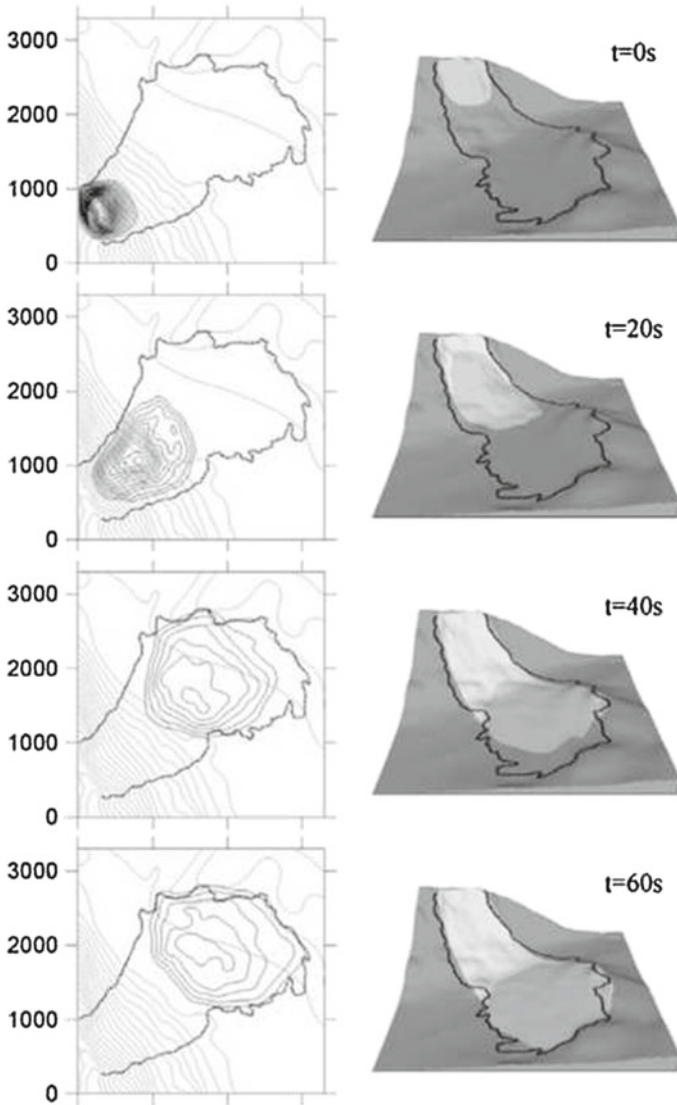


Fig. 13.38 Analysis of the Frank slide *Plane and oblique views of the simulated flow position at 20 s intervals. The flow depth contours are at 5 m intervals. The thick, solid line indicates the extent of the real event (digitized from the Canada Department of Mines: Map 57A (Frank, Alberta 1917)), from [60]. © Canadian Geotech. Journal*

S. MCDUGALL and O. HUNGR [59] performed back analyses of a historical and recent landslides to see whether the model equations adequately reproduce the soil mass movements in the landslides, see **Fig. 13.38**. They used

- the Frank slide in Canada: “On April 29, 1903, approximately 30 million m^3 of rock descended Turtle Mountain into the Crow’s-nest River Valley, partially burying the town of Frank, Alberta and killing about 70 people. It was Canada’s worst landslide disaster, EVANS (2001) [28]. The simulation shown in Fig. 13.38 is based on a detailed digital elevation model of the present-day topography, provided by the Geological Survey of Canada. The topography of the deposition zone was modified to approximate the pre-slide condition by removing approximately 30 million m^3 from the area according to estimated deposit depths. The starting position of the 30 million m^3 slide mass was similarly estimated.

The model provided a good match of the general extent and distribution of the final deposit, using a frictional rheology with $\delta = 14^\circ$ and $\phi = 40^\circ$. The low value of the bed friction angle points at the existence of pore water pressure in the flowing material and would require a solid-fluid mixture model for adequate physical description. Computations have shown that the flow must have come to rest in about 100 s. For more details see [59].

- The second landslide analyzed by S. MCDUGALL and O. HUNGR [60] is the 1999-Nomash River rock slide-debris avalanche in British Columbia. This landslide began with the collapse of 300,000 m^3 of crystalline limestone, with the head scarp located about 430 m above the river on the Western side of the V-valley and then continuing down, roughly along the thalweg to stop after more than a kilometer. The computations performed without supposing mass being entrained from the ground on the Western slope always made the computed avalanche to stop before it turned its motion down the main valley. Water did not seem to be the cause for the farther continuing motion of the real avalanche motion. However, “steep talus-like deposits at the foot of the source slope” [60], have led S. MCDUGALL and O. HUNGR to postulate a volume entrainment density per unit area, compare also Fig. 13.39,

$$V = E|v|h, \quad (13.138)$$

where $|v|$ is the modulus of the depth-averaged topography parallel velocity and h is the avalanche depth as a function of space. By trial and error $E = 1.9 \times 10^{-3}$ (m^{-1}) was found to be optimal for matching trim lines with snapshots of computed avalanche margins. Details are shown in Fig. 13.39 and its caption.

The above description of avalanching motions of granular materials in small table top, laboratory and outdoor experiments were complemented by two landslide events in Nature by CH.- Y. KUO et al. [52, 53]. In [53], the theory that was used in the computational validation attempts were based on the assumptions of COULOMB internal frictional and basal MOHR–COULOMB sliding behavior, which allowed *anisotropic stress responses* for the normal stresses σ_{xx} , σ_{yy} tangential to the basal surface, in the approximation of this MOHR–COULOMB model expressed as (13.95)–(13.103), so that in general the down-slope and cross-slope normal pressures differ from one another. Such a stress anisotropy is denied by the geophysical mass flow group of the New York State University at Buffalo, [65, 66], who choose

Fig. 13.39 Oblique surfacial views of the 1999-Nomash-River rock slide-debris avalanche in British Columbia, Canada (Photographs courtesy D. AYOTTE). *Top* photograph looking down valley, *bottom* photograph showing the erosion in the track, from [60]. © Canadian Geotech. Journal



$$\sigma_{xx} = \sigma_{yy} = K_{act/pas} \sigma_{zz} \tag{13.139}$$

with the active and passive earth pressure coefficient selected according to whether

$$\frac{\partial u}{\partial x} + \frac{\partial u}{\partial y} \tag{13.140}$$

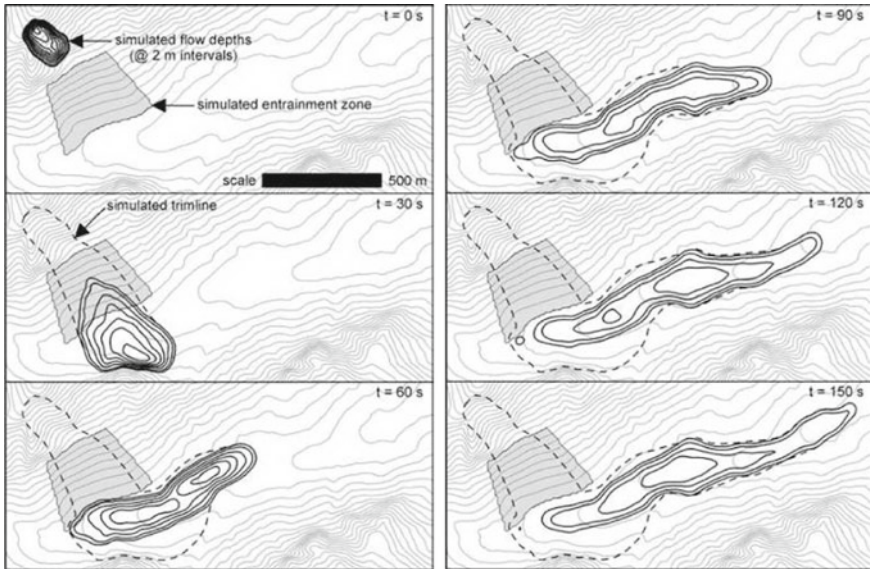


Fig. 13.40 Simulation of the Nomash River landslide accounting for entrainment of material from the source slope. The surface elevation contours are shown at 20 m intervals. Dashed lines show the computed trim lines, from [60]. © Canadian Geotech. Journal

is positive or negative. They have advertized their model in B. PITMAN et al. (2003) [65] and B. PITMAN and L. LEE (2005) [66] and employ their own software TITAN2D. Comparison of their solid-fluid mixture model with data from field observations are not known to us (in 2014). Neither seems the stress (an)isotropy law (13.139), (13.140) have been corroborated by detailed laboratory experiments; for details see [70], p. 455 ff (**Fig. 13.40**).

A further careful analysis of the simulation and validation of the landslide of the Hsiaolin catastrophe, Taiwan is reported by CH.- Y. KUO et al. (2011) [53]. Accordingly, Typhoon Morakot struck southern Taiwan in the summer of 2009, causing the most severe flooding since the 1950s. In the early morning of August 9, rainfall triggered the Hsiaolin landslide, which itself caused 474 of the total 724 deaths by overrunning the Hsiaolin village. Good pre- and post event topographies (5×5 m grid resolution) of the region, where the catastrophic mass flow took place allowed estimation of $(11 + 2)$ million m^3 of moving mass without entraining mass. CH.- Y. KUO et al. [53] based their computation on their extended SH formulation in topography-following coordinates by Y.- CH. TAI and CH.- Y. KUO (2008) [81] and Y.- CH. TAI et al. (2012) [83], a formulation, which avoids the calculation of the CHRISTOFFEL symbols, see for comparison I. LUCA et al. [55, 56], but restricted their analysis to the simplified material behavior of the shallow water assumption, i.e. by putting $K_{\text{act/pas}} = 1$ (vanishing angle of internal friction) and employing a basal

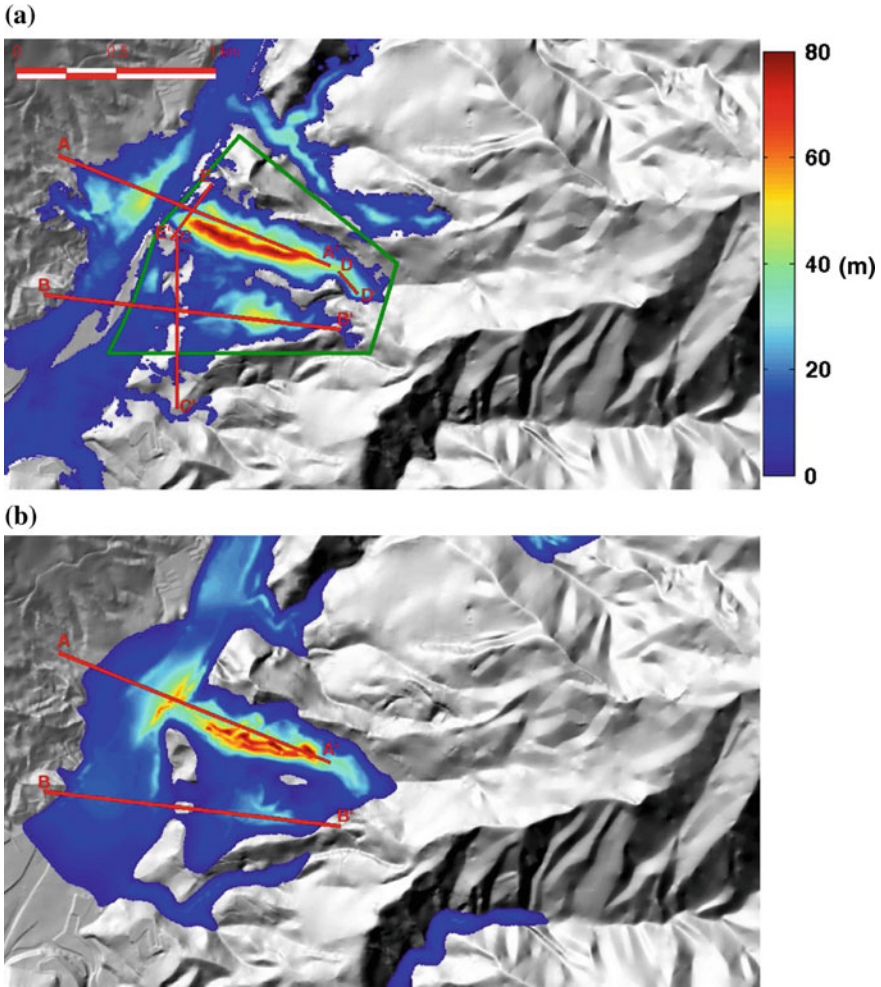


Fig. 13.41 **a** Actual deposit and **b** simulated deposit of the Hsiaolin landslide, Taiwan. The deposit depths are coded with the same *color axis*. The area boxed in the bold *dark green* polygon is the region for the minimization scheme, from [53] © American Geophysical Union, J. Geophys. Research, Solid Earth

COULOMB or VOELLMY drag parameterization (see [53], formulae (5) and (8)).¹⁴ They employed an optimization procedure using the method of least squares,

$$h_{\text{stat}}^2 = \min_{\mu, \alpha} \frac{1}{A} \int_A \{h(\mathbf{x}, \mu, \alpha) - h_{\text{meas}}(\mathbf{x})\}^2, \quad (13.141)$$

¹⁴Details on conditions of validity of this assumption are given in [57].

where A is the area of the deposition, μ the MOHR–COULOMB friction and α the VOELLMY coefficient. Moreover, $h(\mathbf{x}, \mu, \alpha)$ is the computed deposition height obtained for given μ and α and $h_{\text{meas}}(\mathbf{x})$ the corresponding measured height. The above minimum for h_{stat}^2 is first computed for $\alpha = 0$ and variable μ ; then $\mu = \mu_{\text{opt}}$ is held fixed and a second optimization yields an optimal value for $\alpha = \alpha_{\text{opt}}$. **Figure 13.41** shows a comparison between, (a) the actual deposit and (b) the simulated deposit. The area boxed by the bold green polygon is the region for which the minimization procedure is applied (for a more detailed and more objective judgment, the reader may consult [53]). We emphasize that, apart from the many difficulties in the interpretation of the topographic data and the insecurities of the pre- and post event surveyor data the results leave the reader insecure with regard to the chosen constitutive response. More specifically, the computations have been performed with an isotropic stress postulate ($K_x = K_y = 1$), which in laboratory data (see Fig. 13.34) have shown a significant dependence on the earth pressure dependent stress anisotropy. It would be worthwhile to conduct such a comparison to judge the reliability of the assumption made in [53]. For additional model verification, see [57].

References

1. Ambraseys, N., Sarma, S.: Liquefaction by soils induced by earthquakes. *Bull. Seismol. Soc. Am.* **59**(2), 651–664 (1969)
2. Amstutz, Ed, Staub, A.: Dr. A. Voellmy zum 65. Geburtstag. *Schweiz. Bauzeitung* **85**(28), 481 (1965)
3. Armstrong, B.R., Williams, K.: *The Avalanche Book*. Fulcrum Publishing Golden, CO, Golden (1986), (1992)
4. Ansey, Ch., Meunier, M.: Estimating bulk rheological properties of flowing avalanches from the field data. *J. Geophys. Res.* **109**, NoF1:F001004 (2003). doi:[10.1029/2003JF0036](https://doi.org/10.1029/2003JF0036)
5. Bardet, J.P., Kapuskar, M.: Liquefaction and sand boils in San Francisco during 1989 Loma Prieta earthquake ASCE. *J. Geotech. Eng.* **119**, 543–562 (1993)
6. Bassi, F., Ghidoni, A., Rebay, S., Tesini, P.: High-order accurate p-multigrid discontinuous Galerkin solution of the Euler equations. *Int. J. Numer. Meth. Fluids* **60**, 847–865 (2008)
7. Bowen, R., Wang, C.C.: *Introduction to Vectors and Tensors*. Vol. I Linear and Multilinear Algebra; Vol. 2 Vector and Tensor Analysis. Plenum Press, New York (1976)
8. Brillouin, L.: *Tensors in Mechanics and Elasticity*. Academic Press, New York (1964)
9. Bouchut, F., Westdickenberg, M.: Gravity driven shallow water models for arbitrary topography. *Commun. Appl. Math. Sci.* **2**(3), 359–389 (2004)
10. Casagrande, A.: Characteristics of cohesionless soils affecting the stability of slopes and earth fills. *J. Boston Soc. Civil Eng.* (1936)
11. Chen, H., Lee, C.F.: Numerical simulation of debris flows. *Can. Geotech. J.* **37**, 146–160 (2000)
12. Chiou, M., Wang, Y., Hutter, K.: Influence of obstacles on rapid granular flows. *Acta Mech.* **175**, 105–122 (2005)
13. Chiou, M.: *Modelling dry granular avalanches past different obstruct (Elektronische Ressource): numerical simulations and laboratory analyses*. Ph.D. thesis, TU Darmstadt (2005)
14. Cockburn, B., Karniadakis, G.E., Shu, C.-W.: The development of discontinuous galerkin methods. In: Cockburn, B., Karniadakis, G.E., Shu, C.-W. (eds.) *Discontinuous Galerkin Methods. Lecture Notes in Computational Science and Engineering*, vol. 11, pp. 3–50. Springer, Heidelberg (2000)

15. Denlinger, R.P., Iverson, R.M.: Flow of variably fluidized granular material across three-dimensional terrain 2. Numerical predictions and experimental tests. *J. Geophys. Res.* **106**, 553–566 (2001)
16. Denlinger, R.P., Iverson, R.M.: Granular avalanches across irregular three-dimensional terrain. 1. Theory and computation. *J. Geophys. Res.* **109** (2004). doi:[10.11029/2003JF00085](https://doi.org/10.11029/2003JF00085)
17. Dent, J.D., Burrell, K.J., Schmidt, D.S., Louge, M.Y., Adams, E.E., Jazbutis, T.G.: Density, velocity and friction measurements in a dry-snow avalanche. *Ann. Glaciol.* **26**, 247–252 (1998)
18. De Toni, S., Scotton, P.: Two-dimensional mathematical and numerical model for the dynamics of granular avalanches. *Cold Reg. Sci. Technol.* **43**, 36–48 (2005)
19. Dolejsi, V., Feistauer, M.: A semi-implicit discontinuous Galerkin finite element method for the numerical solution of inviscid compressible flow. *J. Comp. Phys.* **198**, 727–746 (2004)
20. Eckart, W., Faria, S., Hutter, K., Kirchner, N., Pudasaini, S.P., Wang, Y.: Continuum description of granular materials. Spring School at the Department of Structural and Geotechnical Engineering, Polytechnic Institute, Turin, Italy, 8–12 April 2002
21. Eckart, W., Gray, J.M.N.T. and Hutter, K.: Particle image velocimetry (PIV) for granular avalanches on inclined planes. In: Hutter, K., Kirchner, N. (eds.) *Dynamic Response of Granular and Porous Materials Under Catastrophic Deformations*. Springer, Berlin (2003)
22. Eglit, M.E.: Theoretical approaches to the calculation of the motion of snow avalanches. In: *Itogi Nauki, Moscow, Viniti 60–97*. English translation in *Glaciological Data Report GD-16*, 63–118 (1974)
23. Eglit, M.E., Shveshnikova, E.I.: Mathematical modeling of snow avalanches (in Russian). English translation *Data of Glaciological Studies* **38**, 79–84 (1980)
24. Eglit, M.E.: Calculation of the parameters of avalanches in the region of breaking and halting (in Russian). English translation *Data of Glaciological Studies* **53**, 35–39 (1982)
25. Eglit, M.E.: Some mathematical models of snow avalanches. In: Shahinpoor, M. (ed.) *Advances in mechanics and the flow of granular materials*, vol. 2, pp. 577–588. Claustral-Zellerfeld and Gulf Publishing Company, Houston (1983)
26. Eglit, M.E.: Mathematical modeling of dense avalanches. In: *25 Years of Snow Avalanche Research at NGI. Anniversary Conference*, Voss, Norway, 12–26 May 1998
27. Erismann, T., Abele, G.: *Dynamics of Rockslides and Rockfalls*. Springer, Berlin, (2001)
28. Evans, S.G.: Landslides. In: Brooks, G.R. (ed.) *A synthesis of geological hazards in Canada*. *Geol. Surv. Can. Bull.* **548**, 43–79 (2001)
29. Gray, J.M.N.T., Hutter, K.: Physik granularer Lawinen. *Physikalische Blätter*, **54**, 37–44 (1998)
30. Gray, J.M.N.T., Wieland, M., Hutter, K.: Gravity driven free surface flow of granular avalanches over complex basal topography. *Proc. R. Soc. Lond.* **A455**, 1841–1874 (1999)
31. Greve, R., Hutter, K.: The motion of a granular avalanche in a convex and concave curved chute: Experiments and theoretical predictions. *Philos. Trans. R. Soc. Lond.* **A342**, 573–604 (1993)
32. Griault, V., Riviere, B., Wheeler, M.F.: A splitting method using discontinuous Galerkin for the transient incompressible Navier–Stokes equations. *ESIAM: M2AN*, **39**(6), 1115–1147 (2005)
33. Grigoriyan, S.S., Ostoumov, A. V.: On the mechanics of the formation and collaps of mountainous slag heaps. (in Russian) *Inst. Mekh. Moskov. Gos. Univ. Moscow. Report Nr 1724* (1975a)
34. Grigoriyan, S.S., Ostoumov, A. V.: Calculation of the parameters of the motion and the force action on an avalanche dike. (in Russian) *Inst. Mekh. Moskov. Gos. Univ. Moscow. Report Nr 1695* (1975b)
35. Grigoriyan, S.S.: A new law of friction and mechanism for large-scale slag heaps and landslides (English translation in *Soviet Phys. Dokl.* **24**, 110–111 (1979))
36. Harrison, J., Falcon, N.: The Saidmarreh Landslip southwest Iran. *Geogr. J.* **89**, 42–47 (1937)
37. Huber, A.: Schwallwellen in Seen als Folge von Felsstürzen, Mitteilung Nr. 47 der Versuchsanstalt für Wasserbau, Hydrologie und Glaziologie an der ETH Zürich (1980)
38. Hui, W.H.: The unified coordinates system in computational fluid mechanics. *Commun. Comput. Phys.* **2**(4), 577–610 (2007)

39. Hui, W.H., Koudriakov, S.: Computation of the shallow water equations using the unified coordinates. *SIAM, J. -Sci. Comput.* **23**(5) 1615–1654 (2002)
40. Hungr, O., McDougall, S.: Two numerical models for landslide dynamic analysis. *Comput. Geosci.* **35**, 978–992 (2009)
41. Hutter, K., Koch, T.: Motion of a granular avalanche in an exponentially curved chute. Experiments and theoretical predictions. *Philos. Trans. Royal. Soc. Lond.*, **A 334**, 93–138 (1991)
42. Hutter, K., Siegel, M., Savage, S.B., Nohguchi, Y.: Two-dimensional spreading of a granular avalanche down an inclined plane. I. *Theory Acta. Mech.* **100**, 37–68 (1993)
43. Hutter, K., Wang, Y., Pudasaini, S.P.: The Savage-Hutter avalanche model. How far can it be pushed? *Philos. Trans. R. Soc.* **A363**, 1507–1528 (2005)
44. Hutter, K., Baillifard, O.: A continuum formulation of lava flows from fluid ejection to solid deposition. In: Hutter, K., Wu, T.T., Shu, Y.Ch. (eds.) *From Waves in Complex Systems to Dynamics of Generalized Continua*, pp. 219–283. World Scientific, Singapore (2011)
45. Iverson, R.M., Denlinger, R.P.: Flow of variable fluidized granular masses across three-dimensional terrain: 1 Coulomb mixture theory. *J. Geophys. Res.* **106**, 537–552 (2004). doi:[10.1029/2000JB900329](https://doi.org/10.1029/2000JB900329)
46. Iverson, R.M., Logan, M., Denlinger, R.P.: Granular avalanches across three-dimensional terrain. 2. Experimental tests. *J. Geophys. Res.* **109** F01015, (2004). doi:[10.1029/2003JF00084](https://doi.org/10.1029/2003JF00084)
47. Kerswell, R.R.: Dam break with Coulomb friction: a model for granular slumping? *Phys. Fluids*, **17**, 057101 (2005)
48. Klingbeil, E.: *Tensorrechnung für Ingenieure (Hochschultaschenbücher) Bibliographisches Institut Mannheim* (1966)
49. Koch, T.: *Bewegung einer granularen Lawine auf einer geneigten und gekrümmten Fläche. Entwicklung und Anwendung eines theoretischen numerischen Verfahrens und dessen Überprüfung durch Laborexperimente. Ph.D. thesis. Technische Hochschule Darmstadt*, 255 p (1994)
50. Kolymbas, D.: Behaviour of liquefied sand. *Philos. Trans. R. Soc. Lond.* **A356**, 2609–2622 (1998)
51. Kolymbas, D.: Liquefaction and cold volcanism. *Acta Geotechnica* (2014). doi:[10.1007/s11440-013-0268-x](https://doi.org/10.1007/s11440-013-0268-x)
52. Kuo, C.Y., Tai, Y.C., Bouchut, F., Mangeney, A., Pelanti, M., Chen, R.F., Chang, K.J.: Simulation of Tsaoling landslide, Taiwan, based on Saint Venant equations over general topography. *Eng. Geol.* **104**, 181–189 (2009)
53. Kuo, C. Y., Tai, Y. C., Chen, C.C., Chang K. J., Siau, A, Y., Dong, J.J., Han, R.H., Shimamoto, T., Lee, C.T.: The landslide stage of the Hsialin catastrophe: simulation and validation. *J. Geophys. Res.* **116** F04007, (2011). doi:[10.1029/2010JF001921](https://doi.org/10.1029/2010JF001921)
54. Kuribayashi, E., Tatsuoka, F.: History of earthquake-induced soil liquefaction in Japan. *Bull. of Public Works Research Institute Ed. Ministry of Construction*, **38**, Tokyo (1977)
55. Luca, I., Tai, Y-Ch., Kuo, Chih-Yu.: Non-Cartesian topography based avalanche equations and approximations of gravity driven ideal and viscous fluids. *Math. Models Methods Appl. Sci.* **19**, 127–171 (2009)
56. Luca, I., Hutter, K., Tai, Yih-Chin, Kuo, Chih-Yu.: A hierarchy of avalanche models on arbitrary topography. *Acta Mechanica* **205**, 121–149 (2009)
57. Luca, I., Tai, Y.-Ch., Kuo, Chih-Yu.: *Rapid Geophysical Mass Flows down Arbitrary Topography*, p. 287. Springer, Berlin (2016)
58. MacCormack, R.W.: An efficient explicit-implicit characteristic method for solving the compressible Navier–Stokes equations. *SIAM-AMS Proc.* **11**, 130–155 (1978)
59. McDougall, S., Hungr, O.: A model for the analysis of rapid landslide motion across three-dimensional terrain. *Can. Geotech. J.* **41**, 1084–1097 (2004)
60. McDougall, S., Hungr, O.: Dynamic modelling of entrainment in rapid landslides. *Can. Geotech. J.* **42**(5), 1437–1448 (2005)
61. McElwaine, J., Nishimura, K.: Ping-pong wall avalanche experiments. *Ann. Glaciol.* **32**, 241–250 (2001)

62. Mohr, O.: Welche Umstände bedingendie Elastizitätsgrenze und den Bruch eines Materials? *Zeitschrift des Vereins Deutscher Ingenieure*, **24**, 1524–1530, 1572–1577 (1914)
63. Jiang, G.S., Tadmor, E.: Non-oscillatory schemes for multi-dimensional hyperbolic conservation laws. *SIAM J. Sci. Comput.* **9**(6), 1892–1917 (1997)
64. Morgemstern, N.: Submarine slumping and the initiation of turbidity currents, pp. 189–220. *Proceedings of the International Res. Conference Marine Geotechnique*, Univ Illinois (1967)
65. Pitman, B., Patra, A.K., Bauer, A.C., Nichita, C.C., Sheridan, M., Bursik, M.: Computing granular avalanches and landslides. *Phys. Fluids* **15**, 3638–3646 (2003)
66. Pitman, B., Lee, L.: A two-fluid model for avalanche and debris flows. *Philos. Trans. R. Soc. Lond.* **A363**, 1573–1601 (2005)
67. Pudasaini, S.P.: Dynamics of flow avalanches over curved and twisted channels: theory, numeric and experimental validation. Ph.D. Dissertation, Darmstadt University of Technology, Germany (2003)
68. Pudasaini, S.P., Wang, Y., Hutter, K.: Dynamics of avalanches along general mountain slopes. *Ann. Glaciol.* **38**, 357–362 (2005)
69. Pudasaini, S.P., Wang, Y., Hutter, K.: Modeling debris flows down general channels. *Nat. Hazards Earth Syst. Sci.* **5**, 799–819 (2005)
70. Pudasaini, S.P., Hutter, K.: *Avalanche Dynamics—Dynamics of Rapid Flows of Dense Granular Avalanches*, p. 602. Springer, Berlin (2007)
71. Reynolds, O.: On the dilatancy of media composed of rigid particles in contact. *Philos. Mag. Ser.* **5**(20), 469–481 (1885)
72. Savage, S.B., Hutter, K.: The motion of a finite mass of granular material down a rough incline. *J. Fluid Mech.* **199**, 177–215 (1989)
73. Savage, S.B., Hutter, K.: Dynamics of avalanches of granular materials from ignition to run-out. Part I: *Anal. Acta Mechanica* **86**, 201–233 (1991)
74. Shahbazi, K., Fischer, P.F., Ethier, C.R.: A high-order discontinuous Galerkin method for the unsteady incompressible Navier–Stokes equations. *J. Comput. Phys.* **222**, 391–407 (2007)
75. Sino-Geotechnics, Research and Development Foundation, Taipei Taiwan (1996)
76. Sokolnikoff, I.S.: *Tensor Analysis Theory and Applications*. Wiley, New York (1951)
77. Straub, S.: *Schnelles granulares Fliessen in subaerischen pyroclastischen Strömen*. Ph.D. Dissertation Bayerische Julius Maximilians Universität, Würzburg, Germany (1994)
78. Tai, Y.-Ch., Wang, Y., Gray, J.M.N.T., Hutter, K.: Methods of similitude in granular avalanche flows. In: Hutter, K., Wang, Y., Beer, H. (eds) *Advances in Cold-region Thermal Engineering and Sciences*, pp. 415–428. Springer, Berlin (1999)
79. Tai, Y.-Ch.: Dynamics of granular avalanches and their simulations with shock-capturing and front-tracking numerical schemes Ph. D. dissertation, Darmstadt University of Technology, Darmstadt, Germany (2000)
80. Tai, Y.-Ch., Gray, J.M.N.T., Hutter, K.: Dense granular avalanches: mathematical description and experimental validation. In: Balmforth, N.J., Provinciale, A. (eds.) *Geophysical Fluid Mechanics*, pp 339–366. Springer, Berlin (2001)
81. Tai, Y.-Ch., Kuo, Ch-Y: A new model of granular flows over general topography with erosion and deposition. *Acta Mechanica* **199**, 71–96 (2008)
82. Tai, Y.-Ch., Lin Y.C.: A focused view of the behavior of granular flows down a confined inclined chute into the horizontal runout zone. *Phys. Fluids*, **20**, 123302, (2008). doi:[10.1063/1.3033490](https://doi.org/10.1063/1.3033490)
83. Tai, Y.-Ch., Kuo, Ch-Y, Hui, W.-H.: An alternative depth integrated formulation for granular avalanches over temporally varying topography with small curvature. *Geophys. Astrophys. Fluid Dyn.* **106**(6), 596–629 (2012)
84. Voellmy, A.: Über die Zerstörkraft von Lawinen. *Schweizerische Bauzeitung*, **73**, 159–162, 212–217, 246–249, 280–285 (1955)
85. Wang, Y., Hutter, K.: Comparisons of numerical methods with respect to convectively dominated problems. *Int. J. Numer. Meth. Fluids* **37**, 721–745 (2001)
86. Wang, Y., Hutter, K.: Granular material theories revisited. In: Balmforth, N.J., Provenzale, A. (eds.) *Geomorphological Fluid Mechanics*, pp. 79–107. Springer, Heidelberg (2001)

87. Wang, Y., Hutter, K., Pudasaini, S.: The Savage-Hutter theory: a system of partial differential equations for avalanche flows of snow, debris, and mud. *Z. Angew. Math. Mech.* **84**(8), 507–527 (2004)
88. Wieland, M., Gray, J.M.N.T., Hutter, K.: Channelized free surface flow of cohesionless granular avalanches in a chute with shallow lateral curvature. *J. Fluid Mech.* **392**, 73–100 (1999)

Chapter 14

Uniqueness and Stability

Abstract This chapter on uniqueness and stability provides a first flavor into the subject of laminar-turbulent transition. Two different theoretical concepts are in use and both assume that the laminar-turbulent transition is a question of loss of stability of the laminar motion. With the use of the energy method one tries to find conditions for the laminar flow to be stable. Energy stability criteria operate with the construction of upper bounds of the rate of the perturbed kinetic energy $K(t)$ of the fluid system, in order to obtain by time integration an inequality of the form $K(t) < K(0)\exp(-t/\tau)$. Here, $\tau > 0$ guarantees decay and $\tau < 0$ growth rates of the perturbed energy, $\tau = 0$ guarantees neutral stability of the perturbation flows. The difficulty of the method is that the condition $\tau = 0$ generally provides poor, i.e., very safe estimates for stability. More successful for pinpointing the laminar-turbulent transition has been the method of linear instability analysis, in which a lowest bound, is searched for, at which the onset of deviations from the laminar flow is taking place. For plane channel flows the RAYLEIGH and ORR–SOMMERFELD equations with associated boundary conditions for an ideal and viscous fluid, respectively, are derived and the associated eigenvalue problems are discussed, which leads to the stability chart, separating REYNOLDS number dependent stable and unstable flow regimes.

Keywords Kinetic energy of the difference motion · Uniqueness · Energy stability of laminar channel flows · RAYLEIGH equation · ORR–SOMMERFELD equation

List of Symbols

Roman Symbols

$c = \omega/\alpha$	Phase speed
$D[\mathbf{v}]$	Stretching, strain rate deviator $D[\mathbf{v}] = \frac{1}{2}[\text{grad } \mathbf{v} + \text{grad }^T \mathbf{v}]$
d	Width of a canal, radius of a sphere
EI	Bending stiffness of an EULER beam
$\langle f \rangle$	Spatial average of the function f (see (14.38))
$\mathbf{h}(x, y)$	Auxiliary vector function
K	Kinetic energy per unit mass
L	Length of an (EULER) beam

$M(x)$	Bending moment in an (EULER) beam
$-m, m > 0$	Lower bound for the eigenvalues of $\mathbf{D}[\mathbf{u}]$
P	Axial load of an (EULER) beam
$P(x, y)$	Pressure in a plane channel
p'	Perturbation pressure
p, p^*	Pressure associated with $\mathbf{v}(\mathbf{x}, t)$ and $\mathbf{v}^*(\mathbf{x}, t)$, respectively
\mathcal{R}^n	Real space of dimension n
$\mathbb{R} = U_e d / \nu$	REYNOLDS number
r	Radial distance
$\mathbf{t}^R, \mathbf{t}^{R*}$	CAUCHY viscous stress deviator in two different motions
U_e, U_0	Mean flow velocity through a channel of width d
$\mathbf{u} = \mathbf{v}^* - \mathbf{v}$	Difference of two velocity fields
$V(t)$	Domain of a body
$\mathbf{v}(\mathbf{x}, t), \mathbf{v}^*(\mathbf{x}, t)$	Velocity fields satisfying the NAVIER–STOKES equations
u', v'	Perturbation velocity components in a channel
$y(x)$	Transverse displacement of a beam
x, y, z	Cartesian coordinates

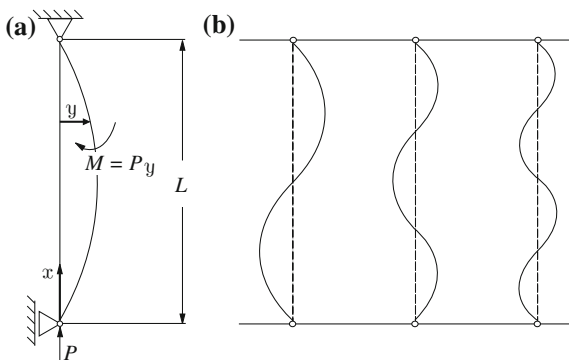
Greek Symbols

α	Wave number
ν	Kinematic viscosity
ρ	Mass density
ρK	Kinetic energy of a body per unit volume
$\iota = \sqrt{-1}$	Imaginary unit
ψ	Streamfunction in two dimensional flow
$\Psi(y)$	Amplitude function of the streamfunction ψ
ω	Frequency
$\partial V(t)$	Boundary domain of a body of volume $V(t)$
$\nabla^2 = \Delta$	(Two dimensional) LAPLACE operator

14.1 Introduction

Stability in mechanics characterizes states of deformations and stresses in material bodies, in which a body configuration, which smoothly changes as the result of smooth changes of the exciting loads, suddenly transits rapidly or instantly into another configuration that is far distant from the previous one. A famous example is the so-called EULER beam, **Fig. 14.1**, a straight rod of constant cross section loaded at its hinged ends in the direction of, and toward, the rod axis. For small loads, P , the straight rod is a persistent, i.e., stable equilibrium configuration; the beam will become somewhat shorter, but no transverse deflection will occur. A fortiori,

Fig. 14.1 **a** EULER beam, axially loaded by P and **b** its bifurcated configurations



if a small deflection is artificially induced, and the beam is left to adjust to this perturbation, the transverse deflection will return to its zero value. Evidently, the zero deflection is a unique stable configuration. If, however, the load has the value $P_n = EI(n\pi/L)^2$, the beam may possess the zero deflection or any sinusoidal, displaced axis $y(x) = \sin[(n\pi/L)x]$. Here, n is an integer, EI the bending rigidity and L the length of the shaft. It is clear from Fig. 14.1 and its figure legend that $y \equiv 0$ is solution of the differential equation (14.1). However, when P is given as one of the EULER loads P_n , a second sinusoidal, solution exists. One speaks in this situation of a possible *bifurcation* from the trivial $y \equiv 0$, solution to the bifurcated, EULER solution with non-zero transverse deflection $y = \alpha \sin[(n\pi/L)x]$, where α is an undetermined amplitude. The simple, linear, homogeneous differential equation does not tell us which of the solutions the EULER beam may prefer at buckling. A deeper analysis shows that for $P \neq P_n$, $y \equiv 0$ is the only solution, whilst at $P = P_n$, only $y = \alpha \sin[(n\pi/L)x]$ is the assumed solution. One speaks for the configuration $y \equiv 0$ of the *stable*, trivial, solution, which becomes *unstable* when P equals one of the EULER loads P_n .

The differential equation of its bending is

$$y'' = -\frac{M(x)}{EI}, \quad M = P y \quad \longrightarrow \quad y'' + \frac{P}{EI}y = 0, \quad (14.1)$$

subject to hinged endpoints possesses the only zero solution $y = 0$, but if $P = P_n = \left(\frac{n\pi}{L}\right)^2$, then it also has the sinusoidal solution $y = \alpha \sin[(n\pi/L)x]$.

The EULER beam is likely the simplest example with the aid of which the concepts of stability and uniqueness can be explained. These concepts occur in any subject of science and engineering, also in fluid mechanics. Indeed, the stability/instability descriptions form an important special field of fluid mechanics, which e.g. chiefly contributed to the conceptual understanding of the transition from laminar to turbulent flow, which today is understood as a loss of stability of the laminar flow and the associated transition to the turbulent flow configuration.

In this chapter we shall only scratch the surface of the title topic, given the extensive literature that exists about this subject.¹ There are different mathematical procedures how the question of the stability and/or uniqueness of a basic flow can analytically be attacked. Common to these procedures is the assumption that the bifurcated solution from the basic flow is a perturbation field, which sets in as a small deviation from the basic flow and will evolve in time and space. If the evolution of the perturbed variables dies out in time, the basic flow will eventually be the sole contribution of the total field quantities that will survive. If this happens, stability of the basic flow will then have been demonstrated. If the perturbed fields grow in time, then the total solution consisting of the basic fields plus the perturbations will constitute a new solution: The basic flow will in this case not be *stable*; it is then called *unstable*. Details of the mathematical methods in use to analyse this situation differ according to whether the perturbations are small or large, i.e., of the order of magnitude of the basic flow. If they are small, perturbation equations can be linearized in the perturbation quantities. This procedure leads to linear stability analyses. For these, analytical-numerical techniques are well known today, but results provide only information on the transition from the basic flow to the perturbed flow. Stability/instability transition is expressed as a *growth rate of the perturbed field variables* exclusively under the conditions of the instability *onset*. When the values of the perturbation variables are not small, linearization of the total fields is *not* permissible. Fully nonlinear equations must be handled and proofs of stability (here, at this moment, interpreted as boundedness of the perturbation fields) require advanced mathematical tools of analysis.

Stability/instability analyses and proofs for uniqueness following the linearization procedure use the methods of linear ordinary and partial differential equations subject to boundary and initial conditions, a special field of highly developed applied mathematics. The full nonlinear theory makes chiefly use of differential relations of *kinetic energy of the perturbation fields* and searches for bounds of its growth rate. The values of these bounds deliver statements of stability, if such growth rates are negative. They cannot provide information on the stability/instability transition (which are often termed *neutral stability*). By contrast, the linear stability/instability methods capture the conditions of this neutral stability and formulate this transition (and only the transition) precisely. Mathematically, it is generally expressed as an eigenvalue problem for a complex valued phase speed, of which the sign of the imaginary value provides information on the growth or attenuation of the perturbed fields.

In what follows, we shall give an introduction to these concepts and no more. In the next section we shall start with the derivation of the balance equation for the kinetic energy of the perturbed motion. Next, we shall take up this balance law of kinetic energy to prove under restricted conditions the uniqueness of the

¹There is a large number of books treating stability as a whole subject. Among these we mention S. CHANDRASEKHAR [2], F. CHARRU [3], P.G. DRAZIN [4], P.G. DRAZIN and W.H. REID [6], C. GODRECHE and C. MANNEVILLE [8], C.C. LIN [12], D.D. JOSEPH [10, 11], S.S. SRITHARAN [21], H.L. SWINNEY and J.P. GOLLUB [22].

flow of a specific initial boundary value problem of the NAVIER–STOKES equations. Section 14.4 is devoted to energy stability criteria. These criteria will then be applied in Sect. 14.5 for a study of stability of laminar channel flow. Finally, in Sect. 14.6 linear stability analysis of laminar channel flow will be tackled on the basis of work by LORD RAYLEIGH and W.M.F ORR and A. SOMMERFELD. Our aim, however will be only to give a flavor of this fascinating subject of fluid mechanics.

14.2 Kinetic Energy of the Difference Motion

Let $V(t)$ be a region in \mathcal{R}^3 with boundary $\partial V(t)$ that is filled with a density preserving viscous fluid. Assume, moreover, that on $\partial V(t)$ the velocity is prescribed (e.g. via the no-slip condition).

Let $\mathbf{v}(\mathbf{x}, t)$ and $\mathbf{v}^*(\mathbf{x}, t)$ be two velocity fields, which satisfy the NAVIER–STOKES equations within $V(t)$ and the velocity boundary conditions on $\partial V(t)$; let p and p^* be the corresponding pressure fields. The *difference motion* in $V(t)$ is defined by

$$\mathbf{u} = \mathbf{v}^* - \mathbf{v}. \quad (14.2)$$

Its kinetic energy in $V(t)$ is given by

$$\rho K = \frac{\rho}{2} \int_{V(t)} |\mathbf{u}|^2 dv \quad (14.3)$$

and is called the *kinetic energy of the difference motion*. The momentum equation for the velocities \mathbf{v} and \mathbf{v}^* are

$$\begin{aligned} \rho \left\{ \frac{\partial \mathbf{v}}{\partial t} + (\text{grad } \mathbf{v})\mathbf{v} \right\} &= -\text{grad } p + \text{div } \mathbf{t}^R, \\ \rho \left\{ \frac{\partial \mathbf{v}^*}{\partial t} + (\text{grad } \mathbf{v}^*)\mathbf{v}^* \right\} &= -\text{grad } p^* + \text{div } \mathbf{t}^{R*}. \end{aligned}$$

By taking the difference of these equations one obtains

$$\rho \left\{ \frac{\partial \mathbf{u}}{\partial t} + (\text{grad } \mathbf{v}^*)\mathbf{v}^* - (\text{grad } \mathbf{v})\mathbf{v} \right\} = -\text{grad } (p^* - p) + \text{div } (\mathbf{t}^{R*} - \mathbf{t}^R).$$

The nonlinear term on the left-hand side can be transformed as follows

$$\begin{aligned} &(\text{grad } \mathbf{v}^*)\mathbf{v}^* - (\text{grad } \mathbf{v})\mathbf{v} \\ &= (\text{grad } \mathbf{v}^* - \text{grad } \mathbf{v})\mathbf{v}^* + (\text{grad } \mathbf{v})(\mathbf{v}^* - \mathbf{v}) \\ &= (\text{grad } \mathbf{u})\mathbf{v}^* + (\text{grad } \mathbf{v})\mathbf{u}, \end{aligned}$$

so that

$$\begin{aligned} & \rho \left\{ \frac{\partial \mathbf{u}}{\partial t} + (\text{grad } \mathbf{u}) \mathbf{v}^* + (\text{grad } \mathbf{v}) \mathbf{u} \right\} \\ &= -\text{grad} (p^* - p) + \text{div} (\mathbf{t}^{R^*} - \mathbf{t}^R). \end{aligned} \quad (14.4)$$

Scalar multiplication of this equation with the difference velocity \mathbf{u} yields a balance equation for the difference motion; it has the form

$$\begin{aligned} & \rho \left\{ \frac{\partial}{\partial t} \left(\frac{|\mathbf{u}|^2}{2} \right) + \underbrace{\mathbf{u} \cdot ((\text{grad } \mathbf{u}) \mathbf{v}^*) + \mathbf{u} \cdot ((\text{grad } \mathbf{v}) \mathbf{u})}_{(i)} \right\} \\ &= \underbrace{-\mathbf{u} \cdot \text{grad} (p^* - p)}_{(ii)} + \underbrace{\mathbf{u} \cdot \text{div} (\mathbf{t}^{R^*} - \mathbf{t}^R)}_{(iii)}. \end{aligned} \quad (14.5)$$

In this equation the underbraced terms can be transformed as follows:

$$\begin{aligned} (i) &= u_i \frac{\partial u_i}{\partial x_k} v_k^* + u_i \frac{\partial v_i}{\partial x_k} u_k = \frac{1}{2} \frac{\partial}{\partial x_k} (u_i u_i v_k^*) - \frac{1}{2} u_i u_i \underbrace{\frac{\partial v_k^*}{\partial x_k}}_{=0} \\ &+ \frac{1}{2} \underbrace{\left(u_i \frac{\partial v_i}{\partial x_k} u_k + u_i \frac{\partial v_k}{\partial x_i} u_k \right)}_{\mathbf{u} \cdot \mathbf{D}[\mathbf{v}]\mathbf{u}} \\ &= \frac{1}{2} \text{div} (|\mathbf{u}|^2 \mathbf{v}^*) + \mathbf{u} \cdot \mathbf{D}[\mathbf{v}]\mathbf{u}, \\ (ii) &= -\text{div} (\mathbf{u}(p^* - p)) + (p^* - p) \underbrace{\text{div } \mathbf{u}}_{=0} = -\text{div} (\mathbf{u}(p^* - p)), \\ (iii) &= u_i \frac{\partial \tau_{ik}}{\partial x_k} = \frac{\partial}{\partial x_k} (u_i \tau_{ik}) - \tau_{ik} \frac{\partial u_i}{\partial x_k}, \quad \tau_{ik} := (\mathbf{t}^{R^*})_{ik} - (\mathbf{t}^R)_{ik} \\ &= \frac{\partial}{\partial x_k} (u_i \tau_{ik}) - \tau_{ik} \frac{1}{2} \left(\frac{\partial u_i}{\partial x_k} + \frac{\partial u_k}{\partial x_i} \right) \\ &= \text{div} (\mathbf{u}(\mathbf{t}^{R^*} - \mathbf{t}^R)) - \text{tr} \left((\mathbf{t}^{R^*} - \mathbf{t}^R) \mathbf{D}[\mathbf{u}] \right). \end{aligned}$$

Substituting these expressions into (14.5) yields the balance law for the kinetic energy of the difference motion in the form

$$\begin{aligned} & \rho \left\{ \frac{\partial}{\partial t} \left(\frac{|\mathbf{u}|^2}{2} \right) + \frac{1}{2} \text{div} (|\mathbf{u}|^2 \mathbf{v}^*) + \mathbf{u} \cdot \mathbf{D}[\mathbf{v}]\mathbf{u} \right\} \\ &= -\text{div} (\mathbf{u}(p^* - p)) + \text{div} (\mathbf{u}(\mathbf{t}^{R^*} - \mathbf{t}^R)) - \text{tr} \left((\mathbf{t}^{R^*} - \mathbf{t}^R) \mathbf{D}[\mathbf{u}] \right). \end{aligned} \quad (14.6)$$

We quote that

$$\mathbf{D}[\mathbf{v}] = \frac{1}{2} (\text{grad } \mathbf{v} + (\text{grad } \mathbf{v})^T), \quad (14.7)$$

$$\mathbf{D}[\mathbf{u}] = \mathbf{D}[\mathbf{v}^*] - \mathbf{D}[\mathbf{v}] =: \mathbf{D}^* - \mathbf{D},$$

because of the linearity of the operator $\mathbf{D}[\cdot]$. Integration of (14.6) over $V(t)$ yields

$$\rho \frac{dK}{dt} = - \int_{V(t)} \left\{ \rho \mathbf{u} \cdot \mathbf{D}[\mathbf{v}]\mathbf{u} + \text{tr} \left((\mathbf{t}^{R*} - \mathbf{t}^R) \mathbf{D}[\mathbf{u}] \right) \right\} dv. \quad (14.8)$$

In the derivation of this equation, the divergence theorem was used, e.g.,

$$\begin{aligned} \int_{V(t)} \text{div} \left(\rho \frac{|\mathbf{u}|^2}{2} \mathbf{v}^* \right) dv &= \int_{\partial V(t)} \frac{\rho |\mathbf{u}|^2}{2} (\mathbf{v}^* \cdot \mathbf{n}) da = 0, \\ \int_{V(t)} \text{div} (\mathbf{u}(p^* - p)) dv &= \int_{\partial V(t)} (p^* - p) (\mathbf{u} \cdot \mathbf{n}) da = 0, \end{aligned}$$

due to $\mathbf{u} = \mathbf{v}^* - \mathbf{v} = \mathbf{0}$ on the boundary $\partial V(t)$.

Moreover,

$$\begin{aligned} \int_{V(t)} \rho \frac{\partial}{\partial t} \left(\frac{|\mathbf{u}|^2}{2} \right) dv &= \int_{V(t)} \frac{\partial}{\partial t} \left(\frac{\rho |\mathbf{u}|^2}{2} \right) dv \\ &= \frac{d}{dt} \int_{V(t)} \frac{\rho |\mathbf{u}|^2}{2} dv - \int_{\partial V(t)} \underbrace{\left(\frac{\rho |\mathbf{u}|^2}{2} \right)}_{=0} \Big|_{\partial V(t)} (\mathbf{v} \cdot \mathbf{n}) da. \end{aligned}$$

It is emphasized that application of the boundary condition $\mathbf{u}|_{\partial V(t)} = \mathbf{0}$ at the body surface was essential in obtaining (14.8). However, the fluid may even be nonlinearly viscous.

Let us now specialize Eq.(14.8) for NEWTONIAN density preserving fluids. In this case,

$$\mathbf{t}^R = 2\rho\nu\mathbf{D}[\mathbf{u}], \quad \mathbf{t}^{R*} - \mathbf{t}^R = 2\eta\mathbf{D}[\mathbf{u}], \quad \eta := \rho\nu,$$

so that

$$\begin{aligned} \text{tr} \left((\mathbf{t}^{R*} - \mathbf{t}^R) \mathbf{D}[\mathbf{u}] \right) &= 2\rho\nu \text{tr} ((\mathbf{D}[\mathbf{u}]) (\mathbf{D}[\mathbf{u}])) \\ &= 2\rho\nu \text{tr} \left(\left(\frac{1}{2} (\mathbf{L} + \mathbf{L}^T) \right) \left(\frac{1}{2} (\mathbf{L} + \mathbf{L}^T) \right) \right), \quad \mathbf{L} := \text{grad } \mathbf{u} \end{aligned}$$

$$\begin{aligned}
&= \frac{1}{2} \rho \nu \{ \text{tr} (\mathbf{L}\mathbf{L}) + \text{tr} (\mathbf{L}\mathbf{L}^T) + \text{tr} (\mathbf{L}^T\mathbf{L}) + \text{tr} (\mathbf{L}^T\mathbf{L}^T) \} \\
&\stackrel{(*)}{=} \rho \nu \{ \text{tr} (\mathbf{L}\mathbf{L}) + \text{tr} (\mathbf{L}\mathbf{L}^T) \} \\
&\stackrel{(+)}{=} \{ \text{div} (\mathbf{u}\mathbf{L}^T) + \text{tr} (\mathbf{L}\mathbf{L}^T) \}.
\end{aligned}$$

The step $\stackrel{(*)}{=}$, follows because $\text{tr} (\mathbf{L}\mathbf{L}) = \text{tr} (\mathbf{L}^T\mathbf{L}^T)$ as well as $\text{tr} (\mathbf{L}\mathbf{L}^T) = \text{tr} (\mathbf{L}^T\mathbf{L})$. On the other hand $\stackrel{(+)}{=}$, implies

$$\text{tr} (\mathbf{L}\mathbf{L}) = u_{i,j} u_{j,i} = \left[(u_i u_{j,i})_{,j} - \underbrace{u_i u_{j,j}}_{=0} \right] = (u_i u_{j,i})_{,j} = \text{div} (\mathbf{u}\mathbf{L}^T),$$

and this yields

$$\int_{V(t)} \rho \nu \text{div} (\mathbf{u}\mathbf{L}^T) \, dv = \int_{\partial V(t)} \rho \nu (\mathbf{u} \cdot \text{grad} (\text{div} \mathbf{u})) \, da = 0,$$

according to the divergence theorem and the boundary condition $\mathbf{u}|_{\partial V} = \mathbf{0}$. It follows that (14.8) takes for a NEWTONIAN fluid the form

$$\begin{aligned}
\frac{dK}{dt} &= - \int_{V(t)} \{ \nu \text{tr} (\mathbf{L}\mathbf{L}^T) + \mathbf{u} \cdot \mathbf{D}[\mathbf{v}]\mathbf{u} \} \, dv \\
&= - \int_{V(t)} \{ \nu \text{tr} ((\text{grad} \mathbf{u})(\text{grad} \mathbf{u})^T) + \mathbf{u} \cdot \mathbf{D}[\mathbf{v}]\mathbf{u} \} \, dv, \quad (I). \quad (14.9)
\end{aligned}$$

A slightly altered form of this equation can be derived as follows:

$$\begin{aligned}
\mathbf{u} \cdot \mathbf{D}[\mathbf{v}]\mathbf{u} &= u_i \frac{1}{2} (v_{i,j} + v_{j,i}) u_j = \frac{1}{2} u_i v_{i,j} u_j + \frac{1}{2} u_i v_{j,i} u_j \\
&= \frac{1}{2} (u_i v_i u_j)_{,j} - \frac{1}{2} v_i (u_i u_j)_{,j} + \frac{1}{2} (u_i v_j u_j)_{,i} - \frac{1}{2} v_j (u_i u_j)_{,i} \\
&= (u_i v_i u_j)_{,j} - v_i (u_i u_j)_{,j} \\
&= \text{div} ((\mathbf{u} \cdot \mathbf{v})\mathbf{u}) - \mathbf{v} \cdot ((\text{grad} \mathbf{u})\mathbf{u}).
\end{aligned}$$

When substituting this into (14.9), the divergence theorem can be used to transform the volume integral into a surface term, which vanishes due to the boundary condition, $\mathbf{u}|_{\partial V} = \mathbf{0}$. Thus, instead of (14.9), one may also write

$$\frac{dK}{dt} = \int_{V(t)} \{ \mathbf{v} \cdot ((\text{grad} \mathbf{u})\mathbf{u}) - \nu \text{tr} ((\text{grad} \mathbf{u})(\text{grad} \mathbf{u})^T) \} \, dv, \quad (II). \quad (14.10)$$

The two formulae (I) and (II) differ in form, how the basic flow \mathbf{v} arises in the integral on the right-hand side. It is apparent that for positive dK/dt the flow may become unstable. This becomes in (II) manifest via a large modulus of \mathbf{v} ; by contrast, this is achieved in (I) by a too large modulus of the shear velocity $\mathbf{D}[\mathbf{v}]$.

These formulae will now be used in subsequent solutions for a search of uniqueness or/and stability of the flow.

14.3 Uniqueness

In the year 1929 E. FOÁ proved the following theorem²:

Theorem 14.1 *If two flows, which obey the NAVIER–STOKES equations of a density preserving fluid possess in a bounded material region $V(t)$ the same velocity distributions at time $t = 0$ and they have for all times $t > 0$ coinciding velocities along the boundary $\partial V(t)$ of $V(t)$, then the two flows in $V(t)$ are identical. ■*

For the proof the two velocity fields will be denoted by \mathbf{v}^* and \mathbf{v} , and the difference motion is described by $\mathbf{u} = \mathbf{v}^* - \mathbf{v}$. Since the two fields agree with one another at $t = 0$ in $V(t)$ and $\partial V(t)$, one has

$$K(0) = 0. \quad (14.11)$$

Furthermore, on the boundary one has

$$\mathbf{u}|_{\partial V(t)} = \mathbf{0}, \quad \forall t \geq 0. \quad (14.12)$$

Thus, the prerequisites of the above theorem are satisfied. Because $\text{tr}(\mathbf{L}\mathbf{L}^T) \geq 0$, $\forall \mathbf{L}$, Eq. (14.9) implies

$$\frac{dK}{dt} \leq - \int_{V(t)} \mathbf{u} \cdot \mathbf{D}[\mathbf{v}]\mathbf{u} \, dv. \quad (14.13)$$

Now, since $\mathbf{D}[\mathbf{v}]$ is a deviator ($\text{div} \mathbf{v} = 0$), the sum of its eigenvalues vanishes. Otherwise stated, the smallest eigenvalue is negative. Let's call the lower bound of this eigenvalue in $V(t)$ for $t \leq T$, $-m$ with $m > 0$. Then we have for $0 \leq t \leq T$

$$\mathbf{u} \cdot \mathbf{D}[\mathbf{v}]\mathbf{u} \geq -m|\mathbf{u}|^2. \quad (14.14)$$

²E. FOÁ: L' Industria, **43**, 426 (1929), Milan.

Consequently, we have a fortiori

$$\begin{aligned} \frac{dK}{dt} &\leq - \int_{V(t)} \mathbf{u} \cdot \mathbf{D}[\mathbf{v}]\mathbf{u} \, dv \leq m \int_{V(t)} |\mathbf{u}|^2 \, dv = 2mK \\ \longrightarrow \frac{dK}{dt} - 2mK &\leq 0. \end{aligned} \quad (14.15)$$

This is an ordinary differential inequality, which can also be written as

$$\frac{d}{dt} (K \exp(-2mt)) \leq 0. \quad (14.16)$$

Integration over the interval $0 \leq t \leq T$ yields

$$K(t) \exp(-2mt) \leq 0, \quad \text{since } K(0) = 0. \quad (14.17)$$

Now, $K(t)$ can never be negative by definition, hence $K(t) = 0$; this means that $\mathbf{u}(t) = \mathbf{0}$. This proves the uniqueness of the basis solution:

$$\mathbf{u} = \mathbf{0}, \quad \forall t \in [0, T]. \quad (14.18)$$

14.4 Stability

In this section we will derive stability criteria in order to apply them later to special flows. Let us call $\mathbf{v}(\mathbf{x}, t)$ the basic flow and $\mathbf{v}^*(\mathbf{x}, t)$ the perturbed flow of $\mathbf{v}(\mathbf{x}, t)$; $\mathbf{u} = \mathbf{v}^* - \mathbf{v}$ is a perturbation of the basic flow. We assume that the basic flow and the perturbation flow satisfy the same boundary conditions on $\partial V(t)$, so that $\mathbf{u}|_{\partial V(t)} = \mathbf{0}$. Now, however, we assume that $K(0) \neq 0$. If one can demonstrate that for all $t \geq 0$, $dK/dt < 0$, then one has proved that the basic flow is stable. This gives a lower bound for stability.

In the following we shall deduce from relation (I) a stability criterion (III), and similarly from relation (II) a stability criterion (IV).³

a) Derivation of relation (III)

Let \mathbf{h} and \mathbf{u} be differentiable vector fields. Then one may deduce

$$\begin{aligned} 0 &\leq (u_{i,k} + u_i h_k) (u_{i,k} + u_i h_k) = u_{i,k} u_{i,k} + 2 u_i h_k u_{i,k} + |\mathbf{u}|^2 |\mathbf{h}|^2 \\ &= u_{i,k} u_{i,k} + (u_i u_i h_k)_k - |\mathbf{u}|^2 h_{k,k} + |\mathbf{u}|^2 |\mathbf{h}|^2 \\ &= \text{tr} ((\text{grad } \mathbf{u}) (\text{grad } \mathbf{u})^T) + \text{div} (|\mathbf{u}|^2 \mathbf{h}) + |\mathbf{u}|^2 (|\mathbf{h}|^2 - \text{div} (\mathbf{h})). \end{aligned}$$

³See e.g. Handbuch der Physik III/1 'Strömungsmechanik (I)', p. 153 ff.

If this inequality is integrated over $V(t)$ and the divergence theorem is applied where possible and the boundary condition, $\mathbf{u}|_{\partial V} = \mathbf{0}$, is accounted for, then one obtains

$$\int_{V(t)} \text{tr} ((\text{grad } \mathbf{u}) (\text{grad } \mathbf{u})^T) \, dv \geq \int_{V(t)} |\mathbf{u}|^2 (\text{div } \mathbf{h} - |\mathbf{h}|^2) \, dv. \quad (14.19)$$

If this inequality is used in Eq. (14.9) (I), we obtain

$$\begin{aligned} \frac{dK}{dt} &\leq - \int_{V(t)} \{ \nu (\text{div } \mathbf{h} - |\mathbf{h}|^2) |\mathbf{u}|^2 + \mathbf{u} \cdot \mathbf{D}[\nu]\mathbf{u} \} \, dv \\ \frac{dK}{dt} &\stackrel{(14.14)}{\leq} - \int_{V(t)} \nu (\text{div } \mathbf{h} - |\mathbf{h}|^2) |\mathbf{u}|^2 \, dv + 2mK. \end{aligned} \quad (14.20)$$

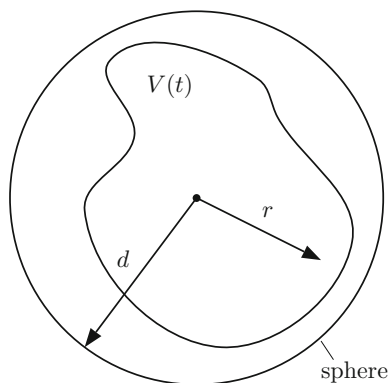
To derive a concrete formula, let us select now a specific vector field \mathbf{h} . To this end we choose a sphere with radius d , which encloses the entire $V(t)$, **Fig. 14.2**. Let r be the radial distance from the center of the sphere and choose

$$\mathbf{h} = C \tan(Cr) \hat{\mathbf{e}}_r, \quad (14.21)$$

in which $\hat{\mathbf{e}}_r$ is the radial unit vector and C is a constant, which shall later be taken as $C = \pi/d$. The field \mathbf{h} is continuously differentiable in $V(t)$ and we have in spherical coordinates

$$\begin{aligned} \text{div } \mathbf{h} &= \frac{2}{r} C \tan(Cr) + \frac{C^2}{\cos^2(Cr)}, \\ \text{div } \mathbf{h} - |\mathbf{h}|^2 &= \frac{2C}{r} \tan(Cr) + \frac{C^2}{\cos^2(Cr)} (1 - \sin^2(Cr)) \end{aligned}$$

Fig. 14.2 Sphere with radius d which encloses $V(t)$ at all times $t \in [0, T)$ the distance measured from the center of the sphere is given by r



$$= \frac{2C^2}{Cr} \tan(Cr) + C^2 \geq 3C^2. \quad (14.22)$$

The last inequality holds, since $(\tan x)/x \geq 1, \forall x \in [0, \pi]$. With $C = \pi/d$ the inequality (14.22) holds for all points in the sphere with radius d .

If (14.22) is used in (14.20), one obtains

$$\begin{aligned} \frac{dK}{dt} &\leq -3C^2\nu \int_{V(t)} |\mathbf{u}|^2 dv + 2mK = \left(2m - \frac{6\pi^2\nu}{d^2}\right) K, \\ \rightarrow \frac{dK}{dt} - \left(2m - \frac{6\pi^2\nu}{d^2}\right) K &\leq 0. \end{aligned} \quad (14.23)$$

Integration over t yields

$$K(t) \leq K(0) \exp\left(\left(2m - \frac{6\pi^2\nu}{d^2}\right)t\right), \quad (III), \quad (14.24)$$

which is the statement that was earlier announced. One easily recognizes that $K(t)$ is exponentially growing, when the argument of the exponential function is positive. Thus, the basic flow is stable, provided that

$$m < \frac{3\pi^2\nu}{d^2}, \quad (\text{stability!}).$$

Strictly, (14.24) only states that $K(t)$ is a decreasing function, if $m = (3\pi^2\nu)/d^2 =: m_0$ for all $t < T$, a fact which one associates with stability. Else, the bound m_0 may be too 'rough' to infer anything on instability. So $m < m_0$ is a sufficient condition for stability.

b) Derivation of relation (IV)

In this subsection, we base the analysis on the inequality

$$0 \leq (\nu u_{i,k} - v_i u_k)(\nu u_{i,k} - v_i u_k) = \nu^2 u_{i,k} u_{i,k} - 2\nu v_i u_{i,k} u_k + |\mathbf{u}|^2 |\mathbf{v}|^2.$$

This implies

$$\nu^2 \operatorname{tr}((\operatorname{grad} \mathbf{u})(\operatorname{grad} \mathbf{u})^T) + |\mathbf{u}|^2 |\mathbf{v}|^2 \geq 2\nu \mathbf{v} \cdot ((\operatorname{grad} \mathbf{u}) \mathbf{u}),$$

or

$$\mathbf{v} \cdot ((\operatorname{grad} \mathbf{u}) \mathbf{u}) \leq \frac{1}{2\nu} \left\{ \nu^2 \operatorname{tr}((\operatorname{grad} \mathbf{u})(\operatorname{grad} \mathbf{u})^T) + |\mathbf{u}|^2 |\mathbf{v}|^2 \right\}. \quad (14.25)$$

If this inequality is substituted into inequality (14.10) (II), then one obtains

$$\begin{aligned} \frac{dK}{dt} &\leq \frac{1}{2\nu} \int_{V(t)} \{ |\mathbf{u}|^2 |\mathbf{v}|^2 + (\nu^2 - 2\nu^2) \operatorname{tr} ((\operatorname{grad} \mathbf{u}) (\operatorname{grad} \mathbf{u})^T) \} dv \\ &= \frac{1}{2\nu} \int_{V(t)} \{ |\mathbf{u}|^2 |\mathbf{v}|^2 - \nu^2 \operatorname{tr} ((\operatorname{grad} \mathbf{u}) (\operatorname{grad} \mathbf{u})^T) \} dv. \end{aligned} \quad (14.26)$$

Let v_0 be the largest modulus of the velocity of the basic flow in $V(t)$ during $0 \leq t < T$. Then, (14.26) implies

$$\begin{aligned} \frac{dK}{dt} &\leq \frac{1}{2\nu} \left\{ 2v_0^2 K - \nu^2 \int_{V(t)} \operatorname{tr} ((\operatorname{grad} \mathbf{u}) (\operatorname{grad} \mathbf{u})^T) dv \right\} \\ &\stackrel{(14.19)}{\leq} \frac{1}{2\nu} \left\{ 2v_0^2 K - \nu^2 \int_{V(t)} \left(|\mathbf{u}|^2 \underbrace{(\operatorname{div} \mathbf{h} - |\mathbf{h}|^2)}_{> 3C^2 = \frac{3\pi^2}{d^2}} \right) dv \right\} \\ &\leq \frac{1}{2\nu} \left\{ 2v_0^2 K - \frac{3\pi^2}{d^2} \nu^2 2K \right\}, \end{aligned}$$

or

$$\frac{dK}{dt} - \frac{1}{\nu} \left\{ v_0^2 - \frac{3\pi^2\nu^2}{d^2} \right\} K \leq 0, \quad (14.27)$$

from which by integration one obtains

$$K(t) \leq K(0) \exp \left(\left(v_0^2 - \frac{3\pi^2\nu^2}{d^2} \right) t \right), \quad (IV). \quad (14.28)$$

This is the statement (IV), a second inequality, from which stability of the flow can be deduced:

$$\text{Stability} \iff v_0^2 < \frac{3\pi^2\nu^2}{d^2} \longrightarrow \frac{v_0 d}{\nu} < \sqrt{3} \pi \approx 5.44. \quad (14.29)$$

The quantity $v_0 d/\nu$ is a REYNOLDS number and the statement says that the flow of the viscous fluid is stable provided this REYNOLDS number is smaller than 5.44. Experience teaches that this limit value is far too low.

The two stability criteria (III) (14.24) and (IV) (14.28) make two physically different statements. In (III) the amount of shearing is limited; in (IV) the velocity itself is limited. These facts suggest that neither of the two describes this bifurcation of the flow adequately. An appropriate criterion should involve both.

14.5 Energy Stability of the Laminar Channel Flow

Consider plane viscous channel flow with the steady velocity profile, **Fig. 14.3**,

$$\mathbf{v} = U(z)\hat{\mathbf{e}}_x, \quad U(z) = \frac{3}{2}U_0 \left(1 - 4\left(\frac{z}{d}\right)^2\right), \quad U'' = -\frac{12U_0}{d^2}. \quad (14.30)$$

The parabolic velocity profile is a solution of the NAVIER–STOKES equations, if it is driven by the pressure gradient

$$\Delta P = 12\nu \frac{U_0}{d^2}. \quad (14.31)$$

Let us now perturb this basic flow by writing

$$\mathbf{v} = U(z)\hat{\mathbf{e}}_x + \mathbf{u}, \quad \text{grad } p = \Delta P\hat{\mathbf{e}}_x + \rho \text{grad } \pi. \quad (14.32)$$

The NAVIER–STOKES equation for the difference motion is then given by

$$\frac{\partial \mathbf{u}}{\partial t} + (\text{grad } \mathbf{u} + \text{grad } (U\hat{\mathbf{e}}_x)) (\mathbf{u} + U\hat{\mathbf{e}}_x) = -\text{grad } \pi + \nu \Delta \mathbf{u}. \quad (14.33)$$

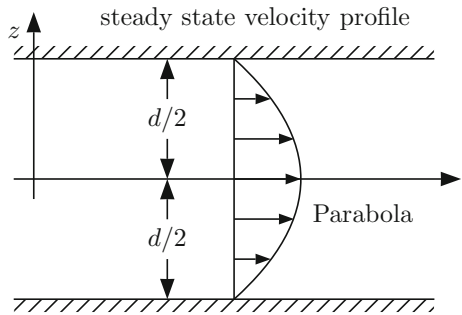
The basic flow satisfies already the equation $\Delta P - (12\nu U_0)/(d^2) = 0$. Now,

$$(\text{grad } U \hat{\mathbf{e}}_x)U \hat{\mathbf{e}}_x = 0, \quad \text{and} \quad (\text{grad } U \hat{\mathbf{e}}_x)\mathbf{u} = w U' \hat{\mathbf{e}}_x, \quad (14.34)$$

in which $U' = dU/dz$ and w is the z -component of the perturbation velocity $\mathbf{u} = (u, v, w)$. Therefore, (14.33) reduces to

$$\frac{\partial \mathbf{u}}{\partial t} + (\text{grad } \mathbf{u})\mathbf{v} + w U' \hat{\mathbf{e}}_x = -\text{grad } \pi + \nu \Delta \mathbf{u}. \quad (14.35)$$

Fig. 14.3 Plane laminar channel flow of a viscous fluid



This is the momentum equation for the difference motion. Scalar multiplication of this equation with \mathbf{u} yields

$$\frac{\partial}{\partial t} \left(\frac{|\mathbf{u}|^2}{2} \right) + \underbrace{\mathbf{u} \cdot (\text{grad } \mathbf{u}) \mathbf{v}}_{(i)} + uwU' = \underbrace{-\mathbf{u} \cdot \text{grad } \pi}_{(ii)} + \nu \underbrace{\mathbf{u} \cdot \Delta \mathbf{u}}_{(iii)}, \quad (14.36)$$

in which the underbraced terms are expressible as

$$\begin{aligned} (i) &= u_i u_{i,j} v_j = \frac{1}{2} (u_i u_i v_j)_{,j} - \frac{|\mathbf{u}|^2}{2} v_{j,j} \underset{=0}{=} \frac{1}{2} \text{div} (|\mathbf{u}|^2 \mathbf{v}), \\ (ii) &= -u_i \pi_{,i} = -(u_i \pi)_{,i} - \underbrace{u_{i,i}}_{=0} \pi = -\text{div} (\mathbf{u} \pi), \\ (iii) &= (u_i u_{i,jj}) = (u_i u_{i,j})_{,j} - u_{i,j} u_{i,j} \\ &= \text{div} (\mathbf{u} \text{grad } \mathbf{u}) - \text{tr} ((\text{grad } \mathbf{u}) (\text{grad } \mathbf{u})^T). \end{aligned}$$

Substitution of these results into (14.36) leads to the evolution equation

$$\begin{aligned} \frac{\partial}{\partial t} \left(\frac{|\mathbf{u}|^2}{2} \right) + uwU' &= -\nu \text{tr} ((\text{grad } \mathbf{u}) (\text{grad } \mathbf{u})^T) \\ &+ \text{div} \left\{ \nu \mathbf{u} \cdot \text{grad } \mathbf{u} - \mathbf{u} \pi - \frac{|\mathbf{u}|^2 \mathbf{v}}{2} \right\}. \end{aligned} \quad (14.37)$$

This equation will now serve as principal equation for the derivation of the stability/instability state of the channel flow. To this end, let us define spatial averages as

$$\langle f \rangle := \lim_{L \rightarrow \infty} \frac{1}{4dL^2} \int_{-d/2}^{d/2} \int_{-L}^L \int_{-L}^L f \, dx dy dz. \quad (14.38)$$

Application of this averaging process to (14.37) will eliminate the last divergence term on the right-hand side of (14.37), since the divergence theorem will transform it to

$$\oint \left\{ \nu \mathbf{u} \text{grad } \mathbf{u} - \mathbf{u} \pi - \frac{|\mathbf{u}|^2 \mathbf{v}}{2} \right\} \cdot \mathbf{n} \, da, \quad (14.39)$$

which vanishes along the channel wall because of the boundary condition, $\mathbf{u}|_{\partial V} = \mathbf{0}$. As an integral over the cross section at $x = -L$ and $x = +L$ the surface integrals in Eq. (14.39) are of order $\{\cdot\}dL$ since $\{\cdot\}$ is bounded. It follows from (14.38) in this case that

$$\lim_{L \rightarrow \infty} \frac{1}{4dL^2} \oint \{\cdot\} \cdot \mathbf{n} \, da = \mathcal{O}(1/L) \rightarrow 0.$$

Averaging (14.37) according to (14.38), thus, yields

$$\frac{d}{dt} \left\langle \frac{|\mathbf{u}|^2}{2} \right\rangle + \langle uwU' \rangle = -\nu \langle \text{tr} ((\text{grad } \mathbf{u}) (\text{grad } \mathbf{u})^T) \rangle.$$

With

$$\langle uwU' \rangle = - \left\langle uw \frac{12U}{d^2} z \right\rangle = - \frac{12U_0}{d^2} \langle uwz \rangle,$$

we, thus, obtain

$$\frac{d}{dt} \left\langle \frac{|\mathbf{u}|^2}{2} \right\rangle = \underbrace{\frac{12U_0}{d^2} \langle uwz \rangle}_{\text{energy supply due to the basic flow}} - \underbrace{\nu \langle \text{tr} ((\text{grad } \mathbf{u}) (\text{grad } \mathbf{u})^T) \rangle}_{\text{energy dissipation by viscous effects}}. \quad (14.40)$$

The question, whether the channel flow is stable or unstable, depends, according to this equation, upon the amount how the energy supply due to the basic flow and the energy dissipation balance each other.

Equation (14.40) can also be written as

$$\begin{aligned} \frac{d}{dt} \left\langle \frac{|\mathbf{u}|^2}{2} \right\rangle &= -2\nu \langle \text{tr} ((\text{grad } \mathbf{u}) (\text{grad } \mathbf{u})^T) \rangle \\ &\times \left\{ \frac{1}{2} - \frac{12U_0}{\nu d^2} \frac{\langle uwz \rangle}{2 \langle \text{tr} ((\text{grad } \mathbf{u}) (\text{grad } \mathbf{u})^T) \rangle} \right\}. \end{aligned} \quad (14.41)$$

In this form stability or instability now depends on the sign of the curly bracket in (14.41). To investigate this statement, let us define two numbers, λ and Λ , such that

$$\begin{aligned} \frac{d^3}{\lambda} &= \max \left\{ \frac{\langle uwz \rangle}{\langle \text{tr} ((\text{grad } \mathbf{u}) (\text{grad } \mathbf{u})^T) \rangle} \right\}, \\ \frac{\Lambda}{d^2} &= \min \left\{ \frac{2 \langle \text{tr} ((\text{grad } \mathbf{u}) (\text{grad } \mathbf{u})^T) \rangle}{\langle |\mathbf{u}|^2 \rangle} \right\}. \end{aligned} \quad (14.42)$$

In order that these numbers exist (i.e. are bounded), it must be ascertained that \mathbf{u} on $z = \pm d/2$ satisfies the boundary condition, $\mathbf{u} = \mathbf{0}$. Moreover, \mathbf{u} and π must be

almost periodic functions.⁴ With these assertions Eqs. (14.41) and (14.42) imply

$$\begin{aligned} \frac{d}{dt} \left\langle \frac{|\mathbf{u}|^2}{2} \right\rangle &\leq -2\nu \langle \text{tr} ((\text{grad } \mathbf{u}) (\text{grad } \mathbf{u})^T) \rangle \left\{ \frac{1}{2} - \frac{6U_0}{\lambda\nu} \right\} \\ &\leq -\frac{\nu}{d^2} \Lambda \langle |\mathbf{u}|^2 \rangle \left\{ \frac{1}{2} - \frac{6U_0}{\lambda\nu} \right\}. \end{aligned}$$

This implies, after integration,

$$\langle |\mathbf{u}|^2 \rangle (t) \leq \langle |\mathbf{u}|^2 \rangle (0) \exp \left\{ -\frac{\nu \Lambda}{d^2} \left(1 - \frac{12U_0 d}{\lambda\nu} \right) t \right\}. \tag{14.43}$$

It is recognized that a stability statement is only possible if one can adequately determine λ . This is quite complicated as we shall now see. To this end we shall first look at the lower half of the channel, $-d/2 \leq z \leq 0$ and apply the SCHWARZ inequality

$$\int_a^b |\varphi \chi| dz \leq \sqrt{\int_a^b |\varphi|^2 dz} \sqrt{\int_a^b |\chi|^2 dz}$$

for two integrable functions $\varphi(z)$ and $\chi(z)$. If one applies the SCHWARZ inequality to the functions $\varphi = 1$ and $\chi = \partial u / \partial z$ one may write

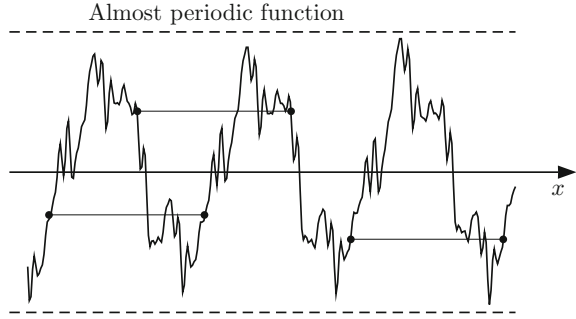
$$\begin{aligned} u(x, y, z, t) = \int_{-d/2}^z 1 \frac{\partial u}{\partial z'} dz' &\leq \int_{-d/2}^z 1 \left| \frac{\partial u}{\partial z'} \right| dz' \\ &\stackrel{\text{Schwarz}}{=} \sqrt{z + \frac{d}{2}} \sqrt{\int_{-d/2}^z \left(\frac{\partial u}{\partial z'} \right)^2 dz'}. \end{aligned} \tag{14.44}$$

With the abbreviated notation

$$\bar{f} := \lim_{L \rightarrow \infty} \int_{-L}^L \int_{-L}^L f \, dx dy,$$

⁴An almost periodic function is uniformly bounded and its value at any position x, y is (for fixed z, t) in a distant point again assumed with almost the same value, see Fig. 14.4.

Fig. 14.4 A picture of an almost periodic function. If the segment $\bullet\text{---}\bullet$ is moved through the graph as indicated by the three segments, its length is not constant but only nearly constant



equation (14.44) implies

$$\begin{aligned}
 \overline{u^2} &\leq \left(z + \frac{d}{2}\right) \int_{-d/2}^z \overline{\left(\frac{\partial u}{\partial z'}\right)^2} dz' \leq \left(z + \frac{d}{2}\right) \int_{-d/2}^0 \overline{\left(\frac{\partial u}{\partial z'}\right)^2} dz' \\
 &\leq \left(z + \frac{d}{2}\right) \int_{-d/2}^0 \overline{\left\{\left(\frac{\partial u}{\partial z'}\right)^2 + \left(\frac{\partial u}{\partial x}\right)^2 + \left(\frac{\partial u}{\partial y}\right)^2\right\}} dz' \\
 &= \left(z + \frac{d}{2}\right) \int_{-d/2}^0 \overline{\text{grad}^2 u} dz. \tag{14.45}
 \end{aligned}$$

Similarly,

$$\overline{w^2} \leq \left(z + \frac{d}{2}\right) \int_{-d/2}^0 \overline{\text{grad}^2 w} dz. \tag{14.46}$$

Furthermore, the following estimate applies:

$$\begin{aligned}
 \overline{uwz} &\leq \frac{1}{4L^2} \iint |z| |uw| dx dy = \frac{1}{4L^2} |z| \iint \sqrt{u^2 w^2} dx dy \\
 &\stackrel{*}{\leq} \frac{1}{8L^2} \iint (u^2 + w^2) dx dy = \frac{|z|}{2} (\overline{u^2} + \overline{w^2}) \\
 &\stackrel{(14.15), (14.16)}{\leq} \frac{|z|}{2} \left(z + \frac{d}{2}\right) \int_{-d/2}^0 \overline{\{\text{grad}^2 u + \text{grad}^2 w\}} dz' \\
 &\leq \frac{|z|}{2} \left(z + \frac{d}{2}\right) \int_{-d/2}^0 \overline{\{\text{grad}^2 u + \text{grad}^2 v + \text{grad}^2 w\}} dz'. \tag{14.47}
 \end{aligned}$$

The step indicated by ' \leq^* ' can be proved as follows: We start with

$$((u^2)^{1/2} \pm (w^2)^{1/2})^2 \geq 0 \implies u^2 + w^2 \pm 2|u||w| \geq 0.$$

From this follows the inequality

$$u^2 + w^2 \geq 2(u^2 w^2)^{1/2} \quad \text{or} \quad (u^2 w^2)^{1/2} \leq \frac{1}{2}(u^2 + w^2).$$

Integrating (14.47) from $z' = -d/2$ to $z' = 0$, thus, yields

$$\int_{-d/2}^0 \overline{uwz} \, dz \leq \underbrace{\int_{-d/2}^0 \frac{|z|}{2} \left(z + \frac{d}{2}\right) dz}_{d^3/96} \int_{-d/2}^0 \overline{\text{tr}((\text{grad } \mathbf{u})(\text{grad } \mathbf{u})^T)} \, dz'. \quad (14.48)$$

The same estimate is also obtained, if the integration is carried out from $z = 0$ to $z = d/2$,

$$\int_0^{d/2} \overline{uwz} \, dz \leq \frac{d^3}{96} \int_0^{d/2} \overline{\text{tr}((\text{grad } \mathbf{u})(\text{grad } \mathbf{u})^T)} \, dz. \quad (14.49)$$

Adding (14.48) and (14.49) yields

$$\begin{aligned} \langle uwz \rangle &\leq \frac{d^3}{96} \langle \text{tr}((\text{grad } \mathbf{u})(\text{grad } \mathbf{u})^T) \rangle \\ \longrightarrow \frac{\langle uwz \rangle}{\langle \text{tr}((\text{grad } \mathbf{u})(\text{grad } \mathbf{u})^T) \rangle} &\leq \frac{d^3}{96}, \end{aligned}$$

or with the statement (14.42)

$$\frac{d^3}{\lambda} = \max \left\{ \frac{\langle uwz \rangle}{\langle \text{tr}((\text{grad } \mathbf{u})(\text{grad } \mathbf{u})^T) \rangle} \right\} \leq \frac{d^3}{96} \longrightarrow \lambda \geq 96. \quad (14.50)$$

This is a definite estimate for λ as was anticipated in (14.43). With this value of λ , (14.43) implies that the steady laminar channel flow is stable, if

$$\frac{12 U_0 d}{96\nu} < 1 \implies \frac{U_0 d}{\nu} < 8. \quad (14.51)$$

With $\langle v \rangle = U_0$ the last inequality can be written as

$$\frac{\langle v \rangle d}{\nu} \leq 8. \quad (14.52)$$

This says that if the REYNOLDS number formed with the mean velocity is smaller than 8, then the basic steady laminar channel flow is stable. One may say ‘certainly stable’ because the bound (14.52) is far too low simply by observational experience. It is in fact the major difficulty of the energy stability method to find bounds as high as possible, which guarantee stability of the basic flow.

14.6 Linear Stability Analysis of Laminar Channel Flow

14.6.1 Basic Concepts

Energy stability analyses had their success in fluid dynamics in problems described by nonlinear initial-boundary-value problems of partial differential equations. In such formulations nonlinear deviations from basic flows are of interest; the answer to the question, whether these deviations remain bounded and reduce in size as time proceeds, or bifurcate further to different flow configurations generally affords nonlinear analysis techniques.

In linear stability analyses the focus is primarily in the onset of the bifurcated flow. This fact is interpreted as the emerging instability of the basic flow, if the bifurcated flow shows a positive growth rate at that instant. More precisely, if the perturbation velocity components are (exponentially) growing, then the basic flow is called *linearly unstable*, however, if they are (exponentially) decaying, then the basic flow is *stable*, sometimes called *absolutely stable*. Finally, if the perturbed velocity components are *steady* or *stationary*, then the basic flow is called *neutrally stable*.

The mathematical prerequisite of linear stability analysis is linearization of the governing equations in the variables of deviation from the basic field variables. This linearization of the perturbation equations in the perturbed fields is the reason, why only the onset of bifurcated flows can be predicted, but nothing beyond it. HERRMANN SCHLICHTING and KLAUS GERSTEN [18], pp.424 ff give an excellent review up-to the year 2000. They are strong supporters of this *method of small disturbances* and prefer it to the *energy method*. In fact they state: ‘This energy method, which was mainly developed by H.A. Lorentz (1907) proved unsuccessful: therefore we will not discuss it further here’. This somewhat strong statement does not lessen, however, the excellent review of the state of the art of the turbulence science at the beginning of the 21st century, which the authors provide.

To derive the governing equations for the perturbed field quantities, let U, V, W, P be the Cartesian velocity components and the pressure of the basic flow, which satisfies the NAVIER–STOKES equations and the boundary and initial conditions of a moving viscous mass of fluid. Moreover, let the corresponding quantities for the

disturbances be u' , v' , w' , p' such that

$$(u, v, w) = (U + u', V + v', W + w'), \quad p = P + p'. \quad (14.53)$$

In a linear stability analysis it is assumed that the perturbation quantities (with primes) are small in comparison to the basic quantities.⁵ The expressions (14.53) are now substituted into the NAVIER–STOKES equations and the boundary and initial conditions of the initial-boundary-value problem formulated here for a linearly viscous fluid. In this process it is assumed that only the variables in the differential equations and initial conditions are perturbed but not in the boundary conditions. In the evolving equations all product terms of the primed quantities are dropped, because they are considered small as compared to the linear (primed) terms. The emerging initial-boundary-value problem is then a set of linear partial differential equations and associated boundary and initial conditions which must be solved.

As an example, let us consider again laminar two-dimensional steady channel flow, for which the basic flow is governed by

$$U = U(y) \left[= \frac{3}{2} U_e \left(1 - 4 \left(\frac{y}{d} \right)^2 \right) \right], \quad V = W = 0, \quad (14.54)$$

$$P = P(x, y) \left[= 12\nu \frac{U_e}{d^2} x \right],$$

in which the expressions in square bracket hold for a steady plane laminar channel flow (see (14.30) and (14.31)), however, here we use y as the transverse coordinate, rather than z . Above, the expressions serve as examples of more general parallel laminar flows).

Inserting the representations (14.53) into the NAVIER–STOKES equations, with the basic fields satisfying (14.54), and assuming that the basic fields also satisfy the NAVIER–STOKES equations, and, furthermore, dropping all products of the primed quantities, yields after somewhat lengthy calculations

$$\begin{aligned} \frac{\partial u'}{\partial t} + U \frac{\partial u'}{\partial x} + v' \frac{dU}{dy} + \frac{1}{\rho} \frac{\partial p'}{\partial x} &= \nu \nabla^2 u', \\ \frac{\partial v'}{\partial t} + U \frac{\partial v'}{\partial x} + \frac{1}{\rho} \frac{\partial p'}{\partial y} &= \nu \nabla^2 v', \\ \frac{\partial u'}{\partial x} + \frac{\partial v'}{\partial y} &= 0, \end{aligned} \quad (14.55)$$

$$\text{in which} \quad \nabla^2 = \frac{\partial^2}{\partial x^2} + \frac{\partial^2}{\partial y^2}.$$

⁵This statement has to be understood in the sense that if e.g. $V = 0$, then v' is obviously not small in comparison to V , but it may still be small in comparison to another variable of the same dimension, e.g. U .

These are three equations for u' , v' , p' . The appropriate boundary conditions require for this two-dimensional channel flow that the perturbation velocities u' , v' vanish at the walls (no slip condition). It should be mentioned here that, even though the basic flow is two-dimensional, velocities in the third spatial direction, w' , could occur and might give rise to the bifurcation at smaller REYNOLDS numbers than Eq. (14.55). It was, however, proved by H.B. SQUIRE [20] as early as 1933 that plane parallel flow becomes unstable with respect to *three-dimensional perturbations* at higher REYNOLDS numbers than two-dimensional perturbations. It follows that *two-dimensional perturbations dominate*.

14.6.2 The Orr–Sommerfeld and the Rayleigh Equations

W.F.M. ORR in 1907 and ARNOLD SOMMERFELD⁶ in 1908, respectively, transformed equations (14.55)_{1,2} for analyzing wave modes into a single equation for the stream function $\psi(x, y, t)$ of the two-dimensional velocity field. To this end, Eq. (14.55) are in a first step transformed to the vorticity equation (by eliminating the pressure, p') and in a second step by replacing the continuity equation by introducing the stream function ψ and writing

$$u' = \frac{\partial \psi}{\partial y}, \quad v' = -\frac{\partial \psi}{\partial x}, \quad (14.56)$$

which satisfy the continuity equation identically. Wave solutions for ψ are sought in the form

$$\psi(x, y, t) = \Psi(y) \exp(\iota(\alpha x - \omega t)). \quad (14.57)$$

In this equation, $\Psi(y)$ is a y -dependent amplitude for the stream function, α is a wave number and ω a frequency; we assume α to be real and positive, $\alpha > 0$, whilst ω could be complex valued. Following the custom in wave theory

$$c = \frac{\omega}{\alpha} = c_r + \iota c_i \quad (14.58)$$

is a complex valued *phase speed*; its real part is the true wave speed of the perturbation stream function, whilst its imaginary part (or the imaginary part of ω) measures the growth or attenuation in time of the stream function. For $\omega_i > 0$ (or $c_i > 0$) one has $-\iota^2 c_i = c_i > 0$; the function $\psi(x, y, t)$ grows with time. This says that the basic motion is unstable. By contrast, for $\omega_i < 0$ (or $c_i < 0$) the function $\psi(x, y, t)$ decays with time. This means that u' and v' , given by

⁶For a short biography of SOMMERFELD, see Fig. 14.5.



Orr-Sommerfeld equation

$$(U - c) (\Psi'' - \alpha^2 \Psi) - U'' \Psi = -\frac{\iota}{\alpha \mathbb{R}} (\Psi'''' - 2\alpha \Psi'' + \alpha^4 \Psi),$$

$$(\cdot)' = \frac{d(\cdot)}{dy}$$

Fig. 14.5 ARNOLD JOHANNES WILHELM SOMMERFELD (5. Dec. 1868 – 26. April 1951)

ARNOLD JOHANNES WILHELM SOMMERFELD was a German theoretical physicist who pioneered developments in atomic quantum physics, and also mentored a large number of students for the new area of theoretical physics. He was born near Königsberg (now Kaliningrad), East Prussia, studied at its University ‘Albertina’ under the supervision of FERDINAND LINDEMANN and benefited there from instructions by ADOLF HURWITZ, DAVID HILBERT and ERNST WIECHERT. He received his Ph.D in 1891. He went to Göttingen and completed his Habilitation there under FELIX KLEIN in 1895. Subsequently, he assumed a teaching assignment of mathematics at the School of Mining in Clausthal–Zellerfeld and in 1900 an associate professorship at the Technische Hochschule in Aachen. It was there, where he developed hydrodynamics as a formal theory; he maintained his interest in fluid dynamics for a long time. Proof for this is the *slide bearing theory*, which he and OSBORN REYNOLDS developed independently (see Sect. 7.3.6 in Chap. 7, Vol. 1) and the fact that two of his Ph.D students (LUDWIG HOPF, WERNER HEISENBERG) wrote their Ph.D dissertations on hydrodynamic topics. In 1906 he assumed the new chair of theoretical physics at the Technische Hochschule Munich, where he taught for 32 years.

ARNOLD SOMMERFELD served as Ph.D supervisor for more NOBEL prize winners in physics than any other supervisor to date, and he was proposed for the NOBEL prize 81 times—more often than any other physicists before and after him.

ARNOLD SOMMERFELD was a very successful academic teacher of theoretical physics as a whole, i.e., classical and modern physics. Among his Ph.D students were WERNER HEISENBERG, WOLFGANG PAULI as well as PETER DEBYE, HANS BETHE, PAUL SOPHUS EPSTEIN, WALTER HEITLER, JOSEPH MEIXNER and many others. Apart from his slide bearing theory, his significant hydrodynamic achievement was the derivation of the ORR–SOMMERFELD equation, the viscous extension of the RAYLEIGH equation for 2D channel flow of ideal fluids [15, 16, 19].

The text is based on www.wikipedia.org

$$u' = \frac{\partial \psi}{\partial y} = \frac{d\Psi}{dy}(y) \exp(\iota(\alpha x - \omega t)),$$

$$v' = -\frac{\partial \psi}{\partial x} = -\iota \alpha \Psi(y) \exp(\iota(\alpha x - \omega t)),$$
(14.59)

will approach zero values as the time tends to infinity. Inserting the above expressions into (14.55) and then eliminating the pressure from the emerging equations yields the following ordinary differential equation for the amplitude $\Psi(y)$ of the stream function

$$(U^* - c^*) ((\Psi^*)'' - (\alpha^*)^2 \Psi^*) - (U^*)'' \Psi^* = -\frac{\iota}{\alpha^* \mathbb{R}} ((\Psi^*)'''' - 2\alpha^* (\Psi^*)'' + (\alpha^*)^4 \Psi^*), \quad (\cdot)' = \frac{d(\cdot)}{dy^*}, \quad (14.60)$$

in which all quantities carrying an asterisk are dimensionless and where the following non-dimensionalizations

$$(x^*, y^*) = \frac{1}{d}(x, y), \quad \left(\alpha^*, \frac{d}{dy^*}\right) = d \left(\alpha, \frac{d}{dy}\right), \quad (u^*, v^*) = \frac{1}{U_e}(u', v'), \quad (14.61)$$

$$t^* = t \frac{U_e}{d}, \quad \Psi^* = \frac{\Psi}{d U_e}, \quad c^* = \frac{c}{U_e}, \quad U^* = \frac{U}{U_e}$$

have been introduced; d is a typical length and U_e a characteristic velocity.

Equation (14.60) is the dimensionless form of the ORR–SOMMERFELD equation. Its left-hand side is due to the inertial terms, whereas those on the right-hand side represent the influence of the linear viscous material behavior. This is recognizable by the pre-factor $\iota/(\alpha^* \mathbb{R})$, where

$$\mathbb{R} = \frac{U_e d}{\nu} \quad \text{is the REYNOLDS number,} \quad (14.62)$$

characteristic of the mean flow.

The boundary conditions that must be applied at both walls in a channel flow, or at one wall and infinitely far away from the wall in a boundary layer flow, are vanishing velocity components u', v' ; thus,⁷

$$\begin{aligned} y = 0, d : \quad u' = v' = 0 &\implies \Psi = 0, \quad \Psi' = 0, \\ y \rightarrow \infty : \quad u' = v' = 0 &\implies \Psi = 0, \quad \Psi' = 0. \end{aligned} \quad (14.63)$$

⁷These coordinates differ from those used in Fig. 14.3 or (14.30) by the translation $y = y^* - \frac{d}{2}$, for which (14.30)₂ reads

$$U(y^*) = \frac{3}{2} U_0 \left(4 \left(\frac{y^*}{d} \right) - 4 \left(\frac{y^*}{d} \right)^2 \right).$$

Thus, (14.63) is formally valid. Moreover, the prime, Ψ' , in (14.63) and consecutive formulae designates now $d\Psi/dy$.

A theoretical limit of the ORR–SOMMERFELD equation is the so-called RAYLEIGH equation [17], derived by him in 1880, prior to the derivations of (14.60) by ORR and SOMMERFELD, and given by

$$(U - c)(\Psi'' - \alpha^2\Psi) - U''\Psi = 0 \quad (14.64)$$

in which asterisks have now been, and henceforth will be omitted, and which follows from (14.60) for $\mathbb{R} \rightarrow \infty$ (or $\nu \rightarrow 0$). Since this equation is of second order, only two of the four boundary conditions can be posed, e.g.,

$$\Psi = 0, \quad \text{at } y = 0 \text{ and } y = d, \text{ or } y \rightarrow \infty. \quad (14.65)$$

Equation (14.64), subject to the boundary conditions (14.65) is the linear perturbation equation for a parallel flow of an inviscid fluid.

14.6.3 The Eigenvalue Problem

The ORR–SOMMERFELD and RAYLEIGH equations with associated boundary conditions are descriptions of eigenvalue problems. This means that non-trivial solutions generally only exist, if a parameter of the equation assumes a certain value.⁸ This parameter is in (14.60) and (14.64) with associated boundary conditions (14.63) and (14.65), respectively, the complex phase speed $c = c_r + \iota c_i$ and is the *eigenvalue* of the boundary value problem. Its real part, c_r , is the phase velocity and its imaginary part c_i is the rate factor, which, according to (14.57) and (14.58), determines the linear stability ($c_i < 0$) or instability ($c_i > 0$) of the basic flow. The value $c_i = 0$ describes *neutral (indifferent) stability*.

For (14.60) and (14.63) nontrivial solutions can be sought by selecting values for U and U'' (provided by the basic flow), the REYNOLDS number \mathbb{R} (equally provided by the basic flow and the viscosity of the fluid) and the characteristic length, d . If for given \mathbb{R} and $\alpha d = \alpha^*$ the value of c_i can be determined by solving the eigenvalue problem, it can be decided, whether the pair of values (\mathbb{R}, α^*) , representing a point in the first quadrant of the plane (\mathbb{R}, α^*) characterizes a state of stability or instability of the basic flow. Repeating this computation for a rectangular net of (\mathbb{R}, α^*) -values, separates domains in the (\mathbb{R}, α^*) -plane of stability or instability. The curve separating these domains defines neutral stability for which $c_i = 0$. **Figure 14.6**, which is a copy from HERRMANN SCHLICHTING and KLAUS GERSTEN [18], displays qualitatively the curves of neutral stability for a plane boundary layer for two-dimensional perturbations of a density preserving viscous fluid. The curve with label *a* belongs to the neutral stability curve for a velocity profile of the basic motion with an inflection point. Alternatively, the curve with label *b* shows the characteristic course for

⁸Please note that Eqs. (14.60), (14.63) as well as (14.64), (14.65) possess the zero solutions $\Psi = 0$. This is so because of the homogeneity of the boundary value problems.

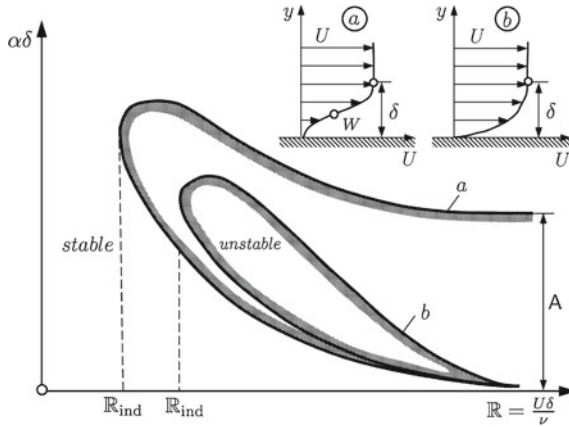


Fig. 14.6 Curves of neutral stability of a plane boundary layer flow for a density preserving fluid under two dimensional perturbations. **a** The inset ① shows a velocity profile of the basic motion with an inflection point which is always unstable for an inviscid fluid predicted by the Rayleigh equation (14.64). The corresponding neutral stability curve, labeled a is determined by the ORR–SOMMERFELD equation (14.60) for a viscous fluid. The asymptotes of the curve of neutral stability for $\mathbb{R} \rightarrow \infty$ are obtained from the RAYLEIGH equation (14.64) for an inviscid fluid. **b** The inset ② shows a velocity profile of the basic motion without inflection point. The neutral stability curve, labeled b is obtained by the ORR–SOMMERFELD equation (14.60) for a viscous fluid. Unstable domains are indicated by shading and indifferent stability states are indicated by \mathbb{R}_{ind} (dashed lines), after [18]

a velocity profile without inflection point. The shaded side indicates the unstable regime. The point on the neutral stability curve, where the REYNOLDS number is smallest (see the tangent to the neutral stability curve perpendicular to the REYNOLDS axis), is of special interest. This is the smallest REYNOLDS number, below which all linear modes are damped, whilst above this value some modes are amplified. This REYNOLDS number on the neutral stability curve is called the *indifference REYNOLDS number* characterizing the *limit of stability*.

The neutral stability curves in Fig. 14.6 are of qualitative nature (note that the two axes, \mathbb{R} and α^* do not show any scales for \mathbb{R} and α^*). To obtain precise results, the eigenvalue problems of (14.60), (14.63–14.65) must be solved. LORD RAYLEIGH was able to solve his boundary value problem (14.64). However, according to H. SCHLICHTING and K. GERSTEN [18], he ‘was basically only able to prove that the presence of a point of inflection is a *necessary condition* for the appearance of unstable waves, but W. TOLLMIEIN in 1935 showed much later that the presence of a point of inflection is a *sufficient condition* for the presence of amplified waves. The point of inflection criterion is of fundamental importance for stability theory, since, provided that we include a correction due to the neglected viscosity effects, it provides a first rough classification of all laminar flows’ [18]. This property has also been observed in convergent/divergent channels, as these flows show favorably decreasing/increasing pressure gradients, which in the velocity profile have/have-not

a point of inflection. This fact is stated in [18] as a theorem: ‘*Velocity profiles with points of inflection are unstable*’.

The effects of viscosity to the solutions of the eigenvalue problems (14.60), (14.63) due to ORR–SOMMERFELD are qualitatively similar to those of the boundary value problem of the RAYLEIGH equation (14.64) with the boundary conditions (14.65) which describes the inviscid behavior (label *a*). The neutral stability curves in Fig. 14.6 for viscous flows are of type *b* instead. They differ most strikingly from those of type *a* by the fact that for infinitely large REYNOLDS numbers, $\mathbb{R} \rightarrow \infty$, the neutral stability curve for inviscid fluids approaches two horizontal asymptotes with $\alpha^* = 0$ and $\alpha^* = A$. This says that for inviscid fluids all perturbations at $\mathbb{R} \rightarrow \infty$ with $\alpha^* = 0$ ($\lambda \rightarrow \infty$) are prone of destabilization. More precisely, at $\mathbb{R} \rightarrow \infty$ all perturbations with $0 < \alpha^* < A$ are unstable. By contrast, for viscous fluids: in this case ‘at infinitely large REYNOLDS numbers, the region of unstable perturbation wavelengths shrinks to nothing, and it is only for finitely large REYNOLDS numbers that a region of unstable waves exists’, [18].

A second result, due to LORD RAYLEIGH [17] and W. TOLLMIEEN [24–26] is also stated as a theorem in [18]: ‘*In boundary-layer profiles, the velocity of propagation for neutral perturbations ($c_i = 0$) is smaller than the maximum velocity of the mean flow*’. This law states ‘that there is a point inside the flow of neutral perturbations where $U - c = 0$ ’. Note that this point is a singular point of the RAYLEIGH equation (14.64), where $|\Psi''|$ becomes infinitely large, unless U'' vanishes there simultaneously’. In the context of matched asymptotic expansions this says that in viscous fluids with small viscosity (large REYNOLDS numbers) the RAYLEIGH equation (14.64) describes the outer flow behavior within the critical layer where $U = c$. The two distinct behaviors described by perturbation series in the perturbation parameter \mathbb{R}^{-1} must be matched together.

The extensive literature on the stability/instability transitions of the RAYLEIGH and ORR–SOMMERFELD equations is discussed by H. SCHLICHTING and K. GERSTEN [18] pp. 433 ff. We restrict ourselves here to mentioning just a few important memoirs. An overview of solutions of the RAYLEIGH equations from a mathematical point of view is e.g. given by P.G. DRAZIN and L.N. HOWARD (1966) [5] and P.G. DRAZIN and W.H. REID (1981) [6]. Early, primarily analytical attempts of solving the ORR–SOMMERFELD equation are given by O. TIETJENS (1922) [23] and W. HEISENBERG (1924) [9]. W. TOLLMIEEN (1929–47) [24–26] presented detailed analytical calculations, whilst J.M. GERSTING and D.F. JANKOWSKI (1972) [7] and R. BETCHOV and W.O. CRIMINALE (1967) [1] summarized the numerical integration techniques.

With this very brief introduction into the onset of turbulence as a problem of fluid flow stability/instability transition we stop here. H. SCHLICHTING and K. GERSTEN [18] discuss a wealth of further studies on experiments and validation of the stability/instability transition of flows based on the NAVIER–STOKES equations, e.g., construction of neutral stability curves and influences, such as effects of pressure gradients, heat transfer etc., and the effects of three-dimensionality of the flow.

References

1. Betchov, R., & Criminale, W. O. (1967). *It Stability of Parallel Flows*. New York: Academic Press.
2. Chandrasekhar, S. (1981). *Hydrodynamic and Hydromagnetic Stability*. New York: Dover. ISBN 0-486-64071-X.
3. Charru, F. (2011). *Hydrodynamic Instabilities*. Cambridge: Cambridge University Press. ISBN 1139500546.
4. Drazin, P. G. (2002). *Introduction to Hydrodynamic Stability*. Cambridge: Cambridge University Press. ISBN 0-521-00965-0.
5. Drazin, P. G., & Howard, L. N. (1966). Hydrodynamic stability of parallel flow of inviscid fluid. *Adv. Appl. Mech.*, *9*, 1–89.
6. Drazin, P. G., & Reid, W. H. (1981). *Hydrodynamic Stability*. Cambridge: Cambridge University Press. ISBN 0-521-28980-7.
7. Gersting, J. M., & Jankowski, D. F. (1972). Numerical methods for Orr-Sommerfeld problems. *Int. J. Numer. Methods Eng.*, *4*, 195–206.
8. Godreche, C., & Manneville, P. (1998). *Hydrodynamics and Nonlinear Instabilities*. Cambridge: Cambridge University Press. ISBN 0521455030.
9. Heisenberg, W. (1924). Über stabilität und turbulenz von flüssigkeitsströmen. *Annu. d. Physik.*, *74*, 577–627.
10. Joseph, D.D.: Stability of Fluid Motions I. In: Tracts in Natural Philosophy, vol. 27, Springer, Berlin (1976). ISBN 3-540-07514-3
11. Joseph, D.D. (1976), Joseph, D.D.: Stability of Fluid Motions II. In: Tracts in Natural Philosophy, vol. 28, Springer, Berlin (1976). ISBN 3-540-07516-X
12. Lin, C.C.: The Theory of Hydrodynamic Stability (corrected ed.). Cambridge University Press, Cambridge (1966). OCLC 952854
13. Lorentz, H.A.: Abhandlung über theoretische Physik I, 43.71. Leipzig (1907). Revision of a paper published by *Zittingsverlag, Akad. V. Wet. Amsterdam*, *6*, 28 (1897)
14. Orr, W.M.F.: The stability or instability of steady motions of a perfect liquid and of a viscous liquid. Part I: A perfect liquid, Part II: A viscous liquid. *Proc. Roy. Irish. Acad.* *27*, 9–38 and 69–138 (1907)
15. Orr, W. M. F. (1907). The stability or instability of steady motions of a liquid. *Part I. Proc. Royal Irish Academy*, *A27*, 9–68.
16. Orr, W. M. F. (1907). The stability or instability of steady motions of a liquid. *Part II Proc. Royal Irish Academy*, *A27*, 69–138.
17. Rayleigh, L.: On the stability or instability of certain fluid motions. *Proc. London Math. Soc.* *11*, 57 (1880) and *19*, 67 (1887)
18. Schlichting, H., Gersten, K.: *Boundary Layer Theory*. 8th revised and enlarged edition. pp. 799. Springer, Berlin (2000)
19. Sommerfeld, A.: Ein Beitrag zur hydrodynamischen Erklärung der turbulenten Flüssigkeitsbewegungen. In: Proceedings of the 4th International Congress Mathematics III, pp. 116–124. Roma (1908)
20. Squire, H. B. (1933). On the stability of three-dimensional distribution of viscous fluid between parallel walls. *Proc. Roy. Soc. London*, *A142*, 621–628.
21. Sritharan, S.S.: *Invariant Manifold Theory for Hydrodynamic Transition*. Pitman Research Notes in Mathematics Series 241, Wiley, New York (1990). ISBN 0-582-06781-2[1]
22. Swinney, H.L., Gollub, J.P., (eds.): *Hydrodynamic Instabilities and the Transition to Turbulence* (2nd ed.). Springer, Berlin (1985). ISBN 978-3-540-13319-3
23. Tietjens, O.: Beiträge zur Entstehung der Turbulenz. Dissertation Universität Göttingen (1922) see also ZAMM, Zeitschr. Angew. Math. Mech. *5*, 200–217 (1925)
24. Tollmien, W.: Über die Entstehung der Turbulenzklasse. Mitteilung, Nachr. Ges. Wiss. Göttingen , Math. Phys. Klasse Engl. Translation in NACA-TM-609 (1931)

25. Tollmien, W.: Ein allgemeines Kriterium der Instabilität der laminaren Geschwindigkeitsverteilungen. *Nachr. Ges. Wiss. Göttingen, math. Phys. Klasse, Fachgruppe I*, **1**, 79–114 (1935). Engl. Translation in NACA-TM-792 (1936)
26. Tollmien, W.: Asymptotische Integration der Störungsdifferentialgleichungen ebener laminarer Strömungen bei hohen Reynoldsschen Zahlen. *ZAMM, Z. angew. Math. Mech.* **25**, 33–45 and **27**, 70–83 (1947)

Chapter 15

Turbulent Modeling

Abstract In this chapter a detailed introduction to the modeling of turbulence is given. Filter operations are introduced to separate the physical balance laws into evolution equations for the averaged fields on the one hand, and into fluctuating or pulsating fields on the other hand. The mathematical properties of the filter define the structure of the averaged equations. REYNOLDS introduced the steady statistical filter, leading to the REYNOLDS averaged NAVIER–STOKES equations. This procedure generates averages of products of fluctuating quantities, for which closure relations must be formulated. Depending upon the complexity of these closure relations, so-called zeroth, first and higher order turbulence models are obtained: simple algebraic gradient-type relations for the flux terms, one or two equation models, e.g., $k - \varepsilon$, $k - \omega$ models, in which evolution equations for the averaged correlation products for k and ε are formulated, etc. This is done for density preserving fluids as well as so-called BOUSSINESQ and convection fluids on a rotating frame (Earth), which are important models to describe atmospheric and oceanic flows.

Keywords Statistical filter operator · REYNOLDS averaged NAVIER–STOKES equations · Closure relations for fluctuating correlation terms · $k - \varepsilon$, $k - \omega$ models · BOUSSINESQ, convection fluids

List of Symbols

Roman Symbols

c_α	Species mass ratio of constituent α
$c_D^{b,s}$	Basal/free surface drag coefficient
D	Strain rate tensor (deviator), stretching tensor
$D^{(\theta)}$	Total (laminar + turbulent) thermal diffusivity
	$D^{(\theta)} = \left(\chi^{(\theta)} + \frac{\nu_t}{\sigma_\theta} \right)$
$D^{(c)}$	Total species diffusivity $D^{(c)} = \left(\chi^{(c)} + \frac{\nu_t}{\sigma_c} \right)$
$D^{(k)}$	Total diffusivity of the turbulent kinetic energy
	$D^{(k)} = \left(\nu + \frac{\nu_t}{\sigma_k} \right)$

$D^{(\varepsilon)}$	Total diffusivity of the turbulent dissipation rate $D^\varepsilon = \left(\nu + \frac{\nu_t}{\sigma_\varepsilon} \right)$
e	Specific turbulent enstrophy $e = \frac{1}{2}(\boldsymbol{\omega} \cdot \boldsymbol{\omega})$
f'	Fluctuation of f in statistical averaging (RANS)
f''	Fluctuation of f in a FAVRE averaging
\mathbf{g}	Gravity vector
\underline{g}	Density of a physical quantity
$\underline{\mathbf{g}}' \otimes \mathbf{v}'$	Correlation flux of the average of \mathbf{g}' with \mathbf{v}'
$\dot{\mathbf{j}}_{c_\alpha}$	Mass flux of species α
\mathbf{j}_t	Turbulent species mass flux $\mathbf{j}_t := \overline{\rho \mathbf{c}' \mathbf{v}'}$
k	Turbulent kinetic energy per unit mass (see (15.29)) $k = \frac{1}{2} \overline{\mathbf{v}' \cdot \mathbf{v}'}$
ℓ	Turbulent mixing length
$\mathcal{M}_\perp^{\text{ground}}$	Flow rate of fluid mass into the ground
p, p^{atm}	Pressure, atmospheric pressure
\mathbf{q}	Heat flux vector
\mathbf{q}_t	Turbulent heat flux vector $\mathbf{q}_t = \rho u' \mathbf{v}'$
$Q_{\text{ir}}^{\text{a}}, Q_{\text{ir}}^{\text{w}}$	Black body radiation of the atmosphere and water at the free surface
Q_ℓ, Q_s	Latent/sensible heat fluxes between water and air
\mathbf{R}	Turbulent REYNOLDS stress tensor $\mathbf{R} := -\rho \overline{(\mathbf{v}' \otimes \mathbf{v}')} $
r	Specific energy supply, specific radiation
\mathbf{t}^R	Frictional (viscous) stress
u, u'	Specific internal energy, its fluctuation
V	Typical velocity
\mathbf{v}	Velocity vector
$\langle \mathbf{v} \rangle$	Average velocity over a sample, over time or over space
\mathbf{v}'	Fluctuation (pulsation) of \mathbf{v}
\mathbf{W}_\parallel	Wind velocity parallel to the free surface
z^g	Supply density of g
z_{c_α}	Mass supply density of species α

Greek Symbols

ν, ν_t	Kinematic viscosity, turbulent viscosity
ρ	Mass density
ε	Turbulent dissipation rate (see (15.30))
θ	Temperature (absolute or Celsius)
ϕ^g	Flux of g
ϕ	Total turbulent dissipation rate
Φ^k, Φ^ε	Flux of turbulent kinetic energy—of turbulent dissipation rate
κ	Curvature of ρ as a function of θ , $\kappa = \left. \frac{d^2 \rho}{d\theta^2} \right _{\bar{\theta}}$
$\chi_t^{(\theta)}, \chi_t^{(c)}$	Turbulent eddy diffusivities of heat and mass ratio
σ_θ, σ_c	PRANDTL/SCHMIDT number
$\sigma_k, \sigma_\varepsilon$	Prandtl numbers for k and ε

π^k, π^ε	Production rate densities of the turbulent kinetic energy —of the turbulent dissipation rate
π^g	Production density of g
$\boldsymbol{\omega} = \text{curl } \mathbf{v}$	Vorticity vector
$\boldsymbol{\omega}'$	Fluctuation of $\boldsymbol{\omega}$
$\boldsymbol{\Omega}$	Angular velocity of the non-inertial frame (angular velocity of the Earth)

Miscellaneous Symbols

$\langle \cdot \rangle_T$	Time average of (\cdot) over a ‘time’ interval T
$\langle \cdot \rangle_R$	Space average of (\cdot) over a ‘radius’ R
$\langle \cdot \rangle_S$	Statistical average over probability space
$\{f\}$	FAVRE average $\{f\} = \langle \rho f \rangle / \langle \rho \rangle$
$\langle \cdot \rangle$	REYNOLDS average of (\cdot)
$II_{\overline{D}}$	Second invariant of \overline{D}

15.1 A Primer on Turbulent Motions

In daily life turbulent motions are ubiquitous fluid dynamical elements which can be observed in various forms e.g. in wind gusts and surface water flows in rivers, lakes and the ocean. ‘Scientists have investigated turbulent phenomena for hundreds of years. For instance, LEONARDO DA VINCI (1452–1519) (see **Fig. 15.1**) studied turbulent flows and produced several hand-drawings, showing eddies of various sizes [and how they interact]. Based on such observations today we have knowledge of energy cascade models describing the turbulent kinetic energy of flow as a function of eddy size [...], [4].

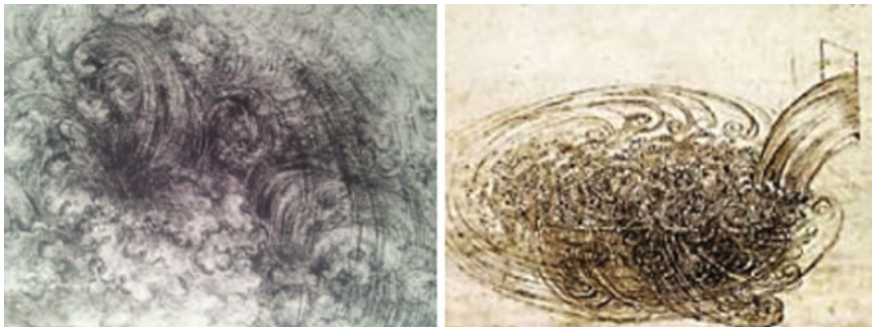


Fig. 15.1 Drawings of turbulent eddies in water motions by LEONARDO DA VINCI. *The right panel shows a free water jet issuing from a square hole into a pool; it represents, perhaps the world’s first use of visualization as a scientific tool to study a turbulent flow. LEONARDO wrote (translation by UGO PIOMELLI, University of Maryland) ‘Observe the motion of the surface of the water, which resembles that of hair, which has two motions, of which one is caused by the weight of the hair, the other by the direction of the curls, thus the water has eddying motion, one part of which is due to the principal current, the other to the random and reverse motion. According to L. LUMLEY, Cornell University, LEONARDO may have prefigured the now famous REYNOLDS decomposition nearly 400 years prior to OSBORNE REYNOLDS’ own flow visualization and analysis’. Figure and text courtesy [5]*



Fig. 15.2 OSBORNE REYNOLDS in 1903 (23. Aug. 1842–21. Feb. 1912)

OSBORNE REYNOLDS was a mathematician with degree from Cambridge University (1867) and prominent innovator in the understanding of fluid dynamics. He was appointed professor of engineering at Owens College in Manchester, the first professor in UK university history to hold the title of ‘Professor of Engineering’. REYNOLDS most famously studied the conditions in which the flow of fluid in pipes transitioned from laminar flow to turbulent flow. His studies of condensation and heat transfer between solids and fluids brought radical revision in boiler and condenser technology. He also proposed a mathematical procedure which is now known as REYNOLDS-averaging of turbulent flows. This led to the ‘bulk’ description of turbulent flows as expressed in the REYNOLDS-Averaged NAVIER–STOKES equations. His final theoretical model, published in the mid 1890s is still the standard mathematical framework used today. Another subject which REYNOLDS studied in the 1880s was the mechanical behavior of granular materials.

The text is based on www.wikipedia.org

The first basic thoughts and experiments on turbulence are likely due to JOSEPH VALENTIN BOUSSINESQ (1872) [3] and OSBORNE REYNOLDS (1883)¹. [14], who both studied the flow of a fluid through pipes with circular cross sections. BOUSSINESQ proposed that the turbulent stress can be parameterized just as its laminar counterpart as the product of the mean turbulent strain rate multiplied with a scalar quantity of the dimension of a viscosity [$\text{m}^2 \text{s}^{-1}$], called the turbulent viscosity. REYNOLDS recognized (by adding dye through a pipette to the fluid) that basically two flow

¹For a biographical sketch of REYNOLDS see **Fig. 15.2**

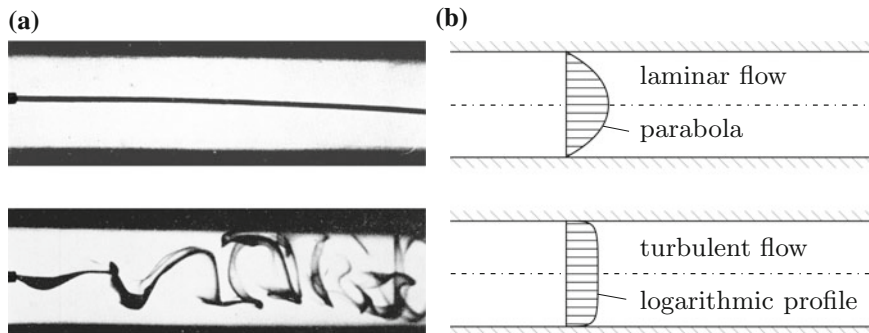


Fig. 15.3 Laminar and turbulent flow in a cylindrical pipe. **a** To visualize the flow dye is added to the water through a capillary pipette. The nozzle of this pipette is visible at the left end of the photographs on the left (courtesy Royal Society London [14]). **b** Mean velocity profiles in a circular pipe under steady laminar and turbulent conditions, respectively, from [7]

regimes exist: In one case, the so-called *laminar* flow, the dye forms coherent thin filaments; in the second case, known as *turbulent* flow, the dye filament is torn very quickly after it left the nozzle of the pipette and is spread over the entire cross section of the pipe, **Fig. 15.3**. The transition from laminar to turbulent flow is a sudden event—a fluid flow instability. The critical quantity that characterizes the change is the REYNOLDS number

$$\mathbb{R} = \frac{VD}{\nu}, \quad \text{if } \mathbb{R} > 2000, \text{ then the flow is turbulent,}$$

where V , D , ν are the mean axial velocity, the inner pipe diameter and the kinematic viscosity of the fluid. The velocity profiles, averaged over a time interval (which eliminates fluctuations) look as shown in **Fig. 15.3b**. The transition from the laminar to the turbulent flow regime takes place for $500 < \mathbb{R} < 2000$. Exactly at which REYNOLDS number this transition takes place depends largely upon the set-up and performance of the experiment. For $\mathbb{R} > 2000$ the flow is essentially turbulent, unless very careful precursory measures are taken.

15.1.1 Averages and Fluctuations

In **Fig. 15.3b** the velocity profile for the turbulent flow is drawn for the *mean* axial velocity; the true velocity is fraught with strong fluctuations. For steady driving and adequately constructed mean values of the velocity, the mean profiles are also steady and have homogeneous random appearances. Such fluctuations are seen for turbulent flows in time series of the velocity at a fixed point, **Fig. 15.4** as well as spatial variations at fixed time. The time and space scales of these pulsations are for most

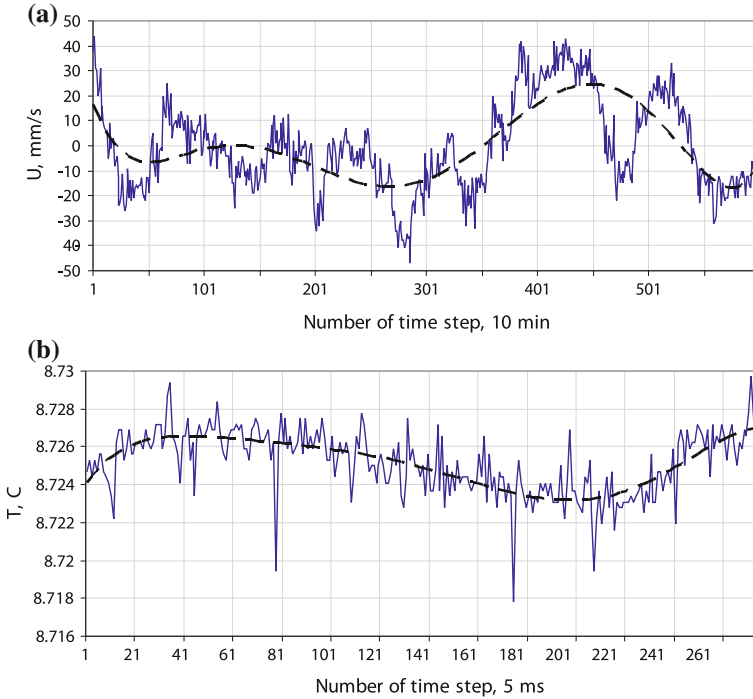


Fig. 15.4 Typical examples of measured signals. **a** Time variation of the northward component of the current speed during the period of 100h, measured by ADCP in the middle of Lake Constance at a depth of 2m on 24–28 October 2001. Courtesy ANDREAS LORKE, data delivered to [2]. **b** Water temperature in a laboratory flume, measured with the time step of 5ms

applications not relevant; rather, one is interested in some average behavior, for which space and time scales extend over many typical ‘periods’ of the turbulent fluctuations. This suggests to additively decompose the velocity into two contributions, the mean value $\langle \mathbf{v} \rangle$ and the fluctuations \mathbf{v}' ,

$$\mathbf{v} = \langle \mathbf{v} \rangle + \mathbf{v}'. \quad (15.1)$$

Of course, this composition is not unique and the split between $\langle \mathbf{v} \rangle$ and \mathbf{v}' depends on how $\langle \mathbf{v} \rangle$ is defined. For a temporal average

$$\langle \mathbf{v} \rangle_T := \frac{1}{T} \int_{t-T/2}^{t+T/2} \mathbf{v}(\mathbf{x}, \tau) d\tau, \quad (15.2)$$

this mean value depends on the large-scale interval of averaging, T , and, consequently, so does also the ‘subscale’ fluctuation velocity, \mathbf{v}' . In computing such an

average from a given time series, it must be observed that the interval T , over which the averaging operation is performed, is not too small, so that the turbulent pulsations are indeed ‘eliminated’. Conversely, this interval should neither be too large, because if so, important non-turbulent time dependent phenomena may thereby be lost. It transpires that the decomposition of \mathbf{v} into $\langle \mathbf{v} \rangle$ and \mathbf{v}' depends on the selection of T , and via this choice it defines, which scales of the time variations belong to the mean processes and which are part of the fluctuations. Moreover, this decomposition will also depend on the mathematical properties of the averaging operator, which is often also called *filter*.

15.1.2 Filters

Above, in relation (15.2) the temporal filter was introduced. For the *spatial filter*, one integrates the field in question over a spherical (or nearly spherical) volume $V(\mathbf{x}, r)$ with center at \mathbf{x} and radius r , and defines the mean value as

$$\langle \mathbf{v} \rangle_R := \frac{1}{V} \int_{V(\mathbf{x}, r)} \mathbf{v}(\boldsymbol{\xi}, t) d\boldsymbol{\xi}. \quad (15.3)$$

The volume $V(\mathbf{x}, r)$ under consideration is a compact set, defining the region of influence as nearly spherical, which is sufficiently compact that a typical parameter can be defined for a sphere, which may replace the actual volume. For (15.3) variations of \mathbf{v} with wave length smaller than $\mathcal{O}(V^{1/3})$ are filtered away. The quantity $\langle \mathbf{v} \rangle_R$ is a function of position \mathbf{x} and time t , and may also depend on $V(\mathbf{x}, r)$. It is obvious that (15.2) and (15.3) define different averages, $\langle \mathbf{v} \rangle_T$ and $\langle \mathbf{v} \rangle_R$, and one may easily see that in general $\langle \langle \cdot \rangle_{T,R} \rangle_{T,R} \neq \langle \cdot \rangle_{T,R}$.

The filter that was used first in describing the turbulent fluid behavior is the *statistical filter*, used by OSBORNE REYNOLDS. It is based on the assumption that, on a local scale, the fluctuations have the properties of a *stationary random process*.

Let $u(\mathbf{x}, t)$ denote the value at (\mathbf{x}, t) of the scalar function u , for example the first component of the velocity field. The value $u(\mathbf{x}, t)$ can be any real number. If $\rho(\mathbf{x}, t, \hat{u})$ denotes the density of the probability that $u(\mathbf{x}, t)$ takes the value \hat{u} at the point (\mathbf{x}, t) , where \hat{u} is any real number, one has

$$\int_{-\infty}^{\infty} \rho(\mathbf{x}, t, \hat{u}) d\hat{u} = 1. \quad (15.4)$$

The expectation value for the value of the function u at (\mathbf{x}, t) is

$$\langle u \rangle_S(\mathbf{x}, t) = \int_{-\infty}^{\infty} \hat{u} \rho(\mathbf{x}, t, \hat{u}) d\hat{u}, \quad (15.5)$$

in which the subscript is an identifier of the statistical averaging. In a certain sense, the expectation value $\langle u \rangle_S(\mathbf{x}, t)(\mathbf{x}, t)$ is the most probable value of u at (\mathbf{x}, t) .

The statistical filter has been the only filter used in early turbulence research; it is still important today and has the following properties, which the reader may easily prove with the use of (15.5):

1. *Linearity*: Let u, v be two quantities of a turbulent field and a a real number. Then,

$$\langle u + aw \rangle_S = \langle u \rangle_S + a \langle w \rangle_S. \quad (15.6)$$

2. *Commutability with differentiation*

$$\langle \partial u \rangle_S = \partial \langle u \rangle_S, \quad \text{where } \partial \in \left\{ \frac{\partial}{\partial x}, \frac{\partial}{\partial y}, \frac{\partial}{\partial z}, \frac{\partial}{\partial t} \right\}. \quad (15.7)$$

3. *Invariance under multifold averaging*

$$\langle \langle u \rangle_S \rangle_S = \langle u \rangle_S. \quad (15.8)$$

Of course, this condition implies

$$\langle \langle \dots \langle u \rangle_S \dots \rangle_S \rangle_S = \langle u \rangle_S. \quad (15.9)$$

Of the three filters introduced above, only the statistical filter satisfies all these properties. In the ensuing analysis we shall assume that the chosen filter satisfies all three conditions. This hypothesis is called the *ergodic hypothesis*. The reader may also verify the following computational rules

$$\begin{aligned} \langle u' \rangle_S &= \langle u \rangle'_S = 0, \\ \langle \langle u \rangle_S v \rangle_S &= \langle u \rangle_S \langle v \rangle_S, \\ \langle \langle u \rangle v' \rangle_S &= 0, \\ \langle u v \rangle_S &= \langle u \rangle_S \langle v \rangle_S + \langle u' v' \rangle_S. \end{aligned} \quad (15.10)$$

In what follows the subscript S in $\langle \cdot \rangle$ will henceforth be dropped. In modern turbulence theory models are being developed, which request the invariance of the multifold filtering as well as others which negate it. The **Reynolds-Averaged-Navier-Stokes (RANS)** models satisfy the conditions of the statistical filter. Models, for which $\langle u' \rangle \neq 0$, equally do not satisfy (15.9). These models are summarized under the heading **Large Eddy Simulation (LES)** models.

15.1.3 Reynolds Versus Favre Averages

The ultimate purpose of the above calculations is to employ them in the derivation of averaged balance laws of mass, momentum, energy and further averaged statements

if necessary. In this regard the conservation law of mass points at a subtlety, which we shall now explain. Therefore, consider the conservation laws of mass,

$$\frac{\partial \rho}{\partial t} + \operatorname{div}(\rho \mathbf{v}) = 0, \quad (15.11)$$

which, when RANS-averaged, takes the form

$$\left\langle \frac{\partial \rho}{\partial t} \right\rangle + \langle \operatorname{div}(\rho \mathbf{v}) \rangle = 0. \quad (15.12)$$

Employing the computational rules (15.10), transforms (15.12) into

$$\frac{\partial \langle \rho \rangle}{\partial t} + \operatorname{div}(\langle \rho \rangle \langle \mathbf{v} \rangle) + \operatorname{div}(\langle \rho' \mathbf{v}' \rangle) = 0. \quad (15.13)$$

The third term on the left-hand side is the divergence of the correlation mass flux $\langle \rho' \mathbf{v}' \rangle$ which only vanishes for a density preserving fluid ($\rho' = 0$). For a gas or a compressible fluid this term does not vanish, but we would wish it to be zero in order to preserve the conservation law for mass under turbulent conditions (for the mean quantities). This can be reached as follows:

Definition 15.1 The density weighted average $\{f\}$ of a quantity f is defined as

$$\{f\} := \frac{\langle \rho f \rangle}{\langle \rho \rangle}, \quad f = \{f\} + f''. \quad (15.14)$$

$\{f\}$ is the so-called FAVRE average of f and $f'' = f - \{f\}$ is its fluctuation. ■

We leave the following statements to prove to the reader:

$$\{f\} = \langle f \rangle + \frac{\langle \rho' f' \rangle}{\langle \rho \rangle}, \quad f'' = f' - \frac{\langle \rho' f' \rangle}{\langle \rho \rangle}. \quad (15.15)$$

For a density preserving material, $\rho' = 0$; so, (15.15) implies in this case that

$$\{f\} = \langle f \rangle, \quad f'' = f' \quad \text{for a density preserving material.} \quad (15.16)$$

This implies that FAVRE averages must only be performed for compressible materials for which the balance law of mass (15.13) reduces to

$$\frac{\partial \langle \rho \rangle}{\partial t} + \operatorname{div}(\langle \rho \rangle \langle \mathbf{v} \rangle) = 0, \quad (15.17)$$

in which (15.15)₁ has been used.

15.2 Balance Equations for the Averaged Fields

The purpose in studying turbulent motions in fluid mechanics is to determine the distribution and evolution of the field variables such as velocity, pressure, temperature and tracer mass concentration. Experience shows that in many circumstances these fields often fluctuate both in time and space with varied periods and wave lengths. In engineering and geophysical applications not all those scales can or should be resolved. Field equations of averages of the true fields are sought which, in turbulent flows, are fluctuating. Turbulent motion manifests itself often as a cascade of vortical structures, of which the sizes are restricted by the extent of the domains, where the motions take place. In a particular bounded domain the largest gyre that can occur is of the size of the largest extent of the domain—in the ocean or a lake given by the coasts or shores. By fluid flow instabilities these gyres break down into smaller vortices of cascading dimensions down to very small eddies, whose remaining energy will be absorbed into heat. In geophysical applications—oceanography and meteorology—the sizes of these vortical structures are from approximately 1 mm to several kilometers (in the ocean up to thousands of kilometers).

Complete resolution of all vortical structures is computationally impossible. In a theoretical description the motion can only be resolved to a certain length and period, usually twice the grid size by which the governing equations or boundary geometry is discretized. In fluid dynamics (of water and air) it is the conviction of most scientists that on the smallest time scales the NAVIER–STOKES equations are the adequate description of the fluid motion by which the turbulent eddies through all sizes can be well reproduced. This has been demonstrated by comparison of results obtained by **Direct Numerical Simulations (DNS)** with measured velocity fields in a wealth of examples since the late 80s of the last century. The resolution of all time and space scales in a numerical computation is impossible, however. As one alternative one, therefore, averages the NAVIER–STOKES equations by selecting the smallest space and time scales that one can afford to resolve and thereby filters those pulsations of the processes out, which are of ‘subscale structure’. However, the loss of information is partly counteracted by parameterizing the correlation terms in a way similar to constitutive closure relations, yet slightly more flexible.

We shall demonstrate this procedure for a BOUSSINESQ fluid and/or a free convection fluid.² Let us start with a general balance statement

$$\frac{d}{dt} \int_{\omega} g(\mathbf{x}, t) dv = \int_{\partial\omega} \phi^g(\mathbf{x}, t) da + \int_{\omega} (\pi^g + z^g) dv, \quad (15.18)$$

²A BOUSSINESQ fluid is a fluid, which is kinematically volume preserving ($\text{div } \mathbf{v} = 0$) with constant density except in the gravity term where ρ may vary with position and time. In a *free convection fluid* the density function in the ‘acceleration terms’ ($\rho_0 d\mathbf{v}/dt$, $\rho_0 du/dt$, $\rho_0 dc^\alpha/dt$) varies with z ($\rho = \rho_0(z) + \rho'(x, y, z, t)$), where in applications z is the vertical direction of the gravity and $\rho_0(z)$ is prescribed. This approximation is popular in geophysical flows.

in which g is a specific physical quantity (mass density, momentum density, ...), $\phi^g(\mathbf{x}, t)$ is its flux into the body region ω through its boundary $\partial\omega$, and $\pi^g(\mathbf{x}, t)$ and $z^g(\mathbf{x}, t)$ are the specific production and specific supply rate densities of g , respectively.

For differentiable fields the global balance law (15.18) transforms to the local law

$$\begin{aligned} \frac{\partial g}{\partial t} + \operatorname{div} (g\mathbf{v} - \phi^g) - \pi^g - z^g &= 0, & (g \text{ is a scalar field}), & \quad (15.19) \\ \frac{\partial \mathbf{g}}{\partial t} + \operatorname{div} (\mathbf{g} \otimes \mathbf{v} - \phi^g) - \boldsymbol{\pi}^g - \mathbf{z}^g &= 0, & (\mathbf{g} \text{ is a vector field}). & \end{aligned}$$

The transformation from (15.18) to (15.19) is standard if the fields arising in (15.18) are differentiable. This is explicitly demonstrated in Chap. 3.

Subjecting these equations to a statistical filter with the properties (15.6)–(15.10) the following REYNOLDS averaged balance laws are obtained:

$$\begin{aligned} \frac{\partial \bar{g}}{\partial t} + \operatorname{div} (\bar{g}\bar{\mathbf{v}} - \bar{\phi}^g) - \bar{\pi}^g - \bar{z}^g &= -\operatorname{div} (\overline{g'\mathbf{v}'}) & (g \text{ is a scalar field}), \\ \frac{\partial \bar{\mathbf{g}}}{\partial t} + \operatorname{div} (\bar{\mathbf{g}} \otimes \bar{\mathbf{v}} - \bar{\phi}^g) - \boldsymbol{\pi}^{*g} - \bar{\mathbf{z}}^g &= -\operatorname{div} (\overline{\mathbf{g}' \otimes \mathbf{v}'}) & (\mathbf{g} \text{ is a vector field}). \end{aligned} \quad (15.20)$$

Here and henceforth notation has been simplified by denoting the averaging operation by an overbar. The various quantities arising in (15.19) are defined in **Table 15.1** for the conservation statements of mass, linear momentum and the balance laws of internal energy and an additional scalar quantity c_α . In (15.20) the production $\boldsymbol{\pi}^{*g}$ may consist of an averaged quantity plus a correlation term as is e.g. the case for the production density of internal energy.

If one substitutes the entries of Table 15.1 into the balances (15.20) describing the turbulent average behavior the following equations are obtained:

- For the conservation of mass:

$$\frac{\partial \bar{\rho}}{\partial t} + \operatorname{div} (\bar{\rho}\bar{\mathbf{v}}) = -\operatorname{div} (\overline{\rho'\mathbf{v}'}),$$

Table 15.1 Density of a physical quantity g , its flux ϕ^g , supply z^g and production π^g densities for mass, momentum, internal energy and a scalar field

Balance law	g	ϕ^g	z^g	π^g
Mass	ρ	0	0	0
Momentum	$\rho\mathbf{v}$	$\mathbf{t}^R - p\mathbf{1}$	$\rho\mathbf{g}$	0
Internal energy	ρu	$-\mathbf{q}$	ρr	$\operatorname{tr}(\mathbf{t}^R \mathbf{D})$
Scalar field	ρc_α	\dot{J}_{c_α}	z_{c_α}	π_{c_α}

\mathbf{t}^R = stress deviator, \mathbf{D} = strain rate tensor, ρ = density, p = pressure, \mathbf{v} = velocity, u = internal energy, \mathbf{q} = heat flux vector, r = energy supply rate density, \mathbf{g} = gravity constant

which for constant ρ reduces to

$$\operatorname{div} \bar{\mathbf{v}} = 0. \quad (15.21)$$

The specification ‘ $\rho = \text{const.}$ ’ means that the variability of the density is ignored kinematically, as this is e.g. done for a BOUSSINESQ fluid or a free convection fluid.

- For the conservation of linear momentum:

$$\left. \begin{aligned} \frac{\partial \bar{\mathbf{v}}}{\partial t} + \operatorname{div} (\bar{\mathbf{v}} \otimes \bar{\mathbf{v}}) \\ \frac{d\bar{\mathbf{v}}}{dt} \equiv \frac{\partial \bar{\mathbf{v}}}{\partial t} + (\operatorname{grad} \bar{\mathbf{v}}) \bar{\mathbf{v}} \end{aligned} \right\} + \frac{1}{\rho} \operatorname{grad} \bar{p} - \frac{1}{\rho} \operatorname{div} \bar{\mathbf{t}}^R - \mathbf{g} = -\operatorname{div} (\overline{\mathbf{v}' \otimes \mathbf{v}'}). \quad (15.22)$$

- For the balance law of internal energy:

$$\left. \begin{aligned} \frac{\partial \bar{u}}{\partial t} + \operatorname{div} (\bar{u} \bar{\mathbf{v}}) \\ \frac{d\bar{u}}{dt} \end{aligned} \right\} - \frac{1}{\rho} \operatorname{tr} (\bar{\mathbf{t}}^R \bar{\mathbf{D}}) + \frac{1}{\rho} \operatorname{grad} \bar{q} \\ = -\operatorname{div} (\overline{u' \mathbf{v}'}) + \frac{1}{\rho} \operatorname{tr} (\bar{\mathbf{t}}^R \bar{\mathbf{D}}) + r. \quad (15.23)$$

- For the balance law of a scalar field c_α , ($\alpha = 1, 2, 3, \dots, \nu$):

$$\left. \begin{aligned} \rho \left(\frac{\partial \bar{c}_\alpha}{\partial t} + \operatorname{div} (\bar{c}_\alpha \bar{\mathbf{v}}) \right) \\ \rho \left(\frac{\partial \bar{c}_\alpha}{\partial t} + \operatorname{grad} (\bar{c}_\alpha \bar{\mathbf{v}}) \right) \end{aligned} \right\} + \operatorname{div} (\bar{\mathbf{j}}_{c_\alpha}) - \bar{\pi}_{c_\alpha} - \bar{z}_{c_\alpha} = -\rho \operatorname{div} (\overline{c'_\alpha \mathbf{v}'_\alpha}), \quad (\alpha = 1, \dots, \nu). \quad (15.24)$$

In what follows the counting index α will be dropped as only one typical scalar field \bar{c} will be stated.

At this point, the following remarks are helpful:

1. In Eqs. (15.21)–(15.24) the density, wherever it arises, is to be understood either as a constant ($\rho = \rho^*$ for a BOUSSINESQ fluid) or as a time independent function of z ($\rho = \rho_0(z)$ for a free convection fluid). In both cases its fluctuation does not arise or is ignored.
2. Equations (15.21)–(15.24) are $5 + \nu$ equations for the $5 + \nu$ variables $\bar{\mathbf{v}}, \bar{u}, \bar{p}$ and \bar{c}_α ($\alpha = 1, \dots, \nu$). All the remaining quantities must be described by phenomenological relations. For a NAVIER–STOKES fluid or a more complex nonlinear viscous fluid such constitutive relations must be postulated for $\bar{\mathbf{t}}^R, \bar{\mathbf{q}}$ (and \bar{u}). In addition, for the turbulent correlation terms

$$\overline{\mathbf{v}' \otimes \mathbf{v}'}, \quad \overline{u' \mathbf{v}'}, \quad \operatorname{tr} (\bar{\mathbf{t}}^R \bar{\mathbf{D}}'), \quad \overline{c'_\alpha \mathbf{v}'_\alpha}, \quad (15.25)$$

turbulent closure relations are to be formulated.

15.3 Turbulent Closure Relations

Definitions:

- The quantity

$$\mathbf{R} := -\rho \overline{(\mathbf{v}' \otimes \mathbf{v}')} \quad (15.26)$$

is called the REYNOLDS *stress tensor*. It is symmetric and has first been introduced by OSBORNE REYNOLDS in 1894 [15].

- The flux vector of internal energy

$$\mathbf{q}_t := \rho \overline{u' \mathbf{v}'} = \rho c_v \overline{\theta' \mathbf{v}'} \quad (15.27)$$

is called the *turbulent heat flux vector*, and θ' is the temperature fluctuation.

- The flux vector

$$\mathbf{j}_t := \rho \overline{\mathbf{v}' c'} \quad (15.28)$$

is called the *turbulent species mass flux* (if c is a mass ratio).

- The *turbulent kinetic energy (density)* is defined as

$$k := \frac{1}{2} \overline{\mathbf{v}' \cdot \mathbf{v}'}. \quad (15.29)$$

- The *turbulent dissipation rate density* is defined by

$$\varepsilon := \frac{1}{\rho} \text{tr} \left(\overline{\mathbf{t}^{R'} \mathbf{D}'} \right) \quad \left(\stackrel{(2)}{=} 4\nu \overline{II_{D'}} \right), \quad (15.30)$$

in which $II_{D'} = \frac{1}{2} \text{tr} (\mathbf{D}' \mathbf{D}')$ is the second invariant of the strain rate deviator \mathbf{D}' and the step $\stackrel{(2)}{=}$ holds for a NEWTONian fluid only.

15.3.1 Reynolds Stress Hypothesis and Turbulent Dissipation Rate

The definition of the REYNOLDS stress tensor implies that $\text{tr} \mathbf{R} = -\rho \text{tr} \overline{(\mathbf{v}' \otimes \mathbf{v}')} = -\rho \overline{\mathbf{v}' \cdot \mathbf{v}'} = -2\rho k$, in which k is the turbulent kinetic energy, defined in (15.29). Thus, we may alternatively write instead of (15.26)

$$\mathbf{R} = -\rho \left\{ \underbrace{\overline{\mathbf{v}' \otimes \mathbf{v}'}}_{\mathbf{R}_D = \text{deviator}} - \frac{2}{3} k \mathbf{1} \right\} - \frac{2}{3} \rho k \mathbf{1}. \quad (15.31)$$

Thus, for a BOUSSINESQ fluid or a free convection fluid, since for these the strain rate tensor is deviatoric, one may request a turbulent closure relation of the form $\mathbf{R}_D = \mathbf{R}_D(\overline{\mathbf{D}})$, implying that

$$\mathbf{R} = -\frac{2}{3}\rho k\mathbf{1} + \mathbf{R}_D(\overline{\mathbf{D}}) = \begin{cases} -\frac{2}{3}\rho k\mathbf{1} + 2\rho\nu_t\overline{\mathbf{D}}, & \text{NEWTONIAN FLUID} \\ -\frac{2}{3}\rho k\mathbf{1} + \rho F(II_{\overline{\mathbf{D}}})\overline{\mathbf{D}}, & \text{nonlinear viscous fluid.} \end{cases} \quad (15.32)$$

Here, ν_t is a turbulent viscosity in analogy to the laminar kinematic viscosity as proposed in a simple context but corresponding to (15.32), by JOSEPH BOUSSINESQ (1872) [3]. $F(II_{\overline{\mathbf{D}}})$ is dimensionally a kinematic viscosity [$\text{m}^2 \text{s}^{-1}$] and generally monotonic function of $II_{\overline{\mathbf{D}}}$.

In anticipation of the analysis of mixing length parameterizations, we wish to emphasize here that the turbulent closures (15.32) for the REYNOLDS stress tensor are of gradient type ($\overline{\mathbf{D}}$ is the symmetrized velocity gradient) just as is the constitutive assumption for the material behavior of the viscous stress under laminar flows. We have, however, not yet said anything about how the turbulent viscosity in the vicinity of a spatial point might depend on the detailed structure of the turbulence in the vicinity of this point. Suggestions, how such dependences might affect the turbulent closure relations, have begun by LUDWIG PRANDTL by making the turbulent viscosity depend upon his *turbulent mixing length* in 1925 [11].

With the definition of $\overline{\phi} = \text{tr}(\overline{\mathbf{t}^R \mathbf{D}})$ this total dissipation rate density can be written as

$$\frac{1}{\rho}\overline{\phi} := \frac{1}{\rho}\text{tr}(\overline{\mathbf{t}^R \mathbf{D}}) = \frac{1}{\rho}\text{tr}(\overline{\mathbf{t}^R \mathbf{D}}) + \frac{1}{\rho}\text{tr}(\overline{\mathbf{t}^{R'} \mathbf{D}'}) \quad (15.33)$$

$$= 2\nu\text{tr}(\overline{\mathbf{D} \mathbf{D}}) + 2\nu\text{tr}(\overline{\mathbf{D}' \mathbf{D}'}) \quad \text{for a Newtonian fluid}$$

$$= \underbrace{4\nu II_{\overline{\mathbf{D}}}}_{\substack{\text{dissipation rate due} \\ \text{to the mean velocity}}} + \underbrace{4\nu II_{\overline{\mathbf{D}'}}}_{\substack{\text{turbulent} \\ \text{dissipation rate } \varepsilon}}, \quad (15.34)$$

in which ν is the material kinematic viscosity $\nu = \eta/\rho$. The second quantity of the above definition is the turbulent dissipation rate density, defined in (15.30). Splitting $\overline{\phi}/\rho$ in (15.33) into mean flow and turbulent fluctuation contributions as in (15.34) for a nonlinear REYNOLDS stress parameterization is more elaborate and will not be given here.

15.3.2 Averaged Density Field ρ

The averaged conservation equation of momentum (15.22), when simplified to a BOUSSINESQ or free convection fluid requires knowledge of $\overline{\rho}/\rho^*$ or $\overline{\rho}/\rho_0$. We start with the equation of state in its simplest form $\rho = \hat{\rho}(\theta)$. If we substitute $\theta = \overline{\theta} + \theta'$, assume that $|\theta'| \ll |\theta|$ and employ TAYLOR series expansion, we obtain

$$\rho(\bar{\theta} + \theta') = \rho(\bar{\theta}) + \left. \frac{d\rho}{d\theta} \right|_{\bar{\theta}} \theta' + \frac{1}{2} \left. \frac{d^2\rho}{d\theta^2} \right|_{\bar{\theta}} (\theta')^2 + \dots, \quad (15.35)$$

and after averaging

$$\overline{\rho(\bar{\theta} + \theta')} = \overline{\rho(\bar{\theta})} + \frac{1}{2} \left. \frac{d^2\rho}{d\theta^2} \right|_{\bar{\theta}} \overline{(\theta')^2} + \dots, \quad (15.36)$$

in which $\overline{\rho(\bar{\theta})} \equiv \rho(\bar{\theta})$. This result is interesting: to lowest order $\overline{\rho(\bar{\theta})}$ is simply $\rho(\bar{\theta})$, but when temperature fluctuations are not small, then the second term on the right-hand side of (15.36) with the autocorrelation $\overline{(\theta')^2}$ is also important. This contribution may be written as

$$\frac{1}{2} \overline{\kappa(\theta')^2}, \quad \kappa := \left. \frac{d^2\rho}{d\theta^2} \right|_{\bar{\theta}}, \quad (15.37)$$

where κ is the curvature of the density as a function of temperature (which for a quadratic equation of state (for water between 0 and 30°C) can be taken to be constant). If this second-order term is not negligible, it must be expressed in terms of the original independent fields. We conclude that the higher-order approximation of the density function has led to a new temperature correlation for which an additional closure condition is needed.

It is now pretty clear, how $\bar{\rho}$ can be evaluated when $\rho = \rho(\theta, a)$, where a is either the pressure p or the salinity s or any other tracer substance. We leave it to the reader to show that

$$\overline{\rho(\theta, a)} = \rho(\bar{\theta}, \bar{a}) + \frac{1}{2} \overline{\kappa_{\theta\theta}(\theta')^2} + \kappa_{\theta a} \overline{a'\theta'} + \frac{1}{2} \overline{\kappa_a(a')^2} + \dots, \quad (15.38)$$

with

$$\kappa_{\theta\theta} = \left. \frac{\partial^2\rho}{\partial\theta^2} \right|_{(\bar{\theta}, \bar{a})}, \quad \kappa_{\theta a} = \left. \frac{\partial^2\rho}{\partial\theta\partial a} \right|_{(\bar{\theta}, \bar{a})}, \quad \kappa_a = \left. \frac{\partial^2\rho}{\partial a^2} \right|_{(\bar{\theta}, \bar{a})}. \quad (15.39)$$

Note that the above are three second order correlation terms for all of which closure relations must be formulated at this level of approximation. We shall not pursue this avenue because second order correlation terms would also have to be formulated for the flux terms.

15.3.3 Turbulent Heat Flux q_t and Turbulent Species Mass Flux j_t

The decisive postulation in the REYNOLDS stress parameterization in (15.32) is the closure proposition

$$\mathbf{R}_D(\overline{\mathbf{D}}) = 2\rho\nu_t\overline{\mathbf{D}}, \quad (15.40)$$

as essentially already proposed by JOSEPH BOUSSINESQ. It assumes \mathbf{R}_D to be collinear (affine) to $\overline{\mathbf{D}} = \frac{1}{2}(\text{grad } \bar{\mathbf{v}} + \text{grad } {}^T\bar{\mathbf{v}})$ and can, thus, be characterized as a *gradient-type closure condition*. The REYNOLDS stress is a momentum *flux* quantity. It has become customary in turbulence modeling to parameterize (all) flux quantities in this fashion; so also for \mathbf{q}_t and \mathbf{j}_t . This suggests closure conditions analogous to FOURIER's law of heat conduction and FICK's first law of mass flux as follows³:

$$\mathbf{q}_t := \overline{\rho \mathbf{v}' u'} = \rho c_v \overline{\mathbf{v}' \theta'} = -\rho c_v \chi_t^{(\theta)} \text{grad } \bar{\theta}, \quad (15.41)$$

$$\mathbf{j}_t := \overline{\rho \mathbf{v}' c'} = -\rho \chi_t^{(c)} \text{grad } \bar{c}. \quad (15.42)$$

Here, c_v has been assumed to be a constant. The coefficients $\chi_t^{(\theta)}$ and $\chi_t^{(c)}$ are called *turbulent eddy diffusivities* of heat and mass ratio, respectively, which have the dimension $[\text{m}^2 \text{s}^{-1}]$. These turbulent closure quantities are again not constants but subject to similar extensions of the type of mixing length propositions as suggested by LUDWIG PRANDTL for the REYNOLDS stress tensor.

With (15.40)–(15.42) the turbulent fluxes of momentum, energy and species mass ratio have been systematically chosen to be of gradient type with respect to the corresponding field variables, viz.,

$$\begin{aligned} - \mathbf{R}_D & \text{ is proportional to } \overline{\mathbf{D}}, \\ - \mathbf{q}_t & \text{ is proportional to } \text{grad } \bar{\theta}, \\ - \mathbf{j}_t & \text{ is proportional to } \text{grad } \bar{c}. \end{aligned} \quad (15.43)$$

The general form is, of course, motivated by the NAVIER–STOKES–FOURIER–SCHMIDT constitutive parameterizations of the material response. Moreover, such closure relations of zeroth order are also made for higher order closure schemes, e.g. $k - \varepsilon$ or $k - \ell$ or $k - \omega$ models, as soon will be demonstrated. However, they cannot be claimed to represent any notion of universality. More on this shall be said in Chap. 16 where PRANDTL's mixing length parameterizations and extensions of it shall be scrutinized.

The averaging procedure of the NAVIER–STOKES equations has brought into evidence a number of new turbulent quantities, which can be grouped as

$$\text{Group 1: } \left\{ k, \varepsilon, \nu_t, \chi_t^{(\theta)}, \chi_t^{(c)} \right\}, \quad (15.44)$$

$$\text{Group 2: } \left\{ \overline{(\theta')^2}, \overline{(a')^2}, \overline{\theta' a'} \right\}, \quad (15.45)$$

where e.g. $a = p$ and $a = s$ for pressure and salinity. Those in group 1 are scalar coefficients, of which numerical values or functional relations need to be prescribed, whereas the variables in the second group arise when the density function $\rho(\theta, a)$ is averaged to second order, see (15.36). In the lowest order approximation, in which

³For short biographies of JEAN BAPTISTE JOSEPH FOURIER and ADOLPH EUGEN FICK, see Figs. 18.1 and 17.31.

$\overline{\rho(\theta, a)} \approx \rho(\bar{\theta}, \bar{a})$, these variables are of no relevance.⁴ If we consider this case, there remain, however, still the five quantities of the first group. They may, in general, be functions of $\bar{\theta}$, \bar{c} and all invariants of $\overline{\mathbf{D}}$, $\text{grad } \bar{\theta}$ and $\text{grad } \bar{c}$, but it is customary in turbulence theory to assume $\{\nu_t, \chi_t^{(\theta)}, \chi_t^{(c)}\}$ to be functions of $\{k, \varepsilon, \bar{\theta}, \bar{c}\}$, and in heterogeneous turbulence also of the spatial coordinates; hence

$$\{\nu_t, \chi_t^{(\theta)}, \chi_t^{(c)}\} = \text{fcts}(k, \varepsilon, \bar{\theta}, \bar{c}, \mathbf{x}). \quad (15.46)$$

Moreover, it is also customary to introduce the ratios between the eddy viscosity and the turbulent diffusivities of heat and mass,

$$\sigma_\theta := \frac{\nu_t}{\chi_t^{(\theta)}}, \quad \sigma_c := \frac{\nu_t}{\chi_t^{(c)}} \quad (15.47)$$

and to call σ_θ *turbulent PRANDTL number* and σ_c *turbulent SCHMIDT⁵ number*, respectively. The turbulent heat and mass fluxes can then be written as

$$\overline{\mathbf{v}'\theta'} = -\frac{\nu_t}{\sigma_\theta} \text{grad } \bar{\theta}, \quad \overline{\mathbf{v}'c'} = -\frac{\nu_t}{\sigma_c} \text{grad } \bar{c}. \quad (15.48)$$

As long as one chooses for $\{\nu_t, \sigma_\theta, \sigma_c\}$ independent functional representations of $\{k, \varepsilon, \bar{\theta}, \bar{c}\}$, (15.48) is equivalent to (15.46). If, however, σ_θ and σ_c are assumed to be constant, which is often the case, then the functional dependencies of $\chi_t^{(\theta)}$ and $\chi_t^{(c)}$ are affine to that of ν_t . This is a kind of similarity rule, sometimes not being experimentally corroborated, but often employed. In this simple case, one then only needs to find a relation for

$$\nu_t = \hat{\nu}_t(k, \varepsilon, \bar{\theta}, \bar{c}, \mathbf{x}). \quad (15.49)$$

If ν_t neither depends on $\bar{\theta}$ nor on \bar{c} , then, apart from a dependence on \mathbf{x} (15.50) reduces to

$$\nu_t = \hat{\nu}_t(k, \varepsilon, \cdot), \quad \text{or, even simpler } \nu_t = \hat{\nu}_t(k, \cdot), \quad (15.50)$$

where the dot stands for a possible \mathbf{x} -dependence. If the parameterization of ν_t on k, ε , and \mathbf{x} or on k (and \mathbf{x}) are known, one then only needs additional algebraic or differential equations for k and ε to fix the turbulent viscosity. Depending upon, which case prevails, one then speaks of *one-* or *two-equation models*. In early turbulence modeling the turbulent viscosity was often assumed to be at most a function of position.

⁴What is meant here is that no new turbulent closure must be given if the equation of state is prescribed.

⁵For a biographical sketch of SCHMIDT see Fig. 15.5.

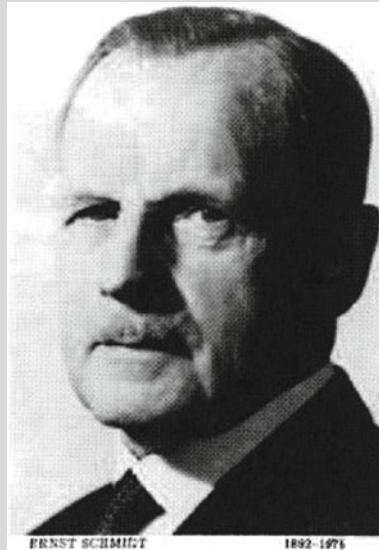


Fig. 15.5 ERNST HEINRICH WILHELM SCHMIDT (11. Feb. 1892–22. Jan. 1975)

ERNST HEINRICH WILHELM SCHMIDT was a German thermodynamicist and University teacher. He studied at the Technical Universities (Hochschule (TH)) of Dresden and Munich civil engineering but quickly changed to electrical engineering and applied physics. In 1911/12 he served in the German military and was drafted in the first World War from 1914–1918. In 1919, he completed his studies in Munich and graduated with diploma in electrical engineering. In 1920 he was promoted to Dr.-Ing in Munich and subsequently worked under OSKAR KNOBLAUCH as laboratory assistant of applied physics at TH Munich. He obtained the habilitation degree from TH Munich and immediately captured the professorship for thermodynamics at TH Danzig (now Gdańsk, Poland). In November 1933 he signed a supporting statement of the University and TH professors in Germany for ADOLF HITLER and joined the supporting members of the NSDAP. With the assignment of HERMANN GÖRING ERNST SCHMIDT was installed in 1943 as plenipotentiary for jet propulsion. As such, he established the largest German research network for solid-propulsion rockets.

ERNST SCHMIDT was professor of engine research between 1937 and 1945, and again professor of thermal sciences from 1945 to 1952, both at TH Braunschweig. From 1952–1961 he was full professor for thermodynamics at the TH Munich, where he retired in 1972.

The SCHMIDT number is named after him. It measures the ratio of the diffusive momentum to diffusive mass transfer. SCHMIDT, moreover, focused his research on thermodynamics of rocket engines, which are extensively treated in [18].

The text is based on www.wikipedia.org and <http://www.deutsche-biographie.de/pnd118795228.html>

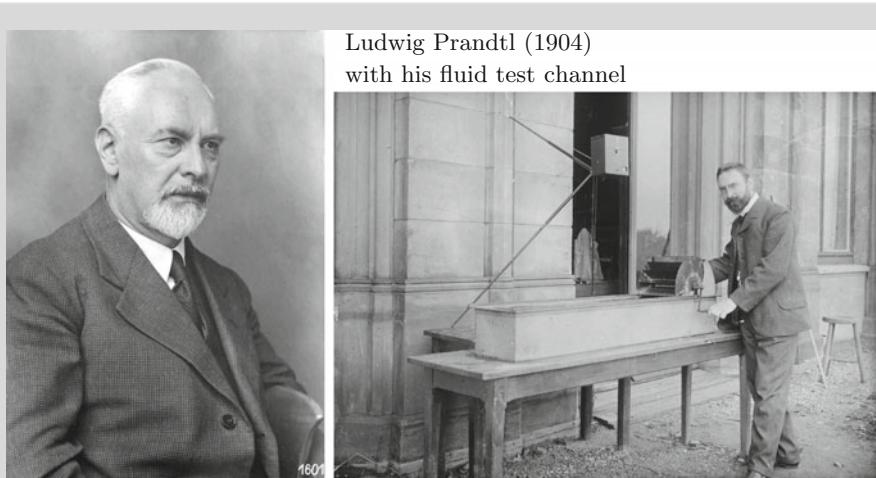


Fig. 15.6 LUDWIG PRANDTL (4. Feb. 1875–15. Aug. 1953)

LUDWIG PRANDTL was a German engineer, a pioneer in the development of rigorous systematic mathematical analyses which he used to underlay the science of aerodynamics. He wrote his doctoral dissertation on SAINT VENANT torsion in shafts under AUGUST FÖPPL (1854–1924), where he presented his membrane analogy between torsion of beams and bending of soap films under transverse pressure, spanned over a wire of the form of the boundary of the beam's cross section (see Fig. 8.3 in Vol. 1). In the 1920s he developed the mathematical basis for subsonic aerodynamics including transonic velocities. His studies identified the boundary layer, thin-airfoils, and lifting-line theories. In 1901 PRANDTL became a professor of fluid mechanics at the *Technische Hochschule Hannover*, where he developed many of his most important theories. In 1904 he delivered a groundbreaking paper, *Fluid Flow with Very Little Friction*, in which he described the boundary layer, its importance for drag and streamlining and the flow separation as a result of the boundary layer, clearly explaining the concept of stall for the first time. In 1918–1919, he published the LANCHESTER–PRANDTL wing theory. Considerable work was included on the nature of induced drag and wingtip vortices and turbulence. Other works examined the problem of compressibility at high subsonic speeds, known as the PRANDTL–GLAUERT correction. He also worked on meteorology, plasticity and structural mechanics.

The above photo with Prandtl's test channel is taken from [21].

The text is based on www.wikipedia.org

15.3.4 One- and Two-Equation Models

PRANDTL⁶ in his seminal papers [11, 12], which gave quantitative turbulence modeling an early start, did not postulate closure conditions for k and ε but described

⁶For a biographical sketch of PRANDTL see Fig. 15.6

the eddy viscosity as a function of the mean velocity gradient and a mixing length, $\nu_t = \ell^2 |\partial \bar{v}_1 / \partial x_2|$, for simple shearing which in three-dimensional flows may be extrapolated to have the form

$$\nu_t = 2\ell^2 \sqrt{\Pi_D}, \quad (15.51)$$

(which was *not* proposed in this form by LUDWIG PRANDTL. He initially only formulated it for turbulent simple shear). This formula requires parameterization of the mixing length ℓ . This was done by LUDWIG PRANDTL himself in his paper of 1933 [12], by postulating a balance law of the form

$$\frac{\partial \ell}{\partial t} + \text{div}(\ell \bar{\mathbf{v}}) + 2\ell \sqrt{\Pi_D} + \dots = 0 \quad (15.52)$$

for the mixing length.

PRANDTL's proposal is an example of a one-equation model. If ℓ is determined by (15.52), the turbulent viscosity and diffusivities are known by the equations

$$\nu_t = 2\ell^2 \sqrt{\Pi_D}, \quad \chi_t^{(\theta)} = \frac{\nu_t}{\sigma_\theta}, \quad \chi_t^{(c)} = \frac{\nu_t}{\sigma_c}, \quad (15.53)$$

and, since dimensionally $[k] = [\nu_t^2 / \ell^2]$, one may also set

$$k = c_k 4\ell^2 \Pi_D. \quad (15.54)$$

In (15.53) and (15.54), σ_θ , σ_c and c_k are fitting constants.

An alternative to the above closure relations (15.52) and (15.53) is to propose evolution equations for two quantities: k , ε or the mixture length ℓ or any turbulent scalar quantity that characterizes the turbulent intensity e.g., the turbulent vorticity ω . These quantities are dimensionally related by

$$[\varepsilon] = \frac{[k^{3/2}]}{[\ell]}, \quad [\omega] = \frac{[k]}{[\ell^2]}, \quad (15.55)$$

and equation models have been proposed for the turbulent variable pairs (k, ℓ) , (k, ε) , (k, ω) and are called $k - \ell$ model, $k - \varepsilon$ model and $k - \omega$ model, respectively. For each of these, balance law-type equations have been proposed. The most popular is the $k - \varepsilon$ model [9, 10]. This model has extensively been tested against experiments [16, 17], however, the $k - \omega$ model has also gained popularity in geophysical applications, [23, 24].

For all these models a direct connection with the turbulent viscosity must still be established. This is obtained with the aid of dimensional analysis by appropriately constructing the physical dimension of the quantity under question. The reader may easily check the dimensional relations

$$[\nu_t] = \frac{[k^2]}{[\varepsilon]} = [k^{1/2}][\ell] = \frac{[k]}{[\omega^{1/2}]},$$

from which we may postulate the parameterizations

$$\nu = c_\mu \frac{k^2}{\varepsilon} = c'_\mu k^{1/2} \ell = c''_\mu k \omega^{-1/2}, \quad (15.56)$$

in which c_μ, c'_μ, c''_μ are coefficients adjusted by experiments. Interestingly, in spite of this, these coefficients exhibit some notion of universality, i.e., their numerical values are assumed to hold for (nearly) all turbulent processes.

15.4 $k - \varepsilon$ Model for Density Preserving and Boussinesq Fluids

In the $k - \varepsilon$ model evolution equations are constructed for the turbulent kinetic energy k , and the turbulent dissipation rate, ε and the actual values for the turbulent diffusivity ν_t are computed with the aid of (15.56) viz.,

$$\nu_t = c_\mu \frac{k^2}{\varepsilon}. \quad (15.57)$$

Since $[\nu_t] = [k^2]/[\varepsilon]$, it follows that c_μ is a dimensionless scalar, which, in the $k - \varepsilon$ model is taken to be a constant. For k and ε , partial differential equations of balance type are derived. These will also contain scalar parameters and must equally be determined numerically by validating the model.

Historically, the $k - \varepsilon$ model has originally been developed in the 1970s by K. HANJALIC and B.E. LAUNDER [6], W.P. JONES and B.E. LAUNDER [9] and B.E. LAUNDER and D.B. SPALDING [10]. It has, in the last decades, attracted great attention in the engineering and geophysical and hydraulic engineering community. W. RODI [16, 17] describes its applicability in geophysics and the hydraulic engineering community, J. WEIS [22] and L. UMLAUF [20] put it in proper perspective with other two-equation models. A derivation using continuum mechanical principles is given in HUTTER and K. JÖHNK [7]. Here we provide a summary only.

15.4.1 *The Balance Equations*

In the $k - \varepsilon$ closure scheme the balance laws of mass, momentum, energy and tracer mass for the mean motion are complemented by the balance laws for turbulent kinetic energy and turbulent dissipation rate. They are given by

$$\begin{aligned}\frac{d}{dt} \int_{\omega} k \, dv &= - \int_{\partial\omega} \phi^k \cdot \mathbf{n} \, da + \int_{\omega} \pi^k \, dv, \\ \frac{d}{dt} \int_{\omega} \varepsilon \, dv &= - \int_{\partial\omega} \phi^\varepsilon \cdot \mathbf{n} \, da + \int_{\omega} \pi^\varepsilon \, dv,\end{aligned}\tag{15.58}$$

or in local form

$$\begin{aligned}\frac{\partial k}{\partial t} + \operatorname{div}(k\bar{\mathbf{v}}) &= -\operatorname{div}(\phi^k) + \pi^k, \\ \frac{\partial \varepsilon}{\partial t} + \operatorname{div}(\varepsilon\bar{\mathbf{v}}) &= -\operatorname{div}(\phi^\varepsilon) + \pi^\varepsilon,\end{aligned}\tag{15.59}$$

in which ϕ^k and ϕ^ε are flux and π^k , π^ε are production terms. The imaginative part of the proposal of the $k - \varepsilon$ model is the postulation of these flux and production terms as are the parameterizations for \mathbf{R} , \mathbf{q}_t , \mathbf{j}_t in (15.32), (15.41) and (15.42), which are repeated as follows

$$\begin{aligned}\frac{\mathbf{R}}{\rho} &= -\overline{\mathbf{v}' \otimes \mathbf{v}'} = -\frac{2}{3} k \mathbf{1} + 2\nu_t \bar{\mathbf{D}}, \\ \frac{\mathbf{q}_t}{\rho c_v} &= \overline{\mathbf{v}' \theta'} = -\frac{\nu_t}{\sigma_\theta} \operatorname{grad} \bar{\theta}, \\ \frac{\mathbf{j}_t}{\rho} &= \overline{\mathbf{v}' c'} = -\frac{\nu_t}{\sigma_c} \operatorname{grad} \bar{c},\end{aligned}\tag{15.60}$$

in which the relations in (15.47) have been applied. These parameterizations all involve the turbulent (momentum) viscosity ν_t and PRANDTL and SCHMIDT numbers σ_θ and σ_c , which are assumed to be constants. This serves as motivation also to parameterize the flux terms in (15.59) in the same form, viz.,

$$\begin{aligned}\phi^k &= -\left(\frac{\nu_t}{\sigma_k} + \nu\right) \operatorname{grad} k = -D^{(k)} \operatorname{grad} k, \\ \phi^\varepsilon &= -\left(\frac{\nu_t}{\sigma_\varepsilon} + \nu\right) \operatorname{grad} \varepsilon = -D^{(\varepsilon)} \operatorname{grad} \varepsilon\end{aligned}\tag{15.61}$$

with two new PRANDTL numbers, σ_k and σ_ε , respectively, to be numerically determined; ν_t is the turbulent and ν the material kinematic viscosity.⁷

⁷To write down the local forms (15.59) and the gradient type representations (15.61) one presupposes *locality* and *differentiability* of k , ε , ϕ^k , ϕ^ε , π^k , π^ε . More precisely, (15.58) is assumed to hold for any region ω , how-so ever small and the fields involved are smooth. Neither of these assumptions seems to us to be obvious, even though they appear to never have been explicitly questioned.

The judicious selection of the production rate densities π^k and π^ε is the heart of the construction of the $k - \varepsilon$ model. For a BOUSSINESQ fluid the resulting relations are

$$\begin{aligned}\pi^k &= 4\nu_t II_{\overline{\mathbf{D}}} - \varepsilon + \frac{\overline{\rho} \overline{\alpha}_\theta}{\rho^*} \frac{\nu_t}{\sigma_\theta} \mathbf{g} \cdot \text{grad } \overline{\theta}, \\ \pi^\varepsilon &= 4c_1 k II_{\overline{\mathbf{D}}} - c_2 \frac{\varepsilon^2}{k} + c_3 \frac{\overline{\rho} \overline{\alpha}_\theta}{\rho^*} \frac{c_\mu}{\sigma_\theta} k \mathbf{g} \cdot \text{grad } \overline{\theta},\end{aligned}\quad (15.62)$$

in which

$$\overline{\alpha}_\theta = - \frac{1}{\overline{\rho}} \left. \frac{\partial \rho(\theta)}{\partial \theta} \right|_{\overline{\theta}}, \quad II_{\overline{\mathbf{D}}} = \frac{1}{2} \text{tr} (\overline{\mathbf{D}} \overline{\mathbf{D}}) \quad (15.63)$$

are the coefficient of thermal expansion and $II_{\overline{\mathbf{D}}}$ is the second invariant of $\overline{\mathbf{D}}$. The first and the second terms on the right-hand side of (15.62) are the classical production terms of the $k - \varepsilon$ model of density preserving fluids, whereas the last terms are due to the buoyancy effects of the BOUSSINESQ fluid.

A detailed derivation of the $k - \varepsilon$ model will not be given here; however, a sketch of the derivation is provided; for details the reader is, however, referred to [7].

Turbulent kinetic energy: To briefly outline the procedure, let us commence with the derivation of the equation of the turbulent kinetic energy. To this end, one scalarly multiplies the momentum equation for the fluctuation velocities⁸

$$\begin{aligned}\frac{\partial \mathbf{v}'}{\partial t} + \text{div} (\overline{\mathbf{v}} \otimes \mathbf{v}' + \mathbf{v}' \otimes \overline{\mathbf{v}}) + \text{div} (\mathbf{v}' \otimes \mathbf{v}' - \overline{\mathbf{v}' \otimes \mathbf{v}'}) \\ + \frac{1}{\rho} \text{grad } p' - \text{div} (\nu \text{grad } \mathbf{v}') = \mathbf{0}\end{aligned}\quad (15.64)$$

with the fluctuation velocity \mathbf{v}' and then applies the filter operation $\overline{(\cdot)}$ to the emerging equation. The result is

$$\begin{aligned}\underbrace{\frac{\partial \mathbf{v}'}{\partial t} \cdot \mathbf{v}'}_{\textcircled{1}} + \underbrace{\text{div} (\mathbf{v}' \otimes \overline{\mathbf{v}}) \cdot \mathbf{v}'}_{\textcircled{2}} + \underbrace{\text{div} (\overline{\mathbf{v}} \otimes \mathbf{v}') \cdot \mathbf{v}'}_{\textcircled{3}} \\ + \underbrace{\text{div} (\mathbf{v}' \otimes \mathbf{v}') \cdot \mathbf{v}'}_{\textcircled{4}} + \underbrace{\frac{1}{\rho^*} \text{div } p' \mathbf{v}'}_{\textcircled{5}} - \underbrace{\nu (\text{div grad } \mathbf{v}') \cdot \mathbf{v}'}_{\textcircled{6}} = 0,\end{aligned}\quad (15.65)$$

in which a term linear in \mathbf{v}' has been omitted, since $\overline{\mathbf{v}'} = \mathbf{0}$. The individual underbraced terms are expressible as

⁸This is the difference of the momentum equation for $\overline{\mathbf{v}} + \mathbf{v}'$ and the momentum equation for $\overline{\mathbf{v}}$.

$$\begin{aligned}
\textcircled{1} &= \frac{\partial k}{\partial t}, \\
\textcircled{2} &= \operatorname{div}(k\bar{\mathbf{v}}), \\
\textcircled{3} &= -\frac{1}{\rho} \operatorname{tr}(\mathbf{R}\bar{\mathbf{D}}) = 4\nu_t II_{\bar{\mathbf{D}}} = 4c_\mu \frac{k^2}{\varepsilon} II_{\bar{\mathbf{D}}}, \\
\textcircled{4} &= \operatorname{div}\left(\frac{1}{2}\overline{(\mathbf{v}' \cdot \mathbf{v}')\mathbf{v}'}\right), \\
\textcircled{5} &\approx 0, \\
\textcircled{6} &= \nu \operatorname{div} \operatorname{grad} k - \varepsilon.
\end{aligned} \tag{15.66}$$

All these expressions are exact and obtained by algebraic manipulations except the pressure term $\textcircled{5}$, which is approximate. Note, that the term $\textcircled{4}$ is the divergence of the average of a triple correlation. We define this vectorial quantity as

$$\mathbf{q}^k = \overline{\left(\frac{1}{2}\mathbf{v}' \cdot \mathbf{v}'\right)\mathbf{v}'} \tag{15.67}$$

and postulate for it the gradient law

$$\mathbf{q}_k = -\chi_t^k \operatorname{grad} k = -\frac{\nu_t}{\sigma_k} \operatorname{grad} k = -c_\mu \frac{k^2}{\sigma_k \varepsilon} \operatorname{grad} k. \tag{15.68}$$

Combining this expression with the first part of (15.66) $_6$ then generates the flux of the turbulent kinetic energy, which was already stated in (15.61) without motivation. The remaining terms in (15.66) then define the first two terms on the right-hand side of (15.62) $_1$. The last (third) terms on the right-hand sides of (15.62) arise only in a BOUSSINESQ fluid and will later be explained.

Turbulent dissipation rate: The balance law for the turbulent dissipation rate ε is intimately based on the fact that vorticity, i.e., $\boldsymbol{\omega} = \operatorname{curl} \mathbf{v}$, is the cause for the formation of eddies. This is evidenced by the relation

$$\begin{aligned}
\varepsilon &\stackrel{(15.34)}{:=} 4\nu II_{\bar{\mathbf{D}'}} = 2\nu \operatorname{tr}(\bar{\mathbf{D}'\mathbf{D}'}) \\
&= \frac{\nu}{2} \operatorname{tr}\left[\overline{(\operatorname{grad} \mathbf{v}' + \operatorname{grad}^T \mathbf{v}')(\operatorname{grad} \mathbf{v}' + \operatorname{grad}^T \mathbf{v}')}\right] \\
&= \frac{\nu}{2} \overline{|\operatorname{grad} \mathbf{v}' + \operatorname{grad}^T \mathbf{v}'|^2} \\
&= \nu |\operatorname{curl} \mathbf{v}'|^2 = \nu \overline{\boldsymbol{\omega}' \cdot \boldsymbol{\omega}'} = 2\nu e,
\end{aligned} \tag{15.69}$$

where

$$e = \frac{1}{2} \overline{(\boldsymbol{\omega}' \cdot \boldsymbol{\omega}')} \tag{15.70}$$

is called the *specific turbulent enstrophy*. Equation (15.69) is the salient expression of the connection between turbulent dissipation and vorticity.

To derive an evolution equation for ε , it is therefore tempting to proceed formally as with the balance law for the turbulent kinetic energy. One starts with the momentum equation for the fluctuation velocities (15.64), takes its curl and, thus, obtains the *vorticity transport equation for the turbulent velocity*⁹

$$\begin{aligned} \frac{\partial \boldsymbol{\omega}'}{\partial t} + \operatorname{div} (\boldsymbol{\omega}' \otimes (\bar{\mathbf{v}} + \mathbf{v}') - (\bar{\mathbf{v}} + \mathbf{v}') \otimes \boldsymbol{\omega}' + \bar{\boldsymbol{\omega}} \otimes \mathbf{v}' - \mathbf{v}' \otimes \bar{\boldsymbol{\omega}}) \\ - \nu \operatorname{div} \operatorname{grad} \boldsymbol{\omega}' - \operatorname{div} (\overline{\boldsymbol{\omega}' \otimes \mathbf{v}' - \mathbf{v}' \otimes \boldsymbol{\omega}'}) = \mathbf{0}. \end{aligned} \quad (15.71)$$

It is now clear that an evolution equation for ε or e will emerge, if one multiplies (15.71) scalarly with $\boldsymbol{\omega}'$ and then applies to the emerging equation the filter operation (\cdot) . This yields the relation

$$\begin{aligned} \text{(i)} \quad & \frac{\partial \varepsilon}{\partial t} + \overline{2 \nu \boldsymbol{\omega}' \cdot \operatorname{div} [\boldsymbol{\omega}' \otimes (\bar{\mathbf{v}} + \mathbf{v}')] } \\ \text{(ii)} \quad & - \overline{2 \nu \boldsymbol{\omega}' \cdot \operatorname{div} [(\bar{\mathbf{v}} + \mathbf{v}') \otimes \boldsymbol{\omega}']} \\ \text{(iii)} \quad & + \overline{2 \nu \boldsymbol{\omega}' \cdot \operatorname{div} [\bar{\boldsymbol{\omega}} \otimes \mathbf{v}' - \mathbf{v}' \otimes \bar{\boldsymbol{\omega}}]} \\ \text{(iv)} \quad & - \overline{2 \nu^2 \boldsymbol{\omega}' \cdot \operatorname{div} (\operatorname{grad} \boldsymbol{\omega}')} \\ \text{(v)} \quad & - \overline{2 \nu \boldsymbol{\omega}' \cdot \operatorname{div} (\boldsymbol{\omega}' \otimes \mathbf{v}' - \mathbf{v}' \otimes \boldsymbol{\omega}')} \\ & = 0. \end{aligned} \quad (15.72)$$

The individual terms in the five lines of (15.72) are transformed and interpreted in a relatively complex detailed computation, see e.g. Chap. 11 in [7]. The result can be summarized as follows:

$$\begin{aligned} \text{(i)} \quad & \frac{\partial \varepsilon}{\partial t} + \operatorname{div} (\varepsilon \bar{\mathbf{v}}) + \operatorname{div} \mathbf{q}^\varepsilon, \quad \mathbf{q}^\varepsilon := \overline{\nu (\boldsymbol{\omega}' \cdot \boldsymbol{\omega}') \mathbf{v}'}, \\ \text{(ii)} \quad & = -4 c_1 k II_{\mathcal{D}}, \quad c_1 = \text{const.}, \\ \text{(iii)} \quad & \approx 0, \\ \text{(iv)} \quad & = -\operatorname{div} (\nu \operatorname{grad} \varepsilon) + 2 \nu^2 \overline{|\operatorname{grad} \boldsymbol{\omega}'|^2} \\ & \approx -\operatorname{div} (\nu \operatorname{grad} \varepsilon) + c_2 \frac{\varepsilon^2}{k}, \quad c_2 = \text{const.}, \\ \text{(v)} \quad & = 0. \end{aligned} \quad (15.73)$$

Notice that statement (i) contains a flux term \mathbf{q}^ε ; similarly, (iv) also involves a flux term given by $\nu \operatorname{grad} \varepsilon$. With the gradient type parameterization

⁹The derivation of this equation is given in the solution to the homework Nr. 7 of Chap. 7 on p. 518 of [7].

$$\mathbf{q}^\varepsilon = -\chi_t^\varepsilon \text{grad } \varepsilon = -c_\varepsilon \frac{k^2}{\varepsilon} \text{grad } \varepsilon, \quad \chi_t^\varepsilon = \frac{\nu_t}{\sigma_\varepsilon} = \frac{c_\mu k^2}{\sigma_\varepsilon \varepsilon}, \quad \sigma_\varepsilon = \frac{c_\mu}{c_\varepsilon} \quad (15.74)$$

the two flux terms can be combined to form

$$\phi^\varepsilon = -\left(\frac{\nu_t}{\sigma_\varepsilon} + \nu\right) \text{grad } \varepsilon = -D^{(\varepsilon)} \text{grad } \varepsilon, \quad (15.75)$$

already stated in (15.61). In summary, the balance of turbulent dissipation takes the final form

$$\frac{\partial \varepsilon}{\partial t} + \text{div}(\varepsilon \bar{\mathbf{v}}) = \text{div}\left(\left(c_\varepsilon \frac{k^2}{\varepsilon} + \nu\right) \text{grad } \varepsilon\right) + \underbrace{4c_1 k II_{\mathcal{D}} - c_2 \frac{\varepsilon^2}{k}}_{\pi^\varepsilon}, \quad (15.76)$$

in which the specific production rate density π^ε has already been anticipated in the first two terms of (15.62)₂. Its third term is only present in a BOUSSINESQ fluid. This completes the presentation of the $k - \varepsilon$ equations for a density-preserving fluid.

15.4.2 Boussinesq Fluid Referred to a Non-inertial Frame

Recall that a BOUSSINESQ fluid is kinematically density preserving, but accounts for small density variations in the gravity term. Moreover, in geophysical applications non-inertial effects are accounted for by the CORIOLIS¹⁰ acceleration, whilst centripetal accelerations are generally absorbed in the gravity term.¹¹ This implies that the momentum equation for the velocity fluctuations, relation (15.64), must on the left-hand side be complemented by

$$2 \boldsymbol{\Omega} \times \mathbf{v}' - \frac{\rho' \mathbf{g}}{\rho^*},$$

where $\boldsymbol{\Omega}$ is the angular velocity of the frame. After scalar multiplication with \mathbf{v}' and then averaging,

$$\underbrace{(2 \boldsymbol{\Omega} \times \mathbf{v}') \cdot \mathbf{v}'}_0 - \frac{\mathbf{g}}{\rho^*} \cdot \overline{\rho' \mathbf{v}'} = -\frac{1}{\rho^*} \overline{\rho' \mathbf{v}'} \cdot \mathbf{g} \quad (15.77)$$

is obtained. It follows, the balance law of turbulent kinetic energy has the additional production rate density (15.77), so that

¹⁰For a short biography of GASPARD DE CORIOLIS, see Fig.8.10, Vol. 1. An interesting historical addendum is the book ‘*Pendulum—Léon Foucault and the Triumph of Science*’ by AMIR D. ACZEL [1].

¹¹Obviously, this is not so in laboratory experiments on rotating platforms.

$$\begin{aligned} \frac{\partial k}{\partial t} + \operatorname{div}(k \bar{\mathbf{v}}) - \operatorname{div} \left(\left(\frac{c_\mu k^2}{\sigma_k \varepsilon} + \nu \right) \operatorname{grad} k \right) \\ - 4 c_\mu \frac{k^2}{\varepsilon} II_{\bar{\mathbf{D}}} + \varepsilon - \frac{1}{\rho^*} \overline{\rho' \mathbf{v}'} \cdot \mathbf{g} = 0. \end{aligned} \quad (15.78)$$

The balance law for the turbulent dissipation rate is obtained if the curl of the equation for the velocity fluctuations is formed, which is then scalarly multiplied by the vorticity fluctuation $\boldsymbol{\omega}' = \operatorname{curl} \mathbf{v}'$, and the resulting equation is subsequently filtered. This generates the two additional terms

$$2\nu \left\{ \overline{\operatorname{curl}(2\boldsymbol{\Omega} \times \mathbf{v}') \cdot \operatorname{curl} \mathbf{v}' - \operatorname{curl} \left(\frac{\mathbf{g} \rho'}{\rho^*} \right) \cdot \operatorname{curl} \mathbf{v}'} \right\} \quad (15.79)$$

in the balance of turbulent dissipation rate. The common factor 2ν enters because of (15.69). With (15.79) the balance law of the turbulent dissipation rate is, therefore, given by

$$\begin{aligned} \frac{\partial \varepsilon}{\partial t} + \operatorname{div}(\varepsilon \bar{\mathbf{v}}) - \operatorname{div} \left(\left(c_\varepsilon \frac{k^2}{\varepsilon} + \nu \right) \operatorname{grad} \varepsilon \right) - 4 c_1 k II_{\bar{\mathbf{D}}} + c_2 \frac{\varepsilon^2}{k} \\ - 2\nu \left[\overline{\operatorname{curl} \left(\frac{\mathbf{g} \rho'}{\rho^*} \right) \cdot \operatorname{curl} \mathbf{v}'} \right] + 2\nu \left[\overline{\operatorname{curl}(2\boldsymbol{\Omega} \times \mathbf{v}') \cdot \operatorname{curl} \mathbf{v}'} \right] = 0. \end{aligned} \quad (15.80)$$

The new terms in (15.78) and (15.80) are, respectively, due to the small density variations in the buoyancy term and CORIOLIS acceleration inferred by the non-inertial frame.

In the turbulence literature the parameterization

$$- 2\nu \left[\overline{\operatorname{curl} \left(\frac{\mathbf{g} \rho'}{\rho^*} \right) \cdot \operatorname{curl} \mathbf{v}'} \right] = - \frac{\mathbf{g}}{\rho^*} \cdot c_3 \frac{\varepsilon}{k} \overline{\rho' \mathbf{v}'} \quad (15.81)$$

is suggested. The following argument may serve to justify this proposal. On the left-hand side ρ' and \mathbf{v}' are the only arising fluctuating variables. So, it is tempting to postulate that the left-hand side of (15.81) is affine (collinear) to $\overline{\rho' \mathbf{v}'}$ with an adjustment using k and ε to match the dimensions on the two sides of the equation. This requires the right-hand side to involve the explicit factor ε/k with a dimensionless coefficient c_3 as a modeling constant. In geophysical applications c_3 is small and often set to zero: $c_3 = 0$. For more details of the ‘derivation’ of (15.81), see e.g. [7].

The term in (15.80) due to the CORIOLIS acceleration is generally ignored. This assumption may be justified by the argument that the CORIOLIS acceleration does not produce any turbulent kinetic energy; so, the corresponding production in the turbulent dissipation equation should equally vanish. An alternative motivation for this choice is again given in [7].

In summary, the above arguments suggest that *under fairly weak simplifying assumptions of the differential equation for the turbulent dissipation a BOUSSINESQ fluid is the same as the corresponding equation for a density preserving fluid.*

For the simplest form of the thermal equation of state $\rho = \hat{\rho}(\theta)$ a TAYLOR series expansion yields

$$\rho = \hat{\rho}(\theta) = \hat{\rho}(\bar{\theta} + \theta') \approx \hat{\rho}(\bar{\theta}) + \left. \frac{\partial \hat{\rho}}{\partial \theta} \right|_{\bar{\theta}} \theta' + \dots, \quad (15.82)$$

implying a linear approximation

$$\begin{aligned} \bar{\rho} &= \hat{\rho}(\bar{\theta}), \\ \rho' &= \frac{\partial \hat{\rho}}{\partial \theta}(\bar{\theta}) \theta' = -\bar{\rho} \bar{\alpha}_\theta \theta', \end{aligned} \quad (15.83)$$

where

$$\bar{\alpha}_\theta = \hat{\alpha}_\theta(\bar{\theta}) = -\frac{1}{\hat{\rho}(\bar{\theta})} \frac{\partial \hat{\rho}}{\partial \theta}(\bar{\theta}) \quad (15.84)$$

is the averaged coefficient of thermal expansion. The added term in (15.78) due to the density variations in the balance law of turbulent kinetic energy can with (15.83)₂ be written as

$$-\frac{\mathbf{g}}{\rho^*} \cdot \overline{\rho' \mathbf{v}'} = \frac{\bar{\rho}}{\rho^*} \bar{\alpha}_\theta \mathbf{g} \cdot \overline{\theta' \mathbf{v}'} \stackrel{*}{=} -\frac{\bar{\rho}}{\rho^*} \bar{\alpha}_\theta(\bar{\theta}) \mathbf{g} \cdot \frac{\nu_t}{\sigma_\theta} \text{grad } \bar{\theta}, \quad (15.85)$$

in which at step ‘ $\stackrel{*}{=}$ ’ the gradient-type law (15.60)₂, i.e.,

$$\overline{\theta' \mathbf{v}'} = -\frac{\nu_t}{\sigma_\theta} \text{grad } \bar{\theta} \quad (15.86)$$

was employed, in which ν_t is the turbulent viscosity and σ_θ the PRANDTL number for adjustment with experiments. Similarly, the corresponding term in the balance law of turbulent dissipation in (15.80) [see also (15.81)] takes the form

$$-\frac{\mathbf{g}}{\rho^*} \cdot c_3 \frac{\varepsilon}{k} \overline{\rho' \mathbf{v}'} = \frac{c_3 c_\mu}{\sigma_\theta} \frac{\bar{\rho}}{\rho^*} \bar{\alpha}_\theta k \mathbf{g} \cdot \text{grad } \theta. \quad (15.87)$$

15.4.3 Summary of the $k - \varepsilon$ Equations

It is helpful to collect all governing field equations of the turbulent motion of a BOUSSINESQ fluid at one place. These equations are as follows:

- Balance of mass

$$\operatorname{div} \bar{\mathbf{v}} = 0. \quad (15.88)$$

- Balance of linear momentum

$$\begin{aligned} \frac{\partial \bar{\mathbf{v}}}{\partial t} + \operatorname{div} (\bar{\mathbf{v}} \otimes \bar{\mathbf{v}}) + 2\boldsymbol{\Omega} \times \bar{\mathbf{v}} \\ = -\frac{1}{\rho^*} \operatorname{grad} \bar{p} + \operatorname{div} (2(\nu + \nu_t)\bar{\mathbf{D}}) + \frac{\bar{\rho}}{\rho^*} \mathbf{g}. \end{aligned} \quad (15.89)$$

- Balance of energy

$$\begin{aligned} \frac{\partial \bar{\theta}}{\partial t} + \operatorname{div} (\bar{\mathbf{v}}\bar{\theta}) \\ = \operatorname{div} \left(\left(\chi^{(\theta)} + \frac{\nu_t}{\sigma_\theta} \right) \operatorname{grad} \bar{\theta} \right) + \frac{4\nu}{c_v} II_{\bar{\mathbf{D}}} + \frac{r}{c_v}. \end{aligned} \quad (15.90)$$

- Balance of species mass (we write c for c_α)

$$\frac{\partial \bar{c}}{\partial t} + \operatorname{div} (\bar{\mathbf{v}}\bar{c}) = \operatorname{div} \left(\left(\chi^{(c)} + \frac{\nu_t}{\sigma_c} \right) \operatorname{grad} \bar{c} \right) + \bar{\Phi}^c. \quad (15.91)$$

- Balance of turbulent kinetic energy

$$\begin{aligned} \frac{\partial k}{\partial t} + \operatorname{div} (\bar{\mathbf{v}}k) \\ = \operatorname{div} \left(\left(\nu + \frac{\nu_t}{\sigma_k} \right) \operatorname{grad} k \right) + 4\nu_t II_{\bar{\mathbf{D}}} - \varepsilon + \frac{\bar{\rho} \bar{\alpha}_\theta}{\rho^*} \frac{\nu_t}{\sigma_\theta} \mathbf{g} \cdot \operatorname{grad} \bar{\theta}. \end{aligned} \quad (15.92)$$

- Balance of turbulent dissipation rate¹²

$$\begin{aligned} \frac{\partial \varepsilon}{\partial t} + \operatorname{div} (\bar{\mathbf{v}}\varepsilon) \\ = \operatorname{div} \left(\left(\nu + \frac{\nu_t}{\sigma_\varepsilon} \right) \operatorname{grad} \varepsilon \right) + 4c_1 k II_{\bar{\mathbf{D}}} - c_2 \frac{\varepsilon^2}{k} + \frac{\bar{\rho} \bar{\alpha}_\theta}{\rho^*} \frac{c_3 c_\mu}{\sigma_\theta} k \mathbf{g} \cdot \operatorname{grad} \bar{\theta}. \end{aligned} \quad (15.93)$$

In these equations no expression has been proposed for the production rate density $\bar{\Phi}^c$ of species c . Its postulation depends on the particular problem at hand, which is the reason why it remains unspecified here. For salinity, however, we have $\bar{\Phi}^c = 0$. Moreover, it should be mentioned that the buoyancy related terms in the balance

¹²Notice that in [8] the last term on the right-hand side of (15.93) is in error (misprint).

Table 15.2 Numerical values for the closure constants of the $k - \varepsilon$ model

$c_\mu = 0.09$	$c_1 = 0.126$	$c_2 = 1.92$
$c_3 \approx 0$	$\sigma_k = 1.4$	$\sigma_\varepsilon = 1.3$

relations of turbulent kinetic energy and turbulent dissipation rate have formally been ignored.

To the many empirical constants which arise in the above equations, numerical values must be assigned. These are collected in **Table 15.2**. The numerical values of these coefficients have been obtained by relatively simple model calculations (for details see [17]).

15.4.4 Boundary Conditions

The form of the boundary conditions, which have to be formulated in a solution scheme of the partial differential equations of the $k - \varepsilon$ model, depend on the particular physical situation at hand. In what follows, we will focus attention to problems as they arise in meteorology, oceanography, limnology and conceptually related problems of geophysical or environmental contexts.

‘The field equations (15.88)–(15.93) constitute a set of $7 + \nu$ (‘ ν ’ for ν species mass balances (15.91)) equations for the unknown fields \bar{v} (3), \bar{p} (1), $\bar{\theta}$ (1), \bar{c}_α ($\alpha = 1, 2, \dots, \nu$), k (1), ε (1) unknowns. They form a system of nonlinear partial differential equations, for which boundary conditions must be prescribed. The equations are of parabolic type (they are of first order in time and of second order in the space variables (via the flux parameterizations)). Consequently, boundary conditions must be formulated at the solid and at the free surface for all diffusive-type equations’ [8].

Boundary conditions of momentum: The bottom surface is generally treated as rigid and material, only for extremely shallow regions (e.g. of the atmosphere, the ocean or lakes) the bottom surface may move and material of the basal soil be dislodged. Excluding these cases, the fixed *bottom surface* may allow a certain discharge of water, $Q_\perp^{\text{boundary}}$, into the ground and the velocity tangential to the bed may either be zero (no-slip condition) or related to the basal traction. Let us introduce the notation

$$\begin{aligned}
 v_\perp^s &:= \mathbf{v}^s \cdot \mathbf{n}, \\
 \mathbf{v}_\parallel^s &:= \mathbf{v}^s - (\mathbf{v}^s \cdot \mathbf{n})\mathbf{n} = \mathbf{v}^s - v_\perp^s \mathbf{n}, \\
 p_\perp^s &:= -\mathbf{n} \cdot \mathbf{t}^s \mathbf{n}, \\
 \mathbf{t}_\parallel^s &:= \mathbf{t}^s \mathbf{n} - (\mathbf{n} \cdot \mathbf{t}^s \mathbf{n})\mathbf{n} = \mathbf{t}^s \mathbf{n} + p_\perp^s \mathbf{n},
 \end{aligned} \tag{15.94}$$

in which s is a label for a surface ($s = b$ for the bottom surface) and \mathbf{n} is the unit normal vector perpendicular to the surface and exterior to the domain, in which the

boundary value problem is to be solved. v_{\perp}^s , \mathbf{v}_{\parallel}^s , p_{\perp}^s and \mathbf{t}_{\parallel}^s are, in turn, the water velocity normal and parallel to the surface, and the surface normal pressure and the shear traction parallel to it. With the notation (15.94), the *basal boundary conditions* read (s = b stands for ‘bottom surface’)

$$\overline{v_{\perp}^b} = \mathcal{M}_{\perp}^{\text{ground}}, \quad \mathbf{t}_{\parallel}^b = -\rho^* c_D^b |\overline{\mathbf{v}_{\parallel}^b}| \overline{\mathbf{v}_{\parallel}^b}. \quad (15.95)$$

For $\mathcal{M}_{\perp}^{\text{ground}} = 0$ the bottom surface is impermeable for the water, this is the usual case. Should ground water accretion be substantial, then $\mathcal{M}_{\perp}^{\text{ground}} \neq 0$ follows from a coupling of the $k - \varepsilon$ equations with a ground water model. ρ^* is the water density at 4°C and $c_D^b \approx 1.5 \times 10^{-3}$ is the basal drag coefficient, $c_D^b \rightarrow \infty$ corresponds to the no-slip condition, $\overline{\mathbf{v}_{\parallel}^b} = \mathbf{0}$, and $c_D^b = 0$ models frictionless sliding, for which $\mathbf{t}_{\parallel}^b = \mathbf{0}$.

At the *free surface*, momentum is transferred by wind and atmospheric pressure. Such traction boundary conditions are usually described as follows:

$$\mathbf{t}_{\parallel}^s = \rho_a c_D^s |\mathbf{W}_{\parallel}| \mathbf{W}_{\parallel}(\mathbf{x}^s, t), \quad p_{\perp}^s = p^{\text{atm}}(\mathbf{x}, t), \quad (15.96)$$

in which $\rho_a \approx 1.4 \text{ kg m}^{-3}$ is the density of air at atmospheric pressure, $c_D^s \approx 1.2 \times 10^{-3}$ is the drag coefficient and \mathbf{W}_{\parallel} the wind velocity parallel to the water surface, ordinarily 10m above the surface. Wind velocities measured at different heights above the water surface affect the value of c_D^s , adjustments are then necessary, see the specialized literature, e.g. [7], Chap. 13. A dependence of the atmospheric pressure on the spatial coordinate and time can often be ignored for lakes, because their extents are generally small in comparison to the spatial variability of the atmospheric pressures. Only in storm surge situations $\text{grad } p^{\text{atm}}(\mathbf{x}, t) \neq 0$ and must be accounted for.

Boundary conditions for the temperature field: At the bottom surface one usually requests that

$$\overline{\theta}(\mathbf{x}^b, t) = [\theta(z^b, t)]^{\text{static}}, \quad (15.97)$$

where $[\theta(z^b, t)]^{\text{static}}$ is the static temperature distribution prescribed and held constant. Alternatively, one may also request continuity of the heat flow across the bottom surface

$$\mathbf{q}^s \cdot \mathbf{n} = Q_{\perp}^{\text{geotherm}}, \quad (15.98)$$

where (15.98) is to be preferred over (15.97) in regions of high volcanic activity. When the thermal regime of a water basin (lake or ocean) is coupled to the thermal regime of the ground then continuity of both the heat flow and the basal surface temperature are required, viz.,

$$\overline{[\theta(\mathbf{x}^b, t)]} = 0, \quad \overline{[\mathbf{q}^b \cdot \mathbf{n}]} = 0, \quad (15.99)$$

in which $\llbracket f \rrbracket$ is the difference of the values of f on the side of the ground (f^+) and of the water (f^-). This situation requires a mathematical model for the lake domain and its complement (i.e. the exterior region to the lake).

The most difficult setting of a boundary condition is the energetic transfer at the free surface of a lake or the ocean. The proper handling of this problem is pursued with a radiation balance, which may be expressed as

$$\bar{q}^s \cdot \mathbf{n} = Q_{\text{ir}}^{\text{a}} - Q_{\text{ir}}^{\text{w}} + Q_{\ell} + Q_{\text{s}}. \quad (15.100)$$

Here, Q_{ir}^{a} and Q_{ir}^{w} are the black body radiation above the surface and water, whilst Q_{ℓ} and Q_{s} are the latent and sensible heat fluxes between water and air. For their explicit parameterizations, see the specialized literature, e.g. [7], pp. 582–584.

Boundary conditions for the species concentration: Boundary conditions for tracer substances depend on the kind of biochemical-physical processes to which these substances are subjected and whether bio-chemical-hydro-mechanical processes are in focus. Boundary conditions to be established depend largely upon the complexity of the problem at hand. In the simplest cases either the concentration or its derivative normal to the free surface or a combination of these is generally prescribed at the free surfaces.

Boundary conditions for k and ε : In general, these are rather difficult to postulate, because the peculiar conditions of turbulence near boundaries are not directly accessible. Commonly one wishes to prescribe numerical values for k and ε or their fluxes (derivatives of k and ε perpendicular to the surface). Such values or formulae can often only be obtained by consideration of the dynamics of the boundary layer.

At the *bottom surface* where the flow is weakly turbulent or turbulence has died out all together, one may require

$$k = 0, \quad \varepsilon = 0 \quad \text{at the bottom.} \quad (15.101)$$

However, close to solid walls the $k - \varepsilon$ model requires the introduction of wall functions to properly describe the turbulent boundary layer. This means that (15.101) is an approximation and should be taken as a gross simplification of the correct behavior.

At the *free surface* a physically appropriate postulation of the boundary conditions is more complicated and also more critical. A fairly simple and also physically transparent assumption is to request that there is no diffusive loss of turbulent kinetic energy and turbulent energy dissipation through the free surface. With the gradient type relations (15.61) this says

$$\frac{\partial k}{\partial \mathbf{n}} = \mathbf{0}, \quad \frac{\partial \varepsilon}{\partial \mathbf{n}} = \mathbf{0} \quad \text{at the free surface.} \quad (15.102)$$

The reader is asked to consult the specialized literature e.g. [7, 19].

15.4.5 Closing Remarks

In this chapter an introduction into turbulence modeling has been given. The basic ‘philosophy’ in such modeling is that a sufficient level of approximation of the true fluctuation dynamics is replaced by an averaging or smoothing operation, by which those variations of the physical variables are eliminated, which are thought to exert a negligible influence upon the processes under consideration. The first such averaging operation has been introduced by JOSEPH BOUSSINESQ (1872) [3] and in a more detailed mathematical form by OSBORNE REYNOLDS [14]. The averaging operations have been introduced in this chapter either by spatial or temporal or statistical filters, which have different mathematical properties and, therefore, yield averaging equations in which the differences in eliminated fluctuations are accounted for by adequately selected closure conditions. The statistical averaging operator as a filter of homogeneous processes is based on ensemble averaging; it is defined by the mathematical properties (15.6)–(15.9) and computational rules summarized in (15.10). The acronym for the form of the emerging equations is RANS, for REYNOLDS-Averaged-NAVIER–STOKES equations. This filter satisfies the so-called ergodic property, according to which multiple averaging does not yield smoother and smoother computed processes. Of course, such behavior cannot universally be expected from physical processes. Results, based on computations founded on RANS equations must be interpreted as approximations, possibly subject to amendment. Therefore, the statistical filter is today sometimes replaced by more general averaging rules, which do not obey ergodicity. The so-called Large Eddy Simulations (LES) are such more general averaging rules, which have *not* been dealt with in this chapter.

The balance laws for mass, momentum, energy and for a scalar field, when subject to the RANS-averaging operation again possess balance equation structure. Their detailed forms (15.21)–(15.24) contain in comparison to the non-averaged analogous equations additional 4 correlation terms (15.25), three of which have flux nature and one is an energy production rate. In an attempt of turbulent closure of the REYNOLDS stress tensor \mathbf{R} , (15.31), and the mean turbulent dissipation rate $\frac{1}{\rho}\overline{\Phi}$ two new quantities arise, the turbulent kinetic energy, k , defined as (15.29) and the turbulent dissipation rate ε , defined in (15.30), but naturally introduced in (15.34), for which independent closure statements must be postulated. It should be stated here that in the earliest zeroth order closure attempt, see the following Chap. 16, no closure relations needed to be postulated, because these variables did not arise in the simpler flow configurations, which were under focus there.

Nevertheless, the earliest proposals for the scalar stress components under plane or axisymmetric flow due to JOSEPH BOUSSINESQ (1872) [3] introduced a turbulent viscosity ε , suggested by

$$\tau_{12} = \rho\varepsilon \frac{\partial u_1}{\partial x_2}.$$

Follow-up suggestions for the turbulent heat flux, q , (15.41), and turbulent mass flux (15.42) were then analogously proposed with gradient-type proposals (15.43), ‘setting in motion’ the victorious advance of the gradient-type closure relations. This apparent ‘gradient-mania’ found its continuation in the first order closure scheme, as we have demonstrated when deriving and motivating the balance laws for the turbulent kinetic energy, k and the turbulent dissipation rate, ε , and the closure postulates for the flux of turbulent kinetic energy (15.68) and turbulent dissipation rate (15.73). Here, too, it seems as if the second and third generations of turbulence modelers would have forgotten already PRANDTL’s attempts in his 1933 and 1945 [12, 13] papers with the intention to reach better agreement of the theoretical mean velocity distributions with gradient free parameterizations of flux terms, see Chap. 16.

References

1. Aczel, A.D.: *Pendulum – Léon Foucault and the Triumph of Science*. Washington Square Press, New York (2003). ISBN 0-74344-6439-6
2. Bäuerle, E., Chubarenko, B., Chubarenko I., Halder, J., Hutter, K., Wang, Y.: Autumn physical limnological experimental campaign in the Mainau Island Limnological Zone of Lake Constance (Constance Data Band) 12 October–19 November 2001. Report of the ‘Sonderforschungsbereich 454 Bodenseelittoral’, 85 p. (2001)
3. Boussinesq, J.: *Essay sur la théorie des eaux courantes*. Mémoires présentés par div. Savants l’Académie des Sciences de l’Institut de France. Tome 23 (avec supplément in Tome 24) (1872)
4. Egolf, P.W.: Difference-quotient turbulent model: a generalization of Prandtl’s mixing length theory. *Phys. Rev. E* **49**(2), 1260–1268 (1994)
5. Gad-el-Hak, M.: *Flow Control: Passive, Active and Research Flow Management*. Cambridge University Press, Cambridge (2000)
6. Hanjalic, K., Launder, B.E.: A Reynolds stress model of turbulence and its application to thin shear flows. *J. Fluid Mech.* **52**, 609–638 (1972)
7. Hutter, K., Jöhnk, K.: *Continuum Methods of Physical Modeling*, 635 pp. Springer, Berlin (2004)
8. Hutter, K., Wang, Y., Chubarenko, I.: *Physics of Lakes, Volume 1: Foundation of the Mathematical and Physical Background*, 434 pp. Springer, Berlin (2011)
9. Jones, W.P., Launder, B.E.: The prediction of laminarisation with a two equation model of turbulence. *J. Heat Mass Transf.* **15**, 301–314 (1972)
10. Launder, B.E., Spalding, D.B.: The numerical computation of turbulent flow. *Comput. Methods Appl. Mech. Eng.* **3**, 269–288 (1974)
11. Prandtl, L.: Bericht über Untersuchungen zur ausgebildeten Turbulenz. *Zeitschrift für angewandte Mathematik und Mechanik (ZAMM)* **5**(2), 136–39 (1925)
12. Prandtl, L.: Neuere Ergebnisse der Turbulenzforschung. *Zeitschr. VDI* **77**, 105–113 (1933)
13. Prandtl, L.: Über ein neues Formelsystem für die ausgebildete Turbulenz. *Nachr. Akad. Wiss. Göttingen Math.-Phys. Klasse*, pp. 6–19 (1945)
14. Reynolds, O.: An experimental investigation of circumstances, which determine whether the motion of water shall be direct or sinuous, and the law of resistance in parallel channels. *Philos. Trans. R. Soc. Lond.* **A 174**, 935–982 (1883)
15. Reynolds, O.: On the dynamical theory of turbulent incompressible viscous fluids and the determination of the criterion. *Philos. Trans. R. Soc. Lond.* **A 186**, 123–164 (1894)
16. Rodi, W.: Examples of calculation methods for flow and mixing in stratified fluids. *J. Geophys. Res.* **C5**(92), 5305–5328 (1987)

17. Rodi, W.: Turbulence Models and their Application in Hydraulics IAHR Monograph Series. A.A. Balkema, Rotterdam/Brookfield (1993)
18. Schmidt, E.H.W.: Einführung in die technische Thermodynamik und in die Grundlagen der chemischen Thermodynamik, 10th edn. Springer, Berlin (1963)
19. Svensson, U.: A mathematical model for the seasonal variation of the thermocline, Report 1002, Department of WaterResources Engineering, University of Lund, Sweden, 187 pp. (1978)
20. Umlauf, L.: Turbulence Parameterization in Hydro-Biological Models for Natural Waters. Ph.D. Dissertation, Department of Mechanics, Darmstadt University of Technology, Darmstadt, Germany, 231 p. (2001)
21. Vogel-Prandtl, J.: Ludwig Prandtl, a Personal Biography Drawn from Memories and Correspondence. Universitätsverlag Göttingen, 248 p. (2014)
22. Weis, J.: Ein algebraisches Reynolds Spannungs-Modell. Ph.D. Dissertation, Department of Mechanics, Darmstadt University of Technology, Darmstadt, Germany, 111 p. (2001)
23. Wilcox, D.C.: Reassessment of the scale-determining equation for advanced turbulence models. AIAA J. **26**(11), 1299–1310 (1988)
24. Wilcox, D.C.: Turbulence Modeling for CFD, 2nd edn. DCW Industries, Inc., La Canada (1998)

Chapter 16

Turbulent Mixing Length Models and Their Applications to Elementary Flow Configurations

Abstract In comparison to Chap. 15, this chapter goes back one step by scrutinizing the early zeroth order closure relations as proposed by PRANDTL, VON KÁRMÁN and collaborators. The basis is BOSSINESQ's (Mém. Prés. Div. Savant Acad. Sci. Paris, 23:46 [3]) ansatz for the shear stress in plane parallel flow, τ_{12} , which is postulated to be proportional to the corresponding averaged shear rate $\partial v_1 / \partial x_2$ with coefficient of proportionality $\rho \varepsilon$, where ρ is the density and ε a kinematic turbulent viscosity or turbulent diffusivity (m^2s^{-1}). In turbulence theory the flux terms of momentum, heat and suspended mass are all parameterized as gradient-type relations with turbulent diffusivities treated as constants. PRANDTL realized from data collected in his institute that ε was not a constant but depended on his mixing length squared and the magnitude of the shear rate (PRANDTL, ZAMM 5:136–139, [23]). This proposal was later improved ("Prandtl (1942), Abriss der Strömungslehre" PRANDTL [25]) to amend the unsatisfactory agreement at positions where shear rates disappeared. The 1942-law is still local, which means that the REYNOLDS stress tensor at a spatial point depends on spatial velocity derivatives at the same position. PRANDTL, in a second proposal of his 1942-paper suggested that the turbulent diffusivity should depend on the velocity difference at the points where the velocity of the turbulent path assumes maximum and minimum values. This proposal introduces some non-locality, and it yielded better agreement with data, but PRANDTL left the non-gradient-type dependence in order to stay in conformity with BOUSSINESQ. It does become neither apparent nor clear that Prandtl or the modelers at that time would have realized that non-local effects would be the cause for better agreement of the theoretical formulations with data. The proposal of complete nonlocal behavior of the REYNOLDS stress parameterization came in 1991 by P. EGOLF and subsequent research articles during 20 years, in which also the local strain rate (=local velocity gradient) is replaced by a difference quotient. We motivate and explain the proposed Difference Quotient Turbulence Model (DQTM) and demonstrate that for standard two-dimensional configurations analyzed in this chapter its performance is superior to other zeroth order models.

This chapter has been criticized by Prof. P. EGOLF. This led to improvements. The authors thoroughly thank for this help.

Keywords Local/nonlocal turbulent stress closure · Criticisms on zeroth order local stress closures · PRANDTL turbulent plane wake · Axisymmetric isothermal jet · Turbulent jet in parallel co-flow · Plane POISEUILLE flow

List of Symbols

Roman Symbols

A, B	Constants of integration in plane POISEUILLE flow
a	Half width of a two-dimensional channel
b	Half width of a plane or axial turbulent jet
c	Turbulent convection parameter
D	Strain rate, stretching tensor (deviator)
d	Diameter of a cylinder immersed in a parallel flow
\overline{F}	Mean force per unit width exerted on a circular cylinder by a viscous fluid
$f_1(\eta), f_2(\eta), f_{12}(\eta)$	Dimensionless functions describing the transverse variation of \overline{v}_1^* , \overline{v}_2^* , $\overline{v'_1 v'_2}$
$f_{ii}, ii = 11, 22, 33$	Dimensionless auto-correlation functions for $(v'_i)^2$
\mathbf{g}, g	Gravity vector—constant
$g_1(\eta)$	Scaled transverse distribution of \overline{v}_1^* for plane POISEUILLE flow: $g_1(\eta) = f_1(\eta)/f_1(0)$
g_{ii}	$g_{ii} = \sqrt{f_{ii}}$ ($ii = 11, 22, 33$) (see (16.91) and (16.102)).
$k_1 = 4\beta$	Auxiliary parameter
k	Turbulent kinetic energy ($\frac{1}{2}\overline{v'_i v'_i}$), dimensionless constant
kd	Characteristic length of the similarity representation of field variables (16.22)–(16.25)
ℓ, ℓ'	PRANDTL mixing lengths
m_0, m_1	Axial mass flow at the exit nozzle of a round jet—at a general cross section
\mathcal{O}	Order symbol
p, \overline{p}, p_0	Pressure, mean—constant reference—
p	Virtual origin of a jet stream, production of turbulent kinetic energy
p_0, p_1, p_2, p_{12}	Exponent of $(x_1 - p)/(kd)$ in the similarity representations of $b, \overline{v}_1^*, \overline{v}_2^*, \overline{v'_1 v'_2}$
$\mathbf{R} = \overline{\rho v'_1 \otimes v'_2}$	REYNOLDS stress tensor
R_{12}	REYNOLDS shear stress $R_{12} = \tau_{12} = -\overline{\rho v'_1 v'_2} = \nu_t \frac{\partial \overline{v}_1}{\partial x_2}$
\mathbf{R}_D	REYNOLDS stress deviator
\mathbb{R}	REYNOLDS number
\mathbf{t}^R	Viscous stress tensor (deviator)
U_G	Undisturbed parallel flow velocity far upstream
$U + U_G$	Mean exit velocity at the nozzle of a jet exit
$\mathbf{v} = (v_1, v_2, v_3)$	Velocity field components of \mathbf{v} in an orthogonal, not-necessarily orthonormal coordinate system

$\bar{v}_{\max}, \bar{v}_{\min}$	Maximum/minimum mean velocity in the turbulent domain at a fixed value of x_1
\bar{v}_1, \bar{v}_2	x_1 -, respectively, x_2 -component of the mean velocity field
$\frac{v_0}{v_1^*}$	Steady jet stream velocity at the exit nozzle
$\overline{(v'_i)^2}$	Reduction of \bar{v}_1 from U_G
$\mathbf{x} = (x_1, x_2, x_3)$	Auto-correlation functions of the velocity components v'_i ($i = 1, 2, 3$)
x_0	Position vector with its components
$x_{2\max}$	Characteristic length (equivalent to kd)
	Position x_2 (at fixed x_1), where \bar{v}_1 assumes a Maximum

Greek Symbols

$\alpha = f_1(0)/\mathbb{R}^*$	Parameters in the DQTM equation (16.171) for plane POISEUILLE flow
$\beta = \sigma (f_1(0))^2$	Auxiliary parameter, dimensionless parameter in the similarity representation of $b(x_1)$ (see (16.25))
ξ_1	Shifted coordinate x_1 with origin at $x_1 = -p$
$\eta = \frac{x_2}{b(x_1)}$	Dimensionless scaled transverse coordinate for a jet stream
η_0	Parameter in representation (16.46) to adjust $f_1(\eta)$ to the experiments
ξ, η	Dimensionless Cartesian coordinates for plane POISEUILLE flow: $\xi = x_1/a, \eta = x_2/a$
$\eta = \rho\nu$	Dynamic viscosity
ν, ν_t	Kinematic material/turbulent viscosity
ρ	Mass density
χ	Unspecified field quantity
$\bar{\chi}$	Mean value of χ in turbulent processes
χ'	Fluctuation of χ in a REYNOLDS averaging process
$\overline{\chi'\psi'}$	Correlation product of χ and ψ
χ_2	Characteristic length in the x_2 -direction, e.g., $b(x_1)$
$\chi = \beta(\alpha)/4$	Order parameter in plane POISEUILLE flow
$db/dx_1 = \tan \alpha$	Auxiliary variable

16.1 Motivation/Introduction

As pointed out in Chap. 15, turbulent motions are, in principle, analyzed by performing a statistical average of the governing variables into mean quantities and fluctuations according to

$$\chi = \bar{\chi} + \chi', \quad \chi \in [v_1, v_2, v_3, p, t_{ij}^R, \dots], \quad (16.1)$$

where v_1, v_2, v_3 are any three independent components of the velocity field. Moreover, $\bar{\chi}$ denotes the mean value of χ , interpreted as an ensemble average, and χ' is the deviation of χ from its mean value $\bar{\chi}$, called the *fluctuation* or *pulsation* of χ . For REYNOLDS averaging they have the properties that

$$\overline{\chi'} = 0, \quad \overline{\partial\chi} = \partial\bar{\chi}, \quad \overline{\bar{\chi}} = \bar{\chi}, \quad \overline{\chi\psi} = \bar{\chi}\bar{\psi} + \overline{\chi'\psi'}. \quad (16.2)$$

Performing for a density preserving fluid the averages of the equations of balances of mass and momentum yields, on use of the computational rules (16.2),

$$\operatorname{div} \bar{\mathbf{v}} = 0, \quad (16.3)$$

$$\left\{ \rho \frac{\partial \bar{\mathbf{v}}}{\partial t} + \rho \operatorname{div} \left[(\bar{\mathbf{v}} \otimes \bar{\mathbf{v}}) + \overline{(\mathbf{v}' \otimes \mathbf{v}')} \right] \right\} = -\operatorname{grad} \bar{p} + \operatorname{div} \bar{\mathbf{t}}^R + \rho \mathbf{g}, \quad (16.4)$$

as have also been shown in (15.21) and (15.22), in which $\{\bar{\mathbf{v}}, \bar{p}, \bar{\mathbf{t}}^R, \rho, \mathbf{g}\}$ are the averaged velocity vector, pressure, frictional (or viscous) stress tensor and the constant density and gravity vector. Moreover, $\mathbf{v} \otimes \mathbf{v}$ is the dyadic product of the velocity vector with itself. Defining by (15.26), i.e.,

$$\mathbf{R} = -\rho \overline{\mathbf{v}' \otimes \mathbf{v}'} \quad (16.5)$$

the symmetric turbulent stress tensor, the averaged momentum equation can also be written as

$$\left. \begin{array}{l} \rho \left(\frac{\partial \bar{\mathbf{v}}}{\partial t} + \operatorname{div} (\bar{\mathbf{v}} \otimes \bar{\mathbf{v}}) \right) \\ \rho \left(\frac{\partial \bar{\mathbf{v}}}{\partial t} + (\operatorname{grad} \bar{\mathbf{v}}) \bar{\mathbf{v}} \right) \end{array} \right\} = -\operatorname{grad} \bar{p} + \operatorname{div} \bar{\mathbf{t}}^R + \operatorname{div} \mathbf{R} + \rho \mathbf{g}. \quad (16.6)$$

Because regularly, $\|\operatorname{div} \bar{\mathbf{t}}^R\|$ is much smaller than $\|\operatorname{div} \mathbf{R}\|$, the viscous stress is often ignored in (16.6) for a fully developed turbulent flow. Furthermore, the gravity force is often also absorbed into a hydrostatic pressure such that

$$\bar{p} = p_{\text{stat}} + p_{\text{dyn}}, \quad \text{such that} \quad \operatorname{grad} p_{\text{stat}} = \rho \mathbf{g}. \quad (16.7)$$

The classical viscous stress in a NEWTONian fluid is given by $\mathbf{t}^R = 2\rho\nu\mathbf{D}$ so that its average is given by

$$\bar{\mathbf{t}}^R = 2\rho\nu\bar{\mathbf{D}} \quad (16.8)$$

having in three (two) dimensions five (two) independent components because $\operatorname{tr} \bar{\mathbf{D}} = 0$. An analogous parameterization of \mathbf{R} for fully developed turbulence is, however, not appropriate, because, according to (16.5), the *turbulent kinetic energy*, k , defined by

$$k := \frac{1}{2} \overline{v'_i v'_i} = \frac{1}{2} \text{tr} (\overline{\mathbf{v}' \otimes \mathbf{v}'}) = -\frac{1}{2\rho} \text{tr} \mathbf{R}, \quad (16.9)$$

does not need to vanish in general (even though the fluid has been assumed to be density preserving). Consequently, a consistent zeroth order stress parameterization must be of the form (see also (15.32)₁)

$$-\overline{\mathbf{v}' \otimes \mathbf{v}'} = \frac{1}{\rho} \mathbf{R} = -\frac{2}{3} k \mathbf{1} + 2\nu_t \overline{\mathbf{D}}. \quad (16.10)$$

In the above, ν and ν_t are the material and turbulent viscosities, respectively and are often of quite different orders of magnitude (e.g. $\nu \approx 10^{-6} \text{m}^2 \text{s}^{-1}$ and $\nu_t \geq 10^{-3} \text{m}^2 \text{s}^{-1}$, for water). The first proposal of the form (16.10) is due to JOSEPH BOUSSINESQ (1872) [3]. In his parameterization, the turbulent kinetic energy was not modeled ($k = 0$), so his proposal corresponds to $\frac{1}{\rho} \mathbf{R} = 2\nu_t \overline{\mathbf{D}}$, or in Cartesian tensor notation $\frac{1}{\rho} R_{ij} = \nu_t (\overline{v_{i,j}} + \overline{v_{j,i}})$. BOUSSINESQ was looking at uniaxial axisymmetric plane flow in pipes or plane parallel flow, thus situations with the shear stress being of the form

$$R_{12} = \tau_{12} = \nu_t \frac{\partial \overline{v}_1}{\partial x_2}, \quad (16.11)$$

since $\overline{v}_2 = \overline{v}_3 = 0$. Here and henceforth we have changed the notation: For turbulent simple shear flows, $\overline{v}_1(x_2, x_3)$, the turbulent shear stress τ_{12} or τ is often used instead of R_{12} . In what follows, the analysis will follow PETER EGOLF [8]. According to this reference, several authors [2, 8, 29] have since the 70's of the last century criticized the phenomenological gradient approaches such as (16.10) or (16.11). PETER EGOLF mentions several criticisms, which we shall now report.¹

- **Criticism 1:** The analogy between molecular and turbulent transport is questionable. In molecular dynamics the size of the molecules is small compared to the mean free path between the molecules. In contrast to this, the largest interacting eddies may have any size, i.e. may not be small as compared with the characteristic length scale of the flow under consideration. A fortiori, the 'mixing length' is not even small as compared with the characteristic length scale of the flow under consideration.

In the kinetic theory of gases the viscosity is proportional to the product of the root-mean-square velocity and the mean free path of the molecules. LUDWIG PRANDTL (1925) [23] in his *mixing length theory* introduced the mean velocity by a first order expansion amounting to an eddy-exchange in a layer of thickness ℓ , defining the mixing length ℓ :

$$\tau_{12}(x_1, x_2) = \rho \ell^2 \left| \frac{\partial \overline{v}_1}{\partial x_2} \right| \frac{\partial \overline{v}_1}{\partial x_2}, \quad \varepsilon_{\text{turb}} = \ell^2 \left| \frac{\partial \overline{v}_1}{\partial x_2} \right|. \quad (16.12)$$

¹Quotation is not exactly word by word.

This mixing-length proposal found its successful application in free turbulence and in plane viscous boundary layers as well as in atmospheric flows (planetary boundary layers, geostrophic flows, HOLTON (1979) [16]).² So, ‘length \times velocity’ on the molecular dynamic side is replaced by ‘length² \times Strain rate’ on the turbulent side. Whereas these expressions are dimensionally equal, they express different emphases of the physics.

- **Criticism 2:** Comparing measured and calculated mean velocity profiles \bar{v}_1 as functions of x_2 revealed deviations at the points of vanishing derivatives, $\partial\bar{v}_1/\partial x_2 = 0$. This was recognized by LUDWIG PRANDTL, and in 1942 [25] he proposed an extended version of the eddy viscosity by making the eddy viscosity also dependent on the curvature of the velocity profile at the considered point, viz.,

$$\tau_{12}(x_1, x_2) = \rho\ell^2 \left\{ \left(\frac{\partial\bar{v}_1}{\partial x_2} + \ell' \frac{\partial^2\bar{v}_1}{\partial x_2^2} \right)^2 \right\}^{1/2} \frac{\partial\bar{v}_1}{\partial x_2}, \quad (16.13)$$

where he assumed the second mixing length ℓ' to be statistically equally distributed in the positive and negative directions, so that in this *mean gradient theory* the cross terms in the curly bracket of (16.13) cancel out, viz.,

$$\tau_{12} = \rho\ell^2 \left\{ \left(\frac{\partial\bar{v}_1}{\partial x_2} \right)^2 + (\ell')^2 \left(\frac{\partial^2\bar{v}_1}{\partial x_2^2} \right)^2 \right\}^{1/2} \frac{\partial\bar{v}_1}{\partial x_2}. \quad (16.14)$$

Computations with (16.14) instead of (16.13) yielded better agreement with data, see H. GÖRTLER [12].

- **Criticism 3:** Model predictions with (16.13) or (16.14) are still deficient since they predict characteristic length scales which are much smaller than the largest eddies observed in the flow under consideration. LUDWIG PRANDTL (1942), therefore, tried in the *free shear layer theory* to relate the eddy viscosity to the overall flow conditions, namely the width b of the turbulent zone and the greatest mean velocity difference

$$\tau_{12} = \kappa\rho b(\bar{v}_{1\max} - \bar{v}_{1\min}) \frac{\partial\bar{v}_1}{\partial x_2}, \quad (16.15)$$

in which κ is a constant.

In this expression PRANDTL’s viscosity is now ‘length \times velocity’ ($= b \times (\bar{v}_{1\max} - \bar{v}_{1\min})$) as in molecular dynamics. More importantly, however, if we compare the eddy viscosity of (16.15) with the earlier ones, e.g. (16.12) and (16.13), it is recognized that LUDWIG PRANDTL replaces local expressions by nonlocal ones, in which the eddy viscosity is replaced by a nonlocal term in (16.15) [the term

²For LUDWIG PRANDTL’s derivation in the German language along with K.H.’s translation into English, see Appendix to this chapter.

($\bar{v}_{1\max} - \bar{v}_{1\min}$)]. This is in partial anticipation of PETER EGOLF's [8] analogous but extended difference expression. H. GÖRTLER³ (1942) [12] calculated velocity functions with the approach (16.15), which he found to be in good agreement with experimental results, but still with one exception:

- **Criticism 4:** At the boundary of the mixing zone there are deviations, because the eddy viscosity in (16.15) does not vanish there. To alter (16.15) and improve the turbulent shear stress proposition, let us write (16.15) in the form

$$\tau_{12}(x_1, x_2) = \kappa \rho b^2 \frac{\partial \bar{v}_1}{\partial x_2} \left(\frac{\bar{v}_{1\max} - \bar{v}_{1\min}}{b} \right). \quad (16.16)$$

When we assume the difference of the positions, at which $\bar{v}_{1\max}$ and $\bar{v}_{1\min}$ arise, to be the distance b (the half width of the turbulent jet), then the last term may be called a *difference quotient*. Formula (16.16) contains the differential, $\partial \bar{v}_1 / \partial x_2$, and a difference quotient, the last term in (16.16). It bears the disadvantage that the differential quotient does not involve the position x_2 for which $\tau_{12}(x_1, x_2)$ is calculated. However, the difference quotient introduces non-local effects, which are not present in earlier parameterizations of τ_{12} except in (16.15) which is due to LUDWIG PRANDTL. This is so, since in the evaluation of (16.16) at least two spatial points are involved namely that, where τ_{12} is evaluated and those where $\bar{v}_{1\min}$ and $\bar{v}_{1\max}$ are evaluated.

- **The difference quotient model of Peter Egolf [8]:** One can go further than in the parameterization (16.16) and also replace $\partial \bar{v}_1 / \partial x_2$ by a difference quotient by writing

$$\tau_{12}(x_1, x_2) = -\overline{\rho v'_1 v'_2} = \rho \chi_2 \frac{db}{dx_1} (\bar{v}_1 - \bar{v}_{1\min}) \left(\frac{\bar{v}_{1\max} - \bar{v}_1}{x_{2\max} - x_2} \right), \quad (16.17)$$

in which $\chi_2 \in [x_2, b]$ is a variable or characteristic length scale of the flow, perpendicular to the main flow direction and $x_{2\max}$ denotes the location where the mean downstream velocity attains its maximum, $\bar{v}_{1\max}$. Note that this rather unusual model does not make use of the eddy viscosity concept (16.11).

PETER EGOLF [8] writes 'The difference quotient, which for certain locations is a mean quotient over a very large domain, introduces a non-locality. For that reason criticism 1 does not apply to this model'. Computed results for turbulent shear flows 'show no deviations from measurements at the points of vanishing derivatives (criticism 2)'. The shortcoming of too small computed mixing lengths (criticism 3) does not apply either, 'because χ_2 is a large length scale, e.g., the width b of the entire turbulent zone. Moreover, if we let \bar{v}_1 approach the value $\bar{v}_{1\min}$ at the boundary, the turbulent shear stress in (16.17) will vanish as it should, (criticism 4)'. From this discussion, PETER EGOLF [8] concludes, 'that the difference quotient model is a natural continuation of LUDWIG PRANDTL'S ideas on momentum transfer'.

³For a short biography of H. GÖRTLER see Fig. 16.1.

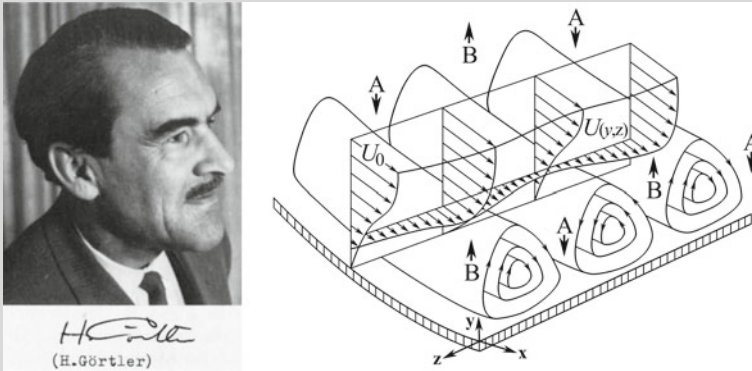


Fig. 16.1 HENRY GÖRTLER also HEINRICH GÖRTLER (26. Oct. 1909 – 31. Dec. 1987). (Right) GÖRTLER vortices: ‘A: down-wash regions; B: up-wash regions’.

HENRY GÖRTLER, born in Calgary (Canada) came in 1923 to Giessen, Germany. He studied architecture and then mathematics and physics at the University in Munich with ARNOLD SOMMERFELD and afterwards at the University of Giessen with JAFFÉ and HARALD GEPPERT and wrote his doctoral dissertation on ‘Asymptotische Eigenwertgesetze bei Differentialgleichungen vierter Ordnung’ (‘Asymptotic laws of eigenvalues of fourth order differential equations’) (1936) [11]. In 1937 he became a close collaborator of Ludwig Prandtl in Göttingen, where he worked on boundary layer theory. Noteworthy are the GÖRTLER series in the computation of two-dimensional laminar boundary layers (1957) and the TAYLOR-GÖRTLER vortices [instability of a three-dimensional boundary layer as an extension of the instability of two-dimensional laminar boundary layers (TOLLMIEÑ-SCHLICHTING waves), see the above right panel of the figure, showing a GÖRTLER vortex © [13]].

In 1944 GÖRTLER became associate professor and in 1949 full professor at the University of Freiburg, Germany, where he founded the Institute of Applied Mathematics. He was a member of the academy of Sciences in Heidelberg (1961) and Leopoldina (1963) and received the CARL-FRIEDRICH GAUSS Medal (1967). Moreover, he received an honorary doctorate from the university of Calgary and was president of the ‘Gesellschaft für Angewandte Mathematic und Mechanik’ (GAMM) (1955–58).

The text is based on www.wikipedia.org

The above developments of LUDWIG PRANDTL’s mixing-length postulates lay open two modeling operations, which are in conflict with today’s schemes of continuum material modeling as well as modern turbulence closure procedures: These are loss of (i) the locality principle and absence of (ii) Euclidean invariance. Both these properties are explicitly spelled out above and clearly evidenced by the above criticisms, and they are manifest in the formulae (16.15) and (16.17). Interestingly, one of the authors of this book (K.H.) has through most of his career as continuum modeler never looked at turbulence from such a point of view. And indeed, modern higher order turbulence closure schemes, see [17], neither apply principles of non-linearity consequentially, but accept the violation of Euclidean invariance, which is so obvious in formulae (16.15) and (16.17).

It is nevertheless conceptually tempting to scrutinize P. EGOLF’s extension of L. PRANDTL’s shear stress formulae, in particular, because it will be seen that computational results are more satisfactory when compared with experiments and analytical results based on LUDWIG PRANDTL’s proposal, see e.g., [12, 26].

On the other hand, it seems to be pretty clear from the analysis in this chapter that it will be practically impossible to apply L. PRANDTL’s or P. EGOLF’s ad hoc non-locality concept in a fully three dimensional turbulence field theory.

16.2 The Turbulent Plane Wake

A turbulent plane wake is created e.g. if a constant parallel flow U_G in the x_1 -direction passes a circular cylinder of, say, diameter d and generates a (symmetric) velocity profile as shown in Fig. 16.2. Sufficiently far downstream from the cylinder the mean perturbed flow is given by

$$\bar{v}_1 = U_G - \bar{v}_1^*, \tag{16.18}$$

in which \bar{v}_1^* is the reduction of the mean flow velocity behind the cylinder. To guarantee fully turbulent velocity disturbances, experience tells that the REYNOLDS number must be in the range

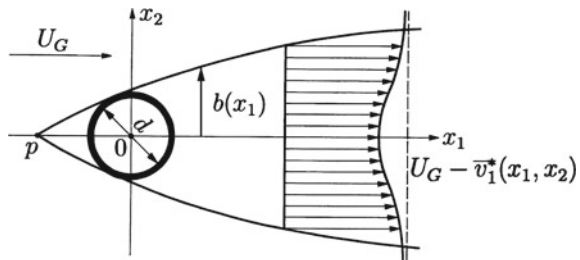
$$\mathbb{R} \equiv \frac{U_G d}{\nu} > 800. \tag{16.19}$$

Moreover, at positions far downstream, i.e. for

$$\xi_1 = \frac{x_1 - p}{d} \gg 0, \tag{16.20}$$

it can be expected that a self similar flow regime with \mathbb{R} -similarity occurs. This regime has its origin at $x_1 = p$, upstream of the axis of the cylinder. The Cartesian coordinates x_1 and x_2 have their origin in the center of the cylinder and are oriented parallel and perpendicular to the approaching velocity U_G , respectively.

Fig. 16.2 Turbulent plane wake flow behind a cylinder



The balance laws of mass and momentum are applied to the density preserving fluid, without gravity, with negligible viscosity and for steady state conditions. This yields for the continuity and EULER equations (see HINZE [14], Chap. 6), after applying a scale analysis, the equations

$$\begin{aligned} \frac{\partial}{\partial x_1} \left(\frac{\bar{v}_1^*}{U_G} \right) + \frac{\partial}{\partial x_2} \left(\frac{\bar{v}_2^*}{U_G} \right) &= 0, \\ \frac{\partial}{\partial x_1} \left(\frac{\bar{v}_1^*}{U_G} \right) - \frac{\partial}{\partial x_2} \left(\frac{v'_1 v'_2}{U_G^2} \right) &= 0. \end{aligned} \quad (16.21)$$

Similarity solutions are found for (16.21) by transforming these equations into ordinary differential equations in a suitably chosen new coordinate $\eta = \hat{\eta}(x_1, x_2)$. Based on precursory use by O. HINZE [14], P. EGOLF [8] has found that this goal is achieved by the following relations.

$$\bar{v}_1^* = U_G \left(\frac{x_1 - p}{kd} \right)^{p_1} f_1(\eta), \quad (16.22)$$

$$\bar{v}_2^* = U_G \left(\frac{x_1 - p}{kd} \right)^{p_2} f_2(\eta), \quad (16.23)$$

$$\overline{v'_1 v'_2} = -U_G^2 \left(\frac{x_1 - p}{kd} \right)^{p_{12}} f_{12}(\eta), \quad (16.24)$$

$$\eta = \frac{x_2}{b(x_1)}, \quad b(x_1) = \beta \left(\frac{x_1 - p}{kd} \right)^{p_0} kd. \quad (16.25)$$

In the above, the quantity $b(x_1)$ denotes a characteristic width of the turbulent free shear flow and k is a constant. Moreover, U_G, p, p_1, p_2, p_{12} are constants, while $f_1(\eta), f_2(\eta), f_{12}(\eta)$ are profile functions for the velocity components \bar{v}_1^*, \bar{v}_2^* and the shear stress $\rho v'_1 v'_2$. It is easy to show that

$$\begin{aligned} \frac{\partial}{\partial x_1} &= \frac{\partial \eta}{\partial x_1} \frac{d}{d\eta} = -p_0 \left(\frac{1}{x_1 - p} \right) \eta \frac{d}{d\eta}, \\ \frac{\partial}{\partial x_2} &= \frac{\partial \eta}{\partial x_2} \frac{d}{d\eta} = \frac{1}{\beta kd} \left(\frac{1}{x_1 - p} \right)^{p_0} \frac{d}{d\eta}. \end{aligned} \quad (16.26)$$

Substituting (16.22) and (16.23) into (16.21)₁, the balance law of mass yields

$$\begin{aligned} &\frac{\partial}{\partial x_1} \left[\left(\frac{x_1 - p}{kd} \right)^{p_1} f_1(\eta) \right] + \frac{\partial}{\partial x_2} \left[\left(\frac{x_1 - p}{kd} \right)^{p_2} f_2(\eta) \right] = 0, \\ \rightarrow &p_1 \left(\frac{x_1 - p}{kd} \right)^{p_1-1} \frac{1}{kd} f_1(\eta) + \left(\frac{x_1 - p}{kd} \right)^{p_1} \frac{df_1(\eta)}{d\eta} \frac{\partial(\eta(x_1, x_2))}{\partial x_1} \\ &+ \left(\frac{x_1 - p}{kd} \right)^{p_2} \frac{df_2(\eta)}{d\eta} \frac{\partial(\eta(x_1, x_2))}{\partial x_2} = 0, \quad \text{insert (16.26)} \end{aligned}$$

$$\begin{aligned} \rightarrow \quad & \frac{1}{kd} \left(\frac{x_1 - p}{kd} \right)^{p_1 - 1} \left[p_1 f_1(\eta) - p_0 \eta \frac{df_1(\eta)}{d\eta} \right] \\ & + \frac{1}{\beta kd} \left(\frac{x_1 - p}{kd} \right)^{p_2 - p_0} \frac{df_2(\eta)}{d\eta} = 0. \end{aligned} \quad (16.27)$$

The left-hand side of this equation can be viewed as a function of x_1 and η , but the x_1 -dependence drops out if all exponents of the function $(x_1 - p)/(kd)$ are the same. So, one must request $p_1 - 1 = p_2 - p_0$, or

$$p_0 + p_1 - p_2 = 1. \quad (16.28)$$

With this choice (16.27) reduces to the ordinary differential equation

$$p_1 f_1(\eta) - p_0 \eta \frac{df_1(\eta)}{d\eta} + \frac{1}{\beta} \frac{df_2(\eta)}{d\eta} = 0. \quad (16.29)$$

Proceeding in the same way with the momentum Eq. (16.21)₂ leads to

$$\begin{aligned} & \frac{\partial}{\partial x_1} \left[\left(\frac{x_1 - p}{kd} \right)^{p_1} f_1(\eta) \right] - \frac{\partial}{\partial x_2} \left[\left(\frac{x_1 - p}{kd} \right)^{p_{12}} f_{12}(\eta) \right] = 0, \\ \rightarrow \quad & p_1 \left(\frac{x_1 - p}{kd} \right)^{p_1 - 1} \frac{1}{kd} f_1(\eta) + \left(\frac{x_1 - p}{kd} \right)^{p_1} \frac{df_1(\eta)}{d\eta} \frac{\partial(\eta(x_1, x_2))}{\partial x_1} \\ & - \left(\frac{x_1 - p}{kd} \right)^{p_{12}} \frac{df_{12}(\eta)}{d\eta} \frac{\partial(\eta(x_1, x_2))}{\partial x_2} = 0, \quad \text{insert (16.26)} \\ \rightarrow \quad & \frac{1}{kd} \left(\frac{x_1 - p}{kd} \right)^{p_1 - 1} \left[p_1 f_1(\eta) - p_0 \eta \frac{df_1(\eta)}{d\eta} \right] \\ & + \frac{1}{\beta kd} \left(\frac{x_1 - p}{kd} \right)^{p_{12} - p_0} \frac{df_{12}(\eta)}{d\eta} = 0. \end{aligned} \quad (16.30)$$

Requesting again that the x_1 -dependence of the left-hand side drops out, implies

$$p_0 + p_1 - p_{12} = 1, \quad (16.31)$$

$$p_1 f_1(\eta) - p_0 \eta \frac{df_1(\eta)}{d\eta} + \frac{1}{\beta} \frac{df_{12}(\eta)}{d\eta} = 0. \quad (16.32)$$

The above computations have led to two ordinary differential equations for the functions f_1 , f_2 , f_{12} and 4 constants p_0 , p_1 , p_2 , p_{12} , but they do obviously not suffice to uniquely determine these functions and parameters. At least Eqs. (16.28)–(16.32) do not conflict with one another. This says that these equations possess the potential of similarity solutions (ordinary differential equations for the functions f_1 , f_2 , f_{12} are the prerequisite for this), but at least two additional equations must be found amongst

the parameters p_0, p_1, p_2, p_{12} . These functions are furnished by the following postulates:

- It is requested that the turbulent shear stress, scaled with the mean velocity in the principal flow direction, is independent of x_1 , [14]

$$\frac{d}{dx_1} \left(\frac{\overline{v'_1 v'_2}}{\overline{v_1^{*2}}} \right) = 0 \implies \frac{d}{dx_1} \left(\frac{-U_G^2 \left(\frac{x_1 - p}{kd} \right)^{p_{12}} f_{12}(\eta)}{U_G^2 \left(\frac{x_1 - p}{kd} \right)^{2p_1} f_1^2(\eta)} \right) = 0, \quad (16.33)$$

in which (16.22)₁ and (16.24) have been used. This requires

$$2p_1 - p_{12} = 0. \quad (16.34)$$

- Next, note that, owing to (16.21)₂,

$$\frac{d}{dx_1} \int_{-\infty}^{\infty} \left(\frac{\overline{v_1^*}}{U_G} \right) dx_2 = - \frac{\tau_{12}}{\rho U_G^2} \Big|_{-\infty}^{\infty} = 0,$$

the integral

$$\int_{-\infty}^{\infty} \frac{\overline{v_1^*}}{U_G} dx_2 = \text{const.}, \quad (16.35)$$

along a path perpendicular to the flow direction, is a constant, since the turbulent shear stresses vanish at $x_2 = \pm\infty$.

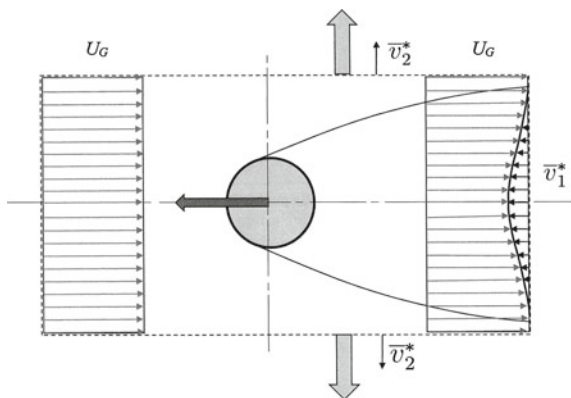
- Important in obtaining self-similarity is the assumption that the mean disturbance is at least one order of magnitude smaller than the undisturbed mean flow,

$$\frac{\overline{v_1^*}}{U_G} \ll 1. \quad (16.36)$$

Now, considering the momentum fluxes through a rectangle (**Fig. 16.3**), of which the sides normal to the flow direction extend from $x_2 = -\infty$ to $x_2 = \infty$, these fluxes are in steady state given by

$$\int_{-\infty}^{\infty} \rho [U_G^2 - (U_G - \overline{v_1^*})^2] dx_2 \approx 2\rho U_G \int_{-\infty}^{\infty} \overline{v_1^*} dx_2, \quad (16.37)$$

Fig. 16.3 Explaining the momentum flux through the boundary of a rectangle. At $x_2 = \pm\infty$ no horizontal momentum flux can occur, since the velocity is tangential to the flow path. Courtesy P. EGOLF and D.A. WEISS [9], © Phys. Rev. E, reproduced with changes



and the approximation (16.36) has been used. [The contributions along the flow parallel paths vanish at $x_2 = \pm\infty$, because the unit normal to the wall is perpendicular to the flow path there.]

Equation (16.37) can be interpreted in the sense that the rectangle of Fig. 16.3 loses so much more momentum at the inflow section as it loses at the outflow section. Therefore, the loss of momentum flux in the x_1 -direction is given by

$$-\rho U_G \int_{-\infty}^{\infty} \bar{v}_1^* dx_2.$$

The expression on the right-hand side of (16.37) is the loss of momentum from far upstream to far downstream within the rectangle due to viscous effects and due to the reacting force of the cylinder, which equally distributes between the two effects. Thus, the mean drag force acting on the cylinder can, in dimensionless form, be written as

$$\frac{\bar{F}}{\rho U_G^2 d} = \frac{1}{d} \int_{-\infty}^{\infty} \frac{\bar{v}_1^*}{U_G} dx_2 = \text{const.}, \tag{16.38}$$

and in steady state this force is constant. Introducing (16.22)–(16.25) in (16.38) yields

$$\frac{\bar{F}}{\rho U_G^2 d} = \frac{\beta kd}{d} \left(\frac{x_1 - p}{kd} \right)^{p_0+p_1} \underbrace{\int_{-\infty}^{\infty} f_1(\eta) d\eta}_{\text{const.}} = \text{const.}, \tag{16.39}$$

and this becomes independent of x_1 provided that

$$p_0 + p_1 = 0. \tag{16.40}$$

Let us now collect all equations for the exponents at one place:

$$\begin{aligned} p_0 + p_1 - p_2 &= 1, & p_0 &= 1/2, \\ p_0 + p_1 - p_{12} &= 1, & p_1 &= -1/2, \\ & \text{with the solution} & & \\ 2p_1 - p_{12} &= 0, & p_2 &= -1, \\ p_0 + p_1 &= 0, & p_{12} &= -1. \end{aligned} \tag{16.41}$$

With these values of p_0, p_1, p_2, p_{12} one obtains for (16.22)–(16.25)

$$\begin{aligned} \bar{v}_1^* &= U_G \left(\frac{kd}{x_1 - p} \right)^{1/2} f_1(\eta), & \bar{v}_2^* &= U_G \left(\frac{kd}{x_1 - p} \right) f_2(\eta), \\ \overline{v_1'v_2'} &= -U_G^2 \left(\frac{kd}{x_1 - p} \right) f_{12}(\eta), & & \\ \eta &= \frac{x_2}{b(x_1)}, & b(x_1) &= \beta \left(\frac{x_1 - p}{kd} \right)^{1/2} kd, \end{aligned} \tag{16.42}$$

and for (16.29) and (16.32)

$$\begin{aligned} f_1(\eta) + \eta \frac{df_1}{d\eta} - \frac{2}{\beta} \frac{df_2(\eta)}{d\eta} &= 0, \\ f_1(\eta) + \eta \frac{df_1}{d\eta} - \frac{2}{\beta} \frac{df_{12}(\eta)}{d\eta} &= 0. \end{aligned} \tag{16.43}$$

It is seen from (16.42) that

$$\text{as } x_1 \rightarrow \infty, \quad \bar{v}_1^* \sim (\sqrt{x_1})^{-1}, \quad \bar{v}_2^* \sim x_1^{-1}, \quad \overline{v_1'v_2'} \sim x_1^{-1}, \quad b \sim \sqrt{x_1}.$$

The singularities of the functions (16.42) as $x_1 \rightarrow p$ are irrelevant since the similarity solutions are not physically representative there. The two ordinary differential equations (16.43) are, however, insufficient to determine the functions f_1, f_2, f_{12} and, thus, require a closure condition. Surprisingly, though, this condition cannot come from a postulate on the turbulent shear stress as $f_{12}(\eta)$ can be expressed in terms of $f_1(\eta)$. Indeed, if one writes (16.43)₂ as

$$\frac{df_{12}(\eta)}{d\eta} = \frac{\beta}{2} \left[f_1(\eta) + \eta \frac{df_1(\eta)}{d\eta} \right] = \frac{\beta}{2} \frac{d}{d\eta} (\eta f_1(\eta)),$$

this ordinary differential equation integrates to

$$f_{12} = \frac{\beta}{2} \eta f_1(\eta), \quad (16.44)$$

where a constant of integration has been set to zero because $f_{12}(\eta) = -f_{12}(-\eta)$ for $f_1(\eta) = f_1(-\eta)$.

Similarly, from (16.43)₁ we may deduce

$$\frac{df_2(\eta)}{d\eta} = \frac{\beta}{2} \left[f_1(\eta) + \eta \frac{df_1(\eta)}{d\eta} \right] = \frac{\beta}{2} \frac{d}{d\eta} (\eta f_1(\eta)),$$

implying

$$f_2(\eta) = \frac{\beta}{2} \eta f_1(\eta) \quad (16.45)$$

and a constant of integration is again dropped because $f_2(\eta) = -f_2(-\eta)$.

It is seen from (16.44) and (16.45) that $f_2(\eta)$ and $f_{12}(\eta)$ are determined once $f_1(\eta)$ is prescribed as a symmetric function of η . A turbulence closure can in this case not be spelled out in terms of a parameterization of the turbulent shear stress because the latter is intimately related to the velocity distributions \bar{v}_1^* or/and \bar{v}_2^* . The simplest ansatz is

$$f_1(\eta) = \exp\left(-\left(\frac{\eta}{2\eta_0}\right)^2\right), \quad (16.46)$$

in which η_0 follows from an adjustment with data of \bar{v}_1 - and \bar{v}_2 -velocities. In principle, optimal coincidence may be reached between experimental data and theory by replacing (16.46) by an exponential sum and adjusting the free parameters to the available data.

On the other hand, based on (16.44), one may write

$$\begin{aligned} \tau_{12}(x_1, x_2) &= -\rho \overline{v_1' v_2'}(x_1, x_2) = -\rho U_G^2 \left(\frac{kd}{x_1 - p} \right) f_{12}(\eta) \\ \frac{\tau_{12}(x_1, x_2)}{\rho U_G^2} &= \frac{\beta}{2} \left(\frac{kd}{x_1 - p} \right) \frac{x_2}{\beta kd} \frac{1}{\left(\frac{x_1 - p}{kd} \right)^{1/2}} \left(\frac{x_1 - p}{kd} \right)^{1/2} \frac{\bar{v}_1^*(x_1, x_2)}{U_G} \\ &= \frac{1}{2} \left(\frac{x_2}{x_1 - p} \right) \frac{\bar{v}_1^*(x_1, x_2)}{U_G}. \end{aligned} \quad (16.47)$$

Now, whereas no stress parameterization is needed, it can at least be tested whether P. EGOLF's [8] Difference Quotient Turbulence Model (DQTM) proposal (16.17) generates the solution (16.47). If one substitutes

$$\chi_2 = x_2, \quad x_{2\max} = b, \quad \bar{v}_{1\min} = 0, \quad \bar{v}_{1\max} = U_G \quad (16.48)$$

as obvious choices into (16.17), then

$$\begin{aligned} \overline{v'_1 v'_2} &= -x_2 \frac{db}{dx_1} (U_G - \overline{v}_1^*(x_1, x_2)) \frac{U_G - [U_G - \overline{v}_1^*(x_1, x_2)]}{b(x_1, x_2) - x_2}, \\ \frac{\overline{v'_1 v'_2}}{U_G^2} &= -x_2 \frac{1}{b} \frac{db}{dx_1} (U_G - \overline{v}_1^*(x_1, x_2)) \frac{\overline{v}_1^*(x_1, x_2)}{1 - \frac{x_2}{b}}, \end{aligned}$$

or in the limit as $b \rightarrow \infty$, when $\overline{v}_1^*(x_1, x_2) \ll U_G$ and $x_2/b \rightarrow 0$, and with

$$\begin{aligned} \frac{1}{b} \frac{db}{dx_1} &= \left(\frac{p_0}{x_1 - p} \right) = \frac{1}{2} \left(\frac{1}{x_1 - p} \right), \\ \frac{\overline{v'_1 v'_2}}{U_G^2} &= \frac{1}{2} \left(\frac{x_2}{x_1 - p} \right) \frac{\overline{v}_1^*}{U_G}, \end{aligned} \tag{16.49}$$

which agrees with (16.47). It follows that the DQTM-model is for large x_1 asymptotically in conformity with the similarity solution (16.44) and (16.45).

This positive result should not delude over the fact that the approximate turbulent equations (16.21) generate structurally the same Eqs.(16.29) and (16.32), for the similarity functions f_1, f_2, f_{12} . Indeed, simple inspection of these equations reveals that (modulo boundary conditions) f_2 and f_{12} must be affine to one another. So, conditions to being able to construct solutions, in which a closure model for the turbulent shear stress can be formulated must be based on a generalization of (16.21).

16.3 The Axisymmetric Isothermal Steady Jet

Consider an axisymmetric steady turbulent flow of an incompressible viscous fluid out of a circular orifice into a quiescent infinite three-dimensional domain, **Fig. 16.4**. For REYNOLDS numbers

$$\mathbb{R} = \frac{v_0 d_0}{\nu} \geq 25\,000 \tag{16.50}$$

fully turbulent jets are observed. Under such prerequisites the jet has a linearly growing width in the downstream direction. Let d_0 be the nozzle diameter, v_0 the mean exit velocity at the nozzle from the pipe in the x_1 direction of a two-dimensional coordinate system with axial and radial coordinates and vanishing azimuthal mean velocity component, $\overline{v}_3 = 0$, and

$$\frac{\partial}{\partial x_3}(\overline{\varphi}) = 0, \quad \text{for } \overline{\varphi} \in \{\overline{v}_1, \overline{v}_2, \overline{v'_1 v'_2}, \dots\}. \tag{16.51}$$

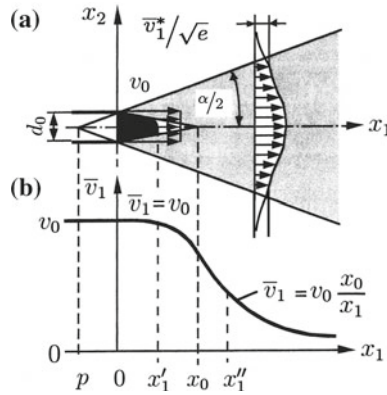


Fig. 16.4 Turbulent round axisymmetric jet emerging from a nozzle with diameter d_0 . **a** According to current understanding, the fictitious core length x_0 is used as length scale in the description of the problem. **b** In a meridional plane the time averaged velocity component in the longitudinal direction on the centerline is shown. In the core region $x_1 < x'_1$ it is constant, v_0 . Beyond a transition region ($x'_1 < x_1 < x'_1''$) in the self-similarity domain ($x'_1 < x_1$) the axial velocity component follows a GAUSSIAN-type curve. The boundary of the jet is then given by \bar{v}_1^*/\sqrt{e} . Courtesy P. EGOLF and D.A. WEISS [9], © Phys. Rev. E, reproduced with changes

The turbulent REYNOLDS Eqs. (15.21) and (15.22), for a NEWTONIAN fluid read in this case

$$\frac{\partial \bar{v}_1}{\partial x_1} + \frac{1}{x_2} \frac{\partial}{\partial x_2} (x_2 \bar{v}_2) = 0, \tag{16.52}$$

$$\bar{v}_1 \frac{\partial \bar{v}_1}{\partial x_1} + \bar{v}_2 \frac{\partial \bar{v}_1}{\partial x_2} + \frac{1}{\rho} \frac{\partial \bar{p}}{\partial x_1} + \frac{\partial}{\partial x_1} \overline{v_1'^2} + \frac{1}{x_2} \frac{\partial}{\partial x_2} (x_2 \overline{v_1' v_2'}) = 0, \tag{16.53}$$

$$\bar{v}_1 \frac{\partial \bar{v}_2}{\partial x_1} + \bar{v}_2 \frac{\partial \bar{v}_2}{\partial x_2} + \frac{1}{\rho} \frac{\partial \bar{p}}{\partial x_2} + \frac{\partial}{\partial x_1} \overline{v_1' v_2'} + \frac{1}{x_2} \frac{\partial}{\partial x_2} (x_2 \overline{v_2'^2}) - \frac{1}{x_2} \overline{v_3'^2} = 0. \tag{16.54}$$

These equations represent, in turn, the continuity equation, the axial and radial components of the momentum equations, in which the materially dependent viscous terms have been ignored as REYNOLDS numbers are very large, see (16.50).

In Eq. (16.54) the terms

$$\bar{v}_1 \frac{\partial \bar{v}_2}{\partial x_1}, \quad \bar{v}_2 \frac{\partial \bar{v}_2}{\partial x_2}, \quad \frac{\partial}{\partial x_1} (\overline{v_1' v_2'})$$

can be neglected in comparison to the remaining terms, owing to the boundary layer character of the flow and since $|\bar{v}_2| \ll |\bar{v}_1|$. This then implies that the radial momentum equation reduces to

$$\frac{1}{\rho} \frac{\partial \bar{p}}{\partial x_2} + \frac{1}{x_2} \frac{\partial}{\partial x_2} (x_2 \overline{v_2'^2}) - \frac{1}{x_2} \overline{v_3'^2} = 0. \tag{16.55}$$

Moreover, note that in (16.53) and (16.55) all three quadratic fluctuation terms, $\overline{v_1'^2}$, $\overline{v_2'^2}$, $\overline{v_3'^2}$, arise. At this stage, therefore, the assumption of orthotropy of the fluctuations

$$\overline{v_2'^2} = \overline{v_3'^2} \quad (16.56)$$

is introduced. With this assumption, Eq. (16.55) reduces to

$$\frac{1}{\rho} \frac{\partial \overline{p}}{\partial x_2} + \frac{\partial}{\partial x_2} \left(\overline{v_2'^2} \right) = 0 \implies \overline{p} + \rho \overline{v_2'^2} = p_0, \quad (16.57)$$

in which $p_0 = \text{const.}$ is the unperturbed pressure far from the turbulent domain. This equation can be used to eliminate from (16.53) the pressure, so that

$$\overline{v_1} \frac{\partial \overline{v_1}}{\partial x_1} + \overline{v_2} \frac{\partial \overline{v_1}}{\partial x_2} + \frac{\partial}{\partial x_1} \left(\overline{v_1'^2} - \overline{v_2'^2} \right) + \frac{1}{x_2} \frac{\partial}{\partial x_2} \left(x_2 \overline{v_1' v_2'} \right) = 0, \quad (16.58)$$

which can further be simplified by assuming isotropy of the kinetic fluctuations,

$$\overline{v_1'^2} = \overline{v_2'^2}, \quad (16.59)$$

implying

$$\overline{v_1} \frac{\partial \overline{v_1}}{\partial x_1} + \overline{v_2} \frac{\partial \overline{v_1}}{\partial x_2} + \frac{1}{x_2} \frac{\partial}{\partial x_2} \left(x_2 \overline{v_1' v_2'} \right) = 0. \quad (16.60)$$

The axial momentum equation will be assumed in this reduced form.

Experimental observations suggest that ‘for all $x_1 > x_1''$ (Fig. 16.4) a self-similarity domain exists, [...], where the mean physical quantities can be made dimensionless to become functions of only one variable. This leads to the possibility of transforming the two partial differential equations (16.52) and (16.60) into a single ordinary differential equation. The following self-similarity relations are assumed to hold. Distances from the pole, $(x_1 - p)$, are replaced by x_1 because in the self-similarity domain $x_1 \gg |p|$; we then have

$$\overline{v_1} = v_0 \left(\frac{x_1}{x_0} \right)^{p_1} f_1(\eta), \quad \overline{v_2} = v_0 \left(\frac{x_1}{x_0} \right)^{p_2} f_2(\eta), \quad (16.61)$$

$$\overline{v_1' v_2'} = -v_0^2 \left(\frac{x_1}{x_0} \right)^{p_{12}} f_{12}(\eta), \quad (16.62)$$

$$\eta = \frac{x_2}{b}, \quad b = \beta \left(\frac{x_1}{x_0} \right)^{p_0} x_0, \quad (16.63)$$

according to P. EGOLF and D.A. WEISS [9], in which v_0 and x_0 are constants.

The ensuing computations parallel the analogous computations in Sect. 16.2. The expressions (16.61)–(16.63) are substituted into Eqs. (16.52) and (16.60), and it is required that the exponents of x_1/x_0 of all the terms in the emerging equations are identical, so that the x_1 -dependence drops out and only ordinary differential equations in the variable η survive. This computation is relatively long and only the outcome of this process is given here. The results are⁴

$$\begin{aligned} p_0 + p_1 - p_2 &= 1, \\ p_0 + 2p_1 - p_{12} &= 1, \\ p_0 + p_1 &= 0 \end{aligned} \quad (16.64)$$

for the exponents and

$$\begin{aligned} p_1 f_1 - p_0 \eta \frac{df_1}{d\eta} + \frac{1}{\beta} \frac{1}{\eta} \frac{d}{d\eta} (\eta f_2) &= 0, \\ p_1 f_1^2 - p_0 \eta f_1 \frac{df_1}{d\eta} + \frac{1}{\beta} \left(f_2 \frac{df_1}{d\eta} - \frac{1}{\eta} \frac{d}{d\eta} (\eta f_{12}) \right) &= 0 \end{aligned} \quad (16.65)$$

for the residual equations of continuity and momentum balance: Relations (16.64) are short by one equation to uniquely determine the exponents p_0, p_1, p_2, p_{12} . From the requirement of self-similarity of the REYNOLDS stresses in the sense that

$$\frac{\overline{v'_1 v'_2}}{\overline{v_1^*}^2} = -f_{12}(\eta), \quad (16.66)$$

it follows, owing to (16.61) and (16.62), that

$$\overline{v_1^*}(x_1) = \overline{v_1}(x_1, 0) \quad \text{and} \quad 2p_1 - p_{12} = 0. \quad (16.67)$$

Equations (16.64), (16.67)₂ now yield the unique solutions

$$p_0 = 1, \quad p_1 = -1, \quad p_2 = -1, \quad p_{12} = -2 \quad (16.68)$$

and, correspondingly, from (16.65)

$$f_1 + \eta \frac{df_1}{d\eta} - \frac{1}{\beta} \frac{1}{\eta} \frac{d(\eta f_2)}{d\eta} = 0, \quad (16.69)$$

$$f_1^2 + \eta f_1 \frac{df_1}{d\eta} - \frac{1}{\beta} \left(f_2 \frac{df_1}{d\eta} - \frac{1}{\eta} \frac{d(\eta f_{12})}{d\eta} \right) = 0. \quad (16.70)$$

These are two equations for the three unknowns f_1, f_2, f_{12} . Therefore, a turbulence closure model is required to close the system of equations. Before this problem is attacked with P. EGOLFS [8] difference quotient turbulence model (DQTM), the

⁴Equation (16.64)₃ follows in the same way as (16.40) was derived.

following rearrangement of Eq. (16.69) is made

$$\begin{aligned}
 (\eta f_1(\eta))' &= \frac{1}{\beta} \frac{1}{\eta} (\eta f_2(\eta))' && \longrightarrow \\
 \beta \eta (\eta f_1(\eta))' &= (\eta f_2(\eta))' && \longrightarrow \text{integration} \\
 \eta f_2(\eta) &= \beta \int_0^\eta \xi (\xi f_1(\xi))' d\xi && \longrightarrow \text{integration by parts} \quad (16.71) \\
 f_2(\eta) &= \beta \left\{ \eta f_1 - \frac{1}{\eta} \int_0^\eta \xi f_1(\xi) d\xi \right\},
 \end{aligned}$$

in which $(\cdot)' = \partial/\partial\eta$. It follows that $f_2(\eta)$ is known, once $f_1(\eta)$ is determined.

To formulate the missing turbulent closure relation, recall Eq. (16.17), the DQTM appropriate for the axisymmetric jet, in which the substitutions

$$x_{2\max} = 0, \quad \bar{v}_{1\min} = 0 \quad \bar{v}_{1\max} = \bar{v}_1^*(x_1) \quad (16.72)$$

are made, and b is taken to be the semi-width of the jet with

$$\beta = \frac{db}{dx_1} = \tan\left(\frac{\alpha}{2}\right). \quad (16.73)$$

Owing to Fig. 16.4 these are plausible selections. With the assignments (16.72), (16.73) and the aid of (16.17) and (16.62) it is straightforward to show that

$$f_{12} = -\beta \frac{1}{\eta} f_1(1 - f_1). \quad (16.74)$$

So, f_{12} is equally determined by $f_1(\eta)$. Substituting (16.71) and (16.74) into (16.70) leads to the integro-differential equation for f_1

$$\int_0^\eta f_1(\xi) \xi d\xi = 1 - 2f_1 - \eta \frac{f_1^2}{f_1'}. \quad (16.75)$$

Differentiating this expression with respect to η yields, finally, the highly nonlinear differential equation

$$\eta f_1^2 f_1'' - 2(f_1')^3 - 3\eta f_1 (f_1')^2 - f_1^2 f_1' = 0. \quad (16.76)$$

A solution to this equation is

$$f_1 = \exp\left(-\frac{\eta^2}{2}\right), \quad (16.77)$$

as P. EGOLF and D.A. WEISS [9] say. The reader may corroborate this by substitution.

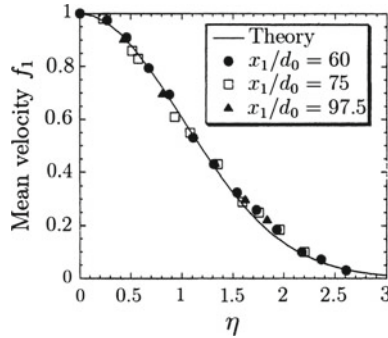


Fig. 16.5 Axisymmetric steady jet: Theoretical representation and experimental data of the time-averaged axial velocity distribution in the radial direction η . The theoretical curve follows (16.77); the experimental data are taken from [30]. The measured points lie very close to the GAUSSian distribution function (16.77). Courtesy P. EGOLF and D.A. WEISS [9], © *Phys. Rev. E*, reproduced with changes

Experimental data are taken from P. EGOLF and D.A. WEISS [9]. The graph of **Fig. 16.5** shows excellent agreement between the theoretical GAUSSian distribution of the axial velocity component and the experimental points, taken at three distances from the nozzle.

With $f_1(\eta)$ determined, so are, according to (16.71) and (16.74) also $f_2(\eta)$ and $f_{12}(\eta)$:

$$\begin{aligned} f_2 &= \beta \left\{ \eta \exp\left(-\frac{1}{2}\eta^2\right) - \frac{1}{\eta} \left(1 - \exp\left(\frac{1}{2}\eta^2\right)\right) \right\} \\ &= \beta \left(\eta f_1 - \frac{1}{\eta} (1 - f_1) \right), \end{aligned} \quad (16.78)$$

$$f_{12} = -\beta \frac{1}{\eta} \left(\exp\left(-\frac{1}{2}\eta^2\right) - \exp\left(-\eta^2\right) \right). \quad (16.79)$$

Experiments on the radial velocity component in a meridional plane were also published by I. WYGANSKI and J. FIEDLER [30]. **Figure 16.6** displays the experimental points together with the graph of the mathematical curve (16.78). However, Fig. 16.6 also contains additional results, namely the experimental results of Fig. 16.5 when inserting these into the expression on the right of (16.78), to obtain mean velocities in the radial direction shown for three distances; these points are presented by open symbols. It is no surprise that these show less agreement with the theoretical curve.

P. EGOLF and D.A. WEISS [9] also show the graph of the theoretical turbulent shear stresses (16.79) together with the different extracted experimental data (see **Fig. 16.7**); those represented by the symbol D indicate the distances downstream from the nozzle and measured in units of d_0 , whilst those with the symbol I show the shear stress by taking the data of f_1 in Fig. 16.5 and applying (16.74).

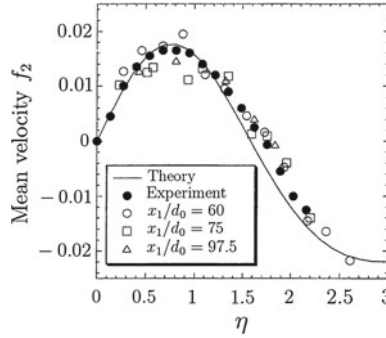


Fig. 16.6 Axisymmetric steady jet: Theoretical results (16.78) shown as solid curve and experimental points from [30] for the radial mean velocity component (solid circles). Note, the radial velocity component is less than 2% of the axial mean velocity component. In domains where $f_2 < 0$ the turbulent jet is fed by the ambient fluid. This is the region of entrainment. Courtesy P. EGOLF and D.A. WEISS [9], © Phys. Rev. E, reproduced with changes

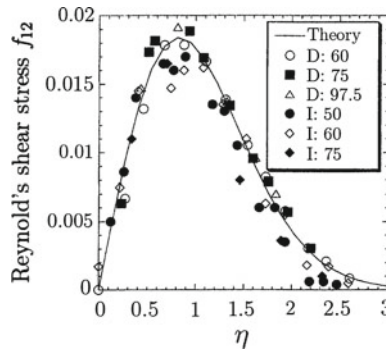


Fig. 16.7 Radial distribution of the REYNOLDS stress function. The number after the letter D denotes the distance downstream from the nozzle measured in units of d_0 . The three Reynolds shear stresses, represented by I , were calculated by taking the data of f_1 shown in Fig. 16.5 and then applying Eq.(16.79). Courtesy P. EGOLF and D.A. WEISS [9], © Phys. Rev. E, reproduced with changes

The above computations demonstrate a convincing performance of the turbulent spreading properties of a steady round jet regarding the mean axial and radial velocities as well as the REYNOLDS stress τ_{12} . There is even convincing evidence regarding the turbulent entrainment rate, the REYNOLDS normal stress and certain contributions to the turbulent energy balance.

Entrainment rate, ordinarily simply called entrainment, can be determined from the axial mass flow

$$m_1 = 2\pi\rho \int_0^\infty \bar{v}_1 x_2 dx_2. \tag{16.80}$$

It represents the total axial flux of mass by the jet for given x_1 . When being scaled with the outgoing mass flow at the nozzle exit

$$m_0 = \rho\pi \frac{d_0^2}{4} v_0, \quad (16.81)$$

then,

$$\frac{m_1}{m_0} = \frac{8\beta^2 x_0 x_1}{d_0^2} \int_0^\infty \exp(-\frac{1}{2}\xi^2) \xi d\xi = k_1 \left(\frac{x_1}{d_0}\right) = \frac{8\beta^2}{m^2} \left(\frac{x_1}{x_0}\right), \quad (16.82)$$

implying that the so-called *mixing number*, m , is given by

$$m = \frac{d_0}{x_0}. \quad (16.83)$$

It is the dimensionless ratio of the nozzle diameter d_0 to the fictitious core distance x_0 and possesses values in the interval $0.16 < m < 0.19$ [7], when jets emerge from round nozzles.

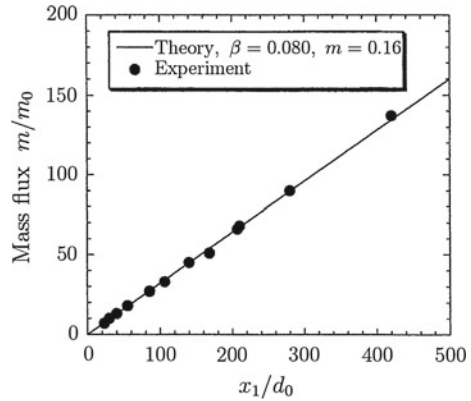
According to P. EGOLF and D.A. WEISS [9] 'F.P. RICOU and D.B. SPALDING (1961) [28] also report a linear behavior of the mass flux as a function of the axial distance x_1 . After a reviewing process they conclude that the values of the constant k_1 obtained [see Eq.(16.82)] range from about 0.22 up to 0.404 according to the investigators [listed by them]. Their own experimentally determined value of the constant is $k_1 = 0.32$. They further comment that [...] the constant k_1 can only be determined by experimental means. [It will be] shown that with high accuracy [one] has

$$m = 2\beta \quad \longleftrightarrow \quad k_1 = 4\beta. \quad (16.84)$$

F.P. RICOU and D.B. SPALDING do not mention the spreading angle or the spreading parameter. However, from $k_1 = 0.32$ [...] β is now determined to be 0.080, which certainly must be close to its actual value (compare e.g. in [30] $\beta = 0.074$ or in [22] $\beta = 0.082$). The experimental results of F.P. RICOU and D.B. SPALDING are shown in **Fig. 16.8**. There is no doubt that the mass flow is very accurately a linear function of x_1 , [9].

Longitudinal turbulent normal stress: In the above analysis, because of the isotropy assumption for $\overline{v_i^2}$, $i = 1, 2, 3$ (see (16.56) and (16.59)) no information can be obtained for these turbulent normal stresses. A separate closure condition is needed. In this subsection a proposal of the class (16.17) is suggested. P. EGOLF and D.A. WEISS [9] took formula (16.17), in which the index 2 is replaced by the index 1; in this way the following DQTM-parameterization is obtained

Fig. 16.8 Linear dependence of the mass flux in axial direction on the distance x_1 . The DQTM-theory matches very well numerically the linear dependence. Here, the theoretical results obtained are compared with data from [28]. Courtesy P. EGOLF and D.A. WEISS [9], © Phys. Rev. E, reproduced with changes



$$\overline{v_1'^2} = -\sigma\chi_1(\overline{v_1} - \overline{v_{1\min}}) \frac{\overline{v_{1\max}} - \overline{v_1}}{x_{1\max} - x_1}, \tag{16.85}$$

$$\overline{x_{1\max}} := \{x_1 \mid \overline{v_1} = \max_{x_1}\{\overline{v_1}\}\}, \tag{16.86}$$

with the following suggestive assignments, see Fig. 16.4,

$$\chi_1 = x_0, \quad x_{1\max} = x_0, \quad \overline{v_{1\min}} = 0, \quad \overline{v_{1\max}} = v_0 \tag{16.87}$$

together with

$$\sigma = \frac{db}{dx_1} = \beta = \tan\left(\frac{1}{2}\alpha\right). \tag{16.88}$$

‘It is meaningful that the characteristic length in the x_1 -direction is identical to the only available length in this direction, the core distance x_0 ’ [9]. With (16.87), (16.88), Eq. (16.85) and the definitions

$$\overline{v_1^*} := v_0 \left(\frac{x_0}{x_1}\right), \quad f_{11} := \frac{\overline{v_1'^2}}{\overline{v_1^*}^2}, \tag{16.89}$$

one obtains for (16.85)

$$\overline{v_1'^2} = - \underbrace{\frac{db}{dx_1}}_{\beta} x_0 \overline{v_1} \frac{v_0 - \overline{v_1}}{x_0 - x_1} = -\beta x_0 v_0 \left(\frac{x_0}{x_1}\right) f_{11} \frac{v_0 - v_0 \left(\frac{x_0}{x_1}\right)}{x_0 \left(1 - \frac{x_1}{x_0}\right)}$$

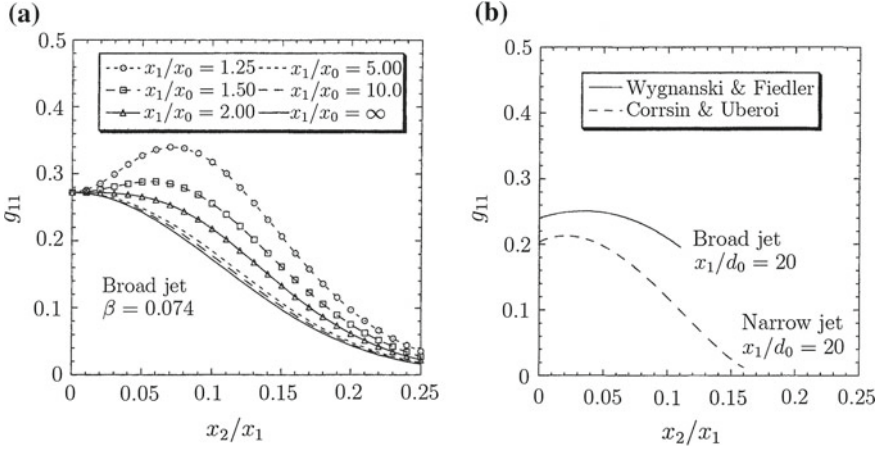


Fig. 16.9 Fluctuation intensities g_{11} plotted against x_2/x_1 . **a** Computed according to (16.91), **b** experimentally given by [30] and [5]. Note, the experimentally observed off-axis peaks in (b) are also seen in the theoretical curves (a). Courtesy P. EGOLF and D.A. WEISS [9], © Phys. Rev. E, reproduced with changes

$$\begin{aligned}
 &= -\beta x_0 v_0 \underbrace{\frac{x_0}{x_1} f_1}_{\bar{v}_1^*} v_0 \frac{1 - \frac{x_0}{x_1} f_1}{x_0 \left(1 - \frac{x_1}{x_0}\right)} = -\beta \bar{v}_1^* f_1 \underbrace{\frac{v_0 x_0}{x_1}}_{\bar{v}_1^*} \frac{\frac{x_1}{x_0} - f_1}{1 - \frac{x_1}{x_0}} \\
 &= \beta \bar{v}_1^{*2} \left(\frac{\frac{x_1}{x_0} - f_1}{\frac{x_1}{x_0} - 1} \right) f_1. \tag{16.90}
 \end{aligned}$$

Therefore,

$$g_{11} := \sqrt{f_{11}} := \sqrt{\beta} \left(\frac{\frac{x_1}{x_0} - f_1}{\frac{x_1}{x_0} - 1} \right)^{1/2} f_1^{1/2}. \tag{16.91}$$

The function $g_{11}((x_1/x_0), \eta)$ was evaluated and plotted in [9] against x_2/x_1 for various values of x_1/x_0 , see **Fig. 16.9a** and for experiments **Fig. 16.9b**. It is seen that for growing values of x_1/x_0 a self-similar bell shaped profile is approached. Indeed,

$$\begin{aligned}
 &\text{as } \frac{x_1}{x_0} \rightarrow \infty, \quad f_1(\eta) \rightarrow f_1(0) = 1 \\
 \implies &g_{11} \rightarrow \sqrt{\beta f_1(0)} = \sqrt{\beta} = \text{const.} . \tag{16.92}
 \end{aligned}$$

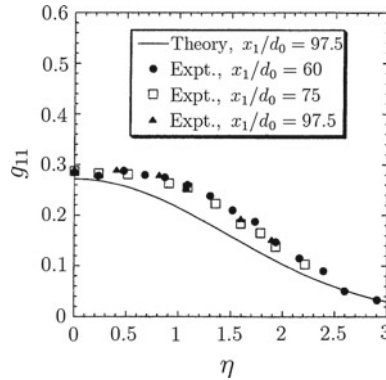


Fig. 16.10 Relative fluctuation intensity g_{11} plotted against η for various values of x_1/d_0 . Experimental data are taken from [30]. The deviation of the theoretical function from the experimental results at mean distances η is related to the production of turbulent kinetic energy and an incomplete turbulent transport of this kind of energy. Courtesy P. EGOLF and D.A. WEISS [9], © *Phys. Rev. E*, reproduced with changes

As indicated in Fig. 16.9b ‘the jet measured by S. CORRSIN and M.S. UBEROI (1949) [5] is narrower than the one that was experimentally investigated by I. WYGANSKI and J. FIEDLER [30]. This [...] corresponds to the presented theory, which states that the fluctuation intensity on the axis [$x_2/x_1 = 0$] is smaller for a narrower jet. However, this only qualitatively confirms the result

$$\frac{\sqrt{\overline{v_1'^2}}}{\overline{v_1^*}} = \sqrt{\beta} \quad (16.93)$$

by measurements. More reliable comparisons of theoretical predictions and experimental data of the normal stress in the axial direction are shown in Fig. 16.10. The deviation of measurements from the theoretical results varies to a great extent on the experimental work taken into consideration in each case. [...] it is believed that deviations [from self-similarity], occurring at medium values of x_2/x_1 only, are caused by the underlying production of turbulent kinetic energy and that fluctuation energy has not been perfectly distributed over the whole width of the jet [via] transportation by the mean motion and turbulent convection ...’ [9].

Finally, we note that the numerical value of $\beta \equiv \sigma$ has been determined in Fig. 16.10 by curve fitting with a value $\beta = 0.074$. By contrast, a theoretical value can be obtained by evaluating $g_{11}(\eta = 0)$, see Fig. 16.10; this yields $\sqrt{\beta} = 0.28$, thus, $\beta = 0.079$. This is rewarding corroboration of the value of β by two independent approaches.

Transverse turbulent normal stresses $\overline{v_2'^2} = \overline{v_3'^2}$: With the radial and azimuthal turbulent intensities being equal, one may write for these

$$\overline{v_2'^2} = \overline{v_3'^2} = \frac{\gamma}{\beta} \overline{v_1'^2} \quad (16.94)$$

with $\gamma < \beta$ for axisymmetric orthotropy and $\gamma = \beta$ for isotropy. Formula (16.94) assumes that $\overline{v_2'^2}$, $\overline{v_3'^2}$ follow the radial distribution similarly to that of $\overline{v_1'^2}$. The axial momentum balance yields [22]

$$M(x_1) = 2\pi\rho \int_0^\infty \left(\overline{v_1^2} + \overline{v_1'^2} - \frac{\overline{v_2'^2} + \overline{v_3'^2}}{2} \right) x_2 dx_2 = M(0), \quad (16.95)$$

$$M(0) = \frac{\pi d_0^2}{4} \rho v_0^2. \quad (16.96)$$

Substituting into (16.95) the relations (16.61), (16.90) and (16.89), one obtains

$$\begin{aligned} \frac{M(x_1)}{\overline{v_1^*}^2} &= \frac{2\pi\rho}{v_0^2 \left(\frac{x_0}{x_1}\right)^2} \int_0^\infty \left\{ v_0^2 \left(\frac{x_0}{x_1}\right)^2 f_1^2 + \left(\frac{\frac{x_1}{x_0} - f_1}{\frac{x_1}{x_0} - 1}\right) \beta f_1 v_0^2 \left(\frac{x_0}{x_1}\right)^2 \right. \\ &\quad \left. - \frac{\gamma}{\beta} \left(\frac{\frac{x_1}{x_0} - f_1}{\frac{x_1}{x_0} - 1}\right) \beta f_1 v_0^2 \left(\frac{x_0}{x_1}\right)^2 \right\} \underbrace{b^2(x_1)}_{\beta^2 (x_1/x_0)^2 x_0^2} \eta d\eta \\ &= \frac{\pi d_0^2 \rho v_0^2}{4v_0^2 \left(\frac{x_0}{x_1}\right)^2}, \end{aligned} \quad (16.97)$$

from which

$$\begin{aligned} &\int_0^\infty \left\{ f_1^2 + (\beta - \gamma) \left(\frac{\frac{x_1}{x_0} - f_1}{\frac{x_1}{x_0} - 1}\right) f_1 \right\} \eta d\eta \\ &= \frac{d_0^2 v_0^2}{8v_0^2} \left(\frac{x_1}{x_0}\right)^2 \frac{1}{\beta^2} \frac{1}{\left(\frac{x_1}{x_0}\right)^2} \frac{1}{x_0} = \frac{1}{8\beta^2} \left(\frac{d_0}{d_1}\right) \left(\frac{v_0}{\overline{v_1^*}}\right)^2 \end{aligned} \quad (16.98)$$

is obtained. Substituting for f_1 the GAUSSIAN profile (16.77) and employing the transformation $\eta^2 = \xi$ leads to

$$\begin{aligned} &(\gamma - \beta - 1) \underbrace{\int_0^\infty \exp(-\xi) d\xi}_{=1} + \frac{x_1}{x_0} \left\{ \underbrace{\int_0^\infty \exp(-\xi) d\xi}_{=1} + (\beta - \gamma) \underbrace{\int_0^\infty \exp\left(-\frac{\xi}{2}\right) d\xi}_{=2} \right\} \\ &= \frac{1}{4\beta^2} \left(\frac{d_0}{x_0}\right)^2 \left(\frac{x_1}{x_0} - 1\right), \end{aligned} \quad (16.99)$$

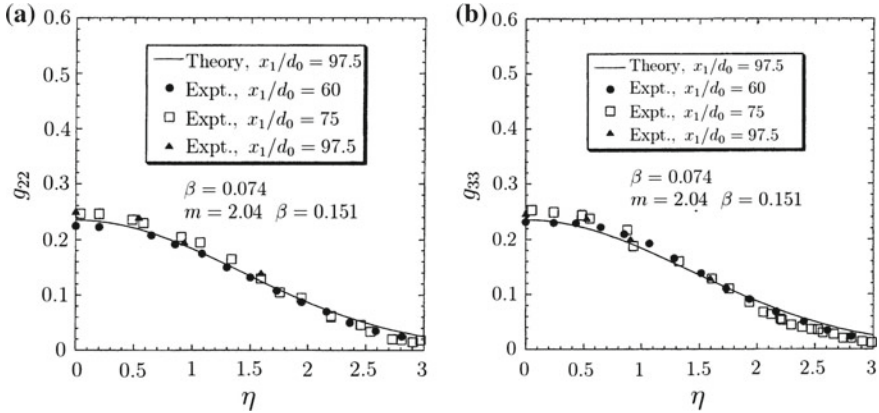


Fig. 16.11 Relative turbulent intensities **a**, g_{22} in the radial and **b** g_{33} in the azimuthal directions. *Experimental data are from [30]. Courtesy P. EGOLF and D.A. WEISS [9], © Phys. Rev. E, reproduced with changes*

which can readily be transformed into

$$\gamma = \beta - \frac{\left(1 - \frac{x_1}{x_0}\right) \left(1 - \frac{m^2}{4\beta^2}\right)}{\left(\frac{2x_1}{x_0} - 1\right)}, \quad \text{where } \left(\frac{d_0}{x_0}\right)^2 = m^2. \quad (16.100)$$

Isotropic turbulence implies, according to (16.100),

$$\text{Isotropy} \iff \gamma = \beta \iff m = 2\beta, \quad (16.101)$$

which has been differently derived in (16.84).

P. EGOLF and D.A. WEISS [9] evaluate and plot

$$f_{22} = g_{22}^2 := \frac{\overline{v_2'^2}}{\overline{v_1^{*2}}} \quad \text{and} \quad f_{33} = g_{33}^2 := \frac{\overline{v_3'^2}}{\overline{v_1^{*2}}} \quad (16.102)$$

against η for β and m -values as shown as insets ($m > 2\beta$) and compare the theoretical results with the experimental data from [30]. Their plots are displayed in **Fig. 16.11** as panels (a) (radial, g_{22}) and (b) (azimuthal, g_{33}). The theoretical curves mimic the GAUSSIAN profile as already displayed for g_{11} in Fig. 16.10. The experimental points for g_{22} and g_{33} are closer to the theoretical curves than g_{11} in Fig. 16.10, even though they slightly overestimate the g_{22} - and g_{33} -values at small $\eta < 1$ and underestimate them for larger values of $\eta > 2$.

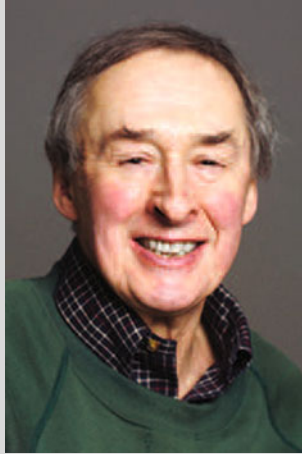


Fig. 16.12 JOHN LEASK LUMLEY (11. Nov. 1930–30. May 2015)

JOHN LEASK LUMLEY received his M.S.E. and Ph.D. degrees from Johns Hopkins University in 1954 and 1957, respectively. His Ph.D. supervisor was STANLEY CORRSIN (1920–1986). He started his academic career at the Pennsylvania State University, where he became Evan Pugh Professor of Aerospace Engineering. He was also in charge of research on turbulence and transition at the Applied Research Laboratory. In 1977 LUMLEY joined Cornell University where he has been Professor emeritus of Mechanical and Aerospace Engineering until his death. He made seminal contributions to engineering in the study of turbulent fluid flow: Complex and chaotic, ubiquitous in nature and engineering devices, turbulence is found in cumulus clouds, smoke stacks and jet exhausts. Experts agree that ‘more than any other person, he defined the field of turbulence during the second half of the 20th century’.

LUMLEY made important contributions regarding buoyant plumes and smokestacks, turbulent dispersion of pollution in the atmosphere, the propagation of waves in the atmosphere and oceans, turbulence in the presence of atmospheric inversions, the flow of air over objects, the diffusion of salt in water known as ‘salt-fingering’, and the effects of electromagnetic fields on turbulence. His theoretical contributions are key to our modern knowledge of turbulence; they include statistical processes, the identification of structures in turbulence, the cascade dynamics of turbulence, and modeling of generic fluid flows, such as jets and wakes and turbulent flows near walls.

His 1972 book, ‘A First Course in Turbulence with Henk Tennekes’ [29], was the first book to place dimensional analysis and scaling arguments as central to the subject. In 1964, with HANS PANOFSKY [20], he wrote the influential book ‘The Structure of Atmospheric Turbulence’ and in 1998 with PHIL HOLMES and GAL BERKOOZ they co-authored ‘Turbulence, Coherent Structures, Dynamical Systems, and Symmetry’ [15].

In 1990, LUMLEY received the Fluid Dynamics Prize of the American Physical Society. Other awards include the Fluid and Plasma Dynamics Award of the American Institute of Aeronautics and Astronautics in 1982 and the Timoshenko Medal in 1993. LUMLEY was a fellow in the American Institute of Aeronautics and Astronautics, the American Academy of Arts and Sciences, and a member of the National Academy of Engineering.

The text is based on www.wikipedia.org

Production of turbulent kinetic energy: When deriving the balance law of turbulent kinetic energy by taking the inner product of the momentum equation with the velocity vector and subsequently averaging the emerging equation, the resulting equation is the turbulent kinetic energy equation, see e.g. O. HINZE [14], H. TENNEKES and J.L. LUMLEY⁵ [29], K. HUTTER and K. JÖHNK [17]. It contains the following terms for an axisymmetric flow,

$$p = \overline{v'_1 v'_2} \frac{\partial \bar{v}_1}{\partial x_2} + \overline{v_1'^2} \frac{\partial \bar{v}_1}{\partial x_1} + \overline{v_2'^2} \frac{\partial \bar{v}_2}{\partial x_2}, \quad (16.103)$$

$$k = \frac{1}{2} \frac{\overline{v_1'^2} + \overline{v_2'^2} + \overline{v_3'^2}}{\bar{v}_1^{*2}}, \quad (16.104)$$

$$c = \frac{df_1}{d\eta} \frac{\partial \eta}{\partial x_1} \bar{v}_1^{*3} k + 3f_1 \bar{v}_1^{*2} \frac{d\bar{v}_1^*}{dx_1} k + f_1 \bar{v}_1^{*3} \frac{dk}{d\eta} \frac{\partial \eta}{\partial x_1} \\ + \frac{1}{x_2} f_2 \bar{v}_1^{*3} k + \frac{df_2}{d\eta} \frac{\partial \eta}{\partial x_2} \bar{v}_1^{*3} k + f_2 \bar{v}_1^{*3} \frac{dk}{d\eta} \frac{\partial \eta}{\partial x_2}, \quad (16.105)$$

among others, which cannot be handled in this context, see e.g. [14] and [9]. Note that all terms on the right-hand sides of (16.103), (16.104), (16.105) have been dealt with in the preceding sections, so that p , k , c can be computed for the axisymmetric jet.

The dimensionless form of p is

$$\pi = \frac{px_1}{\bar{v}_1^{*3}} \quad (16.106)$$

and can straightforwardly be computed from (16.103) and earlier expressions for f_1 , f_2 , f_{11} , f_{22} . The result is

$$\pi = x_1 \left\{ -f_{12} \frac{df_1}{d\eta} \frac{\partial \eta}{\partial x_2} + f_{11} \frac{1}{\bar{v}_1^*} \left(\frac{\partial \bar{v}_1^*}{\partial x_1} f_1 + \bar{v}_1^* \frac{df_1}{d\eta} \frac{\partial \eta}{\partial x_1} \right) \right. \\ \left. + f_{22} \frac{df_2}{d\eta} \frac{\partial \eta}{\partial x_2} \right\}, \quad (16.107)$$

which, with the expressions

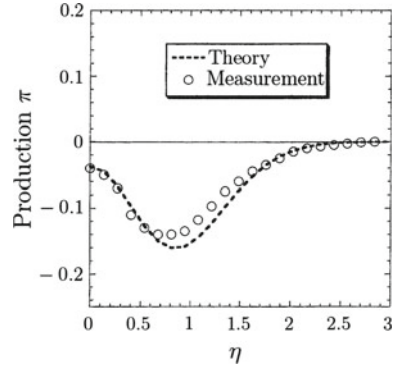
$$\frac{\partial \eta}{\partial x_1} = -\eta \frac{1}{x_1}, \quad \frac{\partial \eta}{\partial x_2} = \frac{1}{\beta x_1}, \quad \frac{d\bar{v}_1^*}{dx_1} = -\frac{1}{x_1} \bar{v}_1^*, \quad (16.108)$$

takes the form

$$\pi = -\frac{1}{\beta} f_{12} \frac{df_1}{d\eta} - f_{11} \left(f_1 + \eta \frac{df_1}{d\eta} \right) + \frac{1}{\beta} f_{22} \frac{df_2}{d\eta}. \quad (16.109)$$

⁵For a biographical sketch of LUMLEY see **Fig. 16.12**.

Fig. 16.13 Dimensionless turbulent production $\pi(\eta)$ plotted against η . Dashed curve is from DQTM computations, open circles from data obtained by I. WYGANSKI and J. FIEDLER [30]. Courtesy P. EGOLF and D.A. WEISS [9], © *Phys. Rev. E*, reproduced with changes



Inserting (16.74) for f_{12} and (16.79) for f_2 as well as (16.102) for f_{22} and f_{33} (with the isotropy assumption) yields

$$\pi = \left(\frac{1}{\eta} f_1 \frac{df_1}{d\eta} + \beta \frac{1}{\eta^2} f_1 \right) (1 - f_1) + \beta \frac{1}{\eta} f_1 \frac{df_1}{d\eta}. \tag{16.110}$$

Replacing in this expression $df_1/d\eta$ by $-\eta f_1$ owing to (16.77), finally yields for the dimensionless pressure

$$\pi = f_1^3 - f_1^2 \left(1 + \beta + \beta \frac{1}{\eta^2} \right) + \beta \frac{1}{\eta^2} f_1, \tag{16.111}$$

which is a relatively simple polynomial expression for π in terms of f_1 . The function $\pi(\eta)$ is plotted in Fig. 16.13 together with data points from [30]. The modulus of π shows a relative maximum at finite non-zero η .

Substituting (16.77) for f_1 into (16.111) and performing a TAYLOR series expansion of the emerging expression about $\eta = 0$ produces

$$\pi \approx \eta^2 \left(\beta^2 - \frac{1}{2} \right) - \frac{1}{2} \beta. \tag{16.112}$$

It follows that for $\eta = 0$

$$\pi(0) = -\frac{1}{2} \beta. \tag{16.113}$$

With $\beta = 0.074$ one obtains $\pi = -0.037$ as shown in Fig. 16.13.

A second term, which can be computed for the axisymmetric steady jet is the turbulent kinetic energy itself, (16.104), which can easily be written in the form

$$k(x_1, x_2) = \frac{\beta + 2\gamma}{2} \left(\frac{x_1}{x_0} - f_1 \right) \left(\frac{x_1}{x_0} - 1 \right) f_1 \stackrel{\text{isotropy}}{=} \frac{3}{2} \beta \left(\frac{x_1}{x_0} - f_1 \right) \left(\frac{x_1}{x_0} - 1 \right) f_1, \tag{16.114}$$

of which the expression on the far right holds for isotropic turbulence. For large distances $x_1 \gg x_0$ from the orifice the last expression in (16.114) reduces to

$$k = \frac{3}{2}\beta f_1. \tag{16.115}$$

The third quantity is the ‘turbulent convection parameter’ c , listed in (16.105). Its dimensionless version is

$$\chi = \frac{cx_1}{v_1^*{}^3}. \tag{16.116}$$

With Eq. (16.108), this expression takes the form

$$\chi = -\eta \frac{df_1}{d\eta} k - 3f_1 k - \eta f_1 \frac{dk}{d\eta} + \frac{1}{\beta} \frac{1}{\eta} f_2 k + \frac{1}{\beta} \frac{df_2}{d\eta} k + \frac{1}{\beta} f_2 \frac{dk}{d\eta}, \tag{16.117}$$

which, with the aid of (16.78)₂ and (16.115), becomes

$$\begin{aligned} \chi(\eta) &= \frac{3}{2}\beta \left(\frac{2}{\eta} f_1 \frac{df_1}{d\eta} - f_1^2 - \frac{1}{\eta} \frac{df_1}{d\eta} \right) \stackrel{(16.77)}{=} \frac{3}{2}\beta f_1(\eta)(1 - 3f_1(\eta)), \\ \chi(0) &= \frac{3}{2}\beta f_1(0)(1 - 3f_1(0)) = -3\beta. \end{aligned} \tag{16.118}$$

This result is in excellent agreement with experimental results of I. WYGANSKI and J. FIEDLER [30]. Their experimentally based curve in Fig. 16.14 shown by open circles—is referred to in several articles and textbooks in the years subsequent to their work, see e.g. O. HINZE [14].

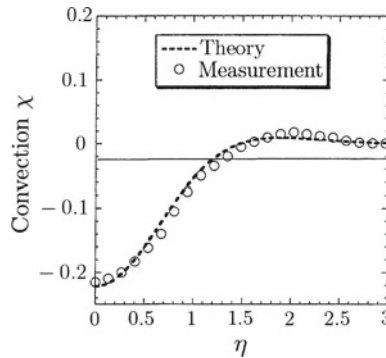


Fig. 16.14 Dimensionless turbulent convection term. Dashed curve as calculated with the DQTM-parameterization (16.17); open circles as extracted from measurements given in [30]. At $\eta = 1.2$ the convection parameter χ changes sign. The $\chi(\eta)$ -function reaches a maximum value at $\eta = 2.1$ and approaches $\chi \rightarrow 0$ as $\eta \rightarrow \infty$. Courtesy P. EGOLF and D.A. WEISS [9], © Phys. Rev. E, reproduced with changes

16.4 Turbulent Round Jet in a Parallel Co-flow

The axisymmetric jet dealt with in the last section is restricted to the situation of a jet inflow into a quiescent ambient fluid. P. EGOLF [8] has also looked at the situation of a jet entering a fluid moving with a constant velocity parallel to the jet exit velocity. If U_G , see Fig. 16.15, is the speed of its background velocity and U the mean jet speed at the nozzle beyond U_G , then an approach analogous to that in the previous section shows that similarity solutions do not exist in general, but can still be constructed in the limits, when

$$\frac{U}{U_G} \rightarrow 0 \quad \text{and} \quad \frac{U}{U_G} \rightarrow \infty. \tag{16.119}$$

In the first case the jet velocity at the nozzle is small in comparison to the ambient velocity; in the second case it is reverse, i.e., the ambient velocity is small as compared to that of the jet. This case has been analyzed in Sect. 16.3 of this chapter. The proof of this fact may e.g. by following mathematically the approach of Sect. 16.3: Existence of similarity solutions is postulated and a contradiction is derived. Necessary conditions for the exponents p_0, \dots, p_{12} (compare (16.61), (16.62), (16.63)) are established for which similarity solutions will not exist. This happens to be the case if U/U_G is bounded from below and above, i.e., if it is of finite value. In the limits (16.119), however, similarity solutions can be constructed. The solution for the limit $U/U_G \rightarrow \infty$ has essentially been shown in Sect. 16.3. The other case is the topic of this section.

For the axisymmetric steady flow the balances of mass and momentum of the mean turbulent motion are given by (16.52), (16.60) together with (16.18),

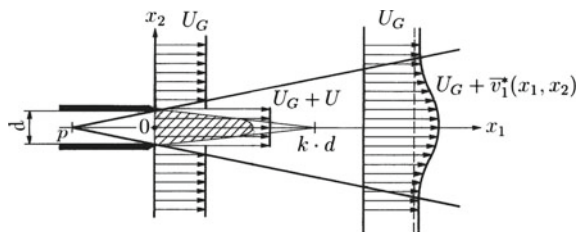


Fig. 16.15 Turbulent circular jet entering an ambient region with constant velocity U_G parallel to the jet. The relative mean velocity to the velocity of the ambient fluid is U , so that its absolute speed is $U + U_G$. The perturbed velocity above U_G downstream of the nozzle is $\vec{v}_1^*(x_1, x_2)$. The diameter of the nozzle is d and the distance of influence of the flow out of the pipe is kd . Courtesy P. EGOLF [8], © Phys. Rev. E., reproduced with changes

$$\frac{\partial \bar{v}_1^*}{\partial x_1} + \frac{1}{x_2} \frac{\partial(x_2 \bar{v}_2^*)}{\partial x_2} = 0, \tag{16.120}$$

$$\bar{v}_1^* \frac{\partial \bar{v}_1^*}{\partial x_1} + \bar{v}_2^* \frac{\partial \bar{v}_1^*}{\partial x_2} + \frac{1}{x_2} \frac{\partial(x_2 \bar{v}_1' v_2')}{\partial x_2} = 0, \tag{16.121}$$

in which $\bar{v}_1 = U_G + \bar{v}_1^*$; here, \bar{v}_1^* is the axial perturbation speed and U_G the constant parallel speed of the surrounding fluid.

If we now use the product decompositions of \bar{v}_1^* , \bar{v}_2^* , $\bar{v}_1' v_2'$, $\eta = x_2/b$ and b as shown in (16.22)–(16.25), substitute these in (16.120) and (16.121) and request similarity behavior, then the continuity equation leads to

$$p_0 + p_1 - p_2 = 1, \quad \text{and} \quad p_1 f_1 - p_0 \eta \frac{df_1}{d\eta} + \frac{1}{\beta} \frac{1}{\eta} \frac{d(\eta f_2)}{d\eta} = 0, \tag{16.122}$$

as before in (16.64)₁ and (16.65)₁. However, the approximate axial momentum equation transforms to

$$\begin{aligned} \frac{1}{kd} \left\{ \left(\left(\frac{U_G}{U} \right) + \left(\frac{x_1 - p}{kd} \right)^{p_1} f_1 \right) \left(\frac{x_1 - p}{kd} \right)^{p_1 - 1} \left(p_1 f_1 - p_0 \eta \frac{df_1}{d\eta} \right) \right. \\ \left. + \frac{1}{\beta} \left(\frac{x_1 - p}{kd} \right)^{p_2 + p_1 - p_0} f_2 \frac{df_1}{d\eta} \right. \\ \left. - \frac{1}{\beta} \left(\frac{x_1 - p}{kd} \right)^{p_{12} - p_0} \frac{1}{\eta} \frac{d(\eta f_{12})}{d\eta} \right\} = 0 \end{aligned} \tag{16.123}$$

and is more difficult to explore. Requesting next also that the REYNOLDS stress, scaled with the mean velocity in the principal flow direction, is independent of x_1 , see (16.33), then relation (16.34) must equally hold,

$$2p_1 - p_{12} = 0. \tag{16.124}$$

Finally, one may equally request that the force on the cylinder, induced by the flow is x_1 -independent. This has also been explained earlier, between (16.37)–(16.39) and yielded

$$p_0 + p_1 = 0. \tag{16.125}$$

Returning to (16.123), notice that this equation involves U_G/U , and it is this term, which destroys its similarity property. Indeed, the equation consists of 4 terms, each with its own exponent of $(x_1 - p)/(kd)$. For instance, for finite values of U_G/U one would have to request that $p_1 - 1 = 2p_1 - 1$ or $1 = 2$, unless $p_1 = 0$, $p_0 = 0$, $p_{12} = 0$, $p_2 = -1$, which is obviously inconsistent! So, there is only hope for similarity behavior in the limits (16.119).

(a) Large jet velocity such that $U_G/U \rightarrow 0$

Dropping U_G/U in (16.123) and comparing the exponents of $(x_1 - p)/(kd)$ in the emerging equation generates again (16.122), and the new equation

$$p_0 + 2p_1 - p_{12} = 1. \quad (16.126)$$

The four Eqs. (16.122)₁, (16.124), (16.125), (16.126) [and two non-conflicting remaining equations] generate the solution

$$p_0 = 1, \quad p_1 = -1, \quad p_2 = -1, \quad p_{12} = -2, \quad (16.127)$$

which agree with (16.68). This must obviously be so, because the condition $U_G/U = 0$ corresponds with a jet merging into a quiescent ambient. It is, therefore, consequential that the DQTM-solutions for f_1 , f_2 , f_{12} also agree with (16.77), (16.71) and (16.74). The reader may prove this by himself/herself.

(b) Small jet velocity such that $U_G/U \rightarrow \infty$

Rewriting (16.123) as

$$\begin{aligned} & \left\{ 1 + \frac{U}{U_G} \left(\frac{x_1 - p}{kd} \right)^{p_1} f_1 \right\} \left(\frac{x_1 - p}{kd} \right)^{p_1 - 1} \left(p_1 f_1 - p_0 \eta \frac{df_1}{d\eta} \right) \\ & + \frac{1}{\beta} \frac{U}{U_G} \left(\frac{x_1 - p}{kd} \right)^{p_2 + p_1 - p_0} f_2 \frac{df_1}{d\eta} \\ & - \frac{1}{\beta} \frac{U}{U_G} \left(\frac{x_1 - p}{kd} \right)^{p_{12} - p_0} \frac{1}{\eta} \frac{d}{d\eta} (\eta f_{12}) = 0 \end{aligned} \quad (16.128)$$

and ignoring all terms linear in U/U_G leads to a single ordinary differential equation for f_1 ,

$$\frac{d}{d\eta} (\eta f_1(\eta)) = 0, \quad \forall \eta \in [0, \infty) \quad \longrightarrow \quad f_1(\eta) \equiv 0, \quad (16.129)$$

which is simply the trivial solution.⁶ No jet can be formed in this limit. It follows, for a non-trivial solution some of the terms involving U/U_G in (16.128) should survive. Several choices are possible, but only one is appropriate. A natural selection is to drop the second term in the curly bracket in the first line of (16.128), and balancing

$$\left(\frac{x_1 - p}{kd} \right)^{p_1 - 1} \quad \text{and} \quad \left(\frac{x_1 - p}{kd} \right)^{p_{12} - p_0}; \quad (16.130)$$

⁶Another non-trivial solution is $f_1 = c/\eta$. However, this solution is equally inadmissible, since it generates a singularity at $\eta = 0$, which is unphysical.

this yields

$$p_1 - 1 = p_{12} - p_0 \implies p_0 + p_1 - p_{12} = 1. \tag{16.131}$$

Together with (16.122), (16.125), (16.126), which still hold, the following p -values,

$$p_0 = \frac{1}{3}, \quad p_1 = -\frac{2}{3}, \quad p_2 = -\frac{4}{3}, \quad p_{12} = -\frac{4}{3}, \tag{16.132}$$

are obtained. With them, the exponents of the $(x_1 - p)/(kd)$ -terms take the values

$$p_1 - 1 = p_{12} - p_0 = -\frac{5}{3}, \quad p_2 + p_1 - p_0 = 2p_1 - 1 = -\frac{7}{3}. \tag{16.133}$$

This implies that, asymptotically for large values of $(x_1 - p)/(kd)$,

$$\left(\frac{x_1 - p}{kd}\right)^{-5/3} \text{ is larger than } \left(\frac{x_1 - p}{kd}\right)^{-7/3}, \tag{16.134}$$

so that in this limit the underscored terms in (16.128) can be dropped in comparison to the remaining terms. This leads now to the asymptotic similarity behavior for which (16.122)₂, obtained from the continuity equation and the reduced momentum equation (16.128), yields

$$\begin{aligned} 2f_1 + \eta \frac{df_1}{d\eta} - \frac{3}{\beta} \frac{1}{\eta} \frac{d(\eta f_2)}{d\eta} &= 0, \\ \implies \frac{d}{d\eta} (\eta f_2) &= \frac{\beta}{3} \frac{d}{d\eta} (\eta^2 f_1), \\ \implies f_2 &= \frac{\beta}{3} \eta f_1, \end{aligned} \tag{16.135}$$

$$2f_1 + \eta \frac{df_1}{d\eta} + \frac{3}{\beta} \left(\frac{U}{U_G}\right) \frac{1}{\eta} \frac{d(\eta f_{12})}{d\eta} = 0, \tag{16.136}$$

in which the p -values (16.132) have been substituted. These are two equations for three unknowns.

The DQTM-model of EGOLF [8] is now introduced in the form (16.17), in which $\chi_2 = b$ is used. This yields

$$\begin{aligned} \frac{\overline{v'_1 v'_2}}{U^2} &= b \frac{db}{dx_1} \left[\frac{U_G}{U} + \frac{\overline{v_1^*}(x_1, x_2)}{U} \right] \left[\frac{U_G}{U} + \frac{\overline{v_1^*}(x_1, 0)}{U} - \left(\frac{U_G}{U} + \frac{\overline{v_1^*}(x_1, x_2)}{U} \right) \right] \frac{1}{x_2} \\ &\approx \underbrace{b \frac{db}{dx_1}}_{\frac{1}{3}\beta} \frac{U_G}{U} \frac{\overline{v_1^*}(x_1, 0) - \overline{v_1^*}(x_1, x_2)}{U x_2} \end{aligned} \tag{16.137}$$

and implies with (16.22)–(16.25)

$$f_{12} = \frac{1}{3}\beta \frac{U_G}{U} \frac{1 - f_1}{\eta}. \quad (16.138)$$

Substitution of this equation into (16.136) yields

$$2f_1 + \left(\eta + \frac{1}{\eta}\right) \frac{df_1}{d\eta} = 0, \quad (16.139)$$

which is an ordinary differential equation for f_1 alone and possesses the solution

$$f_1 = \frac{1}{1 + \eta^2}, \quad (16.140)$$

which enjoys the symmetry property that $f_1(\eta) = f_1(-\eta)$. Based on (16.138) and (16.135), Eq. (16.140) generates the functions

$$f_2 = \frac{\beta}{3} \frac{\eta}{1 + \eta^2}, \quad (16.141)$$

$$f_{12} = -\frac{\beta}{3} \left(\frac{U_G}{U}\right) \frac{\eta}{1 + \eta^2}, \quad (16.142)$$

which are both anti-symmetric: $f_2(\eta) = -f_2(-\eta)$, $f_{12}(\eta) = -f_{12}(-\eta)$ and proportional to each other.

Graphs of the functions (16.140)–(16.142) are shown in **Fig. 16.16**. The mean velocity profile in the main direction, f_1 , shows a maximum at $\eta = 0$ and decreases algebraically to zero as $\eta \rightarrow \infty$. Because of symmetry requirements the mean scaled radial velocity $f_2(\eta)$ and the REYNOLDS shear stress f_{12} vanish for $\eta = 0$ and as

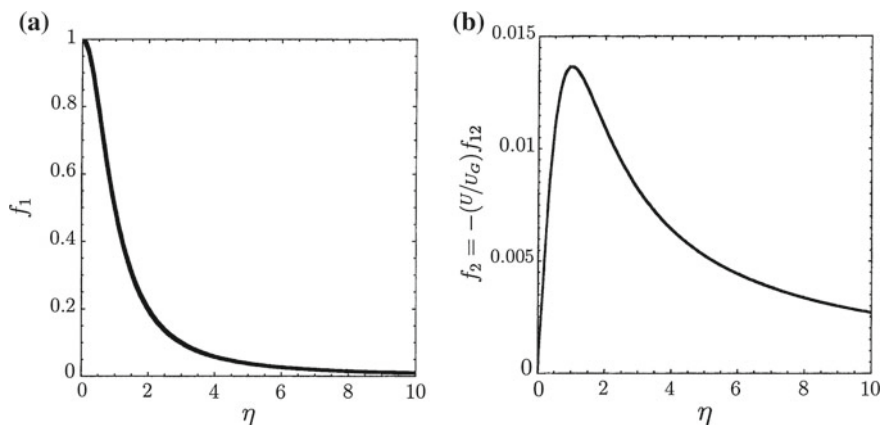


Fig. 16.16 Distribution of f_1 , f_2 and $f_{12}(\eta)/(U_G/U)$ as functions of η , according to (16.140), (16.141) and (16.142)

η approaches ∞ . Moreover, f_2 is positive for $\eta > 0$ and negative for $\eta < 0$ and, therefore, does not exhibit the entrainment phenomenon.

16.5 A Study of Turbulent Plane Poiseuille Flow

Consider plane steady turbulent flow between two parallel rigid planes a distance $2a$ apart. Let x_1 and x_2 be Cartesian coordinates parallel and orthogonal to the flow direction, see **Fig. 16.17**. Moreover, consider the balance laws of mass and momentum under the restriction that $\bar{v}_2 = 0$ and $\partial(\cdot)/\partial x_3 = 0$ for all field variables of the system under consideration. It then follows from the continuity equation that \bar{v}_1 is only a function of x_2 . This implies that the convective acceleration terms in the horizontal directions,

$$\bar{v}_1 \frac{\partial \bar{v}_1}{\partial x_1} + \bar{v}_2 \frac{\partial \bar{v}_1}{\partial x_2} = 0, \quad \bar{v}_1 \frac{\partial \bar{v}_2}{\partial x_1} + \bar{v}_2 \frac{\partial \bar{v}_2}{\partial x_2} = 0, \tag{16.143}$$

vanish identically. Therefore, the horizontal momentum equations (15.22) for a NEWTONIAN fluid reduce to the force balances

$$\begin{aligned} \frac{1}{\rho} \frac{\partial \bar{p}}{\partial x_1} - \nu \frac{\partial^2 \bar{v}_1}{\partial x_2^2} + \frac{\partial \overline{v_1' v_2'}}{\partial x_2} &= 0, \\ \frac{1}{\rho} \frac{\partial \bar{p}}{\partial x_2} + \frac{\partial \overline{v_2'^2}}{\partial x_2} &= 0, \end{aligned} \tag{16.144}$$

in which we have used the viscous stress representations

$$(t_D)_{ij} = \rho \nu \left(\frac{\partial \bar{v}_i}{\partial x_j} + \frac{\partial \bar{v}_j}{\partial x_i} \right), \tag{16.145}$$

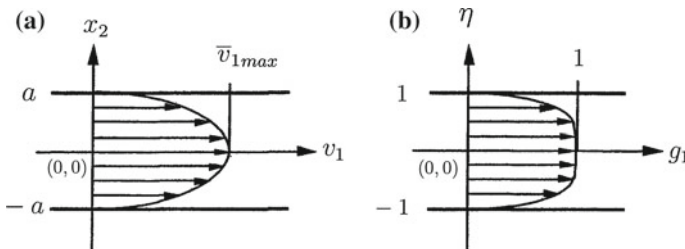


Fig. 16.17 Laminar and turbulent POISEUILLE flow between two plane parallel plates. **a** In the laminar case, the velocity profile is parabolic, **b** In turbulent steady flow the profile flattens more and more as the REYNOLDS number increases

where ν is the kinematic viscosity. It is easy to show that all material stress components vanish with the above assumptions, except $(t_D)_{12} = \tau$. Moreover, it is also readily seen that only the REYNOLDS stresses $R_{12} = \tau_{12} = \tau_t$ and $R_{22} = \sigma_t$ survive.

Introducing the dimensionless space coordinates

$$\xi = x_1/a, \quad \eta = x_2/a \quad (16.146)$$

and the *shear velocity*

$$v^* = \sqrt{\frac{|\tau_0|}{\rho}}, \quad \tau_0 = \pm \rho \nu \left. \frac{\partial \bar{v}_1}{\partial x_2} \right|_{\pm a} \quad (16.147)$$

as well as the REYNOLDS numbers

$$\mathbb{R} = \frac{\bar{v}_{1\max} a}{\nu}, \quad \mathbb{R}^* = \frac{v^* a}{\nu} \implies \mathbb{R} = \frac{\bar{v}_{1\max}}{v^*} \mathbb{R}^*. \quad (16.148)$$

Equations (16.144) are now made dimensionless by defining the quantities⁷

$$f_1(\eta, \mathbb{R}^*) = \frac{\bar{v}_1}{v^*}, \quad (16.149)$$

$$P(\xi, \eta, \mathbb{R}^*) = \frac{\bar{p} - p_0}{\rho(v^*)^2}, \quad (16.150)$$

$$f_{12}(\eta, \mathbb{R}^*) = \frac{\overline{v'_1 v'_2}}{(v^*)^2}, \quad (16.151)$$

$$f_{22}(\eta, \mathbb{R}^*) = \frac{\overline{v'^2_2}}{(v^*)^2}. \quad (16.152)$$

With these, Eqs. (16.144) take the forms

$$\begin{aligned} \frac{\partial P}{\partial \xi} - \frac{1}{\mathbb{R}^*} \frac{\partial^2 f_1}{\partial \eta^2} + \frac{\partial f_{12}}{\partial \eta} &= 0, \\ \frac{\partial P}{\partial \eta} + \frac{\partial f_{22}}{\partial \eta} &= 0. \end{aligned} \quad (16.153)$$

The second of these equations implies that $P + f_{22}(\eta) = F(\xi, \mathbb{R}^*)$. Alternatively, the first equation says $\partial P / \partial \xi = G(\eta, \mathbb{R}^*)$ [where G can easily be inferred from (16.153)₁]. Thus,

$$\frac{\partial P}{\partial \xi} = G(\eta, \mathbb{R}^*) = \frac{\partial F(\xi, \mathbb{R}^*)}{\partial \xi}. \quad (16.154)$$

⁷Note, P is a function of ξ , since \bar{p} depends on ξ . f_{12} and f_{22} have no ξ -dependence by assumptions analogous to (16.33).

This implies that G and $\partial F/\partial \xi$ can neither depend on ξ nor on η and, thus, must be the same function of \mathbb{R}^* alone. Consequently, integration of F yields

$$F = A(\mathbb{R}^*)\xi + C(\mathbb{R}^*). \quad (16.155)$$

Therefore, we have from (16.153)₂

$$P + f_{22} = A(\mathbb{R}^*)\xi + C(\mathbb{R}^*). \quad (16.156)$$

and from (16.153)₁

$$\begin{aligned} & \frac{\partial}{\partial \eta} \left\{ \frac{1}{\mathbb{R}^*} \frac{\partial f_1}{\partial \eta} - f_{12} \right\} = A(\mathbb{R}^*) \\ \longrightarrow & \frac{1}{\mathbb{R}^*} \frac{\partial f_1(\eta, \mathbb{R}^*)}{\partial \eta} - f_{12}(\eta, \mathbb{R}^*) - A(\mathbb{R}^*)\eta + B(\mathbb{R}^*) = 0. \end{aligned} \quad (16.157)$$

The parameter $A(\mathbb{R}^*)$ and the constants of integration $B(\mathbb{R}^*)$ and $C(\mathbb{R}^*)$ must be determined.

The boundary conditions at the two walls request

$$\{f_1; f_{12}; f_{22}\}(\pm 1, \mathbb{R}^*) = 0 \quad (16.158)$$

and

$$P(0, -1, \mathbb{R}^*) = 0 \quad \text{for normalization of the pressure.} \quad (16.159)$$

Relations (16.158) say that the mean velocity \bar{v}_1 and the turbulent stresses τ_t and σ_t vanish at the walls, so that the total stress τ_{tot} is given by the viscous τ and the turbulent or REYNOLDS shear stress τ_t ,

$$\tau_{\text{tot}} = \tau + \tau_t = \rho\nu \frac{\partial \bar{v}_1}{\partial x_2} - \overline{\rho v'_1 v'_2}. \quad (16.160)$$

Near the wall, the turbulent fluctuations disappear. From this and (16.147), one may deduce

$$\frac{\tau_{\text{tot}}}{\rho} \Big|_{\pm a} = \nu \frac{\partial \bar{v}_1}{\partial x_2} \Big|_{\pm a} = \mp (v^*)^2, \quad (16.161)$$

which yields, together with the definition (16.149),

$$\nu \frac{v^*}{a} \frac{df_1}{d\eta} \Big|_{\pm 1} = \mp (v^*)^2 \implies \frac{df_1}{d\eta} \Big|_{\pm 1} = \mp \frac{v^* a}{\nu} = \mp \mathbb{R}^*. \quad (16.162)$$

Substituting these results into (16.157) yields

$$A + B = -1 \text{ and } -A + B = 1 \implies A = -1, B = 0. \quad (16.163)$$

Therefore, (16.156) with $C = 0$ (due to (16.159)) and (16.157) take the forms

$$\begin{aligned} P(\xi, \eta, \mathbb{R}^*) + f_{22}(\eta, \mathbb{R}^*) + \xi &= 0, \\ \frac{1}{\mathbb{R}^*} \frac{df_1(\eta, \mathbb{R}^*)}{d\eta} - f_{12}(\eta, \mathbb{R}^*) + \eta &= 0. \end{aligned} \quad (16.164)$$

The second of these equations can be integrated subject to the boundary conditions that $f_1(\pm 1, \mathbb{R}^*) = 0$. This leads to

$$f_1(\eta, \mathbb{R}^*) = \mathbb{R}^* \left\{ \int_{-1}^{\eta} f_{12}(\bar{\eta}, \mathbb{R}^*) d\bar{\eta} + \frac{1}{2} (1 - \eta^2) \right\}, \quad (16.165)$$

owing to the symmetry requirement $f_{12}(\eta) = -f_{12}(-\eta)$ for the shear stress. To fulfill the boundary conditions $f_1(-1, \mathbb{R}^*) = 0$, the integration constant in (16.165) has been set equal to $\frac{1}{2}$. For laminar flows ($f_{12} = 0$), $f_1(\eta)$ takes the form

$$f_1(\eta, \mathbb{R}^*) = \frac{\mathbb{R}^*}{2} (1 - \eta^2), \quad (16.166)$$

which is the HAGEN–POISEUILLE profile.

There remains the implementation of the DQTM parameterization of the shear stress; with (16.17) it may be expressed as

$$\begin{aligned} \tau_t &= -\rho \overline{v'_1 v'_2} \\ &= \rho \sigma \chi_2 [\bar{v}_1(x_1, x_2) - \bar{v}_{1\min}(x_1)] \frac{\bar{v}_{1\max}(x_1) - \bar{v}_1(x_1, x_2)}{x_{2\max} - x_2}, \end{aligned} \quad (16.167)$$

in which σ is the spreading parameter. In (16.17), where free turbulence was dealt with, we chose $\sigma = db/dx_1$, where b is the spreading width of the turbulent region. 'In POISEUILLE flow the spreading by turbulent convection is only a flow internal feature, [whilst] in a jet flow it also defines the boundary of the turbulent domain. The turbulence intensities are small compared with the mean downstream velocity [$|\bar{v}_1| \gg (\overline{v_1'^2})^{1/2}$]' [10]. Since $\bar{v}_{1\min} = 0$ and $\bar{v}_{1\max} = \bar{v}_1(0, \mathbb{R}^*)$, substitution of (16.149) into (16.167) yields [we do not show the dependence on \mathbb{R}^*]

$$f_{12}(\eta) = \frac{\sigma}{\eta} f_1(\eta) (f_1(0) - f_1(\eta)). \quad (16.168)$$

Thus, one obtains from (16.164)₂ the differential equation

$$\frac{1}{\mathbb{R}^*} \frac{df_1(\eta)}{d\eta} - \sigma \frac{1}{\eta} f_1(\eta) [f_1(0) - f_1(\eta)] + \eta = 0. \quad (16.169)$$

Turbulent closure relations would also have to be formulated for f_{22} and P that would be substituted into (16.164)₁. Because Eq. (16.169) is independent of (16.164)₁ and not affected by (16.164)₂, the ensuing analysis will be restricted to the exploitation of (16.169).

With the new functions

$$g_1(\eta) \equiv \frac{f_1(\eta)}{f_1(0)}, \quad g_{12}(\eta) = f_{12}(\eta) \quad (16.170)$$

and the abbreviations

$$\alpha \equiv \frac{f_1(0)}{\mathbb{R}^*}, \quad \beta \equiv \sigma (f_1(0))^2, \quad (16.171)$$

the differential equation (16.169) transforms into

$$\alpha \eta \frac{dg_1(\eta)}{d\eta} - \beta g_1(\eta) + \beta (g_1(\eta))^2 + \eta^2 = 0 \quad (16.172)$$

and must be solved subject to the following symmetry, normalization and boundary conditions

$$g_1(\eta) = g_1(-\eta), \quad g_1(0) = 1, \quad g_1(1) = 0, \quad (16.173)$$

as well as (16.162) or

$$\left. \frac{dg_1}{d\eta} \right|_{\pm 1} = \mp \frac{\mathbb{R}^*}{f_1(0)} = \mp \frac{1}{\alpha}, \quad (16.174)$$

owing to (16.171). This says that the slope of the mean velocity profile at the plates is directly proportional to the REYNOLDS number \mathbb{R}^* . These results are due to P. EGOLF and D.A. WEISS [10]. They state that ‘this is in qualitative agreement with experimental observations of a decreasing boundary layer thickness in terms of an increasing REYNOLDS number’, [10].

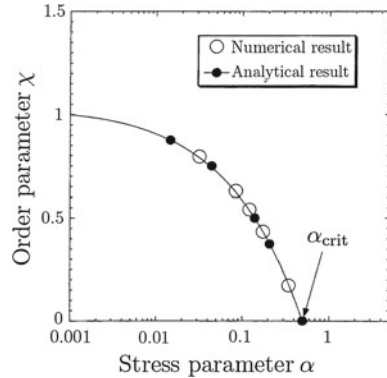
P. EGOLF and D.A. WEISS performed the numerical integration of (16.172) by a shooting procedure, starting at $\eta = -1$, selecting a certain value of β , using α as shooting parameter and varying it until the profile would hit $(\eta, g_1) = (+1, 0)$ on the opposite side and fulfill the boundary condition (16.173)₃. The function

$$\chi = \beta(\alpha)/4, \quad (16.175)$$

which has been evaluated by this procedure, is shown in **Fig. 16.18**. It is referred to as *order parameter*.

As this figure suggests, if $\alpha \rightarrow 0$, then β approaches 4 and χ approaches 1. Moreover, as numerically indicated, the values for β are positive and smaller and/or equal to 4, a value, which can be shown analytically to be correct [10]. Owing to the

Fig. 16.18 Analytically and numerically derived functional relation between the stress parameters α and β (or the order parameter χ). α is inversely related to the REYNOLDS number, see equation (16.174). Corresponding mean velocity profiles and REYNOLDS stresses are shown in Fig. 16.19. Courtesy P. EGOLF and D.A. WEISS [10], © *Phys. Rev. E*. reproduced with changes



symmetry condition (16.173)₁, it suffices to study the behavior of g_{12} in the interval $0 \leq \eta < 1$.

EGOLF and WEISS [10] solved Eqs. (16.164)₂ and (16.168), or alternatively (16.172) and (16.168) with definitions (16.170) subject to boundary condition (16.173), (16.174) and plotted mean velocity profiles g_1 and REYNOLDS shear stresses $g_{12} \equiv f_{12}$ as functions of η for the values of β as shown as insets in Fig. 16.19. These graphs show that with increasing parameter β , the time averaged velocity profiles flatten and the REYNOLDS shear stresses converge toward a linear distribution in η .

P. EGOLF and D.A. WEISS [10] also attack the solution of (16.172) subject to the conditions (16.170), (16.171). These solutions were constructed by them for low, moderate and high REYNOLDS numbers. In these regimes, analytical, or partly analytical solutions could be found.

Low Reynolds numbers: For this limit $\beta = 0$ and $\alpha = \frac{1}{2}$, see Fig. 16.18 and formulae (16.171), (16.172), for which

$$g_1(\eta) = 1 - \eta^2. \tag{16.176}$$

This represents the laminar velocity profile for REYNOLDS numbers below the critical values.

Moderate Reynolds numbers: In this case $\beta > 0, \alpha > 0$. The following transformation

$$g_1 = H \frac{h'}{h}, \quad H \equiv \frac{\alpha}{\beta} \eta \tag{16.177}$$

is considered, implying for (16.172)

$$\alpha^2 \eta h'' + (\alpha^2 - \alpha\beta)h' + \beta\eta h = 0. \tag{16.178}$$

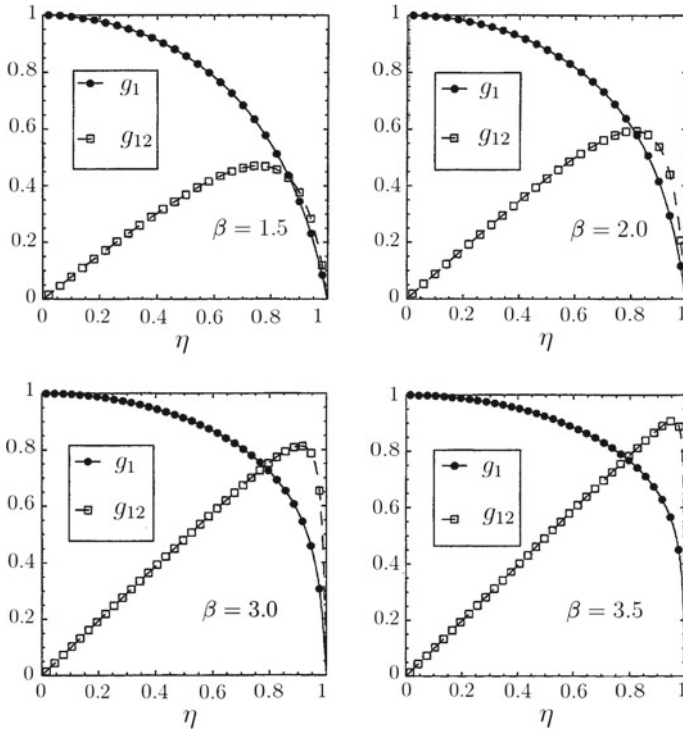


Fig. 16.19 Four time-averaged velocity profiles g_1 and REYNOLDS shear stress distributions (for $0 < \eta < 1$) g_{12} for different turbulent intensities $0 \leq \beta \leq 4$. Note that with growing β the velocity profile flattens and the turbulent shear stresses approach a linear distribution with η . Courtesy P. EGOLF and D.A. WEISS [10], © Phys. Rev. E, reproduced with changes

Applying the further transformation

$$\psi \equiv \lambda \eta, \quad \lambda \equiv \frac{\sqrt{\beta}}{\alpha} \tag{16.179}$$

leads to the following BESSEL differential equation

$$\psi \frac{\partial^2 h}{\partial \psi^2} + \left(1 - \frac{\beta}{\alpha}\right) \frac{\partial h}{\partial \psi} + \psi h = 0. \tag{16.180}$$

P. EGOLF and D.A. WEISS [10] show that the general solution for g_1 , defined in (16.177), is given by

$$g_1(\psi) = \frac{\psi}{2\kappa} \frac{pJ_{\kappa-1}(\psi) + qY_{\kappa-1}(\psi)}{pJ_{\kappa}(\psi) + qY_{\kappa}(\psi)}, \tag{16.181}$$

where

$$\kappa = \frac{\beta}{2\alpha} \quad (16.182)$$

and J_κ and Y_κ are the BESSEL functions of first and second kind, respectively and order κ . For $\psi \rightarrow 0$, i.e., $\eta \rightarrow 0$ the function $g_1(\psi)$ must reach its maximum value, see (16.173)₂,

$$\lim_{\psi \rightarrow 0} g_1(\psi) = 1. \quad (16.183)$$

This implies, since $\lim_{\psi \rightarrow 0} Y(\psi) \rightarrow \infty$, that $q = 0$, so that

$$g_1(\psi) = \frac{\psi}{2\kappa} \frac{J_{\kappa-1}(\psi)}{J_\kappa(\psi)} = \frac{J_{\kappa-1}(\psi)}{J_{\kappa-1}(\psi) + J_{\kappa+1}(\psi)}. \quad (16.184)$$

The second boundary condition, (16.173)₃ now requires that $\psi(\eta = 1) = \lambda = \sqrt{\beta}/\alpha$, and, consequently, from (16.184)

$$J_{\kappa-1}\left(\frac{\sqrt{\beta}}{\alpha}\right) = 0, \quad \implies \quad \frac{\sqrt{\beta}}{\alpha} = j_{\kappa-1,1}, \quad (16.185)$$

in which $j_{\kappa-1,1}$ is the first zero of the BESSELS function $J_{\kappa-1}$. Because $2\kappa = \beta/\alpha$, according to (16.182), one can solve these equations for α and β separately:

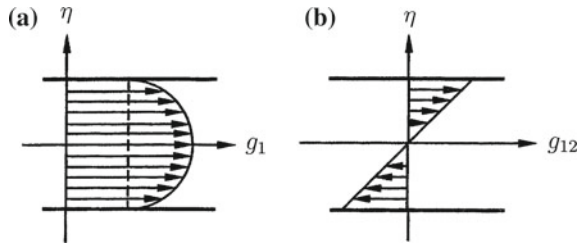
$$\alpha = \frac{2\kappa}{(j_{\kappa-1,1})^2}, \quad \beta = \frac{4\kappa^2}{(j_{\kappa-1,1})^2}. \quad (16.186)$$

To given κ , pairs of (α, β) can be calculated by means of tables (e.g., ABRAMOWITZ–STEGUN [1]. Using this source, P. EGOLF and D.A. WEISS [10] also find the representations

$$J_\kappa(\psi) = \left(\frac{\psi}{2}\right)^\kappa \sum_{k=0}^{\infty} \frac{\left(-\frac{\psi^2}{4}\right)^k}{k! \Gamma(\kappa + k + 1)}, \quad (16.187)$$

$$g_1(\psi) = \frac{1}{\kappa} \frac{\sum_{k=0}^{\infty} \frac{\left(-\frac{\psi^2}{4}\right)^k}{k! \Gamma(\kappa + k)}}{\sum_{k=0}^{\infty} \frac{\left(-\frac{\psi^2}{4}\right)^k}{k! \Gamma(\kappa + k + 1)}}, \quad (16.188)$$

Fig. 16.20 Time-averaged mean velocity and turbulent shear stress distributions for infinite REYNOLDS number. The velocity distribution is a perfect half circle, the shear stress is triangular



$$g_{12} = \beta j_{\kappa-1,1} \frac{1}{\psi} \frac{J_{\kappa-1} J_{\kappa+1}}{(J_{\kappa-1} + J_{\kappa+1})^2}. \tag{16.189}$$

Here $\Gamma(x)$ is the Gamma function and $k!$ the factorial of k .

Infinite Reynolds number: With the definition of α and $\alpha \rightarrow 0$, Fig. 16.18 suggests $\beta = 4$ ($\chi = 1$); consequently, (16.172) reduces to the quadratic equation

$$g_1^2(\eta) - g_1(\chi) + \frac{\eta^2}{4} = 0, \implies g_1 = \frac{1}{2} \left(1 + \sqrt{1 - \eta^2} \right). \tag{16.190}$$

P. EGOLF and D.A. WEISS [10] prove that this in fact is the pointwise limit of the solution of (16.184) for $\kappa \rightarrow \infty$. Substituting the variable change

$$\zeta = 2g_1 - 1$$

the solution (16.190) can be written as

$$\zeta^2 + \eta^2 = 1, \tag{16.191}$$

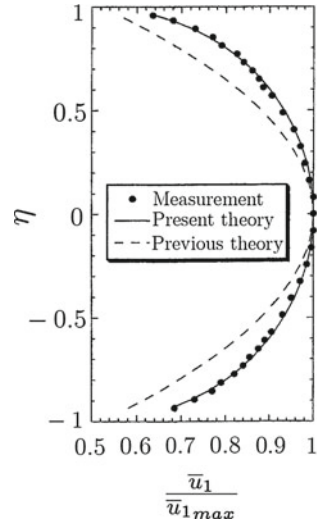
an equation describing the unit circle. **Figure 16.20a, b** displays the time-averaged velocity profile and the corresponding turbulent shear stress for a motion from left to right. With the representation (16.190)₂ (and $\beta = 4$) we obtain

$$g_{12}(\eta) = \frac{4}{\eta} \frac{1 + \sqrt{1 - \eta^2}}{2} \left(1 - \frac{1 + \sqrt{1 - \eta^2}}{2} \right) = \eta, \tag{16.192}$$

which indeed reproduces the linear distribution displayed in Fig. 16.20.

Comparison with experiments: The computational result that the turbulent mean velocity profiles for very high REYNOLDS numbers converge toward a semi circle, is a marvelous test against experiments. Such data are given by J. LAUFER [18] and H. REICHARDT [26]. P. EGOLF and D.A. WEISS [10] chose the data of the latter, which are displayed in Fig. 16.21 ‘The experiments confirm the model results convincingly, but the good results are a little misleading. In the domain surrounding $\eta = \pm 0.6$ some measured quantities are somewhat smaller than the functional values. On the other

Fig. 16.21 Measured time-averaged velocity profile for fully turbulent flow. Data from [26] with $v^* = 15.2 \text{ cm s}^{-1}$ compared with the circle solution, denoted by ‘present theory’. The measurements were performed in a channel with height 24.6 cm, which is transformed to $\eta \in [-1, 1]$. The width of the channel was 98 cm. The dashed parabolic profile is due to an earlier model, given by REICHARDT [27]. Courtesy EGOLF and WEISS [10], © Phys. Rev. E. reproduced with changes



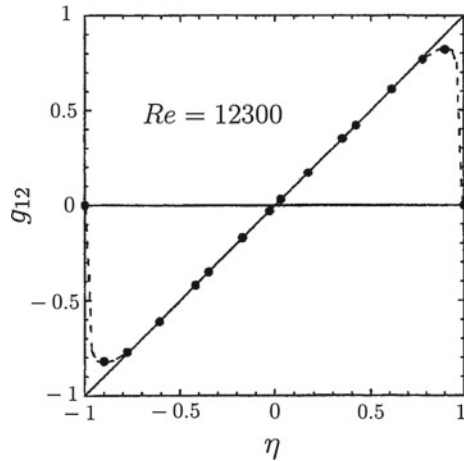
hand, exactly there—where the excitation of the flow system is further increased—the mean velocity profiles begin to exceed the theoretical functions...’ [10].

P. EGOLF and D.A. WEISS [10] mention the ‘Princeton Super Pipe Data’ [31] as ‘the newest results of the axisymmetric POISEUILLE flow measured [until the year 2000] at highest REYNOLDS numbers, for example $\mathbb{R} = 17,629,500$. The mean velocity profile between $\eta = -0.5$ and $\eta = 0.5$ also follows the circle profile with a maximum relative error of 1.2 %. Only in the turbulent boundary layer, at larger absolute values of η , the relative deviation takes higher values. From theory and experiments it is known that in the boundary layer, closer to the wall, the results of pipe and channel flow are practically identical. [...] so, also in the plane case, at higher REYNOLDS numbers, it is expected that the experimental values could exceed the theoretical ones shown in Fig. 16.21. But the solution in the core region, which is roughly defined by the interval $-0.5 < \eta < 0.5$, hardly alters any more when the excitation is further increased. Therefore, in Fig. 16.21 only in the core region the agreement between theory and experiment is reliable’ [10].

Figure 16.22 displays a comparison of the calculated REYNOLDS stresses with experimental data. The theoretical results are again in good agreement with the experimental data set; and they are as expected from Fig. 16.19.

The graphs in Fig. 16.19 and the results obtained for $\mathbb{R}^* \rightarrow \infty$ provide a justification for the denotation ‘order parameter’ to χ . The \bar{v}_1^* -velocity and REYNOLDS stress distributions across a channel profile depend on the α or β -parameter and, thus, also on the REYNOLDS number $\mathbb{R}^* = v_1^* a / \nu$. For $\beta = 0$ (low REYNOLDS number flow) the DQTM model for POISEUILLE flow delivers a *parabola* as the longitudinal velocity profile, whose curvature is largest at the channel axis that becomes continuously flatter as one moves toward the upper and lower walls. The corresponding shear stress distribution is linear! As β (and \mathbb{R}^*) grow, the longitudinal velocity distribution

Fig. 16.22 REYNOLDS shear stress g_{12} at $\mathbb{R} = 12\,300$. The distribution is already very close to the distribution for $\mathbb{R} = \infty$. The experimental data are taken from [18] and [21]. Courtesy P. EGOLF and D.A. WEISS [10], © Phys. Rev. E. reproduced with changes



deviates more and more from the parabola and approaches a semi-circular profile, which it exactly reaches as $\mathbb{R}^* \rightarrow \infty$. Correspondingly, the turbulent shear stress g_{12} that is skew-symmetric in η builds up from the zero function at $\beta = 0$, building a hump with zero values at $\eta = 0$ and $\eta = 1$ with maximum value closer to the wall than the channel axis. For growing $\beta \in (0, 4)$ ($\mathbb{R}^* \in [0^+, \infty)$) the maximum of this hump grows and its position moves toward the wall approaching an exactly *circular* mean velocity profile and linear shear stress distribution as $\mathbb{R}^* \rightarrow \infty$. These results are marvelously corroborated by data from L. LAUFER [18] and S.I. PAI [21], as evidenced in Figs. 16.21 and 16.22.

P. EGOLF and D.A. WEISS mention results obtained with the ‘Princeton Super Pipe Data’ taken at $\mathbb{R} = 17\,629\,500$. Small deviations of these data for $0.5 < \eta \leq 1$ from the exact circle are also observed there as in Fig. 16.22. More important than those small deviations, also observable in Fig. 16.22, seem to us the positive conclusion that the DQTM closure scheme yields a significant improvement over the classical PRANDTL-type modeling.

16.6 Discussion

This chapter is devoted to a number of zero order turbulence models for free turbulence and plane channel flow. Mathematically, the study is restricted to steady flows and situations, in which the processes can be reduced to two spatial dimensions—either exactly or approximately. The basis of our analysis is the Göttinger school, primarily under LUDWIG PRANDTL, who himself proposed his own turbulence closure relations, originally based upon BOUSSINESQ’s proposition of the turbulent eddy viscosity concept. LUDWIG PRANDTL introduced in 1925 [23] his mixing length concept, in which in two dimensions $\varepsilon_{\text{turb}} = \ell^2 |d\bar{v}_1/dx_2|$. For L. PRANDTL’s presentation

of this model, see Appendix A to this chapter. This concept was criticized even by L. PRANDTL himself by adding a second length scale ℓ' , involving the curvature effects of the velocity profile (see (16.14)). However, with these proposals optimal validation by experiment delivered values of the mixing lengths much smaller than the largest eddies in the flow under consideration. This fact makes it likely that L. PRANDTL regarded the mixing length not just as a phenomenological quantity, but assigned a direct physical meaning to it. In his next proposal in 1942 he then might have thought that the physical dimension of $\varepsilon_{\text{turb}}$ is $[\text{m}^2\text{s}^{-1}]$; incorporation of effects of the largest and smallest eddies (of a whole cascade) into $\varepsilon_{\text{turb}}$ may be achieved by constructing a viscosity with $\bar{v}_{1\text{max}}, \bar{v}_{1\text{min}}$ within the cross section of the free turbulent flow and the width b of the turbulent spread: $\varepsilon_{\text{turb}} \stackrel{\text{prop}}{=} b[\bar{v}_{1\text{max}} - \bar{v}_{1\text{min}}]$. This expression has the correct physical dimension, but to have the flexibility to adjust its value by validation with experiments, L. PRANDTL conjectured

$$\varepsilon_{\text{turb}}^{\text{Prandtl}} = \kappa b [\bar{v}_{1\text{max}} - \bar{v}_{1\text{min}}]. \quad (16.193)$$

and it is hoped that $\kappa = \mathcal{O}(1)$, see (16.15). That H. GÖRTLER [12] found good agreement with experiments in his validation attempt is rewarding; more important is the fact that L. PRANDTL gave up the strict locality concept and made his suggested $\varepsilon_{\text{turb}}$ at point \mathbf{x} to depend on field quantities at points $\mathbf{y} \neq \mathbf{x}$ (but *nota bene* also still at the same time). The shear stress formula, however, was in his case product-composed of the non-local expression of $\varepsilon_{\text{turb}}^{\text{Prandtl}}$ with the local mean velocity gradient:

$$\frac{\tau_{12}}{\rho} = \underbrace{(\varepsilon_{\text{turb}}^{\text{Prandtl}})}_{\text{non-local}} \underbrace{\frac{\partial \bar{v}_1}{\partial x_2}}_{\text{local}} \quad (16.194)$$

It is not known to us whether any-one or L. PRANDTL himself was thinking along these lines; fact is that we have not found statements, neither in PRANDTL's paper [25] nor in GÖRTLER's paper [12] that would mention the non-locality. The least in the 21-st century, in which invariance principles of continuum theories are well known, this might have raised resistance because a generalization to arbitrary three-dimensional processes can hardly be visualized. H. GÖRTLER found the largest deviations from measurements in the vicinity of the boundary of the mixing zone, because the eddy viscosity (16.193) does not vanish there.

It is at this point where P. EGOLF in 1992 [7] replaced (16.194) by a completely non-local expression, namely by

$$\tau_{12} = -\rho \overline{v'_1 v'_2} = \rho \chi_2 \frac{db}{dx_1} (\bar{v}_1 - \bar{v}_{1\text{min}}) \frac{\bar{v}_{1\text{max}} - \bar{v}_1}{x_{2\text{max}} - x_2}, \quad (16.195)$$

in which $\chi_2 \in [x_2, b]$ is a length parameter and $x_{2\text{max}}$ is that position in the cross section, where $\bar{v}_1 = \bar{v}_{1\text{max}}$. Moreover, ρ, χ_2 are still local quantities but the remaining factors are of non-local typ. Here, any notions of turbulent viscosity and local velocity

gradient are gone, but since \bar{v}_1 at the boundary of the mixing zone equals $\bar{v}_{1\min}$, τ_{12} , evaluated with (16.195) will vanish there.

The remainder of the chapter demonstrates that (nearly) all cases, for which turbulent mean velocities are computed, results are more convincing than with the older closure options. The procedures that have been followed are simple steady two-dimensional (plane or axisymmetric) flows, for which far away from initiating or disturbing elements exact or approximate similarity solutions of the governing equations can be constructed. They are expressible in general as functions f_1, f_2, f_{12}, \dots of a variable η perpendicular to the main flow direction, and f_2 and f_{12} have been shown to be expressible in terms of a functional of $f_1(\eta)$. The following problems have been attacked:

1. *The turbulent plane wake*: What just has been said above does not fully apply: Here, f_2 and f_{12} are expressible as functionals of f_1 . However, the equations do not reveal a boundary value problem for f_1 . The function f_1 can only be determined by constructing an optimal fit with experimental data. The mathematical determination of $f_1(\eta)$ remains unsolved.
2. *Axisymmetric isothermal steady jet into a quiescent ambient* is fully analytically determinable, provided the terms

$$\bar{v}_1 \frac{\partial \bar{v}_2}{\partial x_1}, \quad \bar{v}_2 \frac{\partial \bar{v}_2}{\partial x_2}, \quad \frac{\partial}{\partial x_1} (\overline{v'_1 v'_2})$$

are ignored. The first is the convective acceleration in the x_1 -direction, which is parallel to the direction of the principal flow. The second is small, since \bar{v}_2 is small and the third term expresses the slow variation of the shear stress in the longitudinal direction of the jet. The functions $f_1(\eta)$, $f_2(\eta)$ and $-f_{12}(\eta)$ marvelously match data (Figs. 16.5, 16.6, 16.7) of I. WYGANSKI and J. FIEDLER [30], as do the functions $g_{ii}(\eta)$ which are representative of $(v'_i)^2$ ($i = 1, 2, 3$). The mathematical method allows in this case also the computation of the density of turbulent kinetic energy, its production rate and convection parameter (see Eqs. (16.9)–(16.12)). Because these quantities were also experimentally determined by I. WYGANSKI and J. FIEDLER, validation of the computational results on the basis of their experiments is a particular convincing test of the closure model.

3. *Turbulent round jet in a parallel co-flow*: This case is similar to handle as the case of the jet-flow into a quiescent ambient fluid. It so happens that the general case, for which the speed of the jet and the outer fluid velocity parallel to the jet speed does not permit similarity solutions; on the other hand, if the jet speed is much larger than the speed of the ambient fluid, the functions f_1, f_2 and f_{12} agree with the solutions of a jet flow into a quiescent ambient fluid; else, f_1, f_2 and f_{12} as functions of η are as given in (16.140)–(16.142).
4. *Turbulent plane POISEUILLE flow*: This case is a bounded flow; it differs from the earlier cases insofar as $f_1(\eta, \mathbb{R}^*), P(\xi, \eta, \mathbb{R}^*), f_{12}(\eta, \mathbb{R}^*), f_{22}(\eta, \mathbb{R}^*)$, which are representative of $\bar{v}_1, \bar{p}, \overline{v'_1 v'_2}, (\overline{v'_2})^2$ are determinable as functionals of $\eta = x_2/a$ ($2a =$ distance of the walls) and ξ and the REYNOLDS number $\mathbb{R}^* = \bar{v}^* a/\nu$.

Owing to the wall boundary conditions $\{f_1; f_{12}; f_{22}\}(\pm 1, \mathbb{R}^*) = 0$ the equations

$$P(\xi, \eta, \mathbb{R}^*) + f_{22}(\eta, \mathbb{R}^*) + \xi = 0, \quad (16.196)$$

$$f_1(\eta, \mathbb{R}^*) = \mathbb{R}^* \left\{ \int_{-1}^{\eta} f_{12}(\bar{\eta}, \mathbb{R}^*) d\bar{\eta} + \frac{1}{2} (1 - \eta^2) \right\} \quad (16.197)$$

can be derived. These equations have been obtained without a closure condition for the turbulent shear stress $-\overline{v_1'v_2'}$, but with a linear viscous material behavior. For laminar flow, $f_{12} \equiv 0$ and (16.197) implies

$$f_{12}(\eta, \mathbb{R}^*) = \frac{\mathbb{R}^*}{2} (1 - \eta^2) \quad (\text{laminar flow}),$$

which is the HAGEN-POISEUILLE profile, as we have already seen. If some turbulence is present, DQTM parameterization must be added. This then yields $f_{12}(\eta, \mathbb{R}^*)$ as a function of f_1 . When this relation is combined with (16.197), a differential equation for a function $g_1(\eta)$ (proportional to f_1 or \bar{v}_1) subject to boundary conditions involving two parameters, α and β (see (16.172)). Solutions to this boundary value problem only exist when $\beta = \beta(\alpha)$ [expressed in (16.175) as $\chi = \beta/4\chi(\alpha)$]. This function is called *order parameter*. It measures the distribution of the longitudinal velocity f_1 and of the shear stresses f_{12} as shown in Figs. 16.18 and 16.19. In other words, depending upon \mathbb{R}^* , the transverse distribution of \bar{v}_1 and τ_{12} depend on \mathbb{R} . An exact parabolic velocity profile and strictly linear shear stress distribution are only possible for $\mathbb{R}^* = 0$, and a precisely semi-circular longitudinal velocity profile and a linear shear stress distribution are obtained when $\mathbb{R}^* \rightarrow \infty$. Excellent agreement of these computed with corresponding measured profiles is displayed in Figs. 16.21 and 16.22. In between these profiles are continuously deformed; this transition is monitored by the continuous change of the order parameter.

Appendix A: Prandtl's Mixing Length

We present here PRANDTL's ansatz of the turbulent mixing length (16.12) in PRANDTL's original German form and K.H.'s translation into the English language.

– Bericht über Untersuchungen zur ausgebildeten Turbulenz

....

II. Weiter möchte ich von einem Ansatz berichten, der dazu dienen sollte, die Verteilung der Grundströmung einer turbulenten Bewegung unter den verschiedensten Bedingungen hydrodynamisch zu berechnen. Nach verschiedenen vergeblichen Versuchen konnte hier ein erfreulicher Erfolg erzielt werden, und es zeigte sich überdies, daß der Ansatz für die durch den Impulsaustausch hervorbrachte

– Report about investigations regarding fully developed turbulences

....

II. Furthermore, I wish to report about an ansatz which should serve as a means to hydrodynamically compute under various conditions the distribution of the mean flow of a turbulent motion. After several fruitless attempts a gratifying success could be reached in this regard, and it turned out, in addition, that the formula of concern for the fictitious shear

scheinbare Schubspannung τ , um die es sich hier handelt, auch einer recht anschaulichen Begründung fähig ist. In der BOUSSINESQschen Formel

$$\tau = \rho \varepsilon \frac{\partial u}{\partial y} \quad (16.198)$$

ist ε ein Maß für den turbulenten 'Austausch' und ist seiner Dimension nach, die gleich derjenigen von ν ist, das Produkt einer Länge und einer Geschwindigkeit. Diese Länge und die Geschwindigkeit lassen sich nun vorstellungsmäßig fassen. Die letztere ist die Quergeschwindigkeit w , mit der im Mittel die von beiden Seiten herankommenden Flüssigkeitsballen durch die Schicht mit dem zeitlichen Mittelwert der Qergeschwindigkeit u hindurchtreten.

Die von der Seite der größeren Geschwindigkeiten kommenden Flüssigkeitsballen bringen auch größere Werte der Geschwindigkeit u mit, die von der Seite der kleineren Geschwindigkeiten dagegen kleinere, so daß immer mehr Impuls in der einen Richtung transportiert wird als in der entgegengesetzten (abgesehen von der Stelle von $u = u_{\max}$). Die gesuchte Länge ℓ ist nun dadurch charakterisiert, daß sie die Entfernung von der betrachteten Schicht angibt, in der die durchschnittlichen u -Geschwindigkeiten, die die Flüssigkeitsballen bei ihrem Durchtritt haben, als zeitlicher Mittelwert der Strömungsgeschwindigkeit angetroffen werden. Genähert sind diese Geschwindigkeiten also $u + l\partial u/\partial y$ und $u - l\partial u/\partial y$. Daß ℓ der Größenordnung nach mit dem Durchmesser der Flüssigkeitsballen übereinstimmt, sei nebenher erwähnt (genauer ist es der 'Bremsweg' des Flüssigkeitsballens in der übrigen Flüssigkeit, der aber dem Durchmesser proportional ist). Ueber die Länge ℓ kann einstweilen nur ausgesagt werden, daß sie an der Wand gegen Null gehen muß, da hier nur noch Ballen, deren Durchmesser kleiner als der Wandabstand ist, sich wie besprochen bewegen können. Im übrigen soll ℓ einen möglichst regelmäßigen Verlauf haben. Ist β der durchschnittliche verhältnismäßige Anteil der Fläche, der von den von der einen Seite durchtretenden Flüssigkeitsballen eingenommen wird, so tritt an dieser Seite sekundlich ein Impuls $\beta \rho w \cdot \ell \partial u/\partial y$ durch die Flächeneinheit, von der anderen Seite ungefähr der gleiche

stress τ that is generated by the momentum exchange, can also clearly be motivated. In the BOUSSINESQ formula

ε is a measure for the turbulent 'exchange' and, according to its dimension, which is the same as that of ν , is the product of a length and a velocity. This length and the velocity can now conceptually be understood. The latter is the transverse velocity w by which, on average, the fluid packages enter from both sides the fluid layer that moves with a temporal mean of the transverse velocity u .

The fluid packages coming from the side with the larger velocities also carry with them larger values of the velocity u , those from the side with the smaller velocities, however, smaller ones, so that always more momentum is transported in one direction than in the other (except at a position where $u = u_{\max}$). The sought length ℓ is now characterised by the fact that it provides the distance from the considered layer in which the average u -velocities, which the fluid packages have on their passage, are encountered as a temporal mean value. Approximations of those velocities are therefore $u + l\partial u/\partial y$ and $u - l\partial u/\partial y$. That ℓ agrees in order of magnitude with the diameter of the fluid packages is only remarked here parenthetically (more accurately, it is the 'stopping distance' of the fluid package in the remaining fluid, which, however, is proportional to the diameter). About the length ℓ one can presently only say, that it must go to zero at the wall, since only packages, of which the diameter is smaller than the distance from the wall, can move as discussed. Besides, ℓ should have a behaviour as regular as possible. If β is the averaged relative fraction of area that is encountered by the fluid packages passing from one side, then the momentum per second entering from this side is $\beta \rho w \cdot \ell \partial u/\partial y$, from the opposite side about the same amount, so that we

Betrag, so daß wir den BOUSSINESQ'schen Ansatz also bestätigen und $\varepsilon = 2\beta w\ell$ setzen können. Es handelt sich jetzt noch darum, für die Mischgeschwindigkeit w einen brauchbaren Ansatz zu machen. Diese Mischgeschwindigkeit wird immer rasch abgebremst und muß immer wieder neu geschaffen werden. Wir nehmen daher an, daß sie beim Zusammentreffen von zwei Ballen mit verschiedener Geschwindigkeit u erzeugt wird und darum dem Geschwindigkeitsunterschied, also dem Betrage von $l\partial u/\partial y$ proportional ist. Damit wird aber, falls wir alle unbekanntenen Zahlenfaktoren auf die nicht genauer bekannte Länge ℓ werfen, die scheinbare Schubspannung τ

$$\tau = \rho\ell^2 \left| \frac{\partial u}{\partial y} \right| \cdot \frac{\partial u}{\partial y}.$$

Dieser Ansatz bedarf noch einer Berichtigung für den Fall, daß $\partial u/\partial y = 0$ wird. Für die Erzeugung der Geschwindigkeit w wirkt die Nachbarschaft in einer gewissen Breite zusammen; sie wird nicht Null, wenn $\partial u/\partial y = 0$ ist, wird vielmehr einem statistischen Mittelwert von $|\partial u/\partial y|$ proportional gesetzt werden können, also proportional $|\partial u/\partial y|$; verändert sich das Geschwindigkeitsprofil in der Strömungsrichtung, wie bei verengten und erweiterten Kanälen, so wird die Stelle, über die gemittelt wird, auch um einen gewissen Betrag stromauf gelegt werden müssen, da der Vorgang der Ausbildung der Geschwindigkeit w Zeit beansprucht.

...

can corroborate BOUSSINESQ's ansatz and set $\varepsilon = 2\beta w\ell$.

The remainder now consists in making a useful hypothesis for the mixing velocity w . This mixing velocity is always very quickly attenuated and must continuously be newly created. We therefore suppose that it is generated in an encounter of two packages with different velocity u and thus is proportional to the velocity difference, whence the modulus of $l\partial u/\partial y$. With this, and provided we throw all unknown factors on this not exactly known length ℓ , the fictitious shear stress τ becomes

This formula still needs to be amended for the case that $\partial u/\partial y = 0$. For the creation of velocity w the neighbourhood of a certain width is active; it does not become zero, if $\partial u/\partial y = 0$, it may rather be set proportional to an average value of $|\partial u/\partial y|$, thus proportional to $|\partial u/\partial y|$ itself; if the velocity profile changes in the direction of the flow, as is the case in contracting and diverging channels, then the position about which the average is taken will have to be moved somewhat upstream, because the process of the creation of the velocity w will take some time.

...

References

1. Abramowitz, M., Stegun, I.A.: Handbook of Mathematical Functions. Dover Publications, USA (1964)
2. Bernard, P.S., Handler, R.A.: Reynolds stress and the physics of turbulent momentum transfer. *J. Fluid Mech.* **220**, 90–124 (1990)
3. Boussinesq, J.: Essai sur la théorie des eaux courantes. *Mém. Près. Div. Savant Acad. Sci. Paris.* **23**, 46 (1872)
4. Corrsin, S.: Limitations of gradient transport models in random walks and in turbulence. *Adv. Geophys.* **18A**, 25–60 (1974)
5. Corrsin, S., Uberoi, M.S.: Further Experiments on the Flow and Heat Transfer in a Heated Turbulent Air Jet. Technical note Technical Note (United States. National Advisory Committee for Aeronautics), no. 1865. Washington, National Advisory Committee for Aeronautics (1949)
6. Egolf, P.W.: A new model on turbulent shear flows. *Helv. Phys. Acta.* **64**, 944–946 (1991)

7. Egolf, P.W.: Die mittlere Geschwindigkeit längs der Achse eines isothermen Freistrahles. *Gesundheits-Ingenieur* (1992)
8. Egolf, P.W.: Difference-quotient turbulence model: a generalization of Prandtl's mixing-length theory. *Phys. Rev. E*, **49**(2), 1260–1268 (1994)
9. Egolf, P.W., Weiss, D.A.: Difference-quotient turbulence model: the axisymmetric isothermal jet. *Phys. Rev. E*, **58**(1), 459–470 (1998)
10. Egolf, P.W., Weiss, D.A.: Difference-quotient turbulence model: analytical solutions for the core region of plane Poiseuille flow. *Phys. Rev. E*, **62**(1), 553–563 (2000)
11. Görtler, H.: Asymptotische Eigenwertgesetze bei Differentialgleichungen vierter Ordnung. Volume 26 of *Mitteilungen aus dem Mathematischen Seminar der Universität Giessen, Universität Giessen, Mathematisches Seminar* (1936)
12. Görtler, H.: Berechnung von Aufgaben der freien Turbulenz auf Grund eines neuen Näherungsansatzes. *Zeitschr. Angew. Math. Mech. (ZAMM)*, **22**(5), 244–254 (1942)
13. Gschwind, P.: Strömungs- und Transportvorgänge in gewellten Kanälen mit ineinander liegender Anordnung der Wände. PhD thesis, Universität Stuttgart (2000)
14. Hinze, O.: *Turbulence*, 2nd edn. MacGraw Hill, New York (1975)
15. Holmes, P., Lumley, J.L., Berkooos, G.: *Turbulence coherence Structures, Dynamical Systems and Symmetry*. Cambridge University Press Press, Cambridge (1998) ISBN 978-0-521-63419-9
16. Holton, J.R.: *An Introduction to Dynamic Meteorology*. International Geophysics Series, vol. 23. Academic Press, New York (1979)
17. Hutter, K., Jöhnk, K.: *Continuum Methods of Physical Modeling*. Springer, Berlin (2004)
18. Laufer, J.: National Advisory Committee for Aeronautics. Technical Report No. 1774 (1951)
19. Liepmann, D., Gharib, M.: The role of streamwise vorticity in the near-field entrainment of round jets. *J. Fluid Mech.* **245**, 643–668 (1992)
20. Lumley, J.L., Panowsky, H.A.: *The Structure of Atmospheric Turbulence*. Wiley, New York (1964)
21. Pai, S.I.: On turbulent flow between parallel plates. *J. Appl. Mech.* **20**, 109 (1953)
22. Panchapakesan, N.R., Lumley, J.L.: Turbulence measurements in axisymmetric jets of air and helium Part 1. Air jet. *J. Fluid Mech.* **247**, 197–223 (1993)
23. Prandtl, L.: Bericht über Untersuchungen zur ausgebildeten Turbulenz. *Zeitschr. Angew. Math. Mech. (ZAMM)*, **5**(2), 136–139 (1925)
24. Prandtl, L.: Neuere Ergebnisse der Turbulenzforschung. *Zeitschr. VDI*, **77**, 105–113 (1933)
25. Prandtl, L.: *Abriss der Strömungslehre*, 3rd edn. Vieweg, Braunschweig (1942)
26. Reichardt, H.: Vollständige Darstellung der turbulenten Geschwindigkeitsverteilung in glatten Leitungen. *Zeitschr. Angew. Math. Mech.* **31**(7), 208 (1951)
27. Reichardt, H.: *Gesetzmäßigkeiten der freien Turbulenz*. VDI-Forschungsheft 414, 2. erweiterte Auflage II + 30 S. mit 18 Abb. Düsseldorf (1951)
28. Ricou, F.P., Spalding, D.B.: Measurements of entrainment by axisymmetrical turbulent Jets. *J. Fluid Mech.* **11**, 21–32 (1961)
29. Tennekes, H., Lumley, J.L.: *A First Course in Turbulence*. MIT Press, Cambridge (1972)
30. Wyganski, I., & Fiedler, J. (1969). Some measurements in the self-preserving jet. *J. Fluid Mech.*, **38**, 577–612.
31. Zagrola, M.V., Perry, A.E., Smits, A.J.: Log laws and power laws: the scaling of the overlap region. *Phys. Fluids*, **9**, 2094–2100 (1997)

Chapter 17

Thermodynamics—Fundamentals

Abstract This chapter is devoted to thermodynamics; first, fundamentals are attacked and, second, a field formulation is presented and explored. Class experience has taught us that thermodynamic fundamentals are difficult to understand for novel readers. Utmost caution is therefore exercised to precisely introduce terminology such as ‘states’, ‘processes’, ‘extensive’, ‘intensive’ and ‘molar state variables’ as well as concepts like ‘adiabatic’, and ‘diathermic walls’, ‘empirical’ and ‘absolute temperature’, ‘equations of state’ and ‘reversible’ and ‘irreversible processes’. The core of this chapter is, however, the presentation of the first and second law of thermodynamics. The first law balances the energies. It states that the time rate of change of the kinetic plus internal energies are balanced by the mechanical power of the stresses and the body forces plus the thermal analogies, which are the flux of heat through the boundary plus the specific radiation referred to as energy supply. This conservation law then leads to the definitions of the caloric equations of state and the definitions of specific heats. The Second Law of Thermodynamics is likely the most difficult to understand and it is introduced here as a balance law for the entropy and states that all physical processes are irreversible. We motivate this law by going from easy and simple systems to more complex systems by generalization and culminate in this tour with the Second Law as the statement that entropy production rate cannot be negative. Examples illustrate the implications in simple physical systems and show where the two variants of entropy principles may lead to different answers.

Keywords Reversible/irreversible processes · Empirical/absolute temperature · First, second law of thermodynamics · Thermodynamic states—processes · Extensive, intensive, molar state variables · Adiabatic/non-adiabatic systems · Diathermic wall · Thermal equations of state · VAN DER WAALS gas · Caloric equation of state · Specific heats

List of Symbols

Roman Symbols

- | | |
|-----------|---|
| A, B, C | Identifiers for thermodynamic systems |
| a, b | Two constants in the thermal equation of state for VAN DER WAALS fluids |

$A_{\Delta t}$	Work of the non-conservative external forces on a body
C	Capacity in an electric circuit, elastic constant of a spring, mass concentration of a tracer
c_v	Specific heat at constant volume $c_v = \left(\frac{\partial u}{\partial T}\right)_V$
c_p	Specific heat at constant pressure $c_p = \left(\frac{\partial h}{\partial T}\right)_V$
C_V^m, C_p^m	Specific molar heats of a VAN DER WAALS gas
\mathbf{D}	Strain rate tensor, stretching tensor (deviator) $\mathbf{D} = \frac{1}{2}(\mathbf{L} + \mathbf{L}^T)$
D, D_c	Diffusivity,—of a tracer
E	Specific total energy per unit mass
\mathbf{E}	Distortion (rate) tensor $\mathbf{E} = \mathbf{D} - \frac{1}{3}(\text{tr})\mathbf{1}$
e	Specific total energy per unit mass $e = \frac{1}{2} \mathbf{v} ^2 + u$
E_G	$E_G = T + U - \psi$, Kinetic + internal energy – potential of the conservative force
\mathbf{F}	Force acting on a finite body or a mass point
\mathbf{f}	Specific body force per unit mass
$f_{\text{trans}}, f_{\text{rot}}, f_{\text{osc}}$	Translational, rotational and oscillation degrees of freedom
\mathbf{g}, g	Gravity vector, gravity constant
$h = u + p/\rho$	Specific enthalpy per unit mass
I_0	Initial electric current (strength)
L	Inductivity of a condenser, power of working of \mathbf{F} formed with \mathbf{v} , power of working of a body
L_1	Power of working of the conservative external forces
$\mathbf{L} = \text{grad } \mathbf{v}$	Spatial velocity gradient
M	Mole mass, mass of a rigid body
\dot{m}_a, \dot{m}_e	Inflow and outflow (rate) of mass through a system
N	Normal force (positive as a pressure) acting on a body at and \perp to a basal surface, Integrating denominator of a two-dimensional PFAFFian form
n	Number of mole masses
\mathbf{n}	Unit normal vector at a point of the boundary ∂V of a body V
p, p_c	Pressure, critical—for a VAN DER WAALS gas
$pV_m = R_m T$	Thermal equation of state for an ideal gas
Q	(Total) heating supplied to a body at its boundary
Q_A, Q_B	Heating of systems A and B
$Q_{\Delta t}$	Heating of external sources applied to a body during a time step Δ
q	Heat supplied at a body point per unit mass
\mathbf{q}	Heat flux vector supplied to a body at a point on ∂V
$(q_{12})_p$	Heat added to a system between states 1 and 2 at constant pressure
R	Resistivity of an electric circuit
$R = R_m/M$	Gas constant of an ideal gas whose mole mass is M
R_m	Universal or molar gas constant $R_m = 8.31451 \pm 0.00007 \text{ [J mol}^{-1}\text{K}^{-1}\text{]}$

R	Gas constant of an ideal gas $R = c_p(T) - c_v(T)$
S	Entropy of a finite system
\dot{S}, \dot{s}	GIBBS relation for a system $\dot{S} = \frac{1}{T} (\dot{U} + p\dot{V})$, – for a unit mass $\dot{s} = \frac{1}{T} (\dot{u} + p\dot{v})$
s	Specific entropy per unit mass
$T = \frac{1}{2}m \mathbf{v} ^2$	Kinetic energy of a mass point
T	Tangential sliding force of a moving body along a surface, kinetic energy at a point per unit mass
$T(\vartheta)$	Absolute temperature as a function of the empirical temperature ϑ
$T_r = 273.16[\text{K}]$	Temperature at the triple point of water
t	CELSIUS temperature: $t = T - 273.15[\text{C}^\circ]$
t_F	Fahrenheit temperature $t_F = T - 32[\text{F}^\circ] = T - T_0$
T_0	Temperature of the ice point
T_c	Critical temperature of a VAN DER WAALS gas
\mathbf{t}	CAUCHY stress tensor
\mathbf{t}^R	Frictional (viscous) CAUCHY stress tensor (deviator)
$\mathbf{t} \cdot \mathbf{v}$	Stress power
\mathbf{t}_n	Traction vector on ∂V of V
U, u	Internal energy of a body, specific internal energy per unit mass
$u(y, t)$	Velocity component along the x -axis as a function of the y -axis and time t
u_0	Boundary value of $u(0, t)$
V, V_m	Volume of a body, mole volume
\mathbf{v}, v	Velocity vector, y -component of \mathbf{v}
\mathbf{x}	Displacement vector, position vector
$\dot{\mathbf{x}}_0$	Initial velocity
Z	State variable
$z_1 = Z/m$	Specific state variable per unit mass
$z_2 = Z/V$	Specific state variable per unit volume
Z/n	Molar state variable
$z = Z_m/M$	Specific state variable

Greek and Miscellaneous Symbols

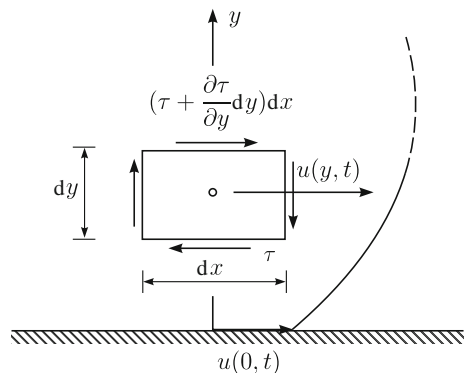
γ	Damping constant, specific entropy production per unit volume
$\Delta m_e, \Delta m_a$	Mass entering/leaving a system
$\eta = \rho\nu$	Dynamic viscosity
η_{th}	Thermal efficiency
$\eta_c = \eta_{\text{th}}^{\text{rev}}$	CARNOT factor, CARNOT efficiency
\dot{H}_V	Rate of entropy of a body V
ν	Kinematic viscosity
$\rho\gamma$	Specific entropy production per unit mass
$\rho\mathbf{f} \cdot \mathbf{v}$	Power of working of the body force

ρs	Specific entropy per unit volume
ϑ	Empirical temperature
$\Theta(\vartheta)$	Empirical temperature
Φ	Dissipation function
Φ_V	Dissipation function due to pure volume changes
Φ_G	Dissipation function due to pure form changes
$-\dot{\psi}$	Power of working of the conservative external forces of a body
τ	Shear stress
∂V	Surface of a body V

17.1 Concepts and Some Historical Remarks

Up to now we have devoted our attention to questions of fluid mechanical concern; in particular, we determined with the aid of the **mechanical laws** the **motion** of liquids (such as water, oil, etc.) and gases (air, etc.). Apart from applying the general laws of **conservation of mass** and **linear** and **angular momenta**, we also made use of material technological-statements, as e.g. the postulation of a connection between shear stress and shear angle in simple shear, or the relation between the stress tensor and the strain rate (stretching) tensor in viscous fluids (Chap. 7). The formulation of these laws has, however, been introduced in a rather bold fashion without support by other physical principles; these laws find at last their support by experimental tests. In so doing, the goal is to make the mechanical balance laws integrable by complementary statements, which describe the **material behavior**, at least in principle, to arrive at a closed system of equations. In this sense such laws or equations are also called **closure conditions**. To explain this situation by means of a very simple example, consider an unsteady parallel flow along a moving wall parallel to the x -direction, see **Fig. 17.1**. With the assumptions of the velocity components u , v in the x - and y -directions and the pressure p

Fig. 17.1 Flow along a moving wall. Velocity profile $u(y, t)$ and fluid element $dx dy$ with the shear tractions acting on it



$$u = u(y, t), \quad v = 0, \quad p = \text{constant},$$

respectively, formulation of the balance of linear momentum in the x -direction for the illustrated rectangular element yields

$$\rho \frac{\partial u}{\partial t} dx dy = \frac{\partial \tau}{\partial y} dx dy,$$

or

$$\rho \frac{\partial u}{\partial t} = \frac{\partial \tau}{\partial y}, \quad (17.1)$$

which is a relation between velocity u and shear stress τ . Only if we complement the above equation with the material equation

$$\tau = \eta \frac{\partial u}{\partial y}, \quad (17.2)$$

in which η is the dynamic shear viscosity that changes from material to material, we obtain from (17.1) by substitution of (17.2) a differential equation for u alone, namely

$$\frac{\partial u}{\partial t} = \nu \frac{\partial^2 u}{\partial y^2}, \quad (17.3)$$

which, subject to adequate boundary conditions, becomes integrable. For instance, for a harmonically oscillating wall and a velocity field that dies out to a state of rest at $y = \infty$ these boundary conditions read

$$\begin{aligned} u(y, t) &= u_0 \cos \omega t, & y &= 0, \\ u(y, t) &= 0, & y &\rightarrow \infty, \end{aligned} \quad (17.4)$$

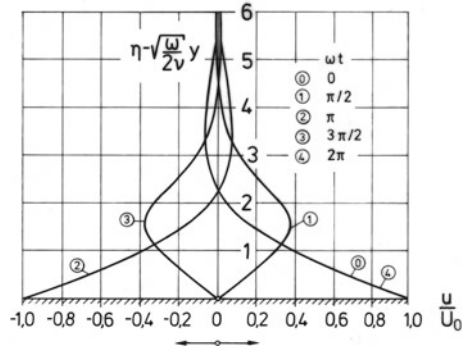
and the solution of (17.3) takes in this case the form

$$u(y, t) = u_0 \exp\left(-\sqrt{\frac{\omega}{2\nu}} y\right) \cos\left(\omega t - \sqrt{\frac{\omega}{2\nu}} y\right), \quad (17.5)$$

which is graphically displayed in **Fig. 17.2**. That (17.5) is indeed a solution of (17.3) subject to the boundary conditions (17.4) may be corroborated by simple substitution of (17.5) into (17.3) and (17.4).

Thermodynamics is less concerned with the construction of such solutions—even though this is equally its ultimate goal—but rather with the theoretical foundation of material laws such as (17.2). Thermodynamics formulates physical principles, according to which it can be decided, whether a postulated **material law is physically meaningful** or senseless. It took a rather long time until such an interpretation of the basic goals of thermodynamics crystallized. For its roots we have to go back to

Fig. 17.2 Flow along a moving wall. *Distributions of the horizontal velocity perpendicular to the wall for a harmonically oscillating wall, plotted for different times*



the explanation of phenomena such as **energy conservation** and **energy transfer** in heat engines; this then merged into a **theory of heat**.

To reach the above goal two principal laws had to be recognized. The first concerns the **extension of the notion of energy to non-mechanical forms**. The decisive quantities are in this regard the **internal energy** and **heat** and the recognition of their equivalence. The balance law, expressing conservation of the sum of all mechanical, thermal, (electrical and chemical) energy forms, is expressed as the **First Law of Thermodynamics**. It describes how the individual forms of energy balance, i.e., transfer into one another, provided such transfers are allowable at all. Regarding the transfer of the individual energy forms the First Law is *symmetric*. Changes of mechanical energy into thermal energy is in principle equally possible as the reverse changes from thermal into mechanical energy.

Many observations and long experiences, however, showed that the transfer from a non-thermal to a thermal energy form is favored by nature; this is the basic expression of the **Principle of Irreversibility** which finds its mathematical formulation in the **Second Law of Thermodynamics**. This law essentially expresses the fact that physical processes favor a direction in their evolution. This is sometimes expressed by saying that physical processes cannot be traversed in the reversed direction of time. If such time reversal is possible, the respective process must be exceptionally seldom and physically idealized. For the mathematization of the notion of irreversibility the concept of **entropy** was created. This is a physical quantity, which is very difficult to intellectually grasp; indeed, its meaning and interpretation can probably best be disclosed by the mathematical laws, which are formulated for it.¹

¹For didactic reasons it is recommended here to most readers to initially accept these mathematical laws and not to ask too deeply for their physical meaning or background, but to accept their functional and mathematical implications and to understand their consequences analytically. The reason for this recommendation is that the laws are only physically fully justifiable for simplified cases, but must be accepted as axioms in the general case.

Without dwelling into details (because they would hardly be understood at the present stage of the development), we mention that in a modern formulation of the Second Law, apart from the **entropy density** also **entropy flux**, **entropy production** and **entropy supply** are defined for which a **balance law** is formulated. To this end, consider a material volume V with boundary ∂V for which the following balance statement holds²

$$\left\{ \begin{array}{l} \text{Time rate of change} \\ \text{of the entropy in, } V \end{array} \right\} = \left\{ \begin{array}{l} \text{Flux of the entropy} \\ \text{through the boundary } \partial V \text{ of } V \end{array} \right\} \\ + \left\{ \begin{array}{l} \text{Production of entropy} \\ \text{within the volume } V \end{array} \right\} \\ + \left\{ \begin{array}{l} \text{Supply of entropy from} \\ \text{outside to the volume } V \end{array} \right\}. \quad (17.6)$$

In this form the Second Law finds its expression in the statement that *the entropy production in the body is not allowed to take negative values for whichever physical process that may take place within the body.*³ This exclusiveness of the sign of the entropy production is expression of the irreversibility. If the production vanishes, the process is **reversible**, if it is negative, the process is physically **not realizable**. Moreover, if the entropy flux from the outside vanishes, it follows from statement (17.6) that the time rate of change of the entropy in V cannot be negative, but must grow or remain constant.

These statements are simple mathematical inferences drawn from the balance (17.6) and the requirement that the entropy production is not allowed to become negative. They must in the subsequent text be ‘filled’ with physical content. The fact that *the balance (17.6) must hold for all possibly thinkable processes* finds its consequences in the fact that this apparently implies *constraints for the material equations*. Such a constraint is, for instance the requirement that the shear viscosity is a positive quantity. Expressed somewhat more generally, *the material functionals for a body must be so structured that they make it impossible for a body in any process deduced from the equations to violate the fundamental axioms of physics.*

²Such a balance may be formulated for any quantity and need not be restricted to physical quantities or entropy. Let in (17.6) e.g. ‘entropy’ be replaced by ‘money of any form in a bank’. Its amount will grow if customers physically enter the building, make a deposit and leave. This is the flux of money through the boundary. If within the building notes are printed or coins are pressed, then money is produced; this production also can take negative values, if worn-out notes are destroyed. Finally, if a customer makes a payment electronically from outside to a deposit of the bank, then money is supplied. Of course, in this example of a balance law, the production ordinarily vanishes, because only special banks are authorized to print notes and press coins. The law governing the growth of money in the bank is then a conservation law.

³That the entropy production must be non-negative is a convention associated with the definition of the entropy. It would at this stage be better to request the entropy production to have only one sign.

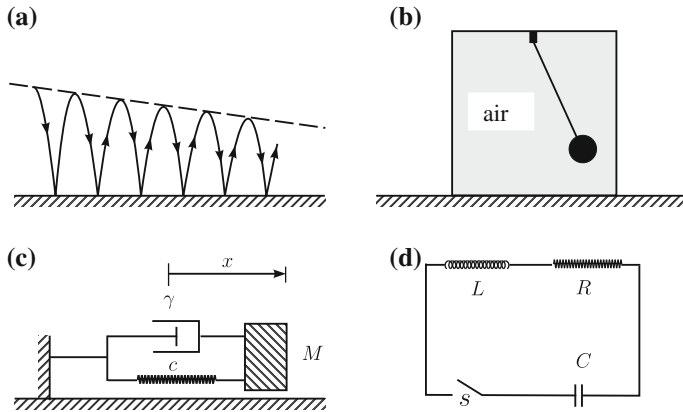


Fig. 17.3 Irreversible Processes. **a** Consecutive decrease of the jumping heights of a bouncing ping-pong ball. **b** Oscillations of a mathematical pendulum in air. **c** Mass oscillator with spring and dashpot. **d** Electrical circuit with capacity, resistivity and induction coil

Irreversible processes are overwhelmingly observed in Nature. Obvious are those, which cannot be observed in temporally reversed situation. One example is the bouncing **ping-pong ball**, whose height of jump decreases from one jump to the next and whose evolution in reverse sequence has never been observed, see **Fig. 17.3a**. Another example is a **pendulum oscillating in air**, of which the amplitude decreases with time, whereby the air is heated, see **Fig. 17.3b**. The initial energy of the pendulum is transferred after some time to the air and the pendulum is in its position at rest. It has never been observed that the pendulum would be excited from its rest position by still air whilst the latter is being cooled.

The examples, which demonstrate the irreversibility in the governing equations and which are probably familiar to the reader are illustrated in **Fig. 17.3c, d**: the **mechanical** and **electrical oscillators**. For a mass point M , which is exposed to a spring force proportional to its elongation x , cx , and a damping force, proportional to the rate of elongation \dot{x} , $\gamma\dot{x}$, application of NEWTON's fundamental law yields the differential equation

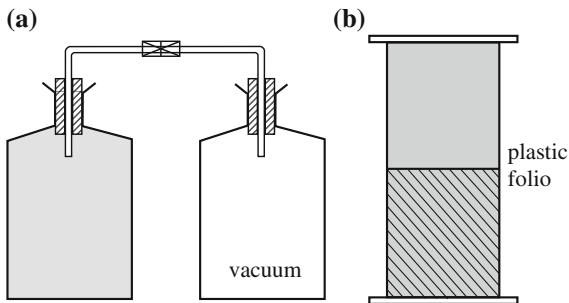
$$\ddot{x} + \frac{\gamma}{M}\dot{x} + \frac{c}{M}x = 0. \quad (17.7)$$

For the electrical circuit (**Fig. 17.3d**) with condenser of capacity C , resistance of resistivity R and inductance of inductivity L , application of KIRCHHOFF's law after closure of the circuit yields for the electric current the ordinary differential equation

$$\ddot{I} + \frac{R}{L}\dot{I} + \frac{1}{LC}I = 0. \quad (17.8)$$

In these equations dots denote differentiation with respect to time, and so it is obvious that time reversal that changes dt into $-dt$ will change the sign in the second terms

Fig. 17.4 Irreversible expansion and mixing. **a** Flow of a gas from one bottle into a vacuum bottle. **b** Diffusive mixing of two originally separated gases



on the left-hand sides of (17.7) and (17.8), but leave the other terms unchanged. With the initial conditions

$$\begin{aligned} x(t = 0) &= 0, & I(t = 0) &= 0, \\ \dot{x}(t = 0) &= \dot{x}_0, & \dot{I}(t = 0) &= \dot{I}_0, \end{aligned} \tag{17.9}$$

the solutions can be written as

$$\begin{aligned} x &= \frac{\dot{x}_0}{\omega} \exp\left(-\frac{\gamma}{2M}t\right) \sin \omega t, & I &= I_0 \exp\left(-\frac{R}{2L}t\right) \sin \Omega t \\ \omega &= \sqrt{\frac{c}{M} - \frac{\gamma^2}{4M^2}}, & \Omega &= \sqrt{\frac{1}{LC} - \frac{R^2}{4L^2}}. \end{aligned} \tag{17.10}$$

For positive γ or R , they represent damped oscillations. In the mechanical example, kinetic energy at time $t = 0$ is transformed into **frictional heat**, in the example of the electric circuit the energy originally stored in the condenser is transformed into **Joule heat**. The processes evolving reversed in time (change of the sign of γ and R) would result in temporally amplified oscillations, which has never been observed.

An irreversible process can also be illustrated by the flow of a gas into a vacuum container, see **Fig. 17.4a**. A bottle filled with a gas—usually NO_2 is used, because of its brown color it is easily visible—is connected by a tube with a second bottle (initially under vacuum) until the gas in the bottle is subjected to the same pressure. However, one has never observed that the gas would by itself collect itself in one of the two bottles.

Analogously, two masses of different gasses confined in a bottle and separated by a foil will, after removal of the foil, (slowly) mix until a homogeneous mixture of both gasses is reached. This mixing process is called **diffusion**, and it can, if left un-accelerated by adequate means, last very long. A de-mixing of the mixed gasses by themselves has never been observed. Analogously, one has never observed that a solution of sugar in water at moderate concentration would spontaneously separate the sugar from the water.

Historically, the formulations of the First and Second Laws of Thermodynamics must be located in the 19th century, when one recognized that heat is some sort of energy. In fact, this recognition came long after the realization of the steam

engine, which transforms heat into mechanical work. Its first construction in Europe is attributed to the French physicist DENIS PAPIN (1647–1712) and falls into the period around 1690. As already mentioned in the introduction, it was, however NICOLAS LÉONARD SADI CARNOT (1796–1832)⁴ who first formulated the generation of usable work from heat in a general form. In so doing he formulated the notions of a **perfect machine** and **reversible processes**, which are today known as CARNOT's **circular processes**. He also arrived at a certain limited formulation of the Second Law.

CARNOT's memoirs were largely only published 40 years after his death. This is the likely reason, that most thermodynamicists attribute the merit of having first hypothesized the equivalence of heat and energy to ROBERT MAYER (1814–1878),⁵ and to have spelled out the fact that *in a closed system the total energy is conserved*, where 'closed' means 'materially bounded'.

Independently of MAYER's theoretical considerations of 1842 and 1845 JAMES PRESCOTT JOULE (1818–1889)⁶ laid down between 1843 and 1848 the experimental foundations of the First Law by determining the mechanical heat equivalent. CLIFFORD AMBROSE TRUESDELL (1919–2000), however, has shown in his historical studies (1980) that these attributions must be regarded as exaggerations, since MAYER's works only allow the interconvertibility of heat and work for isothermal processes; moreover, he mentions that JOULE's experimental results were subject to such large fluctuations that LORD KELVIN doubted the correctness of JOULE's inferences. It appears that around 1850 the First Law and the Second Law were 'somewhat in the air', but had yet still not clearly been spelled out.

On the basis of the works by MAYER, JOULE and above all CARNOT, JULIUS EMANUEL CLAUSIUS (1822–1888)⁷ then succeeded in the years (1850–1865) to tailor the two thermodynamic laws in a mathematical form, first for reversible circular processes (1850) and later (1862) for irreversible processes. In so doing, he expressed the First Law as a balance between heat, work and internal energy and introduced for the formulation of the Second Law the new thermodynamic quantity, which he called entropy (1865). In his memoir of 1865 he spelled out the famous sentences⁸:

- *'Die Energie der Welt ist konstant: The energy of the world is constant', and*
- *'Die Entropie der Welt strebt einem Maximum zu: The entropy of the world strives for a maximum'.*

⁴For a short biography of NICOLAS LÉONARD SADI CARNOT, see **Fig. 17.5**.

⁵For a short biography of JULIUS ROBERT VON MAYER, see **Fig. 17.6**.

⁶For a short biography of JAMES PRESCOTT JOULE, see **Fig. 17.7**.

⁷For a short biography of RUDOLF JULIUS EMANUEL CLAUSIUS, see **Fig. 17.8**.

⁸These sentences may possibly have led natural philosophers to spell out inferences of grandeur and world-embrace which seem to be large and unjustified exaggerations, given the relatively simple thermodynamic concepts dealt with by CLAUSIUS for which the above two sentences apply. In CLAUSIUS' context the world is a very simple physical system which is not apt to describe the complexity of the universe.



Fig. 17.5 NICOLAS LÉONARD SADI CARNOT (1. June 1796–24. Aug. 1832)

NICOLAS LÉONARD SADI CARNOT was a French physicist and engineer who, with his theoretical works on heat engines and the related cyclic (CARNOT) processes, founded what became *thermodynamics*. He was born in Paris into a family of politics and science and was persuaded by his father to study the technical sciences. He entered École Polytechnique in Paris in 1812, but left it in 1814 for a military career in the French army's corps of engineers. In 1819 he asked for discharge to fully concentrate on science: Chemistry, physics, mathematics, natural sciences and political economy.

In his studies CARNOT concentrated on steam engines performing cyclic processes. Empirical studies by NEWCOMEN (1664–1729) of these had in the early 18th century (in 1712 in the form of piston-operated steam engines) been studied by JAMES WATTS (1736–1819). SADI CARNOT felt it necessary to scrutinize the phenomenon of the 'generation of motion by the moving of heat'. The results of these efforts were shown in 1824 in a memoir 'Réflexions sur la puissance motrice du feu et sur les machines propres à développer cette puissance', [6]. This was the only paper that was published in CARNOT's life time. Only in 1890 an English translation appeared [7], and in 1892 WILHELM OSTWALD (1853–1932) published a translation into the German language [8].

EMILE CLAPEYRON (1799–1864) was the first to reflect in 1834 on CARNOT's paper, but in spite of his positive reflection, did hardly find any response. Only around the 1850s the situation improved: WILLIAM THOMSON (LORD KELVIN) was motivated in 1848 by SADI CARNOT's reflections to introduce his temperature scale. Similarly, RUDOLF CLAUSIUS noted in POGGENDORFFS 'Annalen der Physik und Chemie' of 1850 and emphasized CARNOT's scientific exceptional contribution. Surprisingly, neither WILLIAM THOMSON (LORD KELVIN) nor RUDOLF CLAUSIUS were aware of CARNOT's 1824-memoir, but only knew EMILE CLAPEYRON's paper. WILHELM OSTWALD in 1892 explicitly stated that SADI CARNOT's 1824-treatise intellectually presented what is today called the Second Law of Thermodynamics.

SADI CARNOT died in 1832 at the young age of 36 due to scarlet and 'brain fever' during a cholera epidemic in Paris.

The text is based on www.wikipedia.org



Fig. 17.6 JULIUS ROBERT VON MAYER (25. Nov. 1814–20. March 1878)

JULIUS ROBERT VON MAYER, a German physician and physicist (by devotion), is often claimed to be one of the founders of thermodynamics. He is best known for enunciating in 1841 one of the original statements of the conservation of ‘energy’ (expressed as ‘forces’ in his paper), which is now often called the first version of the First Law of Thermodynamics, namely that ‘energy in a body can neither be created nor destroyed’. This memoir submitted to POGGENDORFF’s ‘Annalen der Physik und Chemie’ contained a number of fundamental physical flaws and was initially rejected by the scientific community.

If energy of motion (kinetic energy) can be transformed into thermal energy (heat) water would have to be transformed into heat by simply shaking it. This experiment led JULIUS MAYER to the determination of the *mechanical equivalent of heat*, which he published in 1842 in the LIEBIG ‘Annalen der Chemie und Pharmacie’ [36]. JULIUS MAYER improved his first value of mechanical equivalence of heat from 365 to eventually 425 kg*m/kcal [kg* = force kilogram]. Today’s value is 4.184 KJ/kcal (=426.6 kg*m/kcal). This relation says that work and heat are equivalent to one another; these are different forms of energy, which can always be transformed to one another by the ‘universal’ ratio of 4.184 kJ/kcal. This is, in fact, a first version of the First Law of Thermodynamics that was perfected by HERMANN HELMHOLTZ (1821–1896) in the year 1847.

JULIUS MAYER was convinced about the significance of his discovery, but his lack of professionalism in expressing himself scientifically and his speculative tendencies as well as his obedient religiosity did not further his scientific recognition; the contemporary physicists refused his conservation law of energy. One doubted MAYER’s qualification in physical knowledge. In the aftermaths of these circumstances and because of the concurrent death in 1848 of two of his children, his mental state was thrown into turmoil. After an attempt of suicide on 18 May 1850 he was hospitalized in two nerve clinics; upon his release, he was a broken man. He retreated to his privacy, acted as a foster parent to the two daughters of his elder brother after the latter’s death and devoted his time to his medical practice. Only after 1860 he opened his life faint-heartedly to the public and recognized that his scientific stand had somewhat increased. So, he received a late recognition of his achievements, even though he was no longer able to properly enjoy it.

The text is based on www.wikipedia.org

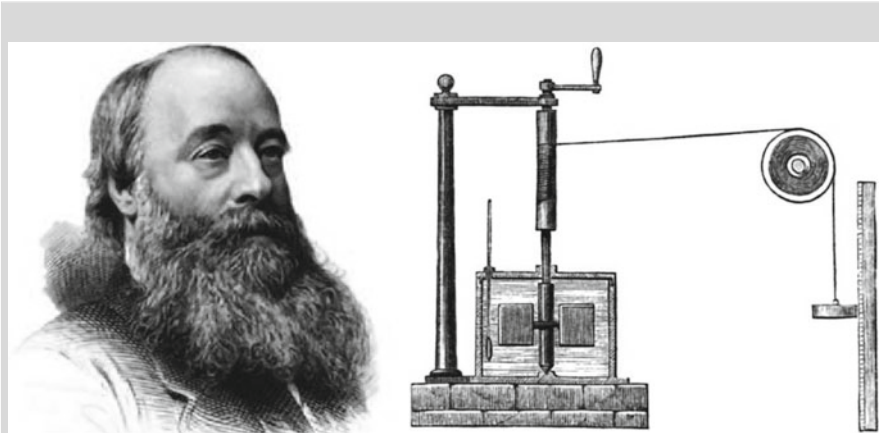


Fig. 17.7 JAMES PRESCOTT JOULE (24. Dec. 1818–11. Oct. 1889)

JAMES PRESCOTT JOULE and his apparatus for measuring the mechanical equivalent of heat in which the ‘work’ of the falling weight is converted into the ‘heat’ of agitation in the water. The falling of the weight is transmitted to a rotation of the paddles in the water chamber. JAMES PRESCOTT JOULE was an English physicist and brewer. JAMES JOULE studied the nature of heat, and discovered its relation to mechanical work. This led to the law of conservation of energy, the development of the first law of thermodynamics. The SI derived unit of energy, the ‘Joule’, is named after JAMES PRESCOTT JOULE. He worked with WILLIAM THOMSON (LORD KELVIN) to develop the absolute scale of temperature the ‘Kelvin’-temperature. JAMES JOULE also made observations of magnetostriction, and he found the relation between the electric current through a resistor and the associated dissipated heat, which is now called JOULE’s first law.

The son of a wealthy brewer, Joule was tutored as a young man by the famous scientist JOHN DALTON and was strongly influenced by chemist WILLIAM HENRY and Manchester engineers PETER EWART and EATON HODGKINSON. He was also fascinated by electricity. However, he left this field in the benefit of work on the convertibility of energy. In 1843 he estimated the mechanical equivalent of heat and reported his results to the British Association for the Advancement of Science in August 1843 and was there met by silence. By forcing water through a perforated cylinder he could measure the slight viscous heating of the fluid; it led to a mechanical equivalent of 4.14 J/cal. Subsequently he perfected the experiments: these were so constructed that to thermally isolated water mass a precise amount of mechanical energy was added and subsequently the raise in temperature was measured. This led to a mechanical equivalent of heat of 4.41 J/cal. This had already been demonstrated in 1841 by JULIUS ROBERT MAYER. A further improvement of JAMES JOULE’s measurements in 1850 yielded 4.159 J/cal which is closer to today’s standard value 4.1860 J/cal. For original literature see [19–24].

The text is based on www.wikipedia.org



- (I) Heat can never pass from a colder to a warmer body without some other change, connected therewith, occurring at the same time.
- (II) The energy of the universe is constant. The entropy of the universe tends to a maximum

Fig. 17.8 RUDOLF JULIUS EMANUEL CLAUDIUS (2. Jan. 1822–24. Aug. 1888)

RUDOLF JULIUS EMANUEL CLAUDIUS was a German physicist and mathematician and is considered one of the founders of the science of thermodynamics, in particular a first rational version of its Second Law. He studied mathematics and physics in Berlin, where he also became a Private Docent. 1855 he was called to the newly founded Eidg. Polytechnicum (now Swiss Federal Institute of Technology) in Zurich, where he stayed until 1867, when he moved to the University Würzburg and in 1869 to Bonn, where he stayed until his death.

His most famous paper, ‘Über die bewegende Kraft der Wärme’ (‘On the Moving Force of Heat and the Laws of Heat which may be deduced therefrom’) [9] was published in 1850, and dealt with the mechanical theory of heat. In this paper, he recognized—as WILLIAM THOMSON (LORD KELVIN) did—that SADI CARNOT’s 1824-concept and MAYER’s, JOULE’s and HELMHOLTZ’ energy conservation law were in conflict. He restated the two laws of thermodynamics to overcome this contradiction. He gave the conservation law of energy a new framing by establishing a new relation between heat Q and work W and internal energy U : $dU = dQ + W$. He recognized that heat was not an unchangeable substance, but merely a form of energy, which can be transformed to other energy forms (e.g., kinetic energy) in a combined statement. He formulated in 1854/56 [10, 11] a first version of the second law with the statement (I) above. This is the expression that thermal processes are directed; otherwise stated, thermal processes are not reversible. The heat transfer relative to the temperature at this transfer (expressed as dQ/T) is a measure for the transfer of heat into work and thus, for the quality of the process, expressed by $S = dQ/T$.

In 1865, CLAUDIUS gave the first mathematical version of the concept of entropy, and also gave it its name [14]. He chose the word ‘entropy’ because the meaning, from Greek, $\epsilon\eta$ + $\tau\rho\epsilon\iota\eta\sigma$, is ‘content transformative’ or ‘transformation content’ (German: ‘Verwandlungsinhalt’). This landmark paper in which he introduced the concept of entropy ends with the above statement (II) of the first and second laws of thermodynamics, [13, 14].

CLAUDIUS also contributed profoundly to the kinetic theory of gases and electrolytic dissociation. The concept of free wavelength was also introduced by him. These works led JAMES CLERK MAXWELL and LUDWIG BOLTZMANN to significant discoveries, which laid the theoretical foundation of the kinetic theory of gases. And he researched on electrodynamics of moving bodies, for which only ALBERT EINSTEIN 1905 found its solution through the special theory of relativity. See also [12, 13].

The text is based on www.wikipedia.org

Independently and almost simultaneously (1851) WILLIAM THOMSON (LORD KELVIN)⁹ was led to a different formulation of the Second Law; he extended CLAUSIUS' theory to general fluids. He was coining the word **thermodynamics**, introduced already in 1848 on the basis of the developments of CARNOT the **absolute temperature**, and demonstrated the *universality of a temperature scale that is independent of the particular properties of real thermometers*.

Two new approaches, which complemented and extended this phenomenological theory of spatially homogeneous processes, were introduced in the second half of the 19th century. One of them is the **statistical mechanics** or **statistical thermodynamics**, which led with JAMES CLERK MAXWELL's (1831–1879)¹⁰ **second theory of kinetic gases** to a field theory for gases. In this theory temperature, heat, work, energy, stress and heat flux are defined as statistical expectation values of fluctuating quantities of molecules bouncing into each other. MAXWELL formulated in his kinetic theory also a field equation for the energy and, thus, gave the First Law the form that is employed today. His formulation is neither restricted to homogeneous processes nor states in the vicinity of thermodynamic equilibrium. LUDWIG BOLTZMANN (1844–1906)¹¹ later used MAXWELL's second theory (1872, 1875, 1896) to derive his '**H-theorem**',¹² which in the kinetic theory is the analogue to the Second Law, see also [2]. With it, one arrives at a natural definition of the entropy within the kinetic theory.

The other, second, new approach was constructed by JOSIAH WILLARD GIBBS (1839–1903).¹³ He formulated the classical phenomenological theory for the **thermodynamic equilibria** and applied it to systems consisting of several phases. He discovered the so-called **phase rule** and introduced the **chemical potentials** to describe the thermostatics of **mixtures**. Considerations of the equilibria of chemically reacting materials made it then necessary to also consider the behavior of the entropy at the absolute zero of the temperature; it was necessary to identify a constant of integration, which was done by WALTER HERMANN NERNST (1864–1941)¹⁴ and later by MAX PLANCK (1858–1947).¹⁵ This theorem is often called the **Third Law of Thermodynamics**.

⁹For a short biography of LORD KELVIN, see **Fig. 17.9**.

¹⁰For a short biography of JAMES CLERK MAXWELL, see **Fig. 17.10**.

¹¹For a short biography of LUDWIG EDUARD BOLTZMANN, see **Fig. 17.11**.

¹² H is to be understood as capital Greek η and not as capital Roman h , since η is the common mathematical symbol for entropy.

¹³For a short biography of JOSIAH WILLARD GIBBS, see **Fig. 17.12**.

¹⁴For a short biography of WALTER HERMANN NERNST, see **Fig. 17.13**.

¹⁵For a short biography of MAX KARL ERNST LUDWIG PLANCK, see **Fig. 17.14**.



Fig. 17.9 WILLIAM THOMSON, first BARON KELVIN (26. June 1824–17. Dec. 1907)

A KELVIN- HELMHOLTZ instability rendered visible by clouds over Mount Duval in Australia
 WILLIAM THOMSON, first BARON THOMSON or LORD KELVIN, or KELVIN of Largs was a mathematical physicist and engineer. He was professor of Natural Philosophy at Glasgow University for more than 50 years and did important work in the mathematical analysis of electricity and the formulation of the first and second law of thermodynamics. He also had a successful career as an electrical telegraph engineer which propelled him into the public eye and ensured his wealth, fame and honour. Largely for this work he was knighted by Queen VICTORIA (1866), becoming Sir WILLIAM. Moreover, for his scientific key role in developing the basis of the absolute temperature and the KELVIN temperature scale, and because of his opposition to the Irish Home Rule, he received ennoblement as Baron KELVIN of Largs or Lord KELVIN (1892).

As a child WILLIAM THOMSON lost his mother at the age of 6 years (1830). The 4 boys and 2 girls were educated by their father who in 1834 became professor at Glasgow University. So, son William started his university education in Glasgow at the age of 10. In the academic year 1839/40 he won the class prize in Astronomy for his essay on the figure of the Earth. When coming across FOURIER's *Théorie analytique de la chaleur* he committed himself to study continental mathematics. He left Glasgow University in 1841 without a degree and went to Cambridge, where he graduated in 1845. In 1846, already at the age of 22, he was appointed to the chair of Natural Philosophy in the University of Glasgow, a position he kept until 1899.

WILLIAM THOMSON's important work on the first and second law of thermodynamics was done in the years from 1847 onwards during about 10 years. Besides his fundamental work on absolute zero, he and James Prescott JOULE collaborated, one result being the JOULE-THOMSON effect. He also phrased the second law in the form: *It is impossible, by means of inanimate material agency, to derive mechanical effect from any portion of matter by cooling it below the temperature of the coldest of the surrounding objects.*

THOMSON did also major work on electricity and developed his THOMSON bridge, KELVIN generator, mirror galvanometer and many more. He was deeply involved in the proper build-up of the telegraph cable across the Atlantic. He was also an enthusiastic yachtsman and contributed to the perfection to many marine instruments. His interest in tides led to the description of KELVIN waves and the THOMSON tide predicting machine.

THOMSON published more than 600 scientific papers and filed 70 patents. His book ‘Treatise on Natural Philosophy’ (1867) with Peter Guthrie TAIT did much in unifying the modern physics of that time.

The text is based on www.wikipedia.org

Towards the end of the 19th and the beginning of the 20th century the classical phenomenological thermodynamics reached a certain stage of completion with works by MAX PLANCK, GEORGE HARTLEY BRYAN (1864–1928) CONSTANTINE CARATHÉODORY (1873–1950)¹⁶ and PIERRE MAURICE MARIE DUHEM (1861–1916).¹⁷ PLANCK proposed in his works a form of the second law, which today is known as the **Clausius–Planck Inequality** and can be regarded as the precursor of the **Clausius–Duhem Inequality**. Indeed, the two collapse to the same statement for homogeneous systems. GEORGE HARTLEY BRYAN was the first who drew in his work on the foundations of thermodynamics attention to the fact that the internal energy as an independent essential quantity must necessarily be introduced to properly formulate the First Law, and CARATHÉODORY gave in 1909 an axiomatic justification of thermodynamics by introducing an axiom concerning the reachability by a system of thermodynamic states under adiabatic isolation. Unfortunately, his postulate cannot be extended to general systems.

The true breakthrough to a thermodynamic field theory was reached when PIERRE MAURICE MARIE DUHEM was formulating the Second Law for a material body essentially, but not yet completely, in the form (17.6) of a balance law. Mathematically, his Second Law can be written as

$$\dot{H}_V \geq - \int_{\partial V} \frac{\mathbf{q} \cdot \mathbf{n}}{T} dA. \quad (17.11)$$

Here, \dot{H}_V denotes the time rate of change of the entropy of the body in V and \mathbf{q} is the heat flux vector, so that $-\mathbf{q} \cdot \mathbf{n}$ is the heat supplied to the body through the boundary $\partial V = 0$ of V per unit time and T is the absolute temperature. Inequality (17.11) expresses the fact that *the heat gained by a body divided by the absolute temperature is a lower bound for the entropy growth*. MAX PLANCK restricts attention to homogeneous processes for which $-\int_{\partial V} \mathbf{q} \cdot \mathbf{n} = Q$, which transforms (17.11) to the CLAUDIUS–PLANCK inequality

$$\dot{H}_V \geq \frac{Q}{T}, \quad (17.12)$$

and CLAUDIUS’ analysed circular processes \mathcal{C} for which $\int_{\mathcal{C}} \dot{H}_V dt = 0$, so that CLAUDIUS’ form of the Second Law takes the form

$$\int_{\mathcal{C}} \frac{Q}{T} dt \leq 0. \quad (17.13)$$

¹⁶For a short biography of CONSTANTINE CARATHÉODORY, see Fig. 17.15.

¹⁷For a short biography of PIERRE MAURICE MARIE DUHEM, see Fig. 17.16.

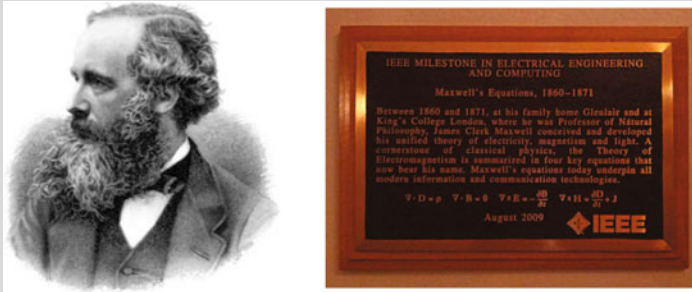


Fig. 17.10 JAMES CLERK MAXWELL (13. June 1831–5. Nov. 1879) (Left) MAXWELL'S Portrait; (Right) Commemoration of MAXWELL's equations at King's College. One of three identical IEEE Milestone Plaques, the others being at Maxwell's birthplace in Edinburgh and the family home at Glenlair. © James Clerk Maxwell Foundation

JAMES CLERK MAXWELL was a Scottish scientist in the field of mathematical physics. His most notable achievement was to formulate the classical theory of electromagnetic radiation, bringing together for the first time electricity, magnetism, and light as manifestations of the same phenomenon. MAXWELL's equations for electromagnetism, see Fig. 17.10b have been called the 'second great unification in physics', after the first one, realized by ISAAC NEWTON. With the publication of 'A Dynamical Theory of the Electromagnetic Field' in 1865, MAXWELL demonstrated that electric and magnetic fields travel through space as waves moving at the speed of light. The unification of light and electrical phenomena led also to the prediction of the existence of radio waves.

MAXWELL helped develop the MAXWELL- BOLTZMANN distribution, a statistical means of describing probability aspects of the kinetic theory of gases. He is also known for presenting the first durable colour photograph in 1861 and for his foundational work on graphical statics in the determination of the internal stress distribution in statically determinate trusses (MAXWELL- CREMONA maps). His discoveries in electrodynamics furthered advanced special relativity and quantum mechanics; so his contributions to the science are considered to be of comparable universality as those of ISAAC NEWTON and ALBERT EINSTEIN.

MAXWELL entered in Oct. 1850 Cambridge University. In 1854 he graduated from Trinity College with a degree in mathematics and was made a fellow in 1855. He worked experimentally on the colours of light and demonstrated that white light would result from a mixture of red, green and blue light. His paper 'Experiments on colour, as perceived by the eye, with remarks on colour blindness' was presented in March 1855 to the Royal Society of Edinburgh. In 1856 he applied to the Chair of Natural Philosophy at Marischall College in Aberdeen (now University of Aberdeen). He stayed there until 1860 and focused his attention to the 200 years old problem of the Nature of Saturn's rings. He proved that a regular solid ring would not be stable, while a fluid ring would be forced by wave action to break into blobs. MAXWELL, thus, concluded that the rings must be composed of numerous small particles, which he called 'brick-bats'. His prediction was confirmed in 1980 by observations during the voyager's flyby.

In 1860 Marischall college merged with King's College in Aberdeen; so MAXWELL was laid-off. He subsequently assumed the Chair of Natural Philosophy at King's College in London. The following years (1860–1865) he developed ideas on the *viscosity of gases* and *dimensional analysis*. Particularly noteworthy are, however, his advances on the fields of electricity and magnetism. This was done in his multi-part papers 'On the physical lines of forces' (1861/62), in which he provided conceptual models for *electromagnetic induction* and *magnetic flux* and discussed *electrostatics*, *displacement current* and *polarization of light*.

In 1865 MAXWELL resigned the chair of King's College, London and moved back to his home town, Glenlair, close to Edinburgh, where he wrote his textbook 'Theory of Heat', which is still available today in its ninth edition, [33]. In 1871 he became the first Cavendish Professor of Physics at Cambridge, where he was principally involved with the build-up and installation of the institute and edited the work of HENRY CAVENDISH (1731–1810). Maxwell died on 5. Nov. 1879 of abdominal cancer at the age of 48.

For MAXWELL's papers, see e.g. [24–35] and [45]

The text is based on www.wikipedia.org

Naturally, the route of the developments was in the reverse direction. DUHEM did not derive his form of the Second Law by using the CLAUSIUS or PLANCK inequalities. He could have at most *motivated* his inequality by using them. Similarly, the CLAUSIUS-DUHEM inequality, one of today's forms of the Second Law, cannot be derived but only motivated by using DUHEM's inequality. One may motivate it as follows: The left-hand side of (17.11) may alternatively be written as

$$\dot{H}_V = \frac{d}{dt} \int \rho s dV,$$

where s is the **specific entropy**. This assignment makes the entropy an additive quantity. The right-hand side of the imbalance (17.11) is the supply of entropy through the boundary ∂V of V and given by the heat in-flow divided by the absolute temperature. If there is, in addition, a volumetric supply of entropy from the outside, then one may postulate it as a volumetric heat supply divided by the absolute temperature, integrated over the volume. So, the right-hand side of (17.11) can be generalized to

$$-\int_{\partial V} \frac{\mathbf{q} \cdot \mathbf{n}}{T} dA + \int_V \frac{\rho q}{T} dV,$$

where q is the heat supply per unit mass within the body. So, a natural extension of (17.11) is

$$\frac{d}{dt} \int_V \rho s dV \leq - \int_{\partial V} \frac{\mathbf{q} \cdot \mathbf{n}}{T} dA + \int_V \frac{\rho q}{T} dV. \quad (17.14)$$

To free this statement from the imbalance we now write it as an equality

$$\frac{d}{dt} \int_V \rho s dV = - \int_{\partial V} \frac{\mathbf{q} \cdot \mathbf{n}}{T} dA + \int_V \frac{\rho q}{T} dV + \underbrace{\int_V \rho \gamma dV}_{P_V}, \quad (17.15)$$

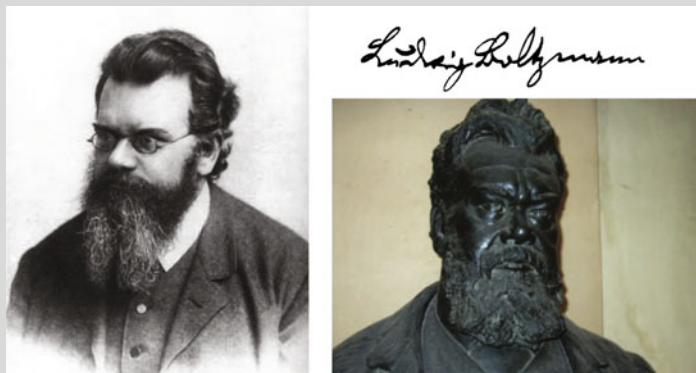


Fig. 17.11 LUDWIG EDUARD BOLTZMANN (20. Feb. 1844–5. Sept. 1906) (Left) Boltzmann 1902; (right) his signature; (right below) Boltzmann's bust in the courtyard arcade of the main building, University of Vienna

LUDWIG EDUARD BOLTZMANN was an Austrian physicist and philosopher whose greatest achievement was in the development of statistical mechanics, which explains and predicts how the properties of atoms (such as mass, charge, and structure) determine the physical properties of matter (such as viscosity, thermal conductivity, and diffusion).

LUDWIG EDUARD BOLTZMANN, born in Vienna studied physics at the University of Vienna, starting in 1863. He received his doctoral degree in 1866 working under the supervision of JOSEPH STEFAN on kinetic theory of gases. In 1867 he became a Privatdozent and STEFAN introduced him to MAXWELL's work. In 1869 at age 25 he was appointed full Professor of Mathematical Physics at the University of Graz. In 1869 he spent several months in Heidelberg working with ROBERT BUNSEN and LEO KÖNIGSBERGER. In 1871, he was KIRCHHOFF with GUSTAV and HERMANN VON HELMHOLTZ in Berlin. In 1873 BOLTZMANN joined the University of Vienna as Professor of Mathematics, where he stayed until 1876. Then, BOLTZMANN went back to Graz to take up the chair of Experimental Physics. Among his students in Graz were SVANTE ARRHENIUS, see Fig. 12.7, and WALTHER NERNST, see Fig. 17.13. He spent 14 happy years in Graz and it was there that he developed statistical mechanics. In 1890 he was appointed to the Chair of Theoretical Physics at the University of Munich. In 1893, he succeeded his teacher JOSEPH STEFAN as Professor of Theoretical Physics at the University of Vienna. In 1900, he went to the University of Leipzig, on the invitation of WILHELM OSTWALD but after the retirement of ERNST MACH, BOLTZMANN returned back to Vienna in 1902. His students there included KARL PRZIBRAM, PAUL EHRENFEST and LISE MEITNER.

Boltzmann was subject to rapid alternation of depressed moods, likely the symptoms of undiagnosed bipolar disorder, which dominated much of his later life. On Sept. 1906, during an attack of depression he committed suicide. Boltzmann was an influential researcher and teacher both in physics and natural philosophy, which has been on his unquestioned believe of the existence of atoms and molecules as structural elements of our Nature. This was in contrast to the leading defenders at the time of what is called *energetics*, among them the physicist. ERNST MACH, see Fig. 19.9, the physical chemist WILHELM OSTWALD and the mathematical chemist GEORG HELM.

They saw energy, and not matter, as the chief compositing agents of the universe and denied the existence of atoms and molecules. These opposite positions occupied the natural philosophy community strongly in the 1890s. BOLTZMANN's most important contributions in the kinetic theory, the MAXWELL- BOLTZMANN distribution in the kinetic theory of dilute gases, the BOLTZMANN statistics with the definition of entropy S as $S = k_B W$, where k_B is the BOLTZMANN constant and W the probability, i.e., the frequency of occurrence of a macro state, and, at last, the success of statistical physics is proof of this.

The text is based on www.wikipedia.org

and call P_V the **total** and γ the **specific entropy productions**. Equation (17.15) is nothing else than the mathematical form of the balance (17.6), and DUHEM's postulate now corresponds to the statement

$$P_V \geq 0, \quad (17.16)$$

or, if (17.15) holds for any subvolume

$$\gamma \geq 0. \quad (17.17)$$

The material equations for a body must be so structured that in no process the entropy production assumes a negative value.

The additional supply term (involving the radiation q in the above imbalances has been introduced in 1957 by CLIFFORD A. TRUESDELL (1919–2000) who called the imbalance (17.14) the CLAUDIUS- DUHEM inequality. We also mention for completeness that even further generalizations of the entropy balance have been postulated. These cannot well be motivated at this early stage of the developments and will therefore be introduced later in this book.

17.2 General Notions and Definitions

17.2.1 Thermodynamic System

A thermodynamic investigation starts such that one identifies and delimits the region in the space in which the investigation is conducted. In this spirit we mean by a **system a bounded spatial region** or a **bounded material substance**. The substance delimited by these boundaries or the corresponding control volume are called a **thermodynamic system**. Everything that does not belong to the system is defined as its **environment**. Directly or indirectly idealized properties are often assigned to the system boundaries; these pertain, in particular to the permeability of these boundaries with respect to matter and/or energy. The properties of these specializations are given in the following

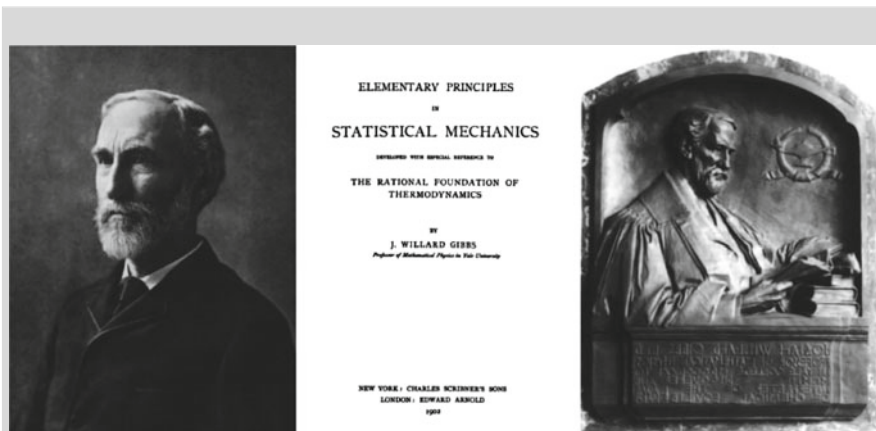


Fig. 17.12 JOSIAH WILLARD GIBBS (11. Feb. 1839–28. April 1903) (Left) Photograph of JOSIAH WILLARD GIBBS taken around 1895; (middle) Front cover of his book on Statistical Mechanics; (right) Bronze memorial tablet at the entrance to the JOSIAH WILLARD GIBBS Laboratories, Yale University

JOSIAH WILLARD GIBBS was an American scientist, who made important theoretical contributions to chemical thermodynamics, physics and mathematics. He studied at the University of New Haven and was from 1863–1866 tutor at the Yale College. Subsequently, he went to Europe to continue his studies in Paris, Berlin and Heidelberg. 1871 he was appointed professor at Yale University in New Haven.

His work on the application of thermodynamics was instrumental in transforming physical chemistry into a rigorous deductive science. Together with JAMES CLERK MAXWELL and LUDWIG BOLTZMANN he created statistical mechanics (a term that he coined), explaining the laws of thermodynamics as consequences of statistical properties of large ensembles of particles. This work is summarized in his book [18] of which the front page is reproduced above. JOSIAH WILLARD GIBBS also worked on the application of the MAXWELL equations to problems on physical optics. As a mathematician, he invented the modern vector calculus (as did at the same time and independently OLIVER HEAVISIDE). They replaced thereby the previously popular calculus of quaternions due to WILLIAM ROWAN HAMILTON (1805–1865).

Between 1876 and 1878 GIBBS wrote a series of articles summarized under the heading ‘On the Equilibrium of Heterogeneous Substances’, which counts as one of the great achievements of mathematical physics of the 19th century and built the foundation of physical thermodynamics to interpret physicochemical manifestations. Among his findings are the so-called GIBBS relation and the GIBBS phase rule. These articles appeared in the ‘*Transactions of the Connecticut Academy*’. The article ‘On the Equilibrium of Heterogeneous Substances’ was translated into the German Language by the chemist WILHELM OSTWALD (1853–1932). JOSIAH WILLARD GIBBS’ collected work is given in [4, 26, 47].

The text is based on www.wikipedia.org



Fig. 17.13 WALTHER HERMANN NERNST (25. June 1864–8. Nov. 1941)

WALTHER HERMANN NERNST was a German physicist who is known for his theories behind the calculation of *chemical affinity* as embodied in the *Third Law of Thermodynamics*, for which he won in 1920 the Nobel Prize in chemistry. He helped establish the modern field of physical chemistry and contributed to electrochemistry, thermodynamics and solid state physics.

WALTHER NERNST was born in west Prussia, now Poland and studied physics and mathematics in Zürich, Berlin, Graz and Würzburg, where he received his doctoral degree in physics in 1887 under FRIEDRICH KOHLRAUSCH [37]. In 1889 he finished his habilitation at the University of Leipzig with the physical chemist WILHELM OSTWALD [38]. 1890 he was 'Private docent' (assistant professor) at the University of Heidelberg, but moved in 1891 to the University of Göttingen, where he was associate professor and from 1895–1905 full professor. In the same year he moved to the University Berlin as full professor and director of the Institute of Physical Chemistry until 1933, when he was forced out because he was a vocal critic of ADOLF HITLER and Nazism.

WALTHER NERNST is best known for the *Third Law of Thermodynamics*, which he established in 1905 and called the 'New Heat Theorem'. It describes the behavior of matter as temperatures approach absolute zero. This law is sometimes stated as follows. *The entropy of a perfect crystal at absolute zero is exactly equal to zero. An equivalent statement is: It is impossible by any procedure, no matter how idealized, to reduce the absolute temperature of any system to zero in a finite number of finite operations.*

The text is based on www.wikipedia.org

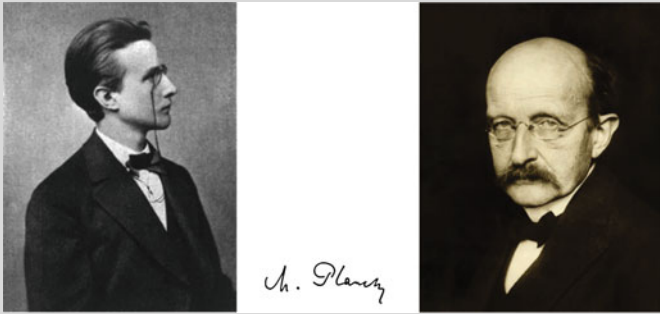


Fig. 17.14 MAX KARL ERNST LUDWIG PLANCK (23. April 1858–4. Oct. 1947) (Left) Planck as a young man, 1878; (middle) his signature; (right) Planck in 1933

MAX KARL ERNST LUDWIG PLANCK was a prominent German physicist, who originated quantum theory, which won him the Nobel Prize in Physics in 1918. He made many contributions to theoretical physics, but his fame as a physicist rests primarily on his role as an originator of the quantum theory. His name is also known through his presidency of the Kaiser Wilhelm Gesellschaft and its re-naming in 1948 as the MAX PLANCK Gesellschaft (Society, MPS), which now includes more than 800 institutions over a wide range of scientific specialties.

Born in Kiel, Germany, MAX PLANCK spent his childhood in Munich and passed his high-school degree (Abitur) at the ‘Maximilian’s Gymnasium’ in 1874. Despite his talents as a singer, pianist and cellist, he chose physics for his academic education in Munich and Berlin. At the Friedrich Wilhelm University KIRCHHOFF GUSTAV (see Fig. 3.42), HERMANN VON HELMHOLTZ (Fig. 4.10) and KARL WEIERSTRASS were among his teachers. However, he did self-education by studying RUDOLF CLAUSIUS’ papers on the theory of heat. He had already learnt of the principle of energy conservation, as a high school scholar and chose CLAUSIUS’ second law as basis of his doctoral work with dissertation ‘On the Second Law of the mechanical theory of heat’ (1879) [41]. In 1880 he passed his habilitation degree with a thesis ‘On the states of equilibria of isotropic bodies’. These articles were hardly recognized by the physics community; nevertheless PLANCK continued his research on the theory of heat, in particular entropy and its role in mixtures of gases and fluid solutions.

From 1885–1889 MAX PLANCK was professor at the Christian-Albrechts University in Kiel. Here, he participated in an academic competition ‘on the nature of energy’. He won second prize with his monograph ‘The principle of the conservation of energy’ [42]. In 1889 PLANCK was offered the chair of theoretical physics at the Friedrichs Wilhelm University in Berlin, first as associate and then as full professor, that had become vacant KIRCHHOFF after’s death in 1887 and BOLTZMANN’s rejection of the first offer.

In Berlin in 1894 PLANCK turned his attention to the problem of black body radiation. The problem had already been stated by G. KIRCHHOFF in 1859. The decisive solution covering

the range of all wave lengths was presented to the Deutsche Physikalische Gesellschaft (DFG) (German Physical Society) in Dec. 1900 and was based on PLANCK's postulate that electromagnetic energy could be emitted only in quantized form; it had to be an integer multiple of an elementary unit, $\dot{E} = h$, where h , a frequency, is PLANCK's constant. This was the birth of quantum mechanics.

In this book we shall work in parts on extensions of PLANCK's work on the second law of thermodynamics, [40–43]

The text is based on www.wikipedia.org

Definition 17.1

- An **open system** allows exchange of matter and energy with its environment.
- A system is called **materially closed**, if across its boundary no transport of matter can occur.
- A system is called **absolutely closed** if across its boundary neither matter nor energy can be exchanged.
- A system is called **adiabatic**, if it does not exchange any heat with *its environment*.

Of special significance in these definitions is the difference between **material closeness** and **absolute closeness**. Apparently a material volume, as introduced in continuum mechanics is a materially closed but not necessarily absolutely closed system, since it can exchange heat and therefore energy with the surroundings. If one interprets the mass of a gas confined in a cylinder as a system, see Fig. 17.17a, then this defines a materially closed system; in spite of possible volume changes the mass of the gas remains constant. However, a turbine, see Fig. 17.17b, is an open system, since vapor or fluid enters and leaves the turbine via openings, so there are mass flows into and out of the system.

17.2.2 Thermodynamic States, Thermodynamic Processes

The delineation of a system against its environment is a first step of its description. Within the system boundaries physical processes are taking place which are described by a certain number of physical quantities. At a certain time t these quantities have certain values by which the **state of the system at time t** is characterized. If the values of these quantities are followed for some time, then they describe a **thermodynamic process** within the system. Therefore, one may interpret a thermodynamic state as a time slice or snapshot of a thermodynamic process.

In classical thermodynamics, which restricts itself to the description of macroscopically measurable properties of systems, a relatively small number of variables describe the properties of the systems. It is one step of the description of a thermodynamic system to identify the physical quantities for a particular problem which characterize a thermodynamic process. For the confined gas in the cylinder of Fig. 17.17 these variables are the volume V , the pressure p and the mass m of the system.



Fig. 17.15 CONSTANTINE CARATHÉODORY (13. Sept. 1873–2. Feb. 1950)

CONSTANTINE CARATHÉODORY was a Greek mathematician who spent most of his professional career in Germany. He made significant contributions to the theory of functions of a real variable, the calculus of variations, and measure theory. His work also includes important results in conformal representations and theory of boundary correspondence. In 1909, CARATHÉODORY pioneered the Axiomatic Formulation of Thermodynamics along a primarily geometrical approach.

CARATHÉODORY was born in Berlin into a family of an Osmanian diplomat from Constantinople and grew up in Brussels, where he studied civil engineering and then worked until 1902 internationally on several construction sites, when he decided to study mathematics. His Ph.D. topic was ‘Variational Calculus’ under HERMANN MINKOWSKI in Göttingen. There he also received his Habilitation under FELIX KLEIN. He was professor of mathematics, mathematical physics and engineering at the Technical Universities Hannover and Breslau (now Wrocław) as well as the Universities Göttingen and Munich, where he retired in 1938. He also had an assignment at the University in Smyrna. His scientific contributions to mathematics and mathematical physics are exceptional. We restrict attention here to *Thermodynamics*:

In 1909, CARATHÉODORY published a pioneering work ‘Investigations on the Foundations of Thermodynamics’ [5] in which he treated the Laws of Thermodynamics axiomatically. It is sometimes said that he was using only mechanical concepts and the theory of PFAFF’s differential forms (named after JOHANN FRIEDRICH PFAFF (1765–1825)). However, in reality he also relied heavily on the concept of an adiabatic process. Its physical meaning rests on the concepts of heat and temperature. CARATHÉODORY’s ‘first axiomatically rigid foundation of thermodynamics’ [5] was acclaimed by MAX BORN [3], but criticized by Max Planck [44].

In his theory he simplified the basic concepts, for instance heat is not an essential concept but a derived one. He formulated the axiomatic principle of irreversibility in thermodynamics stating that inaccessibility of states is related to the existence of entropy, where temperature is the integration function. The Second Law of Thermodynamics was expressed via the following axiom: “In the neighborhood of any initial state, there are states which cannot be approached arbitrarily close through adiabatic changes of state.” In this connection he coined the term adiabatic accessibility, see [25].

The text is based on www.wikipedia.org



Fig. 17.16 PIERRE MAURICE MARIE DUHEM (10. June 1861–14. Sept. 1916)

PIERRE MAURICE MARIE DUHEM was a French physicist, mathematician, historian and philosopher of science, best known for his writings on the indeterminacy of experimental criteria and on scientific development in the Middle Ages. DUHEM also made major contributions to the sciences of his days, particularly in the fields of hydrodynamics, elasticity, and thermodynamics. He studied at the *École Normale Supérieure* and taught theoretical physics at the Universities of Lille, Rennes and Bordeaux.

His philosophical ideas are expressed in *The Aim and Structure of Physical Theory* [15], which appeared in 1914. In this work, he opposed Newton's statement that the Principia's law of universal mutual gravitation was deduced from 'phenomena', including Kepler's second and third laws. Newton's claims in this regard had already been attacked by critical proof-analyses of the German logician Leibniz and then most famously by Immanuel Kant, following Hume's logical critique of induction. But the novelty of Duhem's work was his proposal that Newton's theory of universal mutual gravity flatly contradicted KEPLER's Laws of planetary motion because the interplanetary mutual gravitational perturbations caused deviations from KEPLERian orbits.

DUHEM is well known for his work on the *History of Science*, which is documented in his 10 volume treatise *Le système du monde: histoire des doctrines cosmologiques de Platon à Copernic* (*The System of World: A History of Cosmological Doctrines from Plato to Copernicus*) (1914). He was instrumental in working out the role played by the Middle Ages to the sciences of his time.

DUHEM is also known for his work in *thermodynamics*, being in part responsible for the development of his form of the Second Law, in this book expressed by Eq. (17.11). This was a generalization of the *Second Law* in RUDOLF CLAUSIUS' form and eventually led to the CLAUSIUS- DUHEM inequality. He is also known via the GIBBS- DUHEM relation and the DUHEM- MARGULES equation. DUHEM thought that from the first principles of thermodynamics physicists should be able to derive all the other fields of physics—e.g., chemistry, mechanics, and electromagnetism, but he failed in achieving this. With the physicist, ERNST MACH and the physical chemist WILHELM OSTWALD, DUHEM also shared a scepticism with regard to the existence of atoms.

The text is based on www.wikipedia.org

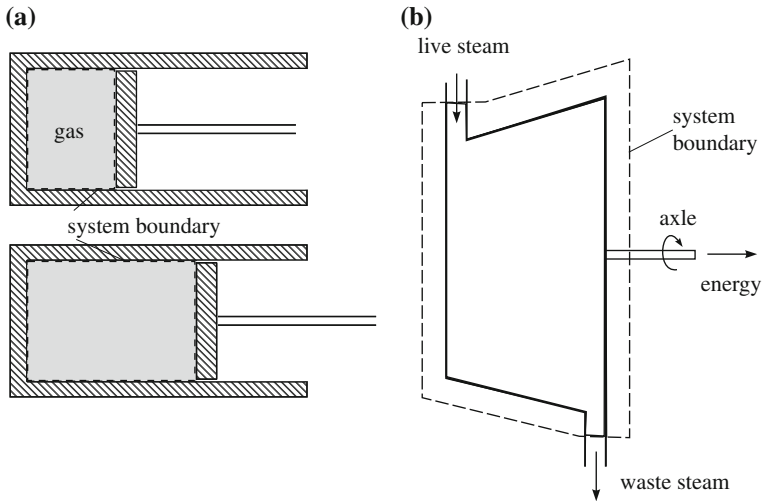


Fig. 17.17 System identifications. **a** Gas in a cylinder as an example of a materially closed system. Despite volume changes the mass of the gas inside the system remains constant. **b** Steam turbine as an example of an open system

The variables, which describe the state of a system, are called **state variables**. Sometimes, one differentiates between **external** and **internal** state variables; the former characterize the **mechanical state**, i.e., position, velocity, acceleration; the latter describe the **thermodynamic state** and, thus, comprise mass, volume, pressure, etc. The differentiation between external and internal state variables is, however, artificial, not unique and not necessarily meaningful, since the state variables interact and, thus, cannot really be separated into two different groups.

In the above discussion we have defined a ‘state’ for a *system as a whole*. This is obviously only meaningful, if the state variables are typical for the *system as a whole*. In this sense one speaks of **homogeneous systems** and **homogeneous states**. Inhomogeneous systems may occasionally be subdivided into a number of nearly homogeneous sub-systems. In this way a material body may be divided into infinitesimal volume elements of an infinite number of nearly homogeneous systems. The homogeneity of the states in the individual volume elements, however, is not exactly satisfied, since non-vanishing gradients of the state variables may arise. In thermodynamics one generally assumes that the gradients are small in these cases so that they are not affecting the state of the system.

A special state is the thermodynamic equilibrium.

Definition 17.2

- An **equilibrium state** is a state of a thermodynamic system, which does not change in time when external actions on the system are absent.

The theory of thermostatic equilibria is also called **thermostatistics**. A system that consists of two or more substances is called a **heterogeneous system**.

In thermodynamics the participating substances are also called **phases**; however, it is not mandatory that the different phases are different chemical substances. At the phase boundaries the values of the phase variables may change discontinuously. A container filled with water and its vapor is a heterogeneous two-phase system; the chemical composition of water and water vapor is the same, but across the phase boundary e.g., the density changes abruptly. Mixtures consisting of several chemical elements are also heterogeneous. They belong to the **multiphase systems**, and it is easy to see that such systems are in general heterogeneous, since their composition generally changes from position to position. Non-heterogeneous systems are single phase systems and are therefore also called simple systems. Their thermodynamic state can completely be characterized by volume, mass and pressure. For instance, air can be regarded as a simple system, even though it is composed of different phases (gases). In the following we shall mostly be concerned with such simple systems.

17.2.3 *Extensive, Intensive, Specific and Molar State Variables*

It was already mentioned that a simple system is characterized by the state variables: mass m , volume V and pressure p . In heterogeneous systems, beside these also other state variables occur. We shall here denote state variables by the letter Z .

A homogeneous system can be arbitrarily thought to be divided into partial systems. The original system and the partial systems are described by their state variables. A state variable, of which the value is the sum of the respective state variables of the individual partial systems, is called an **extensive** quantity; else, it is called an **intensive** quantity. The mass m and the volume V of a system are extensive variables; they are today more often also called **additive** variables. A state variable that is divided by the mass or volume of the system,

$$z_1 = \frac{Z}{m}, \quad z_2 = \frac{Z}{V}, \quad (17.18)$$

is called a **specific state variable**. Examples of such state variables are:

$$\begin{array}{ll} \text{mass density} & \rho = \frac{m}{V}, \\ \text{specific volume}^{18} & v = \frac{V}{m}. \end{array} \quad (17.19)$$

If the state variable is, however, divided¹⁸ by the mole number n (i.e., the number of mole masses in the system), then one obtains the **molar state variable**

$$Z_m = \frac{Z}{n}. \quad (17.20)$$

Since, in particular

$$m = Mn,$$

where M is the mole mass, one obtains the connection

$$z = \frac{Z_m}{M}, \quad \text{or} \quad Z_m = zM \quad (17.21)$$

between the specific and molar state variables.

For each homogeneous system that is divisible into sub-systems, we have for the specific state variable z the relation

$$z = \frac{Z_A}{m_A}, \quad (A = 1, 2, \dots). \quad (17.22)$$

This says: the value of the state variable z is independent of the sub-system. If Z is an extensive quantity of the system, one obtains

$$Z = \sum Z_A = z \sum m_A = zm. \quad (17.23)$$

In other words, the state variable Z is proportional to the mass of the system. This property offers an alternative possibility of the notion of extensive or additive property. All these notions will now be summarized in the following definition:

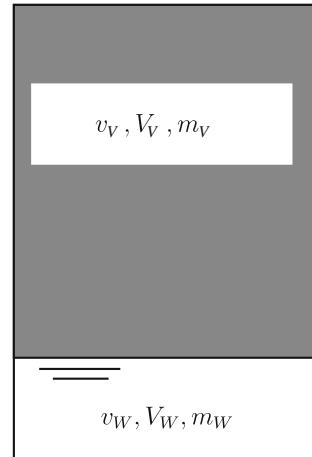
Definition 17.3

- A quantity that is proportional to the mass of a system is called **extensive** or **additive**. If the state variable is independent of the mass of the system, it is called **intensive**.
- A quantity that is measured by units of the mass is called **specific state variable**. If it is measured in units of the mole size, it is called a **molar state variable**.

Examples of extensive or additive variables are the mass—obviously—and the volume; every specific quantity, however, is intensive, as e.g. are the pressure and the temperature. As an example, consider a container with volume V , in which a two phase system, consisting of water and saturated water vapor with total mass m , see **Fig. 17.18**. The partial volumes of water and water vapor are given by V_W and

¹⁸The specific volume is denoted here by v , which is also often used to indicate a velocity component. We trust this notation will not cause confusion.

Fig. 17.18 Two phase systems. Container with volume V , filled with water (index W) and water vapor (index V)



V_V , and the common pressure of the two phases is p . The specific volumes v_W and v_V depend on the pressure; this functional dependence is assumed to be known. We would like to determine the masses m_W and m_V . Because of the additivity property we have

$$V_W + V_V = V, \quad m_W + m_V = m, \quad (17.24)$$

and

$$V_W = m_W v_W(p), \quad V_V = m_V v_V(p). \quad (17.25)$$

These four equations allow determination of the unknowns

$$\begin{aligned} m_V &= \frac{V - m v_W}{v_V - v_W}, & V_V &= m_V v_V, \\ m_W &= \frac{V - m v_V}{v_W - v_V}, & V_W &= m_W v_W. \end{aligned} \quad (17.26)$$

Provided the equations of state $v_W(p)$ and $v_V(p)$ are known, the partial masses and volumes can be calculated.

17.2.4 Adiabatic and Diathermic Walls

In Definition 17.1 materially closed and absolutely closed systems were defined. These notions are now complemented by two further system specializations as follows:

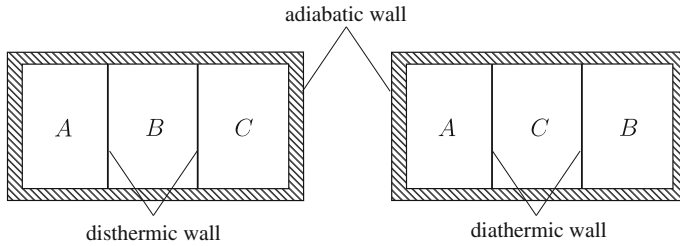


Fig. 17.19 Illustrating thermodynamic equilibria. When A and B are in equilibrium and B and C are in equilibrium, then A is also in equilibrium with C

Definition 17.4

- Two systems, separated by an **adiabatic wall** can be in equilibrium at all values of their state variables.
- Two thermodynamic systems that are in different states of equilibrium and are brought in contact with a **diathermic wall** reach, after a long time a common thermodynamic equilibrium.

Note that these definitions are indirect. This is so, because the description of the notion ‘adiabatic wall’ and ‘diathermic wall’ require knowledge of the temperature and heat flux which have not yet been introduced. Later we shall call a wall adiabatic, if it does not exchange heat with the environment, and two systems will be in equilibrium with one another, if they possess the same temperature.

Consider now the equilibrium between three systems A , B and C , see **Fig. 17.19**. We assume that system A is in equilibrium with system B and system B is in equilibrium with system C . If one separates the systems from one another without changing their states and if one brings them in contact such that systems A and C are in contact with one another via a diathermic wall, then experience tells us that systems A and C are equally in equilibrium with one another. In other words, *if two systems are in equilibrium with a third, then the three systems are also in equilibrium amongst all of them*. This property of **transitivity** of thermodynamic equilibria is sometimes called the **zeroth Law of Thermodynamics**. The notion of thermodynamic equilibrium is also **symmetric**, in other words, if a system A is in equilibrium with system B , then system B is also in equilibrium with system A . And, finally, the thermodynamic equilibrium also possesses the property of **reflexivity**, i.e., system A is trivially in equilibrium with itself. With these three properties thermodynamic equilibria fulfill mathematically the properties of **equivalence relations**. Systems, which are in mutual equilibrium, are described by one and the same equivalence class, whilst systems which are not in equilibrium with the latter belong to different, alien equivalence classes. It is apparent that one would like to characterize equivalence classes by a state variable, of which the value would allow to differentiate between the different equivalence classes. We shall see that this variable is the temperature.

17.2.5 Empirical Temperature, Gas Temperature and Temperature Scales

The notion of the temperature is closely connected with our understanding of the notions ‘cold’ and ‘warm’ or ‘hot’. Such sensations are purely subjective and do not allow a clear and unique definition of the notion ‘temperature’. In fact, our sensation of ‘hot’ and ‘cold’ is not even monotonic but rather relative. We may on occasion feel severe coldness as rather hot, for instance when we touch cold CO_2 -ice and then get blisters. It transpires that the definition of the temperature is difficult and should be chosen independently of the human sensation. It is, however, not possible to define the temperature in a direct manner. It must be defined indirectly via the notion of thermodynamic equilibrium. One says: *Two systems have the same temperature, if they are in thermal equilibrium with one another.* This statement is so expressed that the temperature is only defined for equilibria. One can express this fact also in the reverse way: As long as the temperatures of two systems differ from one another they cannot be in a common equilibrium.

There is also another approach to define temperature, and this approach is also applicable to non-equilibria. According to this approach the **empirical temperature** is any physical quantity, which allows establishment of a unique connection between the value of this quantity and the sensation of heat (or the degree of hotness) of a system. Of course, this connection must be unique; this implies that the functional relation of the empirical temperature must depend monotonically on the sensation of heat, see **Fig. 17.20a**. Empirical temperatures are measured with thermometers in which a physical quantity is uniquely related to the degree of hotness. This variable is for

- the gas thermometer a pressure, for
- the mercury thermometer or the fluid thermometer a volume, and for
- resistivity thermometers an electrical resistivity.

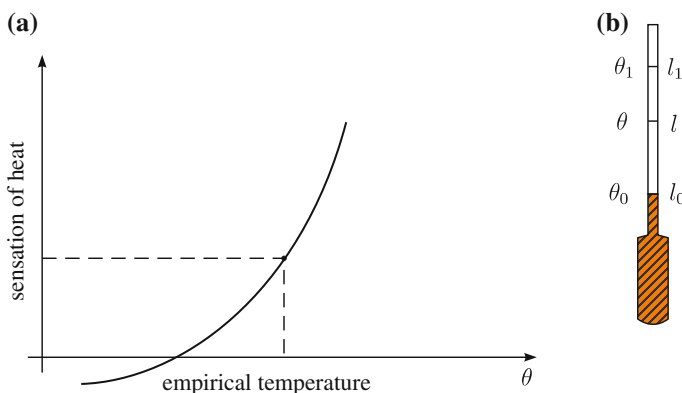


Fig. 17.20 Illustrating the definition of the temperature. **a** The empirical temperature must be connected with the sensation of heat in a monotone fashion. **b** Thermometer that uses the thermal expansion of a fluid as a measure of empirical temperature

For instance, a fluid is apt as thermometer substance, if this fluid experiences a thermal expansion when heat is supplied to it, but does hardly change its volume when being subjected to pressure variations. If the empirical temperature is denoted by θ , one may regard the specific volume alone as a function of θ . If this fluid is kept in a glass container to which a pipette is attached vertically, the position of the fluid meniscus in the pipette can be taken as a measure for the empirical temperature. With reference to Fig. 17.20b two positions l_0 and l_1 can be assigned the empirical temperatures θ_0 and θ_1 , and so one is led via linear interpolation to the representation

$$\theta = \theta_0 + \frac{\theta_1 - \theta_0}{l_1 - l_0}(l - l_0), \quad (17.27)$$

in which larger fluid-wetted capillary lengths indicate higher temperatures.

This example of the fluid thermometer demonstrates the arbitrariness of the relation by which a value of the temperature is assigned to a particular state of the thermometer. It also becomes certainly clear that in general each thermometer is characterized by its own empirical temperature. In order to remove this arbitrariness, one would have to agree to declare a certain empirical temperature as the generally accepted one, or one would have to corroborate the question whether an **absolute** or **universal temperature** exists, with the property that to a certain thermodynamic state of a system always the same value of the temperature can be assigned, no matter with what kind of a thermometer it is measured. Of course, into the definition of such a temperature no specific properties of the thermometer can enter. As we shall see later in this chapter, the Second Law of Thermodynamics will allow the definition of such a temperature. It was introduced by LORD KELVIN in the year 1848 and is called in his honor the **Kelvin temperature**. It can be realized by the definition of an **ideal gas thermometer**. We shall use the convention to denote any empirical temperature by the letter θ and the absolute temperature by the symbol T .

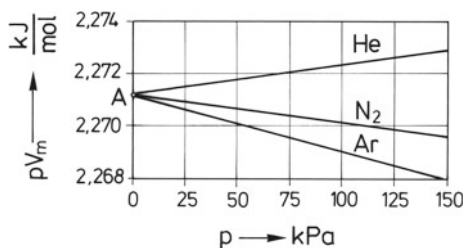
The measurement of the temperature by an ideal gas thermometer is based on the fact that for the gaseous form of a pure substance the thermal equation of state has the form $\theta = \theta(p, V_m)$. Therefore, by measuring the pressure and the mole-volume alone one can deduce the temperature. At small pressure this equation can be written as

$$pV_m = A_0(\theta) + A_1(\theta)p + \dots, \quad (17.28)$$

with coefficients $A_i(\theta)$, $i = 0, 1$ which are only functions of the empirical temperature. For isothermal processes ($\theta = \text{const.}$), the product pV_m only depends upon the pressure. Now, one would expect that the coefficients $A_0(\theta)$, $A_1(\theta)$, \dots for different gases would assume different values. This, they do, but $A_0(\theta)$ is independent of the gas (compare Fig. 17.21), which shows the isotherms of the product pV_m for various gases). Consequently, one is tempted to define by $A_0(\theta)$ a special empirical temperature $\Theta(\theta)$ by setting

$$A_0(\theta) = R_m \Theta(\theta) \quad (17.29)$$

Fig. 17.21 Isotherms of ideal gases. *Isotherms of the product pV_m for the gases He, Ar, N_2 at the triple point of water*



with the **universal** or **molar gas constant** R_m . We shall demonstrate later that Θ can be identified with the absolute temperature T . Equation (17.28) can therefore also be written as

$$pV_m = R_m T + A_1(T)p + \dots, \quad (17.30)$$

where we have now replaced Θ by T . An **ideal gas** is characterized by the thermal equation of state

$$pV_m = R_m T. \quad (17.31)$$

It represents for real gases the limiting behavior at vanishingly small pressure.

The value of the universal molar gas constant R_m depends upon the choice of the temperature scale for the absolute temperature. This scale is the **KELVIN** scale, according to which 1 Kelvin (= 1K) is given by

$$1 \text{ K} = \frac{T_r}{273.16}, \quad T_r = 273.16, \quad (17.32)$$

and T_r is the temperature at the triple point (at which water, ice and water vapor are in thermodynamic equilibrium). Because of historical reasons this temperature has the value $T_r = 273.16$. Provided once the temperature scale is fixed, one can measure the value of pV_m at $T = T_r$ and obtains from this the value

$$R_m = (8.31451 \pm 0.00007) \text{ J mol}^{-1} \text{ K}^{-1}. \quad (17.33)$$

Besides the **KELVIN** temperature there are also other empirical temperatures in use. These are today defined by agreed transformation formulae from and to the **KELVIN** temperature.

The **CELSIUS** temperature¹⁹ t is defined by

$$t = T - 273.15 \text{ [}^\circ\text{C]} \quad (17.34)$$

¹⁹After **ANDREAS CELSIUS** (1701–1744), a Swedish astronomer, mathematician and physicist. For a brief biography, see **Fig. 17.22**.



Fig. 17.22 ANDERS SPOLE CELSIUS (27. Nov. 1701–25. April 1744) (Right) The observatory of ANDERS CELSIUS, from a contemporary engraving

ANDERS SPOLE CELSIUS was a Swedish astronomer, physicist and mathematician. He was professor of astronomy at Uppsala University from 1730 to 1744, but traveled from 1732 to 1735 visiting notable observatories in Germany, Italy and France. He founded the Uppsala Astronomical Observatory in 1741, and in 1742 proposed the Celsius temperature scale which now bears his name. As the son of an astronomy professor and the grandson of a mathematician, he was a talented mathematician from an early age. Anders Celsius studied at Uppsala University, where his father was a teacher, and in 1730 he too, became a professor of astronomy there. He died from tuberculosis in 1744.

In 1730, Celsius published the *Nova Methodus distantiam solis a terra determinandi* (New Method for Determining the Distance from the Earth to the Sun). His research also involved the study of auroral phenomena, which he conducted with his assistant OLOF HIORTER. He was the first to suggest a connection between the aurora borealis and changes in the magnetic field of the Earth. He observed the variations of a compass needle and found that larger deflections correlated with stronger auroral activity. At Nuremberg in 1733, he published a collection of 316 observations of the aurora borealis made by himself and others over the period 1716–1732.

Celsius traveled frequently in the early 1730s, including to Germany, Italy and France, when he visited most of the major European observatories. In Paris he advocated the measurement of an arc of the meridian in Lapland. In 1736, he participated in the expedition organized for that purpose by the French Academy of Sciences, led by the French mathematician PIERRE LOUIS MAUPERTUIS (1698–1759) to measure a degree of latitude. The aim of the expedition was to measure the length of a degree along a meridian, close to the pole, and compare the result with a similar expedition to Peru, today in Ecuador, near the equator. The expeditions confirmed Isaac Newton's belief that the shape of the earth is an ellipsoid flattened at the poles. In 1738, he published the *De observationibus pro figura telluris determinanda* (Observations on Determining the Shape of the Earth). CELSIUS' participation in the Lapland expedition won him much respect in Sweden with the government and his peers, and played a key role in generating interest from the Swedish authorities in donating the resources required to construct a new modern observatory in Uppsala. He was successful in the request, and Celsius founded the Uppsala Astronomical Observatory in 1741. The observatory was equipped with instruments purchased during his long voyage abroad, comprising the most modern instrumental technology of the period.

Celsius was the first to perform and publish careful experiments aiming at the definition of an international temperature scale on scientific grounds. In his Swedish paper ‘Observations of two persistent degrees on a thermometer’ he reports on experiments to check that the freezing point is independent of latitude (and of atmospheric pressure). He determined the dependence of the boiling of water with atmospheric pressure which was accurate even by modern day standards. He proposed the CELSIUS temperature scale in a paper to the Royal Society of Sciences in Uppsala in 1710.

The text is based on www.wikipedia.org

and thus represents the difference between two thermodynamic temperatures. Its unit is therefore Kelvin [t] = K and is denoted by °C. The value 273.15 is the KELVIN temperature of the ice point and deviates from the value 273.16 because of historical reasons. $t = 0$ agrees with the melting point of water and $t = 100$ with the boiling point of water at 1 atm (atmosphere) pressure.

In the United States of America one still uses the **Fahrenheit temperature** t_F with the unit 1°F = (5/9)K, it is related to the KELVIN temperature by

$$t_F - 32^\circ\text{F} = T - T_0, \quad (17.35)$$

where T_0 denotes the temperature of the ice point.

17.3 Thermal Equations of State

A thermodynamic system is characterized by a certain number of state variables which depend on the kind of system under consideration; in general, this number is the larger, the more complex its structure is. If the number of variables introduced to describe the system is larger than the number necessary to describe the thermodynamic state, then the state variables must be related to one another by the **equations of state**.

The states of a simple system, e.g. a fluid, in which electromagnetic properties are irrelevant, can be characterized by pressure p , temperature T and specific volume v (and other variables that are expressible in terms of these). Experience, however, teaches us that two of the above three variables suffice to characterize the system. The **thermal equation of state**, therefore, establishes a connection between these three quantities,

$$F(p, T, v) = 0, \quad (17.36)$$

and, thus, reduces the number of independent variables to two. This functional relation is materially dependent and must be determined experimentally. Under the assumption that relation (17.36) is one-to-one and onto (i.e., bijective), this relation can also be represented in one of the following three representations:

$$p = f(T, v), \quad T = g(p, v), \quad v = h(p, T), \quad (17.37)$$

which allow definition of the following curves:

$$\begin{aligned} \text{Isobar} : \quad p &= f(T, v) = \text{constant}, \\ \text{Isotherm} : \quad T &= g(p, v) = \text{constant}, \\ \text{Isochor} : \quad v &= h(p, T) = \text{constant}. \end{aligned} \quad (17.38)$$

They define the graphs for constant pressure, temperature and volume, respectively.

17.3.1 Ideal Gas

We have defined an **ideal gas** already in the last subsection by the **thermal equation of state**

$$pV_m = R_m T. \quad (17.39)$$

The gas is called ideal, because the general expansion (17.30) terminates after the first term ($A_i = 0$ for $i \geq 1$); correspondingly, the resulting Eq. (17.39) can be applied for real gases only at small pressure p . Practically, the pressures must lie below 1 MPa.

If in (17.39) we introduce with

$$v = V_m/M, \quad (17.40)$$

the connection between the specific volume v , the molar volume V_m and the mole mass M , the thermal equation of state of an ideal gas can also be written as

$$pv = RT, \quad R = R_m/M, \quad (17.41)$$

where R is no longer the universal gas constant, but the gas constant of the individual ideal gas. As evident from (17.41), it can be obtained from the universal gas constant and the mole mass of the substance in question.

The isobars, isotherms and isochors of an ideal gas are given by the relations

$$\begin{aligned} T/v &= \text{constant, (isobar)}, \\ pv &= \text{constant, (isotherm)}, \\ T/p &= \text{constant, (isochor)}. \end{aligned} \quad (17.42)$$

In a (T, v) -diagram the isobars are given by a set of straight lines through the origin, the isotherms are in the (p, v) -diagrams representable as a set of hyperbolas and the isochors in the (p, T) -diagrams are a set of radial straight lines through the origin, see **Fig. 17.23**. Practically, the isotherms are particularly significant, as the isotherms of ideal and real gases differ markedly from one another.

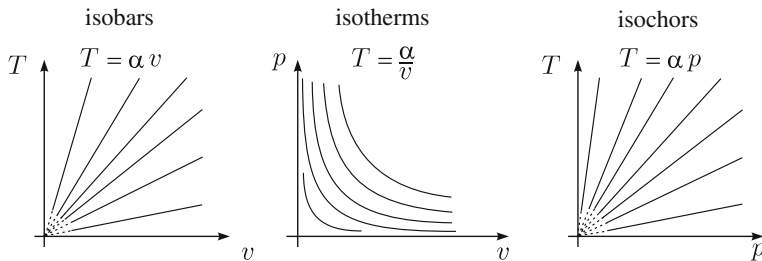


Fig. 17.23 Thermal equation of state. *Isobars, isotherms and isochors of an ideal gas*

17.3.2 Real Gases

Real gases or real fluids show conspicuous differences to the behavior of ideal fluids. Their isotherms in the (p, v) -diagram look as qualitatively shown in **Fig. 17.24**. To explain this figure, we consider the following gedanken experiment. A cylinder, filled with a gas (e.g. CO_2) and absolutely closed with a piston and having diathermic walls is thought to be submerged in a heat bath, of which the temperature is held constant at the value T_1 , which is smaller than the **critical temperature** T_c of the gas. ($T_c = 304 \text{ K}$ for CO_2). This critical temperature belongs in Fig. 17.24 to that isotherm, which touches the dashed curve with horizontal tangent at its highest point. Starting with a certain initial volume the gas is now compressed by moving the piston so slowly (theoretically infinitely slowly) that the temperature in the cylinder agrees at all times with the temperature of the reservoir, T_1 , see **Fig. 17.25**. Such a process is called a **quasi-static isothermal compression**. In this process the pressure first increases monotonically; however, as soon as the volume decreases below a certain value v_2 (which depends on the gas and the temperature T_1 at which the experiment is performed), liquid is accumulated at the bottom of the cylinder.²⁰

This process is called **condensation** because the liquid is denser than the gas. Once the volume is smaller than v_2 , it does not increase for some time, but stays constant. However, one observes that the liquid volume increases as the volume in the cylinder further decreases until at $v = v_1$ the entire cylinder is filled with liquid. If the volume within the cylinder is further decreased, the pressure increases very steeply. Apparently, the compressibility of the liquid is much smaller than that of the gas. If the experiment is conducted at various different values of the temperatures of the bath, one obtains the qualitative behavior sketched in Fig. 17.24. Below the dashed curve of the (p, v) -diagram gas and liquid phases **coexist** arbitrarily long; they are in thermodynamic equilibrium. One speaks of the *coexistence of the liquid with the gas or vapor phase*. One also sees in Fig. 17.24 that in the region of coexistence

²⁰The collection of the fluid at the bottom is the consequence of gravity, because the larger liquid droplets, owing to their correspondingly larger weight can no longer be kept suspended in the gas by the impacts of the molecules of the gas. If the experiment would be performed in outer space without gravity, the liquid droplets would be homogeneously distributed in the entire cylinder and after a very long time they would cluster as larger liquid regions.

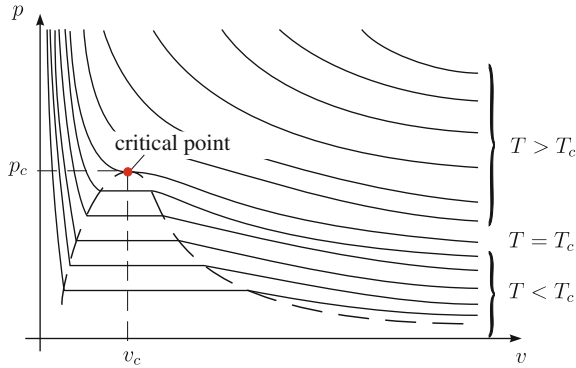


Fig. 17.24 Thermal equation of state. *Graphs of the isotherms for a real fluid*

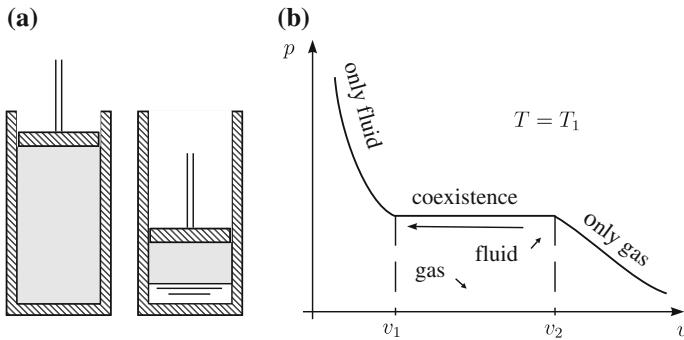


Fig. 17.25 Quasi-static isothermal compression. **a** Fluid confined in a cylinder with piston, on the left as a pure gas at large specific volume, on the right as a two phase medium with vapor and fluid phases at small specific volume. **b** Isotherm for a temperature $T < T_c$, at which phase changes are possible

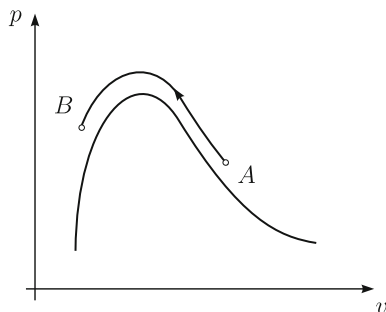
of liquid and gas phases the pressure no longer depends upon the volume but only the temperature. To each temperature there belongs its peculiar **vapor pressure**.

Coexistence between gas (vapor) and liquid only arises below the critical temperature T_c . The isotherm for T_c is called **critical isotherm**. At the point of **critical**

Table 17.1 Critical temperatures T_c and critical pressures p_c for a number of gases

Material	T_c (K)	p_c (Pa)	Material (K)	T_c (Pa)	p_c
He	5.2	0.233×10^6	O ₂	154.0	5.07×10^6
H ₂	33.2	1.31×10^6	Kr	211.0	5.47×10^6
Ne	44.7	2.74×10^6	Xe	290.0	5.88×10^6
N ₂	126.0	3.34×10^6	CO ₂	304.0	7.40×10^6
Ar	151.0	4.86×10^6	NH ₃	406.0	11.35×10^6

Fig. 17.26 Quasi-static thermodynamic process. In a thermodynamic process along the indicated curve AB a gas turns into a liquid without being noticeable



volume v_c and **critical pressure** p_c it possesses an inclination point with horizontal tangent. The values T_c and p_c only depend upon the substance, whilst v_c is proportional to the amount of the substance. Values of the critical temperatures and critical pressures for some gases are shown in **Table 17.1**.

It is possible to imagine a quasi-static transition of a system from a gaseous state to a liquid state by a sequence of quasi-static equilibria, which avoid the region of coexistence of a gas and a liquid, as e.g. along the curve AB shown in **Fig. 17.26**. In this case in point A of the (p, v) -diagram, we have a gas, whilst in point B , we have a liquid. By adequate changes of the variables p , v and T along the indicated curve, the system can be changed from state A to state B without being able to tell with certainty where its gaseous state terminates and where the liquid state commences.

17.3.3 The Phenomenological Model of van der Waals

JOHANNES DIDERIK VAN DER WAALS (1837–1923)²¹ proposed in the year 1873 a thermal equation of state which is capable of mimicking a large part of real gases and liquids, respectively. It reads

$$\left(p + \frac{a}{V_m^2}\right)(V_m - b) = R_m T, \quad (17.43)$$

and is referred to the volume of a mole, V_m . R_m is the universal gas constant and a and b are constants, which depend on the substance. One can make Eq. (17.43) plausible by means of certain model considerations, but it cannot be deduced from physical principles. It is therefore a phenomenological proposal. To motivate Eq. (17.43), we write its left-hand side as $(p + p_B)(V_m - b)$ and so realize that $p_B = a/(V_m)^2$ is an additional pressure, whilst b has the dimension of a volume. In a VAN DER WAALS gas the pressure is increased by the **internal pressure**, p_B , whereas the mole volume is reduced by the so-called **inaccessible volume** b . The occurrence of the internal pressure can be explained by the fact that the smaller mean distance of the liquid

²¹For a short biography of JOHANNES DIDERIK VON DER WAALS, see **Fig. 17.27**.



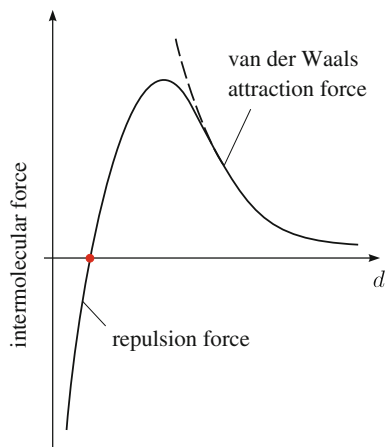
Fig. 17.27 JOHANNES DIDERIK VAN DER WAALS (23. Nov. 1837–8. March 1923)

JOHANNES DIDERIK VAN DER WAALS was a Dutch physicist, who received in 1910 the Nobel Prize for Physics. After his basic education he worked as a teacher at his home town Leiden. Without a formal high school degree (Abitur, Matura) he could not attend a regular university education, but he visited from 1862–1865 lectures and seminars at the University of Leiden and achieved thus an extension of his certificate of teaching mathematics and physics. This also brought him a teaching position at a school in den Haag, where he advanced to the level of school director. A change in the educational law of Holland allowed him to commence a study in Natural Sciences, which he finished in 1873 with a doctoral dissertation in physics, [30, 46]. From 1877 until 1908, he was professor of physics at the University of Amsterdam. VAN DER WAALS studied the behavior of molecules in particular and matter in general. 1869, he discovered the cause of the attraction of atoms and non-polarized molecules, which later were called VAN DER WAALS forces (see Fig. 17.29). 1873 he developed in his dissertation a model describing the continuous transition of matter in gaseous and liquid state of existence. He then proposed a thermal equation of state, which showed that states of gases and liquids not only can be transformed into one another, but are based on the same physical principle. This led to the Nobel Prize for physics of 1910.

The text is based on www.wikipedia.org

molecules as compared to the gas molecules makes the VAN DER WAALS attracting forces between the molecules more effective than in the gas, for which they are negligible, see Fig. 17.29. By the mutual attraction in the coexisting region of gas and liquid the continuum builds something like its own pressure. In Eq. (17.43) this is phenomenologically achieved by the addition of the internal pressure; this is added as a kind of self-pressure to the thermodynamic pressure. On the other hand, the inaccessible volume b is interpreted as the influence of the finite volume which the molecules of real gases and liquids have as opposed to ideal gases of mass points, whose molecules are thought to have vanishing extent. If the molecules are thought as hard, elastic spheres of finite radius, their mobility is restrained. For a given mean

Fig. 17.28 VAN DER WAALS fluid. Isotherms and their MAXWELL corrections (see inset) in the co-existence regime of both phases



kinetic energy (i.e., at given temperature) the number of impacts per unit time is, therefore, larger than for a gas of mass points. One can qualitatively account for this by incorporating into the equation of state of the ideal gas a volume that is smaller than the mole volume by the inaccessible volume of the molecules. This plausibility argument, therefore, also gives us a hint, which value one must expect for b . One may substitute for it the fourfold²² value of the self-volume of the molecules.

The graph of the isotherms for the equation of state of VAN DER WAALS gases is sketched qualitatively in **Fig. 17.28**. No horizontal regions arise, which would allow characterizing the coexistence regime of the gas and liquid. However, there is an isotherm with a point of horizontal tangent and changing inclination. It is tempting to identify this isotherm with the critical temperature T_c . The isotherms with $T > T_c$ show a bijective relation between pressure and volume. For those isotherms whose temperature lies below the critical temperature the functional relation between pressure p and volume V_m is not bijective. Whereas to a given volume V_m there is a unique pressure, the reverse does not hold: to a given pressure p three values of the volume V_m can be assigned. We shall define the **critical point** in the (p, V_m) -diagram as that point of the isotherm belonging to T_c which has a horizontal tangent and a vanishing curvature. Using Eq. (17.43), it can easily be shown that this point is given by

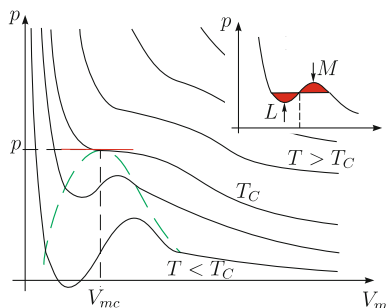
$$T_c = \frac{8a}{27bR_m}, \quad p_c = \frac{a}{27b^2}, \quad V_{mc} = 3b. \quad (17.44)$$

To this end one only needs to compute

$$\frac{dp}{dV_m} = 0, \quad \text{and} \quad \frac{d^2p}{dV_m^2} = 0,$$

²²We cannot give a justification of this value here.

Fig. 17.29 VAN DER WAALS forces. Two molecules are subjected to an interaction force, which at very large distance is a very small attraction, but turns into a repulsion when the molecule distance is very small



and to solve these two equations together with (17.43) for $p = p_c$, $T = T_c$ and $V_m = V_{mc}$. Elimination of a and b from (17.43) with the aid of (17.44) yields the simple VAN DER WAALS relation

$$p_c V_{mc} = \frac{3}{8} R_m T_c. \quad (17.45)$$

Thus, if the VAN DER WAALS gas is a good description of a real gas, then this gas must satisfy the relation

$$\frac{p_c V_{mc}}{R_m T_c} = \frac{3}{8} = 0.375. \quad (17.46)$$

As **Table 17.2** shows, the experimental values all lie below 0.375. As revealed by **Table 17.1**, the critical temperatures of some of these gases differ by orders of magnitude; on this basis the values in **Table 17.2** must be regarded as close to the value (17.46).

Consider now an isotherm for $T < T_c$ in the regime of positive inclination $dp/dV_m > 0$, see insert in **Fig. 17.28** between the points identified as L and M . In this regime, a small volume change in an isothermal process would be amplified as follows: A small volume increase would yield an increase in pressure, which would again cause a volume increase. Analogously, a small volume decrease would yield a pressure decrease, which would again lead to a volume decrease. Hence, such a process cannot be stabilized. The **negative compressibility** of the VAN DER WAALS gas in this regime leads to an **unstable thermodynamic state**. Small changes are amplified—this is a positive feedback—and the system moves farther and farther away from its original state.

As we have already seen, the experimental isotherm in this regime does not behave as a VAN DER WAALS gas; the pressure in this regime is independent of the volume. Neither is it plausible that unstable thermodynamic states should exist. One can modify the VAN DER WAALS model such that one changes the isotherms in the unstable regime such that along the new, corrected isotherm the pressure does not change. In the inset panel of **Fig. 17.28** this is sketched by the shaded alteration of the isotherm.

Table 17.2 Values of the constants $p_c V_{mc}/(R_m T_c)$ for some gases

Material	$\frac{p_c V_{mc}}{R_m T_c}$	Material	$\frac{p_c V_{mc}}{R_m T_c}$
H_2O	0.230	CH_h	0.290
SO_2	0.269	N_2	0.291
C_2H_4	0.270	Ar	0.291
C_2H_2	0.274	O_2	0.292
CO_2	0.275	CO	0.294
C_2H_6	0.285	H_2	0.304
Xe	0.288	4He	0.308

However, we now must ask, how this straight horizontal segment of the isotherm must be positioned to satisfy the thermodynamic requirements. The answer to this question was given by JAMES CLERK MAXWELL: The dashed areas above and below the straight new segment must possess the same areas in order that the Second Law of Thermodynamics is satisfied. This will be later scrutinized in this chapter. With this construction of MAXWELL it is possible to eliminate the non-unique regime in the (p, V_m) -diagram of a VAN DER WAALS gas (this regime in Fig. 17.28 is outlined by the shaded curve) and to define the vapor pressure and the coexistence of the gas and the liquid.

There exists a particularly elegant dimensionless representation of the VAN DER WAALS equation (17.43). If one defines the dimensionless quantities

$$\bar{p} = \frac{p}{p_c}, \quad \bar{v} = \frac{V_m}{V_{mc}} = \frac{v}{v_c}, \quad \bar{T} = \frac{T}{T_c},$$

then (17.43) together with (17.44) can be put into the form

$$\left(\bar{p} + \frac{3}{\bar{v}^2}\right)(3\bar{v} - 1) = 8\bar{T}. \quad (17.47)$$

This form of the VAN DER WAALS equation can be denoted as **universal**, since it does not contain the parameters a and b , which change from substance to substance. The equation says that in VAN DER WAALS gases, for which two values of \bar{p} , \bar{v} , \bar{T} agree with one another, the third value must also agree. In the (\bar{p}, \bar{v}) -diagram all VAN DER WAALS gases have the same coexistence region of gas and liquid. They are in so-called **corresponding states** whenever they agree in two of the dimensionless variables \bar{p} , \bar{v} , \bar{T} . Interestingly, this law of corresponding states is for real fluids satisfied with large precision, even though their behavior is only qualitatively described by the VAN DER WAALS equation that is complemented by MAXWELL's construction in the region of coexistence between gas and liquid.

17.4 Reversible and Irreversible Thermodynamic Processes

Thermodynamic states were already defined in Sect. 17.1. If a thermodynamic state changes in time by some outside action, then a thermodynamic process is generated; we wish to formally lay down this by the

Definition 17.5

- A thermodynamic process in a system is a temporal sequence of events, in which previous events determine ensuing events such that they imply a particular time dependent sequence of thermodynamic states

In this definition it is irrelevant how these states are caused. It is only important that a temporal sequence of exactly identifiable events can be defined, which cause the change of state. The process can be initiated by releasing internal constraints or the removal of an external action.

In the introduction to this chapter we have already spoken of processes and introduced the notion of the principle of irreversibility without clearly formulating this notion. We shall now precisely define reversibility and irreversibility how they were introduced already in the year 1824 by NICOLAS LÉONARD SADI CARNOT.

Definition 17.6

- If a system, in which a thermodynamic process has taken place, can be brought back into its initial state such that no changes remain in its environment, then the process is called **reversible**. If the initial state of the system cannot be re-established without leaving any changes in the environment, then the process is called **irreversible**.

According to this definition the process is not reversible only by the fact that the system can be brought back to its initial state; this is in principle always possible. An essential part of the definition is the statement that after the back transformation of the system to its initial state equally no changes are allowed to remain in the environment of the system. Most natural processes are irreversible, for they usually start with a non-equilibrium state and often end in an equilibrium state, or they connect two equilibrium states.

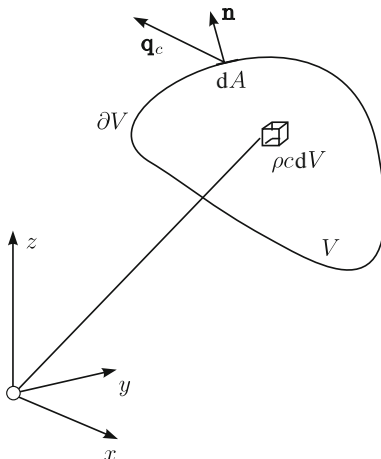
We have already mentioned irreversible processes in Sect. 17.1, see Figs. 17.3 and 17.4. A decisive characterization of the irreversibility of a process was thereby the observation that the process evolving backward in time was physically impossible. Let us describe here a well-known process for which this impossibility of time reversal can easily be identified.

17.4.1 Diffusion

We consider a dye that is in solution with a fluid and wish to describe its spreading, see Fig. 17.30. To this end, we imagine that the molecules of the dye in a point of the fluid move on average with the velocity of the fluid. The number of the molecules

Fig. 17.30 Derivation of the diffusion equation.

Explaining the derivation of the diffusion equation. Body with volume V and boundary ∂V . The volume element dV contains the mass $\rho c dV$ of a tracer substance. Through the surface element dA the amount $\mathbf{q}_c \cdot \mathbf{n} dA$ of the tracer mass is moving



on a material particle can then be regarded as a measure of their concentration. If one denotes the mass ratio of the dye to that of the fluid at the point \mathbf{x} and at time t by $c(\mathbf{x}, t)$, then the total mass of the dye contained in the fluid volume V is given by $\int_V \rho c dV$, and its time rate of change is

$$\frac{d}{dt} \int_V \rho c dV. \tag{17.48}$$

Now, observation shows that the dye is spreading. Per unit time, an amount of dye, thus, moves through the fluid surface ∂V ; this flux is given by

$$\int_{\partial V} \mathbf{q}_c \cdot \mathbf{n} dA, \tag{17.49}$$

in which \mathbf{q}_c is the so-called **diffusive flux** and \mathbf{n} is the unit vector pointing to the exterior to V . The time rate of change of the dye mass (17.48) must therefore be equal to the flux (17.49) through the surface

$$\frac{d}{dt} \int_V \rho c dV = - \int_{\partial V} \mathbf{q}_c \cdot \mathbf{n} dA. \tag{17.50}$$

(The negative sign is due to the fact that $\mathbf{q}_c \cdot \mathbf{n}$ is positive as an outflow). With the aid of the transport theorem proved in Chap. 3 (see p. 88 in Vol. 1)

$$\frac{d}{dt} \int_V \rho c dV = \int_V \rho \frac{dc}{dt} dV \tag{17.51}$$

and applying the divergence theorem to the surface integral (17.49), viz.,

$$\int_{\partial V} \mathbf{q}_c \cdot \mathbf{n} dA = \int_V \operatorname{div} \mathbf{q}_c dV, \quad (17.52)$$

we may also write (17.50) in the form

$$\int_V \left(\rho \frac{dc}{dt} + \operatorname{div} \mathbf{q}_c \right) dV = 0, \quad (17.53)$$

or, since V can be arbitrary

$$\rho \frac{dc}{dt} + \operatorname{div} \mathbf{q}_c = 0. \quad (17.54)$$

This equation, known as FICK's **second law**,²³ is nothing else than the mass balance for the dye.

Equation (17.54) does not suffice to describe the spreading of the dye concentration. It must be complemented by a relation for the diffusive flux. It was the merit of ADOLF EUGEN FICK to have proposed a phenomenological relation for it. He namely realized that the dye in solution or suspension of the fluid moves from regions of high concentration to regions of low concentration. This fact suggests to set the diffusive flux proportional to the concentration gradient with negative constant of proportionality,

$$\mathbf{q}_c = -\rho D \operatorname{grad} c, \quad D > 0. \quad (17.55)$$

$D > 0$ is the **diffusion coefficient** or **diffusivity** and its positivity is a requirement of the Second Law of Thermodynamics as we shall see. This equation is known as FICK's **first law**. Substitution of (17.55) into (17.54) leads to the equation

$$\rho \frac{dc}{dt} = \operatorname{div} (\rho D \operatorname{grad} c),$$

which for a density preserving fluid and constant diffusion coefficient takes the form

$$\frac{dc}{dt} = \frac{\partial c}{\partial t} + (\operatorname{grad} c) \cdot \mathbf{v} = D \Delta c, \quad (17.56)$$

in which $\Delta(\cdot) = \operatorname{div} \operatorname{grad}(\cdot)$ denotes the LAPLACE operator. If the fluid is at rest, the convective term is absent.

Equation (17.56) is called **diffusion equation**; it discloses the irreversibility of the diffusion processes simply by its non-invariance under *time reversal* $t \rightarrow -t$. Indeed, in this transformation the signs of $\partial c / \partial t$ and $(\operatorname{grad} c) \cdot \mathbf{v}$ change, but not the sign of Δc . A diffusion process that is traversed backward in time cannot exist. This

²³According to ADOLF EUGEN FICK (1829–1901) Professor of medicine at the Universities of Zurich and Würzburg. For a short biography see Fig. 17.31.



Fig. 17.31 ADOLPH EUGEN FICK (3. Sept. 1829–21. Aug. 1901)

ADOLPH EUGEN FICK showed in his early life a remarkable talent for mathematics and physics, which he started to study at the University of Marburg. However, under the prodding of his elder brother HEINRICH FICK, he was persuaded that his talents would fall on particular fertile ground in medicine. Therefore, he matriculated in medicine and completed his medical doctorate in 1851 with the dissertation ‘Tractatus de errore optico’, in which he connected astigmatism with the curvature of the cornea. Subsequently, FICK specialized in physiology and assumed a position at the medical school of the University of Zurich, where he received his habilitation in 1853. In 1856 he was promoted to Associate and in 1862 to Full Professor of Physiology. In 1868, FICK moved to the University of Würzburg, where he held the chair of physiology until his retirement in 1899. FICK’s mathematical talent found its trace in many of his scientific works. 1851 he published a fundamental paper on the movement of the eyes. 1855, he formulated his diffusion theory of matter with his two basic laws, known as FICK’s first and second laws. He invented the myographion to measure muscle jerks (1862), designed an instrument, called later ‘Plethysmograph’ to measure the speed of the blood in arteries of humans (1868) and devised a technique for measuring cardiac output (1870). FICK also invented the tonometer to measure the pressure in the eyes (1888), however, the invention of the contact lenses is by his nephew ADOLPH, GASTON EUGEN FICK.

FICK received an honorary doctor degree of the University of Leipzig, and was member of the Academies in Berlin, Munich, Stockholm, Uppsala, Lund and Florence; he also received the Golden Cothenius Medal of the ‘Deutschen Akademie der Naturforscher’ and was named ‘Geheimer Rath’ and received a title of nobility by the ‘Bavarian Crown’, however he was too modest to ever use these attributes.

FICK’s phenomenologically motivated diffusion law received a theoretical foundation through A. EINSTEIN’s work on BROWNIAN motion (1905) [16]. A detailed description on this connection is given by J. PHILIBERT, [39].

In physics, chemistry and engineering FICK’s first law expresses the flux of a species concentration in a bearer fluid to be proportional to the gradient of the concentration field and pointing from high concentration to small concentration.

The text is based on www.wikipedia.org

can be visualized by the fact that non-uniform concentrations are homogenized with time but not vice versa.

The example, incidentally, also shows that there exist irreversible processes for which the temperature does not play a role. The Second Law of thermodynamics should also be able to cope with such phenomena.

17.4.2 Reversible Expansion and Compaction of a Gas

As already said, reversible processes do not exist in Nature. Under idealized conditions one may, however, imagine situations in which these thought processes are traversed reversibly. In the expansion of the gas that is confined in the cylinder of **Fig. 17.32** one can imagine that by the expansion of the gas a weight in the gravity field of the Earth is lifted. The work that is performed by the gas when moving the piston is then stored as potential energy and can be regained. This process can be reversibly conducted only provided the pressures at the piston perform under expansion exactly the same work as the work that is necessary to compress the gas again into its initial state. This is only possible, if the gas pressure in the cylinder performs at all times the same power of working as does the weight. This can be achieved by adequately forming the guiding curve. Of course, the conditions of reversibility also require that the gas is always in a homogeneous state such that all irreversible homogenization processes between the different parts of the system are avoided. The motion must therefore be a sequence of quasi-static changes of thermodynamic states.

17.5 First Law of Thermodynamics

The First Law of Thermodynamics expresses the principle of energy conservation of all energy forms, mechanical, thermal and if present electrical, chemical and nuclear energies. The application of this principle leads us to introduce, besides the common mechanical energy, also other energy forms, namely internal energy and heat. For the formulation of the First Law we first summarize a number of notions that were already defined earlier or are well known from basic mechanics.

17.5.1 Mechanical Energies

Definition 17.7

- By **work** of a system we mean the work done by all forces acting on the system.
- **Power** or **power of working** is work per unit time.

Fig. 17.32 Reversible expansion. *Imagined construction to achieve reversible expansion and compaction of a gas in an isolated cylinder*

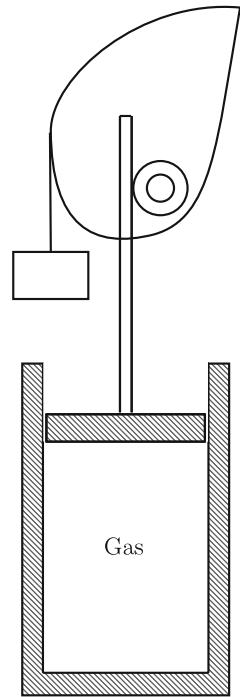
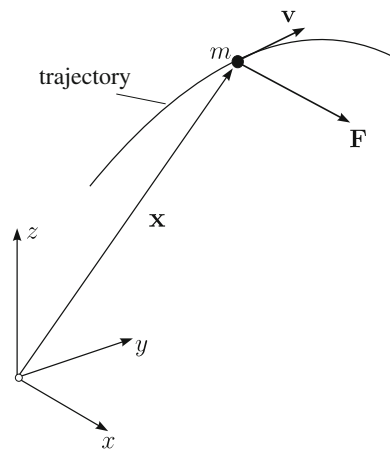


Fig. 17.33 Mass point in motion. *Motion of a mass point with mass m and resulting force \mathbf{F} along its trajectory*

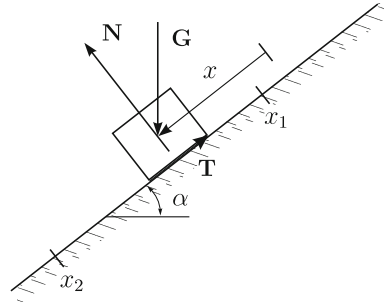


We assume that the reader is familiar with these notions from basic mechanics, but explain them below with the aid of a few examples.

Consider a mass point with mass m which moves with velocity $\dot{\mathbf{x}}$ along its trajectory $\mathbf{x}(t)$ and is subjected to the external force \mathbf{F} , see **Fig. 17.33**. NEWTON's law reads in this case

$$(m\dot{\mathbf{x}})' = m\ddot{\mathbf{x}} = \mathbf{F}. \quad (17.57)$$

Fig. 17.34 Motion of a cube along an inclined plane. The external forces are \mathbf{G} , \mathbf{N} and \mathbf{T} , the coordinate is x and the cube is displaced from x_1 to x_2



$m\dot{\mathbf{x}}$ is the *momentum* and $\ddot{\mathbf{x}}$ the acceleration. One commonly writes \mathbf{v} for the velocity, which we shall now do. If (17.57) is scalarly multiplied with \mathbf{v} , then one obtains

$$\dot{T} = m\dot{\mathbf{v}} \cdot \mathbf{v} = \frac{d}{dt} \left(m \frac{|\mathbf{v}|^2}{2} \right) = \mathbf{F} \cdot \mathbf{v} = L, \quad (17.58)$$

in which

$$T = \frac{m}{2} |\mathbf{v}|^2 \quad \text{and} \quad L = \mathbf{F} \cdot \mathbf{v} \quad (17.59)$$

denote the kinetic energy of the mass point and the power of working of the forces acting on the mass point. Integration of (17.58) along the trajectory yields

$$\int_{t_1}^{t_2} \dot{T}(t) dt = \int_{t_1}^{t_2} L(t) dt = \int_{t_1}^{t_2} \mathbf{F} \cdot \mathbf{v} dt = A_{12},$$

$$T_2 - T_1 = A_{12}. \quad (17.60)$$

The difference of the kinetic energies of the mass point at the times t_2 and t_1 equals the **work** A_{12} done by the forces acting on the mass point during the motion from t_1 to t_2 . We infer from formula (17.60) the equivalence between ‘work’ and ‘kinetic energy’; for, if they are correlated as in Eq. (17.60), they have the same dimension, namely ($\text{kg m}^2\text{s}^{-2}$).

For the rectangular block of **Fig. 17.34**, which slides down the inclined plane, the external forces are given by the weight \mathbf{G} and the reactions \mathbf{N} and \mathbf{T} between sliding mass and supporting plane. With the coordinate x as shown in the figure, the power of working is given by

$$L(t) = (G \sin \alpha - T)v(t),$$

which, together with COULOMB’s²⁴ dry friction law

$$T = \mu N = \mu G \cos \alpha,$$

²⁴For a short biography of CHARLES- AUGUSTINE DE COULOMB see Fig. 13.8.

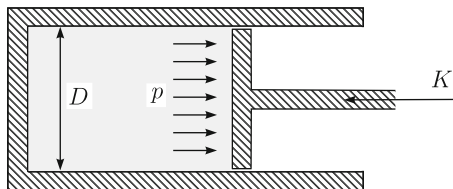


Fig. 17.35 Illustrating the calculation of the work due to volume changes. *The work of the pressure p due to the displacement of the piston is for a circular cylinder with diameter D given by (17.63). [The work of the pressure acting on the gas would be the negative value of that given in (17.63).]*

can also be written as

$$L(t) = G(\sin \alpha - \mu \cos \alpha) \frac{dx}{dt}(t). \quad (17.61)$$

The normal force N does not contribute to the value of the power since it is perpendicular to the displacement increment. The work A_{12} , which the external forces supply during the motion of the sliding mass between positions 1 and 2, is therefore given by

$$A_{12} = G(\sin \alpha - \mu \cos \alpha) \int_{t_1}^{t_2} \frac{dx}{dt}(t) dt = G(\sin \alpha - \mu \cos \alpha)(x_2 - x_1). \quad (17.62)$$

When the piston of a cylinder that is filled with a gas is moved, the forces that act on the piston are the resulting pressure and the external force K acting on the piston, see **Fig. 17.35**. The power of working and the work done by the pressure during the displacement of the piston are given by

$$\begin{aligned} L dt &= dA = p \frac{\pi D^2}{4} dx = p dV, \\ A_{12} &= \frac{\pi D^2}{4} \int_{x_1}^{x_2} p(x) dx = \int_{V_1}^{V_2} p dV, \end{aligned} \quad (17.63)$$

respectively. They can be calculated as soon as the pressure p is known as a function of x . The work (17.63) is called the work done due to volume changes. The work done by the gas has obviously the reverse sign and is given by

$$A_{12}^{\text{gas}} = - \int_{V_1}^{V_2} p dV. \quad (17.63a)$$

With these examples we are now in the position to formulate the total kinetic energy of the material volume V with boundary ∂V as well as the powers of working of the volume and surface forces, see **Fig. 17.36a**, as volume and surface integrals of the respective specific quantities; they are

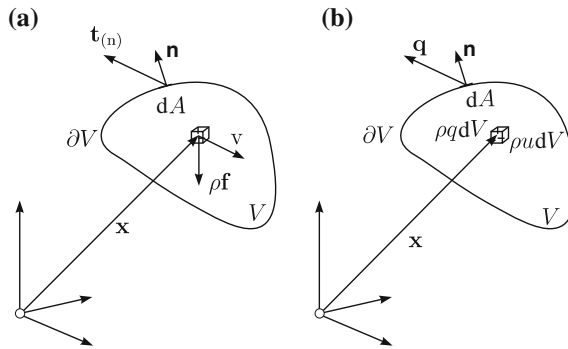


Fig. 17.36 Illustrating the derivation of the First Law. **a** Material volume V with boundary ∂V and volume element dV with indicated velocity \mathbf{v} and specific body force $\rho \mathbf{f}$ and surface element dA with vector of surface traction $\mathbf{t}_{(n)}$. **b** Same as in **a**, but now illustrating a mass element with specific internal energy $\rho u dV$ and specific radiation $\rho q dV$, and surface element dA with heat flux vector \mathbf{q} . The two panels separate the mechanical and thermodynamic quantities

$$T = \int_V \frac{\rho}{2} |\mathbf{v}|^2 dV, \quad (\text{kinetic energy}),$$

$$L_V = \int_V \rho \mathbf{f} \cdot \mathbf{v} dV, \quad (\text{power of working of the volume forces}), \quad (17.64)$$

$$L_{\partial V} = \int_{\partial V} \mathbf{v} \cdot \mathbf{t}_{(n)} dA, \quad (\text{power of working of the surface forces}).$$

$L_V + L_{\partial V}$ is the mechanical power brought by all forces acting on the body. On the basis of the calculations conducted for the above mass point example, see Eq. (17.60), one may now be tempted to set the time rate of change of the kinetic energy equal to this power of working. It is, however, exactly the recognition, which found its realization in the First Law of Thermodynamics, that this is not correct in general and may be correct only in a very simplified idealized case.

17.5.2 Definitions, Important for the First Law

There are two new quantities, which we must introduce to be able to properly formulate the First Law; one is the notion of **heat**, the other that of **internal energy**. In thermodynamics these notions are often introduced indirectly via other quantities already defined. Here, we wish to simply declare heat as a form of rate of energy, which complements the power of working of the external forces as a non-mechanical counterpart. Correspondingly, we declare the internal energy as a primarily thermal,

and if mechanical, then system-internal, deformation-induced energy form that complements the kinetic energy. More formally:

Definition 17.8

- The **internal energy** of a system is an extensive or additive quantity which, together with the kinetic energy forms the total energy of the system
- The **heat** of a system is non-mechanical energy per unit time that is supplied to the system from the outside.

The following remarks are important additions to this definition: First, as the kinetic energy, the internal energy is a *quantity of the system* inherent to the body that, together with the kinetic energy, defines the energetic state of the body. As such *the internal energy can comprise thermal, mechanical, electromagnetic and chemical ‘components’*, depending upon whether such interactions will arise. If a body deforms elastically, then the internal energy contains such a ‘component’. Second, heat is a **process quantity**, which is supplied to a body just as power of working is supplied from the outside. It is customary to choose the notations

- U for the internal energy of the system,
- Q for the heat supplied to the system.

The connection with the kinetic energy T and the power of working L is apparent; accordingly, one calls

- $T + U$ the *total energy* stored in the system,
- $L + Q$ the power of working plus the heat supplied to the system from the outside.

The following statement now forms the content of the First Law of Thermodynamics:

First Law of Thermodynamics, Mathematically Formulated

- *In a materially closed system the time rate of change of the sum of kinetic plus internal energies equals the sum of the mechanical power of the external forces plus the heat supplied to the system from the outside:*

$$\dot{T} + \dot{U} = L + Q. \quad (17.65)$$

This statement is a *postulate* and cannot be deduced from other principal laws of physics, but forms a fundamental law, just as mass balance and NEWTON’s law; it can only be tested for correctness by experimental verification. A disproof of it has never been found; so, the statement (17.65) is accepted as a general physical principle since the middle of the 19th century.

Special cases of the First Law can easily be formulated and have in parts well known forms:

- For a *materially closed system at rest* the kinetic energy T vanishes and (17.65) takes the form

$$\dot{U} = L + Q, \quad (17.66)$$

or after an integration by time from $t = t_1$ to $t = t_2$

$$U_2 - U_1 = \int_{t_1}^{t_2} (L + Q) dt = A_{12} + Q_{12}, \quad (17.67)$$

in which $U_1 = U(t_1)$, $U_2 = U(t_2)$ are the internal energies at the times t_1 and t_2 ; moreover, A_{12} and Q_{12} are the work performed by the external forces and the heat supplied to the body during the time interval $t_2 - t_1$, respectively.

- For an *adiabatic system at rest* both the kinetic energy and the heat supplied to the body vanish, $T = 0$, $Q = 0$, so here we have

$$\dot{U} = L \implies U_2 - U_1 = A_{12}, \quad (17.68)$$

where it is often customary to write A_{12}^{ad} instead of A_{12} , to emphasize that A_{12}^{ad} is the work done on the system under adiabatic conditions.

- In a purely mechanical, *rigid*, adiabatic system, as e.g. a mass point, see Fig. 17.33, we have $\dot{U} = 0$, $Q = 0$ and so

$$\dot{T} = L \implies T_2 - T_1 = A_{12}, \quad (17.69)$$

a statement that was already written down in Eq. (17.60)

- If the external forces are conservative, they can be derived from a potential Ψ . Since in such a case their work is independent of their trajectories, we have $L = -\dot{\Psi}$. One can in this case generally additively compose the power of working into $L = L_1 - \dot{\Psi}$, where L_1 is the power of the non-conservative forces and $-\dot{\Psi}$ that of the conservative forces. The First Law of Thermodynamics (17.65), thus can also be written as

$$\dot{E}_g = \dot{T} + \dot{U} + \dot{\Psi} = L_1 + Q, \quad (17.65a)$$

in which E_g is the sum of the kinetic, internal and potential energies (of the conservative forces).

All these statements concern materially closed systems, i.e., material bodies, which do not exchange mass with the environment. It is possible to formulate the First Law also for open systems—and this we shall occasionally do. In this case, however, kinetic and internal energies also enter through the system boundaries. Consequently, a relation that connects T and U with L and Q so logically and clearly and divides these quantities into system and process quantities, is no longer possible.

Let us, finally, present the First Law in a form as it finds applications in a modern field theory. In so doing we shall use the expressions for the kinetic energy of a material body V with boundary ∂V and power of workings of the volume and surface forces $L_V + L_{\partial V}$ as listed in (17.64). Since the internal energy is an additive (extensive) quantity, we may introduce the internal energy per unit mass,²⁵ u , and then may assign

²⁵The internal energy per unit mass is denoted here by u , which is also often used to identify the velocity component. We trust this notation will not cause confusion.

$\rho u dV$ as internal energy of a volume element dV , see Fig. 17.36b. Thus, the internal energy of the body V is given by

$$U = \int_V \rho u dV. \quad (17.70)$$

The heat that is supplied to the body from the outside also consists of two contributions (as does the power of working of the external forces), a volume and a surface contribution. If q is the heat supplied to the body from outside per unit mass, then its value per unit volume is $\rho q dV$, and the quantity

$$Q_V = \int_V \rho q dV \quad (17.71)$$

is that part of the heat that is supplied to the body via the volume by distant action. Radiation is of this kind and it is effectively used in a microwave oven. One calls q the **specific energy supply** or the **specific radiation** and Q_V the **heat supplied to the body by radiation**.

Finally, heat can also be supplied to a body V by heat flow through the boundary ∂V . If \mathbf{q} is the **heat flux vector** at a boundary point, then $-\mathbf{q} \cdot \mathbf{n} dA$ is the heat flow through the surface area element dA through ∂V into the body (the negative sign accounts for the fact that $\mathbf{q} \cdot \mathbf{n}$ is positive as an outflow). Consequently,

$$Q_{\partial V} = - \int_{\partial V} \mathbf{q} \cdot \mathbf{n} dA \quad (17.72)$$

is that part of the heat supplied to the body via the surface ∂V .

Collecting all these formulations: (17.64) and (17.70)–(17.72) we may write

$$\begin{aligned} T + U &= \int_V \rho \left(\frac{1}{2} |\mathbf{v}|^2 + u \right) dV, \\ L + Q &= (L_{\partial V} + Q_{\partial V}) + (L_V + Q_V) \\ &= \int_{\partial V} (\mathbf{v} \cdot \mathbf{t}_{(n)} - \mathbf{q} \cdot \mathbf{n}) dA + \int_V \rho (\mathbf{f} \cdot \mathbf{v} + q) dV, \end{aligned} \quad (17.73)$$

so that the First Law of Thermodynamics, (17.65), for a material body takes the form

$$\frac{d}{dt} \int_V \rho \left(\frac{1}{2} |\mathbf{v}|^2 + u \right) dV = \int_{\partial V} (\mathbf{v} \cdot \mathbf{t}_{(n)} - \mathbf{q} \cdot \mathbf{n}) dA + \int_V \rho (\mathbf{f} \cdot \mathbf{v} + q) dV, \quad (17.74)$$

in which $\mathbf{t}_{(n)}$ is the surface traction on the surface element with exterior unit normal vector \mathbf{n} , which is related to the CAUCHY stress tensor \mathbf{t} and the pressure and extra stress tensor \mathbf{t}^E (or the so-called frictional stress tensor \mathbf{t}^R) according to

$$\mathbf{t}_{(n)} = \mathbf{t}\mathbf{n} = (-p\mathbf{1} + \mathbf{t}^R)\mathbf{n}, \quad (17.75)$$

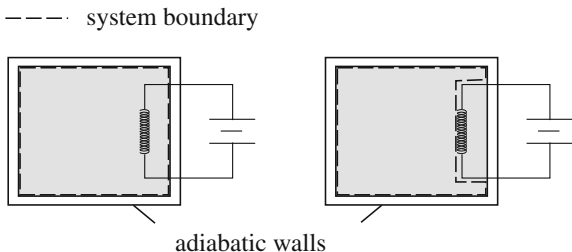
see Eq. (7.6). Equation (17.74) holds for any material body, also material parts of such bodies, so that it may also be applied to an infinitesimal body. Before doing this, a few remarks should be made that set the above deductions in the proper perspective.

- All above stated mathematical relations are different arrangements and interpretations of the First Law, (17.65), which is the truly essential statement in form of a non-provable postulate. The First Law is expressed in terms of the sum $Q + L$ of supplied heat and power of working of external origin. There are no indications to separate these two terms, which therefore must be treated as equals. In this sense *the First Law postulates the unrestricted possibility to transform different forms of energy into one another*. This is different with the sum of the kinetic and internal energies, $T + U$. It is quite clear here what kinetic energy is; consequently also the internal energy is well defined as the difference between total and kinetic energy.
- The equivalence between heat and power of working in exactly this sense will be further explained by the following example of an adiabatic system. Consider a container filled with a gas and materially closed by adiabatic walls. An electric circuit is so arranged that its resistance is in contact with the gas. **Figure 17.37** shows two possible delineations of the system (dashed). If a current flows through the circuit, then power of working is supplied to the system that can be calculated via the electrical power. With the system delineation in the right panel in Fig. 17.37 the system receives this rate of energy in the form of heat. The electrical power supplied to the resistance increases the system's internal energy; its temperature rises and due to the temperature differences the resistance supplies heat to the gas. It is seen that the form of energy supplied to a system, whether as heat or as power of working, depends on the choice of the system's boundaries.
- Finally, we mention that the interpretation of heat as dimensionally the same as power of working goes back to CONSTANTINE CARATHÉODORY. He showed that the entire theory can be based on concepts without the assumption of the existence of a physical quantity that deviates from the ordinary mechanical quantities, namely heat. Prior to this understanding, physicists were of the opinion that heat would consist of a substance to which a certain measurable amount could be assigned. For this reason one did not speak of heat but *amount of heat*, a denotation still occasionally in use today. This understanding of heat as an independent entity with its own physical dimension made it necessary to introduce the so-called heat equivalent, in order to relate to one another or to transform into one another mechanical and thermal energies.

The First Law of Thermodynamics can also be formulated for an *open system*. To this end we recall its form for a material volume V , (17.74). However, we assume now that the velocity field \mathbf{v} and the internal energy in V are continuously differentiable. Under such prerequisites one may define the specific total energy e by

$$e = \frac{1}{2}|\mathbf{v}|^2 + u, \quad (17.76)$$

Fig. 17.37 Explaining heat and power of working. Whether a quantity is interpreted as heat or power of working also depends on the definition of the boundaries of the system



and apply the REYNOLDS transport theorem

$$\frac{d}{dt} \int_V \rho e \, dV = \int_V \frac{\partial(\rho e)}{\partial t} \, dV + \int_{\partial V} \rho e (\mathbf{v} \cdot \mathbf{n}) \, dA, \tag{17.77}$$

(see footnote on p. 88 of Vol. 1). In the integral on the left-hand side it is important to regard V as a material volume that moves with the fluid; in the integrals on the right-hand side, this interpretation is no longer compelling, one may even regard V as a stationary volume, since the differentiation is performed in the integrand function. Physically, the surface integral in (17.77) can then be interpreted as the flux of e through the surface ∂V . Instead of (17.74) one obtains therefore

$$\int_V \frac{\partial(\rho e)}{\partial t} \, dV - \int_{\partial V} (\mathbf{v} \cdot \mathbf{t} - \mathbf{q} - \rho e \mathbf{v}) \cdot \mathbf{n} \, dA - \int_V \rho (\mathbf{f} \cdot \mathbf{v} + q) \, dV = 0, \tag{17.78}$$

in which (17.75)₁ was also used. One recognizes that in the derivation of the First Law the distinction between an open and a closed system is actually only a semantic one. If, in the surface integral of (17.77), we now also apply the divergence theorem

$$\int_{\partial V} (\mathbf{v} \cdot \mathbf{t} - \mathbf{q} - \rho e \mathbf{v}) \cdot \mathbf{n} \, dA = \int_V \operatorname{div} (\mathbf{v} \cdot \mathbf{t} - \mathbf{q} - \rho e \mathbf{v}) \, dV, \tag{17.79}$$

one can write (17.78) alternatively also as

$$\int_V \left(\frac{\partial(\rho e)}{\partial t} - \operatorname{div} (\mathbf{v} \cdot \mathbf{t} - \mathbf{q} - \rho e \mathbf{v}) - \rho (\mathbf{f} \cdot \mathbf{v} + q) \right) \, dV. \tag{17.80}$$

Since this equation holds for all volumes V , the integrand function in parentheses must vanish by itself, so that one obtains the local statement

$$\frac{\partial(\rho e)}{\partial t} + \operatorname{div} (\rho e \mathbf{v} - \mathbf{v} \cdot \mathbf{t} + \mathbf{q}) - \rho (\mathbf{f} \cdot \mathbf{v} + q) = 0. \tag{17.81}$$

Because of its complexity, this equation does not offer an easy physical interpretation. By mathematical transformations, it may however, be simplified considerably. With (17.76) one obtains for the individual terms

$$\frac{\partial(\rho e)}{\partial t} = \frac{\partial \rho}{\partial t} e + \rho \mathbf{v} \cdot \frac{\partial \mathbf{v}}{\partial t} + \rho \frac{\partial u}{\partial t} \quad (17.82)$$

and

$$\begin{aligned} \operatorname{div}(\rho e \mathbf{v} - \mathbf{v} \cdot \mathbf{t} + \mathbf{q}) &= (\operatorname{div} \rho \mathbf{v}) e + \rho \mathbf{v} \cdot (\mathbf{L} \mathbf{v}) + \rho (\operatorname{grad} u) \cdot \mathbf{v} \\ &\quad - \mathbf{v} \cdot \operatorname{div} \mathbf{t} - \operatorname{tr}(\mathbf{L}^T \cdot \mathbf{t}) + \operatorname{div} \mathbf{q} \end{aligned} \quad (17.83)$$

with $\mathbf{L} = \operatorname{grad} \mathbf{v}$. With these, Eq. (17.81) can be put into the form

$$\begin{aligned} &\underbrace{\left(\frac{\partial \rho}{\partial t} + \operatorname{div} \rho \mathbf{v} \right)}_{=0} e + \mathbf{v} \cdot \underbrace{\left(\rho \frac{d\mathbf{v}}{dt} - \operatorname{div} \mathbf{t} - \rho \mathbf{f} \right)}_{=0} \\ &+ \left(\rho \frac{du}{dt} + \operatorname{div} \mathbf{q} - \operatorname{tr}(\mathbf{L}^T \mathbf{t}) - \rho q \right) = 0. \end{aligned} \quad (17.84)$$

Because of mass conservation and balance of linear momentum (see equations (3.44) and (7.5) in Vol. 1), the first two brackets in (17.84) vanish. If one further uses the representation $\mathbf{t} = -p\mathbf{1} + \mathbf{t}^R$, then (17.84) simplifies and becomes

$$\begin{aligned} \rho \frac{du}{dt} &= \underbrace{-p \operatorname{div} \mathbf{v}}_{\text{power of working of pressure}} + \underbrace{\operatorname{tr}(\mathbf{L}^T \mathbf{t}^R)}_{\text{power of working of dissipation } \Phi} \\ &\quad + \underbrace{-\operatorname{div} \mathbf{q}}_{\text{heat conduction}} + \underbrace{\rho q}_{\text{radiation}}. \end{aligned} \quad (17.85)$$

The time rate of change of the internal energy is thus balanced by four terms, (i) the power of working of the pressure, which is given as the product of the pressure with the rate of volume change, $\operatorname{div} \mathbf{v}$, (ii) the power of working of the viscous stresses which vanish for an ideal fluid, since then $\mathbf{t}^R = \mathbf{0}$, (iii) the conductive heat, $-\operatorname{div} \mathbf{q}$ and (iv) the specific radiation, ρq . Incidentally, one can easily show with the use of the balance equation of mass that (17.85) can also be written as

$$\rho \left(\frac{du}{dt} - \frac{p}{\rho^2} \frac{d\rho}{dt} \right) = \Phi - \operatorname{div} \mathbf{q} + \rho q, \quad (17.86)$$

a form of the First Law that is particularly useful when exploiting the Second Law of Thermodynamics.²⁶ Moreover, for a **linearly viscous fluid** the dissipation function can also be put into a different form; indeed, using (see (7.28) in Vol. 1)

²⁶With the enthalpy

$$\begin{aligned} \mathbf{t}^R &= \zeta(\operatorname{div} \mathbf{v})\mathbf{1} + 2\eta\mathbf{E}, \\ \mathbf{E} &= \mathbf{D} - \frac{1}{3}(\operatorname{div} \mathbf{v})\mathbf{1}, \quad \mathbf{D} = \frac{1}{2}(\mathbf{L} + \mathbf{L}^T), \end{aligned} \quad (17.87)$$

we successively obtain

$$\begin{aligned} \Phi &= \operatorname{tr}(\mathbf{L}^T \mathbf{t}^R) = \operatorname{tr}(\mathbf{D} \mathbf{t}^R) \\ &= \operatorname{tr}\left[\left(\mathbf{E} + \frac{1}{3}(\operatorname{div} \mathbf{v})\mathbf{1}\right)(\zeta(\operatorname{div} \mathbf{v})\mathbf{1} + 2\eta\mathbf{E})\right] \\ &= \operatorname{tr}\left[\frac{\zeta}{3}(\operatorname{div} \mathbf{v})^2 \mathbf{1} + 2\eta\mathbf{E}^2 + \zeta(\operatorname{div} \mathbf{v})\mathbf{E} + \frac{1}{3}(\operatorname{div} \mathbf{v})2\eta\mathbf{E}\right] \\ &= \zeta(\operatorname{div} \mathbf{v})^2 + 2\eta \operatorname{tr} \mathbf{E}^2 = \Phi_V + \Phi_G, \end{aligned} \quad (17.88)$$

which, in Cartesian coordinates can also be written as

$$\begin{aligned} \Phi_V &= \zeta \left\{ \left(\frac{\partial u}{\partial x} + \frac{\partial v}{\partial y} + \frac{\partial w}{\partial z} \right)^2 \right\} \\ \Phi_G &= \eta \left\{ \left(\frac{\partial u}{\partial y} + \frac{\partial v}{\partial x} \right)^2 + \left(\frac{\partial v}{\partial z} + \frac{\partial w}{\partial y} \right)^2 + \left(\frac{\partial w}{\partial x} + \frac{\partial u}{\partial z} \right)^2 \right\}. \end{aligned} \quad (17.89)$$

The quantities Φ_V and Φ_G are called dissipation function due to volume changes and dissipation function due to changes of shape. In purely dilating or compacting deformations $\Phi_V \neq 0$ and $\Phi_G = 0$, but in isochoric deformations $\Phi_V = 0$ and $\Phi_G \neq 0$. Obviously also, the first vanishes for a density preserving fluid or when the STOKES assumption ($\zeta = 0$) is made, the second differs from zero for all deformations involving shearing.

Equation (17.85) or (17.86) represent local balances for the internal energy, how it evolves in a body point as a function of time. In order that it can be computed at all, the pressure, the velocity field, the viscosities ζ and η , the heat flux vector and the energy supply must be known. In the form, written down above, the equations hold for **inhomogeneous** systems, of which the thermodynamic states change from position to position. (This alone follows from the fact that differentiations with respect to the spatial coordinates arise.)

A material body can be thought to be composed of infinitesimal elements, and each of these elements can be interpreted as a subsystem on which forces perform work and to which heat is supplied. The individual contributions are shown in equation

(Footnote 26 continued)

$$h =: u + \frac{p}{\rho}$$

this may also be written as

$$\rho \frac{dh}{dt} - \frac{dp}{dt} = \Phi - \operatorname{div} \mathbf{q} + \rho q,$$

which is equivalent to (17.86).

(17.85). If the heat flux vector \mathbf{q} and the specific radiation q vanish in all body points the heat supplied to the body is zero. In this case one calls the material body **locally adiabatic**, since none of its elements is receiving any heat. If a heat exchange between the individual elements is possible, but the supply of heat across the boundary ∂V is prevented, the material body is under **global adiabatic** conditions. Ordinarily, however, the particularizations ‘local’ and ‘global’ are not mentioned, as one tacitly assumes that it is evident from the context which situation prevails.

17.5.3 Caloric Equations of State for Fluids and Gases

We have already met the *thermal equation of state* $p = p(\rho, T) = p(v, T)$, which establishes an experimental relation between p, ρ, T or $p, v = 1/\rho, T$. The analysis in the last subsection has also shown that in a locally adiabatic system free of dissipation ($\Phi = 0$)²⁷, the energy Eq. (17.86) reduces to the equation

$$\rho \left(\frac{du}{dt} - \frac{p}{\rho^2} \frac{d\rho}{dt} \right) = 0. \quad (17.90)$$

This relation now suggests that the internal energy u may be described by a functional relation of the form

$$u = u(T, v) \quad \text{or} \quad u = u(T, \rho). \quad (17.91)$$

This equation, which is also based on experimental facts and, thus, has different forms for different materials represents a **caloric equation of state** of a particular material.

That a relation of the form (17.91) (or of more general form) is necessary, can be seen as follows. For a locally adiabatic, dissipation-free system the balance laws of mass, momentum and energy read

$$\begin{aligned} \frac{d\rho}{dt} + \rho \operatorname{div} \mathbf{v} &= 0, & (\text{see (3.44)}) \\ \rho \frac{d\mathbf{v}}{dt} &= -\operatorname{grad} p + \rho \mathbf{f}, & (\text{see (7.5)}) \\ \rho \frac{du}{dt} &= -p \operatorname{div} \mathbf{v}. & (\text{see (17.90)}) \end{aligned} \quad (17.92)$$

Together, they comprise five equations for the seven unknowns $\rho, \mathbf{v}, p, T, u$. If to these equations the thermal and the caloric equations of state are added, and with their use two unknowns are thought to be eliminated, then the number of unknowns is reduced to five, and one obtains from (17.92) at least formally an integrable system of equations. However, that in a non-locally adiabatic and dissipative system relation (17.91) is *the* form of the caloric equation, that apart from T and $v = 1/\rho$,

²⁷In this situation the stress tensor reduces to a pressure tensor, $\mathbf{t} = -p\mathbf{1}$.

no other independent variables can arise in (17.91), is not obvious at this stage of the developments and will be proved to be a consequence of the Second Law of Thermodynamics, which will allow the derivation of a relation between the thermal and caloric equations of state. According to this so-called GIBBS relation, it is possible with the knowledge of the thermal equation of state to calculate ‘some aspects of the caloric equation of state’, without directly having to measure them.²⁸ The total differential of the internal energy may be calculated with the aid of the chain rule of differentiation, viz.,

$$du = \left(\frac{\partial u}{\partial T} \right)_v dT + \left(\frac{\partial u}{\partial v} \right)_T dv = c_v dT + \left(\frac{\partial u}{\partial v} \right)_T dv. \quad (17.93)$$

In this formula the subscripts v and T attached to the partial derivative terms indicate that the subscripted variable is held constant in the process of differentiation. This notation is customary in thermodynamics, but it is not necessary if one differentiates the function from its values, which one might assume.

The quantity

$$c_v = \left(\frac{\partial u}{\partial T} \right)_v \quad (17.94)$$

is called **specific heat at constant volume** or **heat capacity at constant volume**. If the specific volume does not change in a thermodynamic process, i.e., if

$$\left(\frac{\partial u}{\partial v} \right)_T = 0, \quad (17.95)$$

then the specific internal energy does not depend on the specific volume, and $u = u(T)$.

In ideal gases the specific internal energy depends only upon the temperature. In this case one can set

$$c_v = \frac{du}{dT} = c_v^0(T), \quad (17.96)$$

and obtains after integration

$$u(T) = \int_{T_0}^T c_v^0(T') dT' + u_0, \quad (17.97)$$

where u_0 is the value of the internal energy at the temperature T_0 . For some gases the specific heat (at constant volume), c_v can be assumed to be constant in a certain temperature range; in such cases one obtains instead of (17.97)

²⁸Tables of the specific internal energy as a function of the absolute temperature T and parameterized for various values of the density ρ or the specific volume $v = 1/\rho$ for real fluids are given in books on technical thermodynamics [1].

$$u(T) = c_v^0(T - T_0) + u_0. \quad (17.98)$$

For air $c_v^0 = 0.717 \text{ kJ kg}^{-1} \text{ K}^{-1}$, valid for $-273^\circ \text{C} \leq T \leq 100^\circ \text{C}$ with deviations from measured values less than 1 %.

The fact that the internal energy in ideal gases only depends upon the temperature has been demonstrated for dilute gases as early as 1807 by JOSEPH LOUIS GAY-LUSSAC (1778–1850)²⁹ with experiments on overflow; the results were later (1845) corroborated by JAMES PRESCOTT JOULE (1818–1889). In MAXWELL's kinetic theory the temperature, as well as the internal energy, are defined by the sum of the kinetic fluctuation energies of the molecules, and the potential of the intermolecular forces is ignored. In other words, T and u are proportional to each other; obviously then, in the kinetic theory the internal energy is only a function of the temperature by definition.

In the classical kinetic theory of gases the internal energy is defined as the mean value of the kinetic energy of the fluctuating motion of a large number of molecules that is generated by the molecule encounters. Based on this, one can show that the internal energy is given by

$$u(T) = \frac{1}{2}RT(f_{\text{trans}} + f_{\text{rot}} + 2f_{\text{osc}}),$$

where R is the gas constant of the gas under study and $f_{\text{trans}}, f_{\text{rot}}, f_{\text{osc}}$ are the degrees of freedom of the translational, rotational and oscillating motion of the molecules. The above rule, according to which the internal energy is the sum of the internal energies due to translational, rotational and oscillating motion, is called the **law of equipartition**. With the above formula, one obtains in view of (17.94)

$$c_v = \frac{1}{2}R(f_{\text{trans}} + f_{\text{rot}} + 2f_{\text{osc}}).$$

On the one hand, this formula shows that, according to the classical kinetic theory of gases, the specific heat at constant volume cannot depend on the temperature, and on the other hand, that its value depends on the degree of freedom of the molecules, see **Fig. 17.39a**. For a monatomic gas, of which the molecules possess three translational degrees of freedom, one would expect $c_v = \frac{3}{2}R$. A diatomic gas with a rigid dumbbell structure of the molecules has three translational and two rotational degrees of freedom (the rotational degree of freedom about the dumbbell axis does not count, since the moment of inertia about this axis is vanishingly small); we, thus, obtain here $c_v = \frac{5}{2}R$. If the connection of the molecules is, however, elastic, an additional degree of freedom for the extensional oscillation of the dumbbell-axis must be added, so that $c_v = \frac{7}{2}R$.

²⁹For a brief biography of JOSEPH LOUIS GAY-LUSSAC, see **Fig. 17.38**.



Fig. 17.38 JOSEPH LOUIS GAY-LUSSAC (6. Dec. 1778–9. May 1850) GAY-LUSSAC and BIOT ascend in a hot air balloon (left and right), 1804. Illustrations from the late 19th century

JOSEPH LOUIS GAY-LUSSAC was a French chemist and physicist. He is known mostly for two laws related to gases, and for his work on alcohol-water mixtures, which led to the degrees Gay-Lussac used to measure alcoholic beverages in many countries.

He received his early education from catholic monks and began his education in Paris, finally entering the *École Polytechnique* in 1798, but transferred three years later to the *École des Ponts et Chaussées*. In 1802, he was receiving the position as demonstrator to A.F. FOURCROY at the *École Polytechnique*, where in (1809) he became professor of chemistry. From 1808 to 1832, he was professor of physics at the Sorbonne, a post, which he only resigned for the chair of chemistry at the *Jardin des Plantes*. In 1821, he was elected a foreign member of the Royal Swedish Academy of Sciences. In 1831 he was elected to represent the district Haute-Vienne in the chamber of deputies, and in 1839 he entered the chamber of peers.

In 1802 GAY-LUSSAC first formulated the law, Gay-Lussac's Law, stating that if the mass and volume of a gas are held constant then the gas pressure increases linearly as the temperature rises. The law is sometimes written as $p = kT$, where k is a constant dependent on the mass and volume of the gas and T is the temperature on an absolute scale (in terms of the ideal gas law, $k = n \cdot R/V$).

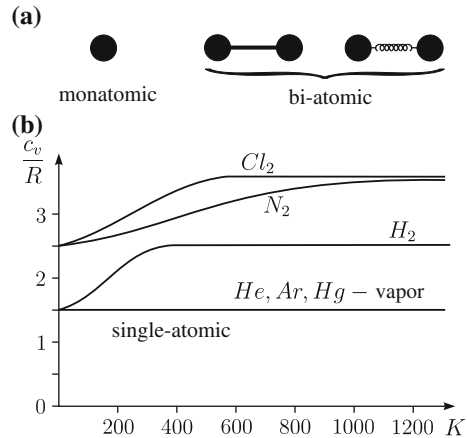
In 1804 he and JEAN-BAPTISTE BIOT made a hot-air balloon ascent to a height of 7,016 m (23,018 ft) in an early investigation of the Earth's atmosphere. He wanted to collect samples of the air at different heights to record differences in temperature and moisture. This caused a surge of popularity as evidenced by the above illustrations.

In 1808 he was the co-discoverer of boron and in 1811 he recognized iodine as a new element, described its properties, and suggested the name *iode*.

The text is based on www.wikipedia.org

Measurements, done with real gases, show the qualitative behavior of Fig. 17.39. The specific heat for the monatomic gases *He*, *Ar*, *Hg*-vapor is indeed given by $c_v = \frac{3}{2}R$; for bi-atomic and multi-atomic gases it is, however, temperature dependent and only fulfills the equipartition law in a certain range of the temperature. The hydrogen gas *H*₂ behaves at low temperature as a monatomic gas with $c_v = \frac{3}{2}R$,

Fig. 17.39 Specific heat at constant volume, c_v . The specific heat of a multi-atomic gas can be estimated with the equipartition law. **a** Model of a monatomic and a bi-atomic gas with and without frozen oscillating degree of freedom. **b** Specific heats c_v/R of various real gases as functions of the KELVIN temperature



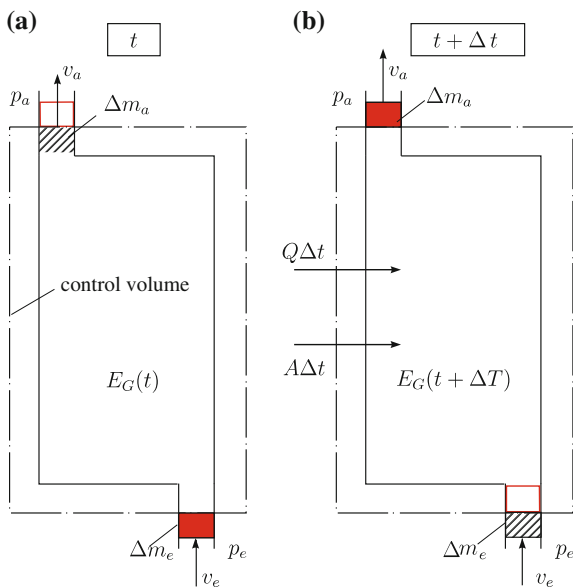
whilst at high temperature as a bi-atomic gas with $c_v = \frac{5}{2}R$, which can only be understood, if one freezes either the oscillating or the rotational degrees of freedom. The specific heats of Cl_2 and N_2 approach at high temperatures the value $c_v = \frac{7}{2}R$ of the equipartition law, and tend to $c_v = \frac{5}{2}R$ for low temperatures; if measurements at yet even lower temperatures would be possible, then $c_v = \frac{3}{2}R$ would be reached.

Various bi-atomic gases behave qualitatively in exactly this way. At low temperature the internal energy corresponds to that of a monatomic gas, in which only the three translational degrees of freedom of the molecule contribute to the specific heat. The rotational and oscillation degrees of freedom are quasi-frozen. With increasing temperature these degrees of freedom are released, first the rotational and afterwards the oscillational degrees of freedom. This order is revealed by measurements of the specific heats of multi-atomic gases as functions of the temperature. The ‘freezing’ and re-‘thawing’ of certain degrees of freedom cannot be explained with the classical kinetic theory of gases; its explanation requires methods of quantum mechanics.

17.5.4 Simple Applications of the First Law

(a) Energy balance for an open system. Consider an open system that is bounded by a fixed spatial control volume; see **Fig. 17.40**. We assume momentarily that fluid is entering this control volume only at one position; similarly we suppose that fluid leaves the volume only through a small cross section. The inflow and outflow cross sections are assumed to be so small that of all physical quantities that mean values taken over the cross section characterize the fluid properties sufficiently accurately. For the balance law of energy in the form

Fig. 17.40 Energy balance in an open system. Material control volume, enclosing the open system **a** at time t and **b** at time $t + \Delta t$



$$\dot{E}_G = \dot{T} + \dot{U} + \dot{\Psi} = L_1 + Q$$

the open system is replaced by the materially closed but moving system of Fig. 17.40. At time t this new system has the mass contained in the (original) control volume, plus a small mass Δm_e of the fluid that enters at the temporal increment Δt the control volume. At time $t + \Delta t$ the materially closed system, however, contains the fluid mass in the control volume at that time plus the small mass Δm_a that left the control volume during the time increment Δt . The two elements of fluid mass Δm_e and Δm_a are in general not the same; this is so only under steady state conditions. If we integrate the equation above over the incremental time Δt , the above equation becomes

$$E_G(t + \Delta t) - E_G(t) = Q_{\Delta t} + A_{\Delta t}, \tag{17.99}$$

in which $E_G = T + U + \Psi$ is the sum of the kinetic, internal and potential energies of the materially closed system, and $Q_{\Delta t}$ and $A_{\Delta t}$ are the heat and the work of the non-conservative forces supplied to the system in the time interval Δt . If we define by $E(t)$ the sum of the kinetic, internal and potential energies, which are contained in the control volume, then we have for the new materially closed system

$$E_G(t + \Delta t) = E(t + \Delta t) + \Delta m_a \left(u_a + \frac{v_a^2}{2} + \Psi_a \right),$$

$$E_G(t) = E(t) + \Delta m_e \left(u_e + \frac{v_e^2}{2} + \Psi_e \right). \tag{17.100}$$

Alternatively, the heat supplied via the materially closed system to the control volume during the time interval is given by

$$Q_{\Delta t} = \int_t^{t+\Delta t} Q(\tau) d\tau \approx Q(t)\Delta t. \quad (17.101)$$

The work $A_{\Delta t}$ performed during the time Δt consists of two contributions, first the work supplied by a machine—pump—to the system

$$A_{\Delta t}^M = \int_t^{t+\Delta t} L(\tau) d\tau \approx L_1(t)\Delta t, \quad (17.102)$$

and, second, the work done by the pressure at the entrance cross section (positive, the fluid is displaced in the same direction as the pressure is acting) and at the exit cross section (negative)

$$\begin{aligned} A_{\Delta t}^p &= L_2(t)\Delta t = p_e A_e v_e \Delta t - p_a A_a v_a \Delta t \\ &= p_e \Delta V_e - p_a \Delta V_a = p_e v_e \Delta m_e - p_a v_a \Delta m_a, \end{aligned} \quad (17.103)$$

in which $A_e, A_a, \Delta V_e, \Delta V_a, v_e, v_a$ are the cross sectional areas, volume increments and specific volumes of the fluid elements at the entrance and exit, respectively. Moreover, $L(t) = L_1(t) + L_2(t)$.

If we substitute these separately derived quantities into the energy balance (17.99), we obtain

$$\begin{aligned} \int_t^{t+\Delta t} (Q(\tau) + L(\tau)) d\tau &= E(t + \Delta t) - E(t) + \Delta m_a \left(u_a + \frac{v_a^2}{2} + \Psi_a \right) \\ &\quad - \Delta m_e \left(u_e + \frac{v_e^2}{2} + \Psi_e \right). \end{aligned} \quad (17.104)$$

If, finally, this equation is divided by Δt and the limit $\Delta t \rightarrow 0$ is performed then, on account of

$$\begin{aligned} \lim_{\Delta t \rightarrow 0} \frac{1}{\Delta t} \int_t^{t+\Delta t} (Q(\tau) + L(\tau)) d\tau &= Q(t) + L(t), \\ \lim_{\Delta t \rightarrow 0} \frac{E(t + \Delta t) - E(t)}{\Delta t} &= \frac{\partial E}{\partial t}, \\ \lim_{\Delta t \rightarrow 0} \frac{\Delta m_k}{\Delta t} &= \frac{dm_k}{dt} = \dot{m}_k \quad (k = a, e), \end{aligned} \quad (17.105)$$

we obtain the equation

$$Q(t) + L_1(t) = \frac{\partial E}{\partial t} + \dot{m}_a \left(u_a + p_a v_a + \frac{v_a^2}{2} + g z_a \right) - \dot{m}_e \left(u_e + p_e v_e + \frac{v_e^2}{2} + g z_e \right), \quad (17.106)$$

in which we have set $\Psi = gz$, which is the gravity potential, the likely most important case of a conservative force system. It is customary to slightly transform equation (17.106). To this end we need

Definition 17.9

- The **specific enthalpy** h is defined as the state variable

$$h = u + pv. \quad (17.107)$$

The internal energy $u = u(T, v)$ as a caloric equation of state is a function of the temperature and the specific volume. With the help of the thermal equation of state $v = v(T, p)$ it may be expressed as a function of the temperature and pressure, so, h too, may be thought of as a function $h = h(T, p)$. In principle h may also be viewed as a function of T and v , however, the Second Law will demonstrate that to regard h as a function of T and p is more natural. The enthalpy is therefore also given as a **caloric equation of state**: $h = h(T, p)$.

With (17.107) equation (17.106) can be written as

$$\frac{\partial E}{\partial t} = Q(t) + L_1(t) - \dot{m}_a \left(h_a + \frac{v_a^2}{2} + g z_a \right) + \dot{m}_e \left(h_e + \frac{v_e^2}{2} + g z_e \right). \quad (17.108)$$

Accordingly, the local time rate of change of the sum of the internal, kinetic plus potential energies in an open control volume is balanced by the heat supplied to and the work of the non-conservative forces done on the system plus the inflow (positive) and the outflow (negative) of the energy fluxes across the boundaries.

The following are two special cases of the balance (17.108):

- **Materially closed systems:** for these we have $\dot{m}_a = \dot{m}_e = 0$ and therefore

$$\frac{\partial E}{\partial t} = Q + L_1, \quad (17.109)$$

an equation, which formally agrees with (17.65a).

- **Steady state processes:** Here $\partial E / \partial t = 0$ and $\dot{m}_a = \dot{m}_e = \dot{m}$, implying that

$$Q + L_1 = \dot{m} \left[(h_a - h_e) + \frac{1}{2}(v_a^2 - v_e^2) + g(z_a - z_e) \right]. \quad (17.110)$$

The sum of the heat and mechanical power of working supplied to the system equals the sum of differences of the enthalpies, kinetic energies and potentials multiplied with the mass flow \dot{m} flowing through the open system per unit time.

Often a control volume receives heat by the mass flow rate \dot{m} , so that one may set $Q = q_{12}\dot{m}$; similarly, often L_1 is proportional to \dot{m} , namely when e.g. L_1 is a technical power, $L_1 = w_{12}^t\dot{m}$. In this case one may write (17.110) as

$$q_{12} + w_{12}^t = (h_2 - h_1) + \frac{1}{2}(v_2^2 - v_1^2) + g(z_2 - z_1). \quad (17.111)$$

Here, the indices e and a have been replaced by the numbers 1 and 2, which in applications is often advantageous, since fluids often flow consecutively through a set of control volumes which need to be adequately identified. The variable w_{12}^t is called the **technical work** done by the fluid; it describes the energy per unit mass of the fluid that is supplied to, or consumed by, the system.

(b) Enthalpy. In Definition 17.9 the specific enthalpy

$$h = u + pv \quad (17.112)$$

was defined as a function of the state variables T and p , $h = h(T, p)$ and called a caloric equation of state. Its differential, dh , can, thus be written as

$$dh = \left(\frac{\partial h}{\partial T}\right)_p dT + \left(\frac{\partial h}{\partial p}\right)_T dp = c_p dT + \left(\frac{\partial h}{\partial p}\right)_T dp. \quad (17.113)$$

The quantity

$$c_p = \left(\frac{\partial h}{\partial T}\right)_p \quad (17.114)$$

is called the **specific heat at constant pressure** or the **specific isobaric heat capacity**. With its help, the specific enthalpy change *at constant pressure* between the temperatures T_1 and T_2 can be computed as

$$h(T_2, p) - h(T_1, p) = \int_{T_1}^{T_2} c_p(T', p) dT' \approx c_p^0(p)(T_2 - T_1), \quad (17.115)$$

where in the expression to the far right it was assumed that in the temperature interval $T_1 \leq T \leq T_2$ the specific heat can be replaced by the value c_p^0 , which only depends on p and, may often be assumed to be constant.

Formula (17.111) now suggests how the specific enthalpy of a simple system could be experimentally determined. To this end we consider quasi-static (thus theoretically infinitely slow) processes for which the kinetic energy vanishes. If neither the center of gravity of the system is moved, whence no mass is lifted or lowered, the potential energy difference will equally vanish. If, finally, the process between the two states 1 and 2 is performed such that no technical work is being performed, w_{12}^t will vanish and (17.111) will reduce to the statement $q_{12} = h_2 - h_1$. If the change of the states of the system from state 1 to state 2 is performed with pure temperature changes at

constant pressure, then this yields, finally,

$$(q_{12})_p = h(T_2, p) - h(T_1, p) = \int_{T_1}^{T_2} c_p(T', p) dT', \quad (17.116)$$

or

$$\frac{\partial (q_{12})_p}{\partial T} = c_p(T, p). \quad (17.117)$$

This result says: The specific heat at constant pressure can be measured by exposing a system that is held at constant pressure to an environment with homogeneous temperature and changing the temperature of the heat bath quasi-statically. If one measures for such temperature changes, the heat supplied to the system as a function of the temperature, then by differentiation of this experimentally determined function with respect to the temperature, c_p is obtained and, consequently also $h(T, p)$ at constant pressure.

The *specific enthalpy* of a *calorically ideal gas*, for which

$$pv = RT \quad \text{and} \quad u = u(T),$$

does not depend on the pressure; indeed

$$h = u(T) + pv = u(T) + RT = h(T). \quad (17.118)$$

For an ideal gas the specific internal energy and the enthalpy are only functions of the temperature. Moreover, because of (17.118)

$$c_p = \frac{\partial h}{\partial T} = \frac{\partial u}{\partial T} + R = c_v + R,$$

or

$$R = c_p(T) - c_v(T). \quad (17.119)$$

Consequently, even though the specific heats themselves can depend upon the temperature, their difference equals the gas constant R of the ideal gas considered which is independent of the temperature.

(c) Two applications

Example 1 Hydraulic power plant

As a simple but instructive application of the first law for steady processes, let us look at the model of a water plant as shown in **Fig. 17.41**. The boundaries of the control volume at the upstream and downstream sides are so chosen that in these sections the fluid velocities are negligibly small. Moreover, we shall assume steady and adiabatic conditions, so that the balance of energy can be taken as stated in (17.111), or

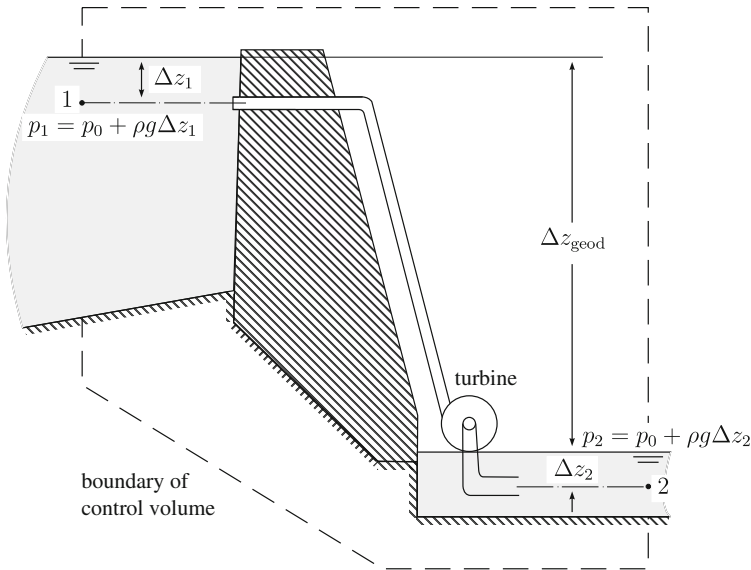


Fig. 17.41 Sketch of a hydraulic power plant. *Application of the First Law for the calculation of the temperature increase of the water between the inflow cross section and return cross section to the river*

$$\begin{aligned}
 w_{12}^t &= (h_2 - h_1) + g(z_2 - z_1) \\
 &= u_2 - u_1 + \frac{p_2}{\rho} - \frac{p_1}{\rho} + g(z_2 - z_1) \\
 &= u_2 - u_1 + g[(z_2 + \Delta z_2) - (z_1 + \Delta z_1)] \\
 &= u_2 - u_1 - g\Delta z_{\text{geod}},
 \end{aligned} \tag{17.120}$$

in which $p_1 = p_2$ was assumed. The power of working provided by the turbine is, thus, essentially given by the loss of potential energy of the water in the gravity field of the Earth. The internal energy is not used; all the more, because of the frictional losses we have $u_2 > u_1$. These frictional losses give rise to an increase of the temperature of the water, which can be estimated as follows: If one denotes by η the degree of efficiency of the plant, this degree is given by

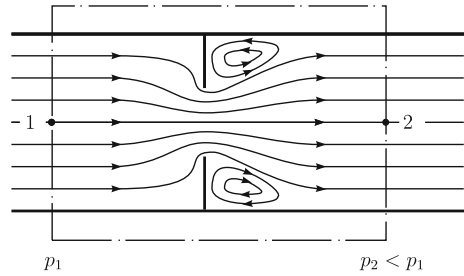
$$\eta = \left| \frac{w_{12}^t}{(w_{12}^t)_{\text{ideal}}} \right| = 1 - \frac{u_2 - u_1}{g\Delta z_{\text{geod}}}. \tag{17.121}$$

If we also set

$$u_2 - u_1 = c_v(T_2 - T_1), \tag{17.122}$$

one may compute from these two relations the temperature rise

Fig. 17.42 Throttle. Cross sectional contraction in a pipe or channel for the explanation of the functioning of an adiabatic throttle



$$T_2 - T_1 = \frac{(1 - \eta)g\Delta z_{\text{geod}}}{c_v}. \quad (17.123)$$

Water power plants have typical hydraulic degrees of efficiency of $\eta = 0.9$, and for water $c_v = 4.19 \text{ kJ kg}^{-1}\text{K}^{-1}$ for a geodetic height of $\Delta z_{\text{geod}} = 100 \text{ m}$ this yields

$$T_2 - T_1 = \frac{0.1 \times 100 \times 9.81}{4.19 \times 10^3} \text{K} = 0.023 \text{K}.$$

By measuring the temperature difference one may, alternatively, estimate the degree of efficiency of the plant.

Example 2 Adiabatic throttle

Consider the flow through the channel section of **Fig. 17.42**. Such a sudden cross sectional narrowing and immediate following widening is called a throttle. Practically, it is often employed at positions of the traps of a valve in pipe systems. By the cross sectional narrowing the fluid is locally accelerated and the pressure is correspondingly lowered. If the cross sections 1 and 2 are positioned sufficiently behind and ahead of the cross-section narrowing and if the channel or pipe is horizontally oriented, the energy equation reduces, because $q_{12} = w_{12}^t = 0$ and $z_1 = z_2$, to

$$h_2 - h_1 = -\frac{1}{2}(v_2^2 - v_1^2), \quad (17.124)$$

or, if one ignores the change of kinetic energy

$$h_1 = h_2. \quad (17.125)$$

The enthalpies ahead and behind the position of the throttle are the same. If p_1 , T_1 and p_2 are known, this result allows determination of the temperature T_2 in cross section 2.

If the gas flowing through the throttle device is an ideal gas, then because of $h = h(T)$, we have $T_1 = T_2$. Thus, even though the pressure drops, $p_2 < p_1$, no temperature change arises. In real gases the enthalpy depends on both, the temperature and the pressure, and from this it follows that in an adiabatic throttle one encounters indeed a temperature change; this fact is called the **Joule-Thomson effect**. Its

measuring, i.e., the measuring of a temperature change through an adiabatic throttle can be used to experimentally determine the pressure dependence of the enthalpy. If, alternatively, the caloric equation $h = h(T, p)$ is known for a real gas, one can calculate the temperature decrease in the passage of an adiabatic throttle. For air at $T_1 = 300 \text{ K}$, $p_1 = 10^6 \text{ Pa}$, $p_2 = 0.7 \times 10^6 \text{ Pa}$ one obtains $T_2 = 299.35 \text{ K}$, thus a temperature decrease of only 0.65 K .

To clear, whether the change of the kinetic energy can indeed be ignored we complement (17.124) with the steady state mass balance equation

$$\rho_1 v_1 A_1 = \rho_2 v_2 A_2 \rightarrow v_2 = \frac{\rho_1}{\rho_2} v_1 \quad (17.126)$$

(with $A_1 = A_2$). If one takes an ideal gas for which

$$h_2 - h_1 = c_p(T_2 - T_1), \quad \frac{p}{\rho} = RT \quad (17.127)$$

holds, then (17.124), (17.126) and (17.127) can be combined to yield

$$T_2 = T_1 - \frac{v_1^2}{2c_p} \left\{ \left(\frac{T_2 p_1}{T_1 p_2} \right)^2 - 1 \right\}, \quad (17.128)$$

in which the second term represents the influence of the kinetic energy. For air we have

$$\begin{aligned} c_v &= 0.717 \times 10^3 \text{ kJ kg}^{-1} \text{ K}^{-1}, \\ R &= 0.287 \times 10^3 \text{ kJ kg}^{-1} \text{ K}^{-1}, \\ c_p &= 1.004 \times 10^3 \text{ kJ kg}^{-1} \text{ K}^{-1}, \end{aligned} \quad (17.129)$$

so that the above example yields with $v_1 = 20 \text{ m s}^{-1}$ the temperature difference

$$T_2 - T_1 = 0.21 \text{ mK}$$

which can iteratively be calculated. It corresponds to a velocity change of 43%: $v_2 = 1.43v_1$.

17.5.5 Specific Heats of Real Gases

According to the definition (17.94) and (17.114) the specific heats at constant volume and at constant pressure are given by

$$c_v = \left(\frac{\partial u}{\partial T} \right)_v, \quad c_p = \left(\frac{\partial h}{\partial T} \right)_p, \quad (17.130)$$

where u and h are prescribed by the functional relations

$$u = u(T, v), \quad h = h(T, p) = u(T, v(T, p)) + pv = \bar{u}(T, p) + pv. \quad (17.131)$$

These formulae allow to relate c_v and c_p to one another, as in (17.119). To this end one writes with (17.131)

$$c_p = \left(\frac{\partial \bar{u}}{\partial T} \right)_p + p \left(\frac{\partial v}{\partial T} \right)_p = \underbrace{\left(\frac{\partial u}{\partial T} \right)_v}_{c_v} + \left(\frac{\partial u}{\partial v} \right)_T \left(\frac{\partial v}{\partial T} \right)_p + p \left(\frac{\partial v}{\partial T} \right)_p, \quad (17.132)$$

from which

$$c_p - c_v = \left\{ \left(\frac{\partial u}{\partial v} \right)_T + p \right\} \left(\frac{\partial v}{\partial T} \right)_p \quad (17.133)$$

is obtained. For an ideal gas the internal energy is independent of the specific volume, so that $(\partial u / \partial v)_T = 0$ and $(\partial v / \partial T)_p = R/p$, as one can easily deduce from the thermal equation of state of an ideal gas. Thus, one obtains $c_p - c_v = R$, as already obtained in Eq. (17.119).

As an additional example we consider a **van der Waals gas** outside the region of coexistence of combined gas-liquid phases. In Sect. 17.3.3 we explained the thermal equation of state by mentioning that in the VAN DER WAALS gas the mutual interaction forces of the molecules must be accounted for; these are neglected in an ideal gas. In other words, the internal energy of the VAN DER WAALS gas differs from that of an ideal gas by the potential of the molecular forces of attraction. When the gas is heated at fixed volume, the mean distance of the molecules does not change. It follows that the potential energy of the forces of attraction does not yield a contribution to $c_v = (\partial u / \partial T)_v$; for a VAN DER WAALS gas the specific heat at constant volume, c_v , has accordingly the same value as for the corresponding ideal gas. However, the potential energy of the molecular attraction grows with growing volume. One, therefore expects $C_p^m - C_v^m > R_m$.³⁰

Now the self-pressure is given by

$$U_B = -A_{V_m \rightarrow \infty} = - \int_{V_m}^{\infty} p_B \, dV = \int_{\infty}^{V_m} \frac{a}{V^2} \, dV = - \frac{a}{V_m}, \quad (17.134)$$

so that the internal energy per mole is given by

$$U_m = U_{\text{ideal}}^m - \frac{a}{V_m}, \quad (17.135)$$

in which U_{ideal}^m is the internal energy per mole of the corresponding ideal gas. From

³⁰Because in Subsection 17.3.3 all quantities are referred to the mole volume, we here calculate the difference of the heats for a body of 1 mole mass. For the same reason we also choose capital letters C_p^m and C_v^m .

$$\left(\frac{\partial U_m}{\partial V_m}\right)_T = \underbrace{\left(\frac{\partial U_{\text{ideal}}^m}{\partial V_m}\right)_T}_{=0} + \frac{a}{V_m^2} = \frac{a}{V_m^2}, \quad (17.136)$$

relation (17.133), written for a mole implies

$$C_p^m - C_v^m = \left(\frac{a}{V_m^2} + p\right) \left(\frac{\partial V_m}{\partial T}\right)_p. \quad (17.137)$$

If one also uses the thermal equation of state (17.43)

$$\left(\frac{a}{V_m^2} + p\right) (V_m - b) = R_m T,$$

one may deduce from it the relation

$$\left(\frac{\partial T}{\partial V_m}\right)_p = \frac{1}{R_m} \left\{ -\frac{2a}{V_m^3} (V_m - b) + \frac{R_m T}{V_m - b} \right\}, \quad (17.138)$$

which, when substituted into (17.137) leads to

$$C_p^m - C_v^m = \frac{R_m}{1 - \frac{2a}{R_m T V_m^3} (V_m - b)^2} > R_m, \quad (17.139)$$

an inequality, one might have expected.

17.6 The Second Law of Thermodynamics—Principle of Irreversibility

17.6.1 Preamble

As explained in the introductory remarks to this chapter, the Second Law of Thermodynamics expresses the fact, that physical processes can only evolve in one direction whereas a process, which is traversed in the opposite direction, is physically not realizable. The First Law—the conservation law of energy—is symmetric in this respect. It allows, in principle, a transformation of mechanical energy into heat and makes the re-gain of this mechanical energy from heat possible by a process that is traversed in the reverse direction. We have given examples to the impossibility of this in Figs. 17.3 and 17.4.

There are different forms, in which the Second Law of Thermodynamics is spelled out. This has essentially historical reasons: The Second Law is a statement based

on observations and experience, and its formulation grew from special conditions to full generality. For this reason it is not so that its most general form could be *derived* from special variants of it. Rather, such generalizations are *motivated* by statements that were derived under more restrictive conditions. The generalized form can, thus, only be justified by the fact that (i) it embraces all results already deduced under simplified conditions and (ii) nothing physically unrealistic follows from it in the generalization.

Statements, all of which characterize the content of the Second Law, without, however, quantifying it, are³¹:

- All natural processes are irreversible.
- All processes involving friction are irreversible (PLANCK).
- The adiabatic expansion of a gas without the performance of any work is irreversible.
- Heat can never by itself be transferred from a body of low temperature to a body of higher temperature (CLAUSIUS 1854).
- It is impossible to construct a periodically operating machine, which achieves no more than lifting a load and cooling a reservoir (PLANCK 1897).
- There exists no machine, which draws heat from a heat bath and transfers it into work by a cyclic process without the presence of a second heat bath at lower temperature, to which the machine supplies heat.

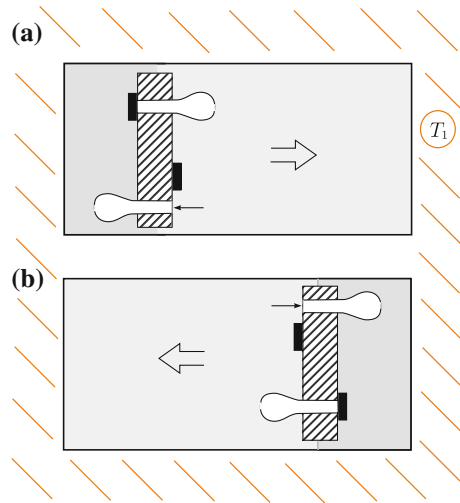
All these qualitative statements hit the core of what the principle of irreversibility speaks out, but do not quantify it. In spite of this, some inferences can be drawn from it. For instance, in view of the sixth of the above statements, it is impossible to construct a submarine boat, which takes the energy for the motor that drives the propeller from the heat content of the surrounding sea water. The reason is that there is no second heat bath present.

A (thought) machine, which violates the Second Law of Thermodynamics is called a **perpetuum mobile of the second kind**. The Second Law of Thermodynamics is therefore equivalent to the statement that a *perpetuum mobile of second kind cannot exist*. (A perpetuum mobile of the first kind violates the First Law of Thermodynamics). The above mentioned submarine boat, if it existed, would be a perpetuum mobile of the second kind, because as a continuously operating machine, it would draw heat from a reservoir and transform it into work without the presence of a second bath to which heat could be supplied.

Because in the literature (mostly of profane nature) perpetua mobili of the second kind are of relatively frequent occurrence, we shall here add two additional examples. The first example is the **trap machine**. Its principle mimics its well-known analogue as ‘fish-trap’ and is here operating as a trap machine of molecules, built into the piston of a closed cylinder that is filled with a gas, but otherwise materially closed,

³¹W. THOMSON [LORD KELVIN] (1824–1907) essentially already spoke out in the year 1851 what RUDOLF J.E. CLAUSIUS and MAX PLANCK expressed in the above statements. His statement reads: “It is impossible, by means of inanimate agency, to derive mechanical effect from any portion of matter by cooling it below the temperature of the coldest of the surrounding objects”.

Fig. 17.43 Trap machine ('fish trap machine'). A cylinder, embedded in an environment with temperature T_1 , contains a gas and a movable piston, into which semi-permeable membranes (the trapping elements) are built, which allow molecules to pass only in the direction of the small arrow indicated in the figure. The pressure difference that is built this way induces a motion of the piston and a correspondingly established working as indicated by the large arrows

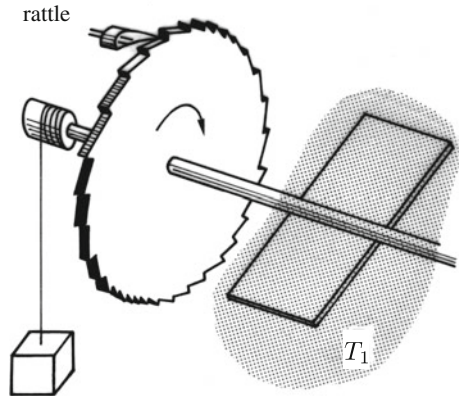


as shown in **Fig. 17.43**. The cylinder is kept in a 'bath' of constant temperature T_1 . The trap is thought to be constructed such that molecules can enter it through the large opening and leave it again through the small opening, but not vice versa; The trap device thus operates as a **semi-permeable wall**. If the piston is initially positioned on the left side of the cylinder, and if the two trap elements with their valves are arranged as in **Fig. 17.43a**, the number of molecules on the left side of the piston will grow and, correspondingly the pressure will increase, whereas in the right part of the cylinder the pressure will decrease. The pressure difference between the two chambers of the cylinder will push the cylinder to the right, which via the piston rod (not shown in the figure) will perform work. If the piston is in the right position a mechanism will change the positions of the traps of the valves as shown in **Fig. 17.43b**; as a consequence the motion of the piston is now to the left, since the displaced molecules will now generate a pressure difference to the left with a corresponding work transmitted via the piston rod, etc. If in this process the expansion of the gas is performed isothermally and reversibly, the power of working in the piston motion from one cylinder end to the other is given by

$$(w_{12})_{\text{rev}} = \int_{v_1}^{v_2} \Delta p \, dv.$$

where v_1 , v_2 are the volumes of one part of the cylinder at the two end positions of the piston. This power of working is brought by withdrawal of heat from the reservoir with temperature T_1 . The process can be continued forever, but it is a perpetuum mobile of the second kind, because it corresponds to the fifth of the above itemized statements: The trap machine performs periodically work (equal to lifting a load) and only cools a reservoir of heat by drawing heat from it. The trap machine fails,

Fig. 17.44 FENMAN's rattle machine. A gear disk on an axis with frictionless supports can only rotate in one direction, because the rattle prevents it from the opposite motion. The paddle, subjected to a gas of temperature T_1 causes, owing to molecular encounters, the rotational motion that raises a weight



because the BROWNIAN motion of the molecules makes them also to pass the trap elements in the 'wrong' direction through the small hole of the trap machine.

RICHARD FEYNMAN, in his 'Lectures on Physics' (Vol. 1, pp. 46.1–9) [17], presents a model of a perpetuum mobile, which is now known as FEYNMAN's **rattle machine**, see Fig. 17.44. It consists of a gear wheel, of which the motion is only possible in one direction. By the rotation of the wheel a weight is lifted. The axis, on which the wheel is mounted carries a paddle and is horizontally suspended in frictionless supports. Moreover, the machine is surrounded by a gas of temperature T_1 . The rotation of the disk is thought to be caused by collisions, which the molecules experience with the shovels of the paddle. Without the rattle at most a fluctuating motion of the disk will arise, since molecule encounters with the paddle are equally probable on both sides of the paddle. With the rattle, however, a rotation can be expected, because the motions that are initiated by the molecular impacts on the 'wrong side of the shovels' are prevented by the rattle. The rotating motion can be used to lift a weight and the power of working used to raise the weight is taken from the gas by lowering its temperature. This is again a violation of the fifth of the itemized above statement (PLANCK). This perpetuum mobile cannot function, since the rattle will also jump and then allow backward motions.

17.6.2 The Second Law for Simple Adiabatic Systems

In this subsection we shall present a first form of the Second Law of Thermodynamics by using a very simple example. The system under consideration will be simple (in the sense defined earlier), non-moving and adiabatic (and hence isolated against supply of heat), for which the First Law of Thermodynamics implied the formulae (17.68), provided processes are conducted reversibly, viz.,

$$U_2 - U_1 + \int_{V_1}^{V_2} p \, dV = 0, \quad u_2 - u_1 + \int_{v_1}^{v_2} p \, dv = 0. \quad (17.140)$$

It is seen that for reversible cyclic processes the work done by the pressure vanishes, since $v_1 = v_2$, so that $u_1 = u_2$. Alternatively one can imagine a cyclic **irreversible** process such that the work done by the pressure vanishes. For this situation we have the following law that is founded on experience:

Statement of experience (SEARS–KESTIN assertion)³²

- *It is impossible in an irreversibly conducted process of a simple adiabatic system, which connects two equilibria and is cyclic with respect to the variables that perform work, to lower the value of the internal energy.*

Let us go deeper into this statement by putting it into the proper perspective relative to formula (17.140), which is valid for reversible processes. So, for irreversible processes the zero on the right-hand side must be replaced by some non-zero value. If the process is cyclic with respect to variables that perform work, then this means that the pressure integral in (17.140) vanishes. For such irreversible processes connecting two equilibria the above statement of experience now requests that $u_2 - u_1 \geq 0$. As this is a statement of experience, we must accept it as a fact and treat it as an axiom.

In an adiabatically conducted reversible process of a system from state 1 to state 2, the system follows a well-defined curve in the (U, V) —or (u, v) -diagram, which, in **Fig. 17.45**, is shown in bold, and which is fixed once the thermal and caloric equations of state are known. On the basis of the statement of experience all final states of irreversible changes of the system from state 1 into state 2 lie therefore ‘above’ the shown reversible adiabatic curve.

Equation (17.140) implies for adiabatic processes

$$\begin{aligned} dU + p \, dV = 0 &\iff du + p \, dv = 0, \\ \dot{U} + p \dot{V} = 0 &\iff \dot{u} + p \dot{v} = 0, \end{aligned} \quad (17.141)$$

or

$$\left(\frac{\partial U}{\partial V}\right)_{\text{ad,rev}} = -p \iff \left(\frac{\partial u}{\partial v}\right)_{\text{ad,rev}} = -p. \quad (17.142)$$

The slope of the reversible adiabatic curve in the (u, v) -diagram is therefore equal to the negative pressure, see **Fig. 17.45**.

This fact offers a possibility to determine the reversible adiabatic curves in the (u, v) -diagram; to this end the thermal, $p = \hat{p}(T, v)$, and caloric, $u = \hat{u}(T, v)$, equations of state must be known. Inverting formally the caloric equation of state for the temperature, $T = \hat{T}(u, v)$, and using this in the thermal equation of state, one obtains $p = \hat{p}(\hat{T}(u, v), v) = \tilde{p}(u, v)$. Thus, from (17.142) one may deduce

³²W. MUSCHIK, Am. J. Phys. **58**(3), 1990, 241–244.

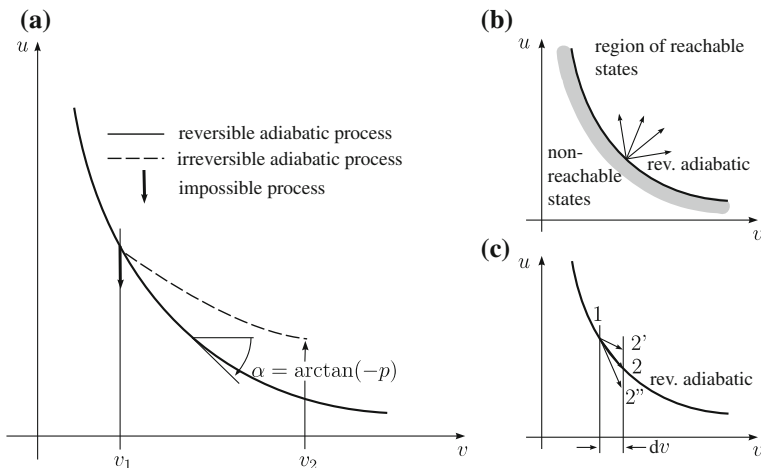


Fig. 17.45 Changes of states in a simple adiabatic system. **a** Changes of states of reversible adiabatic processes follow in the (u, v) -diagram the solid curve. At constant volume, it is impossible, to reduce the internal energy (vertical arrow). All irreversible processes that start in the (u, v) -diagram from a fixed point (dashed) lie above the reversible adiabatic curve. In each point the reversible adiabatic curve has the slope $-p$. **b** In the vicinity of each point of the (u, v) -diagram, there are infinitely many non-reachable states. **c** In a simple adiabatic system, a process $1 - 2'$ is reversible and a process $1 - 2''$ is impossible

$du/dv = -\tilde{p}(u, v)$, which is a differential equation that can be solved by the method of separation of variables.

For an ideal gas with linear caloric equation of state $u(T) = c(T - T_0)$ one obtains e.g.,

$$p = \frac{RT}{v} = \frac{R\left(\frac{u}{c} + T_0\right)}{v} = \tilde{p}(u, v), \tag{17.143}$$

and therefore

$$\left(\frac{\partial u}{\partial v}\right)_{\text{ad, rev}} = -\frac{R\left(\frac{u}{c} + T_0\right)}{v}$$

or

$$\frac{du}{R\left(\frac{u}{c} + T_0\right)} = -\frac{dv}{v}, \tag{17.144}$$

from which, by integration

$$\frac{\frac{u}{c} + T_0}{\frac{u_1}{c} + T_0} = \left(\frac{v_1}{v}\right)^{R/c} \tag{17.145}$$

ensues, in which (u_1, v_1) is a fixed state in the (u, v) -plane, which is the constant of integration that selects the adiabatic curve.

If an infinitesimally conducted process from an equilibrium state 1 connects a second state 2, then the power of working of the pressure due to the associated infinitesimal volume change is not zero but $p dv$. (The second state does not have to be an equilibrium state.) If one requires for this process that $du + p dv \geq 0$, one can with this requirement obtain the result spelled out in the SEARS–KESTIN assertion. To this end one must only consecutively couple such processes to a whole process that is cyclic with respect to the pressure. We will now require that this statement, namely $du + p dv \geq 0$, is satisfied for all physically realizable processes. With the aid of Fig. 17.45b this statement can also be expressed in the following form: *A closed adiabatic system in a certain initial state cannot reach every possible state; those states are not reachable, which possess a smaller internal energy than those states that are reachable by reversible processes from a state of the same initial volume.* Since through each point in the (u, v) -diagram a reversible adiabatic curve can be drawn, in which in all points the equation $du/dv = -p(u, v)$ holds, one may also conclude as follows: *In the vicinity of any point in the (u, v) -diagram there are for a simple adiabatic system infinitely many non-reachable points.* In Fig. 17.45b, for the drawn adiabatic curve this is the shaded region. From Fig. 17.45 and the fact that for an adiabatic system, Eq. (17.140) implies $u_2 - u_1 = -(w_{12})_{\text{ad}}$ one further concludes: *Of all processes in a closed adiabatic system between given initial and final states, the reversible process yields the largest work.* These formulations go back to CONSTANTINE CARATHÉODORY, see biography in Fig. 17.15.

Since the reversible adiabatic processes of a simple system are characterized by relation (17.141), or

$$du + p dv = 0 \quad \Longleftrightarrow \quad dh - v dp = 0,$$

the above described properties concerning the non-reachable states allow to read off from the sign of $du + p dv$ or $dh - v dp$ whether an infinitesimal process is irreversibly or reversibly conducted or is simply impossible (or not realizable). Indeed the following statements hold:

$$du + p dv \left\{ \begin{array}{l} > 0, \Longleftrightarrow \text{irreversible} \\ = 0, \Longleftrightarrow \text{reversible} \\ < 0, \Longleftrightarrow \text{impossible} \end{array} \right\} \text{ process of an adiabatic system.} \quad (17.146)$$

These three infinitesimal changes of states are illustrated in Fig. 17.45c by the arrows 2', 2 and 2''.

The result (17.146) requires the following clarifying comments: The statement only holds in the given form for infinitesimal processes, since the value of

$$\int_1^2 (du + p dv) = u_2 - u_1 + \int_1^2 p dv, \quad \int_1^2 (dh - v dp) = h_2 - h_1 - \int_1^2 v dp \quad (17.147)$$

for finite processes depends upon the path, along which the change of states is reached. Mathematically, this means that $du + pdv$ is not a **total (or complete) differential**. Indeed, if this were so, then

$$df = du + pdv = \frac{\partial f}{\partial u} du + \frac{\partial f}{\partial v} dv \quad (17.148)$$

would have to hold, in which case df is only a total differential, if the **integrability condition**

$$\frac{\partial}{\partial v} \left(\frac{\partial f}{\partial u} \right) = \frac{\partial}{\partial u} \left(\frac{\partial f}{\partial v} \right) \quad (17.149)$$

is satisfied. This condition is necessary in order that the integral $\int_1^2 df$ from an initial state 1 to a final state 2 is independent of the trajectory along which the change of states $1 \rightarrow 2$ is conducted. We shall shortly come back to this point. If the integrability condition (17.149) would hold for $df = du + pdv$, then in view of

$$\frac{\partial f}{\partial u} = 1, \quad \frac{\partial f}{\partial v} = p, \quad (17.150)$$

the relation

$$\left. \frac{\partial p}{\partial u} \right|_v = 0$$

would have to be fulfilled; the pressure could not be a function of the internal energy, a result that obviously disagrees with experience. This is seen for an ideal gas directly from equation (17.143). Incidentally, for a gas, subjected to constant volume and frictional work, one measures not only an increase of the internal energy, but also an increase of the pressure. It follows that $(\partial p / \partial u)|_v$ cannot be zero.

These results hold irrespective of which independent variables are chosen for the thermal and caloric equations of state. If, e.g., $u = u(\vartheta, v)$ and $p = p(\vartheta, v)$, then df , given by

$$df = \frac{\partial u}{\partial \vartheta} d\vartheta + \left(\frac{\partial u}{\partial v} + p \right) dv, \quad (17.151)$$

is not a total differential and for $h = h(\vartheta, v)$, $v(\vartheta, v)$ neither is

$$df = \frac{\partial h}{\partial \vartheta} d\vartheta + \left(\frac{\partial h}{\partial p} - v \right) dp. \quad (17.152)$$

Hidden behind this problem—namely the fact that $(du + pdv)$ or $(dh - vd p)$ are not total differentials—are two concepts of classical thermodynamics of adiabatic systems, namely that of **entropy** and that of **absolute temperature**. Both quantities have found their prominent role in classical thermodynamics out of mathematical causes and less because of physical necessity, even though the two concepts express, once they have been introduced, important physical content.

(a) Appendix about Pfaffian forms in two independent variables To outline the role played by PFAFFian³³ forms we wish to explain a few facts from the theory of ordinary differential equations. Consider the so-called Pfaffian form

$$X(x, y)dx + Y(x, y)dy = 0. \quad (17.153)$$

This is a differential equation in the two independent variables x, y , and the two differentiable functions $X(x, y)$ and $Y(x, y)$ are assumed to be prescribed. In general, one cannot expect that (17.153) is a total differential in the sense discussed above. However it is so that such PFAFFian forms have an **integrating multiplier** (or an **integrating denominator** or **divisor**), which is not necessarily unique. In other words, there exists at least one function $N(x, y)$ with the property that

$$\frac{Xdx + Ydy}{N} = df(x, y) \quad (17.154)$$

is a total differential of a well-defined function f , i.e., the following statement holds

$$df \hat{=} \left\{ \begin{array}{l} \text{complete} \\ \text{differential} \end{array} \right\} \iff \frac{\partial}{\partial x} \left(\frac{Y}{N} \right) = \frac{\partial}{\partial y} \left(\frac{X}{N} \right). \quad (17.155)$$

If this statement holds true, then the integral $\int_1^2 df$ from (x_1, y_1) to (x_2, y_2) is independent of the trajectory along which the integral is computed. The function which achieves this property is called integrating denominator or divisor; its inverse is the integrating factor or multiplier.

To *prove* the statement (17.155) we assume first that df is indeed a complete or total differential. Then, the integral

$$\oint_{\mathcal{L}} df = \oint_{\mathcal{L}} \left\{ \frac{\partial f}{\partial x} dx + \frac{\partial f}{\partial y} dy \right\} = 0 \quad (17.156)$$

vanishes along any simply closed path \mathcal{L} , see **Fig. 17.47**, else the function f would not be unique. If we write

$$\mathbf{K} = (K_x, K_y) =: \left(\frac{\partial f}{\partial x}, \frac{\partial f}{\partial y} \right), \quad ds = (dx, dy), \quad (17.157)$$

³³For a short biography of JOHANN FRIEDRICH PFAFF, see **Fig. 17.46**.



Fig. 17.46 JOHANN FRIEDRICH PFAFF (22. Dec. 1765–21. April 1825)

JOHANN FRIEDRICH PFAFF (sometimes spelled FRIEDERICH) was a German mathematician. He was described as one of Germany's most eminent mathematicians during the 19th century. He was a precursor of the German school of mathematical thinking, which under CARL FRIEDRICH GAUSS and his followers largely determined the lines on which mathematics developed during the nineteenth century.

He received his early education at the Carlsschule, where he met Friedrich Schiller, his lifelong friend. His mathematical capacity was noticed during his early years. He pursued his studies at Göttingen under ABRAHAM GOTTHELF KÄSTNER, and in 1787 he went to Berlin and studied practical astronomy under J.E. BODE. In 1788, Pfaff became professor of mathematics in Helmstedt, and continued his work as a professor until that university was abolished in 1810. After this event, he became professor of mathematics at the University of Halle, where he stayed for the rest of his life.

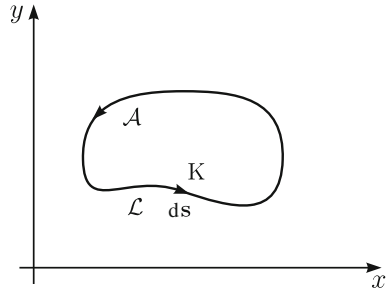
He studied mathematical series and integral calculus, and is noted for his work on partial differential equations of the first order (Pfaffian systems as they are now called) which became part of the theory of differential forms. He was CARL FRIEDRICH GAUSS's formal research supervisor. He knew Gauss well, when they both lived together in Helmstedt in 1798. August Möbius was later his student.

His two principal works are 'Disquisitiones analyticae maxime ad calculum integrelem et doctrinam serierum pertinentes' (4to., Vol. i., Helmstädt, 1797) and 'Methodus generalis, aequationes differentiarum particularum, necnon aequationes differentiales vulgares, utrasque primi ordinis inter quocumque variables, complete integrandi' in: *Abhandlungen der Königlichen Akademie der Wissenschaften zu Berlin* (1814–1815).

His brother JOHANN WILHELM ANDREAS PFAFF was a professor of pure and applied mathematics. Another brother, CHRISTIAN HEINRICH PFAFF, was a professor of medicine, physics and chemistry.

The text is based on www.wikipedia.org

Fig. 17.47 Explaining the integrating denominator of a PFAFFian form *The integral $\oint_{\mathcal{L}} df$ along a simply connected path \mathcal{L} vanishes, if df is a total differential*



then (17.156) can also be written in the form (STOKES law)

$$\oint_{\mathcal{L}} \mathbf{K} \cdot d\mathbf{s} = \iint_{\mathcal{A}} \text{curl } \mathbf{K} \cdot d\mathbf{A} = 0, \tag{17.158}$$

in which $d\mathbf{s}$ is the vectorial line element along the curve \mathcal{L} and $d\mathbf{A}$ is the vectorial surface element (perpendicular to the (x, y) -plane.). In Eq. (17.158) it was assumed that \mathbf{K} is a differentiable two-dimensional vector field, so that the STOKES law can be applied.

The quantity $\text{curl } \mathbf{K}$ is understood to be a vector perpendicular to the (x, y) -plane with the algebraic value $(\partial K_x / \partial y - \partial K_y / \partial x)$. Since the statement (17.158) holds for any simply closed path \mathcal{L} , we necessarily have

$$\text{curl } \mathbf{K} = \mathbf{0} \Rightarrow \frac{\partial}{\partial y} \left(\frac{\partial f}{\partial x} \right) - \frac{\partial}{\partial x} \left(\frac{\partial f}{\partial y} \right) = 0 \Rightarrow \frac{\partial}{\partial y} \left(\frac{X}{N} \right) - \frac{\partial}{\partial x} \left(\frac{Y}{N} \right) = 0. \tag{17.159}$$

So the first part of (17.155) is proved.

To prove the reverse, one assumes that (17.159) holds; then there follows with $\mathbf{K} = (X/N, Y/N)$ also $\text{curl } \mathbf{K} = \mathbf{0}$ in the entire domain, in which X, Y and N are continuously differentiable. With this result, (17.158) must equally hold: (one only needs to read this equation in the backward direction). In other words, the line integral $\int_1^2 \mathbf{K} \cdot d\mathbf{s}$ along an arbitrary path is independent of this path, and therefore the vector field \mathbf{K} is a gradient field

$$\begin{aligned} \mathbf{K} = \text{grad } f &\Rightarrow \frac{\partial f}{\partial x} = \frac{X}{N}, \quad \frac{\partial f}{\partial y} = \frac{Y}{N} \\ &\Rightarrow \oint_{\mathcal{L}} \left\{ \frac{\partial f}{\partial x} dx + \frac{\partial f}{\partial y} dy \right\} = \oint_{\mathcal{L}} df = 0. \end{aligned} \tag{17.160}$$

With this result, the existence of an integrating denominator for the PFAFFian form (17.153) is proved.

(b) Entropy. Let us apply these findings to the PFAFFian forms $(du + pdv)$ and $(dh - vdp)$. Depending upon the choice of the independent variables the forms of the entropy functions differ from one another:

- If u and v are the independent variables, there exists an integrating denominator $N(u, v)$ such that

$$ds = \frac{du + pdv}{N(u, v)} \quad (17.161)$$

is the total differential of a function $s(u, v)$.

- If h and p are the independent variables, the corresponding statement reads

$$ds = \frac{dh - vdp}{N(h, p)}. \quad (17.162)$$

$N(h, p)$ is here the integrating denominator—not necessarily unique—and ds is the total differential of a function $s(h, p)$.

- If one chooses ϑ and v as independent variables, the starting point is (17.151), and the integrating denominator in this case is $N(\vartheta, v)$, yielding the total differential

$$ds = \frac{\frac{\partial u}{\partial \vartheta}}{N(\vartheta, v)} d\vartheta + \frac{\frac{\partial u}{\partial v} + p}{N(\vartheta, v)} dv. \quad (17.163)$$

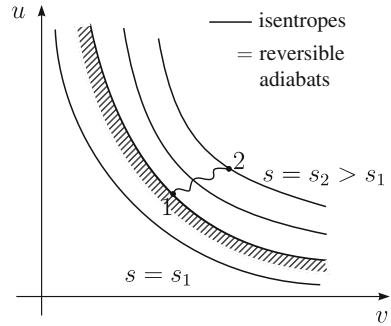
- Finally, one may also choose ϑ and p as independent variables and then obtains with the integrating denominator $N(\vartheta, p)$ as well as the relation (17.152) the expression

$$ds = \frac{\frac{\partial h}{\partial \vartheta}}{N(\vartheta, p)} d\vartheta + \frac{\frac{\partial h}{\partial p} - v}{N(\vartheta, p)} dp. \quad (17.164)$$

The expressions (17.161)–(17.164) are total differentials of functions of two variables, all of which represent physically analogous quantities. They are called **empirical entropies**, because they are not unique owing to the non-uniqueness of the integrating denominators. They must be additive (extensive) quantities, because u and v or h and v are themselves additive.

Relations (17.161)–(17.164) allow the derivation of the following integrability conditions:

Fig. 17.48 Thermodynamics of adiabatic systems. Lines of constant entropy represent in the (u, v) -diagram the reversible adiabatic processes. Starting from a process 1 only states 2 can be reached with not smaller entropy



$$\frac{\partial}{\partial v} \left(\frac{1}{N(u, v)} \right) = \frac{\partial}{\partial u} \left(\frac{p(u, v)}{N(u, v)} \right) \quad \text{for (17.161),}$$

$$\frac{\partial}{\partial p} \left(\frac{1}{N(h, p)} \right) = -\frac{\partial}{\partial h} \left(\frac{v(h, p)}{N(h, p)} \right) \quad \text{for (17.162),}$$

$$\frac{\partial}{\partial v} \left(\frac{\frac{\partial u}{\partial \vartheta}(\vartheta, v)}{N(\vartheta, v)} \right) = \frac{\partial}{\partial \vartheta} \left(\frac{\frac{\partial u}{\partial v}(\vartheta, v) + p(\vartheta, v)}{N(\vartheta, v)} \right) \quad \text{for (17.163),} \quad (17.165)$$

$$\frac{\partial}{\partial p} \left(\frac{\frac{\partial h}{\partial \vartheta}(\vartheta, p)}{N(\vartheta, p)} \right) = \frac{\partial}{\partial \vartheta} \left(\frac{\frac{\partial h}{\partial p}(\vartheta, p) - v(\vartheta, p)}{N(\vartheta, p)} \right) \quad \text{for (17.164).}$$

Of these, the last two relations are of particular practical usefulness. These relations express equality of the cross differentials

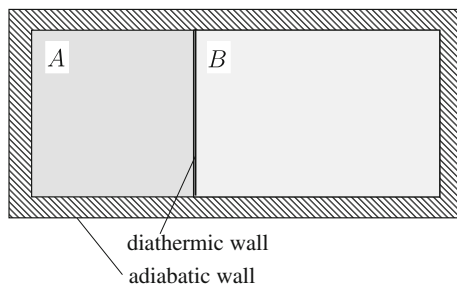
$$\frac{\partial^2 f}{\partial x \partial y} = \frac{\partial^2 f}{\partial y \partial x}.$$

They are called **Maxwell relations**.

For reversible processes of simple adiabatic systems, we have $ds = 0$ or $s = \text{constant}$; this follows immediately from the above Eqs. (17.161)–(17.164) and relation (17.146)₂. For simple systems the reversible adiabats are, therefore, identical with the isentropes. Provided N is a positive function, the Second Law of Thermodynamics, therefore, says that in adiabatic simple systems starting from an initial state 1 only states can be reached, of which the entropy is not smaller, see Fig. 17.48, explicitly,

$$s_2 - s_1 \geq 0, \quad \text{for adiabatic simple systems, if } N > 0. \quad (17.166)$$

Fig. 17.49 Universality of the integrating denominator. An *adiabatic* system $A \cup B$ is split by a *diathermic* wall into two *non-adiabatic* systems



(c) **Absolute or thermodynamic temperature.** The result (17.166), according to which the empirical entropy of an adiabatic system cannot decrease, neither for reversible nor irreversible processes, is tied to the assumption that, always, a strictly positive integrating denominator $N > 0$ can be found. The proof that this is always possible has not yet been given. Furthermore, we might ask, whether inconsistencies with the Second Law might emerge, if for different systems, which interact, the integrating denominators can essentially arbitrarily be chosen. It would, indeed be an advantage, if the integrating denominator used for the entropy differentials would be a universal function, independent of the material properties of the system. If this integrating denominator then would also turn out to be positive, then the statement (17.166) would hold in an absolute sense, i.e., for the ‘true’ entropy, not simply for that empirical entropy, for which (accidentally) $N > 0$ would hold.

To corroborate the existence of a ‘universal’ integrating denominator, let us consider an *adiabatic* total system $A \cup B$ that is composed of two partial systems A and B that are separated from one another by a *diathermic* wall, see Fig. 17.49. If the two partial systems are in equilibrium with one another, then their empirical temperatures must be the same, $\vartheta_A = \vartheta_B$; for across a diathermic wall the temperature must be continuous. This property, as well as the additivity property of the entropy, is now employed to corroborate the material independence of the integrating denominator. To this end, we write relation (17.161) for the three systems A , B and $A \cup B$ as follows

$$\begin{aligned} N_A(s_A, \vartheta) ds_A &= du_A + p dv_A, \\ N_B(s_B, \vartheta) ds_B &= du_B + p dv_B, \\ N(s, \vartheta) ds_{A \cup B} &= du_{A \cup B} + p dv_{A \cup B} = (du_A + du_B) + p(dv_A + dv_B), \end{aligned} \quad (17.167)$$

or

$$N(s, \vartheta) ds = du + p dv. \quad (17.168)$$

In these formulae we assumed N to be a function of the entropy and empirical temperature, and we have set $\vartheta_A = \vartheta_B = \vartheta$, because the systems are in equilibrium with one another. In addition, we have made use of the additivity of the internal energy and the specific volume, and have used the fact that $p = p_{A \cup B} = p_A = p_B$. Equation (17.168) then implies

$$\begin{aligned} ds &= \frac{du + pdv}{N(s, \vartheta)} = \frac{du_A + pdv_A}{N(s, \vartheta)} + \frac{du_B + pdv_B}{N(s, \vartheta)} \\ &= \frac{N_A(s_A, \vartheta)}{N(s, \vartheta)} ds_A + \frac{N_B(s_B, \vartheta)}{N(s, \vartheta)} ds_B. \end{aligned} \quad (17.169)$$

Since in these expressions all quantities are functions of s and ϑ , and, in particular, ds on the left-hand side only depends on s , but not on ϑ , it follows that the right-hand side of (17.169) must equally be independent of ϑ . In other words, one has

$$\frac{\partial}{\partial \vartheta} \left(\frac{N_A}{N} \right) = \frac{\partial}{\partial \vartheta} \left(\frac{N_B}{N} \right) = 0, \quad (17.170)$$

from which

$$\frac{1}{N} \frac{\partial N}{\partial \vartheta} \equiv \frac{1}{N_A} \frac{\partial N_A}{\partial \vartheta} \equiv \frac{1}{N_B} \frac{\partial N_B}{\partial \vartheta}$$

or

$$\frac{\partial}{\partial \vartheta} (\ln N) \equiv \frac{\partial}{\partial \vartheta} (\ln N_A) \equiv \frac{\partial}{\partial \vartheta} (\ln N_B) =: g(\vartheta) \quad (17.171)$$

is obtained. The three expressions on the left-hand side in (17.171) are, therefore functions of the empirical temperature (and possibly the entropy). The following argument, however, makes clear why the entropy cannot arise as a variable. The division of the total system $A \cup B$ into the systems A and B is namely arbitrary, i.e., the diathermic wall can be set at will. Consequently, if a dependence of the expressions in (17.171) on the entropy would exist, then the three expressions could not be the same, this because of the additivity of the entropy; for this reason, g is only a function of ϑ . We may now set $g(\vartheta) > 0$ without any restriction. Integration of (17.171) yields

$$\begin{aligned} N(s, \vartheta) &= \Psi(s)f(\vartheta), \\ N_\alpha(s_\alpha, \vartheta) &= \Psi(s_\alpha)f(\vartheta), \quad \alpha = A, B \end{aligned} \quad (17.172)$$

with

$$f(\vartheta) = \exp \left(\int_{\vartheta_0}^{\vartheta} g(\bar{\vartheta}) d\bar{\vartheta} \right) > 0, \quad (17.173)$$

in which the different Ψ 's are necessarily constants, because of the additivity of s : $N = cf(\vartheta)$. (Substitute (17.172) into (17.169) and request $ds = ds_A + ds_B$.) For all adiabatic systems and except for a multiplicative constant the integrating denominator is, thus, the same function of the empirical temperature. Without restriction, we may now choose $c = 1$; the *associated integrating denominator* will be called **absolute** or **thermodynamic temperature** or **Kelvin temperature**

$$T = f(\vartheta) > 0. \quad (17.174)$$

Because of the exponential property (17.173) it is positive, and because of $g(\vartheta) > 0$ it is a monotonic function of ϑ .³⁴

We summarize: *For simple adiabatic systems there exists an integrating denominator, which is only a function of the absolute temperature. It is positive and independent of the material properties of the systems, i.e., universal and is called absolute temperature. The entropy that is constructed with this integrating denominator is no longer called empirical entropy but **true entropy** or simply **entropy**.* For this we have

$$ds = \frac{1}{T(\vartheta)}(du + pdv) = \frac{1}{T(\vartheta)}(dh - vdp). \quad (17.175)$$

$ds > 0$ characterizes irreversible processes, $ds = 0$ describes reversible processes and $ds < 0$ indicates impossible or physically non-realizable processes. If one integrates the imbalance $ds \geq 0$ between an initial state 1 and a final state 2, one obtains

$$s_2 - s_1 \geq 0 \quad \text{for adiabatic systems.}$$

The entropy of an adiabatic system can never decrease. *For all natural irreversible adiabatic processes the entropy increases, for reversible processes it remains constant.*

This statement also holds, if several non-adiabatic systems are combined to a total adiabatic system, i.e., the entropy of the total system also fulfills the above imbalance. For an absolutely closed system at rest the working supplied to the system under adiabatic conditions vanishes, and the energy balance (First Law of Thermodynamics) reduces to the form stated in (17.68), in which $A_{12} = 0$. Hence,

$$U_2 - U_1 = 0 \quad \text{and} \quad S_2 - S_1 \geq 0. \quad (17.176)$$

All quasi-static (i.e., infinitely slow) processes in absolutely closed systems can only so evolve that the energy remains constant and the entropy is increased until it finally reaches a maximum. This state corresponds to a *thermodynamic equilibrium*. In other words: *The thermodynamic equilibrium of an absolutely closed system is characterized by the maximum of its entropy.* Incidentally, the results (17.176) are due to JULIUS EMANUEL CLAUSIUS, who expressed its content by the statements: ‘*The energy of the world is constant*’ and ‘*The entropy of the world strives for a maximum*’, which we quoted already in Sect. 17.1. Grasping the complexity of the universe today these statements sound rather courageous.

Back to relations (17.175)! In the honor of the American thermodynamicist JOSIAH WILLARD GIBBS (1839–1903), they are called the **Gibbs relations**, see Fig. 17.12. They connect the internal energy (enthalpy), the pressure and specific volume with the entropy, with the absolute temperature acting as integrating denominator of the PFAFFIAN forms $(du + pdv)$ and $(dh - vdp)$, respectively. If ϑ and v are the independent

³⁴Monotonicity is important, since only with it the absolute temperature is a candidate of an objective measure of the sensation of heat and coldness. These arguments are essentially due to CARATHÉODORY [5].

thermodynamic variables, then one obtains the differential of the entropy in the form

$$ds = \frac{1}{T(\vartheta)} \left\{ \frac{\partial u}{\partial \vartheta}(\vartheta, v) d\vartheta + \left[\frac{\partial u}{\partial v}(\vartheta, v) + p(\vartheta, v) \right] dv \right\}. \quad (17.177)$$

If the thermal and caloric equations of state are known as functions of ϑ and v , then the entropy can be determined by integration along an arbitrary curve in the (ϑ, v) -plane. If s and v are the independent variables, Eq. (17.175)₁ implies

$$\left. \frac{\partial u}{\partial s} \right|_v = T(\vartheta), \quad \left. \frac{\partial u}{\partial v} \right|_s = -p. \quad (17.178)$$

The second of these relations shows once more that reversible processes in adiabatic systems are automatically also isentropic.

Since the thermodynamic temperature has universal character, this function can be used for the construction of the absolute temperature scale, independent of the thermal properties of the material. This has first been recognized by LORD KELVIN in 1848, and was worked out by him in the years 1850–1854.

Naturally, the absolute temperature $T(\vartheta)$ must be determined by using functions, which are materially dependent. It may be determined from the integrability condition of (17.177), viz.,

$$\frac{1}{T} \frac{dT}{d\vartheta} = \frac{d \ln T}{d\vartheta} = \frac{\frac{\partial p}{\partial \vartheta}}{\frac{\partial u}{\partial v} + p}, \quad (17.179)$$

which, after integration, becomes

$$T(\vartheta) = T(\vartheta_0) \exp \left\{ \int_{\vartheta_0}^{\vartheta} \frac{\frac{\partial p}{\partial \vartheta}(\bar{\vartheta}, v)}{\frac{\partial u}{\partial v}(\bar{\vartheta}, v) + p(\bar{\vartheta}, v)} d\bar{\vartheta} \right\} \quad (17.180)$$

with the constant of integration $T(\vartheta_0)$. Even though the integrand on the right-hand side depends on the empirical temperature *and* the specific volume, the result is only a function of ϑ ; that is to say, if one knows the internal energy and the pressure for one single material, then the absolute temperature is known except for a multiplicative factor. Alternatively, if one knows the absolute temperature, one may use Eq. (17.179) to evaluate on the basis of knowledge of $p(\vartheta, v)$ the dependence of the internal energy on the specific volume. One obtains

$$\frac{\partial u}{\partial v} = \frac{T}{dT/d\vartheta} \frac{\partial p}{\partial \vartheta} - p. \quad (17.181)$$

Differentiating both sides of this relation with respect to ϑ , one obtains a relation for the specific heat at constant volume as a function of the specific volume (and temperature),

$$\frac{\partial c_v}{\partial v} = \frac{\partial}{\partial \vartheta} \left(\frac{T}{dT/d\vartheta} \frac{\partial p}{\partial \vartheta} - p \right). \quad (17.182)$$

These relations corroborate the statement made already earlier, that *the Second Law of Thermodynamics constrains the form of the caloric equations insofar as they cannot be chosen independently of the thermal equation of state*. Indeed, owing to (17.181) and (17.182), the functional relation for the internal energy is largely predetermined.

Let us apply the above findings to an ideal and a VAN DER WAALS gas. For a caloric ideal gas we get

$$p = \frac{RT(\vartheta)}{v}, \quad u = u(\vartheta) = \int_{\vartheta_0}^{\vartheta} c_v(T(\bar{\vartheta})) d\bar{\vartheta} + u_0, \quad (17.183)$$

and so from (17.163)

$$ds = \frac{c_v(T(\vartheta))}{N(\vartheta)} \frac{dT}{d\vartheta} d\vartheta + \frac{RT(\vartheta)}{N(\vartheta)} \frac{dv}{v}. \quad (17.184)$$

The integrability condition of this GIBBS equation reads

$$\frac{\partial}{\partial v} \left(\frac{c_v(T(\vartheta))}{N(\vartheta)} \frac{dT}{d\vartheta} \right) = \frac{\partial}{\partial \vartheta} \left(\frac{RT(\vartheta)}{N(\vartheta)v} \right). \quad (17.185)$$

Because the expression on the left-hand side is independent of the specific volume, this term vanishes, and, consequently also the right-hand side, implying

$$\frac{T(\vartheta)}{N(\vartheta)} = \text{const.}, \quad T(\vartheta) = cN(\vartheta) \rightarrow T(\vartheta) = \bar{N}(\vartheta), \quad \text{for } c = 1. \quad (17.186)$$

Indeed, R is a constant and v is independent of ϑ . The integrating denominator is, therefore, identical to the ideal gas temperature (except for an unimportant factor, which only affects the temperature scale). One may now regard the absolute temperature, since any gas at sufficient dilution behaves like an ideal gas, as a measure for the empirical temperature, and set

$$T = \vartheta. \quad (17.187)$$

This was the proposal of LORD KELVIN, which is why T is also called the **Kelvin temperature**.

Alternatively, if one substitutes the thermal equation of state (17.183)₁ into relations (17.181), (17.182), one obtains $\partial u/\partial v = 0$ and $\partial c_v/\partial v = 0$. In other words: The internal energy of an ideal gas is indeed independent of the specific volume, as

already assumed in (17.183)₂. Moreover, (17.181) does not yield any further restrictions for the internal energy.

For a VAN DER WAALS gas we write (17.43) as

$$p = \frac{R_m T}{V_m - b} - \frac{a}{V_m^2} = \frac{R_m T}{\frac{M}{\rho} - b} - \frac{a}{M^2 \rho^2}, \quad (17.188)$$

where use has been made of the relation $V_m = M/\rho$. Equation (17.181) then implies

$$\frac{\partial u}{\partial v} = \frac{a}{V_m^2} = \frac{a}{M^2} \rho^2 \quad \rightarrow \quad \frac{\partial u}{\partial \rho} = -\frac{a}{M^2},$$

so that

$$\frac{\partial}{\partial \rho} \frac{\partial u}{\partial \vartheta} = \frac{\partial c_v}{\partial \rho} = \frac{\partial}{\partial \vartheta} \left(-\frac{a}{M^2} \right) = 0. \quad (17.189)$$

The specific heat of a VAN DER WAALS gas at constant density (specific volume) is therefore independent of the density, as for an ideal gas. One may, therefore write

$$\begin{aligned} u &= \int_{\vartheta_0}^{\vartheta} c_v(\bar{\vartheta}) \, d\bar{\vartheta} + \int_{\rho_0}^{\rho} \frac{\partial u}{\partial \bar{\rho}} \, d\bar{\rho} + u(\vartheta_0, \rho_0) \\ &= \int_{\vartheta_0}^{\vartheta} c_v(\bar{\vartheta}) \, d\bar{\vartheta} - \frac{a}{M^2} (\rho - \rho_0) + u(\vartheta_0, \rho_0) \\ &= \int_{\vartheta_0}^{\vartheta} c_v(\bar{\vartheta}) \, d\bar{\vartheta} - \frac{a}{M} \left(\frac{1}{V_m} - \frac{1}{V_m^0} \right) + u(\vartheta_0, V_m^0). \end{aligned} \quad (17.190)$$

These are two forms of the specific heat of a Van der Waals gas.

17.6.3 Generalizations for Non-adiabatic Systems

The results of the preceding section are based on two fundamental assumptions, first the **adiabaticity** of the considered systems and, second, the assumption that the systems are **simple** and their state, therefore, describable by two variables. The consequence of the irreversibility of the processes under such restricting conditions was that physically realizable processes must obey the inequality

$$du + pdv \geq 0 \quad \text{or} \quad \dot{u} + p\dot{v} \geq 0. \quad (17.191)$$

The existence of a state function *entropy* s and that of the absolute temperature T found expression in the GIBBS relation

$$\dot{s} = \frac{1}{T} (\dot{u} + p\dot{v}), \quad (17.192)$$

which relates the total differential of the entropy to those of the internal energy and specific volume, such that the absolute temperature acts as integrating denominator. The validity of (17.192) is a consequence of purely mathematical considerations paired with the additional requirement that the entropy is an additive quantity. The existence of an integrating denominator for the entropy as stated in (17.192) is, however, only compelling, if s depends at most on two variables; its material independence follows from the required additivity of s . It transpires that in extending the Second Law of Thermodynamics beyond adiabatic systems one necessarily needs other and perhaps additional postulates.

To motivate such a generalization let us consider a finite non-adiabatic (but still simple) system at rest, and assume temporarily that the GIBBS relation

$$\dot{S} = \frac{1}{T} (\dot{U} + p\dot{V}) \quad (17.193)$$

is still valid under such more general conditions. We shall interpret S in (17.193) as the entropy of the non-adiabatic system, U as its internal energy and V as its volume. T is the absolute temperature of which its existence is now pre-assumed (as its existence has only been proved for adiabatic systems).

Supposing that (17.193) is meaningful, we now combine it with the energy equation (First Law) for a system at rest, whence with

$$\dot{Q} + L = \dot{U} + p\dot{V}. \quad (17.194)$$

Here, \dot{Q} denotes the heating supplied to the system, L the working of the frictional forces, $-p\dot{V}$ the working of the pressure and \dot{U} the time rate of change of the internal energy. Combination of (17.193) and (17.194) yields

$$\frac{L}{T} = \dot{S} - \frac{\dot{Q}}{T}. \quad (17.195)$$

One form of the early forms of the Second Law of Thermodynamics was the statement $L \geq 0$ (the working of the frictional forces is non-negative), so that with $T \geq 0$ one also obtains

$$\dot{S} - \frac{\dot{Q}}{T} \geq 0 \quad \iff \quad \dot{S} \geq \frac{\dot{Q}}{T}. \quad (17.196)$$

The growth of the entropy in a non-adiabatic system is bounded from below by the quotient formed with the heating supplied to the system from the outside, \dot{Q} , and the absolute temperature, T , of the system.

If the system is adiabatic, then $Q = 0$, and (17.196) reduces to $\dot{S} \geq 0$, valid for adiabatic systems. If the process monitoring is reversible and no internal frictional working and, in particular, no internal heating exchanges are produced, then (17.196) holds with equality sign, so that $\dot{S} = Q/T$. Evidently, one has obtained a generalization of the formulation of the Second Law of Thermodynamics. However, more than a *plausible extension* is not obtained by (17.196), for to reach it, first, the validity of the GIBBS relation was *assumed*, second, the energy equation for simple systems *at rest* was used and, third, only homogeneous systems were considered. For an inhomogeneous system, (17.196) can further be generalized by dividing the system into a finite or infinite number of subsystems and requiring

$$\dot{S} - \int \frac{Q}{T} \geq 0, \quad (17.197)$$

owing to the additivity of the entropy. In (17.197), S is the total entropy of the system, \int is the integral over infinitesimally small sub-systems or the sum over finite sub-systems. The integral $\int(Q/T)$ can be interpreted as the entropy rate supplied to the system from the outside.

17.7 First Applications of the Second Law of Thermodynamics

In this section we first apply some classical examples, in which the Second Law is employed in the form (17.197). This analysis is then followed in Chap. 18 by the standard treatment of the formal entropy principle.

(a) Irreversibility of the heat transfer. Consider the system $A \cup B$ sketched in Fig. 17.50; it consists of two sub-systems A and B , which are separated by a wall, and is thought as a whole to be adiabatically closed. If the two subsystems are at rest, the heat transfer from system A to system B takes place without any production of frictional heat; under such conditions, the first law of thermodynamics, formulated for the total system reads

$$\dot{U}_{AUB} = Q_{AUB} = 0, \quad (17.198)$$

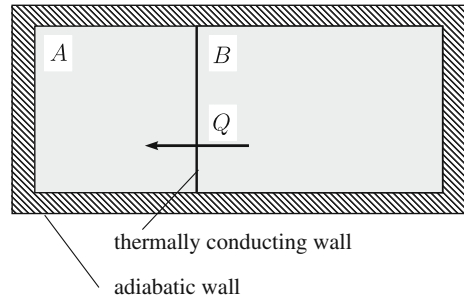
in which the heating supplied to the system vanishes because of the adiabatic isolation. If one now regards the system $A \cup B$ to be composed of the subsystems A and B , one may write

$$Q_A + Q_B = Q_{AUB} = 0 \implies Q_A = -Q_B = Q.$$

The heating supplied to sub-system A is withdrawn from sub-system B .

We suppose that the processes in each of the sub-systems A and B are performed reversibly. The second law (17.196) for the two sub-systems then reads

Fig. 17.50 Irreversibility of the heat transfer. In two systems A and B which are separated by a thermally conducting wall but are adiabatically isolated as a whole heat flows from the hotter system to the colder system



$$\dot{S}_A = \frac{Q_A}{T_A} = \frac{Q}{T_A}, \quad \dot{S}_B = \frac{Q_B}{T_B} = -\frac{Q}{T_B}. \quad (17.199)$$

Here, we have used the fact that the exchange of heating takes place only across the wall, which is common to the two sub-systems, whose temperatures are different from one another.

For system $A \cup B$ the heating exchange between the sub-systems A and B is an internal irreversible process, the whole system $A \cup B$ is, however, adiabatically closed, for which the Second Law was proved to have the form $\dot{S}_{AUB} \geq 0$. Owing to the additivity of the entropy and (17.199), we, thus have

$$\dot{S}_{AUB} = \dot{S}_A + \dot{S}_B = Q \left(\frac{1}{T_A} - \frac{1}{T_B} \right) \geq 0. \quad (17.200)$$

This implies

$$T_B \geq T_A \implies Q > 0,$$

$$T_B \leq T_A \implies Q < 0.$$

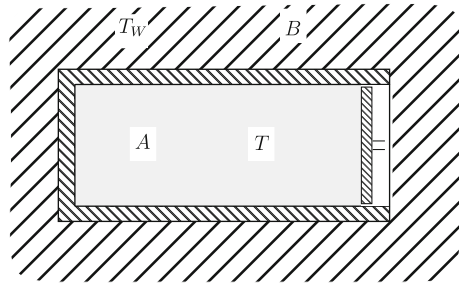
The heat flow, or better the heating transfer takes place for these systems from the hotter to the colder medium.

(b) Isothermal condensation of an ideal gas. Consider a cylinder, filled with an ideal gas that is embedded in an infinite heat bath of temperature T_w . Cylinder A and bath B together form an adiabatic system, see **Fig. 17.51**. If one assumes that the entropy change within the cylinder takes place with a reversibly conducted compression, then the entropy change is given by $dS_A = \frac{1}{T}(du + pdv)$ as for an adiabatic system. With the equations of state of an ideal gas, $u = \hat{u}(T)$, $p = RT/v$ one has

$$dS_A = mR \frac{dv}{v},$$

$$S_A^2 - S_A^1 = mR \ln \frac{v_2}{v_1} = \frac{Q_{1 \rightarrow 2}^{\text{rev}}}{T} < 0. \quad (17.201)$$

Fig. 17.51 Isothermal compression of an ideal gas. If the interior of cylinder A and environment B form an adiabatic system the compression of the ideal gas always yields $T \geq T_W$



m is the mass of the gas contained in the cylinder. In the above the difference of the entropies in the states 1 and 2 is negative because the volume is decreased by compression. Therefore, even though the difference of the entropy in cylinder A decreases, the Second Law of Thermodynamics is not necessarily violated, since for the adiabatic total system $A \cup B$ the inequality

$$(S_2 - S_1)_A + (S_2 - S_1)_B \geq 0 \quad (17.202)$$

must hold. Consider now system B ; by the reception of heat, see (17.201), its internal energy increases by the amount

$$(U_2 - U_1)_B = -Q_{1 \rightarrow 2}^{\text{rev}}, \quad (17.203)$$

and the entropy difference is given by

$$(S_2 - S_1)_B = -\frac{Q_{1 \rightarrow 2}^{\text{rev}}}{T_W} = \frac{|Q_{1 \rightarrow 2}^{\text{rev}}|}{T_W}. \quad (17.204)$$

In this case, the Second Law, thus, requires

$$|Q_{1 \rightarrow 2}^{\text{rev}}| \left\{ \frac{1}{T_W} - \frac{1}{T} \right\} \geq 0. \quad (17.205)$$

This inequality shows that condensation of an ideal gas must always lead to an increase of the temperature; moreover, the process is only isothermal, if it is conducted extremely slowly, for which $T = T_W$; then the entropy of the total system remains unchanged.

(c) Heat engines. Consider a heat engine, which extracts heat from a heat source and transforms it into working by some user, see **Fig. 17.52a**. Let us assume that all the heating can be transferred to the user. We shall prove that this is impossible, because it violates the Second Law of Thermodynamics.

We assume that the heat engine plus the heat source together constitute an adiabatic system for which the inequality

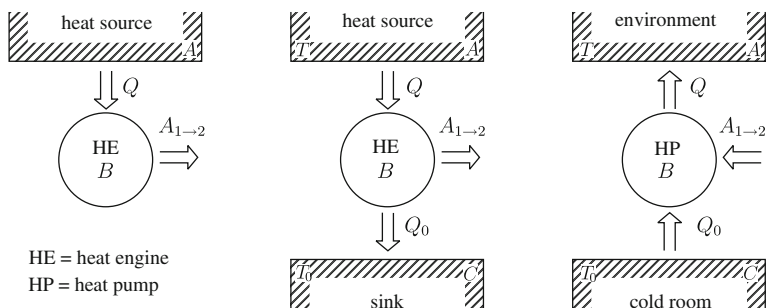


Fig. 17.52 Illustrating the functioning of a heat engine. **a** A machine, which does no more than draw energy (Q) from a source and deliver this as work to a user, violates the Second Law. **b** To be in conformity with the Second Law a certain amount of heat $Q_0 \leq Q$ is dissipated and brought to a sink-bath. This heat counts as being lost. **c** Withdrawal of some heat Q_0 from a cold room requires that some work A_{1-2} is provided to the system from outside

$$\Delta S_A + \Delta S_B \geq 0 \tag{17.206}$$

must hold; here, ΔS_A and ΔS_B are the entropy growths of the two partial systems in a **cyclic process**. For system B such a process is characterized by the fact that after completion of the process (or after the termination of a period) the system is in the same state as at the beginning. This means that $\Delta S_B = 0$; and it implies that the second law for system $A \cup B$ takes the form

$$\Delta S_A \geq 0. \tag{17.207}$$

With the definition of Q as shown in Fig. 17.52a, Q for system A is a heat loss, the heat supplied to system B by system A . Without any restriction the condition of the process in system A may be assumed to be reversible. This means that the Second Law for system A takes the form

$$\Delta S_A + \frac{Q}{T} = 0 \implies T \Delta S_A = -Q < 0.$$

We conclude

$$\Delta S_A \leq 0, \tag{17.208}$$

which is in conflict with (17.207). In other words: *A machine, which in a cyclic process does no more than withdraw energy from an energy reservoir and provide this energy to a user, is in conflict with the Second Law of thermodynamics.*

Apparently, a certain amount of heat must be dissipated to a bath of heat loss. If this heat loss is given by Q_0 , the **thermal efficiency** of a heat engine may be written as

$$\eta_{\text{th}} = \frac{A_{1 \rightarrow 2}}{Q} = \frac{Q - Q_0}{Q} = 1 - \frac{Q_0}{Q} < 1, \quad (17.209)$$

which, according to the Second Law of Thermodynamics must be smaller than unity.

The thermal efficiency of a heat engine is a *maximum*, if all processes are reversibly conducted. We shall now determine this optimal thermal efficiency by the assumption that the heat source is a bath with constant temperature T and that the heat Q_0 is lost to a bath with constant temperature T_0 , see Fig. 17.52b. The individual partial systems are denoted by A, B, C and the total system $A \cup B \cup C$ is assumed to be adiabatically closed. The Second Law for the total system then requires for a cyclic process

$$\begin{aligned} \Delta S_A + \Delta S_B + \Delta S_C &\geq 0, \\ \Delta S_B &= 0 \quad (\text{cyclic process}). \end{aligned} \quad (17.210)$$

Since the processes in the two systems A and C are assumed to be reversibly conducted (in order to achieve the optimal efficiency), the Second Law for these two systems reads

$$\begin{aligned} \Delta S_A &= -\frac{Q}{T}, \quad (Q > 0), \\ \Delta S_C &= \frac{Q_0}{T_0}, \quad (Q_0 > 0). \end{aligned} \quad (17.211)$$

Substitution into (17.210) yields

$$\frac{Q_0}{T_0} - \frac{Q}{T} \geq 0 \quad \Longrightarrow \quad \frac{Q_0}{Q} \geq \frac{T_0}{T}. \quad (17.212)$$

Alternatively, when ignoring the internal energy in system B , the balance of energy yields

$$A_{1 \rightarrow 2} = Q - Q_0. \quad (17.213)$$

Combination of (17.210) with (17.211) yields

$$\eta_{\text{th}} = \frac{A_{1 \rightarrow 2}}{Q} \leq \frac{T - T_0}{T}. \quad (17.214)$$

If all processes are reversibly conducted, then (17.210), (17.211) and (17.213) hold with equality sign, so that

$$\eta_C = \eta_{\text{th}}^{\text{rev}} = \frac{T - T_0}{T}. \quad (17.215)$$

The coefficient η_C is called the **Carnot factor** or the **Carnot efficiency**, according to its discoverer SADI CARNOT (1796–1832), see Fig. 17.5. It shows which fraction of the supplied heating can at most be transformed into mechanical power. It is the

larger, the higher the temperature T of the working system is and the lower the temperature T_0 is at which the heat is lost to the environment. If the source and sink temperatures are the same, then $\eta_C = 0$ and the heat engine is ineffective, or: *heat that is available at the temperature of the sink (environment) is thermodynamically worthless.*

The procedure described above can also be used for **heat pumps** and **cooling machines**. Such machines transfer heat from a ‘cooling room’ of low temperature T_0 to an environment (the outside of the cooling room at a higher temperature). According to the Second Law this is not possible by itself; one must via a heat pump, supply work or, better, power of working, L , see Fig. 17.52c.

If one regards the cooling aggregate C , the heat pump B and the surrounding environment A as an adiabatic system, and if the processes of systems A and C are reversibly conducted, then the Second Law yields for the different systems

$$\begin{aligned} \text{system } A \cup B \cup C : & \quad \Delta S_A + \Delta S_B + \Delta S_C \geq 0, \\ \text{system } A : & \quad \Delta S_A = \frac{Q}{T}, \\ \text{system } B : & \quad \Delta S_B = 0 \quad (\text{cyclic process}), \\ \text{system } C : & \quad \Delta S_C = -\frac{Q_0}{T_0}, \end{aligned}$$

from which by combination one deduces

$$\frac{Q}{T} - \frac{Q_0}{T_0} \geq 0 \quad \Longrightarrow \quad \frac{Q_0}{Q} \leq \frac{T_0}{T}. \quad (17.216)$$

Moreover, the First Law for system B yields

$$Q_0 - Q + A_{1 \rightarrow 2} = 0, \quad (17.217)$$

or after combination with (17.216)

$$\frac{A_{1 \rightarrow 2}}{Q} = 1 - \frac{Q_0}{Q} \geq \frac{T - T_0}{T} = \eta_C.$$

For a cyclically working heat pump, we thus obtain during a cycle

$$A_{1 \rightarrow 2} \geq \eta_C Q. \quad (17.218)$$

Therefore, the CARNOT efficiency indicates, which fraction of heat that is released by the heat pump must *at least* be provided by the power of working. With (17.218) we obtain

$$Q \leq \frac{1}{\eta_C} A_{1 \rightarrow 2}, \quad (17.219)$$

in which $(1/\eta_C)$ is called **degree of provisioning**. The formula says: At most the $(1/\eta_C)$ part of the supplied mechanical power can be provided as heating by the heat pump.

For a cooling machine, one is not interested in the heating Q that is provided, but the heating Q_0 that is removed. One then obtains with (17.218)

$$\frac{Q_0}{A_{1 \rightarrow 2}} = \frac{1}{\frac{Q}{Q_0} - 1} \leq \frac{T_0}{T - T_0} = \frac{T_0}{T} \frac{1}{\eta_C},$$

in which, coupled to (17.219), also the factor T_0/T of (17.216) appears.

The above examples demonstrate by and large the procedures taken by physicists and (mechanical) engineers in handling problems of heat engines, cooling machines and simple irreversible phenomena. Prior to the 1940s the science of thermodynamics had not yet reached the systematic approach of a field theory; this developed later. The 19th and early 20th century's thermodynamicists were occupied with the correct formulations of the First and Second Laws. This period followed by several decades of explorative applied (perhaps 'down to Earth') activities. With the development of the so-called theories of Irreversible and Rational Thermodynamics in the 1940s and 1960s two very flourishing periods brought mathematical and physical extensions to field theories, which will be introduced in the the next chapter.

References

1. Baehr, H.: *Thermodynamik*, 6th edn. Springer, Berlin (1988)
2. Boltzmann, L.: Über die mechanische Bedeutung des zweiten Hauptsatzes der Wärmetheorie. *Sitzungsberichte der Kaiserlichen Akademie der Wissenschaften* 53, S. 195–220 (19xy)
3. Born, M.: *The Born-Einstein Letters*. MacMillan, London (1971)
4. Bunstead, H.A., Van Name, R.G. (eds.): *The Scientific Papers of J. Willard Gibbs*, vol. 2. Dover, New York (1961)
5. Carathéodory, C.: Untersuchungen über die Grundlagen der Thermodynamik. *Math. Ann.* **67**, 355–386 (1909)
6. Carnot, N.L.S.: *Réflexions sur la puissance motrice du feu et sur les machines propres à développer cette puissance*. *Annales Scientifiques de l' Ecole Normale Supérieures*, Sér **2**, 393–457 (1872)
7. Carnot, N.S.L.: *Reflections on the Motive Power of Heat*. Transl: Thurston, Robert Henry (editor and translator). Wiley, New York (1890)
8. Carnot, N.L.S.: *Betrachtungen über die bewegende Kraft des Feuers und die zur Entwicklung dieser Kraft geeigneten Maschinen* (Übersetzer und Hrsg. Wilhelm Ostwald). Wilhelm Engelmann-Verlag (1892)
9. Clausius, R.: Über die bewegende Kraft der Wärme. *Annalen der Physik* **79**, 368–397, 500–524 (1850)
10. Clausius, R.: Über eine veränderte Form des zweiten Hauptsatzes der mechanischen Wärmetheorie. *Annalen der Physik und Chemie* **93**(12), 481–506 (1854)
11. Clausius, R.: On a modified form of the second fundamental theorem in the mechanical theory of heat. *Philos. Mag.* **4** **12**(77), 81–98 (1856)
12. Clausius, R.: Über die Wärmeleitung gasförmiger Körper. *Annalen der Physik* **115**, 1–57 (1862). doi:[10.1002/andp.18621910102](https://doi.org/10.1002/andp.18621910102)

13. Clausius, R.: Über verschiedene für die Anwendung bequeme Formen der Hauptgleichungen der mechanischen Wärmetheorie. *Annalen der Physik* **125**, 353–400 (1865). doi:[10.1002/andp.18652010702](https://doi.org/10.1002/andp.18652010702)
14. Cropper, W.H.: *The Road to Entropy Rudolf Clausius. Great Physicists: The Life and Times of Leading Physicists from Galileo to Hawking*, pp. 93–105. Oxford University Press, Oxford (2004). ISBN 978-0-19-517324-6
15. Duhem, P., Wiener, P.P.: *La Théorie Physique: Son Objet et sa Structure [The Aim and Structure of Physical Theory]*. Jules Vuillemin. Princeton University Press, Princeton (1954). ISBN 978-0-691-02524-7
16. Einstein, A.: *Investigations on the Theory of the Brownian Movement* (1905). Edited with notes by R. Fürth. Dover Publications, New York (1956)
17. Feynman, R.P., Leighton, R.B., Sands, M.: *The Feynman Lectures on Physics. Volume I: Mainly Mechanics, Radiation, and Heat*, 2nd edn. Addison-Wesley, Reading (2005)
18. Gibbs, J.W.: *Elementary Principles in Statistical Mechanics, Developed with Especial Reference to the Rational Foundation of Thermodynamics*. New York: Dover Publications (1960) [1902]
19. Joule, J.P.: On the heat evolved by metallic conductors of electricity, and in the cells of a battery during electrolysis. *Philos. Mag.* **19**, 260 (1841). doi:[10.1080/14786444108650416](https://doi.org/10.1080/14786444108650416)
20. Joule, J.P.: On the calorific effects of magneto-electricity, and on the mechanical value of heat. *Philos. Mag.* **3** **23**, 263, 347 & 435 (1843). doi:[10.1080/14786444308644766](https://doi.org/10.1080/14786444308644766)
21. Joule, J.P.: On the changes of temperature produced by the rarefaction and condensation of air. *Philos. Mag.* **3** **26**(174), 369–383 (1845). doi:[10.1080/14786444508645153](https://doi.org/10.1080/14786444508645153)
22. Joule, J.P.: ‘On the Mechanical Equivalent of Heat’. *Brit. Assoc. Rep.*, trans. Chemical Sect., p. 31, read before the British Association at Cambridge, June (1845)
23. Joule, J.P.: On the existence of an equivalent relation between heat and the ordinary forms of mechanical power. *Philos. Mag.* **3** **27**(179), 205–207 (1845). doi:[10.1080/14786444508645256](https://doi.org/10.1080/14786444508645256)
24. Joule, J.P.: On the mechanical equivalent of heat. *Philos. Trans. R. Soc. Lond.* **140**, 61–82 (1850). doi:[10.1098/rstl.1850.0004](https://doi.org/10.1098/rstl.1850.0004)
25. Lieb, E., Yngvarson, J.: The physics and mathematics of the second law of thermodynamics. [de.arXiv.org > cond-mat > arXiv:cond-mat/9708200](https://arxiv.org/abs/cond-mat/9708200) (1997)
26. Longley, W.R., Van Name, R.G. (eds.): *The collected works of J. Willard Gibbs*. New York: Longmans, Green and Company, 2 volumes (1928) Yale University Press, New Haven (1948, 1957)
27. Maxwell, J.C.: A dynamical theory of the electromagnetic field. *Philos. Trans. R. Soc. Lond.* **155**, 459–512 (1865)
28. Maxwell, J.C.: *A Treatise on Electricity and Magnetism*, vol. II. Clarendon Press, Oxford (1873)
29. Maxwell, J.C.: *A Treatise on Electricity and Magnetism*, vol. I. Clarendon Press, Oxford (1873)
30. Maxwell, J.C.: Van der Waals on the continuity of gaseous and liquid states. *Nature* **10**(259), 477–480 (1874). doi:[10.1038/010477a0](https://doi.org/10.1038/010477a0)
31. Maxwell, J.C.: *On the Stability of the Motion of Saturn’s Rings*
32. Maxwell, J.C.: *An Elementary Treatise on Electricity*. Clarendon Press, Oxford (1881)
33. Maxwell, J.C.: *Theory of Heat*. Longmans Green Co., London (1908)
34. Maxwell, J.C.: *The Scientific Papers of James Clerk Maxwell*, vol. I. Dover Publication, New York (1890)
35. Maxwell, J.C.: *The Scientific Papers of James Clerk Maxwell*, vol. II. University Press, Cambridge (1890)
36. Mayer, R.: Bemerkungen über die Kräfte der unbelebten Natur. *Annalen der Chemie und Pharmacie* **43**, 233 (1842) Engl. Translation: Mayer, J.R.: Remarks on the forces of inorganic nature. *Philos. Mag.* **4** **24**(162), 371–377 (1862)
37. Nernst, W.H.: Über die electromotorischen Kräfte, welche durch den Magnetismus in von einem Wärmestrom durchflossenen Metallplatten geweckt werden. *Annalen der Physik* **267**, 760–789 (1887)

38. Nernst, W.H.: Über die elektromotorische Wirksamkeit der Ionen. *Zeitschrift für Physik u. Chemie* **4**, 129 (1889)
39. Philibert, J.: One and a half century of diffusion: fick, Einstein, before and beyond. *Diffus. Fundam.* **4**, 6.1–6.19 (2006)
40. Planck, M.: *Treatise on Thermodynamics*. Ogg, A. (transl.). London: Longmans, Green & Co. (1903)
41. Planck, M.: Über den zweiten Hauptsatz der mechanischen Wärmetheorie. Ackermann, München (1879)
42. Planck, M.: Das Prinzip von der Erhaltung der Energie. Leipzig (1887) nach: Hoffmann: Max Planck. München S. 32 (2008)
43. Planck, M.: Gegen die neue Energetik. *Annalen der Physik* **57**, 72–78 (1896). doi:[10.1002/andp.18962930107](https://doi.org/10.1002/andp.18962930107)
44. Pogliani, L., Berberan-Santos, M.-N.: Constantin Carathéodory and the axiomatic thermodynamics. *J. Math. Chem.* **28**, 1–3 (2000)
45. Truesdell, A.C., Muncaster, R.G.: *Fundamentals of Maxwell's Kinetic Theory of a Simple Monatomic Gas, Treated as a Branch of Rational Mechanics*, 593 pp. Academic Press, New York (1980)
46. Van der Waals, J.D.: Over de Continuïteit van den Gasen Vloeïstoftoestand (On the continuity of the gas and liquid state). Ph.D. thesis, University Leiden, The Netherlands (1873)
47. Wilson, E.B.: *Vector Analysis. A Text-book for the Use of Students. Founded upon the Lectures of J.W. Gibbs*. Yale University Press, New Haven (1901)

Chapter 18

Thermodynamics—Field Formulation

Abstract This chapter extends and applies the concepts of Chap. 17 to continuous material systems. The Second Law is written in global form as a balance law of entropy with flux, supply and production quantities, which can be written in local form as a differential statement. The particular form of the Second Law then depends upon, which postulates the individual terms in the entropy balance are subjected to. When the entropy flux equals heat flux divided by absolute temperature and the entropy-production-rate density is requested to be non-negative, the entropy balance law appears as the CLAUSIUS–DUHEM inequality and its exploitation follows the axiomatic procedure of open systems thermodynamics as introduced by BERNARD COLEMAN and WALTER NOLL. When the entropy flux is left arbitrary but is of the same function class as the other constitutive relations and the entropy supply rate density is identically zero, then the entropy inequality appears in the form of MÜLLER. In both cases, the second law is expressed by the requirement that the entropy-production-rate density is non-negative, but details of the exploitation of the second law in the two cases are subtly different from one another. For standard media such as elastic and/or viscous fluids the results are the same. However, for complex media they may well differ from one another. Examples illustrate the procedures and results.

Keywords Entropy balance law · Thermodynamic process—equilibrium · CLAUSIUS–DUHEM inequality · MÜLLER’S entropy principle · Exploitation of the entropy principle · Absolute/empirical temperature · Specific heats of ideal gasses · Hyperbolic heat conduction equation

List of Symbols

Roman Symbols

\mathcal{B}	Body, bodily region
$\partial\mathcal{B}$	boundary of \mathcal{B}
c_v	Specific heat at constant volume
c_p	Specific heat at constant pressure
\mathbf{D}	Strain rate tensor, stretching tensor
$f _E$	Value of f in thermodynamic equilibrium

\mathbf{f}	Specific body force
$\llbracket f \rrbracket = f^+ - f^-$	Jump of f across a surface, where f^+ and f^- are the values of f on the positive/negative sides of the surface
$g = p/\rho - Ts$	Free enthalpy = GIBBS free energy
g, \mathbf{g}	Specific body force, gravity vector
$h = u + p/\rho$	Specific enthalpy per unit mass
$\mathbf{L} = \text{grad } \mathbf{v}$	Spatial velocity gradient
M	Mole mass
\mathbf{n}	Unit normal vector on a surface (generally $\partial\mathcal{B}$)
p	Pressure
Q	Heat supply to a (sub)system
q	Specific energy supply per unit mass
\mathbf{q}	Heat flux vector
q_i	Coefficient of the isotropic representation of \mathbf{q} as isotropic function
R	Gas constant of an ideal gas
$R_m = RM$	Universal gas constant
S	Total entropy of a thermodynamic system
s	Specific entropy per unit mass
T	Absolute (KELVIN) temperature
$\mathbf{t} = \mathbf{t}^R - p\mathbf{1}$	CAUCHY stress tensor
$\mathbf{t}^R, \mathbf{t}^E$	Frictional or extra CAUCHY stress tensor
$v = 1/\rho$	Specific mass
\mathbf{v}	Velocity vector
z^s	Specific entropy supply

Greek and Miscellaneous Symbols

α	Thermal expansion coefficient
β	Isochoric stress coefficient
Γ	(Total) dissipation (rate) per unit volume
η	Dynamic shear viscosity
κ	Coefficient in the stress-stretching relation of the REINER–RIVLIN fluid
λ	Second Lamé constant of the viscosity
Λ^ρ	LAGRANGE parameter for the mass balance equation
Λ^ε	LAGRANGE parameter for the energy equation
ρ	Mass density
ϕ_1	Coefficient of the isotropic representation of ϕ as isotropic function
ϕ	Specific entropy flux
Ψ	Symbol for an unspecified constitutive variable
$\psi = u - Ts$	HELMHOLTZ free energy
Π^s, π^s	Total/specific entropy production of a thermodynamic system
$\Theta = \Theta(\theta)$	Absolute (or KELVIN) temperature

θ	Empirical temperature
κ_T	Isobaric compressibility
κ_s	Adiabatic compressibility
$\kappa = c_p/c_v$	Ratio between c_p and c_v for an ideal gas
τ	Characteristic time in the generalized heat conduction equation (see (18.163))
$\Lambda(\theta, \dot{\theta})$	Universal coldness function in a theory with $\dot{\theta}$ as an independent constitutive variable
$1/\Lambda(\theta, 0) = T(\theta)$	Absolute (KELVIN) temperature

This chapter comprises a direct continuation of the formulation of the Second Law of Thermodynamics of the last chapter, but the focus is now on field formulations and the exploitation of two popular forms of the Second Law in this context. It will be demonstrated that field theoretical formulations are well advanced to the extent that the mathematical procedures to exploit the Second Law are well established, and inferences can fairly routinely be obtained, provided the mathematical complexities can be mastered. Scrutiny of the subtle differences of the two formulations of the Second Law, however, also show that scientists have still not agreed on a final common form of the Second Law. Whereas for simple physical situations the different formulations of the Second Law generate identical results, this may not be so for relatively complex situations. This then implies that the ultimate Second Law of Thermodynamics has still not been found and, perhaps may never be found.

18.1 The Second Law of Thermodynamics for Continuous Systems

We now return to the entropy inequality (17.197) in the last chapter.

$$\dot{S} - \int \frac{Q}{T} \geq 0, \quad (18.1)$$

in which S is the total entropy of the system. \int is the integral over (infinitesimal) subsystems. The integral $\int(Q/T)$ can be interpreted as the entropy rate supplied to the system from the outside.

To formalize the imbalance (18.1) somewhat for material bodies, we now define

$$\begin{aligned} S &:= \int_{\mathcal{B}} \rho s \, dV, \\ \int \frac{Q}{T} &:= - \int_{\partial \mathcal{B}} \phi \cdot n \, dA + \int_{\mathcal{B}} \rho z^s \, dV, \\ \Pi^s &:= \int_{\mathcal{B}} \rho \pi^s \, dV, \end{aligned} \quad (18.2)$$

and combine these to the following balance law

$$\frac{d}{dt} \int_{\mathcal{B}} \rho s \, dV = - \int_{\partial \mathcal{B}} \boldsymbol{\phi} \cdot \mathbf{n} \, dA + \int_{\mathcal{B}} \rho (z^s + \pi^s) \, dV. \quad (18.3)$$

The quantity s is called the **specific entropy** per unit mass; $\boldsymbol{\phi}$ is called **entropy flux**, z^s **specific entropy supply** and π^s **specific entropy production**. With the identifications

$$\boldsymbol{\phi} = \frac{\mathbf{q}}{T}, \quad z^s = \frac{q}{T}, \quad (18.4)$$

which are obviously motivated by (18.1), the imbalance

$$\Pi^s \geq 0 \quad (18.5)$$

then generates inequality (18.1). *The Second Law of Thermodynamics corresponds in this form to the statement that thermodynamic processes are physically only possible if the entropy production is non-negative at all times.* This generalization calls for the following remarks:

- The above inequality (18.5) does not suggest, how it could be analytically applied. This procedure still needs to be explained and defined. Indeed, for the motivation of (18.5) several, not at all trivial, facts of simple adiabatic systems were used without verifying their validity in the general case.
- We used unquestioned the following identifications

$$\begin{aligned} \text{entropy flux} &= \frac{\text{heat flux}}{\text{absolute temperature}} : \quad \boldsymbol{\phi} = \frac{\mathbf{q}}{T}, \\ \text{entropy supply} &= \frac{\text{heat supply}}{\text{absolute temperature}} : \quad z^s = \frac{q}{T}. \end{aligned} \quad (18.6)$$

- The total supply of entropy to the body \mathcal{B} , $\int (Q/T)$ is composed of the total entropy flow across the boundary $\partial \mathcal{B}$ of \mathcal{B} (the surface integral) and the bulk entropy supply (integral over the volume of the body \mathcal{B}). Moreover, the existence of the absolute temperature is unquestioned as is the (non-equilibrium) entropy. For simple adiabatic systems, the latter is only uniquely defined once the universality of the integrating denominator of the PFAFFIAN form $du + p \, dv$ was established.
- Inequality (18.5) is a global formulation of the Second Law of Thermodynamics, valid for the body \mathcal{B} as a whole, based on the global entropy balance (18.3). If one considers differentiable thermodynamic processes, then the REYNOLDS transport theorem can be used on the left-hand side of (18.3),

$$\frac{d}{dt} \int_{\mathcal{B}} \rho s \, dV = \int_{\mathcal{B}} \left\{ \frac{\partial(\rho s)}{\partial t} + \text{div}(\rho s \mathbf{v}) \right\} dV = \int_{\mathcal{B}} \rho \frac{ds}{dt} dV$$

and the divergence theorem may be employed in the surface integral,

$$\int_{\partial\mathcal{B}} \boldsymbol{\phi} \cdot \mathbf{n} \, dA = \int_{\mathcal{B}} \operatorname{div} \boldsymbol{\phi} \, dV,$$

so that

$$\int_{\mathcal{B}} (\rho \dot{s} + \operatorname{div} \boldsymbol{\phi} - \rho (z^s + \pi^s)) \, dV = 0. \quad (18.7)$$

As required already for the balance laws of mass, momentum and energy, Eq. (18.7) is thought to be valid for any material part of the body \mathcal{B} , also infinitely small ones, so that

$$\rho \dot{s} + \operatorname{div} \boldsymbol{\phi} - \rho (z^s + \pi^s) = 0 \quad (18.8)$$

can be deduced, an equation from which (18.6) implies

$$\rho \dot{s} + \operatorname{div} \frac{\mathbf{q}}{T} - \frac{\rho q}{T} = \rho \pi^s. \quad (18.9)$$

The Second Law of Thermodynamics, thus finds in the local form its expression in the inequality

$$\pi^s \geq 0, \quad (18.10)$$

which must hold for all possible physical processes of a continuous system.

- Combining (18.8), (18.10) and (18.9), (18.10) yield the imbalances

$$\begin{aligned} \text{(i)} \quad & \rho \dot{s} + \operatorname{div} \boldsymbol{\phi} - \rho z^s \geq 0, \\ \text{(ii)} \quad & \rho \dot{s} + \operatorname{div} \frac{\mathbf{q}}{T} - \frac{\rho q}{T} \geq 0. \end{aligned} \quad (18.11)$$

The first of these is weaker than the second, because nothing specific is assumed about the entropy flux vector and the entropy supply. The second imbalance is more restrictive, since the specifications (18.6) have been employed. The imbalances (18.11) are called **local entropy inequalities** and (18.11)₂ is known as **Clausius–Duhem Inequality**¹; in this inequality the entropy flux and entropy supply are expressed in terms of energy quantities, the heat flux and the energy supply (radiation) and the temperature.

In the motivation of the Second Law of Thermodynamics above (either in its global, (18.5), or local, (18.11), form), we only said that one of these inequalities must be fulfilled, if a thermodynamic process should be physically possible. We shall now make the requirement more concrete. To this end it is, first, necessary to precisely

¹For biographies of CLAUDIUS and DUHEM, see Figs. 17.8 and 17.16, respectively.

define a **thermodynamic process** and, second to clarify under what conditions such processes are physically possible (realizable).

Recall that it is the **goal of thermodynamics** to determine in the body \mathcal{B} , which is exposed to external driving mechanisms, the motion, temperature distribution, etc.,—briefly all field quantities that have been introduced to describe the physical processes in \mathcal{B} —as functions of space and time. To this end, the physical conservation laws of mass, linear momentum, (angular momentum)² and energy must be fulfilled for all time; for only such processes are physically possible. As we have seen already when introducing these laws, the number of physical field variables that arise in these conservation laws, is much larger, in general, than the number of independent equations, which is obtained from these balance laws. Hence, there are, in general, infinitely many field distributions for the physical quantities, by which the conservation laws can be fulfilled. Consequently, constraint equations must be introduced. In other words, some field variables must be expressed in terms of other field variables, until the number of independent fields yields a system of equations, which is at least principally uniquely integrable or solvable. These equations, which relate the field variables, are different for different materials; they are known as **material** or **constitutive equations**. Examples of such material statements are the thermal and caloric equations of state, e.g.,

$$p = \hat{p}(T, v), \quad u = \hat{u}(T, v), \quad (18.12)$$

or the stress-stretching relation for viscous fluids,

$$\mathbf{t}^R = \lambda(\text{tr}\mathbf{D})\mathbf{1} + 2\eta\mathbf{D} + \kappa\mathbf{D}^2, \quad (18.13)$$

see Eq.(7.14). In these equations, $v = 1/\rho$ and $\mathbf{D} = \text{symgrad } \mathbf{v}$. Incidentally, the Second Law in the form of one of the entropy principles will show that the thermal, $p = \hat{p}(T, v)$, and caloric, $u = \hat{u}(T, v)$, equation of state cannot be independently selected.

The balance laws of mass, momentum and energy have the forms

$$\begin{aligned} \frac{d\rho}{dt} + \rho \text{div } \mathbf{v} &= 0, \\ \rho \frac{d\mathbf{v}}{dt} &= \text{div } \mathbf{t} + \rho \mathbf{f}, \\ \rho \frac{du}{dt} &= -\text{div } \mathbf{q} + \text{tr}(\mathbf{t}\mathbf{D}) + \rho q. \end{aligned} \quad (18.14)$$

Here, $\rho, \mathbf{v}, \mathbf{t}, \mathbf{f}$ are the density, velocity, CAUCHY stress tensor and specific body force; u, \mathbf{q}, q and \mathbf{D} are the internal energy, heat flux vector, heat radiation and $\mathbf{D} = \frac{1}{2}(\mathbf{L} + \mathbf{L}^T)$, where $\mathbf{L} = \text{grad } \mathbf{v}$, is the stretching tensor or the tensor of strain rate. The

²The law of angular momentum says that the CAUCHY stress tensor is symmetric (see Sect.3.5, Eq.(3.276) and, thus, is often not mentioned.

reader is advised to clearly scrutinize the content of these equations; they have been discussed already earlier.³ Equations (18.14) constitute together five scalar relations, which in a body must be satisfied by the fields ρ , \mathbf{v} , \mathbf{t} , u , \mathbf{q} and \mathbf{f} , q . Commonly, the specific body force \mathbf{f} and the radiation q are known as quantities, which are supplied to the body from the outside; moreover, \mathbf{t} is symmetric, $\mathbf{t} = \mathbf{t}^T$ to be in conformity with the balance of angular momentum. Thus, one has 14—and if one also adds the temperature T —15 unknown field quantities; of these, $15 - 5 = 10$ must be functionally expressed in terms of 5 fields. If one regards density ρ , velocity \mathbf{v} and (absolute) temperature T as the independent fields, then the remaining free fields must be expressed as functionals of these. For instance, one may consider a fluid, of which internal energy, stress tensor and heat flux vector are functions of the density, temperature, temperature gradient and stretching tensor, viz.,

$$\begin{aligned} u &= \hat{u}(\rho, T, \text{grad}T, \mathbf{D}), \\ \mathbf{t} &= \hat{\mathbf{t}}(\rho, T, \text{grad}T, \mathbf{D}), \\ \mathbf{q} &= \hat{\mathbf{q}}(\rho, T, \text{grad}T, \mathbf{D}). \end{aligned} \tag{18.15}$$

A material, which obeys these constitutive relations, is called a **heat conducting compressible viscous fluid**. One sees that the functions $\hat{u}(\rho, T, \text{grad}T, \mathbf{D})$, etc., are indeed depending on ρ , T and \mathbf{v} , partly via spatial derivatives of these. Relations (18.15) also contain generalizations of the thermal and caloric equations of state; indeed, they postulate an experimental energy relation between the internal energy and the pressure (the latter via the stress tensor \mathbf{t} , but now, apart from the density ρ (or the specific volume $v = 1/\rho$) and the temperature T also containing additional variables. With these preparations we are now in the position, to exactly lay down the definition of thermodynamic processes.

Definition 18.1

- Every prescription of functions $\rho = \rho(\mathbf{x}, t)$, $\mathbf{v} = \mathbf{v}(\mathbf{x}, t)$, $\mathbf{t} = \mathbf{t}(\mathbf{x}, t)$, $u = u(\mathbf{x}, t)$, $\mathbf{q} = \mathbf{q}(\mathbf{x}, t)$ as well as $\mathbf{f} = \mathbf{f}(\mathbf{x}, t)$, $q = q(\mathbf{x}, t)$ with $\mathbf{x} \in \mathcal{B}$ and $t \in [0, \infty)$, which satisfy the balance laws (18.14), is called a **thermodynamic process**.
- If this prescription is also consistent with the material equations, e.g., (18.15), then the process is called an **admissible thermodynamic process**.

³The mass balance is discussed in Sect. 3.2 and is e.g. given in Eqs. (3.44) and (3.45). The momentum equation is discussed in Sects. 3.3 and 7.1, all in Vol. 1. In its form (18.14)₂ this equation arises in (7.5). The energy equation (18.14)₃ is given also in (17.85), in which the CauchyCAUCHY stress is written as $\mathbf{t} = -p\mathbf{1} + \mathbf{t}^R$, so that

$$\rho \frac{du}{dt} = -\text{div} \mathbf{q} - p \text{div} \mathbf{v} + \text{tr}(\mathbf{t}^R \mathbf{D}) + \rho q.$$

The balance laws together with the constitutive relations define the **field equations** of which solutions for the considered material build the admissible thermodynamic processes.

In this connection, the following remarks are in order:

- When postulating the constitutive relations, e.g., (18.15), one is fairly free with the choice of the independent variables. Whether additional space or time derivatives of the density, temperature and velocity vector should or must be introduced, depends upon whether experiments suggest these. (One could, for instance, also introduce additionally $\text{grad } \rho$ and \dot{T} , etc., as independent variables.)
- The kind and number of independent constitutive variables that arise in a material equation, *define* the material class; at the present stage there is no reason to include in a constitutive equation a particular physical variable and to omit this variable in another one. For instance, one could write the constitutive relation for the internal energy instead as in (18.15)₁ as $u = \hat{u}(\rho, T)$ and leave \mathbf{t} , \mathbf{q} as stated in (18.15)_{2,3}. We shall not do this and take the position that such possible reductions ought to be *proven*. We shall lay down this working rule as follows:

Rule of aequi presence *When postulating material equations, all dependent constitutive variables are supposed to depend on the same number of independent variables.*

With this rule of aequipresence a set of independent materials defines a *particular class of materials*.

- In postulating rules such as (18.15), constitutive relations for a material point at position \mathbf{x} are defined by functionals at the same point \mathbf{x} and same time t . This means that variations in the independent constitutive variables are only taken into account via higher order space and/or time derivatives, thought to be evaluated at position \mathbf{x} and time t . This is expression of the fact that such spatial variations are only taken into account in the closest vicinity of the point \mathbf{x} and not at $\mathbf{y} \neq \mathbf{x}$ or $\tau \neq t$ farther away from \mathbf{x} and t . The restriction to this rule expresses the notion of *locality* in space and time. If such functionals account for the material behavior at times τ for all $\tau < t$, one speaks of *hereditary effects* that are accounted for, but maintains the locality principle for the spatial dependence. Purely spatial locality is generally simply referred to as ‘locality’. In this chapter and throughout the remainder of the book we restrict ourselves to the strict rule of locality; recall, however, Chap. 16.
- Apart from the rules of aequipresence and locality one must in the postulation of constitutive relations also observe additional other rules. For instance, it is reasonable to request that the constitutive equations of a material are *independent of the observer*; in other words, two independent observers, who move relative to one another, should for one and the same material formulate constitutive relations, which are independent of the relative motion of the observers. This rule is called the **rule of material objectivity**, or the **rule of material frame indifference**. The mathematical formulation of this rule is beyond the goals of this book. The rule, however, has been observed in (18.15). It says for a heat conducting viscous

fluid e.g. that the full spatial velocity gradient cannot be part of the independent constitutive variables; it is only the symmetric part $\mathbf{D} = \frac{1}{2}(\mathbf{L} + \mathbf{L}^T)$, $\mathbf{L} = \text{grad } \mathbf{v}$ that is permissible as an independent variable. These rules have been tacitly observed in (18.15).⁴

- The postulation of constitutive relations, as introduced so far, does not employ the Second Law of Thermodynamics; similarly, the admissible thermodynamic processes define a whole set of solutions of the field equations, of which the number exceeds the number of the physically possible ones (which satisfy the Second Law of Thermodynamics). It is time that we describe more closely the role that is played by the Second Law. Apparently, its role is to constrain the number of solutions of the field equations. More explicitly, *the Second Law is regarded as a law, which restricts the postulated material equations or simplifies them such that the entirety of the solutions of the field equations obtained with the thus constrained constitutive relations only consists of the physically possible ones.* In other words, the Second Law is primarily a restriction of the material equations, and only secondarily of the processes.

18.2 Two Popular Forms of the Entropy Principle

In today's thermodynamic research there exist a number of approaches by which the Second Law of Thermodynamics is axiomatized. We may even say that these different axiomatic systems form separate thermodynamic schools, whose members defend their views against each other, sometimes rather vividly. In our opinion the only objective way to select the best axiomatics is to judge the results against experiments. Here, we present two entropy principles, which generate identical results for simple single constituent continuous systems, but may deviate in their results for structured continua. These are

- (i) The CLAUSIUS–DUHEM inequality applied to open systems, and
- (ii) The entropy principle of INGOMÜLLER, which applies to closed as well as open systems.

In the approach using the CLAUSIUS–DUHEM inequality the absolute temperature T is taken over from thermostatics. Its existence and form are unquestioned. Moreover, for the entropy supply rates ϕ and z^s a-priori estimates are postulated ($\phi = \mathbf{q}/T$, $z^s = q/T$). In this way a direct link between the Second Law and the physical conservation laws (balances of mass, momenta, energy) is established.

By contrast, in the entropy principle of MÜLLER, the absolute temperature is not introduced, but its existence must be proved, or it must be replaced by a more general concept of 'universal' measure of coldness. The link between the Second Law and

⁴The formal theory of the postulation of material equations is treated in books of continuum thermodynamics, e.g., I. MÜLLER [25], K. HUTTER and K. JÖHNK [15], M.E. GURTIN [10], P. CHADWICK [2], A.J.M. SPENCER (1929–2008) [29], and others. The abstract formulation goes back to WALTER NOLL (1925–) [27].

the remaining physical conservation laws is established without a priori estimates for ϕ and z^s ; instead, ϕ is postulated to be a constitutive variable of the same class as all other material field quantities within the context of aequipresence. Moreover, z^s is determined by stating that external field quantities will not influence the constitutive behavior.⁵

18.2.1 Entropy Principle 1: Clausius–Duhem Inequality

1. In a body, whose thermodynamic processes are described by the balance laws of mass, linear and angular momenta, energy and material equations for the internal energy, the stress tensor and the heat flux vector, there exists an additive (extensive) quantity, called **entropy** s , for which the balance law

$$\rho \dot{s} = -\operatorname{div} \frac{\mathbf{q}}{T} + \frac{\rho q}{T} + \rho \pi^s \quad (18.16)$$

holds.

2. The entropy is a material quantity, which, according to the rule of aequipresence, depends on the same independent constitutive quantities as the material equations for the internal energy, stress tensor and heat flux vector.
3. The entropy flux is also a material quantity and is given by the a priori relation

$$\text{entropy flux} = \frac{\text{heat flux}}{\text{absolute temperature}}. \quad (18.17)$$

4. Similarly,

$$\text{entropy supply} = \frac{\text{energy supply}}{\text{absolute temperature}}. \quad (18.18)$$

5. The entropy production π^s is for all thermodynamic processes, i.e., all solutions of the field equations non-negative,

$$\pi^s \geq 0 \quad \text{for all thermodynamic processes.} \quad (18.19)$$

In this entropy principle the existence of the absolute temperature, which is strictly non-negative is a priori assumed; the Second Law finds its expression in the satisfaction of the CLAUSIUS–DUHEM inequality. In comparison to the Second Law as used in the formulation for adiabatic systems,⁶ in which the absolute temperature is

⁵For expositions on different formulations of the Second Law, see Hutter (1977) [14], HUTTER and WANG (2003) [16].

⁶The exact definitions of the axioms for adiabatic systems from which the existence of the absolute (universal) temperature follows, is given by CARATHÉODORY (1873–1950) in 1909 [1]. For a biography of CARATHÉODORY see Fig. 17.15.

a *derived* quantity, this is a loss in rigor. A more general entropy principle should find its extension in exactly this point.

In the following it will be demonstrated how the entropy principle is exploited for a heat conducting viscous fluid. Combining (18.16) and (18.19) shows that the CLAUSIUS–DUHEM *inequality*

$$\rho \dot{s} + \operatorname{div} \left(\frac{\mathbf{q}}{T} \right) - \frac{\rho q}{T} \geq 0 \quad (18.20)$$

must hold for all thermodynamic processes of all heat conducting viscous fluids. In other words, (18.20) must hold for all solutions of the balance laws (18.14), viz.,

$$\begin{aligned} \dot{\rho} + \rho \operatorname{div} \mathbf{v} &= 0, \\ \rho \dot{\mathbf{v}} &= \operatorname{div} \mathbf{t} + \rho \mathbf{f}, \\ \rho \dot{u} &= -\operatorname{div} \mathbf{q} + \operatorname{tr}(\mathbf{tD}) + \rho q, \end{aligned} \quad (18.21)$$

as well as the material equations (18.15) or

$$\begin{aligned} u &= \hat{u}(\rho, T, \operatorname{grad} T, \mathbf{D}), & \mathbf{t} &= \hat{\mathbf{t}}(\rho, T, \operatorname{grad} T, \mathbf{D}), \\ \mathbf{q} &= \hat{\mathbf{q}}(\rho, T, \operatorname{grad} T, \mathbf{D}), & s &= \hat{s}(\rho, T, \operatorname{grad} T, \mathbf{D}). \end{aligned} \quad (18.22)$$

Here, we requested as in item (2) of the entropy principle that the entropy density, s , is given by a constitutive relation that is of the same class as the other constitutive quantities. In particular, the rule of aequipresence was employed, according to which the number of independent variables in the postulated material equations of all constitutive variables is the same, here for u , \mathbf{t} , \mathbf{q} , s . The external forces $\rho \mathbf{f}$ and the heat supplies (radiation) ρq are never treated as independent constitutive variables. They are assumed to be externally provided sources, which can arbitrarily be prescribed.⁷ To be precise, the exploitation of the CLAUSIUS–DUHEM inequality is performed on an *open* thermodynamic system. This view was first clearly spoken out by BERNARD D. COLEMAN and WALTER NOLL.⁸

If one eliminates with the aid of the energy equation (18.21)₃ the radiation q from the CLAUSIUS–DUHEM inequality, then the **dissipation inequality**

⁷The supposition that the external forces and heat supplies can take any value we please, is actually so extraordinary that serious natural philosophers may justly question its validity. Contemplating on this postulate to the very end, it means that we can shift in our thoughts the body in the universe to any position guaranteeing satisfaction of the momentum and energy equation even if, in reality the body might ‘evaporate’ or being destroyed because of the extreme sources to which it is exposed.

⁸BERNARD D. COLEMAN (1930–) and WALTER NOLL (1925–) were the leading researchers in the 60s and 70s of the 20th century in the mathematical formulation of thermodynamic models based on the CLAUSIUS–DUHEM inequality and the exploitation of the Second Law of Thermodynamics. They wrote a great number of relevant articles, individually and together, which inspired many scientists for follow-up articles. This movement led to the science what is called *Rational Thermodynamics*, see e.g. [3, 4, 11, 30, 31] and many books on continuum thermodynamics. This book intends to give a flavor of this movement.

$$\Gamma := \rho(T\dot{s} - \dot{u}) - \frac{\mathbf{q} \cdot \text{grad } T}{T} + \text{tr}(\mathbf{tD}) \geq 0$$

is obtained, in which the quantity Γ will be denoted as **(specific) dissipation**. If in this inequality we next substitute the material equations (18.22) and perform the indicated differentiation processes (using the chain rule of differentiation where needed), the dissipation inequality takes the form

$$\begin{aligned} \Gamma = \rho \left\{ \left(T \frac{\partial \hat{s}}{\partial \rho} - \frac{\partial \hat{u}}{\partial \rho} \right) \dot{\rho} + \left(T \frac{\partial \hat{s}}{\partial T} - \frac{\partial \hat{u}}{\partial T} \right) \dot{T} + \text{tr} \left[T \left(\frac{\partial \hat{s}}{\partial \mathbf{D}} - \frac{\partial \hat{u}}{\partial \mathbf{D}} \right) \dot{\mathbf{D}} \right] \right. \\ \left. + \left(T \frac{\partial \hat{s}}{\partial \text{grad } T} - \frac{\partial \hat{u}}{\partial \text{grad } T} \right) \cdot (\text{grad } T) \right\} - \frac{\hat{\mathbf{q}} \cdot \text{grad } T}{T} + \text{tr}(\hat{\mathbf{t}}\mathbf{D}) \geq 0, \quad (18.23) \end{aligned}$$

in which the symbol $(\hat{\cdot})$ means that in the corresponding variables the functional dependencies (18.22) are thought to be substituted. Inequality (18.23) must be satisfied as an identity for all thermodynamic processes, i.e., all solutions of the field equations (18.21) (if one thinks all the material equations (18.22) to be substituted). As already mentioned, we treat $\rho \mathbf{f}$ and ρq as free source terms. This means that for any values of ρ , T , $\text{grad } T$ and \mathbf{D} as well as possible gradients and time derivatives of these variables that may arise, the momentum equations (18.21)₂ and energy equation (18.21)₃ can always be fulfilled. One simply must choose for $\rho \mathbf{f}$ and ρq values which make (18.21)_{2,3} to be fulfilled. Otherwise stated, these equations do not constitute constraint conditions for the identical satisfaction of inequality (18.23).⁹ On the other hand, $\dot{\rho}$ in (18.23) cannot be arbitrarily selected, since the continuity equation (18.21)₁ must hold, from which one obtains

$$\dot{\rho} = -\rho \text{div } \mathbf{v} = -\rho \text{tr}(\mathbf{D}) = -\rho \text{tr}(\mathbf{1D}),$$

in which $\mathbf{1}$ is the unit tensor. The first and the last term in (18.23) may therefore be combined

$$\text{tr} \left\{ \left[\hat{\mathbf{t}} - \rho^2 \left(T \frac{\partial \hat{s}}{\partial \rho} - \frac{\partial \hat{u}}{\partial \rho} \right) \mathbf{1} \right] \mathbf{D} \right\},$$

so that the dissipation inequality takes the form

$$\begin{aligned} \Gamma := \rho \left\{ \left(T \frac{\partial \hat{s}}{\partial T} - \frac{\partial \hat{u}}{\partial T} \right) \dot{T} + \text{tr} \left[\left(T \frac{\partial \hat{s}}{\partial \mathbf{D}} - \frac{\partial \hat{u}}{\partial \mathbf{D}} \right) \dot{\mathbf{D}} \right] \right. \\ \left. + \left(T \frac{\partial \hat{s}}{\partial \text{grad } T} - \frac{\partial \hat{u}}{\partial \text{grad } T} \right) \cdot (\text{grad } T) \right\} \\ + \text{tr} \left\{ \left[\hat{\mathbf{t}} - \rho^2 \left(T \frac{\partial \hat{s}}{\partial \rho} - \frac{\partial \hat{u}}{\partial \rho} \right) \mathbf{1} \right] \mathbf{D} \right\} - \frac{\hat{\mathbf{q}} \cdot \text{grad } T}{T} \geq 0. \quad (18.24) \end{aligned}$$

⁹This is the point, where the open systems thermodynamics of BERNARD COLEMAN and WALTER NOLL shows its computational advantage: The momentum and energy equations do not exert any influence on the thermodynamic implications.

In this form all necessary field equations of a heat conducting fluid are accounted for as constraint conditions. This also implies that (18.24) must be valid for arbitrary continuously differentiable fields ρ , T , \mathbf{v} , in particular also arbitrary values of \dot{T} , $\dot{\mathbf{D}}$ and $(\text{grad } T)^\cdot$.

The various terms in the balance (18.24) have been so arranged that in the first two lines only such terms arise, which depend explicitly upon \dot{T} , $\dot{\mathbf{D}}$ and $(\text{grad } T)^\cdot$. Since these variables do not occur as independent constitutive variables, the dissipation inequality (18.24) is **linear in the variables \dot{T} , $\dot{\mathbf{D}}$ and $(\text{grad } T)^\cdot$** , which can assume arbitrary values.¹⁰ Consequently, in order that the inequality is not violated, the prefactors of these variables must necessarily vanish, i.e., we have the identities

$$\frac{\partial \hat{s}}{\partial T} = \frac{1}{T} \frac{\partial \hat{u}}{\partial T}, \quad \frac{\partial \hat{s}}{\partial \mathbf{D}} = \frac{1}{T} \frac{\partial \hat{u}}{\partial \mathbf{D}}, \quad \frac{\partial \hat{s}}{\partial \text{grad } T} = \frac{1}{T} \frac{\partial \hat{u}}{\partial \text{grad } T}. \quad (18.25)$$

There remains the **residual inequality**¹¹

$$\Gamma := \text{tr} \left\{ \left[\hat{\mathbf{t}} - \rho^2 \left(T \frac{\partial \hat{s}}{\partial \rho} - \frac{\partial \hat{u}}{\partial \rho} \right) \mathbf{1} \right] \mathbf{D} \right\} - \frac{\mathbf{q} \cdot \text{grad } T}{T} \geq 0. \quad (18.26)$$

The identities (18.25) can further be exploited. If the functions $s = \hat{s}(\cdot)$ and $u = \hat{u}(\cdot)$ are unique functions of their variables, then the ‘cross differentiations’ must be independent of the order of differentiation. From (18.25)_{1,2} one obtains e.g.

$$\frac{\partial^2 \hat{s}}{\partial \mathbf{D} \partial T} = \frac{1}{T} \frac{\partial^2 \hat{u}}{\partial \mathbf{D} \partial T}, \quad \frac{\partial^2 \hat{s}}{\partial T \partial \mathbf{D}} = \frac{1}{T} \frac{\partial^2 \hat{u}}{\partial T \partial \mathbf{D}} - \frac{1}{T^2} \frac{\partial \hat{u}}{\partial \mathbf{D}}. \quad (18.27)$$

¹⁰These variables do not occur in the balance laws of mass and momentum, and only \dot{T} arises in the energy equation, which has a freely assignable radiation term.

¹¹To see this, let the last line of (18.24) be denoted by Φ and make the permissible choices $\dot{\mathbf{D}} = \mathbf{0}$, $(\text{grad } T)^\cdot = \mathbf{0}$. With these, (18.24) becomes

$$\dot{T} \rho \left(T \frac{\partial \hat{s}}{\partial T} - \frac{\partial \hat{u}}{\partial T} \right) \geq -\Phi,$$

which is violated if

$$\dot{T} \leq -\Phi / \rho \left(T \frac{\partial \hat{s}}{\partial T} - \frac{\partial \hat{u}}{\partial T} \right)$$

is chosen. So, (18.25)₁ must hold true.

In a similar fashion one can also argue if one chooses

$$\dot{T} = 0, \quad \dot{\mathbf{D}} = \mathbf{0}, \quad (\text{grad } T)^\cdot \neq \mathbf{0}$$

or

$$\dot{T} = 0, \quad \dot{\mathbf{D}} \neq \mathbf{0}, \quad (\text{grad } T)^\cdot = \mathbf{0},$$

implying (18.25)_{1,3}.

Uniqueness of s and u requires the integrability conditions

$$\frac{\partial^2 \hat{s}}{\partial T \partial \mathbf{D}} = \frac{\partial^2 \hat{s}}{\partial \mathbf{D} \partial T}, \quad \frac{\partial^2 \hat{u}}{\partial T \partial \mathbf{D}} = \frac{\partial^2 \hat{u}}{\partial \mathbf{D} \partial T},$$

which, together with (18.27) implies $\partial \hat{u} / \partial \mathbf{D} = \mathbf{0}$ and owing to (18.25) also $\partial \hat{s} / \partial \mathbf{D} = \mathbf{0}$. Therefore, we have

$$\frac{\partial \hat{u}}{\partial \mathbf{D}} = \frac{\partial \hat{s}}{\partial \mathbf{D}} = \frac{\partial \hat{u}}{\partial \text{grad } T} = \frac{\partial \hat{s}}{\partial \text{grad } T} = \mathbf{0}, \quad (18.28)$$

where the two last results followed from a similar cross differentiation of (18.25)_{1,3}, using $(\text{grad } T)$ as the variable.

The result (18.28) says that the internal energy and the entropy cannot be functions of the stretching tensor \mathbf{D} and the temperature gradient $\text{grad } T$, and, thus, are of the form

$$u = \hat{u}(\rho, T), \quad s = \hat{s}(\rho, T), \quad (18.29)$$

where from (18.25) one also infers the relation

$$\frac{\partial \hat{s}}{\partial T} = \frac{1}{T} \frac{\partial \hat{u}}{\partial T}. \quad (18.30)$$

It follows that, even though we started with the application of the rule of equipresence, i.e., the assumption for a heat conducting viscous fluid of a more general dependence of the internal energy and the entropy, exploitation of the Second Law in the version of the CLAUSIUS–DUHEM inequality led to a reduced functional dependence, which we had *assumed* in simple systems.

There remains the exploitation of the residual inequality (18.26). To this end, recall that its left-hand side for a heat conducting viscous fluid represents a nonlinear function of ρ , T , \mathbf{D} and $\text{grad } T$. For fixed values of ρ and T , the dissipation, Γ , is a function of \mathbf{D} and $\text{grad } T$ with parameters ρ, T ,

$$\Gamma = \hat{\Gamma}_{\rho, T}(\mathbf{D}, \text{grad } T). \quad (18.31)$$

The Second Law, therefore, requests that $\Gamma \geq 0$ for all thermodynamic processes. It can also directly be inferred from (18.26) that

$$\Gamma = 0, \quad \text{if } \mathbf{D} = \mathbf{0} \quad \text{and} \quad \text{grad } T = \mathbf{0}. \quad (18.32)$$

Whenever $\mathbf{D} = \mathbf{0}$ and $\text{grad } T = 0$, no entropy is produced. These are exactly the conditions of homogeneous systems with uniform temperature and velocity fields. This suggests the following

Definition 18.2

- A **thermostatic or thermodynamic equilibrium** of a heat conducting viscous fluid is a time-independent process with homogeneous temperature and velocity fields.

Because the dissipation $\Gamma = \hat{\Gamma}_{\rho,T}(\mathbf{D}, \text{grad } T)$ is a non-negative function of its variables, which assumes its minimum value (namely the value zero) in equilibrium, the following conditions must necessarily be fulfilled¹²

$$\begin{aligned} \frac{\partial \hat{\Gamma}_{\rho,T}}{\partial \mathbf{D}} \Big|_E = \mathbf{0}, \quad \frac{\partial \hat{\Gamma}_{\rho,T}}{\partial \text{grad } T} \Big|_E = \mathbf{0}, \\ \mathbf{A} := \left(\begin{array}{cc} \frac{\partial^2 \hat{\Gamma}_{\rho,T}}{\partial \mathbf{D} \partial \mathbf{D}} & \frac{\partial^2 \hat{\Gamma}_{\rho,T}}{\partial \mathbf{D} \partial \text{grad } T} \\ \text{sym} & \frac{\partial^2 \hat{\Gamma}_{\rho,T}}{\partial \text{grad } T \partial \text{grad } T} \end{array} \right) \Big|_E \end{aligned} \quad (18.33)$$

is positive semi-definite.

The index $(\cdot)|_E$ indicates that the corresponding result holds for conditions of equilibrium, i.e., for $\mathbf{D} = \mathbf{0}$ and $\text{grad } T = \mathbf{0}$.

Let us exploit (18.33)_{1,2} first. With (18.26) it is easy to show that

$$\begin{aligned} \frac{\partial \hat{\Gamma}_{\rho,T}}{\partial \mathbf{D}} \Big|_E = \hat{\mathbf{t}}|_E - \rho^2 \left(T \frac{\partial \hat{s}}{\partial \rho} - \frac{\partial \hat{u}}{\partial \rho} \right) \mathbf{1} = \mathbf{0}, \\ \frac{\partial \hat{\Gamma}_{\rho,T}}{\partial \text{grad } T} \Big|_E = \frac{1}{T} \mathbf{q}|_E = \mathbf{0}, \end{aligned} \quad (18.34)$$

from which one concludes that

$$\hat{\mathbf{t}}|_E = -p\mathbf{1}, \quad p = -\rho^2 \left(T \frac{\partial \hat{s}}{\partial \rho} - \frac{\partial \hat{u}}{\partial \rho} \right), \quad \mathbf{q}|_E = \mathbf{0}. \quad (18.35)$$

In thermodynamic equilibrium the stress tensor is a pure pressure tensor and the heat flux vector vanishes. The variable p is called **thermodynamic pressure**; owing to (18.35) it is given by the entropy and the internal energy and, thus, only a function of

¹²This step is based upon the application of a theorem of analysis on extrema of functions of several variables. If $f(x_1, \dots, x_N)$ is a differentiable function, then the extrema of this function f lie where

$$\frac{\partial f}{\partial x_i} = 0, \quad (i = 1, \dots, N).$$

Moreover, a necessary condition for such an extremum to be a relative minimum is the condition that the matrix

$$A_{ij} \hat{=} \left(\frac{\partial^2 f}{\partial x_i \partial x_j} \right) \Big|_E \text{ is positive definite.}$$

If such a minimum occurs in the neighborhood of an equilibrium, then A_{ij} is positive semi-definite.

ρ and T : $p = \hat{p}(\rho, T)$. Moreover, the results (18.30) and (18.35)₂ can be combined to obtain the relation

$$\frac{\partial \hat{s}}{\partial T} = \frac{1}{T} \frac{\partial \hat{u}}{\partial T}, \quad \frac{\partial \hat{s}}{\partial \rho} = \frac{1}{T} \left(\frac{\partial \hat{u}}{\partial \rho} - \frac{\hat{p}}{\rho^2} \right). \quad (18.36)$$

Because of (18.29) these two expressions can be combined to the total differential of the entropy in the form

$$\begin{aligned} ds &= \frac{\partial \hat{s}}{\partial T} dT + \frac{\partial \hat{s}}{\partial \rho} d\rho = \frac{1}{T} \left\{ \frac{\partial \hat{u}}{\partial T} dT + \left(\frac{\partial \hat{u}}{\partial \rho} - \frac{\hat{p}}{\rho^2} \right) d\rho \right\} \\ &= \frac{\partial \hat{s}}{\partial T} dT + \frac{\partial \hat{s}}{\partial v} dv = \frac{1}{T} \left\{ \frac{\partial \hat{u}}{\partial T} dT + \left(\frac{\partial \hat{u}}{\partial v} + \hat{p} \right) dv \right\}. \end{aligned} \quad (18.37)$$

Here, we replaced in the second line the density by the specific volume, $v \equiv 1/\rho$ as independent variable, viz.,

$$u = \hat{u}(v, T), \quad p = \hat{p}(v, T). \quad (18.38)$$

This equation is identical with the **Gibbs relation** as it was already derived in (17.177) for a simple adiabatic system.

If the entropy is a unique function of its variables, then (18.37) must fulfill integrability conditions. From

$$\frac{\partial^2 \hat{s}}{\partial T \partial \rho} = \frac{\partial^2 \hat{s}}{\partial \rho \partial T},$$

one deduces

$$T \frac{\partial \hat{p}}{\partial T} - \hat{p} = -\rho^2 \frac{\partial \hat{u}}{\partial \rho}. \quad (18.39)$$

Similarly,

$$\frac{\partial^2 \hat{s}}{\partial T \partial v} = \frac{\partial^2 \hat{s}}{\partial v \partial T}$$

leads to the equation

$$T \frac{\partial \hat{p}}{\partial T} - \hat{p} = \frac{\partial \hat{u}}{\partial v}. \quad (18.40)$$

Relations (18.39) and (18.40) show that the *thermal and caloric equations of states are not independent of one another*. This corroborates our earlier statement that the Second Law of Thermodynamics constrains the freedom in the postulation of the thermal and caloric equations of state.

The following remarks are helpful:

- The GIBBS relation in the form (18.37) has been obtained from a general entropy principle (the CLAUSIUS–DUHEM inequality) for a heat-conducting viscous fluid.

Unlike the corresponding relation for a simple adiabatic system the absolute temperature is here a primitive quantity, i.e., a quantity, which is given a priori—not derived as a function of an empirical temperature. In this connection the CLAUSIUS–DUHEM inequality is, therefore, simpler, respectively less far reaching in its inferences than the previously employed simple statement of experience expressed by the SEARS–KESTIN assertion: ‘It is impossible to lower the internal energy of a simple adiabatic system when the specific volume is kept constant’, see MUSCHIK (1990) [26].

- Even though the thermodynamic pressure has been obtained by use of a thermodynamic equilibrium condition, the three functions $s = \hat{s}(\rho, T)$, $u = \hat{u}(\rho, T)$, $p = \hat{p}(\rho, T)$ can also be taken over as entropy, internal energy and pressure *in non-equilibrium*. This follows alone from the fact that these functions are not functions of \mathbf{D} and $\text{grad } T$. If the thermal and caloric equations of state are determined for quasi-static processes—i.e., thermodynamic equilibria—these functions can simply be taken over for non-equilibrium processes. Sometimes this is expressed by the statement that entropy, internal energy and pressure are determined by a co-moving frozen state of equilibrium.
- With the result (18.35) for the stress tensor in thermodynamic equilibrium, it is advantageous to additively decompose the CAUCHY stress tensor as follows:

$$\mathbf{t} = -p\mathbf{1} + \mathbf{t}^E. \quad (18.41)$$

Here, $p = \hat{p}(\rho, T)$ is the thermodynamic pressure (18.35) and its value, which it assumes for the actual values of the density ρ and the temperature T ; \mathbf{t}^E is called **extra stress tensor**; it agrees with the **frictional stress tensor** \mathbf{t}^R , introduced in Chap. 7. However, here, and with the present knowledge, it is not evident that it is ‘reasonable’ for the viscous effects. If one substitutes (18.41) into (18.35), one obtains

$$\mathbf{t}_{|E}^E = \mathbf{0}, \quad \mathbf{q}|_E = \mathbf{0}. \quad (18.42)$$

In thermodynamic equilibrium both the extra stress tensor \mathbf{t}^E and the heat flux vector \mathbf{q} vanish.

- With (18.41) and (18.35) the residual inequality (18.26) assumes the form

$$\Gamma := \text{tr}(\mathbf{t}^E \mathbf{D}) - \frac{\mathbf{q} \cdot \text{grad } T}{T} \geq 0. \quad (18.43)$$

This is about as far as an exploitation of the entropy principle can deliver without explicit assumptions for the material equations. The results, which are obtained are significant and constrain the choice of the constitutive relations of a heat conducting viscous fluid:

- Internal energy u , entropy s and thermodynamic pressure p are functions of the density ρ and temperature T , which are related to one another by the GIBBS relation

$$ds = \frac{1}{T} \left\{ \frac{\partial \hat{u}}{\partial T} dT + \left(\frac{\partial \hat{u}}{\partial \rho} - \frac{\hat{p}}{\rho^2} \right) d\rho \right\}. \quad (18.44)$$

- The thermal and caloric equations of state cannot be independently selected, but must satisfy the relation

$$T \frac{\partial \hat{p}}{\partial T} - \hat{p} = -\rho^2 \frac{\partial \hat{u}}{\partial \rho}, \quad (18.45)$$

in order that the entropy is a unique function of its variables. This must also experimentally be observed if the theory makes sense at all.

- The extra stress tensor and the heat flux vector in thermodynamic equilibrium vanish,

$$\mathbf{t}_{|E}^E = \mathbf{0}, \quad \mathbf{q}|_E = \mathbf{0}. \quad (18.46)$$

Before concluding, let us exploit the residual inequality (18.43) for a fluid, for which material equations for the extra stress tensor and the heat flux vector are given as *linear* functions of the strain rate tensor \mathbf{D} and the temperature gradient $\text{grad } T$. One can then easily see that \mathbf{t}^E cannot depend on $\text{grad } T$, and \mathbf{q} cannot depend on \mathbf{D} . For a viscous fluid, the form of the extra stress tensor has already been given in Chap. 7 (Eq. (7.28)). The heat-flux vector is assumed to be collinear to the temperature gradient:

$$\mathbf{t}^E = \zeta (\text{div } \mathbf{v}) \mathbf{1} + 2\eta \underbrace{\left(\mathbf{D} - \frac{1}{3} (\text{div } \mathbf{v}) \mathbf{1} \right)}_E, \quad (18.47)$$

$$\mathbf{q} = -\kappa \text{grad } T.$$

Here, \mathbf{E} is the deviator of the stretching tensor, defined by

$$\mathbf{E} := \mathbf{D} - \frac{1}{3} (\text{div } \mathbf{v}) \mathbf{1} \quad \text{with } \text{tr } \mathbf{E} = 0,$$

also called the distortion (rate) tensor. The laws (18.47) are called a **Newtonian stress relation** and the **Fourier law of heat conduction**.¹³ Here, $\zeta = \hat{\zeta}(\rho, T)$, $\eta = \hat{\eta}(\rho, T)$ and $\kappa = \hat{\kappa}(\rho, T)$ are the bulk viscosity, the shear viscosity and the heat conductivity, which in the context of a theory linear in \mathbf{D} and $\text{grad } T$ can still be functions of density and temperature.

If one substitutes (18.47) into (18.43), one obtains (compare also Eq. (17.88))

¹³For a remark on NEWTON, see Chap. 7, Eq. (7.21) of Vol. 1 and text immediately below it. Baron JEAN BAPTISTE FOURIER (1768–1830) was a French mathematician and professor at Ecole Normale and Ecole Polytechnique, later—under NAPOLEON—Governor of Egypt. FOURIER series and integrals are also named after him, which are treated in his oeuvre ‘Théorie analytique de chaleur’ (1822). For a biographical sketch of FOURIER see Fig. 18.1.



Fig. 18.1 JEAN BAPTISTE JOSEPH FOURIER (21. March 1768–16. May 1830) (Right) 1820 watercolor caricatures of French mathematicians ADRIEN–MARIE LEGENDRE (left) and JOSEPH FOURIER (right) by French artist JULIEN–LEOPOLD BOILLY, watercolor portrait numbers 29 and 30 of Album de 73 Portraits-Charge Aquarelle’s des Membres de l’Institute. See also Fig. 18.2

JEAN BAPTISTE JOSEPH FOURIER was a French mathematician and physicist. He was the son of a tailor and was educated at the military school in Auxerre. With the age of 18 he became professor at that school. He was active in the French revolution, but followed later NAPOLEON. FOURIER succeeded in 1797 LAGRANGE as professor of Analysis and Mechanics at the École Polytechnique. In physics he is known for the mathematical description of heat transport in solid bodies, for which he won a prize at the Academy in Paris. His ‘Théorie analytique de la chaleur’ (1822) is the basis for the description of the heat (temperature) in continuous bodies. In 1824 and 1827 he described in ‘Mémoire sur les températures du globe terrestre et les espaces planétaire’ for the first time the fundamental mechanisms of the atmospheric Greenhouse effect [8, 9]. With his FOURIER analysis he set the foundation of the progress in modern physics.

In the context of this book the FOURIER law expresses the heat flux vector as proportional to the temperature gradient with the heat conductivity measuring this proportionality.

The text is based on www.wikipedia.org

$$\Gamma = \hat{\Gamma}(x, y, z) = \zeta \frac{x^2}{2} + \eta \frac{y^2}{2} + \kappa \frac{z^2}{2} \geq 0, \tag{18.48}$$

$$\frac{x}{\sqrt{2}} = \text{div } \mathbf{v}, \quad \frac{y}{\sqrt{2}} = \sqrt{2 \text{tr}(\mathbf{E}^2)}, \quad \frac{z}{\sqrt{2}} = \frac{|\text{grad } T|}{\sqrt{T}},$$

where new variables x, y, z have been introduced.

Here, the dissipation Γ is a quadratic function of the three scalar variables x, y, z with coefficients, which themselves may still depend on density and temperature. Performing the differentiations of (18.48) with respect to x, y, z it is readily shown that

$$\frac{\partial \hat{\Gamma}}{\partial x} \Big|_E = \frac{\partial \hat{\Gamma}}{\partial y} \Big|_E = \frac{\partial \hat{\Gamma}}{\partial z} \Big|_E = 0,$$

$$\mathbf{A} = \left(\begin{array}{ccc} \frac{\partial^2 \hat{\Gamma}}{\partial x^2} & 0 & 0 \\ 0 & \frac{\partial^2 \hat{\Gamma}}{\partial y^2} & 0 \\ 0 & 0 & \frac{\partial^2 \hat{\Gamma}}{\partial z^2} \end{array} \right) \Big|_E = \begin{pmatrix} \zeta & 0 & 0 \\ 0 & \eta & 0 \\ 0 & 0 & \kappa \end{pmatrix},$$

in which the index E denotes the thermodynamic equilibrium that is given by $x = y = z = 0$. The matrix \mathbf{A} is positive semi-definite, provided that

$$\zeta \geq 0, \quad \eta \geq 0, \quad \kappa \geq 0. \quad (18.49)$$

In order that in a linear, heat conducting fluid the bulk and shear viscosities as well as the coefficient of heat conduction are in conformity with the second law, these coefficients must be non-negative functions of the variables density, ρ and temperature, T .

With these results, all inferences implied by the Second Law in form of the CLAUSIUS–DUHEM inequality for a linear, heat conducting linear viscous NEWTONian fluid are exploited.

18.2.2 Entropy Principle of Ingo Müller¹⁴

In the last section we formulated the second law in the form of the CLAUSIUS–DUHEM inequality and simplified its mathematical exploitation effectively by using two assumptions. These assumptions were

•

$$\text{entropy supply} = \frac{\text{energy supply}}{\text{absolute temperature}},$$

$$\text{entropy flux} = \frac{\text{heat flux}}{\text{absolute temperature}}.$$

¹⁴Ingo Müller (*1936), a physicist-engineer with doctorate (1966) and habilitation (1971) from the Technische Hochschule Aachen, is among the rational thermodynamicists, who was chiefly involved in research to generalize the entropy principle, to make it more flexible and better apt for thermodynamic processes than the CLAUSIUS–DUHEM inequality with its absolute temperature and the a priori estimate of the entropy flux as \mathbf{q}/T . This is seen already in his doctoral dissertation, in which the GIBBS relation found already a thermodynamic extension [21–23], and his books [24, 25].

- The balance laws of linear momentum and energy accommodate non-vanishing supply terms, which can be prescribed arbitrarily, and when necessary, can take every value we please.

The first assumption is restricting, because it assumes the existence of the absolute temperature; in addition it fails for mixtures and must be modified there. The second assumption is physically presumptuous, because it assumes that our “universe” is natured in such a way that, for a body, when necessary, there exists always a neighbourhood for which the external forces and the radiation take values as we please.

In the endeavour of softening these assumptions INGO MÜLLER in 1971 [23] formulated a weaker form of entropy principle, which, nevertheless, satisfies all necessary requirements of an irreversibility statement and reads as follows:

Entropy Principle 2:

- (1) *In every material body there exists an additive quantity, the specific entropy s , which obeys a balance equation*

$$\rho \frac{ds}{dt} = -\operatorname{div} \phi + \rho z^s + \rho \gamma, \quad (18.50)$$

in which ϕ is the entropy flux, z^s the specific entropy supply and γ the specific entropy production.

- (2) *The specific entropy s and the entropy flux ϕ are material quantities for which, according to the rule of aequipresence, the same material laws hold as for the remaining constitutive quantities.*
- (3) *The entropy production must be a non-negative quantity,*

$$\gamma \geq 0 \quad \text{for all thermodynamic processes,} \quad (18.51)$$

i.e., for all solutions of the field equations (these are the balance equations plus the constitutive relations together).

- (4) *The supply terms, which appear in the balance equations, can not influence the material behaviour.*
- (5) *There exist special material singular surfaces, the so-called ideal walls, between two continua, across which the normal heat flux and normal entropy flux are simultaneously continuous.* ■

This entropy principle is weaker in its prerequisites, but equally also more embracing in its inferences than the CLAUSIUS–DUHEM inequality. This is the reason why we prefer it to the latter. However, the analytical operations, which have to be performed with it, are considerably more complex than with the CLAUSIUS–DUHEM inequality. This is why we demonstrate its analytical exploitation with simpler constitutive classes than with the heat conducting viscous fluid.

(a) Heat Conducting Compressible Fluid. We shall apply this entropy principle for the simplest case, a heat conducting, compressible fluid; then the material equations are

$$\Psi = \hat{\Psi}(\rho, \theta, \text{grad } \theta), \quad \Psi \in \{\varepsilon, s, \mathbf{q}, \mathbf{t}, \phi\}. \quad (18.52)$$

Mass, momentum, energy and entropy balances are given by

$$\begin{aligned} \frac{\partial \rho}{\partial t} + \text{div}(\rho \mathbf{v}) &= 0, \\ \rho \frac{d\mathbf{v}}{dt} - \text{div} \hat{\mathbf{t}} - \rho \mathbf{g} &= \mathbf{0}, \\ \rho \frac{d\hat{\varepsilon}}{dt} + \text{div} \hat{\mathbf{q}} - \text{tr}(\hat{\mathbf{t}}\mathbf{D}) - \rho q &= 0, \\ \rho \frac{d\hat{s}}{dt} + \text{div} \hat{\phi} - \rho z^s &\geq 0, \end{aligned} \quad (18.53)$$

in which ρ , θ (the empirical temperature) and \mathbf{v} are to be considered as independent field quantities and the constitutive equations are thought to be substituted (which is indicated by the notation $(\hat{\cdot})$). A thermodynamic process is a solution of equations (18.53)_{1,2,3}, and the entropy principle demands that the entropy inequality (18.53)₄ must be fulfilled by all fields, which also satisfy the field equations (18.53)_{1,2,3}.¹⁵

It is plausible to think that one can satisfy this statement by the following modification of the original entropy inequality:

$$\begin{aligned} &\rho \frac{d\hat{s}}{dt} + \text{div} \hat{\phi} - \rho z^s \\ &\quad - \Lambda^\rho \left\{ \frac{\partial \rho}{\partial t} + \text{div}(\rho \mathbf{v}) \right\} - \Lambda^{\mathbf{v}} \cdot \left\{ \rho \frac{d\mathbf{v}}{dt} - \text{div} \hat{\mathbf{t}} - \rho \mathbf{g} \right\} \\ &\quad - \Lambda^\varepsilon \left\{ \rho \frac{d\hat{\varepsilon}}{dt} + \text{div} \hat{\mathbf{q}} - \text{tr}(\hat{\mathbf{t}}\mathbf{D}) - \rho q \right\} \\ &\geq 0. \end{aligned} \quad (18.54)$$

In this inequality the balance equations of mass, momentum and energy multiplied by the corresponding so-called LAGRANGE parameters are subtracted, and it is immediately prudent that (18.53) imply (18.54). The converse of this is also true, which was proved by I-SHIH LIU [18]. This proof will be given in the Appendix to this chapter. LIU's theorem states that both statements: (i) 'Satisfy the inequality (18.54) for *unrestricted fields*' and (ii) 'satisfy the inequality (18.53)₄ by simultaneously satisfying the field equations (18.53)_{1,2,3}' are equivalent. It is easy to fulfill the

¹⁵This entropy principle is more general than the principle using the CLAUSIUS–DUHEM inequality and the COLEMAN–NOLL approach by the fact that the form of the constitutive relation for the entropy flux is kept free within the constitutive class under study and not a priori set in relation to heat flux and absolute temperature. It is different also by the fact that the concept of absolute temperature is a derived one, i.e., the measure of coldness of a body is the empirical temperature and the absolute temperature is functionally related to it (if it is meaningful at all). And third, external source terms are required not to affect the material behaviour of a body. This latter point is contrary to the COLEMAN–NOLL approach.

extended inequality, but one must determine the unknown LAGRANGE multipliers, which is again a matter of tedious calculations.

If the constitutive equations (18.52) are substituted in (18.54), and differentiations with respect to time and space coordinates using the chain rule are executed, one obtains the resulting modified inequality in the form

$$\begin{aligned}
 & \rho \left(\frac{\partial \hat{s}}{\partial \theta} - \Lambda^\varepsilon \frac{\partial \hat{\varepsilon}}{\partial \theta} \right) \dot{\theta} + \rho \left(\frac{\partial \hat{s}}{\partial \rho} - \Lambda^\varepsilon \frac{\partial \hat{\varepsilon}}{\partial \rho} - \frac{\Lambda^\rho}{\rho} \right) \dot{\rho} \\
 & + \rho \left(\frac{\partial \hat{s}}{\partial \text{grad } \theta} - \Lambda^\varepsilon \frac{\partial \hat{\varepsilon}}{\partial \text{grad } \theta} \right) (\text{grad } \theta) \cdot \\
 & + \left\{ \frac{\partial \hat{\phi}}{\partial \rho} - \Lambda^\varepsilon \frac{\partial \hat{q}}{\partial \rho} + \mathbf{\Lambda}^v \frac{\partial \hat{t}}{\partial \rho} \right\} \cdot \text{grad } \rho \\
 & + \left\{ \frac{\partial \hat{\phi}}{\partial \text{grad } \theta} - \Lambda^\varepsilon \frac{\partial \hat{q}}{\partial \text{grad } \theta} + \mathbf{\Lambda}^v \frac{\partial \hat{t}}{\partial \text{grad } \theta} \right\} \cdot \text{grad } (\text{grad } \theta) \\
 & - \rho \mathbf{\Lambda}^v \cdot \dot{\mathbf{v}} \\
 & + \left\{ \frac{\partial \hat{\phi}}{\partial \theta} - \Lambda^\varepsilon \frac{\partial \hat{q}}{\partial \theta} + \mathbf{\Lambda}^v \frac{\partial \hat{t}}{\partial \theta} \right\} \cdot \text{grad } \theta \\
 & + \Lambda^\varepsilon \text{tr} \left[\left(\hat{\mathbf{t}} - \rho \frac{\Lambda^\rho}{\Lambda^\varepsilon} \mathbf{I} \right) \mathbf{D} \right] - \rho z^s + \rho \mathbf{g} \cdot \mathbf{\Lambda}^v + \rho q \Lambda^\varepsilon \\
 & \geq 0.
 \end{aligned} \tag{18.55}$$

This inequality is simplified in a first step, in which point (4) of the entropy principle should be evaluated. It says that the material properties should not be influenced by the supply terms, and from this it follows that the LAGRANGE parameters Λ^ρ , $\mathbf{\Lambda}^v$ and Λ^ε cannot depend on z^s , \mathbf{g} and q , implying that

$$z^s = \Lambda^\varepsilon q + \mathbf{\Lambda}^v \cdot \mathbf{g}. \tag{18.56}$$

The entropy supply is a linear combination of the energy supply and the momentum supply, whereby the factors are simply the LAGRANGE multipliers of the corresponding equations. The reader may recall that the entropy supply was postulated in the CLAUSIUS–DUHEM inequality as $z^s = q/\Theta$, where Θ is the absolute temperature; this is obviously a special case of (18.56).

Substituting (18.56) in (18.55), one obtains an inequality which is linear in

$$\boldsymbol{\beta} = [\dot{\theta}, \dot{\rho}, (\text{grad } \theta) \cdot, \text{grad } \rho, \text{grad } (\text{grad } \theta), \mathbf{D}]^T \tag{18.57}$$

and expressible in the form

$$\boldsymbol{\alpha} \cdot \boldsymbol{\beta} + \Gamma \geq 0. \tag{18.58}$$

The vector α is given¹⁶ by the prefactors of β (in the first four lines of (18.55)); Γ embraces the last three lines of (18.55) without the supply terms.

It follows from LIU's theorem that β is arbitrarily choosable at a fixed material point—in other words, it is possible to construct an admissible thermodynamic process with arbitrary β . Thus, necessary and sufficient condition for (18.58) to hold is $\alpha = \mathbf{0}$ (and $\Gamma \geq 0$), or

$$\begin{aligned} \frac{\partial \hat{s}}{\partial \theta} - \Lambda^\varepsilon \frac{\partial \hat{\varepsilon}}{\partial \theta} &= 0, \\ \frac{\partial \hat{s}}{\partial \rho} - \Lambda^\varepsilon \frac{\partial \hat{\varepsilon}}{\partial \rho} - \frac{\Lambda^\rho}{\rho} &= 0, \\ \frac{\partial \hat{s}}{\partial \text{grad } \theta} - \Lambda^\varepsilon \frac{\partial \hat{\varepsilon}}{\partial \text{grad } \theta} &= \mathbf{0}, \\ \frac{\partial \hat{\phi}}{\partial \rho} - \Lambda^\varepsilon \frac{\partial \hat{q}}{\partial \rho} + \Lambda^v \frac{\partial \hat{t}}{\partial \rho} &= \mathbf{0}, \\ \left\{ \frac{\partial \hat{\phi}}{\partial \text{grad } \theta} - \Lambda^\varepsilon \frac{\partial \hat{q}}{\partial \text{grad } \theta} + \Lambda^v \frac{\partial \hat{t}}{\partial \text{grad } \theta} \right\}_{\text{sym}} &= \mathbf{0}, \\ \hat{t} = \rho \frac{\Lambda^\rho}{\Lambda^\varepsilon} \mathbf{I} &= -p \mathbf{I}, \end{aligned} \tag{18.59}$$

equations, which must be fulfilled as identities. These constrain the constitutive equations for \hat{s} , $\hat{\varepsilon}$, \hat{q} , \hat{t} and $\hat{\phi}$ but can also be viewed as determining equations for Λ^ε , Λ^ρ and Λ^v . This last interpretation can be applied to conclude, that the LAGRANGE multipliers, as these are determined alone by constitutive quantities, themselves can only depend on the independent constitutive variables. This implies, specially, that these can not depend on $\dot{\mathbf{v}}$. Equation (18.55) is therefore also linear in $\dot{\mathbf{v}}$, and from this it follows that

$$\Lambda^v = \mathbf{0}. \tag{18.60}$$

The LAGRANGE multiplier of the momentum equation vanishes, or the momentum equation does not modify the analysis of the entropy inequality—at least not in this restricted theory for a compressible heat conducting fluid. This was assumed in the last section in which the entropy principle was employed as CLAUSIUS–DUHEM inequality and the COLEMAN–NOLL approach was used for its exploitation. Finally, the CAUCHY stress is isotropic and known as soon as Λ^ε and Λ^ρ are determined.

The next step in the evaluation of the identities (18.59) consists in the determination of the LAGRANGE multiplier Λ^ε . Here as well one starts from explicit representations of the entropy flux and heat flux as objective vector valued isotropic functions,

¹⁶One could be tempted to regard the term $\Lambda^v \cdot \dot{\mathbf{v}}$ as linear in $\dot{\mathbf{v}}$, however, this is not so—at least not at this stage of the computations—because the LAGRANGE multipliers can depend on $\dot{\mathbf{v}}$ in addition to ρ , θ , $\text{grad } \theta$.

$$\begin{aligned}\phi &= -\phi_1(\rho, \theta, \|\text{grad } \theta\|^2) \text{grad } \theta, \\ \mathbf{q} &= -q_1(\rho, \theta, \|\text{grad } \theta\|^2) \text{grad } \theta.\end{aligned}\quad (18.61)$$

Substituting these assumptions in the second to the last of the relations (18.59) results, by considering (18.60), in

$$\begin{aligned}\phi_1 \mathbf{I} + \frac{\partial \phi_1}{\partial \|\text{grad } \theta\|^2} 2 \text{grad } \theta \otimes \text{grad } \theta \\ = \Lambda^\varepsilon q_1 \mathbf{I} + \Lambda^\varepsilon \frac{\partial q_1}{\partial \|\text{grad } \theta\|^2} 2 \text{grad } \theta \otimes \text{grad } \theta,\end{aligned}\quad (18.62)$$

which must be satisfied for arbitrary values of $\text{grad } \theta$. From this one obtains

$$\phi_1 = \Lambda^\varepsilon q_1 \quad \text{and} \quad \frac{\partial \Lambda^\varepsilon}{\partial \|\text{grad } \theta\|^2} = 0.\quad (18.63)$$

The entropy flux is thus collinear with the heat flux, whereby the factor is given by the LAGRANGE multiplier of the energy equation. In view of (18.63)₂ the latter is not a function of the temperature gradient.

Using (18.63) with (18.61) and (18.60) in (18.59)₄, one obtains

$$\Lambda^\varepsilon \frac{\partial q_1}{\partial \rho} + \frac{\partial \Lambda^\varepsilon}{\partial \rho} q_1 = \Lambda^\varepsilon \frac{\partial q_1}{\partial \rho} \quad \Rightarrow \quad \frac{\partial \Lambda^\varepsilon}{\partial \rho} q_1 = 0,\quad (18.64)$$

from which with $q_1 \neq 0$ (which is to be required) follows that Λ^ε is no longer permitted to be a function of ρ . In summary, one obtains, from relations (18.59)_{4,5}

$$\phi = \Lambda^\varepsilon(\theta) \mathbf{q},\quad (18.65)$$

a result, which approaches the CLAUSIUS–DUHEM assumption $\Lambda^\varepsilon(\theta) = 1/\Theta(\theta)$, very closely where $\Theta(\theta)$ indicates the absolute temperature. Presently, however, $\Lambda^\varepsilon(\theta)$ is still a materially dependent function of the empirical temperature θ .

In order to prove that the LAGRANGE multiplier of the energy, $\Lambda^\varepsilon(\theta)$, is independent of the material properties, (at least within the material class of the heat conducting compressible fluids) let us recall the last property of the entropy principle, namely, that between two such materials there exist material singular surfaces with the property of an ideal wall across which the normal heat flux and normal entropy flux are simultaneously continuous. We now consider two heat conducting compressible fluids, which are separated by a material singular surface through which the empirical temperature is continuous. The jump conditions of entropy and energy read in this case,

$$[[\phi \cdot \mathbf{n}]] = [[\Lambda^\varepsilon \mathbf{q} \cdot \mathbf{n}]] = 0 \quad \text{and} \quad [[\mathbf{q} \cdot \mathbf{n}]] = 0,$$

or

$$[[\Lambda^\varepsilon]] \mathbf{q} \cdot \mathbf{n} = 0 \quad \Rightarrow \quad [[\Lambda^\varepsilon]] = 0 \quad \text{provided that} \quad \mathbf{q} \cdot \mathbf{n} \neq 0.\quad (18.66)$$

In other words, $\Lambda^\varepsilon(\theta)^+ = \Lambda^\varepsilon(\theta)^-$; or, the LAGRANGE multiplier is the same function of empirical temperature on both sides of the ideal wall. Since the fluids on both sides of the ideal wall can be arbitrary within their constitutive class, there follows the material independency of $\Lambda^\varepsilon(\theta)$ within this class. One refers to $\Lambda^\varepsilon(\theta)$ as the **coldness function** (or simply **coldness**) and its reciprocal value as the absolute temperature,

$$\Theta(\theta) = \frac{1}{\Lambda^\varepsilon(\theta)}. \quad (18.67)$$

Thus, the relations (18.59)_{4,5} are exploited.¹⁷

We now turn our attention to the identities (18.59)_{1,2,3}, where we will simultaneously make use of the result $\Lambda^\varepsilon = \Lambda^\varepsilon(\theta)$. Differentiating (18.59)₁ with respect to $\text{grad } \theta$ and (18.59)₃ with respect to θ , one can derive the following chain of equations

$$\begin{aligned} \frac{\partial^2 \hat{s}}{\partial \text{grad } \theta \partial \theta} &= \Lambda^\varepsilon \frac{\partial^2 \hat{\varepsilon}}{\partial \text{grad } \theta \partial \theta} = \frac{\partial^2 \hat{s}}{\partial \theta \partial \text{grad } \theta} \\ &= \Lambda^\varepsilon \frac{\partial^2 \hat{\varepsilon}}{\partial \theta \partial \text{grad } \theta} + \frac{\partial \Lambda^\varepsilon}{\partial \theta} \frac{\partial \hat{\varepsilon}}{\partial \text{grad } \theta}. \end{aligned} \quad (18.68)$$

Since the sequence of differentiation of the functions \hat{s} and $\hat{\varepsilon}$ with respect to θ and $\text{grad } \theta$ must be irrelevant, (18.68) implies, since $\partial \Lambda^\varepsilon(\theta)/\partial \theta \neq 0$, that $\hat{\varepsilon}$ can not be a function of $\text{grad } \theta$, $\partial \hat{\varepsilon}/\partial \text{grad } \theta = 0$. Resubstituting this result in (18.59)₃ shows then that \hat{s} does not depend on $\text{grad } \theta$ either, and—after having shown this for \hat{s} and $\hat{\varepsilon}$ —the same must also hold for Λ^ρ . Thus, one has the classical result

$$s = \hat{s}(\rho, \theta), \quad \varepsilon = \hat{\varepsilon}(\rho, \theta), \quad \Lambda^\rho = \hat{\Lambda}^\rho(\rho, \theta). \quad (18.69)$$

It is still to be demonstrated from (18.59) that the first two identities, which can be combined together, yield

$$d\hat{s} = \Lambda^\varepsilon \left[\frac{\partial \hat{\varepsilon}}{\partial \theta} d\theta + \left(\frac{\partial \hat{\varepsilon}}{\partial \rho} + \frac{\Lambda^\rho}{\rho \Lambda^\varepsilon} \right) d\rho \right] = \frac{1}{\Theta(\theta)} \left[d\hat{\varepsilon} + \hat{p} d\left(\frac{1}{\rho}\right) \right], \quad (18.70)$$

where we have identified the ratio $\rho \Lambda^\rho / \Lambda^\varepsilon$ with the thermodynamic pressure via

$$\hat{p}(\rho, \theta) = -\frac{\Lambda^\rho(\rho, \theta)}{\Lambda^\varepsilon(\theta)} \rho. \quad (18.71)$$

This pressure is the same as that introduced in (18.59)₆. Equation (18.70) is known as *GIBBS equation*, which expresses the total differential of the entropy as the product

¹⁷Notice that the above result was obtained by exploiting only relations (18.59) involving entropy flux and heat flux, but not entropy and internal energy. This is typical. Characteristic is equally the fact that isotropy relations had also to be used to achieve the result.

of the inverse of the absolute temperature times the total differential of the internal energy plus the additional term $\hat{p} d(1/\rho)$.

Naturally, the GIBBS equation must also satisfy an integrability condition, which is obtained from the cross differentiations of the coefficients of (18.70); the result is

$$\frac{d \ln \Lambda^\varepsilon}{d\theta} = \frac{1}{\Lambda^\varepsilon} \frac{d\Lambda^\varepsilon}{d\theta} = \frac{\partial \hat{p} / \partial \theta}{(\partial \hat{\varepsilon} / \partial \rho) \rho^2 - \hat{p}}. \quad (18.72)$$

Integrating this equation yields

$$\ln \frac{\Lambda^\varepsilon}{\Lambda_0^\varepsilon} = -\ln \frac{\Theta}{\Theta_0} = \int_{\theta_0}^{\theta} \frac{\partial \hat{p} / \partial \theta}{(\partial \hat{\varepsilon} / \partial \rho) \rho^2 - \hat{p}(\rho, \bar{\theta})} d\bar{\theta}$$

or

$$\Theta(\theta) = \Theta_0 \exp \left\{ - \int_{\theta_0}^{\theta} \frac{\partial \hat{p} / \partial \theta}{(\partial \hat{\varepsilon} / \partial \rho) \rho^2 - \hat{p}(\rho, \bar{\theta})} d\bar{\theta} \right\}. \quad (18.73)$$

The absolute temperature Θ is thus known as a function of the empirical temperature, if one knows $\hat{p}(\rho, \theta)$ and $(\partial \hat{\varepsilon} / \partial \rho)(\rho, \theta)$ as functions of their variables for **any heat conducting compressible fluid**. The left-hand side of (18.73) is materially independent, and thus so must be its right-hand side. Conversely, when one knows the function $\Theta(\theta)$, the pressure and the internal energy can not be chosen arbitrarily from each other, since relation (18.73) must be obeyed.

Choosing an *ideal gas* as the special fluid for which the equations of state are

$$p = R\rho \Theta(\theta), \quad \varepsilon = \hat{\varepsilon}(\theta), \quad (18.74)$$

where R is the gas constant, then (18.73) exhibits the identity $\Theta(\theta) = \Theta(\theta)$. This can be taken as motivation to set

$$\Theta(\theta) =: T. \quad (18.75)$$

This was suggested by LORD KELVIN.¹⁸ One calls T the *absolute* or **KELVIN temperature**. Using this relation one can replace in all relations the empirical temperature θ by the absolute temperature; this we shall now do.

If with

$$\Psi := \varepsilon - Ts = \hat{\Psi}(\rho, T) \quad (18.76)$$

the HELMHOLTZ free energy is introduced, then the GIBBS equation (18.70) takes the form

¹⁸For a short biography of LORD KELVIN, see Fig. 17.9.

$$\left(\frac{\partial \hat{\Psi}}{\partial \rho} - \frac{\hat{p}}{\rho^2} \right) d\rho + \left(\frac{\partial \hat{\Psi}}{\partial T} + \hat{s} \right) dT = 0, \quad (18.77)$$

which must be satisfied for arbitrary differentials $d\rho$ and dT . Consequently,

$$s = -\frac{\partial \hat{\Psi}}{\partial T}, \quad \hat{p} = \rho^2 \frac{\partial \hat{\Psi}}{\partial \rho}. \quad (18.78)$$

The entropy and the thermodynamic pressure are thus calculable from the prescribed thermodynamic potential $\hat{\Psi}(\rho, \theta)$, the HELMHOLTZ free energy. The restrictions on the constitutive functions, which are imposed by the second law, appear as especially concise in this form.

Thus, the identities (18.59) are exploited and there remains the analysis of the residual inequality $\Gamma \geq 0$, or

$$\Pi^s = T\Gamma = -\frac{\mathbf{q} \cdot \text{grad } T}{T} \geq 0. \quad (18.79)$$

Thermodynamic equilibrium is defined as a process, which produces no entropy and, thus, requires $\text{grad } T = \mathbf{0}$. The necessary conditions for this are the statements

$$\left(\frac{\partial \Pi^s}{\partial \text{grad } T} \right)_{|E} = \mathbf{0}, \quad (18.80)$$

$$\frac{\partial^2 \Pi^s}{(\partial \text{grad } T)^2}_{|E} \quad \text{is positive semi-definite,} \quad (18.81)$$

where $|_E$ indicates evaluation at equilibrium. Performing the differentiation (18.80) in (18.79) results in

$$\mathbf{q}_{|E} = \mathbf{0}. \quad (18.82)$$

The equilibrium heat flux vector vanishes. With the isotropic representations

$$\begin{aligned} \mathbf{t} &= -\hat{p}(\rho, T)\mathbf{I}, \\ \mathbf{q} &= -q_1(\rho, T, \|\text{grad } T\|^2)\text{grad } T \end{aligned} \quad (18.83)$$

one can exploit (18.81). The only relation which results from criterion (18.81) is

$$q_1(\rho, T, 0) \geq 0. \quad (18.84)$$

The nonlinear material equation (18.83) for the stress tensor and the heat flux vector are thus compatible with the entropy principle, if \hat{p} is derived via (18.78) from the Helmholtz free energy, and the thermal conductivity q_1 at $\text{grad } T = \mathbf{0}$ is non-negative.

The entropy principle of MÜLLER, in this example of a heat conducting compressible fluid, has led to the same results, as would have been obtained with the

application of the CLAUSIUS–DUHEM inequality carried out in accordance with the COLEMAN–NOLL approach. However, these results were obtained with the much weaker formulation. It was *proved* here by the entropy principle of INGO MÜLLER that the momentum balance does not influence the exploitation of the entropy principle; the absolute temperature was not assumed a priori *to exist*, but one has *proved* that it can be interpreted as the inverse of the LAGRANGE multiplier of the internal energy balance, and further one has *shown* that it represents a quantity independent of the material. Finally, *rewriting* the relations given at the beginning of this section,

$$\begin{aligned}\text{entropy supply} &= \frac{\text{energy supply}}{\text{absolute temperature}}, \\ \text{entropy flux} &= \frac{\text{heat flux}}{\text{absolute temperature}}\end{aligned}$$

—in connection with the heat conducting compressible fluids—we can say that these relations are now proved statements. These facts mediate to the model equations, which are derived from MÜLLER’s entropy principle, strengthened credibility. But it is also likely that for general material laws both entropy principles—CLAUSIUS–DUHEM inequality with the exploitation of COLEMAN–NOLL on the one hand and the more general entropy principle of Müller on the other hand—do not necessarily furnish the same results. This is so in general and must be scrutinized on a case by case basis. In this regard it is advisable to apply MÜLLER’s entropy principle whenever possible.

(b) Heat Conducting Density Preserving Fluid In a heat conducting density preserving fluid the independent constitutive variables are θ and $\text{grad } \theta$ only; thus

$$\Psi = \hat{\Psi}(\theta, \text{grad } \theta), \quad \Psi \in \{\varepsilon, s, \mathbf{q}, \mathbf{t}^E, \phi\}, \quad (18.85)$$

where

$$\mathbf{t} = -p\mathbf{I} + \mathbf{t}^E, \quad (18.86)$$

in which p is the constraint pressure and \mathbf{t}^E the extra stress tensor which may be taken to be a deviator, $\text{tr } \mathbf{t}^E = 0$. The balance of mass reduces to $\text{div } \mathbf{v} = 0$, so that the entropy inequality, extended by the field-equation constraints, see (18.54) for comparison, becomes

$$\begin{aligned}\rho \frac{d\hat{s}}{dt} + \text{div } \hat{\phi} - \rho z^s \\ - \Lambda^\rho \text{div } \mathbf{v} - \Lambda^v \cdot \left\{ \rho \frac{d\mathbf{v}}{dt} + \text{div } (p\mathbf{I}) - \text{div } (\hat{\mathbf{t}}^E) - \rho \mathbf{g} \right\} \\ - \Lambda^\varepsilon \left\{ \rho \frac{d\hat{\varepsilon}}{dt} + \text{div } \hat{\mathbf{q}} + p \text{div } \mathbf{v} - \text{tr } (\hat{\mathbf{t}}^E \mathbf{D}) - \rho \mathbf{q} \right\} \geq 0.\end{aligned} \quad (18.87)$$

This inequality must hold for arbitrary independent fields, i.e., also deformation fields which do not satisfy the condition $\operatorname{div} \mathbf{v} = 0$. The constitutive relations are thought to be substituted in (18.87); this is made visible by writing any constitutive variable f as \hat{f} .

Performing the differentiations, using the chain rule wherever needed yields the inequality

$$\begin{aligned}
 & \rho \left(\frac{\partial \hat{s}}{\partial \theta} - \Lambda^\varepsilon \frac{\partial \hat{\varepsilon}}{\partial \theta} \right) \dot{\theta} + \rho \left(\frac{\partial \hat{s}}{\partial \operatorname{grad} \theta} - \Lambda^\varepsilon \frac{\partial \hat{\varepsilon}}{\partial \operatorname{grad} \theta} \right) (\operatorname{grad} \theta) \cdot \\
 & + \left\{ \frac{\partial \hat{\phi}}{\partial \operatorname{grad} \theta} - \Lambda^\varepsilon \frac{\partial \hat{q}}{\partial \operatorname{grad} \theta} + \Lambda^v \frac{\partial \hat{\mathbf{t}}^E}{\partial \operatorname{grad} \theta} \right\} \cdot \operatorname{grad} (\operatorname{grad} \theta) \\
 & - \rho \Lambda^v \cdot \dot{\mathbf{v}} - \Lambda^v \cdot \operatorname{grad} p \\
 & + \left\{ \frac{\partial \hat{\phi}}{\partial \theta} - \Lambda^\varepsilon \frac{\partial \hat{q}}{\partial \theta} + \Lambda^v \frac{\partial \hat{\mathbf{t}}^E}{\partial \theta} \right\} \cdot \operatorname{grad} \theta - \Lambda^\varepsilon \left(p + \frac{\Lambda^\rho}{\Lambda^\varepsilon} \right) \operatorname{div} \mathbf{v} \\
 & + \Lambda^\varepsilon \operatorname{tr} \left[\hat{\mathbf{t}}^E \left(\mathbf{D} - \frac{1}{3} I_D \mathbf{I} \right) \right] - \rho z^s + \rho \mathbf{g} \cdot \Lambda^v + \rho q \Lambda^\varepsilon \geq 0. \quad (18.88)
 \end{aligned}$$

Because the material is assumed to be independent of the external sources (item 4) in the entropy principle) one necessarily has

$$z^s = \Lambda^\varepsilon q + \Lambda^v \cdot \mathbf{g}. \quad (18.89)$$

Moreover, since inequality (18.88) is linear in the variables $\dot{\theta}$, $(\operatorname{grad} \theta) \cdot \operatorname{grad} (\operatorname{grad} \theta)$, $\operatorname{div} \mathbf{v}$ and $(\mathbf{D} - \frac{1}{3} I_D \mathbf{I})$, which all may have any arbitrarily assigned values, we have

$$\begin{aligned}
 & \frac{\partial \hat{s}}{\partial \theta} - \Lambda^\varepsilon \frac{\partial \hat{\varepsilon}}{\partial \theta} = 0, \\
 & \frac{\partial \hat{s}}{\partial \operatorname{grad} \theta} - \Lambda^\varepsilon \frac{\partial \hat{\varepsilon}}{\partial \operatorname{grad} \theta} = \mathbf{0}, \\
 & \left\{ \frac{\partial \hat{\phi}}{\partial \operatorname{grad} \theta} - \Lambda^\varepsilon \frac{\partial \hat{q}}{\partial \operatorname{grad} \theta} - \Lambda^v \frac{\partial \hat{\mathbf{t}}^E}{\partial \operatorname{grad} \theta} \right\}_{\operatorname{sym}} = \mathbf{0}, \quad (18.90) \\
 & \Lambda^\rho = -\Lambda^\varepsilon p, \\
 & \hat{\mathbf{t}}^E = \mathbf{0}.
 \end{aligned}$$

These identities show that the LAGRANGE multipliers Λ^ε , Λ^v may be viewed as constitutive quantities. Furthermore, Λ^ρ is determined by Λ^ε and the constraint pressure. These facts imply that in particular Λ^v does not depend on $\dot{\mathbf{v}}$ so that the inequality (18.88) is also linear in $\dot{\mathbf{v}}$. As a consequence

$$\Lambda^v = \mathbf{0}. \quad (18.91)$$

The momentum equation does not influence the thermodynamics.

Using the representations of ϕ and \mathbf{q} as isotropic functions of their variables, it is now straightforward to show that (18.90)₃ implies that Λ^ε is only a function of the empirical temperature, $\Lambda^\varepsilon = \Lambda^\varepsilon(\theta)$, and \mathbf{q} and ϕ are collinear such that

$$\phi = \Lambda^\varepsilon(\theta) \mathbf{q}, \quad (18.92)$$

for details see the paragraph from (18.61)–(18.65). Similarly, with the aid of item (5) of the entropy principle it may also be demonstrated that $\Lambda^\varepsilon(\theta)$ is a universal function of the empirical temperature, (see the arguments leading to (18.67)), so that

$$\Theta(\theta) = \frac{1}{\Lambda^\varepsilon(\theta)} = T \quad (18.93)$$

may be identified with the absolute temperature.

Let us focus the attention now on the identities (18.90)_{1,2}. Differentiating (18.90)₁ with respect to $\text{grad } \theta$ and (18.90)₂ with respect to θ and comparing the two emerging results shows that

$$s = \hat{s}(\theta), \quad \varepsilon = \hat{\varepsilon}(\theta), \quad (18.94)$$

provided that $\Lambda^\varepsilon(\theta)$ is a nontrivial function of θ ; thus the GIBBS relation of a density preserving heat conducting fluid takes the form

$$ds = \Lambda^\varepsilon(\theta) d\varepsilon. \quad (18.95)$$

The results (18.94) and (18.95) are also interesting for the following fact: There is no relation like (18.72) or (18.73) in a density preserving fluid, in which a certain combination of derivatives of the pressure and internal energy would be related to the logarithmic derivative of Λ^ε . The reason for this is that the pressure is a free field here that cannot be related to any constitutive quantity. The above computations express this quite naturally.

With the identities (18.90)–(18.93) being satisfied, inequality (18.88) reduces to

$$-\frac{\mathbf{q} \cdot \text{grad } \theta}{\Theta(\theta)} \geq 0, \quad (18.96)$$

where $\Theta(\theta) > 0$. With $\mathbf{q} = -q_1(\theta, \text{grad } \theta) \text{grad } \theta$ this implies

$$q_1(\theta, 0) \geq 0. \quad (18.97)$$

The proof follows the same lines as that which led to (18.84).

This completes the thermodynamic analysis for a heat conducting density preserving fluid; the results, which this more general entropy principle delivers, are in this case the same as those obtained by the CLAUSIUS–DUHEM inequality.

(c) Viscous Heat Conducting Compressible Fluid The results for this class of fluids obtained with the entropy principle of MÜLLER are the same as those obtained with the CLAUSIUS–DUHEM inequality and the exploitation rules of COLEMAN–NOLL, see MÜLLER (1985) [25].

An example for which the two entropy principles yield different results is given in Sect. 18.4.

18.3 Thermal and Caloric Equations of State

18.3.1 Canonical Equations of State

In the preceding sections the **thermal** and **caloric equations of state**

$$\begin{aligned} p &= \hat{p}(\rho, T), & \text{or} & & p &= \tilde{p}(v, T), \\ u &= \hat{u}(\rho, T), & \text{or} & & u &= \tilde{u}(v, T) \end{aligned} \quad (18.98)$$

were mentioned several times; it was shown with the aid of the Second Law that these equations of state cannot experimentally be determined completely independently of each other, as certain integrability conditions for the entropy must be fulfilled. Neither have we employed uniformity in the choice of the independent variables (in Eq. (18.98); they are either the pair (ρ, T) or (v, T)). The same non-uniformity prevailed also in the dependent variables. As the caloric equation of state we determined once the relation (18.98)₂ for the internal energy $u = \hat{u}(\rho, T)$, and once the equation $h = \hat{h}(p, T)$, where h is the enthalpy $h = u + pv$, with the independent variable pair (p, T) . This fact leads to the justified question, *which variable combinations are to be regarded as the most natural ones*. A partial answer to this question, or better, an indication to it, was brought by in Sect. 17.6.2, when the Second Law was studied for simple adiabatic systems (see the GIBBS relations (17.161)–(17.164) and the corresponding integrability conditions (17.165)). In this subsection we wish to give an answer to the above question.

A first, direct access to answer these questions can be found in the GIBBS relation for heat conducting viscous fluids

$$ds = \frac{1}{T} (du + pdv),$$

which we now write in the (more convenient) form

$$du = Tds - pdv \quad \longrightarrow \quad \dot{u} = T\dot{s} - p\dot{v}. \quad (18.99)$$

It explicitly shows that the total differential of the internal energy is expressed as a linear combination of the differentials ds and dv ; obviously, u in (18.99) is assumed

as a function of s and v : $u = \tilde{u}(s, v)$. Indeed, if one calculates the total differential of this function, viz.,

$$du = \frac{\partial \tilde{u}}{\partial s} ds + \frac{\partial \tilde{u}}{\partial v} dv, \quad (18.100)$$

one recognizes the same linear form as in (18.99). All the more, if the differentials (18.99) and (18.100) are the same, one obtains the relations

$$T = \frac{\partial \tilde{u}}{\partial s}, \quad -p = \frac{\partial \tilde{u}}{\partial v}. \quad (18.101)$$

If one knows the internal energy as a function of the entropy and the specific volume, the absolute temperature T is obtained from $\tilde{u}(s, v)$ by differentiation with respect to the entropy s and the (negative) pressure, $-p$, is obtained from $\tilde{u}(s, v)$ by differentiation with respect to the specific volume v . The internal energy, regarded as a function of s and v is a **thermodynamic potential** for the absolute temperature and the pressure. This inference, deduced from the GIBBS relation, shows the connection of the thermal and caloric equations of state particularly conspicuously. If one manages to determine (experimentally) the function $\tilde{u}(s, v)$, then the thermal equation of state does no longer have to be experimentally determined; it follows from (18.101)₂ by differentiation.

Because the specific volume v is related to the density ρ by $v = 1/\rho$, the GIBBS relation (18.99) may also be written as

$$du = T ds + \frac{p}{\rho^2} d\rho, \quad (18.102)$$

since $dv = -d\rho/\rho^2$. In this case, we obtain with $u = \hat{u}(s, \rho)$

$$du = \frac{\partial \hat{u}}{\partial s} ds + \frac{\partial \hat{u}}{\partial \rho} d\rho \quad (18.103)$$

and by comparison of (18.102) and (18.103)

$$T = \frac{\partial \hat{u}}{\partial s}, \quad p = \rho^2 \frac{\partial \hat{u}}{\partial \rho}. \quad (18.104)$$

This is a result, which one could also have directly obtained from (18.101) by a variable change $v = 1/\rho$. One can see that temperature T and pressure p can be regarded as the components of a two-dimensional vector, which can be obtained by formation of a gradient operator of a thermodynamic potential. Equations (18.101) and (18.104) can also be combined in the more compact form

$$(T, -p) = \nabla_{s,v} \tilde{u}(s, v), \quad \left(T, \frac{p}{\rho^2} \right) = \nabla_{s,\rho} \hat{u}(s, \rho). \quad (18.105)$$

The indices (s, v) and (s, ρ) , respectively indicate, with respect to which variables the functions \tilde{u} and \hat{u} , are differentiated. The variable pairs $(T, -p) \longleftrightarrow (s, v)$ and $(T, p/\rho^2) \longleftrightarrow (s, \rho)$ are called **conjugate pairs**. The former are obtained by gradient operation of a certain thermodynamic energy (potential) with respect to the latter. If such simple relations exist, the conjugate variables are called **canonical**.

Canonical equations of state are caloric equations of state for thermodynamic potentials, which lead to simple relations in the sense of (18.105). The following equations of state are commonly used:

- Internal energy $u = \tilde{u}(s, v), \quad u = \hat{u}(s, \rho),$
- Enthalpy $h = \hat{h}(s, p),$
- HELMHOLTZ free energy $\psi = \tilde{\psi}(T, v), \quad \psi = \hat{\psi}(T, \rho),$
- Free enthalpy or GIBBS free energy $g = \check{g}(T, p).$

Here, we wish to investigate, how these functions are related to one another.

We start with the **enthalpy** how one may achieve a variable change from the density or specific volume as independent variable of a thermodynamic potential to the pressure. To this end we write the GIBBS relation as

$$\dot{u} = T\dot{s} - p\dot{v} = T\dot{s} - (pv)\dot{} + v\dot{p}, \quad (18.106)$$

or

$$\dot{h} = (u + pv)\dot{} = T\dot{s} + v\dot{p}. \quad (18.107)$$

In this relation the left-hand side appears as the time derivative of the function $h = u + pv$, which was defined already earlier as **enthalpy**; the right-hand side appears as a linear combination of the variables \dot{s} and \dot{p} . Therefore, one may interpret the enthalpy as a function of s and p , so that

$$\dot{h} = \frac{\partial \hat{h}}{\partial s} \dot{s} + \frac{\partial \hat{h}}{\partial p} \dot{p}, \quad (18.108)$$

or when comparing this with (18.107)

$$T = \frac{\partial \hat{h}}{\partial s} \quad v = \frac{\partial \hat{h}}{\partial p}, \quad (18.109)$$

or

$$(T, v) = \nabla_{s,p} \hat{h}(s, p), \quad (18.110)$$

with the integrability conditions

$$\frac{\partial \hat{T}(s, p)}{\partial p} = \frac{\partial \hat{v}(s, p)}{\partial s}. \quad (18.111)$$

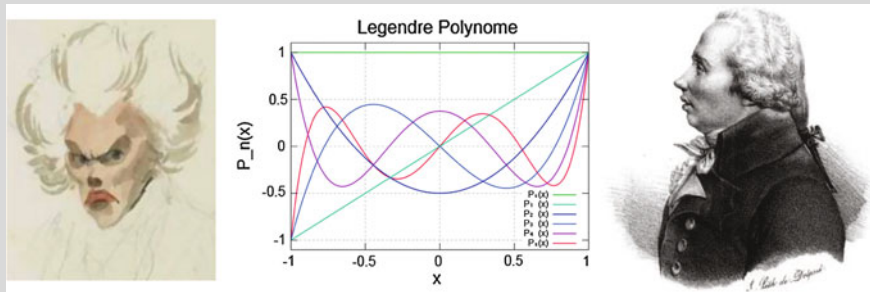


Fig. 18.2 ADRIEN–MARIE LEGENDRE (18 Sept. 1752–10 Jan. 1833) (*Left*) 1820 watercolor caricature of Adrien-Marie Legendre by French artist Julien-Leopold, the only existing portrait known; (*middle*) 5 Legendre polynomials; (*right*) side view sketching of French politician Louis Legendre (1752–1797), whose portrait has been mistakenly used, for nearly 200 years, to represent French mathematician Adrien-Marie Legendre, i.e. up until 2005 when the mistake was discovered, see [6] for details

ADRIEN–MARIE LEGENDRE (also LEGENDRE) was a French mathematician. He made numerous contributions to mathematics. Well-known and important concepts such as the LEGENDRE polynomials (see above figure, middle panel) are named after him. He was born in Paris to a wealthy family. He received his education at the Collège Mazarin in Paris, and defended his thesis in physics and mathematics in 1770. He taught at the École Militaire in Paris from 1775 to 1780 and at the École Normale Supérieure from 1795. At the same time, he was associated with the Bureau des Longitudes. In 1782, the Berlin Academy awarded LEGENDRE a prize for his treatise on projectiles in resistant media. This treatise also brought him to the attention of LAGRANGE. The Académie des Sciences made LEGENDRE an adjoint member in 1783 and an associé in 1785. In 1789 he was elected a Fellow of the Royal Society. LEGENDRE is known for the LEGENDRE transformation, which is used to go from the LAGRANGIAN to the HAMILTONIAN formulation of classical mechanics. In thermodynamics it is also used to obtain the enthalpy and the HELMHOLTZ and GIBBS (free) energies from the internal energy. He is also the namegiver of the LEGENDRE polynomials, solutions to LEGENDRE's differential equation. He is best known as the author of 'Éléments de géométrie', which was published in 1794 and was the leading elementary text on the topic for around 100 years. This text greatly rearranged and simplified many of the propositions from EUCLID's Elements to create a more effective textbook.

The text is based on www.wikipedia.org

(T, v) and (s, p) are canonical pairs of variables, and the enthalpy is the associated potential. Incidentally, a transformation, which achieves an exchange of dependent and independent variables, is called a **Legendre transformation**.¹⁹ The integrability conditions (here (18.111)) are called **Maxwell relations**.

For the **Helmholtz free energy** (T, v) or (T, ρ) are the independent variables. Therefore, the GIBBS equation can be brought into the form

$$\dot{u} = T\dot{s} - p\dot{v} = (Ts)' - s\dot{T} - p\dot{v},$$

¹⁹For a short biography of ADRIEN, MARIE LEGENDRE (1752–1833), see Fig. 18.2

or

$$\dot{\psi} = (u - Ts)' = -s\dot{T} - p\dot{v}. \quad (18.112)$$

Therefore, we have $\psi = \tilde{\psi}(T, v)$ and, consequently, the identity

$$\frac{\partial \tilde{\psi}}{\partial T} \dot{T} + \frac{\partial \tilde{\psi}}{\partial v} \dot{v} = -s\dot{T} - p\dot{v},$$

from which one concludes

$$s = -\frac{\partial \tilde{\psi}(T, v)}{\partial T}, \quad p = -\frac{\partial \tilde{\psi}(T, v)}{\partial v}, \quad (18.113)$$

$$(-s, -p) = \nabla_{T,v} \tilde{\psi}(T, v)$$

with the integrability condition

$$\frac{\partial s(T, v)}{\partial v} = \frac{\partial p(T, v)}{\partial T}. \quad (18.114)$$

If (T, ρ) are the independent variables, one may show, using $v = 1/\rho$

$$\left(-s, \frac{p}{\rho^2}\right) = \nabla_{T,\rho} \hat{\psi}(T, \rho), \quad (18.115)$$

$$- \frac{\partial \hat{s}(T, \rho)}{\partial \rho} = \frac{1}{\rho^2} \frac{\partial \hat{p}(T, \rho)}{\partial T}. \quad (18.116)$$

If one knows the HELMHOLTZ free energy $\psi = u - Ts$ as function of the variable pairs (T, v) and (T, ρ) , respectively, then the negative entropy is obtained by differentiating $\tilde{\psi}(T, v)$ and $\hat{\psi}(T, \rho)$, respectively with respect to the temperature and the negative pressure by differentiating $\tilde{\psi}(T, v)$ with respect to v .

To introduce the **free enthalpy** or the **GIBBS free energy**, the GIBBS relation is written in the form

$$\dot{u} = T\dot{s} - p\dot{v} = (Ts)' - s\dot{T} - (pv)' + v\dot{p},$$

and obtains then

$$\dot{g} = (u + pv - Ts)' = (h - Ts)' = -s\dot{T} + v\dot{p}.$$

Therefore, we have $g = \check{g}(T, p)$ and, consequently,

$$\frac{\partial \check{g}}{\partial T} \dot{T} + \frac{\partial \check{g}}{\partial p} \dot{p} = -s\dot{T} + v\dot{p},$$

Table 18.1 Thermodynamic potentials and MAXWELL relations for a simple fluid

Potential	Independent variables	Conjugate variables	MAXWELL relations
u Internal energy	s, v $du = Tds - pdv$	$(T, -p) = \nabla_{s,v} \tilde{u}(s, v)$	$\frac{\partial \tilde{T}(s, v)}{\partial v} = -\frac{\partial \tilde{p}(s, v)}{\partial s}$
	s, ρ $du = Tds + \frac{p}{\rho^2} d\rho$	$(T, \frac{p}{\rho^2}) = \nabla_{s,\rho} \hat{u}(s, \rho)$	$\frac{\partial \hat{T}(s, \rho)}{\partial \rho} = \frac{1}{\rho^2} \frac{\partial \hat{p}(s, \rho)}{\partial s}$
h Enthalpy	s, p $dh = Tds + vdp$ $h = u + pv$	$(T, v) = \nabla_{s,p} \hat{h}(s, p)$	$\frac{\partial \hat{T}(s, p)}{\partial p} = \frac{\partial \hat{v}(s, p)}{\partial s}$
ψ HELMHOLTZ free energy	T, v $d\psi = -sdT - pdv$	$(-s, -p) = \nabla_{T,v} \tilde{\psi}(T, v)$	$\frac{\partial \tilde{s}(T, v)}{\partial v} = \frac{\partial \tilde{p}(T, v)}{\partial T}$
$\psi = u - Ts$	T, ρ $d\psi = -sdT + \frac{p}{\rho^2} d\rho$	$(-s, \frac{p}{\rho^2}) = \nabla_{T,\rho} \hat{\psi}(T, \rho)$	$-\frac{\partial \hat{s}(T, \rho)}{\partial \rho} = \frac{1}{\rho^2} \frac{\partial \hat{p}(T, \rho)}{\partial T}$
g Free enthalpy or GIBBS free energy $g = h - Ts$	T, p $dg = -sdT + vdp$	$(-s, v) = \nabla_{T,p} \check{g}(T, p)$	$-\frac{\partial \check{s}(T, p)}{\partial p} = \frac{\partial \check{v}(T, p)}{\partial T}$

from which one deduces

$$(-s, v) = \nabla_{T,p} \check{g}(T, p)$$

$$-\frac{\partial \check{s}(T, p)}{\partial p} = \frac{\partial \check{v}(T, p)}{\partial T}. \quad (18.117)$$

Table 18.1 collects the derived results in summarized form.

In closing, we would like to emphasize that we systematically differentiated in the above analysis between a function and the value of this function (writing e.g. \tilde{f} and f , respectively). If this differentiation is not made, it is not clear, which pair of variables is meant in a potential (compare e.g. the two possibilities for the internal energy and the HELMHOLTZ free energy). When performing the partial derivatives of functions of two variables, one often employs for clarity an index, which indicates, which variable is held constant. For instance

$$\left. \frac{\partial s}{\partial \rho} \right|_T \quad \text{stands for} \quad \frac{\partial \hat{s}(T, \rho)}{\partial \rho}.$$

We shall in subsequent chapters occasionally make use of this rule.

18.3.2 Specific Heats and Other Thermodynamic Quantities

As before, we consider a fluid, for which the thermal and caloric equations of state reduce to functional relations in three variables, thus relations for which conditions of Table 18.1 apply. It is customary, apart from the already introduced variables, also to work with the following quantities:

- Thermal expansion coefficient α : $\alpha = \frac{1}{v} \frac{\partial \check{v}(T, p)}{\partial T} = \frac{1}{v} \frac{\partial v}{\partial T} \Big|_p$
- Isobaric compressibility κ_T : $\kappa_T = -\frac{1}{v} \frac{\partial \check{v}(T, p)}{\partial p} = -\frac{1}{v} \frac{\partial v}{\partial p} \Big|_T$
- Adiabatic compressibility κ_s : $\kappa_s = -\frac{1}{v} \frac{\partial \hat{v}(s, p)}{\partial p} = -\frac{1}{v} \frac{\partial v}{\partial p} \Big|_s$
- Isochoric stress coefficient β : $\beta = \frac{1}{p} \frac{\partial \check{p}(T, v)}{\partial T} = \frac{1}{p} \frac{\partial p}{\partial T} \Big|_v$

$$(18.118)$$

These quantities plus the potentials, collected in Table 18.1 are not independent of one another. One e.g. recognizes from a combination of (18.118)₁ and the lowest MAXWELL relations of Table 18.1 that

$$\frac{\partial \check{s}(T, p)}{\partial p} = -\frac{\partial \check{v}(T, p)}{\partial T} = -\alpha \check{v}(T, p). \quad (18.119)$$

Knowledge of such relations is useful in attempts of the experimental determination of the caloric equation of state. To this end we shall now introduce the specific heat as follows:

Definition 18.3

- **Specific heat** is the heat that is reversibly supplied to a system per unit temperature change at fixed volume or fixed pressure, respectively.

If we start from the Second Law in the form (17.196), it reads, owing to the reversibly conducted increment of heat,

$$ds = \frac{dQ}{T} \quad \longrightarrow \quad dQ = T ds. \quad (18.120)$$

Here, dQ denotes the increment of heat, reversibly supplied to the system, which gives rise to a change of entropy ds . Now, s is either a function of T and v or of T

and p , so that the specific heat $c = dQ/dT$ at constant volume or constant pressure may be defined as

$$c_v := T \frac{\partial \tilde{s}(T, v)}{\partial T} = \frac{\partial \tilde{u}(T, v)}{\partial T}, \quad c_p := T \frac{\partial \check{s}(T, p)}{\partial T} = \frac{\partial \check{h}(T, p)}{\partial T}. \quad (18.121)$$

The two expressions in the far right are in this form not understandable. From the GIBBS relation $du = Tds - pdv$ one concludes at constant volume ($dv = 0$) $du = Tds$, which implies $(\partial u/\partial T)|_v = T(\partial s/\partial T)|_v$. One regards the internal energy as a function of T and v . This function is computed as follows (see Table 18.1):

$$\tilde{u}(T, v) = \tilde{u}(\tilde{s}(T, v), v) = \tilde{u}\left(-\frac{\partial \tilde{\psi}(T, v)}{\partial T}, v\right).$$

In much the same way, one obtains from the GIBBS relation $dh = Tds - vdp$ for constant pressure $dh = Tds$, so that, analogously to the above procedure, one concludes $(\partial h/\partial T)|_p = T(\partial s/\partial T)|_p$. The entropy as a function of T and p is obtained as follows (see Table 18.1):

$$\hat{h}(T, p) = \hat{h}(\check{s}(T, p), p) = \hat{h}\left(-\frac{\partial \check{g}(T, p)}{\partial T}, p\right),$$

where $g = \check{g}(T, p)$ is the GIBBS free energy.

We wish to demonstrate now that the specific heats and the quantities, introduced in (18.118) are not independent of each other. For the derivation of the first of these relations we start from the second of the definitions (18.121) for c_p where $s = \check{s}(T, p)$. However, since we wish to correlate c_p and c_v , we set

$$s = \check{s}(T, p) = \tilde{s}(T, v) = \tilde{s}(T, \check{v}(T, p)).$$

The remainder is application of the chain rule of differentiation:

$$\begin{aligned} c_p &= T \frac{\partial \check{s}(T, p)}{\partial T} = T \left\{ \frac{\partial \tilde{s}(T, v)}{\partial T} + \frac{\partial \tilde{s}(T, v)}{\partial v} \frac{\partial \check{v}(T, p)}{\partial T} \right\} \\ &= c_v + T \frac{\partial \tilde{s}(T, v)}{\partial v} \frac{\partial \check{v}(T, p)}{\partial T}. \end{aligned}$$

If, in addition, the MAXWELL relation for ψ (Table 18.1) is used, we deduce from this

$$c_p - c_v = T \frac{\partial \check{p}(T, v)}{\partial T} \frac{\partial \check{v}(T, p)}{\partial T} = \alpha \beta v p T. \quad (18.122)$$

This is a first relation for the difference of the specific heats. Conversely, one can also start from the definition of c_v . Then, one obtains

$$\begin{aligned}
 c_v &= T \frac{\partial \check{s}(T, v)}{\partial T} = T \frac{d\check{s}(T, \tilde{p}(T, v))}{dT} \Big|_v \\
 &= T \left\{ \frac{\partial \check{s}(T, p)}{\partial T} + \frac{\partial \check{s}(T, p)}{\partial p} \frac{\partial \tilde{p}(T, v)}{\partial T} \right\} = c_p - T \frac{\partial \check{v}(T, p)}{\partial T} \frac{\partial \tilde{p}(T, v)}{\partial T}, \quad (18.123)
 \end{aligned}$$

from which one may again obtain (18.122). With

$$p = \tilde{p}(T, v) = \tilde{p}(T, \check{v}(T, p)) = \check{p}(T, p)$$

one deduces by differentiation with respect to T

$$\frac{\partial \check{p}}{\partial T} \stackrel{!}{=} 0 = \frac{\partial \tilde{p}(T, v)}{\partial T} + \frac{\partial \tilde{p}(T, v)}{\partial v} \frac{\partial \check{v}(T, p)}{\partial T}$$

or

$$\frac{\partial \tilde{p}(T, v)}{\partial T} = - \frac{\partial \tilde{p}(T, v)}{\partial v} \frac{\partial \check{v}(T, p)}{\partial T}.$$

Substituted in (18.123), this yields

$$c_v - c_p = T \frac{\partial \tilde{p}(T, v)}{\partial v} \left(\frac{\partial \check{v}(T, p)}{\partial T} \right)^2 = - \frac{\alpha^2 v T}{\kappa_T}, \quad (18.124)$$

in which use was also made of (18.118). This is a second relation for the difference of the specific heats.

A relation between the adiabatic and isothermal compressibility is obtained if one starts from the definition of κ_T

$$\begin{aligned}
 v\kappa_T &= - \frac{\partial \check{v}(T, p)}{\partial p} = - \frac{d\hat{v}(\check{s}(T, p), p)}{dp} \Big|_T = - \frac{\partial \hat{v}(s, p)}{\partial p} - \frac{\partial \hat{v}(s, p)}{\partial s} \frac{\partial \check{s}(T, p)}{\partial p} \\
 &= v\kappa_s - \frac{\partial \check{s}(T, p)}{\partial p} \frac{\partial \hat{v}(s, p)}{\partial s} = v\kappa_s + \underbrace{\frac{\partial \check{v}(T, p)}{\partial T}}_{\alpha v} \frac{\partial \hat{v}(s, p)}{\partial s}. \quad (18.125)
 \end{aligned}$$

Here, use was made of the MAXWELL relation (Table 18.1) and the definition of the thermal expansion coefficient. If one also uses the relation

$$\check{v}(T, p) = \hat{v}(\check{s}(T, p), p),$$

one obtains via differentiation with respect to T

$$\frac{\partial \check{v}(T, p)}{\partial T} = \frac{\partial \hat{v}(s, p)}{\partial s} \frac{\partial \check{s}(T, p)}{\partial T}$$

or

$$\frac{\partial \check{v}(s, p)}{\partial s} = \frac{\frac{\partial \check{v}(T, p)}{\partial T}}{\frac{\partial \check{s}(T, p)}{\partial T}} = \frac{\alpha v T}{c_p}. \quad (18.126)$$

Substitution of this result into (18.125), finally, yields, the relation

$$\kappa_T = \kappa_s + \frac{\alpha^2 v^2 T}{c_p}, \quad (18.127)$$

which we were looking for.

We also wish to demonstrate that the internal energy and the entropy can be computed as functions of T and v , if the specific heat $\check{c}_v(T, v)$ and the pressure $\check{p}(T, v)$ are experimentally determined. To this end, we start from the GIBBS relation and demonstrate that

$$T \frac{\partial \check{s}(T, v)}{\partial v} = \frac{\partial \check{u}(T, v)}{\partial v} + \check{p}(T, v), \quad (18.128)$$

so that

$$\frac{\partial \check{u}(T, v)}{\partial v} = T \frac{\partial \check{p}(T, v)}{\partial T} - \check{p}(T, v). \quad (18.129)$$

Here, use was made of the corresponding MAXWELL relation (see Table 18.1). Integration yields

$$\begin{aligned} \check{u}(T, v) &= \int_{v_0}^v \left[T \frac{\partial \check{p}(T, \bar{v})}{\partial T} - \check{p}(T, \bar{v}) \right] d\bar{v} + F(T) \\ &= \int_{v_0}^v \check{p}(T, \bar{v}) [T\check{\beta}(T, \bar{v}) - 1] d\bar{v} + F(T). \end{aligned} \quad (18.130)$$

If this relation is differentiated with respect to T , the function $F(T)$ can be determined

$$\frac{\partial \check{u}(T, v)}{\partial T} = c_v(T, v) = \frac{\partial}{\partial T} \int_{v_0}^v \check{p}(T, \bar{v}) [T\check{\beta}(T, \bar{v}) - 1] d\bar{v} + \frac{dF}{dT},$$

from which

$$F(T) = \int_{T_0}^T c_v(\bar{T}, v) d\bar{T} - \int_{v_0}^v \check{p}(T, \bar{v}) [T\check{\beta}(T, \bar{v}) - 1] d\bar{v}$$

$$+ \int_{v_0}^v \tilde{p}(T_0, \tilde{v}) \left[T_0 \tilde{\beta}(T_0, \tilde{v}) - 1 \right] d\tilde{v} + u(T_0, v_0)$$

follows. Substitution of this result in (18.130), finally, yields

$$\tilde{u}(T, v) = \int_{T_0}^T c_v(\bar{T}, v) d\bar{T} + \int_{v_0}^v \tilde{p}(T_0, \tilde{v}) \left[T_0 \tilde{\beta}(T_0, \tilde{v}) - 1 \right] d\tilde{v} + u(T_0, v_0). \quad (18.131)$$

Alternatively, from the MAXWELL relation

$$\frac{\partial \tilde{s}(T, v)}{\partial v} = \frac{\partial \tilde{p}(T, v)}{\partial T},$$

we deduce via integration with respect to v

$$\tilde{s}(T, v) = \int_{v_0}^v \frac{\partial \tilde{p}(T, \tilde{v})}{\partial T} d\tilde{v} + S(T) = \int_{v_0}^v \tilde{p}(T, \tilde{v}) \tilde{\beta}(T, \tilde{v}) d\tilde{v} + S(T).$$

Differentiating this last relation with respect to T leads to

$$\frac{\partial \tilde{s}(T, v)}{\partial T} = \frac{c_v(T, v)}{T} = \frac{\partial}{\partial T} \int_{v_0}^v \tilde{p}(T, \tilde{v}) \tilde{\beta} d\tilde{v} + \frac{dS}{dT},$$

or after a further integration with respect to T

$$S(T) = \int_{T_0}^T \frac{c_v(\bar{T}, v)}{\bar{T}} d\bar{T} + \int_{v_0}^v \tilde{p}(T_0, \tilde{v}) \tilde{\beta}(T_0, \tilde{v}) d\tilde{v} - \int_{v_0}^v \tilde{p}(T, \tilde{v}) \tilde{\beta}(T, \tilde{v}) d\tilde{v} + S(T_0, v_0),$$

so that the entropy can be expressed as

$$\tilde{s}(T, v) = \int_{T_0}^T \frac{c_v(\bar{T}, v)}{\bar{T}} d\bar{T} + \int_{v_0}^v \tilde{p}(T_0, \tilde{v}) \tilde{\beta}(T_0, \tilde{v}) d\tilde{v} + \tilde{S}(T_0, v_0). \quad (18.132)$$

In the formulae (18.131) and (18.132) the pressure must only be known as a function of \tilde{v} for a fixed reference temperature, whilst the specific heat must be provided as a function of T and v . If the integration would have been conducted in reverse order, one would have started from

$$\tilde{u}(T, v) = \int_{T_0}^T c_v(\bar{T}, v) d\bar{T} + G(v).$$

Differentiation of this expression with respect to v and use of (18.129) determines

$$G(v) = \int_{v_0}^v \tilde{p}(T, \bar{v}) [T\beta(T, \bar{v}) - 1] d\bar{v} - \int_{T_0}^T c_v(\bar{T}, v) d\bar{T} + \int_{T_0}^T c_v(\bar{T}, v_0) d\bar{T} + \tilde{u}(T_0, v_0)$$

so that in lieu of (18.131) and (18.132), one would have

$$\begin{aligned} \tilde{u}(T, v) &= \int_{v_0}^v \tilde{p}(T, \bar{v}) [T\beta(T, \bar{v}) - 1] d\bar{v} + \int_{T_0}^T c_v(\bar{T}, v_0) d\bar{T} + \tilde{u}(T_0, v_0) \\ \tilde{s}(T, v) &= \int_{v_0}^v \tilde{p}(T, \bar{v}) \tilde{\beta}(T, \bar{v}) d\bar{v} + \int_{T_0}^T \frac{c_v(\bar{T}, v_0)}{\bar{T}} d\bar{T} + \tilde{S}(T_0, v_0). \end{aligned} \quad (18.133)$$

In these relations $\tilde{p}(T, v)$ must be known as bivariate function, whereas $c_v(T, v_0)$ must be prescribed only for a fixed prescribed value of v_0 . Which of the two representations is chosen depends upon, in what way the experimental data are available. Alternatively, the set of data could be used as control set of the reliability of the data.

We leave it as an exercise to the reader to corroborate the representations

$$\begin{aligned} \check{h}(T, p) &= \int_{T_0}^T c_p(\bar{T}, p) d\bar{T} + \int_{p_0}^p \check{v}(T_0, \bar{p}) [1 - \alpha(T_0, \bar{p}) T_0] d\bar{p} + \check{h}(T_0, p_0) \\ &= \int_{T_0}^T c_p(\bar{T}, p_0) d\bar{T} + \int_{p_0}^p \check{v}(T, \bar{p}) [1 - \alpha(T, \bar{p}) T] d\bar{p} + \check{h}(T_0, p_0) \\ \check{s}(T, p) &= \int_{T_0}^T \frac{c_p(\bar{T}, p)}{\bar{T}} d\bar{T} - \int_{p_0}^p \check{v}(T_0, \bar{p}) \alpha(T_0, \bar{p}) d\bar{p} + \check{s}(T_0, p_0) \\ &= \int_{T_0}^T \frac{c_p(\bar{T}, p_0)}{\bar{T}} d\bar{T} - \int_{p_0}^p \check{v}(T, \bar{p}) \alpha(T, \bar{p}) d\bar{p} + \check{s}(T_0, p_0). \end{aligned}$$

Here, too, two representations which must yield identical results are possible.

18.3.3 Application to Ideal Gases

For reasons of better understanding, let us repeat here once more the definition of an ideal gas:

Definition 18.4 *An ideal gas is defined by*

- *the thermal equation of state*

$$p = p(T, v) = \frac{RT}{v}, \quad (18.134)$$

- *$u = u(T)$; the internal energy is only a function of the temperature. $R_m = RM$ where R is the **universal gas constant** and M is the mole mass of the gas.*

The second of these properties follows from the first; indeed

$$\frac{\partial}{\partial v} \tilde{u}(\tilde{s}(T, v), v) = \underbrace{\frac{\partial \tilde{u}(s, v)}{\partial v}}_{-p} + \underbrace{\frac{\partial \tilde{u}(s, v)}{\partial s}}_T \underbrace{\frac{\partial \tilde{s}(T, v)}{\partial v}}_{\frac{\partial \tilde{p}(T, v)}{\partial T}} = 0,$$

in which the expressions underneath the braces can be taken from Table 18.1 and the final result obtains by substitution of the thermal equation of state, see (18.134). Consequently, the internal energy cannot depend on the specific volume. Since

$$h = u + pv = u(T) + RT \quad \longrightarrow \quad h = h(T),$$

the enthalpy of an ideal gas can neither depend upon the specific volume. If one has experimentally determined the specific heats (18.121), which now are merely functions of the temperature, the internal energy and enthalpy follow by integration with respect to T ,

$$\begin{aligned} u(T) &= \int_{T_0}^T c_v(\bar{T}) d\bar{T} + u(T_0), \\ h(T) &= \int_{T_0}^T c_p(\bar{T}) d\bar{T} + h(T_0). \end{aligned} \quad (18.135)$$

Incidentally, one easily shows with the aid of (18.122)₁ and the equation of an ideal gas, (18.134), that

$$c_p - c_v = R. \quad (18.136)$$

Even though the specific heats of ideal gases are functions of the temperature, their difference is a constant. It, thus, suffices to experimentally determine only one of them.

Next, we compute the *entropy*. It can be determined from known specific heat functions. Indeed, we write the GIBBS equation as

$$ds = \frac{1}{T} (du + p dv) \stackrel{(18.134)}{=} c_v(T) \frac{dT}{T} + R \frac{dv}{v},$$

and then obtain after integration

$$s - s_0 = \int_{T_0}^T \frac{c_v(\bar{T})}{\bar{T}} d\bar{T} + R \ln \left(\frac{v}{v_0} \right). \quad (18.137)$$

Analogously,

$$ds = \frac{1}{T} (dh - v dp) = c_p(T) \frac{dT}{T} - R \frac{dp}{p},$$

or

$$s - s_0 = \int_{T_0}^T \frac{c_p(\bar{T})}{\bar{T}} d\bar{T} - R \ln \left(\frac{p}{p_0} \right). \quad (18.138)$$

With the definitions of the HELMHOLTZ free energy ψ and the free enthalpy (GIBBS free energy) g (see Table 18.1), we get

$$\psi = u - Ts = \int_{T_0}^T c_v(\bar{T}) d\bar{T} - T \int_{T_0}^T \frac{c_v(\bar{T})}{\bar{T}} d\bar{T} - TR \ln \left(\frac{v}{v_0} \right) + (u_0 - Ts_0), \quad (18.139)$$

$$g = h - Ts = \int_{T_0}^T c_p(\bar{T}) d\bar{T} - T \int_{T_0}^T \frac{c_p(\bar{T})}{\bar{T}} d\bar{T} + TR \ln \left(\frac{p}{p_0} \right) + (h_0 - Ts_0). \quad (18.140)$$

Finally, we leave it to the reader to corroborate the relations

$$\alpha = \frac{1}{T}, \quad \kappa_T = \frac{1}{p}, \quad \kappa_s = \frac{1}{p} \left[1 - \frac{R}{c_p} \right], \quad \beta = \frac{1}{T} \quad (18.141)$$

for the parameters, defined in (18.118) and valid for ideal gases.

Caloric ideal gases are gases of which the specific heats are constant. For these, one has the simple relation

$$u - u_0 = c_v(T - T_0),$$

$$h - h_0 = c_p(T - T_0), \quad (18.142)$$

$$s - s_0 = c_v \ln \frac{T}{T_0} + R \ln \frac{v}{v_0} = c_p \ln \frac{T}{T_0} - R \ln \frac{p}{p_0}.$$

18.3.4 Isentropic Processes in Caloric Ideal Gases

Isentropic processes are characterized by constant entropy. If (s_0, T_0, v_0) is the state associated to this constant entropy $s = s_0$ we deduce from (18.142)₃ that

$$c_v \ln \left(\frac{T}{T_0} \right) + (c_p - c_v) \ln \left(\frac{v}{v_0} \right) = 0. \quad (18.143)$$

Moreover, if one defines with

$$\kappa = \frac{c_p}{c_v} = \frac{R + c_v}{c_v} = 1 + \frac{R}{c_v} > 1 \quad (18.144)$$

the ratio of the specific heats, then one obtains from (18.143)

$$\ln \left(\frac{T}{T_0} \right) + (\kappa - 1) \ln \left(\frac{v}{v_0} \right) = 0,$$

or after application of the operator $\exp(\cdot)$ on both sides of the equation,

$$\frac{T}{T_0} = \left(\frac{v}{v_0} \right)^{-(\kappa-1)} = \left(\frac{\rho}{\rho_0} \right)^{\kappa-1}, \quad \frac{\rho}{\rho_0} = \left(\frac{T}{T_0} \right)^{1/(\kappa-1)}. \quad (18.145)$$

One can analogously proceed if one starts from the entropy, given in Eq. (18.142). The results are

$$\frac{p}{p_0} = \left(\frac{T}{T_0} \right)^{\kappa/(\kappa-1)}, \quad \frac{T}{T_0} = \left(\frac{p}{p_0} \right)^{(\kappa-1)/\kappa}, \quad \frac{p}{p_0} = \left(\frac{\rho}{\rho_0} \right)^{\kappa}. \quad (18.146)$$

A particularly impressive formula is obtained from (18.146)₃, if in this formula ρ is replaced by $1/v$. The result is

$$pv^{\kappa} = p_0 v_0^{\kappa} = \text{constant}. \quad (18.147)$$

Table 18.2 contains the gas constants, specific heats and $\kappa = c_p/c_v$ for some gases.

Table 18.2 Gas constants, specific heats c_p and c_v and the ratio $\kappa = c_p/c_v$ for some gases

	$R[\text{J/Kg K}]$	$c_p[\text{J/Kg K}]$	$c_v[\text{J/Kg K}]$	κ
Hydrogen	4125	14028	9903	1.41
Helium	2077	5232	3155	1.66
Argon	208	532	324	1.64
Nitrogen	296	1023	727	1.40
Oxygen	260	917	657	1.40
Air	287	1005	718	1.40
Carbon dioxide	189	819	630	1.30
Methane	518	2160	1642	1.32
Acetylene	319	1512	1193	1.27

18.4 Thermodynamics of an Inviscid, Heat Conducting Compressible Fluid—Toward a Hyperbolic Heat Conduction Equation

It would not be correct when leaving the reader with examples only, for which the COLEMAN–NOLL approach to the CLAUSIUS–DUHEM inequality and the more general entropy principle, due to MÜLLER yield identical results. The different axiomatic structures of the two entropy principles should also yield different results, at least when demonstrated by an instructive example from which the superiority of one of the entropy principles is visible.

We consider a *heat conducting inviscid compressible fluid* and follow essentially HUTTER (1977) [14], for which the balance laws of mass, momentum and energy take the forms

$$\begin{aligned}
 \frac{d\rho}{dt} + \rho \operatorname{div} \mathbf{v} &= 0, \\
 \rho \frac{d\mathbf{v}}{dt} &= \operatorname{div} \mathbf{t} + \rho \mathbf{f}, \\
 \rho \frac{du}{dt} &= -\operatorname{div} \mathbf{q} + \operatorname{tr}(\mathbf{tD}) + \rho q,
 \end{aligned}
 \tag{18.148}$$

in which $\{\rho, \mathbf{v}, u, \mathbf{t}, \mathbf{q}, \mathbf{D}, \mathbf{f}, q\}$ are the mass density, the velocity of the fluid particles, the internal energy, the Cauchy stress tensor, the heat flux vector, the strain rate tensor, the external specific body force and the specific energy supply rate density. The constitutive relations will be assumed in the form

$$\begin{aligned}
 u &= \hat{u}(\rho, \theta, \dot{\theta}, g), \\
 \mathbf{q} &= \hat{\mathbf{q}}(\rho, \theta, \dot{\theta}, \operatorname{grad} \theta) = -\kappa(\rho, \theta, \dot{\theta}, g) \operatorname{grad} \theta, \\
 \mathbf{t} &= \hat{\mathbf{t}}(\rho, \theta, \dot{\theta}, \operatorname{grad} \theta) = -p(\rho, \theta, \dot{\theta}, g) \mathbf{1} + Q(\rho, \theta, \dot{\theta}, g) \operatorname{grad} \theta \otimes \operatorname{grad} \theta,
 \end{aligned}
 \tag{18.149}$$

where $g = |\text{grad } \theta|^2 = \text{grad } \theta \cdot \text{grad } \theta$. Note that in (18.149) the strain rate tensor is not an independent constitutive variable. θ is the temperature and will be replaced by the absolute KELVIN temperature T when the CLAUSIUS–DUHEM inequality is used as entropy inequality and the COLEMAN–NOLL approach is employed for its exploitation; else, i.e., when using MÜLLER’s entropy principle, θ is the empirical temperature.

18.4.1 The Coleman-Noll Approach

It is basic in the COLEMAN–NOLL approach of the exploitation of the entropy inequality that the inequality

$$\rho \frac{ds}{dt} + \text{div } \phi - \rho \sigma \equiv \rho \gamma \geq 0, \quad (18.150)$$

in which s is the specific entropy, ϕ its flux, σ its specific supply and γ its specific production rate density; this inequality must be *identically satisfied for all thermodynamic processes*. Such a process is understood to be any time-dependent solution of the field variables satisfying the balance laws of mass, momentum, angular momentum, energy and constitutive relations. In order to establish a connection between the Eqs. (18.148)–(18.150) a priori estimates for ϕ and σ are introduced according to

$$\phi = \frac{q}{T}, \quad \sigma = \frac{q}{T}, \quad (18.151)$$

in which T is the absolute temperature, which replaces here the empirical temperature θ . With (18.151) the entropy inequality (18.150) takes the form

$$\rho \frac{ds}{dt} + \text{div} \left(\frac{q}{T} \right) - \frac{\rho q}{T} \equiv \rho \gamma \geq 0, \quad (18.152)$$

and is referred in this form as CLAUSIUS–DUHEM inequality. For the entropy density a constitutive relation of the class (18.149) is formulated, $s = \hat{s}(\rho, T, \dot{T}, g)$, $g = |\text{grad } T|^2$.

It is important to realize that COLEMAN and NOLL regard body force ρf and energy supply ρq to be external fields *that can be assigned arbitrarily*. This implies that for whatever process that might occur, there are always externally applied body forces and energy supply distributions, which guarantee the balance laws of momentum and energy to be identically satisfied. ‘The fact that practical difficulties prevent us from varying the motion and the temperature arbitrarily, does not affect our argument any more than our inability to produce arbitrary forces acting on mass points prevents us from calculating, on the basis of NEWTON’s law of motion, the force required to

produce a given, but arbitrary motion of a mass point' [from DAY, [5], pp. 22]. As a consequence, in exploiting the entropy inequality as an identity, only the balance of mass must be accounted for.

Eliminating ρq from (18.152) and (18.148)₃, substituting in the emerging inequality the constitutive relations (18.149) and subsequently performing the indicated differentiations produces the inequality

$$\begin{aligned} \rho \left\{ \left[T \frac{\partial \hat{s}}{\partial \rho} - \frac{\partial \hat{u}}{\partial \rho} \right] \dot{\rho} + \left[T \frac{\partial \hat{s}}{\partial T} - \frac{\partial \hat{u}}{\partial T} \right] \dot{T} + \left[T \frac{\partial \hat{s}}{\partial \dot{T}} - \frac{\partial \hat{u}}{\partial \dot{T}} \right] \ddot{T} \right. \\ \left. + \left[T \frac{\partial \hat{s}}{\partial g} - \frac{\partial \hat{u}}{\partial g} \right] \dot{g} \right\} - p \delta_{ij} v_{i,j} + Q T_{,i} T_{,j} v_{i,j} + \frac{\kappa g}{T} \geq 0. \end{aligned} \quad (18.153)$$

This imbalance must hold for all thermodynamic processes, which must, in particular, be in conformity with the balance law of mass (18.148)₁, so that

$$\begin{aligned} \gamma = \rho \left\{ \left[T \frac{\partial \hat{s}}{\partial T} - \frac{\partial \hat{u}}{\partial T} \right] \dot{T} + \left[T \frac{\partial \hat{s}}{\partial \dot{T}} - \frac{\partial \hat{u}}{\partial \dot{T}} \right] \ddot{T} + \left[T \frac{\partial \hat{s}}{\partial g} - \frac{\partial \hat{u}}{\partial g} \right] \dot{g} \right\} \\ - \left\{ \left[\rho^2 \left(T \frac{\partial \hat{s}}{\partial \rho} - \frac{\partial \hat{u}}{\partial \rho} \right) + p \right] \delta_{ij} - Q T_{,i} T_{,j} \right\} v_{i,j} + \frac{\kappa g}{T} \geq 0. \end{aligned} \quad (18.154)$$

The balance laws of momentum and energy do not form constraint conditions for the satisfaction of (18.154), because in the exploitation of the CLAUSIUS–DUHEM inequality arbitrary external body forces $\rho \mathbf{f}$ and external energy supply terms ρq allow identical satisfaction of these laws in whatever thermodynamic process. Thus, (18.154) must be satisfied for arbitrary values of \dot{T} , $T_{,i}$ and \dot{g} and $v_{i,j}$. It follows that

$$\begin{aligned} \frac{\partial \hat{s}}{\partial \dot{T}} - \frac{1}{T} \frac{\partial \hat{u}}{\partial \dot{T}} &= 0, \\ \frac{\partial \hat{s}}{\partial g} - \frac{1}{T} \frac{\partial \hat{u}}{\partial g} &= 0, \\ \frac{\partial \hat{s}}{\partial \rho} - \frac{1}{T} \left(\frac{\partial \hat{u}}{\partial \rho} - \frac{p}{\rho^2} \right) &= 0, \end{aligned} \quad (18.155)$$

and that $Q \equiv 0$. There remains the residual inequality

$$\hat{\gamma} \equiv \left(\frac{\partial \hat{s}}{\partial T} - \frac{1}{T} \frac{\partial \hat{u}}{\partial T} \right) \dot{T} + \kappa \frac{T_{,i} T_{,i}}{T^2} \geq 0. \quad (18.156)$$

Defining thermodynamic *equilibrium* to be a time independent process with uniform temperature and velocity fields, it is seen that $\hat{\gamma}$ assumes its minimum in equilibrium; of necessity then,

$$\begin{aligned} \frac{\partial \hat{\gamma}}{\partial \dot{T}} \Big|_E = 0, \quad \frac{\partial \hat{\gamma}}{\partial T_{,i}} \Big|_E = 0, \\ \left(\begin{array}{cc} \frac{\partial^2 \hat{\gamma}}{\partial \dot{T}^2} & \frac{\partial^2 \hat{\gamma}}{\partial \dot{T} \partial T_{,i}} \\ \frac{\partial^2 \hat{\gamma}}{\partial T_{,i} \partial \dot{T}} & \frac{\partial^2 \hat{\gamma}}{\partial T_{,i} \partial T_{,j}} \end{array} \right) \Big|_E \text{ is positive definite,} \end{aligned} \quad (18.157)$$

which imply the relations

$$\frac{\partial \hat{s}}{\partial T} \Big|_E - \frac{1}{T} \frac{\partial \hat{u}}{\partial T} \Big|_E = 0, \quad \kappa_{|E} \geq 0, \quad \frac{\partial \hat{u}}{\partial \dot{T}} \Big|_E \leq 0. \quad (18.158)$$

Here (18.158)_{2,3} form the so-called ROUTH–HURWITZ criteria of the matrix (18.157)₃. According to this theorem, all principal minors of a matrix must be non-negative in order that the matrix qualifies to be positive-semi definite. With the aid of (18.156), it is easy to show that

$$\begin{aligned} \frac{\partial^2 \hat{\gamma}}{\partial \dot{T}^2} &= \frac{\partial}{\partial \dot{T}} \left(\frac{\partial \hat{s}}{\partial T} - \frac{1}{T} \frac{\partial \hat{u}}{\partial T} \right) + \frac{\partial^2 \kappa}{\partial \dot{T}^2} T_{,i} T_{,i} \\ &= \frac{\partial}{\partial T} \underbrace{\left(\frac{\partial \hat{s}}{\partial \dot{T}} - \frac{1}{T} \frac{\partial \hat{u}}{\partial \dot{T}} \right)}_{=0 \text{ in equil.}} - \frac{1}{T^2} \frac{\partial \hat{u}}{\partial \dot{T}} + \frac{\partial^2 \kappa}{\partial \dot{T}^2} T_{,i} T_{,i}, \\ \frac{\partial^2 \hat{\gamma}}{\partial T_{,i} \partial T_{,j}} &= \frac{\kappa}{T^2} \delta_{ij}, \end{aligned}$$

or in equilibrium,

$$\frac{\partial^2 \hat{\gamma}}{\partial \dot{T}^2} \Big|_E = -\frac{1}{T^2} \frac{\partial \hat{u}}{\partial \dot{T}} \Big|_E, \quad \frac{\partial^2 \hat{\gamma}}{\partial T_{,i} T_{,j}} \Big|_E = \frac{\kappa_{|E}}{T^2} \delta_{ij},$$

which proves (18.158). Since $T > 0$,

$$\frac{\partial \hat{u}}{\partial \dot{T}} \Big|_E \leq 0, \quad \kappa_{|E} \geq 0. \quad (18.159)$$

With (18.155), (18.158), and (18.159), the inferences of the CLAUSIUS–DUHEM inequality are exhausted. Relations (18.155), in particular show that the thermodynamic generalization of the GIBBS equation is the expression

$$ds = \frac{\partial \hat{s}}{\partial T} dT + \frac{1}{T} \left\{ \left(\frac{\partial \hat{u}}{\partial \rho} - \frac{p}{\rho^2} \right) d\rho + \frac{\partial \hat{u}}{\partial g} dg + \frac{\partial \hat{u}}{\partial \dot{T}} d\dot{T} \right\}, \quad (18.160)$$

which in thermostatic equilibrium, since $dg_{|E} = 0$, $d\dot{T}_{|E} = 0$, reduces to

$$ds|_E = \frac{1}{T} \left\{ \frac{\partial \hat{u}}{\partial T} dT + \left(\frac{\partial \hat{u}}{\partial \rho} - \frac{p|_E}{\rho^2} \right) d\rho \right\} = \frac{1}{T} \left\{ d\hat{u}|_E - \frac{p|_E}{\rho^2} d\rho \right\}. \quad (18.161)$$

This is the classical GIBBS relation of thermostatics. The expression (18.160) is more general than the GIBBS relation of classical thermodynamics, because the entropy and internal energy (but not the free energy ψ) may depend on variables, which vanish in thermostatic equilibrium. Moreover, (18.160) is a proven statement.

However, this theory exhibits defects, which should be discussed. The extension of the GIBBS relation to involve non-equilibrium variables is due to the presence of \dot{T} as an independent constitutive variable, which is good. However, it is desirable that \dot{T} is *not* an independent constitutive variable. To see this, consider a process with uniform, time-independent density and velocity fields. Close to thermodynamic equilibrium the energy equation may then be written as

$$\rho \left\{ \frac{\partial \hat{u}}{\partial \dot{T}|_E} \ddot{T} + \frac{\partial \hat{u}}{\partial T} \Big|_E \dot{T} \right\} = \kappa|_E \Delta T, \quad (18.162)$$

where Δ is the LAPLACE operator. Because of inequalities (18.159), Eq.(18.162) is *elliptic*, implying that thermal disturbances propagate with infinite speed. If \dot{T} is missing as an independent constitutive variable, the above equation becomes *parabolic*, and the paradox of an infinite speed of thermal disturbances persists. This does not mean that the COLEMAN–NOLL theory rules out the possibility of a finite speed of propagation of thermal disturbances. For that purpose the FOURIER heat law must be altered, e.g. to the form

$$\begin{aligned} \mathbf{q} + \tau \dot{\mathbf{q}} &= -\frac{\kappa}{\tau} \text{grad } T \\ \longrightarrow \mathbf{q}(t) &= -\int_0^\infty \frac{\kappa}{\tau} \exp\left(-\frac{\xi}{\tau}\right) \text{grad } T(t - \xi) d\xi, \end{aligned} \quad (18.163)$$

where τ is a relaxation time, as has been amply illustrated, see e.g. by MORTON GURTIN and A.C. PIPKIN in 1969 [12] and DANIEL JOSEPH and LUIGI PREZIOSI in 1989 [17] for a review.²⁰

²⁰To obtain a finite thermal pulse speed in this case, \dot{T} is not allowed to be an independent constitutive variable. For instance, for a rigid heat conductor, one has the energy equation

$$\frac{du}{dt} = -\text{div } \mathbf{q}, \quad \text{with } du = c dT,$$

where c is the constant heat capacity. Combining this with (18.163)₁ then yields

$$\frac{\partial^2 T}{\partial t^2} + \frac{1}{\tau} \frac{\partial T}{\partial t} = \frac{\kappa}{\tau c} \nabla^2 T.$$

This is the so-called telegraph equation, which is hyperbolic.

Here we have shown that in BERNARD D. COLEMAN and WALTER NOLL's theory the above paradox has not been removed by the introduction of \dot{T} but worsened.

18.4.2 The Rational Thermodynamics of Ingo Müller

In this approach the entropy inequality is taken over in the form (18.150). The a-priori estimates (18.151) are not made, i.e., the *absolute temperature is a derived quantity* and entropy and entropy flux are formulated as constitutive quantities, here of a heat conducting compressible fluid, viz.,

$$\begin{aligned} s &= \hat{s}(\rho, \theta, \dot{\theta}, g), \\ \phi_i &= \hat{\phi}_i(\rho, \theta, \dot{\theta}, \theta_{,j}) = -\varphi(\rho, \theta, \dot{\theta}, g)\theta_{,i}, \end{aligned} \quad (18.164)$$

in which θ is the empirical temperature. These expressions, which are the most general isotropic functional relations of the constitutive class $\{\rho, \theta, \dot{\theta}, \theta_{,i}\}$, show that entropy flux and heat flux are collinear, see (18.149)₂.

Following an idea by I-SHIIH LIU (1973) [19] it is customary to set

$$\sigma = \lambda_i f_i + \lambda q, \quad (18.165)$$

where λ_i and λ are factors of proportionality, not dependent on f_i and q . The assignment (18.165) is a generalization of relation (18.151)₂ for a theoretical formulation without the absolute temperature as a primitive concept. Notice that (18.165) is not a constitutive concept but a statement that the external supply terms of the theory should not affect the implications of the second law of thermodynamics.

In MÜLLER's concept of the second law the independent fields ρ, v, θ , which satisfy inequality (18.150), must be solutions of the field Eqs. (18.148) and (18.149). These field equations can be interpreted as constraint conditions for inequality (18.150). It is a consequence of LIU's theorem that satisfaction of these conditions can be accomplished by the LAGRANGE parameter method (see Appendix), viz., in this heat conducting compressible fluid model, by writing

$$\begin{aligned} \rho \dot{s} + \phi_{i,i} - \rho(\lambda_i f_i + \lambda q) - \Lambda^\rho \{\dot{\rho} + \rho v_{i,i}\} \\ - \Lambda^{v_i} \{\rho \dot{v}_i - t_{ij,j} - \rho f_i\} \\ - \Lambda \{\rho \dot{u} - t_{ij} v_{(i,j)} + q_{i,i} - \rho q\} \geq 0. \end{aligned} \quad (18.166)$$

In other words, the entropy inequality is enlarged by subtracting from it the scalar products of Λ^ρ with the mass balance, of Λ^{v_i} with the momentum balance and of Λ with the energy balance. The LAGRANGE parameters $\Lambda^\rho, \Lambda^{v_i}$ and Λ are new unknown parameters to be determined in the exploitation process of (18.166), in

which $\rho, \theta, \dot{\theta}, \theta_{,i}$ are now arbitrary fields. $\Lambda^\rho, \Lambda^{v_i}$ and Λ are functions of these variables plus f_i and q .

Apart from the auxiliary quantities $\hat{s}, \hat{\phi}$ and σ new parameters $\Lambda^\rho, \Lambda^{v_i}, \Lambda$ and λ_i, λ have now been introduced. Substituting the constitutive equations into (18.166) and performing all differentiations where appropriate yields the long-hand form of the extended entropy inequality as follows:

$$\begin{aligned}
 & \rho \left\{ \frac{\partial \hat{s}}{\partial \rho} \dot{\rho} + \frac{\partial \hat{s}}{\partial \theta} \dot{\theta} + \frac{\partial \hat{s}}{\partial \dot{\theta}} \ddot{\theta} + \frac{\partial \hat{s}}{\partial \theta_{,i}} \dot{\theta}_{,i} \right\} \\
 & + \left\{ \frac{\partial \hat{\phi}_i}{\partial \rho} \rho_{,i} + \frac{\partial \hat{\phi}_i}{\partial \theta} \theta_{,i} + \frac{\partial \hat{\phi}_i}{\partial \dot{\theta}} \dot{\theta}_{,i} + \frac{\partial \hat{\phi}_i}{\partial \theta_{,k}} \theta_{,ik} \right\} \\
 & - \rho (\lambda_i f_i + \lambda q) \\
 & - \Lambda^\rho \{ \dot{\rho} + \rho v_{i,i} \delta_{ij} \} \\
 & - \Lambda^{v_i} \left\{ \rho \dot{v}_i - \frac{\partial \hat{t}_{ij}}{\partial \rho} \rho_{,j} - \frac{\partial \hat{t}_{ij}}{\partial \theta} \theta_{,j} - \frac{\partial \hat{t}_{ij}}{\partial \dot{\theta}} \dot{\theta}_{,j} - \frac{\partial \hat{t}_{ij}}{\partial \theta_{,k}} \theta_{,kj} - \rho f_i \right\} \\
 & - \Lambda \left\{ \rho \frac{\partial \hat{u}}{\partial \rho} \dot{\rho} + \rho \frac{\partial \hat{u}}{\partial \theta} \dot{\theta} + \rho \frac{\partial \hat{u}}{\partial \dot{\theta}} \ddot{\theta} + \rho \frac{\partial \hat{u}}{\partial \theta_{,i}} \dot{\theta}_{,i} \right. \\
 & \quad \left. - t_{ij} v_{i,j} - \frac{\partial \hat{q}_i}{\partial \rho} \rho_{,i} - \frac{\partial \hat{q}_i}{\partial \theta} \theta_{,i} - \frac{\partial \hat{q}_i}{\partial \dot{\theta}} \dot{\theta}_{,i} - \frac{\partial \hat{q}_i}{\partial \theta_{,k}} \theta_{,ik} - \rho q \right\} \geq 0. \quad (18.167)
 \end{aligned}$$

This imbalance is linear in the variables

$$\{ \dot{\rho}; \ddot{\theta}; \dot{\theta}_{,k}; \theta_{ik}; \rho_{,k}; \dot{v}_i, v_{i,k}; f_i; q \}. \quad (18.168)$$

The standard procedure of its exploitation is to collect the terms of (18.167) in the order and sequence of (18.168) and the residual terms not involving (18.168). In certain, not too complex, cases it may turn out to be more economical to directly operate with (18.167); the above inequality is of this kind. Recall that (18.167) has the form $\alpha \cdot \mathbf{x} + \beta \geq 0$, in which α and β do not depend on \mathbf{x} which may assume any value. LIU's theorem says in this case that α and β satisfy the conditions

$$\alpha = \mathbf{0} \quad \text{and} \quad \beta \geq 0. \quad (18.169)$$

In what follows, we now exploit the conditions $\alpha = \mathbf{0}$.

1. The only term involving \dot{v}_i is $\Lambda^{v_i} \rho \dot{v}_i$, which must vanish for any value of \dot{v}_i . This requires that

$$\Lambda^{v_i} = 0 \quad (i = 1, 2, 3). \quad (18.170)$$

This result implies that the momentum equation does not affect the second law.

2. The terms that are linear in $\ddot{\theta}$ yield

$$\frac{\partial \hat{s}}{\partial \hat{\theta}} - \Lambda \frac{\partial \hat{u}}{\partial \hat{\theta}} = 0. \quad (18.171)$$

3. The terms linear in $\rho_{,i}$ yield

$$\frac{\partial \hat{\phi}_i}{\partial \rho} - \Lambda \frac{\partial \hat{q}_i}{\partial \rho} = 0. \quad (18.172)$$

4. The terms linear in $\theta_{,i}$ yield

$$\frac{\partial \hat{\phi}_i}{\partial \theta_k} - \Lambda \frac{\partial \hat{q}_i}{\partial \theta_k} = 0. \quad (18.173)$$

5. The terms linear in $\dot{\rho}$ yield

$$\Lambda^\rho = \rho \left\{ \frac{\partial \hat{s}}{\partial \rho} - \Lambda \frac{\partial \hat{u}}{\partial \rho} \right\}. \quad (18.174)$$

Equations (18.171)–(18.174) can be viewed as equations determining Λ and Λ^ρ . This implies that Λ and Λ^ρ are of the function class of the constitutive relations. Hence, they do not, in particular, depend on \mathbf{f} and q .

6. Inequality (18.167) is now linear also in \mathbf{f} and q . Therefore,

$$\rho(\lambda_i - \Lambda^{v_i})f_i + \rho(\lambda - \Lambda)q = 0, \quad \forall \mathbf{f}, q \quad (18.175)$$

implying

$$\lambda_i = \Lambda^{v_i} = 0, \quad \lambda = \Lambda. \quad (18.176)$$

7. Caution must be observed, when the terms that are linear in $\dot{\theta}_{,i}$ are considered. Straightforward computation shows

$$\begin{aligned} \dot{\theta}_{,i} &\equiv \frac{\partial}{\partial x_i} \left(\frac{\partial \theta}{\partial t} + \theta_j v_j \right) = \frac{\partial^2 \theta}{\partial x_i \partial t} + \frac{\partial^2 \theta}{\partial x_i \partial x_j} v_j + \frac{\partial \theta}{\partial x_j} v_{j,i} \\ &= (\theta_{,i})' + \theta_{,j} v_{j,i}. \end{aligned}$$

It follows that $(\theta_{,i})'$ and $v_{i,j}$ are arbitrary, and this implies that the following identities be satisfied

$$\rho \left\{ \frac{\partial \hat{s}}{\partial \theta_{,i}} - \Lambda \frac{\partial \hat{u}}{\partial \theta_{,i}} \right\} + \left\{ \frac{\partial \hat{\phi}_i}{\partial \hat{\theta}} - \Lambda \frac{\partial \hat{q}_i}{\partial \hat{\theta}} \right\} = 0, \quad (18.177)$$

$$\left\{ -\Lambda^\rho \rho \delta_{ij} + \Lambda t_{ij} + \left\{ \frac{\partial \hat{\phi}_i}{\partial \hat{\theta}} - \Lambda \frac{\partial \hat{q}_i}{\partial \hat{\theta}} \right\} \theta_{,j} \right\} v_{j,i} = 0, \quad \forall v_{j,i}, \quad (18.178)$$

or when Eq. (18.174) is used

$$\left(\frac{\partial \hat{\phi}_i}{\partial \theta} - \Lambda \frac{\partial \hat{q}_i}{\partial \theta} \right) \theta_{,j} - \rho^2 \left\{ \frac{\partial \hat{s}}{\partial \rho} - \Lambda \frac{\partial \hat{u}}{\partial \rho} \right\} \delta_{ij} + \Lambda t_{ij} = 0. \quad (18.179)$$

There remains the residual inequality

$$\left\{ \frac{\partial \hat{\phi}_i}{\partial \theta} - \Lambda \frac{\partial \hat{q}_i}{\partial \theta} \right\} \theta_{,i} + \rho \left\{ \frac{\partial \hat{s}}{\partial \theta} - \Lambda \frac{\partial \hat{u}}{\partial \theta} \right\} \dot{\theta} \geq 0. \quad (18.180)$$

If $\hat{\phi}_i = -\varphi \theta_{,i}$ and $\hat{q}_i = -\kappa \theta_{,i}$ are substituted into (18.173), one obtains

$$(-\varphi + \Lambda \kappa) \delta_{ij} + 2 \left(-\frac{\partial \varphi}{\partial g} + \Lambda \frac{\partial \kappa}{\partial g} \right) \theta_{,i} \theta_{,k} = 0,$$

or

$$\varphi = \Lambda \kappa, \quad \text{and} \quad \frac{\partial \Lambda}{\partial g} \kappa = 0 \longrightarrow \frac{\partial \Lambda}{\partial g} = 0, \quad \kappa \neq 0, \quad (18.181)$$

so that

$$\Lambda = \Lambda(\rho, \theta, \dot{\theta}).$$

Equation (18.172) now implies $\partial \Lambda / \partial \rho = 0$, so that

$$\Lambda = \Lambda(\theta, \dot{\theta}) \implies \phi = \Lambda(\theta, \dot{\theta}) \mathbf{q}. \quad (18.182)$$

This result says that heat flux and entropy flux are collinear and Λ is a function of the empirical temperature and its time rate of change.

If one requires in addition that the normal component of the entropy flux and the normal component of the heat flux at an ideal (diathermic) material wall, separating two heat conducting simple fluids I and II, are continuous if the empirical temperature is continuous,

$$[[\mathbf{q} \cdot \mathbf{e}]] = 0, \quad \text{and} \quad [[\Lambda \mathbf{q} \cdot \mathbf{e}]] = 0, \quad \text{if} \quad [[\theta]] = 0,$$

then $[[\Lambda(\theta, \dot{\theta})]] = 0$, i.e.,

$$\Lambda^I(\theta, \dot{\theta}) = \Lambda^{II}(\theta, \dot{\theta}), \quad (18.183)$$

in other words, $\Lambda(\theta, \dot{\theta})$ is the same function for the two simple heat conducting compressible materials on both sides of the ideal diathermic wall. More precisely, $\Lambda(\theta, \dot{\theta})$ is for such materials the same universal function.

Substitution of (18.182) into (18.177)–(18.178) leads to the statements

$$\frac{\partial \ln \Lambda}{\partial \dot{\theta}} = \frac{Q}{\kappa}, \quad \Lambda^\rho = -\Lambda \frac{p}{\rho}, \quad \frac{\partial \hat{s}}{\partial g} = \Lambda \left(\frac{\partial \hat{u}}{\partial g} + \frac{Q}{2\rho} \right), \quad (18.184)$$

which, together with (18.171) and (18.174), yield

$$ds = \frac{\partial \hat{s}}{\partial \theta} d\theta + \Lambda(\theta, \dot{\theta}) \left\{ \left(\frac{\partial \hat{u}}{\partial \rho} - \frac{p}{\rho^2} \right) d\rho + \frac{\partial \hat{u}}{\partial \dot{\theta}} d\dot{\theta} + \left(\frac{\partial \hat{u}}{\partial g} + \frac{Q}{2\rho} \right) dg \right\} \quad (18.185)$$

as GIBBS relation for thermodynamic processes of heat conducting simple compressible fluids based on MÜLLER's entropy principle. Please compare (18.185) with (18.160), the corresponding GIBBS relation derived with the CLAUSIUS–DUHEM inequality and the COLEMAN–NOLL approach for its exploitation! They are *not* the same!

Returning to the residual entropy inequality (18.180) and substituting (18.182), one obtains

$$\begin{aligned} \gamma &\equiv \rho \left(\frac{\partial \hat{s}}{\partial \theta} - \Lambda \frac{\partial \hat{u}}{\partial \theta} \right) \dot{\theta} + \frac{\partial \Lambda}{\partial \theta} q_i \theta_{,i} \geq 0, \\ \rightarrow \gamma &\equiv \rho \left(\frac{\partial \hat{s}}{\partial \theta} - \Lambda \frac{\partial \hat{u}}{\partial \theta} \right) \dot{\theta} - \frac{\partial \Lambda}{\partial \theta} \kappa \theta_{,i} \theta_{,i} \geq 0. \end{aligned} \quad (18.186)$$

γ takes its minimum value in thermostatic equilibrium ($\dot{\theta} = 0, \theta_{,i} = 0$). Of necessity then

$$\frac{\partial \hat{\gamma}}{\partial \dot{\theta}} \Big|_E = 0, \quad \frac{\partial \hat{\gamma}}{\partial \theta_{,i}} \Big|_E = 0, \quad (18.187)$$

$$\left(\begin{array}{cc} \frac{\partial^2 \hat{\gamma}}{\partial \dot{\theta}^2} & \frac{\partial^2 \hat{\gamma}}{\partial \dot{\theta} \partial \theta_{,i}} \\ \frac{\partial^2 \hat{\gamma}}{\partial \theta_{,i} \partial \dot{\theta}} & \frac{\partial^2 \hat{\gamma}}{\partial \theta_{,i} \partial \theta_{,j}} \end{array} \right) \Big|_E \text{ is positive definite.}$$

These conditions imply the relations

$$\begin{aligned} \frac{\partial \hat{s}}{\partial \theta} \Big|_E &= \Lambda \Big|_E \frac{\partial \hat{u}}{\partial \theta} \Big|_E, & (q_k) \Big|_E &= -\kappa \Big|_E (\theta_{,k}) \Big|_E = 0, \\ \frac{\partial \Lambda}{\partial \theta} \Big|_E \kappa \Big|_E &\leq 0, & \frac{\partial \Lambda \Big|_E}{\partial \dot{\theta}} \frac{\partial \hat{u}}{\partial \dot{\theta}} \Big|_E &\geq \frac{\partial \Lambda}{\partial \dot{\theta}} \Big|_E \frac{\partial \hat{u} \Big|_E}{\partial \dot{\theta}}. \end{aligned} \quad (18.188)$$

Let us return to the GIBBS relation (18.185). This differential, ds , of the entropy is a total differential in the sense that

$$ds = \frac{\partial \hat{s}}{\partial \theta} d\theta + \frac{\partial \hat{s}}{\partial \rho} d\rho + \frac{\partial \hat{s}}{\partial \dot{\theta}} d\dot{\theta} + \frac{\partial \hat{s}}{\partial g} dg$$

and as such must satisfy the integrability conditions

$$\frac{\partial^2 \hat{s}}{\partial x_i \partial x_j} = \frac{\partial^2 \hat{s}}{\partial x_j \partial x_i}, \quad \text{where } x_i := \{\theta; \rho; \dot{\theta}; g\}.$$

Performing all these cross differentiations yields the following chain of integrability conditions for Λ :

$$\frac{\partial \ln \Lambda}{\partial \dot{\theta}} = \frac{\frac{\partial p}{\partial \dot{\theta}}}{\rho^2 \frac{\partial \hat{u}}{\partial \rho} - p} = \frac{2 \frac{\partial p}{\partial g}}{\kappa - \rho \frac{\partial \kappa}{\partial \rho}} = \frac{-\frac{\partial Q}{\partial \dot{\theta}}}{Q + 2\rho \left(\frac{\partial \hat{u}}{\partial g} \right)} = \frac{Q}{\kappa}. \quad (18.189)$$

These relations represent an essential contribution of the entropy principle to the thermodynamic constitutive theory. We have demonstrated that with the axiom of the existence of ideal material walls between two heat conducting fluids, see (18.183), the four different fractions in (18.189) must represent the same universal function of θ and $\dot{\theta}$. This property is a strong possibility for experimental tests of the phenomenological parameters of this theory.

In thermostatic equilibrium the entropy s is only a function of θ and ρ . Indeed for $\dot{\theta} \equiv 0$ and $g \equiv 0$ and with (18.188)₁, the GIBBS relation (18.185) reduces to

$$ds|_E = \Lambda(\theta, 0) \left\{ \frac{\partial \hat{u}|_E}{\partial \theta} d\theta + \left(\frac{\partial \hat{u}|_E}{\partial \rho} - \frac{p|_E}{\rho^2} \right) d\rho \right\}. \quad (18.190)$$

The LAGRANGE parameter $\Lambda(\theta, 0)$ is integrating factor of the PFAFFIAN form $\{\cdot\}$ in (18.190). This expression is exactly of the form, which CONSTANTIN CARATHÉODORY [1] proved in 1909 for adiabatic equilibrium systems, if $\Lambda(\theta, 0)$ is identified with the absolute temperature. This was sufficient reason for I. MÜLLER to make the identification

$$T(\theta) = \frac{1}{\Lambda(\theta, 0)}. \quad (18.191)$$

With this identification $\Lambda(\theta, \dot{\theta})$ can justly be considered a thermodynamic generalization of the absolute temperature. Müller coined for it the term **coldness function** or simply **coldness**.

Of course, the GIBBS equation in equilibrium, (18.190), also implies an integrability condition which reads

$$\frac{d \ln T}{d\theta} = \frac{-\frac{\partial \hat{p}_{|E}}{\partial \theta}}{\rho^2 \frac{\partial \hat{u}_{|E}}{\partial \rho} - p_{|E}}$$

$$\rightarrow T = T_0(\theta_0) \exp \left\{ \int_{\theta_0}^{\theta} \frac{-\frac{\partial \hat{p}_{|E}}{\partial \xi}}{\rho^2 \frac{\partial \hat{u}_{|E}}{\partial \rho} - p_{|E}} d\xi \right\}. \quad (18.192)$$

It is evident, the absolute temperature T is a function of the empirical temperature. So, if we take $T_0(\theta_0) > 0$, then also T will be positive. Moreover, $T(\theta)$ can be constructed from the measured series of $p_{|E}(\theta)$ and $\partial \hat{u}(\theta, \rho)/\partial \rho$. Conversely, if $T(\theta)$ is known, the pressure $p_{|E}(\theta, \rho)$ and $\partial \hat{u}(\theta, \rho)/\partial \rho$ cannot be independently prescribed; they must be in conformity with (18.192).

MÜLLER's theory of a simple heat conducting fluid enjoys better behavior than the COLEMAN–NOLL theory, when linear thermal waves are considered. For a thermodynamic process with uniform and time-independent density and velocity fields the linear heat equation has the form

$$\rho \frac{\partial \hat{u}}{\partial \theta} \Big|_E \ddot{\theta} + \rho \frac{\partial \hat{u}}{\partial \theta} \Big|_E \dot{\theta} = \kappa_{|E} \Delta \theta. \quad (18.193)$$

Contrary to the theory of COLEMAN–NOLL, see (18.162), this equation may be hyperbolic. Indeed, if $(\partial \hat{u}_{|E}/\partial \dot{\theta})$ is positive, then (18.193) is hyperbolic. Such a requirement is possible provided that $\partial \Lambda/\partial \dot{\theta} \neq 0$. Thus, $\dot{\theta}$ is an important variable of the constitutive theory. With $\partial \hat{u}_{|E}/\partial \theta \geq 0$, (an inequality that must hold for reasons of stability the inequality (18.188)₄, therefore, also implies $\partial \Lambda_{|E}/\partial \dot{\theta} < 0$).

We conclude that $\dot{\theta}$ is a genuine variable of the coldness function $\Lambda(\theta, \dot{\theta})$. In fact, were we to set $\partial \Lambda/\partial \dot{\theta} = 0$ wherever it occurs, we could replace Λ by $1/T(\theta)$ in all formulas and then would obtain results identical to those of COLEMAN and Noll. However, this does not mean that MÜLLER's entropy principle will always lead to results identical with those of COLEMAN and NOLL whenever $\partial \Lambda/\partial \dot{\theta} = 0$. The reader may easily construct the counter example. Starting from the constitutive assumptions of the form $C = \hat{C}(\rho, \dot{\rho}, \rho_{,i}, \theta, \theta_{,i})$ (no $\dot{\theta}$ dependence) he may prove that MÜLLER's theory will yield the GIBBS relation

$$ds = \frac{1}{T(\theta)} \left\{ \frac{\partial \hat{u}}{\partial \theta} d\theta \right\} + \frac{\partial \hat{s}}{\partial \rho} d\rho, \quad (18.194)$$

while the COLEMAN–Noll approach will result in

$$ds = \frac{1}{T} \left\{ \frac{\partial \hat{u}}{\partial T} dT + \left(\frac{\partial \hat{u}}{\partial \rho} - \frac{p}{\rho^2} \right) d\rho \right\}. \quad (18.195)$$

A great number of analyses concerning the Second Law in the forms of the CLAUSIUS–DUHEM and MÜLLER’s entropy inequalities and procedures of their exploitation have been performed in the 70 and 80s of the last century. Irrespective of the material response considered, MÜLLER’s theory is more general than most of the other thermodynamic theories in the following points:

- The entropy flux and entropy supply are not a priori given, but their determination is a basic ingredient of the theory.
- The *absolute temperature* is not a primitive, but a *derived quantity* which is determinable as a function of the empirical temperature. Regularly this function is *universal* that is, independent of the material, yet there are exceptions.
- The GIBBS equation of thermostatics is a *derived* specialization of a *proven* thermodynamic GIBBS relation. Hence, the GIBBS relation is a proven statement (as it already was in thermostatics) [14].

That this leads to essential results is demonstrated by HUTTER in [14] and in greater detail by MÜLLER in [25]. One property that emerges from MÜLLER’s entropy principle is that incorporation of the time rate of change of the temperature into the set of independent constitutive variables may lead to finite speed of thermal pulses. This is not so, if the COLEMAN–NOLL approach is applied. This does not say that the COLEMAN–NOLL approach does not lead to a hyperbolic system of equations for thermal pulses; for that purpose, the Fourier heat law must be replaced by a history dependent parameterization of the heat flow vector on the temperature gradient. Moreover, it cannot be proved in general that the coldness would be a universal function. In fact there are counterexamples to this effect. For instance, for a fluid of the constitutive class $\mathcal{C} = \hat{\mathcal{C}}(\rho; \dot{\rho}; \rho_{,i}; \theta; \dot{\theta}; \theta_{,i})$, I-Shih Liu (1973) [19] proved that

$$\phi = \Lambda q, \quad \sigma = \Lambda q, \quad \Lambda = \hat{\Lambda}(\rho, \dot{\rho}, \theta, \dot{\theta}), \quad (18.196)$$

i.e., heat flux and entropy flux are still collinear, but Λ is no longer a universal function.

Further critiques of general nature, raised mostly by physicists are stated in [14].

Appendix: Proof of Liu’s Theorem²¹

We now return to the balance equations (18.53) and the material equations (18.52). Substituting the material equations (18.52) into the balance equations (18.53), the resulting balance equations of mass, momentum and energy—known as field equations—can be written in the form

²¹See I-SHIH LIU [18], or I. MÜLLER [25]. Actually, LIU’s theorem is a special case of a much broader theorem well known in operations research. A proof in that context can be found in A. SCHRIJVER [28], but the theorem dates back to G. FARKAS [7] and H. MINKOWSKI [20], see also R.A. HAUSER and N. KIRCHNER [13].

$$\mathbf{Ax} + \mathbf{b} = \mathbf{0}, \quad (18.197)$$

in which \mathbf{x} , \mathbf{A} and \mathbf{b} are given by

$$\mathbf{x} = \{ \dot{\theta}, \rho, (\text{grad } \theta); \text{grad } \rho, \text{grad } (\text{grad } \theta) \},$$

$$\mathbf{A} = \begin{pmatrix} 0 & 1 & 0 & 0 & 0 \\ 0 & 0 & 0 & -\frac{\partial \hat{\mathbf{t}}}{\partial \rho} & -\frac{\partial \hat{\mathbf{t}}}{\partial \text{grad } \theta} \\ \rho \frac{\partial \hat{\varepsilon}}{\partial \theta} & \rho \frac{\partial \hat{\varepsilon}}{\partial \rho} & \rho \frac{\partial \hat{\varepsilon}}{\partial \text{grad } \theta} & \frac{\partial \hat{\mathbf{q}}}{\partial \rho} & \frac{\partial \hat{\mathbf{q}}}{\partial \text{grad } \theta} \end{pmatrix}, \quad (18.198)$$

$$\mathbf{b}^T = \left(\rho \text{div } \mathbf{v}, \rho \dot{\mathbf{v}} - \frac{\partial \hat{\mathbf{t}}}{\partial \theta} \text{grad } \theta - \rho \mathbf{g}, \rho \frac{\partial \hat{\varepsilon}}{\partial \theta} - \text{tr } (\hat{\mathbf{D}}) - \rho q \right).$$

Likewise the entropy inequality takes the form

$$\boldsymbol{\alpha} \cdot \mathbf{x} + \beta \geq 0 \quad (18.199)$$

with

$$\boldsymbol{\alpha}^T = \left(\rho \frac{\partial \hat{s}}{\partial \theta}, \rho \frac{\partial \hat{s}}{\partial \rho}, \rho \frac{\partial \hat{s}}{\partial \text{grad } \theta}, \frac{\partial \phi}{\partial \rho}, \left(\frac{\partial \phi}{\partial \text{grad } \theta} \right)_{\text{sym}} \right), \quad (18.200)$$

$$\beta = \frac{\partial \phi}{\partial \theta} \cdot \text{grad } \theta.$$

Equations (18.197) and the inequality (18.199) are linear in the variables \mathbf{x} , since these variables are not contained in the set of constitutive variables. If one considers a solution of the balance equations at a position in space and time in the form $\mathbf{Ax} + \mathbf{b} = \mathbf{0}$, then from the dimension of \mathbf{A} it is apparent that this equation allows a whole variety of higher dimensions from which \mathbf{x} can originate, if \mathbf{A} and \mathbf{b} are fixed. Indeed, \mathbf{A} possesses in any case more columns than rows. This being assured it is, however, still not clear whether to all these values of \mathbf{x} at fixed \mathbf{A} and \mathbf{b} there belong in reality globally meaningful fields as solutions of the balance equations. Actually, it can be applied even for an empty solution set. This is shown in R.A. HAUSER and N. KIRCHNER [13]. In many cases the desired proof is carried out with the conditions of CAUCHY and KOVALEVSKAYA being fulfilled. This is the case here, but we mention it only without proof.

Theorem *Let a matrix \mathbf{A} and vectors \mathbf{x} , \mathbf{b} and $\boldsymbol{\alpha}$, as well as a scalar β be given. In view of their dimensions these are assumed compatible with the statements*

$$\mathbf{Ax} + \mathbf{b} = \mathbf{0} \quad \text{and} \quad \boldsymbol{\alpha} \cdot \mathbf{x} + \beta \geq 0. \quad (18.201)$$

Assume, moreover, that the linear equation system (18.201)₁ has for \mathbf{x} a non-empty solution set \mathbb{S} . Then the following statements are equivalent:

(a) *For all $\mathbf{x} \in \mathbb{S}$ the inequality $\boldsymbol{\alpha} \cdot \mathbf{x} + \beta \geq 0$ holds.*

(b) *There exists a vector $\lambda \neq \mathbf{0}$, such that*

$$\alpha^T - \lambda^T A = \mathbf{0} \quad \text{and} \quad \beta - \lambda \cdot \mathbf{b} \geq 0. \tag{18.202}$$

Proof (i) From (b) follows (a): We multiply the first equation from (b) with an arbitrary \mathbf{x} of dimension of α and add this to the second inequality from (b). This yields

$$\begin{aligned} \beta - \lambda \cdot \mathbf{b} + (\alpha^T - \lambda^T A)\mathbf{x} &\geq 0 \\ \lambda \cdot \underbrace{(\mathbf{Ax} + \mathbf{b})}_{=0 \text{ since } \mathbf{x} \in \mathbb{S}} + (\alpha \cdot \mathbf{x} + \beta) &\geq 0 \quad \longrightarrow \quad (\alpha \cdot \mathbf{x} + \beta) \geq 0, \end{aligned}$$

which proves statement (a).

(ii) From (a) follows (b): This is shown by contradicting the opposite assumption: Let us therefore assume, (a) holds, but there does not exist a suitable λ with $\alpha^T - \lambda^T A = \mathbf{0}$. Then the vector α^T is linearly independent of the rows of the matrix A . This lets us find a vector with the property $A\mathbf{x}_0 = \mathbf{0}$, but at the same time $\alpha \cdot \mathbf{x}_0 \neq 0$. One now adds a suitable multiple $\delta\mathbf{x}_0$ of this vector to a solution of $A\mathbf{x} + \mathbf{b} = \mathbf{0}$, one obtains again a solution vector because $A(\mathbf{x} + \delta\mathbf{x}_0) = A\mathbf{x}$. On the other hand, one is now able to violate the inequality $\alpha \cdot (\mathbf{x} + \delta\mathbf{x}_0) + \beta \geq 0$ arbitrarily. Thus a contradiction to the assumption that the statement (a) holds has been obtained. Therefore, there exists really a λ with $\alpha^T - \lambda^T A = \mathbf{0}$, and thus one necessarily has $\beta - \lambda \cdot \mathbf{b} \geq 0$. ■

In a postscript to this law let us mention that the statement $\alpha^T - \lambda^T A = \mathbf{0}$ in our example corresponds to the identities (18.59), and the second relation (18.202), $\beta - \lambda \cdot \mathbf{b} \geq 0$ corresponds to the residual inequality (18.79) which has been obtained from the last two rows of (18.55).

References

1. Caratheodory, C.: Untersuchungen über die Grundlagen der Thermodynamik. *Mathematische Annalen* **67**, 355–386 (1909)
2. Chadwick, P. *Continuum Mechanics, Concise Theory and Problems*. George Atten & Unwin Ltd., 174 p. (1976) Also: Dover, New York, 187 p. (1999)
3. Coleman, B.D., Noll, W.: The thermodynamics of elastic materials with heat conduction and viscosity. *Arch. Ration. Mech. Anal.* **13**, 167–178 (1963)
4. Coleman, B.D., Noll, W.: The thermodynamics of materials with memory *Arch. Ration. Mech. Anal.* **17**, 1–46 (1964)
5. Day, W.A.: *The Thermodynamics of Simple Materials With Fading Memory*. *Tracts in Natural Philosophy*, vol. 22. Springer, Berlin (1972)
6. Duren, P.: Changing faces: the mistaken portrait of Legendre. *Not. AMS* **56**(11), 1440–1443 (2009)
7. Farkas, G.: A Fourier-file mechanikai etv alkalmazai. *Mathematikai és Természettudományi, Ertesítő.* **12**, 457–472 (1894)

8. Fourier, J.: Remarques Générales Sur Les Températures Du Globe Terrestre Et Des Espaces Planétaires. *Annales de Chimie et de Physique* **27**, 136–67 (1824)
9. Fourier, J.: Mémoire Sur Les Températures Du Globe Terrestre Et Des Espaces Planétaires. *Mémoires de l'Académie Royale des Sciences* **7**, 569–604 (1827)
10. Gurtin, M.: *An Introduction to Continuum Mechanics*, p. 265. Academic Press, Cambridge (1981)
11. Gurtin, M.E., Giudugli, P.P.: The thermodynamics of constrained materials. *Arch. Ration. Mech. Anal.* **51**, 192–208 (1973)
12. Gurtin, M.E., Pipkin, A.C.: A general theory of heat conduction with finite wave speed. *Arch. Ration. Mech. Anal.* **31**, 113–126 (1969)
13. Hauser, R.A., Kirchner, N.: A historical note on the entropy principle of Müller and Liu. *Contin. Mech. Thermodyn.* **14**, 223–226 (2002)
14. Hutter, K.: The foundation of thermodynamics, its basic postulates and implications. A review of modern thermodynamics. *Acta Mech.* **27**, 1–54 (1977)
15. Hutter, K., Jöhnk, K.: *Continuum Methods of Physical Modeling*, p. 635. Springer, Berlin (2004)
16. Hutter, K. and Wang, Y.: Phenomenological thermodynamics and entropy principles. Chapter 4 in: Greven, A., Keller, G. and Warnecke, G. (eds.) *Entropy*. Princeton University Press, Princeton-Oxford. ISBN 0-691-11338-6. pp. 57–78 (2003)
17. Joseph, D.D., Preziosi, L.: Heat waves. *Rev. Mod. Phys.* **61**, 47–71 (1989)
18. Liu, I-Shih: Method of Lagrange multipliers for exploitation of the entropy principle. *Arch. Ration. Mech. Anal.* **46**, 131–148 (1972)
19. Liu, I-Shih: A non-simple heat conducting fluid. *Arch. Ration. Mech. Anal.* **50**, 26–33 (1973)
20. Minkowski, H.: *Geometrie der Zahlen*, 256 p. Teubner, Leipzig (1896)
21. Müller, I.: Zur Ausbreitungsgeschwindigkeit von Störungen in kontinuierlichen Medien. *Doctoral Dissertation, Technische Hochschule Aachen*, 111 p (1966)
22. Müller, I.: Zum Paradox der Wärmeleitungstheorie. *Zeitschrift für Physik* **198**, 329–344 (1967)
23. Müller, I.: Die Kältefunktion, eine universelle Funktion in der Thermodynamik viskoser wärmeleitender Flüssigkeiten. *Arch. Ration. Mech. Anal.* doi:[10.1007/BF00281528](https://doi.org/10.1007/BF00281528)
24. Müller, I.: *Thermodynamik. Die Grundlagen der Materialtheorie*. Bertelsmann, Universitätsverlag, 232 p. (1973)
25. Müller, I.: *Thermodynamics*. Pitman, 521 p (1985)
26. Muschik, W.: Second law: Sears–Kestin statement and Clausius inequality *Am. J. Phys.* **58**(3), 241–244 (1990)
27. Noll, W.: *Foundations of Mechanics and Thermodynamics - Selected Papers*. Springer, Berlin (1974)
28. Schrijver, A.: *Theory of Linear and Integer Programming*, Wiley-Interscience Series in Discrete Mathematics, 471 p. Wiley, Chichester (1996)
29. Spencer, A.J.A.: *Continuum Mechanics*. Longman, London-New York, 183 p (1980)
30. Truesdell, C.A.: The non-linear field theories of mechanics. In: Flügge, S. (ed) *Encyclopedia of Physics*, Vol III/3, p. 602. Springer, Berlin (1965)
31. Truesdell, C. A.: *Rational Thermodynamics*, 2nd ed., 578 p. Springer, Berlin (1984)

Chapter 19

Gas Dynamics

Abstract This chapter on gas dynamics illustrates a technically important example of a fluid field theory, where the information deduced by the second law of thermodynamics delivers important properties, expressed e.g. by the thermal and caloric equations of state of, say, ideal and real gases. Problems of acoustics, steady isentropic flow processes and their stream filament theory are briefly touched. The description of the propagation of small perturbations in a gas serves in its one-dimensional form ideally as a model for the propagation of sound e.g. in a flute or organ pipe, and it can be used to explain the DOPPLER shift occurring when the sound source is moving relative to the receiver. Moreover, with the stream filament theory, the sub- and supersonic flow through a nozzle can be explained. In a final section the three dimensional theory of shocks is derived as the set of jump conditions on surfaces for the balance laws of mass, momentum, energy and entropy. Their exploitation is illustrated for steady surfaces for simple fluids under adiabatic flow conditions. This leads to the well-known RANKINE–HUGONIOT relations. These problems are classics; gas dynamics, indeed forms an important advanced technical field that was developed in the 20th century as a subject of aerodynamics and astronautics and important specialties of mechanical engineering.

Keywords Acoustic waves · Generation of sounds · D’ALEMBERT’s and BERNOULLI’s solution · Acoustic DOPPLER effect · Isentropic stream filament theory · LAVAL nozzle · Theory of shocks · Stationary shocks · RANKINE–HUGONIOT relations

List of Symbols

Roman Symbols

A	Cross section of a stream filament or narrow pipe
c	Speed of sound, adiabatic speed of sound [$c^2 = \partial \hat{p}(\rho, s) / \partial \rho _s$]
f	Thermodynamic field quantity
f^\pm	Restriction of f to positions on the positive/negative side of a singular surface
f	Body force per unit mass
h	Specific enthalpy per unit mass

$\iota = \sqrt{-1}$	Imaginary unit
k, k_n	Wave number, $k = \omega/c$
$L(t)$	Technical power added to a conduit between two cross sections 1 and 2
M, M^*	MACH number ($M = v /c$, critical MACH number ($M^* = v^*/c$, see (19.111))
m_1, m_2	Mass flow through the cross sections 1 and 2 of a stream filament
\mathbf{n}	Unit normal vector on a surface
p, p_0	Pressure, equilibrium pressure,
$\int_{p_0}^p d\tilde{p}/\rho(\tilde{p})$	Pressure function
$\dot{Q}(t)$	Heat flow supplied to the wall of a thin stream filament or thin pipe
q	Specific energy supply per unit mass, specific radiation
\mathbf{q}	Heat flux vector
R	Universal gas constant: $R = 287.04 \text{ kg}^{-1} \text{ K}^{-1}$
r	Radial distance
S	Surface in \mathbb{R}^3
s	Entropy density per unit mass
T, T_0	Temperature, KELVIN temperature
t	Time
\mathbf{t}	CAUCHY stress tensor
U	Body force potential: $\mathbf{f} = -\text{grad } U$
u	Specific internal energy per unit mass
u_0	Tangential velocity of a moving surface, see (19.58)
\mathbf{u}	Velocity of a point on a surface
\mathbf{v}	Material velocity vector
v_{\max}	Maximum velocity out of a vessel, see (19.85): $v_{\max} = \sqrt{2c_p T_0} = \sqrt{\frac{2\kappa}{\kappa-1} RT_0}$
$v^* = c^*$	Critical outflow speed from a vessel: $v^* = c^* = 2RT_0\kappa/(\kappa + 1)$
v_n, v_t	Velocity components normal/tangential to a singular surface

Greek and Miscellaneous Symbols

$\Delta(\cdot)$	LAPLACE operator: $\Delta(\cdot) = \nabla^2 = \text{div grad } (\cdot)$
$\Delta\omega = u_0\omega/c$	DOPPLER (frequency) shift ($\omega = ck$)
κ	Isentropic exponent of a caloric ideal gas
ρ, ρ_0	Mass density, equilibrium mass density
Φ	Velocity potential, $\mathbf{v} = -\text{grad } \Phi$
ψ	HELMHOLTZ free energy, initial value of $\dot{\Phi}(x, 0) = \psi(x)$
$\Phi(r, t)$	D'ALEMBERT'S solution of the spherical wave equation, see Eq. (19.38) radiating from $x = 0$: $\Phi(r, t) = \frac{1}{2}f(r - ct)$
$\Theta = \rho v$	Mass flow along a flow filament
$\chi(x)$	Initial value of $\Phi(x, 0) = \chi(x)$
σ	Degree of radiation: $\sigma = \xi^2/(1 + \xi^2)$, $\xi = \omega_n/\omega_k$
π^s	Specific entropy production per unit mass
σ	Specific supply quantity of a general balance law

ω, ω_k	Circular frequency
$\oint_{\mathcal{C}} \mathbf{v} \cdot d\mathbf{x}$	Circulation of \mathbf{v} for the closed loop \mathcal{C}
$\llbracket f \rrbracket$	Jump of f across the singular surface \mathcal{S} : $\llbracket f \rrbracket = f^+ - f^-$
$\langle\langle f \rangle\rangle$	Average value of f on the positive/negative side of a singular surface \mathcal{S} , see RANKINE–HUGONOT relations (19.134): $\langle\langle f \rangle\rangle = \frac{1}{2}(f^+ + f^-)$

19.1 Introductory Remarks

In this chapter the step from general thermodynamics to gas dynamics will be made by also accounting for the movements that are taking place in the gas. In the last chapter on thermodynamics the major focuses were the state variables; it was shown that the thermal and caloric equations of state are coupled to one another as a consequence of the Second Law of Thermodynamics. In other words, if the caloric state variables as e.g. the HELMHOLTZ free energy is known as a function of density and temperature, then the pressure is basically determinable by differentiation of the HELMHOLTZ free energy with respect to the density, see Table 18.1. In this chapter it is our intention to treat simple gas-dynamic problems, in which besides the state variables, density and temperature, also the velocity field arises as one of the unknown quantities. These are five field quantities, ρ , T , \mathbf{v} , for which the balance laws of mass, momentum and energy serve as five equations. This counting of the variables, however, also assumes that the pressure and internal energy are given as assigned functions of the density and temperature and that also a constitutive relation for the viscous stresses is at the disposal. In the sequel we shall ignore the influence of the frictional stresses. The balance laws of mass, momentum and energy then take the forms (17.92), whereby additions of the equations of state for pressure and energy makes these equations integrable, at least in principle as a set of five partial differential equations for ρ , T and \mathbf{v} , which, when being complemented by initial and boundary conditions, form a properly posed initial-boundary-value problem (IBVP).

Our goal in this chapter is less ambitious. We shall limit attention to simple flows in a gas, in particular we shall treat

- simple problems of linear acoustics,
- stationary, isentropic flow processes of linear acoustics,
- stream-filament theory in stationary flows, and
- theory of shocks.

Obviously these can provide only an exemplary first impression of the complex topic of gas dynamics. **Acoustics** is a technically important research field, which in the context of increased demands of environmental protection has acquired more and more significance. Often the focus in acoustics lies in noise absorption and noise reduction.

In gas dynamics there exist a large number of technically significant problems, in which non-linear effects are important. In the **stream filament theory** we shall encounter the most important non-linearities of gas dynamics. These type of flows are fluid motions through thin tubes and pipes, where ‘thin’ means that the cross section is only slowly varying in a meaning to be made precise shortly.

Singular surfaces in a continuous body are material or nonmaterial orientable surfaces in the body across which some physical quantities may suffer a jump. In particular, a singular surface, across which the velocity field is discontinuous, $[[\mathbf{v}]] \neq \mathbf{0}$, is called a **singular surface of first order**. If the normal component of the velocity is discontinuous, $[[\mathbf{v} \cdot \mathbf{n}]] \neq 0$, the surface is called a **shock**. These are conceptually and technically important and will be looked at in this chapter for stationary shocks in simple fluids under adiabatic conditions.

19.2 Propagation of Small Perturbations in a Gas

19.2.1 Fundamental Equations

Let us start the ensuing study with

Definition 19.1

- A flow is called **isentropic**, if the entropy of the fluid particles remains constant, $ds/dt = 0$.
- A flow is called **homentropic**, if the entropy remains constant in the entire domain that is occupied by the fluid.

Under isentropic conditions the value of the entropy can change from particle to particle; under homentropic conditions this is not possible; the entropy is constant throughout the domain of the fluid. If a gas is at rest ($\mathbf{v} = \mathbf{0}$) and in thermodynamic equilibrium, i.e., if temperature and density are temporally and spatially constant, then also the entropy is temporally and spatially constant (since $s = \hat{s}(\rho, T)$). If the gas is only brought gently out of its equilibrium, then most likely an oscillatory movement will ensue, in which temperature, density and velocity will oscillate about this state of rest. Now, the periods in the acoustic frequency regime are so small that no temperature adjustment by heat conduction between the single particles of air can be achieved. One may, therefore, assume that no heat flow is generated, corresponding ideally to **adiabatic conditions**. If one considers the balance of energy (17.92)₃, which for this situation takes the form

$$\rho \frac{du}{dt} = -p \operatorname{div} \mathbf{v} = \frac{p}{\rho} \frac{d\rho}{dt} \quad (19.1)$$

and replaces the internal energy u by the HELMHOLTZ free energy ψ via $u = \psi + Ts$, and, finally employs the relations of Table 18.1, Eq. (19.1) becomes

$$\rho \left(\dot{\psi} + T\dot{s} + \dot{T}s - \frac{\partial \hat{\psi}}{\partial \rho} \dot{\rho} \right) = \rho \left(\frac{\partial \hat{\psi}}{\partial \rho} \dot{\rho} + \frac{\partial \hat{\psi}}{\partial T} \dot{T} + T\dot{s} + \dot{T}s - \frac{\partial \hat{\psi}}{\partial \rho} \dot{\rho} \right) = 0, \quad (19.2)$$

which reduces to

$$\rho T \dot{s} = 0 \quad \text{or} \quad \dot{s} = 0. \quad (19.3)$$

Adiabatic and isentropic states in a single gas are, therefore, equivalent¹; expressed differently, this means that the energy equation can be replaced by the equation $\dot{s} = 0$. Balance laws of mass, momentum and energy can, thus, be written as

$$\begin{aligned} \frac{\partial \rho}{\partial t} + \operatorname{div}(\rho \mathbf{v}) &= 0, \\ \frac{\partial \mathbf{v}}{\partial t} + (\operatorname{grad} \mathbf{v})\mathbf{v} &= -\frac{1}{\rho} \operatorname{grad} p, \\ \frac{\partial s}{\partial t} + (\operatorname{grad} s)\mathbf{v} &= 0. \end{aligned} \quad (19.4)$$

They constitute in this form five equations for the six unknowns ρ , \mathbf{v} , p , s and must be complemented by the equation of state

$$p = \hat{p}(s, \rho). \quad (19.5)$$

With this equation one may write, since $\dot{s} = 0$,

$$\operatorname{grad} p = \left. \frac{\partial \hat{p}}{\partial \rho} \right|_s \operatorname{grad} \rho. \quad (19.6)$$

The pressure can now be eliminated from (19.4). The derivative of the pressure function $\hat{p}(\rho, s)$ with respect to the density equals the square of the speed of sound. This is important enough to be noted as

Definition 19.2

- The quantity

$$c := \sqrt{\left(\left. \frac{\partial \hat{p}(\rho, s)}{\partial \rho} \right) \right|_s} \quad (19.7)$$

is called **speed of sound** or **adiabatic speed of sound**. It is generally a function of density and entropy.

¹This statement remains valid also for a heat conducting viscous fluid, provided the dissipative working is ignored, as was shown in Sect. 18.2.

Equations (19.4)–(19.6) constitute in this general form a system of nonlinear partial differential equations, of which the integration is very difficult. For small perturbations from a thermodynamic equilibrium one may, however, assume that nonlinear terms in the governing equations may be ignored. This **linearization process** is our next goal.

If ρ_0 , s_0 and $\mathbf{v}_0 = \mathbf{0}$ denote the values of density, entropy and velocity in equilibrium and ρ' , s' and \mathbf{v}' deviations thereof, we have

$$\rho = \rho_0 + \rho', \quad s = s_0 + s', \quad \mathbf{v} = \mathbf{v}'. \quad (19.8)$$

Substitution of (19.8) into (19.4)–(19.6) and omission of all products of primed quantities (they are regarded to be of higher order small) leads for (19.4)_{1,2} to the *linearized* mass and momentum balances.

$$\frac{\partial \rho}{\partial t} + \rho_0 \operatorname{div} \mathbf{v} = 0, \quad \frac{\partial \mathbf{v}}{\partial t} + \frac{c_0^2}{\rho_0} \operatorname{grad} \rho = 0, \quad (19.9)$$

in which primes, identifying perturbation quantities are omitted. The speed of sound, c_0 and the density ρ_0 in (19.9) are regarded as constants, of which the values are treated as fixed, if values for density and temperature (or entropy) of the underlying thermodynamic equilibrium are known. The third equation (19.4)₃ is not needed.

By eliminating the velocity \mathbf{v} from (19.9), i.e., differentiation of (19.9)₁ with respect to time and substitution of $\partial \mathbf{v} / \partial t$ from (19.9)₂ one obtains

$$\frac{\partial^2 \rho}{\partial t^2} - c_0^2 \Delta \rho = 0, \quad (19.10)$$

where

$$\Delta := \operatorname{div} \operatorname{grad} \quad (19.11)$$

is the **Laplace operator**, which in Cartesian coordinates is given by

$$\Delta f = \frac{\partial^2 f}{\partial x^2} + \frac{\partial^2 f}{\partial y^2} + \frac{\partial^2 f}{\partial z^2} \quad (19.12)$$

and in spherical coordinates takes the form

$$\Delta f = \frac{\partial^2 f}{\partial r^2} + \frac{2}{r} \frac{\partial f}{\partial r} + \frac{1}{r^2 \sin \varphi} \frac{\partial^2 f}{\partial \varphi^2} + \frac{1}{r^2} \frac{\partial^2 f}{\partial \vartheta^2} + \frac{\cot \vartheta}{r^2} \frac{\partial f}{\partial \vartheta}. \quad (19.13)$$

If the thermal equation of states, $\rho = \hat{\rho}(p, s)$, is used with

$$\begin{aligned} d\rho|_s &= \left. \frac{\partial \hat{\rho}}{\partial p} \right|_s dp = \frac{1}{\partial p / \partial \hat{\rho}|_s} dp = \frac{1}{c_0^2} dp, \\ \frac{\partial \rho}{\partial t} &= \frac{1}{c_0^2} \frac{\partial p}{\partial t}, \quad \text{grad } \rho = \frac{1}{c_0^2} \text{grad } p, \end{aligned}$$

then (19.10) implies

$$\frac{\partial^2 p}{\partial t^2} - c_0^2 \Delta p = 0, \quad (19.14)$$

which is a second form of the acoustic equation, expressed as an equation for the perturbation pressure.

If one forms the curl of (19.9)₂ we obtain $\partial(\text{curl } \mathbf{v})/\partial t = 0$ (as $\text{curl grad } \rho = \mathbf{0}$) or, since in this linear approximation the partial time derivative agrees with the material time derivative

$$(\text{curl } \mathbf{v})' = \mathbf{0} \quad \rightarrow \quad \text{curl } \mathbf{v} = \mathbf{0}. \quad (19.15)$$

The operator on the left-hand side states that the vorticity (strength of vortices) remains constant along particle trajectories, that on the right assumes that the corresponding flow has emerged from a **vorticity free state**. Here, we shall assume such conditions. Consequently, then, the velocity field can be derived from a potential ϕ ,

$$\mathbf{v} = -\text{grad } \phi. \quad (19.16)$$

If this is substituted in (19.9)₂ and the density is eliminated from (19.9)_{1,2}, one obtains

$$\text{grad} \left(\frac{\partial^2 \phi}{\partial t^2} - c_0^2 \Delta \phi \right) = 0, \quad (19.17)$$

which can also be written as

$$\frac{\partial^2 \mathbf{v}}{\partial t^2} - c_0^2 \Delta \mathbf{v} = 0. \quad (19.18)$$

Alternatively, one can also integrate (19.17) and then obtains

$$\frac{\partial^2 \phi}{\partial t^2} - c_0^2 \Delta \phi = 0, \quad (19.19)$$

in which an arbitrary constant of integration has been set to zero, because the potential at time $t = 0$ can be normed to this value. It is seen that (19.10), (19.14), (19.18) and (19.19) show that density, pressure, velocity and velocity potential all satisfy the acoustic wave equation. These equations are also called **Helmholtz equations**.²

Let us add the following comments:

²HERMANN LUDWIG FERDINAND VON HELMHOLTZ (1821–1894) physician and physicist, was professor of physiology in Königsberg (Kaliningrad), Bonn, Heidelberg and since 1871 professor of physics in Berlin. For a brief biography, see Fig. 4.10 in Vol. 1.

- In (19.16) the velocity potential was introduced with the negative sign (which contradicts the common usage). This choice is advantageous, because the momentum equation (19.9)₂ implies in this case

$$\text{grad} \left(\rho_0 \frac{\partial \phi}{\partial t} - p \right) = \mathbf{0}.$$

It can directly be integrated to

$$\rho_0 \frac{\partial \phi}{\partial t} = p,$$

in which an arbitrary function of time has been set to zero, if the motion starts from a state of rest. With the choice (19.16), the velocity field is directly proportional to the time derivative of this potential. This is computationally convenient.

- For an exact proof of our statement that the flow field \mathbf{v} , subject to the stated conditions, is **irrotational** (free of vorticity), consider the balance law of momentum (3.92), in which the viscous stresses are ignored ($\mathbf{t}^R = \mathbf{0}$) and the body force is derivable from a potential, $\mathbf{f} = -\text{grad } U$:

$$\frac{d\mathbf{v}}{dt} = - \left(\frac{\text{grad } p}{\rho} + \text{grad } U \right). \quad (19.20)$$

For isentropic changes of states the thermal equation of state can be written as $p = \hat{p}(\rho, s_0) = \tilde{p}(\rho)$. We may, thus, introduce the **pressure function**

$$P(\rho) = \int_{p_0}^p \frac{d\tilde{p}}{\tilde{\rho}(\tilde{p})},$$

a form, which is restricted to barotropic fluids with the property

$$\text{grad } P = \frac{\text{grad } p}{\tilde{\rho}(p)}. \quad (19.21)$$

If this result is substituted in Eq. (19.20), then

$$\frac{d\mathbf{v}}{dt} = -\text{grad} (P + U) \quad (19.22)$$

is obtained. That is, the acceleration is the gradient of a potential.

Consider now an arbitrary simply closed material curve ℓ and compute the time derivative of the **circulation**

$$\begin{aligned}
\frac{d}{dt} \oint_{\ell} \mathbf{v} \cdot d\mathbf{x} &= \oint_{\ell} \dot{\mathbf{v}} \cdot d\mathbf{x} + \oint_{\ell} \mathbf{v} \cdot (d\mathbf{x}) \\
&= \oint_{\ell} \dot{\mathbf{v}} \cdot d\mathbf{x} + \oint_{\ell} d\left(\frac{|\mathbf{v}|^2}{2}\right) \\
&= \oint_{\ell} d\left\{\frac{|\mathbf{v}|^2}{2} - P - U\right\} = 0.
\end{aligned} \tag{19.23}$$

The integral on the right-hand side vanishes, because the path of integration is closed and the integrand is a unique function. That is, the circulation along particle trajectories remains constant. We now employ STOKES' integral theorem in three-dimensional space

$$\frac{d}{dt} \oint_{\ell} \mathbf{v} \cdot d\mathbf{x} = \frac{d}{dt} \int_{A_{\ell}} \text{curl } \mathbf{v} \cdot d\mathbf{a}, \tag{19.24}$$

in which A_{ℓ} is the area spanned by ℓ . Since A_{ℓ} can be contracted to an infinitely small area, (19.23) and (19.24) imply

$$\frac{d}{dt} (\text{curl } \mathbf{v}) = \mathbf{0}. \tag{19.25}$$

The last two statements together define **Kelvin's vorticity theorem**. According to it, the circulation around an arbitrary closed material line is temporally constant. If the flow is irrotational initially, it remains irrotational for all time. This terminates the proof of (19.16). We emphasize that the assumption of isentropic conditions is an important prerequisite of the result.

In Chap. 18, Sect. 18.3.4 isentropic processes in caloric ideal gases were shown to obey the thermal equation of state

$$\frac{P}{P_0} = \left(\frac{\rho}{\rho_0}\right)^{\kappa}. \tag{19.26}$$

With the definition of the speed of sound (19.7), Eq. (19.26) may be used to evaluate

$$c = \sqrt{\kappa RT}, \tag{19.27}$$

which can easily be computed for the gases listed in (19.7). Typical values for c in the temperature range around 300 K yield $c \in [250, 450] \text{ m s}^{-1}$. For air with $R = 287.04 \text{ J kg}^{-1} \text{ K}^{-1}$, $\kappa = 1.402$ and $T = 293 \text{ }^{\circ}\text{K}$, one obtains the value $c = 348.48 \text{ m s}^{-1}$.



Fig. 19.1 JEAN- BAPTISTE LE ROND D'ALEMBERT (16. Nov. 1717–29. Oct. 1783)

JEAN- BAPTISTE LE ROND D'ALEMBERT was a French mathematician, mechanician, physicist, philosopher, and music theorist. Until 1757 he was also co-editor with DENIS DIDEROT of the *Encyclopédie*.

Born in Paris, D'ALEMBERT was the illegitimate child of the writer CLAUDINE GUÉRIN de Tencin and the chevalier LOUIS- CAMUS DESTOUCHES, an artillery officer. He became the foster child of the wife of a glazier, Madame ROUSSEAU, with whom D'ALEMBERT lived for 48 years. DESTOUCHES secretly paid for the education of JEAN LE ROND, but did not want his paternity officially recognized. D'ALEMBERT first attended a private school, supported by his father, who left him an annuity of 1200 lives on his death in 1726. At the age of twelve he entered 'Collège Mazarin'. Here he studied philosophy, law, and the arts, graduating in arts in 1735. He then entered law school for two years, but was equally interested in medicine and mathematics.

D'ALEMBERT was an excellent mathematician with interest of its application to solve problems of mechanics and physics. His most successful contribution to theoretical mechanics was what later became analytical dynamics. His fundamental thoughts were outlined in his 'Traité de dynamique' [4]. In this article he developed the D'ALEMBERT principle, which is to be regarded as a rule how to treat the equations of motion in a material body; it reduced the dynamics of bodies to problems of equilibrium. This led to the LAGRANGEAN equations. D'ALEMBERT published in 1744 an article on the equilibrium and motion of fluids, and in 1747 he submitted a further article to the Berlin Academy of Science on the theory of winds on Earth and concluded that the distribution of winds on Earth was the result of the atmospheric tides [5]. In the same year he studied the vibration of an oscillating string and deduced the wave equation as the equation of its motion. He recognized that the oscillations of a string are determined by the prescription of the initial and boundary conditions, see **Figs. 19.2** and **19.3**. He also applied the method of separation of variables, attributed to DANIEL BERNOULLI and LEONHARD EULER. In his 'Essai d' une nouvelle théorie de la résistance des fluids' (1752) [6] he analyzed the steady motion of a rigid body through an ideal, incompressible fluid, employed thereby complex functions—before the formal introduction of the theory of complex variables with the CAUCHY-RIEMANN equations—and formulated the D'ALEMBERT 'paradox': that in three-dimensional steady potential flow

the force exerted by the fluid on the body vanishes. He was also deeply involved in celestial mechanics and constructed some solutions to the three body problem. He was elected member of the *Académie Française* in 1754 of which he became Permanent Secretary in 1772. The text is based on www.wikipedia.org and Fachlexikon: Forscher und Erfinder, Nikol Verlagsgesellschaft mbH & Co. KG

19.2.2 Plane and Spherical Waves

Plane waves are obtained when all variables depend only on a single space coordinate, say x . One is then led to the wave equation

$$\frac{\partial^2 \Phi}{\partial t^2} = c^2 \frac{\partial^2 \Phi}{\partial x^2} \quad -\infty < x < \infty, \quad (19.28)$$

in which Φ stands for any of the variables ρ , p , ϕ and $c = c_0$ is the constant acoustic speed. We wish to solve (19.28) on the infinite line, subject to the initial conditions

$$\Phi(x, 0) = \chi(x), \quad \dot{\Phi}(x, 0) = \psi(x). \quad (19.29)$$

A general solution of the wave equation (19.28) due to JEAN BAPTISTE LE ROND D'ALEMBERT³ can be written as

$$\Phi(x, t) = f(x - ct) + g(x + ct), \quad (19.30)$$

in which f and g are differentiable functions. These two functions can be determined with the aid of the initial conditions. Indeed, substitution of (19.30) into (19.29) yields

$$f(x) + g(x) = \chi(x), \quad c(-f(x) + g(x))' = \hat{\psi}(x), \quad (19.31)$$

in which primes indicate differentiation with respect to the arguments $x \pm ct$, χ and $\hat{\psi}$ are functions, which for $x \rightarrow \pm\infty$ fall sufficiently fast to zero. Integrating (19.31)₂ yields

$$-f(x) + g(x) = \frac{1}{c} \int_{-\infty}^x \hat{\psi}(\xi) d\xi =: \psi(x), \quad (19.32)$$

in which a constant of integration has been set to zero, because f and g must each vanish as $x \rightarrow \pm\infty$. Equations (19.31)₁ and (19.32) form a linear system of equations for $f(x)$ and $g(x)$, which has the solution

$$f(x) = \frac{1}{2}(\chi(x) - \psi(x)), \quad g(x) = \frac{1}{2}(\chi(x) + \psi(x)), \quad (19.33)$$

³For a brief biography of JEAN BAPTISTE LE ROND D'ALEMBERT (1717–1783), see Fig. 19.1.

which together with (19.32) implies

$$\begin{aligned} f(x-ct) &= \frac{1}{2}\chi(x-ct) - \frac{1}{2c} \int_{-\infty}^{x-ct} \hat{\psi}(\xi) d\xi, \\ g(x+ct) &= \frac{1}{2}\chi(x+ct) + \frac{1}{2c} \int_{-\infty}^{x+ct} \hat{\psi}(\xi) d\xi. \end{aligned} \quad (19.34)$$

Substitution of these results in (19.30) leads to the general solution of the plane wave equation according to D'ALEMBERT

$$\Phi(x, t) = \frac{1}{2} (\chi(x-ct) + \chi(x+ct)) + \frac{1}{2c} \int_{x-ct}^{x+ct} \hat{\psi}(\xi) d\xi. \quad (19.35)$$

The physical significance of the solutions (19.30) and (19.35), respectively, is recognized by the following discussion: For constant argument $\xi_+ = x - ct$, i.e., an observer propagating with the speed of sound in the positive x -direction the value of $f(\xi_+)$ remains constant; $f(x - ct)$ thus, represents a propagating wave which moves to the right, i.e., in the positive x -direction. Completely analogously, for constant argument $\xi_- = x + ct$, the value of $g(\xi_-)$ remains constant; $g(x + ct)$, thus, represents a propagating wave, which moves with the speed of sound to the left; i.e., in the negative x -direction.

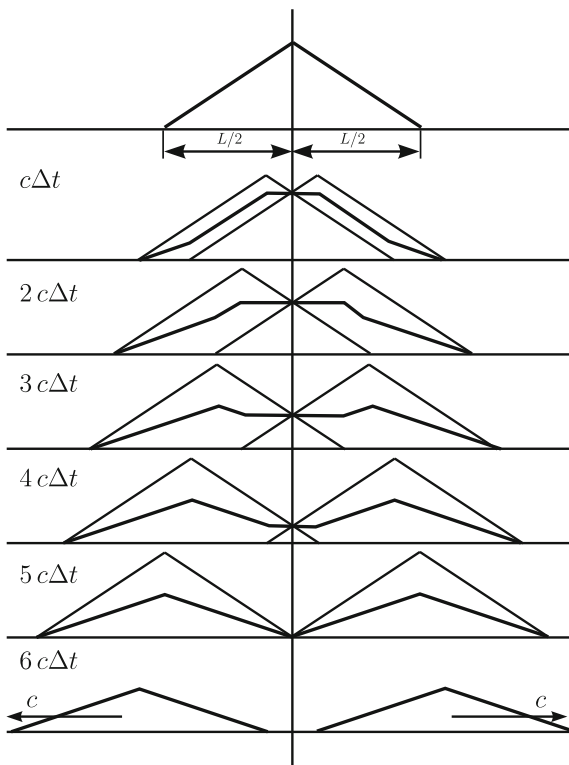
Example 1

If one considers as initial condition a motion from a state at rest, one has $\psi(x) = 0$; so, the last integral term on the right of (19.35) vanishes. Consequently, a given initial perturbation $\chi(x)$ will travel with half the amplitude to the left and right; for any fixed time the two profiles, cut in half and correspondingly positively and negatively shifted (along the x -axis), will be added where they overlap. **Figure 19.2** displays how these two waves, which propagate to the right and left, evolve from an initially triangular profile. Once the two perturbations have moved far enough to the left and right and no longer interact, they propagate as independent triangles each with half the height to the left and right.

Example 2

Example 1 is insofar special as the domain in which the wave propagates, is assumed to be of infinite extent to the left and the right. The two waves have finite extent, they reach the two ends of the line only after an infinitely long time; so, no boundary

Fig. 19.2 Construction of D’ALEMBERT’S solution. A triangular perturbation Φ , released from rest propagates to the left and right with the height cut in half



conditions have to be taken into account. In realistic problems the solution $\Phi(x, t)$ must not only satisfy initial conditions but equally also certain boundary conditions. To be able to formulate these, the solution must be extended into the domain where the physical solution does not exist, such that the boundary conditions are met.

If one takes as an example the one-sided half line $x > 0$ and assumes a perturbation, which is initially zero ($\hat{\psi} = 0$), we obtain as in Example 1

$$\Phi(x, t) = \frac{1}{2} (\chi(x - ct) + \chi(x + ct)),$$

and if one requests as reflection condition the vanishing of the perturbation, thus, $\Phi(0, t) = 0$, then the last equation implies⁴

$$\chi(ct) = -\chi(-ct) \quad \longrightarrow \quad \chi(x) = -\chi(-x).$$

⁴This is e.g. the appropriate condition if Φ is the horizontal velocity.

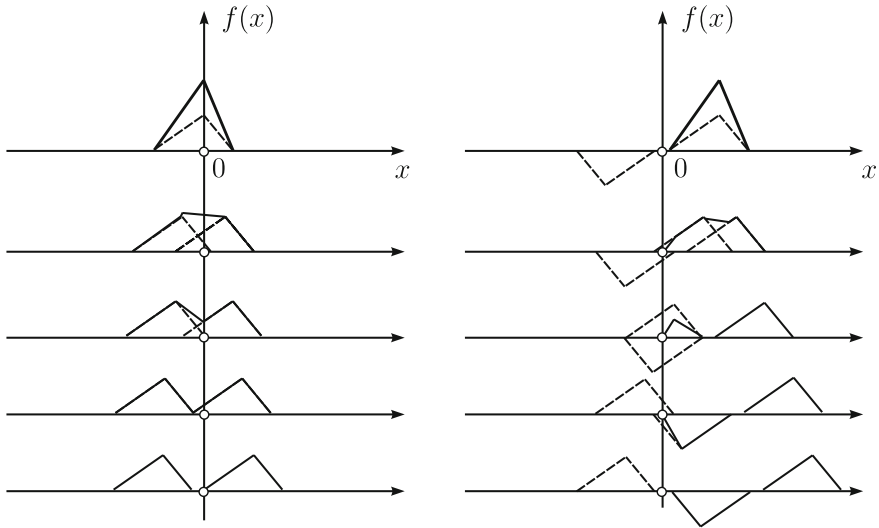


Fig. 19.3 Construction of the D’ALEMBERT solution when reflection occurs at $x = 0$. For a wave propagating on the half line $x > 0$, which is reflected at $x = 0$, the condition $\Phi(0, t) = 0$ is satisfied by mirrored continuation of Φ to values of $x < 0$

The perturbation $\chi(x)$ for $x > 0$ must, therefore, anti-symmetrically be extended into the half-line $x < 0$.

If one cuts in halves the function $\chi(x)$, which is declared for all values of x , and then lets the two halves move to the left and right, then the perturbation lying on the positive x -axis (**Fig. 19.3**) splits into two oppositely moving waves. As soon as the part moving to the left encounters the origin, its mirror picture occupies the positive x -axis, so that the amplitude at $x = 0$ remains zero. After some time, nothing is left of the wave traveling to the left. Instead its mirror picture travels on the positive x -axis to the right. At $x = 0$ a reflection has taken place with simultaneous change of the sign of the perturbation.

Spherical waves are e.g. formed, if a point source in three dimensions emits acoustic signals. Technically, this can for instance be reached, if an elastic sphere ‘breathes’ in the acoustic frequency regime. The waves are in this case radially propagated. In spherical coordinates the wave function cannot have any φ - and ϑ -dependences (if the coordinate origin is in the center of the sphere); so, the LAPLACE operator (19.13) reduces to

$$\Delta\Phi|_{\varphi,\vartheta} = \frac{\partial^2\Phi}{\partial r^2} + \frac{2}{r}\frac{\partial\Phi}{\partial r} = \frac{1}{r}\frac{\partial^2}{\partial r^2}(r\Phi). \tag{19.36}$$

The wave equation, therefore, assumes the form

$$\frac{\partial^2(r\Phi)}{\partial t^2} = c^2 \frac{\partial^2(r\Phi)}{\partial r^2} \quad (19.37)$$

and is formally equivalent to Eq. (19.28) of plane waves, if in this latter equation Φ is replaced by $r\Phi$ and x is replaced by r . The only formal difference to plane waves is that the domain of the solution for a source in the coordinate origin is restricted to values of $r > 0$ and that only outgoing waves are possible, whereas for plane waves x may embrace the whole line and waves propagating to the left and to the right are possible.

Because the surface of the sphere can only emit waves which propagate in the positive r -direction, D'ALEMBERT'S solution has here the form

$$\Phi(r, t) = \frac{1}{r} f(r - ct), \quad (19.38)$$

where the function f is determined by the source function in $r = r_0$.

Example 3

We assume that a **spherical radiator** with radius r_0 and surface speed⁵

$$v^{(n)} = v_n \exp(i\omega_n t), \quad \text{for } r = r_0 \quad (19.39)$$

with constant v_n vibrates, and we ask how pressure and particle velocity are distributed in the outer space $r > r_0$. This problem can be solved, if the velocity potential Φ in (19.38) is expressed by the trial function

$$\Phi(r, t) = \frac{c_n}{r} \exp[i(\omega_n t - k_n r)] \quad (19.40)$$

with constant c_n . The circular frequency and the wave number k_n must obviously be connected with the speed of sound; this can successfully be done with

$$\exp[i(\omega_n t - k_n r)] = \exp\left[-ik_n \left(r - \frac{\omega_n}{k_n} t\right)\right]. \quad (19.41)$$

According to (19.38), (ω_n/k_n) in (19.41) must agree with c ; this means that

$$\frac{\omega_n}{k_n} = c. \quad (19.42)$$

If the speed of sound c and the circular frequency ω_n are given, the wave number follows from (19.42). The ratio $(\omega_n/k_n) = c$ is called in wave theory the **phase speed**; it, thus, has been shown that the sound and phase speed agree with one another.

⁵The index $(\cdot)_n$ in (19.39) will shortly become understood below.

With the aid of the trial solution (19.40), the complex valued radial particle velocity can be evaluated by differentiation with respect to r ; this yields

$$v(r, t) = -\frac{\partial\Phi}{\partial r} = \frac{c_n}{r^2}(1 + \iota k_n r) \exp[\iota(\omega_n t - k_n r)]. \quad (19.43)$$

If this is evaluated for $r = r_0$ and the resulting expression compared with (19.39), c_n can be connected with v_n . If the result is again substituted in (19.43), one obtains

$$v^{(n)}(r, t) = v_n \frac{1 + \iota k_n r}{1 + \iota k_n r_0} \left(\frac{r_0}{r}\right)^2 \exp[\iota(\omega_n t - k_n(r - r_0))]. \quad (19.44)$$

Finally, using the relation $\rho_0 \partial\Phi/\partial t = p$, the pressure takes the form,

$$p^{(n)}(r, t) = v_n \frac{\iota\omega_n \rho_0 r_0^2}{1 + \iota k_n r_0} \frac{1}{r} \exp[\iota(\omega_n t - k_n(r - r_0))]. \quad (19.45)$$

If the spherical radiator oscillates with a stimulus velocity having the FOURIER representation

$$v(r_0, t) = \sum_n v^{(n)}(r_0, t) = \sum_{n=0}^{\infty} v_n(r_0) \exp(\iota\omega_n t), \quad (19.46)$$

the general solution can be obtained by summation over the components (19.44) and (19.45); this is possible, because of the linearity of the HELMHOLTZ differential equation and the boundary conditions. For the excitation (19.46) we, thus have

$$\begin{aligned} v(r, t) &= \sum_{n=0}^{\infty} v_n \frac{1 + \iota k_n r}{1 + \iota k_n r_0} \left(\frac{r_0}{r}\right)^2 \exp[\iota(\omega_n t - k_n(r - r_0))], \\ p(r, t) &= \sum_{n=0}^{\infty} v_n \frac{\iota\omega_n \rho_0 r_0^2}{1 + \iota k_n r_0} \frac{1}{r} \exp[\iota(\omega_n t - k_n(r - r_0))]. \end{aligned} \quad (19.47)$$

Let us close this example by a few remarks:

- An important measure in acoustics is the effective radiated acoustic power. Its areal density is called **acoustic intensity** and is defined as the product of the pressure with the velocity. In the complex valued notation given here, it is defined by

$$j = \frac{1}{2} \text{Re}(pv^*), \quad (19.48)$$

in which v^* is the complex conjugate to v and $\text{Re}(pv^*)$ is the real part of pv^* . With (19.44) and (19.45) there follows

$$j = \frac{1}{2}\rho_0 c v_n^2 \left(\frac{r_0}{r}\right)^2 \frac{(k_n r_0)^2}{1 + (k_n r_0)^2}, \quad (19.49)$$

or after multiplication with the total area of the sphere

$$P_n = j 4\pi r_0^2 = 2\pi r_0^2 v_n^2 \rho_0 c \frac{(k_n r_0)^2}{1 + (k_n r_0)^2}. \quad (19.50)$$

P_n is the total radiated power of the frequency ω_n of the oscillating sphere. If one defines with

$$\omega_k := c/r_0, \quad (19.51)$$

the so-called **corner angular frequency** of the **spherical radiator**, then the total power P_n takes the elegant form

$$P_n = 2\pi r_0^2 v_n^2 \rho_0 c \frac{(\omega_n/\omega_k)^2}{1 + (\omega_n/\omega_k)^2}. \quad (19.52)$$

- We conclude from (19.52) that the radiation power is small if $\omega_n \ll \omega_k$. Moreover, the fraction in (19.52) reaches the value 1 if $\omega_n/\omega_k \rightarrow \infty$. Obviously for small finite n the fraction is smaller than 1.
- One calls

$$\sigma = \frac{\xi^2}{1 + \xi^2}, \quad \xi = \frac{\omega_n}{\omega_k} \quad (19.53)$$

the **degree of radiation**, which for $\xi \ll 1$ has the asymptotic representation $\sigma = \xi^2$, but $\sigma \approx 1$ for $\xi \rightarrow \infty$. Its logarithm is given by

$$\ln \sigma = 2 \left[\ln \xi - \ln \sqrt{1 + \xi^2} \right]. \quad (19.54)$$

It is proportional to the noise level measured in decibel.

Example 4

The reader has experienced that the horn (siren) of an ambulance or police car sounds higher for a car approaching an observer at standstill and suddenly lower, once the car has passed the observer. This frequency shift, called **Doppler shift**⁶ can be made precise with the spherical wave treated in Example 2.

⁶For a brief biography of CHRISTIAN JOHANN DOPPLER (1803–1853), see **Fig. 19.4**.



Fig. 19.4 CHRISTIAN ANDREAS DOPPLER (29. Nov. 1803–17. March 1853)

CHRISTIAN ANDREAS DOPPLER was an Austrian mathematician and physicist, known through his explanation of the frequency shift of a moving oscillating source when reaching a receiver at rest (or moving with different velocity). He was the son of a stonemason in Salzburg (Austria), but of weak health and, therefore, unfit for this choice of profession. He studied mathematics and physics at the Polytechnic Institute in Vienna and philosophy in Salzburg.

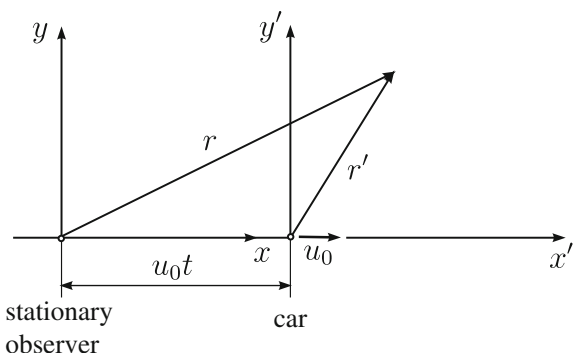
Subsequently, in 1829, he worked in Vienna as an assistant, and from 1835 was teacher of mathematics and physics, eventually at the Polytechnic Institute in Prague (a junior college). 1841 he was called as full professor for mathematics and physics at the Charles-University in Prague, taught for some time mathematics, physics and mechanics at the Academy of Mines and Forests (in today's Slovakia) and then moved in 1849 to Vienna where he was appointed by the Emperor FRANZ JOSEPH head of the first ever Institute of Experimental Physics at the University of Vienna in 1850. CHRISTIAN DOPPLER died at the age of 49 in Venice from pulmonary disease.

CHRISTIAN DOPPLER's scientific work comprises of approximately 50 articles, but his most notable article is 'Über das farbige Licht der Doppelsterne und einiger anderer Gestirne des Himmels' (On the colored light of the binary stars and some other stars of the heavens), which he read on 25. May 1842 in front of the Königlich Böhmisches Gesellschaft der Wissenschaften in Prague, which was also published in the same year. There is a facsimile edition with an English translation by ALEC EDEN [7].

The text is based on www.wikipedia.org

We idealize the siren on the moving car as a spherical radiator and assume that the car moves relative to the observer with *constant* speed u_0 in the positive x' -direction. The observer is immobile relative to the spatially fixed coordinate system (x, y, z) ; the acoustic source moves together with the primed system, see **Fig. 19.5**.

Fig. 19.5 Moving acoustic point source. A car moves with constant speed u_0 in the x' -direction. The observer is in the origin of the fixed coordinate system (x, y, z)



In the moving system the solution of the acoustic wave equation for the siren as a spherical radiator has the form

$$\Phi(r', t) = \frac{C}{r'} \exp [\iota(\omega t' - kr')]. \tag{19.55}$$

For an immobile observer this equation only needs to be written in his coordinates. With the aid of Fig. 19.5 one has

$$r' = \sqrt{(x - u_0 t)^2 + y^2 + z^2},$$

so that (19.55) takes the form

$$\Phi(x, y, z, t) = C \frac{\exp [\iota(\omega t - k\sqrt{(x - u_0 t)^2 + y^2 + z^2})]}{\sqrt{(x - u_0 t)^2 + y^2 + z^2}}. \tag{19.56}$$

This relation explains now, why an observer in the (x, y, z) -system experiences different sounds depending upon his position relative to the moving car. If his position is in the origin of the coordinate system (x, y, z) , then (19.56) yields

$$\Phi(0, 0, 0, t) = \frac{C}{u_0 t} \exp [\iota(\omega - u_0 k)t]. \tag{19.57}$$

The observer experiences the sound of the siren with shifted frequency

$$\omega_{\text{obs}} = \omega - u_0 k. \tag{19.58}$$

For $u_0 \leq 0$ then $\omega_{\text{obs}} \geq \omega$, so that the sound is higher when the car is approaching the observer, but lower when it is leaving his position. The quantity

$$\Delta\omega = u_0 k = \frac{u_0 \omega}{c}, \quad \left(\frac{\omega}{k} = c\right) \tag{19.59}$$

is called the **Doppler frequency shift**. If the frequency of the radiator signal and the speed of sound are known, then the DOPPLER shift allows measurement of the velocity u_0 . This property is exploited in many technical applications, not only in the acoustic frequency range.

For an observer who is far distant from the x -axis the frequency does not change, because with $(x - u_0 t)^2 \ll (y^2 + z^2)$, (19.56) takes the form

$$\Phi(x, y, z, t) = C \frac{\exp \left[i(\omega t - k\sqrt{y^2 + z^2}) \right]}{\sqrt{y^2 + z^2}}, \quad (19.60)$$

which agrees with (19.40), if one identifies $\sqrt{y^2 + z^2}$ with the distance between source and observer.

19.2.3 *Eigen Oscillations Determined with Bernoulli's Method*

Any wind-instrument can in first approximation be regarded as a one-dimensional acoustic oscillator. The simplest case is an **organ pipe**, of which the equation of oscillation is given by

$$\frac{\partial^2 \Phi}{\partial t^2} = c^2 \frac{\partial^2 \Phi}{\partial x^2}, \quad 0 \leq x \leq l, \quad (19.61)$$

which is to be solved subject to initial conditions

$$\Phi(x, 0) = \Phi_0(x), \quad \dot{\Phi}(x, 0) = \dot{\Phi}_0(x), \quad (19.62)$$

where $\Phi_0(x)$ and $\dot{\Phi}_0(x)$ are prescribed functions. Let the pipe have length l . If Φ is the velocity we have

$$\Phi(0, t) = \Phi(l, t) = 0. \quad (19.63)$$

The solution of the initial boundary value problem (IBVP) (19.61)–(19.63) can be constructed with the D'ALEMBERT method. More convenient is the **separation technique**

$$\Phi(x, t) = f(x)g(t). \quad (19.64)$$

Substitution of this expression in Eq. (19.61) leads to

$$\underbrace{\ddot{g}(t)}_{\text{fct}(t)} = c^2 \underbrace{\frac{f''(x)}{f(x)}}_{\text{fct}(x)} = -\omega^2, \quad (19.65)$$

in which the point (prime) denotes differentiation with respect to time (spatial coordinate). The expression on the left is only a function of time t , that in the middle only a function of position x . Both can only be equal to one another, if they are equal to the same constant, $-\omega^2$ say, which still must be determined. Equation (19.65) implies the two ordinary differential equations

$$\ddot{g}(t) + \omega^2 g(t) = 0, \quad f''(x) + \frac{\omega^2}{c^2} f(x) = 0 \quad (19.66)$$

with the solutions

$$\begin{aligned} g(t) &= C_1 \sin \omega t + C_2 \cos \omega t, \\ f(x) &= D_1 \sin \left(\frac{\omega}{c} x \right) + D_2 \cos \left(\frac{\omega}{c} x \right), \end{aligned} \quad (19.67)$$

where C_1, C_2, D_1, D_2 are constants of integration. The boundary conditions (19.63) are equivalent to the statements $f(0) = f(l) = 0$, so that according to (19.67)₂ we obtain

$$D_2 = 0, \quad \frac{\omega_n l}{c} = n\pi, \quad (n = 1, 2, 3, \dots). \quad (19.68)$$

To every n there belongs an $\omega = \omega_n$ so that also $\Phi = \Phi_n(x, t)$ or

$$\Phi_n(x, t) = (A_n \sin \omega_n t + B_n \cos \omega_n t) \sin \left(\frac{\omega_n x}{c} \right) \quad (n = 1, 2, 3, \dots), \quad (19.69)$$

in which $A_n = C_1 D_1$ and $B_n = C_2 D_1$ has been chosen. ω_n is called n th **eigenvalue** or n th **eigenfrequency**, and Φ_n is the associated **eigenfunction** or **eigenoscillation form**; there is a countable infinite set for these.

The most general solution is obtained by superposition of all eigensolutions,

$$\Phi(x, t) = \sum_{n=1}^{\infty} \{A_n \sin(\omega_n t) + B_n \cos(\omega_n t)\} \sin \left(\frac{n\pi x}{l} \right) \quad (19.70)$$

with constants $A_n, B_n, n = 1, 2, \dots, \infty$. For the determination of these free constants, A_n and B_n , the solution (19.70) is substituted into the initial conditions (19.62) from which

$$\sum_{n=1}^{\infty} B_n \sin \left(\frac{n\pi x}{l} \right) = \Phi_0(x), \quad \sum_{n=1}^{\infty} \omega_n A_n \sin \left(\frac{n\pi x}{l} \right) = \dot{\Phi}_0(x) \quad (19.71)$$

is obtained. The expressions on the left-hand side are the FOURIER sine series of the prescribed functions on the right-hand side. One can find an expression for B_n by multiplication of (19.71)₁ with $\sin(m\pi x/l)$ and integration of the resulting expression from $x = -l$ to $x = l$:

$$\int_{-l}^l \sum_{n=1}^{\infty} B_n \sin\left(\frac{n\pi x}{l}\right) \sin\left(\frac{m\pi x}{l}\right) dx = \int_{-l}^l \Phi_0(x) \sin\left(\frac{m\pi x}{l}\right) dx,$$

from which one easily deduces

$$B_m = \frac{1}{l} \int_{-l}^l \Phi_0(x) \sin\left(\frac{m\pi x}{l}\right) dx. \quad (19.72)$$

To obtain this result, the orthogonality relations of the trigonometric functions

$$\int_{-l}^l \sin\left(\frac{n\pi x}{l}\right) \sin\left(\frac{m\pi x}{l}\right) dx = \begin{cases} l, & m = n, \\ 0, & m \neq n \end{cases} \quad (19.73)$$

were used. Analogously, if one multiplies (19.71)₂ with $\sin(m\pi x/l)$ and integrates the emerging expression from $x = -l$ to $x = l$, A_m can be evaluated:

$$A_m = \frac{1}{\omega_m l} \int_{-l}^l \dot{\Phi}_0(x) \sin\left(\frac{m\pi x}{l}\right) dx, \quad (19.74)$$

where again the orthogonality relation (19.73) was employed.

An organ pipe that is stimulated by $\Phi_0(x)$ and $\dot{\Phi}_0(x)$ and is closed at its upper end, i.e., at $x = l$, will respond, in general, with the entire **spectrum** of the eigenoscillations; ω_1 is the frequency of the **fundamental tone** and $\omega_2, \omega_3, \dots$ are those of the harmonic **overtones**. The **sound** of the organ pipe is formed by superposition of the fundamental tone with the overtones; depending upon how the stimulation takes place (this corresponds to the prescription of $\Phi_0(x)$ and $\dot{\Phi}_0(x)$), some overtones stand out more than others and thus determine the **timbre** of the sound. With wind instruments without valves (e.g. alphorn or French horn) certain overtones may, with adequate blowing, stand out loudly, whilst others may only softly be stimulated. This way one excites **natural tones** of instruments and can play this way also melodies, being composed only of such natural tones. In instruments with valves the length l of the resonating ‘pipe’ is altered by changing this length which, correspondingly also changes their eigenfrequencies. With such instruments one is generally able to play the full scale of notes in a certain frequency range.

In the above example we considered a pipe that is closed at both ends and solved the acoustic equation subjected to the boundary conditions (19.63). For a (standing) pipe, which is closed below and open above, the boundary conditions are

$$\Phi(0, t) = 0, \quad \frac{\partial \Phi}{\partial x}(\ell, t) = 0. \quad (19.75)$$

The general separation solution (19.64) leads in this case equally to the solution of the form (19.67), however, the boundary conditions (19.75) now request $f(0) = 0$ and $f'(l) = 0$, which leads to

$$D_2 = 0, \quad \frac{\omega_n l}{c} = \frac{2n + 1}{2} \pi, \quad (n = 0, 1, 2, \dots). \tag{19.76}$$

The eigenfrequencies are in this case, therefore, given by

$$\omega_n = \frac{2n + 1}{2} \frac{\pi c}{l}, \quad (n = 0, 1, 2, \dots). \tag{19.77}$$

The corresponding eigenfunctions appear again as (19.70), whereby ω_n is now given by (19.77). The forms of the eigenoscillations of the two pipes are displayed in Fig. 19.6. The wave lengths of the pipes with open upper end are longer than those with closed upper end, and the eigenfrequencies, i.e., the level of the tones, are lower, the ground tone by a full octave. In addition, the frequency relations of neighboring

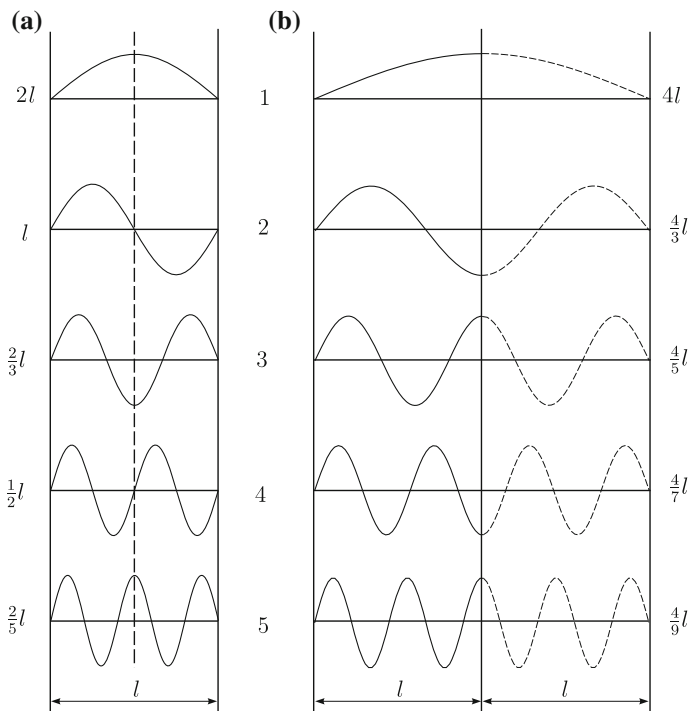


Fig. 19.6 Eigenfunctions of linear pipes. **a** For pipes which are closed at the bottom and top. **b** For pipes which are closed at the bottom and open at the top (in the figure two pipe lengths are shown). Both panels show the forms of the oscillations for the ground tone and the next four overtones and the wave lengths of the tones of the pipe length, l

overtones are different, which is one reason why open and closed pipes have different timbres and different sounds.

19.3 Steady, Isentropic Stream Filament Theory

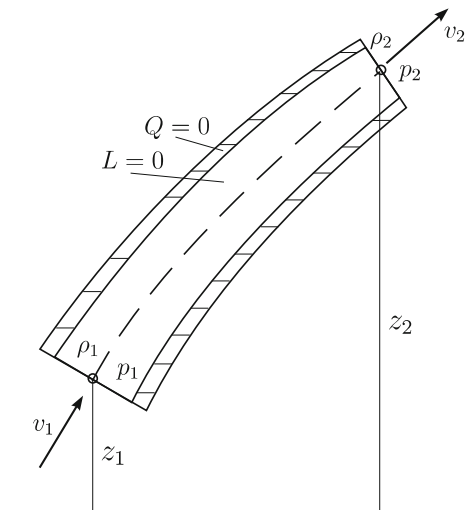
Stream filament flows in gas dynamics are flows through thin pipes or tubes, for which the tube cross-section changes only slowly along the tube axis. The velocity, density and pressure fields are treated as uniform over the cross sections. At sufficient discharge through the conduits the velocity field is with sufficient approximation axially directed, and density and pressure as well as this axial velocity are merely functions of time and the coordinate along the conduit axis.

Consider stationary flow through a tube with adiabatic walls; see **Fig. 19.7**. This means that the pipe wall is thermally insulated so that heat flow through the wall is completely prevented. The First Law of Thermodynamics, formulated for a pipe section between the cross sections 1 and 2 is then given by Eq. (17.108) or

$$Q(t) + L(t) = \dot{m}_2 \left(h_2 + \frac{v_2^2}{2} + gz_2 \right) - \dot{m}_1 \left(h_1 + \frac{v_1^2}{2} + gz_1 \right), \quad (19.78)$$

in which $Q(t)(= 0)$ is the heat flow supplied to the wall from the outside, which vanishes for an adiabatic pipe wall. Moreover, $L(t)$ is the technical power added to the conduit between cross sections 1 and 2; \dot{m}_1 and \dot{m}_2 are the mass flow densities through the cross sections 1 and 2; h_1, h_2 are the enthalpy densities; v_1, v_2 the velocities parallel to the axis and gz_1, gz_2 the gravity potentials, all in cross sections 1 and 2. For

Fig. 19.7 Thin stream filament section. *Between the cross sections 1 and 2 the conduit wall is assumed to be adiabatic and it is supposed that within the tube no technical working is performed*



$Q = L = 0$ and with $\dot{m}_1 = \dot{m}_2$ Eq. (19.78) is considerably simplified. If, in addition the flowing gas is assumed to be subjected to adiabatic, i.e., isentropic conditions, then we have, owing to $T ds = dh - dp/\rho = 0$,

$$dh = \frac{dp}{\rho} \quad \longrightarrow \quad h = \int \frac{dp}{\rho}. \quad (19.79)$$

With all these prerequisites, the energy equation (19.78) takes the form

$$\frac{v^2}{2} + \int \frac{dp}{\rho} + gz = \text{constant}. \quad (19.80)$$

This equation has been derived before for density preserving and/or barotropic fluids and was then called BERNOULLI equation.

For a caloric ideal gas under isentropic conditions Eq. (18.147) applies, $(p/p_0) = (\rho/\rho_0)^\kappa$, $\kappa = c_p/c_v$. Therefore, we have

$$\int_{p_0}^p \frac{dp}{\rho} = \kappa \frac{p_0}{\rho_0^\kappa} \int_{\rho_0}^{\rho} \tilde{\rho}^{(\kappa-2)} d\tilde{\rho} = \frac{\kappa}{\kappa-1} \frac{p_0}{\rho_0} \left\{ \left(\frac{\rho}{\rho_0} \right)^{\kappa-1} - 1 \right\}. \quad (19.81)$$

For a caloric ideal gas the BERNOULLI equation can, thus, be written in the following equivalent forms:

$$\begin{aligned} \frac{v^2}{2} - \frac{v_0^2}{2} &= \frac{\kappa}{\kappa-1} \frac{p_0}{\rho_0} \left\{ 1 - \left(\frac{\rho}{\rho_0} \right)^{\kappa-1} \right\} \\ &= \frac{\kappa}{\kappa-1} \frac{p_0}{\rho_0} \left\{ 1 - \left(\frac{p}{p_0} \right)^{(\kappa-1)/\kappa} \right\} \\ &= \frac{\kappa}{\kappa-1} RT_0 \left\{ 1 - \frac{T}{T_0} \right\}, \end{aligned} \quad (19.82)$$

in which for (19.82)_{2,3} relations (18.146) have been employed and the contribution of the gravity force has been omitted, because of the small gas density that makes this contribution minute. Let us explain the theory with a simple example.

Example 5

Let us consider the flow of a gas out of a very large container in somewhat greater detail. We suppose that the container has adiabatic walls; that the gas contained in it has temperature T_0 , density ρ_0 , pressure p_0 and vanishing velocity $v_0 = 0$. To this vessel an exit pipe is connected, out of which the gas can flow in a controlled manner (by a valve). The state of the gas at the exit cross section of the pipe is given by T , p , ρ and v . Provided the container is sufficiently large, the

conditions of the gas during the out-flow process do hardly change; equally, except for a short initiating phase, the out-flow process is time independent, so that stationary conditions can be assumed. Equations (19.82), therefore, imply with $v_0 = 0$

$$v = \sqrt{\frac{2\kappa}{\kappa - 1} R(T_0 - T)} = \sqrt{\frac{2\kappa}{\kappa - 1} R \left(T_0 - T_0 \cdot \left(\frac{p}{p_0} \right)^{(\kappa-1)/\kappa} \right)}, \quad (19.83)$$

or, if one uses the relation

$$\frac{\kappa}{\kappa - 1} = \frac{c_p}{c_p - c_v} = \frac{c_p}{R},$$

which holds true for ideal gases,

$$v = \sqrt{2c_p(T_0 - T)} = \sqrt{2c_p \left(T_0 - T_0 \left(\frac{p}{p_0} \right)^{R/c_p} \right)}. \quad (19.84)$$

This formula shows that, because the absolute temperature must be positive, the out-flow velocity is bounded from above by

$$v_{\max} = \sqrt{2c_p T_0} = \sqrt{\frac{2\kappa}{\kappa - 1} R T_0}. \quad (19.85)$$

It belongs to the temperature $T = 0$ and pressure $p = 0$ and corresponds to out-flow conditions into vacuum.

Equations (19.83) and (19.84) can be brought into forms, which are more convenient for computations. To this end one preferably starts from (19.82), which with $v_0 = 0$ takes the form

$$\frac{\kappa}{\kappa - 1} \frac{p}{\rho} + \frac{v^2}{2} = \frac{\kappa}{\kappa - 1} \frac{p_0}{\rho_0} = \frac{v_{\max}^2}{2}. \quad (19.86)$$

(Here one has made use of the ideal gas equation $p_0/\rho_0 = RT_0$.) If now also use is made of the isentropic relations (18.146), the chain of Eq.(19.86) leads to the relations

$$\begin{aligned} \frac{T}{T_0} &= 1 - \frac{v^2}{v_{\max}^2}, \\ \frac{\rho}{\rho_0} &= \left(1 - \frac{v^2}{v_{\max}^2} \right)^{1/(\kappa-1)}, \\ \frac{p}{p_0} &= \left(1 - \frac{v^2}{v_{\max}^2} \right)^{\kappa/(\kappa-1)}, \end{aligned} \quad (19.87)$$

of which the functional dependences are displayed in **Fig. 19.8**. In the neighborhood of $(v/v_{\max}) = 0$ the normed temperature, density and pressure are in this approximation given by concave parabolas of rank 2. This approximation reads for the pressure

$$\frac{p}{p_0} \sim 1 - \frac{\kappa}{\kappa - 1} \frac{v^2}{v_{\max}^2}, \quad \frac{v}{v_{\max}} < 0.2. \tag{19.88}$$

However, it only constitutes a satisfactory approximation for $v/v_{\max} < 0.2$. For $v/v_{\max} = 1$, density ratio ρ/ρ_0 and pressure ratio p/p_0 have vanishing slopes and enjoy convex curvature. An approximating formula can also be given here, which, however, cannot be derived by Taylor series expansion. For the pressure, given in (19.87), one can write

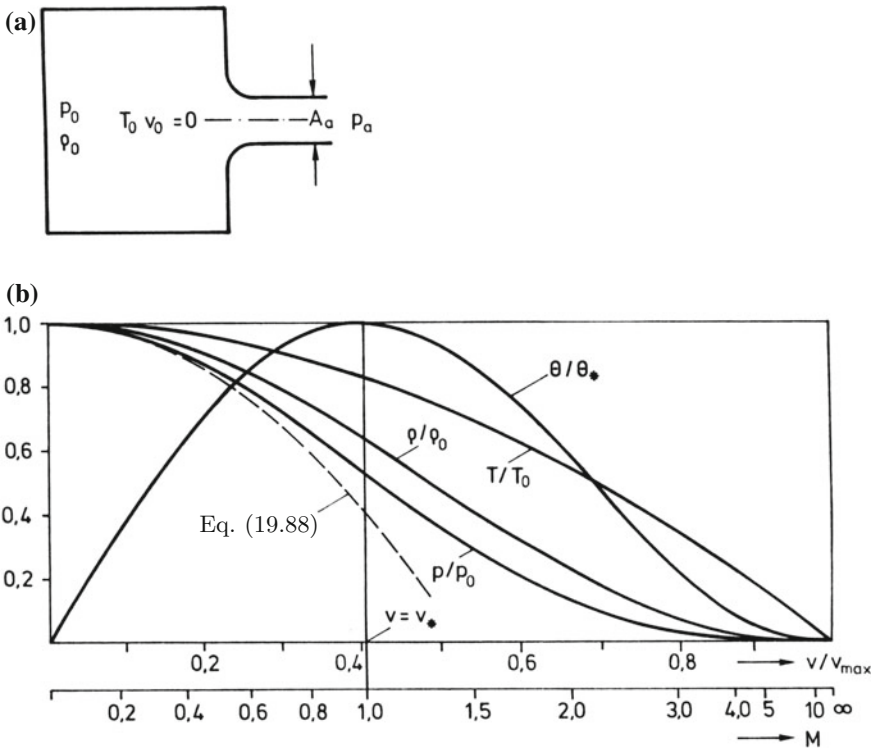


Fig. 19.8 Flow of a gas out of a vessel. The functions for pressure, density, temperature and mass flow, normed by the conditions within the vessel are plotted against the dimensionless velocity v/v_{\max} , where $v_{\max} = \sqrt{2\kappa(\kappa - 1)}$ is the maximum velocity appropriate for vacuum conditions. The dashed curve represents the approximate dimensionless pressure function (19.88), of which the validity is restricted to $v/v_{\max} < 0.2$. Pressure, density and mass flow have in $v/v_{\max} = 1$ a horizontal tangent and convex curvature

$$\begin{aligned}
 \frac{p}{p_0} &= \left(1 - \frac{v}{v_{\max}}\right)^{\kappa/(\kappa-1)} \left(1 + \frac{v}{v_{\max}}\right)^{\kappa/(\kappa-1)} \\
 &= \left(1 - \frac{v}{v_{\max}}\right)^{\kappa/(\kappa-1)} \left\{2 - \left(1 - \frac{v}{v_{\max}}\right)\right\}^{\kappa/(\kappa-1)} \\
 &\cong 2 \left(1 - \frac{v}{v_{\max}}\right)^{\kappa/(\kappa-1)} \left\{1 - \frac{\kappa}{2(\kappa-1)} \left(1 - \frac{v}{v_{\max}}\right)\right\}.
 \end{aligned}$$

The results, derived above can also differently be given, if the velocities are scaled with the speed of sound. To this end, we start with Definition 19.2, or Eq. (19.7) of the speed of sound, which for isentropic changes of states of a caloric ideal gas is given by

$$c^2 = \frac{dp}{d\rho} = \frac{d}{d\rho} \left(p_0 \left(\frac{\rho}{\rho_0} \right)^\kappa \right) = \kappa \frac{p_0}{\rho_0} \left(\frac{p}{p_0} \right)^{(\kappa-1)/\kappa} = \kappa RT, \quad (19.89)$$

(see (18.145)–(18.147)). Equation (19.82)₂ can then be written as

$$\frac{v^2}{2} = \frac{c_0^2 - c^2}{\kappa - 1} \rightarrow \frac{v_{\max}^2}{2} = \frac{c_0^2}{\kappa - 1}, \quad (19.90)$$

where $v_0 = 0$ has also been used; alternatively, or when (19.89) is used

$$\frac{v^2}{2} = \frac{\kappa}{\kappa - 1} R(T_0 - T) = \frac{c^2}{\kappa - 1} \left(\frac{T_0}{T} - 1 \right). \quad (19.91)$$

If this equation is solved for T/T_0 , one obtains

$$\begin{aligned}
 \frac{T}{T_0} &= \left\{ 1 + M^2 \frac{\kappa - 1}{2} \right\}^{-1}, \\
 \frac{\rho}{\rho_0} &= \left\{ 1 + M^2 \frac{\kappa - 1}{2} \right\}^{-1/(\kappa-1)}, \\
 \frac{p}{p_0} &= \left\{ 1 + M^2 \frac{\kappa - 1}{2} \right\}^{-\kappa/(\kappa-1)},
 \end{aligned} \quad (19.92)$$

where for (19.82)_{2,3} Eq. (18.146) has also been employed. M is defined as

$$M = \frac{v}{c} \quad (19.93)$$

and is called **Mach number**.⁷ One differentiates between **subsonic flows** ($M < 1$), **sonic flows** ($M = 1$) and **supersonic flows** ($M > 1$). **Trans-sonic conditions** describe flows in the transition regime for which $M \in [M - \varepsilon, M + \varepsilon]$, where

⁷For a short biography of ERNST WALDFRIED JOSEF WENZEL MACH, see Fig. 19.9.

$0 < \varepsilon < 0.1$ and **hypersonic conditions** for which $M \geq 3$. If one plots T/T_0 , ρ/ρ_0 and p/p_0 against the MACH number, one obtains curves as shown in **Fig. 19.10**, where the solid curves are for air ($\kappa = 1.4$), whereas the dashed-dotted curves are for $\kappa = 1.2$.

It is evident that the value of the adiabatic exponent exerts its influence particularly in the supersonic regime. For small MACH numbers the formulae (19.92) can be approximated by Taylor series expansions about $M = 0$. In this way one obtains for the density

$$\frac{\rho}{\rho_0} \sim 1 - \frac{1}{2}M^2 + \dots, \quad M^2 \ll 1. \quad (19.94)$$

With this formula it can be estimated, in which way in a gas conditions of density preserving are approximately fulfilled. Finally, using (19.84)₁ and (19.89)₁, v/v_{\max} can be written as a function of M . One obtains

$$\frac{v}{v_{\max}} = \frac{\kappa - 1}{2} M \left\{ 1 + \frac{\kappa - 1}{2} M^2 \right\}^{-1/2} \quad (19.95)$$

and can with this formula connect the graphs of Figs. 19.8 and 19.10. This is done in Fig. 19.8 by a second, nonlinear abscissa for the MACH number.

We close this paragraph with two remarks:

- Special out-flow conditions prevail, if the velocity v reaches exactly the (local) speed of sound, hence $v^* = c^*$. This speed is called **critical out-flow speed**; it is denoted here with an asterisk and can be computed with the aid of (19.90). Indeed, with

$$\frac{v_*^2}{2} = \frac{c_0^2 - v_*^2}{\kappa - 1} \quad (19.96)$$

we obtain by solving for v_*

$$v_*^2 = c_*^2 = \frac{2c_0^2}{\kappa + 1} = 2 \frac{p_0}{\rho_0} \frac{\kappa}{\kappa + 1} = 2RT_0 \frac{\kappa}{\kappa + 1}. \quad (19.97)$$

- An important combination of the variables displayed in Figs. 19.8 and 19.10 is the mass flow $\Theta = \rho v$; it is scaled with (19.87) and is given by

$$\frac{\Theta}{\rho_0 v_{\max}} = \frac{v}{v_{\max}} \left(1 - \frac{v^2}{v_{\max}^2} \right)^{1/(\kappa-1)}. \quad (19.98)$$

Its maximum is at $v/v_{\max} = \sqrt{(\kappa - 1)(\kappa + 1)}$ and takes the value

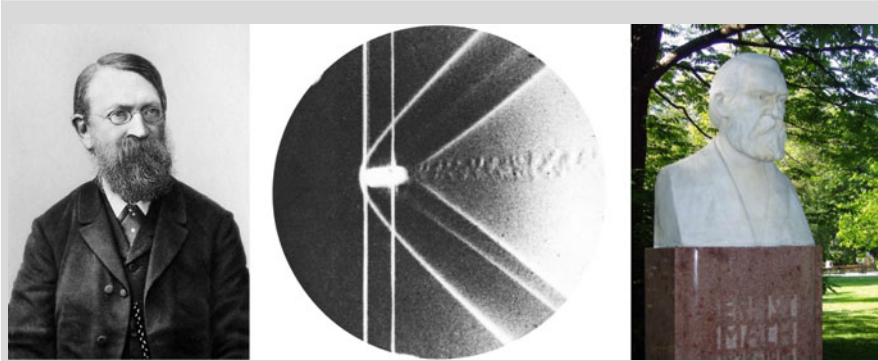


Fig. 19.9 ERNST WALDFRIED JOSEF WENZEL MACH (18. Feb. 1838–19. Feb. 1916). (Left) ERNST MACH, 1900; (middle) ERNST MACH’s photography of a bow shock wave around a supersonic bullet, in 1888; (right) Bust of MACH in the Rathauspark (City Hall Park) in Vienna, Austria

ERNST WALDFRIED JOSEF WENZEL MACH was an Austrian physicist and philosopher, noted for his contributions to physics such as the Mach number and the study of shock waves. As a philosopher of science, he was of major influence on logical positivism, American pragmatism and through his criticism of Newton, a forerunner of Einstein’s relativity.

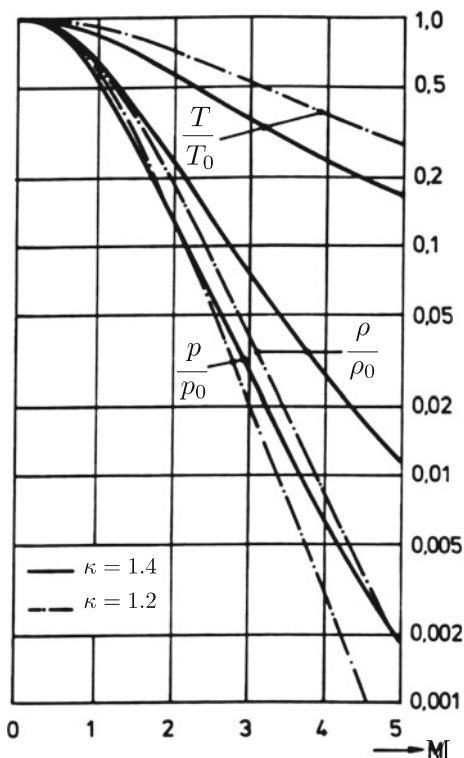
ERNST MACH received his education up to the age of 14 at home from his parents. He then entered a Gymnasium (high school), where he stayed for three years. In 1855 he became a student at the University of Vienna where he studied physics and for one semester medical physiology, receiving his doctorate in physics in 1860 and his Habilitation in 1861. His early work focused on the Doppler effect in optics and acoustics. In 1864 he took a job as Professor of Mathematics at the University of Graz, and in 1866 was appointed Professor of Physics there. During that period, MACH continued his work in psycho-physics and in sensory perception. In 1867, he took the chair of Experimental Physics at Charles University, Prague, where he stayed for 28 years before returning to Vienna.

MACH’s main contribution to physics involved his description and photographs of spark shock-waves and then ballistic shock-waves. He described how and when a bullet or shell created a compression wave. Using Schlieren photography, he and his son LUDWIG were able to photograph the shadows of invisible shock waves. MACH also made many contributions to psychology and physiology among others especially his discovery of a non-acoustic function of the inner ear which helps control human balance.

In the field of aerodynamics MACH conducted important explorations in the field of supersonic flows around bodies. His paper (1877) correctly describes the sound effects observed during the supersonic motion of a projectile. He deduced and experimentally confirmed the existence of a shock wave which has the form of a cone with the projectile at the apex (see above figure panel in the middle). The ratio of the speed of projectile to the speed of sound v_p/v_s is now called MACH number. He also contributed to cosmology the hypothesis known as Mach’s principle. In natural philosophy MACH shared his views with DUHEM and OSTWALD: They did not believe in the existence of atoms.

The text is based on www.wikipedia.org

Fig. 19.10 Flow of a gas out of a vessel. Temperature, density and pressure (scaled for conditions in the vessel) plotted against the Mach number for two different values of adiabatic exponents $\kappa = 1.4$ (solid, for air) and $\kappa = 1.2$ (dashed-dotted)



$$\left(\frac{\Theta}{\rho_0 v_{\max}}\right)_{\max} = \sqrt{\frac{\kappa - 1}{\kappa + 1}} \left(\frac{2}{\kappa + 1}\right)^{1/(\kappa - 1)} = \frac{\Theta_*}{\rho_0 v_{\max}}. \tag{19.99}$$

If one substitutes this expression in (19.98), one obtains

$$\frac{\Theta}{\Theta_*} = \sqrt{\frac{\kappa + 1}{\kappa - 1}} \frac{v}{v_{\max}} \left\{ \frac{\kappa + 1}{2} \left(1 - \frac{v^2}{v_{\max}^2}\right) \right\}^{1/(\kappa - 1)}. \tag{19.100}$$

This function is also shown in Fig. 19.8. For $\kappa = 1.4$ its maximum lies at $v/v_{\max} \approx 0.408$.

In the above analysis computations were based on single stream filaments; however, we did not touch the fact that this flow filament was embedded in the flow of a fluid through a narrow pipe, a tube or a nozzle. We now wish to study this and consider a gas which flows through a conduit with variable cross section A . Let the flow be steady state, so that mass balance may be stated as

$$Q = \rho v A = \text{constant}, \tag{19.101}$$

by differentiation this yields

$$\frac{d\rho}{\rho} + \frac{dv}{v} + \frac{dA}{A} = 0. \quad (19.102)$$

For isotropic conditions the BERNOULLI equation (19.80) must be added to this which, after omission of the gravity potential, is given by

$$\frac{v^2}{2} + \int_{p_0}^p \frac{d\bar{p}}{\rho(\bar{p})} = \text{constant}, \quad (\text{along streamlines}). \quad (19.103)$$

If this equation is differentiated,

$$v dv + \frac{dp}{\rho} = v dv + c^2 \frac{d\rho}{\rho} = 0 \quad (19.104)$$

is obtained. Combining Eqs. (19.102) and (19.104) leads to

$$\frac{dA}{A} = (M^2 - 1) \frac{dv}{v} \quad (19.105)$$

with MACH number $M = v/c$. This equation allows the following interpretation:

- For subsonic flow, i.e., for $M < 1$, the assumption $dA \leq 0$ implies the inequality $dv \geq 0$. In other words, in a converging pipe segment the velocity increases, in a diverging segment it decreases.
- For supersonic flow, i.e., for $M > 1$, the assumption $dA \leq 0$ implies $dv \leq 0$. Here, the response is reverse. In a converging pipe segment the velocity decreases, whereas it grows within a diverging pipe segment.

This property can be used in an adequately designed nozzle to continuously accelerate the flow. To this end, consider the **Laval nozzle**⁸; this nozzle consists of a converging section, into which gas is flowing, and a diverging section in the out-flow regime; see **Fig. 19.11**. If one manages that the flow is subsonic in the converging section, exactly sonic at the position of the smallest cross section and supersonic in the outflow section, then the gas will be accelerated throughout the entire nozzle. Laval nozzles are, therefore, elements, with the aid of which gas can be accelerated to supersonic flow.

Let us now assume that the gas flows out of a vessel through a convergent nozzle. Moreover, let the pressure in the vessel be p_0 , the outside pressure $p_a < p_0$ and assume that $p_1 > p_*$, where p_* is the critical pressure at which the fluid speed reaches

⁸The concept of the LAVAL nozzle was developed in 1878 by the German engineer and manufacturer ERNST KÖRTING (1842–1921) and independently in 1883 by the Swedish engineer CARL GUSTAV PATRIK DE LAVAL (1845–1913) for use in steam turbines and rocket engine nozzles. It is named after LAVAL only.

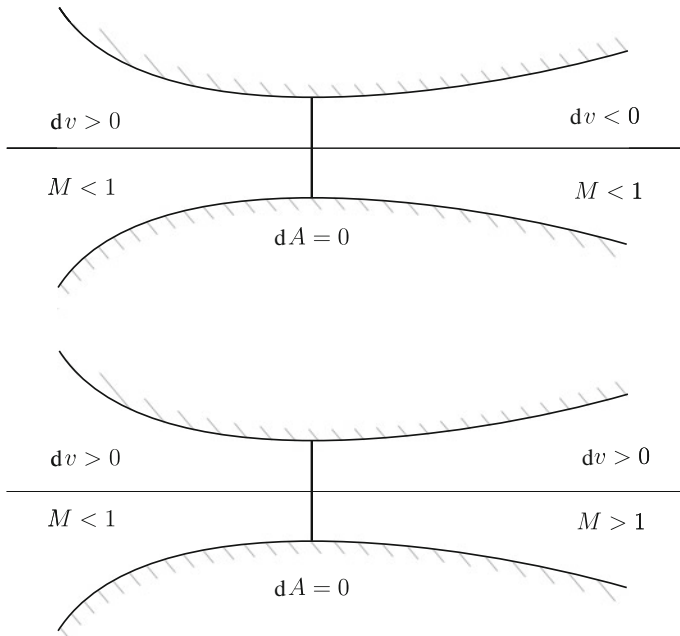


Fig. 19.11 Flow through a nozzle. A convergent-divergent conduit segment is called a Laval nozzle

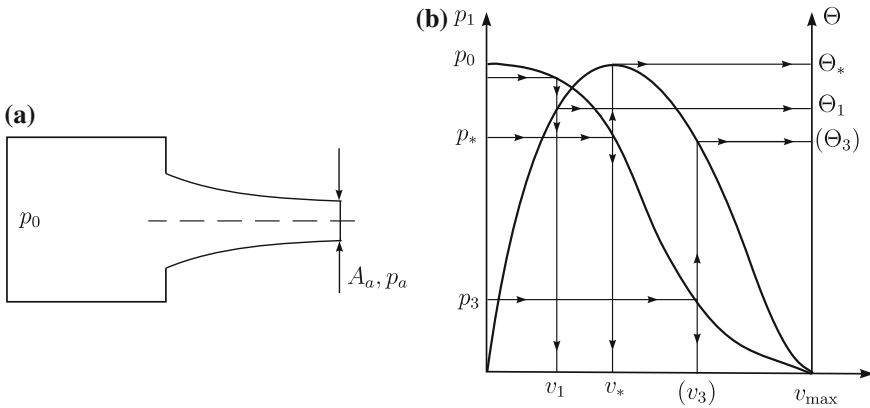


Fig. 19.12 Out-flow of a gas from a vessel through a convergent nozzle. **a** Vessel with nozzle, interior pressure p_0 , external pressure p_a and exit cross sectional area A_a . **b** Pressure p and specific mass flow (per stream filament cross section) as functions of the speed v . The indices 1, *, 3 characterize three different conditions in the exit cross section

exactly the sonic speed, see (19.97). Furthermore, let the out-flow velocity be v_1 , the density in the exit cross section $A_a \rho_a$, and the mass flow $\Theta_1 A_a$. **Figure 19.12**, in which the pressure curve and the curve of the specific mass flow, are displayed once more,

illustrates, which values Θ_1 and v_1 assume, if p_1 is prescribed as external pressure. The largest mass flow is reached, if the external pressure is the same as the critical pressure, $p_a = p_*$; then $\Theta = \Theta_*$ is a maximum. If the external pressure is below the critical pressure, $p_a < p_*$ (for instance conditions p_3, Θ_3, v_3 in Fig. 19.12), the flow of the gas through the converging nozzle cannot take place. The reason is as follows: Because in this case the velocity would have to rise from the value zero to the value v_3 in the exit cross section, and the pressure would have to fall from the value p_0 to the value p_3 , the mass flow density Θ would assume its largest value Θ_* somewhere in between the vessel and the exit cross section; the mass flow $Q_* \bar{A}$ in this cross section \bar{A} would then be larger than the mass flow in the exit cross section $\Theta_3 A_a$, a fact which would violate in a convergent nozzle the mass balance under steady flow. However, such a flow state is not possible in a convergent nozzle. Instead, the pressure will continuously drop from the kettle to the exit cross section and assume there the critical pressure p_* , independently of the pressure $p_1 < p_*$. This way, the mass balance can be fulfilled. Because, however, the external pressure is smaller than p_* , the gas will expand in the jet leaving the nozzle. This post-expansion takes place, due to reasons which cannot be explained here; what happens is that the jet boundary deforms in waves as indicated in Fig. 19.13. This can often be observed in rockets.

The explanations make clear that the critical conditions are technically significant. For this reason we shall now describe these conditions. We start with formula (19.82)₂ with $v_0 = 0$, which is here repeated,

$$v^2 = \frac{2\kappa}{\kappa - 1} \frac{p_0}{\rho_0} \left\{ 1 - \left(\frac{p}{p_0} \right)^{(\kappa-1)/\kappa} \right\}. \tag{19.106}$$

If this relation is written for critical conditions ($v = v_* = c_*$, $p = p_*$) and

$$c_*^2 = \kappa RT^* = \kappa \frac{p_*}{\rho_*} \tag{19.107}$$

is used, one easily deduces

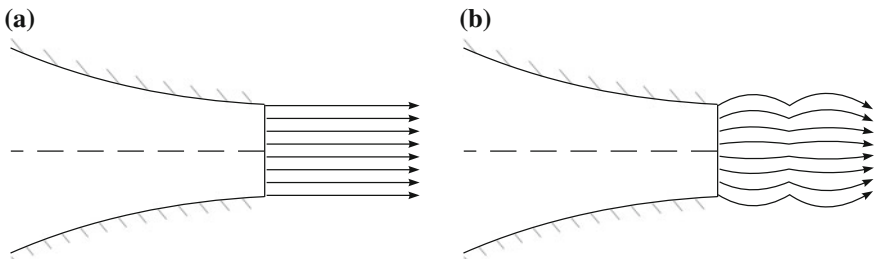


Fig. 19.13 Characteristic flows of a jet from a nozzle. **a** Smooth flat boundary of a jet leaving the nozzle, if the external pressure is larger than the critical pressure, $p_a > p_*$. **b** Wavy jet boundary, if the external pressure is smaller than the critical pressure, $p_a < p_*$

$$\kappa \frac{p_*}{\rho_*} = \frac{2\kappa}{\kappa - 1} \frac{p_0}{\rho_0} \left\{ 1 - \left(\frac{p_*}{p_0} \right)^{(\kappa-1)/\kappa} \right\}, \quad (19.108)$$

or, when (18.146)₃ is used,

$$\begin{aligned} 1 - \left(\frac{p_*}{p_0} \right)^{(\kappa-1)/\kappa} &= \frac{\kappa - 1}{2} \frac{p_*}{\rho_*} \frac{\rho_0}{p_0} = \frac{\kappa - 1}{2} \frac{p_*}{p_0} \left(\frac{\rho_0}{\rho_*} \right) \\ &= \frac{\kappa - 1}{2} \left(\frac{p_*}{p_0} \right) \left(\frac{p_0}{p_*} \right)^{1/\kappa} = \frac{\kappa - 1}{2} \left(\frac{p_*}{p_0} \right)^{(\kappa-1)/\kappa}. \end{aligned} \quad (19.109)$$

This equation allows solution for p_*/p_0 and then, with the help of (18.146), determination of ρ_*/ρ_0 and T/T_0 , respectively, viz.,

$$\begin{aligned} \frac{p_*}{p_0} &= \left(\frac{2}{\kappa + 1} \right)^{\kappa/(\kappa-1)} = \begin{cases} 0.5283, \\ 0.5764, \end{cases} \\ \frac{\rho_*}{\rho_0} &= \left(\frac{2}{\kappa + 1} \right)^{1/(\kappa-1)} = \begin{cases} 0.6339, \\ 0.7071, \end{cases} \\ \frac{T_*}{T_0} &= \frac{2}{\kappa + 1} = \begin{cases} 0.833, \\ 0.909, \end{cases} \end{aligned} \quad (19.110)$$

in which the upper (lower) figures hold for $\kappa = 1.4$ ($\kappa = 1.2$). The quantities on the left depend upon the conditions in the kettle; those on the right-hand side depend, however, only on the material, i.e., the gas under consideration. The formulae allow determination of the critical density, temperature and critical pressure, if the corresponding quantities are known in the kettle. If one introduces now the **critical Mach number**

$$M^* = v/c_* = v / \sqrt{2 \frac{p_0}{\rho_0} \frac{\kappa}{\kappa + 1}}, \quad (19.111)$$

one obtains with (19.82)₁

$$\frac{v^2}{2} = \frac{M_*^2 c_*^2}{2} = M_*^2 \frac{p_0}{\rho_0} \frac{\kappa}{\kappa + 1} = \frac{\kappa}{\kappa - 1} \frac{p_0}{\rho_0} \left\{ 1 - \left(\frac{\rho}{\rho_0} \right)^{\kappa-1} \right\},$$

from which one obtains

$$\frac{\rho}{\rho_0} = \left\{ 1 - M_*^2 \frac{\kappa - 1}{\kappa + 1} \right\}^{1/(\kappa-1)}. \quad (19.112)$$

Analogously, using (18.146) also p/p_0 and T/T_0 can be computed as functions of the critical MACH number. The result is

$$\begin{aligned} \frac{\rho}{\rho_0} &= \left\{ 1 - M_*^2 \frac{\kappa - 1}{\kappa + 1} \right\}^{1/(\kappa-1)}, \\ \frac{p}{p_0} &= \left\{ 1 - M_*^2 \frac{\kappa - 1}{\kappa + 1} \right\}^{\kappa/(\kappa-1)}, \\ \frac{T}{T_0} &= \left\{ 1 - M_*^2 \frac{\kappa - 1}{\kappa + 1} \right\}. \end{aligned} \quad (19.113)$$

These formulae give ρ , p , T as functions of κ , M_* and the quantities ρ_0 , p_0 and T_0 in the kettle.

Combining (19.110) and (19.113) allows elimination of the kettle quantities ρ_0 , p_0 , T_0 . The simple computations yield

$$\begin{aligned} \frac{\rho}{\rho_*} &= \left\{ 1 - \frac{\kappa - 1}{2} (M_*^2 - 1) \right\}^{1/(\kappa-1)}, \\ \frac{p}{p_*} &= \left\{ 1 - \frac{\kappa - 1}{2} (M_*^2 - 1) \right\}^{\kappa/(\kappa-1)}, \\ \frac{T}{T_*} &= \left\{ 1 - \frac{\kappa - 1}{2} (M_*^2 - 1) \right\}. \end{aligned} \quad (19.114)$$

Finally, the steady state continuity equation $\rho v A = \rho_* v_* A_*$ yields

$$\frac{\rho v A}{\rho c_* A_*} = \frac{v A}{c_* A_*} = M_* \frac{A}{A_*} = \frac{\rho_*}{\rho}. \quad (19.115)$$

From this equation and (19.114)₁ one may deduce

$$\frac{A_*}{A} = M_* \left\{ 1 - \frac{\kappa - 1}{2} (M_*^2 - 1) \right\}^{1/(\kappa-1)}, \quad (19.116)$$

which can be interpreted as the integral of the differential equation (19.105).

We have seen above that in a nozzle, which contracts in the direction of the flow, the velocity of the gas cannot go beyond the critical velocity (compare Fig. 19.8 and formula (19.99)). It was also demonstrated that an increase of the speed of the gas beyond c_* is nevertheless principally possible in a nozzle, if it contracts first in the direction of the flow and then extends somewhat, see Fig. 19.14. In Fig. 19.14a it is assumed that the areal ratio, A_0/A_* of such a converging-diverging nozzle is equal to the ratio, Θ_*/Θ_3 , of the specific mass flow belonging to the pressure p_3 in Fig. 19.8, so that the continuity equation $A_*\Theta_* = A_a\Theta_3$ holds. If the external pressure p_3 is prescribed, the flow velocity in the converging part of the nozzle grows monotonically up to the value v_* . This monotonic growth is continued in the connecting divergent part of the nozzle up to the final value v_3 . The pressure thereby decreases steadily in the direction of flow and the velocity of the gas grows continuously.

Figure 19.14b contains, apart from this kind of pressure curve, also further pressure curves, which are then established, when the external pressure p does not agree with

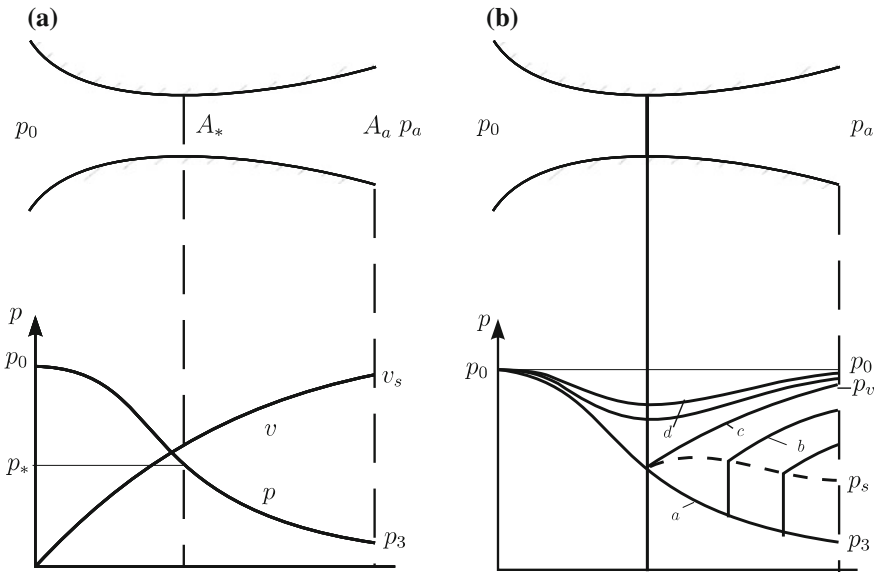


Fig. 19.14 Flow through a Laval nozzle. **a** The external pressure p_a and the exit cross section of the nozzle A_a are exactly such that a continuous decreasing pressure curve is built in the direction of the flow and also the corresponding velocity distribution is continuous. **b** Various continuous and discontinuous pressure curves can be generated in a convergent-divergent nozzle, if the external pressure p_a is varied. Compare also main text

the reference pressure p_3 which justifies the areal ratio A_a/A_* of the nozzle. The following scenarios must be differentiated:

- If the external pressure p_a is below p_3 , then the pressure distribution is in the entire nozzle that of Fig. 19.14a. The gas expands in this case once it has left the nozzle as a free jet.
- If the external pressure is somewhat above p_3 , the gas just outside the nozzle will be compressed. Within the nozzle the velocity and pressure distributions will be as shown in Fig. 19.14a. This is only changed, when p_a reaches a certain value p_s , which we still must determine.
- If $p_s < p < p_v$, then **compression shocks** arise in the nozzle. The pressure only follows curve 'a' in Fig. 19.14b until the compression shock arises, whose position in the diagram must also be determined. When shock conditions are reached, the pressure will instantly rise and the pressure will follow curve 'b'. In the compression shock the gas will be abruptly decelerated from supersonic to subsonic conditions.
- When $p_a \rightarrow p_v$ see Fig. 19.14b, the shock approaches the position of the smallest cross section and the strength of the shock attenuates. For $p_a = p_v$ the pressure jump across the shock vanishes. In this case the flow in the converging part of the nozzle is then expansive until the pressure p_* is reached and the velocity is

accelerated until v_* is reached. In the diverging part of the nozzle the flow is decelerated and the pressure is increased, see Fig. 19.14b, curve 'c'.

- When $p_v < p < p_0$, then the gas in the most narrow cross section neither reaches the critical pressure p_* nor the critical velocity, see Fig. 19.14b, curve 'd'. The velocity then stays below the critical velocity in the entire nozzle. The flow within the nozzle is then qualitatively behaving like a density preserving fluid. This near-incompressible behavior is the better, the smaller $|p_a - p_o|$ is.

Recall that for $p_a < p_v$ the mass flow equals $Q_* A_*$, independent of the external pressure. One says that the nozzle is 'blocked' in this case, because the mass flow through the nozzle cannot be influenced by changes of the external pressure; it then decreases until it vanishes when $p_a = p_o$, because the gas is then everywhere at rest.

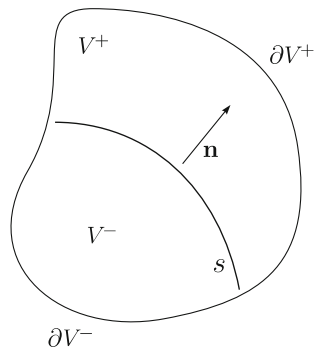
19.4 Theory of Shocks

19.4.1 General Concepts

As indicated by the discussion in the previous section **compression shocks** or **compaction shocks** may arise in the divergent regime of a Laval nozzle; this fact was mentioned but neither derived nor justified. In this section we shall only deal with stationary adiabatic shocks. However, because the theory of shocks is not considerably more complicated for more general cases, we shall in the ensuing introductory paragraphs derive those facts of shock theory which are common to all continuum theories and will subsequently specialize these.

In the previous chapters the basic prerequisites were that the thermodynamic fields ρ , T and \mathbf{v} , etc. are differentiable throughout the entire body. This assumption shall now be weakened by assuming that the thermodynamic fields in the body are still differentiable, except that these fields may on special surfaces within the body be discontinuous. Cracks are discontinuities of the displacement field. They cannot arise in liquids or gases. A thermodynamic quantity could, however, grow to infinity as a certain surface is approached, or it could assume different but finite values, if this surface is approached from one or the other side of it. In this case the considered physical quantity experiences a **finite jump** when the surface is crossed. This is for instance the case if the density changes abruptly. The interfacial surface between oil and water is of this nature. The strongest type of singularity is formed when a material breaks under the applied load and may perform cracks. In this case the displacement field is no longer unique after crack formation. Such discontinuities are called **dislocations**. The next level are singular surfaces at which the thermodynamic quantities experience jumps and no cracks are formed. Even weaker are those singularities, for which the thermodynamic quantities themselves are continuous across the singular surface, but their derivatives normal to the surface suffer a jump. The strongest singularities which we shall consider in this chapter are jumps of the thermodynamic quantities themselves.

Fig. 19.15 Explaining the definition of a singular surface S within a material body V . S partitions the volume V into V^+ and V^- with boundaries ∂V^+ and ∂V^- , respectively. V^\pm are defined once the orientation of the unit normal vector \mathbf{n} has been selected



Let V be a material body (here a gas or liquid), which is divided into two partial volumina by an orientable surface.⁹ If the surface S is smooth, i.e., if it possesses in each of its points a unique tangent plane, then by choice of the unit normal vector \mathbf{n} the positive part V^+ and the negative part, V^- of V can be defined, see **Fig. 19.15**: V^+ must lie on that side of S , into which the unit normal vector points. We agree on the following definition:

Definition 19.3

- A **singular surface** is an orientable surface across which a thermodynamic field or its temporal and/or spatial derivative suffer a finite jump, i.e., if the surface is approached from one or the other side toward the same point, the values of the thermodynamic field or their time and/or their spatial derivatives are not the same.
- If $f(\mathbf{x}, t)$ is a thermodynamic field, then f^+ and f^- denote the function values $f(\mathbf{x}^+, t)$ and $f(\mathbf{x}^-, t)$, respectively, where \mathbf{x}^\pm are two points in the immediate neighborhood of the surface point $\mathbf{x} \in S$, respectively.
- The jump of f , i.e.,

$$[[f]] := f(\mathbf{x}^+, t) - f(\mathbf{x}^-, t) = f^+ - f^-$$

is the difference of the values of f on the positive and negative sides of the surface point $\mathbf{x} \in S$.

A singular surface can be **material** or **non-material**. If it is material, it moves with the normal velocity of the particles, which define it. If it is non-material, it

⁹We must restrict ourselves to orientable surfaces, because physically a body or body part has always an outside and inside, which are always separated by an orientable surface. Examples of non-orientable surfaces are the MÖBIUS strip or the KLEIN bottle, see **Fig. 19.16**. AUGUST FERDINAND MÖBIUS (17. Nov. 1790–26. Sept. 1868) was a German mathematician and theoretical astronomer and FELIX KLEIN (25. April 1849–22. June 1925) was a mathematician, who chiefly established the distinguished mathematical school in Göttingen in the late 19th and early 20th century.

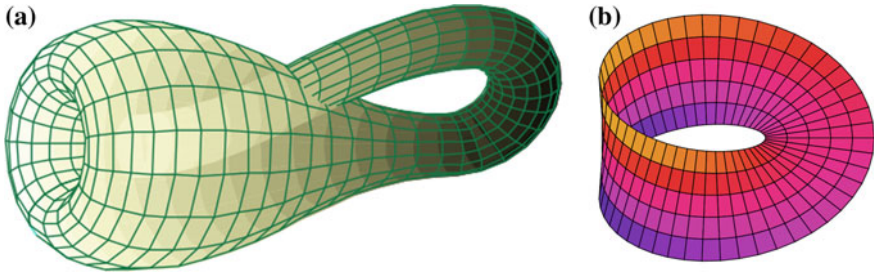


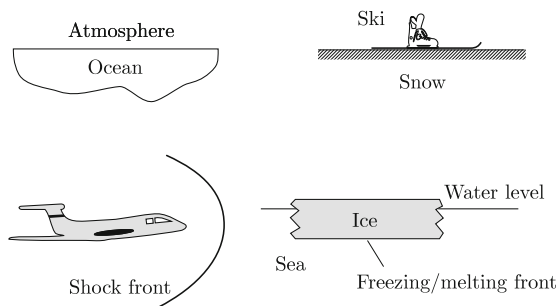
Fig. 19.16 Examples of non-orientable surfaces. **a** A two-dimensional representation of the KLEIN bottle immersed in three-dimensional space, against which a system for determining a normal vector cannot be consistently defined. **b** A parametric plot of a MÖBIUS strip, which is a surface with only one side and only one boundary component. Whereas a MÖBIUS strip is a surface with boundary, a KLEIN bottle has no boundary. © www.wikipedia.org

possesses its own normal velocity, i.e., in this case the particles can move across the singular surface, as it is e.g. the case for a shock wave.

Let us list a few examples of singular surfaces (see **Fig. 19.17**):

- The surface of separation of two immiscible fluids is a material surface. The free surface of a lake or an ocean is such a material surface, if the body is defined by the system ‘atmosphere-ocean’. The density across the singular surface changes discontinuously, if one crosses the surface from one side to the other. This example ignores the possibility of evaporation and/or precipitation. If these processes are accounted for, the lake surface is non-material, since water molecules can be transported through the surface.
- Consider the singular surface between ice and water in a frozen lake. This interface may be material or non-material; if the lake is in a freezing (thawing) phase, that is, if the ice cover thickness is growing (thinning), since ice particles from one side become water particles on the other side of the surface (or vice versa). The singular surface, thus, does not always consist of the same particles.
- The sliding surface of two bodies, which slide on one another, is a material surface. For a ski sliding over a snow cover the lower surface of the ski defines this singular

Fig. 19.17 Examples of singular surfaces



surface; however, the sliding surface is also defined by the snow cover; both of these are material. If the sliding motion generates heat, such that contacting snow particles melt, then the lower surface of the ski is still material and the ski also moves orthogonally to this surface with normal velocity given by the melting rate of the snow particles. On the other hand, the snow below the ski is at absolute rest, but the interface on the snow side moves according to the melting rate of the particles.¹⁰ This surface is non-material. Note also that the ski moves, whereas the snow is always at rest in this example.

- The shock surface in a sonic boom is a non-material surface.

19.4.2 Jump Conditions

The balance laws of mass, momentum and energy for a material body have the global form

$$\frac{d}{dt} \int_V \Psi dV = \int_{\partial V} \Phi \cdot \mathbf{n} dA + \int_V (\sigma + \gamma) dV, \quad (19.117)$$

in which the individual quantities are defined in **Table 19.1**, which also lists connections to other chapters, where more details are given. The balance law (19.117) is now manipulated with the assumption that the fields Ψ , Φ , σ and γ in V^\pm are continuously differentiable and across S experience a finite jump. To this end the term on the left-hand side (19.117) needs to be transformed. This transformation builds the content of the **Reynolds transport theorem**. The integral is divided into two integrals over V^+ and V^- and then, the classical transport theorem is applied to (19.117) for V^+ and V^- separately. This yields the following chain of expressions

$$\begin{aligned} \frac{d}{dt} \int_V \Psi dV &= \frac{d}{dt} \int_{V^+} \Psi dV + \frac{d}{dt} \int_{V^-} \Psi dV \\ &= \int_{V^+} \frac{\partial \Psi}{\partial t} dV + \int_{\partial V^+} \Psi (\mathbf{v} \cdot \mathbf{n}) dA - \int_S \Psi^+ (\mathbf{u} \cdot \mathbf{n}) dA \\ &\quad + \int_{V^-} \frac{\partial \Psi}{\partial t} dV + \int_{\partial V^-} \Psi (\mathbf{v} \cdot \mathbf{n}) dA + \int_S \Psi^- (\mathbf{u} \cdot \mathbf{n}) dA \\ &= \int_V \frac{\partial \Psi}{\partial t} dV + \int_{\partial V} \Psi (\mathbf{v} \cdot \mathbf{n}) dA - \int_S [\Psi (\mathbf{u} \cdot \mathbf{n})] dA. \end{aligned} \quad (19.118)$$

¹⁰It is assumed here that snow particles turning into water particles fall immediately into the pore space of the snow space, otherwise the singular surface is material. Alternatively, one may interpret melting as formation of a water layer between the snow cover and the sole of the ski. In this interpretation, two singular surfaces must be introduced, a material surface separating the ski sole and upper water layer and a non-material surface separating the dry snow from the water in the thin layer above it.

Table 19.1 Physical quantity Ψ , its flux Φ , supply σ and production γ densities

Balance law	Ψ	Φ	σ	γ	Remarks equation nr.
Mass	ρ	0	0	0	(3.51) ^a
Momentum	$\rho \mathbf{v}$	\mathbf{t}	$\rho \mathbf{f}$	0	(7.4), (7.6)
Energy	$\rho \left(\frac{v^2}{2} + u \right)$	$(\mathbf{v} \cdot \mathbf{t} - \mathbf{q})$	$\rho (\mathbf{f} \cdot \mathbf{v} + q)$	0	(17.74), (17.75)
Entropy	ρs	$-\mathbf{q}/T$	$\rho q/T$	$\rho \pi^s$	(18.3), (18.6)

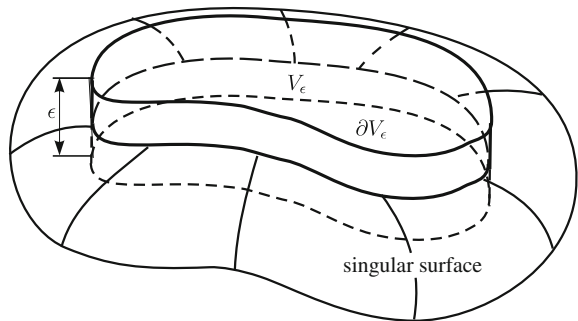
^aIn (3.51) V is a volume fixed in space. If a material volume is considered, the balance of mass reads $(d/dt) \int_V \rho dV = 0$

If we now choose for V an infinitely thin cylinder V_ϵ , which embraces the singular surface—a so-called pillbox enclosing the singular surface with lid on the positive and bottom on the negative side, see **Fig. 19.18**, the following limiting statements apply

$$\begin{aligned}
 \lim_{\epsilon \rightarrow 0} \int_{V_\epsilon} (\sigma + \gamma) dV &\rightarrow 0, & \lim_{\epsilon \rightarrow 0} \int_{V_\epsilon} \frac{\partial \Psi}{\partial t} dV &\rightarrow 0, \\
 \lim_{\epsilon \rightarrow 0} \int_{\partial V_\epsilon} \Phi \cdot \mathbf{n} dA &\rightarrow \int_S \llbracket \Phi \cdot \mathbf{n} \rrbracket dA, & & (19.119) \\
 \lim_{\epsilon \rightarrow 0} \int_{\partial V_\epsilon} \Psi (\mathbf{v} \cdot \mathbf{n}) dA &\rightarrow \int_S \llbracket \Psi (\mathbf{v} \cdot \mathbf{n}) \rrbracket dA,
 \end{aligned}$$

which all hold, because the fields $\sigma, \gamma, \Psi, \partial \Psi / \partial t$ only experience finite jumps.¹¹ If one uses the results (19.119), (19.118) and (19.117), the balance law (19.117) reduces to

Fig. 19.18 Material cylindrical volume V_ϵ with boundary ∂V_ϵ . The cylinder cuts the singular surface such that ‘lid’ and ‘bottom’ lie on opposite sides of S . If its height $\epsilon \rightarrow 0$ then (19.120) is obtained



¹¹Actually, slightly more general dependences are allowed, see e.g. K. HUTTER and K. JÖHNIK [8].

$$\int_S \{ \llbracket \Psi(\mathbf{v} - \mathbf{u}) \cdot \mathbf{n} \rrbracket - \llbracket \Phi \cdot \mathbf{n} \rrbracket \} dA = 0,$$

an expression, which must be valid for cylinders with arbitrarily large generating surfaces S , from which there follows

$$- \llbracket \Phi \cdot \mathbf{n} \rrbracket + \llbracket \Psi(\mathbf{v} - \mathbf{u}) \cdot \mathbf{n} \rrbracket = 0 \quad (19.120)$$

as **local jump condition**. If one substitutes in (19.120) the expressions listed in Table 19.1, the following jump conditions for mass, momentum, energy and entropy are obtained:

$$\begin{aligned} \text{Mass:} & \llbracket \rho(\mathbf{v} - \mathbf{u}) \cdot \mathbf{n} \rrbracket = 0, \\ \text{Momentum:} & \llbracket \rho \mathbf{v}((\mathbf{v} - \mathbf{u}) \cdot \mathbf{n}) \rrbracket - \llbracket \mathbf{t} \mathbf{n} \rrbracket = \mathbf{0}, \\ \text{Energy:} & \llbracket \rho \left(\frac{v^2}{2} + u \right) (\mathbf{v} - \mathbf{u}) \cdot \mathbf{n} \rrbracket - \llbracket (\mathbf{v} \cdot \mathbf{t} - \mathbf{q}) \mathbf{n} \rrbracket = 0, \\ \text{Entropy:} & \llbracket \rho s (\mathbf{v} - \mathbf{u}) \cdot \mathbf{n} \rrbracket + \llbracket \frac{\mathbf{q} \cdot \mathbf{n}}{T} \rrbracket \geq 0. \end{aligned} \quad (19.121)$$

It is seen that the jump conditions involve only the normal component of the velocity of the surface S . (The tangential contribution is irrelevant). The quantity

$$V_s = (\mathbf{u} - \mathbf{v}) \cdot \mathbf{n} \quad (19.122)$$

is called the **propagation speed**. This is the speed relative to the speed of a particle perpendicular to the surface. Equation (19.122) implies several special cases, which we collect in the following definition.

Definition 19.4

- A singular surface is **material**, if its normal velocity agrees with the normal velocities of the particles on either side of the surface,

$$(\mathbf{v} - \mathbf{u}) \cdot \mathbf{n} = 0. \quad (19.123)$$

A **sliding surface**, thus, is material if the normal speeds of the particles are the same on both sides of the surface.

- A singular surface, across which the velocity is discontinuous, $\llbracket \mathbf{v} \rrbracket \neq \mathbf{0}$, is called a **singular surface of first order**. If the normal component of the velocity is discontinuous across the surface, the surface is called a **shock**. The moving singular surface is called in this case a **shock wave**.
- If the tangential component of the material velocity across the surface is discontinuous but the normal component is continuous, i.e., if

$$\llbracket \mathbf{v} \cdot \mathbf{n} \rrbracket = 0, \quad \llbracket \mathbf{v} \times \mathbf{n} \rrbracket \neq \mathbf{0},$$

then the singular surface is called a **vortex sheet**.

With these definitions and the jump conditions (19.121) simple inferences can now be drawn:

On a material singular surface the jump conditions (19.121) reduce to

$$[[\mathbf{tn}]] = \mathbf{0}, \quad [[(\mathbf{vt} - \mathbf{q}) \cdot \mathbf{n}]] = 0, \quad \left[\left[\frac{\mathbf{q} \cdot \mathbf{n}}{T} \right] \right] \geq 0. \quad (19.124)$$

These are the jump conditions of momentum, energy and entropy; the jump condition of mass is trivial; it states that $[[\rho]]$ may have any value. Equation (19.124)₁ states that the stress vector (traction) across a singular surface is continuous; Eq. (19.124)₂ equates the jump of the conductive heat flow to the power of working of the sliding tractions. This can particularly clearly be recognized if one accounts for the fact that, owing to $[[\mathbf{tn}]] = \mathbf{0}$, we also have $[[\mathbf{vt} \cdot \mathbf{n}]] = [[\mathbf{v} \cdot \mathbf{tn}]] = [[\mathbf{v}]] \cdot \mathbf{tn}$ so that the jump condition of energy, (19.124)₂, can also be written in the form

$$[[\mathbf{q} \cdot \mathbf{n}]] = [[\mathbf{v}]] \cdot \mathbf{tn}. \quad (19.125)$$

Provided the temperature is continuous across the singular surface, relation (19.124)₃ yields,

$$[[\mathbf{v}]] \cdot \mathbf{tn} \geq 0, \quad \text{if } [[T]] = 0. \quad (19.126)$$

If the two materials on the two sides of the singular surface adhere to each other, the jump of the velocity vanishes, $[[\mathbf{v}]] = \mathbf{0}$, and no entropy is produced. Incidentally, (19.126)₁ states that the power of the sliding tractions is non-negative.

In an inviscid, simple fluid (gas or liquid) the stress tensor is reduced to a pressure tensor, $\mathbf{t} = -p\mathbf{1}$. If, in addition also $\mathbf{v} \cdot \mathbf{n}$ is continuous (vortex sheet, sliding surface) the jump conditions take the forms

$$\begin{aligned} \text{Mass:} & \quad [[\rho]] (\mathbf{v} - \mathbf{u}) \cdot \mathbf{n} = 0, \\ \text{Momentum:} & \quad [[\mathbf{v}]] (\rho(\mathbf{v} - \mathbf{u}) \cdot \mathbf{n}) + [[p]] \mathbf{n} = \mathbf{0}, \\ \text{Energy:} & \quad \left[\left[\frac{v^2}{2} + u \right] \right] (\rho(\mathbf{v} - \mathbf{u}) \cdot \mathbf{n}) + [[\mathbf{q} \cdot \mathbf{n}]] + [[p]] \mathbf{v} \cdot \mathbf{n} = 0, \\ \text{Entropy:} & \quad [[s]] \rho(\mathbf{v} - \mathbf{u}) \cdot \mathbf{n} + \left[\left[\frac{\mathbf{q} \cdot \mathbf{n}}{T} \right] \right] \geq 0. \end{aligned} \quad (19.127)$$

On a **sliding surface** one has $(\mathbf{v} - \mathbf{u}) \cdot \mathbf{n} = 0$ but possibly $[[\rho]] \neq 0$ (jump condition of mass). Thus, (19.127) imply

$$[[p]] = 0, \quad [[\mathbf{q} \cdot \mathbf{n}]] = 0, \quad [[T]] = 0.$$

For an inviscid fluid the pressure, the normal component of the conductive heat and the temperature are continuous across such a surface. If across such a singular surface a mass flow exists, even though $[[\mathbf{v} \cdot \mathbf{n}]] = 0$, then the singular surface is a **vortex sheet** and (19.127)₁ necessarily requires that ρ is continuous, $[[\rho]] = 0$. With this,

(19.127)₂ implies, since $[[\mathbf{v}]]$ is parallel to the singular surface, that

$$[[\mathbf{v}]] = \mathbf{0}, \quad [[p]] = 0. \tag{19.128}$$

In other words, the velocity per se and not only its normal component is continuous, i.e., *shocks are necessarily connected with a jump of the normal velocity component* $[[\mathbf{v} \cdot \mathbf{n}]] \neq 0$, or: *singular surfaces of first order are necessarily shocks*.

19.4.3 Stationary Shocks in Simple Fluids Under Adiabatic Conditions

We now wish to consider an important gas dynamic special problem, namely a simple fluid (for which $\mathbf{t} = -p\mathbf{1}$) under local adiabatic conditions (for which the heat flux vector vanishes, $\mathbf{q} = \mathbf{0}$) and for stationarity of the shock ($\mathbf{u} = \mathbf{0}$). With these restrictive conditions the jump conditions (19.121) become

$$\begin{aligned} \text{Mass:} & \quad \hat{\rho}\hat{v}_n = \rho v_n, \\ \text{Momentum:} & \quad \hat{\rho}\hat{v}_n^2 + \hat{p} = \rho v_n^2 + p, \\ & \quad \hat{\rho}\hat{v}_t\hat{v}_n = \rho v_t v_n, \\ \text{Energy:} & \quad \hat{\rho}\left(\hat{u} + \frac{\hat{v}^2}{2}\right)\hat{v}_n + \hat{p}\hat{v}_n = \rho\left(u + \frac{v^2}{2}\right)v_n + p v_n, \\ \text{Entropy:} & \quad \hat{\rho}\hat{s}\hat{v}_n \geq \rho s v_n. \end{aligned} \tag{19.129}$$

In these equations the variables ahead (behind) the shock are identified with (without) a caret ‘^’. In addition, the velocities are split into components tangential (v_t) and normal (v_n) to the singular surface. Incidentally, Eq. (19.129) are also obtained by considering a small volume, which crosses the shock surface and writing for it the corresponding balances. This is sketched in **Fig. 19.19**.

It is easy to derive from (19.129) the reduced equations

$$\begin{aligned} \text{Mass:} & \quad \hat{\rho}\hat{v}_n = \rho v_n, \\ \text{Momentum:} & \quad \hat{\rho}\hat{v}_n^2 + \hat{p} = \rho v_n^2 + p, \\ & \quad \hat{v}_t = v_t, \\ \text{Energy:} & \quad \hat{u} + \frac{\hat{p}}{\hat{\rho}} + \frac{\hat{v}_n^2}{2} = u + \frac{p}{\rho} + \frac{v_n^2}{2}, \\ \text{or} & \quad \hat{h} + \frac{\hat{v}_n^2}{2} = h + \frac{v_n^2}{2}, \\ \text{Entropy:} & \quad \hat{s} \geq s. \end{aligned} \tag{19.130}$$

These are the reduced shock conditions for stationary shocks of simple fluids under isentropic (adiabatic) changes of state. From these, a number of inferences can be drawn which we now wish to derive.

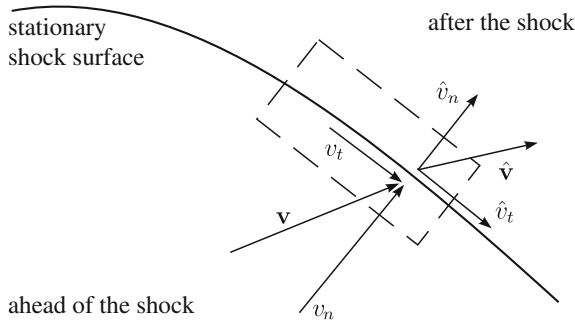


Fig. 19.19 Shock surface in a stationary shock. Particle velocities ahead ($\mathbf{v} : v_t, v_n$) and after ($\hat{\mathbf{v}} : \hat{v}_t, \hat{v}_n$) the shock (The denotations ‘ahead’ and ‘after’ the shock are to be understood such that fluid particles are ‘ahead’ of the shock, if they have not yet gone through the shock. They are ‘after’ the shock if they have already passed the shock surface)

From (19.130) the normal velocities v_n and \hat{v}_n can be eliminated, so that equations emerge, which involve only thermomechanical quantities. Momentum and energy balances (19.130)_{2,4} imply the relations

$$\hat{p} - p = \rho v_n^2 - \hat{\rho} \hat{v}_n^2, \quad \hat{h} - h = \frac{1}{2} (v_n^2 - \hat{v}_n^2).$$

Division of the second by the first expression yields

$$\begin{aligned} \frac{\hat{h} - h}{\hat{p} - p} &= \frac{1}{2} \frac{v_n^2 - \hat{v}_n^2}{\rho v_n^2 - \hat{\rho} \hat{v}_n^2} = \frac{1}{2} \frac{(v_n + \hat{v}_n)(v_n - \hat{v}_n)}{\rho v_n^2 - (\hat{\rho} \hat{v}_n) \hat{v}_n} \\ &= \frac{1}{2} \frac{(v_n + \hat{v}_n)(v_n - \hat{v}_n)}{\rho v_n (v_n - \hat{v}_n)} = \frac{v_n + \hat{v}_n}{2 \rho v_n} \\ &= \frac{1}{2} \left(\frac{1}{\rho} + \frac{\hat{v}_n}{\rho v_n} \right) = \frac{1}{2} \left(\frac{1}{\rho} + \frac{1}{\hat{\rho}} \right), \end{aligned}$$

or

$$\hat{h} - h = \frac{1}{2} \left(\frac{1}{\rho} + \frac{1}{\hat{\rho}} \right) (\hat{p} - p), \tag{19.131}$$

where also (19.130)₁ has been used. If one considers next $u = h - p/\rho$ and also uses (19.130)₁, then

$$\begin{aligned}
\hat{u} - u &= \hat{h} - \frac{\hat{p}}{\hat{\rho}} - \left(h - \frac{p}{\rho} \right) = \hat{h} - h + \frac{p}{\rho} - \frac{\hat{p}}{\hat{\rho}} \\
&= \frac{1}{2} \left(\frac{1}{\rho} + \frac{1}{\hat{\rho}} \right) (\hat{p} - p) + \frac{p}{\rho} - \frac{\hat{p}}{\hat{\rho}} \\
&= \frac{1}{2} \left(\frac{\hat{p}}{\rho} + \frac{\hat{p}}{\hat{\rho}} - \frac{p}{\rho} - \frac{p}{\hat{\rho}} + 2\frac{p}{\rho} - 2\frac{\hat{p}}{\hat{\rho}} \right) \\
&= \frac{1}{2} \left(\frac{\hat{p}}{\rho} - \frac{\hat{p}}{\hat{\rho}} + \frac{p}{\rho} - \frac{p}{\hat{\rho}} \right) = \frac{1}{2} \left(\frac{1}{\rho} - \frac{1}{\hat{\rho}} \right) (p + \hat{p}) \quad (19.132)
\end{aligned}$$

is obtained. This, as well as Eq. (19.131) form together the so-called **Rankine–Hugoniot relations**,¹² which are separately stated here once more:

$$\begin{aligned}
\hat{u} - u &= -\frac{1}{2}(\hat{p} + p) \left(\frac{1}{\hat{\rho}} - \frac{1}{\rho} \right), \\
\hat{h} - h &= \frac{1}{2} \left(\frac{1}{\hat{\rho}} + \frac{1}{\rho} \right) (\hat{p} - p). \quad (19.133)
\end{aligned}$$

They allow computation of the jump of the caloric state variables u and h by thermal equations of state on both sides of the shock, whereby not only jumps of p and $1/\rho$ arise, but equally also mean values. If these are denoted as

$$[\Psi] = \hat{\Psi} - \Psi, \quad \langle \Psi \rangle = \frac{1}{2}(\hat{\Psi} + \Psi),$$

pregnant forms of the RANKINE–HUGONIOT relations are given by

$$[u] = -\langle p \rangle \left[\frac{1}{\rho} \right], \quad [h] = \left\langle \frac{1}{\rho} \right\rangle [p]. \quad (19.134)$$

Remark These relations are surprisingly analogous to the following relations which can be obtained from the GIBBS relation

$$T ds = du + p d \left(\frac{1}{\rho} \right) = dh - \left(\frac{1}{\rho} \right) dp = 0,$$

which for isentropic (adiabatic) conditions become

$$du = -pd \left(\frac{1}{\rho} \right), \quad dh = \left(\frac{1}{\rho} \right) dp. \quad (19.135)$$

The correspondence is obtained via the pair analogues $d(\cdot)$ and $[(\cdot)]$ as well as (\cdot) and $\langle \langle \cdot \rangle \rangle$. For this reason the shock surfaces are sometimes called **dynamic adiabatic conditions**. We do not wish to see more behind this than a ‘crib’.

¹²For brief biographies of WILLIAM JOHN MACQUORN RANKINE (1820–1872) and PIERRE HENRI HUGONIOT (1851–1887), see Figs. 19.20 and 19.21, respectively.

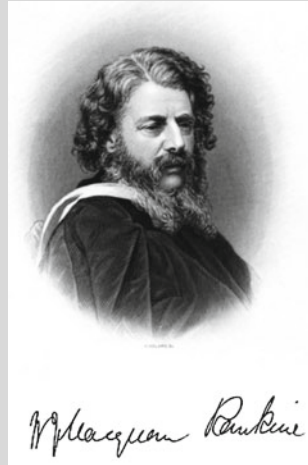


Fig. 19.20 WILLIAM JOHN MACQUORN RANKINE (5. July 1820–24. Dec. 1872)

WILLIAM JOHN MACQUORN RANKINE was a Scottish mechanical and civil engineer, physicist and mathematician. He was a founding contributor, with RUDOLF CLAUSIUS and WILLIAM THOMSON (LORD KELVIN), to the science of thermodynamics, particularly focusing on the first of the three thermodynamic laws.

Rankine developed a complete theory of the steam engine and of all heat engines. His manuals of engineering science were used for many decades after their publication in the 1850s and 1860s. He published several hundred papers and notes on science and engineering topics, from 1840 onwards, and his interests were extremely varied, including botany, music theory and number theory, and, later, most major branches of science, mathematics and engineering. He was an enthusiastic amateur singer, pianist and cellist who composed his own humorous songs. He was born in Edinburgh and died in Glasgow, a bachelor.

RANKINE received his basic education in Glasgow and studied at the Military and Naval Academy Edinburgh. In 1836 he began his studies at the University of Edinburgh focusing on natural history and natural philosophy. Here, under FORBES, he was awarded prizes for essays on physical inquiry and wave theory of light. He left the University in 1838 without a degree and worked as an engineer apprentice in railway systems in Scotland and Ireland. In the 1840s he returned to the mechanics of heat engines and succeeded in finding the relations between saturated vapor pressure and temperature and the thermal equation of state for gases. In the 1850s, he made use of energy concepts akin to the first law and introduced his own thermodynamic function, which he, later, realized to be identical to the entropy of CLAUSIUS. Today he is primarily remembered through the RANKINE–HUGONIOT equation for propagation of shock waves, which govern the behavior of shock waves normal to the oncoming flow.

Especially through his activities in railway engineering, RANKINE has recognized early-on that fatigue and rupture of railway axles are caused by the initiation of cracks; he showed that the axles had failed by progressive growth of a brittle crack or other stress concentration sources on the shaft.

The text is based on www.wikipedia.org



Fig. 19.21 PIERRE- HENRI HUGONIOT (5. June 1851–? Feb. 1887)

PIERRE- HENRI HUGONIOT was an inventor, mathematician, and physicist who worked on fluid mechanics, especially on issues related to material shock.

HUGONIOT was the son of a metallurgist and demonstrated early talents for science. At the age of only 17 years he became ‘Préparateur de Physique’ at the faculty of Science in Strasbourg. After going into the marine artillery upon his graduation from the École Polytechnique in 1872 he became professor of mechanics and ballistics at the School of Artillery Lorient (1879–1882) and Deputy Director of the Central Laboratory of the Artillery Navy (1882–1884). He was promoted to captain in January 1884, and in April was appointed assistant professor of mechanical engineering at the École Polytechnique. He conducted research on the trigger gas accompanying the detonation of cannons.

This led in 1885 to his mathematical description of shock waves. He invented this theory based on conservation of mass, momentum, and energy, which allowed for improvements in fluid flow studies (with applications to aerospace). The Rankine–Hugoniot equation (or adiabatic dynamics of gas) is the product of these efforts and has been named in his honor. These papers were published *post mortem* (he died, probably by overwork) by the mathematician ROGER LIOUVILLE. His ideas were further explored in France by J. CROUSSARD (1907) and E. JOUGUET (1910) and ‘Mécanique des Explosives’ (1917) [9–11]. A recent biography is [2].

The text is based on www.wikipedia.org

Photo: W.H. Hager (personal communication). See also his biographical dictionary ‘Hydraulicians in Europe 1800–2000’, Int Assoc. Hydr. Engr. & Research (IAHR 2003)

Caloric Ideal Gases

The above computations have been done for shocks of simple fluids. Let us now focus on caloric ideal gases for which

$$\frac{p}{\rho} = RT, \quad h = c_p T + h_0, \quad u = c_v T + u_0 \quad (19.136)$$

with constant specific heats. These relations imply

$$h - h_0 = \frac{c_p}{R} \frac{p}{\rho} = \frac{c_p}{c_p - c_v} \frac{p}{\rho} = \frac{\kappa}{\kappa - 1} \frac{p}{\rho},$$

from which one may conclude

$$\hat{h} - h = \frac{\kappa}{\kappa - 1} \left(\frac{\hat{p}}{\hat{\rho}} - \frac{p}{\rho} \right) = \frac{1}{2} \left(\frac{1}{\rho} + \frac{1}{\hat{\rho}} \right) (\hat{p} - p), \quad (19.137)$$

in which (19.133)₂ has also been used. Equation (19.137) is a relation between the pressures and densities on both sides of the shock which can also be expressed in the forms

$$\frac{\hat{p} - p}{\hat{\rho} - \rho} = \kappa \frac{\hat{p} + p}{\hat{\rho} + \rho}, \quad \frac{\hat{p}}{p} = \frac{(\kappa + 1) \frac{\hat{\rho}}{\rho} - (\kappa - 1)}{(\kappa + 1) - (\kappa - 1) \frac{\hat{\rho}}{\rho}}, \quad (19.138)$$

as was shown by THÉODORE VON KÁRMÁN.¹³ With the aid of the equation of state (19.136)₁ the second of the VON KÁRMÁN relations can directly be used to determine the temperature change across the shock. For the ratio \hat{T}/T one obtains

$$\frac{\hat{T}}{T} = \frac{\rho}{\hat{\rho}} \frac{\hat{p}}{p} = \frac{\rho}{\hat{\rho}} \frac{(\kappa + 1) \frac{\hat{\rho}}{\rho} - (\kappa - 1)}{(\kappa + 1) - (\kappa - 1) \frac{\hat{\rho}}{\rho}}. \quad (19.139)$$

For the computation of the entropy jump across the shock, we start with the GIBBS relation

$$ds = \frac{1}{T} \left(c_p dT - \frac{dp}{\rho} \right).$$

Moreover, the equation of state of ideal gases, $p = RT\rho$, implies

$$\frac{dT}{T} = \frac{dp}{p} - \frac{d\rho}{\rho}.$$

¹³One obtains

$$\begin{aligned} \frac{\kappa}{\kappa - 1} (\hat{p}\rho - p\hat{\rho}) &= \frac{1}{2} (\hat{\rho} + \rho)(\hat{p} - p), \\ \frac{\kappa}{\kappa - 1} \{ (\hat{p} - p)(\hat{\rho} + \rho) - (\hat{\rho} - \rho)(\hat{p} + p) \} &= (\hat{\rho} + \rho)(\hat{p} - p), \\ (\hat{p} - p)(\hat{\rho} + \rho) \left\{ \frac{\kappa}{\kappa - 1} - 1 \right\} - \frac{\kappa}{\kappa - 1} (\hat{\rho} - \rho)(\hat{p} + p) &= 0, \\ (\hat{p} - p)(\hat{\rho} + \rho) &= \kappa (\hat{\rho} - \rho)(\hat{p} + p). \end{aligned}$$

This relation leads to the first of the VON KÁRMÁN relations.

We eliminate the temperature between the last two equations and so obtain

$$ds = c_p \left(\frac{dp}{p} - \frac{d\rho}{\rho} \right) - R \frac{dp}{p} = c_v \frac{dp}{p} - c_p \frac{d\rho}{\rho},$$

which can be integrated to

$$s - s_0 = c_v \ln \frac{p}{p_0} - c_p \ln \frac{d\rho}{\rho}, \quad (19.140)$$

so that the entropy jump across the shock surface can be written as

$$\begin{aligned} \hat{s} - s &= c_v \ln \frac{\hat{p}}{p} - c_p \ln \frac{\hat{\rho}}{\rho} = \ln \left[\left(\frac{\hat{p}}{\rho} \right)^{-\kappa} \frac{\hat{p}}{p} \right] \\ &= c_v \ln \left[\left(\frac{\hat{\rho}}{\rho} \right)^{-\kappa} \frac{(\kappa + 1) \left(\frac{\hat{p}}{\rho} \right) - (\kappa - 1)}{(\kappa + 1) - (\kappa - 1) \left(\frac{\hat{p}}{\rho} \right)} \right]. \end{aligned} \quad (19.141)$$

The Second Law of Thermodynamics requires $\hat{s} - s \geq 0$ (see (19.130)₆) so that we easily obtain from the last expression of the first line of (19.141)

$$\frac{\hat{p}}{p} \geq \left(\frac{\hat{\rho}}{\rho} \right)^\kappa. \quad (19.142)$$

Please recall that the gas is subjected on both sides of the shock to adiabatic changes of states, for which the isentropic law

$$\frac{p_2}{p_1} = \left(\frac{\rho_2}{\rho_1} \right)^\kappa \quad (19.143)$$

must hold. The indices 1 and 2 refer to two points on the same side of the shock.

Figure 19.22 shows how \hat{p}/ρ and \hat{p}/p vary according to the VON KÁRMÁN relations (19.138) and the isentropic relation (19.143) between ρ_2/ρ_1 , and p_2/p_1 . The RANKINE–HUGONIOT curve has for $\hat{p}/\rho = (\kappa + 1)/(\kappa - 1)$ a vertical asymptote and at $\hat{p}/\rho = (\kappa - 1)/(\kappa + 1)$ a zero. Furthermore, the following statements can easily be proved:

- Both curves have a point of contact in (1, 1) with common tangent.
- For $\hat{p}/\rho > 1$, i.e., $\rho_2/\rho_1 < 1$ the RANKINE–HUGONIOT curve lies above the isentropic curve; for $\hat{p}/\rho < 1$, i.e., $\rho_2/\rho_1 > 1$ it is reverse.
- For the isentropic exponent $\kappa = 1.4$, **Table 19.2** gives a few values for the two relations.

Fig. 19.22 Shock and isentropic relations. RANKINE–HUGONIOT relation [(19.138), solid] and isentropic relation [(19.143), dashed], schematically displaced. In point (1, 1) the two curves have a common tangent

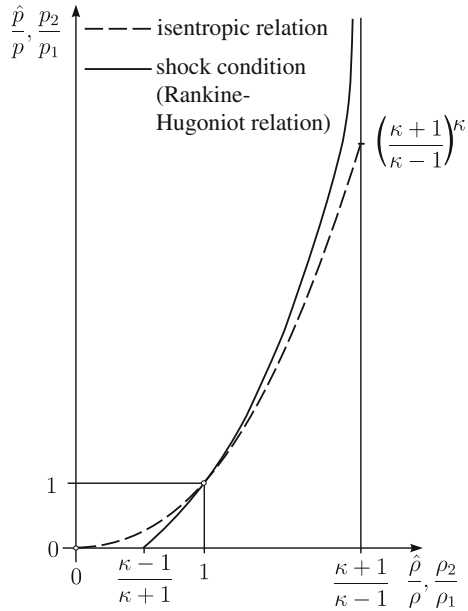
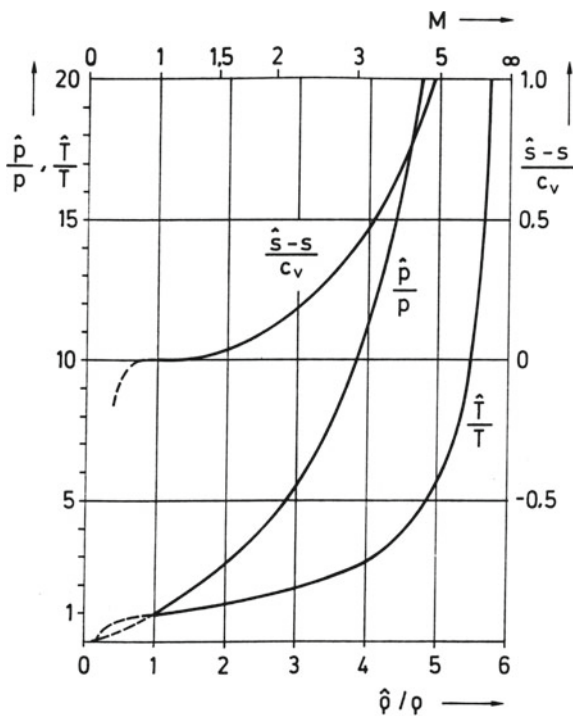


Table 19.2 RANKINE–HUGONIOT and isentropic relations for $\kappa = 1.4$

$\hat{\rho}/\rho$	$\hat{\rho}_2/\rho_1$	RANKINE–HUGONIOT relation		Isentropic relation p_2/p_1
		\hat{p}/p	\hat{T}/T	
$\frac{\kappa-1}{\kappa+1}$	$\frac{1}{6}$	0	0	0.0814
	1	1	1	1
	2	2.75	5.5	2.64
	3	5.66	17.0	4.66
	4	11.5	46.0	6.96
	5	29.0	145.0	9.52
	6	∞	∞	12.29

Let us return to the statement (19.142) of the Second Law. According to this formula, only shocks are possible, for which the RANKINE–HUGONIOT curve lies above the isentropic curve. Therefore, $\hat{\rho}/\rho > 1$ must hold. Otherwise stated, the density of the gas after the shock must be larger than ahead of the shock. Correspondingly, the speed of the gas after the shock must be larger than that before the shock, as dictated by the mass balance relation (19.130)₁. One calls shocks, of which the density behind the shock is larger than ahead of it, compaction shocks; for these we just have proved that *in calorically ideal gases only compaction shocks are possible*. This is a consequence of the Second Law. The balance laws of mass, momentum and energy for themselves would permit also rarefaction shocks.

Fig. 19.23 Shock relations for calorically ideal gases. Ratios \hat{p}/p , \hat{T}/T and $(\hat{s} - s)/c_v$ (after the shock) plotted against $\hat{\rho}/\rho$ and M . The solid curves are thermodynamically possible, the dashed curve is not; that is, for the dashed curve the Second Law of Thermodynamics is violated



It is informative to graphically display all shock equations (19.138), (19.139) and (19.141) in a single graph. This is done in Fig. 19.23, in which the abscissa shows the density ratio (below with linear scale) and the MACH number M ahead of the shock (above with nonlinear scale [Their relation is given in Eq. (19.139)]. One recognizes in these plots, and can corroborate these facts with the corresponding formulae, that \hat{p}/p , \hat{T}/T , $(\hat{s} - s)/c$ approach the value ∞ , if $\hat{\rho}/\rho \rightarrow (\kappa + 1)/(\kappa - 1)$ and that also the MACH number tends to infinity in this case. On the other hand, the jump in entropy is very small, if the density ratio does not deviate too much from the value 1; indeed by power series expansion of the expression on the right-hand side of (19.141) with respect to $(\hat{\rho}/\rho - 1)$, one obtains

$$\frac{\hat{s} - s}{c_v} = \frac{\kappa^2(\kappa - 1)}{6} \left(\frac{\hat{\rho}}{\rho} - 1 \right)^3 + \dots \tag{19.144}$$

In the vicinity of $(\hat{\rho}/\rho - 1)$ the graph of the function $(s - s_0)/c_v$ is a cubic parabola of $(\hat{\rho}/\rho - 1)$, with horizontal tangent and vanishing curvature at $(\hat{\rho}/\rho = 1)$: For weak shocks the entropy jump is of third order small. In spite of this, the jump of entropy across the shock is never zero, even though the flows ahead of the shock and behind it have been assumed as isentropic.

19.5 Final Remarks

In this chapter simple gas-dynamic problems have been presented for ideal compressible fluids as they arise in linear acoustics, in the steady isentropic stream filament theory and in the theory of shock waves. Only four rather elementary problems have been touched. For more complete accounts the reader is encouraged to consult the literature, e.g. [1, 3, 12–14].

References

1. Becker, E.: *Gasdynamik*. Teubner, Stuttgart (1965) Engl. Translation (1988)
2. Chéret, R.: The life and work of Pierre Henri Hugoniot. In: Johnson J.N., Chéret R. (eds.) *Classic Papers in Shock Compression Science*, pp. 149–160. Springer, New York (1998)
3. Courant, R., Friedrichs, K.O.: *Supersonic Flow and Shock Waves*. Applied Mathematical Sciences, vol. 21, Springer, Berlin, fifth printing (1999)
4. d'Alembert, le Rond J.-B.: *Traité de dynamique*. Paris (1743)
5. d'Alembert, le Rond J.-B.: *Réflexions sur la cause générale des vents (Reflections on the general causes of winds)* (Paris, David l'ainé) (1747)
6. d'Alembert, le Rond J.-B.: *Essai d'une nouvelle théorie de la résistance des fluides (Essay on a new theory of resistance of fluids)* (1752)
7. Eden, A.L.: *Christian Doppler: Leben und Werk*. Salzburg: Landespressebüro, ISBN 3-85015-069-0 (1988)
8. Hutter, K., Jöhnk, K.: *Continuum Methods of Physical Modeling*, pp. 635. Springer, Berlin (2004)
9. Hugoniot, P.-H.: *Mémoire sur la propagation du mouvement dans un fluide indéfini*. *Journal de Mathématiques pures et appliquées* (4th series), **3**, 477–492 and **4**, 153–168 (1887)
10. Hugoniot, P.-H.: *Sur la propagation du mouvement dans les corps et spécialement dans les gaz parfaits (première partie)*. *Journal de l'école Polytechnique*, **57**, 3–97 (1887)
11. Hugoniot, P.-H.: *Sur la propagation du mouvement dans les corps et spécialement dans les gaz parfaits (deuxième partie)*. *Journal de l'école Polytechnique* (in French), **58**, 1–125 (1889)
12. Oswatitsch, K.: *Grundlegende Gasdynamik*. Springer, Wien (1976)
13. Oswatitsch, K.: *Contributions to the development of Gasdynamics: Selected Papers*. Translated on the occasion of K. Oswatitsch's 70th Birthday, Vieweg, Paperback (2013)
14. Zierep, J.: *Vorlesungen über Gasdynamik*. Verlag G. Braun, Karlsruhe, 298 pp. (1963)

Chapter 20

Dimensional Analysis, Similitude and Physical Experiments at Laboratory Scale

Abstract This chapter is devoted to the subjects ‘Dimensional analysis, similitude and physical experimentation at laboratory scale’, topics often not systematically taught at higher technical education. However, no insider would deny the usefulness of these specialties. Books treating these subjects separately and in sufficient detail have appeared since the mid 20th century. We give an account of dimensional analysis, define dimensional homogeneity of functions of mathematical physics, the properties of which culminate in BUCKINGHAM’s theorem (which is proved in an appendix to the chapter); its use is illustrated by a diversity of problems from general fluid dynamics, gas dynamics and thermal sciences, e.g., propagation of a shock from a point source, rising gas bubbles, RAYLEIGH–BÉNARD instability, etc. The theory of physical models develops rules, how to down- or up-scale physical processes from the size of a prototype to the size of the model. The theory shows that in general such scaling transformations are practically never exactly possible, so that scale effects enter in these cases, which distort the model results in comparison to those in the prototype. In hydraulic applications, this leads to the so-called FROUDE and REYNOLDS models, in which the FROUDE or REYNOLDS numbers, respectively, remain mapping invariants but not the other. Application on sediment transport in rivers, heat transfer in forced convection, etc. illustrate the difficulties. The chapter ends with the characterization of dimensional homogeneity of the equations describing physical processes by their governing differential equations. The NAVIER–STOKES–FOURIER–FICK fluid equations serve as illustration.

Keywords Similitude and model experiments • Dimensional homogeneity • BUCKINGHAM’s theorem • Viscosity in a kinetic gas • Motion of a shock front after an explosion • RAYLEIGH–BÉNARD instability • Sediment transport in a shallow lake • Model theory and differential equations • NAVIER–STOKES–FOURIER–FICK fluid

List of Symbols

Roman Symbols

- A Amplitude of a harmonic variation of a function,
e.g. $\hat{\omega} = A \sin(\pi \hat{z})$
- [A] Physical dimension of A

A_j	Derived physical unit ($j = 1, \dots, n$)
$[A]_j$	Dimension of the derived physical unit A_j
$\mathbb{B}r$	BRINKMAN number
c_p	Specific heat at constant pressure
C_D	Drag coefficient
c	Speed of sound in a fluid, specific heat
c_s	Concentration of the sediments in a solid-fluid mixture
c_α	Mass concentration of constituent α
D	Characteristic length of a submerged body; typical dimension of a gas bubble, rising in a vertical fluid pipe
$D_T = \kappa/(\rho_0 c)$	Thermal diffusivity [$\text{m}^2 \text{s}^{-1}$]
$\mathbf{D} = \text{sym grad } \mathbf{v}$	Strain rate tensor, stretching tensor
$D^{\alpha\beta}$	Diffusion constant describing the diffusion between constituents α and β
D^{th}	Thermal diffusivity number: $D^{\text{th}} = [\kappa]/([\rho][c_p])$
D^{spec}	Representative species diffusivity ($D^{\alpha\beta} = [D^{\text{spec}}]\tilde{D}^{\alpha\beta}$)
\mathfrak{d}	Typical dimension of a molecule, representative diameter of sediment grains
\mathfrak{d}^*	Representative dimensionless diameter of the sediment grains
$E^{(3)}$	Energy, released in a point explosion in \mathbb{R}^3
$E^{(2)}$	Energy per unit length, released from a straight linear source per unit length (in $\mathbb{R}^{(2)}$)
$E^{(1)}$	Energy released from a point for a straight linear shock propagation (in \mathbb{R})
\mathbf{E}	Distortion (rate) tensor $\mathbf{E} = \mathbf{D} - \frac{1}{3}(\text{div } \mathbf{v})\mathbf{1}$
\mathbb{E}_d	Dissipation number
$\mathbb{E}u$	EULER number
$\mathbb{E}k$	EKMAN number $\mathbb{E}k = [\nu]/([\omega][L]^2)$
f, \bar{f}	Value of the variable f in Nature (prototype) and in a model
$[f]$	Constant reference value of f with physical dimension, physical dimension of f
\mathfrak{f}	Intermolecular ‘force’ (interaction force) at unit distance from the molecular center
$\mathbb{F}r$	FROUDE number: $\mathbb{F}r = V^2/(gD)$ [sometimes $\mathbb{F}r = V/\sqrt{gD}$]
$\mathbb{F}_{[\omega]}$	FROUDE number based on $[\omega]$: $\mathbb{F}_{[\omega]} = [\omega][V]/[g]$
G_i	Fundamental physical unit ($i = 1, \dots, m$)
$[G]_i$	Dimension of the fundamental physical unit G_i
g	Gravity constant
\mathfrak{g}	GIBBS free energy
$\mathfrak{G} = \mathfrak{f}^{-t}$	Strength of a \mathfrak{f} th inverse power force law (see (9.10))
H	Plate distance in RAYLEIGH–BÉNARD convection
h	Water depth measured from a reference surface
K	Modulus of a force on a body

k	Roughness length of the interior pipe surface
k/D	Dimensionless wall roughness
L	Distance between two pipe cross sections
m	Mass of a molecule
$M = V/c$	MACH number
$N = \alpha D/\kappa$	NUSSELT number
$p(\mathbf{x}, t)$	Pressure
$\tilde{p}(\mathbf{x}, t)$	Perturbation pressure
\mathbb{P}	Pressure ratio: $\mathbb{P} = K/(\rho V^2 D^2)$
$\mathbb{P}_{[\omega]}$	Pressure coefficient
$\mathbb{P}e = \mathbb{R}e\mathbb{P}r$	PÉCLET number
$\mathbb{P}r = \nu/D_T$	PRANDTL number
$\mathbb{P}e^{\text{tracer}} = \mathbb{R}e\mathbb{S}$	Tracer PÉCLET number
$R_f^{(1)}$	Distance of a shock front from the source point of an explosion
$R_f^{(2)}$	Radius of a semi-circular shock front in two-dimensions
$R_f^{(3)}$	Radius of a semi-spherical shock front
r	Specific radiation per unit mass
$\mathbb{R}a$	RAYLEIGH number: $\mathbb{R}a = g\alpha\Delta TH^3/(D_T\nu)$
$(\mathbb{R}a)_c$	Critical RAYLEIGH number
$\mathbb{R} = \mathbb{R}e$	REYNOLDS number: $\mathbb{R} = \mathbb{R}e = VD/\nu$
$\mathbb{R}a_{[\omega]}$	Radiation number: $\mathbb{R}a_{[\omega]} = [c_p][\Delta T][\omega]/[r]$
$\mathbb{R}o$	ROSSBY number: $\mathbb{R}o = [V]/([\omega][L])$
$\mathbb{S} = \nu[\mathcal{D}^{\text{spec}}]$	SCHMIDT number
s	Entropy density per unit mass
s	Complex valued variable describing the temporal growth for the vertical velocity component and the temperature
$\hat{s} = sH\tau/D_T$	Dimensionless counterpart of s
t	Time
T_0	Reference temperature
T_B	Temperature distribution in a state of rest
$\tilde{T}(\mathbf{x}, t)$	Perturbation temperature
\mathbf{u}_B	Stationary velocity distribution
$\tilde{\mathbf{u}}$	Perturbation velocity
V	Fluid velocity far upstream
$\mathbb{W} = \rho V^2 D/\sigma$	WEBER number (MORITZ WEBER)
$\bar{w}(z)$	Vertical profile of the vertical velocity component
$\hat{w} = (H/D_T)\bar{w}$	Dimensionless scaled vertical velocity component
x, y	Horizontal Cartesian coordinates
z	Vertical coordinate

Greek Symbols

α	Coefficient of thermal expansion
α, β	Indices, identifiers for constants

$\alpha_k = G_k^o/G_k^n$	Ratio of old to new basic units (examples $\alpha_1 = 1 \text{ m}/100 \text{ cm}$, $\alpha_2 = 1 \text{ h}/3600 \text{ s}$)
β	Exponent of the REYNOLDS number in a parameterization of the heat transfer coefficient
$\beta = \delta T/H$	Vertical mean linear temperature gradient
$\beta = \Delta p$	Pressure difference between two pipe cross sections in steady state
ΔT	Temperature difference between two parallel horizontal plates in the RAYLEIGH–BÉNARD problem: $\Delta T = T_{\text{lower}} - T_{\text{upper}}$
ε	Internal energy
ζ	Bulk viscosity
η	Shear viscosity
$\theta_c = \tau_c/(\Delta\rho g\delta)$	Critical SHIELDS parameter
κ	Thermal conductivity, heat conductivity
$\lambda = n^2\pi^2 + \hat{a}^2$	Auxiliary parameter
$\lambda_f = \hat{f}/f$	Scale factor for f
λ_A	Scale factor of the acceleration A
λ_L	Scale factor of the length L
λ_V	Scale factor of velocity V
$\lambda_g = \bar{g}/g$	Scale factor of the gravity
$\lambda_\nu = \bar{\nu}/\nu$	Scale factor of the kinematic viscosity
$\mu = \rho\nu$	Dynamic viscosity
ν	Kinematic viscosity [$\text{m}^2 \text{s}^{-1}$]
Π, Π_j, \dots	Various Π -products
$\Pi_j(x_i)$	Dimensionless products ($j = 1, \dots, m$) of the physical variables x_1, \dots, x_N
π^α	Production rate (per unit mass) of the mass density of constituent α
ρ	Mass density
ρ_0	Reference value of ρ (a constant)
ρ_s, ρ_f	Densities of the solid and fluid constituents, respectively
σ	Surface tension acting on the interface of two bodies
τ, τ_c	Shear traction, critical shear traction (at the onset of sediment transport)
Φ	Dissipation rate of a NS-fluid: $\Phi = \zeta(\text{div } \mathbf{v})^2 + 2\eta\text{tr}(\mathbf{E}^2)$
ω, ω	Angular velocity of the non-inertial frame

Miscellaneous Symbols

$\llbracket f \rrbracket$	Jump of f across a singular surface: $\llbracket f \rrbracket = f^+ - f^-$
$\frac{d(\cdot)}{dt}$	Material time derivative keeping the reference configuration fixed
$\frac{\partial(\cdot)}{\partial t}$	Local time derivative, keeping the spatial position fixed

$\left(\frac{dv}{dt}\right)_{\text{abs}}$	Acceleration relative to the inertial frame
$\left(\frac{dv}{dt}\right)_{\text{rel}}$	Acceleration relative to the non-inertial frame

20.1 Introductory Motivation¹

Physical problems are described by relations, which are determined by quantities having a certain dimension—length, time, mass, force, temperature, etc. These relations must be so structured that, dependent and independent quantities are combined so as to yield dimensionally correct formulas. In an equation defining a physical process, in which several terms are added, these terms must have the same dimension; this is often expressed as ‘apples and pears cannot be added together’. Such properties of expressions describing physical processes are connected with what is called *dimensional homogeneity*. In other applied sciences and in humanities, dimensional homogeneity is not required to hold, a fact, which allows equations with more general structure.

20.1.1 Dimensional Analysis

Loosely expressed, dimensional analysis is a method by which physical intuition is combined with rigorous mathematical analysis, leading to functional representations, which express upon which combinations of physical parameters an envisaged process can depend. It is particularly useful, when experiments are planned and helps to comprehend the sort and number of variables which one will encounter in the performance of such experiments. If, for instance the quantity y depends upon x_1, x_2, \dots, x_n , where all quantities have physical dimensions, then dimensional analysis shows that the envisaged process can only be described by a functional relation $f(\Pi_y, \Pi_x) = 0$ of all possible independent dimensionless products of $\{y, x_1, x_2, \dots, x_n\}$ (their number is generally less than $n + 1$). The physical part of the problem is the selection of the variables $\{y, x_1, x_2, \dots, x_n\}$. The scientist confronted with a particular physical problem must estimate upon which kind of physical parameters a certain fact may depend. The selection depends on the physical understanding of the studied process. If the chosen variables do not capture the essential physics, the rational mathematical steps will either demonstrate this, or physically meaningless relations (i.e. relations not corroborated by experimental data) will be generated. The mathematical part follows straightforward rules of linear algebra that will be explained below.

¹The topic presented here in this chapter is a popular theme in fluid mechanics and is the subject of several books, e.g., G.I. BARENBLATT [1], HENRY GÖRTLER [17], H.L. LANGHAAR [26], JOSEPH SPURK [40], K. HUTTER and K. JÖHNK [20] and others. A mathematical theory, based on a system of axioms with an extensive list of related references is given by D.E. CARLSON [13, 14].

Example 20.1 Viscosity in a Kinetic Gas²

In the kinetic theory of gases the balance laws of mass, momentum and energy are deduced by building moments of the BOLTZMANN equation; likewise, it is also possible to obtain the functional dependence of the shear viscosity from the BOLTZMANN equation. The decisive element in this derivation is the collision operator, of which the form depends upon the law of interaction in binary collisions. Three mechanical parameters describe this interaction, namely

$$\begin{aligned} m &: \text{mass of the molecule,} \\ \vartheta &: \text{typical dimension of the molecule,} \\ f &: \text{intermolecular 'force' (interaction force) at a unit distance} \end{aligned} \quad (20.1)$$

of the molecule center,

and these may influence the interaction only in certain combinations.

It is known by experience that the viscosity of a gas depends upon the density and the temperature. Since the latter is a measure for the kinetic energy of the fluctuating motion of the molecules, and because it is identified as internal energy ε , which is proportional to the temperature, one may assume the viscosity as a function of the form

$$\mu = \mu(\rho, \varepsilon; m, \vartheta, f), \quad \text{or} \quad f(\mu, \rho, \varepsilon; m, \vartheta, f) = 0, \quad (20.2)$$

in which the last three variables characterize the dependence of the viscosity upon the properties of the interaction of the molecules during collisions, whilst the first three characterize the global response of the molecules in a representative volume element. We shall employ the identifications $y = \mu, x_{1-5} = (\rho, \varepsilon, m, \vartheta, f)$. Dimensional analysis will show that these six variables give rise to three independent dimensionless products, namely e.g.,

$$\Pi_1 = \frac{\mu \vartheta^2}{m \sqrt{\varepsilon}}, \quad \Pi_2 = \frac{\rho \vartheta^3}{m}, \quad \Pi_3 = \frac{f \vartheta}{m \varepsilon}. \quad (20.3)$$

With these, the viscosity can be written as

$$\mu = \frac{m \sqrt{\varepsilon}}{\vartheta^2} f(\Pi_2, \Pi_3) = \frac{m \sqrt{\varepsilon}}{\vartheta^2} f\left(\frac{\rho \vartheta^3}{m}, \frac{f \vartheta}{m \varepsilon}\right), \quad (20.4)$$

where f is still an unspecified function. The number of variables is reduced from six to three, a dramatic reduction!

Formula (20.4) allows us to study qualitatively the behavior of the viscosity when the three parameters of the molecule, m, ϑ, f , are varied. For instance, because $\rho = n m$, where n denotes the number density of molecules, the first argument in the function f of (20.4) is given by $n \vartheta^3$ and, thus, independent of the molecules' mass

²See CLIFFORD A. TRUESDELL and ROBERT G. MUNCASTER [44], where this example is presented with fewer details.

and equal to the volume density of the molecules. Moreover, if the molecules do not exert any force on each other, if their distance is finite, then necessarily $f = 0$, and Π_3 in (20.3) drops out and Eq. (20.4) reduces to

$$\mu = \frac{m\sqrt{\varepsilon}}{\varrho^2} \hat{f} \left(\frac{\rho\varrho^3}{m} \right) = \frac{m\sqrt{\varepsilon}}{\varrho^2} \hat{f} (n\varrho^3). \quad (20.5)$$

In other words, in a gas, in which the molecules do not execute any forces upon each other at finite distances, the viscosity grows with the square root of the internal energy (or temperature). This is e.g. the case for molecules behaving as frictionless, perfect elastic (hard) spheres. If, moreover, the volume of the molecule, $n\varrho^3$, is negligibly small, then $\hat{f}(0)$ in (20.5) is a constant and the viscosity takes the form

$$\mu \propto \frac{m\sqrt{\varepsilon}}{\varrho^2} \quad \text{for ideal spheres.} \quad (20.6)$$

Such a square root temperature dependence is obeyed e.g. by monatomic gases.

20.1.2 *Similitude and Model Experiments*³

A *physical model* is a mapping of Nature or at least a sub-process that occurs in Nature to smaller scale. ‘Projection mapping’ or simply ‘projection’ instead of ‘mapping’ would be the better denotation, since some information is generally lost in the mapping. Analogously, every theory expressed in mathematical equations and describing processes of any kind equally represents a *mathematical model*; ‘theory’ would therefore also better be called ‘model’. It is imputed that it adequately describes certain processes which are observed in Nature. Physical and mathematical models generally describe partial facts of the reality, those which are important for the purposes for which they have been designed. In this sense all theories or physical models are projections of Nature, which enjoy some similarities of but do not completely correspond to Nature. Complete correspondence is usually not possible for conceptual reasons because it is generally impossible to preserve the *scale invariance* (i.e., invariance of the real processes by down- or up-scaling to the modeled processes). Because of these inescapable facts it is vital that those aspects of the physical processes, which are the intended focus of the study in question, are (nearly) preserved.

That physical models are subjected to loss of information by, say, geometrical downscaling, is inescapable. To explain the situation, recall from the example above, and accept in anticipation the fact that any physical process, which is described by a set of dimensional parameters y, x_1, x_2, \dots, x_n , must be *dimensionally homogeneous*, i.e., expressible by a functional equation of the form

³From K. HUTTER et al.: Physics of Lakes, Vol. 3 [21], pp. 313–314.

$$\tilde{f}(\Pi_y, \Pi_{x_1}, \Pi_{x_2}, \dots, \Pi_{x_N}) = 0, \quad \text{or} \quad \Pi_y = f(\Pi_{x_1}, \Pi_{x_2}, \dots, \Pi_{x_N}), \quad (20.7)$$

where Π_y and Π_{x_j} ($j = 1, \dots, N \leq n$) are dimensionless products of the variables $\{y, x_1, \dots, x_n\}$. If by a physical or mathematical model the same process as that described by the prototype (by Eq. (20.7)) is to be identically reproduced by a down-scaled model, all the Π -products of the model must have the same values as in the prototype. This defines complete similarity; it is exactly preserved in a process whose dimensional analysis leads to a functional expression of the form $\Pi_y = f(\Pi_x)$ between only two Π -products. In all other cases this cannot be guaranteed. Those Π -products, which are not preserved in the downscaling, may have a falsifying effect in inferences drawn from model results at the scale of the prototype; they are referred to as *scale effects*. By defining the Π -products adequately, such errors may be kept to a minimum.

As far as mathematical models are concerned, scientists and engineers often presume as if the model would describe Nature per se. This interpretation is for instance often given to the NAVIER–STOKES (NS) equations; in turbulence modeling it finds its enthusiastic defenders among all those who apply the Direct Numerical Simulation (DNS) technique to these equations. More specifically, turbulent modelers are of the opinion that every turbulent flow of a fluid (the implication is mostly applied to water and air) can adequately be modeled by the NS-equations, if one simply succeeds in constructing solutions on all scales, even the smallest possible ones. The stipulation is that all eddies, no matter how small, can be resolved by the NS-equations, if only the grid size used in the numerical solution technique is smaller than the smallest eddies which can arise. Naturally, also the NS-equations find their limitation as a model of Nature, namely certainly at the length scales of the molecules themselves, when classical physics loses its validity.

The stipulation, that a set of equations for the description of certain physical processes is correct in an absolute sense, suggests on the other hand, the following question: Is it possible to identify certain structures in the equations, which suggest certain invariance properties? For instance, is it possible by a scale analysis of the physical variables to non-dimensionalize the field equations and boundary conditions? The answer is yes and because of this, non-dimensional quantities will enter the field equations and boundary conditions as parameters. These parameters are nothing else than the Π -products, which are realized by the model equations. For every set of values of these Π -products a whole *class of solutions* of the governing equations is defined. This suggests a *principle of similitude*. Physical processes, which are characterized by different length-, time-, velocity-, force-scales etc., for which, however, the Π -products underlying the governing equations, have the same values, are similar to each other.⁴

⁴The method of using model equations for the description of certain processes as basis of dimensional analysis has been coined *inspectional analysis* after GARRETT BIRKHOFF [8], and it is regarded as being separate from classical dimensional analysis. This method is popular in hydraulic engineering and its use ‘is recommended as a more rigorous approach to the theory of similitude’, DONALD R.F. HARLEMAN [19]. Its use in downscaling processes from the prototype to the model size, obviously, assigns the notion of absolute truth to the equations—and they must obviously be

20.1.3 Systems of Physical Entities

Physical quantities have dimensions such as length, time, mass, velocity, force, temperature etc. Some of these must be introduced as *basic* or *fundamental* entities, others are then obtained as derived quantities. Depending upon which quantities one chooses as fundamental, different physical systems are chosen. As one of the most important laws mention might be made of NEWTON's second law, which may be stated as

$$\text{Force} = \text{Mass} \times \text{Acceleration}, \quad (20.8)$$

which is not the most general form of NEWTON's law, but sufficient to illustrate the point. With this law the most important transformation can be performed. If the mass is set to unity, 1, and the acceleration equal to the Earth's gravity constant, g , then the force unit is equal to g . Thus: *The weight of a unit mass equals exactly g units of the force.*

Until about the middle of the 20th century and also somewhat later, many different dimensional systems were in use; today the *International System (IS) of units* is almost exclusively used. It is an extension of the MKS-system (Meter, Kilogram, Second) to include thermal, chemical and electromagnetic entities. It has the following *fundamental* entities:

Meter	[m]	as unit of length,	
Second	[s]	as unit of time,	
Kilogram	[Kg]	as unit of mass,	
Kelvin	[K]	as unit of absolute temperature,	(20.9)
Ampère	[A]	as unit of electric current,	
mole	[mole]	as unit of substance,	
Candela	[cd]	as unit of light intensity.	

Quantities, which appear in SI units as very large or very small numbers, are expressed as multiples or fractions of the SI units in powers of 10 and are denoted by a prefix. **Table 20.1** collects these standard prefix notations: 1 micrometer (μm) is 10^{-6}m ; 1 Hectopascal (1 HPa) is 10^2 Pascals, and today a standard unit of atmospheric pressure; 1 femto second (1 fs) is 10^{-15}s , etc.

For any of the fundamental quantities (20.9) the SI system of units is fixed according to definitions now agreed upon by the United Nations. All other dependent quantities, such as velocity, acceleration, specific heat, etc., are expressed as certain products of powers of the fundamental units, e.g.,

(Footnote 4 continued)

known beforehand. In this book we regard inspectional analysis, if used, as part of dimensional analysis.

Table 20.1 Prefixes to characterize powers of 10 units in the IS system

Prefix	Symbol	Power	Prefix	Symbol	Power
Exa	E	10 ¹⁸	deci	d	10 ⁻¹
Peta	P	10 ¹⁵	centi	c	10 ⁻²
Tera	T	10 ¹²	milli	m	10 ⁻³
Giga	G	10 ⁹	micro	μ	10 ⁻⁶
Mega	M	10 ⁶	Nano	n	10 ⁻⁹
Kilo	K	10 ³	Piko	p	10 ⁻¹²
Hecto	H	10 ²	Femto	f	10 ⁻¹⁵
Deka	Da	10 ¹	Atto	a	10 ⁻¹⁸

$$\begin{aligned}
 \text{velocity} & \quad [\text{m s}^{-1}], \\
 \text{force} & \quad [\text{m Kg s}^{-2}] \equiv [\text{N}], \\
 \text{acceleration} & \quad [\text{m s}^{-2}], \\
 \text{work} & \quad [\text{m}^2 \text{Kg s}^{-2}] = [\text{N m}] \equiv [\text{J}], \\
 \text{diffusivity} & \quad [\text{m}^2 \text{s}^{-1}], \\
 \text{power} & \quad [\text{m}^2 \text{Kg s}^{-3}] = [\text{N m s}^{-1}] = [\text{J s}^{-1}] \equiv [\text{W}], \\
 \text{pressure} & \quad [\text{Kg m}^{-1} \text{s}^{-2}] = [\text{N m}^{-2}] \equiv [\text{Pa}].
 \end{aligned}
 \tag{20.10}$$

For some of these derived quantities their own denotations have become customary to quantify their units. In the IS system 1 *force unit* is that force which subjects 1 [Kg] mass to an acceleration of 1 [m s⁻²]; this force unit is called 1 NEWTON ([N]) as indicated in (20.10)₂. Analogously, the *unit of work* is the work done by 1 unit of force displaced by 1 [m] and called 1 JOULE. Obviously, 1 [J] = 1 [Nm] = 1 [m² Kg s⁻²], as shown in (20.10)₄. The *unit of power*, i.e., 1 unit of work per unit of time, is called WATT ([W]) and obviously given by 1 [W] = 1 [J s⁻¹] = 1 [Nm s⁻¹] = 1 [m² Kg s⁻³]. The unit for *pressure*, defined as force per unit area in the IS system is 1 PASCAL = [Pa] = 1 [Nm⁻²] = 1 [Kg m⁻¹ s⁻²]; however, in meteorology, oceanography and limnology 1 *bar* = 10⁵ [Pa] was and still is more common as unit for pressure measures. Moreover, pressures in weather forecasts are often given in Hectopascals, since 1 Hectopascal = 1 millibar. Transformation rules can easily be found in the internet, as can the units used in the United States of America.

The above text shows that the numerical values for a physical quantity depend upon which physical entities are selected as fundamental and which units are chosen for these. In the old CGS system, centimeter, gram and second are chosen as fundamental units of length, mass and time and, consequently, 1 [*dyne*] = 1 [g cm s⁻²] is its force unit and *erg* its work unit: 1 [erg] = 1 [dyne cm] = 1 [g cm s⁻¹]. In this system the fundamental quantities are the same as in the MKS-system, only their units have changed. It is, however, not compelling that the number of fundamental quantities are seven. For instance, it is known from the kinetic theory of gases that temperature is a measure of the averaged fluctuation energy of the molecules. So, its dimension is [ρv^2] = [Kg m⁻¹ s⁻²]. The introduction of the temperature as a fundamental physical quantity is not coercive as it could be reduced to the fundamental quantities of the MKS quantities. This fact is clearly seen in the history of the theory of heat, in which

the equivalence of energy and heat had first to be recognized. It led to the first law of thermodynamics, and more precisely, to the conceptual equivalence of heat and energy by ROBERT MAYER and PRESCOTTE JOULE, for biographical descriptions, see Figs. 17.6 and 17.7.

20.2 Theory of Dimensional Equations

20.2.1 Dimensional Homogeneity

Definition 20.1 An equation is called ‘homogeneous in its dimensions’ or ‘dimensionally homogeneous’, if the form of this equation does not depend upon the choice of the fundamental units. ■

Example 20.2 Torricelli’s Formula

As an example, consider the flow of an ideal density preserving fluid out of a container via a short horizontal tube of constant cross section at the bottom of the container. This flow is described in detail in Chap. 3, Example 3.6, Figs. 3.28 and 3.29 by use of the dynamic BERNOULLI equation, see Eqs. (3.139)–(3.145). In steady state the cross sectional averaged velocity in the exit-cross section is given by the so-called TORRICELLI formula (3.146),

$$v = \sqrt{2gh} \quad (\text{TORRICELLI formula}), \quad (20.11)$$

in which g is the Earth’s gravity constant and h the difference of the levels between the free surface point 1 and point 2 at the exit-cross section of the pipe, see also Fig. 3.30 for a biographical description of EVANGELISTA TORRICELLI.

Equation (20.11) holds in the given form irrespective in which units the height h and gravity constant g are measured—Lengths: in km, m, cm, miles; Time: in sec, hours, days, months—the velocity evaluated with the use of (20.11) is always correctly obtained in units of length and time that were chosen. If instead we use $g = 9.81 \text{ [m s}^{-2}\text{]}$ and substitute this above, then

$$v = \sqrt{2 \times 9.81} \sqrt{h} = 4.43 \sqrt{h} \quad (h \text{ in [m]}). \quad (20.12)$$

This form of the equation for v is still correct, however, it is in its application referred to the Earth’s surface at positions where $g = 9.81 \text{ m s}^{-2}$. Furthermore, it restricts itself to a particular system of units. Only if the value for h is substituted in [m] and the emerging value for v is interpreted in $[\text{m s}^{-1}]$, formula (20.12) generates a correct value of the fluid velocity in the exit-cross section, see Fig. 3.28. The reason for these constraints is that the assignment $g = 9.81$ is fraught with a physical dimension, expressed in SI units. It is evident, Eq. (20.11) is stated in dimensionally homogeneous form, but (20.12) is not.

Dimensionally homogeneous functions are a special class of functions. Moreover, application of dimensional analysis to practical problems is based on the experience that the solution of a problem of physics leads to dimensionally homogeneous functions only, provided the independent variables are correctly selected. This property is based on the fact that the *fundamental equations of physics are dimensionally homogeneous* and that deductions performed with such equations again lead to dimensionally homogeneous equations. However, there is no a priori reason to assume that a postulated functional relation describing a certain physical process is dimensionally homogeneous; this is only so, if the functional relation involves all parameters, which describe the physical phenomenon in focus. For instance,

Example 20.3 Drag Force on a Body

The drag force K of a body, submerged in a steadily moving fluid with constant speed at infinity and held fixed (or a steadily moving ship in a still ocean) will likely depend on the following parameters:

$$\begin{array}{ll}
 \rho & \text{density of the fluid,} \\
 \nu & \text{kinematic viscosity of the fluid,} \\
 V & \text{fluid velocity approaching the body,} \\
 g & \text{gravity constant,} \\
 c & \text{speed of sound of the fluid,} \\
 \sigma & \text{surface tension between the body and the fluid,} \\
 D & \text{characteristic length of the submerged body.}
 \end{array} \tag{20.13}$$

These variables give rise to the general functional relation

$$f(K, V, D, \rho, g, \nu, c, \sigma) = 0, \quad \text{or} \quad K = f(V, D, \rho, g, \nu, c, \sigma). \tag{20.14}$$

With $y = K$, $x = \{V, D, \rho, g, \nu, c, \sigma\}$, this equation has the alternative form $f(y, x_1, x_2, \dots, x_7) = 0$ and can be viewed as an equation expressing K as a function of the variables $\{x_1, x_2, \dots, x_7\}$. With these variables the following five dimensionless quantities can be formed⁵.

$$\begin{array}{lll}
 \Pi_1 & \text{REYNOLDS number} & \mathbb{R} = \frac{VD}{\nu}, \\
 \Pi_2 & \text{FROUDE number} & \mathbb{Fr} = \frac{V^2}{gD}, \\
 \Pi_3 & \text{MACH number} & \mathbb{M} = \frac{V}{c}, \\
 \Pi_4 & \text{WEBER number} & \mathbb{W} = \frac{\rho V^2 D}{\sigma}, \\
 \Pi_5 & \text{pressure ratio} & \mathbb{P} = \frac{K}{\rho V^2 D^2}.
 \end{array} \tag{20.15}$$

⁵For short biographies on REYNOLDS, see Fig. 15.2; on FROUDE, see Fig. 7.25; on MACH, see Fig. 19.9, and on WEBER, see Fig. 20.1.



Fig. 20.1 MORITZ GUSTAV WEBER (18. July 1871–10. June 1951)

MORITZ GUSTAV WEBER grew up in Hannover and studied in Göttingen under Felix Klein. After his graduation in 1904 he left for Berlin, where he worked as government official civil servant for the railway system on the first project of electrification of the city railway and the water supply system of the railway station Charlottenburg. In the same year he became full professor of mechanics at the Techn. Hochschule Hannover (now Tech. University Hannover) and in 1913 full professor of mechanics of ship and ship-machine design. He remained there until his retirement in 1936.

MORITZ WEBER focused in his scientific activities on (i) the motion of the Comet Halley, (ii) the principle of D'ALEMBERT (iii) the LAGRANGEan equations of motion and (iv) problems of oscillations of coupled bodies. His particular interest was devoted to the mechanical theory of similitude and to rational rules of physical modeling, for which he developed systematic procedures. The dimensionless Π -product (20.15)₄, denoted WEBER number, is a measure that weighs on a free surface element the pressure perpendicular to the element surface relative to the surface tension tangential to the interface and perpendicular to the element periphery.

WEBER's first publication in 1919 focuses on mechanics of similitude and appeared in the Annual Report of the Society of Ship Construction Technique. He expressed in this article that mechanics of similitude paired with dimensional analysis are not only useful in the construction of ships, but equally also for model experiments in technical physics such as thermodynamics, electro technique and strength of materials.

According to his understanding the principles of similitude in physics would go beyond their mere direct use in designing and exploiting experiments, as was already indicated by ISAAC NEWTON. This view is outlined in his article of 1930 [49]: 'The general principle of similitude of physics and its connection with the sciences of dimensional analysis and model theory'.

The text is based on www.wikipedia.org

They are mutually independent, since Π_1 contains only ν , Π_2 only g , Π_3 only c , Π_4 only σ and Π_5 only K . Four of them bear names of scientists from the 19th and 20th century, moreover, there are no more than five independent so-called Π -products which can be formed from the eight independent physical variables listed in (20.15). Therefore, a dimensionless homogeneous representation of (20.14) may be written as

$$K = \rho V^2 D^2 \tilde{f}(\mathbb{R}, \mathbb{F}r, \mathbb{M}, \mathbb{W}). \quad (20.16)$$

The function \tilde{f} is a function only of four variables instead of the previously seven ones. This reduction is the property of the dimensional homogeneity and does not involve any simplifying approximations. Further reduction of the number of variables in (20.16) is based on the neglect of dependencies on variables which have likely a minor or negligible influence. For completely submerged bodies gravity can hardly influence the drag force; a dependence on $\mathbb{F}r$ can be dropped. Similarly, for subsonic velocities $V/c \ll 1$ a MACH number dependence is unlikely in this case; and if the body is completely submerged, a dependence of f on \mathbb{W} can also be dropped. Approximately, one therefore obtains

$$K = \rho V^2 D^2 \hat{f}(\mathbb{R}). \quad (20.17)$$

Example 20.4 Drag Force on a Ship

To determine the drag force on the hull of a floating ship, we identify the force K in the above example with this drag force and may then write $\mathbb{P} = f(\mathbb{R}, \mathbb{F}r)$, or

$$K = \rho V^2 D^2 \tilde{f}(\mathbb{R}, \mathbb{F}r) = \frac{1}{2} C_D \rho V^2 A, \quad C_D = C_D(\mathbb{R}, \mathbb{F}r), \quad (20.18)$$

in which the factor $\frac{1}{2}$ has been introduced for conventional reasons of the definition of the drag coefficient C_D . A is taken as the cross sectional area drawn by the ship perpendicular to the direction of the upstream flow. It is customary to additively separate the frictional and gravity contributions according to

$$C_D(\mathbb{R}, \mathbb{F}r) = C'_D(\mathbb{R}) + C''_D(\mathbb{F}r). \quad (20.19)$$

Both coefficients C'_D and C''_D can be separately determined by experiments. However, as it is impossible to keep both the FROUDE and REYNOLDS numbers simultaneously invariant, the drag coefficient C'_D will be determined by a REYNOLDS model, whereas C''_D follows from a FROUDE model.

The above discussion makes the following definition plausible.

Definition 20.2 A set of dimensionless products of given physical variables is complete, if each product in this set is independent of any other and if any such dimensionless product of dimensional variables, which does not belong to the set, can be expressed as a product of powers of the dimensionless products of the set. ■

20.2.2 Buckingham's Theorem

The above example of functional dependence of the drag force on Π -products as stated in (20.16) made it clear that, if an equation is formed by terms, all of which are dimensionally homogeneous, then this equation is trivially dimensionally homogeneous, because it does not depend upon the choice of the fundamental quantities and their units by prerequisite. Therefore, the following statement holds true: *Sufficient condition for an equation to be dimensionally homogeneous is that this equation can be reduced to an equation of dimensionless products.* EDGAR BUCKINGHAM (1867–1940)⁶. [12] has shown that the above statement is not only necessary. He proved that it is also sufficient. We, therefore have the following theorem:

Theorem 20.1 (BUCKINGHAM) *If an equation is dimensionally homogeneous, it can be reduced to a relation of dimensionless products.* ■

This theorem is proved in the Appendix to this chapter.

Let us re-analyze the case of Eq. (20.14) (drag force on a body) with a focus of deriving the dimensionless Π -products more formally. We shall do this by ignoring the speed of sound of the fluid and the surface tension between fluid and body. Thus, we start now with the functional representation

$$f(K, V, D, \rho, g, \nu) = 0. \quad (20.20)$$

To derive the dimensionless Π -products from the independent variables stated in the functional relation (20.20) the following trial solution is proposed:

$$\Pi = K^{k_1} V^{k_2} D^{k_3} \rho^{k_4} g^{k_5} \nu^{k_6}. \quad (20.21)$$

As before, Π is a dimensionless product formed of all the variables occurring in (20.20). The exponents $k_j, j = 1, \dots, 6$ are to be determined, and it is hoped that all combinations of k -values are found which determine the dimensionless products. The dimension, i.e., exponent of the Π -product on the left-hand side of (20.20) is $[\Pi] = 0$; so with the physical dimensions $M = \text{mass}$, $L = \text{length}$ and $T = \text{time}$, the dimensions of (20.21) can be deduced from the equation

$$[\Pi] = [MLT^{-2}]^{k_1} [LT^{-1}]^{k_2} [L]^{k_3} [ML^{-3}]^{k_4} [LT^{-2}]^{k_5} [L^2T^{-1}]^{k_6}. \quad (20.22)$$

⁶For a short biography of BUCKINGHAM see Fig. 20.2.



Fig. 20.2 EDGAR BUCKINGHAM (8. July 1867–29. April 1940)

EDGAR BUCKINGHAM was a physicist and soil scientist. He graduated from Harvard with a bachelor's degree in physics in 1887. He did additional graduate work at the University of Strasbourg and the University of Leipzig, where he studied under chemist WILHELM OSTWALD. BUCKINGHAM received a Ph.D. from Leipzig in 1893. He worked at the USDA Bureau of Soils from 1902 to 1906 as a soil physicist and from 1906–1937 at the (US) National Bureau of Standards (now the National Institute of Standards and Technology, or NIST). His fields of expertise included soil physics, gas properties, acoustics, fluid mechanics, and blackbody radiation. He is also the originator of the BUCKINGHAM Π -theorem in the field of dimensional analysis.

BUCKINGHAM's first work on soil physics is on soil aeration, particularly the loss of carbon dioxide from the soil and its subsequent replacement by oxygen. He found that the rate of gas diffusion in soil did not significantly depend on the soil structure, compactness or water content of the soil. He determined the diffusion coefficient as a function of air content. This relation is still commonly cited in many textbooks and used in modern research. The outcomes of his research on gas transport were: the exchange of gases in soil aeration takes place by diffusion and is independent of the variations of the outside barometric pressure.

In his work on soil moisture BUCKINGHAM found that soils of various textures could strongly inhibit evaporation, particularly where capillary flow through the uppermost layers was prevented. Moreover, he showed that evaporative losses in soil were initially higher from the arid soil, then after three days the evaporation under arid conditions became less than under humid conditions, with the total loss ending up greater from the humid soil. BUCKINGHAM believed this occurred due to the self-mulching behavior exhibited by the soil under arid conditions.

BUCKINGHAM is famous for his work on unsaturated flow and capillary action. He recognized the importance of the potential of the forces arising from interactions between soil and water, which he called capillary potential. He combined capillary theory and an energy potential in soil physics theory, and was the first to expound the dependence of soil hydraulic conductivity on capillary potential. This dependence later came to be known as relative permeability in petroleum engineering. He also applied a formula equivalent to Darcy's law to unsaturated flow.

The text is based on www.wikipedia.org

The exponents of $[M]$, $[L]$ and $[T]$ on the right-hand side of this equation must each sum up to zero, because $[IT]$ is dimensionless and so, its exponent is zero. This requirement yields the three equations

$$\begin{aligned} [M] : \quad & 0 = k_1 + k_4, \\ [L] : \quad & 0 = k_1 + k_2 + k_3 - 3k_4 + k_5 + 2k_6, \\ [T] : \quad & 0 = -2k_1 - k_2 - 2k_5 - k_6 \end{aligned} \tag{20.23}$$

or in matrix form

$$\underbrace{\begin{pmatrix} 1 & 0 & 0 & 1 & 0 & 0 \\ 1 & 1 & 1 & -3 & 1 & 2 \\ -2 & -1 & 0 & 0 & -2 & -1 \end{pmatrix}}_{\text{dimensional matrix}} \begin{pmatrix} k_1 \\ k_2 \\ k_3 \\ k_4 \\ k_5 \\ k_6 \end{pmatrix} = \begin{pmatrix} 0 \\ 0 \\ 0 \end{pmatrix}. \tag{20.24}$$

This is a homogeneous system of linear equations for k_1, \dots, k_6 . According to a theorem in algebra of the theory of linear equations (20.23) possess $N - m$ independent fundamental solutions, where N is the number of unknowns ($=6$ in this case) and m is the rank of the *dimensional matrix*. Thus, there are $N - m$ different independent Π -products. The rank of a rectangular matrix is defined as the largest size of the square sub-matrices with non-vanishing determinant, which in this case is $m = 3$, as can easily be seen from (20.24) whose matrix possesses more than one 3×3 sub-matrix with non-vanishing determinant.

It is mathematically not difficult to determine three different fundamental solutions for the homogeneous system (20.23). Knowing the rank of the dimensional matrix, one selects 3 different values for three exponents k_j e.g.,

$$\begin{aligned} k_1 = 1, \quad k_2 = 0, \quad k_3 = 0, \\ k_1 = 0, \quad k_2 = 1, \quad k_3 = 0, \\ k_1 = 0, \quad k_2 = 0, \quad k_3 = 1, \end{aligned}$$

with the aid of which the values for k_4, k_5 and k_6 follow (in the same order) as

$$\begin{aligned} k_4 = -1, \quad k_5 = 0, \quad k_6 = -2, \\ k_4 = 0, \quad k_5 = -\frac{1}{3}, \quad k_6 = -\frac{1}{3}, \\ k_4 = 0, \quad k_5 = \frac{1}{3}, \quad k_6 = -\frac{2}{3}. \end{aligned} \tag{20.25}$$

This yields the Π -products

$$\Pi_1 := \frac{K}{\rho \nu^2}, \quad \Pi_2 := \frac{V}{(g\nu)^{1/3}}, \quad \Pi_3 := \frac{Dg^{1/3}}{\nu^{2/3}}. \tag{20.26}$$

They can easily be checked to be dimensionless, however, these Π -products are physically not transparent. It is, therefore, often more convenient to ‘guess’ three independent Π -products, which transpire the physics more directly. With some limited knowledge in fluid mechanics already, it is tempting to try in this case with

$$\mathbb{P} := \frac{K}{\rho V^2 D^2}, \quad \mathbb{R} := \frac{VD}{\nu}, \quad \mathbb{Fr} := \frac{V^2}{gD}. \tag{20.27}$$

\mathbb{P} is a force (pressure) ratio, \mathbb{R} is the classical REYNOLDS number, \mathbb{Fr} the FROUDE number, and it is straightforward to see that

$$\mathbb{P} = \frac{2 \Pi_1}{(\Pi_2 \Pi_3)^2}, \quad \mathbb{R} = \Pi_2 \Pi_3, \quad \mathbb{Fr} = \frac{\Pi_2^2}{\Pi_3}. \tag{20.28}$$

The above examples make plausible, and the proof of BUCKINGHAM’s theorem (see Appendix to this chapter) rigorously corroborates the content of

Theorem 20.2 *The number of dimensionless products in a complete set of physical variables equals the total number of variables minus the rank of the dimensional matrix.* ■

Example 20.5 Pressure Drop in Pipes

This problem has been dealt with in Chap. 10, Sect. 10.3.1. Here, we shall demonstrate, how easily and straightforwardly formula (10.55) for the pressure drop can be obtained. Let Δp be the pressure drop between two cross sections in a straight circular pipe that transports a density preserving fluid under steady conditions. Moreover, let L be the distance between the two cross sections and D the internal diameter of the pipe. Denote by k the mean roughness length of the interior wall, V the mean velocity of the fluid within the cross section, ρ the fluid density and ν the kinematic viscosity of the fluid. The pressure drop between the two cross sections can, thus, be functionally expressed by

$$f(\Delta p, L, D, k, V, \rho, \nu) = 0. \tag{20.29}$$

The dimensional matrix of the variables of (20.29) is given by

$$\begin{array}{c|cccc|ccc} & \Delta p & L & D & k & V & \rho & \nu & \\ \hline M & 1 & 0 & 0 & 0 & 0 & 1 & 0 & \\ L & -1 & 1 & 1 & 1 & 1 & -3 & 2 & \\ T & -2 & 0 & 0 & 0 & -1 & 0 & -1 & \\ \hline & & & & & & & & \end{array} \quad \det |\cdot| \neq 0.$$

It has rank 3, and so, this problem is characterized by four Π -products, which e.g. can easily be found to be

$$\mathbb{P} = \frac{\Delta p}{\frac{1}{2}\rho V^2}, \quad \mathbb{R} = \frac{VD}{\nu}, \quad \frac{L}{D}, \quad \frac{k}{D}. \tag{20.30}$$

With these we may write

$$\Delta p = \frac{1}{2} \rho V^2 f\left(\mathbb{R}, \frac{L}{D}, \frac{k}{D}\right). \tag{20.31}$$

A linear dependence of Δp on L can easily be corroborated by experiment. This implies

$$\Delta p = \frac{1}{2} \rho V^2 \frac{L}{D} \lambda\left(\mathbb{R}, \frac{k}{D}\right). \tag{20.32}$$

The function $\lambda(\mathbb{R}, k/D)$ has been experimentally determined. A standardization of this, based on formulae derived by LUDWIG PRANDTL [32] and JOHANNES NIKURADSE [29] is given as Fig. 10.14 in Chap. 10. Section 10.3.1 also gives a different and more detailed presentation of formula (20.32).

Example 20.6 Viscosity in a Kinetic Gas Once Again

Let us go back to Example 20.1 and verify the statements made at the beginning of this chapter and given without proof. In Eq. (20.2)₂ the function f was stated to describe the viscosity μ of the gas to depend on the three molecular parameters m, ϑ, f and on the ‘global’ parameters ρ and ε , where ε is the internal energy of the molecules interpreted as the mean kinetic energy of their fluctuating motion, used here as measure of the temperature of the kinetic gas. The dimensional matrix is given by

M	μ	ρ	ε	m	ϑ	f	$\det \cdot \neq 0$	(20.33)
L	-1	-3	2	0	1	1		
T	-1	0	-2	0	0	-2		

which has rank 3, so that according to the Π -theorem three independent dimensionless Π -products must exist, namely for instance

$$\frac{\mu\vartheta^2}{m\sqrt{\varepsilon}}, \quad \frac{\rho\vartheta^3}{m}, \quad \frac{f\vartheta}{m\varepsilon}, \tag{20.34}$$

as the reader may easily corroborate. Thus, given the variable set (20.2) we have now proven confidence in Eq. (20.4) and the approximations (20.5), (20.6).

Another interesting case of molecular force influence of the viscosity of a kinetic gas exists, if the molecules repel each other by a force, which is proportional to the ξ -th power of the inverse distance of the molecules. NEWTON’s second law then reads

$$f = \frac{\mathfrak{G}}{r^\mathfrak{k}}, \quad \mathfrak{k} > 0, \quad \mathfrak{G} > 0. \tag{20.35}$$

The exponent \mathfrak{k} is dimensionless and so $[\mathfrak{G}] = [f r^\mathfrak{k}] = [M L^{\mathfrak{k}+1} T^{-2}]$. The dimensional matrix, based on $\{\mu, \rho, \varepsilon, m, \mathfrak{G}\}$ is, thus, given by

$$\begin{array}{c|ccccc} & \mu & \rho & \varepsilon & m & \mathfrak{G} \\ M & 1 & 1 & 0 & 1 & 0 \\ L & -1 & -3 & 2 & 0 & \mathfrak{k} + 1 \\ T & -1 & 0 & -2 & 0 & -2 \end{array} \quad \det |\cdot| \neq 0. \tag{20.36}$$

So, there are two dimensionless Π -products in this case, e.g.

$$\Pi_1 = \frac{m\sqrt{\varepsilon}}{\mu} \left(\frac{m\varepsilon}{\mathfrak{G}}\right)^{2/(\mathfrak{k}-1)}, \quad \Pi_2 = \frac{m\varepsilon}{\mathfrak{G}} \left(\frac{\rho}{m}\right)^{(1-\mathfrak{k})/3}. \tag{20.37}$$

Consequently,

$$\mu = m\sqrt{\varepsilon} \left(\frac{m\varepsilon}{\mathfrak{G}}\right)^{2/(\mathfrak{k}-1)} \tilde{f} \left(\frac{m\varepsilon}{\mathfrak{G}} \left(\frac{\rho}{m}\right)^{(1-\mathfrak{k})/3}\right). \tag{20.38}$$

Therefore, only inverse power molecules with $\mathfrak{k} \neq 1$ are meaningful. Moreover, if μ is independent of ρ , then $\tilde{f} = \text{const.}$ and

$$\mu \propto m\sqrt{\varepsilon} \left(\frac{m\varepsilon}{\mathfrak{G}}\right)^{2/(\mathfrak{k}-1)}. \tag{20.39}$$

The kinetic theory of ideal and dilute gases presupposes such conditions.

20.2.3 A Set of Examples from Fluid Mechanics

Example 20.7 Motion of a Shock Front after an (Atomic) Explosion Close to the Ground

This example is well known among fluid dynamicists, as it caused embarrassment to the Government of the United States. The basis is the Manhattan Project during the Second World War, when first atomic bomb tests were conducted in the desert of New Mexico. The example is reported in [1].

Consider a half space, $x, y, z > 0$; we regard it as the atmosphere bounded by the plane ground, see **Fig. 20.3**. Let a boundary point be the center of the semi-sphere

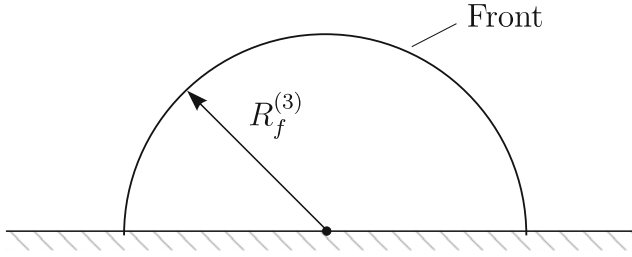


Fig. 20.3 Semi-spherical fire ball with radius $R_f^{(3)}$ due to a point explosion (The superscript in $R_f^{(3)}$ identifies the dimension of the space in which the wave propagates)

in Fig. 20.3, where at time $t = 0$ a large quantity of energy $E^{(3)}$ is released.⁷ We assume that the volume, in which the energy is released, can be identified with an instantaneous point source; moreover, it is assumed that the source is isotropic in the upper half space, $z > 0$, from the point source at the basal surface. These prerequisites are needed for the formation of a half-spherical shock wave. Its front will at time $t > 0$ be a distance $R_f^{(3)}(t)$ away from the center. We wish to find the evolution of the front position as a function of time. This front moving process will likely depend on $E^{(3)}$, t and the density ρ_0 of air ahead of the shock front, so that $R_f^{(3)} = f(t, \rho_0, E^{(3)})$. The corresponding dimensional matrix is

$$\begin{array}{c|cccc}
 & t & R_f^{(3)} & \rho_0 & E^{(3)} \\
 \hline
 M & 0 & 0 & 1 & 1 \\
 L & 0 & 1 & -3 & 2 \\
 T & 1 & 0 & 0 & -2
 \end{array} \tag{20.40}$$

and has rank 3 and allows determination of the single-family⁸ dimensionless product

$$\Pi = \frac{R_f^{(3)}}{\left(\frac{E^{(3)}}{\rho_0}\right)^{1/5} t^{2/5}} = \text{const.} \tag{20.41}$$

Thus,

$$R_f^3(t) = \text{const.} \times \left(\frac{E^{(3)}}{\rho_0} t^2\right)^{1/5}. \tag{20.42}$$

⁷The superscript (3) indicates that the space in which this phenomenon is studied is three-dimensional.

⁸Of all the possible Π -products, which only differ by powers from one another, we select that, which is linear in $R_f^{(3)}$.

The expansion of the semi-spherical front grows with $t^{2/5}$. The free constant can be determined, if one measures the radius of the front $R_f^{(3)}$ at different times. This is best done in doubly logarithmic representation, i.e.,

$$\ln R_f^{(3)} = \ln(\text{const}) + \frac{1}{5} \ln \left(\frac{E^{(3)}}{\rho_0} \right) + \frac{2}{5} \ln(t). \tag{20.43}$$

In a plot with $x = \ln(t)$ and $y = \ln(R_f^{(3)})$ this equation represents a straight line with inclination $2/5$. It crosses the y -axis at $\ln(\text{const}) + \frac{1}{5} \ln(E^{(3)}/\rho_0)$. Incidentally, the gas dynamical problem is known and shows that $\text{const} \approx 1$. If one knows this, then the experimental determination of $R_f^{(3)}$ allows evaluation of the strength of the explosion. This was done by G.I. TAYLOR by using a movie film of the nuclear test in the desert of New Mexico, when the Americans were testing their atomic bombs in the Manhattan Project during the Second World War. For the nuclear agency of the USA this caused much embarrassment as TAYLOR said, since the strength of the bomb was kept secret, whilst the movie was not classified, [42, 43].

Repetition of the above computation shows that in the two and one-dimensional cases the formulae analogous to (20.42) are

$$R_f^{(2)}(t) = \text{const} \times \left(\frac{E^{(2)}}{\rho_0} t^2 \right)^{1/4}, \tag{20.44}$$

$$R_f^{(1)}(t) = \text{const} \times \left(\frac{E^{(1)}}{\rho_0} t^2 \right)^{1/3}.$$

The speed of expansion of the blast wave changes with the dimension of the space, in which the wave expands.

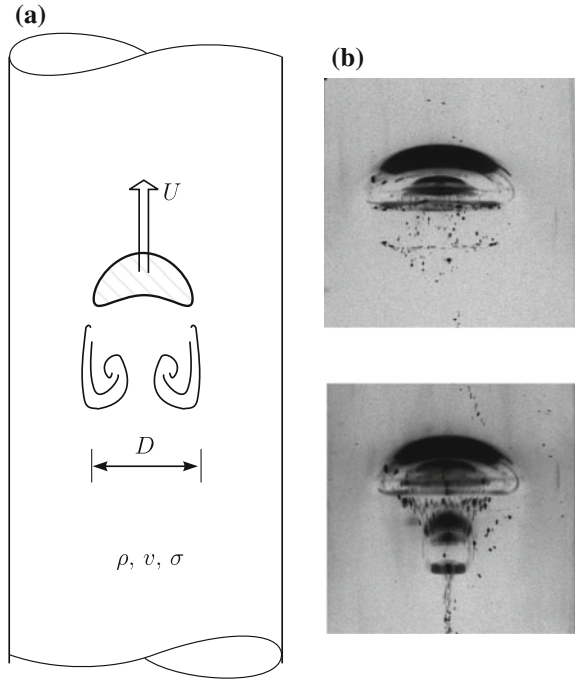
Example 20.8 Rising Gas Bubbles

Gas bubbles, which are rising in a quiescent viscous fluid, reach soon after their release a constant rising velocity (see **Fig. 20.4**). Parameters, upon which the ultimate velocity U depends are the Earth's acceleration, g , a typical bubble diameter, D , the fluid density, ρ , its kinematic viscosity, ν , and, for small bubbles the surface tension, σ . We neglect the kinematic viscosity of the gas in the bubble as well as the relative density difference $\|(\rho_{\text{fluid}} - \rho_{\text{gas}})/\rho_{\text{fluid}}\| \approx 1$. Moreover, we ignore thermal effects and the exchange of matter between the bubble and the fluid. The dimensional matrix of the above variables

	U	g	D	ν	σ	ρ	
M	0	0	0	0	1	1	
L	1	1	1	2	-1	-3	
T	-1	-2	0	-1	-2	0	

(20.45)

Fig. 20.4 **a** Sketch of a bubble with trailing vortex ring. The bubble diameter is D and it is assumed to be small in comparison to the pipe diameter. **b** Photos of rising bubbles in silicon oil (Model of demonstration, Institute of Mechanics, Darmstadt University of Technology, Photo and model courtesy of Prof. K.G. ROESNER)



has rank 3 and, thus, gives rise to three dimensionless products, which we choose as

$$\mathbb{F}r = \frac{U}{\sqrt{gD}}, \quad \mathbb{R} = \frac{UD}{\nu}, \quad \mathbb{W} = \frac{\rho U^2 D}{\sigma}, \quad (20.46)$$

which are the FROUDE, REYNOLDS and WEBER numbers. For not too small drops a dependence of $\mathbb{F}r$ on \mathbb{W} is unlikely, so that

$$\mathbb{F}r = f(\mathbb{R}).$$

For a power law

$$\mathbb{F}r = C\mathbb{R}^\alpha, \quad (20.47)$$

with unknowns C and α , one deduces with the definitions (20.46)

$$U = C^{\frac{1}{1-\alpha}} g^{\frac{1}{2(1-\alpha)}} \nu^{\frac{\alpha}{\alpha-1}} D^{\frac{2\alpha+1}{2-2\alpha}}. \quad (20.48)$$

Observation of rising bubbles with various diameters indicates that, very roughly, U varies linearly with D ; thus, (20.48) implies

$$\frac{2\alpha + 1}{2 - 2\alpha} = 1 \implies \alpha = \frac{1}{4}.$$

so that

$$U = C^{4/3} g^{2/3} \nu^{-1/3} D. \quad (20.49)$$

The constant C can be determined by experiment and yields the value $C = 2/(3 \times 10^{1/4}) = 0.3749$.

Example 20.9 RAYLEIGH–BÉNARD⁹ Instability)

RAYLEIGH–BÉNARD convection is treated in nearly all books dealing with fluid-flow instability. It is treated at length by S. CHANDRASEKHAR [15] for the linear theory and by D. JOSEPH [22] and B. STRAUGHAN [41] with non-linear energy stability techniques.

Consider a viscous BOUSSINESQ fluid, which is kept between two infinitely long rigid plates at a distance H . Initially the fluid is thought to be at rest. The lower plate is heated and the upper plate is cooled below the temperature of the lower plate. The temperatures of the plates are T_{lower} and T_{upper} , and the temperature difference of the plates is $\Delta T = T_{\text{lower}} - T_{\text{upper}}$, set at a certain value. The coefficient of thermal expansion of the fluid that is kinematically treated as incompressible (volume preserving) and the kinematic viscosity are given by α [K^{-1}] and ν [$L^2\text{T}^{-1}$], respectively. These are conditions of a BOUSSINESQ fluid, for which the velocity field is treated as solenoidal even though the density varies as $\Delta\rho = -\alpha\Delta T\rho_0$.

Observations show that for sufficiently small values of ΔT the fluid between the two plates is at rest. In this thermal regime of the fluid layer the transport of heat from the lower to the upper plate is by thermal conduction. When the temperature difference ΔT of the plate is sufficiently high, i.e., when ΔT reaches a threshold value, ΔT_{thres} , a convection flow (in cells, rolls or more complex bounded regions) is formed. The structure of this convective flow depends upon the initial conditions and the side boundaries, which hold the fluid between the two plates together. When the side walls are very far away (theoretically infinitely far away), convective rolls with horizontal axes are preferentially formed; if side boundaries are present, triangular, hexagonal or more complex cells are established, in which the fluid is vertically circulating as e.g. shown in **Fig. 20.7**. When the horizontal extent of the container carrying the fluid is relatively small the cells are still bounded, but take non-regular forms.

⁹For brief biographies of LORD RAYLEIGH and HENRI CLAUDE BÉNARD, see **Figs. 20.5** and **20.6**, respectively.

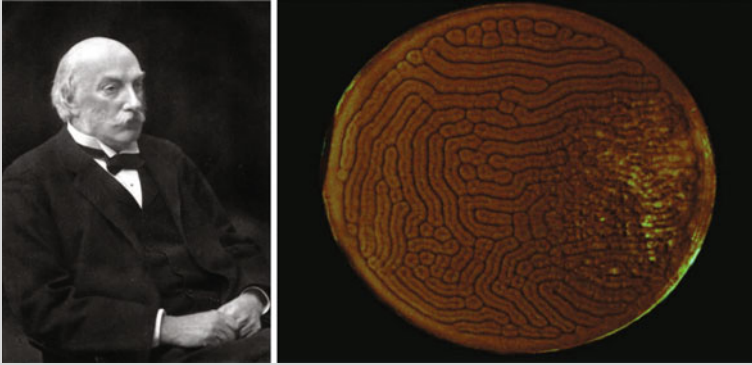


Fig. 20.5 JOHN WILLIAM STRUTT, 3. BARON RAYLEIGH (12. Nov. 1842–30. June 1919) (*Left*) 3. Baron Rayleigh; (*right*) Ilya Lisenker, Terese Decker Team-3 Spring 2010. Rayleigh–Benard convection cells visualized in a mixture of olive oil and canola oil with aluminum and magnesium filings

JOHN WILLIAM STRUTT, 3. BARON RAYLEIGH was a physicist, who, with WILLIAM RAMSAY, discovered argon, an achievement for which he earned the *Nobel Prize for Physics* in 1904. He also discovered the phenomenon now called *Rayleigh scattering*, which can be used to explain why the sky is blue, and predicted the existence of the *surface waves* in solid bodies, now known as *Rayleigh waves*, see RAYLEIGH’s textbook, ‘*The Theory of Sound*’, [35, 36].

JOHN WILLIAM STRUTT, suffered from frailty and poor health in his early years. He attended the University of Cambridge in 1861 where he studied mathematics at Trinity College. He obtained a Bachelor of Arts degree in 1865, and a Master of Arts in 1868. He was subsequently elected to a Fellowship of Trinity College. In 1873, on the death of his father, JOHN STRUTT, 2nd BARON RAYLEIGH, he inherited the Barony of RAYLEIGH. He was the second Cavendish Professor of Physics at the University of Cambridge, from 1879 to 1884 (following JAMES CLERK MAXWELL). He first described dynamic soaring by seabirds in 1883, in the British journal *Nature*. From 1887 to 1905 he was Professor of Natural Philosophy at Cambridge.

LORD RAYLEIGH was elected Fellow of the Royal Society in June 1873, and served as its president from 1905 to 1908. In 1919, RAYLEIGH served as President of the Society for Psychological Research. He died on 30 June of that year and was succeeded, as the 4th LORD RAYLEIGH, by his son ROBERT JOHN STRUTT, another well-known physicist. LORD RAYLEIGH’s scientific works are not only immense by substance but equally also by volume. His scientific collected papers fill six volumes and have been re-published in 2011 by Cambridge University Press [37].

The analysis in the main text (pp. 559–566) gives a flavor of the simplest possible plane convective analysis of RAYLEIGH’s computations, and the above panel shows a geometrically more complex visualization.

The text is based on www.wikipedia.org

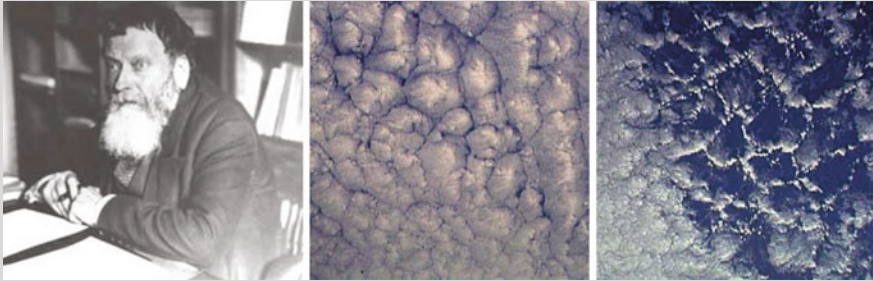


Fig. 20.6 HENRI CLAUDE BÉNARD (25. Oct. 1874–29. March 1939) Two kinds of BÉNARD convection cells can frequently be distinguished in satellite images, open cells (*right*) and closed cells (*middle*). Courtesy Environmental Technology Laboratory, Boulder, Colorado

HENRI CLAUDE BÉNARD was a French physicist who focused his research activities on experimental fluid dynamics. He is best known for the discovery of the regular convective cells, which are known today as BÉNARD *cells*. Their formation as a bifurcation from a motionless configuration have been theoretically predicted for a BOUSSINESQ fluid by LORD RAYLEIGH. This is the reason why this bifurcation phenomenon is referred to as RAYLEIGH–BÉNARD convection.

HENRI BÉNARD studied between 1894 and 97 at the École Normale Supérieure and graduated with doctorate at the Collège de France and with support from MARCEL BRILLOUIN, [3–6]. The second part of the dissertation dealt with the rotation of the polarization plane in sugar solutions; this work had practical implications in measuring the concentration of sugar, e.g. in grapes [27, 39].

In 1902 BÉNARD taught in Lyon and started there work that led to an early understanding of what later became known as VON KÁRMÁN vortex street [7]. This led to a priority dispute in the 1920s between HENRI BÉNARD and THEODORE VON KÁRMÁN. As a consequence HENRI BÉNARD revisited his work on thermal convection, claiming agreement between his results and the theory of LORD RAYLEIGH [34].

HENRI BÉNARD became in 1910 professor at the University in Bordeaux and in 1922 Maitre de conférences (habilitation) at the Sorbonne with promotion to full professor in 1926. In 1929 he became head of the Laboratory of Hydrodynamics. Moreover, in 1935 he was called to the Committee for Atmospheric Turbulence and 1937 professor at the École de l’Aéronautique.

The text is based on www.wikipedia.org

We conjecture that the transition from the conductive to the convective regime can be described by a functional relation of the form

$$f(H, g, \nu, \alpha, \Delta T, D_T) = 0, \quad (20.50)$$

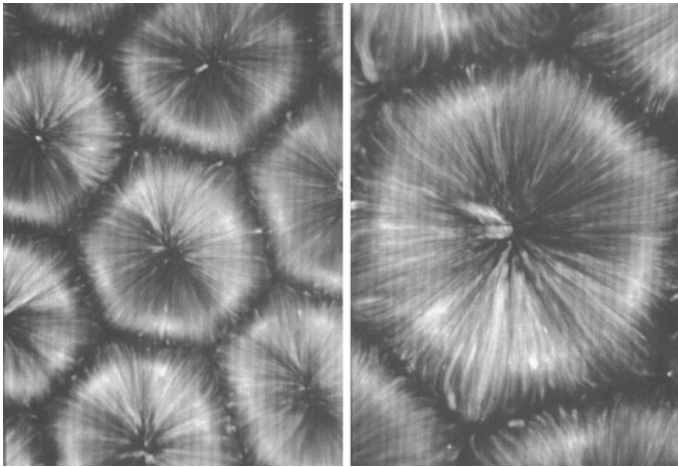


Fig. 20.7 RAYLEIGH–BÉNARD cells can most simply be made visible in shallow shells using silicon oil and aluminium powder. They are, however also briefly visible when eggs are fried (shortly before the white of the egg is coagulating) [Courtesy of M.G. VELARDE and C. NORMAND [47]]

in which H is the gap width and g the gravity constant [9.81 m s^{-2}]; ν , α , D_T are the kinematic viscosity, the coefficient of thermal expansion and the thermal diffusivity, all assumed to be constant. ΔT is the temperature difference between the plates. The transition of the conductive, motionless flow state to the convective motion can physically easily be understood as the heavier and colder fluid at the top tends to form lobes. These lobes will eventually ‘break through’ and induce a downward convective motion that is counterbalanced for mass balance reasons by an upward motion of warmer fluid merging into a cell like rotation of the fluid.

The dimensional matrix of the variables (20.50) is given by

$$\begin{array}{c|cccccc}
 & H & g & \nu & \alpha & \Delta T & D_T \\
 \hline
 M & 0 & 0 & 0 & 0 & 0 & 0 \\
 L & 1 & 1 & 2 & 0 & 0 & 2 \\
 T & 0 & -2 & -1 & 0 & 0 & -1 \\
 K & 0 & 0 & 0 & -1 & 1 & 0 \\
 \hline
 & _ & _ & _ & _ & _ & _
 \end{array}
 \quad \det |\cdot| \neq 0, \quad (20.51)$$

in which M , L , T , K stand for ‘mass’, ‘length’, ‘time’ and ‘temperature’ (Kelvin). This matrix has rank 3. Thus, there exist three independent Π -products, which may be selected as

$$\mathbb{R}a = \frac{g \alpha \Delta T}{D_T \nu} H^3, \quad \mathbb{R} = \frac{\sqrt{g H} H}{\nu}, \quad \mathbb{P}r = \frac{\nu}{D_T}. \quad (20.52)$$

$\mathbb{R}a$ is the so-called RAYLEIGH number, \mathbb{R} is a REYNOLDS number and $\mathbb{P}r$ the PRANDTL number. It follows that the critical RAYLEIGH number, identifying the transition from the conductive to the convective regime is given by a relation of the form

$$\mathbb{R}a = f(\mathbb{R}, \mathbb{P}r). \quad (20.53)$$

It is likely that the REYNOLDS number does not influence the bifurcation locus in a given problem simply since \mathbb{R} is formed with the shallow water velocity \sqrt{gH} and the gap width as the characteristic length. It seems, indeed, to be plausible that this velocity is not a relevant quantity in bounded, primarily convection driven flow. So, (20.53) reduces to

$$\mathbb{R}a = f(\mathbb{P}r), \quad (20.54)$$

which is likely a sufficient relation to describe the bifurcation from the conductive to the convective thermo-viscous flow state.

This understanding is corroborated if one tries to explicitly determine the function $f(\mathbb{P}r)$ in (20.54). To this end, consider a density preserving fluid in the BOUSSINESQ approximation, i.e., a kinematically incompressible fluid, whose gravity force may nevertheless vary due to the thermal expansion of its particles under temperature changes. Consider a fluid, in which the temperature has small variations ΔT about a constant value T_0 , leading to variations in the local fluid density.

$$T = T_0 + \Delta T \quad \longrightarrow \quad \rho = \rho_0 + \Delta\rho. \quad (20.55)$$

In the so-called BOUSSINESQ approximation the density change $\Delta\rho$ due to the temperature change ΔT is given by

$$\Delta\rho = -\alpha \Delta T \rho_0, \quad (20.56)$$

in which α is the (constant) coefficient of thermal expansion; it implies a change in the gravity force

$$\Delta\mathbf{g} = -\rho_0 \alpha \Delta T \mathbf{g}, \quad (20.57)$$

in which \mathbf{g} is the (constant) value of the gravity acceleration, $\|\mathbf{g}\| = 9.81 \text{ [m s}^{-2}\text{]}$. The field equations of a BOUSSINESQ fluid subjected to small temperature changes are now given by

$$\begin{aligned} \text{Mass:} & \quad \nabla \cdot \mathbf{u} = 0, \\ \text{Momentum:} & \quad \rho_0 \left\{ \frac{\partial \mathbf{u}}{\partial t} + (\text{grad } \mathbf{u}) \cdot \mathbf{u} \right\} \\ & \quad = -\nabla p + \eta \nabla^2 \mathbf{u} + \rho_0 (1 - \alpha \Delta T) \mathbf{g}, \\ \text{Energy:} & \quad \frac{\partial T}{\partial t} + (\text{grad } T) \mathbf{u} = D_T \nabla^2 T, \end{aligned} \quad (20.58)$$

where u, T, p are the velocity, temperature and pressure fields, η is the dynamic viscosity and $D_T = \text{constant} = \kappa/(\rho_0 c)$ is the coefficient of thermal diffusion.

Consider the fluid to be between two parallel horizontal plates, **Fig. 20.8**; assume, moreover, that the basic state is motionless, the lower plate is held at the temperature T_0 , whilst the upper plate temperature is monitored to be kept at $T_0 - \Delta T$, $\Delta T = \beta H$,



Fig. 20.8 Basic state (*left*) with no motion, but a vertical temperature gradient, (*right*) convective regime with bounded cells (rolls, finite cells) of convective fluid motion

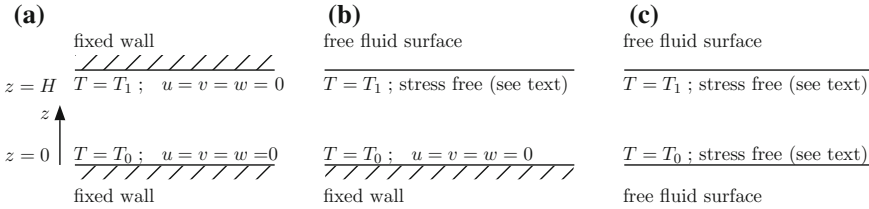


Fig. 20.9 Combinations of boundary conditions, which can in principle, be applied to the layer of liquid. The combinations of **a**, **b** can experimentally be realized, the situation in panel **c** is not experimentally realizable and, therefore, somewhat artificial

where H is the gap width. We, thus, assume that the temperature regime is given by $\beta = \Delta T/H$.

The fluid system (20.58) is subjected to *boundary conditions*. Those of the temperature are prescribed, but the mechanical boundary conditions depend upon the kind of mechanical support. At a fixed wall without slip one may request $u = v = w = 0$, whilst at a free fluid surface one has stress free conditions. These can be combined to the boundary conditions sketched in **Fig. 20.9**.

The base state with no motion and linear temperature profile in the vertical direction can be assumed to be given by

$$\mathbf{u}_B = \mathbf{0} \quad \text{and} \quad T_B = T_0 - \beta z, \tag{20.59}$$

and, indeed, the field equations (20.58) are satisfied for (20.59), if

$$\frac{dp_B}{dz} = -\rho_0 g(1 + \alpha \beta z) \quad \longrightarrow \quad p_B = p_B(z) = -\rho_0 g \left(z + \frac{1}{2} \alpha \beta z^2 + p_0 \right), \tag{20.60}$$

in which p_0 is the (constant) pressure at the lower boundary $z = 0$. In the ensuing analysis (20.60) will not be needed any further.

The *linearized perturbed state* will be a fluid state beyond the base state,

$$\mathbf{u} = \mathbf{u}_B + \tilde{\mathbf{u}}(\mathbf{x}, t), \quad T = T_B(z) + \tilde{T}(\mathbf{x}, t), \quad p = p_B(z) + \tilde{p}(\mathbf{x}, t). \tag{20.61}$$

If this ansatz is substituted in (20.58), nonlinear terms in the tilde-quantities are systematically omitted and if (20.60) is observed, the linearized governing equations

$$\begin{aligned}
 \text{Mass:} & \quad \nabla \cdot \tilde{\mathbf{u}} = 0, \\
 \text{Momentum:} & \quad \rho_0 \frac{\partial \tilde{\mathbf{u}}}{\partial t} = -\nabla \tilde{p} + \eta \nabla^2 \tilde{\mathbf{u}} - \rho_0 \alpha \tilde{T} \mathbf{g}, \\
 \text{Energy:} & \quad \frac{\partial \tilde{T}}{\partial t} + (\nabla T_B) \cdot \tilde{\mathbf{u}} = D_T \nabla^2 \tilde{T}
 \end{aligned} \tag{20.62}$$

are obtained, or in Cartesian component form

$$\text{Mass:} \quad \frac{\partial \tilde{u}}{\partial x} + \frac{\partial \tilde{v}}{\partial y} + \frac{\partial \tilde{w}}{\partial z} = 0, \tag{20.63}$$

$$\begin{aligned}
 \text{Momentum:} \quad \frac{\partial \tilde{u}}{\partial t} &= -\frac{1}{\rho_0} \frac{\partial \tilde{p}}{\partial x} + \nu \nabla^2 \tilde{u}, \\
 \frac{\partial \tilde{v}}{\partial t} &= -\frac{1}{\rho_0} \frac{\partial \tilde{p}}{\partial y} + \nu \nabla^2 \tilde{v},
 \end{aligned} \tag{20.64}$$

$$\begin{aligned}
 \frac{\partial \tilde{w}}{\partial t} &= -\frac{1}{\rho_0} \frac{\partial \tilde{p}}{\partial z} + \nu \nabla^2 \tilde{w} + \alpha g \tilde{T}, \\
 \text{Energy:} \quad \frac{\partial \tilde{T}}{\partial t} - \beta \tilde{w} &= D_T \nabla^2 \tilde{T}.
 \end{aligned} \tag{20.65}$$

Here, $\nu = \eta/\rho_0$ is the (constant) kinematic viscosity.

Equations (20.63)–(20.65) constitute five equations for the unknowns $\tilde{u}, \tilde{v}, \tilde{w}, \tilde{p}, \tilde{T}$. They will now be reduced to two equations for the variables \tilde{w} and \tilde{T} . Taking

$$\frac{\partial}{\partial x}(20.64)_1 + \frac{\partial}{\partial y}(20.64)_2 + \frac{\partial}{\partial z}(20.64)_3$$

and using $\text{div } \tilde{\mathbf{u}} = 0$, yields

$$0 = -\frac{1}{\rho_0} \nabla^2 \tilde{p} + \alpha g \frac{\partial \tilde{T}}{\partial z}. \tag{20.66}$$

The components \tilde{u}, \tilde{v} have disappeared from (20.66); to eliminate the pressure, we, thus, apply the operator ∇^2 to Eq. (20.64)₃ and then substitute in the emerging equation $\nabla^2 \tilde{p}$ from (20.66). This computation yields

$$\frac{\partial}{\partial t} (\nabla^2 \tilde{w}) = \alpha g \left(\nabla_H^2 \tilde{T} \right) + \nu \nabla^4 \tilde{w}, \tag{20.67}$$

in which ∇_H^2 is the horizontal Laplace operator. Equations (20.65) and (20.67) constitute a system of partial differential equations (PDE) for \tilde{w} and \tilde{T} , that was attempted to be constructed.

Solutions to this system will be sought by the *normal mode analysis*. To this end, the following test solution is tried

$$\begin{aligned}\tilde{w}(x, y, z, t) &= f(x, y)\bar{w}(z)\exp(st), \\ \tilde{T}(x, y, z, t) &= f(x, y)\theta(z)\exp(st).\end{aligned}\tag{20.68}$$

The variable s describes the growth rate and may, in general be complex valued. If $\text{Re}(s) > 0$, the functions \tilde{w} and \tilde{T} will grow and eventually become exponentially unbounded. This describes the instability. If $\text{Re}(s) < 0$, the solution (20.68) will die out in time: The ground state will be stable. For a complex valued s the functions \tilde{w} and \tilde{T} are oscillatory (neutral stability, when $\text{Re} = 0$) plus exponentially decaying or growing, depending whether the real part of s is positive or negative.

The functions $\bar{w}(z)$ and $\theta(z)$ describe the mode structure of \tilde{w} and \tilde{T} in the z -direction. Finally, $f(x, y)$ describes the horizontal structure of \tilde{w} and \tilde{T} .

Substituting the functional representations (20.68) into (20.65) and (20.67) yields the following partial differential equations for f and \bar{w} :

$$s\{(\nabla_H^2 f)\bar{w} + f\bar{w}''\} = \alpha g(\nabla_H^2 f)\theta + \nu\left\{\left[\left(\nabla_H^2 + \frac{\partial^2}{\partial z^2}\right)^2 f\right]\bar{w}\right\},\tag{20.69}$$

$$sf\theta - \beta f\bar{w} = D_T\{(\nabla_H^2 f)\theta + f\theta''\},\tag{20.70}$$

in which primes denote differentiations with respect to z . Equation (20.70) is better written as

$$s\theta(z) - \beta\bar{w}(z) = D_T\theta(z)\left(\frac{\nabla_H^2 f}{f}\right) + D_T\theta''(z).\tag{20.71}$$

This equation turns into an ordinary differential equation, if one chooses

$$\frac{\nabla_H^2 f}{f} = \text{constant} = -a^2.\tag{20.72}$$

With this choice, Eq. (20.69) takes the form

$$\begin{aligned}s\{-a^2 f\bar{w} + f\bar{w}''\} &= \alpha g(-a^2 f)\theta + \nu\left(\frac{d^2}{dz^2} - a^2\right)^2 \bar{w}f, \\ \frac{s}{\nu}\left(\frac{d^2}{dz^2} - a^2\right)\bar{w} &= -\alpha g a^2 \frac{\theta}{\nu} + \left(\frac{d^2}{dz^2} - a^2\right)^2 \bar{w}, \\ \left(\frac{d^2}{dz^2} - a^2\right)\left(\frac{d^2}{dz^2} - a^2 - \frac{s}{\nu}\right)\bar{w} &= \alpha g a^2 \frac{\theta}{\nu},\end{aligned}\tag{20.73}$$

and (20.71) reduces to

$$\underbrace{\left(\frac{d^2}{dz^2} - a^2 - \frac{s}{D_T}\right)}_O \theta = -\frac{\beta}{D_T}\bar{w}.\tag{20.74}$$

Pre-multiplying (20.73) with the operator \mathcal{O} , finally, yields the single sixth order linear ordinary differential equation (ODE)

$$\left(\frac{d^2}{dz^2} - a^2 - \frac{s}{D_T}\right) \left(\frac{d^2}{dz^2} - a^2\right) \left(\frac{d^2}{dz^2} - a^2 - \frac{s}{\nu}\right) \bar{w} = -\frac{a^2 \alpha g \beta}{D_T \nu} \bar{w} \quad (20.75)$$

for \bar{w} . It is seen that the choice (20.72) has led to a single ODE of the sixth order in the variable z .

Introducing the dimensionless variables

$$\begin{aligned} \hat{z} &= \frac{z}{H}, & \frac{d}{d\hat{z}} &= H \frac{d}{dz}, \\ \hat{a} &= Ha, & \hat{s} &= \frac{sH^2}{D_T}, & \hat{w} &= \frac{H}{D_T} \bar{w} \end{aligned} \quad (20.76)$$

transforms (20.75) into

$$\left(\frac{d^2}{d\hat{z}^2} - \hat{a}^2 - \hat{s}\right) \left(\frac{d^2}{d\hat{z}^2} - \hat{a}^2\right) \left(\frac{d^2}{d\hat{z}^2} - \hat{a}^2 - \frac{\hat{s}D_T}{\nu}\right) \hat{w} = -\frac{\hat{a}^2 \alpha H^4 g \beta}{D_T \nu} \hat{w}$$

or

$$\left(\frac{d^2}{d\hat{z}^2} - \hat{a}^2 - \hat{s}\right) \left(\frac{d^2}{d\hat{z}^2} - \hat{a}^2\right) \left(\frac{d^2}{d\hat{z}^2} - \hat{a}^2 - \frac{\hat{s}}{\mathbb{P}r}\right) \hat{w} = -\hat{a}^2 \mathbb{R}a \hat{w}, \quad (20.77)$$

in which

$$\mathbb{P}r = \frac{\nu}{D_T}, \quad \mathbb{R}a = \frac{\alpha H^4 g \beta}{D_T \nu}. \quad (20.78)$$

The RAYLEIGH number contains the applied thermal gradient β and is used as control parameter, to be externally varied by the experimenter. The PRANDTL number is a pure material parameter. **Table 20.2** gives some values. As would be expected (and will be corroborated below), for small values of $\mathbb{R}a$ (=small values of β), the base state is stable, but for large values of β convection (in form of rolls or cells) will occur. The sixth order ODE (20.77) requires six boundary conditions (i.e. three at each boundary), which all must be expressed in terms of \bar{w} , which is difficult in the realistic cases shown in panels a and b of Fig. 20.9. To illustrate the mathematical steps, which must be taken, consider the case of panel c. In this (physically rather unrealistic) case, when both fluid surfaces are open to air, we let the boundary conditions be given by

$$\hat{w} = 0, \quad \frac{d^2 \hat{w}}{d\hat{z}^2} = 0, \quad \frac{d^4 \hat{w}}{d\hat{z}^4} = 0, \quad \text{at } \hat{z} = 0. \quad (20.79)$$

This was the choice, which Lord RAYLEIGH took in 1916 [34]. For a detailed analysis see e.g., S. CHANDRASEKHAR [15]. Because (20.77) and (20.79) contain only even z -derivatives of the function \hat{w} and Eq. (20.77) has constant coefficients

Table 20.2 Approximate values for PRANDTL numbers

Sun	Liquid metals	Gas	Water	Oils	Earth mantle
-8	-2	0	7	2	23

and the boundary conditions (20.79) are repetitive with even derivatives, the function

$$\hat{w} = A \sin(n\pi\hat{z}), \quad n = 1, 2, 3, \dots \tag{20.80}$$

will solve this two-point-boundary-value problem, provided that

$$(-n^2\pi^2 - \hat{a}^2 - \hat{s}) (-n^2\pi^2 - \hat{a}^2) \left(-n^2\pi^2 - \hat{a}^2 - \frac{\hat{s}}{\mathbb{P}r}\right) A = -\hat{a}^2 \mathbb{R}a A, \tag{20.81}$$

valid for any value of the amplitude A . If we introduce the abbreviation

$$\lambda = n^2\pi^2 + \hat{a}^2, \tag{20.82}$$

then (20.81) takes the form

$$(\hat{s} + \lambda) \left(\frac{\hat{s}}{\mathbb{P}r} + \lambda\right) = \frac{\hat{a}^2 \mathbb{R}a}{\lambda}. \tag{20.83}$$

This is a quadratic equation for \hat{s} with the solution

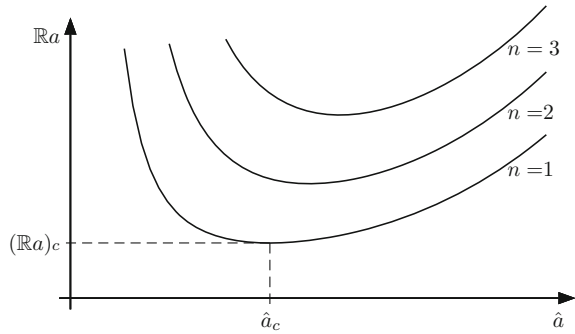
$$\hat{s} = -\frac{\lambda(\mathbb{P}r + 1)}{2} \pm \frac{1}{2} \sqrt{\lambda^2(\mathbb{P}r + 1)^2 + 4\mathbb{P}r \left(\frac{\hat{a}^2 \mathbb{R}a}{\lambda} - \lambda^2\right)}. \tag{20.84}$$

Now, if \hat{s} is real (which we assume) then \hat{s} is positive provided that

$$\frac{\hat{a}^2 \mathbb{R}a}{\lambda} - \lambda^2 > 0 \implies \mathbb{R}a > (\mathbb{R}a)_n(\hat{a}) = \frac{\lambda^3}{\hat{a}^2} = \frac{(n^2\pi^2 + \hat{a}^2)^3}{\hat{a}^2}. \tag{20.85}$$

Interestingly, this result is independent of the PRANDTL number. It corresponds in (20.54) to $f(\mathbb{P}r) = \text{const}$. For $\mathbb{R}a = (\mathbb{R}a)_n$, $\hat{s} = 0$, and there is no growth of \tilde{w} with time. These are conditions of neutral stability. These conditions are plotted in Fig. 20.10. As the RAYLEIGH number increases from a value below $(\mathbb{R}a)_c$ the base state (no convection, fluid at rest) first becomes unstable at $\mathbb{R}a = (\mathbb{R}a)_c$ to a convective state, described by the eigenmode with mode number $n = 1$ in the vertical direction and \hat{a}_c . $(\mathbb{R}a)_c$ and \hat{a}_c are found by minimizing $(\mathbb{R}a)_1(\hat{a})$ with respect to \hat{a} . The result is

Fig. 20.10 Curves of neutral stability for $\mathbb{R}a$ against \hat{a} for $n = 1, 2, 3$



$$\hat{a}_c^2 = \frac{\pi^2}{2}, \quad (\mathbb{R}a)_c = \frac{\left(\pi^2 + \frac{\pi^2}{2}\right)^3}{\left(\frac{\pi^2}{2}\right)} = \frac{27}{4}\pi^4 = 657.5. \quad (20.86)$$

This is the most unstable mode. Its distribution in the z -direction is $\hat{w} = \sin(\pi z)$, and the variation of this mode in the (x, y) -plane is given by Eq. (20.72), or

$$\nabla_H^2 f + a_c^2 f = 0. \quad (20.87)$$

This equation has many possible solutions, all of the same energy level. The simplest of these has no y -dependence and is given by

$$f(x, y) = \cos\left(\frac{2\pi x}{\hat{L}_x}\right), \quad \text{where } \frac{4\pi^2}{\hat{L}_x^2} = \hat{a}_c^2, \quad (20.88)$$

which yields with (20.85) $\hat{L}_x = \sqrt{8}$. These roll waves have their axes parallel to the y -axis and are periodic in the x -direction with period as shown in Fig. 20.11.

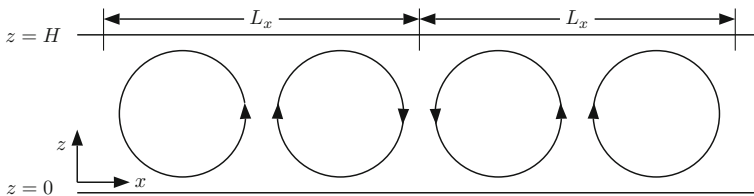


Fig. 20.11 Roll wave solution of the most unstable RAYLEIGH-BÉNARD problem with free-free boundaries

20.3 Theory of Physical Models

In this section we will be concerned with the rules of building physical models. We first will present a set of propositions which provide guidelines, which ought to be observed, if downscaling of physical processes to smaller scales will lead to results of model experiments which optimally mimic corresponding processes at the prototype scale. In a second subsection it will be shown, how differential equations derived for certain processes can help in the interpretation of the complexity of processes for which they have been designed. We follow in parts HUTTER and JÖHNK [20] and HUTTER et al. [21].

20.3.1 Analysis of the Downscaling of Physical Processes

In model theory one differentiates between *geometrically similar* and *geometrically distorted* models. If practically possible, models are constructed in geometrically similar reduction; such models are obtained, if all three space directions are reduced by the same scale. *Distorted* models are obtained if this is not the case; frequent cases are super-elevated models; this is almost always necessary in hydraulics, physical oceanography and physical limnology, when the water depths in the model become so small that effects of surface tension can be recognized and then would influence the model processes, whilst this is not so at the prototype size.

We quote from [20]. “Generally, there exists a point to point correlation between the *model* and the *prototype*. In geometrical language, corresponding points between model and Nature (prototype) are called *homologous points*. A set of homologous points will lead to homologous regions and domains. If time dependent processes are analyzed, one must introduce the notion of homologous times. To this end NEWTON’s second law is used; accordingly, differences of times are declared as homologous, if a material point on homologous trajectories passes two homologous points at homologous times. Analogously, one can speak of homologous distributions of mass, velocities, moments of inertia, etc. When constructing models it is, however, not necessary that all the homologies are preserved. One may restrict oneself to those which have an influence on the physical quantity under study. This, for instance, is so for an airplane wing of which the drag force is sought; it is not needed for its determination to reproduce a homologous distribution of mass, however, this is necessary if one wishes to determine the yield stress of the wing or its behavior in flow induced vibrations, etc.

Before a problem is subjected to a model study, it is advantageous to first contemplate about which variables might have an influence upon the processes to be studied. Via a dimensional analysis one thus determines the number of dimensionless products, which correspond to the chosen variables. If Π_d denotes the dependent dimensionless variable and Π_1, \dots, Π_p the independent dimensionless products, then

$$\Pi_d = f(\Pi_1, \dots, \Pi_p) \quad (20.89)$$

gives the physical variable to be analyzed as a function of all dimensionless variables Π_1, \dots, Π_p .

If a model has to correctly reproduce the processes arising in the prototype, then the values of Π_1, \dots, Π_p are not allowed to change when going from the prototype conditions to those of the model: for only then the function $f(\Pi_1, \dots, \Pi_p)$ for Π_1, \dots, Π_p will deliver the same result for the dependent variable. If such conditions are satisfied, the model is called *completely similar*. Therefore:

Proposition 20.1 *A model is capable to reproduce a process in Nature with complete similarity, if all the dimensionless products which describe the process, have the same values in the model as well as in Nature.* ■

Even though this theorem embraces the entire content of *model similarity*, it contains a club-foot, it namely supposes that the engineer or physicist recognizes all variables which describe a physical process. This need not be the case, if the insight into the physical problem is incomplete. Conversely, it may occasionally not be possible to map a process in Nature completely similarly to the model, because one does not always succeed to reproduce a process in Nature at small scale and thereby preserve all values of the Π -products in the [above proposition]. With utmost rigor this is in fact [virtually] never possible as we shall shortly see. Physical processes in Nature and in the model can completely similarly be mapped into one another at least mathematically, if all Π -products that describe the processes remain invariant in the mapping from Nature to model. This is only successful in a rear number of cases; one is regularly forced to hold only a reduced number of Π -products invariant when performing the mapping from the prototype to the model and to let the remaining Π -products vary as dictated by the laws of the mapping. In these circumstances it is hoped, and often this can also be demonstrated, that the Π -products which do not remain invariant in the mapping will not, or at least not much, influence the physical processes that are studied. If they nevertheless should do this, then one speaks in such cases of *scale effects*. If a process depends only on Π -products which all remain invariant in a model mapping, then this process is called *scale invariant*", [20].

Early in this chapter the drag force exerted on the hull of a ship was determined and it was made clear that the dimensionless drag coefficient is a function of the FROUDE and REYNOLDS numbers,

$$C_D = C_D(\text{Fr}, \text{Re}) \quad \text{with } \text{Fr} = \frac{V^2}{gL}, \quad \text{Re} = \frac{VL}{\nu}, \quad (20.90)$$

in which V, L, g, ν are the velocity of the ship, a characteristic length, the gravity constant and the kinematic viscosity of the water. How can this drag coefficient be determined by use of a scaled model?

Let overbarred quantities denote physical quantities in the model; then, *invariance of the FROUDE number in the mapping from the prototype to the model requires*

$$\frac{V^2}{gL} = \frac{\bar{V}^2}{\bar{g}\bar{L}} \quad \longrightarrow \quad \lambda_V = \frac{\bar{V}}{V} = \sqrt{\frac{\bar{L}}{L}} \sqrt{\frac{\bar{g}}{g}} = \sqrt{\lambda_L \lambda_g}. \quad (20.91)$$

Here, we have introduced length-, gravity- and velocity scales,

$$\lambda_L := \frac{\bar{L}}{L}, \quad \lambda_g := \frac{\bar{g}}{g}, \quad \lambda_V := \frac{\bar{V}}{V}. \quad (20.92)$$

Thus, FROUDE number invariance has led to the relation

$$\lambda_V = \sqrt{\lambda_L \lambda_g}. \quad (20.93)$$

λ_L is the scale of length of the geometrically similar model; its gravity is reduced by the gravity scale λ_g and in FROUDE similitude the scale for velocity then follows the rule (20.93); it is no longer freely assignable. With the dimensional equation $[T] = [L/V]$ also the scale for time is deducible

$$\lambda_T = \frac{\bar{T}}{T} = \frac{\bar{L}}{\bar{V}} \frac{V}{L} = \frac{\bar{L}}{L} \frac{V}{\bar{V}} = \lambda_L \frac{1}{\lambda_V} = \sqrt{\frac{\lambda_L}{\lambda_g}} \quad (20.94)$$

as is the acceleration scale

$$\lambda_A = \frac{\bar{A}}{A} = \frac{\bar{V}}{V} \frac{T}{\bar{T}} = \lambda_V \frac{1}{\lambda_T} = \sqrt{\lambda_L \lambda_g} \sqrt{\frac{\lambda_g}{\lambda_L}} = \lambda_g. \quad (20.95)$$

For most situations on the planet Earth the gravity constant may be regarded as constant ($\lambda_g = 1$), or else artificial measures need be taken (experiments under microgravity, on a centrifuge).

For invariance of the REYNOLDS number one must have

$$\frac{VL}{\nu} = \frac{\bar{V}\bar{L}}{\bar{\nu}} \quad \longrightarrow \quad \lambda_V = \frac{\bar{V}}{V} = \frac{L}{\bar{L}} \frac{\bar{\nu}}{\nu} = \frac{1}{\lambda_L} \lambda_\nu, \quad (20.96)$$

where the viscosity scale is defined as

$$\lambda_\nu := \frac{\bar{\nu}}{\nu}. \quad (20.97)$$

Thus, the velocity scale is given here by

$$\lambda_V := \frac{\lambda_\nu}{\lambda_L}, \quad (20.98)$$

which is the ratio of the viscosity scale divided by the length scale; time and acceleration scales are here given by

$$\begin{aligned} \lambda_T &= \frac{\bar{T}}{T} = \frac{\bar{L}}{L} \frac{V}{\bar{V}} = \lambda_L \frac{1}{\lambda_V} = \frac{\lambda_L^2}{\lambda_\nu}, \\ \lambda_A &= \frac{\bar{A}}{A} = \frac{\bar{V}}{V} \frac{T}{\bar{T}} = \lambda_V \frac{1}{\lambda_T} = \frac{\lambda_V}{\lambda_L} \frac{\lambda_\nu}{\lambda_L^2} = \frac{\lambda_\nu}{\lambda_L^3}. \end{aligned} \tag{20.99}$$

These transformations are summarized in **Table 20.3**.

Models for which the FROUDE (REYNOLDS) number is a scale invariant are called FROUDE (REYNOLDS) models; analogously, the corresponding similarity property is called FROUDE (REYNOLDS) similitude. Complete similarity for (20.90) requires that $\mathbb{F}r$ and $\mathbb{R}e$ are simultaneous mapping invariants. This requires additionally that the velocity scales are the same, namely

$$\sqrt{\lambda_L \lambda_g} = \frac{\lambda_\nu}{\lambda_L} \quad \longrightarrow \quad \lambda_\nu^2 = \lambda_L^3 \lambda_g. \tag{20.100}$$

It is easy to verify with the aid of Table 20.3 that also time and acceleration scales are the same in this case. However, it is very unlikely that this can practically be achieved. Indeed, with $\lambda_g = 1$ relation (20.100) requires that $\lambda_\nu = \lambda_L^{3/2}$. The viscosity scale must be the $\frac{3}{2}$ -power of the length scale; experiments would, thus have to be conducted with a fluid whose viscosity would have to be adjusted to the length scale. “For FROUDE similitude and when $\lambda_g = 1$ homologous velocities and time differences are scaled by the square root of the length scale, whilst the acceleration remains the same. By contrast, when REYNOLDS similitude is implemented with $\lambda_\nu = 1$, homologous velocities in the model are larger than in the prototype by the factor of λ_L^{-1} . Homologous time differences are shortened by the square of the length scale and accelerations are enlarged by the third power of the inverse length scale”, [20].

“To develop the general theory, let us embed Nature and model in EUCLIDian spaces with Cartesian coordinates (x, y, z) and $(\bar{x}, \bar{y}, \bar{z})$, respectively. Homologous

Table 20.3 Rules of transformations for FROUDE and REYNOLDS similitude if the length scale is λ_L , the gravity scale λ_g and the viscosity scale λ_ν

	FROUDE similitude	REYNOLDS similitude
Length	λ_L	λ_L
Velocity	$\sqrt{\lambda_L \lambda_g}$	$\frac{\lambda_\nu}{\lambda_L}$
Time	$\sqrt{\frac{\lambda_L}{\lambda_g}}$	$\frac{\lambda_L^2}{\lambda_\nu}$
Acceleration	λ_g	$\frac{\lambda_\nu^2}{\lambda_L^3}$

points and homologous times are then given by

$$\bar{x} = \lambda_x x, \quad \bar{y} = \lambda_y y, \quad \bar{z} = \lambda_z z, \quad \bar{t} = \lambda_t t. \quad (20.101)$$

$\lambda_x, \lambda_y, \lambda_z$ are the scale factors in the spatial directions x, y, z and λ_t is that for time t . For $\lambda_x = \lambda_y = \lambda_z$ the model is geometrically similar, else, the model is distorted. λ_t can be chosen as the ratio of the times that elapse when a material point traces the distance between two homologous points in the model and prototype, respectively. If $f(x, y, z, t)$ and $f(\bar{x}, \bar{y}, \bar{z}, \bar{t})$ describe a physical process in Nature and in the model, respectively, then the principal expression of similarity is:

Definition 20.3 The function f is called similar to the function \bar{f} , if the ratio \bar{f}/f remains unchanged when for the arguments (x, y, z, t) and $(\bar{x}, \bar{y}, \bar{z}, \bar{t})$ homologous points and times are chosen. The ratio $\bar{f}/f = \lambda_f$ is called the scale of f . ■

In the following we shall discuss the various rules of similitude. Important are the notions of *kinematic* and *dynamic* similitude.

Definition 20.4 Two systems are called **kinematically similar**, if their motions are similar, i.e., if homologous particles are to be found at homologous times in homologous points. ■

If kinematic similarity prevails, then corresponding velocities and accelerations are similar. The scale factors are easily computable from

$$\bar{u} = \frac{d\bar{x}}{d\bar{t}}, \quad \bar{v} = \frac{d\bar{y}}{d\bar{t}}, \quad \bar{w} = \frac{d\bar{z}}{d\bar{t}}. \quad (20.102)$$

Since $d\bar{x} = \lambda_x dx, \dots, d\bar{t} = \lambda_t dt$ one obtains

$$\bar{u} = \frac{\lambda_x dx}{\lambda_t dt} = \frac{\lambda_x}{\lambda_t} u, \quad \bar{v} = \frac{\lambda_y}{\lambda_t} v, \quad \bar{w} = \frac{\lambda_z}{\lambda_t} w. \quad (20.103)$$

The scale factors for the *velocities* are therefore

$$\lambda_u = \frac{\lambda_x}{\lambda_t}, \quad \lambda_v = \frac{\lambda_y}{\lambda_t}, \quad \lambda_w = \frac{\lambda_z}{\lambda_t}, \quad (20.104)$$

and for the *accelerations* one obtains in an analogous manner

$$\lambda_{a_x} = \frac{\lambda_x}{\lambda_t^2}, \quad \lambda_{a_y} = \frac{\lambda_y}{\lambda_t^2}, \quad \lambda_{a_z} = \frac{\lambda_z}{\lambda_t^2}. \quad (20.105)$$

This should show how scales for homologous quantities are computed. This brings us now to the

Definition 20.5 Two systems are called **dynamically similar** if homologous parts are subject to similar forces, i.e., if the force scale is invariant. ■

Basis for this definition is NEWTON’s second law. So, with similar distributions of masses according to $\bar{m} = \lambda_m m$ there follows from NEWTON’s law

$$\bar{F}_x = \bar{m}\bar{a}_x, \quad \bar{F}_y = \bar{m}\bar{a}_y, \quad \bar{F}_z = \bar{m}\bar{a}_z, \tag{20.106}$$

or

$$\frac{\bar{F}_x}{F_x} = \frac{\bar{m}\bar{a}_x}{ma_x} = \lambda_m \frac{\lambda_x}{\lambda_t^2}, \dots \tag{20.107}$$

In NEWTONian mechanics the scale factors for the forces are thus given by

$$\lambda_{F_x} = \lambda_m \frac{\lambda_x}{\lambda_t^2}, \quad \lambda_{F_y} = \lambda_m \frac{\lambda_y}{\lambda_t^2}, \quad \lambda_{F_z} = \lambda_m \frac{\lambda_z}{\lambda_t^2}. \tag{20.108}$$

The scales for the velocities and accelerations are not freely assignable, but must be computed from the scale factors of geometry and time. Analogously, for dynamic similitude the scale factor for the forces is obtained automatically from the scale factors for length, time and mass.

It has already been said that in a model experiment of a fluid mechanical problem the FROUDE and REYNOLDS numbers cannot simultaneously be held invariant. Thus, we ask for a rule, which will allow us to select which of the two numbers should be kept invariant in a particular situation to reach at least approximate similitude. This decision is facilitated, if one asks whether the gravity force has a decisive influence on the flow processes. The acceleration of the Earth arises namely only in the definition of the FROUDE number. If in a hydrodynamic problem the bounding walls are rigid and prescribed as is e.g. the case for pipe flow that is driven by pumps, then the piezometric pressure $P = p + \rho g z$ as a whole is the unknown quantity (and not p and $\rho g z$ individually). Gravity does not arise as an independent variable in this case; it follows that pipe flow is governed by REYNOLDS similitude. On the other hand, if the fluid is bounded by a free surface, then the variable z in the piezometric pressure is an unknown and gravity will affect the flow field. If, in addition surface tension is active to the extent that its effect is recognizable, then besides the FROUDE and REYNOLDS numbers also the WEBER number will affect the similarity. We thus have the following:

Rule: For dynamical ‘similitude’ of flows of density preserving fluids it is sufficient in a model reproduction that

- in regions with **fixed boundaries** and geometrically similar boundary values the REYNOLDS number is kept invariant, whilst
- in regions with **free boundaries** and geometrically similar boundary values the REYNOLDS, FROUDE and (possibly) WEBER numbers must be the same.

Now, we have already seen, when discussing the drag force on a ship, that simultaneous satisfaction of the invariance of the FROUDE and REYNOLDS numbers is not possible. If one therefore imputes FROUDE similitude, then the REYNOLDS number will assume a different value in the model than in Nature. However, if the quantities to be measured should not depend upon the REYNOLDS number (or at least not in observable magnitude), then FROUDE similitude is applicable without special precaution. Else, i.e. when both FROUDE and REYNOLDS effects are of comparable importance, scale effects will arise with which one may cope as follows: One must at least build two FROUDE models with differing scales; with these, identical experiments are performed, each associated with its own REYNOLDS number. With interpolation/extrapolation (linear in this case) one can find in this way functional dependences of any measured quantity upon the REYNOLDS number. This principle, naturally, can also be applied when models with several scales are applied for non-linear interpolation, or when several Π -products arise, [20]. Because construction of laboratory models is generally costly, one is often forced to dispense with the construction of models at two (or more) different scales.

20.3.2 Applications

Example 20.10 Sediment Transport in a Shallow Lake

Consider sediment transport in a very shallow lake or in a lagoon. Depending on the strength of the circulation due to wind, the primary horizontal current might erode grains from the lake bottom and, thus, generate a variable load of suspended sediments in the lake water. It is rather intuitive that the erosion inception of the sediment in the bed will likely depend on the shear traction exerted on the lake side of the basal surface τ_c , the true densities ρ_s and ρ_f , of the sediment grains and the fluid, and the concentration c_s , gravity constant g , fluid viscosity ν , and the nominal diameter of the sediment grains \mathfrak{d} . So, inception of sediment transport can likely be described by an equation

$$f(\tau_c, \rho_s, \rho_f, g, \mathfrak{d}, \nu, c_s) = 0 \tag{20.109}$$

evaluated at the bed surface. We shall employ the identifications $y = \tau_c, x_{1-6} = (\rho_s, \rho_f, g, \mathfrak{d}, \nu, c_s)$. Exclusive c_s , which is already dimensionless, the dimensional matrix of the variables (20.109) is given by

	τ_c	ρ_s	ρ_f	g	\mathfrak{d}	ν	
M	1	1	1	0	0	0	
L	-1	-3	-3	1	1	2	
T	-2	0	0	-2	0	-1	

$\det |\cdot| \neq 0$



Fig. 20.12 ALBERT FRANK SHIELDS (26. June 1908–1. July 1974)

ALBERT FRANK SHIELDS, was born in Cleveland, Ohio. Following graduation from high school, he worked for 1 year to earn money to support his further education. In 1927 he enrolled at Cornell University [Ithaca, N.Y.] and remained there for two semesters before transferring to Stevens Institute of Technology [Hoboken, New Jersey], where he obtained his bachelor's and master's degrees, both in mechanical engineering, in 1931 and 1933, respectively [23]. In 1933, he received a fellowship of the German Academic Exchange Service of the Technical University (TH) Berlin. His plans included pursuit of research at the Prussian research Institute for Hydraulic Engineering and Shipbuilding (PRI, Director: Prof R. SEIFERT) that would serve as the basis for his dissertation, which would be submitted to TH Berlin for the degree of Doctor of engineering [23].

KENNEDY reports in his *'The Albert Shields Story'* [23] that SHIELDS could not pursue a thesis on his favored subjects, which he had been dealt with in his master's degree. 'The only available research assignment that would not entail some expenses that SHIELDS would have to bear, was concerned with sediment transport by river flow, and in particular bed-load transport, which he took up. The fortunate circumstance was that two earlier phases of the PRI bed-load investigation had been conducted by two other American Freeman scholars, HANS KRAMER (1894–1957) and HUGH J. CASEY (1898–1981) with their Ph. Dissertations, [16, 24, 25]. Unfortunately, the American master's degree was not recognized as equivalent to the German Diploma, preventing pursuing the doctoral degree. According to [23], the PRI director, Professor SEIFERT, reluctantly allowed SHIELDS to discontinue his research in order to work toward his Diploma.

His missing 'Diplomarbeit' (master's thesis) was done under the famous professor H. FÖT-TINGER (1877–1945) and consisted of truly original work done under the supervision of Dr. WEINIG [50]. However, SHIELDS needed to find a job to support his further research, which he only found in the French Saarland region; furthermore, he missed to obtain professor SEIFERT's permission. The result was that professor SEIFERT forbade him access to PRI. Fortunately, after enough agony and humiliating apologies, see [23], the thesis could be completed; the exam took place on May 30 1936 and the candidate passed with the score 'gut bestanden' ($\sim B^-$), for SHIELDS a disappointingly low grade.

SHIELDS took after his degree quite some efforts in Europe and the US to find employment in sediment transport, but had no luck. He found in 1937 a full time job with the S&S Corrugated Paper Machinery Co. Inc., of Brooklyn, N. Y. He remained with this company until retirement in 1973 and never returned to sediment transport research.

The text is based on www.wikipedia.org

and possesses the rank 3 and, therefore, gives rise to three independent dimensionless products, e.g., together with $\Pi_4 := c_s$, we, thus, have

$$\Pi_1 = \frac{\tau_c}{\bar{\rho} g \vartheta}, \quad \Pi_2 = \frac{\rho_s}{\rho_f}, \quad \Pi_3 = \frac{(g\nu)^{1/3} \vartheta}{\nu}, \quad \Pi_4 = c_s. \quad (20.110)$$

$\bar{\rho}$ may be a linear combination of ρ_s and ρ_f ; in fact, since the detritus layer is submerged in the lake water, the proper density for the definition of Π_1 is $\bar{\rho} = \rho_s - \rho_f$. Moreover, since $(g\nu)^{1/3}$ has the dimension of a velocity, Π_3 may be interpreted as a particle REYNOLDS number. When written as $\Pi_3 = (g/\nu^2)^{1/3} \vartheta$, the prefactor of ϑ has the dimension of an inverse length. With this identification Π_3 allows the interpretation of a dimensionless particle diameter ϑ^* . In the sediment transport literature Π_1 and Π_3 are used in the forms

$$\Pi_1^* = \frac{\tau_c}{(\rho_s - \rho) g \vartheta} = \frac{\tau_c}{\Delta \rho g \vartheta}, \quad \Pi_3^* = \left(\frac{g}{\Delta \nu^2} \right)^{1/3} \vartheta, \quad \Delta \equiv \left(\frac{\rho_s}{\rho} - 1 \right), \quad (20.111)$$

where ρ is the mixture density. It is not difficult to see that for small mass fractions, c_s , the mixture density may approximately be replaced by ρ_f . We may now write

$$f(\Pi_1^*, \Pi_2, \Pi_3^*, \Pi_4) = 0 \quad \text{or} \quad \frac{\tau_c}{\Delta \rho g \vartheta} = \tilde{f}(\Pi_2, \Pi_3^*, \Pi_4). \quad (20.112)$$

The number of variables is now reduced from 7 to 4. However, even further reduction is possible. For sediment transport in the geophysical environment Π_2 is very nearly a constant on the entire Globe ($\sim 2700/1000 = 2.7$), and Π_4 is very small ($\leq 10^{-2}$); so, the Π_4 -dependence may be dropped. Thus, we may write

$$\theta_c \equiv \frac{\tau_c}{\Delta \rho g \vartheta} = \hat{f}(\Pi_3^*) = \hat{f}(Re^*) = \hat{f}(\vartheta^*). \quad (20.113)$$

θ_c is called (critical) SHIELDS¹⁰ parameter (1936) [38] and represents the dimensionless shear stress at which value the detritus bed, consisting of particles with diameter ϑ starts to erode. Had we omitted the fluid viscosity ν in the variable set, Π_3^* (or Π_3) cannot be defined, and \hat{f} in (20.113) is necessarily constant in this case, so that

¹⁰For a brief biography of ALBERT FRANK SHIELDS, see **Fig. 20.12**.

$$\tau_c = \text{const.} \times \Delta \rho g \bar{d}. \quad (20.114)$$

The experimenter's burden would simply be to determine this constant. The experimental facts are, however, such that (20.114) is not correct. It follows, inclusion of ν as a parameter in the list (20.109) is vital. Not including the Earth's acceleration, g is disastrous as it eliminates Π_1^* and Π_3^* , reducing (20.112)₁ to $f(\Pi_2, \Pi_4) = 0$, a meaningless expression, not able to describe erosion inception.

The result (20.113) does not say that this equation indeed describes the correct dependence of the SHIELDS parameter as a function of Re^* or \bar{d}^* . It only states that θ_c is a function of $Re^* = \bar{d}^*$, if the original variables are chosen as given in (20.109) as the basic variables describing erosion inception. The proof that (20.109) is a correct functional relation for sediment transport inception must come from experiments which will determine $\hat{f}(Re^*)$. This has been done in numerous laboratory experiments and involves the most prominent hydraulic engineers. Explicit formulae, which have been validated by experiments, are summarized in [21], pp. 542 ff.

The identification of the function $\hat{f}(Re^*)$ in formula (20.113) is the major achievement of experimental sediment transport research that is still going on. DAVID VETSCH [48] provides in Chap. 2 of his dissertation a detailed review of the literature up to 2012. He restricts consideration to bed local transport in alluvial gravel-bed rivers with particle grain sizes from sand ($0.062 < \bar{d} < 2$ mm), over gravel to ($2 < \bar{d} < 60$ mm) to stones and small rock. Finer sediment in suspension—termed *wash load*—are not considered as neither are exchange processes from suspended to bed-load fractions and vice versa. ‘The definition of the point of inception [of the sediment motion] is not clear and varies considerably among the various studies. This means that in practical cases of turbulent flow there is no single criterion for the beginning of movement of sediment. BUFFINGTON and MONTGOMERY (1997) [11] give an extensive review on the issue. There is also a large data collection available by BROWNLIE (1985) [9] and BROWNLIE and BROOKS (1981) [10]’, [48].

The criterion for incipient motion is usually determined by threshold quantities such as a critical shear stress, a critical shear velocity or critical lifting force. It is expressed as a separation line in a log-log plot of the critical SHIELDS parameter θ_c (a dimensionless critical shear stress) against the dimensionless particle diameter $\bar{d} \equiv Re^*$. **Figure 20.13**, a copy of Fig. 2.2 from David Vetsch's Ph.D dissertation [48], collects experimental results of a number of authors stated in the inset of the figure. They are identified by distinct symbols and colors. The following statements may emerge from a scrutiny of the figure:

- The spread of the data suggests that the transition from non-moving to moving bed load is not a sharp separation, but seems to occur in a regime of a certain band width.
- Data taken by SHIELDS (1936) are restricted to the regime $6 < Re^* < 700$; similarly, data of MEYER-PETER-MÜLLER (1948) have been collected for $60 < Re^* < 220$. BATHURST et al.'s data of 1987 are restricted to the large Re^* -regime for $900 < Re^* < 9000$. According to VETSCH [48] ‘BATHURST et al. [2] studied the threshold condition for steep mountain streams. To point out the sensitivity of

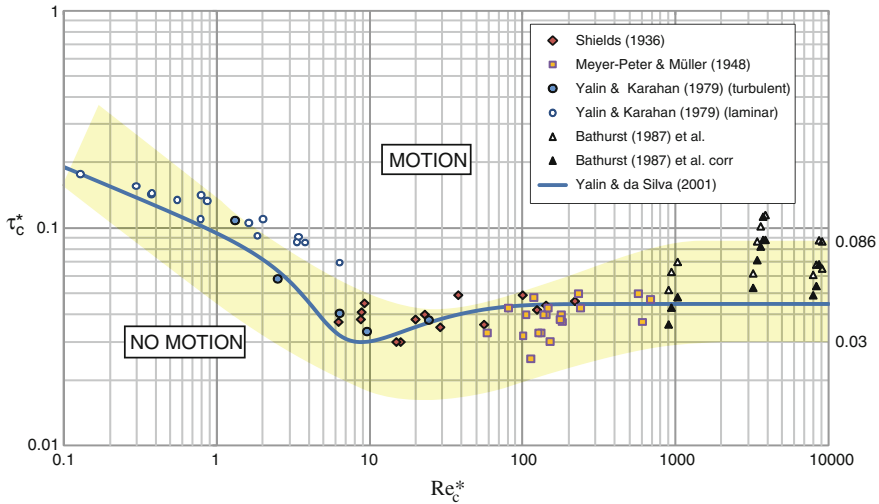


Fig. 20.13 Selected experimental results of incipient motion characterizing the transition from no (sediment) motion to motion. A facsimile copy of the SHIELDS diagram from the latter dissertation and the dissertation front page are shown by KENNEDY in [23]. The colorized area covers the data collected by Buffington and Montgomery (1997) [11]. The data are taken from [2, 28, 38, 51, 52]. Courtesy D. VETSCH © Versuchsanstalt für Wasserbau, Hydrologie und Glaziologie an der ETH Zurich, reproduced with permission

the approach for the calculation of the dimensionless shear stress [the value of the SHIELDS parameter] the results of the latter are drawn in Fig. 20.13 based on the formula [open triangles] and according to that of SHIELDS (denoted as BATHURST (1987) corr.’ [filled triangles].

- ‘Investigation into fine sediments such as sand and silt cover the left part of the SHIELDS diagram for $0.1 < Re^* < 10$ (open and filled triangles in Fig. 20.13). YALIN and KARNAHAN (1979) [51] extended the SHIELDS diagram based on measurements with focus on viscous dominated flow conditions, and they carried out flume experiments with a glycerin-water mixture to obtain laminar flow and with water for turbulent flow’, [48].

For numerical models, expressions by VAN RIJN [45, 46] are frequently used to calculate the critical shear stress to which a single formula has been developed.

The solid blue curve in Fig. 20.13 is an approximate mathematical proposition to this by YALIN and DA SILVA (2001) [52] and can be expressed as

$$\tau_c = 0.13(D^*)^{-0.392} \exp(-0.015(D^*)^2) + 0.045(1 - \exp(-0.068)D^*), \tag{20.115}$$

where

$$D^* = \mathfrak{d} \left(\frac{\Delta \rho g}{\rho_f \nu^2} \right)^{1/3}. \tag{20.116}$$

Example 20.11 Heat Transfer by Forced Convection

Consider a rigid body (say a sphere or a cylinder or any other body) with nominal diameter D immersed in a moving fluid and kept at rest. [As an example one may think of hot wire anemometry to measure the velocity of the fluid.] Let the velocity sufficiently distant from the body, subject to free stream be V . The transfer of heat from the body to the fluid may depend on the density ρ , kinematic viscosity ν , specific heat c , on the conductivity of heat of the fluid κ and the temperature difference ΔT between the body and the fluid distant from it. Of practical interest here is the amount of heat transferred from the body to the water, expressed as power of working P , that has to be prescribed by the body. For a sphere this may be written to be proportional to the area of the section crossed by the fluid πD^2 , and the temperature difference ΔT ,

$$P = \alpha \pi D^2 \Delta T, \tag{20.117}$$

where α is the heat transfer coefficient with dimension $[MT^{-3}K^{-1}]$. We shall now seek a functional dependence of α on Π -products. The dimensional matrix of the physical variables introduced above is given by

	α	V	ΔT	D	ρ	ν	c	κ	
M	1	0	0	0	1	0	0	1	
L	0	1	0	1	-3	2	2	1	det $ \cdot \neq 0$.
T	-3	-1	0	0	0	-1	-2	-3	
K	-1	0	1	0	0	0	-1	-1	

Its rank is 4, since the determinant of the indicated 4×4 submatrix does not vanish; thus, there are 4 independent Π -products, which may be selected as follows:

$$\begin{aligned} \mathbb{N} &\equiv \frac{\alpha D}{\kappa} && \text{NUSSELT number,} \\ \mathbb{R}e &\equiv \frac{V D}{\nu} && \text{REYNOLDS number,} \\ \mathbb{P}r &\equiv \frac{\nu}{\nu} && \text{PRANDTL number,} \\ \mathbb{B}r &\equiv \frac{\rho \nu V^2}{\kappa \Delta T} && \text{BRINKMANN number,} \end{aligned}$$

so that $\mathbb{N} = f(\mathbb{R}e, \mathbb{P}r, \mathbb{B}r)$ or, if the fluid in the model is the same as in Nature,

$$\mathbb{N} = f(\mathbb{R}e, \mathbb{B}r) \quad \longrightarrow \quad \alpha = \frac{\kappa}{D} f(\mathbb{R}e, \mathbb{B}r). \tag{20.118}$$

This equation tells us, first, that the heat transfer coefficient depends, apart from κD^{-1} , on the REYNOLDS and BRINKMANN numbers, of which a first proposal could be a power law representation

$$\alpha = c \frac{\kappa}{D} \mathbb{R}e^\beta \mathbb{B}r^\gamma. \tag{20.119}$$

Second, request of invariance of the BRINKMANN number in a downscaling from Nature to the model yields

$$\lambda_{\Delta T} = \frac{\Delta \bar{T}}{\Delta T} = \frac{\bar{V}^2}{V^2} = \lambda_V^2 \stackrel{\text{REYNOLDS}}{=} \lambda_L^{-2}, \tag{20.120}$$

provided the same fluid is used in model and prototype and REYNOLDS similitude is employed. However, this result is disappointing because it tells us that for $\lambda_L = 10^{-1}$ the temperature scale must be $\lambda_{\Delta T} = 10^2$; temperature differences in the model would have to be a factor of 100 times larger than in Nature, if heat transport in the model obeys REYNOLDS similitude. Fortunately, in hot-wire anemometry α depends only weakly on $\mathbb{R}e$, since the flow around the sphere is turbulent; so, in a first approximation its $\mathbb{R}e$ -dependence may be dropped in (20.119) [$\beta = 0$]. Under those circumstances $\lambda_{\Delta T}$ may be chosen independently of λ_L ; so, (20.120) does not apply in this case.

A different but nevertheless related situation of heat convection prevails, when e.g. heated water from a tributary enters a main river or a lake at its river mouth. When the spreading of the heat, discharged by the tributary into the lake in the vicinity of the river mouth is modeled by laboratory experiments, the existence of the free water surface gives rise to the addition in the dimensional matrix of the acceleration due to gravity, g . This implies that $\mathbb{N} = f(\mathbb{F}r, \mathbb{R}e, \mathbb{P}r, \mathbb{B}r)$. Dependences on the REYNOLDS and PRANDTL numbers will be ignored as above, so that $\mathbb{N} \approx f(\mathbb{F}r, \mathbb{B}r)$. Maintaining FROUDE and BRINKMANN numbers invariant now yields

$$\lambda_{\Delta T} = \lambda_V^2 \stackrel{\text{FROUDE}}{=} \lambda_L. \tag{20.121}$$

This result is as disappointing as (20.120), because temperature differences between a tributary and a lake are at most $\sim 10^\circ\text{C}$, implying that for $\lambda_L = 10^{-2}$ these differences would have to be no larger than 0.1°C in the model. This would require sensibly acclimatized laboratories, even at less severe downscaling.

20.4 Model Theory and Differential Equations

In this section the position is taken that the differential equations, which are written down to describe a certain class of physical processes, have been tested, so that their appropriateness in describing the physical processes under consideration is without

any doubt.¹¹ Under such prerequisites, these equations and associated boundary conditions are obviously dimensionally homogeneous, but, additionally, when written in dimensionless form, disclose the Π -products, which describe the physical content of the equations. In this form, since the equations are by assumption describing a certain class of processes, they provide, via the identifiable Π -products, a possibility to judge the adequacy of the down-scaling of certain processes described by them.

20.4.1 *Avalanching Motions down Curved and Inclined Surfaces*

Interesting cases, in which the governing differential equations and boundary conditions offer insight into the physics of the fluid mechanical processes, are the depth integrated balance equations of mass and momentum in the shallow flow approximation as derived in Chap. 13 “Shallow rapid granular avalanches”. In the formulation of SAVAGE–HUTTER the relevant equations are (13.106)–(13.111) with earth pressure coefficients as listed in (13.97) and (13.98). These equations contain two dimensionless constitutive parameters, the angle of internal friction, ϕ , and the bed friction angle, δ , and two geometric parameters, ε , and λ , measures for the shallowness and downhill curvature of the avalanching mass. For a model topography, geometrically similar to the prototype, it is likely that these typical measures will not change in the down scaling.¹² If this assumption is correct, which shall now be assumed, then the above stated equations contain no other Π -products than the angles of internal friction, ϕ , and the basal friction angle, δ . This makes downscaling of a granular avalanche flow particularly simple. For geometrically similar basal topographies of the prototype and the model it suffices to perform experiments with laboratory sand and bed surface roughness, which agree with that of the prototype. This may be the reason, why laboratory avalanche models have been so successful, [33].

If the resistive frictional force also contains a viscous contribution proportional to the velocity or to the velocity squared, this (restricted) scale invariance is not preserved.

20.4.2 *Navier–Stokes–Fourier–Fick Equations*

In fluid engineering and geophysical fluid mechanics the Navier–Stokes–Fourier–Fick (NSFF) equations (or their extensions under turbulence—the REYNOLDS equations) are the most important equations, which are able to describe a large class of fluid motions in this field.

¹¹ See also footnote 4, this chapter in Sect. 20.1.3 on p. 591, in which this method is referred to as ‘inspectional analysis’.

¹² This assumption is often simply implemented by taking the SH-equations with $\varepsilon = 1$ and $\lambda = 1$.

These equations emerge from the application of the balance laws of mass, momentum, energy for these mixtures of water or air and a number of tracer substances suspended in the fluid or gas. The equations read

$$\begin{aligned}
 \frac{\partial \rho}{\partial t} + \operatorname{div}(\rho \mathbf{v}) &= 0, \\
 \rho \left\{ \frac{\partial \mathbf{v}}{\partial t} + (\operatorname{grad} \mathbf{v}) \mathbf{v} \right\} &= -\operatorname{grad} p + \rho \mathbf{g} + \operatorname{grad}(\zeta \operatorname{div} \mathbf{v}) + 2 \operatorname{div}(\eta \mathbf{E}), \\
 \rho T \frac{ds}{dt} &= \operatorname{div}(\kappa \operatorname{grad} T) + \Phi + \rho r, \\
 \rho \frac{dc_\alpha}{dt} &= \operatorname{div} \left(\rho \sum_{\beta \neq \alpha} D^{\alpha\beta} \operatorname{grad} c_\beta \right) + \rho \pi^\alpha, \quad \alpha = 1, \dots, n-1.
 \end{aligned}
 \tag{20.122}$$

Equations (20.122)_{1,2,3} are the mixture balance laws of mass, momentum and energy following the barycentric motion, momentum and energy. Equations (20.122)₄ are $n-1$ mass balances for the mass concentrations c_α . Moreover,

$$\begin{aligned}
 \mathbf{E} &= \mathbf{D} - \frac{1}{3}(\operatorname{div} \mathbf{v}) \mathbf{1}, \quad \mathbf{D} := \operatorname{sym} \operatorname{grad} \mathbf{v}, \\
 s &= -\frac{\partial \mathbf{g}}{\partial T}, \quad \frac{1}{\rho} = \frac{\partial \mathbf{g}}{\partial p}, \\
 \Phi &= \zeta(\operatorname{div} \mathbf{v})^2 + 2\eta \operatorname{tr} \mathbf{E}^2, \\
 (\mathbf{g}, \zeta, \eta, \kappa) &= f_{cts}(T, s, p).
 \end{aligned}
 \tag{20.123}$$

In the above, $\rho, \mathbf{v}, p, \mathbf{g}, T, r, c_\alpha, \mathbf{j}_\alpha, \pi_\alpha$ are, in turn, the mixture density, barycentric velocity, pressure, Earth's acceleration, KELVIN temperature, specific energy supply rate density (radiation density), mass concentration of tracer α . \mathbf{D} is the mixture stretching (strain rate) tensor, \mathbf{E} its deviator, s the entropy and \mathbf{g} the free enthalpy (GIBBS free energy); $\zeta, \eta, \kappa, D^{\alpha\beta}$ are the bulk and shear viscosities, the heat conductivity and species diffusivities. The stress tensor, heat flux vector and diffusive mass flux vectors are given by

$$\begin{aligned}
 \mathbf{t}^R &= \zeta(\operatorname{div} \mathbf{v}) \mathbf{1} + 2\eta \mathbf{E}, \\
 \mathbf{q} &= -\kappa \operatorname{grad} T, \\
 \mathbf{j}_\alpha &= -\rho \sum_{\beta \neq \alpha} D^{\alpha\beta} \operatorname{grad} c_\beta, \quad D^{\alpha\beta} = D^{\beta\alpha},
 \end{aligned}
 \tag{20.124}$$

and the mixture density is given by the following 'thermal equation of state'

$$\rho = \nu_f \rho_f(T, s, p) + \sum_{\beta=1}^{n-1} \nu_\beta \rho_s,
 \tag{20.125}$$

in which $\rho_f(T, s, p)$ is the thermal equation of state of the pure fluid (natural water) as a function of the temperature, salinity (mineralization) and pressure. ν_f and ν_β are the volume fractions of the fluid and of $(n - 1)$ components of suspended fine particles with true mass density ρ_s . (So, together with the salt, there are n tracer components ($\alpha \in [s, \beta = 1, \dots, n - 1]$). Now, because of saturation, we have $\sum_\beta \nu_\beta + \nu_f = 1$, and $\nu_\beta = (\rho/\rho_s) c_\beta, \forall \beta \in [1, \dots, n - 1]$. With these relations it follows from (20.125) that

$$\rho = \frac{\rho_f}{1 - \sum_\beta c_\beta (1 - \rho_f/\rho_s)}, \quad \nu_\beta = \frac{\rho}{\rho_s} c_\beta. \quad (20.126)$$

Finally, we use the approximation

$$\rho T \frac{ds}{dt} \approx \rho c_p(T) \frac{dT}{dt}, \quad (20.127)$$

see [21].

20.4.3 Non-dimensionalization of the NSFF Equations

(a) Non-rotating Inertial Frame. Field equations such as the NSFF equations can most easily be put into dimensionless form by splitting each field quantity f into a product

$$f = [f] \tilde{f}, \quad (20.128)$$

in which $[f]$ possesses the same dimension as f , is constant and should have a numerical value such that \tilde{f} assumes a value which is of order unity. It is exactly this requirement, which reflects a considerable degree of individuality in the selection of the scales $[f]$. Two different choices for the mass density are e.g.

$$\rho = [\rho] \tilde{\rho}, \quad \rho = [\rho] (1 + [\sigma] \tilde{\sigma}). \quad (20.129)$$

The first is adequate when density variations are large as it may be appropriate for air. $\tilde{\rho}$ then spans a relatively large interval from 0 (near vacuum) to, say, 1. The second choice is appropriate for water in the ocean or lakes, where density variations are small, only a small fraction of the density of water. Here, $[\rho] \approx 1000 \text{ kg m}^{-3}$ may be an adequate reference value of the density of water from which the real density deviates only by small amounts. This deviation is expressed as $[\sigma] \tilde{\sigma}$, where $[\sigma]$ is of the order 10^{-3} – 10^{-2} and $\tilde{\sigma}$ is of order unity. In this text we shall choose

$$\begin{aligned}
\mathbf{x} &= [L]\tilde{\mathbf{x}}, & t &= [\tau]\tilde{t}, & \rho &= [\rho]\tilde{\rho}, \\
\zeta &= [\zeta]\tilde{\zeta}, & c_p &= [c_p]\tilde{c}_p, & \mathbf{v} &= [V]\tilde{\mathbf{v}}, \\
\eta &= [\eta]\tilde{\eta}, & r &= [r]\tilde{r}, & p &= [p]\tilde{p}, \\
\kappa &= [\kappa]\tilde{\kappa}, & \mathbf{g} &= [g]\tilde{\mathbf{g}}, & T &= T_0 + [\Delta T]\theta, \\
\mathbf{D} &= [D]\tilde{\mathbf{D}}, & \mathbf{E} &= [D]\tilde{\mathbf{E}}, & \omega &= [\omega]\tilde{\omega}, \\
D^{\alpha\beta} &= [D^{\text{spec}}]\tilde{D}^{\alpha\beta},
\end{aligned} \tag{20.130}$$

in which $\tilde{\rho}$ is given by (20.129)₂. Then the NSFF equations may be written as

$$\begin{aligned}
[\sigma] \left\{ \mathbb{S}t \frac{\partial \tilde{\sigma}}{\partial \tilde{t}} + \text{div} (\tilde{\sigma} \tilde{\mathbf{v}}) \right\} + \text{div} \tilde{\mathbf{v}} &= 0, \\
\tilde{\rho} \left\{ \mathbb{S}t \frac{\partial \tilde{\mathbf{v}}}{\partial \tilde{t}} + (\text{grad} \tilde{\mathbf{v}}) \tilde{\mathbf{v}} \right\} &= -\mathbb{E}u \text{grad} \tilde{p} \\
&+ \frac{1}{\mathbb{R}e} \left\{ \frac{[\zeta]}{[\eta]} \text{grad} (\tilde{\zeta} \text{div} \tilde{\mathbf{v}}) + 2 \text{div} (\tilde{\eta} \tilde{\mathbf{E}}) \right\} + \frac{\tilde{\rho}}{\mathbb{F}r} \tilde{\mathbf{g}}, \\
\tilde{\rho} \tilde{c}_p \left\{ \mathbb{S}t \frac{\partial \theta}{\partial \tilde{t}} + (\text{grad} \theta) \cdot \tilde{\mathbf{v}} \right\} &= \frac{1}{\mathbb{P}e} \text{div} (\tilde{\kappa} \text{grad} \theta) \\
&+ \frac{1}{\mathbb{E}d} \left\{ \frac{[\zeta]}{[\eta]} \tilde{\zeta} (\text{div} \tilde{\mathbf{v}})^2 + 2 \tilde{\eta} \text{tr} \tilde{\mathbf{E}}^2 \right\} + \frac{1}{\mathbb{R}a} \tilde{\rho} \tilde{r}, \\
\tilde{\rho} \left\{ \mathbb{S}t \frac{\partial c_\alpha}{\partial \tilde{t}} + (\text{grad} c_\alpha) \tilde{\mathbf{v}} \right\} &= \frac{1}{\mathbb{R}e\mathbb{S}} \sum_{\beta} \text{div} (\tilde{\rho} \tilde{D}^{\alpha\beta} \text{grad} c_\beta), \quad \alpha = 1, \dots, n,
\end{aligned} \tag{20.131}$$

in which the hallow quantities represent the characteristic dimensionless Π -products arising in this non-dimensionalization. They are collected in **Table 20.4**. The derivation of (20.131) is a bit cumbersome and lengthy but not difficult.

In the scalings (20.130) the typical time $[\tau]$ was chosen independently of the characteristic length $[L]$ and characteristic velocity $[V]$. Analogously, also for the pressure an independent scale was chosen. If observations suggest that $[\tau]$ may be interpretable as a time, which a particle needs to propagate a distance $[L]$ with velocity $[V]$, then one may choose $[\tau] = [L]/[V]$ i.e., $\mathbb{S}t = 1$. Such a scaling is appropriate when instationary and convective features are of similar significance. If an exterior flow around a solid body is considered, then the stagnation pressure $[\rho V^2]$ may be used as scale for $[p]$, which corresponds to the choice $\mathbb{E}u = 1$. In such cases ‘only’ 6 dimensionless Π -products arise. Such reduction of the Π -products is helpful, because it reduces the number of possible scale invariances, which one ought to fulfill.

Finally, with regard to scaling properties, Eq. (20.131)_{3,4} show that

$$\mathbb{P}e = \mathbb{R}e\mathbb{P}r \quad \text{and} \quad \mathbb{P}e^{\text{tracer}} = \mathbb{R}e\mathbb{S}$$

must be scale invariants, if heat and mass diffusion processes are to be properly modeled. Because the FROUDE and REYNOLDS numbers cannot be simultaneous model invariants and free surface flows are best scaled with FROUDE models, we conclude

Table 20.4 Characteristic dimensionless parameters arising in the NSFF equations

$Ed := 2\Re\mathbb{T}_h := \frac{[c_p][\Delta T][V][L]}{[V^2][\eta]/[\rho]}$	Dissipation number
$Eu := \frac{[\rho]}{[\rho][V^2]}$	EULER number, pressure coefficient
$Fr := \frac{[V^2]}{[g][L]}$	FROUDE number, inverse RICHARDSON number
$Pe = \Re ePr := \frac{[\rho][c_p][V][L]}{[\kappa]}$	PÉCLET ^a number
$Pe^{\text{tracer}} = \Re eS$	Tracer PÉCLET number
$Pr^{th} := \frac{[\eta]/[\rho]}{[\kappa]/([\rho][c_p])} = \frac{[\nu]}{[D^{th}]}$	PRANDTL number
$Pr^{\text{tracer}} := \frac{[V][L]}{[D]}$	PRANDTL (SCHMIDT) number of tracer diffusion
$\mathbb{R}_a := \frac{[c_p][\Delta T][V]}{[L][r]}$	Radiation number
$\Re e := \frac{[V][L]}{[\eta]/[\rho]}$	REYNOLDS number
$S := \frac{[\eta]/[\rho]}{[D^{\text{spec}}]} = \frac{[\nu]}{[D^{\text{spec}}]}$	SCHMIDT ^b number
$St := \frac{[L]}{[V][\tau]}$	STROUHAL ^c number
$\mathbb{T}h = \frac{[c_p][\Delta T]}{[V^2]}$	Temperature number

^aFor a brief biography of JEAN CLAUDE EUGÉNE PÉCLET, see **Fig. 20.14**^bFor a brief biography of ERNST HEINRICH WILHELM SCHMIDT, see **Fig. 15.5**^c(CENEK) VINCENCE STROUHAL (10 April 1850–26 Jan. 1922) was a Czech experimental physicist, specialized in hydrodynamics. He was one of the founders of the physics department of Charles University in Prague**Proposition 20.2**

- *Measuring temperature in FROUDE models gives no guarantee of appropriate transfer to corresponding quantities in Nature, or: In FROUDE models no homologous temperature field can be generated.*
- *Measurements of tracer concentrations in FROUDE models do not permit a transfer to corresponding tracer concentrations in Nature, or: in FROUDE models no homologous tracer fields can be generated.* ■

This result implies that quantitative comparison between flow velocities, temperature and species distributions in FROUDE models and their prototypes are inadmissible unless the up-scaling is performed with experimental results obtained with models of at least two different down-scalings. This obviously limits the usefulness of model studies of combined fluid dynamics and diffusive processes to principal studies.



Fig. 20.14 JEAN CLAUDE EUGÈNE PÉCLET (10. Feb. 1793–6. Dec. 1857)

JEAN CLAUDE EUGÈNE PÉCLET was a French physicist. Born in Besançon, France, he became, in 1812, one of the first students of the École Normale in Paris with GAY-LUSSAC and DULONG being his professors. In 1816, he was elected professor at the Collège de Marseille and taught physical sciences there until 1827. Being nominated *maître de conférences* (habilitated with fixed employment) at the École Normale, he returned to Paris. In 1829, he became a professor of physics at the École Centrale des Arts et Manufactures that was being founded by the businessman ALPHONSE LAVALLÉE, by PÉCLET, and by three other scientists, PHILIPPE BENOÎT, JEAN-BAPTISTE DUMAS and THÉODORE OLIVIER. His salary was then 3000 Francs per year, plus a share of the profits of this private engineering school. In 1840, PÉCLET became inspecteur général de l'instruction publique.

The PÉCLET number is named after him. He was CORIOLIS's brother-in-law and he died in Paris. He is known through his educational books [30, 31]. He was characterized by clarity of expression, sharp minded views and well-performed experiments.

The text is based on www.wikipedia.org and W H. Hager: *Hydraulicians in Europe 1800–2000*, IAHR monograph (2003)

(b) Rotating, Non-inertial Frame. If the body, in which the fluid is kept and of which the motion is to be studied, is rotating, a new characteristic time $[\tau]$ may be introduced, which is given by the angular velocity of the rotating frame $[\tau] = [\omega]^{-1}$. For the Earth $[\omega] = \Omega \sin \phi$, where Ω is the angular velocity of the Earth and ϕ is the latitude angle. In an Earth-bound laboratory, rotating about a vertical axis with steady angular velocity, the absolute angular velocity is $[\omega + \Omega \sin \phi] \approx [\omega]$, since ordinarily $|\omega| \gg |\Omega \sin \phi|$. With the scales (20.130), in which $[\tau]$ is replaced by $[\omega]^{-1}$, and with the absolute acceleration given by

Table 20.5 Characteristic dimensionless parameters arising in the NSFF equations when $[\tau] = [\omega]^{-1}$

$\mathbb{R}o \equiv \frac{1}{St} _{[\tau]=[\omega]^{-1}} = \frac{[V]}{[\omega][L]}$	ROSSBY number
$\mathbb{P}_{[\omega]} \equiv \frac{[p]}{[\rho][L][\omega][V]}$	Pressure coefficient
$\mathbb{E}k \equiv \frac{[\nu]}{[\omega][L]^2}$	EKMANN number
$\mathbb{F}r_{[\omega]} \equiv \frac{[\omega][V]}{[g]}$	FROUDE number
$\mathbb{R}a_{[\omega]} \equiv \frac{[c_p][\Delta T][\omega]}{[r]}$	Radiation number

$$\left(\frac{d\mathbf{v}}{dt}\right)_{\text{abs}} = \left(\frac{d\mathbf{v}}{dt}\right)_{\text{rel}} + \underbrace{2\boldsymbol{\omega} \times \mathbf{v}}_{\text{Coriolis acc.}} + \underbrace{\boldsymbol{\omega} \times (\boldsymbol{\omega} \times \mathbf{x})}_{\text{centripetal acc.}} + \underbrace{\dot{\boldsymbol{\omega}} \times \mathbf{x}}_{\text{Euler acc.}}, \tag{20.132}$$

the NSFF equations take the dimensionless forms

$$\begin{aligned} \frac{\partial \tilde{\rho}}{\partial \tilde{t}} + \mathbb{R}o \operatorname{div}(\tilde{\rho} \tilde{\mathbf{v}}) &= 0, \\ \tilde{\rho} \left\{ \frac{\partial \tilde{\mathbf{v}}}{\partial \tilde{t}} + \mathbb{R}o(\operatorname{grad} \tilde{\mathbf{v}}) \tilde{\mathbf{v}} + 2\tilde{\boldsymbol{\omega}} \times \tilde{\mathbf{v}} + \frac{1}{\mathbb{R}o} \left\{ \tilde{\boldsymbol{\omega}} \times (\tilde{\boldsymbol{\omega}} \times \tilde{\mathbf{x}}) + \frac{[\dot{\boldsymbol{\omega}}]}{[\omega]^2} \dot{\tilde{\boldsymbol{\omega}}} \times \tilde{\mathbf{x}} \right\} \right\} \\ &= -\mathbb{P}_{[\omega]} \operatorname{grad} \tilde{p} + \mathbb{E}k \left\{ \frac{[\zeta]}{[\eta]} \operatorname{grad}(\tilde{\zeta} \operatorname{div} \tilde{\mathbf{v}}) + 2 \operatorname{div}(\tilde{\eta} \tilde{\mathbf{E}}) \right\} + \frac{1}{\mathbb{F}r_{[\omega]}} \tilde{\rho} \tilde{\mathbf{g}}, \end{aligned} \tag{20.133}$$

$$\begin{aligned} \tilde{\rho} \tilde{c}_p \left\{ \frac{\partial \theta}{\partial \tilde{t}} + \mathbb{R}o(\operatorname{grad} \theta) \cdot \tilde{\mathbf{v}} \right\} &= \frac{\mathbb{E}k}{\mathbb{P}r} \operatorname{div}(\tilde{\kappa} \operatorname{grad} \theta) \\ &+ \frac{\mathbb{E}k}{\mathbb{T}_h} \left\{ \frac{[\zeta] \tilde{\zeta}}{[\eta]} (\operatorname{div} \tilde{\mathbf{v}})^2 + 2 \tilde{\eta} \operatorname{tr}(\tilde{\mathbf{E}}^2) \right\} + \frac{1}{\mathbb{R}a_{[\omega]}} \tilde{\rho} \tilde{r}, \\ \tilde{\rho} \left\{ \frac{\partial c^\alpha}{\partial \tilde{t}} + \mathbb{R}o(\operatorname{grad} c^\alpha) \cdot \tilde{\mathbf{v}}_\alpha \right\} &= \frac{\mathbb{E}k}{\mathbb{P}r_{\text{tracer}}} \sum_{\beta} (\tilde{\rho} \tilde{D}^{\alpha\beta}) \operatorname{grad} c^\beta, \end{aligned}$$

in which $\rho = [\rho] \tilde{\rho}$, $\dot{\boldsymbol{\omega}} = [\dot{\boldsymbol{\omega}}] \dot{\tilde{\boldsymbol{\omega}}}$, and where the new Π -products are given in **Table 20.5**. The rotation of the frame of reference is steady, $[\dot{\boldsymbol{\omega}}] \equiv 0$; likewise, the bulk viscosity is commonly ignored, $[\zeta] = 0$. Moreover, in geophysical fluid dynamics the centrifugal force is generally absorbed in the gravity term or it is ignored. This fact points at a subtle difficulty in laboratory experiments of geophysical flows on rotating platforms, where the centrifugal terms may exert an effective force expression, different in direction of the Earth's gravity.

Examples of rotating laboratory studies have been reported in specialized reports of hydraulic engineering. Such experiments were primarily performed in the late-60s to mid-80s of the last century. HUTTER et al. [21] give an account of these modeling efforts in their Chap. 30, pp. 375–393. It is our impression that the enthusiasm of those times about experiments on rotating platforms has not continued, probably for reasons of costs and dizziness of the experimenters, when working on the rotating platforms with angular frequencies of one revolution in 4–6 s. The future will likely have to be sought in a combination of electronic computations and non-rotating local experimental analyses.

20.5 Discussion and Conclusions

The primary focus of this chapter has been twofold, namely (i) to lay down the basic elements of dimensional analysis and (ii) to apply the rules of dimensional homogeneity of the governing equations of mathematical physics to thoughtful interpretations of laboratory experiments, when up- or downscaling these to the size of similar processes in Nature (i.e. the size of the prototype).

The first goal entails the recognition that physical processes are mathematically described by dimensionally homogeneous functions. *Dimensional analysis* is that sub-branch of linear algebra, which proves that a dimensionally homogeneous functional relation involving a certain number of variables with physical dimensions can always be transformed into an associated functional relation of alternative, mutually independent, variables, which are dimensionless. The number of these dimensionless product combinations of the original variables (with physical dimensions)—the so-called Π -products—is generally smaller than the number of the original variables. BUCKINGHAM's theorem is the decisive statement, which ascertains that (1) any dimensionally homogeneous functional relation can be put into dimensionless form, and (2) the number of Π -products for a set of given physical parameters is determined by the rank of the dimensional matrix as follows:

$$\left\{ \begin{array}{l} \text{Number of independent} \\ \text{dimensionless } \Pi\text{-products} \end{array} \right\} = \left\{ \begin{array}{l} \text{Number of physical parameters} \\ - \text{rank of dimensional matrix} \end{array} \right\}$$

The theorem is of immense practical help as with it, one may obtain first rough information about the general behavior of envisaged processes. The method, however, requires knowledge and proposition of the physical parameters, which may influence the outcome of the results for the envisaged process. This is likely the most difficult part of the identification of the Π -products influencing the behavior of the process. Examples illustrate the procedure in this selection and corroborate the usefulness of this analysis, which has an imaginative and a rational, mathematical component.

An alternative approach to guessing the decisive physical parameters that might affect an envisaged physical process may be *inspectional analysis*. This method starts with the formulated equation set, which is thought to describe the process mathe-

matically. This may be a set of partial differential equations, boundary and initial conditions or any other set of equations for the problem. This set of equations is dimensionally homogeneous by construction, but it is a mathematical *model* and may miss some effects of the envisaged processes. Nevertheless, the mere fact that the set of equations has been constructed gives them a high degree of trustworthiness. Transforming these equations to dimensionless form allows identification of the dimensionless parameters arising in this mathematical problem. This transformation to dimensionless form was demonstrated for the NAVIER–STOKES–FOURIER–FICK equations referred to an inertial and an Earth-bound non-inertial frame, respectively. It was shown how the number of Π -products can be reduced by selecting special parameter combinations for certain Π -products. Additional examples from geophysical fluid mechanics are given in [20, 21].

BUCKINGHAM's theorem is the basis for the design of experiments of physical processes at smaller (or larger) scale. Flow processes in a scaled experiment can only evolve homologously to the processes in the prototype, provided all dimensionless Π -products remain invariant in the geometric and dynamic downscaling from the prototype to the model. However, this theoretical request can in practice only seldom be fulfilled. For instance, it was shown that FROUDE and REYNOLDS numbers cannot simultaneously be fulfilled. Whenever full invariance of all the Π -products cannot be maintained in the downscaling, experiments are said to exhibit *scale effects*. Such effects may be seen in free surface flows (rivers, lakes), when water depths in the model are less than 1 cm, so that surface tension effects become visible. One method to minimize scale effects is to select Π -products by combination such that those Π -products, which cannot be kept invariant are only of a small influence. This can only be achieved by trial and error. A second method is to perform experiments with models at different geometric reduction and then inter- and extrapolate the results due to the non-invariant Π -products; however, this is generally too costly. A promising procedure is to solve the initial-value-problems numerically; this way the exact values of the Π -products can be solved. It is likely that this method of computational fluid mechanics may become competitive in future.

Appendix A: Algebraic Theory of Dimensional Analysis¹³

A.1 Transformation of Basic Units

In this Appendix our goal is to derive the *theorem of* BUCKINGHAM [12]. The reader is requested to have knowledge of Linear Algebra.

Let m be the number of independent, i.e., fundamental dimensions, such as length $[L]$, mass $[M]$, time $[T]$, temperature $[\theta]$, Derived dimensions are formed as products of the fundamental dimensions. If the dimension of a *fundamental unit* is denoted by

¹³This Appendix follows a corresponding text in [20] with some improvements.

$$[G]_i, \quad (i = 1, 2, \dots, m), \quad (20.134)$$

then the dimensions of the derived units A_j can be written as

$$[A]_j = [G]_1^{a_{1j}} [G]_2^{a_{2j}} \cdots [G]_m^{a_{mj}} \quad (20.135)$$

$$= \prod_{i=1}^m [G]_i^{a_{ij}}, \quad (j = 1, 2, \dots, n). \quad (20.136)$$

They are products of powers of the fundamental dimensions.

Let the value of the derived quantity $[A]_j$ in (20.136) relative to particularly chosen units be given by the positive real number x_j , and let the fundamental basic unit $[G]_k$ in one set of units be $[G]_k^o$ and in another set be $[G]_k^n$ ('o' stands for 'old' and 'n' stands for 'new'). Then the relation

$$1 \cdot G_k^o = \alpha_k \cdot G_k^n \quad (20.137)$$

describes the connection between the old and new fundamental units: 1 m = 100 cm. Let the value of $[A]_j$ in the old and new system be x_j and \bar{x}_j , respectively. The old and new values of the derived quantity are then related by

$$\begin{aligned} x_j & [(G_1^o)^{a_{1j}} (G_2^o)^{a_{2j}} \cdots (G_m^o)^{a_{mj}}] \\ &= x_j \left[(\alpha_1^{1j} G_1^n)^{a_{1j}} (\alpha_2^{2j} G_2^n)^{a_{2j}} \cdots (\alpha_m^{mj} G_m^n)^{a_{mj}} \right] \\ &= \bar{x}_j [(G_1^n)^{a_{1j}} (G_2^n)^{a_{2j}} \cdots (G_m^n)^{a_{mj}}], \end{aligned} \quad (20.138)$$

so that

$$\bar{x}_j = x_j \prod_{k=1}^m \alpha_k^{a_{kj}}, \quad (j = 1, 2, \dots, n). \quad (20.139)$$

A.2 Exact Definition of Dimensional Homogeneity

Let y be a function of n variables i.e., $y = f(x_1, \dots, x_n)$. If the units of the basic dimensions are changed, then y and x_j become \bar{y} and \bar{x}_j . An equation is now called dimensionally homogeneous, if $y = f(x_1, \dots, x_n)$ can be transformed to

$$\bar{y} = f(\bar{x}_1, \bar{x}_2, \dots, \bar{x}_n), \quad (20.140)$$

in which f is the same function as before. Mathematically this means that the equation $y = f(x_1, \dots, x_n)$ is *invariant under the group of transformations which is generated by all possible changes of units of the fundamental dimensions*. This group

of transformations¹⁴ is described by (20.138), in which α_k may be arbitrary positive constants. For the dependent and independent variables relation (20.138) can symbolically be summarised by the dimensional matrix

$$\begin{array}{c|cccccc}
 & y & x_1 & x_2 & x_3 & \dots & x_n \\
 [G]_1 & a_{10} & a_{11} & a_{12} & a_{13} & \dots & a_{1n} \\
 [G]_2 & a_{20} & a_{21} & a_{22} & a_{23} & \dots & a_{2n} \\
 \vdots & \vdots & \vdots & \vdots & \vdots & & \vdots \\
 [G]_m & a_{m0} & a_{m1} & a_{m2} & a_{m3} & \dots & a_{mn}
 \end{array} \tag{20.141}$$

If one writes

$$\bar{y} = K_o y, \quad \bar{x}_j = K_j x_j,$$

one obtains, in view of (20.138),

$$K_o = \prod_{k=1}^m \alpha_k^{a_{k0}}, \quad K_j = \prod_{k=1}^m \alpha_k^{a_{kj}}.$$

Therefore, the following identity must hold

$$\bar{y} = K_o y = K_o f(x_1, x_2, \dots, x_n) = f(K_1 x_1, K_2 x_2, \dots, K_n x_n). \tag{20.142}$$

Thus we have

Proposition 20.3 *The function $f(x_1, \dots, x_n)$ is dimensionally homogeneous if and only if the equation*

$$K_o f(x_1, x_2, \dots, x_n) = f(K_1 x_1, K_2 x_2, \dots, K_n x_n) \tag{20.143}$$

with

$$K_o = \prod_{k=1}^m \alpha_k^{a_{k0}}, \quad K_j = \prod_{k=1}^m \alpha_k^{a_{kj}} \tag{20.144}$$

is identically fulfilled in the variables $x_1, x_2, \dots, x_n, \alpha_1, \alpha_2, \dots, \alpha_m$. ■

Notice that all K 's are fixed if the α_k 's and the dimensional matrix are known.

Let us give *two important applications* of Proposition 20.3; consider first

$$(i) \quad y = f(x_1, x_2, \dots, x_n) = x_1 + x_2 + \dots + x_n.$$

The function $f(x_1, \dots, x_n)$ is here the sum of its independent variables; in this case (20.143) reads

¹⁴We leave it to the reader to prove that the group properties (as mathematical statements) are satisfied.

$$K_0(x_1 + x_2 + \cdots + x_n) = K_1x_1 + K_2x_2 + \cdots + K_nx_n,$$

and since this equation must hold identically for all x_j , one must have

$$K_0 = K_1 = K_2 = \cdots = K_n \quad (20.145)$$

or because of (20.144)

$$a_{k_0} = a_{k_1} = a_{k_2} = \cdots = a_{k_n}, \quad (k = 1, 2, \dots, m).$$

Thus we have the

Lemma 20.1 *A sum*

$$y = x_1 + x_2 + \cdots + x_n \quad (20.146)$$

is dimensionally homogeneous if and only if all of its members have the same dimension. [Apples and pears cannot be added] ■

Consider as a second example the composition

$$(ii) \quad y = x_1^{k_1} \times x_2^{k_2} \times \cdots \times x_n^{k_n} = \prod_{j=1}^n x_j^{k_j} \quad (20.147)$$

with arbitrary k_j , ($j = 1, \dots, n$). Such compositions are products of powers of the variables x_1, \dots, x_n . We call them for simplicity products. Then we have

Lemma 20.2 *The product*

$$y = \prod_{j=1}^n x_j^{k_j} \quad (20.148)$$

is dimensionally homogeneous if and only if the exponents are solutions of the linear equations

$$\sum_{j=1}^n a_{ij}k_j = a_{i0}, \quad (i = 1, 2, \dots, m). \quad (20.149)$$

■

Proof The matrix a_{ij} is the dimensional matrix of the independent variables; the vector a_{i0} is the column of the dependent variables. To prove the Lemma we assume that the product of powers (20.148) is dimensionally homogeneous; in a change of the fundamental units it will thus obey (20.143), so that

$$K_0 \left(\prod_{j=1}^n x_j^{k_j} \right) = \prod_{j=1}^n (K_j x_j)^{k_j} = \left(\prod_{j=1}^n K_j^{k_j} \right) \times \left(\prod_{j=1}^n x_j^{k_j} \right) \quad (20.150)$$

is fulfilled, from which

$$K_0 = \prod_{j=1}^n K_j^{k_j} \quad (20.151)$$

is obtained. If one also takes (20.144) into account, one obtains

$$\prod_{k=1}^m \alpha_k^{a_{k0}} = \left(\prod_{k=1}^m \alpha_k^{a_{k1}} \right)^{k_1} \times \cdots \times \left(\prod_{k=1}^m \alpha_k^{a_{kn}} \right)^{k_n} = \prod_{k=1}^m \alpha_k^{\sum_{j=1}^n a_{kj} k_j}, \quad (20.152)$$

and by comparison of the exponents

$$a_{k0} = \sum_{j=1}^n a_{kj} k_j, \quad (k = 1, 2, \dots, m). \quad (20.153)$$

The exponents of a dimensionally homogeneous power product (20.148) thus necessarily satisfy (20.149). To show the converse, namely that the power product (20.148) is dimensionally homogeneous, if the exponents obey (20.149), we state (20.148), written in terms of the old and new fundamental units, as

$$y = \prod_{j=1}^n x_j^{k_j}, \quad \bar{y} = \prod_{j=1}^n \bar{x}_j^{k_j}. \quad (20.154)$$

With the use of the transformation formulas for \bar{y} and \bar{x}_j the last formula takes the form

$$\begin{aligned} \left(\prod_{i=1}^m \alpha_i^{a_{i0}} \right) y &= \prod_{j=1}^n \left(\prod_{i=1}^m \alpha_i^{a_{ij}} x_j \right)^{k_j} = \prod_{j=1}^n \left(\prod_{i=1}^m \alpha_i^{a_{ij} k_j} \right) x_j^{k_j} \\ &= \left(\prod_{i=1}^m \alpha_i^{\sum_{j=1}^n a_{ij} k_j} \right) \underbrace{\prod_{j=1}^n x_j^{k_j}}_y \end{aligned} \quad (20.155)$$

or

$$\frac{\prod_{i=1}^m \alpha_i^{\sum_{j=1}^n a_{ij} k_j}}{\prod_{i=1}^m \alpha_i^{a_{i0}}} = \prod_{i=1}^m \alpha_i^{\sum_{j=1}^n a_{ij} k_j - a_{i0}} = 1, \quad (20.156)$$

which is satisfied for arbitrary values of α_i if (20.149) are fulfilled. \square

A.3 Calculus of Dimensionless Products

(1) We begin by formulating the condition that allows evaluation, whether a number of dimensionless products are independent of one another. Let these products be given by

$$\begin{aligned}
 \Pi_{(1)} &= x_1^{k_1^{(1)}} \times x_2^{k_2^{(1)}} \times \cdots \times x_n^{k_n^{(1)}}, \\
 \Pi_{(2)} &= x_1^{k_1^{(2)}} \times x_2^{k_2^{(2)}} \times \cdots \times x_n^{k_n^{(2)}}, \\
 &\vdots \\
 \Pi_{(p)} &= x_1^{k_1^{(p)}} \times x_2^{k_2^{(p)}} \times \cdots \times x_n^{k_n^{(p)}}.
 \end{aligned}
 \tag{20.157}$$

They can be arranged in a matrix as follows:

$$\begin{array}{c|cccc}
 & x_1 & x_2 & \cdots & x_n \\
 \hline
 \Pi_{(1)} & k_1^{(1)} & k_2^{(1)} & \cdots & k_n^{(1)} \\
 \Pi_{(2)} & k_1^{(2)} & k_2^{(2)} & \cdots & k_n^{(2)} \\
 \vdots & \vdots & \vdots & & \vdots \\
 \Pi_{(p)} & k_1^{(p)} & k_2^{(p)} & \cdots & k_n^{(p)}
 \end{array}
 \tag{20.158}$$

in which only the exponents of the $x_i, i = 1, 2, \dots, p$ are written down. If $\Pi_{(1)}$ and $\Pi_{(2)}$ are not independent, there exist two numbers h_1 and h_2 , such that $\Pi_{(1)}^{h_1} \Pi_{(2)}^{h_2} = 1$, i.e., $\Pi_{(1)}$ is a certain non-trivial power of $\Pi_{(2)}$ (or vice versa). If this argument is extended to p dimensionless products $\Pi_{(1)}, \dots, \Pi_{(p)}$, we may conclude that the dimensionless products $\Pi_{(1)}, \dots, \Pi_{(p)}$ are dependent on each other, if there exist constants h_1, h_2, \dots, h_p , not all of which vanish, such that

$$\Pi_{(1)}^{h_1} \times \Pi_{(2)}^{h_2} \times \cdots \times \Pi_{(p)}^{h_p} = 1.$$

This statement can be reformulated in the following

Proposition 20.4 *Necessary and sufficient condition that the products $\Pi_{(1)}, \dots, \Pi_{(p)}$ are independent of each other is the fact that the rows of the matrix (20.158) or*

$$\begin{pmatrix}
 k_1^{(1)} & k_2^{(1)} & \cdots & k_n^{(1)} \\
 k_1^{(2)} & k_2^{(2)} & \cdots & k_n^{(2)} \\
 \vdots & \vdots & & \vdots \\
 k_1^{(p)} & k_2^{(p)} & \cdots & k_n^{(p)}
 \end{pmatrix}
 \tag{20.159}$$

are linearly independent. ■

Proof To demonstrate necessity, let us assume that the rows of the matrix (20.159) are linearly dependent but the products (20.157) are independent. Then there must exist constants h_1, \dots, h_p not all of which are identically zero, which satisfy the relation

$$h_1 k_i^{(1)} + h_2 k_i^{(2)} + \dots + h_p k_i^{(p)} = 0, \quad (i = 1, 2, \dots, n). \quad (20.160)$$

This, however, implies, in view of (20.157),

$$\Pi_{(1)}^{h_1} \times \Pi_{(2)}^{h_2} \times \dots \times \Pi_{(p)}^{h_p} = x_1^{\sum_{j=1}^p h_j k_1^{(j)}} \times x_2^{\sum_{j=1}^p h_j k_2^{(j)}} \times \dots \times x_n^{\sum_{j=1}^p h_j k_n^{(j)}}.$$

If one substitutes here (20.160), there follows

$$\Pi_{(1)}^{h_1} \times \Pi_{(2)}^{h_2} \times \dots \times \Pi_{(p)}^{h_p} = x_1^0 x_2^0 \dots x_n^0 = 1, \quad (20.161)$$

which is in conflict with the assumption that the products are independent. Thus the rows of the matrix (20.159) must be linearly independent.

Sufficiency can be proved as follows: if the rows of the matrix (20.159) are linearly independent and the dimensionless products are dependent, an equation of the form

$$\Pi_{(1)}^{h_1} \times \Pi_{(2)}^{h_2} \times \dots \times \Pi_{(p)}^{h_p} = 1$$

must exist for the exponents h_j , not all of which vanish. Then, however, (20.157) implies

$$x_1^{\sum_{j=1}^p h_j k_1^{(j)}} \times x_2^{\sum_{j=1}^p h_j k_2^{(j)}} \times \dots \times x_n^{\sum_{j=1}^p h_j k_n^{(j)}} = 1, \quad (20.162)$$

which can only be correct, if all exponents vanish, which is a contradiction to the assumed linear independence of the matrix (20.159). \square

(2) Next, we consider a power product and ask, under which conditions it is dimensionless (and hence a Π -product). The answer to this question is

$$\sum_{j=1}^n a_{ij} k_j = 0, \quad (i = 1, 2, \dots, m) \quad (20.163)$$

and follows immediately from Lemma 20.2 with $a_{i0} = 0$. The linear, homogeneous equations (20.163) possess $(n - r)$ linearly independent solutions, which we shall denote by

$$k_i^{(1)}, k_i^{(2)}, \dots, k_i^{(n-r)}, \quad (i = 1, 2, \dots, n). \quad (20.164)$$

Here, r denotes the rank of the matrix (a_{ij}) . According to Proposition 20.4 the solution vectors furnish the exponents for all dimensionless products. There are no additional ones, so that one can formulate

Proposition 20.5 *Every fundamental system of solutions of the equations*

$$\sum_{j=1}^n a_{ij}k_j = 0, \quad (i = 1, 2, \dots, m) \tag{20.165}$$

determines the $n - r$ exponents of a complete set of dimensionless products of the variables x_1, \dots, x_n . Conversely, the exponents of a complete set of dimensionless products of the variables x_1, \dots, x_n form a fundamental system of solutions of the above equations. ■

This proposition immediately also implies

Proposition 20.6 *The number of independent products in a complete set of dimensionless products of the variables x_1, \dots, x_n is $(n - r)$, where r denotes the rank of the dimensional matrix. ■*

(3) In the practical application of dimensional analysis one often encounters equations of the form $y = f(x_1, \dots, x_n)$. In fact, this form is the rule rather than the exception. We now consider dimensional products and assume that in the dimensional matrix not all a_{i0} are zero. Then the system of equations for the exponents k_j reads

$$\sum_{j=1}^n a_{ij}k_j = a_{i0}, \quad (i = 1, 2, \dots, m), \tag{20.166}$$

and we have

Proposition 20.7 *If y is not dimensionless, then there exists a product of the form*

$$y = x_1^{k_1} \cdot x_2^{k_2} \cdot \dots \cdot x_n^{k_n} = \prod_{j=1}^n x_j^{k_j}, \tag{20.167}$$

if and only if the dimensional matrix of the variables x_1, \dots, x_n possesses the same rank as the dimensional matrix of the variables y, x_1, \dots, x_n . ■

Proof This follows if the system

$$\sum_{j=1}^n a_{ij}k_j = a_{i0}, \quad (i = 1, 2, \dots, m) \tag{20.168}$$

is considered. In books on linear algebra it is shown that solutions to the above equations exist, if the rank of the matrix (a_{ij}) is the same as the rank of the matrix (a_{ij}, a_{i0}) , augmented by the column of the right-hand side.

With the aid of Proposition 20.7 we now may prove

Proposition 20.8 *If $y = f(x_1, x_2, \dots, x_n)$ is a dimensionally homogeneous equation and if y is dimensional, then there exists a product of powers of x_j , which has the same dimension as y . ■*

Proof We assume that $y = f(x_1, \dots, x_n)$ is dimensionally homogeneous, but there does not exist a product of powers of x_j with the dimension of y . Assume, moreover, that the dimensional matrix (a_{i0}, a_{ij}) possesses the rank R . The assumption that no x_j -product exists with the same dimension as y implies, because of Proposition 20.7, that the rank of (a_{ij}) must be smaller than R . Without limitation of generality we may assume that a non-vanishing determinant of (a_{i0}, a_{ij}) lies in the upper left corner of this matrix; its rank is R . If $R = m$ (m is the number of independent fundamental dimensions), then this determinant is given by

$$\Delta = \begin{vmatrix} a_{10} & a_{11} & a_{12} & a_{13} & \dots & a_{1(m-1)} \\ a_{20} & a_{21} & a_{22} & a_{23} & \dots & a_{2(m-1)} \\ \vdots & & & & & \vdots \\ a_{m0} & a_{m1} & a_{m2} & a_{m3} & \dots & a_{m(m-1)} \end{vmatrix} \neq 0. \quad (20.169)$$

If A_{i0} are the algebraic complements or co-factors of a_{i0} of this matrix, then one may also write

$$\Delta = A_{10}a_{10} + \dots + A_{m0}a_{m0} = \sum_{i=1}^m A_{i0}a_{i0}. \quad (20.170)$$

Alternatively, in the theory of determinants one proves that

$$\sum_{i=1}^m A_{i0}a_{ik} = 0, \quad (\forall k = 1, 2, \dots, n). \quad (20.171)$$

(This result, incidentally, follows for $k = 1, 2, \dots, m-1$ from the fact that the value of the determinant is zero if only two columns of a matrix are the same.) Thus for $k = 1, 2, \dots, m-1$ (20.171) is correct. For $k \geq m$ it holds because the rank of the dimensional matrix is equal to $(a_{ij}) = R = m$.

Since y has been assumed as dimensionally homogeneous, (20.143), (20.144) hold as identities in the variables α_j ($j = 1, 2, \dots, m$). We therefore choose now new fundamental units, such that

$$\alpha_i = G^{A_{i0}}, \quad (i = 1, 2, \dots, m) \quad (20.172)$$

holds with arbitrary positive real G . The factors of transformation K_j are then computed according to (20.144) and yield

$$\begin{aligned} K_j &= \prod_{i=1}^m \alpha_i^{a_{ij}} = \prod_{i=1}^m (G^{A_{i0}})^{a_{ij}} = \prod_{i=1}^m G^{A_{i0}a_{ij}} \\ &= G^{\sum_{i=1}^m A_{i0}a_{ij}} = 1, \quad (j = 1, 2, \dots, n). \end{aligned} \quad (20.173)$$

Thus, by specially choosing α_i all K_j ($j = 1, 2, \dots, n$) have been made equal to unity. For K_0 , one obtains

$$K_0 = \prod_{i=1}^m \alpha_i^{a_{i0}} = G^{\sum_{i=1}^m A_{i0} a_{i0}} \neq 1. \tag{20.174}$$

Consequently, (20.143) takes the form

$$K_0 y = f(x_1, x_2, \dots, x_n), \quad K_0 = G^{\sum_{i=1}^m A_{i0} a_{i0}}, \tag{20.175}$$

in which K_0 can be arbitrarily assigned since $G > 0$ was already freely chosen (because it is an arbitrary transformation of the units of the fundamental dimensions). With the possibility to arbitrarily choose K_0 , it is now also shown that

$$K_0 y = f(x_1, x_2, \dots, x_n) \tag{20.176}$$

cannot be a function. This is in contradiction with the assumption that $y = f(x_1, \dots, x_n)$ is a dimensionally homogeneous function.¹⁵ The initial assumption that no power product of x_j with the dimension $[y]$ can exist, was therefore wrong. The proposition is therefore proved for $R = m$.

If $R < m$, e.g. $R = r$, then Δ is of size r , there is now an $r \times r$ matrix with non-vanishing determinant

$$\Delta = \begin{vmatrix} a_{10} & a_{11} & a_{12} & a_{13} & \dots & a_{1(r-1)} \\ a_{20} & a_{21} & a_{22} & a_{23} & \dots & a_{2(r-1)} \\ \vdots & \vdots & \vdots & \vdots & & \vdots \\ a_{r0} & a_{r1} & a_{r2} & a_{r3} & \dots & a_{r(r-1)} \end{vmatrix}, \quad r < m. \tag{20.177}$$

In a way analogous to that before one now concludes that

$$\begin{aligned} \Delta &= \sum_{i=1}^r A_{i0} a_{i0}, \\ \sum_{i=1}^r A_{i0} a_{ik} &= 0, \quad (k = 1, 2, \dots, n), \end{aligned} \tag{20.178}$$

where A_{i0} are again the algebraic complements of a_{i0} . With $\alpha_i = G^{A_{i0}}$ ($i = 1, \dots, r$), $\alpha_j = 1$ ($r < j < m$) one now obtains

$$K_j = G^{\sum_{i=1}^r A_{i0} a_{ij}} = G^0 = 1, \quad K_0 = G^{\sum_{i=1}^r A_{i0} a_{i0}} \neq 1, \tag{20.179}$$

so that one arrives at the same conclusion as before. Setting $a_j = 1$ for all $j > r$ corresponds again to a permissible change of the fundamental units. Proposition 20.8

¹⁵Dimensional homogeneity is not important, since f does not even satisfy the prerequisites of a function.

therefore says nothing else than that a dimensionally homogeneous equation of the form $y = f(x_1, \dots, x_n)$ can always be brought to the form

$$\Pi = F(x_1, \dots, x_n), \quad (20.180)$$

in which Π is dimensionless and F is a new function. \square

A.4 Proof of Buckingham's Theorem

In closing we wish in this section to prove BUCKINGHAM's *theorem* or BUCKINGHAM Π -*theorem* [12] according to which a dimensionally homogeneous equation of several variables can be reduced to a relation only involving dimensionless quantities. The number of these new variables is usually smaller than the original number of dimensional variables.

Notice in particular that the independent variables in a problem of dimensional analysis are always real and positive quantities. If this were not so, then dimensionless products with fractional exponents would become complex valued. We shall also see that BUCKINGHAM's theorem can only hold, if the independent variables are restricted to positive quantities.

Let x_1, \dots, x_n be the independent variables of a physical problem. These variables represent entities such as velocity, force, moment, temperature, heat flux etc. They may be regarded as the Cartesian coordinates of an EUCLIDIAN space \mathcal{E} . Let, moreover, α_i ($i = 1, 2, \dots, m$) be positive constants and K_j ($j = 1, 2, \dots, n$) variables, defined by

$$K_j = \prod_{i=1}^m \alpha_i^{a_{ij}}, \quad (j = 1, 2, \dots, n), \quad (20.181)$$

in which a_{ij} is the dimensional matrix corresponding to the x_j 's. The equation

$$x_j = K_j x_j', \quad (j = 1, 2, \dots, n) \quad (20.182)$$

then corresponds in the space \mathcal{E} to a coordinate or point transformation; it assigns to each point x_j' a point x_j and vice versa. This point transformation shall subsequently be called K -transformation, and it is easy to show that all K -transformations in \mathcal{E} build a group. Indeed,

(i) With $x_j = K_j^* x_j'$, $x_j' = K_j^{**} x_j''$ there follows

$$\begin{aligned} x_j &= (K_j^* K_j^{**}) x_j'' = K_j x_j'', \\ K_j &= \left(\prod_{i=1}^m \alpha_i^{*a_{ij}} \right) \left(\prod_{i=1}^m \alpha_i^{**a_{ij}} \right) \\ &= \prod_{i=1}^m (\alpha_i^* \alpha_i^{**})^{a_{ij}}, \end{aligned} \quad (20.183)$$

i.e., the composition of two K -transformations is again a K -transformation.

- (ii) There exists a unit–element, namely the identity transformation $x_j = x_j$
- (iii) Since K_j differs from zero, there exists to every K_j an inverse transformation K_j^{-1} . With $x_j = K_j x'_j$ and $x'_j = K_j^{-1} x_j$ one may deduce

$$\begin{aligned} x_j &= K_j \left(K_j^{-1} x_j \right) = K_j K_j^{-1} x_j \implies K_j K_j^{-1} = 1 \\ \implies K_j^{-1} &= \frac{1}{K_j} = \frac{1}{\prod_{i=1}^m \alpha_i^{a_{ij}}} = \prod_{i=1}^m \left(\frac{1}{\alpha_i} \right)^{a_{ij}}. \end{aligned} \quad (20.184)$$

This defines to each K -transformation its inverse.

One may interpret the entities K_1, \dots, K_n , which are generated by x_1, \dots, x_n by all possible K -transformations, as a point in an n dimensional space; this space (or its extension by the K_0 -axis) shall simply be called the K -space.

As a preparation to the BUCKINGHAM theorem we now prove the following lemmas:

Lemma 20.3 *A dimensionally homogeneous dimensionless function*

$$\Pi = f(x_1, \dots, x_n) \quad (20.185)$$

is constant in each K -space. ■

Proof Since Π is dimensionless the exponents of the fundamental dimensions on the left-hand side, a_{io} , must all vanish. Therefore, because of (20.144) $K_0 = 1$, and thus (20.143) reads

$$\Pi = f(K_1 x_1, \dots, K_n x_n). \quad (20.186)$$

In the K -space that is generated by x_1, \dots, x_n , the value of Π must therefore be constant irrespective of the value of the element (K_1, \dots, K_n) . □

Lemma 20.3 implies that every dimensionless product of the variables x_1, \dots, x_n is constant in each K -space. If, therefore, $(\Pi_1, \Pi_2, \dots, \Pi_p)$ is a complete set of dimensionless products, then for fixed x_1, \dots, x_n this set does not change its value for all K_j -values ($j = 1, \dots, n$) in K -space.

Lemma 20.4 *If $\{\Pi_1, \Pi_2, \dots, \Pi_p\}$ is a complete set of dimensionless products of the variables (x_1, \dots, x_n) , then to each set of values that is assigned to the dimensionless products $\{\Pi_1, \Pi_2, \dots, \Pi_p\}$, there belongs one and only one K -space. In other words, two elements $\{x'_j\}$ and $\{x''_j\}$ of the K -space can only differ by a K -transformation.* ■

Proof Let $\{\Pi'_1, \Pi'_2, \dots, \Pi'_p\}$ be a set of values of dimensionless products $\{\Pi_1, \Pi_2, \dots, \Pi_p\}$, and let $\{x'_j\}$ and $\{x''_j\}$ be two points in the \mathcal{E} -space, which belong to the values $\{\Pi'_1, \Pi'_2, \dots, \Pi'_p\}$. Then we have

$$\Pi'_\nu = (x'_1)^{k_1^{(\nu)}} \times \dots \times (x'_n)^{k_n^{(\nu)}} = (x''_1)^{k_1^{(\nu)}} \times \dots \times (x''_n)^{k_n^{(\nu)}}.$$

Since all x'_j on the right-hand side of this equation are positive, one may take the logarithm and obtains, after obvious rearrangements,

$$r_1 k_1^{(\nu)} + r_2 k_2^{(\nu)} + \dots + r_n k_n^{(\nu)} = 0, \quad (\nu = 1, 2, \dots, p) \tag{20.187}$$

with $r_j = \ln(x'_j/x''_j)$. Notice that it is here that we assume the x_j to be positive. Thus, BUCKINGHAM Π - Theorem is only provable for positive $x_j > 0$. Since $\{\Pi_1, \Pi_2, \dots, \Pi_p\}$ is complete, the exponents $k_j^{(1)}, \dots, k_j^{(r)}$ are solutions of the system

$$\sum_{j=1}^n a_{ij} k_j^{(\nu)} = 0, \quad (\nu = 1, 2, \dots, p), \quad (i = 1, 2, \dots, m). \tag{20.188}$$

This is a consequence of Proposition 20.5. Since, however, the solutions of (20.188) are also solutions of (20.187), the coefficients in (20.187) must linearly depend upon those of (20.188). Therefore, there must exist non-zero numbers a_j^* ($j = 1, \dots, m$), which satisfy the equation

$$\sum_{j=1}^m \alpha_j^* a_{ji} = r_i = \ln \left(\frac{x'_i}{x''_i} \right), \quad (i = 1, 2, \dots, n). \tag{20.189}$$

The last equation implies

$$x'_i = x''_i \exp \left(\sum_{j=1}^m \alpha_j^* a_{ji} \right) = x''_i \prod_{j=1}^m (e^{\alpha_j^* a_{ji}}). \tag{20.190}$$

If for simplicity we write $\alpha_j = e^{\alpha_j^*}$, ($j = 1, 2, \dots, m$), then there follows

$$x'_i = \left(\prod_{j=1}^m \alpha_j^{a_{ji}} \right) x''_i = K_i x''_i \quad (i = 1, 2, \dots, n). \tag{20.191}$$

This result shows that x'_i and x''_i belong to the same K -space. □

With all these results we may now prove the following proposition.

Proposition 20.9 (BUCKINGHAM Theorem) *Every dimensionally homogeneous equation can be transformed into an equation involving only dimensionless products.* ■

Proof According to Proposition 20.8 every dimensionally homogeneous equation $y = f(x_1 \dots x_n)$ can be brought into the form $\Pi = F(x_1, \dots, x_n)$ in which Π is

dimensionless. Let $\{\Pi_1, \Pi_2, \dots, \Pi_p\}$ be a complete set of dimensionless products belonging to (x_1, \dots, x_n) . Then, according to Lemma 20.3, to every set of values of $\{\Pi_1, \Pi_2, \dots, \Pi_p\}$ there is only one single K -space. According to Lemma 20.3 to every K -space there is only one single value of Π . Therefore, to every set of values of $\{\Pi_1, \Pi_2, \dots, \Pi_p\}$ there is only a single value of Π i.e., Π is a unique function of $\{\Pi_1, \Pi_2, \dots, \Pi_p\}$. It follows that an arbitrary dimensionally homogeneous function $y = f(x_1, \dots, x_n)$ can be reduced to the form $\Pi = F(\Pi_1, \dots, \Pi_p)$. According to Proposition 20.6, $p = (n - r)$, where r is the rank of the dimensional matrix. The converse of the theorem is equally true, i.e., an equation of dimensionless products is dimensionally homogeneous. However, this statement is trivial. \square

References

1. Barenblatt, G.I.: Dimensional Analysis, 135 pp. Gordon and Breach Science Publisher, New York, etc. (1987)
2. Bathurst, J.C., Graf, W.H., Cao, H.H.: Bed load discharge equations for steep mountain rivers. In: Thorne, C.R., Bathurst, J.C., Hey, R.D. (eds.) *Sediment Transfer in Gravel-Bed Rivers*, pp. 453–477. Wiley, New York (1987)
3. Bénard, H.: Les tourbillons cellulaires dans une nappe liquide. *Rev. Gén. Sciences Pure Appl.* **11**, 1261–1271, **11** 1309–1328 (1900)
4. Bénard, H.C.: Les tourbillons cellulaires dans une nappe liquide propageant de la chaleur par convection en régime permanent. Doctoral Dissertation, Collège de France, 15 March 1910
5. Bénard, H.C.: Les tourbillons cellulaires dans une nappe liquide, transportent de la chaleur par convection en régime permanent. *Annales de Chimie Physique* **7**(23), 62–144 (1900)
6. Bénard, H.C.: Les tourbillons cellulaires dans une nappe liquide : Méthodes optiques d'observation et d'enregistrement. *Journal de Physique Théorique et Appliquée* **10**(1), 254–266 (1901)
7. Bénard, H.C.: *Compt. Rend.* **147**(839–842), 970–972 (1908)
8. Birkhoff, G.: *Hydrodynamics, a Study in Logic, Fact and Similitude*. Dover Publication, New York (1955)
9. Brownliwe, W.R.: Compilation of alluvial channel data. *J. Hydraul. Eng.* **111**(7), 1115–1119 (1985)
10. Brownliwe, W.R., Brooks, N.H.: Prediction of flow depth and sediment discharge in open channels. W. M. Keck Laboratory of Hydraulics and Water Resources, California Institute of Technology, Pasadena (1981)
11. Buffington, J.M., Montgomery, D.R.: A systematic analysis of eight decades of incipient motion studies, with special reference to gravel-bedded rivers. *Water Resources Research*, **33**(8), 1993–2029, W. M. Keck Laboratory of Hydraulics and Water Resources, California Institute of Technology, Pasadena (1981)
12. Buckingham, E.: On physically similar systems; Illustrations of the use of dimensional equations. *Phys. Rev.* **44**, 335–376 (1914)
13. Carlson, D.E.: On some new results in dimensional analysis. *Arch. Ration. Mech. Anal.* **68**, 191–220 (1978)
14. Carlson, D.E.: A mathematical theory of physical units, dimensions and measures. *Arch. Ration. Mech. Anal.* **70**, 289–305 (1979)

15. Chandrasekhar, S.: *Hydrodynamic and Hydromagnetic Stability*, 643 pp. Dover Publications Ninc. New York (1981)
16. Casey, H.-J.: Über Geschiebebewegung. Mitteilung der preussischen Versuchsanstalt für Wasserbau und Schiffsbau, Heft, vol. 19. Berlin, Germany (1920)
17. Görtler, H.: *Dimensionsanalyse*. 247 pp. Springer, Berlin, etc. (1974)
18. Hager, W.: *Hydraulicians in Europe 1800–2000*, IAHR monograph (2003)
19. Harleman, D.R.F.: Physical hydraulic models. In: *Estuarine Modeling: An Assessment*, EPA. Water Pollution Control Research Service, 16070, DZ, 02/71 (1971)
20. Hutter, K., Jöhnk, K.: *Continuum Methods of Physical Modeling, Continuum Mechanics, Dimensional Analysis, Turbulence*, 635 pp. Springer, Berlin, etc. (2004)
21. Hutter, K., Wang Y., Chubarenko, I.: *Physics of Lakes Vol. 3: Methods of Understanding Lakes as Components of the Geophysical Environment*, 605 pp. Springer, Berlin (2014)
22. Joseph, D.D.: *Stability of Fluid Motions I and II. Tracts in Natural Philosophy*, vols. 27 and 28. Springer, New York, etc. (vol I, 282 pp., vol. II, 274 pp.) (1976)
23. Kennedy J.F.: The Albert Shields story. *J. Hydraul. Eng. ASCE*, 766-772 (1995)
24. Kramer, H.: *Modellgeschiebe und Schleppkraft*. Dr.-Ing Dissertation, Sächsische Technische Hochschule, Dresden, Germany (1932)
25. Kramer, H.: *Trans. ASCE* **100**, 798–878 (1935)
26. Langhaar, H. L.: *Dimensional Analysis and Model Theory*, 166 pp. Wiley, New York (1964)
27. Mascard, E., Bénard, H.C.: Sur le pouvoir rotatoire du sucre. *Ann. Chim. Phys. Ser. 7*(17), 125–144 (1899)
28. Meyer-Peter, E., Müller, R.: Neuere Versuchsergebnisse über den Geschiebetrieb. *Schweiz. Bauzeitung*, **103** (1948). Or: Formulas for bed-load transport. In: 2nd Meeting IAHR, Stockholm, Sweden, IAHR, pp. 39–64 (1948)
29. Nikuradse, J.: Strömungsgesetze in rauhen Röhren. *Forschungsarbeiten im Ing.-wesen*, vol. 361, 22b p. (1933)
30. Péclet, J.-C.: *Traité élémentaire de physique*. Tome 1 et 2 Hachette, Paris (1838)
31. Péclet, J.-C.: *Traité de la chaleur considérée dans ses applications*. Tome 1, 2, 3., 4th edn. Masson, Paris (1878)
32. Prandtl, L.: Neuere Ergebnisse der Turbulenzforschung. *Zeitschr. VDI* **77**, 105–113 (1933)
33. Pudasaini, S.P., Hutter, K.: *Avalanche Dynamics – Dynamics of Rapid Flows of Dense Granular Avalanches*, vol. XXIV, 602 p. Springer, Berlin etc. (2007)
34. Rayleigh, L. (Strutt, J. W.): On convection currents in a horizontal layer of fluid, when the higher temperature is on the under side. *Philos. Mag. Ser. 6*, **32**(192), 529–546 (1916)
35. Rayleigh, L., (Strutt, J. W.): *The Theory of Sound*, vol. I. Macmillan, London (1877, 1894) (alternatively: (Cambridge University Press, reissued 2011), ISBN 978-1-108-03220-9)
36. Rayleigh, L., (Strutt, J. W.): *The Theory of Sound*, vol.II. Macmillan, London (1878, 1896) (alternatively: (Cambridge University Press, reissued 2011), ISBN 978-1-108-03221-6)
37. Rayleigh, L.: ISBN 978-0-511-70396-6; ISBN 978-0-511-70397-3; ISBN 978-0-511-70398-0; ISBN 978-0-511-70399-7; ISBN 978-0-511-70400-0; ISBN 978-0-511-70401-7
38. Shields, A.F.: Anwendung der Ähnlichkeitsmechanik und der Turbulenzforschung auf die Geschiebebewegung. In: *Mitteilungen der Preussischen Versuchsanstalt für Wasserbau und Schiffbau*, Heft, vol. d26, pp. 1–26 (1936). (Engl. transl. by Ott, W.P., van Uchelen, J.C., available as Hydrodynamics Laboratory, Publication Nr. 167, Hydrodynamics Lab. Cal. Inst. Tech., Pasadena)
39. Simon, L.-J.: Sur les phénylhydrazones du glucose et leur multi-rotation. *Compt. Rend. Acad. Sci.* **132**, 564–566
40. Spurk, J.H.: *Dimensionsanalyse in der Strömungslehre*, 270 pp. Springer, Berlin, etc. (1992)
41. Straughan, B.: *The Energy Method, Stability and Non-linear Convection*. *Applied Mathematical Sciences*, vol. 91, 242 pp. Springer, New York, etc. (1992)
42. Taylor, G.I.: The formation of a blast wave by a very intense explosion. Part I: theoretical discussion. Part II: the atomic explosion of 1945. *Proc. R. Soc. Lond.* **A 201d**, 159–186 (1945)
43. Taylor, G.I.: The formation of a blast wave by a very intensive explosion. Civil Reference Research Committee, Report RC 210, 27 June 1941

44. Truesdell, A.C., Muncaster, R.G.: *Fundamentals of Maxwell's Kinetic Theory of a Simple Monatomic Gas, Treated as a Branch of Rational Mechanics*, 593 pp. Academic Press, New York etc. (1980)
45. Van Rijn, L.C.: Sediment transport. Part II. Suspended load transport. *J. Hydraul. Res. ASCE*. **110**(11) (1984)
46. Van Rijn, L.C.: Unified view of sediment transport by currents and waves: I. Initiation of motion, bed roughness and bed-load transport. *J. Hydraul. Eng. ASCE*. **133**(6), 649–667 (2001)
47. Velarde, M.G., Normand, C.: Convection. *Sci. Am.* **243**(1), 92 (1980)
48. Vetsch, D.: *Numerical Simulation of Sediment-Transport with Meshfree Methods*. (Ph.D. Dissertation) Mitteilung Nr 219 der Versuchsanstalt für Wasserbau, Hydrologie und Glaziologie der Eidg. Tech. Hochschule, Zürich (2012)
49. Weber, M.G.: *Das allgemeine Ähnlichkeitsprinzip der Physik und sein Zusammenhang mit der Dimensionslehre und der Modellwissenschaft (The general principle of similitude of physics and its connection with the sciences of dimensional analysis and model theory)*. Jahrbuch der Schiffbautechnischen Gesellschaft (1930)
50. Weinig, F., Shields, A.F.: Graphisches Verfahren zur Ermittlung der der Sickerströmung durch Staudämme. *Wasserkraft und Wasserwirtschaft*, **31**(18), 233–240 (1936) (in German)
51. Yalin, M.S., Karnahan, E.: Inception of sediment transport. *J. Hydraul. Div.* **105**(11), 1433–1443 (1979)
52. Yalin, M.S., da Silva, A.M.F.: *Fluvial processes*. IAHR Monograph, IAHR, 197pp. Delft, The Netherlands (2001)

List of Biographies

Name	Figure no.	Page no.
Svante August Arrhenius	Fig. 12.7	75
Henri Claude Bénard	Fig. 20.6	562
Ludwig Eduard Boltzmann	Fig. 17.11	336
Edgar Buckingham	Fig. 20.2	552
Constantine Carathéodory	Fig. 17.15	342
Nicolas Léonard Sadi Carnot	Fig. 17.5	327
Anders Spole Celsius	Fig. 17.22	352
Rudolf Julius Emanuel Clausius	Fig. 17.8	330
Charles-Augustine de Coulomb	Fig. 13.8	124
Jean-Baptiste le Rond d'Alembert	Fig. 19.1	492
Christian Andreas Doppler	Fig. 19.4	500
Pierre Maurice Marie Duhem	Fig. 17.16	343
Adolph Eugen Fick	Fig. 17.31	365
Jean Baptiste Joseph Fourier	Fig. 18.1	439
Joseph Louis Gay-Lussac	Fig. 17.38	381
Josiah Willard Gibbs	Fig. 17.12	338
Sidney Goldstein	Fig. 11.9	29
Henry Görtler	Fig. 16.1	270
Pierre-Henri Hugoniot	Fig. 19.21	531
James Prescott Joule	Fig. 17.7	329
Adrien-Marie Legendre	Fig. 18.2	455
John Leask Lumley	Fig. 16.12	291
Ernst Waldfried Josef Wenzel Mach	Fig. 19.9	512
Julius Robert von Mayer	Fig. 17.6	328
James Clerk Maxwell	Fig. 17.10	334
Christian Otto Mohr	Fig. 13.16	138
Walther Hermann Nernst	Fig. 17.13	339
Ernst Kraft Wilhelm Nusselt	Fig. 12.5	62

Name	Figure no.	Page no.
Carl Wilhelm Oseen	Fig. 11.8	23
Jean Claude Eugène Péclet	Fig. 20.14	589
Johann Friedrich Pfaff	Fig. 17.46	401
Max Karl Ernst Ludwig Planck	Fig. 17.14	340
Ludwig Prandtl	Fig. 15.6	245
William John Macquorn Rankine	Fig. 19.20	530
John William Strutt, 3. Baron Rayleigh	Fig. 20.5	561
Osborne Reynolds	Fig. 15.2	230
Ernst Heinrich Wilhelm Schmidt	Fig. 15.5	244
Albert Frank Shields	Fig. 20.12	578
Arnold Johannes Wilhelm Sommerfeld	Fig. 14.5	219
Geoffrey Ingram Taylor	Fig. 11.5	19
William Thomson (Lord Kelvin)	Fig. 17.9	332
Adolf Voellmy	Fig. 13.14	132
Johannes Diderik van der Waals	Fig. 17.27	358
Moritz Gustav Weber	Fig. 20.1	549

Name Index

A

Abele, 122
Abramowitz, 307
Aczel, 252
Ahlkrona, 107
Ambraseyes, 126
Ambraseys, 127
Angström, 74
Ansey, 125
Armstrong, 116
Arrhenius, 23, 74–76, 95, 336
Ayotte, 189

B

Baillifart, 122
Bamber, 103
Baral, 107
Bardet, 127
Barenblatt, 541
Batchelor, 21, 22
Bathurst, 580, 581
Bénard, 560, 562, 563, 570
Berkooz, 291
Bernoulli, 507, 514, 547
Bessel, 306, 307
Betchov, 223
Bethe, 219
Birkhoff, 544
Blasius, 39
Boltzmann, 75, 76, 330, 331, 336, 338, 340, 542
Born, 342

Bouchut, 185
Boussinesq, 137, 230, 236, 238, 240, 242, 249, 250, 252, 254, 259, 267, 310, 314, 315, 560, 564
Boussinesq, 159
Bowen, 144
Breach, 37, 38
Brillouin, 144
Brinkmann, 583
Brooks, 580
Brown, 365, 395
Brownlie, 580
Bryan, 333
Buckingham, 551, 552, 554, 591, 592, 602–604
Buffington, 580
Bunsen, 336

C

Calov, 96
Carathéodory, 333, 342, 374, 398, 407, 430, 477
Carlson, 541
Carnot, 325–327, 331, 362, 416, 417
Casagrande, 126
Casey, 578
Cauchy, 141, 373, 426, 427, 437, 444, 467, 480
Cavendish, 335
Celsius, 351, 352
Chadwick, 429
Chandrasekhar, 200, 560, 568

Charru, 200
 Chen, 185
 Chester, 37, 38
 Chiou, 174
 Christoffel, 145, 146, 190
 Clapeyron, 102, 327
 Clausius, 102, 326, 327, 330, 331, 333, 335,
 337, 340, 343, 393, 407, 425, 429–
 431, 434, 436, 437, 440–445, 449,
 451, 452, 467–470, 476, 479, 530
 Coleman, 431, 432, 442, 444, 449, 452, 467,
 468, 471, 472, 476, 478, 479
 Coriolis, 252, 253
 Corrsin, 288, 291
 Coulomb, 123, 125, 133, 134, 136–138, 142,
 143, 147, 150, 151, 153, 157, 158,
 160, 161, 175, 179, 184, 185, 188,
 191, 192, 368
 Criminale, 223
 Coussard, 531

D

D'Alembert, 492–497, 502
 Da Silva, 581
 Da Vinci, 229
 Day, 469
 De Toni, 185
 De Waele, 76, 77
 Debye, 219
 Denlinger, 185, 186
 Dirichlet, 91
 Doppler, 499, 500, 502
 Drazin, 200, 223
 Duhem, 333, 335, 337, 343, 425, 429–431,
 434, 436, 437, 440–445, 449, 451,
 452, 467–470, 476, 479, 512

E

Eckart, 125
 Eden, 500
 Edlund, 75
 Egholm, 107
 Eglit, 137, 184
 Egolf, 267, 269, 271, 272, 275, 277, 279–
 288, 290, 293–295, 298, 304–311
 Ehrenfest, 336
 Einstein, 23, 145, 330, 365
 Epstein, 219
 Erismann, 122
 Euclid, 602
 Euler, 37, 165–167, 171, 185, 198, 199, 272
 Evans, 38, 188

Ewart, 329

F

Falcon, 126
 Farkas, 479
 Favre, 235
 Feynman, 395
 Fick, 242, 364, 365, 592
 Fiedler, 283, 288, 293, 294, 312
 Fletcher, 14
 Forbes, 530
 Föttinger, 578
 Fourier, 59, 242, 332, 438, 439, 471, 479,
 498, 503, 592
 Fowler, 50
 Friedrichs, 50, 171
 Frobenius, 77
 Froude, 58, 87, 140, 548–550, 554, 559,
 572–574, 576, 588, 590, 592

G

Gaukler, 133
 Gauss, 279, 283, 289, 290
 Gay-Lussac, 380, 381
 Gersten, 216, 221–223
 Gersting, 223
 Gibbs, 331, 338, 379, 407, 409, 411, 412,
 436, 437, 446, 447, 451–457, 459,
 461, 465, 470, 471, 476–479, 529,
 532
 Glauert, 245
 Glen, 76, 77
 Godreche, 200
 Goldstein, 28, 29, 37
 Gollub, 200
 Görtler, 268–270, 541
 Gray, 141, 161, 179, 184
 Greve, 96, 102, 103, 106, 107
 Grigoriyan, 137
 Gurtin, 429, 471

H

Hagen, 303
 Hamilton, 338
 Hanjalic, 247
 Harleman, 544
 Harrison, 126
 Hauser, 479, 480
 Heaviside, 338
 Heisenberg, 219, 223
 Heitler, 219

Helm, 337
 Helmholtz, 447, 448, 454, 456, 457, 465,
 485, 487, 489
 Henry, 329
 Herterich, 96
 Herzfeld, 102, 103, 106
 Hilbert, 219
 Hill, 20
 Hindmarsh, 107
 Hinze, 272, 292, 294
 Hodgkinson, 329
 Hoff, 75
 Holmes, 291
 Holton, 268
 Hopf, 219
 Howard, 223
 Huber, 170
 Hugoniot, 176, 529, 531, 533, 534
 Hui, 185
 Hungr, 185, 187, 188
 Hurwitz, 219
 Hutter, 50, 59, 76, 77, 96, 98, 101–104, 107,
 122, 131, 134, 137, 141, 157, 159,
 165, 166, 171, 174, 177, 185, 247,
 292, 429, 430, 467, 479, 524, 541,
 543, 571, 584, 591
 Huybrechts, 96, 103

I

Iverson, 185, 186

J

Jöhnk, 524
 Jankowski, 223
 Jeffreys, 29
 Jiang, 185
 Jöhnk, 247, 292, 429, 541, 571
 Johnson, 50, 76, 77, 107
 Jones, 247
 Joseph, 200, 471, 500, 560
 Joughin, 104, 105
 Jouguet, 531
 Joule, 326, 329, 332, 380, 546, 547

K

Kaplun, 4
 Kapuskar, 127
 Karnahan, 581
 Kelvin, 447, 468, 530
 Kirchhoff, 324, 336, 340
 Kirchner, 107, 479, 480

Klein, 219, 521, 522
 Klingbeil, 144
 Knoblauch, 244
 Koch, 141
 Kohlrausch, 339
 Kolymbas, 127, 129
 Königsberger, 336
 Körating, 514
 Kourdriakov, 185
 Kovalevskaya, 480
 Kramer, 578
 Kunze, 129
 Kuo, 185, 188, 190
 Kuribayashi, 127

L

Lagerström, 4
 Lagrange, 165, 166, 168–171, 184, 185, 439,
 442–446, 449, 450, 472, 477
 Lamb, 29
 Lanchester, 245
 Langhaar, 541
 Langley, 74
 Laplace, 364, 471, 496, 566
 Larson, 50
 Laufer, 308, 310
 Launder, 247
 Laval, 514
 Lax, 171
 Lee, 185, 190
 Legendre, 455
 Leibniz, 64, 151
 Le Meur, 103
 Leonardo, 229
 Liao, 37–39, 42, 43
 Liebig, 328
 Lighthill, 29
 Lin, 185, 200
 Liouville, 531
 Liu, 442, 444, 472, 473, 479
 Lorke, 232
 Lötstedt, 107
 Love, 127
 Luca, 185, 190
 Lumley, 229, 291, 292

M

MacCormack, 166, 167
 Mach, 510–514, 517, 535, 548–550
 Manneville, 200
 Manning, 133
 Mathieu, 29

Maxwell, 330, 331, 334–336, 338, 359, 361,
457–462, 561
Maxworthy, 38
Mayer, 326, 328–330, 547
McBirney, 59
McDougall, 185, 187, 188
McMeeking, 76, 107
Meitner, 336
Meixner, 219
Meunier, 125
Millikan, 14, 15
Minkowski, 479
Möbius, 521, 522
Mohr, 138–140, 142, 156–158, 161, 185,
188, 192
Montgomery, 580
Morgenstern, 126
Morland, 50, 76–78, 97, 98
Mougin, 133
Müller, 429, 440, 441, 448, 449, 452, 467,
468, 472, 476–479
Muncaster, 542
Murase, 59
Muschik, 437

N

Napoleon, 439
Navier, 3, 4, 13, 39, 201, 205, 210, 216, 217,
223, 230, 236, 238, 242, 259, 544,
592
Nernst, 331, 339
Neumann, 91
Newcomen, 327
Newton, 15, 29, 61, 84, 90, 133, 135, 137,
203, 204, 239, 240, 266, 279, 300,
438, 440, 468, 545, 546, 549, 555,
571, 576
Nikuradse, 555
Noll, 429, 431, 432, 442, 444, 449, 452, 467,
468, 471, 472, 476, 478, 479
Normand, 563
Norton, 76, 77
Nusselt, 61, 62, 64, 90

O

Ockendon, 38
Orovan, 19
Orr, 201, 218, 220–223
Oseen, 4, 22–25, 27, 28, 30, 31, 34, 35, 37,
38
Ostwald, 75–77, 327, 336, 338, 339, 512,
552

P

Pai, 310
Papin, 326
Pauli, 219
Pearson, 37, 38
Péclet, 588, 589
Pfaff, 342, 400–403, 407, 424, 477
Philibert, 365
Piomelli, 229
Pipkin, 471
Pitman, 190
Planck, 331, 333, 335, 340, 393, 395
Poggendorff, 327, 328
Poiseuille, 300, 303, 309
Polanyi, 19
Pouillet, 74
Prandtl, 313
Prandtl, 29, 240, 242, 243, 245, 246, 248,
254, 260, 267–271, 310, 311, 555,
563, 568, 569
Preziosi, 471
Proudman, 37, 38
Przibram, 336
Pudasaini, 131, 165, 177, 178, 185, 186

R

Ramsay, 561
Rankine, 176, 529, 530, 533, 534
Rayleigh, 127, 201, 219, 221–223, 560, 561,
563, 568–570
Reichardt, 308, 309
Reid, 200, 223
Reiner, 120
Renolds, 305
Reynolds, 3, 4, 13, 14, 16, 28–30, 34, 36–
39, 42, 120, 140, 209, 216, 218–223,
229–231, 233, 237, 239–242, 259,
271, 278, 279, 281, 284, 296, 299–
302, 304–306, 308–310, 424, 548–
550, 554, 559, 563, 564, 572–574,
576, 577, 579, 582, 584, 587, 588,
592
Richardson, 588
Richter, 59
Ricou, 285
Ritter, 138
Rittmann, 59
Rivlin, 120
Robin, 101
Rodi, 247
Roesner, 559
Roos, 38

S

Saint-Venant, 137
Sarma, 126, 127
Sato, 96, 107
Savage, 134, 137, 141, 157, 166, 584
Schlichting, 216, 221–223
Schmidt, 242–244, 248, 588
Schoof, 107
Schrijver, 479
Schwarz, 213
Scotton, 185
Seifert, 578
Shanks, 30
Shields, 578–581
Smith, 76–78, 97, 98
Sokolnikoff, 144
Sommerfeld, 201, 218–223
Spalding, 247, 285
Spencer, 429
Spurk, 541
Squire, 218
Sritharan, 200
Stefan, 96, 336
Stegun, 307
Stokes, 3–6, 8, 9, 13–16, 22, 24, 27, 28, 30, 31, 33–36, 39, 41, 42, 61, 65, 66, 83, 88, 107, 201, 205, 210, 216, 217, 223, 230, 236, 238, 242, 259, 491, 544, 592
Straub, 130
Straughan, 560
Strickler, 133
Strutt, 561
Swinney, 200

T

Tadmor, 185
Tai, 185, 190
Tait, 333
Tatsuoka, 127
Taylor, 18, 19, 40, 135, 240, 254, 293, 558
Tennekes, 292
Thomson, 327, 329, 331, 332, 393, 530
Tietjens, 223
Tollmien, 222, 223

Torricelli, 547
Truesdell, 542
Tschirki, 117

U

Uberoi, 288
Umlauf, 247

V

Van der Waals, 357–361, 391, 409, 410
Van Dyke, 30, 37, 38
Van Rijn, 581
Velarde, 563
Venant, 245
Veollmy, 133
Very, 74
Vetsch, 580
Voellmy, 131, 132, 134, 137, 192
Von Kármán, 532, 533, 562
Vulliet, 50, 79

W

Wang, 144, 171, 174, 430
Watts, 327
Weber, 548, 549, 559, 576
Weierstrass, 340
Weinig, 578
Weis, 96, 107, 247
Weiss, 275, 279, 280, 282–288, 290, 293, 294, 304–310
Westdickenberg, 185
White, 37
Whitehead, 33
Wiechert, 219
Wieselsburger, 38
Williams, 116
Willmarth, 38
Wyganski, 283, 288, 293, 294, 312

Y

Yakowitz, 98
Yalin, 581

Subject Index

A

Acceleration

- absolute, 589
- Centripetal, 589
- Coriolis, 253, 589
- Euler, 589
- relative, 589

Accumulation (rate), 55, 102

- function, 54, 98, 103, 104
- function, dimensional, 90
- function, initial, 77
- function, surface, 104

Acoustic intensity, 498

Acoustics, 485

Activation energy, 75, 76

Additive (extensive) quantity, 345, 346, 371, 372, 403, 411, 430, 441

Adiabatic, 507

- change of state, 527, 533
- condition, 407, 486, 527, 529
- curve, 396, 398
- dynamic condition, 529
- expansion of gas, 393
- exponent, 511, 513
- globally, 378
- locally, 378
- non-locally, 378
- process, 396, 398
- shock, 520
- speed of sound, 487
- state, 487
- system, 372, 395, 397, 399, 404, 405, 407, 408
- throttle, 389

wall, 347, 506, 507

Angle of internal friction, 138–140, 142, 157, 161, 165, 167, 173, 178, 179, 190

Anisotropic stress response, 188

Antarctica, 50, 87, 88, 96, 106, 107

Arrhenius

- type rate factor, 74
- parameterization, 95
- relation, 76

Aspect ratio, 58, 59, 84, 140, 154

- of avalanche, 147

Autocorrelation, 241

Avalanche, 141, 142, 147, 150, 157, 159

- dense flow, 116
- deposition, 131
- down a Plexiglas-chute, 131
- down inclined plane, 169
- equation, 159
- granular, 162
- ice, 119
- model, 161
- model, granular, 141
- modeling, 131
- past tetrahedral wedge, 175
- powder, 118
- powder snow, 117, 120
- power snow, 116
- rapid granular, 115
- rock, 115, 122
- simulation, 165
- snow, 115, 116, 119, 122, 130, 134
- Voellmy's model, 132

Axel Heiberg Island, 51

B

- Balance (law), 54, 428
 - of energy, mixture, 585
 - of mass, mixture, 585
 - of momentum, mixture, 585
 - general statement, 236
 - global form, 237, 523
 - of a scalar field, averaged, 238
 - of additional scalar quantity, 237
 - of angular momentum, 427, 430
 - of averaged field, 236
 - of energy, 50, 52, 382, 384, 387, 407, 416, 426, 485–487
 - of energy for an open system, 382
 - of energy for heat conducting compressible fluid, 442
 - of energy for inviscid heat conducting compressible fluid, 467–469
 - of energy for turbulent motion, 255
 - of energy, averaged, 234
 - of entropy, 333, 337, 430, 441
 - of entropy for heat conducting compressible fluid, 442
 - of entropy for inviscid heat conducting compressible fluid, 468, 469
 - of entropy, global form, 424
 - of entropy, local form, 425
 - of internal energy, 59, 237, 376, 377
 - of internal energy, averaged, 238
 - of internal energy, locally adiabatic, dissipation-free, 378
 - of kinetic energy, 200
 - of kinetic energy of difference motion, 202
 - of kinetic energy of the perturbed motion, 200
 - of linear momentum, 237, 321, 430
 - of linear momentum, averaged, 238
 - of mass, 50, 52, 57, 58, 115, 122, 135, 137, 147, 148, 151, 159, 160, 168, 176, 185, 237, 300, 376, 390, 426, 430, 485, 487, 488, 513
 - of mass for heat conducting compressible fluid, 442
 - of mass for inviscid heat conducting compressible fluid, 467–469
 - of mass for turbulent dissipation (rate), 256
 - of mass for turbulent kinetic energy, 255
 - of mass for turbulent motion, 255, 295
 - of mass, averaged, 234, 235, 237, 266
 - of mass, depth-integrated form, 152–154
 - of mass, locally adiabatic, dissipation-free, 378
 - of mechanical, thermal energy, 322
 - of mixing length, 246
 - of momentum for inviscid heat conducting compressible fluid, 467, 469
 - of momentum, 3, 50, 52, 58, 61, 115, 122, 135, 137, 147, 148, 151, 176, 185, 281, 376, 426, 485, 487, 488, 490
 - of momentum for heat conducting compressible fluid, 442
 - of momentum for inviscid heat conducting compressible fluid, 468
 - of momentum for turbulent motion, 255, 295
 - of momentum, averaged, 234, 266
 - of momentum, depth-integrated form, 153–155, 161
 - of momentum, locally adiabatic, dissipation-free, 378
 - of momentum, 300
 - of species mass for turbulent motion, 255
 - of turbulent dissipation (rate), 250, 252–255, 260
 - of turbulent dissipation, global form, 247
 - of turbulent dissipation, local form, 248
 - of turbulent kinetic energy, 251, 252, 254, 256, 260, 284, 292
 - of turbulent kinetic energy, global form, 247
 - of turbulent kinetic energy, local form, 248
 - Reynolds averaged, 237
- Barotropic fluid, 490, 507
- Barycentric velocity, 585
- Bed friction angle, 136, 138, 139, 143, 154, 161, 165, 167, 173, 177–179, 181, 188
- Bernoulli
 - dynamic equation, 547
 - equation, 507, 514
 - method, 502
- Bessel
 - differential equation, 306
 - function, 307
 - function of first kind, 307
 - function of second order, 307
- Bifurcation, 199, 564
 - locus, 564
 - of flow, 209
- Black black radiation, 258
- Blasius flow, 39
- Body force, 468, 469, 490

- specific, 370, 426, 427, 467
- Boltzmann equation, 542
- Boltzmann's constant, 76
- Boundary condition, 4, 10, 12, 15, 27, 28, 31–34, 39, 42, 54, 61, 66, 67, 71, 90, 92, 93, 95, 153, 201, 204, 207, 211, 212, 220, 221, 256, 302–304
 - along grounding line, 70
 - at free surface, 257
 - basal, 63, 148, 257
 - dynamic, base, 142
 - dynamic, free surface, 142
 - energetic transfer, 258
 - fixed bottom surface, 92
 - for k and ε , 258
 - for species concentration, 258
 - for temperature, 257
 - free surface, 61, 67, 92, 148
 - free surface, traction free, 150
 - heat, 90
 - kinematic, 149, 152
 - kinematic, free surface, 142
 - modulo, 278
 - momentum, 256
 - Neumann, 91
 - shear and normal tractions, 63
 - thermal, 64, 82, 91, 98
 - traction, 257
 - traction free, 155
 - un-deformable base, 55
 - upstream, 33
 - zero traction, 54
- Bounded material region, 337
- Bounded spatial region, 337
- Boussinesq
 - ansatz, 315
 - approximation, 564
 - assumption, 159
 - equation, 137
 - fluid, 236, 238, 240, 247, 249, 250, 252, 254, 560, 564
 - formula, 314
- Brazil nut effect, 130
- Brinkmann number, 582, 583
- Buckingham
 - Π -theorem, 552, 602, 604
- Buckingham's
 - theorem, 551, 554, 591, 592, 602–604
- C**
 - Caloric equation of state, 378, 379, 385, 396, 399, 408, 426, 427, 436–438, 452–454, 458
 - Canonical equation of state, 452, 454
 - Capillary
 - force, 121
 - fringe, 122
 - Carnot
 - circular process, 326
 - efficiency, 416, 417
 - factor, 416
 - Center of gravity, 386
 - Characteristic
 - length, 572, 587
 - time, 589
 - velocity, 587
 - Characteristic equation, 163
 - Characteristic speed, 163, 164
 - Chemical potential, 331
 - Christoffel symbol, 145, 146, 190
 - of second kind, 145
 - Circulation, 490, 491
 - Class of material, 428
 - Clausius–Clapeyron behavior, 102
 - Clausius–Duhem inequality, 333, 335, 337, 425, 429–431, 434, 436, 437, 440–444, 449, 451, 452, 467–470, 476
 - Clausius–Planck inequality, 333
 - Closeness
 - absolute, 341
 - material, 341
 - Closure condition, 241, 242, 245, 259, 276, 285, 320
 - gradient-type, 242
 - Closure property, 155
 - Closure proposition
 - for Reynolds stress, 241
 - Closure relation, 241
 - constitutive, 236
 - of higher order, 242
 - of zeroth order, 242
 - turbulent, 238–240, 282, 304
 - Coefficient
 - of heat conduction, 440
 - of thermal expansion, 249, 254, 560, 563, 564
 - Coefficient of friction, 123, 147
 - Cohesion, 121, 122
 - Cohesionless, 121, 138, 161
 - Cohesive, 121
 - Cold-temperate-transition surface, 102
 - Coldness, 407, 446, 477
 - function, 477, 478
 - function, universal, 479
 - Coldness function, 446
 - Coleman–Noll

- approach, 442, 444, 449, 467, 468, 476, 478, 479
 - exploitation rule, 452
 - exploritation, 449
 - theory, 471, 478
 - Commutability with differentiation, 234
 - Complete differential, 399, 400
 - Conductivity
 - thermal, 448
 - Conjugate
 - pair, 454
 - variable, 454, 457
 - Conservation (law), 171, 430
 - of additional scalar quantity, 237
 - of angular momentum, 320, 426
 - of energy, 322, 366, 392, 429
 - of internal energy, 237
 - of linear momentum, 237, 238, 320, 376, 426
 - of mass, 141, 235, 237, 320, 376, 426, 429
 - of mass point, 235
 - of mass under turbulent condition, 235
 - of momentum, 141, 429
 - of momentum, averaged, 240
 - Constitutive
 - assumption, 478
 - class, 185, 441, 442, 446, 472, 479
 - closure relation, 236
 - equation, 426, 428, 442–444, 473
 - function, 448
 - law, 59, 86
 - modeling, 126
 - postulate, 120
 - quantity, 430, 450, 451, 472
 - relation, 54, 57, 66, 70, 86, 127, 184, 238, 427–429, 431, 437, 441, 442, 450, 467–469, 474, 485
 - response, 52, 58, 192
 - theory, 478
 - variable, 428, 429, 431, 433, 449, 471, 480
 - Continuity equation, 56, 68, 86, 93, 95, 272, 279, 296, 298, 300, 432, 518
 - depth integrated, 64
 - Contravariant basis vector, 145, 146
 - Cooling machine, 417, 418
 - Coordinate stretching, 50
 - Coriolis
 - acceleration, 252, 253, 589
 - Corner angular frequency, 499
 - Correlation
 - mass flux, 235
 - temperature, 241
 - term, 236–238, 259
 - term, second order, 241
 - triple, 250
 - Coulomb
 - type friction law, 136
 - type friction stress parameterization, 175
 - basal drag parameterization, 190
 - basal dry friction, 157
 - basal sliding law, 150
 - dry friction, 160, 179
 - dry friction law, 143, 147, 153, 161, 368
 - dry friction sliding law, 142
 - friction, 123
 - friction force, 133, 134
 - frictional behavior, 184
 - internal frictional behavior, 188
 - law, 122, 123
 - resistive force, 133
 - sliding, 125
 - sliding force, 137
 - sliding law, 151
 - Coulomb friction, 133
 - Coulumb
 - law, 124
 - Covariant unit vector, 145, 146
 - Creep response function, 54, 97, 102
 - dimensionless, 58, 76
 - Creep(ing) flow, 89
 - downhill, 77
 - gravity-driven, 84
 - of very viscous body, 52, 84
 - of very viscous fluid, 107
 - on a horizontal basis, 85
 - three-dimensional, 47
 - Critical
 - isotherm, 356
 - point, 359
 - pressure, 356, 357
 - temperature, 355–357, 359, 360
 - volume, 357
 - Critical out-flow flow speed, 511
 - Curvilinear coordinate, 144–148, 151, 161, 184
 - orthogonal, 141
 - Cyclic process, 393, 415–417
- D**
- D'Alembert's
 - method, 502
 - solution, 495–497

- Debris flow, 115, 117–119, 130
 - solid-water, 186
 - water-saturated, 186
- Deformation equation, 39
 - zeroth order, 40
- Degree of efficiency
 - hydraulic, 389
 - of plant, 388, 389
- Degree of provisioning, 418
- Degree of radiation, 499
- Density current, 120
- Density preserving, 135, 511, 576
 - body, 52, 58
 - fluid, 120, 152, 235, 247, 249, 252, 254, 364, 377, 449, 451, 507, 520, 547, 554, 564
 - material, 141, 161, 235
- Derivative
 - material, 53
 - material time, 58
 - substantive, 57
- Determinant, 600, 601
- Detritus
 - bed, 579
 - layer, 579
- Deviator
 - stretching tensor, 438
- Difference quotient, 269
 - model, 269
 - model of Peter Egolf, 269
- Difference Quotient Turbulence Model (DQTM), 277, 278, 281, 282, 285, 286, 293, 294, 297, 298, 303, 309, 310, 313
- Diffusion, 325, 362
 - artificial, 170, 173
 - coefficient, 364, 552
 - coefficient, thermal, 564
 - equation, 363, 364
 - numerical, 170
 - process, irreversibility, 364
- Diffusive flux, 363
- Diffusivity, 364, 545
 - dimensionless, 58
 - dimensionless thermal, 87
 - of heat, turbulent, 243
 - of mass, turbulent, 243
 - species, 585
 - thermal, 102, 563
 - turbulent, 246, 247
 - turbulent eddy, 242
- Dilatancy, 120
- Dimensional
 - matrix, 599, 600, 602
- Dimensional analysis, 246, 541, 542, 544, 548, 552, 571, 591, 599, 602
 - algebraic theory, 592
- Dimensional equation, 573
 - theory, 547
- Dimensional homogeneity, 541, 547, 550, 591, 601
 - exact definition, 593
- Dimensional matrix, 553–558, 563, 577, 582, 583, 591, 594, 595, 599, 605
- Dimensionally homogeneous, 543, 547, 548, 551, 584, 592–596, 600, 603, 605
 - equation, 548, 600, 602, 604
 - form, 547
 - function, 548, 591, 601, 605
 - functional relation, 591
 - power product, 596
 - product, 595
 - sufficient condition, 551
 - sum, 595
- Dimensionless function, 603
- Dimensionless product, 541, 542, 544, 551, 554, 557, 559, 571, 572, 579, 591, 597–599, 602–605
- Dipole, 28
 - flow, 32
- Direct Numerical Simulation (DNS), 236
- Dirichlet type boundary condition, 91
- Dispersive effect, 173
- Dissipation, 50, 58, 59, 87, 98, 129, 434, 435, 439
 - by viscous effect, 212
 - due to strain heating, 59
 - equation, turbulent, 253, 254
 - function, 376, 377
 - inequality, 431–433
 - number, 587
 - rate density, 240
 - rate density, turbulent, 239, 240
 - rate, turbulent, 239, 240, 247, 248, 250, 253, 255, 256, 259, 260
 - specific, 432
 - turbulent, 250
- Distorted model
 - geometrically, 571
- Distortion (rate) tensor, 438
- Divergence theorem, 203, 204, 207, 211, 364, 375, 425
- Doppler
 - frequency shift, 502
 - shift, 499, 502
- Drag coefficient, 28, 38, 42–44, 91, 550, 572

- basal, 257
- dimensionless, 572
- of a sphere, 38
- second order, 37
- third order, 37
- water surface, 257
- Dry friction, 123, 124, 133
 - sliding law, 142
- Dynamically similar, 576

- E**
- Earth pressure coefficient, 124, 136, 138, 139, 157, 158, 160, 177, 184, 189
- Eigenfrequency, 503–505
- Eigenfunction, 503, 505
- Eigenoscillation, 503–505
- Eigensolution, 503
- Eigenvalue, 163, 205, 221, 503
 - problem, 200, 221, 222
- Einstein summation convention, 145
- Ekman number, 590
- Energy conservation, 322
- Energy supply, 212, 377, 425, 430, 440, 443, 449, 468, 469
 - rate density, 237, 467, 585
 - specific, 373
- Energy transfer, 322
- Enthalpy, 376, 385, 387, 390, 407, 452, 454, 455, 457
 - density, 506
 - free, 454, 456, 457, 465, 585
 - of ideal gas, 464
 - of real gas, 389
 - specific, 385–387
- Entrainment, 284
 - phenomenon, 300
 - rate, 284
 - rate, turbulent, 284
- Entropy, 322, 323, 399, 407, 430, 486, 524–527, 585
 - density, 323
 - empirical, 403, 407
 - flow, 424
 - flux, 323, 424, 425, 430
 - flux vector, 425
 - production, 323, 337, 424, 430, 441
 - production, specific, 337, 424, 441
 - specific, 335, 424
 - supply, 323, 424, 425, 430, 440, 443, 449, 479
 - supply rate, 429
 - supply, bulk, 424
 - supply, specific, 424, 441
 - true, 407
- Entropy inequality, 423, 442, 444, 468, 469, 472, 480
 - extended, 449, 473
 - local, 425
 - residual, 433, 434, 437, 438, 448, 469, 475, 476
- Entropy principle, 426, 429, 437, 441–443, 445, 448, 450, 451, 477
 - of Müller, 449
 - of Clausius–Duhem, 429–431, 436, 441, 444, 449, 467, 468
 - of Müller, 429, 440, 441, 448, 452, 467, 468, 476, 478, 479
- Equilibrium state, 344, 362, 398
- Equivalence relation, 348
- Ergodic hypothesis, 234
- Erosion inception, 580
- Euclidian
 - space, 602
- Euler
 - beam, 198, 199
 - constant, 37
 - equation, 272
 - load, 199
 - number, 587
 - solution, 199
 - transformation, 37
- Eulerian
 - approach, 166
 - description limit, 185
 - discretization, 165
 - finite difference scheme, 167, 171, 185
 - finite discretization, 166
 - integration scheme, 166
 - integration technique, 171
 - scheme, 166
- Evolution equation, 211, 246
 - $k - \varepsilon$, 247
 - for ε , 251
 - free surface, 69
 - surface, 73, 96
- Extensive quantity, 345, 346

- F**
- Favre average, 234, 235
- Feynman's rattle machine, 395
- Fick's
 - first law, 364, 365
 - first law of mass flux, 242
 - second law, 364, 365

- Field equation, 52, 54, 56, 57, 60, 66, 86, 87, 90, 95, 331, 428–430, 432, 433, 441, 442, 479
- Filter, 233, 234, 259
 - operation, 249, 251
 - spatial, 233, 259
 - statical, 234
 - statistical, 233, 234, 237, 259
 - temporal, 233, 259
- Flow filament, 513
- Fluctuation, 265, 266, 280, 302
 - energy, 288
 - intensity, 287, 288
 - kinetic, 280
 - quadratic term, 280
- Fluctuation energy, 122
- Fluidization, 125–127
 - acoustic, 128
 - parameter, 129
 - partial, 127
- Fluidized bed, 21, 44
- Fourier
 - heat law, 471, 479
 - law, 439
 - law of heat conduction, 242, 438
 - representation, 498
 - series, 438
 - sine series, 503
 - type heat flux, 59
- Frame
 - inertial, 586, 592
 - non-Inertial, 589
 - non-inertial, 252, 253, 592
- Free convection fluid, 236, 238, 240
- Free shear layer theory, 268
- Frictional (stress) tensor, 266, 373, 437
- Frictional heat, 122
- Frictional heating, 98
- Frobenius expansion, 77
- Froude model, 587, 588
- Froude number, 58, 87, 108, 140, 549, 550, 554, 559, 572, 573, 576, 587, 590
 - invariance, 573
- Froude similitude, 573, 574, 577
- Fundamental
 - basic unit, 593
 - dimension, 592, 593, 600, 601, 603
 - entity, 545
 - equation, 548
 - quantity, 545, 546, 551
 - solution, 553
 - system of solutions, 599
 - unit, 545–547, 592, 593, 595, 596, 600, 601
- Fundamental tone, 504
- G**
- Gas constant, 380, 447, 466
 - molar, 351
 - universal, 351, 354, 357, 387, 464
 - universal molar, 351
- Gaussian
 - type curve, 279
 - distribution, 283
 - distribution function, 283
 - profile, 289, 290
- Geodetic height, 389
- Geometrically similar model, 571, 573, 575
- Geothermal heat, 102
 - flux, 98, 106
- Gibbs
 - equation, 409, 446, 447, 455, 465, 470
 - equation of thermostatics, 479
 - free energy, 454, 456, 457, 459, 465, 585
 - relation, 379, 407, 411, 412, 436, 437, 451–454, 456, 459, 461, 476–479, 529, 532
 - relation for thermodynamic processes, 476
 - relation of classical thermodynamics, 471
 - relation of thermostatics, 471
- Glacier, 50, 51, 55, 78, 80, 83, 107
 - Alpine, 82
 - confined valley, 51
 - flow, 56, 65
 - ice, 73
 - Petermann, 106
 - Piedmont, 51, 107
 - typical scales, 59
- Grading
 - inverse, 129–131
 - of particles, 130
 - reverse, 130
- Greenland, 50, 87, 88, 102–107
- Grounding line, 70, 77, 106, 107
- H**
- Hagen-Poiseuille
 - profile, 303, 313
- Heat, 322, 366, 370, 371, 373–375, 383
 - bath, 355
 - conducting compressible fluid, 447
 - conduction, 376

flux, 348
 flux vector, 53, 237, 333, 370, 373, 377, 426, 427, 430, 435, 438, 439, 448, 467, 527, 585
 flux vector, turbulent, 239
 frictional, 325
 Joule, 325
 radiation, 376, 426
 supply, 335
 Heat capacity, 58, 471
 at constant volume, 379
 specific isobaric, 386
 temperature dependent, 54
 Heat conductivity, 54, 58, 438, 439, 585
 Heat flux
 equilibrium, 448
 latent, 258
 sensible, 258
 Heat pump, 417, 418
 Heat transfer
 coefficient, 582
 coefficient, basal, 55
 coefficient, surface, 55
 Helmholtz, 328, 330, 336, 340
 differential equation, 498
 equation, 489
 free energy, 447, 448, 454–457, 465, 485, 487
 High resolution shock-capturing numerical method, 165, 169
 Hill vortex, 20, 44
 Homentropic
 condition, 486
 flow, 486
 Homogeneous in its dimension, 547
 Homologous, 571
 particle, 575
 point, 571, 575
 region, 571
 temperature, 588
 time, 571, 574, 575
 tracer, 588
 trajectory, 571
 velocity, 574
 Homotopy analysis method, 4, 39
 H-theorem, 331
 Hydrostatic pressure, 108, 266
 assumption, 155, 185
 distribution, 56
 equation, 65, 86, 88

I

Ice sheet, 50, 55, 78, 87, 88, 96, 101–103, 107
 depth, typical, 87
 extent, characteristic, 87
 flow, 78
 flow, steady state, 99, 100
 Greenland, 102–105, 107
 grounded, 107
 plow, plane steady, 97
 profile, 78, 98
 temperature range, 87
 three-dimensional, 79
 Ice shelf, 96, 106
 floating, 88, 106, 108
 glacier, 88
 Ross, 106
 Rønne-Filchner, 106
 Ideal, 350
 Ideal gas, 351, 354, 358, 379, 387, 389–391, 397, 399, 410, 413, 414, 447, 464, 508, 532
 caloric, 409, 465, 466, 491, 507, 510, 531
 caloric, under isentropic condition, 507
 equation, 508
 Inaccessible volume, 357
 Indifference Reynolds number, 222
 Inertial member of the NS-equation, 13
 Inner expansion, 31, 36, 37
 Stokes, 36
 Inner region, 21, 32
 Inner solution, 33, 36, 38
 Inspectional analysis, 544, 545, 591
 Integrability condition, 399, 403, 408, 409, 434, 436, 447, 452, 454–456, 477
 Intensive quantity, 345, 346
 Internal energy, 53, 237, 239, 322, 326, 333, 366, 370–374, 378–380, 382, 385, 388, 391, 396, 399, 405, 407–409, 411, 426–428, 434, 435, 437, 447, 451–454, 457, 459, 461, 464, 467, 471, 485, 487, 542, 543, 555
 balance law, 238, 376, 378
 conservation law, 237
 for ideal gas, 380, 391
 local balance, 377
 material equation, 430
 of ideal gas, 409
 per mole, 391
 per mole of ideal gas, 391
 per unit mass, 372
 specific, 370, 379, 387
 Internal pressure, 357

- Internal yield criterion, 156
 International System (IS) of units, 545
 Invariance under multifold averaging, 234
 Inviscid/ideal fluid, 221–223, 526
 Irrotational flow, 490, 491
 Isentropic, 408, 486, 506
 (adiabatic) change of state, 527
 (adiabatic) condition, 529
 adiabatic state, 487
 change of state, 490, 510
 condition, 486, 491, 507
 curve, 533, 534
 exponent, 533
 flow, 535
 law, 533
 process, 466, 485, 491
 relation, 508, 533, 534
 Isobar, 354, 355
 Isochor, 354
 of ideal gas, 354
 Isochoric
 deformation, 377
 stress coefficient, 458
 Isotherm, 350, 354–356, 359
 of ideal gas, 351
 Isotropic
 function, 444
 Isotropic stress postulate, 192
- J**
 Joule-Thomson effect, 389
 Jump condition, 523, 525, 526
 local, 525
 of energy, 445, 525–527
 of entropy, 445, 525–527
 of entropy across shock, 532, 533
 of mass, 525–527
 of momentum, 525–527
- K**
 Kelvin, 326, 327, 329, 331, 332, 350, 351, 353, 382, 393, 408, 409
 scale, 351
 temperature, 350, 351, 353, 409, 447, 468
 Kinematic (surface) equation, 54, 63, 73, 95
 Kinematic surface condition, 90, 149
 Kinematically similar, 575
 Kinetic energy, 201
 of difference motion, 201, 202
 of perturbation field, 200
 of perturbed motion, 200
- Kinetic sieving mechanism, 164
 Kinetic theory
 of dilute gas, 556
 of gas, 267, 542, 546
 of ideal gas, 556
 Klein bottle, 521, 522
 K -space, 603, 605
 K -transformation, 602
- L**
 Lagerström–Kaplan theory, 4, 30
 Lagrange
 multiplier, 443, 444, 449
 parameter, 442
 Lagrangean
 approach, 168, 169
 calclation, 170
 discretization, 165
 finite difference scheme, 171, 185
 integration scheme, 166
 integration technique, 184
 moving grid technique, 171
 moving mesh, 170
 numerical scheme, 168
 scheme, 168, 170
 Lahars, 118, 122
 Landslide, 115, 118, 119, 122, 126, 187, 188
 HsiaoLin, 190, 191
 induced by a typhoon, 184
 induced by an earthquake, 119, 184
 Nomash River, 190
 Laplace
 operator, 364, 471, 488, 496, 566
 Large Eddy Simulation (LES), 234, 259
 Laval nozzle, 514
 Law of equipartition, 380
 Legendre
 transformation, 455
 Leibniz rule, 64, 151
 Liquefaction, 125–127, 129
 full, 127, 128
 Liu's theorem, 442, 444, 472, 473, 479
 Lubricated sliding, 122
 Lubrication, 122
- M**
 Mach, 336, 343
 Mach number, 510, 511, 513, 514, 517, 535, 549, 550
 critical, 517
 Mapping invariant, 574
 Matched asymptotic expansion, 4, 31, 37

- Material
 - volume, 323, 341, 369, 370, 374, 375, 524
- Material behavior, 320
- Material equation, 321, 323, 337, 426–432, 437, 438, 441, 448, 479
- Material law, 321
- Mathematical model, 543, 544, 592
- Maxwell
 - construction, 361
 - correction, 359
 - kinetic theory, 380
 - relation, 404, 455, 457–462
 - second theory, 331
 - second theory of kinetic gas, 331
- Mean gradient theory, 268
- Mechanical law, 320
- Mechanical state, 344
- Method
 - discontinuous Galerkin, 169
 - homotopy analysis, 4, 39
 - of energy stability, 216
 - of matched asymptotic expansion, 4
 - of quantum mechanics, 382
 - of separation of variables, 397
 - of small disturbance, 216
 - shock-capturing, 169
- Metric coefficient
 - contravariant, 145
 - covariant, 144
- Metric tensor, 145
- Millikan's experiment, 15
- Minkowski, 342
- Mixing length
 - turbulent, 264
- Mixing number, 285
- Mixture
 - balance laws, 585
 - density, 579, 585
 - stretching tensor, 585
- MKS-system, 545, 546
- Möbis strip, 521, 522
- Mohr circle, 139, 140, 156, 157, 161
 - diagram, 157
 - representation, 157
- Mohr–Coulomb
 - constitutive model, 185
 - friction, 192
 - model, 188
 - plastic yield, 161
 - sliding behavior, 188
 - yield criterion, 142, 158
- Mud flow, 115, 117, 119, 130
- Muschik, 396
- N**
- Natural tone, 504
- Navier–Stokes
 - equation of a density preserving fluid, 3
 - equations, 4, 5, 8, 13, 31, 38, 39, 43, 44, 201, 210, 216, 217, 223, 236, 242
 - equations of a density preserving fluid, 205
 - fluid, 238
 - operator, 39, 43
- Navier–Stokes–Fourier–Fick equations, 584
- Navier–Stokes–Fourier–Schmidt constitutive parameterization, 242
- Navier–Stokes
 - equations, 544
- Navier–Stokes–Fourier–Fick equations, 592
- Negative compressibility, 360
- Net driving acceleration, 160
- Neumann type boundary condition, 91
- Neutral stability, 200, 221
 - condition, 200
 - curve, 221–223
 - curve of a plane boundary layer flow, 222
- Newton, 324, 334, 367, 371
- Newton's
 - fundamental law, 324
 - law, 61, 367, 371, 545, 576
 - law of motion, 468
 - mechanics, 576
 - second law, 133, 135, 137, 545, 555, 571, 576
- Newtonian
 - density preserving fluid, 203
 - fluid, 1, 204, 239, 240, 266, 279, 300, 440
 - fluid model, 90
 - linear behavior, 15
 - stress relation, 438
- No-slip condition, 9, 12, 14, 15, 21, 43, 55, 82, 201
- Non-locality, 269, 271, 311
- Non-Newtonian
 - fluid, 84
- Non-oscillatory central (NOC) difference scheme, 173, 174
 - shock capturing, 176
- Normal mode analysis, 566
- Normal stress effect, 120, 121, 140
- Nusselt number, 582
 - basal, 64
 - free surface, 61, 90

O

One-equation model, 243, 245, 246
 Organ pipe, 502
 Orr–Sommerfeld equation, 218, 220–223
 Oseen
 ansatz, 25
 approximation, 24
 correction, 4
 differential equation, 35
 equation, 24, 27, 28, 35, 38
 expansion, 28, 31, 34, 35
 -let, 4, 27, 28
 solution, 31, 34, 35, 37
 theory, 22, 31
 -type solution, 37, 38
 Outer expansion, 31, 35–37
 Outer region, 34
 Outer solution, 37, 38
 Overlapping region, 31, 35, 44
 Overtone, 504

P

Péclet number, 587
 Perfect machine, 326
 Perfect sliding, 16, 55
 Perpetuum mobile, 395
 of the first kind, 393
 of the second kind, 393, 394
 Perturbation, 199, 496
 approach, singular, 4
 equation, 200, 216, 221
 expansion, 154
 field, 200
 flow, 206
 initial, 494
 neutral, 223
 of basic flow, 206
 parameter, 50, 88, 223
 propagation in gas, 486
 quantity, 200, 217
 regular, 107
 scheme, 76
 scheme, regular, 50
 series, 223
 solution, 38, 66, 90
 solution, regular, 88
 speed, 296
 technique, 4
 unstable, 223
 variable, 200
 velocity, 210, 216, 218
 Phase rule, 331

Phase speed, 200, 218, 497
 Physical component, 146–148, 150
 Physical model, 543, 544
 theory, 571
 Piezometric pressure, 576
 Plug flow, 65, 159
 Poiseuille flow, 303, 309
 laminar, 300
 turbulent, 300, 312
 Potential
 of intermolecular force, 380
 of molecular force, 391
 thermodynamic, 448
 Potential flow, 10, 27, 32
 Power law, 76, 77, 559, 582
 constitutive law, 59
 fluid, 81, 90
 Glen, 76, 77
 Norton, 76, 77
 velocity profile, 159
 Power of working, 366, 368–370, 375, 395, 417, 582
 mechanical, 385
 of dissipation, 376
 of external force, 373
 of force, 368
 of heat pump, 417
 of pressure, 376, 398
 of sliding traction, 526
 of surface force, 370, 372
 of turbine, 388
 of viscous stress, 376
 of volume force, 369, 372
 Prandtl
 mixing length, 240, 242, 246, 313
 mixing length theory, 267
 number, 248, 254, 563, 568, 569, 582, 583, 587
 number, turbulent, 243
 proposal, 246
 Pressure
 overburden, 136
 thermodynamic, 358, 435, 437, 446, 448
 Pressure coefficient, 587
 Pressure drag, 13, 16
 Pressure tensor, 141, 147, 155
 Principal stress, 156, 157
 Principle of irreversibility, 322, 362, 392, 393
 Process
 impossible, 398, 407
 irreversible, 324–326, 362, 366, 393, 396–398, 407, 413

irreversible adiabatic, 407
 not realizable, 323, 392, 398, 407
 realizable, 398, 410
 reversible, 323, 326, 362, 366, 367, 396,
 398, 404, 407, 412, 415
 reversible adiabatic, 396–398, 404
 reversible cyclic, 396
 Process quantity, 371, 372
 Propagation speed, 525
 Pyroclastic flow, 118, 130

R

Radiation balance, 258
 Radiation number, 587, 590
 Rank, 599, 600
 Rankine–Hugoniot
 curve, 533, 534
 relation, 176, 529, 534
 Rate factor, 54, 58, 79, 80, 98, 102
 Rayleigh
 critical number, 563
 equation, 218, 221–223
 number, 563, 568, 569
 wave, 127
 Rayleigh–Bénard
 cell, 563
 convection, 560
 Instability, 560
 problem, 570
 Reflexivity, 348
 Reiner-Rivlin fluid, 120
 Reynolds, 375

-averaging, 230
 average, 234
 averaged balance laws, 237
 averaging, 266
 decomposition, 229
 effect, 577
 equation, 279, 584
 model, 550, 574
 normal stress, 284
 number, 3, 4, 13, 14, 16, 28, 30, 34, 36–
 39, 42, 44, 140, 209, 216, 218, 220–
 223, 231, 271, 278, 279, 300, 301, 304,
 305, 308, 309, 312, 549, 550, 554, 559,
 563, 564, 572–574, 576, 577, 579, 582,
 583, 587, 588, 592
 particle, 579
 shear stress, 284, 299, 302, 305, 306, 310
 similitude, 574, 576, 583
 stress, 242, 281, 284, 296, 301, 309
 stress function, 284

stress hypothesis, 239
 stress parameterization, 240, 241
 stress tensor, 239, 240, 242, 259
 transport theorem, 363, 375, 424, 523
 Reynolds-Averaged-Navier–Stokes
 (RANS)
 -averaging, 259
 equations, 259
 model, 234
 Richardson number, 587
 Rock fall, 117, 119
 Rossby number, 590
 Rule of aequipresence, 428, 430, 431, 434,
 441
 Rule of material frame indifference, 428
 Rule of material objectivity, 428

S

Saturation, 586
 Savage-Hutter (SH)
 avalanche model, 161
 equations, 137, 141, 159, 162, 164, 166,
 171, 175, 176, 181, 184
 equations, one-dimensional, 165, 166,
 169
 formulation, 190
 model, 134, 135, 139, 185
 one-dimensional theory, 161
 theory, 156, 158
 Scale analysis, 50, 84, 272, 544
 Scale effect, 544, 572, 577, 592
 Scale invariance, 543, 584, 587
 Scale invariant, 572, 574, 587
 Scaling, 147, 148, 587
 analysis, 116
 down-, 140, 543, 544, 571, 583, 584, 591,
 592
 procedure, 56, 108
 process, 59
 property, 587
 transformation, 147
 up-, 543, 588, 591
 Schmidt number, 248, 588
 turbulent, 243
 Schwarz inequality, 213
 Segregation, 129, 130
 Self-similarity, 274, 281, 288
 domain, 279, 280
 relation, 280
 Separation of variables
 method, 397
 Separation technique, 502

- Shallow
 - flow approximation, 159, 584
 - flow avalanche, 131
 - flow model, 131
 - granular flow, 153
 - granular material, 151
 - water approximation, 190
 - water avalanche model, 182
 - water equation, 165, 181
- Shallow creeping flow, 49
- Shallow flow approximation, 47, 50, 66, 71, 79, 82–84, 106, 107
- Shallow ice approximation, 88, 93
 - second order, 88
- Shallow shelf approximation, 107
- Shallow water approximation, 50
- Shallowness
 - of geometry, 115
 - of the avalanching mass, 140, 584
 - parameter, 116
 - property, 50
- Shear angle, 320
- Shear deformation, 120
- Shields diagram, 581
- Shields parameter, 579–581
 - critical, 579, 580
- Shock, 525
 - compaction, 520
 - compression, 519, 520
- Shock wave, 522, 525
 - dispersed, 164
 - half-spherical, 557
 - theory, 536
- Similarity, 271, 575, 576
 - behavior, 296, 298
 - complete, 544, 572, 574
 - duction, 278
 - kinematic, 575
 - model, 572
 - property, 296, 574
 - solution, 272, 273, 276, 278, 295, 312
- Similitude, 543
 - approximate, 576
 - dynamic, 575, 576
 - Froude, 573, 574, 577
 - kinematic, 575
 - principle, 544
 - Reynolds, 574, 576, 583
 - rule, 575
 - theory, 544
- Singular surface, 96, 486, 520–526
 - material, 441, 445, 486, 521, 525, 526
 - moving, 525
 - non-material, 486, 521
 - of first order, 486, 525, 527
- Sliding law, 14, 15, 55, 70, 77, 82, 91
 - basal, 69
 - dimensional, 63
 - exponent, 80
 - viscous, 15
- Sliding surface, 523, 525, 526
 - of two bodies, 522
- Solid friction, 122
- Sonic flow, 510
- Specific heat, 382, 387, 458–462, 464–467, 545, 582
 - at constant pressure, 386, 387
 - at constant volume, 379, 380, 382, 390, 391, 409
 - of ice, 87
 - of ideal gas, 465
 - of monatomic gas, 381
 - of multi-atomic gas, 382
 - of real gas, 390
 - of van der Waals gas, 410
- Specific turbulent enstrophy, 250
- Speed of sound, 487, 488, 491, 494, 497, 511
 - adiabatic, 487
 - of fluid, 548, 551
- Spherical radiator, 499
- Stability analysis, 200
 - energy, 209, 216
 - linear, 200, 201, 216, 217
 - linear, laminar channel flow, 216
- Stable, 199, 216
 - absolutely, 216
 - basic flow, 208
 - certainly, 216
 - channel flow, 212, 215, 216
 - equilibrium configuration, 198
 - flow, 209
 - neutrally, 216
- Stagnation pressure, 587
- State variable, 344–346, 348, 353, 385, 485
 - caloric, 485, 529
 - external, 344
 - internal, 344
 - molar, 345, 346
 - specific, 345, 346
- Statistical thermodynamics, 331
- Stationary, 216
 - adiabatic shock, 520
 - condition, 508
 - flow, 485, 506
 - isentropic flow process, 485
 - random process, 233

- shock, 486, 527, 528
- volume, 375
- Stationary random process, 233
- Statistical mechanics, 331
- Steady state, 3, 78, 97, 98, 274, 275, 513, 547
 - condition, 272, 383
 - continuity equation, 518
 - ice sheet flow, 99, 100
 - mass balance equation, 390
 - process, 385
- Stokes, 377, 402
 - approximation, 8, 15, 24, 61, 66, 83, 88, 108
 - assumption, 377
 - drag, 13
 - equation, 5, 33, 108
 - expansion, 31–33, 35
 - flow, 4, 6, 9, 13, 43, 65
 - inner expansion, 36
 - integral theorem, 491
 - law, 402
 - let, 4, 27, 28, 33
 - model, 107
 - operator, 6, 42
 - Oseen expansion, 30, 31
 - paradox, 33
 - solution, 16, 27, 28, 30, 31, 34, 41
 - solution, validity, 13
 - stream function, 6
 - theory, 14, 22, 30
- Stokes drag, 13
- Strain heating, 58, 87
- Strain rate, 120, 158
 - deviator, 239
 - mean turbulent, 230
 - tensor, 237, 240, 320, 426, 438, 467, 468
 - tensor, mixture, 585
 - vertical, 87
- Stream filament, 513
 - cross section, 515
 - flow, 506
 - section, 506
 - theory, 486, 506
 - theory, steady isentropic, 536
- Stream function, 6, 8, 10, 20, 22, 32, 218, 220
 - in the interior of the sphere, 18
 - perturbation, 218
 - spherical, 8
- Streamline, 20, 36, 69, 163
- Stress (tensor), 320, 378, 427, 430, 435, 448, 526, 585
 - Cauchy, 141, 373, 426, 427, 437, 444, 467
 - dimensionless, 579
 - extra, 373, 437, 438, 449
 - fictitious shear, 314, 315
 - frictional, 11, 266, 373, 437, 485
 - in thermodynamic equilibrium, 437
 - internal shear, 142, 143
 - longitudinal turbulent normal, 285
 - normal, 120, 121, 156, 184, 188
 - Reynolds, 239, 240, 242, 259, 281, 284, 296, 305, 309
 - Reynolds normal, 284
 - Reynolds shear, 306, 310
 - shear, 17, 18, 65, 68, 156, 157, 267, 272
 - transverse turbulent normal, 288
 - turbulent, 266, 267, 302
 - turbulent shear, 269, 274, 276, 277, 283, 306, 308
 - viscous, 266, 300, 376, 485, 490
- Stress deviator, 53, 54, 56, 58, 76, 85, 120, 237
- Stress state, 139, 156, 157
 - active, 140, 157
 - passive, 140, 157
 - passive basal, 157
- Stress strain rate relation, 120
- Stress (tensor)/shear, 321
- Stretching tensor, 53, 120, 426, 427, 434
 - mixture, 585
- Strouhal number, 588
- Subcritical flow, 164, 177
- Submarine slide, 126
- Subsonic flow, 510, 514
- Super-elevated model, 571
- Supercritical flow, 164, 175–177
- Supersonic flow, 510, 514
- Surface force, 369
- Surface tension, 16, 121, 122, 548, 551, 558, 571, 576
 - gradient, 21
- Suspended matter/sediment, 586
- System, 337
 - absolutely closed, 341, 347, 355, 407
 - adiabatic, 341, 347
 - adiabatically closed, 412, 413
 - closed, 326, 375
 - closed adiabatic, 398
 - heterogeneous, 345
 - heterogeneous two-phase, 345
 - homogeneous, 333, 344–346, 412
 - materially bounded, 326

- materially closed, 341, 344, 347, 371, 372, 383–385, 393
 - materially closed but moving, 383
 - materially closed by adiabatic wall, 374
 - materially closed, at rest, 371
 - non-heterogeneous, 345
 - open, 341, 344, 375, 383
 - simple, 345
 - thermodynamic, 337, 341, 344
 - with a bounded material substance, 337
 - with a bounded spatial region, 337
- T**
- Taylor
 - series, 14, 40
 - series expansion, 40, 85, 135, 240, 254, 293, 509, 511
 - Temperate ice, 96, 102, 106
 - Temperature, 52, 54–56, 59, 63, 64, 67, 69, 70, 74, 76–79, 82, 96–106, 232, 236, 241, 257, 331, 346, 349, 350, 393–395, 485, 486, 488, 509, 555
 - absolute, 331, 333, 335, 350, 351, 379, 399, 405–409, 411, 424, 429, 430, 437, 440–443, 446, 447, 449, 451, 453, 468, 472, 477–479, 508, 545
 - burning, 118
 - Celsius, 351
 - critical, 355–357, 359, 360
 - empirical, 349–351, 405, 406, 408, 409, 437, 442, 445–447, 451, 468, 472, 475, 478
 - Fahrenheit, 353
 - fluctuation, 239, 241
 - granular, 122
 - ideal gas, 409
 - Kelvin, 350, 351, 353, 382, 406, 409, 447, 468, 585
 - melting, 82, 96
 - thermodynamic, 353, 405, 406, 408
 - universal, 350, 430
 - Theory of heat, 322
 - Thermal efficiency
 - of heat engine, 415, 416
 - optimal, 416
 - Thermal equation of state, 254, 350, 351, 353–357, 378, 379, 385, 391, 392, 396, 399, 408, 409, 426, 427, 436–438, 452, 453, 458, 464, 487, 488, 490, 491, 529, 532, 586
 - for ideal gas, 354, 391, 532
 - for mixture, 585
 - Thermo-viscous
 - body, 74
 - flow state, 564
 - response, 54
 - Thermodynamic equilibrium, 331, 344, 348, 349, 351, 355, 407, 435, 437, 438, 440, 448, 471, 486, 488
 - Thermodynamic potential, 453, 454, 457
 - Thermodynamic process, 341, 362, 424, 426, 427, 430–432, 434, 441, 442, 468, 469, 478
 - admissible, 427, 429, 444
 - differentiable, 424
 - irreversible, 362
 - physically possible, 425
 - quasi-static, 357
 - reversible, 362
 - Thermodynamic state, 333, 341, 344, 345, 350, 353, 362, 366, 377
 - unstable, 360
 - Thermodynamic system, 337
 - Thermodynamics
 - first law, 322, 325, 326, 392, 418, 506, 547
 - irreversible, 418
 - rational, 418
 - second law, 126, 322, 323, 325, 326, 331, 333, 350, 361, 366, 376, 379, 385, 392, 393, 395, 404, 405, 409, 411–418, 423–426, 429, 430, 434, 436, 440, 448, 452, 458, 472, 473, 479, 485, 533, 534
 - third law, 331
 - zeroth law, 348
 - Thermometer, 349, 350
 - fluid, 349, 350
 - gas, 349
 - ideal gas, 350
 - mercury, 349
 - real, 331
 - resistivity, 349
 - substance, 350
 - Thermostatic equilibrium, 434
 - Thermostatics, 345, 429, 471, 479
 - of mixture, 331
 - Torricelli formula, 547
 - Total differential, 399, 400, 402, 403, 453
 - of entropy, 411, 436, 446, 476
 - of internal energy, 379, 452
 - Total variation diminishing (TVD), 169, 171
 - algorithm, 171
 - Minmod limiter, 173
 - shock capturing technique, 171
 - slope limiter, 185

Traction
 normal, 55, 63
 shear, 55, 56, 63, 77, 136, 143

Traction free, 142

Transitivity, 348

Trans-sonic condition, 510

Trap machine, 393, 394

Truesdell, 326, 337

Turbidity current, 115, 126, 130

Turbulent cascade model, 229

Turbulent convection, 288, 303
 term, 294

Turbulent dissipation, 239, 240
 rate, 239

Turbulent fluctuation, 232, 240

Turbulent friction, 133

Turbulent heat flux, 243, 260
 vector, 239

Turbulent kinetic energy, 229, 239, 247,
 249–252, 254–256, 258, 260, 266,
 267, 288, 293
 equation, 292
 production, 288, 292

Turbulent Manning-Gaukler term, 133

Turbulent mass flux, 243

Turbulent mixing length, 240, 246, 267, 269,
 313
 balance law, 246
 model, 264
 Prandtl, 246
 proposal, 268
 theory, 267

Turbulent model
 $k - \ell$, 242, 246
 $k - \omega$, 242, 246
 $k - \varepsilon$, 242, 246, 247, 249, 254
 $k - \varepsilon$, density preserving fluid, 247
 $k - \varepsilon$, evolution equation, 247

Turbulent modeling, 227

Turbulent species mass flux, 239

Two-equation model, 243, 245, 247

U

Un-lubricated friction, 122, 123

Un-lubricated sliding, 122

Unit normal vector, 256, 521
 exterior, 54, 373

Unstable, 199, 200, 205, 223
 basic motion, 218
 channel flow, 212
 linearly, 216
 regime, 222

wave, 222

V

Van der Waals
 equation, 361
 fluid, 359
 force, 360
 gas, 357, 359–361, 391, 409, 410
 model, 360
 phenomenological model, 357
 relation, 360

Vapor pressure, 356

Viscosity, 16, 77, 221, 230, 267, 542, 543,
 574
 artificial, 168, 169
 bulk, 438, 440, 585, 590
 dimensionless, 77
 dynamic, 564
 dynamic shear, 321
 eddy, 243, 246, 268
 effective, 61
 in a kinetic gas, 542, 555, 558
 kinematic, 3, 231, 240, 301, 548, 554,
 558, 560, 563, 566, 572, 582
 laminar kinematic, 240
 material kinematic, 240, 249
 numerical, 174
 of a gas, 542
 scale, 573, 574
 shear, 323, 438, 440, 542, 585
 turbulent, 230, 240, 243, 246, 248, 249,
 254, 259

Viscosity law
 finite, 76, 97

Viscous (diffusive) member of the NS-
 equation, 13

Viscous drag, 12, 13, 16

Viscous fluid, 16, 22, 39, 50, 209, 222, 223,
 238, 320, 426, 438, 558
 around a fixed body, 38
 density preserving, 201
 heat conducting, 429, 431, 436, 437, 441,
 452, 487
 heat conducting compressible, 427
 incompressible, 278
 linear, 240, 376
 nonlinear, 240

Viscous friction, 123

Viscous sliding condition, 43

Voellmy coefficient, 192

Voellmy's model, 131, 132, 134, 137

Volcano

- cold, 126–128
- mud, 126
- Volume flux, 65
- Volume force, 369
- Von Kármán relation, 532, 533
- Vortex sheet, 526
- Vorticity, 26, 30, 250, 489
 - equation, 4, 7, 24, 218
 - fluctuation, 253
 - free state, 489
 - transport equation, 251
 - turbulent, 246, 250
- Vorticity theorem
 - Kelvin, 491

W

Wall

- adiabatic, 348, 374
- diathermic, 348, 355, 405, 406
- ideal, 441, 445, 446
- ideal diathermic, 475
- semi-permeable, 394

Wave

- acoustic, 489, 501
- equation, 493, 496
- length, 505
- number, 497
- plane, 493, 497
- shock, 522, 525
- spherical, 493, 496, 499
- Wave number, 218
- Weber number, 549, 559, 576
- Whitehead paradox, 33
- William, 332
- Work, 326, 331, 368, 369
 - by a pump, 384
 - by pressure, 384
 - due to volume change, 369
 - frictional, 399
 - mechanical, 326
 - of a system, 366
 - of frictional force, 411
 - of non-conservative force, 383
 - of pressure, 369, 411
 - of turbine, 388
 - technical, 386
 - usable, 326